UC San Diego

UC San Diego Electronic Theses and Dissertations

Title

Blast damage mitigation of steel structures from near- contact charges

Permalink

https://escholarship.org/uc/item/4r70s0gg

Author

Wolfson, Janet Crumrine

Publication Date

2008

Peer reviewed|Thesis/dissertation

eScholarship.org Powered by the California Digital Library
University of California

UNIVERSITY OF CALIFORNIA, SAN DIEGO

Blast Damage Mitigation of Steel Structures from Near-Contact Charges

A dissertation submitted in partial satisfaction of the
requirements for the degree of Doctor of Philosophy

in

Structural Engineering

by

Janet Crumrine Wolfson

Committee in Charge

Professor Gil Hegemier, Chair
Professor David Benson
Professor Vistasp M. Karbhari
Professor Vitali Nesterenko
Professor Frieder Seible

2008

Copyright

Janet Crumrine Wolfson, 2008

All rights reserved.

The Dissertation of Janet Crumrine Wolfson is approved, and it is acceptable in quality and form for publication on microfilm:

Chair

University of California, San Diego

2008

DEDICATION

I dedicate this dissertation to three men who influenced my life.

My Grandfather, Gerald Crumrine, for teaching me algebra in the 8th grade and instilling in me the purpose of math.

My father, for pushing me to try harder and do better.

My husband, for having the faith in me that I can achieve anything that I want to, all I have to do is try.

TABLE OF CONTENTS

SIGNATURE PAGE iii
DEDICATION iv
TABLE OF CONTENTS v
LIST OF ABBREVIATIONS xx
LIST OF SYMBOLS xxii
LIST OF FIGURES xxiii
LIST OF TABLES xlii
ACKNOWLEDGEMENTS xlix
VITA li
ABSTRACT lii
1. EXECUTIVE SUMMARY 1
1.1 INTRODUCTION 1
1.2 GENERIC CELLULAR STEEL STRUCTURE 2
1.3 SUBSTRUCTURE BEHAVIOR FROM NEAR-CONTACT CHARGES 3
1.4 BLAST MITIGATION TECHNIQUES 7
1.4.1 Laboratory Tests (Initial Retrofit Techniques) 8
1.4.2 Scaled Field Tests (proof-of-concept) 10
1.5 SIMPLIFIED COMPUTATIONAL ANALYSES 15
1.5.1 Simplified Momentum Calculations 15
1.5.2 Computational Analyses 17
1.5.3 Velocity Comparisons 20
1.6 FULL SCALE FIELD TESTS (EMRTC) 22
2. DISSERTATION OUTLINE 28
3. BLAST DAMAGE FAILURE MODES 30
3.1 INTRODUCTION 30
3.2 FAILURE MODES 31
3.2.1 Bolts and Connections 31
3.2.2 Formation and Propagation of Flyer Plates 33
3.2.3 Punch-Through (Secondary) Flyer Plates 35
3.2.4 Damage Levels Observed in Laboratory Tests 37
3.2.5 Brittle and Ductile Fracture Modes 38

3.3 EMRTC FIELD TESTS 1 AND 2 40
3.3.1 Introduction 40
3.3.2 Test Set-Up 40
3.3.3 Charge Set-Up 44
3.3.4 Instrumentation 46
3.3.5 Phantom Cameras 47
3.3.6 Test results 47
3.3.7 Field Test Summary 59
3.4 LAB TESTS 60
3.4.1 Introduction 60
3.4.1 Test Set-Up 62
3.4.2 Loading Methodologies 65
3.4.3 Instrumentation 67
3.4.4 Strain Gage Data 68
3.4.5 Conclusion 74
3.5 BIBLIOGRAPHY 75
4. KEDD DEVELOPMENT 76
4.1 INTRODUCTION 76
4.2 KINETIC ENERGY DEFEAT DEVICE (KEDD) DEVELOPMENT 76
4.2.1 Concept 76
4.2.2 KEDD Laboratory Tests Set-Up 83
4.2.3 KEDD Full Scale Field Test Set-Up 88
4.2.4 KEDD Scaled Field Tests Set-Up (proof-of-concept Tests) 94
4.3 KEDD LABORATORY TESTS 100
4.3.1 Introduction 100
4.3.2 Comparison of Test Results 100
4.3.3 KEDD Comparisons 101
4.3.4 KEDD Conclusions (From Laboratory Tests) 115
5. SCALED TESTS AND CALCULATIONS 116
5.1 INTRODUCTION 116
5.2 TEST SET-UPS 117
5.2.1 Charge Set-Up 118
5.2.2 Time of Arrival Pins 119

5.2.3 Velocity Comparisons 121
5.3 2 PLATE TEST 122
5.3.1 Introduction 122
5.3.2 Test Set-up 122
5.3.3 Calculation Set-up 122
5.3.4 Simplified Momentum Calculation 125
5.3.5 Baseline Test 127
5.3.6 KEDD on Top 135
5.3.7 KEDD on Bottom 146
5.3.8 2 Rows of KEDD's on Top 157
5.3.9 KEDD on Top and Bottom 166
5.3.10 3 Rows of KEDD's on Top 175
5.3.11 Wall of Water Simplified Calculation 184
5.4 2 PLATE TEST COMPARISONS 189
5.4.1 Field Test Comparisons 189
5.4.2 Simplified Calculations Summary 198
5.5 CONCEPTUAL DESIGN GUIDELINES 202
5.6 BIBLIOGRAPHY 203
6. FULL-SCALE RETROFITTED FIELD TESTS (EMRTC) FIELD TEST 3 205
6.1 TEST SET-UP 205
6.2 CHARGE SET-UP 208
6.3 PHANTOM CAMERAS 209
6.4 TEST RESULTS 211
6.5 ADDITIONAL MITIGATION TECHNIQUES 233
6.6 SUMMARY 235
6.7 BIBLIOGRAPHY 236
7. CONCLUSIONS AND RECOMMENDATIONS 237
7.1 CONCLUSION 237
7.2 RECOMMENDATIONS 239
A. APPENDIX A- CHAPTER 3 241
A.1 BRITTLE AND DUCTILE FRACTURE MODES 241
A.2 FIELD TESTS 242
A.2.2 Field Test 2 247

A.3 LAB TESTS 252
A.3.1 test Set-up 252
A.3.2 Blast Generator Description 254
A.3.3 Instrumentation 256
A.3.4 Bandpass Filters 260
A.3.5 Strain Gage Data 265
B. APPENDIX B – CHAPTER 4 280
B.1 KEDD FIELD SCALE FIELD TEST SET-UP 280
B.1.1 KEDD Scaled Field Tests Set-Up (Proof of Concept Tests) 282
C. APPENDIX C – CHAPTER 5 286
C.1 CALIBRATION TEST 286
C.1.2 4 Plate Test 292
C.1.3 2 Plate Test 297
C.1.4 KEDD on Top – 2- Row Test Results 301
C.1.5 2 Plate Test Comparisons 304
C.1.6 3 Plate Test 307
D. APPENDIX D– CHAPTER 6 313
D.1.1 Test Set-Up 313
D.1.2 Charge Set-Up 314
D.1.3 Instrumentation 314
D.2 TEST RESULTS 319
E TEST RESULTS – BALLISTIC TESTS – TYPE 1 321
E.1 STEEL TOWER SINGLE PLATE: TEST 1 (SP1) 321
E.1.1 Introduction 321
E.1.2 Instrumentation 321
E.1.3 Blast Generator Data 324
E.1.4 Specimen Behavior 324
E.2 STEEL TOWER SINGLE PLATE: TEST 2 (SP2) 326
E.2.1 Introduction 326
E.2.2 Instrumentation 326
E.2.3 Blast Generator Data 328
E.2.4 Specimen Behavior 328

E.3 STEEL TOWER SINGLE PLATE: TEST 3 (SP3) 330
E.3.1 Introduction 330
E.3.2 Instrumentation 330
E.3.3 Blast Generator Data 335
E.3.4 Specimen Behavior 335
E.4 STEEL TOWER SINGLE PLATE: TEST 4 (SP4) 337
E.4.1 Introduction 337
E.4.2 Instrumentation 337
E.4.3 Blast Generator Data 342
E.4.4 Specimen Behavior 342
E.5 STEEL TOWER SINGLE PLATE: TEST 5 (SP5) 345
E.5.1 Introduction 345
E.5.2 Instrumentation 345
E.5.3 Blast Generator Data 350
E.5.4 Specimen Behavior 350
E.6 STEEL TOWER SINGLE PLATE: TEST 6 (SP6) 352
E.6.1 Introduction 352
E.6.2 Instrumentation 352
E.6.3 Blast Generator Data 356
E.6.4 Specimen Behavior 356
E.7 STEEL TOWER SINGLE PLATE: TEST 7 (SP7) 357
E.7.1 Introduction 357
E.7.2 Instrumentation 357
E.7.3 Blast Generator Data 362
E.7.4 Specimen Behavior 362
E.8 STEEL TOWER SINGLE PLATE: TEST 8 (SP8) 364
E.8.1 Introduction 364
E.8.2 Instrumentation 364
E.8.3 Blast Generator Data 369
E.8.4 Specimen Behavior 369
E.9 STEEL TOWER SINGLE PLATE: TEST 9 (SP9) 372
E.9.1 Introduction 372
E.9.2 Instrumentation 372

E.9.3 Blast Generator Data 377
E.9.4 Specimen Behavior 377
E.10 STEEL TOWER SINGLE PLATE: TEST 10 (SP10) 380
E.10.1 Introduction 380
E.10.2 Instrumentation 380
E.10.3 Blast Generator Data 385
E.10.4 Specimen Behavior 385
E.11 STEEL TOWER SINGLE PLATE: TEST 11 (SP11) 387
E.11.1 Introduction 387
E.11.2 Instrumentation 387
E.11.3 Blast Generator Data 392
E.11.4 Specimen Behavior 392
E.12 STEEL TOWER SINGLE PLATE: TEST 12 (SP12) 394
E.12.1 Introduction 394
E.12.2 Instrumentation 394
E.12.3 Blast Generator Data 398
E.12.4 Specimen Behavior 398
E.13 STEEL TOWER SINGLE PLATE: TEST 13 (SP13) 401
E.13.1 Introduction 401
E.13.2 Instrumentation 401
E.13.3 Blast Generator Data 406
E.13.4 Specimen Behavior 406
E.14 STEEL TOWER SINGLE PLATE: TEST 14 (SP14) 408
E.14.1 Introduction 408
E.14.2 Instrumentation 408
E.14.3 Blast Generator Data 413
E.14.4 Specimen Behavior 413
E.15 STEEL TOWER SINGLE PLATE: TEST 15 (SP15) 415
E.15.1 Introduction 415
E.15.2 Instrumentation 415
E.15.3 Specimen Behavior 419
E.16 STEEL TOWER SINGLE PLATE: TEST 16 (SP16) 421
E.16.1 Introduction 421

E.16.2 Instrumentation 421
E.16.3 Blast Generator Data 426
E.16.4 Specimen Behavior 426
E.17 STEEL TOWER SINGLE PLATE: TEST 17 (SP17) 428
E.17.1 Introduction 428
E.17.2 Instrumentation 428
E.17.3 Generator Data 433
E.17.4 Specimen Behavior 433
E.18 STEEL TOWER SINGLE PLATE: TEST 18 (SP18) 435
E.18.1 Introduction 435
E.18.2 Instrumentation 435
E.18.3 Blast Generator Data 440
E.18.4 Specimen Behavior 440
E.19 STEEL TOWER SINGLE PLATE: TEST 19 (SP19) 442
E.19.1 Introduction 442
E.19.2 Instrumentation 442
E.19.3 Blast Generator Data 447
E.19.4 Specimen Behavior 447
E.20 STEEL TOWER SINGLE PLATE: TEST 20 (SP20) 449
E.20.1 Introduction 449
E.20.2 Instrumentation 449
E.20.3 Blast Generator Data 454
E.20.4 Specimen Behavior 454
E.21 STEEL TOWER SINGLE PLATE: TEST 21 (SP21) 456
E.21.1 Introduction 456
E.21.2 Instrumentation 456
E.21.3 Blast Generator Data 461
E.21.4 Specimen Behavior 461
E.22 STEEL TOWER SINGLE PLATE: TEST 22 (SP22) 464
E.22.1 Introduction 464
E.22.2 Instrumentation 464
E.22.3 Blast Generator Data 468
E.22.4 Specimen Behavior 468

E.23 STEEL TOWER SINGLE PLATE: TEST 23 (SP23) 470
E.23.1 Introduction 470
E.23.2 Instrumentation 470
E.23.3 Blast Generator Data 472
E.23.4 Specimen Behavior 472
E.24 STEEL TOWER SINGLE PLATE: TEST 24 (SP24) 474
E.24.1 Introduction 474
E.24.2 Instrumentation 474
E.24.3 Blast Generator Data 477
E.24.4 Specimen Behavior 477
E.25 STEEL TOWER SINGLE PLATE: TEST 25 (SP25) 480
E.25.1 Introduction 480
E.25.2 Instrumentation 480
E.25.3 Specimen Behavior 485
E.26 STEEL TOWER SINGLE PLATE: TEST 26 (SP26) 487
E.26.1 Introduction 487
E.26.2 Instrumentation 487
E.26.3 Blast Generator Data 495
E.26.4 Specimen Behavior 495
E.27 STEEL TOWER SINGLE PLATE: TEST 27 (SP27) 497
E.27.1 Introduction 497
E.27.2 Instrumentation 497
E.27.3 Blast Generator Data 505
E.27.4 Specimen Behavior 505
E.28 STEEL TOWER SINGLE PLATE: TEST 28 (SP28) 508
E.28.1 Introduction 508
E.28.2 Instrumentation 508
E.28.3 Blast Generator Data 511
E.28.4 Specimen Behavior 514
E.29 STEEL TOWER SINGLE PLATE: TEST 29 (SP29) 516
E.29.1 Introduction 516
E.29.2 Instrumentation 516
E.29.3 Blast Generator Data 519

E.29.4 Specimen Behavior 524
E.30 STEEL TOWER SINGLE PLATE: TEST 30 (SP30) 526
E.30.1 Introduction 526
E.30.2 Instrumentation 526
E.30.3 Blast Generator Data 529
E.30.4 Specimen Behavior 534
E.31 STEEL TOWER SINGLE PLATE: TEST 31 (SP31) 536
E.31.1 Introduction 536
E.31.2 Instrumentation 536
E.31.3 Blast Generator Data 539
E.31.4 Specimen Behavior 543
E.32 STEEL TOWER SINGLE PLATE: TEST 32 (SP32) 545
E.32.1 Introduction 545
E.32.2 Instrumentation 545
E.32.3 Blast Generator Data 548
E.32.4 Specimen Behavior 553
E.33 STEEL TOWER SINGLE PLATE: TEST 33 (SP33) 555
E.33.1 Introduction 555
E.33.2 Instrumentation 555
E.33.3 Blast Generator Data 563
E.33.4 Specimen Behavior 563
E.34 STEEL TOWER SINGLE PLATE: TEST 51 (SP51) 565
E.34.1 Introduction 565
E.34.2 Instrumentation 565
E.34.3 Blast Generator Data 567
E.34.4 Specimen Behavior 569
F TEST RESULTS – BALLISTIC TESTS – TYPE 2 571
F.1 STEEL TOWER SINGLE PLATE: TEST 35 (SP35) 571
F.1.1 Introduction 571
F.1.2 Instrumentation 571
F.1.3 Blast Generator Data 573
F.1.4 Specimen Behavior 573
F.2 STEEL TOWER SINGLE PLATE: TEST 36 (SP36) 575

F.2.1 Introduction 575
F.2.2 Instrumentation 575
F.2.3 Bolt Type 577
F.2.4 Blast Generator Data 577
F.2.5 Specimen Behavior 579
F.3 STEEL TOWER SINGLE PLATE: TEST 37 (SP37) 581
F.3.1 Introduction 581
F.3.2 Instrumentation 581
F.3.3 Blast Generator Data 583
F.3.4 Specimen Behavior 585
F.4 STEEL TOWER SINGLE PLATE: TEST 38 (SP38) 587
F.4.1 Introduction 587
F.4.2 Instrumentation 587
F.4.3 Bolt Type 589
F.4.4 Blast Generator Data 589
F.4.5 Specimen Behavior 591
F.5 STEEL TOWER SINGLE PLATE: TEST 39 (SP39) 593
F.5.1 Introduction 593
F.5.2 Instrumentation 593
F.5.3 Blast Generator Data 595
F.5.4 Specimen Behavior 597
F.6 STEEL TOWER SINGLE PLATE: TEST 40 (SP40) 599
F.6.1 Introduction 599
F.6.2 Instrumentation 599
F.6.3 Blast Generator Data 601
F.6.4 Specimen Behavior 603
F.7 STEEL TOWER SINGLE PLATE: TEST 41 (SP41) 605
F.7.1 Introduction 605
F.7.2 Kinetic Energy Defeat Device (KEDD) 605
F.7.3 Instrumentation 605
F.7.4 Blast Generator Data 607
F.7.5 Blast Generator Data 609
F.8 STEEL TOWER SINGLE PLATE: TEST 42 (SP42) 611

F.8.1 Introduction 611
F.8.2 Kinetic Energy Defeat Device (KEDD) 611
F.8.3 Instrumentation 611
F.8.4 Strain Gage Locations 612
F.8.5 Blast Generator Data 613
F.8.6 Blast Generator Data 615
F.9 STEEL TOWER SINGLE PLATE: TEST 43 (SP43) 617
F.9.1 Introduction 617
F.9.2 Instrumentation 617
F.9.3 Specimen Behavior 621
F.10 STEEL TOWER SINGLE PLATE: TEST 44 (SP44) 623
F.10.1 Introduction 623
F.10.2 Kinetic Energy Defeat Device (KEDD) 623
F.10.3 Instrumentation 623
F.10.4 Blast Generator Data 627
F.10.5 Blast Generator Data 627
F.11 STEEL TOWER SINGLE PLATE: TEST 45 (SP45) 629
F.11.1 Introduction 629
F.11.2 Instrumentation 629
F.11.3 Blast Generator Data 631
F.11.4 Specimen Behavior 633
F.12 STEEL TOWER SINGLE PLATE: TEST 46 (SP46) 635
F.12.1 Introduction 635
F.12.2 Kinetic Energy Defeat Device (KEDD) 635
F.12.3 Instrumentation 635
F.12.4 Blast Generator Data 639
F.12.5 Specimen Behavior 639
F.13 STEEL TOWER SINGLE PLATE: TEST 47 (SP47) 641
F.13.1 Introduction 641
F.13.2 Kinetic Energy Defeat Device (KEDD) 641
F.13.3 Instrumentation 641
F.13.4 Blast Generator Data 643
F.13.5 Blast Generator Data 645

F.14 STEEL TOWER SINGLE PLATE: TEST 48 (SP48) 647
F.14.1 Introduction 647
F.14.2 Kinetic Energy Defeat Device (KEDD) 647
F.14.3 Instrumentation 647
F.14.4 Bolt Type 649
F.14.5 Blast Generator Data 651
F.14.6 Specimen Behavior 651
F.15 STEEL TOWER SINGLE PLATE: TEST 49 (SP49) 653
F.15.1 Introduction 653
F.15.2 Kinetic Energy Defeat Device (KEDD) 653
F.15.3 Instrumentation 653
F.15.4 Blast Generator Data 657
F.15.5 Specimen Behavior 657
F.16 STEEL TOWER SINGLE PLATE: TEST 50 (SP50) 659
F.16.1 Introduction 659
F.16.2 Instrumentation 659
F.16.3 Blast Generator Data 660
F.16.4 Specimen behavior 660
G FIELD TEST REPORTS 662
G.1 TEST 1 (CALIBRATION SHOT 1) 662
G.1.1 Introduction 662
G.1.2 Instrumentation 662
G.1.3 Specimen Behavior 663
G.2 TEST 2 (CALIBRATION SHOT 2) 666
G.2.1 Introduction 666
G.2.2 Instrumentation 666
G.2.3 Specimen Behavior 667
G.3 TEST 3 (CALIBRATION SHOT 3) 670
G.3.1 Introduction 670
G.3.2 Instrumentation 670
G.3.3 Specimen Behavior 671
G.4 TEST 4 (CALIBRATION SHOT 4) 674
G.4.1 Introduction 674

G.4.2 Instrumentation 674
G.4.3 Specimen Behavior 675
G.5 TEST 5 (FOUR-PLATE TEST) 678
G.5.1 Introduction 678
G.5.2 Instrumentation 678
G.5.3 Specimen Behavior 679
G.6 TEST 6 (TWO-PLATE TEST – NO KEDD) 681
G.6.1 Introduction 681
G.6.2 Instrumentation 681
G.6.3 Specimen Behavior 682
G.7 TEST 7 (TWO-PLATE TEST –KEDD ON BOTTOM) 687
G.7.1 Introduction 687
G.7.2 Kinetic Energy Defeat Device 687
G.7.3 Instrumentation 688
G.7.4 Specimen behavior 689
G.8 TEST 8 (TWO-PLATE TEST – KEDD ON TOP) 692
G.8.1 Introduction 692
G.8.2 Kinetic Energy Defeat Device 692
G.8.3 Instrumentation 693
G.8.4 Specimen Behavior 694
G.9 TEST 9 (THREE-PLATE TEST – KEDD ON TOP) 697
G.9.1 Introduction 697
G.9.1 Kinetic Energy Defeat Device 697
G.9.2 Instrumentation 698
G.9.3 Specimen Behavior 699
G.10 TEST 10 (THREE-PLATE TEST) 704
G.10.1 Introduction 704
G.10.2 Instrumentation 704
G.10.3 Specimen Behavior 706
G.11 TEST 11 (TWO-PLATE TEST – KEDD ON TOP) 711
G.11.1 Introduction 711
G.11.2 Kinetic Energy Defeat Device 711
G.11.3 Instrumentation 712

G.11.4 Specimen Behavior 713
G.12 TEST 12 (TWO-PLATE TEST – KEDD ON BOTTOM) 716
G.12.1 Introduction 716
G.12.3 Instrumentation 717
G.12.4 Specimen behavior 718
G.13 TEST 13 (TWO-PLATE TEST) 722
G.13.1 Introduction 722
G.13.2 Instrumentation 722
G.13.3 Specimen Behavior 723
G.14 TEST 14 (TWO-PLATE TEST) 727
G.14.1 Introduction 727
G.14.2 Instrumentation 727
G.14.3 Specimen Behavior 728
G.15 TEST 15 (TWO-PLATE TEST –2 ROWS OF KEDD'S ON TOP) 732
G.15.1 Introduction 732
G.15.2 Kinetic Energy Defeat Device 732
G.15.3 Instrumentation 733
G.15.4 Specimen Behavior 734
G.16 TEST 16 (TWO-PLATE TEST –1 ROWS OF KEDD'S ONE TOP AND BOTTOM) 737
G.16.1 Introduction 737
G.16.2 Kinetic Energy Defeat Device 737
G.16.3 Instrumentation 738
G.16.4 Specimen Behavior 739
G.17 TEST 17 (TWO-PLATE TEST –3 ROWS OF KEDD'S ON TOP) 743
G.17.1 Introduction 743
G.17.2 Kinetic Energy Defeat Device 743
G.17.3 Instrumentation 744
G.17.4 Specimen Behavior 745
G.18 TEST 18 (TWO-PLATE TEST) 748
G.18.1 Introduction 748
G.18.2 Instrumentation 748
G.18.3 Specimen Behavior 749
G.19 TEST 19 (TWO-PLATE TEST –2 ROWS OF KEDD'S ON TOP) 753

G.19.1 Introduction 753
G.19.2 Kinetic Energy Defeat Device 753
G.19.3 Instrumentation 754
G.19.4 Specimen Behavior 755
G.20 TEST 20 (TWO-PLATE TEST –3 ROWS OF KEDD'S ON TOP) 758
G.20.1 Introduction 758
G.20.2 Kinetic Energy Defeat Device 758
G.20.3 Instrumentation 759
G.20.4 Specimen Behavior 760
G.21 TEST 21 (TWO-PLATE TEST –1 ROWS OF KEDD'S ONE TOP AND BOTTOM) 764
G.21.1 Introduction 764
G.21.2 Kinetic Energy Defeat Device 764
G.21.3 Instrumentation 765
G.21.4 Specimen Behavior 766
H EMRTC FIELD TEST REPORTS 770
H.1 EMRTC TEST 1 770
H.1.2 Charge Details 771
H.1.3 Instrumentation 773
H.1.4 Specimen Behavior 775
H.2 EMRTC TEST 2 777
H.2.1 Introduction 777
H.2.2 Charge Details 779
H.2.3 Instrumentation 779
H.2.4 Specimen Behavior 784
H.3 EMRTC TEST 3 788
H.3.1 Introduction 788
H.3.2 KEDD Field Tests Set-Up 790
H.3.3 Charge Details 791
H.3.4 Instrumentation 793
H.3.5 Test Results 797

List of Abbreviations

ARA	Applied Research Associates
BG	Blast Generator
CMU	Concrete Masonry Unit
COR	Coefficient of Restitution
CTH	Eularian based Hydracode developed by Sandia Labs
Dplot	Graphing Software developed by HydeSoft Computing
EMRTC	Energetic Materials research Testing Center at New Mexico Tech
ft/s or ft/sec	feet per second
IM1	Impacting Mass 1
IM2	Impacting Mass 2
IM3	Impacting Mass 3
in.	inch
K&C	Karagozian and Case
KEDD	Kinetic Energy Defeat Device
kg	kilogram
km/s	kilometer per second
ksi	1,000 pounds per square inch
lbs	pound
LS-DYNA	Computer code developed by Livermore Software Technology Company
m/s	meters per second
m_1	Mass 1
m_2	Mass 2
μs	microsecond

msec or ms	milisecond
MTS	MTS System Corperation
n/a	Not Applicable
PVC	Polyvinyl Chloride
SAIC	Science Applications International Corperation
TEMA	Tack Eye Motion Analysis
TNT	Trinitrotoluene
TOA	Time Of Arrival
TSWG	Technical Support Working Group
UCSD	University of California, San Diego
V_1	Velocity 1
V_2	Velocity 2
V_3	Velocity 3

LIST OF SYMBOLS

c	Speed of sound
E	Young's Modulus
f	frequency
λ	wavelength
ρ	density

LIST OF FIGURES

Figure 1.1: Schematic drawing of generic cellular steel structure 4
Figure 1.2: Field Test 2 pre-test 5
Figure 1.3: Failure Mode 1 – bolt failures 6
Figure 1.4: Failure modes 2 and 3 – initial and secondary flyer plates 6
Figure 1.5: Laboratory KEDD's 9
Figure 1.6: Comparison test series post test photos 9
Figure 1.7: Test set-ups from all tests (from left to right) 12
Figure 1.8: First plates from all tests (from left to right) 13
Figure 1.9: Second plates from all tests (from left to right) 14
Figure 1.10: Momentum calculation – First step 16
Figure 1.11: Momentum calculation – Second step 17
Figure 1.12: 2 Plate Test, two row of KEDD's on top, test set-up 19
Figure 1.13: 2 Plate Test, two rows of KEDD's on top 21
Figure 1.14: Comparing velocity with CTH, field tests, and momentum calculations 22
Figure 1.15: EMRTC field Test 3 structure elevation 24
Figure 1.16: Test specimen during the test with initial flyer plates (time = 9.638 ms) 25
Figure 1.17: Test specimen during the test with initial flyer plates (time = 13.838 ms) 25
Figure 1.18: High speed video capturing water expulsion by the KEDD system (time = 14.338 ms) 26
Figure 1.19: Test specimen post-test 27
Figure 3.1: Failure Mode 1 - Bolt failures 32
Figure 3.2: Bolt failures, in progress, from a lab test 32
Figure 3.3: Failure Mode 2 34
Figure 3.4: Failure Mode 2 – Initial flyer plates 34
Figure 3.5: Failure Modes 2 and 3 – Initial and Secondary flyer plates 36
Figure 3.6: Computer simulation of Failure Modes 1, 2, and 3 by SAIC 36
Figure 3.7: Failure modes for laboratory tests 37
Figure 3.8: Examples of brittle fragments 38
Figure 3.9: Example of ductile fractures 39
Figure 3.10: Example of combined brittle fracture and ductile deformation 39
Figure 3.11: EMRTC field Test 1 set-up elevation 41
Figure 3.12: EMRTC field Test 1 42
Figure 3.13: Elevated concrete supports EMRTC Test 2 43
Figure 3.14: EMRTC field Test 2 set-up elevation view 43
Figure 3.15: EMRTC field Test 2 set-up (photo) 44
Figure 3.16: Location of Charge on test specimen 45
Figure 3.17: Test charge for EMRTC field tests 45
Figure 3.18: Time of Arrival pins for EMRTC Test 2 49
Figure 3.19: Time of Arrival pins (close up) for EMRTC Test 2 49
Figure 3.20: Image from Phantom camera at initial detonation 50
Figure 3.21: Image from Phantom camera after initial detonation, with shock front 50
Figure 3.22: Flyer plate created from EMRTC Test 1 52
Figure 3.23: Top plate (pieced together) from EMRTC Test 1 52
Figure 3.24: Failures from EMRTC Test 1 – post-test 53
Figure 3.25: EMRTC Test 2 – post-test 56
Figure 3.26: EMRTC Test 2 – secondary (pass through) flyer plate 56

Figure 3.27: EMRTC Test 2 flyer plates 57
Figure 3.28: Portion of top plate from EMRTC Test 2 57
Figure 3.29: EMRTC Test 2 reassembled top plate 58
Figure 3.30: Demonstration of localized failures from EMRTC Test 2 58
Figure 3.31: Schematic drawing of laboratory test set-up using generic cellular steel structure 61
Figure 3.32: Ballistic Loading Type 1 and 2 test set-up – south elevation 63
Figure 3.33: Ballistic Loading Type 1 and 2 test set-up 63
Figure 3.34: Progression of damage for a Ballistic Loading Type 1 test 66
Figure 3.35: Progression of damage for a Ballistic Loading Type 2 test 67
Figure 3.36: Strain rate data and trendlines for all plates and bolt types 70
Figure 3.37: Strain rate data and trendlines for 1/4", 1/2" and 3/4" plates 70
Figure 3.38: Displacement of end supports at 28 m/s 72
Figure 3.39: Strain rate data for A307 bolts 73
Figure 3.40: Strain rate data for Grade 5 bolts 73
Figure 3.41: Strain rate data for all bolts 74
Figure 4.1: Initial CTH calculation problem set-up 78
Figure 4.2: Initial KEDD CTH calculation (velocity 800 m/sec) 79
Figure 4.3: Impactor and rear disk velocity histories 80
Figure 4.4: Initial KEDD ALE LS-DYNA calculation (velocity 30 m/sec) 82
Figure 4.5: Sand-filled KEDD container design 84
Figure 4.6: KEDD array (laboratory) 85
Figure 4.7: Pilot test sand-filled KEDD array 85
Figure 4.8: Pilot test water-filled KEDD array 87
Figure 4.9: KEDD end cap (EMRTC) 90
Figure 4.10: KEDD - water (EMRTC) 90
Figure 4.11: KEDD array (EMRTC) 91
Figure 4.12: KEDD hanger assembly (EMRTC) 93
Figure 4.13: 2 Rows of KEDD's on top (EMRTC) 93
Figure 4.14: KEDD - water (field) 95
Figure 4.15: KEDD hanger assembly 95
Figure 4.16: KEDD array 96
Figure 4.17: KEDD layout 98
Figure 4.18: KEDD layout 99
Figure 4.19: KEDD top and bottom layout 99
Figure 4.20 Comparison test series post test photos 102
Figure 4.21: Progression of failure of the comparison test series 103
Figure 4.22: Maximum principal strains and strain rates at Gage 17 for this test series 105
Figure 4.23: Maximum principal strains and strain rates at Gage 18 for this test series 106
Figure 4.24: Comparison of failures 108
Figure 4.25 Comparison of residual deflections 108
Figure 4.26: Maximum principal strains and strain rates at Gage 17 for this test series 109
Figure 4.27: Maximum principal strains and strain rates at Gage 18 for this test series 109
Figure 4.28: Photos comparing damages with and without a KEDD - remained attached 111
Figure 4.29: Bar graph comparing incoming kinetic energy of impacting mass at damage level remained attached 112
Figure 4.30: Damage comparisons (partial failure) 113
Figure 4.31: Damage comparisons (partial failure) 114

Figure 4.32: Bar graph comparing incoming kinetic energy of impacting mass at damage level partial failure 114
Figure 5.1: Test set-up showing exposed area of steel plate 117
Figure 5.2: Explosive material and detonator..... 119
Figure 5.3: A Time of Arrival pin connected to a glass rod..... 120
Figure 5.4: Time of Arrival pin arrays a) 2 1/2" (lower) spacing b) 1/2" (higher) spacing 121
Figure 5.5: 2 Plate Test set-up – schematic drawing..... 123
Figure 5.6: 2 Plate Test, 1 row KEDD top test set-up..... 124
Figure 5.7: Momentum calculation – First step..... 125
Figure 5.8: Momentum calculation – Second step 126
Figure 5.9: Baseline tests, first plate a) Test 6 b) Test 13 c) Test 14 d) Test 18 128
Figure 5.10: Baseline tests, second plate a) Test 6 b) Test 13 c) Test 14 d) Test 18..... 129
Figure 5.11: Velocity profile for 2 Plate Tests 6 and 13 130
Figure 5.12: 2 Plate Tests baseline velocities..... 131
Figure 5.13: 2 Plate Test, baseline test set-up 132
Figure 5.14: 2 Plate Test, baseline – velocity profile of top and bottom plate..... 133
Figure 5.15: 2 Plate Test, baseline – velocity magnitude..... 134
Figure 5.16: KEDD on top test set-ups a) Test 8 b) Test 11 136
Figure 5.17: KEDD on top, first plate a) Test 8 b) Test 11..... 137
Figure 5.18: KEDD on top, second plate a) Test 8 b) Test 11 138
Figure 5.19: Velocity profile for KEDD on top Tests 8 and 11 139
Figure 5.20: 2 Plate Tests KEDD on top velocities..... 140
Figure 5.21: 2 Plate Test, one row of KEDD's on top, test set-up..... 141
Figure 5.22: 2 Plate Test, one row of KEDD's on top close up of velocity magnitude 142
Figure 5.23: 2 Plate Test, one row of KEDD's on top 143
Figure 5.24: 2 Plate Test, one row of KEDD's on top – velocity profile of top and bottom plate..... 145
Figure 5.25: KEDD on top – 1 row, velocities (field, CTH, and Calculation)..... 146
Figure 5.26: KEDD on bottom test set-ups a) Test 7 b) Test 12 148
Figure 5.27: KEDD on bottom, first plate a) Test 7 b) Test 12..... 149
Figure 5.28: KEDD on bottom tests, second plate a) Test 7 b) Test 12 150
Figure 5.29: Velocity profile for KEDD on bottom Tests 7 and 12..... 152
Figure 5.30: 2 Plate KEDD on bottom test velocities 152
Figure 5.31: 2 Plate Test, one row of KEDD's on bottom, test set-up..... 154
Figure 5.32: 2 Plate Test, one row of KEDD's on bottom..... 155
Figure 5.33: 2 Plate Test, KEDD on bottom – 1 row – velocity profile of top and bottom plate 156
Figure 5.34: KEDD on bottom – 1 row, velocities (field, CTH, and calculation) 156
Figure 5.35: Two rows of KEDD's on top test set-ups (Test 15)..... 158
Figure 5.36: Two rows of KEDD's on top, first plate a) Test 15 b) Test 19..... 159
Figure 5.37:Two rows of KEDD's on top, second plate a) Test 15 b) Test 19 160
Figure 5.38: 2 Plate Test, two rows of KEDD's on top velocities 162
Figure 5.39: 2 Plate Test, two row of KEDD's on top, test set-up..... 163
Figure 5.40: 2 Plate Test, two rows of KEDD's on top 164
Figure 5.41: 2 Plate Test, two rows of KEDD's on top – velocity profile of top and bottom plate..... 165
Figure 5.42: KEDD on top – 2 row, velocities (field, CTH, and calculation)..... 166

Figure 5.43: One row of KEDD's on top and bottom test set-ups a) Test 16 b) Test 21 .. 167
Figure 5.44: One row of KEDD's on top and bottom, first plate a) Test 16 b) Test 21..... 168
Figure 5.45: One row of KEDD's on top and bottom, second plate a) Test 16 b) Test 21 . 169
Figure 5.46: 2 Plate Test, one row of KEDD's on top and bottom velocities..... 170
Figure 5.47: 2 Plate Test, one row of KEDD's on top and bottom, test set-up..... 171
Figure 5.48: 2 Plate Test, one row of KEDD's on top and bottom 172
Figure 5.49: Comparing liquid trapped between first and second plates 173
Figure 5.50: 2 Plate Test, one row of KEDD's on top and bottom – velocity profile of top and bottom plate..... 174
Figure 5.51: One row of KEDD's on top and bottom, velocities (field, CTH, and calculation) 175
Figure 5.52: Three rows of KEDD's on top test set-ups a) Test 17 b) Test 20..... 176
Figure 5.53: Three rows of KEDD's on top, first plate a) Test 17 b) Test 20..... 177
Figure 5.54:Three rows of KEDD's on top, second plate a) Test 17 b) Test 20..... 178
Figure 5.55: 2 Plate Test, three rows of KEDD's on top velocities 180
Figure 5.56: 2 Plate Test, three row of KEDD's on top, test set-up..... 181
Figure 5.57: 2 Plate Test, three rows of KEDD's on top 182
Figure 5.58: 2 Plate Test, Three rows of KEDD's on top – velocity profile of top and bottom plate..... 183
Figure 5.59: Three rows of KEDD's on top, velocities (field, CTH, and Calculation)..... 184
Figure 5.60: One solid wall of water, test set-up..... 185
Figure 5.61: One solid wall of water..... 186
Figure 5.62: Close-up of velocity magnitude for a solid wall of water..... 187
Figure 5.63: One solid wall of water – velocity profile of top and bottom plate 188
Figure 5.64: First plates from all tests (from left to right)..... 192
Figure 5.65: Second plates from all tests (from left to right) 193
Figure 5.66: Comparison of second plates a) Two rows of KEDD's on top..... 194
Figure 5.67: Comparison of second plates a) Two rows of KEDD's on top..... 194
Figure 5.68:Average velocities of all 2 Plate Tests..... 196
Figure 5.69: 2 Plate Test calculations – second plate velocities 200
Figure 5.70: Comparing velocity reduction of the second plate with CTH, field tests, and momentum calculations..... 201
Figure 6.1: EMRTC field Test 3 structure elevation (photo) 206
Figure 6.2: EMRTC field Test 3 structure elevation (drawing) 207
Figure 6.3: EMRTC Test 3 charge in place..... 208
Figure 6.4: EMRTC Field Test 3 camera location (Not to Scale)..... 209
Figure 6.5: Image from the Phantom camera at initial detonation 210
Figure 6.6: Image from the Phantom camera showing the bottom two rows of cells 210
Figure 6.7: Test specimen post-test..... 212
Figure 6.8: Test specimen post-test with Key Plan 213
Figure 6.9: Test specimen post-test cells 1 and 2..... 215
Figure 6.10: Test specimen during the test with initial flyer plates (time = 9.638 ms)..... 216
Figure 6.11: Test specimen during the test with initial flyer plates (time = 13.838 ms)..... 216
Figure 6.12: Test specimen post-test cell 3 220
Figure 6.13: Test specimen post-test cells 7 and 8..... 221
Figure 6.14: Test specimen post-test cell 9 223
Figure 6.15: Test specimen and miscellaneous flyer plates 225
Figure 6.16: Miscellaneous flyer plates 225

Figure 6.17: High speed video capturing water expulsion by the KEDD system 228
Figure 6.18: Jets formed by KEDD system 229
Figure 6.19: Test specimen post-test cells 4and 5 230
Figure 6.20: Test specimen post-test cells 4, 5, and 6 232
Figure A.1: Examples of brittle fragments 241
Figure A.2: Examples of brittle failures 241
Figure A.3: Example of ductile fractures 242
Figure A.4: EMRTC field Test 1 set-up section 242
Figure A.5: EMRTC field Test 1 set-up plan view 243
Figure A.6: EMRTC field Test 1 set-up detail 243
Figure A.7: EMRTC field Test 1 set-up (photo) 244
Figure A.8: Test 1set-up with explosive charge in place 244
Figure A.9: Flyer plate created from EMRTC Test 1 245
Figure A.10: EMRTC Test 1 – post-test 245
Figure A.11: Portion of structure from EMRTC Test 1 246
Figure A.12: Failures from EMRTC Test 1 – post-test 246
Figure A.13: EMRTC field Test 2 set-up section 247
Figure A.14: EMRTC field Test 2 set-up details 248
Figure A.15: EMRTC field Test 2 set-up plan view 249
Figure A.16: Test charge for EMRTC Test 2 249
Figure A.17: Top plate fragment found approximately 16’ from test specimen 250
Figure A.18: Top plate fragment found approximately 400’ from test specimen 250
Figure A.19: Failures from EMRTC Test 2 – post-test 251
Figure A.20: Demonstration of localized failures from EMRTC Test 2 251
Figure A.21: Ballistic Loading Type 1 and 2 test set-up – east elevation 253
Figure A.22: Ballistic Loading Type 1 and 2 test set-up 254
Figure A.23: a) Blast Generator unit prior to installation. b) Profile and front view of programmer. 255
Figure A.24: Location of BG accelerometers 257
Figure A.25: TEMA target locations a) Photo b) Drawing 259
Figure A.26: Strain gage locations 259
Figure A.27: Unfiltered acceleration data from a typical test 261
Figure A.28: Filtered acceleration data from a typical test. 261
Figure A.29: Collection of maximum principal strain data 263
Figure A.30: Collection of maximum principal strain data using a bandpass filter 263
Figure A.31: Collection of minimum principal strain data 264
Figure A.32: Collection of minimum principal strain data using a bandpass filter 264
Figure A.33: Strain rate vs. impact velocity for 1/4” thick plate 269
Figure A.34: Comparing displacements of end supports 269
Figure A.35: Comparing displacements of end supports 270
Figure A.36: Strain rate vs. impact velocity for 1/2” thick plate 274
Figure A.37: Comparing displacements of end supports 275
Figure A.38: Comparing displacements of end supports 275
Figure A.39: Strain rate vs. impact velocity for 3/4” thick plate 277
Figure A.40: Strain rate vs. impact velocity for 7/8” thick plate 279
Figure B.1: KEDD hanger assembly drawing (EMRTC) 280
Figure B.2: KEDD hanger assembly (EMRTC) 281
Figure B.3: 2 Rows of KEDD’s on top (EMRTC) 281

Figure B.4: KEDD hanger assembly drawing 282
Figure B.5: KEDD layout a) 1 row bottom b) 1 row top 283
Figure B.6: KEDD layout a) 2-row top b) 3-row top 283
Figure B.7: KEDD 2-row top layout (3-d drawing) 284
Figure B.8: KEDD 3-row top layout (3-d drawing) 284
Figure B.9: KEDD top and bottom layout a) drawing b) photo 285
Figure C.1: Calibration Test set-up – photo 286
Figure C.2: Calibration Test set-up – schematic drawing 287
Figure C.3: Calibration Test set-up –drawing 288
Figure C.4: Fragment velocities from Calibration Tests 289
Figure C.5: Fragments formed from Calibration Test 1 290
Figure C.6: Fragments formed from Calibration Test 2 290
Figure C.7: Fragments formed from Calibration Test 3 291
Figure C.8: Fragments formed from Calibration Test 4 291
Figure C.9: 4 Plate Test set-up – photo 292
Figure C.10: 4 Plate Test set-up –Drawing 293
Figure C.11: 4 Plate Test set-up – schematic drawing 294
Figure C.12: 4 Plate Test a) Post test b) Second, third and fourth plate 295
Figure C.13: First three plates of 4 Plate Test 296
Figure C.14: 2 Plate Test set-up –drawing 297
Figure C.15: Baseline test set-ups a) Test 6 b) Test 13 c) Test 14 d) Test 18 298
Figure C.16: Baseline tests, first and second plate a) Test 6 b) Test 13 c) Test 14 d) Test 18 299
Figure C.17: KEDD on top test set-ups a) Test 8 b) Test 11 300
Figure C.18: KEDD on top tests, first and second plate a) Test 8 b) Test 11 300
Figure C.19: KEDD on bottom tests, first and second plate a) Test 7 b) Test 12 301
Figure C.20: Two rows of KEDD's on top test set-ups 301
Figure C.21: Two rows of KEDD's on top tests, first and second plate a) Test 15 b) Test 19 302
Figure C.22: One row of KEDD's on top and bottom, first and second plate 303
Figure C.23:Two rows of KEDD's on top, second plate a) Top view b) Bottom view 304
Figure C.24: One row of KEDD's on top and bottom, second plate a) Top view b) Bottom view 305
Figure C.25:Three rows of KEDD's on top, second plate a) Top view b) Bottom view 306
Figure C.26: 3 Plate Test set-up –drawing 308
Figure C.27: 3 Plate Test set-up – photo 309
Figure C.28: 3 Plate Test set-up – schematic drawing 309
Figure C.29: 3 Plate Test comparisons 312
Figure D.1: EMRTC field Test 3 set-up (drawing) 313
Figure D.2: EMRTC Test 3 charge box 314
Figure D.3: Time of Arrival pin arrays a) 3 pin array b) 4 pin array 316
Figure D.4: Time of Arrival pin locations for EMRTC Test 3 317
Figure D.5: Time of Arrival pins a) Pin support in outer cells b) Pins located in center cells 318
Figure D.6: Flyer plates at extreme distances 319
Figure D.7: Flyer plates at extreme distances 320
Figure E.1: 1/4" thick steel plate pre test for Test 1 321
Figure E.2: Phantom cameras for tests a) Camera One b) Camera Two 322

Figure E.3: Target layout on plate and impacting mass for Test 1 322
Figure E.4: Accelerometer location for Test 1 323
Figure E.5: Strain gage layout for Test 1 323
Figure E.6: Steel plate post test for Test 1 324
Figure E.7: Progression of damage for Test 1 325
Figure E.8: 1/4" thick steel plate pre test for Test 2 326
Figure E.9: Phantom cameras for Test 2 a) Camera One b) Camera Two c) Camera Three 327
Figure E.10: Target layout on plate and impacting mass for Test 2 327
Figure E.11: Accelerometer location for Test 2 328
Figure E.12: Steel plate post test for Test 2 329
Figure E.13: Progression of damage for Test 2 329
Figure E.14: 1/4" thick steel plate pre test for Test 3 330
Figure E.15: Phantom Cameras for Test 3 a) Camera One b) Camera Two c) Camera Three 331
Figure E.16: Target layout on plate and impacting mass for Test 3 331
Figure E.17: Accelerometer location for Test 332
Figure E.18: Filtered accelerometer data for Test 3 332
Figure E.19: Strain gage layout for Test 3 333
Figure E.20: Maximum principal strains and strain rates for Test 3 334
Figure E.21: Minimum principal strains and strain rates for Test 3 334
Figure E.22: Steel plate post test for Test 3 335
Figure E.23: 1/4" thick steel plate pre test for Test 4 337
Figure E.24: Phantom Cameras for Test 4 a) Camera One b) Camera Two c) Camera Three 338
Figure E.25: Target layout on plate and impacting mass for Test 4 338
Figure E.26: Accelerometer location for Test 4 339
Figure E.27: Filtered accelerometer data for Test 4 339
Figure E.28: Strain gage layout for Test 4 340
Figure E.29: Maximum principal strains and strain rates for Test 4 341
Figure E.30: Minimum principal strains and strain rates for Test 4 341
Figure E.31: Steel plate post test for Test 4 343
Figure E.32: Steel plate post test for Test 4 343
Figure E.33: Progression of damage for Test 4 344
Figure E.34: 1/4" thick steel plate pre test for Test 5 345
Figure E.35: Phantom Cameras for Test 5 a) Camera One b) Camera Two c) Camera Three 346
Figure E.36: Target layout on plate and impacting mass for Test 5 346
Figure E.37: Accelerometer location for Test 5 347
Figure E.38: Filtered accelerometer data for Test 5 347
Figure E.39: Strain gage layout for Test 5 348
Figure E.40: Maximum principal strains and strain rates for Test 5 349
Figure E.41: Minimum principal strains and strain rates for Test 5 349
Figure E.42: Steel plate post test for Test 5 350
Figure E.43: Progression of damage for Test 5 from Camera 1 351
Figure E.44: Progression of damage for Test 5 from Camera 2 351
Figure E.45: 1/2" thick steel plate pre test for Test 6 352
Figure E.46: Target layout on plate and impacting mass for Test 6 353

Figure E.47: Accelerometer location for Test 6 353
Figure E.48: Filtered accelerometer data for Test 6 354
Figure E.49: Strain gage layout for Test 6 355
Figure E.50: Maximum principal strains and strain rates for Test 6 355
Figure E.51: Minimum principal strains and strain rates for Test 6 356
Figure E.52: 1/2” thick steel plate pre test for Test 7 357
Figure E.53: Phantom Cameras for Test 7 a) Camera One b) Camera Two c) Camera Three 358
Figure E.54: Target layout on plate and impacting mass for Test 7 358
Figure E.55: Accelerometer location for Test 7 359
Figure E.56: Filtered accelerometer data for Test 7 359
Figure E.57: Strain gage layout for Test 7 360
Figure E.58: Maximum principal strains and strain rates for Test 7 361
Figure E.59: Minimum principal strains and strain rates for Test 7 361
Figure E.60: Steel Plate post test for Test 7 362
Figure E.61: Progression of damage for Test 7 from Camera 1 363
Figure E.62: Progression of damage for Test 7 from Camera 2 363
Figure E.63: Progression of damage for Test 7 from Camera 3 363
Figure E.64: 1/2” thick steel plate pre test for Test 8 364
Figure E.65: Phantom Cameras for Test 8 a) Camera One b) Camera Two c) Camera Three 365
Figure E.66: Target layout on plate and impacting mass for Test 8 365
Figure E.67: Accelerometer location for Test 8 366
Figure E.68: Filtered accelerometer data for Test 8 366
Figure E.69: Strain gage layout for Test 8 367
Figure E.70: Maximum principal strains and strain rates for Test 8 368
Figure E.71: Minimum principal strains and strain rates for Test 8 368
Figure E.72: Steel plate post test for Test 8 370
Figure E.73: Progression of damage for Test 8 from Camera 1 370
Figure E.74: Progression of damage for Test 8 from Camera 2 370
Figure E.75: Progression of damage for Test 8 from Camera 3 371
Figure E.76: 1/2” thick steel plate pre test for Test 9 372
Figure E.77: Phantom Cameras for Test 9 a) Camera One b) Camera Two c) Camera Three 373
Figure E.78: Target layout on plate and impacting mass for Test 9 373
Figure E.79: Accelerometer location for Test 9 374
Figure E.80: Filtered accelerometer data for Test 9 374
Figure E.81: Strain gage layout for Test 9 375
Figure E.82: Maximum principal strains and strain rates for Test 9 376
Figure E.83: Minimum principal strains and strain rates for Test 9 376
Figure E.84: Steel plate post test for Test 9 378
Figure E.85: Progression of damage for Test 9 from Camera 1 378
Figure E.86: Progression of damage for Test 9 from Camera 2 378
Figure E.87: Progression of damage for Test 9 from Camera 3 379
Figure E.88: 1/2” thick steel plate pre test for Test 10 380
Figure E.89: Phantom Cameras for Test 10 a) Camera One b) Camera Two c) Camera Three 381
Figure E.90: Target layout on plate and impacting mass for Test 10 381

Figure E.91: Accelerometer location for Test 10 382
Figure E.92: Filtered accelerometer data for Test 10 382
Figure E.93: Strain gage layout for Test 10 383
Figure E.94: Maximum principal strains and strain rates for Test 10 384
Figure E.95: Minimum principal strains and strain rates for Test 10 384
Figure E.96: Steel plate post test for Test 10 386
Figure E.97: Progression of damage for Test 10 from Camera 1 386
Figure E.98: 1/2" thick steel plate pre test for Test 11 387
Figure E.99: Phantom Cameras for Test 11 a) Camera One b) Camera Two c) Camera Three 388
Figure E.100: Target layout on plate and impacting mass for Test 11 388
Figure E.101: Accelerometer location for Test 11 389
Figure E.102: Filtered accelerometer data for Test 11 389
Figure E.103: Strain gage layout for Test 11 390
Figure E.104: Maximum principal strains and strain rates for Test 11 391
Figure E.105: Minimum principal strains and strain rates for Test 11 391
Figure E.106: Steel plate post test for Test 11 392
Figure E.107: Progression of damage for Test 11 from Camera 1 393
Figure E.108: 1/4" thick steel plate pre test for Test 12 394
Figure E.109: Phantom Cameras for Test 12 395
Figure E.110: Target layout on plate and impacting mass for Test 12 395
Figure E.111: Accelerometer location for Test 12 396
Figure E.112: Filtered accelerometer data for Test 12 396
Figure E.113: Strain gage layout for Test 12 397
Figure E.114: Maximum principal strains and strain rates for Test 12 399
Figure E.115: Minimum principal strains and strain rates for Test 11 399
Figure E.116: Steel plate post test for Test 12 400
Figure E.117: Progression of damage for Test 12 from Camera 1 400
Figure E.118: Progression of damage for Test 12 from Camera 3 400
Figure E.119: 1/4" thick steel plate pre test for Test 13 401
Figure E.120: Phantom Cameras for Test 13 402
Figure E.121: Target layout on plate and impacting mass for Test 13 402
Figure E.122: Accelerometer location for Test 13 403
Figure E.123: Filtered accelerometer data for Test 13 404
Figure E.124: Strain gage layout for Test 1 404
Figure E.125: Maximum principal strains and strain rates for Test 1 405
Figure E.126: Minimum principal strains and strain rates for Test 13 405
Figure E.127: Steel plate post test for Test 13 406
Figure E.128: Progression of damage for Test 13 from Camera 1 407
Figure E.129: Progression of damage for Test 13 from Camera 3 407
Figure E.130: 1/4" thick steel plate pre test for Test 14 408
Figure E.131: Phantom Cameras for Test 14 409
Figure E.132: Target layout on plate and impacting mass for Test 14 409
Figure E.133: Accelerometer location for Test 14 410
Figure E.134: Filtered accelerometer data for Test 14 410
Figure E.135: Strain gage layout for Test 14 411
Figure E.136: Maximum principal strains and strain rates for Test 14 412
Figure E.137: Minimum principal strains and strain rates for Test 14 412

Figure E.138: Steel plate post test for Test 14 414
Figure E.139: Progression of damage for Test 14 from Camera 1 414
Figure E.140: Progression of damage for Test 14 from Camera 3 414
Figure E.141: 1/2” thick steel plate pre test for Test 15 415
Figure E.142: Phantom Cameras for Test 15 416
Figure E.143: Target layout on plate and impacting mass for Test 15 416
Figure E.144: Strain gage layout for Test 15 417
Figure E.145: Maximum principal strains and strain rates for Test 15 418
Figure E.146: Minimum principal strains and strain rates for Test 15 418
Figure E.147: Steel plate post test for Test 15 419
Figure E.148: Progression of damage for Test 15 from Camera 1 420
Figure E.149: Progression of damage for Test 15 from Camera 3 420
Figure E.150: 1/4” thick steel plate pre test for Test 16 421
Figure E.151: Phantom Cameras for Test 16 422
Figure E.152: Target layout on plate and impacting mass for Test 16 422
Figure E.153: Accelerometer location for Test 16 423
Figure E.154: Filtered accelerometer data for Test 16 423
Figure E.155: Strain gage layout for Test 16 424
Figure E.156: Maximum principal strains and strain rates for Test 16 425
Figure E.157: Minimum principal strains and strain rates for Test 16 425
Figure E.158: Steel plate post test for Test 16 426
Figure E.159: Progression of damage for Test 16 from Camera 1 427
Figure E.160: Progression of damage for Test 16 from Camera 2 427
Figure E.161: Progression of damage for Test 16 from Camera 3 427
Figure E.162: 1/4” thick steel plate pre test for Test 17 428
Figure E.163: Phantom Cameras for Test 17 429
Figure E.164: Target layout on plate and impacting mass for Test 17 429
Figure E.165: Accelerometer location for Test 17 430
Figure E.166: Filtered accelerometer data for Test 17 430
Figure E.167: Strain gage layout for Test 17 431
Figure E.168: Maximum principal strains and strain rates for Test 17 432
Figure E.169: Minimum principal strains and strain rates for Test 17 432
Figure E.170: Steel plate post test for Test 17 433
Figure E.171: Progression of damage for Test 17 from Camera 1 434
Figure E.172: Progression of damage for Test 17 from Camera 2 434
Figure E.173: Progression of damage for Test 17 from Camera 3 434
Figure E.174: 1/2” thick steel plate pre test for Test 18 435
Figure E.175: Phantom Cameras for Test 18 436
Figure E.176: Target layout on plate and impacting mass for Test 18 436
Figure E.177: Accelerometer location for Test 18 437
Figure E.178: Filtered accelerometer data for Test 18 437
Figure E.179: Strain gage layout for Test 18 438
Figure E.180: Maximum principal strains and strain rates for Test 18 439
Figure E.181: Minimum principal strains and strain rates for Test 18 439
Figure E.182: Steel plate and Impacting Mass post test for Test 18 440
Figure E.183: Progression of damage for Test 18 441
Figure E.184: Progression of damage for Test 18 441
Figure E.185: 1/2” thick steel plate pre test for Test 19 442

Figure E.186: Phantom Cameras for Test 19 443
Figure E.187: Target layout on plate and impacting mass for Test 19..... 443
Figure E.188: Accelerometer location for Test 19 444
Figure E.189: Filtered accelerometer data for Test 19 444
Figure E.190: Strain gage layout for Test 19 445
Figure E.191: Maximum principal strains and strain rates for Test 19 446
Figure E.192: Minimum principal strains and strain rates for Test 19..... 446
Figure E.193: Steel plate post test for Test 19..... 447
Figure E.194: Progression of damage for Test 19 from Camera 1..... 448
Figure E.195: Progression of damage for Test 19 from Camera 2..... 448
Figure E.196: Progression of damage for Test 19 from Camera 3..... 448
Figure E.197: 1/2” thick steel plate pre test for Test 20..... 449
Figure E.198: Phantom Cameras for Test 20 450
Figure E.199: Target layout on plate and impacting mass for Test 20..... 450
Figure E.200: Accelerometer location for Test 20 451
Figure E.201: Filtered accelerometer data for Test 20 451
Figure E.202: Strain gage layout for Test 20 452
Figure E.203: Maximum principal strains and strain rates for Test 20 453
Figure E.204: Minimum principal strains and strain rates for Test 20..... 453
Figure E.205: Steel plate post test for Test 20..... 454
Figure E.206: Progression of damage for Test 20 from Camera 1..... 455
Figure E.207: Progression of damage for Test 20 from Camera 2..... 455
Figure E.208: Progression of damage for Test 20 from Camera 3..... 455
Figure E.209: 3/4” thick steel plate pre test for Test 21..... 456
Figure E.210: Phantom Cameras for Test 21 457
Figure E.211: Target layout on plate and impacting mass for Test 21..... 457
Figure E.212: Accelerometer location for Test 21 458
Figure E.213: Filtered accelerometer data for Test 21 458
Figure E.214: Strain gage layout for Test 21 459
Figure E.215: Maximum principal strains and strain rates for Test 21 460
Figure E.216: Minimum principal strains and strain rates for Test 21..... 460
Figure E.217: Steel plate post test for Test 21..... 462
Figure E.218: Progression of damage for Test 21 from Camera 1..... 462
Figure E.219: Progression of damage for Test 21 from Camera 2..... 462
Figure E.220: Progression of damage for Test 21 from Camera 3..... 463
Figure E.221: 3/4” thick steel plate pre test for Test 22..... 464
Figure E.222: Phantom Cameras for Test 22 465
Figure E.223: Target layout on plate and impacting mass for Test 22..... 465
Figure E.224: Strain gage layout for Test 22 466
Figure E.225: Maximum principal strains and strain rates for Test 22 467
Figure E.226: Minimum principal strains and strain rates for Test 22..... 467
Figure E.227: Steel plate post test for Test 22..... 468
Figure E.228: Progression of damage for Test 22 from Camera 1..... 469
Figure E.229: Progression of damage for Test 22 from Camera 2..... 469
Figure E.230: Progression of damage for Test 22 from Camera 3..... 469
Figure E.231: 3/4” thick steel plate pre test for Test 23..... 470
Figure E.232: Phantom Cameras for Test 23 471
Figure E.233: Target layout on plate and impacting mass for Test 23..... 471

Figure E.234: Steel plate post test for Test 23 472
Figure E.235: Progression of damage for Test 23 from Camera 1 473
Figure E.236: Progression of damage for Test 23 from Camera 2 473
Figure E.237: Progression of damage for Test 23 from Camera 3 473
Figure E.238: 1/4” thick steel plate pre test for Test 24 474
Figure E.239: Phantom Cameras for Test 24 475
Figure E.240: Target layout on plate and impacting mass for Test 24 475
Figure E.241: Accelerometer location for Test 2 476
Figure E.242: Filtered accelerometer data for Test 24 476
Figure E.243: Steel plate post test for Test 24 478
Figure E.244: Progression of damage for Test 24 from Camera 1 478
Figure E.245: Progression of damage for Test 24 from Camera 2 479
Figure E.246: Progression of damage for Test 24 from Camera 3 479
Figure E.247: 1/4” thick steel plate pre test for Test 25 480
Figure E.248: Phantom Cameras for Test 25 481
Figure E.249: Target layout on plate and impacting mass for Test 25 481
Figure E.250: Accelerometer location for Test 25 482
Figure E.251: Filtered accelerometer data for Test 25 482
Figure E.252: Strain gage layout for Test 25 483
Figure E.253: Maximum principal strains and strain rates for Test 25 484
Figure E.254: Minimum principal strains and strain rates for Test 25 484
Figure E.255: Steel plate post test for Test 25 485
Figure E.256: Progression of damage for Test 25 from Camera 1 486
Figure E.257: Progression of damage for Test 25 from Camera 2 486
Figure E.258: Progression of damage for Test 25 from Camera 3 486
Figure E.259: 1/2” thick steel plate pre test for Test 26 487
Figure E.260: Phantom Cameras for Test 26 488
Figure E.261: Target layout on plate and impacting mass for Test 26 488
Figure E.262: Accelerometer location for Test 26 489
Figure E.263: Filtered accelerometer data for Test 26 489
Figure E.264: Strain gage layout for Test 26 (drawing) 491
Figure E.265: Strain gage layout for Test 26 (pictures) 491
Figure E.266: Maximum principal strains and strain rates for Test 26 492
Figure E.267: Minimum principal strains and strain rates for Test 26 492
Figure E.268: Combined Axial Strain for Test 26 – Gauges 19 and 21 493
Figure E.269: Combined Axial Strain for Test 26 – Gauges 20 and 22 493
Figure E.270: Truncated Axial and Bending Stresses for Test 26 – Gauges 19 and 21 494
Figure E.271: Truncated Axial and Bending Stresses for Test 26 – Gauges 20 and 22 494
Figure E.272: Steel plate post test for Test 26 495
Figure E.273: Progression of damage for Test 26 from Camera 1 496
Figure E.274: Progression of damage for Test 26 from Camera 2 496
Figure E.275: Progression of damage for Test 26 from Camera 3 496
Figure E.276: 1/2” thick steel plate pre test for Test 27 497
Figure E.277: Phantom Cameras for Test 27 498
Figure E.278: Target layout on plate and impacting mass for Test 27 498
Figure E.279: Accelerometer location for Test 27 499
Figure E.280: Filtered accelerometer data for Test 27 499
Figure E.281: Strain gage layout for Test 27 (drawing) 501

Figure E.282: Strain gage layout for Test 27 (pictures) 501
Figure E.283: Maximum principal strains and strain rates for Test 27 502
Figure E.284: Minimum principal strains and strain rates for Test 27 502
Figure E.285: Combined Axial Strain for Test 27 – Gauges 19 and 21 503
Figure E.286: Combined Axial Strain for Test 27 – Gauges 20 and 22 503
Figure E.287: Truncated Axial and Bending Stresses for Test 27 – Gauges 19 and 21 504
Figure E.288: Truncated Axial and Bending Stresses for Test 27 – Gauges 20 and 22 504
Figure E.289: Steel plate post test for Test 27 506
Figure E.290: Progression of damage for Test 27 from Camera 1 506
Figure E.291: Progression of damage for Test 27 from Camera 2 506
Figure E.292: Progression of damage for Test 27 from Camera 3 507
Figure E.293: 3/4” thick steel plate pre test for Test 28 508
Figure E.294: Phantom Cameras for Test 28 a) Camera One b) Camera Two 509
Figure E.295: Target layout on plate and impacting mass for Test 28 509
Figure E.296: Strain gage layout for Test 28 (drawing) 510
Figure E.297: Strain gage layout for Test 28 (pictures) 510
Figure E.298: Maximum principal strains and strain rates for Test 28 511
Figure E.299: Minimum principal strains and strain rates for Test 28 512
Figure E.300: Combined Axial Strain for Test 28 – Gauges 19 and 21 512
Figure E.301: Combined Axial Strain for Test 28 – Gauges 20 and 22 513
Figure E.302: Truncated Axial and Bending Stresses for Test 28 – Gauges 19 and 21 513
Figure E.303: Truncated Axial and Bending Stresses for Test 28 – Gauges 20 and 22 514
Figure E.304: Steel plate post test for Test 28 515
Figure E.305: Progression of damage for Test 28 from Camera 1 515
Figure E.306: Progression of damage for Test 28 from Camera 2 515
Figure E.307: 3/4” thick steel plate pre test for Test 29 516
Figure E.308: Phantom Cameras for Test 29 517
Figure E.309: Target layout on plate and impacting mass for Test 29 517
Figure E.310: Accelerometer location for Test 29 518
Figure E.311: Filtered accelerometer data for Test 29 518
Figure E.312: Strain gage layout for Test 29 (drawing) 520
Figure E.313: Strain gage layout for Test 29 (pictures) 520
Figure E.314: Maximum principal strains and strain rates for Test 29 521
Figure E.315: Minimum principal strains and strain rates for Test 29 521
Figure E.316: Combined Axial Strain for Test 29 – Gauges 19 and 21 522
Figure E.317: Combined Axial Strain for Test 29 – Gauges 20 and 22 522
Figure E.318: Truncated Axial and Bending Stresses for Test 29 – Gauges 19 and 21 523
Figure E.319: Truncated Axial and Bending Stresses for Test 29 – Gauges 20 and 22 523
Figure E.320: Steel plate post test for Test 29 524
Figure E.321: Progression of damage for Test 29 from Camera 1 525
Figure E.322: Progression of damage for Test 29 from Camera 2 525
Figure E.323: Progression of damage for Test 29 from Camera 3 525
Figure E.324: 3/4” thick steel plate pre test for Test 30 526
Figure E.325: Phantom Cameras for Test 30 527
Figure E.326: Target layout on plate and impacting mass for Test 30 527
Figure E.327: Accelerometer location for Test 30 528
Figure E.328: Filtered accelerometer data for Test 30 528
Figure E.329: Strain gage layout for Test 30 (drawing) 530

Figure E.330: Strain gage layout for Test 30 (pictures) 530
Figure E.331: Maximum principal strains and strain rates for Test 30 531
Figure E.332: Minimum principal strains and strain rates for Test 30 531
Figure E.333: Combined Axial Strain for Test 30 – Gauges 19 and 21 532
Figure E.334: Combined Axial Strain for Test 30 – Gauges 20 and 22 532
Figure E.335: Truncated Axial and Bending Stresses for Test 30 – Gauges 19 and 21 533
Figure E.336: Truncated Axial and Bending Stresses for Test 30 – Gauges 20 and 22 533
Figure E.337: Steel plate post test for Test 30 534
Figure E.338: Progression of damage for Test 30 from Camera 1 534
Figure E.339: Progression of damage for Test 29 from Camera 2 535
Figure E.340: Progression of damage for Test 30 from Camera 3 535
Figure E.341: 7/8” thick steel plate pre test for Test 31 536
Figure E.342: Phantom Cameras for Test 31 537
Figure E.343: Target layout on plate and impacting mass for Test 31 537
Figure E.344: Accelerometer location for Test 3 538
Figure E.345: Filtered accelerometer data for Test 31 538
Figure E.346: Strain gage layout for Test 31 (drawing) 540
Figure E.347: Strain gage layout for Test 31 (pictures) 540
Figure E.348: Maximum principal strains and strain rates for Test 31 541
Figure E.349: Minimum principal strains and strain rates for Test 31 541
Figure E.350: Combined Axial Strain for Test 31 – Gauges 19 and 21 542
Figure E.351: Truncated Axial and Bending Stresses for Test 31 – Gauges 19 and 21 542
Figure E.352: Steel plate post test for Test 31 543
Figure E.353: Progression of damage for Test 31 from Camera 1 544
Figure E.354: Progression of damage for Test 31 from Camera 2 544
Figure E.355: Progression of damage for Test 31 from Camera 3 544
Figure E.356: 7/8” thick steel plate pre test for Test 32 545
Figure E.357: Phantom Cameras for Test 32 546
Figure E.358: Target layout on plate and impacting mass for Test 32 546
Figure E.359: Accelerometer location for Test 32 547
Figure E.360: Filtered accelerometer data for Test 32 547
Figure E.361: Strain gage layout for Test 32 (drawing) 549
Figure E.362: Strain gage layout for Test 32 (pictures) 549
Figure E.363: Maximum principal strains and strain rates for Test 32 550
Figure E.364: Minimum principal strains and strain rates for Test 32 550
Figure E.365: Combined Axial Strain for Test 32 – Gauges 19 and 21 551
Figure E.366: Combined Axial Strain for Test 32 – Gauges 20 and 22 551
Figure E.367: Truncated Axial and Bending Stresses for Test 32 – Gauges 19 and 21 552
Figure E.368: Truncated Axial and Bending Stresses for Test 32 – Gauges 20 and 22 552
Figure E.369: Steel plate post test for Test 32 553
Figure E.370: Progression of damage for Test 32 from Camera 1 554
Figure E.371: Progression of damage for Test 32 from Camera 2 554
Figure E.372: Progression of damage for Test 32 from Camera 3 554
Figure E.373: 7/8” thick steel plate pre test for Test 33 555
Figure E.374: Phantom Cameras for Test 33 a) Camera One b) Camera Two c) Camera Three 556
Figure E.375: Target layout on plate and impacting mass for Test 33 556
Figure E.376: Accelerometer location for Test 33 557

Figure E.377: Filtered accelerometer data for Test 33 557
Figure E.378: Strain gage layout for Test 33 (drawing) 559
Figure E.379: Strain gage layout for Test 33 (pictures) 559
Figure E.380: Maximum principal strains and strain rates for Test 3 560
Figure E.381: Minimum principal strains and strain rates for Test 33 560
Figure E.382: Combined Axial Strain for Test 33 – Gauges 19 and 21 561
Figure E.383: Combined Axial Strain for Test 33 – Gauges 20 and 22 561
Figure E.384: Truncated Axial and Bending Stresses for Test 33 – Gauges 19 and 21 562
Figure E.385: Truncated Axial and Bending Stresses for Test 33 – Gauges 20 and 22 562
Figure E.386: Steel plate post test for Test 33 563
Figure E.387: Progression of damage for Test 33 from Camera 1 564
Figure E.388: Progression of damage for Test 33 from Camera 2 564
Figure E.389: Progression of damage for Test 33 from Camera 3 564
Figure E.390: 1/4” thick steel plate pre test for Test 51 565
Figure E.391: Phantom Cameras for Test 51 566
Figure E.392: Target layout on plate and impacting mass for Test 51 566
Figure E.393: Strain gage layout for Test 51 (drawing) 567
Figure E.394: Maximum principal strains and strain rates for Test 51 568
Figure E.395: Minimum principal strains and strain rates for Test 51 568
Figure E.396: Steel plate post test for Test 51 569
Figure E.397: Progression of damage for Test 51 from Camera 1 569
Figure E.398: Progression of damage for Test 51 from Camera 2 570
Figure E.399: Progression of damage for Test 51 from Camera 3 570
Figure F.1: 1/4” thick steel plate pre test for Test 35 571
Figure F.2: Phantom Cameras for Test 35 a) Camera One b) Camera Two c) Camera Three 572
Figure F.3: Target layout on plate and impacting mass for Test 35 572
Figure F.4: Steel plate post test for Test 35 573
Figure F.5: Progression of damage for Test 35 from Camera 1 574
Figure F.6: Progression of damage for Test 35 from Camera 2 574
Figure F.7: Progression of damage for Test 35 from Camera 3 574
Figure F.8: 1/2” thick steel plate pre test for Test 36 575
Figure F.9: Phantom Cameras for Test 36 a) Camera One b) Camera Two c) Camera Three 576
Figure F.10: Target layout on plate and impacting mass for Test 36 576
Figure F.11: Strain gage layout for Test 36 577
Figure F.12: Maximum principal strains and strain rates for Test 36 578
Figure F.13: Minimum principal strains and strain rates for Test 36 578
Figure F.14: Steel plate post test for Test 36 579
Figure F.15: Progression of damage for Test 36 from Camera 1 579
Figure F.16: Progression of damage for Test 36 from Camera 2 580
Figure F.17: Progression of damage for Test 36 from Camera 3 580
Figure F.18: 1/2” thick steel plate pre test for Test 37 581
Figure F.19: Phantom Cameras for Test 37 a) Camera One b) Camera Two c) Camera Three 582
Figure F.20: Target layout on plate and impacting mass for Test 37 582
Figure F.21: Strain gage layout for Test 37 583
Figure F.22: Maximum principal strains and strain rates for Test 37 584

Figure F.23: Minimum principal strains and strain rates for Test 37 584
Figure F.24: Steel plate post test for Test 37 585
Figure F.25: Progression of damage for Test 37 from Camera 1 585
Figure F.26: Progression of damage for Test 37 from Camera 2 586
Figure F.27: Progression of damage for Test 37 from Camera 3 586
Figure F.28: 1/2” thick steel plate pre test for Test 38 587
Figure F.29: Phantom Cameras for Test 38 a) Camera One b) Camera Two c) Camera Three 588
Figure F.30: Target layout on plate and impacting mass for Test 38 588
Figure F.31: Strain gage layout for Test 38 589
Figure F.32: Maximum principal strains and strain rates for Test 38 590
Figure F.33: Minimum principal strains and strain rates for Test 38 590
Figure F.34: Steel plate post test for Test 38 591
Figure F.35: Progression of damage for Test 38 from Camera 1 591
Figure F.36: Progression of damage for Test 38 from Camera 2 592
Figure F.37: Progression of damage for Test 38 from Camera 3 592
Figure F.38: 1/2” thick steel plate pre test for Test 39 593
Figure F.39: Phantom Cameras for Test 39 a) Camera One b) Camera Two 594
Figure F.40: Target layout on plate and impacting mass for Test 39 594
Figure F.41: Strain gage layout for Test 39 595
Figure F.42: Maximum principal strains and strain rates for Test 39 596
Figure F.43: Minimum principal strains and strain rates for Test 39 596
Figure F.44: Steel plate post test for Test 39 597
Figure F.45: Progression of damage for Test 39 from Camera 1 597
Figure F.46: Progression of damage for Test 39 from Camera 2 598
Figure F.47: 1/4” thick steel plate pre test for Test 40 599
Figure F.48: Phantom Cameras for Test 40 a) Camera One b) Camera Two c) Camera Three 600
Figure F.49: Target layout on plate and impacting mass for Test 40 600
Figure F.50: Strain gage layout for Test 40 601
Figure F.51: Maximum principal strains and strain rates for Test 40 602
Figure F.52: Minimum principal strains and strain rates for Test 40 602
Figure F.53: Steel plate post test for Test 40 603
Figure F.54: Progression of damage for Test 40 from Camera 1 604
Figure F.55: Progression of damage for Test 40 from Camera 2 604
Figure F.56: Progression of damage for Test 40 from Camera 3 604
Figure F.57: 1/4” thick steel plate and KEDD pre test for Test 41 605
Figure F.58: Phantom Cameras for Test 41 a) Camera One b) Camera Two c) Camera Three 606
Figure F.59: Target layout on plate and impacting mass for Test 41 606
Figure F.60: Strain gage layout for Test 41 607
Figure F.61: Maximum principal strains and strain rates for Test 41 608
Figure F.62: Minimum principal strains and strain rates for Test 41 608
Figure F.63: Steel plate post test for Test 41 609
Figure F.64: Progression of damage for Test 41 from Camera 1 610
Figure F.65: Progression of damage for Test 41 from Camera 2 610
Figure F.66: Progression of damage for Test 41 from Camera 3 610
Figure F.67: 1/4” thick steel plate and KEDD pre test for Test 42 611

Figure F.68: Phantom Cameras for Test 42 a) Camera One b) Camera Two c) Camera Three 612
Figure F.69: Target layout on plate and impacting mass for Test 42 612
Figure F.70: Strain gage layout for Test 42 613
Figure F.71: Maximum principal strains and strain rates for Test 42 614
Figure F.72: Minimum principal strains and strain rates for Test 42 614
Figure F.73: Steel plate post test for Test 42 615
Figure F.74: Progression of damage for Test 42 from Camera 1 616
Figure F.75: Progression of damage for Test 42 from Camera 2 616
Figure F.76: Progression of damage for Test 42 from Camera 3 616
Figure F.77: 1/4” thick steel plate pre test for Test 43 617
Figure F.78: Phantom Cameras for Test 43 a) Camera One b) Camera Two 618
Figure F.79: Target layout on plate and impacting mass for Test 43 618
Figure F.80: Strain gage layout for Test 43 619
Figure F.81: Maximum principal strains and strain rates for Test 43 620
Figure F.82: Minimum principal strains and strain rates for Test 43 620
Figure F.83: Steel plate post test for Test 43 621
Figure F.84: Progression of damage for Test 43 from Camera 1 622
Figure F.85: Progression of damage for Test 43 from Camera 2 622
Figure F.86: 1/4” thick steel plate and KEDD pre test for Test 44 623
Figure F.87: Phantom Cameras for Test 44 a) Camera One b) Camera Two c) Camera Three 624
Figure F.88: Target layout on plate and impacting mass for Test 44 624
Figure F.89: Strain gage layout for Test 44 625
Figure F.90: Maximum principal strains and strain rates for Test 44 626
Figure F.91: Minimum principal strains and strain rates for Test 44 626
Figure F.92: Steel plate post test for Test 44 627
Figure F.93: Progression of damage for Test 44 from Camera 1 628
Figure F.94: Progression of damage for Test 44 from Camera 2 628
Figure F.95: Progression of damage for Test 44 from Camera 3 628
Figure F.96: 1/2” thick steel plate pre test for Test 45 629
Figure F.97: Phantom Cameras for Test 45 a) Camera One b) Camera Two c) Camera Three 630
Figure F.98: Target layout on plate and impacting mass for Test 45 630
Figure F.99: Strain gage layout for Test 45 631
Figure F.100: Maximum principal strains and strain rates for Test 45 632
Figure F.101: Minimum principal strains and strain rates for Test 45 632
Figure F.102: Steel plate post test for Test 45 633
Figure F.103: Progression of damage for Test 45 from Camera 1 634
Figure F.104: Progression of damage for Test 45 from Camera 2 634
Figure F.105: Progression of damage for Test 45 from Camera 3 634
Figure F.106: 1/4” thick steel plate and KEDD pre test for Test 46 635
Figure F.107: Phantom Cameras for Test 46 636
Figure F.108: Target layout on plate and impacting mass for Test 46 636
Figure F.109: Strain gage layout for Test 46 637
Figure F.110: Maximum principal strains and strain rates for Test 46 638
Figure F.111: Minimum principal strains and strain rates for Test 46 638
Figure F.112: Steel plate post test for Test 46 639

Figure F.113: Progression of damage for Test 46 from Camera 1 640
Figure F.114: Progression of damage for Test 46 from Camera 2 640
Figure F.115: Progression of damage for Test 46 from Camera 3 640
Figure F.116: 1/4" thick steel plate and KEDD pre test for Test 47 641
Figure F.117: Phantom Cameras for Test 47 642
Figure F.118: Target layout on plate and impacting mass for Test 47 642
Figure F.119: Strain gage layout for Test 47 643
Figure F.120: Maximum principal strains and strain rates for Test 47 644
Figure F.121: Minimum principal strains and strain rates for Test 47 644
Figure F.122: Steel plate post test for Test 47 645
Figure F.123: Progression of damage for Test 47 from Camera 1 646
Figure F.124: Progression of damage for Test 47 from Camera 2 646
Figure F.125: Progression of damage for Test 47 from Camera 3 646
Figure F.126: 1/4" thick steel plate and KEDD pre test for Test 48 647
Figure F.127: Phantom Cameras for Test 48 648
Figure F.128: Target layout on plate and impacting mass for Test 48 648
Figure F.129: Strain gage layout for Test 48 649
Figure F.130: Maximum principal strains and strain rates for Test 48 650
Figure F.131: Minimum principal strains and strain rates for Test 48 650
Figure F.132: Steel plate post test for Test 48 651
Figure F.133: Progression of damage for Test 48 from Camera 1 652
Figure F.134: Progression of damage for Test 48 from Camera 2 652
Figure F.135: Progression of damage for Test 48 from Camera 3 652
Figure F.136: 1/4" thick steel plate and KEDD pre test for Test 49 653
Figure F.137: Phantom Cameras for Test 49 654
Figure F.138: Target layout on plate and impacting mass for Test 49 654
Figure F.139: Strain gage layout for Test 49 655
Figure F.140: Maximum principal strains and strain rates for Test 49 656
Figure F.141: Minimum principal strains and strain rates for Test 49 656
Figure F.142: Steel plate post test for Test 49 657
Figure F.143: Progression of damage for Test 49 from Camera 1 658
Figure F.144: Progression of damage for Test 49 from Camera 2 658
Figure F.145: Progression of damage for Test 49 from Camera 3 658
Figure F.146: 1/4" thick steel plate pre test for Test 50 659
Figure F.147: Target layout on plate and impacting mass for Test 50 660
Figure F.148: Steel plate post test for Test 50 661
Figure G.1: Test 1 set-up 662
Figure G.2: Test 1 Time of Arrival Pins 663
Figure G.3: Test 1 plate post test 664
Figure G.4: Test 1 plate fragmentation 664
Figure G.5: Test 1 plate fragmentation 665
Figure G.6: Test 1 plate petalling details 665
Figure G.7: Test 2 set-up 666
Figure G.8: Test 2 Time of Arrival Pins 667
Figure G.9: Test 2 plate post test 668
Figure G.10: Test 2 plate fragments 668
Figure G.11: Test 2 plate fragments 669
Figure G.12: Test 3 set-up 670

Figure G.13: Test 3 Time of Arrival Pins 671
Figure G.14: Test 3 plate post test 672
Figure G.15: Test 3 plate and fragments 672
Figure G.16: Test 3 a plate fragment 673
Figure G.17: Test 4 set-up 674
Figure G.18: Test 4 Time of Arrival Pins 675
Figure G.19: Test 4 plate and fragments 676
Figure G.20: Test 4 plate fragments 676
Figure G.21: Test 4 top plate post test 677
Figure G.22: Test 5 set-up 678
Figure G.23: Test 5 Time of Arrival pins 679
Figure G.24: Test 5 a) Entire test specimen post test b) Second, third and fourth plates post test 680
Figure G.25: Test 5 top plate 680
Figure G.26: a) Test 6 set-up b) Charge for Test 6 681
Figure G.27: Test 6 Time of Arrival pins 682
Figure G.28: Test 6 post test 683
Figure G.29: Test 6 top plate 683
Figure G.30: Test 6 top flyer plate 684
Figure G.31: Test 6 bottom flyer plate 684
Figure G.32: Test 6 bottom plate 685
Figure G.33: Test 6 bottom plate petalling details 685
Figure G.34: Test 6 top and bottom plates 686
Figure G.35: Test 6 top and bottom flyer plates 686
Figure G.36: a) Test 7 set-up b) Charge for Test 7 687
Figure G.37: a) Individual KEDD b) Test 7 Array of 9 KEDD's 688
Figure G.38: Test 7 Time of Arrival pins 689
Figure G.39: Test 7 post test 690
Figure G.40: Test 7 top plate 690
Figure G.41: Test 7 bottom plate 691
Figure G.42: Test 7 top and bottom plate 691
Figure G.43: a) Test 8 set-up b) Charge for Test 8 692
Figure G.44: a) Individual KEDD b) Test 8 Array of 9 KEDD's 693
Figure G.45: Test 8 Time of Arrival pins 694
Figure G.46: Test 8 post test 695
Figure G.47: Test 8 top plate 695
Figure G.48: Test 8 bottom plate 696
Figure G.49: Test 8 top and bottom plate 696
Figure G.50: a) Test 9 set-up b) Test 9 with charge 697
Figure G.51: a) Individual KEDD b) Test 9 Array of 9 KEDD's 698
Figure G.52: Test 9 Time of Arrival pins 699
Figure G.53: Test 9 post test 700
Figure G.54: Test 9 post test 700
Figure G.55: Test 9 top plate 701
Figure G.56: Test 9 top plate petalling details 701
Figure G.57: Test 9 middle plate 702
Figure G.58: Test 9 bottom plate 702
Figure G.59: Test 9 top, middle, and bottom plates 703

Figure G.60: a) Test 10 set-up b) Charge for Test 10 704
Figure G.61: Test 10 Time of Arrival pins 705
Figure G.62: Test 10 post test 706
Figure G.63: Test 10 top plate 707
Figure G.64: Test 10 top plate fragmentation details 707
Figure G.65: Test 10 top plate fragmentation details 708
Figure G.66: Test 10 middle plate 708
Figure G.67: Test 10 bottom plate 709
Figure G.68: Test 10 top plate petalling details 709
Figure G.69: Test 10 top, middle, and bottom plate 710
Figure G.70: a) Test 11 set-up b) Charge for Test 11 711
Figure G.71: a) Individual KEDD b) Test 11 Array of 9 KEDD's 712
Figure G.72: Test 11 Time of Arrival pins 713
Figure G.73: Test 11 post test 714
Figure G.74: Test 11 top plate 714
Figure G.75: Test 11 bottom plate 715
Figure G.76: Test 11 top and bottom plate 715
Figure G.77: a) Test 12 set-up b) Test 12 set-up with charge 716
Figure G.78: a) Individual KEDD b) Test 12 Array of 9 KEDD's 717
Figure G.79: Test 12 Time of Arrival pins 718
Figure G.80: Test 12 bottom plate in test bed 719
Figure G.81: Test 12 top plate in test bed 719
Figure G.82: Test 12 top plate 720
Figure G.83: Test 12 flyer plate from top plate 720
Figure G.84: Test 12 bottom plate 721
Figure G.85: Test 12 top and bottom plate 721
Figure G.86: a) Test 13 set-up b) Charge for Test 13 722
Figure G.87: Test 13 Time of Arrival pins 723
Figure G.88: Test 13 test specimen post test 724
Figure G.89: Test 13 top plate 724
Figure G.90: Test 13 top plate fragments 725
Figure G.91: Test 13 bottom plate 725
Figure G.92: Test 13 top and bottom plate 726
Figure G.93: a) Test 14 set-up b) Charge for Test 14 727
Figure G.94: Test 14 Time of Arrival pins 728
Figure G.95: Test 14 test specimen post test 729
Figure G.96: Test 14 top plate in test bed 729
Figure G.97: Test 14 top plate 730
Figure G.98: Test 14 bottom plate 730
Figure G.99: Test 14 bottom plate petalling and shearing details 731
Figure G.100: Test 14 top and bottom plate 731
Figure G.101: a) Test 15 set-up b) Charge for Test 15 732
Figure G.102: a) Individual KEDD b) Test 15 - Two rows of KEDD's 733
Figure G.103: Test 15 Time of Arrival pins 734
Figure G.104: Test 15 post test 735
Figure G.105: Test 15 top plate 735
Figure G.106: Test 15 bottom plate 736
Figure G.107: Test 15 top and bottom plate 736

Figure G.108: a) Test 16 set-up b) Charge for Test 16 737
Figure G.109: a) Individual KEDD b) Test 16 - Two rows of KEDD's (one on top and bottom) 738
Figure G.110: Test 16 Time of Arrival pins 739
Figure G.111: Test 16 post test 740
Figure G.112: Test 16 top plate in test bed 740
Figure G.113: Test 16 top plate 741
Figure G.114: Test 16 bottom plate 741
Figure G.115: Test 16 top and bottom plate 742
Figure G.116: a) Test 17 set-up b) Charge for Test 17 743
Figure G.117: a) Individual KEDD b) Test 17 - Three rows of KEDD's 744
Figure G.118: Test 17 Time of Arrival pins 745
Figure G.119: Test 17 post test 746
Figure G.120: Test 17 top plate 746
Figure G.121: Test 17 bottom plate 747
Figure G.122: Test 17 top and bottom plate 747
Figure G.123: a) Test 18 set-up b) Charge for Test 18 748
Figure G.124: Test 18 Time of Arrival pins 749
Figure G.125: Test 18 test specimen post test 750
Figure G.126: Test 18 section of top plate embedded in wall 750
Figure G.127: Test 18 top plate 751
Figure G.128: Test 18 bottom plate 751
Figure G.129: Test 18 bottom plate fragment 752
Figure G.130: Test 18 top and bottom plate 752
Figure G.131: a) Test 19 set-up b) Charge for Test 19 753
Figure G.132: a) Individual KEDD b) Test 19 - Two rows of KEDD's 754
Figure G.133: Test 19 Time of Arrival pins 755
Figure G.134: Test 19 post test 756
Figure G.135: Test 19 top plate 756
Figure G.136: Test 19 bottom plate in test bed 757
Figure G.137: Test 19 top and bottom plate 757
Figure G.138: a) Test 20 set-up b) Charge for Test 20 758
Figure G.139: a) Individual KEDD b) Test 20 - Three rows of KEDD's 759
Figure G.140: Test 20 Time of Arrival pins 760
Figure G.141: Test 20 post test 761
Figure G.142: Test 20 top plate in test bed 761
Figure G.143: Test 20 top plate 762
Figure G.144: Test 20 top plate flyer plate 762
Figure G.145: Test 20 bottom plate 763
Figure G.146: a) Test 21 set-up b) Charge for Test 21 764
Figure G.147: a) Individual KEDD b) Test 21 - Two rows of KEDD's (one on top and bottom) 765
Figure G.148: Test 21 Time of Arrival pins 766
Figure G.149: Test 21 post test 767
Figure G.150: Test 21 top plate in test bed 767
Figure G.151: Test 21 bottom plate in test bed 768
Figure G.152: Test 21 bottom plate with flyer plate in test bed 768
Figure G.153: Test 21 crack in bottom plate 769

Figure G.154: Test 21 top and bottom plate 769
Figure H.1: EMRTC Test 1 structure (photo) 770
Figure H.2: EMRTC Test 1 structure with sand bags 770
Figure H.3: EMRTC Test 1 structure (drawing) 771
Figure H.4: EMRTC Test 1 charge 772
Figure H.5: Test article and charge 772
Figure H.6: Test 1 pressure gage locations 773
Figure H.7: Test article pictures from Phantom Camera 774
Figure H.8: EMRTC Test 1 post test a) Flyer plate b) Reassembled top plate 775
Figure H.9: EMRTC Test 1 post-test 776
Figure H.10: EMRTC Test 1 post-test, concrete foundation 776
Figure H.11: EMRTC Test 2 structure (photo) 777
Figure H.12: EMRTC Test 2 structure (drawing) 778
Figure H.13: EMRTC Test 2 charge 779
Figure H.14: EMRTC Test 2 Time of Arrival pins 780
Figure H.15: EMRTC Test 2 Time of Arrival pin dimensions 780
Figure H.16: EMRTC Test 2 Time of Arrival pin array locations 781
Figure H.17: Test article pictures from Phantom Camera 783
Figure H.18: EMRTC Test 2 post test 784
Figure H.19: EMRTC Test 2 close up of secondary flyer plate 785
Figure H.20: EMRTC Test 2 initial flyer plate 785
Figure H.21: EMRTC Test 2 flyer plates a) Initial flyer plate b) Secondary flyer plate 786
Figure H.22: EMRTC Test 2 flyer plates 786
Figure H.23: EMRTC Test 2 top plate fragments 787
Figure H.24: EMRTC Test 2 reassembled top plate 787
Figure H.25: EMRTC Test 3 structure elevation (photo) 788
Figure H.26: EMRTC Test 3 structure elevation (drawing) 789
Figure H.27: EMRTC Test 3 structure (drawing) 790
Figure H.28: KEDD – EMRTC Test 3 791
Figure H.29: 2 Rows of KEDD's on top EMRTC Test 3 791
Figure H.30: EMRTC Test 3 charge box 792
Figure H.31: EMRTC Test 3 charge in place 792
Figure H.32: Time of Arrival pin arrays a) 3 pin array b) 4 pin array 793
Figure H.33: Time of Arrival pin locations for EMRTC Test 3 794
Figure H.34: Time of Arrival pins a) Pin support in outer cells b) Pins located in center cells 795
Figure H.35: Test specimen post-test 797
Figure H.36: Test specimen post-test with Key Plan 798
Figure H.37: Test specimen post-test cells 1 and 2 800
Figure H.38: Test specimen post-test cell 3 801
Figure H.39: Test specimen post-test cells 7 and 8 803
Figure H.40: Test specimen post-test cell 9 804
Figure H.41: Test specimen and miscellaneous flyer plates 805
Figure H.42: Test specimen and miscellaneous flyer plates 806
Figure H.43: Miscellaneous flyer plates 806
Figure H.44: Flyer plates at extreme distances 807
Figure H.45: Flyer plates at extreme distances 807
Figure H.46: Close up of flyer plate 808

Figure H.47: Jets formed by KEDD system 810
Figure H.48: Test specimen post-test cells 4and 5 811
Figure H.49: Test specimen post-test cells 4, 5, and 6 812

LIST OF TABLES

Table 1.1: Comparing velocity with CTH, field tests, and momentum calculations..... 20
Table 3.1: Time of Arrival pin data..... 48
Table 3.2: Impacting mass and accessories..... 64
Table 4.1: KEDD lab tests..... 100
Table 4.2: KEDD test comparison data..... 102
Table 4.3: KEDD test comparison data..... 107
Table 4.4: KEDD test data..... 110
Table 4.5: Kinetic energy data for damage – remained attached..... 111
Table 4.6: Kinetic energy data for damage – partial failure..... 113
Table 5.1: Test matrix..... 116
Table 5.2: 2 Plate Test baseline velocity data..... 130
Table 5.3: 2 Plate Tests, KEDD on top velocity data..... 139
Table 5.4: 2 Plate Test KEDD on bottom, velocity data..... 151
Table 5.5: 2 Plate Test, two rows of KEDD's on top velocity data..... 161
Table 5.6: 2 Plate Test, one row of KEDD's on top and bottom velocity data..... 170
Table 5.7: 2 Plate Test, three rows of KEDD's on top velocity data..... 179
Table 5.8: Velocity reductions due to KEDD's..... 195
Table 5.9: Velocity reduction of the second plate (CTH calculations)..... 199
Table 5.10: Comparing velocity reduction of the second plate with CTH, field tests, and momentum calculations..... 200
Table 5.11: Diameter and spacing of KEDD system for different plate thicknesses..... 203
Table A.1: Ballistic Loading Tests – Type 1 test matrix..... 252
Table A.2: Ballistic Loading Tests – Type 2 test matrix..... 253
Table A.3: Bolt material properties..... 253
Table A.4: Frequencies used for acceleration bandpass filter..... 262
Table A.5: 1/4" Plate – test matrix..... 266
Table A.6: 1/4" Plate – strain rate data..... 268
Table A.7: 1/2" Plate – test matrix..... 271
Table A.8: 1/2" Plate – strain rate data (Part 1)..... 273
Table A.9: 1/2" Plate – strain rate data (Part 2)..... 274
Table A.10: 3/4" Plate – test matrix..... 276
Table A.11: 3/4" Plate – strain rate data..... 277
Table A.12: 7/8" Plate – test matrix..... 278
Table A.13: 7/8" Plate – strain rate data..... 279
Table E.1: Stain rate information for Test 3..... 333
Table E.2: Stain rate information for Test 4..... 340
Table E.3: Stain rate information for Test 5..... 348
Table E.4: Stain rate information for Test 6..... 354
Table E.5: Stain rate information for Test 7..... 360
Table E.6: Stain rate information for Test 8..... 367
Table E.7: Stain rate information for Test 9..... 375
Table E.8: Stain rate information for Test 10..... 383
Table E.9: Stain rate information for Test 11..... 390
Table E.10: Stain rate information for Test 12..... 397
Table E.11: Stain rate information for Test 13..... 403
Table E.12: Stain rate information for Test 14..... 411

Table E.13: Stain rate information for Test 15 417
Table E.14: Stain rate information for Test 16 424
Table E.15: Stain rate information for Test 17 431
Table E.16: Stain rate information for Test 18 438
Table E.17: Stain rate information for Test 19 445
Table E.18: Stain rate information for Test 20 452
Table E.19: Stain rate information for Test 21 459
Table E.20: Stain rate information for Test 22 466
Table E.21: Stain rate information for Test 25 483
Table E.22: Stain rate information for Test 26 490
Table E.23: Stain rate information for Test 27 500
Table E.24: Stain rate information for Test 28 511
Table E.25: Stain rate information for Test 29 519
Table E.26: Stain rate information for Test 30 529
Table E.27: Stain rate information for Test 31 539
Table E.28: Stain rate information for Test 32 548
Table E.29: Stain rate information for Test 33 558
Table E.30: Stain rate information for Test 51 567
Table F.1: Stain rate information for Test 36 577
Table F.2: Stain rate information for Test 37 583
Table F.3: Stain rate information for Test 38 589
Table F.4: Stain rate information for Test 39 595
Table F.5: Stain rate information for Test 40 601
Table F.6: Stain rate information for Test 41 607
Table F.7: Stain rate information for Test 42 613
Table F.8: Stain rate information for Test 43 619
Table F.9: Stain rate information for Test 44 625
Table F.10: Stain rate information for Test 45 631
Table F.11: Stain rate information for Test 46 637
Table F.12: Stain rate information for Test 47 643
Table F.13: Stain rate information for Test 48 649
Table F.14: Stain rate information for Test 49 655
Table G.1: Time of Arrival Data for Test 1 663
Table G.2: Time of Arrival Data for Test 2 667
Table G.3: Time of Arrival Data for Test 3 671
Table G.4: Time of Arrival Data for Test 4 675
Table G.5: Time of Arrival Data for Test 5 679
Table G.6: Time of Arrival Data for Test 6 682
Table G.7: Time of Arrival Data for Test 7 688
Table G.8: Time of Arrival Data for Test 8 693
Table G.9: Time of Arrival Data for Test 9 698
Table G.10: Time of Arrival Data for Test 10 705
Table G.11: Time of Arrival Data for Test 11 712
Table G.12: Time of Arrival Data for Test 12 717
Table G.13: Time of Arrival Data for Test 13 723
Table G.14: Time of Arrival Data for Test 14 728
Table G.15: Time of Arrival Data for Test 15 733
Table G.16: Time of Arrival Data for Test 16 738

Table G.17: Time of Arrival Data for Test 17 744
Table G.18: Time of Arrival Data for Test 18 749
Table G.19: Time of Arrival Data for Test 19 754
Table G.20: Time of Arrival Data for Test 20 759
Table G.21: Time of Arrival Data for Test 21 765
Table H.1: Sensors used for EMRTC Test 1 774
Table H.2: Time of Arrival pin data 782
Table H.3: EMRTC Field Test 3 Time of Arrival pin data 796

ACKNOWLEDGEMENTS

I would like to thank my advisor, Dr. Gilbert Hegemier for his support and guidance in this research endeavor. His advice and counsel were integral to my successful completion of this document. I would also like to thank my committee members, Dr. David Benson, Dr. Vistasp M. Karbhari, Dr. Vitali Nesterenko and Dr. Frieder Seible, for reading my dissertation and their feedback.

This project would not have been completed if it were not for the support of the Technical Support Working Group, TSWG, and their highly competent staff. I would specifically like to thank Mike Purcell and Phil Thompson who assisted in the coordination of this project and helped to push for its success. In addition to those mentioned above there are other people and organizations that helped me completed this research project. Dr. Joseph Baum and Dr. Chuck Charman at Science Applications International Coorperation (SAIC) for their computational support on some of the field test articles. Ken Morrill and Joe Magallanes, at Karagozian and Case (K&C) also supported this research, through computational analyses of both laboratory and field tests. Without the help of either of those organizations this project would not have been as successful.

Not only did I receive help in regards to computational support, I was taught many things about live field tests. Jason Metzger, Tom Villanova, and Mike Stanley at the Energetic Materials Research and Testing Center at New Mexico Tech (EMRTC) were extremely helpful in the coordination of the three field tests at their testing center. Ruben Martinez of K&C, oversaw the design and construction of these test articles.

Live field testing was also performed in conjunction with the Rocky Mountain Division of Applied Research Associates (RMD-ARA). Fred Sanstrom, Bryan Bockman,

Scott Hardesty, Martin Slack, Bud Reed, and others were extremely helpful with any questions that I had; whether they applied to live field testing or not. I am extremely grateful for their help and advice in the Proof of Concept tests and the 3rd EMRTC field test.

I would also like to thank my support group at UCSD. Without the help of Karen Arnett, I do not know if I would ever have gotten any of this work completed. Thank you for keeping me on budget, on time, and out of trouble. To Lauren Stewart, Mike Oesterle, and Tona Rodriguez-Nikl thank you for all of your help, advice, and friendship over the last five years. Life at school would have been very different without you. I would also like to thank Jim Newell for his advice, patience, and friendship as a sounding board over these past years.

Finally, I would like to thank my family and friends for their patience with me. I know that many of you never want to hear me talk about strain rates or KEDD's ever again, I will try to not talk about this anymore. I never thought that this would actually come to fruition, but as it nears I know that all of you have helped me along my way.

To my wonderful husband David, and our dog Chewbacca; thank you for the love that you gave me every time I came home. It was that support that enabled me to finish my dissertation. I look forward to our next great adventure.

VITA

1996 Associate of Arts, Yuba Community College

2000 Bachelor of Science, California Polytechnic State University, San Luis Obispo

2006 Master of Science, University of California, San Diego

2008 Doctor of Philosophy, University of California, San Diego

PUBLICATIONS

Protection of Our Bridge Infrastructure against Man-made and Natural Hazards, F. Seible, G. Hegemier, J. Wolfson, K. Arnett, R. Conway and J. D. Baum, July 2006, Keynote paper for the Third International Conference on Bridge Maintenance, Safety and Management (IABMAS'06).

Protection of Our Bridge Infrastructure against Man-made and Natural Hazards, Frieder Seible, Gil Hegemier, Vistasp M. Karbhari, Janet Wolfson, Karen Arnett, Robert Conway, and Joseph D. Baum, September 2006, Structure and Infrastructure Engineering (SIE).

The UCSD Blast Simulator, G. Hegemier, F. Seible, K. Arnett, T. Rodriguez-Nikl, M. Oesterle, J. Wolfson, M. Gram and Al Clark, March 2007, 77th Shock and Vibration Symposium (SAVIAC).

Cellular Tower Response to Blast Loading; J.D. Baum, O.A. Soto, C.L. Charman, E.L. Mestreau and J. Wolfson, September 2007, International Symposium on Interaction of the Effects of Munitions with Structures (ISIEMS 2007)

Modeling of Steel Plate Response to Blast Loading Using a Coupled CFD/CSD Methodology; J.D. Baum, C.L. Charman, J. Wolfson, G. Hegemier, O.A. Soto, M.E. Giltrud and E.L. Mestreau, 5th International Conference on computation Fluid Dynamics (ICCFD5) Pending

Kinetic Energy Defeat Device (KEDD) Proof of Concept Tests, - TSWG Test Report; J. Wolfson, G. Hegemier, F. Seible, Department of Structural Engineering, University of California, San Diego, December 11, 2007.

Explosive Loading Laboratory Testing for Blast Simulator Operations and Steel Cellular Bridge Tower Testing, - TSWG Test Report; J. Wolfson, G. Hegemier, F. Seible, Department of Structural Engineering, University of California, San Diego, Pending.

ABSTRACT OF THE DISSERTATION

BLAST DAMAGE MITIGATION OF CELLULAR STEEL STRUCTURES FROM NEAR-CONTACT CHARGES

by

JANET CRUMRINE WOLFSON

Doctor of Philosophy in Structural Engineering

University of California, San Diego, 2008

Professor Gil Hegemier, Chair

A series of experiments have been performed on a built-up cellular steel structure to determine the structural response of the system when subjected to an explosive load at close range. Initial full scale field tests demonstrated how the structure reacted under an extreme loading event; specifically, in the failure of the bolts and support structure, and the formation of flyer plates. Flyer plates are formed out of the support steel of the structure. They can range in size from several inches square to several feet square depending on the size of the charge and standoff. These flyer plates, if unimpeded, can travel at extremely high velocities;

they will then impact additional steel plates forming secondary flyer plates, which can cause significant damage to the entire structure.

Laboratory tests were performed on structural components, plates and bolts, to evaluate their failure mechanisms. Comparisons were made between the type of bolts used and plate thicknesses in developing behavior phenomena. Strain rate data was gathered that can be used to improve existing material behavior. This data reflects overall system behavior as opposed to component behavior. Based on the knowledge gained from these experiments a new retrofit technique was developed that can mitigate damage during an extreme event. The new so-called Kinetic Energy Defeat Device (KEDD) utilizes non-viscous liquids in a periodic array to redirect the kinetic energy of a projectile through the formation of high speed jets. This re-direction of energy can slow the velocity of the incoming projectile, thereby, limiting the damage to the structure.

Full scale and scaled field tests, along with laboratory tests have been performed to determine the effectiveness of this device. Tests with and without the KEDD system have been compared evaluating the type of failure that occurs and the speed at which the projectiles travel.

1. EXECUTIVE SUMMARY

1.1 INTRODUCTION

Over the past decade, world-wide terrorist attacks have demonstrated the vulnerability of our critical infrastructure to conventional and improvised explosives. In response, extensive research has been conducted in an effort to further develop effective protective technologies for building structures. As a result, methods have been created to increase redundancy, harden critical members, and increase stand-off distances. We ask the question: what happens to that class of structures for which, in contrast to building systems, only a few critical members exist and where increasing the stand-off distance is not feasible.

There is a class of steel structures in use today that cannot be hardened using conventional means. In addition, these structures are susceptible to large near-contact charges, where the charge cannot be mitigated by increasing the standoff distance between it and the structure. They are called cellular steel structures; they consist of an array of built-up members that together form the structural system. This system was designed to resist conventional loads (dead, live, wind, snow, and seismic) for which it is very robust; however, when exposed to these types of explosive loads there is no redundancy in this type of structure. An explosive charge placed in one location can easily affect the global stability of the entire structure. The ability of these structures to withstand a terrorist attack is of great importance. A few of these structures are part of our American cultural heritage, and most are integral to everyday commerce.

A series of meetings were held, in various locations throughout the United States in the Fall of 2004 through the Spring of 2005, to speak to owners, representatives, and leading experts about the research needs for the protective design of cellular steel structure. Many

topics were addressed during these sessions; however, it was determined that sufficient data was not available regarding the behavior of these structures to near-contact charges. A detailed computational model that had been developed for cellular steel structures was presented during this series of meetings; however, different meeting attendees debated the validity of this model. Results of full-scale field tests were requested to determine the predictive capabilities of existing computational codes.

The University of California, San Diego (UCSD) was tasked with leading the research endeavor to determine the behavior of cellular steel structures exposed to near-contact charges and to develop an effective blast mitigation technique. Working with industry partners (owners, representatives, and experts) research objectives were established. Those objectives are: 1) develop a generic structure that is representative of such structures; 2) determine, through full-scale live field tests, the phenomenology, or behavior, of cellular steel structures when exposed to near-contact charges; 3) develop a retrofit solution that is effective against the type of damage witnessed in subsequent field tests and that meets constructability and long term maintenance issues associated with these structures; 4) evaluate the predictive capabilities of current computational codes based on the results of field tests; and 5) to validate the retrofit concept with a multi-celled full-scale field test. The methodology and results of this research is presented below.

1.2 GENERIC CELLULAR STEEL STRUCTURE

The first research objective is to establish a generic cellular steel structure that can be evaluated and tested. It is developed in conjunction with UCSD and industry representatives who determined that the structure would be three cells across and four cells deep. Each cell has the interior dimensions of 3’-6” x 3’-6”. The cells, or bays, are constructed out of 7/8”

A36 steel plates and are supported at the corners by 8” x 8” x 1/2” A36 steel angles. These are connected together with 1” diameter A307 (low strength) bolts at a spacing of 4” on center as shown in Figure 1.1. Many of these structures use rivets to connect the plates and angles; however, it would have been challenging and expensive to construct these specimens using rivets. A307 bolts have similar material properties to the historic rivets that are found in this type of structure and were deemed an acceptable connection method.

1.3 SUBSTRUCTURE BEHAVIOR FROM NEAR-CONTACT CHARGES

The second objective of this research endeavor was to determine the behavior of the generic cellular steel structure exposed to a near-contact charge. A series of tests were performed at the Energetic Materials and Research Testing Center and New Mexico Tech (EMRTC) in Summer 2005 on three bays of the generic cellular steel structure. The specimens were fabricated from 7/8” thick A36 steel and supported at the edges by 8” x 8” x 1/2” steel angles. For the first test, the cell was open on the bottom; in the second test the specimen was placed on elevated supports and an additional steel plate was added at the bottom of the cell. A test specimen, prior to detonation, is shown in Figure 1.2.

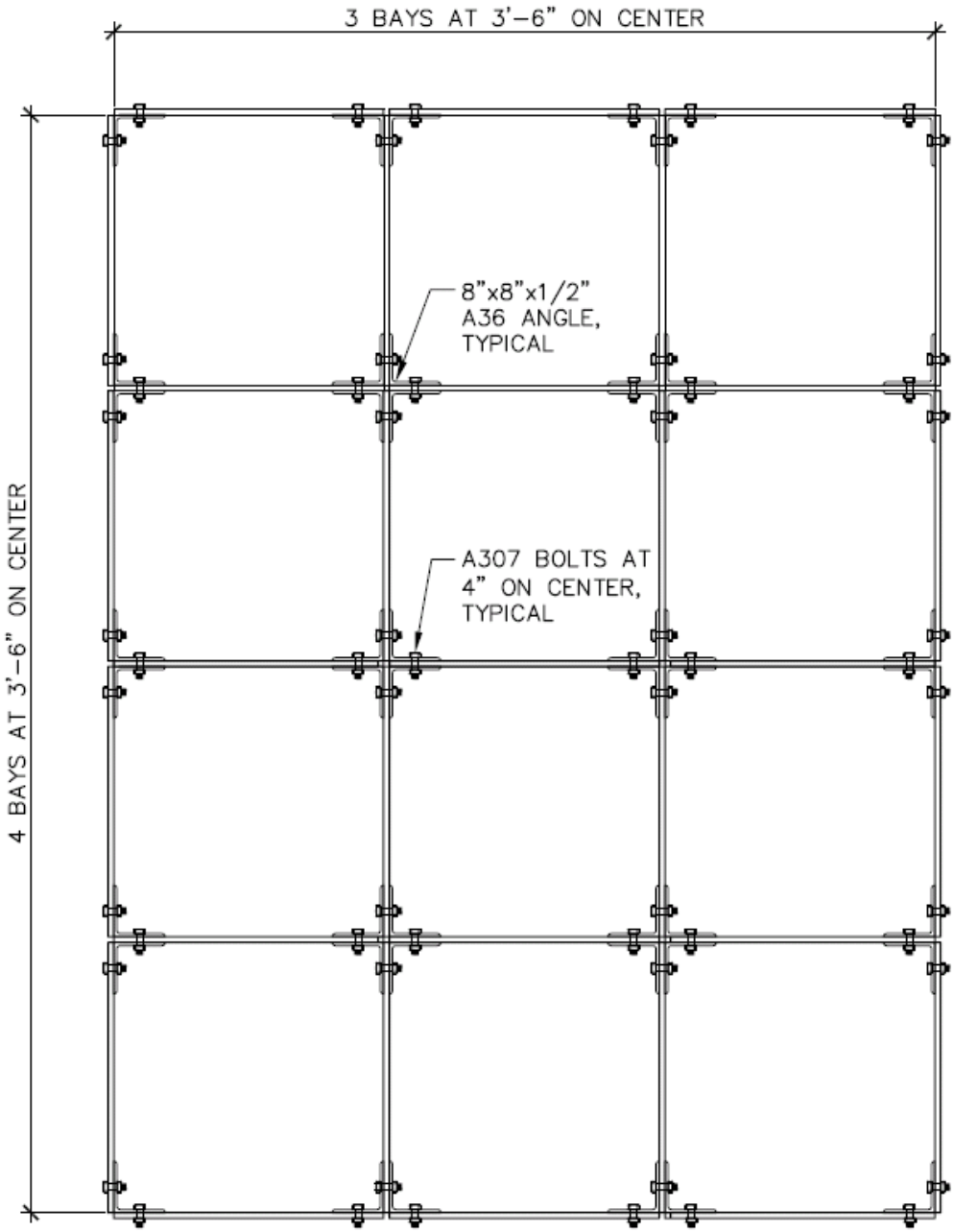

Figure 1.1: Schematic drawing of generic cellular steel structure

These tests were used to evaluate the failure modes for the overall specimen when exposed to a near-contact charge. The first observed mode was in the failure of the bolts that connect the individual components of these built-up structures. The observed bolt failures where in direct shear, and combinations of tension, bending, and shear (Figure 1.3). The second observed failure mode was the formation of an initial flyer plate. A flyer plate is created when a fragment of the first steel plate separates from the remaining structure and travels at high velocities. If unimpeded, the flyer plate will impact subsequent steel plates forming secondary flyer plates, which is the third failure mode. These secondary flyer plates can result in significant damage to the entire structure. If the flyer plates, whether initial or secondary, are traveling at a high enough velocity they will continue to create additional flyer plates, out of subsequent structural members, until the combined damage causes a global failure of the structure. Examples of an initial and secondary flyer plate created in a live field test can be seen in Figure 1.4. The creation of large flyer plates in this test series contradicted some existing computer models. Those models have since been updated based on the data gathered, and are being used to predict the behavior for future tests.

Figure 1.2: Field Test 2 pre-test

Figure 1.3: Failure Mode 1 – bolt failures

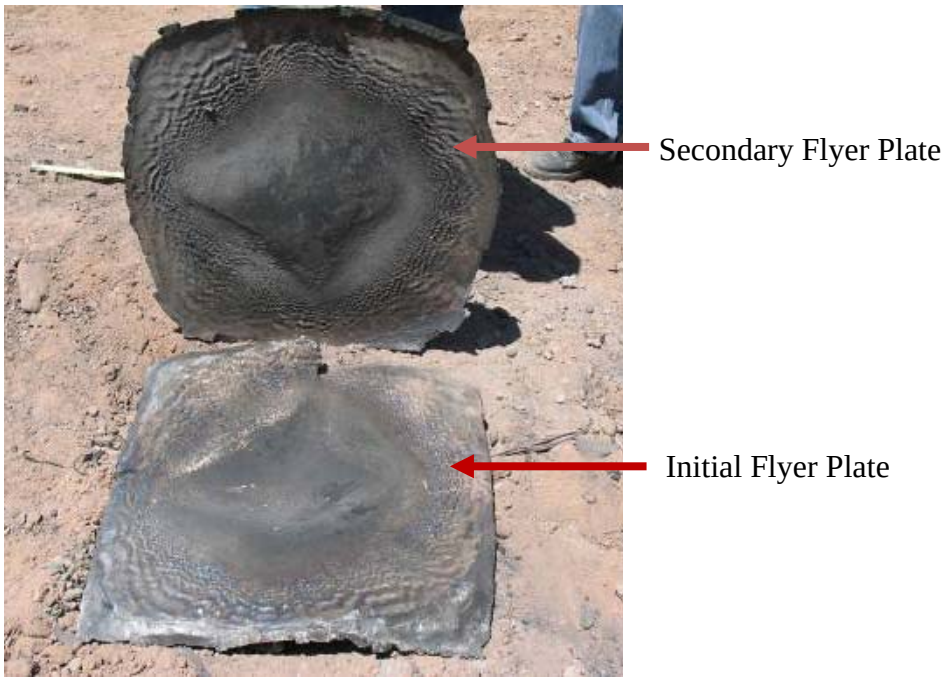

Figure 1.4: Failure modes 2 and 3 – initial and secondary flyer plates

Once it was determined, from the field tests, that a flyer plate was formed in the plates from a near-contact charge, a series of laboratory tests were performed using the Explosive Loading Laboratory at UCSD. These tests studied the failure mechanisms of the connecting bolts from an incoming flyer plate; this effect is discussed further in Chapter 3.

1.4 BLAST MITIGATION TECHNIQUES

The third research objective was to develop a blast mitigation device that can reduce the level of damage from the observed failure modes. There are two typical methods used in the development of blast retrofits. Those methods utilize mass or mechanical (plastic) deformation. Examples of added mass include the addition of concrete, steel, or a combination of both. The mechanical methods typically attempt to absorb energy through the use of foams or collapsing structures. When the initial blast mitigation technique was developed, both of these methods were evaluated; however, each method presented their own application difficulties. If additional mass was added to the structure then considerations needed to account for accessibility through the retrofitted area. Performance studies would need to be evaluated to determine the affects of this mass on the local and global behavior of this structure under loading conditions, other than an explosive load. Foams were also considered, but were limited by the amount of space within the structure. If a collapsing mechanism was used in the structure, then issues arise as to how the forces of those systems interact with and connect to the structure. In addition, both of these traditional methods are expensive; it was the desire of UCSD to develop a system that could protect against the formation of flyer plates, as well as be cost effective. It was through evaluating these more traditional solutions that it was determined that a blast mitigation technique was required that could re-direct the kinetic energy. To this end, a Kinetic Energy Defeat Device (KEDD) was

developed. This technique utilizes a non-viscous liquid to redirect the kinetic energy of a projectile. Such a liquid, when shock loaded in compression and employed in a periodic array of filled and empty adjacent cells, can re-direct energy in a direction perpendicular to the incoming projectile. This redirection of energy is accomplished by the formation of high speed jets. The goal of the KEDD system is to reduce the velocity of the flyer plates and subsequent formation of additional flyer plates, thereby reducing the amount of damage that can occur to the structure. (Additional discussion on investigated, and considered, KEDD layouts in included in Chapter 4.)

1.4.1 LABORATORY TESTS (INITIAL RETROFIT TECHNIQUES)

A series of laboratory tests were performed evaluating two different Kinetic Energy Defeat Devices (KEDD's). One involved a sand-filled KEDD system, the other was a water-filled KEDD system as shown in Figure 1.5. It was determined that a water-filled KEDD system can decrease the damage to a steel plate when compared to a test without a device, (i.e. a baseline test). The use of a sand-filled KEDD system does not behave in the same manner as the water-filled device; the sand-filled KEDD system can actually result in more damage to the structural element. Figure 1.6 shows the results of three tests, all of which used the same design parameters. The sand-filled KEDD system exhibits the most damage, as evidenced by the loss of all the connecting bolts [Figure 1.6(b)]. This can be attributed by the granular interlock that occurs in the sand. The difference between the sand-filled and water-filled KEDD system is demonstrated by the intact connection of the plate to its support when the water-filled KEDD system was utilized [Figure 1.6(c)]. This can be compared to an as-built specimen where half of the support bolts fail from the same type of impact [Figure 1.6(a)].

These photos demonstrate that the water-filled KEDD system protects the structure through re-directing the incoming kinetic energy while protecting the support connections.

a) Sand-filled KEDD system **b) Water-filled KEDD system**

Figure 1.5: Laboratory KEDD's

a) Baseline Test **b) Sand filled KEDD system** **c) Water filled KEDD system**

Figure 1.6: Comparison test series post test photos

1.4.2 SCALED FIELD TESTS (PROOF-OF-CONCEPT)

A series of scaled field tests were conducted to determine the effectiveness of the Kinetic Energy Defeat Device (KEDD) and to determine their optimum location and layout. Five different KEDD system configurations were evaluated and compared to baseline tests. The two basic layouts of the KEDD system are “on top” and “on bottom”. When the KEDD is located “on top” it is placed at the top of the cell directly behind the first plate, multiple rows of KEDD’s on top will be evaluated. The KEDD on bottom layout places the KEDD at the bottom of the cell, directly in front of the second plate. Tests that show the five different layouts of this test series are exhibited in Figure 1.7. Each of these specimens was exposed to the same charge and the same standoff distance. Figure 1.8 shows the remains of the first plates after testing and Figure 1.9 the second plates.

The failure modes and the effectiveness of the KEDD can be best observed via these photos. Figure 1.8(a) shows results from a baseline test, with significant fragmentation of the first plate from the charge. Figure 1.8(b), (d), and (f) show that the tests with 1, 2, and 3 rows of KEDD’s on top typically fail in the same manner, with significant bowing in the first plate and a large hole where the flyer plate is created. Figure 1.8(c) (KEDD’s on bottom) shows some bending of the plate, but also significant shearing along the edges of the plate. Figure 1.8(e) with KEDD’s on top and bottom shows significant damage, similar to the KEDD’s on the bottom test [(Figure 1.8(c)]. In this test a large flyer plate was formed out of the center of the plate, in addition shearing and petalling of the plate can be observed. If the effectiveness of the KEDD system was based solely on damage to the first plate, the option where the KEDD is placed on top would be the preferred location.

Figure 1.9 shows the failures of the second plates. Both the baseline test [Figure 1.9(a)] and the test with the KEDD on the bottom [Figure 1.9(c)] exhibited similar failure

modes. When the flyer plate impacted the second plate, a significant amount of petalling and deformation occurred. In the baseline test, a large flyer plate was formed. In the test with the KEDD on the bottom, a very small flyer plate was created. The second plates in the other tests all behaved in a similar manner [see Figure 1.9(b), (d), (e), and (f)]. When the flyer plate impacted the second plate it caused that plate to deform and release from its supports. It then collapsed onto the plywood base at varying velocities, dependant on the velocity of the incoming flyer plate. The deformation of the second plate was minimized when three KEDD's on top were used; however, some cracks were found in the plate for these tests. Through the use of the KEDD's on top, whether alone or in conjunction with a KEDD on bottom, the deformation, of the second plate was significantly reduced. If the effectiveness of the KEDD system was based solely on the deformation of the second plate the tests with the KEDD's on top would appear to be the preferred location; however, the test with a row of KEDD's at the top and the bottom might be considered equally as ideal a location.

Based on the comparison of damage of the second plates in conjunction with velocity data that was gathered (Chapter 5) it was determined that the optimum location, and layout, of the KEDD system was 2 rows of KEDD's located at the top of the cell (Figure 1.7(d) and Figure 1.15).

a)

b)

c)

d)

e)

f)

Figure 1.7: Test set-ups from all tests (from left to right)

a) Baseline Test b) KEDD's on top c) KEDD's on bottom

d) Two rows of KEDD's on top e) KEDD's on top and bottom f) Three rows of KEDD's on top

a)

b)

c)

d)

e)

f)

Figure 1.8: First plates from all tests (from left to right)

a) Baseline Test b) KEDD's on top c) KEDD's on bottom

d) Two rows of KEDD's on top e) KEDD's on top and bottom f) Three rows of KEDD's on top

a)

b)

c)

d)

e)

f)

Figure 1.9: Second plates from all tests (from left to right)

a) Baseline Test b) KEDD's on top c) KEDD's on bottom

d) Two rows of KEDD's on top e) KEDD's on top and bottom f) Three rows of KEDD's on top

1.5 SIMPLIFIED COMPUTATIONAL ANALYSES

The fourth research objective was to evaluate the predictive capabilities of current computational codes. To achieve that, a set of simplified momentum calculations were developed to predict the outgoing velocity of the secondary flyer plate. A series of computational analyses were also performed using the eularian hydracode CTH. The velocity of the secondary flyer plates (second plate) were predicted by CTH and the simplified momentum calculations were compared to the actual velocities determined in the scaled field tests. These simplified calculations were performed to determine a "lower bound" method to estimate velocity which is a conservative determination of the velocity of the second plate.

1.5.1 SIMPLIFIED MOMENTUM CALCULATIONS

The actual interaction between the steel plates and the KEDD's can only be determined by solving the momentum and energy equations, simultaneously. To this end, a simplified, "lower bound" estimation developed. In order to simplify this calculation, an estimation of the energy term is assumed through the use of a Coefficient of Restitution (COR). This value was determined based on data gathered in the proof-of-concept tests. These tests showed a 40% reduction in velocity when the first plate impacts the second plate, which led to a COR (for these calculations) of 60%. This simplified, "lower bound" calculation was set-up in a two step process. The first step is to determine the velocity of the mass of the steel plate and the KEDD after impact, as shown in Figure 1.10.

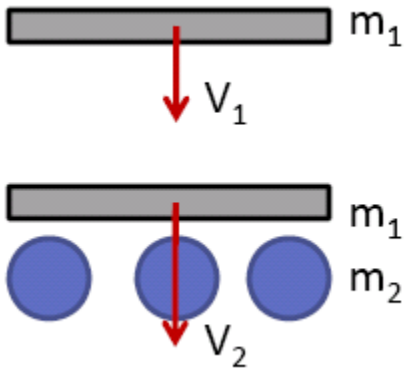

Figure 1.10: Momentum calculation – First step

Momentum is calculated by the mass of the system multiplied by the velocity, and it must always be conserved. The momentum of the flyer plate before it impacts the KEDD system must be equal to the momentum after impact with the retrofit device. Let the mass of the flyer plate be m_1 and its initial velocity is V_1. The mass of the KEDD system is m_2 and the outgoing velocity of the impacting mass and the KEDD system is V_2. (For calculation purposes, the reader is reminded that the steel plate had a length of 9" and was 1/4" thick. The KEDD's were 2" in diameter and filled with water). The momentum balance is:

$$m_1 V_1 = (m_1 + m_2)V_2 \quad \text{or} \quad V_2 = \frac{m_1}{m_1 + m_2} V_1 \qquad (4.1)$$

The next step in the calculation would be to assume that all of the water is dispersed before the first plate impacts the second plate, which is shown pictorially in Figure 1.11. It assumes that a COR of 60% is used, as explained above and shown below, which accounts for the energy that is absorbed through the plate-on-plate impact. The equation for the outgoing velocity of the second plate, V_3, is

$$V_3 = (1\text{-}0.4)V_2 \qquad (4.2)$$

If these momentum calculations were performed on the test set-up that used 2 rows of KEDD's on top, they would predict a velocity of 560 ft/sec for the second plate. The velocity determined in the field test, of the second plate, was 215 ft/sec. This results in a 62% difference with velocity of the second plate seen in the field tests, which is a conservative prediction of the outgoing velocity.

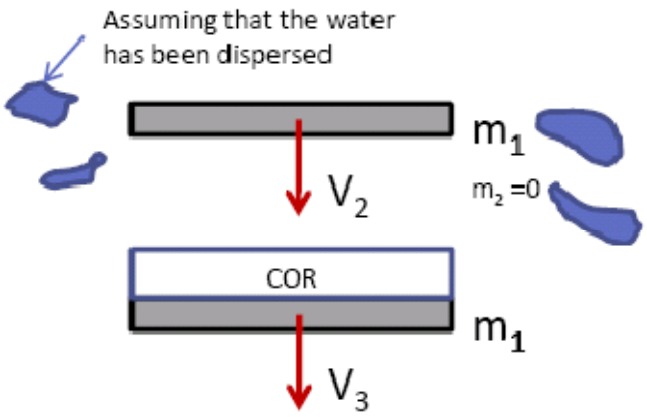

Figure 1.11: Momentum calculation – Second step

1.5.2 COMPUTATIONAL ANALYSES

Computational analyses were performed, by the Author, to estimate the outgoing velocity of the secondary flyer plate using the eularian based hydracode CTH. Analyses were performed on a section of the scaled field tests using the same plate thickness, KEDD arrangement and spacing.

Each analysis was set-up in the same manner. They evaluated a 9" section of the first and second steel plate (in the X direction). The height of the test set-up was 12" (in the Y direction), which was the same distance in the field test. The thickness of the first and second steel plates was 1/4". The diameter of the KEDD was 2" and they were spaced at 3", on center. (Figure 1.12) The calculations were two dimensional rectangular using the traditional

eularian “flat mesh” with a size of 16 inches in the X direction and 18 inches in the Y direction, which yields a mesh size in both the X and Y direction of 0.0315 inches. Outflow boundary conditions were used on all sides of the mesh. The water was modeled using the Sandia National Laboratories Equation of State (EOS) for state. The EOS accounts for the thermodynamic behavior of the water. The steel material was modeled using the widely used Mie-Grüneisen equation of state. The deviatoric response of the material was modeled with a von-Mises perfectly-plastic model. Initial calculations showed that the second plate was sheared in different locations by the formation of high speed ejecta; however, the field tests showed deformation, but not fracture of the plates. In order to achieve results that reflected those seen in the field experiments, the strength of the steel was artificially increased.

A depiction of the computational set-up is shown in Figure 1.12. A steel plate is at the top of the computational frame, with an initial velocity of 1,400 ft/sec. A second plate is at rest 12” below the first plate. An array of five KEDD’s is shown below the plate, representing the two rows of KEDD’s on top test.

A series of six computational frames from the two rows of KEDD’s on top calculation is shown in Figure 1.13. The first column plots the velocity magnitude of each cell and the second column shows a graphical representation of the different materials throughout the simulation. In Figure 1.13(b) the first plate is red in color, the second plate is blue, and the water is shown as grey. The material plots were taken at the same time step as the velocity magnitude and are used to show the relative location of the different materials at a given time step in the calculation. These calculations simulate the formation of high speed ejecta that redirects the energy in the system as depicted in Figure 1.13.

The tips of the jets moving outward from the KEDD’s, in the X direction, have a velocity of approximately 3,280 ft/sec (1 km/sec) which is over twice the velocity of the

incoming plate. Vertical jets are also formed. The first row, in Figure 1.13, shows both types of jets and that the vertical jets have formed and are interacting with, and activating, the second row of KEDD's. The next row in the figure shows that the first plate has interacted with all of the KEDD's. There are now two sets of transverse ejecta, on each side, created from the two rows of KEDD's, along with five vertical jets. The final row demonstrates the amount of water mass that was ejected before the impact of the two plates, only a small portion of the liquid remains. The formation of the thin high speed jets observed in this calculation, is most likely a result of the over simplification of these over-restrained 2-dimmensional calculations. If a 3-dimmensional calculation had been performed, these jets should behave in a more realistic manner and the strength of the steel would not have to be increased. Additionally, these calculations are not capturing the energy absorbed in the shearing and deformation exhibited in the field tests; however, they provide a simplified estimation of the system behavior.

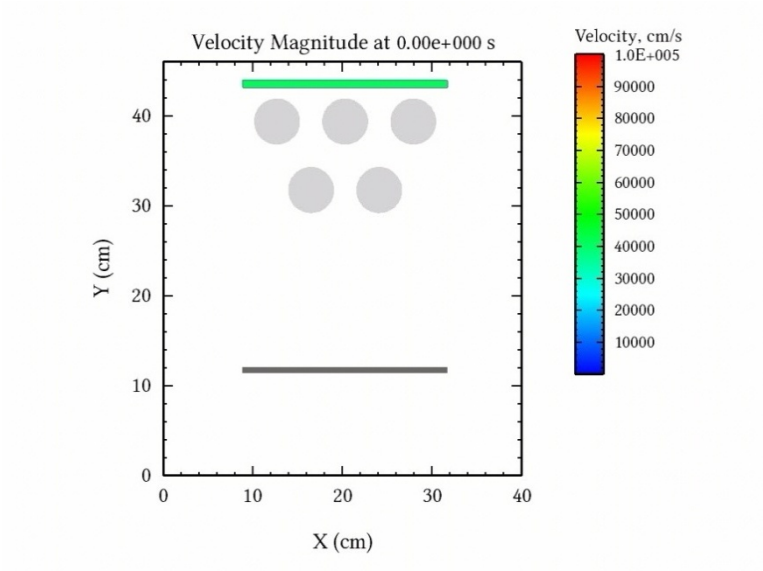

Figure 1.12: 2 Plate Test, two row of KEDD's on top, test set-up

1.5.3 VELOCITY COMPARISONS

The approximate outgoing velocity of the second pate, as determined by CTH, was 380 ft/sec, and the velocity of the second plate in the field tests was 215 ft/sec which is a difference of 43% (between the two). The simplified momentum calculations, predict a velocity of 560 ft/sec for the second plate. When the velocity from the field test is compared to the momentum calculation there is a 62% difference between the results.

An analysis, similar to the one previously discussed along with the simplified momentum calculation, was performed for all the test configurations. These were compared to the data gathered from the live field tests and is shown in **Table** 1.1 and Figure 1.14. This chart shows that with the exception of the KEDD on top and bottom test, the CTH and momentum calculations predict a higher velocity of the second plate. This would lead to a conservative estimation of velocity reduction through the use of the KEDD system.

Table 1.1: Comparing velocity with CTH, field tests, and momentum calculations

Description	Velocity of Second Plate		
	CTH	Field Test	Momentum Calculations
Baseline	1,034 ft/s	1,060 ft/s	1,058 ft/s
KEDD on Bottom	658 ft/s	609 ft/s	690 ft/s
KEDD on Top and Bottom	445 ft/s	586 ft/s	512 ft/s
KEDD on Top	670 ft/s	453 ft/s	690 ft/s
Two KEDD's on Top	380 ft/s	215 ft/s	560 ft/s
Three KEDD's on Top	240 ft/s	152 ft/s	437 ft/s
Wall of Water	355 ft/s	N/A	418 ft/s

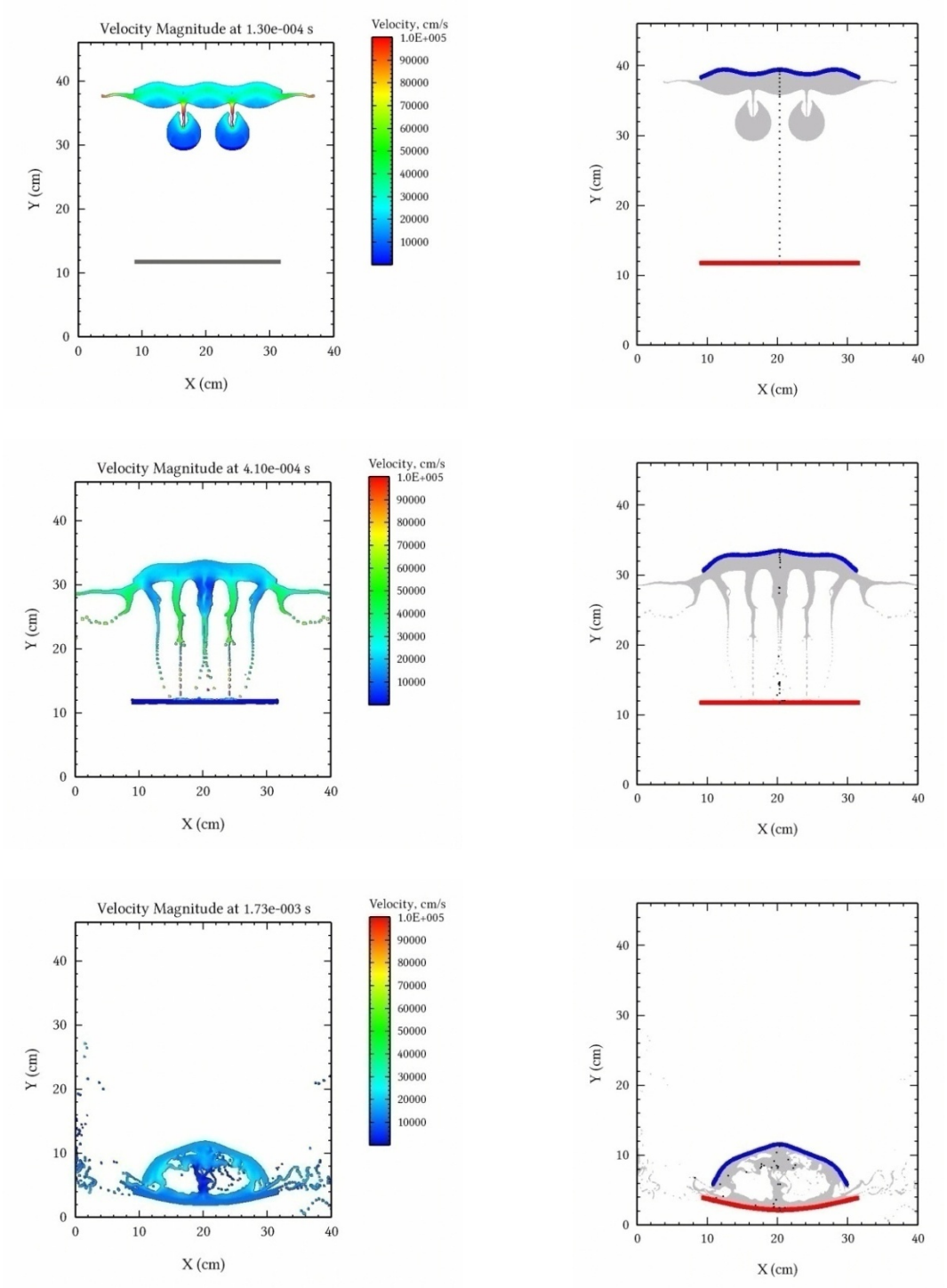

a) Velocity magnitude **b) Materials**

Figure 1.13: 2 Plate Test, two rows of KEDD's on top

Based on the tests conducted in this series, the optimum design for the KEDD system is 2 rows of KEDD's placed directly behind the steel plate (2 rows of KEDD's on top). This should significantly decrease the velocity of the flyer plate and help contain the damage to a localized region. This was the recommended layout for the final full-scale field test.

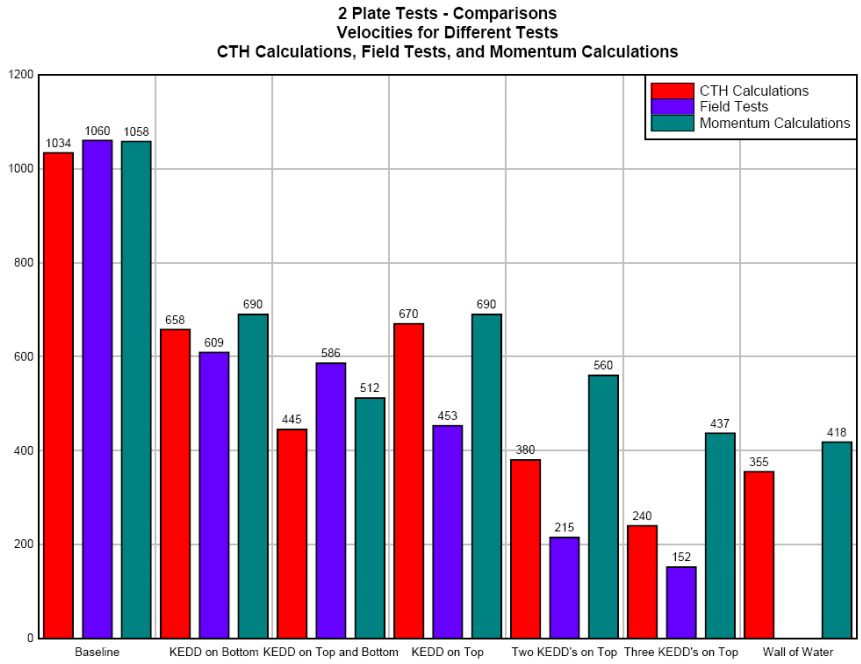

Figure 1.14: Comparing velocity with CTH, field tests, and momentum calculations

1.6 FULL SCALE FIELD TESTS (EMRTC)

The final research objective was to validate the retrofit concept with a multi-celled full-scale field test. This test specimen consisted of nine cells in a square pattern (3 x 3). The construction was similar to the previous large-scale field tests except for the top plate. The top plate of the specimen was separated into two sections that each spanned across all three cells. The purpose of this test was to evaluate the effectiveness of a blast mitigation technique when compared to portions of the as-built structure. The blast mitigation technique involved two

rows of KEDD's placed in each of the center cells. The test set-up, including the KEDD's is shown in Figure 1.15.

High speed video was captured with one Phantom camera (Vision Research). It was located south of the test bed and was placed to record a close-up of the specimen. The camera was located a short distance from the test specimen and was placed behind a steel barricade. It was set-up perpendicular to the test specimen and used an angled mirror to capture the images. Because a mirror was used, the frames in the video are reversed from the actual configuration.

The high speed video captured images from the bottom two cells during the first one second of the explosion. It shows that there are two well formed flyer plates that move through the structure. Figure 1.16 shows a frame, from the high speed video that captures flyer plates moving through the third cell at 9.638 ms after initial detonation. Figure 1.17 shows the same flyer plates at 13.838 ms near the bottom of the cell. If the distance that the flyer plates travel is assumed to be 22" (which is conservative), then the estimated velocity of those plates is over 440 ft/sec. This demonstrates the capability of these structures to create large, fast moving, flyer plates regardless of the layout of the near-contact charge.

The high speed video also captured some of the water expulsion of the KEDD system in the second cell as shown in Figure 1.18 which occurred at 14.338 ms, approximately 0.5 ms after the flyer plates in the outer cells had impacted the bottom plate. The outer flyer plates have traveled over 6' more than the flyer plate in the center cell over the same time scale. If it is assumed that the flyer plate in the center cell has traveled 4' when the first row of KEDD's was activated in the center cell, then the velocity of that plate at 14.338 ms is approximately 280 ft/s. This results in a difference in velocity, from the flyer plates to the activation of the first row of KEDD's in the second cell, of approximately 36%. The water ejecta is

highlighted by the blue circle in Figure 1.18. The water appears to be the entire width of the cell and is moving down its length.

Figure 1.15: EMRTC field Test 3 structure elevation

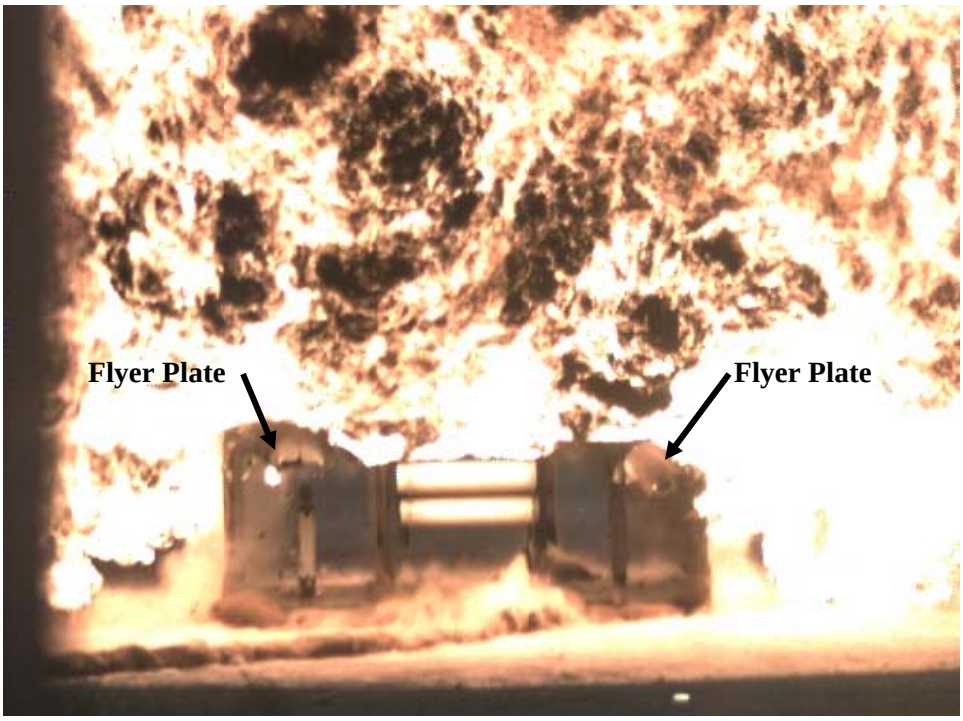

Figure 1.16: Test specimen during the test with initial flyer plates (time = 9.638 ms)

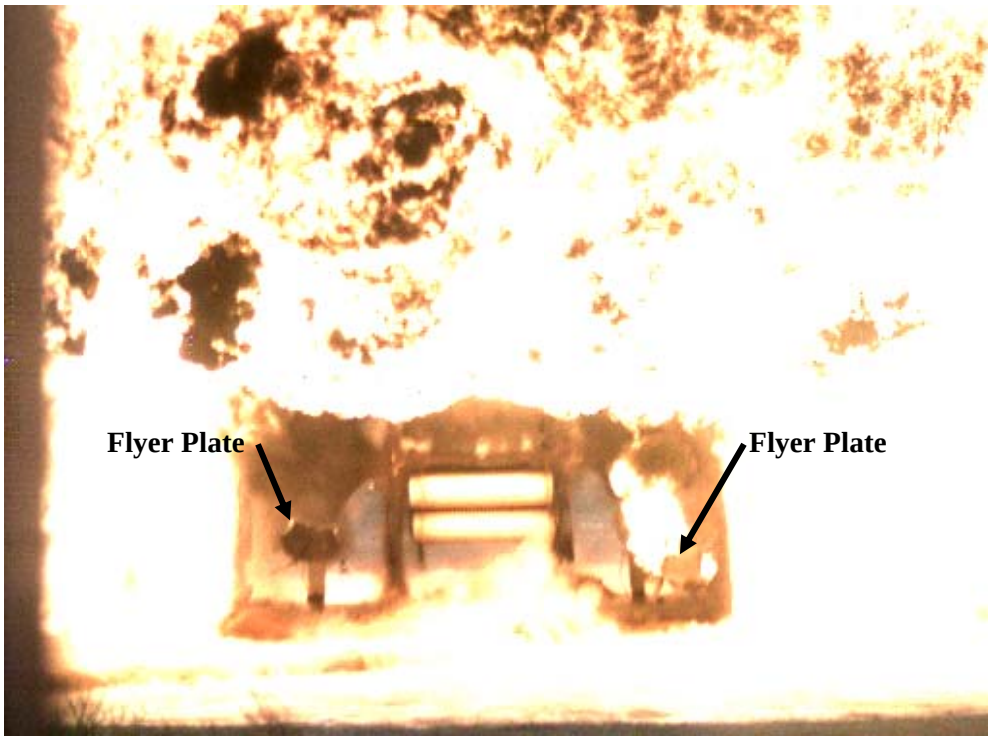

Figure 1.17: Test specimen during the test with initial flyer plates (time = 13.838 ms)

Figure 1.18: High speed video capturing water expulsion by the KEDD system (time = 14.338 ms)

Severe damage occurred to the outer cells of the test specimen. The center cell suffered less damage due to the blast mitigation technique that was used. Figure 1.19, shows the entire test specimen after the explosive event. The sections of the specimen, to the right and left of the center cell in the photo, are what remain of the as-built outer cells. These sections collapsed to the sides when the A307 bolts that connected them to the center section, failed. The center column of cells, seen in the center in Figure 1.19 shows significantly less damage to the retrofitted cells. The bottom cell of the center column is fully intact and with the exception of the top plate, the damage that occurred to the rest of the retrofitted cells was minor.

Figure 1.19: Test specimen post-test

There are still additional design considerations that will need to be evaluated before the KEDD device can be implemented into specific structures, but this test, along with the previous tests have demonstrated that this is a viable solution. A further design improvement could be to increase the strength of the bolts and angles to allow for additional plastic deformation of the plate. These methods used in conjunction with the KEDD system, should significantly improve the performance of a cellular steel structure when subjected to a near-contact charge.

2. DISSERTATION OUTLINE

This dissertation is divided into 7 different chapters. The first is an executive summary that provides initial background information about the research that was conducted. It includes a discussion of the research objectives and how they were developed in conjunction with industry representatives. It highlights the information presented in Chapters 3-7.

Chapter 3 discusses the different blast damage failure modes that were seen in the various test series. It begins with a discussion of the nomenclature of failures that will be used throughout the dissertation; then the behavior of the structural system seen in two field tests is shown, including the damage that occurred. Component tests conducted in the UCSD Explosive Loading Laboratory are explained and results from representative tests are shown. The chapter concludes with data on the strain rate behavior of the laboratory test set-up and how the results can be applied to future material models.

Chapter 4 discussed the blast mitigation technique that was developed. It covers the initial concept of the Kinetic Energy Defeat Device (KEDD) and the development of the set-ups used in the laboratory, full scale and scaled field tests. Laboratory tests show the initial effectiveness of this system.

Chapter 5 shows the results from the scaled, or Proof-of-concept, field tests. It shows the validity of the concept and determines the ideal location and arrangement of the system to be used in the full scale field tests. Simplified momentum calculations and computational analyses were performed (by the Author) in conjunction with these tests. These methods establish a lower bound value that could be used in initial developments of KEDD systems.

Chapter 6 describes the full scale field test that was performed at the Energetic Materials Research and Testing Center at New Mexico Tech (EMRTC). The effectiveness of

the system, compared to an as-built section, is presented with the test results. It includes images from a high speed video camera that shows the creation of flyer plates and relates the time of their formation to the activation of the KEDD system. It was determined, based on the scaled and full scale filed tests, that the most effective arrangement and location of the retrofit system is two rows of KEDD's placed directly behind the top plate.

Conclusions and Recommendations are located in Chapter 7.

In addition to the seven chapters of the dissertation, as discussed above, there are eight appendices associated with this research. Appendix A is a companion to Chapter 3 and it provides additional information associated with those discussions. It also includes a discussion on the Blast Generators (BG's) and additional data that was gathered during those tests but not presented in the dissertation. Appendix B is a companion to Chapter 4 and it includes drawings of the KEDD systems and their supports.

Appendix C is a companion to Chapter 5. It discusses the four types of tests that were performed in conjunction with the scaled field tests. Three of those tests are presented in their complete form. Those tests are: Calibration Tests, 3 Plate Tests, and a 4 Plate Test. It also contains comparison pictures of the 2 Plate Tests.

Appendix D is a companion to Chapter 6 and it provides additional photos from the field test and data on the instrumentation that was placed in the cell.

Appendix E consists of 34 Test Reports associated with the tests presented in Chapter 3. Appendix F consists of 17 Test Reports associated with some of the tests in Chapter 3 and all of the tests in Chapter 4. Appendix G consists of 21 test reports associated with Chapter 5. Appendix H consists of 3 field test reports. They include the two field tests discussed in Chapter 3 and the full scale filed test covered in Chapter 6.

3. BLAST DAMAGE FAILURE MODES

3.1 INTRODUCTION

In order to develop an effective retrofit device, one must first understand the structural behavior of the system when exposed to near-contact charges. The industry representatives, that are considered experts in built-up cellular steel structures, could not agree on a predictive model quantify the specimen behavior when exposed to a near-contact charge. In order to validate/disprove the predictive model a series of field and laboratory tests were performed to characterize the failure modes. Once the primary failure modes were determined, blast mitigation techniques were developed.

An initial description of the different failure modes seen in the field and lab is presented so that a nomenclature of terms can be defined. Two field tests showed that a small sized near-contact explosive charge created significant damage to a structure. What begins as a local effect, a charge placed near one portion of the structure, can create a steel fragment called a flyer plate. That flyer plate if unimpeded, can move throughout the entire structure creating additional, or secondary, flyer plates. This can lead to a global failure of the system. Laboratory tests will show that the support bolts that connect a structural component to the specimen can fail very quickly and affect the behavior of the entire system. If stronger bolts are used in place of the existing rivets, then the strength of the structural system is increased. The laboratory tests also provided data that relates the strain rate behavior of the steel plate to the structural connections and overall system behavior. That data can be used to develop better material models based on the overall behavior of the specimen components i.e. plate thickness and bolt type.

3.2 FAILURE MODES

3.2.1 BOLTS AND CONNECTIONS

A structure subjected to a near-contact charge can behave differently than when subjected to a charge at a greater stand-off distance. This research focused on the structural response when exposed to a near-contact charge. One of the first failure modes that have been observed, both under controlled laboratory experiments (Section 3.4) and live field tests (Section 3.3 and Chapter 6), is the failure of the bolts and connecting angles that support the structure. A wide variety of failure modes were observed by locating bolt pieces dispersed throughout the test bed in the test series that are presented in this chapter. Examples of failures include: direct shear (90 degree angle to the bolt axis) with high strain-rate effects [Figure 3.1(a)], combined mode of necking of the bolt shaft before shearing at a 45 degree angle [Figure 3.1(b)], and bolt heads shearing at the weld connecting the head to the shaft. The laboratory tests provided examples of bolts in the process of failure. Figure 3.2 consists of a frame from a high speed digital video that shows the failure of bolts during a laboratory test. Once the bolts fail, the supporting angles begin to carry the weight of the structure and the blast pressures. This causes the angles to rotate, allowing the front face of the plate to move free of the structure and sections of that plate separate and form steel fragments.

a) Direct Shear **b) Combined Mode**

Figure 3.1: Failure Mode 1 - Bolt failures

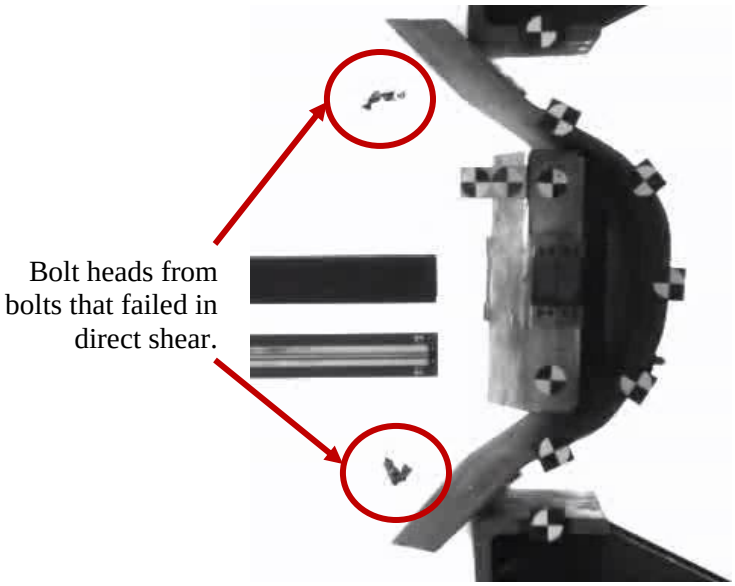

Figure 3.2: Bolt failures, in progress, from a lab test

3.2.2 FORMATION AND PROPAGATION OF FLYER PLATES

Following the failure of the bolts and support angles, the front plate and the transverse plates of the generic cellular steel structure (Figure 1.1) are left to resist the blast pressures that are being applied. A steel fragment, or flyer plate, is formed out of a portion of the first plate of the structure from a near-contact charge. If the charge extends over a larger area, then the formation of multiple flyer plates can be expected. The flyer plate (plates) moves through the structure at a higher velocity (up to 3,280 ft/s or 1km/sec) than the remaining pieces of the first plate. Examples of flyer plates were created in the field tests, simulated in the laboratory, and are well predicted by post-test computational analyses (1). Figure 3.3 shows an actual flyer plate from a field test at the Energetic Materials Research and Testing Center (EMRTC), discussed in more detail in a subsequent section. (The dent in the flyer plate is from impact with a sensor after the formation of the flyer plate occurred.) Figure 3.4 shows the creation of a flyer plate in a computational analysis performed by Science Applications International Corporation (SAIC). It captures the first failure mode (bolt failure) and the separation between the flyer plate and the remaining plates. Multiple flyer plats were created when a near-contact charge was placed over a larger distance and multiple cells (similar to placing a charge across the top of the generic cellular steel structure shown inFigure 1.1). Figure 3.4 shows images from a high speed video capturing the creation of two, symmetrical flyer plates (a retrofit device is shown in the center cell and will be discussed in detail in Chapter 6).

a) Initial flyer plate

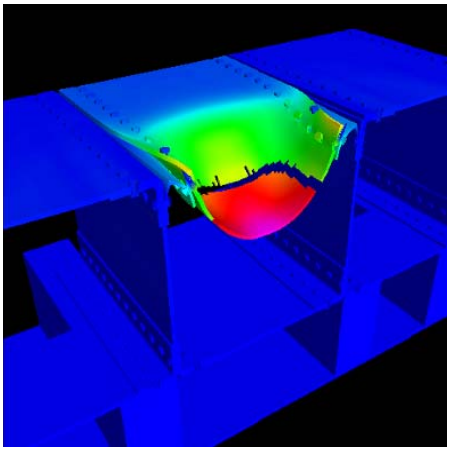

b) Post-test calculation capturing failure modes 1 and 2

Figure 3.3: Failure Mode 2

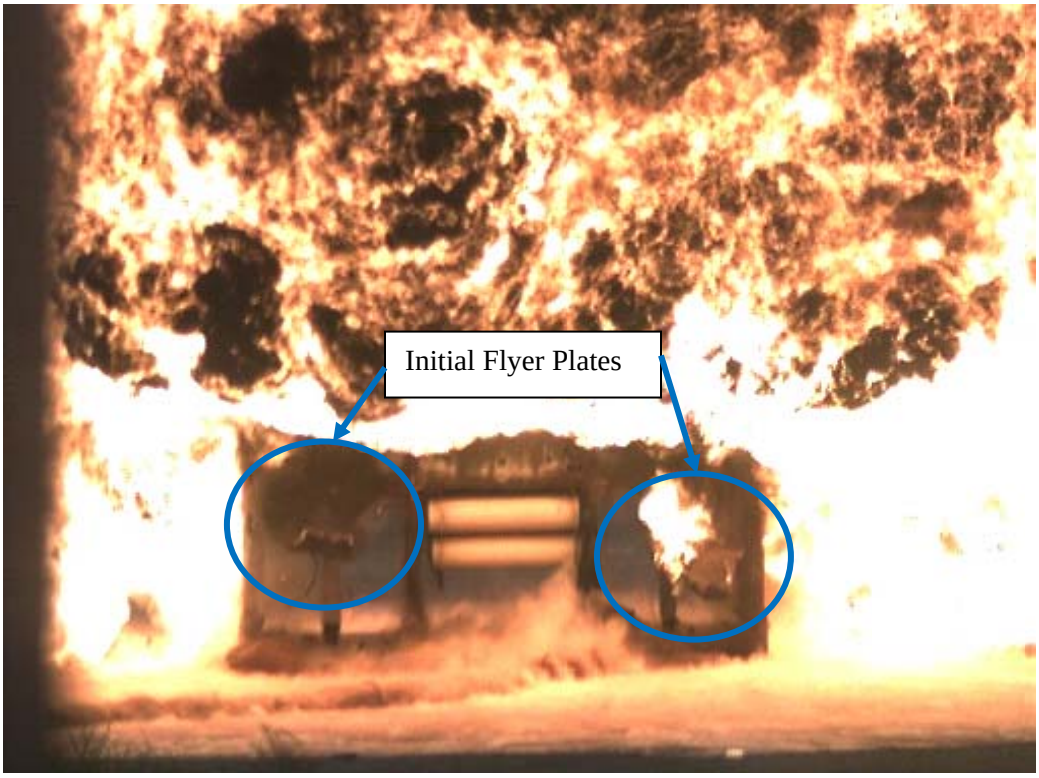

Figure 3.4: Failure Mode 2 – Initial flyer plates

3.2.3 PUNCH-THROUGH (SECONDARY) FLYER PLATES

After the initial flyer plate has been created by the explosive charge, it is free to move through the structure. When this plate reaches a subsequent steel plate, the impact of the first flyer plate creates a secondary flyer plate. These two flyer plates then move together until they encounter another steel plate and form yet another flyer plate. According to the calculations that have been performed by SAIC (2), for near-contact charges there is little inherent strength in the structure that can slow these plates sufficiently to limit the damage to an acceptable level. Examples of initial and secondary flyer plates created by a near-contact charge can be seen in Figure 3.5. Figure 3.6 shows another computational post-test analysis. It captures the three observed failure modes. The bolts of the first plate fail (Failure Mode 1) and the initial flyer plate is created (Failure Mode 2). That fragment moves at a high velocity until it impacts the second plate. A pass-through (or secondary) flyer plat is created through impact and separates from the second plate. The initial and secondary flyer plates (Failure Modes 2 and 3) then move together towards impact with the next steel plate.

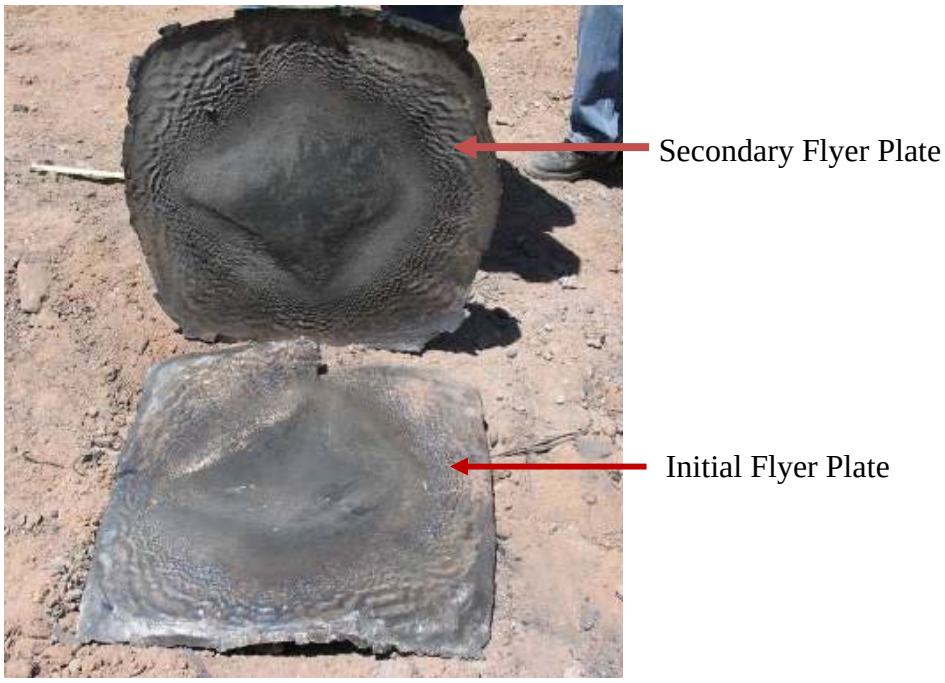

Figure 3.5: Failure Modes 2 and 3 – Initial and Secondary flyer plates

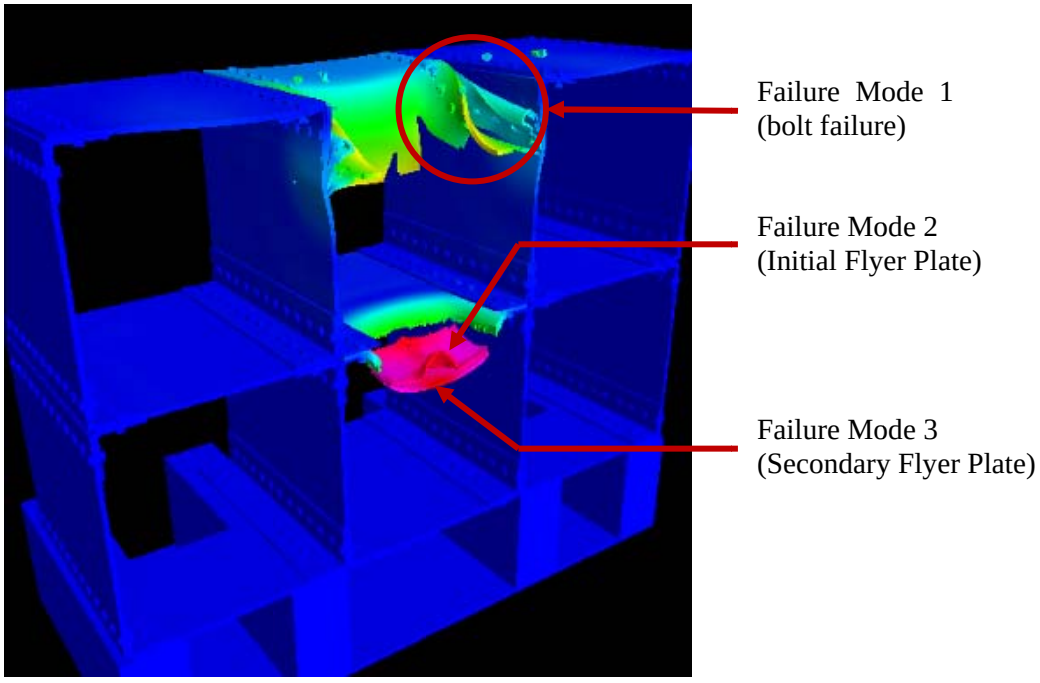

Figure 3.6: Computer simulation of Failure Modes 1, 2, and 3 by SAIC

3.2.4 DAMAGE LEVELS OBSERVED IN LABORATORY TESTS

The laboratory tests exhibited three levels of damage for which a nomenclature needs to be established. In these tests it is assumed that the initial flyer plate is impacting the second steel plate and will be discussed further in Section 3.4. The behavior of the steel plate and support connections were evaluated in the test series. The damage levels relate to the loss of the support bolts (Failure Mode 1) connecting the steel plate to the structure. The first type is "Remained Attached", as shown in Figure 3.7(a), where there was no loss of connecting bolts. The second type is "Partial Failure", as shown in Figure 3.7(b), where seven of the fourteen connecting bolts were damaged. (For this damage type it does not matter if the top or bottom row of bolts failed in order to be classified as "Remained Attached".) The third type is "Complete Failure", as shown in Figure 3.7(c), where all fourteen bolts failed. These damage levels will be discussed frequently when discussing the laboratory tests.

a) Remained Attached **b) Partial Failure** **c) Complete Failure**

Figure 3.7: Failure modes for laboratory tests

3.2.5 BRITTLE AND DUCTILE FRACTURE MODES

The failure modes discussed previously relate to how the structural components fail, whether it is from the failure of the bolts or from initial and secondary flyer plates. The manner in which the flyer plates are created is through dynamic fracture. There are two principal types of dynamic fracture modes: brittle and ductile (3). When a specimen exhibits a brittle fracture, it tends to have edges. In the field tests this will be demonstrated by flyer plates of irregular shapes (Figure 3.8). A ductile fracture exhibits significant plastic deformation and petalling before failure. This is typically seen in tests where a secondary, or pass through, flyer plate is created (Figure 3.9). When a plate exhibits substantial ductility significant amounts of energy is absorbed in the deformation of the plates. There is an additional type of deformation that will be described in later chapters. It is a combination of brittle fracture and ductile deformation. Figure 3.10 is an example of a specimen that exhibits brittle and ductile behaviour during the formation of a flyer plate. The opening shows the sharp edges as expected with a brittle fracture while the ductile behaviour is demonstrated by the plastic deformation of the plate.

Figure 3.8: Examples of brittle fragments

Figure 3.9: Example of ductile fractures

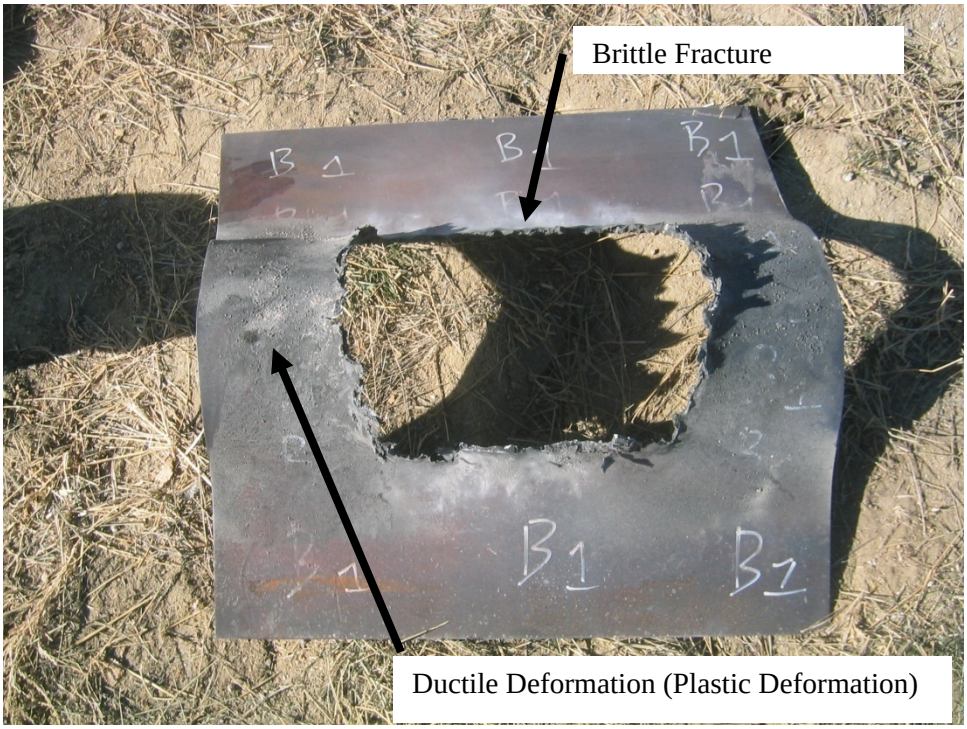

Figure 3.10: Example of combined brittle fracture and ductile deformation

3.3 EMRTC FIELD TESTS 1 AND 2

3.3.1 INTRODUCTION

These tests were developed form the generic steel structure as discussed in Chapter1 and was developed in conjunction with industry partners. Two full scale field tests were performed to determine how the cellular steel structure behaves when exposed to a near-contact charge. These tests showed that large flyer plates are created from the charge and that they travel at very high velocities. The main objective of these tests was to validate pre-test analytical calculations, and enable the development of better high-fidelity computer models. The specific information in regards to the test set-up, charge size, and behavior is discussed below

It should be noted that the actual construction drawings of the test specimens were created by Karagozian & Case (K&C) (4) (5). They also determined the charge size and standoff distance with additional input from UCSD. This first test occurred in May 2005 and was not attended by a UCSD representative. The information provided below, with regards from the first test, were provided by EMRTC after the test. The second test occurred in July 2005 and was attended by UCSD representatives.

3.3.2 TEST SET-UP

The test specimen represented a full scale portion of the generic cellular steel structure. It is constructed out of 7/8” thick A36 steel plates where each plate is 3’ – 6” wide and 8’ long. They were supported, at the interior corners, by 8” x 8” x 1/2” A36 steel angles. The plates were connected to the angles by 1” diameter A307 bolts placed at 4” on center.

The first test article was arranged to be a three sided box representing the outer portion of a typical structure as show in the construction drawing in Figure 3.11 and a photo in Figure 3.12. The test specimen was connected to a 2’ thick unreinforced concrete foundation through 1” diameter threaded rods placed at 8” on center. They were embedded into the foundation a minimum of 8” and secured with epoxy adhesive (Red Head Epcon C6).

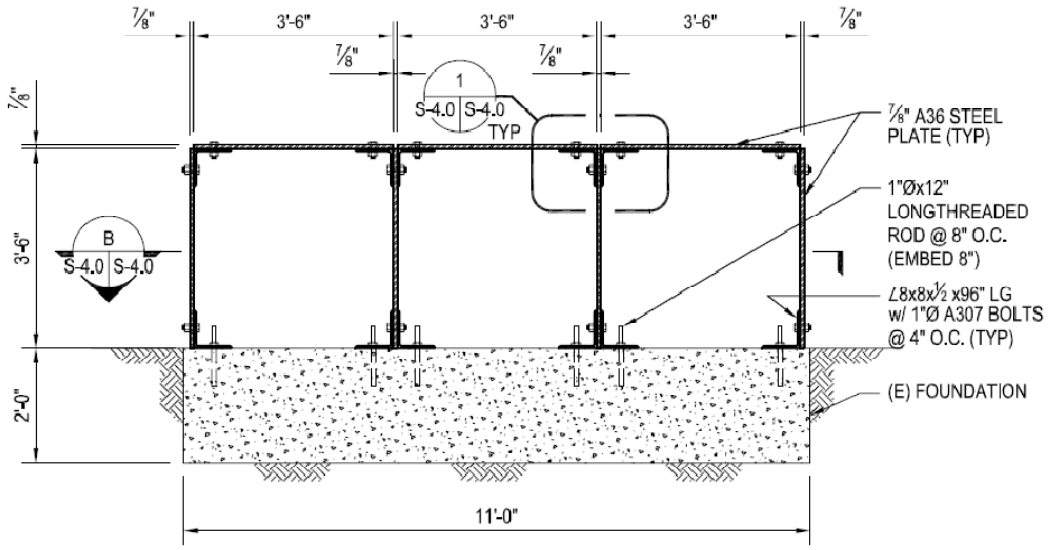

Figure 3.11: EMRTC field Test 1 set-up elevation

The second test specimen was similar in construction to the first test; however, the specimen was placed on elevated supports and an additional steel plate was added at the bottom of each cell. The additional plates were not the same in all bays. The second plate in the center cell was a 7/8” A36 steel plate that was 3’ – 6” wide and 8’ long. Based on results from the first field test, only partial plates were used in the outer bays. They were both constructed out of 7/8” A36 steel plates that were 3’ – 6’ wide and 4’ long. They were placed 2’ in from the front edge of the cell which placed the center of the second plate below the center of the first plate. The concrete pedestals, or elevated supports, were built out of

reinforced concrete; the formwork and reinforcing are shown in Figure 3.13. 1" diameter anchor rods were embedded 8" into the concrete pedestals and attached to the test specimen at 8" on center. Figure 3.14 shows a construction drawing of the specimen elevation. The completed specimen, including the explosive used for this test, is shown in Figure 3.15 and Figure 1.2.

Figure 3.12: EMRTC field Test 1

Figure 3.13: Elevated concrete supports EMRTC Test 2

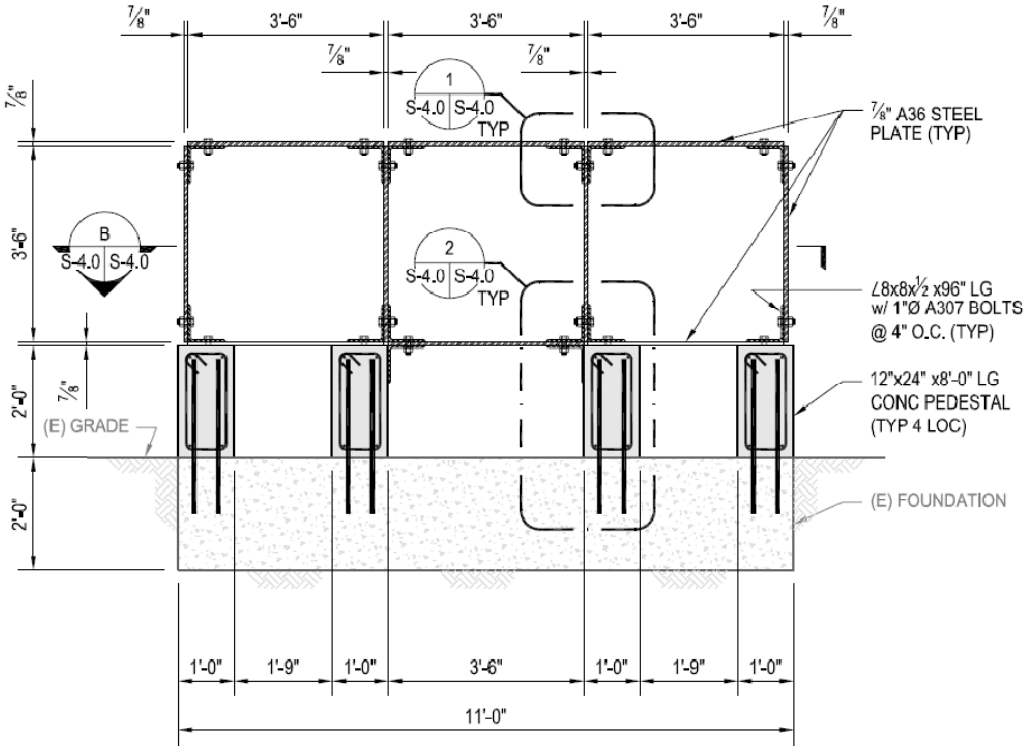

Figure 3.14: EMRTC field Test 2 set-up elevation view

Figure 3.15: EMRTC field Test 2 set-up (photo)

3.3.3 CHARGE SET-UP

Both field tests used an explosive charge that was equivalent to X pounds of TNT[1], placed at a close standoff distance. The explosive was placed inside a 3/4" plywood box with the interior dimensions of 26" x 26" x 18". It was placed uniformly in the box until it reached a height of 13" (for the first test and 12" for the second test) above that level it was placed in a conical shape. A booster charge, also built in a conical shape, was placed at the top of the mound (Figure 3.17). This shape was used to produce a planar wave and ensure proper detonation. The charge was centered 4' in from the edge center plate prior to detonation as is shown in Figure 3.16. The drawing is looking down at the top of the test specimen.

[1] For specific information see EMRTC Test Program: Test #1 or Test #2 Summary Report (through TSWG)

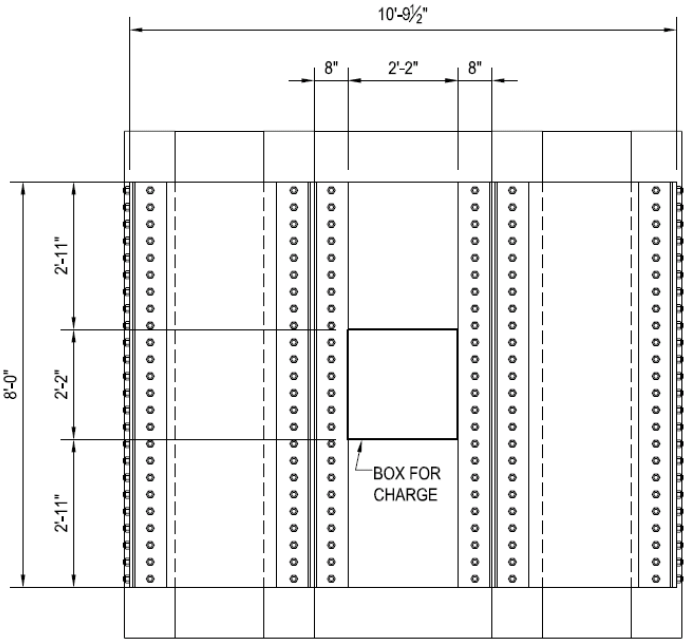

Figure 3.16: Location of Charge on test specimen

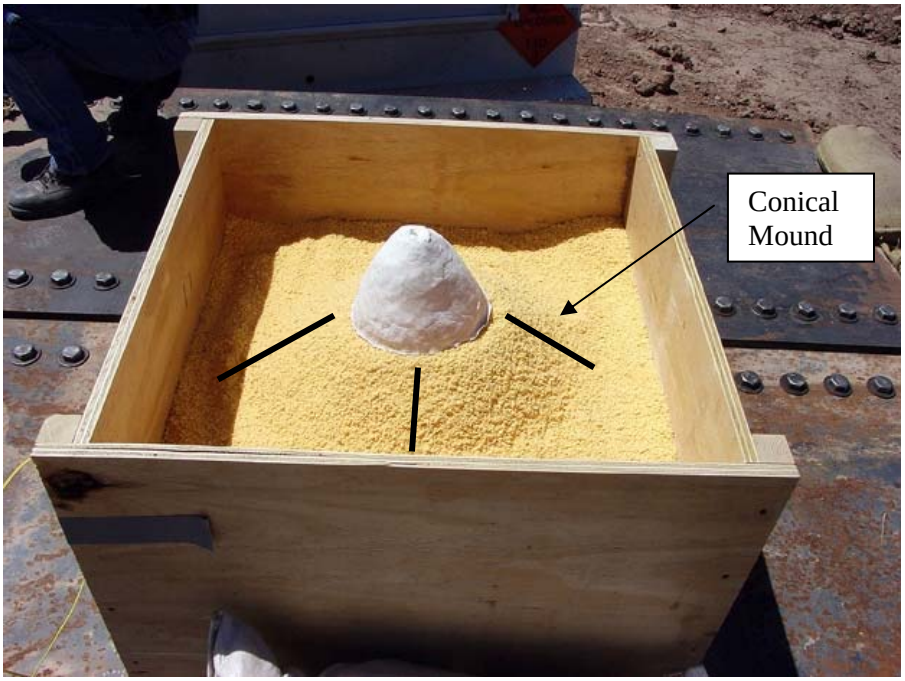

Figure 3.17: Test charge for EMRTC field tests

3.3.4 INSTRUMENTATION

3.3.4.1 FIELD TEST 1

Four PCB pressure sensors were used for this test; they were placed at the center and edge of both the central and left bays. Two PVDF-Piezo film gages were placed adjacent to the centerline PCB gages. Unfortunately, the gages placed in the center span were destroyed in the test. The remaining sensors failed to capture any useful data.

3.3.4.2 FIELD TEST 2

Time of Arrival (TOA) pins were used to determine the velocity of the initial and secondary flyer plates. The velocity is calculated by placing pins in sets at specified intervals, in this case 1/2" intervals. The time is recorded when each pin is impacted, the difference is calculated, and divided by the spacing to calculate the velocity. There were three sets of TOA arrays used in this test placed: directly behind the first plate, in front of the second plate, and behind the second plate. Each set of pins was spaced at 5" and were mounted to a frame built of expanded polystyrene. The arrays of TOA pins in the structure are shown in Figure 3.18 and Figure 3.19.

Due to a miscalculation by the instrumentation personal, the duration of the recording time for the data acquisition system was set to a time frame smaller than needed. This resulted in a lack of data from the second and third array of TOA pins. The only data recorded was from the top array, and one pin in the middle array as exhibited in Table 3.1. The first array of TOA pins appears to capture the bulge in the steel plate, before the flyer plate actually separates. This is demonstrated in the symmetry of the data around the center of the plate. From that data, the flyer plate was traveling at approximately 1,300 ft/sec before it fractured

from the plate. Based on the one useful pin on the middle array, the velocity of the flyer plate before it impacted the second plate is approximately 3,400 ft/sec.

3.3.5 PHANTOM CAMERAS

High speed video was captured with one Phantom camera (Vision Research). It was located southeast of the test bed and was placed to record the entire response of the explosive event. Figure 3.20 and Figure 3.21 shows images from Field Test 1. They are similar enough to Field Test 2 that additional photos are not necessary.

3.3.6 TEST RESULTS

3.3.6.1 FIELD TEST 1

The steel structure was permanently deformed due to the near-contact charge. The top plate was fractured into many pieces and a large flyer plate was created. The flyer plate impacted the bottom of the test bed and was located approximately 50’ east of the original test location as shown in Figure 3.22. The flyer plate had approximately the same dimensions (24” x 24”) as the plywood box that contained the explosive charge (26” x 26”) (which is also the clear space between the angled supports). The rectangular imprint exhibited in the flyer plate was from the pressure gage mount that was placed directly below the charge. Significant ductile deformation was seen in the top plate along with the brittle fracture associated with the flyer plate. A flat portion of the first plate, which was connected to the edge of the flyer plate, is shown in Figure 3.23. The clear fracture along the edge is not a related to the bolt location. The entire top plate is shown reassembled in that photo.

Table 3.1: Time of Arrival pin data

Location	Group	Pin #	Time of Arrival (μs)	Velocity (ft/s)
Top	A	T1	55.961	1344.78
		T2	24.977	
	B	T3	41.537	1296.17
		T4	9.391	
	C	T5	31.143	1337.91
		T6	0.000	
	D	T7	31.401	1346.30
		T8	0.452	
	E	T9	44.334	1276.43
		T10	11.691	
	F	T11	58.831	-
		T12	n/a	
Middle	A	M1	n/a	n/a
		M2	n/a	
	B	M3	n/a	n/a
		M4	n/a	
	C	M5	n/a	n/a
		M6	n/a	
	D	M7	n/a	n/a
		M8	n/a	
	E	M9	916.791	-
		M10	n/a	
	F	M11	n/a	n/a
		M12	n/a	
Bottom	A	B1	n/a	n/a
		B2	n/a	
	B	B3	n/a	n/a
		B4	n/a	
	C	B5	n/a	n/a
		B6	n/a	
	D	B7	n/a	n/a
		B8	n/a	
	E	B9	n/a	n/a
		B10	n/a	
	F	B11	n/a	n/a
		B12	n/a	

Figure 3.18: Time of Arrival pins for EMRTC Test 2

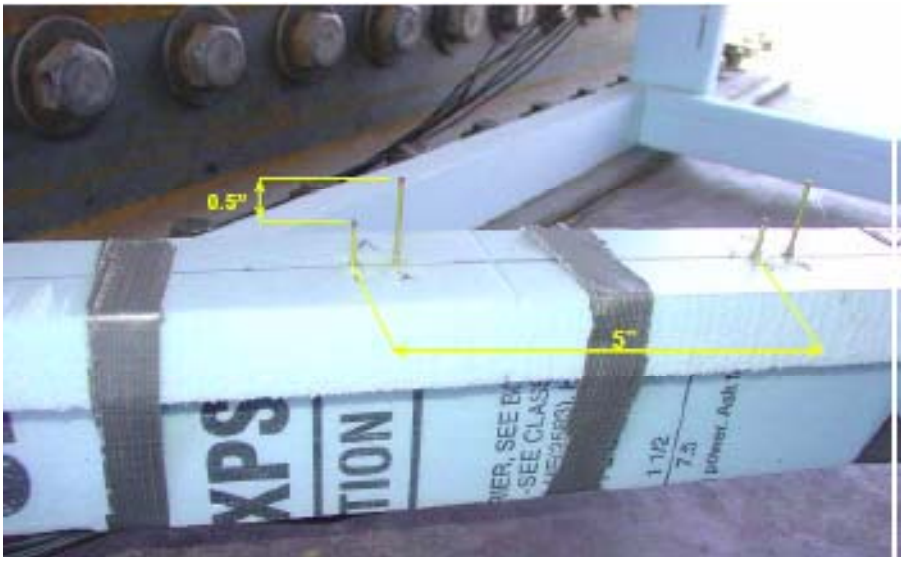

Figure 3.19: Time of Arrival pins (close up) for EMRTC Test 2

Figure 3.20: Image from Phantom camera at initial detonation

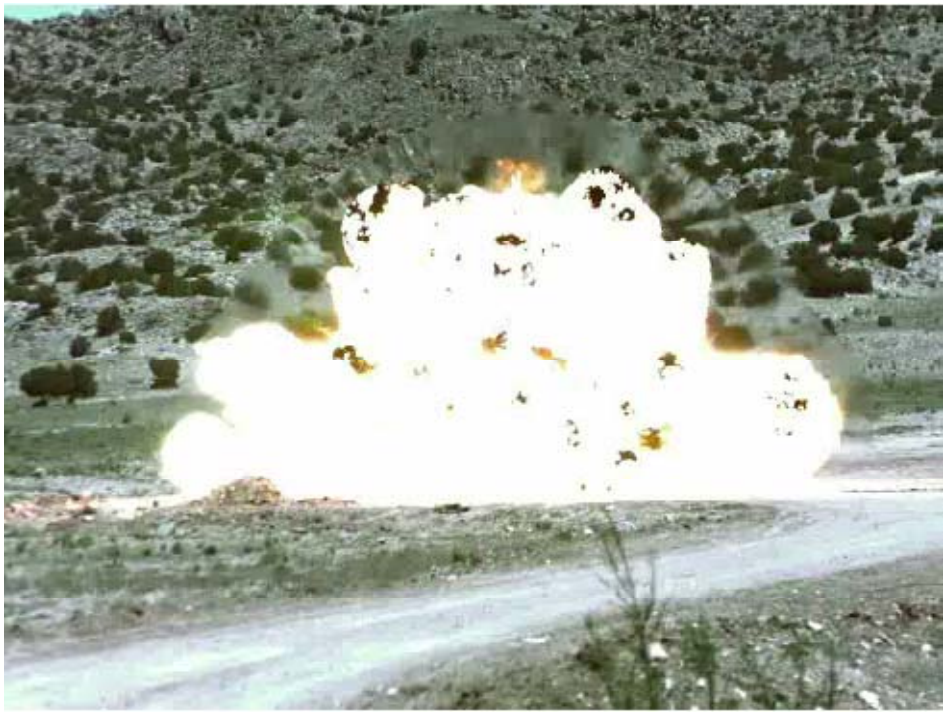

Figure 3.21: Image from Phantom camera after initial detonation, with shock front

The specimen split into three distinct elements two of which rolled away from the test bed. The adhesively anchored threaded rods failed and pulled out from their foundation. The concrete foundation was pulverized where the initial flyer plate impacted it, which gives one a sense of the force associated with that impact. The 1” diameter low strength bolts (A307) that connected the different cells together were damaged. Pieces of bolts were found dispersed throughout the test bed. Most of the bolts appeared to have failed in shear (Figure 1.3). The failure of the bolts and anchor rods allowed the segments of the structure to move from their initial position. In addition to the loss of the support bolts in those areas, there was significant torsional deformation of the support angle in the center bay (Figure 3.24).

The creation of the flyer plate coincided with the expectations of this test. It was important to determine that a flyer plate, of significant size was created. This test showed that it was approximately the same size as the box that the charge was placed in. This structural response did not correlate to some predictive models, yet matched others. This phenomenology has been added to existing high fidelity computational models to improve their predictive capabilities. While the test was successful in determining the behavior of the structure under this type of loading, the design of the test specimen needed to be improved for the second test. Those changes were discussed above.

Figure 3.22: Flyer plate created from EMRTC Test 1

Figure 3.23: Top plate (pieced together) from EMRTC Test 1

Figure 3.24: Failures from EMRTC Test 1 – post-test

3.3.6.2 FIELD TEST 2

This specimen behaved in a similar manner as the previous test. The steel structure was permanently deformed and the first plate fractured into several pieces creating a large flyer plate. The flyer plate impacted the second plate and created a secondary, or pass through, flyer plate. Figure 3.25 shows the remains of the test specimen. The steel plate seen in the front of the photo, in front of the center bay, is the initial flyer plate. It traveled 3' – 6" through the cell, fractured the second plate, and impacted the foundation. The force of that impact caused the plate to rebound from the foundation and land as shown in the photo. Figure 3.26 shows the remains of the second plate. The secondary flyer plate can be seen in the middle of the picture. The steel plate exhibits shearing along the edges where the flyer plate was created (brittle fracture). There are also signs of ductile fracture as shown by the rounded edges where the flyer plate was created.

The initial flyer plate that was formed had dimensions of 24” x 24 1/4”. The secondary flyer plate was slightly larger at 25 1/4” x 25 1/2”. As in the previous test, the shape of the flyer plate is related to the shape of the charge, or the shape of the incoming flyer plate. Figure 3.26 shows that the bolt holes, of the second plate where the secondary flyer plate is created, are intact and that they did not affect the shape of the flyer plate. They were created in the middle of the center span directly below where the charge was placed (as shown in Figure 3.15). Figure 3.27 shows the similarity between the two flyer plates. The bulge seen in the initial flyer plate can also be seen in the secondary flyer plate. The pass through flyer plate is more irregular around the edges than the initial flyer plate. This is attricubted to the different ways in which the plates were formed. The initial flyer plate has square edges due to the force of the planar wave that created the flyer plate. The secondary flyer plate has rounded edges that were formed from the impact of the initial flyer plate. It reflects the deformation and failure mechanisms of the second plate.

Once the secondary flyer plate was removed from the structure, the condition of the concrete foundation was investigated. The flat concrete foundation was pulverized underneath the secondary flyer plate indicating that the velocity of that plate was significant. The first plate suffered additional damage beyond the creation of the flyer plate; it behaved in a very ductile manner exhibited by the permanent plastic deformation shown in Figure 3.28. That photo also depicts the final location of a section of the first plate. In Figure 3.25 the initial flyer plate landed on one side of the specimen while the remaining portion of the first plate (shown in Figure 3.28) was on the opposite side. While most portions of the top plate landed near the test specimen, two separate pieces were located much further away. One small fragment was located approximately 16’ northeast of ground zero, while the other was found approximately 400’ away. The remaining fragments from the top plate were reassembled and

shown in Figure 3.29. This photo demonstrates both types of dynamic fractures. Ductile failure is shown in the petalling of the plate, while brittle fractures are exhibited in the sharp edges seen in the portions of the top plate that were ejected from the test article.

Additional damage occurred to the test specimen beyond what has already been discussed. The support structure that holds the specimen together, the bolts and angles, was also damaged. The support angles along the top and bottom failed in torsion; allowing the horizontal portion of the angle to bend, thereby, allowing the plate to fall through (Figure 3.26). The bolts that supported the angle were found around the test bed in various forms of failures (Figure 1.3).

While the damage to the center bay, where the charge was located, was significant, very little damage occurred to the rest of the structure (Figure 3.30). While the vertical support bolts are missing on one side, they are all intact on the other. In addition, the horizontal bolts connecting the two angles appear to be undamaged. This correlates well with the damage seen in the previous field test. In that test the outer portions of the cells were unscathed, except for the damage due to the inadequacy of the connection to the foundation. These tests show that when the charge is localized over one cell the adjacent cells see very little damage. Not only are the horizontal plates intact, their vertical supports see very little damage as well. This could be attributed to the fact that those plates are not affected by the planar wave created by the charge. The final test will place a continuous explosive charge across all cells to determine the effects on the vertical plates as well as the horizontal plates (Chapter 6).

Figure 3.25: EMRTC Test 2 – post-test

Figure 3.26: EMRTC Test 2 – secondary (pass through) flyer plate

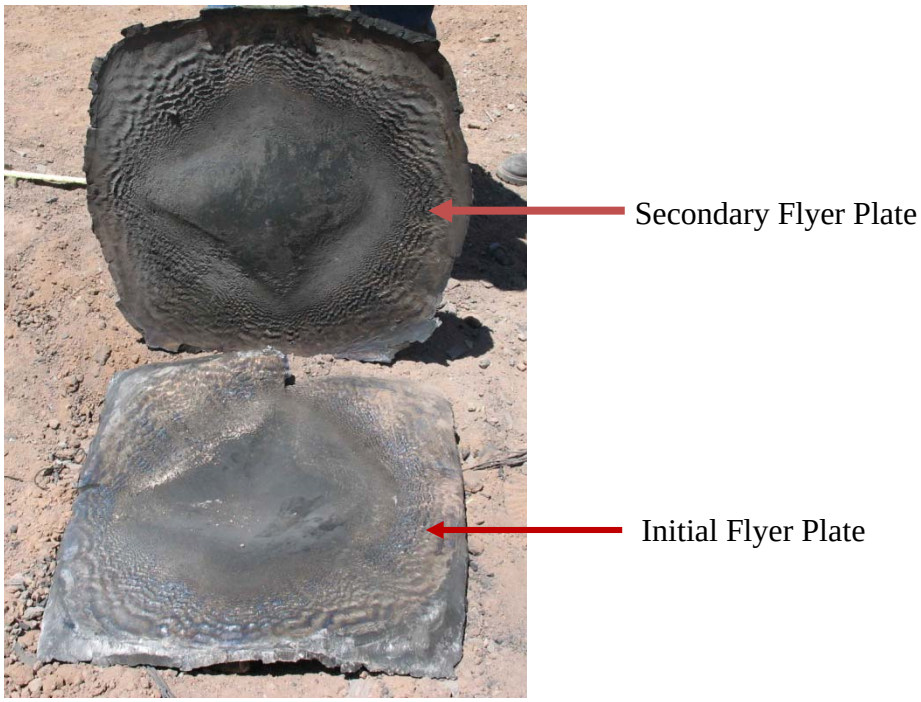

Figure 3.27: EMRTC Test 2 flyer plates

Figure 3.28: Portion of top plate from EMRTC Test 2

Figure 3.29: EMRTC Test 2 reassembled top plate

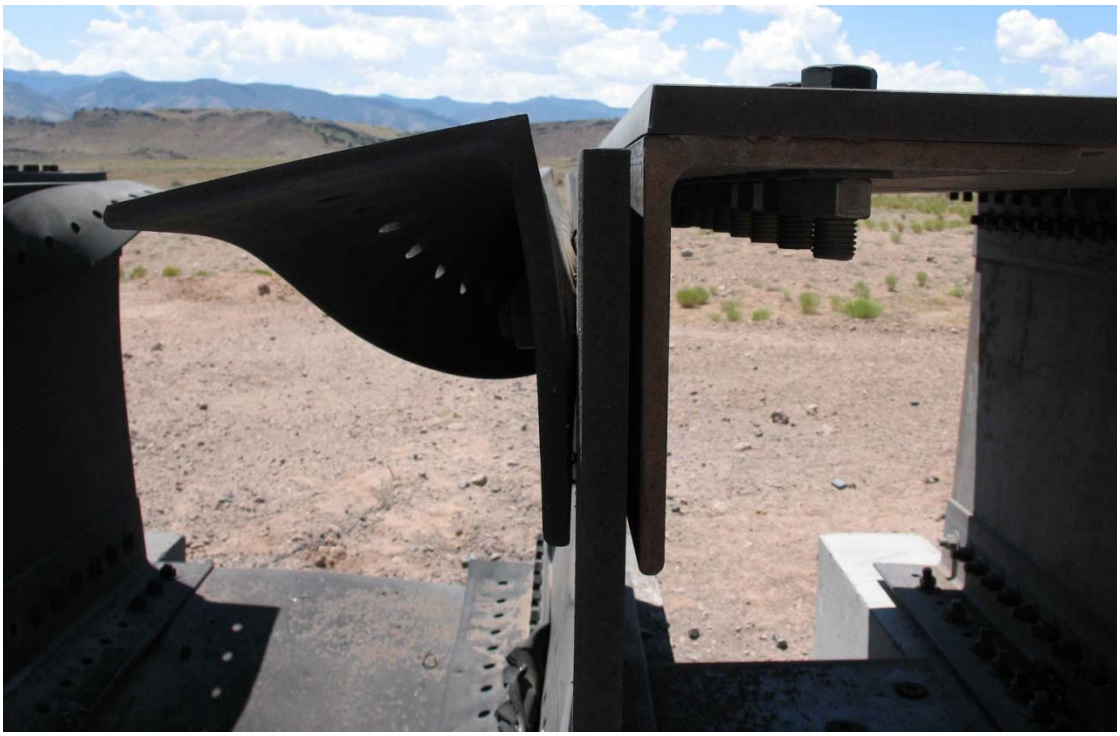

Figure 3.30: Demonstration of localized failures from EMRTC Test 2

3.3.7 FIELD TEST SUMMARY

These tests showed that when these structures are subjected to a near-contact charge a large fragment, or flyer plate, is formed that travels through the specimen at a high velocity. A blast mitigation system was developed based on the failure modes exhibited in these tests (bolt failures, initial and secondary flyer plates) and will be discussed in Chapter 4.

3.4 LAB TESTS

3.4.1 INTRODUCTION

Thirty-seven laboratory tests were performed using the UCSD blast simulator to evaluate the behavior of the second plate inside of the generic cellular steel structure, as exhibited in Figure 3.31. It assumes that a flyer plate is created from the first plate, and it moves through the structure and impacts the second plate. Eleven different impact velocities were chosen to study the specimen behavior. The specific aspects that were studied involved determining the behavior of the specimen when the steel plate fails, finding the threshold velocities at which the specimen partially fails, and evaluating the behavior of the specimen when there is not enough energy to damage the connections. Four different plate thicknesses were used to evaluate these behaviors. While the generic steel structure uses 7/8" A36 steel plates, not all structures use that size steel plate. In order to properly understand the behavior of the different specimens, for a wide variety of structures, multiple plate thicknesses were used. The thicknesses of the steel plates that were used are: 1/4", 1/2", 3/4" and 7/8". Each of these specimens behaved differently than the other as shown by the maximum strain rates in the specimen that will be discussed in subsequent sections.

The plate thickness and impact velocity were not the only variable that changed; bolt type and loading methods were also altered in this test series. As stated before, some of the real structures are constructed using riveted connections; however, low strength, A307, bolts are used to represent the strength of the rivets. The specimen behavior was also evaluated using high strength bolts. Grade 5 bolts, which are similar to A325 bolts, are high strength bolts that have been used when rivets are replaced in traditional retrofits. It is important to evaluate the behavior of the steel plate with the different connections in order to determine

what, if any, effect they have on the specimen. The manner in which the impacting mass (flyer plate) impacted the specimen (second plate) was altered during this test series as well. The differences in the loading methodology will be presented below. The specimen behaved in a similar manner despite the different loading methodologies.

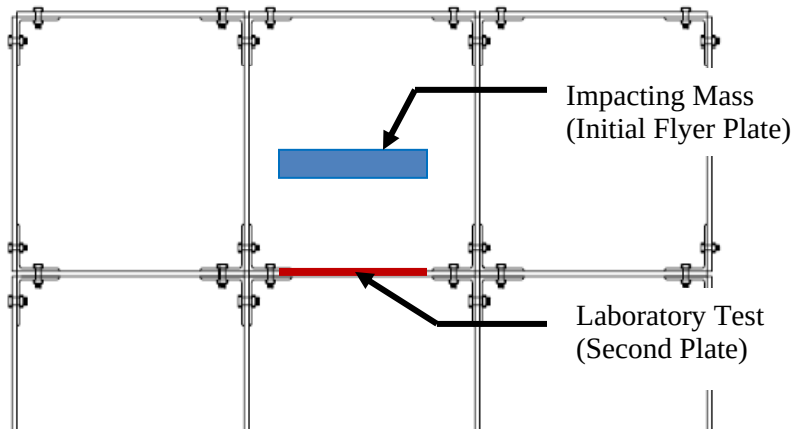

Figure 3.31: Schematic drawing of laboratory test set-up using generic cellular steel structure

There were a wide variety of permutations of the test specimen that occurred during this test series. They were performed to determine the different effects on the specimen. In order to ensure that these effects were consistent, most of these tests were conducted at least two times with similar parameters. The goal was to have three separate tests with the same velocity, plate thickness, and bolt type. While this did not occur for all tests, the majority of the tests that were performed conform to that goal. Each of the tests that were performed is presented in Appendix A. The tables are separated by loading methods, Ballistic Loading Tests – 1 and 2. They show the test number, plate thickness, and bolt type; along with the goal and actual velocity of the impacting mass (flyer plate). Specific information on the specimen behavior of each test can be found in Appendix E and F.

This test series gathered additional information other than specimen behavior. Most of the test specimens had strain gages attached to the steel plate in varying locations. Strain rate data was gathered from these tests and trends in the behavior of the specimen were determined. Specifically, evaluating the effects of strain rate behavior based on the impact velocity of the steel plates and the bolts that were used to connect them. Details on the strain rate behavior of the specimen will be presented below.

3.4.1 TEST SET-UP

Each of the test specimens are 2'-8" wide and 3'-8 1/2" tall. They are simply supported at the top and bottom along the 2'-8" side with seven 1/2" diameter holes spaced at 4" on center. Fourteen bolts (either A307 or Grade 5) connect the plate to a set of semi-rigid end supports. Specific information about the material properties of the bolts used throughout the test can be found in Appendix A.

The semi-rigid end supports are connected to a 6' x 12' x 2" thick steel plate that rests up against a 6' x 12' x 2'-9" concrete block that was placed directly in front of the existing moveable reaction wall in the lab. The entire test set-up is tied to the moveable reaction wall by ten 1 3/8" thick Dywidag bars spaced at 2' intervals. These bars have been prestressed to approximately 108 kips and hold the test set-up together. The bottom semi-rigid end support of the test set-up is connected to the 2" thick steel plate by sixteen 1 1/4" A490 steel bolts and two Dywidag bars. The top semi-rigid end support is connected to the 2" thick steel plate by fourteen 1 1/4" A490 steel bolts and two Dywidag bars. Figure 3.32 shows a drawing of the south elevation of the test set-up and Figure 3.33 shows a photo with a specimen in place before a test.

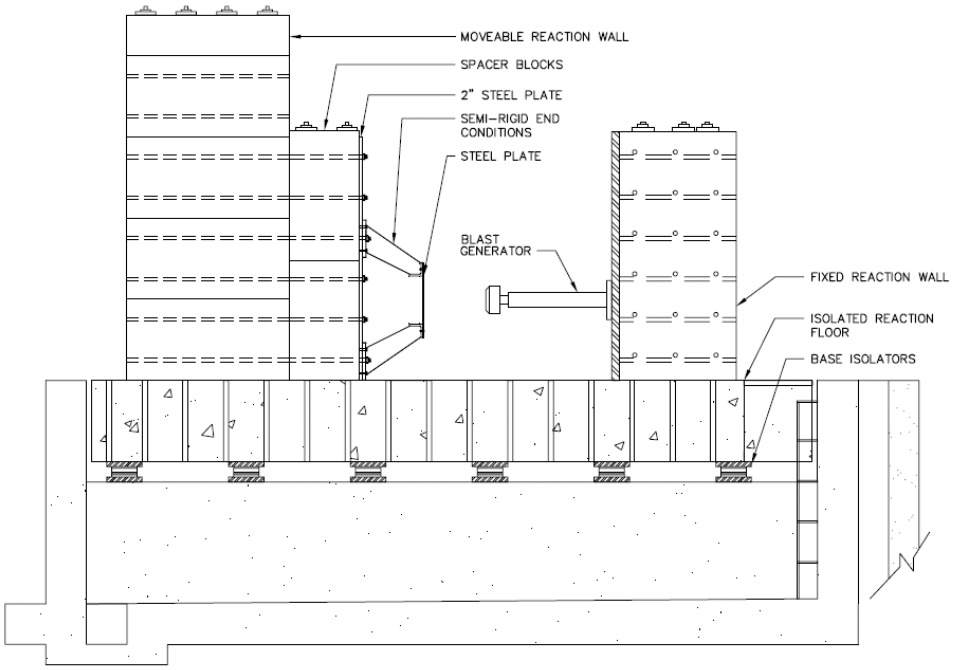

Figure 3.32: Ballistic Loading Type 1 and 2 test set-up – south elevation

Figure 3.33: Ballistic Loading Type 1 and 2 test set-up

A total of three different impacting masses were used in this test series, and were launched with one Blast Generator (BG) (6)(7)(8)(9)(10)(11). (Additional information of the Blast Generator is located in Appendix A) Table 3.2 shows the description, dimensions, and weight of each of the different masses. The table also includes the additional accessories that were associated with the test series. A programmer was attached to the front of the impacting mass for every test. The Rod and Collar was attached to Impacting Mass 1 (IM1) or Impacting Mass 2 (IM2) for the Ballistic Test – Type 1 series. Impacting Mass 3 (IM3) was used, along with the push plate, in Ballistic Tests – Type 2 series. These testing series will be discussed in more detail in the next section.

Table 3.2: Impacting mass and accessories

Description	Height	Width	Depth	Material	Weight
Impacting Mass 1 (IM1)	16. in.	16. in.	6.5 in.	Steel	472 lb
Impacting Mass 2 (IM2)	16. in.	16. in.	6.5 in.	Steel	472 lb
Impacting Mass 3 (IM3)	16. in.	16. in.	3 in.	Aluminum	73 lb
Push Plate	16. in.	16. in.	.625 in.	Steel	45 lb
Programmer	14.5 in.	15.375 in.	1.5 in.	Polyurethane	25 lb
Rod and Collar	-	-	-	-	93 lb

The impacting mass was designed to impact the plate in the center both vertically and horizontally. However, due to an error, the impacting mass is not in the center of the plate along the 2'-8" direction (horizontally); it is approximately 1" off. Instead of having 8" on either side of the plate, the east side has 7" of free plate while the west side has 9". This did not affect the overall behavior of the plate in the longitudinal direction, the stress on the bolts that are being evaluated, or the strain rate data. Specific information about these tests can be found in Appendix E and F.

3.4.2 LOADING METHODOLOGIES

New methods for using the UCSD blast simulator were developed for this test series. In traditional tests the total weight of the BG rod, collar, and impacting mass is less than the test specimen that it impacts. This arrangement allows the BG system to apply an impulsive load to the specimen. This occurs because there is enough energy transfer between the BG and the specimen to allow the deceleration pressure in the blast generator to pull the rod, collar, and programmer away from the specimen after impact. That is not the case in these test series. There is a significant mass discrepancy between the BG assembly and the weight of the steel plate. This allows for a dynamic load to be applied to the specimen instead of an impulsive load. The two loading methods described below: Ballistic Loading Tests – Type 1 and 2 will describe how the dynamic load is applied to the steel plate and the difference between the two methods.

3.4.2.1 BALLISTIC LOADING TESTS – TYPE 1

In these tests the larger impacting masses (IM1 or IM2) were attached to the rod and collar of the Blast Generator (BG). The test was designed to accelerate that mass, at a specific velocity, into the steel plate. The impacting mass was attached to the BG through a series of "break away" bolts. These bolts have a reduced cross section which will allow the impacting mass and programmer to separate from the BG when enough deceleration pressure is applied. This allows the BG to return to its initial position while the mass continues forward impacting the steel plate. Figure 3.34 shows an example of a test where the impacting mass is pushed through the steel plate. The fourth frame in the series shows the impacting mass separating from the blast generator. It also shows that the impacting mass has separated from the horizontal support rods. Upon final separation between the impacting mass and the BG, the

BG will return to its original position while the impacting mass will continue to move forward, until stopped by some other means (either the steel plate or the reaction mass)

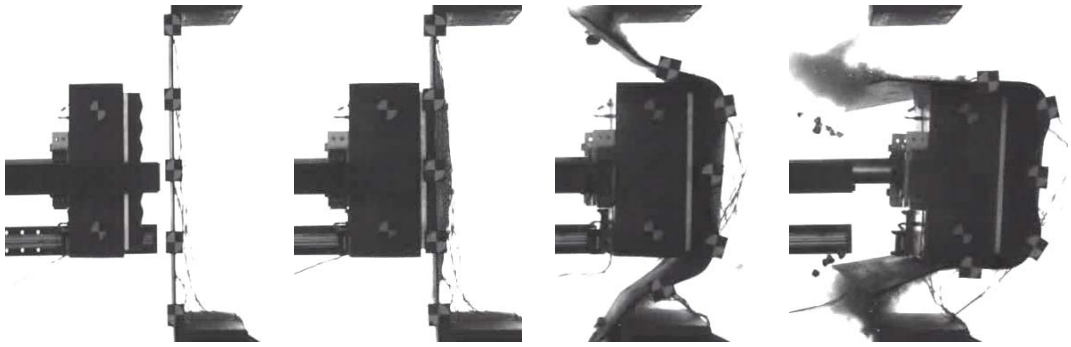

Figure 3.34: Progression of damage for a Ballistic Loading Type 1 test

3.4.2.2 BALLISTIC LOADING TESTS – TYPE 2

Instead of initially attaching the impacting mass to the specimen, only to have it separate later, the impacting mass is not attached to the BG at all. Instead a smaller mass is accelerated forward by a "pushing" force from the BG. A "push plate" is connected to the rod and collar of the BG. The impacting mass is then placed flush with the push plate. When the BG is accelerated, it pushes the impacting mass to a specified distance and velocity. Once that distance is reached the BG, including the rod, collar, and push plate; retract while the impacting mass continues to move forward, on the near frictionless horizontal steel supports, to impact the steel plate. This method was developed in order to remove all additional forces applied to the mass from the hydraulic system of the blast generators. It continues to simulate the impact of the initial flyer plate on the second plate in the generic cellular steel structure. This test method was used primarily when developing the retrofit devices discussed in the next chapter; however, it was used for a set of six tests utilizing 1/2" plates, to evaluate the structural and strain rate behavior. The results will be compared with the Ballistic Loading Tests – Type 1 when the strain rate behavior is discussed. Figure 3.35 shows the push plate,

the 1/2” test specimen, and the impacting mass. The ballistic separation vital to this loading method can be seen in all four frames.

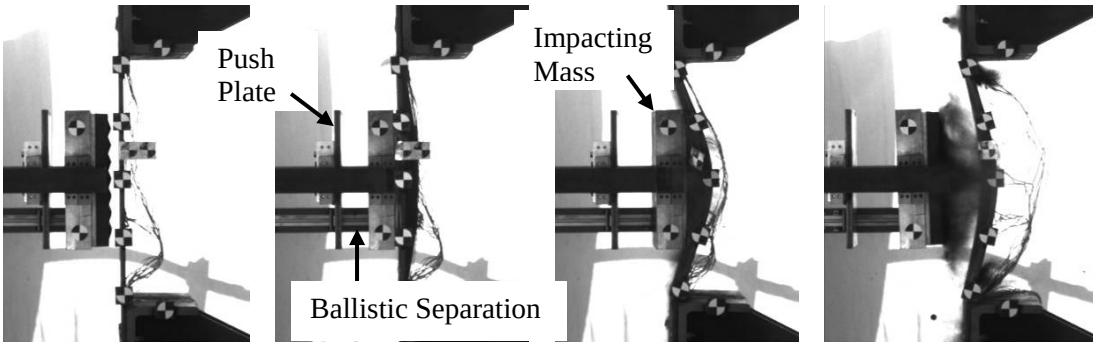

Figure 3.35: Progression of damage for a Ballistic Loading Type 2 test

3.4.3 INSTRUMENTATION

Information of the accelerations, methods to determine impacting velocities and plate displacements is located in Appendix A.

3.4.3.1 DATA ACQUISITION SYSTEM

A high speed data acquisition system from *Hi-Techniques* was used. This system samples at 14 bits and 1 MHz. The data acquisition system has a capacity of 52 channels. It is externally triggered from the MTS Systems controller that is used to fire the BGs.

3.4.3.2 PHANTOM CAMERAS

High speed video was captured with three Phantom v7.1 (Vision Research) cameras. The first camera recorded in black and white at a rate between 5,000 and 10,000 frames per second at a resolution of 512 x 384. The other two cameras recorded in color at rates between 2,500 and 10,000 frames per second at various resolutions. The specifics of each camera

location, the frame rate, and resolutions can be found in Appendix E and F. The cameras were externally triggered from the MTS controller.

These cameras provide visual evidence of the test that can be used to observe the specimen behavior. Phantom camera 1 (black and white) was used to measure displacements and velocities of the entire specimen. Phantom cameras 2 and 3 recorded videos in color to capture different events for different tests. These videos provide impact velocities of the BGs and visuals of the specimen behavior.

3.4.3.3 STRAIN GAGES

The strain in the steel plate was measured using 5mm strain gage rosettes (YEFRA-5 produced by Texas Measurements.) They are high yield, 0˚, 45˚, 90˚ rosettes with a 5mm gage length and a 2mm width. These strain gages will measure strain until the specimen stretches 10 – 15%. There were up to five gages on each test specimen and were placed in a total of twenty-two different locations throughout the test series. For additional information on strain gage locations and filtering methods see Appendix A.

3.4.4 STRAIN GAGE DATA

The following sections will describe the strain rate behavior from forty different tests, where 107 gages yielded useful data. The strain gage data for each test was plotted and the largest strain rate was determined for the maximum and minimum principal strain. A plot of the filtered strain gage data for each applicable test can be found in Appendix E and F. The strain rate was determined by locating the steepest slope in the filtered data before the plate began plastic deformation (near the beginning of the data). All of the strain rates were eventually computed and placed in a table. They were then sorted and compared, using the

different test variables. Those variables included gage location, plate thickness, and bolt type. Each of these variables were plotted against the actual velocity upon impact of the impacting mass. The data provided interesting trends when the plate thickness and the bolt type was compared to velocity and is presented below. There were no discernable trends when evaluating the strain gage location to velocity, and those comparisons are not presented.

3.4.4.1 ALL PLATES

Appendix A describes the strain rate effects when evaluating each plate thickness individually. When those trends are compared to each other additional information concerning the overall behavior of the plates and the test set-up can be obtained and will be discussed herein. All of the strain rate data, and their individual trend lines, are shown in Figure 3.36. In order to determine overall trends in the strain rate behavior for these tests, some data needs to be treated separately. The data from the 1/4" plate with the A307 bolts should be removed, since its behavior is unique and does not add to the overall trends of the other tests. Additionally, the data from the 7/8" plate should be removed because it is only a collection of data at one point. With those points removed, revised trends based on the plate thickness can be determined as shown in Figure 3.37.

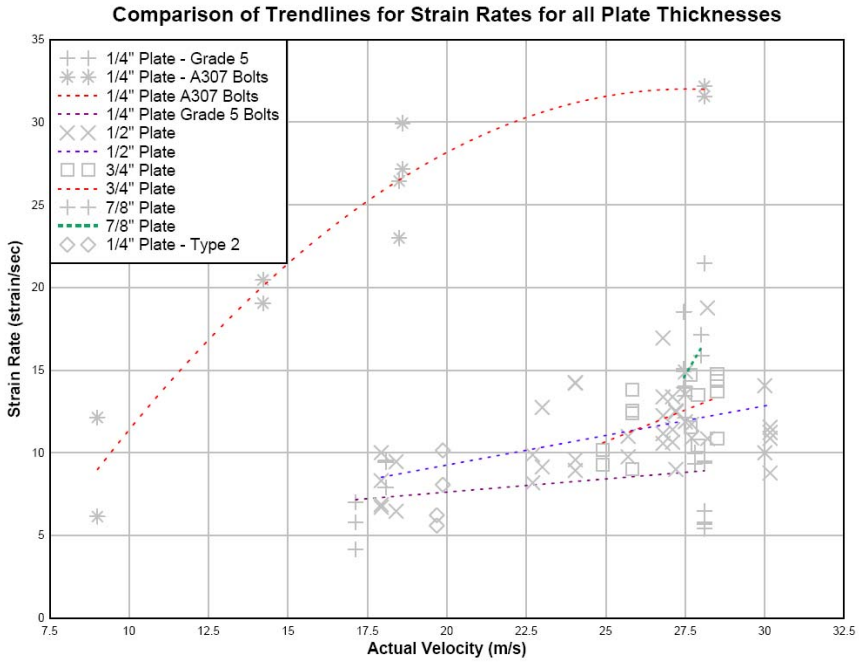

Figure 3.36: Strain rate data and trendlines for all plates and bolt types

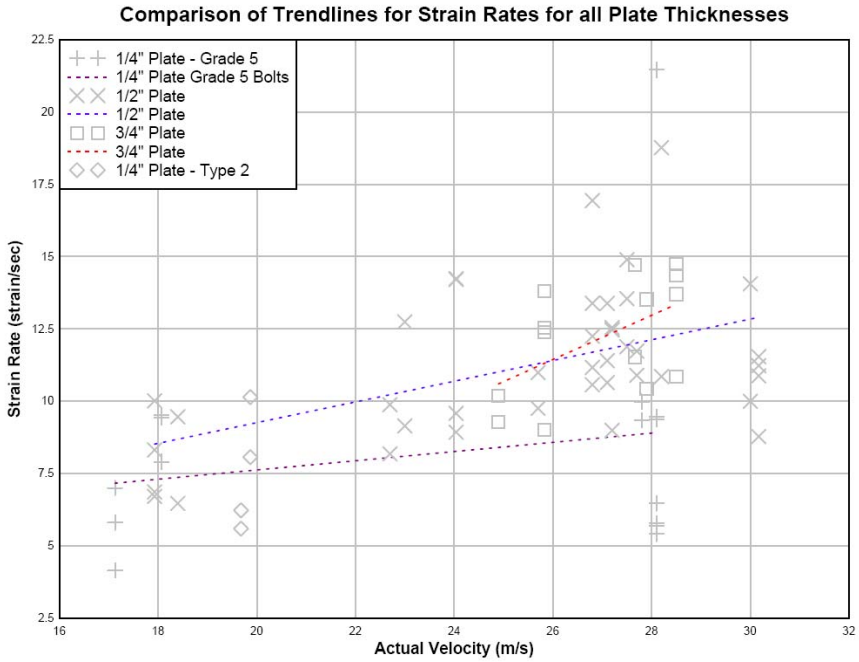

Figure 3.37: Strain rate data and trendlines for 1/4”, 1/2” and 3/4” plates

Each of the trend lines represents a linear relation between strain rate and the velocity of the impacting mass. They were each created by using the linear regression tool in the computer program DPlot. These trends show that an increase in velocity corresponds to an increase in strain. This is most evident in the 3/4" plate. It can be described as follows: as the plate thickens, there are larger increases in the strain rate over the same velocity intervals. This can be verified by evaluating the effects off the end support deformations for a set of tests that occur at velocities around 92 ft/sec (28 m/s). The maximum deformation of the top end support is 0.03" for the 1/4" and 1/2" plates when Grade 5 bolts are used (Figure 3.38). As the end supports displace they release the tension in the plate, which makes it necessary for more force to be applied to increase the strain in the plate. The end supports move the least when the 1/2" plate with the A307 bolts is used. This could be attributed to the weakness of the A307 bolts. They typically fail in 1/2 the time it takes the Grade 5. The displacement of the end supports for the 3/4" plate with A307 bolts is twice as much as the 1/2" plate but almost 1/3 less than the plates with the Grade 5 bolts. This leads to a larger slope in the trend line for the 3/4" plate. As the end support displacement is restricted, the plate is forced to stretch more, therefore causing higher strain rates.

3.4.4.2 BOLT TYPES

In addition to plate thickness, the type of bolt used in the test affects the overall trend of the strain rate vs. impact velocity relation as shown in Figure 3.39 (A307 bolts) and Figure 3.40 (Grade 5). The trend lines, based on blot types, were determined using the same tools that were used when evaluating the trends in plate thickness. The trend line of the A307 bolts has a larger slope than that of the Grade 5 bolts as shown in Figure 3.41. It may seem counter intuitive that the stronger the bolt the smaller affect the velocity has on strain rate. This can be

explained by observing Figure 3.38 again. The bolt types that resulted in the largest deflection of the end support, and over a longer time, were the high strength, Grade 5, bolts. These bolts allow the plate and their supports to displace more, thereby, releasing the tension on the plates by shortening the overall length of the plate, which decreases the strain. Therefore, the more the plate can deform with its supports, the less the plate strains. Compare that with the A307, low strength, bolts. These bolts fail in approximately one half of the time it takes to fail the high strength bolts. That does not allow the end conditions to displace as much as the high strength bolts and does not alleviate the strain in the plate. This leads to the conclusion that more strain is applied to the plate when the lower strength bolts are used, when compared to a plate with high strength bolts at the same velocity.

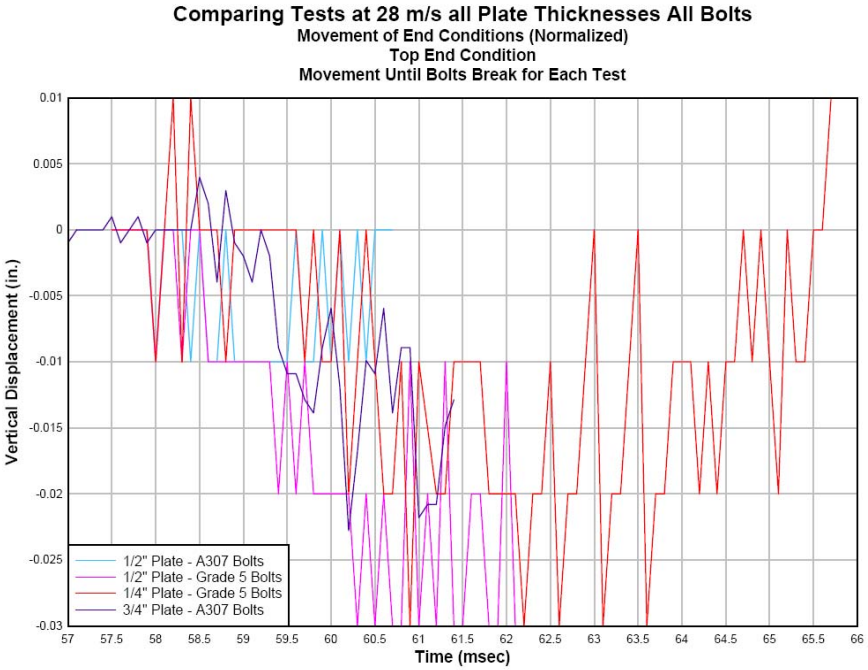

Figure 3.38: Displacement of end supports at 28 m/s

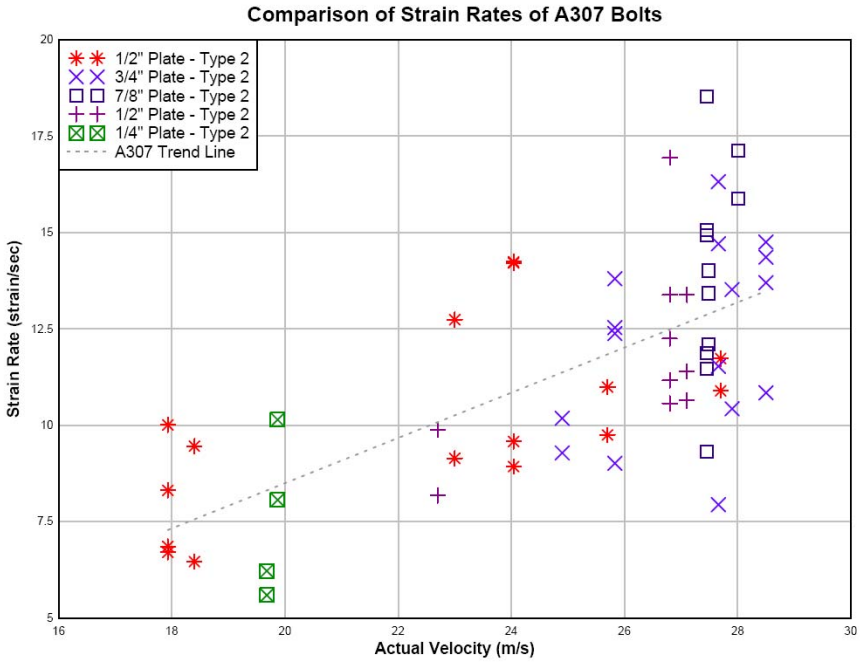

Figure 3.39: Strain rate data for A307 bolts

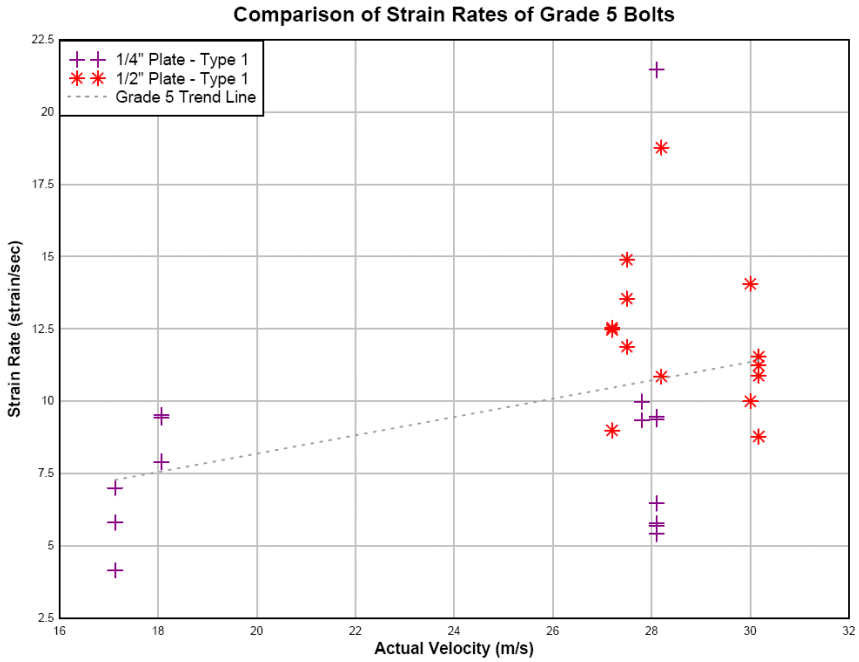

Figure 3.40: Strain rate data for Grade 5 bolts

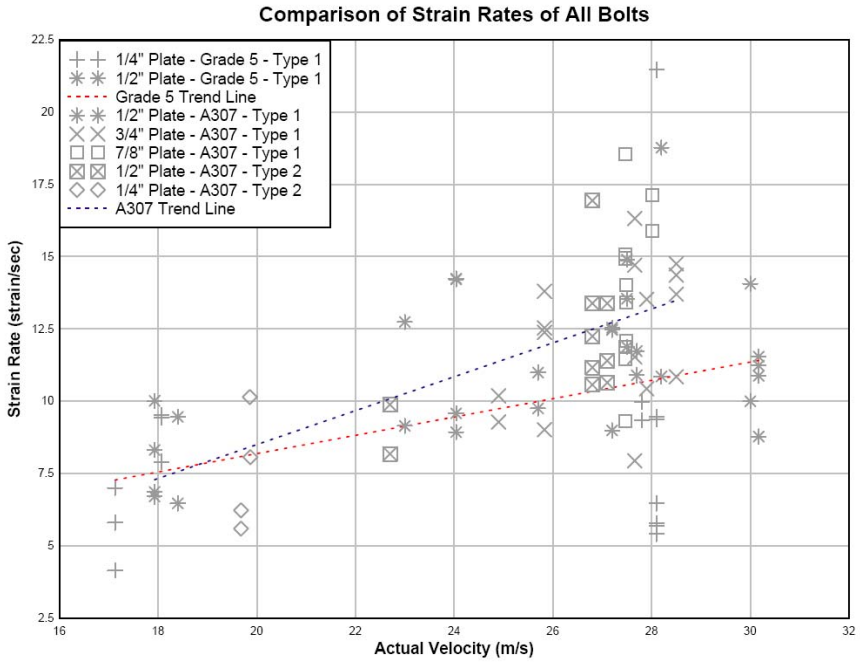

Figure 3.41: Strain rate data for all bolts

3.4.5 CONCLUSION

While both the plate thickness and the bolt type play a role in the strain rates of each plate; bolt type causes a significant effect on the strain rate vs. impact velocity relation. This is an important aspect in developing new material models for the A36 steel along with low and high strength bolts. These strain rate behaviors are unique as they correspond to the effects of the entire system, not just a small sample. This data can be applied to new and existing material models to validate them in regards to structural response. If the material model is velocity dependant, then the data gathered in these tests can be applied directly to the material model. If it is not velocity dependant, then it can be used to tune existing models. In addition, there are the remains of over 600 bolts that are available for future analysis in developing a better material failure model.

3.5 BIBLIOGRAPHY

1. **Baum, Dr. Yossi, Dr. Orlando Soto, Dr. Chuck Charman.** *EMRTC Filed Test Analyses.* Science Applications International Corporation. November 2007.

2. —. *Coupled CFD/CSD Modeling of Scaled Tower Response to Blast Loading.* January 2006.

3. **Meyers, Marc A.** *Dynamic Behavior of Materials.* New York : John Wiley & Sons, Inc., 1994. ISBN 0-471-58262-X.

4. **Martinez, Ruben.** *EMRTC Bridge Section Test Program: Test #1 Summary Report.* Burbank : Karagozian & Case, 2005. p. 46.

5. **Ruben Martinez, Jason Metzger.** *EMRTC Bridge Section Test Program: Test #2 Summary Report.* Socorro, NM : New Mexico Tech, 2005.

6. **Rodriguez-Nikl, Tonatiun.** *Experimental Simulations of Explosive Loading on Structural Components: Reinforced Concrete Columns with Advanced Composite Jackets.* 2006.

7. **Explosive Loading Laboratory.** *Explosiveloading laboratory testing for blast mitigation: Infrastructure developement and blast simulator design. Technical Report.* Department of Structural Engineering, UCSD. 2004.

8. —. *Explosive loading laboratory testing for blast mitigation: Blast simulator commissioning and construction. Technical Report.* Department of Structural Engineering, UCSD. 2005.

9. **Gurtman, G. and Sallay, J.** *Charachterization of UCSD blast simulator programmer material. Technical Report.* Science Applications International Corporation. San Diego, CA : s.n., 2005.

10. *Laboratory Simulation of Blast Loading on Building and Bridge Structures.* **M.M. Gram, A.J. Clark, G.A. Hegemier, and F. Seible.** s.l. : Ninth International Conference of Structures Under Shock and Impact, 2006.

11. *The UCSD Blast Simulator.* **G. Hegemier, F. Seible, K. Arnett, T. Rodrigues-Nike, M. Oesterle, J. Wolfson, M. Gram and A.J. Clark.** s.l. : 77h Shock and Vibration Symposium, 2007.

12. **Morril, Ken.** *Water Slug Write-up.* Karagozian and Case. Burbank, CA : s.n.

4. KEDD DEVELOPMENT

4.1 INTRODUCTION

The development of an effective retrofit device for cellular steel structures is of upmost importance. There are many factors that affect what type of system can be used to protect such structures from a very real threat of terrorist attacks. Some of the limitations include the constructability of the device, the ability to maintain the existing structure, what effects the retrofit will have on the behavior of the entire structure, and the ability to remove the retrofit if required. It is with this myriad of limitations that the new so-called Kinetic Energy Defeat Device, commonly referred to as a KEDD, was developed. The theory behind this development, and the multitude of tests that have been performed, will be discussed in detail within this chapter.

The initial idea was proven effective during simulations using two different computer codes, which led to the development of two different KEDD concepts evaluated in the laboratory tests, a sand-filled and water-filled KEDD system. These tests demonstrated that the water-filled KEDD system was the more effective when compared to the sand-filled KEDD system. This, and other tests, led to the development of the KEDD system for the final field test (Chapter 6), which in turn aided in the KEDD system that was used in the scaled field tests (Chapter 5).

4.2 KINETIC ENERGY DEFEAT DEVICE (KEDD) DEVELOPMENT

4.2.1 CONCEPT

The Kinetic Energy Defeat Device (KEDD) was developed as a novel solution to a very real and complex problem. It was designed for a specific class of structures wherein

traditional retrofit schemes are not feasible. This device utilizes a non-viscous liquid to re-direct the kinetic energy of a projectile into another direction. Such a liquid, when shock loaded in compression and employed in a periodic array of filled and empty adjacent cells, can transmit energy perpendicular to the incoming projectile. This re-direction of energy is accomplished by the formation of high speed ejecta. The goal of the KEDD system is to reduce the velocity of the flyer plates (seen in Field Test 1 and 2, Failure Modes 2 and 3) thereby, limiting damage to the structure. Initial calculations on this subject were defined by Professor Hegemier and executed by Karagozian & Case (K&C) using the eulerian computation code called CTH (1). Subsequent calculations were defined by Professor Hegemier and the Author. They were executed by the Author with the assistance of Lauren Stewart (Chapter 5). The original computational problem was defined such that a circular steel impacting disk, or flyer plate, traveling at 2,625 ft/sec (800 m/s) impacted a cylinder of non-viscous liquid (water) that was resting on a second circular steel disk. Each disk had a radius of 6.7 in. (17 cm) and was 0.79 in. (2 cm) thick. The cylinder of non-viscous liquid was 11.8 in. (30 cm) tall and had a radius of 5.9 in. (15 cm). These dimensions were chosen so that the weight of the water would equal the weight of the two steel disks. Figure 4.1 shows a schematic of the problem set-up. The goal of the calculation was to determine the outgoing velocity of the second steel plate. If the cylinder of liquid between the two disks did not have the ability to redirect the incoming Kinetic Energy of the steel plate, then the second plate would have an outgoing velocity close to the incoming plate. However, if the liquid cylinder does re-direct the energy, then the velocity of the second plate should be slower than the first plate.

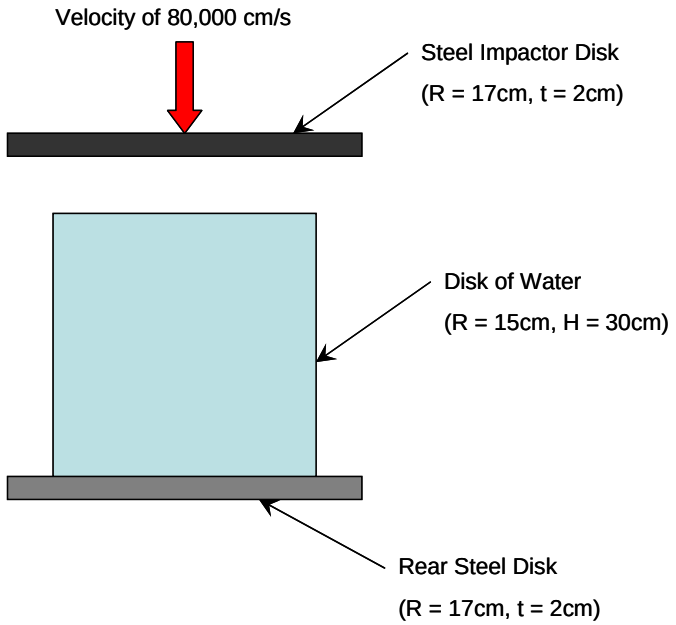

Figure 4.1: Initial CTH calculation problem set-up

The series of computational frames shown in Figure 4.2, demonstrates that the velocity of the initial flyer plate is slowed by the cylinder of water, which is the basis of the KEDD system. The first frame shows the different materials used in the calculation and the initial set-up in the computational code. The second frame shows the formation of high speed jets, or ejecta. The contours shown in the photo relate to the velocity of the different materials. Within approximately 0.1 ms after impact the velocity of the plate has reduced to about 1,312 ft/sec (400 m/s) while the ejecta have a velocity near 3,280 ft/sec (1,000 m/s). By this time, the velocity of the front plate has been decreased by 50%; while the ejecta are traveling at a higher velocity (in the transverse direction) than the flyer plate before impact. The third frame in the series shows that as the plate continues to move through the cylinder of water, the jets continue to form.

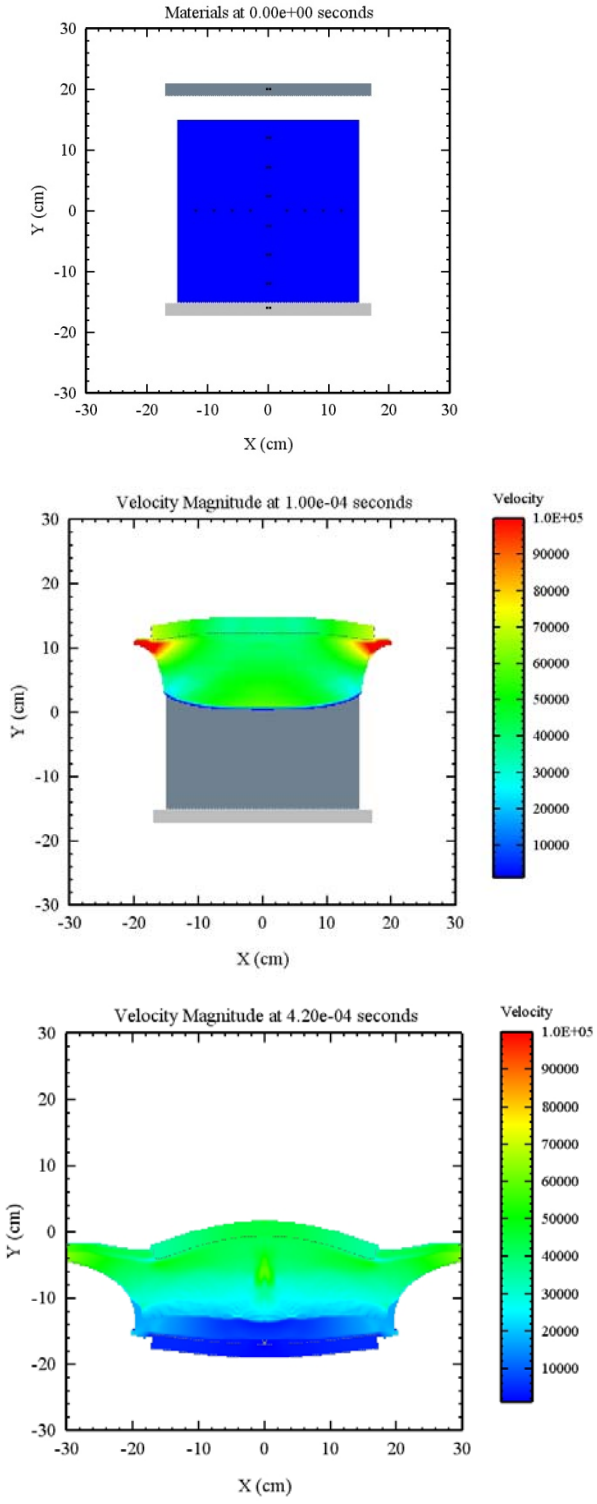

Figure 4.2: Initial KEDD CTH calculation (velocity 800 m/sec)

A plot of velocity vs. time of the two steel plates can be found in Figure 4.3. It shows how the velocities of the front plate, or impactor disk, and back plate, or rear disk, change through the interaction with the cylinder of water. Upon completion of the calculation both plates are traveling at a velocity of approximately 656 ft/sec (200 m/s), which is a reduction in velocity of 75% from the initial velocity. In other words, the calculation predicts a ratio of initial front plate velocity to final back plate velocity of 4 to 1, which results in a ratio of front plate to back plate kinetic energy of 16 to 1, i.e., the back plate energy is an order of magnitude smaller than that associated with the incoming front plate.

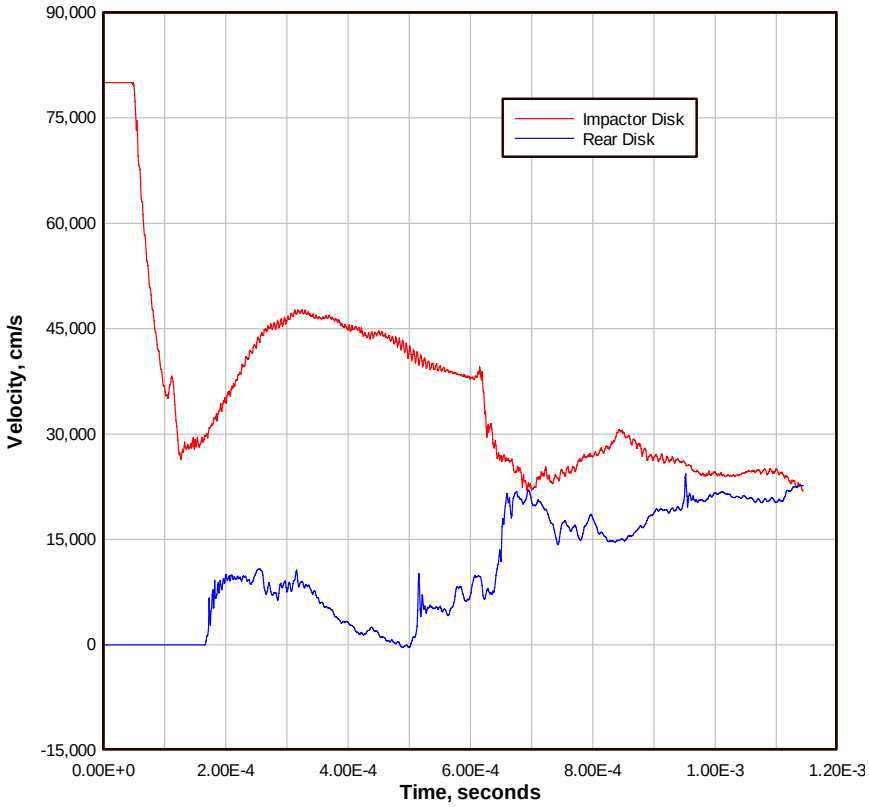

Figure 4.3: Impactor and rear disk velocity histories

Based on the information gathered from this calculation, a pilot experiment was conducted in the UCSD laboratory using one Blast Generator. Due to limits (at the time of the test) on the amount of energy that could be attained, the maximum impact velocity that could be achieved was approximately 98 ft/sec (30 m/s). In order to determine if the basic KEDD theory was consistent at slower velocities, a new calculation was executed by K&C. The set-up for this calculation was the same as the original CTH calculation except for the change in velocity. The slower speed of the impacting mass created problems in the CTH code; therefore, this analysis was performed using the Arbitrary Lagrangian-Eulerian (ALE) option in LS-DYNA (2)(3). A series of four frames from the ALE calculation are shown in Figure 4.4. The same evolution of the liquid expansion process, which was seen in the CTH calculations, can be observed here. The impacting mass impacts the cylinder of non-viscous liquid (water) and the liquid jets out at high velocities from the cylinder, initiating from the impact surface boundary area. This calculation predicted the same front plate to back plate velocity results as the CTH calculation.

Figure 4.4: Initial KEDD ALE LS-DYNA calculation (velocity 30 m/sec)

4.2.2 KEDD LABORATORY TESTS SET-UP

A pilot laboratory exploration on the effectiveness of the KEDD was conducted using the UCSD Blast Simulator. Two different material types were tested: cones of sand, and bottles of water. Due to limits in the blast simulator configuration, the ratio of liquid-to-steel mass was considerably less than what was used in the previous calculations. Therefore, the amount of energy dissipated should be less.

A sand-filled KEDD system was tested first and the results of that test can be found in Appendix F. One of the initial concerns with sand was that the individual grains of sand would "lock up" due to initial confinement. A variety of different geometric arrangements were considered to attempt to combat these effects. Some of the sand-filled KEDD containers that were considered included: rectangles, octagons, circles, and triangles. The triangular, or conical, shape of the KEDD container was decided to be the geometry that would best to mitigate the effect of granular interlock. The idea was that as the cones were compressed, the outer edges would be free to move as the cone diameter decreased along the length of the KEDD. In the design of this experiment, three factors governed the location and size of the cones of sand. The first requirement was that the length of the device did not exceed 8". A goal weight was chosen based on the 1/4" steel plate that would be placed behind the KEDD's. It was chosen to be 50% of the weight of the steel plate, or 50 lbs. In order to achieve all of these design constraints, cones were designed that had a diameter of 2 1/2" at the top and 7/8" at the bottom, and were 8" long. Figure 4.5 shows a drawing of the cone design. Each cone was constructed by the Author out of cardstock and taped closed. A smaller disk of cardstock was placed at the bottom of the cone and taped in place. The cone was filled with sand, and the larger disk was taped into place containing the sand. Cardstock was chosen for the structure of the sand-filled KEDD because it was stronger than everyday

paper, but should fracture easily when compressed. Packing tape was used for similar reasons. A total of 30 sand-filled KEDD's were created to achieve the desired mass. The KEDD system needed to be approximately the same dimensions as the impacting mass (1' – 4" x 1' – 4"). A periodic array of open and filled cells needed to be developed that met the KEDD constraints. (30 KEDD locations in an area approximately 16" square.) The array that was developed placed 2 1/2" diameter sand-filled KEDD's at 3" on center, both horizontally and vertically. This yielded an array of 30 KEDD's over an area of 1' – 6" wide by 1' – 4" high. A drawing of the KEDD array is shown in Figure 4.6. Each sand-filled KEDD weighed approximately 1.8 lbs. There were 30 KEDD's in the array for a total weight of 54 lbs. The array of KEDD's (or KEDD system) was supported by two sheets of 1/4" lightweight Styrofoam at the two ends. One of the two Styrofoam sheets had 2 1/2" diameter holes cut into it to support the front of the sand-filled cone. The other sheet had 1" diameter holes, spaced at 3" on center, to support the back portion of the KEDD. The Styrofoam does not add any strength to the KEDD system and is only used for support. The array was placed in a manner, such that, the 2 1/2" diameter portion faces the incoming impacting mass and the 7/8" diameter portion was placed flush with the plate. The entire KEDD system was supported in place by a sawhorse and wood blocks, which did not affect the impacting mass. The entire KEDD system, including supports, can be seen in Figure 4.7.

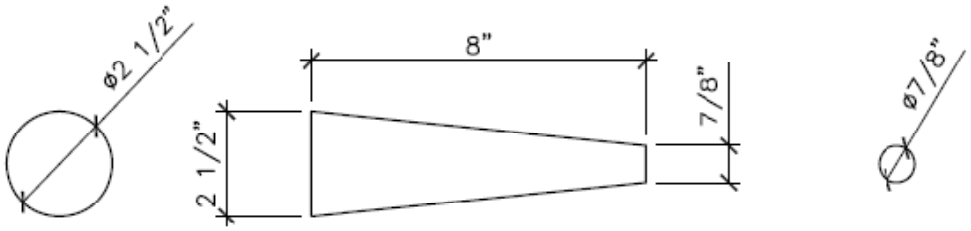

Figure 4.5: Sand-filled KEDD container design

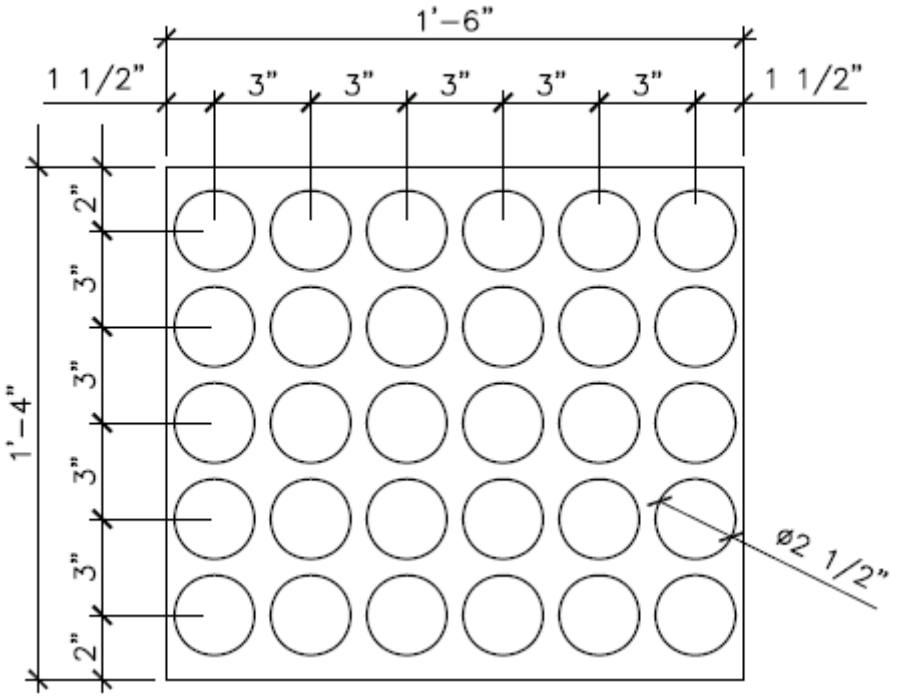

Figure 4.6: KEDD array (laboratory)

Figure 4.7: Pilot test sand-filled KEDD array

Sand was not the only substance evaluated for use in the KEDD. Water was evaluated as well. In order to be consistent in the comparison between the sand and water the same KEDD array was used for both the sand-filled and water-filled KEDD system's. Water bottles were chosen to represent that water-filled KEDD system because of their cylindrical shape and the ease of construction. Other shapes were considered, but eventually discarded. They included: soda cups, milk cartons and jugs of water. Crystal Geyser water bottles were used that are filled with 16.9 ounces of water and are approximately 2 1/2" in diameter at the widest point and 8" long. Each water-filled KEDD system weighed approximately 1.1 lbs. There were 30 KEDD's in the array for a total weight of 33 lbs. The KEDD system was supported by two sheets of 1/4" lightweight Styrofoam along the cylindrical part of the bottle; one sheet near the front and the other near the back. 2 1/2" diameter holes were cut into both pieces of the Styrofoam and were placed at 3" on center in the same manner as the sand-filled KEDD set-up as shown in Figure 4.6. Figure 4.8 shows a front and side view of the actual KEDD system used in the laboratory tests. The water-filled KEDD array was placed such that the bottom of the water bottle was flush with the steel plate and the bottle cap was facing the impacting mass. A drop of red food coloring was used in some of these tests for contrast purposes only.

A variety of heavy liquids were investigated, for use within the KEDD, but discarded for environmental and health concerns. Bentonite and Vermiculite were also considered, but deemed impractical. Combinations of sand with water, and sand with hand soap were also considered, but the solutions separated in short time frames. The two substances would most likely not intermix effectively when shock loaded in compressions and were subsequently discarded.

For the purpose of clarity a KEDD is defined as an individual container filled with a substance. In the laboratory that would be a sand-filled cone or a water-filled bottle. The arrangements of the KEDD's comprise the KEDD system (or KEDD array). A wide variety of KEDD layouts will be presented that shows the flexibility of the KEDD system.

It is important to note that, as opposed to a solid mass of water, there must be an empty cell adjacent to each filled cell in order for this system to work properly. (This will be demonstrated computationally in Chapter 5.) The transverse ejecta process requires a space in which to expand. A continuous wall of liquid or sand, placed in front of the plate will not behave in the same manner and may, in fact, do more damage to the structure.

A series of eight laboratory tests were performed with velocities ranging from 64.5 ft/sec to 86 ft/sec (19.5 m/s to 26.25 m/s). Two of these velocities corresponded directly with velocities of laboratory tests, in the ballistic mode (for a total of ten tests), without the KEDD and will be discussed in a later section.

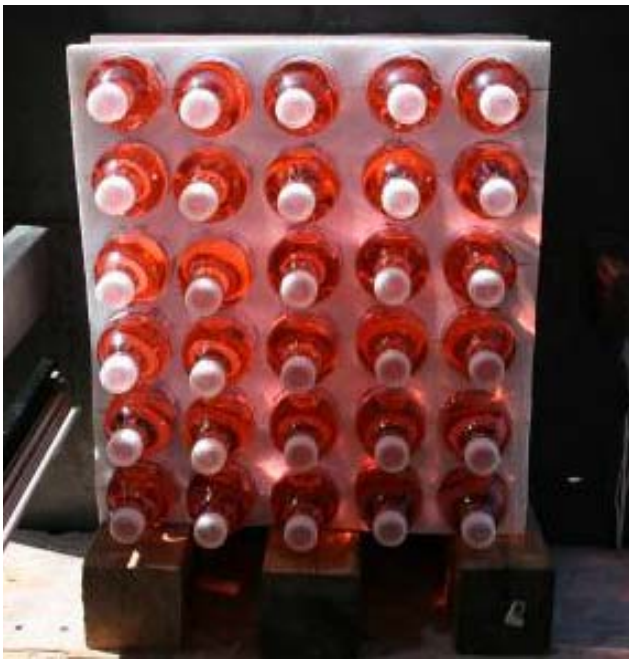

Figure 4.8: Pilot test water-filled KEDD array

4.2.3 KEDD FULL SCALE FIELD TEST SET-UP

The full scale test performed at the Energetic Materials Research and Testing Center at New Mexico Tech (EMRTC) utilized the Kinetic Energy Defeat Device (KEDD) The layout of the KEDD system was motivated by the desire to render the mass of one row of KEDD's as large as possible, while still keeping adequate spacing between the KEDD's. It was also important to have enough space behind the KEDD system to allow a person to maneuver through the structure. The KEDD system works to combat the kinetic energy of the steel fragments that are moving through the structure. For this purpose mass is important; however, the spacing of the KEDD's is equally important. Based on the spacing and the effectiveness of the laboratory test set-up, the initial KEDD layout for the field test was developed.

Many different layouts were evaluated, they included: square pipes, large circular pipes, and multiple rows of smaller circular pipes. In the end it was determined that the different layouts did not dramatically increase the total mass of the KEDD system. The large diameter circular pipes were chosen as the desired KEDD shape due to the availability of containers that could be used, and the ease of construction. The initial KEDD layout was arranged such that the cylinders were parallel to the long dimension of the cell. Eventually, the KEDD's were rotated 90 degrees, so that they were parallel to the short (3' – 6") dimension of the cell. The KEDD arrangement was altered because the KEDD's, in their original layout would need to be of substantial length; which would be difficult to maneuver into place. The new arrangement also increased the efficiency of the KEDD. With the shorter KEDD each one can be individually activated when impacted by a portion of steel, as opposed to the longer KEDD which could only be activated once, before the water began to dissipate.

Having considered all of these conditions it was determined that, for this initial test, the KEDD's should be 8" in diameter and spaced at 10 1/4" on center. The dimensions correlate linearly with the laboratory tests and was designed to have a mass that was 60% the mass of the 3' – 6" x 8' x 7/8" steel plate (steel plate -1000 pounds, KEDD system – 600 pounds). Because the KEDD's needs to support their own weight, over a 3' span while filled with water over a long duration, it was determined that it should be constructed out of Schedule 40 PVC pipe. Other types of pipes were considered, but were deemed either too flexible (would sag over time) or too strong (would not fracture easily to allow the water to dissipate). The pipe must also be able to withstand environmental degradation over time.

The inside diameter of the 8" PVC pipe is 7.943" with an outside diameter of 8.625", and a wall thickness of 0.682". Each pipe had caps constructed out of 3/8" PVC to fit into the ends of the pipes and they extended past the pipe approximately 3/16". One of the end caps had two holes drilled into the ends (Figure 4.9), the KEDD's were filled using those holes (one for air to escape and one for water to enter) and were sealed with 3/8" NPT blind pipe plugs that had Teflon tape around the edges to protect from leaks. The total KEDD length is 3' - 1 3/4" and is shown in Figure 4.10. The dimension was determined based on the ability to install the KEDD in the support system that will be placed inside the structure. The weight of the PVC pipe and caps is 20 lbs, when filled with water the KEDD weighs approximately 88 lbs. It was determined that using two rows of KEDD's is the most efficient layout of the system as this additional mass aids in the dissipation of energy. With two rows of KEDD's the mass of the KEDD system is greater than the mass of the steel plate. For this test 17 individual KEDD's are used in a staggered array (Figure 4.11) which is equal to 1.5 times the weight of the 7/8" steel plate spanning 3' – 6" and 8' in length.

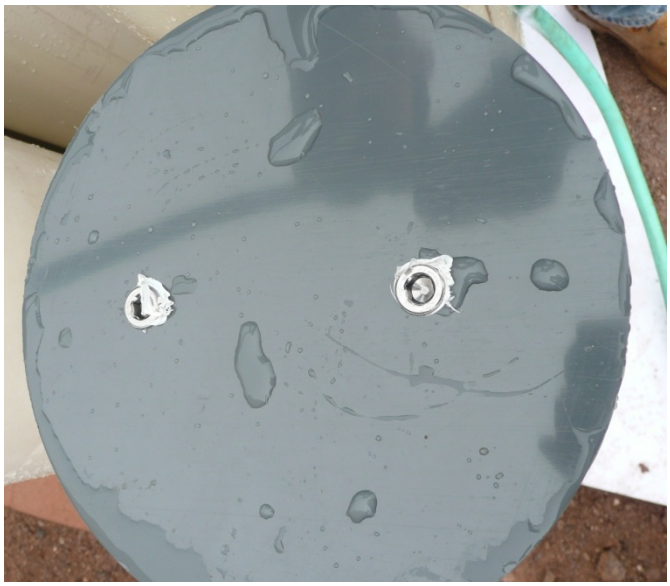

Figure 4.9: KEDD end cap (EMRTC)

Figure 4.10: KEDD - water (EMRTC)

A hanger assembly was developed to support the KEDD's inside the cell. It has many of the same design constraints as the KEDD's. They need to be lightweight, but able to support the weight of the KEDD system. They need to attach to the structure, yet be removable. To meet these design constraints a hanger assembly was developed that attaches to the bolts connecting the plates and angles together. The one disadvantage to this assembly

is that the behavior of the plates, angles, and bolts that make up the cell affects the KEDD system.

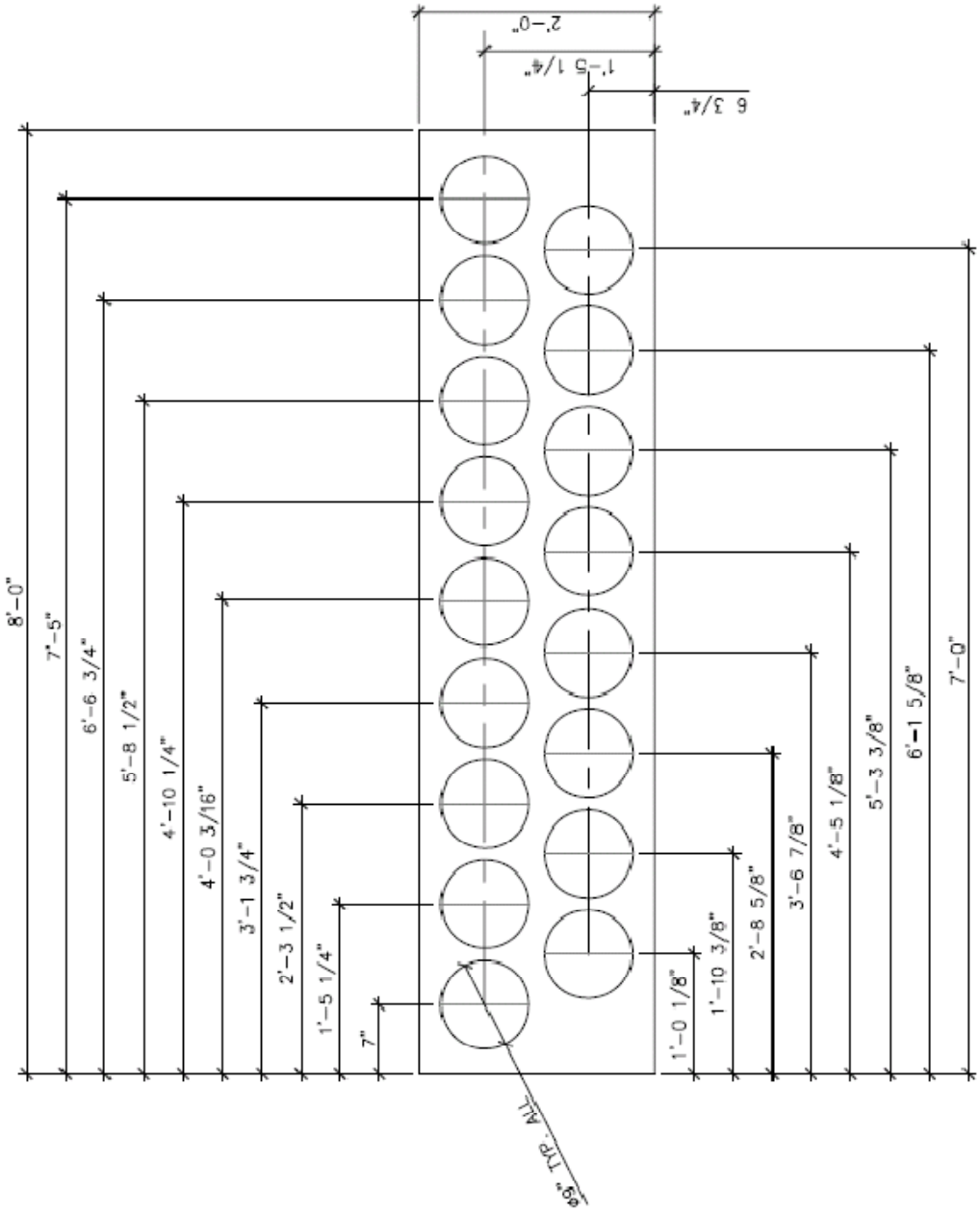

Figure 4.11: KEDD array (EMRTC)

The hangers were constructed from 10 gage sheet metal. It had ovals placed at 10 1/4” on center, starting 7” in from the edge of the hanger for the top row. The second row of ovals was spaced 1’-1/8” from the edge and 6 3/4” from the bottom. Figure 4.12 shows a photo of the standard assembly installed in a cell, the construction drawing for the hanger is located in Appendix B. The original hanger assembly was designed by the Author; however, ARA provided some improvements to the design to ease the construction process. The hangers were designed to connect to the bolts in the structure assuming that the first bolt on the specimen was 2” in from the end of the plate; however, in reality the first bolt was located 4” in from the end. The design locations of the KEDD’s were 2” different than what was anticipated. While this error is unfortunate, it is acceptable and will not adversely affect the overall behavior of the system. An array of KEDD’s in a cell is shown in Figure 4.13. Additional hanger assemblies were placed in each cell as a control measure, as shown in the picture, to determine if they have any effect on the structural behavior of the as-built specimens.

During the construction of the KEDD’s it was determined that the hanger design was less than ideal. In order to maximize the length of the KEDD, the hanger was designed such that that a limited about of overhang, of the KEDD past the support, was provided. When the installation of the KEDD’s began this was brought up as a safety concern. In order to remedy this, one half of the KEDD hangers, were rotated 180 degrees. This allowed for a more secure KEDD support during installation. An example of this is shown in Figure 4.13. The rest of the hangers, in the as-built cells, were left as originally installed. The orientation of the hanger should have no effect on the behavior of the steel plate as long as it does not protrude past the interior angles.

Figure 4.12: KEDD hanger assembly (EMRTC)

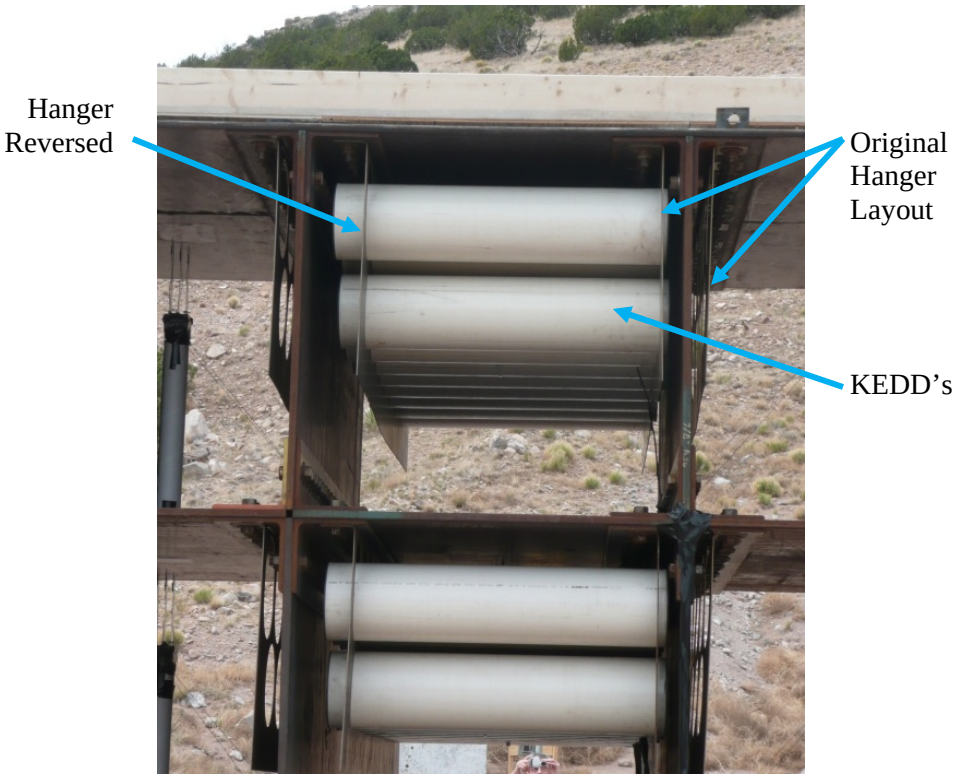

Figure 4.13: 2 Rows of KEDD's on top (EMRTC)

4.2.4 KEDD SCALED FIELD TESTS SET-UP (PROOF-OF-CONCEPT TESTS)

Based on the initial CTH and LS-DYNA calculations, along with the lab experiments, a series of scaled, or Proof-of-concept, field tests were conducted at Applied Research Associates (ARA), Rocky Mountain Division, to explore the viability of the KEDD system. Through the experience gained in the laboratory tests, a similar spacing arrangement was used for the field tests. The KEDD layout for this test series has been scaled down from the full scale tests by 3 1/2. This linear relationship also correlates with the diameter and spacing of the laboratory tests. The original material of the KEDD was to be a corrugated plastic drainage pipe. Unfortunately, the smallest size available was a 3" diameter pipe. Instead a very thin plastic tube that could support the weight of the water of a 1' span was used.

The KEDD system was constructed out of a nominal 2" diameter VisiPack round Heavy Wall Tubing. The inside diameter of the tube was 2.054" with an outside diameter of 2.110" and a wall thickness of 0.028 in. Each plastic tube was placed in an array where the center of the tubes is located 3" away from each other. Each of these tubes were cut to a length of 1', filled with water, and then capped off on both ends by a 2" diameter black Tuff Pak cap produced by VisiPak. Additional staggered rows of KEDD's were used in this test series when additional rows of KEDD's were implemented. These additional rows were located 3" below the center line of KEDD's and were centered between the two KEDD's in the row above. A drawing that shows the three rows of KEDD's is shown in Figure 4.16. The pattern remains the same despite how many rows of KEDD's are used or where the array is placed (either top or bottom). The completed KEDD system, ignoring the weight of the tube and cap, weighed approximately 1.36 lbs each. Figure 4.14 shows a typical KEDD for this test.

Two types of KEDD support assemblies used in these tests. The assembly, used most often, was constructed of 22 gage sheet metal. It had 2 1/4" diameter holes placed at 3" on center starting from the center of the assembly. Figure 4.15 shows a photo of the standard assembly while a drawing is located in Appendix B. The other KEDD support assembly was built out of 2" construction grade Styrofoam and was used when there were multiple rows of KEDD's, it followed the pattern shown in Figure 4.16.

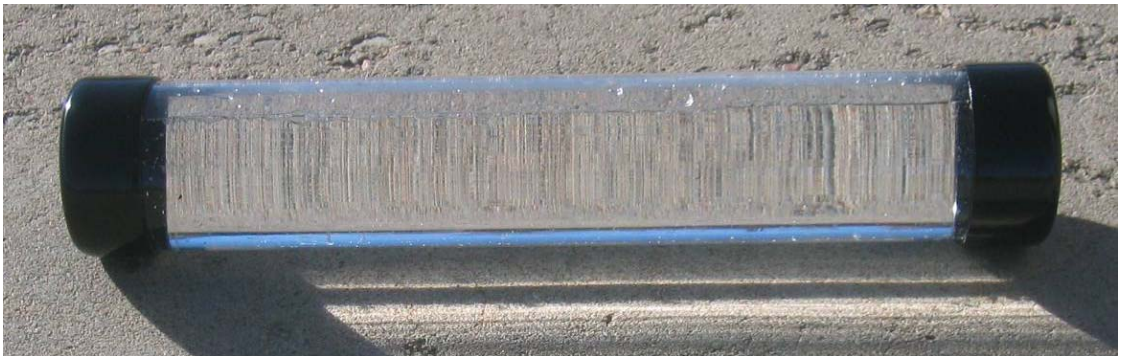

Figure 4.14: KEDD - water (field)

Figure 4.15: KEDD hanger assembly

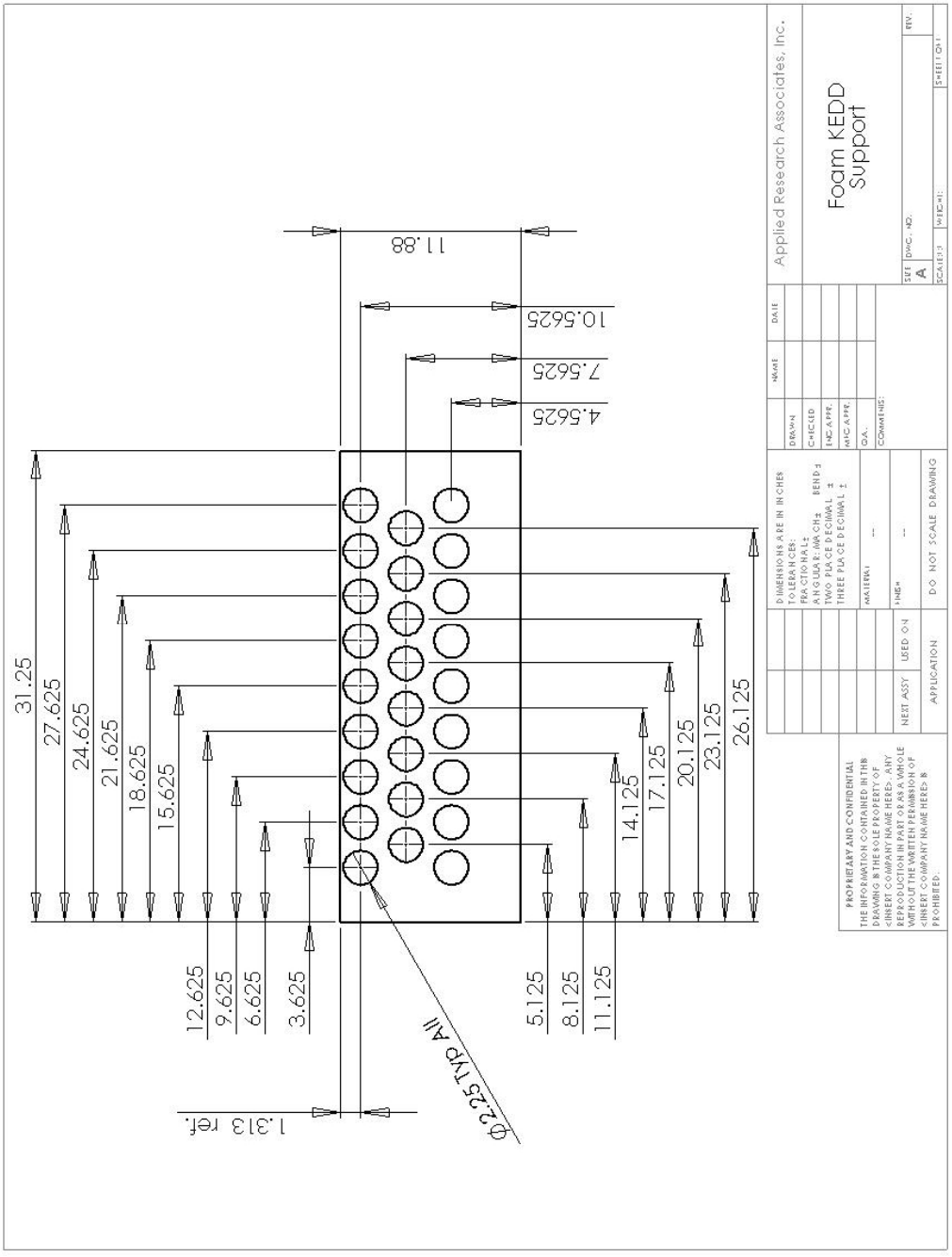

Figure 4.16: KEDD array

In this test series there were five different KEDD system arrangements. They will be presented below with photos from the test set-up. For the majority of these tests only one row of KEDD's were used. Further drawings of these layouts are located in Appendix B.

4.2.4.1 KEDD ON BOTTOM

This system employed one row of KEDD's placed directly in front of a steel plate as shown in Figure 4.17(a). Each KEDD weighed 1.36 lbs; the 9 KEDD's weighed a total of 12.25 lbs, and were supported by the steel hanger assembly. This is approximately 50% of the 23 pound steel plate (1' x 2'-3").

4.2.4.2 KEDD ON TOP

This system employed either one, two, or three rows of KEDD's placed directly in behind a steel plate a shown in Figure 4.17(b) and Figure 4.18. Two of these photos were taken before the top plate was placed, while the Figure 4.18(b) shows the three rows of KEDD's with the steel plate in place. The array that employed one row of KEDD's used the steel hanger assembly to support the KEDD's. The arrays that used two and three rows of KEDD's used foam supports instead. Each KEDD weighed 1.36 lbs; 9 KEDD's weighed a total of 12.25 lbs (one row), 17 KEDD's weighed a total of 23.12 lbs (two rows), and 26 KEDD's weighed a total of 35.36 lbs (three rows). That can be compared to 50%, 100%, and 150% of the 23 pound steel plate (1' x 2'-3").

4.2.4.3 1 ROW OF KEDD'S ON TOP AND BOTTOM

This system used one row of KEDD's placed directly behind the first steel plate, and one row placed directly in front of the second steel plate, as shown in Figure 4.19. Each

KEDD weighed 1.36 lbs; the 18 KEDD's weighed a total of 24.48 lbs. This is approximately 106% the weight of the 23 pound steel plate (1' x 2'-3").

a) 1-row bottom

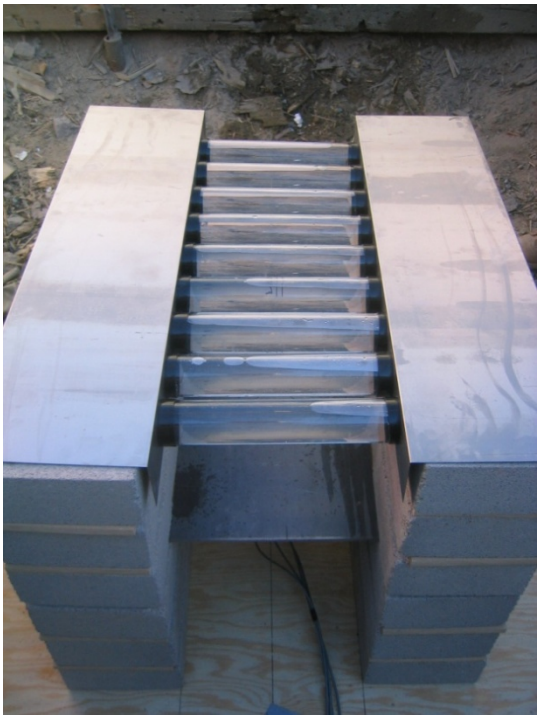

b) 1-row top

Figure 4.17: KEDD layout

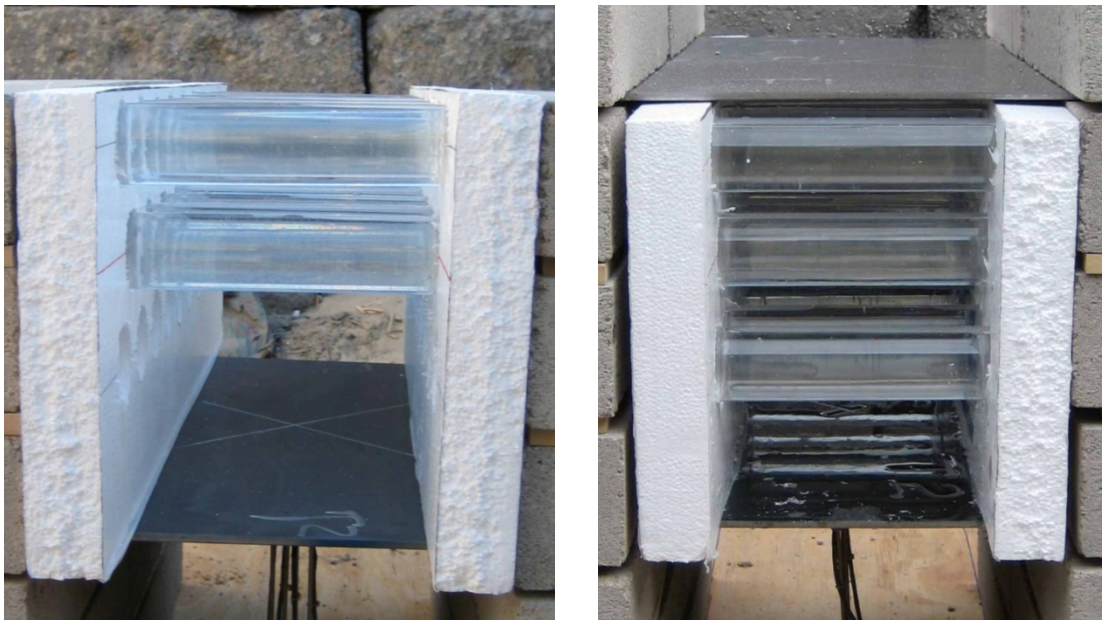

a) 2-row top **b) 3-row top**

Figure 4.18: KEDD layout

Figure 4.19: KEDD top and bottom layout

4.3 KEDD LABORATORY TESTS

4.3.1 INTRODUCTION

Ten tests were performed using the UCSD Blast Simulator to determine the effectiveness of the Kinetic Energy Defeat Device (KEDD) system. It used the Ballistic Impact Tests – Type 2 test set-up that was described in Section 3.4. The tests evaluated both a sand-filled and water-filled KEDD system. Baseline (as-built) tests were also performed for comparison. All of the tests discussed below used a 1/4" thick A36 steel plate that was connected to the end supports by A307 (low strength) bolts. Specific information for these tests can be found in Table 4.1, it includes the test number, bolt type, date tested, and goal and actual velocities. The results from these tests are discussed below.

Table 4.1: KEDD lab tests

Test Number	Plate Thickness	Bolt Type	Goal Velocity	Actual Velocity	Date Tested
40	0.25 in.	A307	64 ft/s (19.5 m/s)	65 ft/s (19.68 m/s)	3/8/2007
41	0.25 in.	A307	64 ft/s (19.5 m/s)	66 ft/s (20.16 m/s)	3/12/2007
42	0.25 in.	A307	64 ft/s (19.5 m/s)	65 ft/s (19.81 m/s)	3/13/2007
43	0.25 in.	A307	66 ft/s (20 m/s)	65 ft/s (19.87 m/s)	3/14/2007
44	0.25 in.	A307	72 ft/s (22 m/s)	85 ft/s (25.82 m/s)	3/15/2007
46	0.25 in.	A307	85 ft/s(26 m/s)	86 ft/s (26.25 m/s)	3/27/2007
47	0.25 in.	A307	66 ft/s (20 m/s)	64 ft/s (19.49 m/s)	3/28/2007
48	0.25 in.	A307	75 ft/s (23 m/s)	77 ft/s (23.34 m/s)	3/29/2007
49	0.25 in.	A307	71 ft/s (21.5 m/s)	70 ft/s (21.30 m/s)	4/4/2007
50	0.25 in.	A307	49 ft/s (15 m/s)	49 ft/s (15.00 m/s)	4/5/2007

4.3.2 COMPARISON OF TEST RESULTS

The following sections will describe the overall specimen behavior when a Kinetic Energy Defeat Device (KEDD) system is used in the laboratory tests. The effectiveness of the KEDD will be discussed, comparing tests at similar velocities and failure modes. The nomenclature of the failure mechanisms were discussed in Chapter 3.

4.3.3 KEDD COMPARISONS

4.3.3.1 DAMAGE COMPARISONS

A direct comparison is needed between a baseline test and tests that utilized a KEDD system, whether it was a sand-filled or a water-filled device. There are three tests that can be compared: Test 40, Test 41, and Test 42. Each of these tests had similar testing parameters and an impact velocity of approximately 20 m/s. Test 40 comprised of a baseline, or as-built test, while Tests 41 and 42 employed a sand-filled and water-filled KEDD system. The test number, KEDD type, impact velocity, and failure mode can be found in Table 4.2, additional information for these tests are located in Appendix F.

While each of these tests had the same initial conditions, the addition of the KEDD systems led to different failure modes after impact. If nothing was done to protect the steel plate (as-built specimen, Test 40) a partial failure of the plate would occur [Figure 4.20(a)]. If a water-filled KEDD system was used as a retrofit device (Test 42) the plate would remain attached to the end supports [Figure 4.20(b)]. When the same test is performed using the sand-filled KEDD system (Test 41), there results are dramatically different. Instead of protecting the specimen, it causes more damage and yields a complete failure [Figure 4.20(c)]. A progression of damage, for all of these tests is shown in Figure 4.21. These frames were captured by the black and white Phantom camera. Figure 4.21(a) is the test without a KEDD, Figure 4.21(b) is the test with a sand filled KEDD system, and Figure 4.21(c) is the test with a water-filled KEDD system.

The water-filled KEDD system re-directs the energy such that less force is applied to the plate. The difference between the sand and water filled tests is that the water is able to disperse in the transverse direction and decrease the velocity of the incoming mass. The sand,

however, is not able to move in the transverse direction as efficiently, and instead moves with the plate, causing more damage than the baseline test. Figure 4.20 shows each of the tests after the completion of the experiment in their respective state of damage. These photos highlight that the use of sand caused more damage to the steel plate than either of the other two tests. The residual deflection of the plate with the water-filled KEDD system was 2 5/16".

Table 4.2: KEDD test comparison data

Test Number	KEDD Type	Impact Velocity	Failure Modes
40	n/a	64.57 ft/sec (19.68 m/s)	Partial Failure
41	Sand	66.14 ft/sec (20.16 m/s)	Complete Failure
42	Water	64.99 ft/sec (19.81 m/s)	Remained Attached

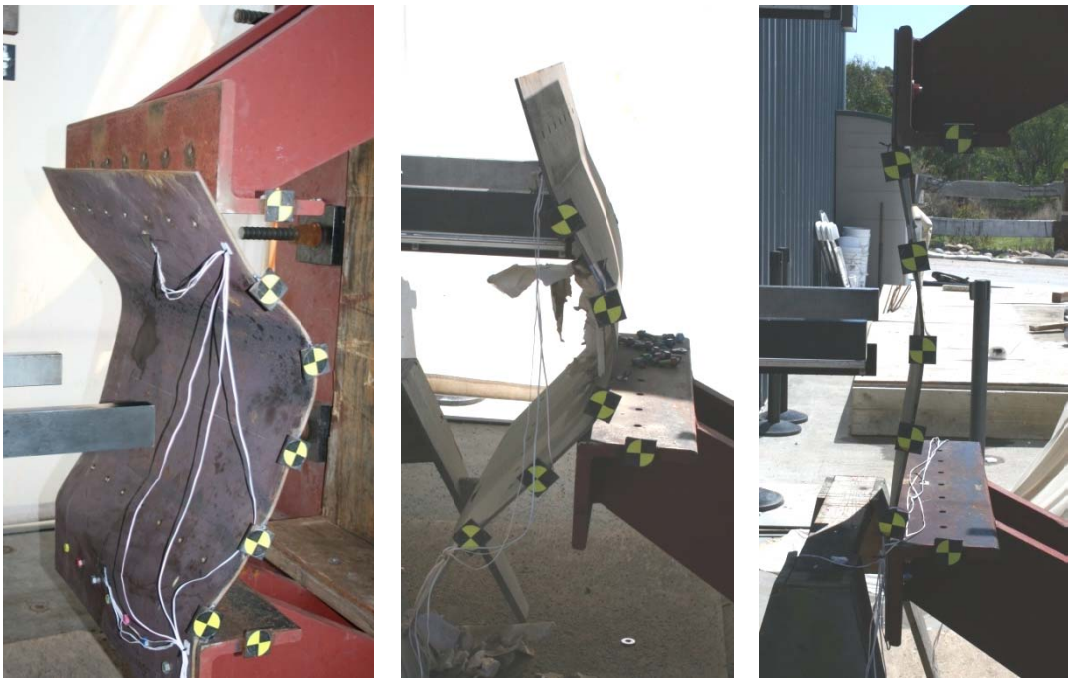

a) Baseline Test -- Test 40 b) Sand filled KEDD -- Test 41 c) Water Filled KEDD -- Test 42

Figure 4.20 Comparison test series post test photos

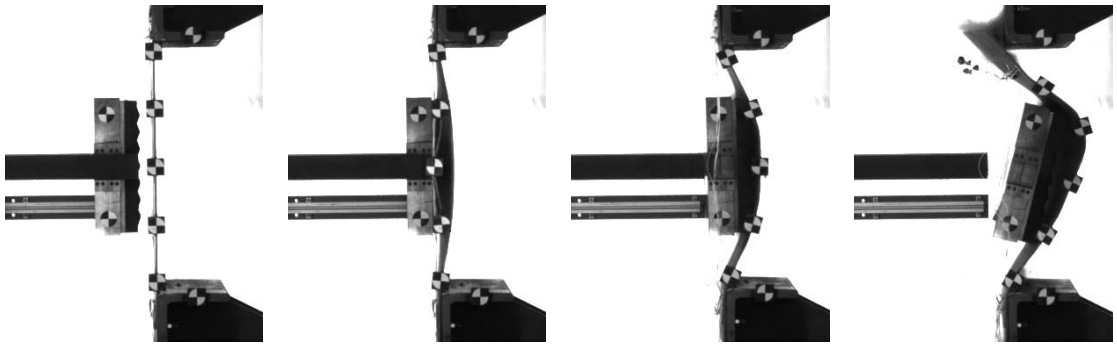

a) Baseline Test -- Test 40

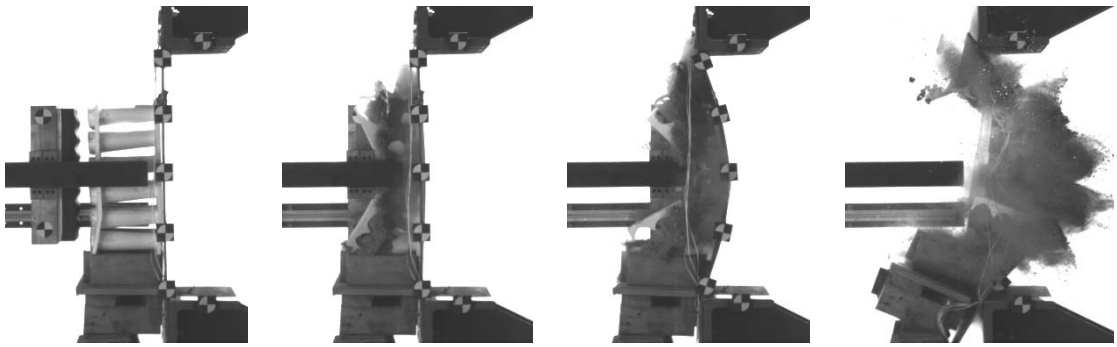

b) Sand filled KEDD -- Test 41

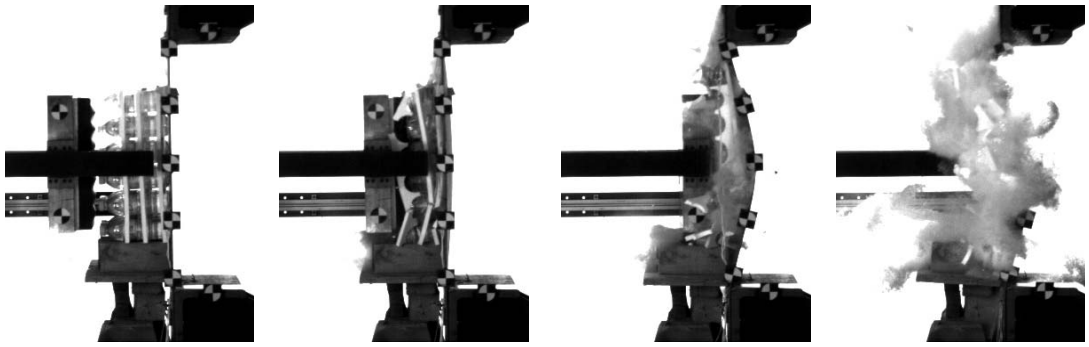

c) Water filled KEDD -- Test 42

Figure 4.21: Progression of failure of the comparison test series

Damage is an important measure in determining the effectiveness of the KEDD system, but it is not the only measure. Strain gage data is also vital as it can describe the

deformation-time history that the plate experiences during the experiment. For this test series there were two strain gages on each plate numbered 17 and 18 (as described in Appendix A). They were placed on the front face of the specimen near the edges of the plate. Information regarding the exact placement of these gages can be found in Appendix F. Figure 4.22 shows the strains and strain rates at Gage 17, and Figure 4.23 shows the strains and strain rates at Gage 18. These gages have been normalized so that all of the initial impacts occur at the same time on the graph. These graphs show that when the incoming mass impacts the as-built specimen (Test 40) the plate has strain rates of 5.59 1/sec and 6.62 1/sec (Gage 17 and 18). When the water-filled KEDD system is placed in front of the steel plate (Test 42) the maximum strain rate is 0.83 1/sec and 1.10 1/sec (Gage 17 and 18). Part of the reduction in strain rate between the two tests can be attributed to how the steel plate is loaded. In the as-built tests, there is nothing to mitigate the impact of the impacting mass and so the plate elongates quickly and produces a sharp spike in the strain data, as exhibited in the orange line on Figure 4.22. This can be compared to the purple line on the same graph. There is no initial sharp spike in strain shown in the data. Instead, there is a period of very little strain followed by an increase in strain. Not only is the maximum strain rate slower when the water-filled KEDD system is used, the maximum strain is also lower; it is between 1,250 -1,500 microstrain. That can be compared to the as-built test whose maximum strain was between 1,800 – 2,100 microstrain. This can be equated to a reduction of strain in the plate by approximately 30%.

The behavior of the plate with the sand-filled KEDD system is very different than the other two tests. Even though maximum strain rate and strain are similar to the water-filled system the amount of damage that occurs to the plate has been increased dramatically. The maximum strain rate and strain for this system is 1.12 1/sec and 1,250 microstrain (Gage 17),

and 0.83 1/sec and 1,600 microstrain (Gage 18). The deformation-time histories show that the locations of the highest strain rate, in the sand-filled tests, occurs at a significantly later time than in the other two tests. They also show that there is a constant increase in strain over a significant duration, i.e. – the plate is slowly elongating. Instead of the sand moving in the transverse direction through the formation of ejecta, the sand experienced granular interlock and traveled in a direction parallel with the incoming mass. The additional mass of the sand (one half of the steel plate) traveling with the impacting mass continues to load the plate and aided in the failure of all of the connections.

These comparisons show that water is an efficient non-viscous liquid for the KEDD system. The granular interlock in the sand was not mitigated through the use of the cones, as had been hoped, and the sand-filled KEDD system led to additional damage to the steel plate over the as-built condition.

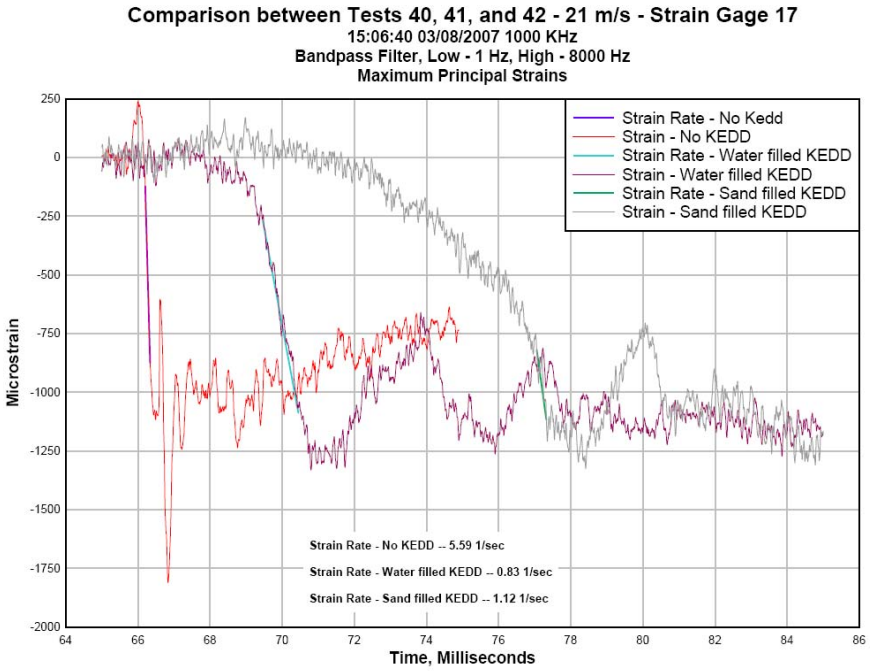

Figure 4.22: Maximum principal strains and strain rates at Gage 17 for this test series

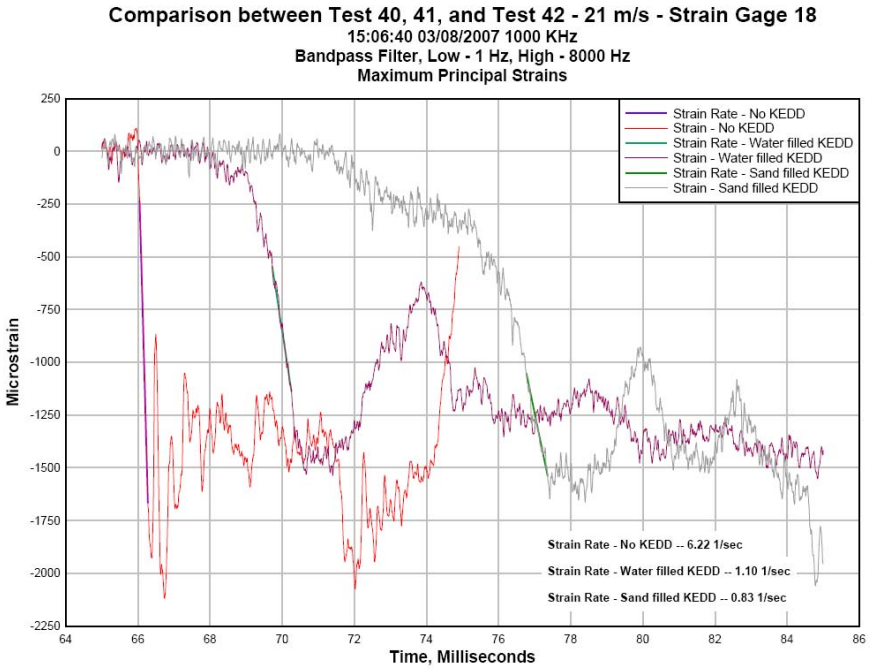

Figure 4.23: Maximum principal strains and strain rates at Gage 18 for this test series

It is important that direct comparisons are made between tests. The comparison between Tests 40, 41 and 42 has helped demonstrate the effectiveness of the water filled KEDD system; however, that was only one test. To further prove that this device can mitigate damage to the structure, another comparison was performed. In this series Tests 43 and 47 were compared. These tests used a 1/4" steel plate with a target velocity of 20 m/s, the actual velocities can be found in Table 4.3. Test 43 was a baseline test, and Test 47 used a water-filled KEDD system. A detailed description of these tests can be found in Appendix F. The baseline test showed that without any retrofit there would be a partial failure of the plate, while the test with the water-filled KEDD system was able to protect the plate from any bolt failures. Figure 4.24 shows a progression of damage captured by the Phantom Camera for each of these tests. Figure 4.24(a) is a test without a KEDD system, and Figure 4.24(b) is

test with a water-filled KEDD system. This series of photos shows the same behaviors of the previous test series. The photos [in Figure 4.24 (a) and Figure 4.25(a)] show that the baseline test failed the top bolts, and the plate was significantly deformed. The test with the KEDD system, however, shows a small residual deflection of 2 1/8" and all of the support bolts are firmly attached to the end supports. The residual deflection of the steel plate in this test was slightly less than Test 42 which had a higher initial velocity.

Table 4.3: KEDD test comparison data

Test Number	KEDD Type	Achieved Velocity	Failure Type
43	n/a	65.19 ft/sec (19.87 m/s)	Partial Failure
47	Water	63.94 ft/sec (19.49 m/s)	Remained Attached

Tests 43 and 47 had strain gages on each plate numbered 17 and 18. They were placed on the front face of the specimen near the edges of the plate. Figure 4.26 shows the strains and strain rates at Gage 17, and Figure 4.27 shows the strains and strain rates at Gage 18 for the two tests. They show the same trends as the previous comparisons. The maximum strain rate in the as-built test was 8.06 1/sec and 10.14 1/sec. The water-filled KEDD system had significantly slower strain rates of 0.72 1/sec and 1/30 1/sec, which were very similar to previous tests.

Once again, these examples show that the amount of damage to the steel plate is reduced when a water-filled KEDD system is used.

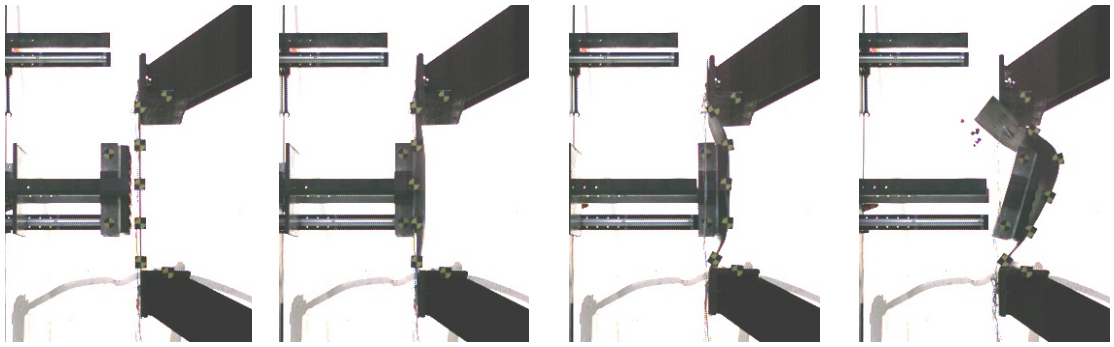

a) Baseline

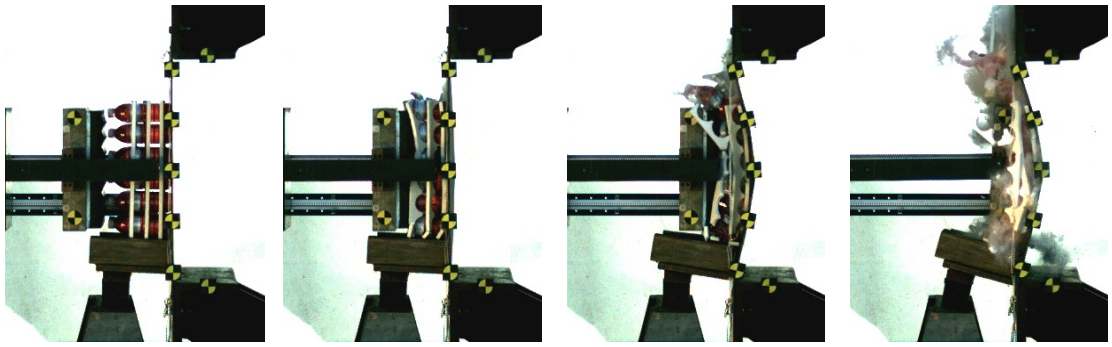

b) Water filled KEDD

Figure 4.24: Comparison of failures

a) Baseline

b) Water filled KEDD

Figure 4.25 Comparison of residual deflections

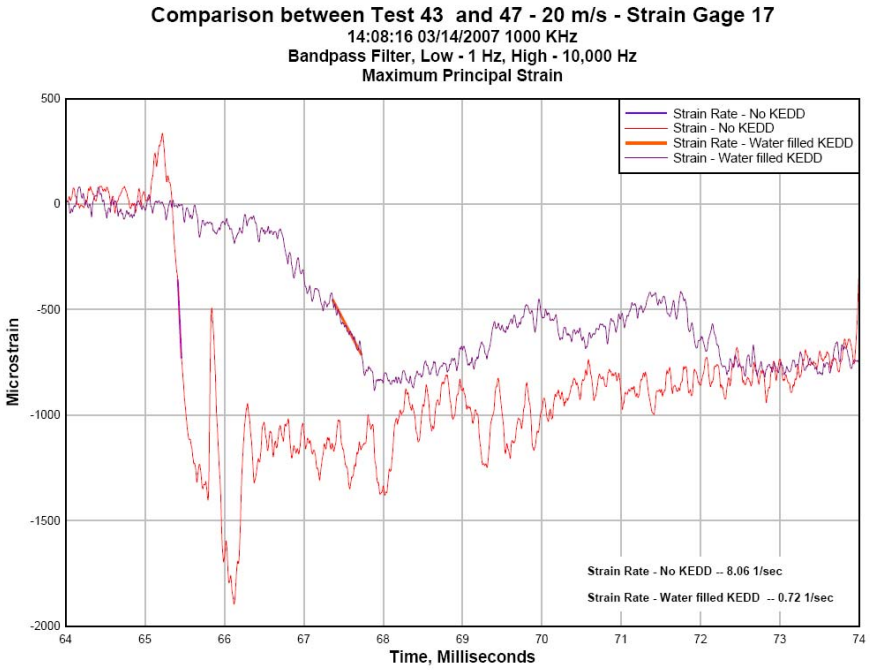

Figure 4.26: Maximum principal strains and strain rates at Gage 17 for this test series

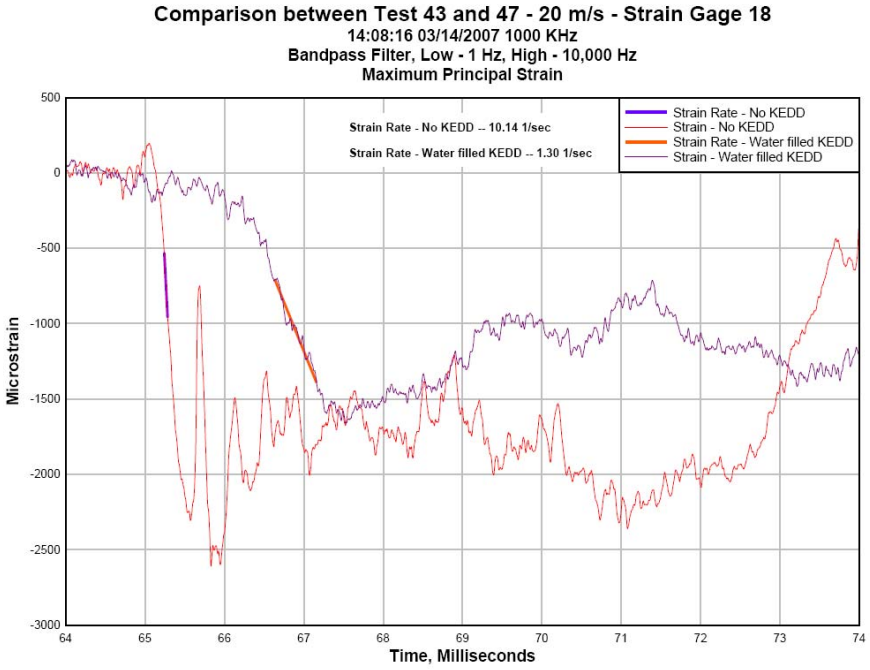

Figure 4.27: Maximum principal strains and strain rates at Gage 18 for this test series

4.3.3.2 KEDD VELOCITY COMPARISONS

The effectiveness of the water-filled KEDD system has been demonstrated via two separate series of tests at the same impact velocity. In particular, the use of the KEDD system has been shown to reduce damage and strain rate. The following discussion compares the behavior of the water-filled KEDD system as the incoming velocity of the impacting mass is increased. Four additional tests were performed at increased velocities, to compare the resulting damage levels when the water-filled KEDD system is utilized. Those velocities are: Test 49 at 76.6 ft/sec (21.3 m/s), Test 48 at 84.7 ft/sec (23.34 m/s), Test 44 at 84.7 ft/sec (25.82 m/s), and Test 46 at 86.1 ft/sec (26.25 m/s). Table 4.4 shows the data for all tests involving a KEDD system and their failure type, including tests that have been discussed. This table shows that when the KEDD system is used, the incoming velocity can reach up to 21.3 m/s and the plate will remain attached to the support.

Table 4.4: KEDD test data

Test Number	KEDD Type	Achieved Velocity	Failure Type
41	Sand	66 ft/s (20.16 m/s)	Complete Failure
42	Water	65 ft/s (19.81 m/s)	Remained Attached
44	Water	85 ft/s (25.82 m/s)	Partial Failure
46	Water	86 ft/s (26.25 m/s)	Partial Failure
47	Water	64 ft/s (19.49 m/s)	Remained Attached
48	Water	77 ft/s (23.34 m/s)	Partial Failure
49	Water	70 ft/s (21.3 m/s)	Remained Attached

In order to compare energy levels of these tests, as opposed to increases in velocity, the kinetic energy of the impacting mass was determined. A chart and table demonstrating the increase on kinetic energy of the incoming flyer plate is provided in Figure 4.29 and Table 4.5. The bars from left to right represent a baseline test (Test 40) and three water-filled KEDD systems (Tests 42, 47 and 49). These tests are comparable because they resulted in the same type of damage “remained attached” as shown in Figure 4.28. The outgoing kinetic energy,

after impacting the KEDD and the plate, could not be determined since the water obscured the targets on the specimen needed to determine velocity, therefore all energy estimates are based on the incoming mass. A baseline test (Test 50) had an incoming velocity of 49 ft/sec (15 m/s), or a kinetic energy of 338J, will result in the same level of damage as a test using a water-filled KEDD system with an incoming velocity of 70 ft/sec (21.3 m/s), or 479J. When these two tests are compared an increase in kinetic energy of 30% can be determined. This same comparison will be made at the next level of damage.

Table 4.5: Kinetic energy data for damage – remained attached

Test	KEDD	Incoming Mass	Incoming Velocity	Kinetic Energy
50	n/a	100 lb (45 kg)	49 ft/sec (15.00 m/s)	338 J
47	water	100 lb (45 kg)	64 ft/sec (19.49 m/s)	439 J
42	water	100 lb (45 kg)	65 ft/sec (19.81 m/s)	448 J
49	water	100 lb (45 kg)	70 ft/sec (21.30 m/s)	479 J

a) Test 50 - No KEDD b) Test 42 – KEDD c) Test 47 – KEDD d) Test 49 – KEDD

Figure 4.28: Photos comparing damages with and without a KEDD - remained attached

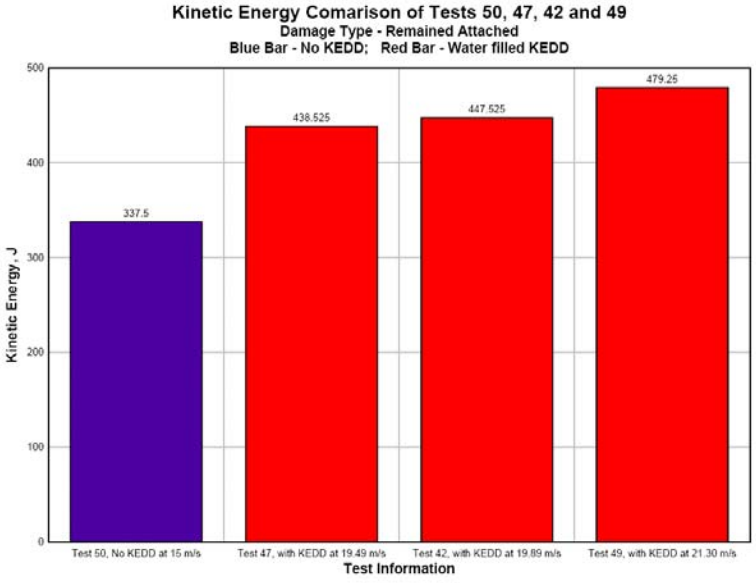

Figure 4.29: Bar graph comparing incoming kinetic energy of impacting mass at damage level remained attached

Once again four tests were used evaluating the increase in kinetic energy (or velocity) of the incoming impacting mass. The tests used are: baseline (Test 40) and three KEDD tests (Test 48, 44, and 46). The impacting velocities and kinetic energies for these tests are located in Table 4.6. Similar to the previous discussion Figure 4.32 contains a chart of the kinetic energy associated with these tests. Figure 4.30 and Figure 4.31 depict the test specimens after the test. They all exhibit the same level of damage "partial failure". A comparison similar to the previous one is shown here depicting the increase in kinetic energy. The baseline test (Test 40) had an incoming velocity of 65 ft/sec (19.68 m/s), or a kinetic energy of 443J, will result in the same level of damage as a test using a water-filled KEDD system with an incoming velocity of 86 ft/sec (26.25 m/s), or 591J. When these two tests are compared an increase in kinetic energy of 25% can be determined for the same level of damage.

Table 4.6: Kinetic energy data for damage – partial failure

Test	KEDD	Incoming Mass	Incoming Velocity	Kinetic Energy
40	n/a	100 lb (45 kg)	65 ft/s (19.68 m/s)	443 J
48	water	100 lb (45 kg)	77 ft/s (23.34 m/s)	525 J
44	water	100 lb (45 kg)	85 ft/s (25.82 m/s)	581 J
46	water	100 lb (45 kg)	86 ft/s (26.25 m/s)	591 J

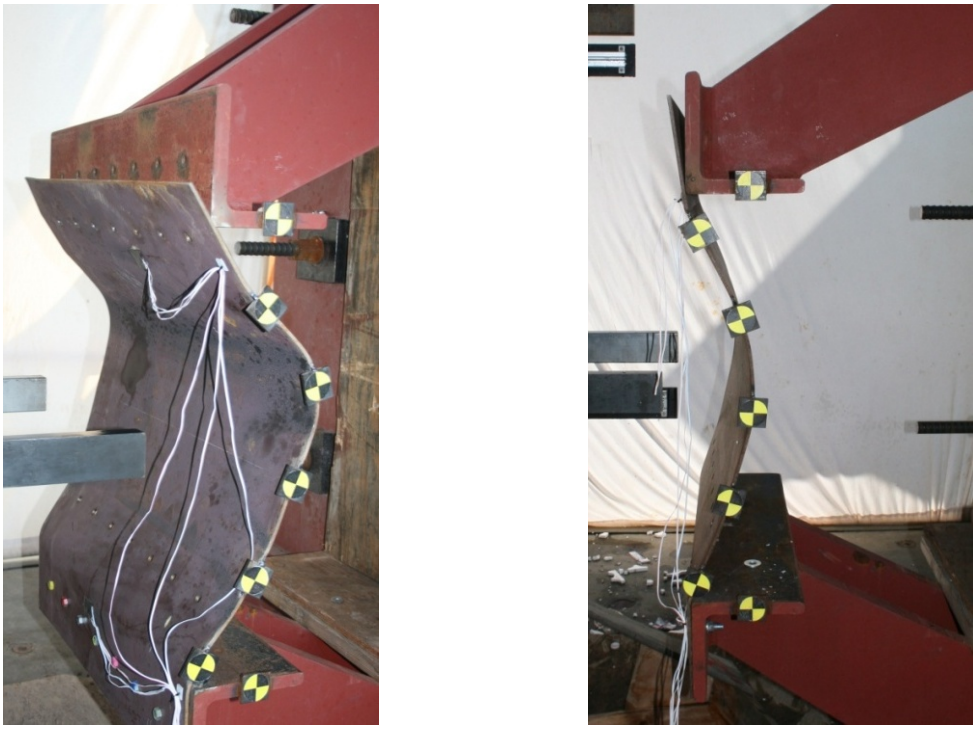

a) No KEDD **b) KEDD (Test 48)**

Figure 4.30: Damage comparisons (partial failure)

a) KEDD (Test 44) **b) KEDD (Test 46)**

Figure 4.31: Damage comparisons (partial failure)

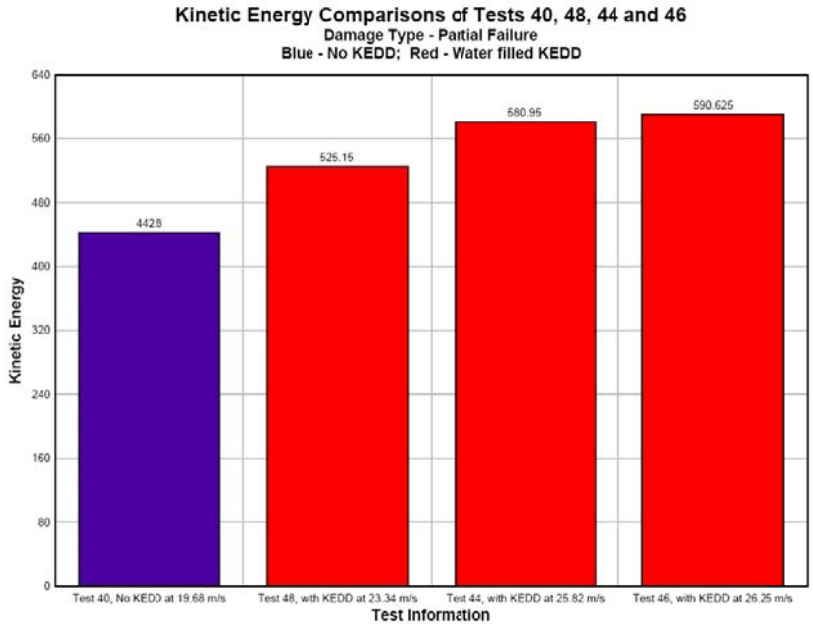

Figure 4.32: Bar graph comparing incoming kinetic energy of impacting mass at damage level partial failure

4.3.4 KEDD CONCLUSIONS (FROM LABORATORY TESTS)

The previous discussions compare the damage levels that would occur to a steel plate when a variety of Kinetic Energy Defeat Devices (KEDD's) are used. It has been shown that a water-filled KEDD system can decrease the damage level when compared to a test without a device, or a baseline test. The discussions have also illustrated that the use of a sand-filled KEDD system does not behave in the same manner as a water-filled system and can result in more damage to the structural element. The effectiveness of the water-filled KEDD system was demonstrated in comparison to two different baseline tests. The plates in the baseline tests partially failed, while in the water-filled KEDD system tests the plates were still intact.

5. SCALED TESTS AND CALCULATIONS

5.1 INTRODUCTION

Twenty-one tests, as part of a Proof-of-concept test series, were performed at the Applied Research and Associates (ARA), Rocky Mountain Division's, test site. The purpose was to determine if the Kinetic Energy Defeat Device (KEDD) system was a viable retrofit solution, and to determine the most effective location for the device within the structure. These included a variety of test set-ups, KEDD positions, and equivalent TNT values as shown in Table 5.1. Individual test reports can be found in Appendix G.

Table 5.1: Test matrix

Test No.	Type	KEDD	KEDD position	Equivalent TNT Charge (lbs)
1	Calibration	No	na	0.034X
2	Calibration	No	na	0.034X
3	Calibration	No	na	0.023X
4	Calibration	No	na	0.011X
5	4 Plate	No	na	0.014X
6	2 Plate	No	na	0.023X
7	2 Plate	Yes	Bottom of cell	0.023X
8	2 Plate	Yes	Top of cell	0.023X
9	3 Plate	Yes	Top of cells	0.034X
10	3 Plate	No	na	0.034X
11	2 Plate	Yes	Top of cell	0.023X
12	2 Plate	Yes	Bottom of cell	0.023X
13	2 Plate	No	na	0.023X
14	2 Plate	No	na	0.023X
15	2 Plate	Yes	Two rows top of cell	0.023X
16	2 Plate	Yes	Top and bottom of cell	0.023X
17	2 Plate	Yes	Three rows top of cell	0.023X
18	2 Plate	No	na	0.023X
19	2 Plate	Yes	Two rows top of cell	0.023X
20	2 Plate	Yes	Three rows top of cell	0.023X
21	2 Plate	Yes	Top and bottom of cell	0.023X

5.2 TEST SET-UPS

The ARA tests were conducted at 1/3.5 scale with respect to the final field test scheduled to be performed at the Energetic Materials Research and Testing Center affiliated with New Mexico Tech (EMRTC) (4). The specimens were fabricated using 1/4" A36 steel plates. Each plate was 2' - 4" wide and 2' - 3" long, and was spaced at 12" between plates (vertically). They were supported by 4" x 8" x 16" (nominal) solid CMU blocks, whose actual dimensions are 3 3/4" x 7 3/4" x 16". They were placed two deep (2'-8") and stacked in rows of three. In order to achieve the exact height of 12" between the steel plates, 3/8" thick spacer blocks, constructed out of Medium Density Fiberboard, were used between each course, or row, of blocks. The area of the steel plate not supported by the CMU blocks is 1' x 2' – 3" as shown in Figure 5.1.

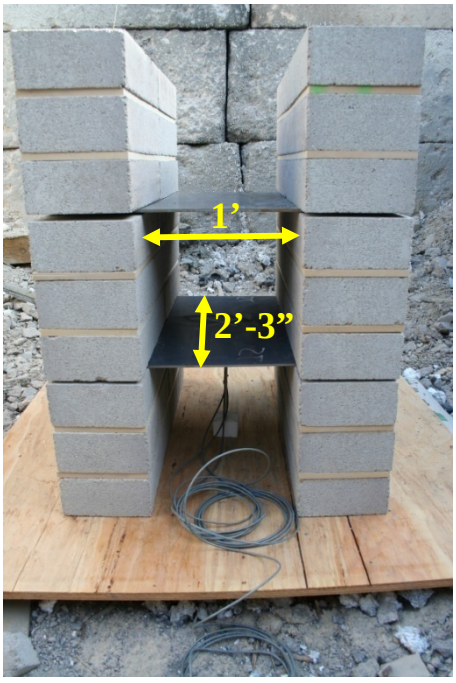

Figure 5.1: Test set-up showing exposed area of steel plate

The specimens were built inside a concrete bunker at the test site. To create a level surface, sand bags were placed in the bunker, and a piece of plywood was placed on top of them, and leveled. The CMU blocks were then placed on the plywood in a manner such that the steel plate would be centered on the plywood. After a course of CMU blocks were placed, a 3/8" thick spacer block was placed upon them. This was repeated three times per plate. Once the 1' height was achieved (three courses were placed), the steel plate was placed on top of the blocks and centered. Another three courses of blocks, and spacers, were placed until the necessary number of plates was installed. Four different test set-ups were used in this test series: Calibration Tests, 4 Plate Test, 2 Plate Tests, and 3 Plate Tests. The test set-ups and the test results for the Calibration Tests, 4 Plate Test, and 3 Plate Tests are located in Appendix C.

5.2.1 CHARGE SET-UP

The 2 Plate Tests used a charge equivalent to 0.023X pounds of TNT as shown in Table 5.1. The explosive was placed into a 9" x 9" square cake pan, made by Wearever. It was consists of a 1mm heavyweight steel construction (5). A RP-81 EBW Detonator from Teledyne RISI, Inc. was placed in the center of the charge. Figure 5.2 shows a photo of the charge with the detonator in the cake pan[1].

[1] For specific information see Kinetic Energy Defeat Device (KEDD) Proof of Concept Tests (through TSWG)

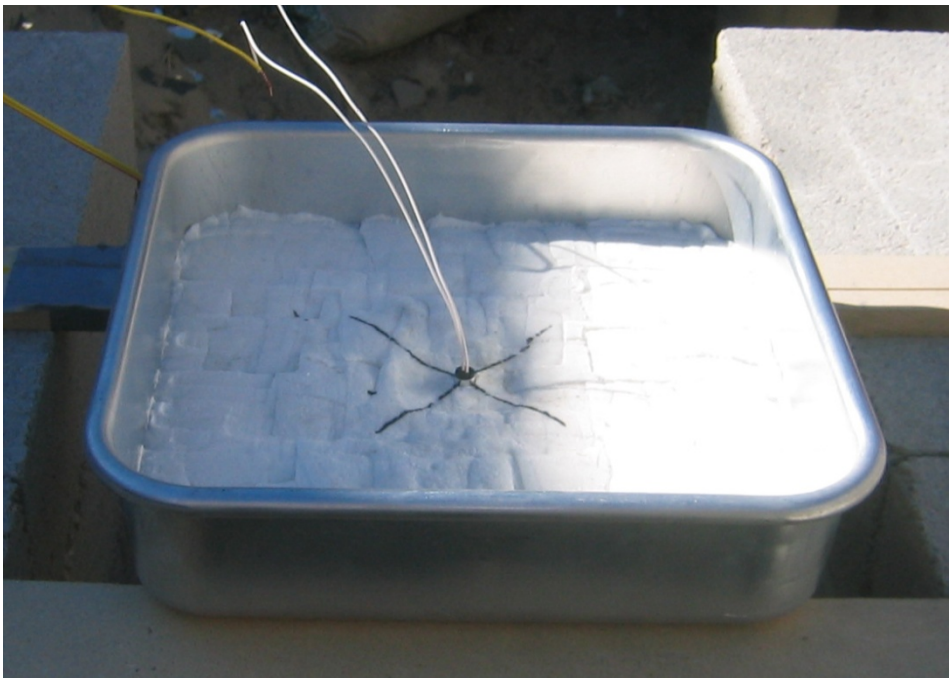

Figure 5.2: Explosive material and detonator

5.2.2 TIME OF ARRIVAL PINS

Time of Arrival (TOA) pins were used for this test series and the full scale test discussed in Chapter 6. They recorded the velocity of the steel plates and flyer plates. The pins were manufactured at the Rocky Mountain office of ARA from rigid coaxial material. Each pin consisted of a conductive rod surrounded by an insulating sheath and a conductive tube. A voltage was applied to the inner conductor rod, the data acquisition system recorded the voltage from the outer conductive tube. When the tip of the inner conductive rod is impacted, a rapid deformation causes a short circuit in the system which creates a voltage step function signal in the outer conductor tube to be recorded. The sub-microsecond timing resolution offers the Time of Arrival information. In order to determine the velocity, a TOA vs. displacement graph can be used. Another method is to determine the time of the first and second impact and then divide that value by the distance between the pins.

The TOA pins were held in place by attaching them to a glass rod, as shown in Figure 5.3. The glass rods were cut at varying lengths. The typical TOA pin series was placed at 10", 7 1/2", 5", and 2 1/2" above the plywood, or steel plate, below. [Figure 5.4(a)] This correlates to spacing between the pins of 2 1/2". This spacing will be deemed as "lower spacing" in future discussions. Another pin series was placed at 11 1/2", 11", 10 1/2", and 10" above the plywood, or steel plate, below [Figure 5.4(b)]. This correlates to spacing between the pins of 1/2". This spacing will be deemed as "higher spacing" in future discussions. The two arrangements were used based on what glass rods were available on site at the time of the test. The goal was to keep the spacing consistent when comparing tests, but unfortunately, that did not occur. Specific information regarding the TOA arrangement for a specific test can be found in Appendix G.

Figure 5.3: A Time of Arrival pin connected to a glass rod

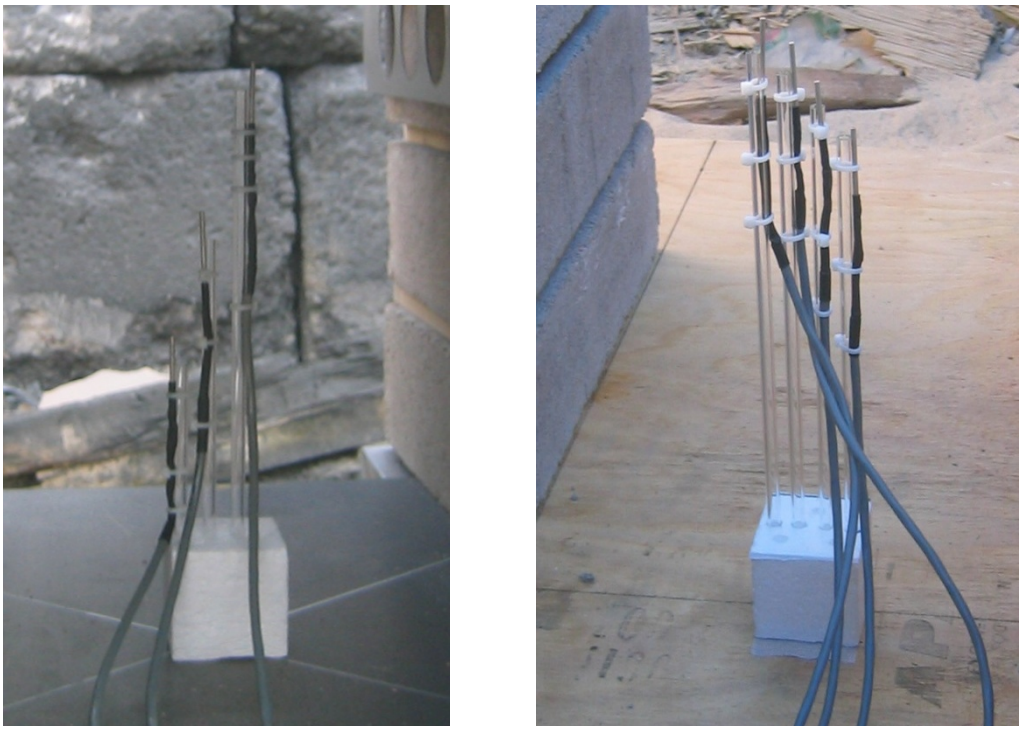

Figure 5.4: Time of Arrival pin arrays a) 2 1/2" (lower) spacing b) 1/2" (higher) spacing

5.2.3 VELOCITY COMPARISONS

In order to determine the effectiveness of the KEDD systems, a comparison must be made in determining the reduction in velocity. The comparison of velocities can be between the impact of two steel plates, between a baseline and KEDD tests, or even comparing different KEDD tests. The reduction in velocity is determined by calculating the difference between the reference test and the comparison test, and then dividing that by the reference test. This equation is shown below. This equation is used any time the percent reduction in velocity is discussed.

$$\boldsymbol{reduction\ in\ velocity} = \frac{\boldsymbol{reference\ test\ \ veloicty - comparison\ test\ velocity}}{\boldsymbol{reference\ test\ \ velocity}}$$

5.3 2 PLATE TEST

5.3.1 INTRODUCTION

Fourteen field tests (Tests 6 - 8 and 11 - 21) were performed using the 2 Plate Test set-up. Baseline (as-built) tests were conducted and compared to tests using one of the five different KEDD locations that were shown in a previous section. The effectiveness of the KEDD was determined by comparing the type of damage that occurred, and the velocity of the flyer plates formed in the second plate. Simplified momentum calculations were developed to determine a "lower bound" estimated velocity of the second plate. These velocities were compared to the velocities determined in the field test. A series of CTH calculations were performed, by the Author, to compare to the data gathered from the field tests presented herein. An additional analysis was performed that compared the effectiveness of a solid wall of water to the three rows of KEDD's on top test set-up. The results from all of these tests and calculations are presented below.

5.3.2 TEST SET-UP

These tests were performed using two 1/4" steel plates. Each plate was spaced 12" above the plywood base, and then 12" above the bottom plate. A schematic drawing and a photo of the test set-up can be found in Figure 5.5.

5.3.3 CALCULATION SET-UP

Computational analyses were performed, by the Author, on seven different set-ups using the hydracode CTH in order to predict the outgoing velocity of the secondary flyer plate (or second plate). This code was written by the Sandia National Laboratories and is a well known, well documented Eularian hydracode(1). In order to evaluate the phenomenology of

the KEDD system five different set-ups, used in the scaled tests, were analyzed. In addition to these set-ups, two additional layouts were analyzed using CTH. They include a baseline calculation and a solid wall of water calculation.

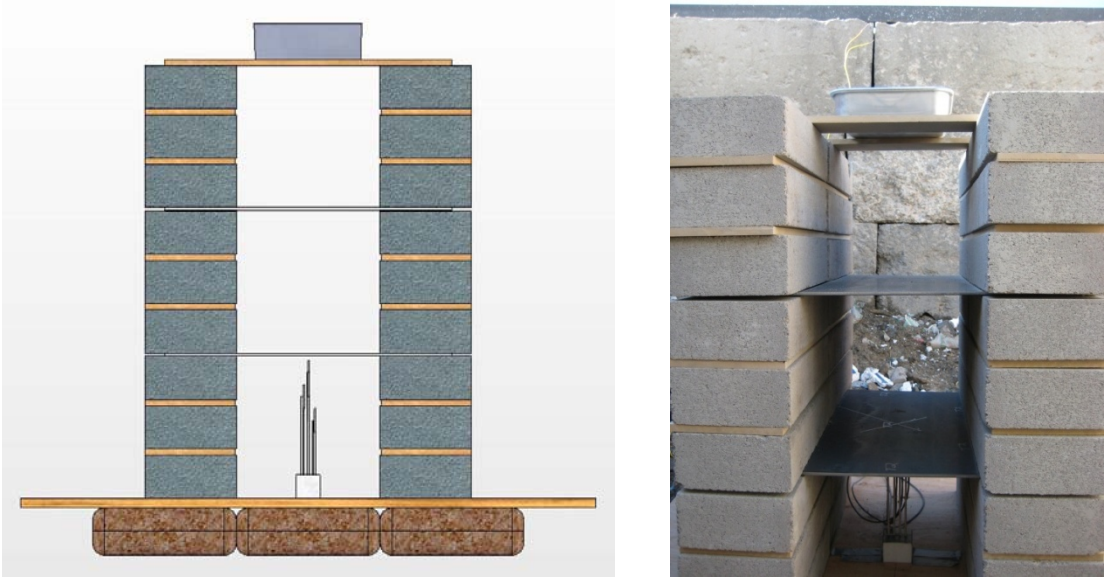

Figure 5.5: 2 Plate Test set-up – schematic drawing

Each of these analyses was set-up in the same manner. They evaluated a 9” section of the first and second steel plate (in the X direction). The height of the test set-up was 12” (in the Y direction), which was the same distance in the field test. The thickness of the first and second steel plates was 1/4”. The radius of the KEDD was 1” and they were spaced at 3”, on center. (Figure 5.6) The calculations were two dimensional rectangular. Using the traditional eularian “flat mesh” with a size of 16 in. (40.64 cm) in the X direction and 18 in. (45.72 cm) in the Y direction. This spacing yields a mesh size in both the x and y direction was 0.0315 in., which corresponds to almost 8 divisions through the thickness of the plate. Outflow boundary conditions were used on all sides of the mesh. In order to keep these calculations consistent with previous calculations performed by Karagozian & Case the following material

models were used for this test. The water material was modeled using the Sandia National Laboratories Equation of State (EOS) for state. It accounts for the thermodynamic behavior of the water. The steel material was modeled using the widely used Mie-Grüneisen equation of state. The deviatoric response of the material was modeled with a von-Mises perfectly-plastic model. Since the purpose of these calculations was to determine the behavior of the KEDD system, not the steel behavior, a Mie- Grüneisen model is sufficient.(1). Initial calculations, show that the steel was sheared in different locations from the formation of high speed ejecta; however, the field tests demonstrated that this was not the case. In order to achieve results that reflected the results seen in the field experiments, the strength of the steel was artificially increased.

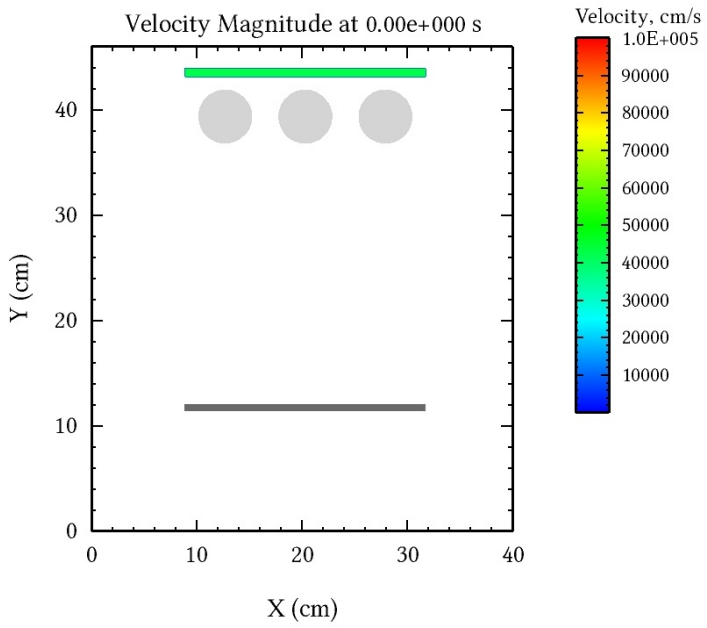

Figure 5.6: 2 Plate Test, 1 row KEDD top test set-up

5.3.4 SIMPLIFIED MOMENTUM CALCULATION

The explanation of this calculation was presented in Chapter 1 and is repeated here for convenience.

Field tests are an important tool, at this stage, in improving and validating the KEDD concept. It is also necessary to correlate the test data with simplified calculations. The actual behavior between the steel plates and the KEDD can only be determined by solving the momentum and energy equations, simultaneously. To this end, a simplified, "lower bound" estimation has been developed. In order to simplify this calculation an estimation of the energy term is assumed through the use of a Coefficient of Restitution (COR). This value was determined based on data gathered in the scaled 2 Plate Tests These tests showed a 40% reduction in velocity when the first plate impacts the second plate, (which will be discussed in the following section) which led to a COR (for these calculations) of 60% or (1-0.4). This simplified, "lower bound" calculation was set-up in a two step process. The first step is to determine the velocity of the mass of the steel plate and the KEDD after impact, as shown in Figure 5.7.

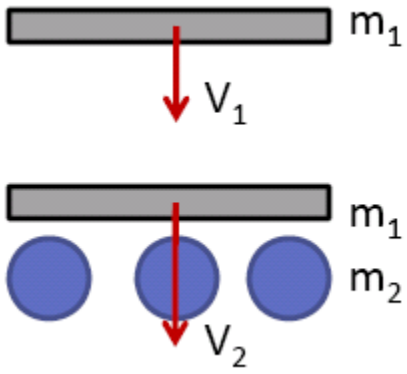

Figure 5.7: Momentum calculation – First step

Momentum is calculated by the mass of the system multiplied by the velocity, and it must always be conserved. The momentum of the flyer plate before it impacts the KEDD system must be equal to the momentum after impact with the retrofit device. Let the mass of the flyer plate be m_1 and its initial velocity is V_1. The mass of the KEDD system is m_2 and the outgoing velocity of the impacting mass and the KEDD system is V_2. (For calculation purposes, the reader is reminded that the steel plate had a length of 9" and was ¼" thick. The KEDD's were 2" in diameter and filled with water.) The momentum equation is:

$$m_1 V_1 = (m_1 + m_2)V_2 \quad \text{or} \quad V_2 = \frac{m_1}{m_1 + m_2} V_1 \tag{4.1}$$

The next step in the calculation would be to assume that all of the water is dissipated before the first plate impacts the second plate, which is shown pictorially in Figure 5.8. It assumes that a COR of 60% is used, as explained above, and shown below. This accounts for the energy that is absorbed by the plate on plate impact. The equation for the outgoing velocity of the second plate, V_3, is

$$V_3 = (1\text{-}0.4)V_2 \tag{4.2}$$

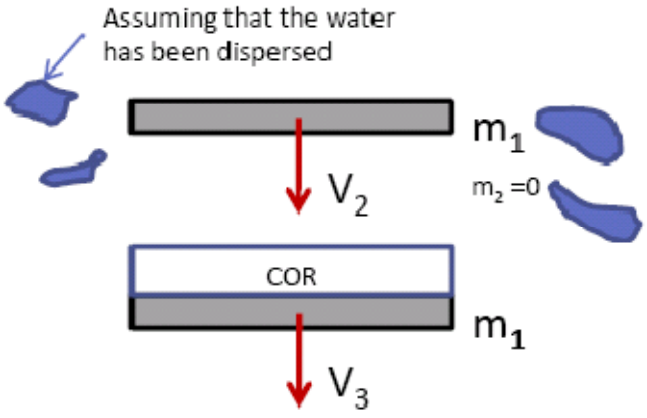

Figure 5.8: Momentum calculation – Second step

5.3.5 BASELINE TEST

5.3.5.1 FIELD TEST RESULTS

Four baseline tests were performed (Test 6, 13, 14, and 18). They were tested with an equivalent to 0.023X pounds of TNT at a close standoff distance and are shown in Figure 5.5. The four tests behaved in a similar manner. The first plates fragmented and formed many individual flyer plates. They tended to behave in a brittle manner with the plate shearing along the edges where they were supported by the solid CMU blocks. (Figure 5.9) After the fragmentation, the initial flyer plates impacted the second plate. These plates failed in a ductile manner, exhibited by the bending and petalling of the plate. (Figure 5.10) The Tests 6 and 13 formed secondary flyer plates that were similar; however, the secondary flyer plate formed in Test 14 was very small, and no flyer plate was located in Test 18. The initial force of the explosion fractures the first plate very rapidly, as shown by: the smaller fragments, the shearing along the edges, and the lack of deformation. As the different fragments impact the second plate they cause more ductile failures and deformation. This could be attributed to the impact on the second plate occurring from the velocity of the fragments and less from the effects of the explosion. This allows the plate to deform, petal, and the secondary flyer plate to separate.

Time of Arrival (TOA) pins captured the velocities of the secondary flyer plates. Two of these velocities varied drastically from the other two tests. Test 6 determined that the average velocity of the secondary flyer plate was 1,036 ft/sec. using the “higher spacing” arrangement of TOA pins. The Test 13 used the “lower spacing” and had a much lower average velocity of 635 ft/sec. A profile showing the different calculated velocities at the distances between the TOA pins is shown in Figure 5.11. The “X” on the plot show the

velocities while the line demonstrates how the velocity is decreasing as the plate/fragment moves through the cell. Test 14 had an average velocity of 1,083 ft/sec; which is in agreement with the Test 6. The average velocity of Test 18 was much higher than all of the previous tests. The TOA pins determined that the velocity of the second plate was 1,605 ft/sec. It is unclear why this is so high. The velocity data from these tests is shown in Table 5.2 and as a bar chart in Figure 5.12.

Figure 5.9: Baseline tests, first plate a) Test 6 b) Test 13 c) Test 14 d) Test 18

Figure 5.10: Baseline tests, second plate a) Test 6 b) Test 13 c) Test 14 d) Test 18

Table 5.2: 2 Plate Test baseline velocity data

Test	Interval Velocity	Average Velocity of Second Plate	Velocity of First Plate	Velocity Change between Plates
6	1096 ft/sec 1126 ft/sec 887 ft/sec	1036 ft/sec	1764 ft/sec	41%
13	593 ft/sec 659 ft/sec 653 ft/sec	635 ft/sec	1764 ft/sec	64%
14	1302 ft/sec 1096 ft/sec 850 ft/sec	1083 ft/sec	1764 ft/sec	39%
18	1984 ft/sec 1225 ft/sec	1605 ft/sec	1764 ft/sec	9%

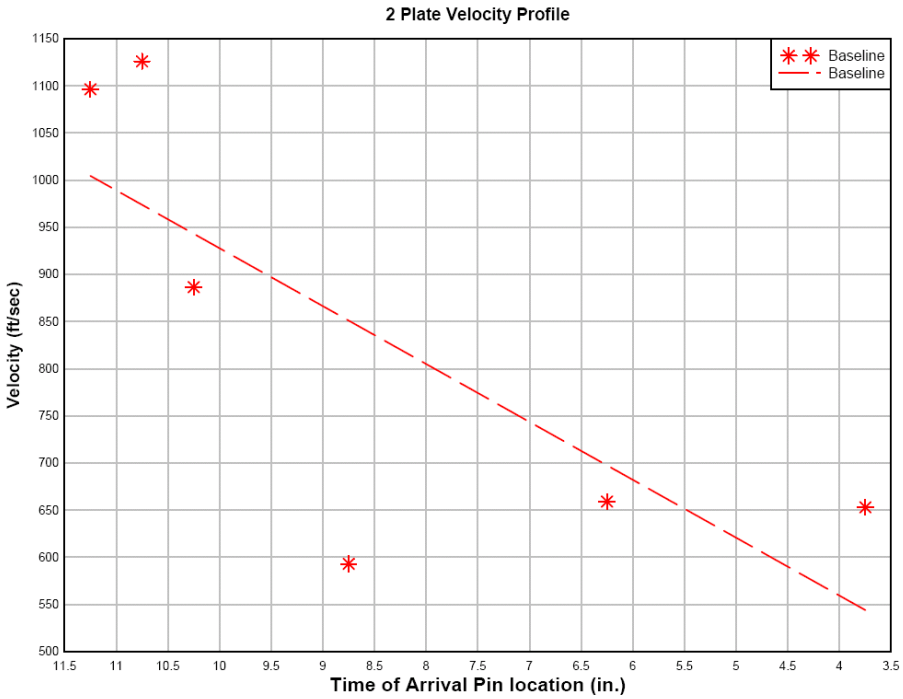

Figure 5.11: Velocity profile for 2 Plate Tests 6 and 13

The reduction in velocity due to the formation of a secondary flyer plate from the initial flyer plate needs to be determined before the effectiveness of the retrofit device, or KEDD system, can be evaluated. Through the use of TOA pins in the third Calibration Test, the velocity of the fragments from the first plate was determined to be 1,764 ft/sec. If that is assumed to be a true value of the velocity of the plate, since there was only one test it is not verifiable, then the percentage of velocity that is absorbed through the impact and deformation of the plates can be determined. Table 5.2 shows the percent difference in velocity between the plates. Ignoring the data from Test 13 due to the location of the TOA pins, and Test 18 due the unusually high velocity, the average reduction in velocity from the impact of the fragments of the first plate to the second plate is 40%. In future discussions the baseline velocity will be the average of Test 6 and 14; which is 1,060 ft/sec.

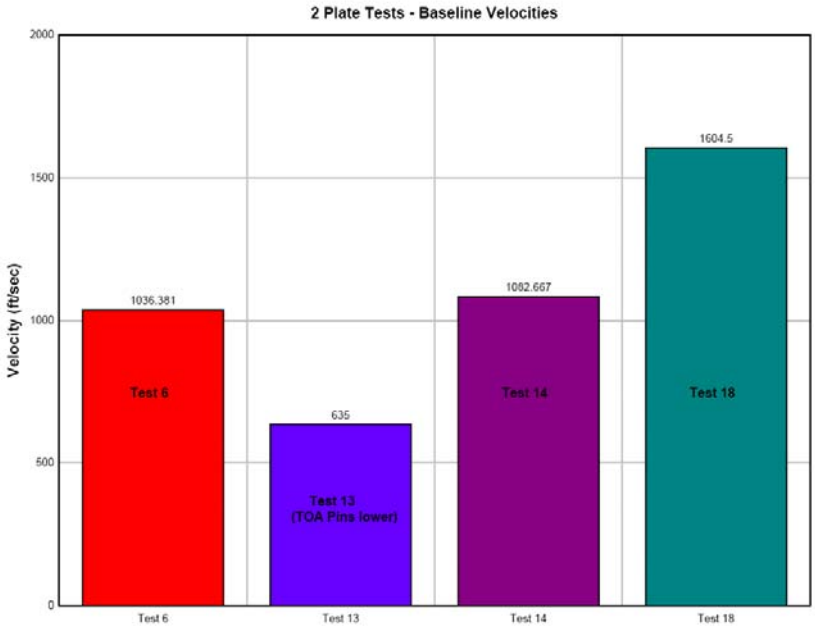

Figure 5.12: 2 Plate Tests baseline velocities

5.3.5.2 SIMPLIFIED CALCULATIONS

The baseline calculation was conducted first. Its purpose was twofold: 1) to calibrate the model with the test results; and 2) to estimate what incoming velocity of the flyer plate would lead to an outgoing velocity near 1,060 ft/sec. (32,309 cm/s). This velocity was chosen to correspond with the baseline field tests. The test set-up had a 1/4" steel plate located 12" from the second steel plate as shown in Figure 5.13.

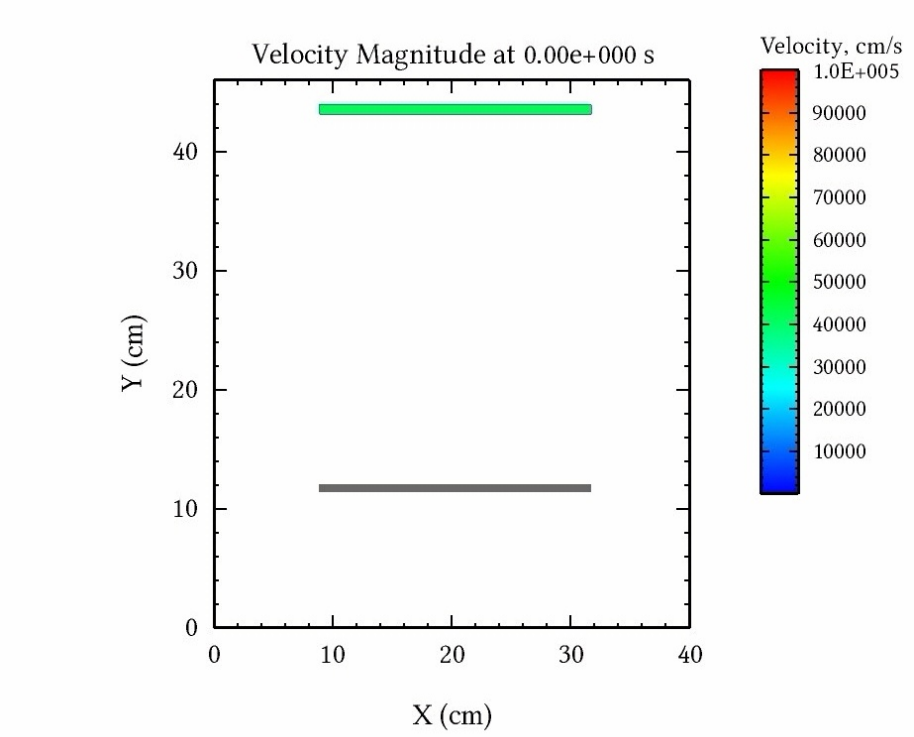

Figure 5.13: 2 Plate Test, baseline test set-up

Three plots from the CTH calculations of the baseline test can be seen in Figure 5.15. The color in the plots represent the velocity magnitude of the specimen, in this case the steel. The velocity magnitude is computed by the square root of the sum of the squares of the X and Y velocity. This value is always a positive value as demonstrated by the color map in these

plots. The map to the right of the plots shows the velocity magnitude for each cell in the calculation. The range of this map is from a minimum value of 0.0033 ft/s (0.1 cm/s) to a maximum value of 328,084 ft/s (or 1 km/s or 10,000,000 cm/s). These maps will stay at the same level for all tests. If a plot shows signs of purple, which will be seen in the KEDD calculations, then the velocity of that particular cell has exceeded 1 km/s. For all tests the incoming velocity of the top plate is in a green range and correlates to a velocity of 1,400 ft/s (42,672 cm/s). This velocity would yield an outgoing velocity of 1,034 ft/s (31,516 cm/s), which is a 2% difference between the computational and test results. A plot of the velocity of the first, or top, and second, or bottom, plate is shown in Figure 5.14.

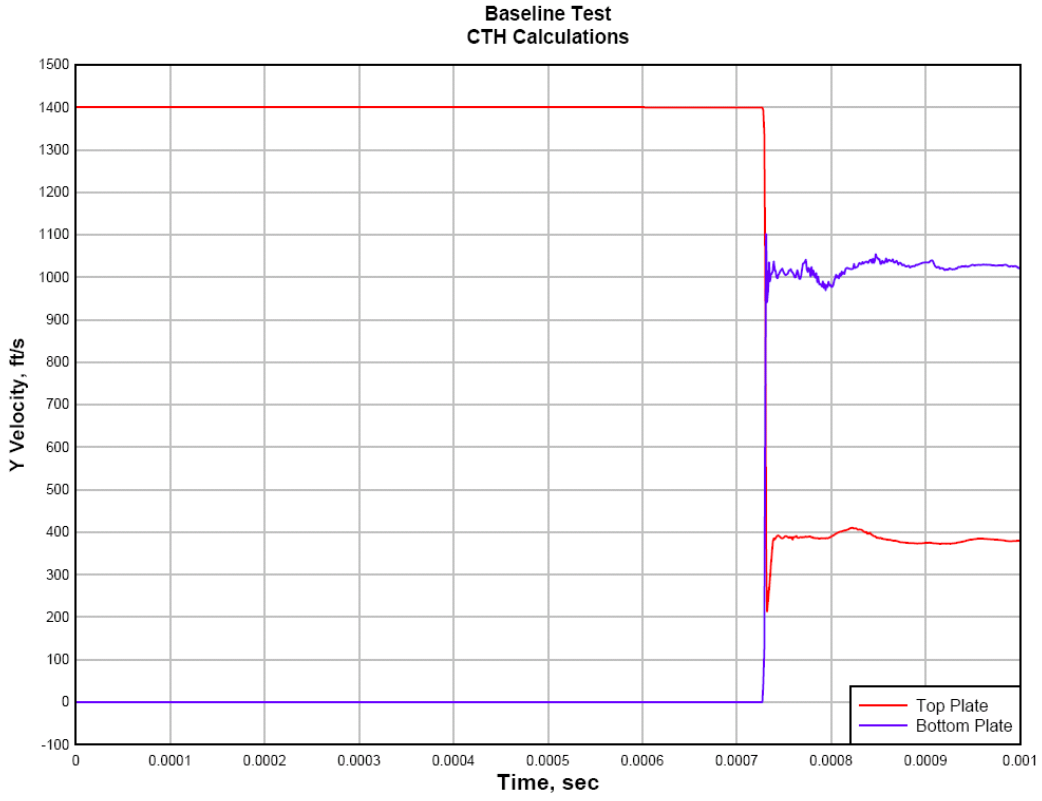

Figure 5.14: 2 Plate Test, baseline – velocity profile of top and bottom plate

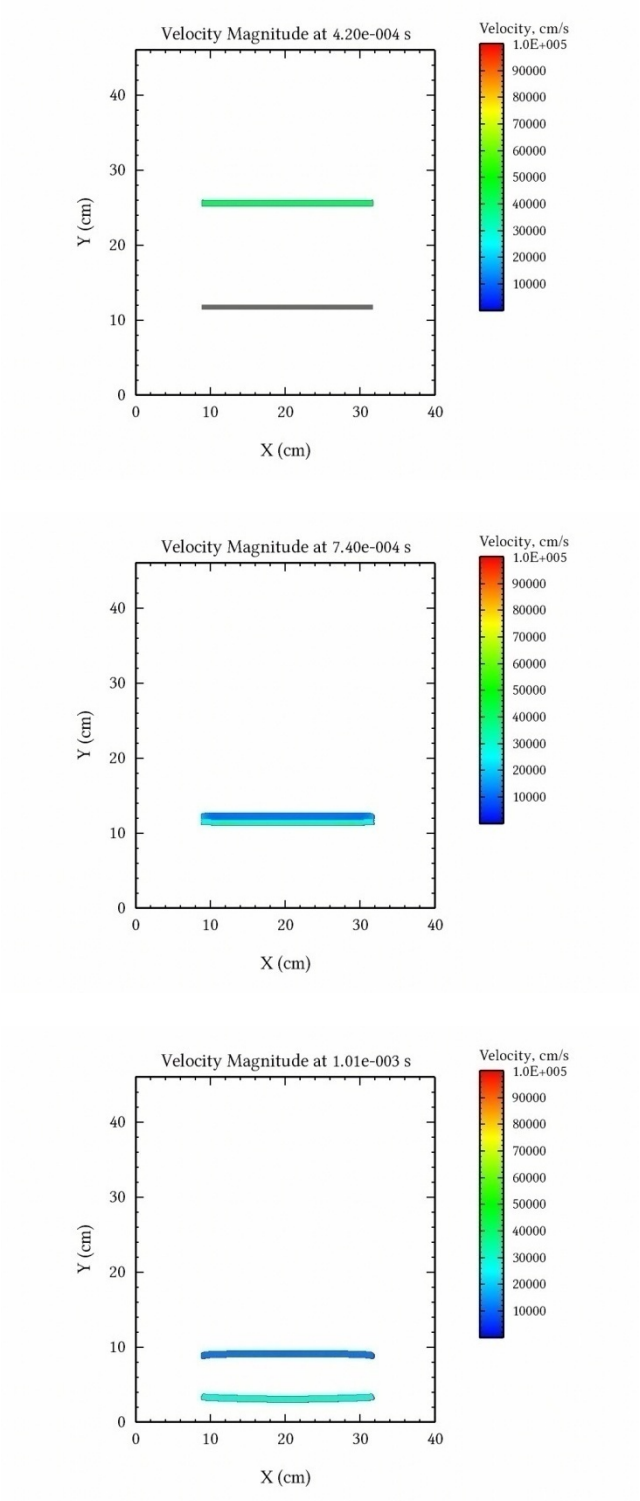

Figure 5.15: 2 Plate Test, baseline – velocity magnitude

5.3.6 KEDD ON TOP

5.3.6.1 FIELD TEST RESULTS

Tests 8 and 11 had a row of KEDD's on the top. Professor Hegemier chose this layout. He felt that the KEDD system did not have to be compressed between two plates to be effective. These specimens were tested with an equivalent to 0.023X pounds of TNT at a close standoff distance as shown in Figure 5.16. The two specimens behaved in a similar manner. Due to the force of the explosion, the first plate exhibited both ductile and brittle failure modes. It bowed significantly (ductile) and had a large flyer plate form in the center of the plate (brittle). The failure modes of the first plates are different than the baseline tests. The ductile deformation absorbs significant energy, but more importantly the plate is intact. This could aid in the load carrying capabilities of the structure after an explosive event. If this trend continues, in future tests, the ability of the KEDD system to alter the failure mechanisms of the first plates will be a very fortunate advantage to the system. The initial flyer plate impacted the second plate where it caused the plate to release from its support. The first plates are shown in Figure 5.17 and the back sides of the second plates are shown in Figure 5.18. The rest of the plate was folded in half from the force of the incoming flyer plate. If the plate was more securely fastened to the supports, this type of damage might not have occurred. The important thing to note is that very little plate cracking occurred. In Test 8, the second plate showed no signs of fracture. The plate in Test 11 had one large fracture on the back side of the plate; however, it contained the flyer plate.

Time of Arrival (TOA) pins captured the velocities of the second plates. The Test 8 determined that the average velocity was 453 ft/sec utilizing the "higher spacing" of the TOA pins. Test 11, using the "lower spacing" determined that the average velocity was 258 ft/sec.

A profile showing the different calculated velocities at the distances between the TOA pins is shown in Figure 5.19. The “X’s” on the plot show the velocities while the line demonstrates how the velocity decreased as it moved through the cell.

Similar to the previous test, a bar chart showing the different average velocities for these tests is furnished in Figure 5.20 where a baseline velocity is used for comparison. Table 5.3 shows the reduction in the velocity of the second plate compared to the average velocity determined from the baseline tests. For Test 8, the reduction in velocity is 57%, in Test 11, the reduction in velocity is 76%. The calculation of the average baseline velocity of 1,060 ft/sec only uses the “higher spacing” arrangement of TOA pins. For comparison purposes the velocity data from Test 11 should be ignored, since the baseline velocity data for the “lower spacing” TOA pins were also discarded. Therefore, the reduction of velocity for these tests is 57% when compared to the baseline tests and the average velocity for this test series is 453 ft/sec.

Figure 5.16: KEDD on top test set-ups a) Test 8 b) Test 11

Figure 5.17: KEDD on top, first plate a) Test 8 b) Test 11

Figure 5.18: KEDD on top, second plate a) Test 8 b) Test 11

Table 5.3: 2 Plate Tests, KEDD on top velocity data

Test	Interval Velocity	Average Velocity	Average Baseline Velocity	Reduction in Velocity by KEDD
8	239 ft/sec 541 ft/sec 579 ft/sec	453 ft/sec	1060 ft/sec	57%
11	434 ft/sec 191 ft/sec 148 ft/sec	258 ft/sec	1060 ft/sec	76%

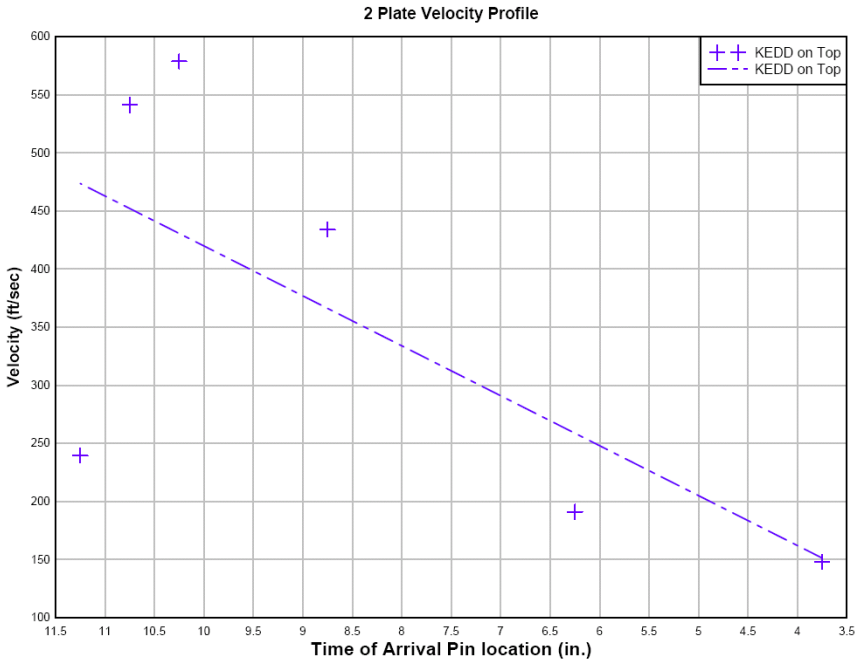

Figure 5.19: Velocity profile for KEDD on top Tests 8 and 11

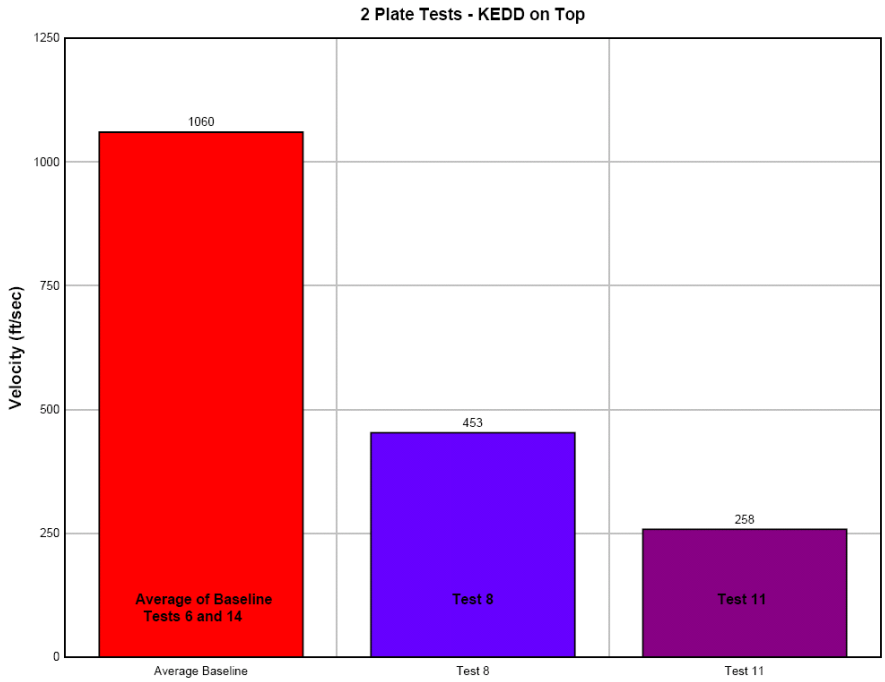

Figure 5.20: 2 Plate Tests KEDD on top velocities

5.3.6.2 SIMPLIFIED CALCULATIONS

The 2 Plate Test configuration with one row of KEDD's on top used the same model set-up as previously where the incoming velocity of the steel plate was 1,400 ft/sec. The test set-up, is shown in Figure 5.21. The first steel plate is placed 3" above the center of the KEDD. Each KEDD is 2" in diameter and is placed 3" on center. The KEDD container is not modeled, only the water inside the KEDD.

A series of six plots from this calculation are shown in Figure 5.23. They show the velocity magnitude of each cell [Figure 5.23 (a)] and a representation of the different materials throughout the calculation [Figure 5.23 (b)]. In Figure 5.23 (b), the first plate is red in color, the second plate is blue, and the water is shaded as grey. These plots were taken at the same time step as the velocity magnitude and are used to show where the different materials are in

the calculation. These calculations accurately predict some of the phenomenology inherent in the KEDD system which correlates with the laboratory data.

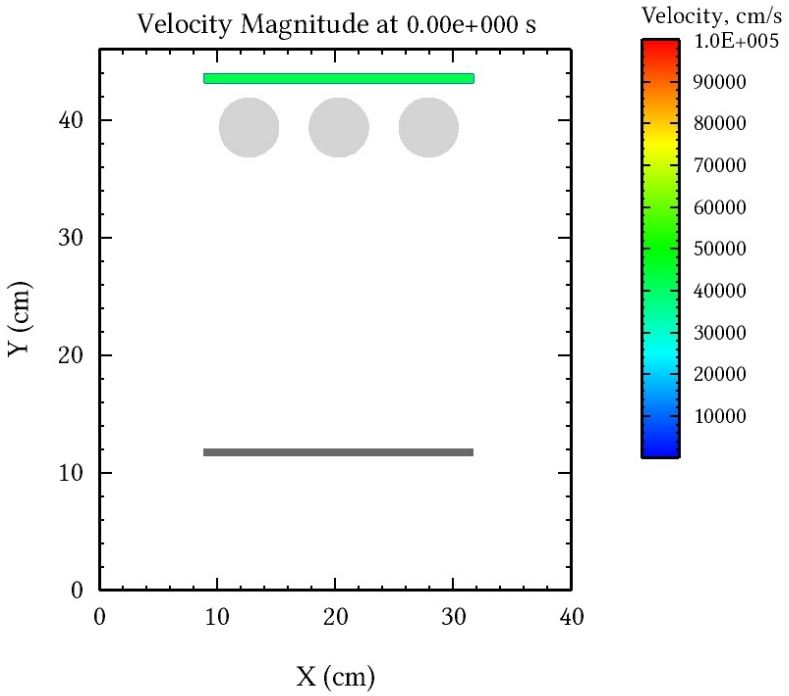

Figure 5.21: 2 Plate Test, one row of KEDD's on top, test set-up

The first row of computational frames shows the formation of the high speed ejecta. The tips of the jets moving outward from the KEDD's, in the X direction, have a velocity around 3,280 ft/sec, or 1 km/sec and are red in color as seen in Figure 5.22. The velocity of these transverse jets is over 2.3 times the incoming velocity of the first plate. These jets continue to form as the calculation progresses and the velocity of the first plate decreases. Through the formation of these transverse ejecta, the water mass is able to dissipate as shown in the third row of plots. There is significantly less water between the steel plates when they are close to impact than there was at the beginning of the calculation. This ability of the water

to disperse is very important in the development of the KEDD system and will be discussed further in the next section involving the KEDD on the bottom calculation.

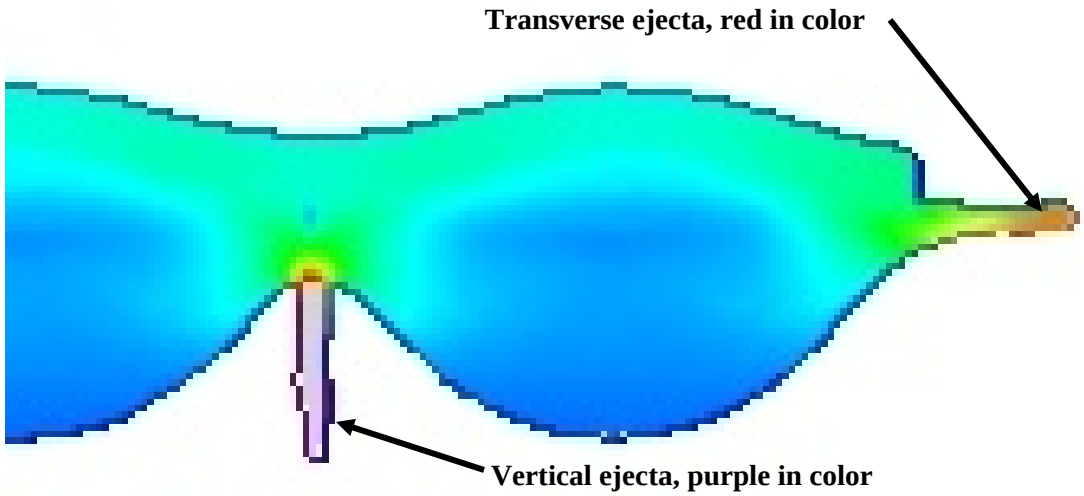

Figure 5.22: 2 Plate Test, one row of KEDD's on top close up of velocity magnitude

While this calculation shows the formation of the transverse ejecta that was expected based on the experimental tests, it does not capture the proper behavior of the vertical ejecta. The transverse jets, formed in these calculations, are easily observed along the outer KEDD's. That same phenomenology is occurring between the inner edges of the KEDD's. Here two jets will form, then impact each other combining to form vertical ejecta. Together the velocity of these jets increase as shown in the first plot of Figure 5.23(a) and Figure 5.22. The calculation shows that these two jets combine together perfectly and with such kinetic energy that the jets shear through the steel plate. In order to defeat this behavior, the strength of the steel was artificially increased. These vertical jets are forming in this manner due to the artificial constraints in the 2-D calculation, it is not likely that they would occur in a 3-D calculation.

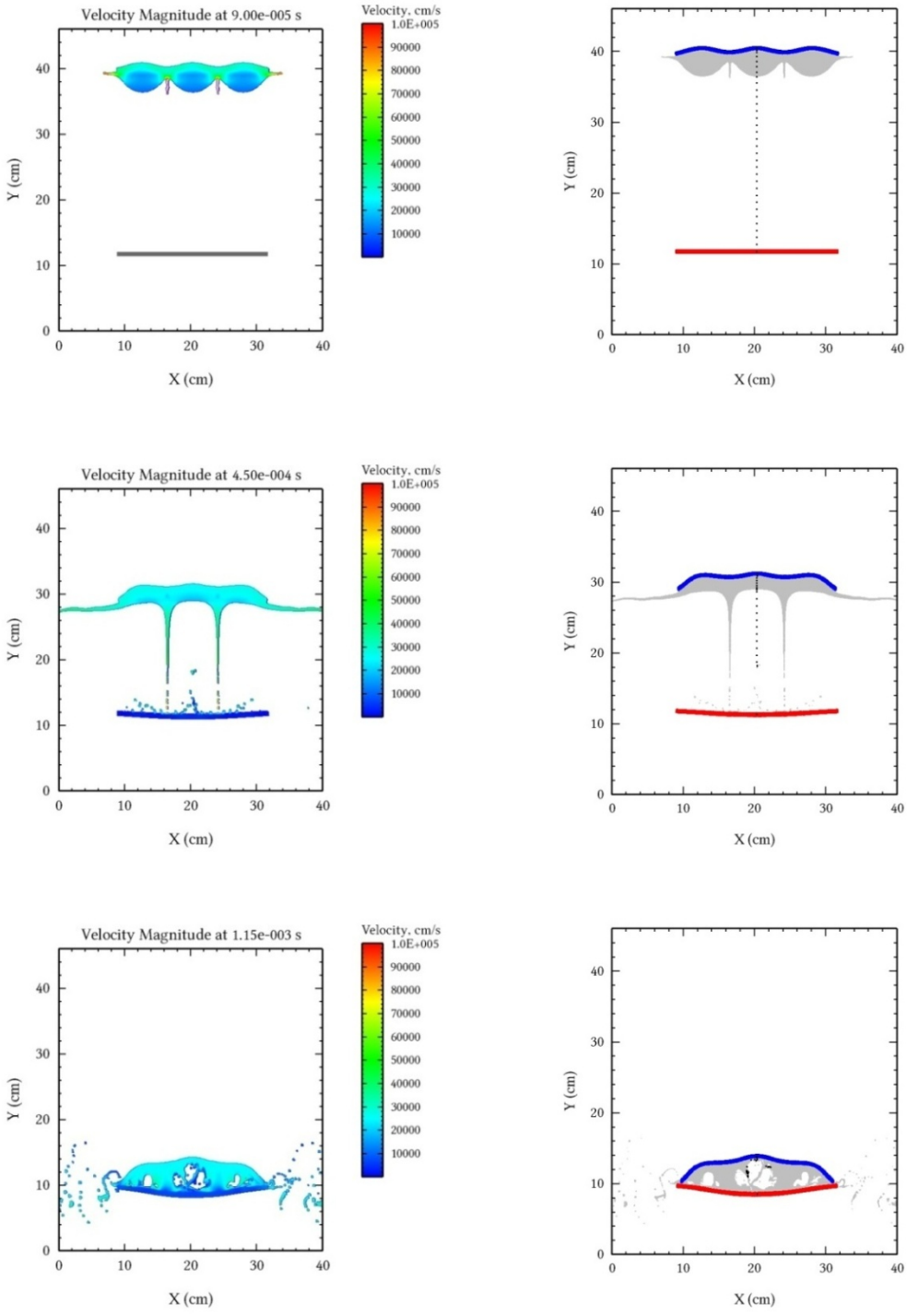

a) Velocity magnitude **b) Materials**

Figure 5.23: 2 Plate Test, one row of KEDD's on top

The CTH calculations are a useful tool to determine some of the behavior of the KEDD system. Without such calculations there is no basis for understanding what is occurring inside one of these cells. To simplify the calculations, many effects were ignored like the charge and its container along with the interaction of the shock wave with the steel plate and the KEDD system.

These calculations show the expected formation of the transverse high speed ejecta and how the dispersal of the water occurs. They also captured velocity data with regards to the first and second steel plate as shown in Figure 5.24. The incoming velocity of the first plate was 1,400 ft/sec (42,662 cm/s). The resulting outgoing velocity of the second plate is 670 ft/sec (20,422 cm/s). This is a reduction in velocity due to one row of KEDD's on top, of 52%. The velocity of the second plate determined from the field tests was 13,807 cm/s (453 ft/sec). The difference in the reduction in velocity of the field tests to the calculations varies by 48%.

The velocity profile shown in Figure 5.24 demonstrates how the KEDD system decreased the speed of the first plate. Upon impact with the KEDD there is a large decrease in velocity. Additional deceleration of the first plate occurs before the velocity levels off. The second plate stays near the same velocity until impact with the first plate. The second plate exhibits an increase in velocity from the interaction of the vertical water jets. The sharp changes in the velocity of the plates, near the end chart, show when the two steel plates impact each other.

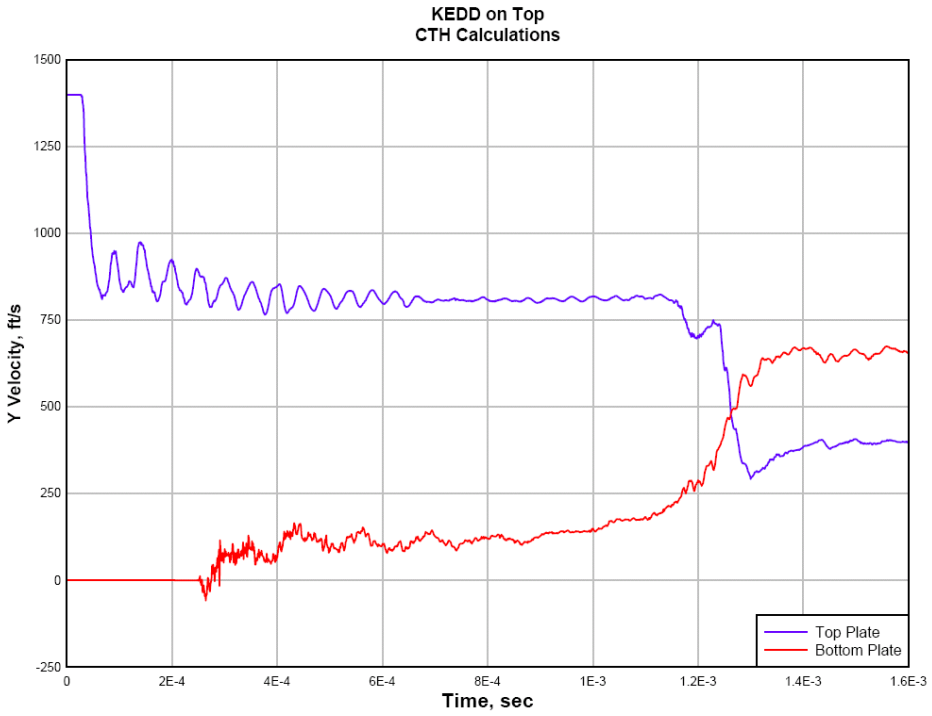

Figure 5.24: 2 Plate Test, one row of KEDD's on top – velocity profile of top and bottom plate

This, simplified "lower bound" momentum calculation furnished an outgoing velocity of the second plate of 690 ft/sec. When this velocity is compared to the velocity of 453 ft/sec determined in the field test there is a 34% difference. If the field test is compared to the velocity determined in the CTH calculations, 670 ft/sec there is a 32% difference. A plot of the different velocities for one row of KEDD's on top is shown in Figure 5.25.

This method appears to offer a good approximation of the behavior. However, it still does not take into account the additional kinetic energy that is absorbed in the plastic deformation and failure of the steel plates and their support structures. This is demonstrated when the results from the simplified calculation is compared to the actual field tests where the average velocity of the second plate was determined to be 453 ft/sec.

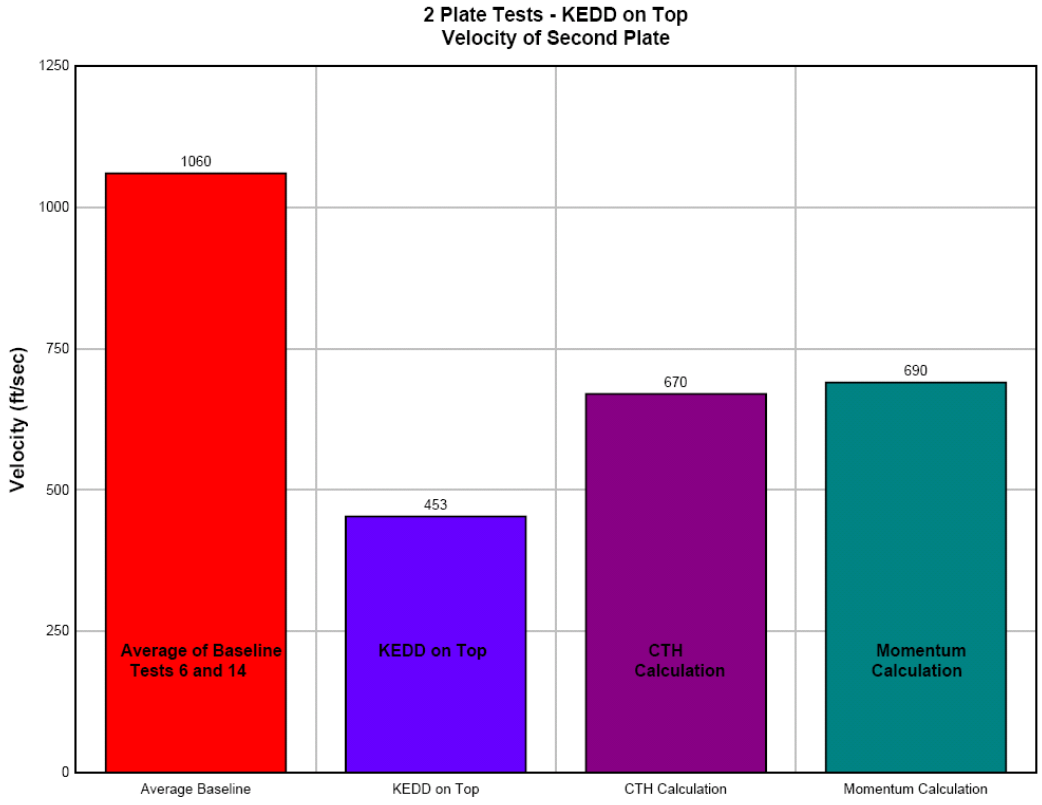

Figure 5.25: KEDD on top – 1 row, velocities (field, CTH, and Calculation)

5.3.7 KEDD ON BOTTOM

5.3.7.1 FIELD TEST RESULTS

Tests 7 and 12 had a row of KEDD's on the bottom. The initial layout of this KEDD system was chosen by the Author. The Author believed that the only way to activate the KEDD system was through compression between the flyer plate and the steel plate, similar to the manner that the KEDD system was tested in the laboratory. (See Section 4.3) These specimens were tested with an equivalent to 0.023X pounds of TNT at a close standoff distance as shown in Figure 5.26. The first plates behaved similarly for these tests; however,

the second plates did not. Due to the force of the explosion the first plate behaved in a slightly ductile manner before a large flyer plate was created in the center of the plate. In Test 7, the first plate sheared into two pieces, while in Test 12, the first plate was connected but bent in half. This could be attributed to the impact of the first plate with a steel pole accidentally left at the entrance to the test bed (Figure 5.27). After the initial flyer plate was formed, it impacted the second plate. The failure of the second plate resulted in a very ductile failure for both tests. In Test 7, the second plate nearly folded in half, while a large section of the plate separated from the rest of the plate on three sides. If this section had completed the shearing along its edges, a flyer plate of significant size would have been produced [Figure 5.28(a)]. Test 12 behaved in a different manner; in this test the second plate bent in half and severe petalling occurred in the center of the plate. A very small flyer plate, approximately 2" long, created [Figure 5.28(b)]. For both of these tests, the basic purpose of the KEDD system was shown to be effective; however, not as effective as the previous test. The flyer plate that was created was very small and traveled at lower velocities than the baseline tests.

The failure mechanisms of the first plates are different than the as-built tests. It is logical to assume, that their failure mechanisms would be similar if the only benefit of the KEDD was to decrease fragment velocity and absorb energy. Again, it is shown; that by placing the KEDD in the cell it affects the failure modes of the first plate, although not as significantly as a test with a KEDD on top. When the flyer plate impacts the KEDD its velocity and the force of the KEDD being activated, causes a very ductile failure. As the KEDD's are impacted, the water moves perpendicular to the incoming flyer plate. However, not all of the water is distributed that way; some of it is trapped between the flyer plate and the second plate which could account for some of the deformation, and will be shown below. A

significant amount of energy is absorbed in the deformation of the plates in the ductile manners shown in these tests, which aids in the decrease of the fragment velocity.

Figure 5.26: KEDD on bottom test set-ups a) Test 7 b) Test 12

Time of Arrival (TOA) pins captured the velocities of the secondary flyer plates which were very similar to each other. Test 7 used the "higher spacing" of TOA pins and determined that the average velocity of the second plate was 592 ft/sec. Test 12 utilized the "lower spacing" arrangement and determined the average velocity of the second plate was 626 ft/sec. It is interesting to note that the velocity of Test 12, over the lower TOA pins, was essentially the same as the baseline test over those same locations. This could be attributed to what fragment actually impacted the TOA pins. For Test 7, it would appear that the large fragment impacted the TOA pins, thereby, determining the average velocity of the plate. For Test 12, the small flyer plate was, most likely, the item that activated the TOA pins. It is possible that it was traveling at a higher velocity before it impacted the TOA pins.

Figure 5.27: KEDD on bottom, first plate a) Test 7 b) Test 12

Figure 5.28: KEDD on bottom tests, second plate a) Test 7 b) Test 12

A profile showing the different calculated velocities at the distances between the TOA pins is shown in Figure 5.29. The “X” on the plot shows the velocities while the line demonstrates the overall trend of those points, as determined by the program DPlot. This plot shows that in Test 7, which has the taller TOA pins, the velocity of the fragments captured over the first interval was over twice the velocity captured over the last interval. The velocity changes from 772 ft/sec to 694 ft/sec to 309 ft/sec each over a 1/2" interval. The initial deflection of the plate may account for the higher initial velocities (similar to Field Test 2). The slower velocities could come from the fragment that was formed. In contrast the velocities in Test 12 were consistent; they were 598 ft/sec, 614 ft/sec, and 667 ft/sec. The velocity data is shown in Table 5.4

A bar chart showing the different average velocities for these tests are shown in Figure 5.30, an as-built, or baseline, velocity was used as a comparison. Table 5.4 shows the reduction in the velocity of the second plate compared to the average velocity determined from the baseline tests. The percent reduction in these velocities is shown in the last column of the table. Through the use of the KEDD system the second plate, and its associated flyer plate, travels on average 43% slower than the baseline fragments.

Table 5.4: 2 Plate Test KEDD on bottom, velocity data

Test	Interval Velocity	Average Velocity	Average Baseline Velocity	Reduction in Velocity by KEDD
7	772 ft/sec	592 ft/sec	1060 ft/sec	44%
	694 ft/sec			
	309 ft/sec			
12	598 ft/sec	626 ft/sec	1060 ft/sec	41%
	614 ft/sec			
	667 ft/sec			

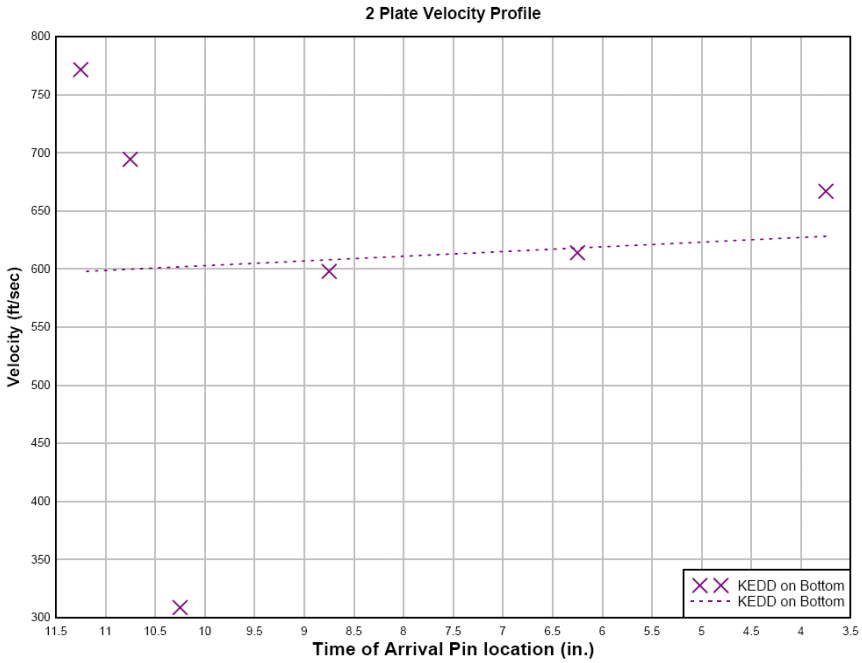

Figure 5.29: Velocity profile for KEDD on bottom Tests 7 and 12

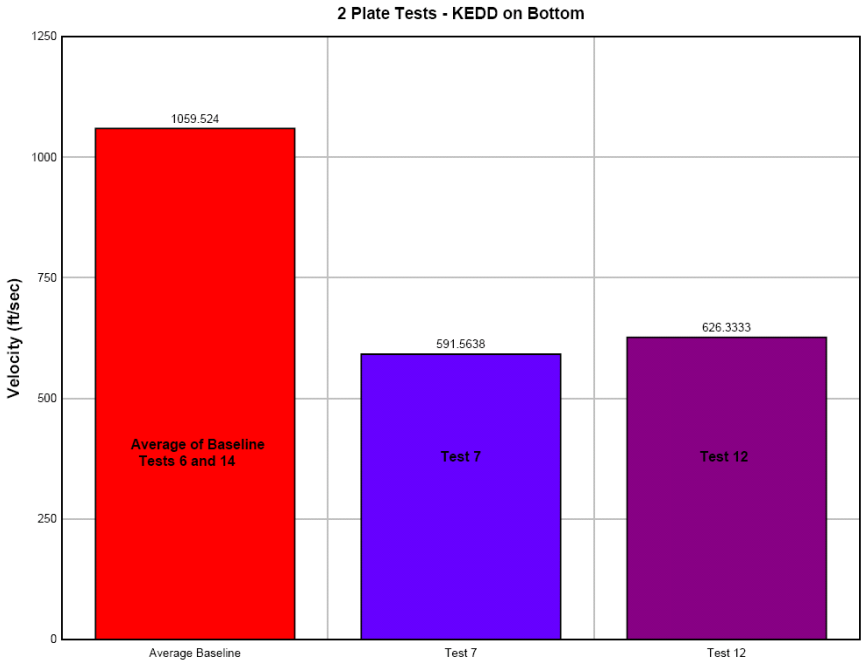

Figure 5.30: 2 Plate KEDD on bottom test velocities

5.3.7.2 SIMPLIFIED CALCULATIONS

This configuration employed the same model set-up as the baseline test where the incoming velocity of the first steel plate was 1,400 ft/sec. The test set-up, before the calculation begins, is shown in Figure 5.31. The first plate is placed 12" above the top surface of the second plate. The row of KEDD's is centered 3" above the second plate. Each KEDD is 2" in diameter and is placed 3" on center. The KEDD container is not modeled, only the water inside the KEDD.

A series of six plots from this calculation are shown in Figure 5.32. They are set-up in the same manner as the previous calculation. The first row of plots shows the formation of the high speed ejecta. The tips of the jets moving outward from the KEDD's, in the X direction, have a velocity around 1 km/sec, or 3,280 ft/sec, similar to the previous test. The KEDD is impacted close to the second steel plate, causing transverse jets to form; however, the water does not have as much time to dissipate as the previous test. Instead a large mass of water is impacted onto the second plate. The second and third rows of plots show that the majority of the water is trapped between the two plates and hence a re-direct of kinetic energy does not occur at the desired effect.

The ability of the water to form high speed transverse ejecta is of upmost importance when determining the ideal location of the KEDD system. When the KEDD is placed too close to the second plate, it is not as effective, as shown in the field tests. This calculation adequately predicted the outgoing velocity of the second plate, 658 ft/sec, according to the plot shown in Figure 5.33. When compared to the velocity determined in the field tests, 609 ft/sec, there is only an 8% difference. The simplified momentum calculations predict a second plate velocity of 690 ft/sec. This leads to a 5% difference between the CTH and simplified

momentum calculations and a 12% difference between the momentum calculation and the test. The different velocities from the tests and the calculations is presented in Figure 5.34.

In the simplified momentum calculations, it is assumed that all of the water has dissipated before the incoming plate impacts the outgoing plate; it yields the same outgoing velocity of the second plate despite the original location of the KEDD's.

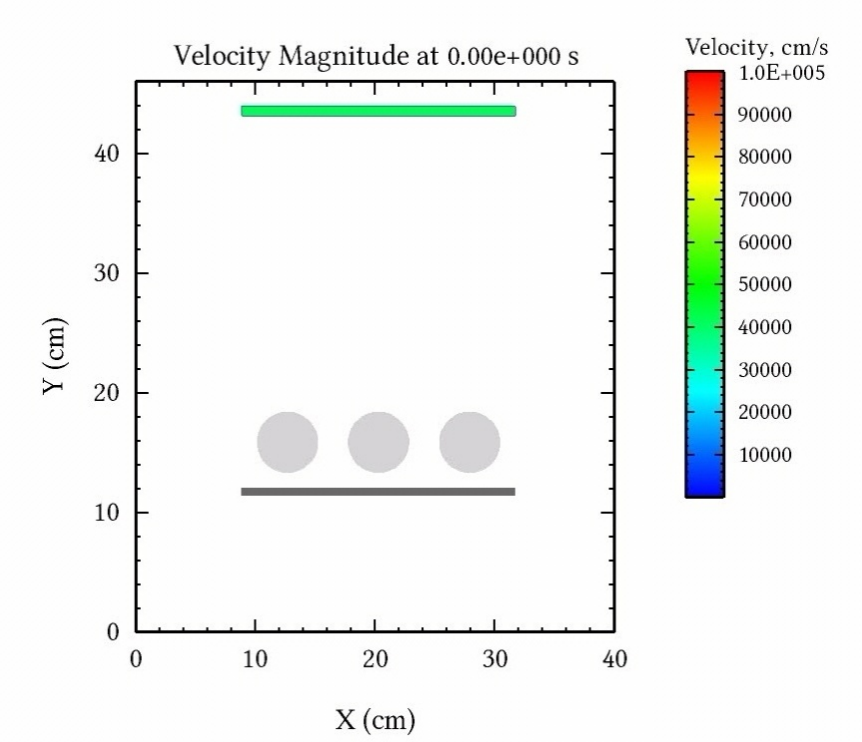

Figure 5.31: 2 Plate Test, one row of KEDD's on bottom, test set-up

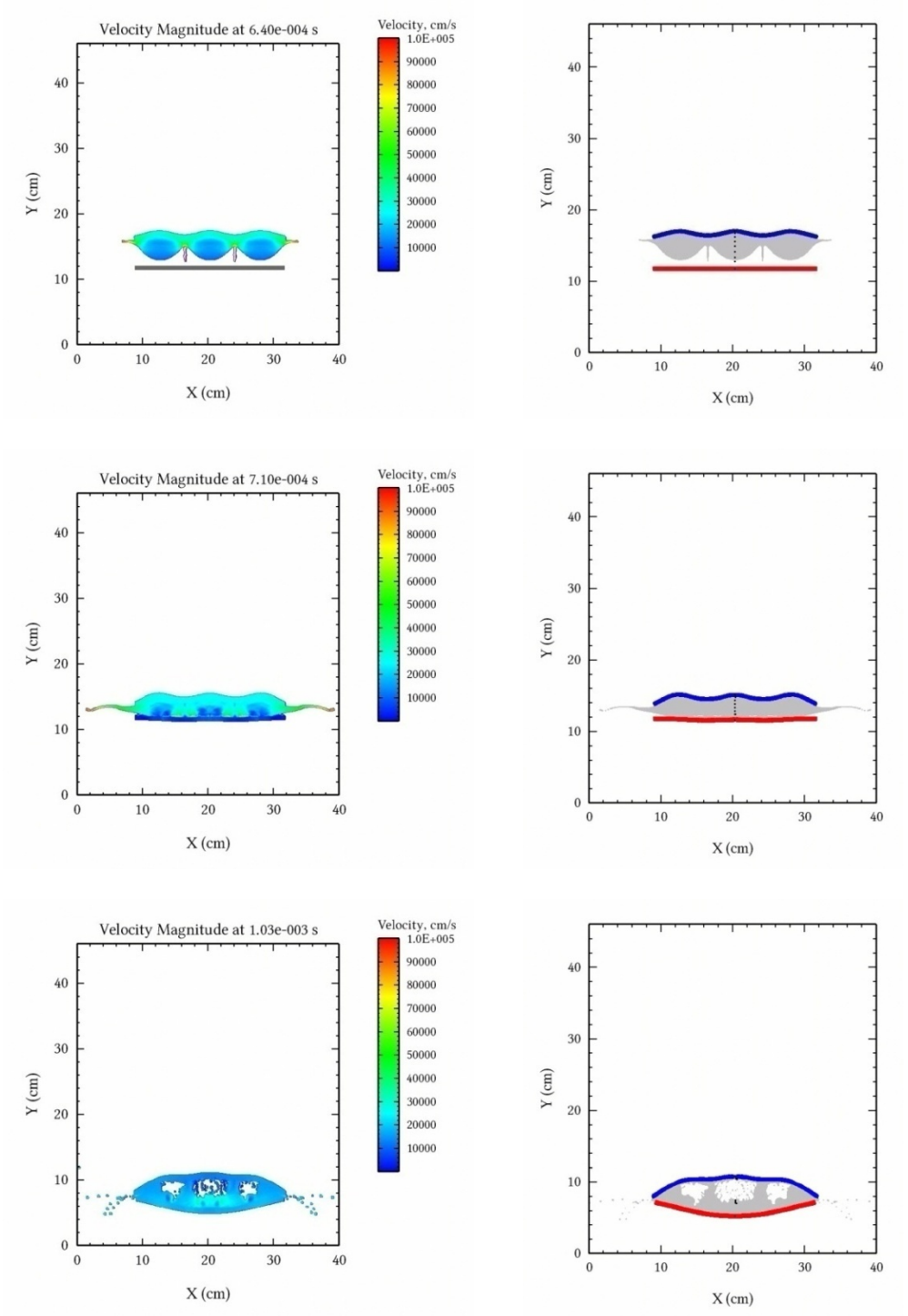

a) Velocity magnitude **b) Materials**

Figure 5.32: 2 Plate Test, one row of KEDD's on bottom

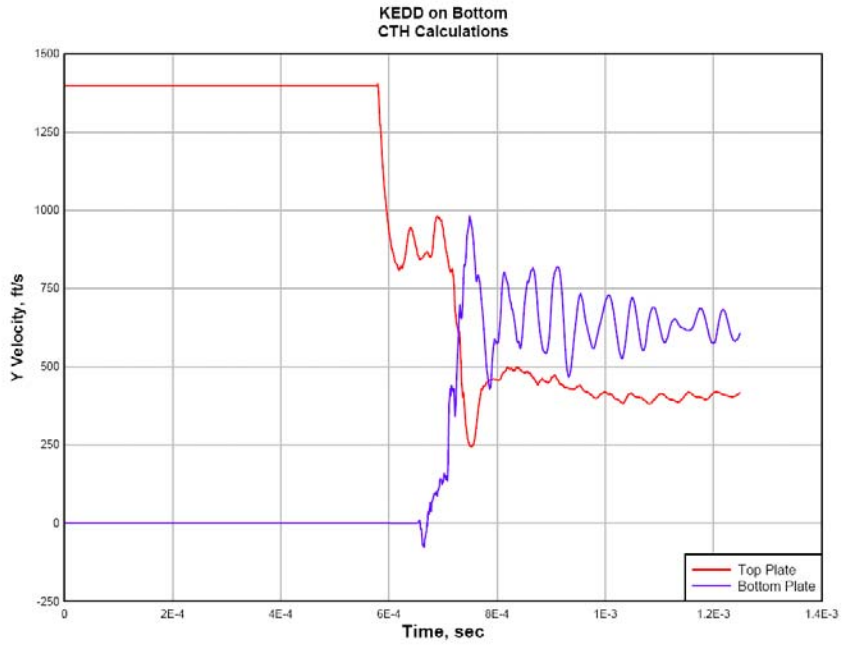

Figure 5.33: 2 Plate Test, KEDD on bottom – 1 row – velocity profile of top and bottom plate

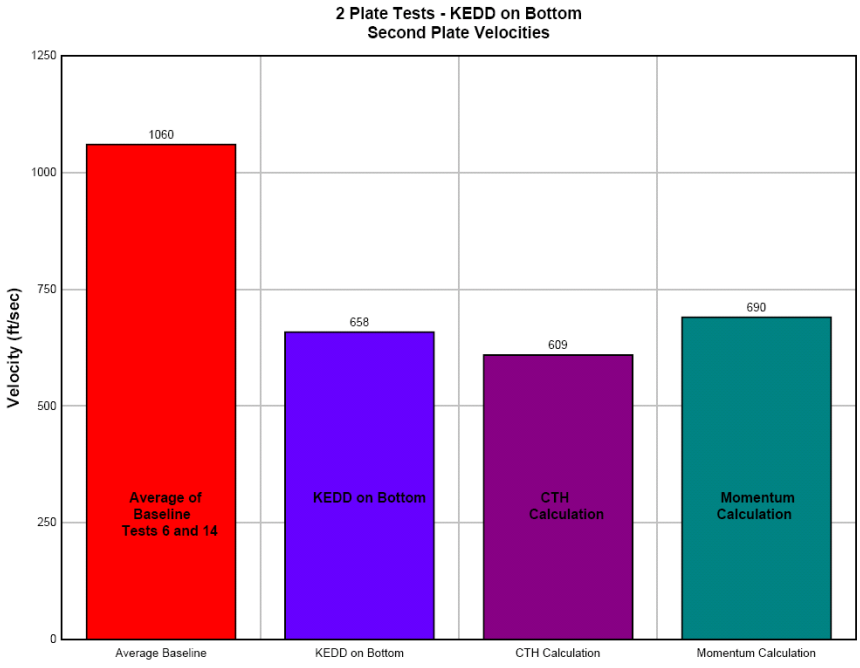

Figure 5.34: KEDD on bottom – 1 row, velocities (field, CTH, and calculation)

5.3.8 2 ROWS OF KEDD'S ON TOP

5.3.8.1 FIELD TEST RESULTS

Tests 15 and 19 had two rows of KEDD's on the top. Since the initial tests, utilizing the one row of KEDD's was successful; it was decided to try two rows. The initial KEDD concept used a mass of water that was equal to the mass of the two steel disks. By doubling the mass of the KEDD, this test becomes a closer approximation to the conceptual calculations. It is expected to double the momentum absorbed through this system, through the additional mass. One would also expect a 50% reduction in the velocity of the second plate when compared to the previous test. This test used the same charge weight and standoff distance as the other 2 Plate Tests as shown in Figure 5.35. Once again, the specimens behaved similarly for these tests; however, there appears to be more damage to the first plate when compared to the tests with one row of KEDD's (Tests 8 and 11). Additional signs of a brittle failure, more than what was seen in tests 8 and 11, were seen in Tests 15 and 19, This is exhibited by the shearing of the first plate in multiple locations. There is no clear reason why these plates suffered more damage than the plates in test 8 and 11. It may have been a random coincidence (which can be expected with field tests.) If tests are performed with additional rows of KEDD's the expected, or typical, behavior of the plate can be determined. Figure 5.36 shows the first plates for the two tests. The flyer plate impacted the second plate where it caused the plate to release from its support, as shown in Figure 5.37. No fractures were found in either of the second plates.

Figure 5.35: Two rows of KEDD's on top test set-ups (Test 15)

Time of Arrival (TOA) pins captured the velocities of the second plates in the "higher spacing" arrangement. The average velocity of the second plate was 215 ft/sec for Test 15, and 465 ft/sec for Test 19. There was one difference in the two pin arrays. Test 15 used four pins and test 19 used three pins.

Figure 5.36: Two rows of KEDD's on top, first plate a) Test 15 b) Test 19

Figure 5.37:Two rows of KEDD's on top, second plate a) Test 15 b) Test 19

As shown in the previous tests, Figure 5.38 exhibits a similar bar chart for the velocities of the second plates as captured by the TOA pins. It demonstrates the vast difference in the velocities for these two tests. It is unknown why the velocity in Test 19 is more than twice the velocity in Test 15. Test 15 is more consistent with the second plate velocity that would be expected when compared to the tests with one row of KEDD's (453 ft/sec) and three rows of KEDD's (152 ft/sec as described in the next section). The TOA pins in Test 19 must have been activated before the plate arrived. Similar to previous tests Table 5.5 shows the velocity data and velocity reduction of the second plate. For Test 15 the reduction in velocity is 80%, in Test 19 the reduction in velocity is 56%. (When compared to the baseline tests) The reduction of velocity shown in Test 19 is similar to the reduction of velocity seen in the test series with one KEDD. Since the weight of the KEDD's were doubled, it seems unlikely that it would not affect the reduction in velocity. Therefore, the data from Test 19 should be ignored. In what follows, when the results of the two rows of KEDD's are discussed, the reduction of velocity is 80% when compared to the baseline test, and the average velocity is assumed to be 215 ft/sec.

Table 5.5: 2 Plate Test, two rows of KEDD's on top velocity data

Test	Interval Velocity	Average Velocity	Average Baseline Velocity	Reduction in Velocity by KEDD
15	184 ft/sec 245 ft/sec 	215 ft/sec	1060 ft/sec	80%
19	298 ft/sec 631 ft/sec 	465 ft/sec	1060 ft/sec	56%

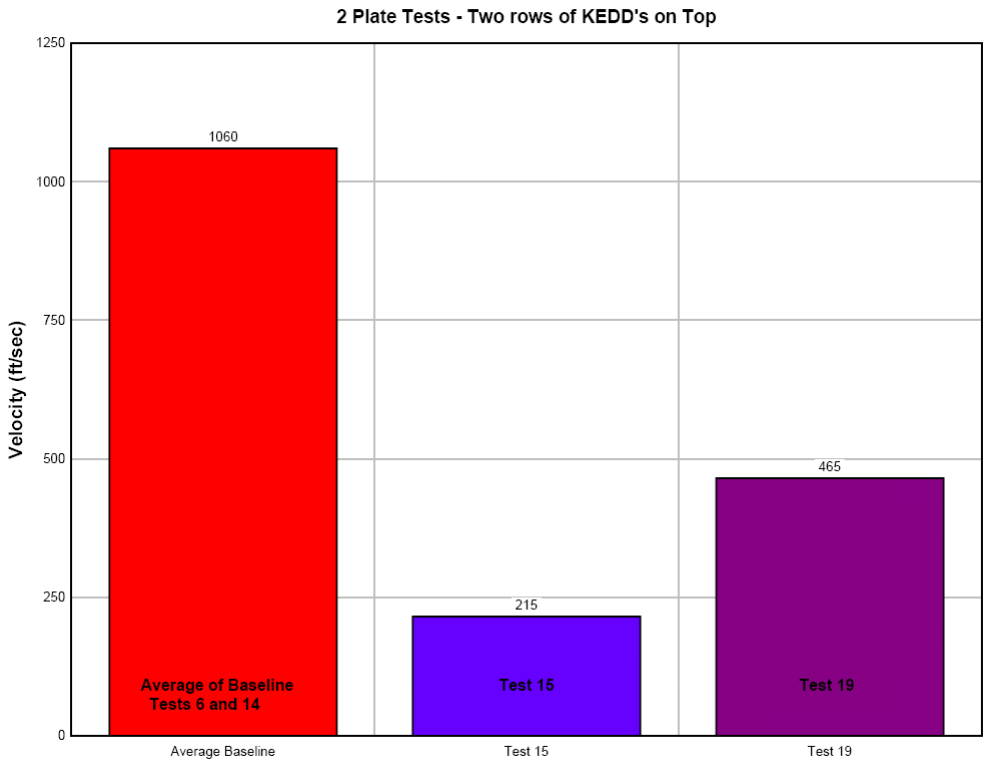

Figure 5.38: 2 Plate Test, two rows of KEDD's on top velocities

5.3.8.2 SIMPLIFIED CALCULATIONS

The 2 Plate Test configuration with two rows of KEDD's on top, used the same model set-up as the test with one row of KEDD's on top. The test set-up, before the calculation begins, is shown in Figure 5.39. The first steel plate is placed 12" above the top surface of the second plate. The first row of KEDD's is centered 2 1/2" below the first plate. The second row of KEDD's is centered 3" below the top row of KEDD's. Each KEDD is 2" in diameter and is placed 3" on center.

A series of six plots from this calculation are shown in Figure 5.40 and are set-up in the same manner as the previous tests. The first row of plots shows the formation of the high speed ejecta, once again, similar to previous tests. The tips of the jets moving outward from

the KEDD's, in the X direction, have a velocity around 1 km/sec, or 3,280 ft/sec. The calculations for this test show that the KEDD system behaves in a similar manner to the case with one row of KEDD's on top. The transverse jets are formed and move at a high velocity. In addition, vertical jets are also formed. The first row of plots in Figure 5.40 shows both types of jets. In this photo, the vertical jets have formed and are interacting with the second row of KEDD's. The next row of plots in this figure show that the steel plate has interacted with all of the KEDD's. There are now two sets of transverse ejecta, on both sides, created from the two rows of KEDD's. Five vertical jets have also formed. The outer two jets were created from the interaction with the two KEDD's on the edge. The middle jet was created from the interaction of the second row of KEDD's. The remaining two jets were created from the initial interaction of the first row of KEDD's The final row of plots demonstrates how much water has been dissipated before the impact of the two plates, only a small portion of the liquid remains.

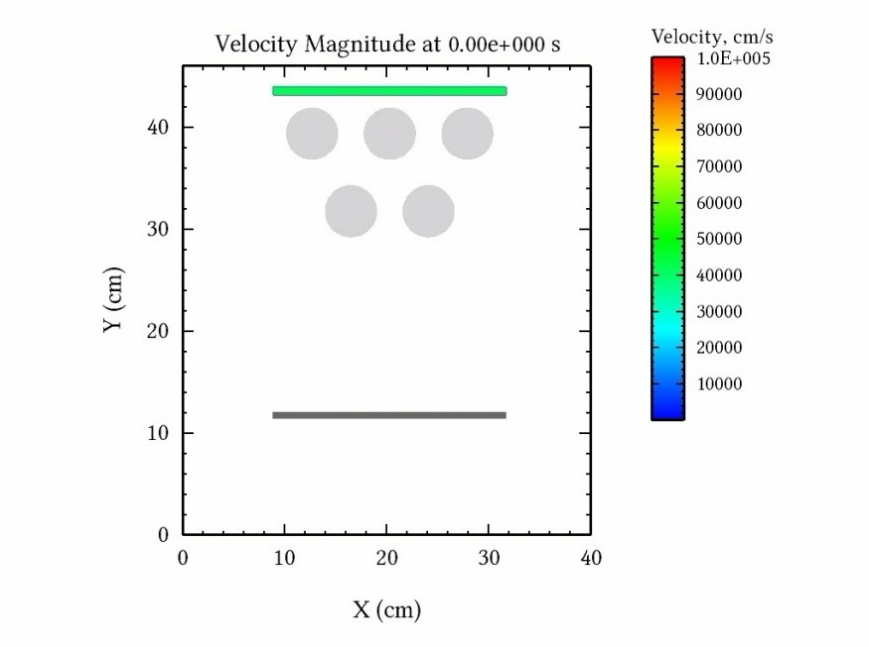

Figure 5.39: 2 Plate Test, two row of KEDD's on top, test set-up

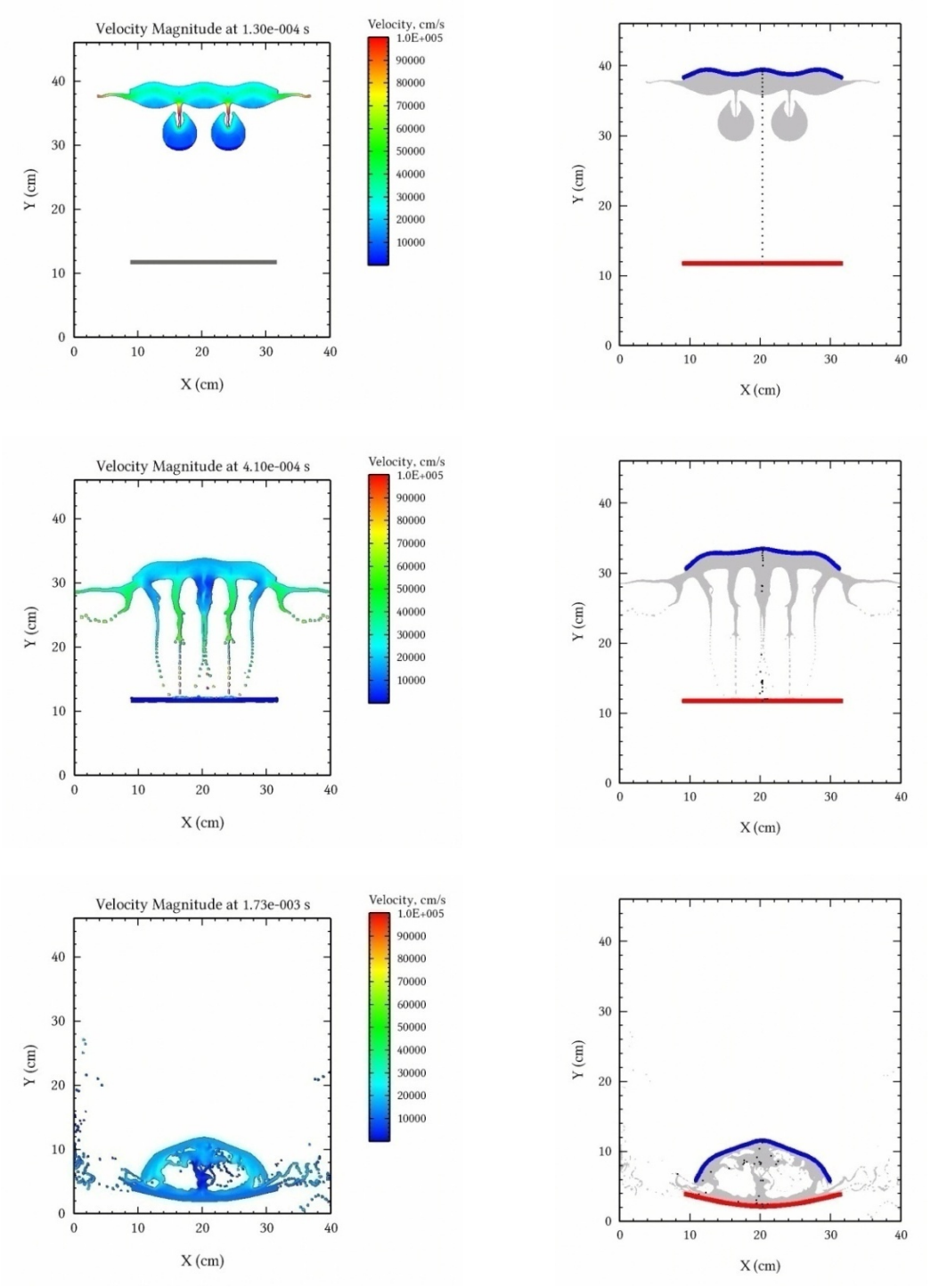

a) Velocity magnitude **b) Materials**

Figure 5.40: 2 Plate Test, two rows of KEDD's on top

The graph in Figure 5.41 shows how the KEDD system changes the velocity of the first plate. The first steel plate has an asymptotic profile. There is an initial steep drop off in velocity, then a slightly more gradual decrease until it reaches its slowest velocity (before impact). It should be noted, that the asymptotic velocity occurs around 0.4 ms. This correlates to the second row of plots in Figure 5.40. At this time step, the water from the vertical jets has just impacted the second plate. The velocity of those jets then increases the velocity of the plate until impact. The actual impact of the plates is not shown on this graph, or was computed in the calculation. The approximate outgoing velocity of the second pate was 380 ft/sec. The velocity of the second plate in the field tests was 215 ft/sec which is a difference of 43% (between the two). The simplified momentum calculations predict a velocity of 560 ft/sec of the second plate. This correlates to a 32% difference with calculations and a 62% difference with field tests. A chart of the different velocities associated with this test is shown in Figure 5.42.

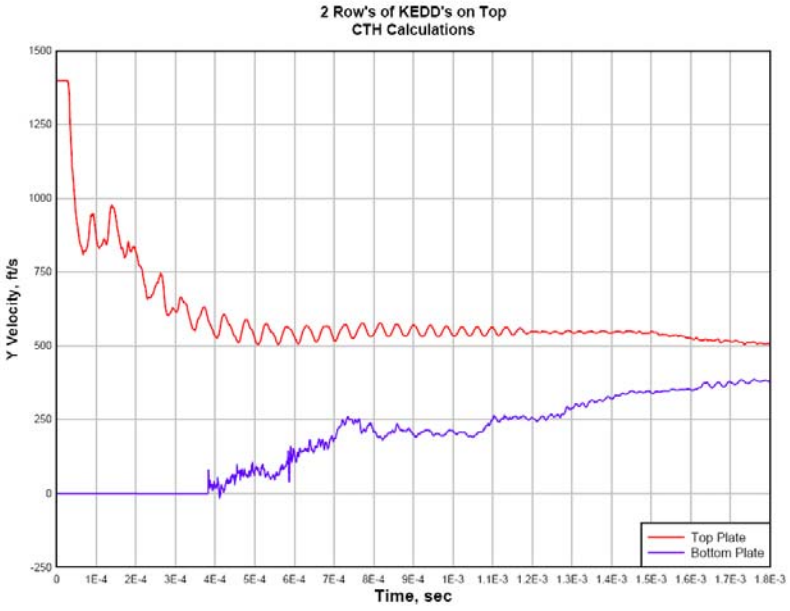

Figure 5.41: 2 Plate Test, two rows of KEDD's on top – velocity profile of top and bottom plate

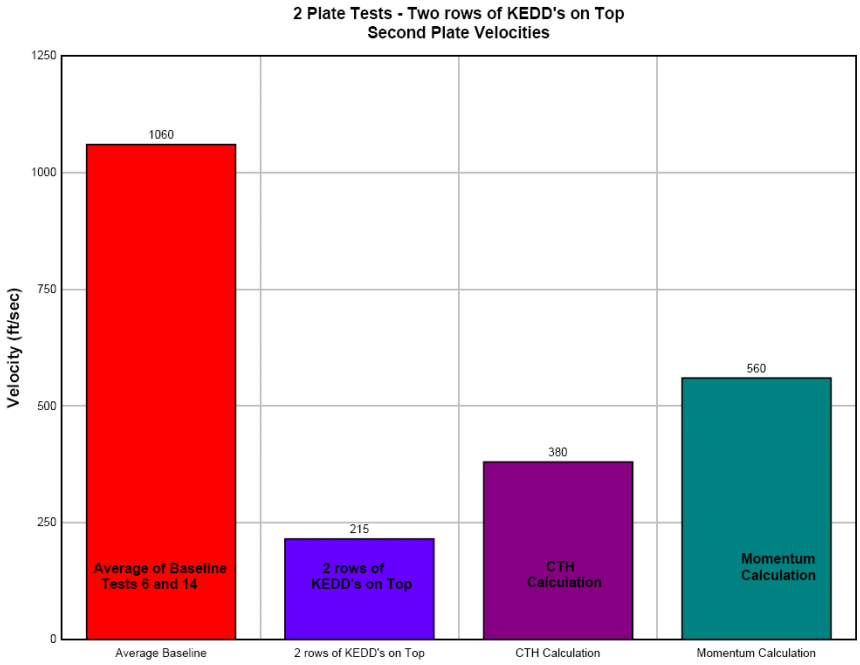

Figure 5.42: KEDD on top – 2 row, velocities (field, CTH, and calculation)

5.3.9 KEDD ON TOP AND BOTTOM

5.3.9.1 FIELD TEST RESULTS

Tests 16 and 21 had one row of KEDD's behind the first plate (top) and in front of the second plate (bottom). In the previous test these permutations (KEDD's Top and KEDD's Bottom) have been evaluated separately. The advantages of placing the KEDD's at the top has been demonstrated, however, it was decided to determine the effects of placing the KEDD's in both locations. These tests used the same charge and standoff distance at Tests 15 and 11 as shown in Figure 5.43. The specimens showed significant amounts of ductile deformation and a large flyer plate was formed from the center of the plate (brittle). Additional signs of brittle failure, in Test 16, can be seen in the shearing of the plate in multiple locations. (Figure 5.44) More ductile deformation is exhibited in the first plate of Test 21 than the comparison test

(Two rows of KEDD's on Top - Test19). The behavior of the first plates is more consistent with the tests where the KEDD is on the bottom, as opposed as the KEDD on the top. (This will be discussed further in the next section.) The flyer plate impacted the second plate where it caused the plate to release from its support, as shown in Figure 5.45. Both of these photos show the flyer plate still enclosed in the steel plate.

Time of Arrival (TOA) pins captured the velocities of the second plate. They determined that the average velocity of the second plate was 630 ft/sec for Test 16, and 541 ft/sec for Test 21, the pins used the "higher layout" arrangement. A bar chart showing the different velocities for these tests are shown in Figure 5.46, demonstrating the similarity in the velocities for these two tests. Table 5.6 shows the velocity data in the same manner as Test 15 and 19. For Test 16 the reduction in velocity is 41%, in Test 21 the reduction in velocity is 49%. These velocities will be averaged and a value of 586 ft/sec will be used in the following discussions. The average reduction in velocity when compared to the baseline tests is 45%.

Figure 5.43: One row of KEDD's on top and bottom test set-ups a) Test 16 b) Test 21

Figure 5.44: One row of KEDD's on top and bottom, first plate a) Test 16 b) Test 21

Figure 5.45: One row of KEDD's on top and bottom, second plate a) Test 16 b) Test 21

Table 5.6: 2 Plate Test, one row of KEDD's on top and bottom velocity data

Test	Interval Velocity	Average Velocity	Average Baseline Velocity	Reduction in Velocity by KEDD
16	968 ft/sec 291 ft/sec	630 ft/sec	1060 ft/sec	41%
21	541 ft/sec	541 ft/sec	1060 ft/sec	49%

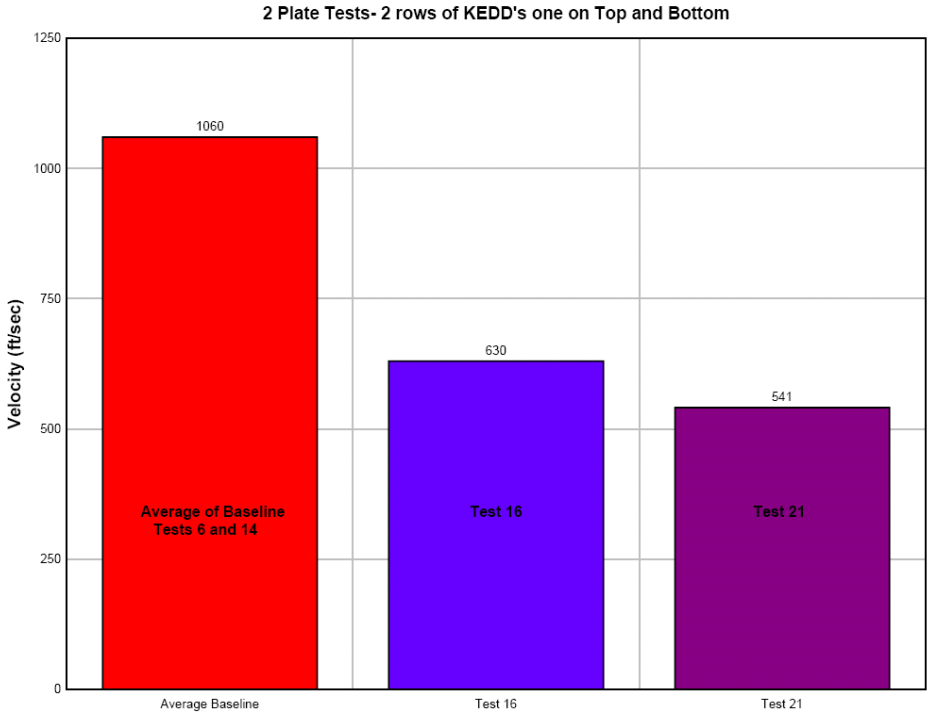

Figure 5.46: 2 Plate Test, one row of KEDD's on top and bottom velocities

5.3.9.2 SIMPLIFIED CALCULATIONS

This configuration used the same model set-up as the two rows of KEDD's on top analysis and is shown in Figure 5.47. The first steel plate is placed 12" above the top surface of the second plate. The first row of KEDD's is centered 2 1/2" below the first plate. The

second row of KEDD's is centered 3" above the second plate. Each KEDD is 2" in diameter and is placed 3" on center.

A series of six plots from this calculation are shown in Figure 5.48 and are set-up in the same manner as the previous tests. The first row of plots shows the formation of the high speed ejecta. The tips of the jets moving outward from the KEDD's, in the X direction, have a velocity around 1 km/sec, or 3,280 ft/sec, as would be expected based on previous calculations. The calculation for this test has similarities with previous tests. The transverse jets are formed and move at a high velocity; vertical jets are also formed. The first row of plots in Figure 5.48 shows both types of jets. The second row of plots shows the vertical jets rebounding off of the bottom plate and interacting with the bottom of the KEDD's. The final row of plots show the remaining water mass trapped between the two plates. That water, along with the plate above will drive the velocity of the second plate.

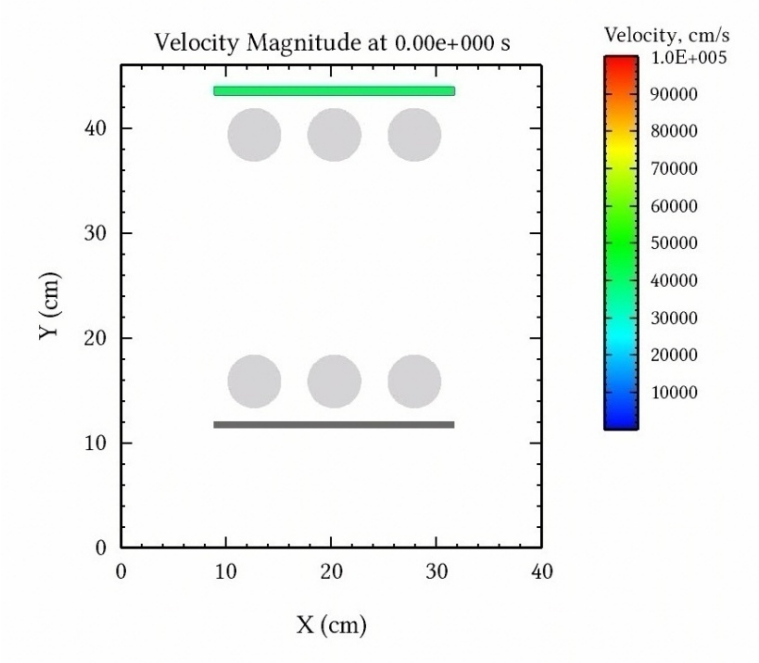

Figure 5.47: 2 Plate Test, one row of KEDD's on top and bottom, test set-up

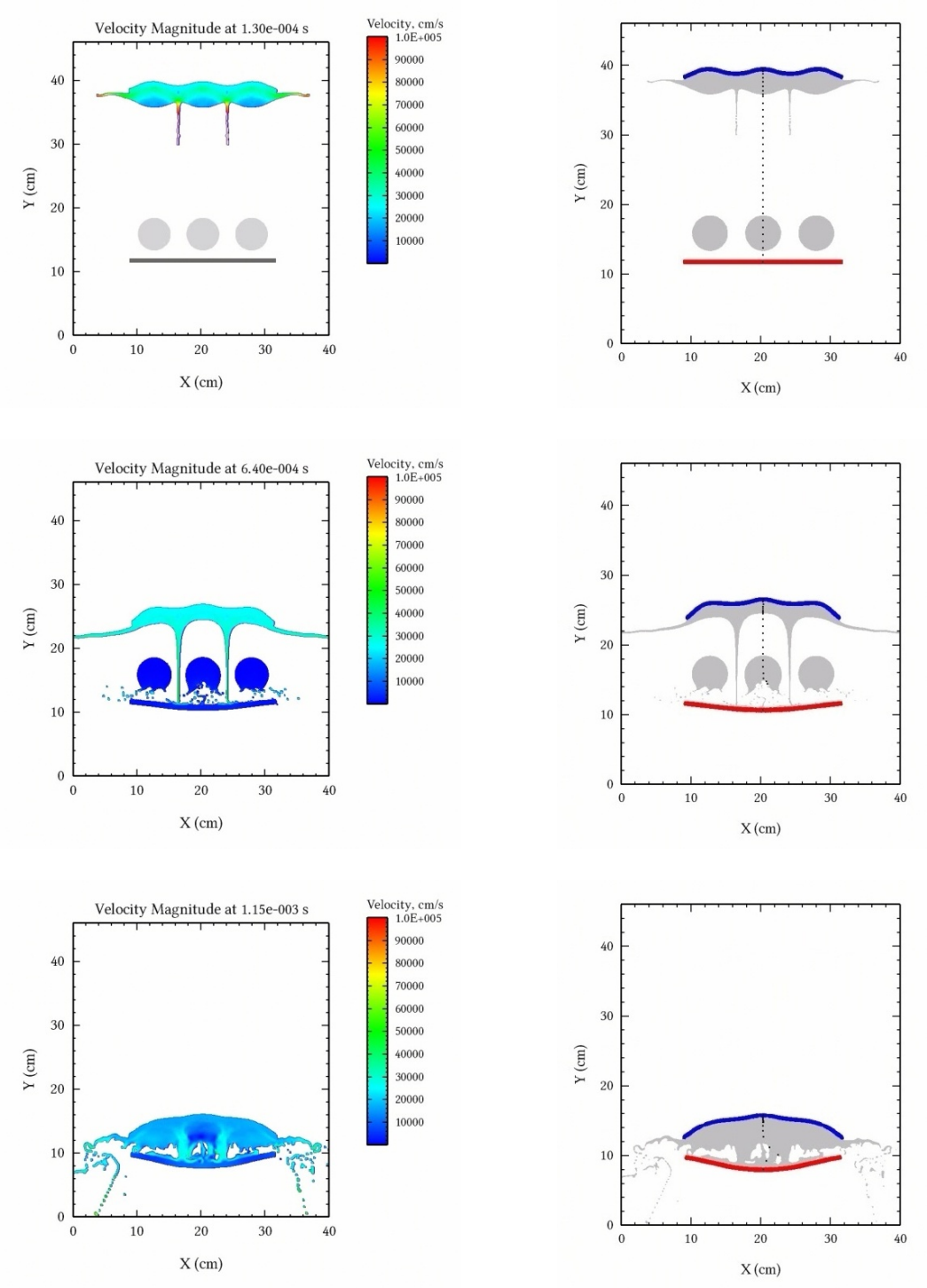

a) Velocity magnitude **b) Materials**

Figure 5.48: 2 Plate Test, one row of KEDD's on top and bottom

In terms of the mass of the KEDD system, this test set-up is very similar to two rows of KEDD's on top, except this calculation has one more KEDD. The behavior at the beginning of the calculation is similar to the KEDD on top tests. Previous calculations and tests have shown that when the KEDD is placed directly in front of a steel plate there is not enough time for all of the water mass to dissipate, instead it will stay trapped between the two plates.

The amount of water mass interacting between the two steel plates from similar tests can be seen in Figure 5.49. Figure 5.49(a) shows the test with the KEDD's on top and bottom, while Figure 5.49(b) shows the test with two rows of KEDD's on top. Even though these are not at the same time steps, the water mass in Figure 5.49(a) is significantly more than in Figure 5.49(b). This additional mass will contribute to the higher velocity of the second plate, as it moves together with the first and second plate.

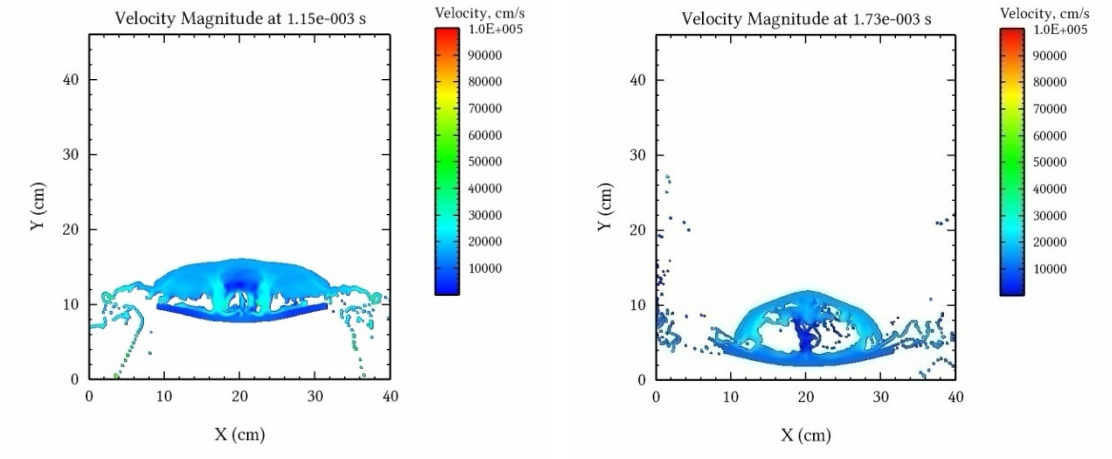

Figure 5.49: Comparing liquid trapped between first and second plates

a) One row of KEDD's top and bottom b) Two rows of KEDD's on top

The velocity profile of the first and second plate is shown in Figure 5.50. There is an initial velocity decrease upon interaction with the KEDD. Additional deceleration of the plate

occurs until the velocity stabilizes at 800 m/s. A second jump in the deceleration of the steel plate occurs upon impact with the KEDD's on the bottom. The initial movement of the second plate is from the force of the high speed vertical jets. Other, smaller velocity decreases occur when the first plate impacts the bottom row of KEDD's and when the first plate impacts the second plate. The average velocity of the second plate after impact is approximately 445 ft/s. In the field the velocity of the second plate had a higher velocity, 586 ft/s. This is a 24% difference between the CTH calculation and the field test. The simplified momentum calculations predicted a velocity of 512 ft/sec. This prediction is 13% lower than the CTH prediction and 14% higher than the field test. Figure 5.51 shows a bar chart of the different velocities determined in this test.

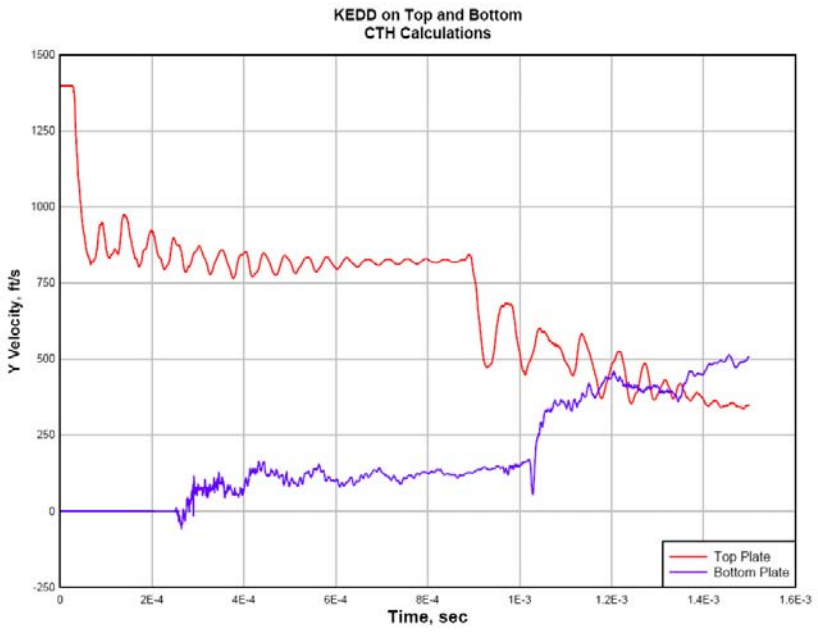

Figure 5.50: 2 Plate Test, one row of KEDD's on top and bottom – velocity profile of top and bottom plate

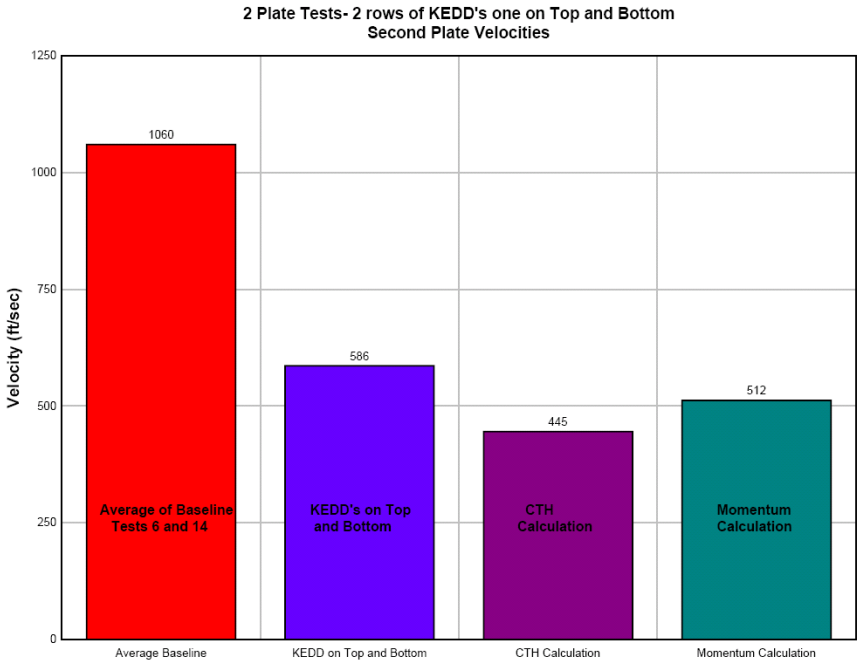

Figure 5.51: One row of KEDD's on top and bottom, velocities (field, CTH, and calculation)

5.3.10 3 ROWS OF KEDD'S ON TOP

5.3.10.1 FIELD TEST RESULTS

Tests 17 and 20 had three rows of KEDD's on the top. Based on the effectiveness of the tests with one and two rows of KEDD's on top, it was decided to determine the effects on the structure when three rows of KEDD's are used. The total mass of the KEDD system is 1.5 times the weight of the steel plate which should continue to aid in the reduction of energy by increasing the mass. The downside with this set-up is that it is not possible to construct this layout in the generic cellular steel structure; however, these tests exhibited some interesting behaviors that enabled the researchers to learn more about this system. These tests used the same charge and standoff distance as Tests 8 and 11 as shown in Figure 5.52. The specimens behaved the same as Tests 8 and 11; however, there appears to be more damage to the first

plate. The first plate exhibited both ductile and brittle failure modes, from the force of the explosion. Large global deformation (ductile) was evident together with a large flyer plate created from the center of the plate (brittle). Other signs of a brittle failure in Test 17 can be seen in the plate tearing in the center of an edge; where the flyer plate was created. In Test 20 a similar behavior occurred; however, instead of tearing the plate, an entire section of the plate was sheared off (Figure 5.53). The flyer plate impacted the second plate where it caused the plate to release from its support, as shown in Figure 5.54. The deformation of the plate might not have been as sever if more realistic boundary conditions were used. The flyer plate can be seen caught in the second plate of Test 17. A similar behavior occurred in Test 20; however, the plate was wide enough to allow the flyer plate to be removed.

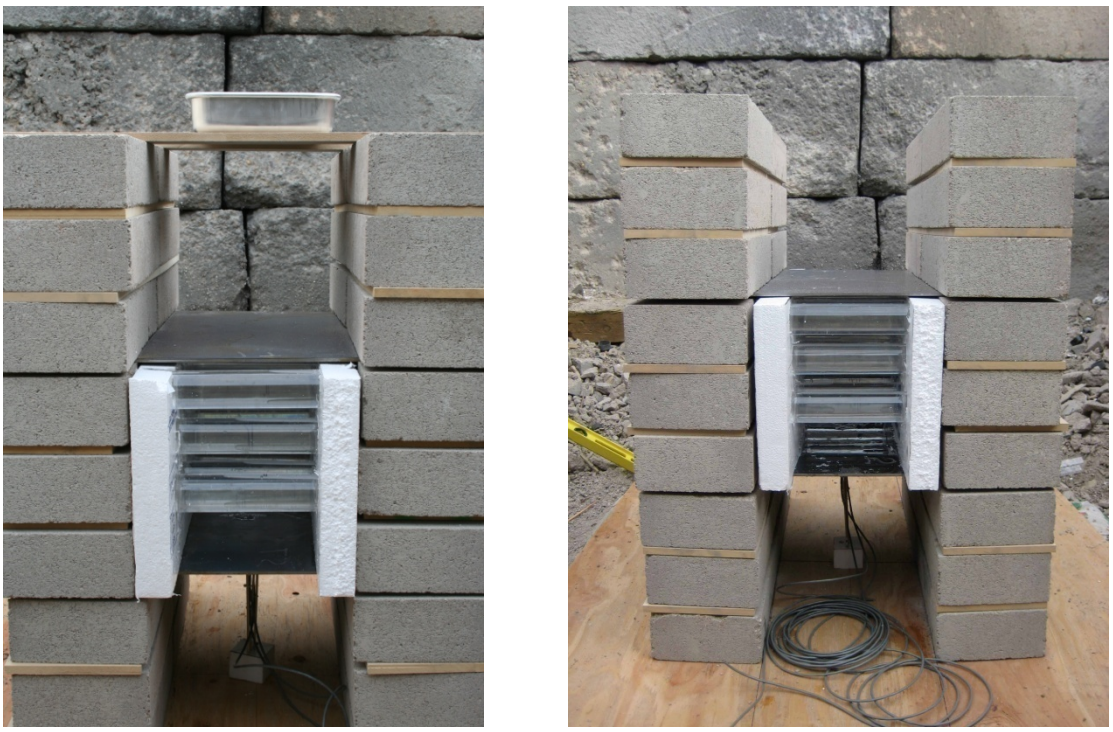

Figure 5.52: Three rows of KEDD's on top test set-ups a) Test 17 b) Test 20

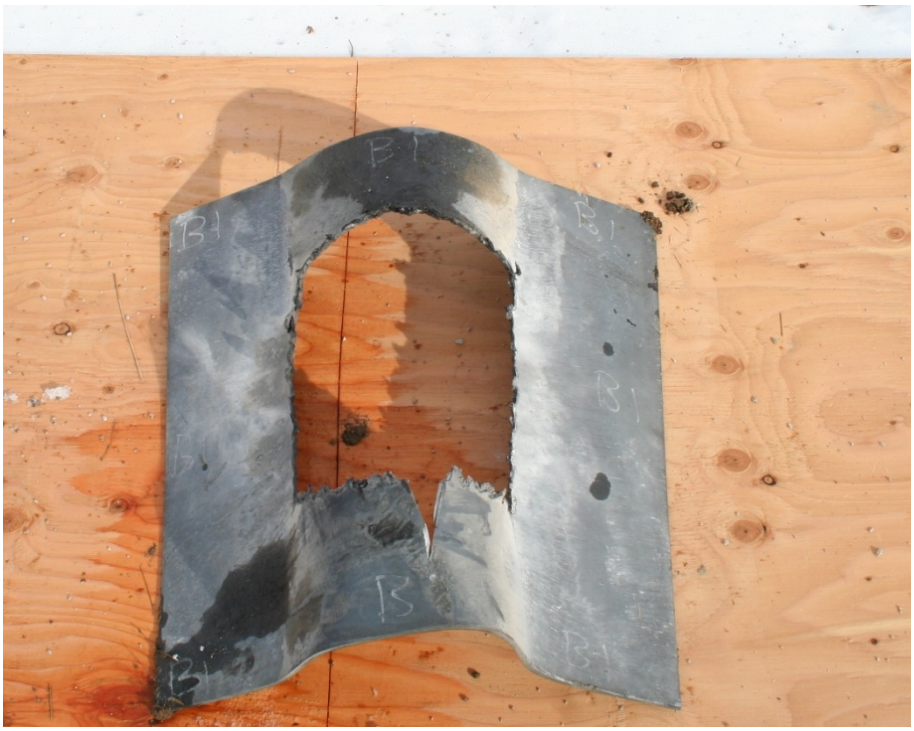

Figure 5.53: Three rows of KEDD's on top, first plate a) Test 17 b) Test 20

Figure 5.54:Three rows of KEDD's on top, second plate a) Test 17 b) Test 20

Time of Arrival (TOA) pins, arranged in the "higher layout", captured the velocities of the secondary flyer plates after they separated from the second plate. They determined that the average velocity of the second plate was 152 ft/sec for Test 17 and 277 ft/sec for Test 20. A bar chart showing the different velocities for these tests are shown in Figure 5.55. It demonstrates the vast difference in the velocities for these two tests. It is unknown why the velocity in Test 20 is almost twice the velocity seen in Test 17. (This also occurred in the two rows of KEDD's tests.) The velocity seen in Test 17 is more consistent with what would be expected when compared to other tests. Table 5.7 shows the velocity data in the same manner as the previous tests. For Test 17 the reduction in velocity, compared to the baseline test, is 86%, in Test 20 the reduction in velocity is 74%. The reduction of velocity shown in Test 20 is equal to the reduction of velocity seen, in the test series with two KEDD's, and a similar argument to exclude Test 20 can be assumed here. Therefore, the data from Test 19 should be ignored. In what follows, when the results of the three rows of KEDD's are discussed the reduction of velocity is 86% when compared to the baseline test, and the average velocity is assumed to be 152 ft/sec.

Table 5.7: 2 Plate Test, three rows of KEDD's on top velocity data

Test	Interval Velocity	Average Velocity	Average Baseline Velocity	Reduction in Velocity by KEDD
17	152 ft/sec	152 ft/sec	1060 ft/sec	86%
20	331 ft/sec	277 ft/sec	1060 ft/sec	74%
	223 ft/sec			

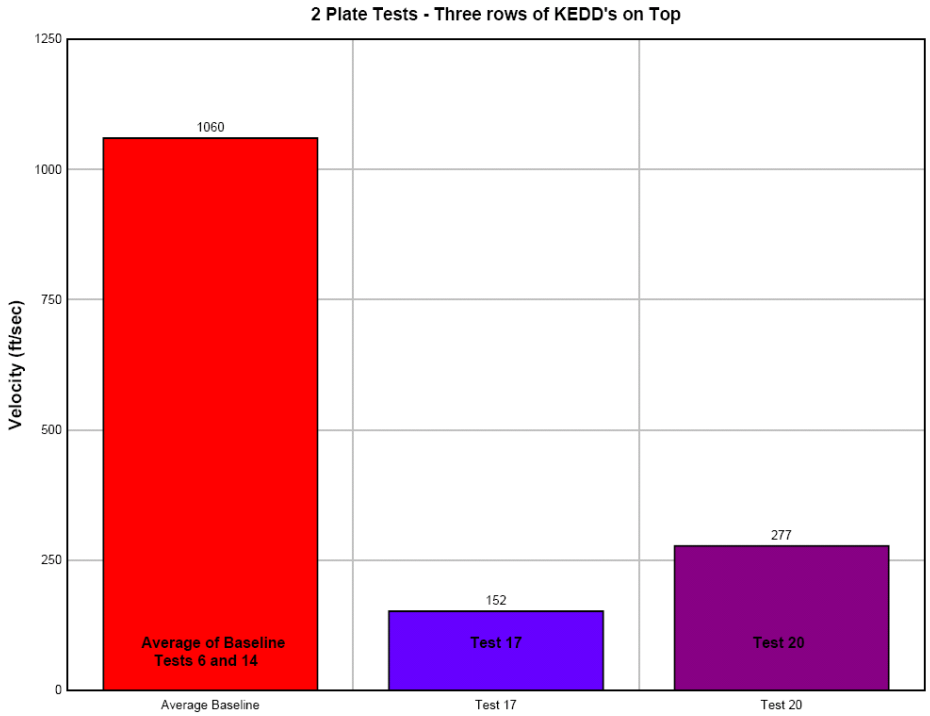

Figure 5.55: 2 Plate Test, three rows of KEDD's on top velocities

5.3.10.2 SIMPLIFIED CALCULATIONS

This configuration used the same model set-up as the previous test and is shown in Figure 5.56. The first steel plate is placed 12" above the top surface of the second plate. The first row of KEDD's is centered 2 1/2" below the first plate, the second and third rows are centered 3" below the previous row. Each KEDD is 2" in diameter and is placed 3" on center.

A series of six plots from this calculation are shown in Figure 5.57, they are set-up in the same manner as the previous calculations. The first row of plots shows the formation of the same high speed ejecta that has been seen in all of the previous test. The calculations for this test show that the KEDD system behaves in a similar manner to the other cases with KEDD's on top. The transverse jets are formed and move at a high velocity. In addition, vertical jets are also formed. The first row of plots in Figure 5.57 shows both types of jets. In

this plot the vertical jets have formed and are interacting with the second row of KEDD's. The next row of plots in this figure show that the steel plate has interacted with the top two rows of KEDD's and the vertical jets are beginning to activate the third row of KEDD's. The final row of computational frames show the two plates before collision. The second plate had started to deform and travel from the impact of the vertical jets. These results indicate that there was not enough empty space, after the final interaction with the KEDD, to allow all of the water mass to dissipate before impacting the second plate. This phenomenon will continue to trap water mass between the first and second plates and will move with them. To achieve the maximum results, the KEDD system should have a larger distance between the last KEDD and the second plate. The ideal separation between the plate and the KEDD's has not been determined..

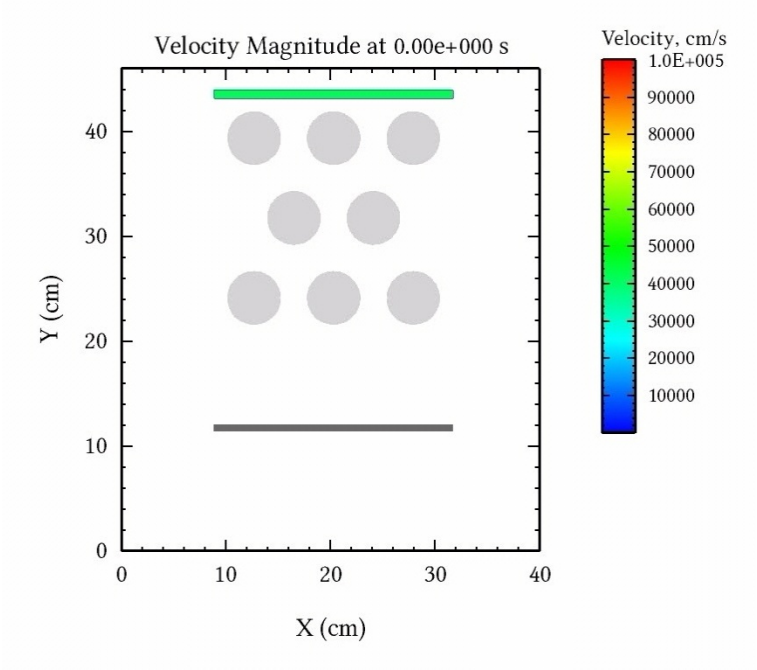

Figure 5.56: 2 Plate Test, three row of KEDD's on top, test set-up

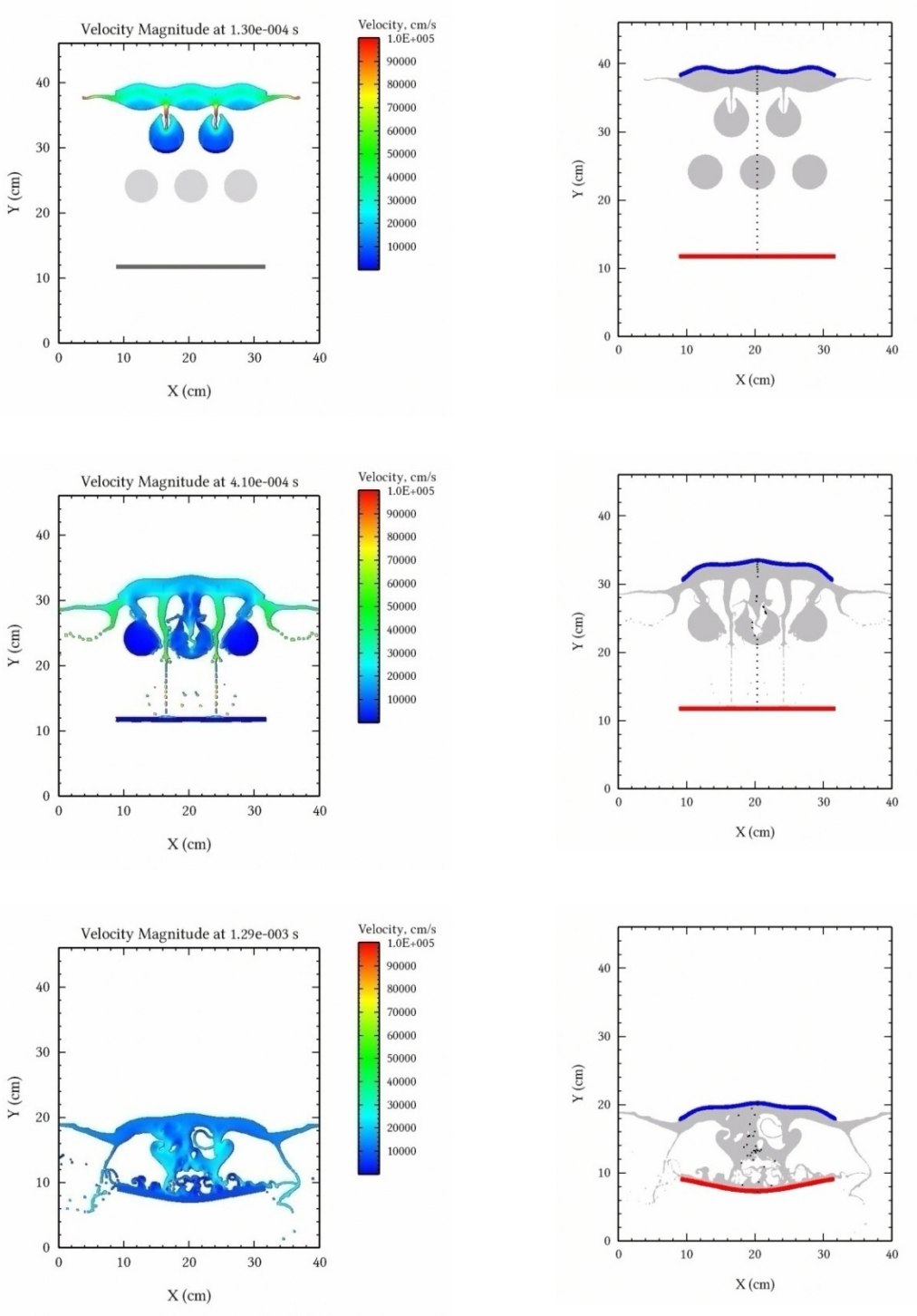

a) Velocity magnitude **b) Materials**

Figure 5.57: 2 Plate Test, three rows of KEDD's on top

The velocity profile of the first and second plate is shown in Figure 5.58. There is an initial velocity decrease upon interaction with the first row of KEDD's. The deceleration of the plate continues at a slower rate until the calculation is stopped. Unlike the test with two rows of KEDD's on top, this graph does not show asymptotic behavior. The second plate; however, behaves in a similar manner to the test with two rows of KEDD's on top. The velocity of the second plate, determined from the CTH calculations, is approximately 240 ft/s. In the field the similar velocity was determined to be 152 ft/s, which is a 37% difference. The simplified momentum calculation predicts a velocity of 437 ft/s. This is a 45% difference between the calculations and CTH, and a 65% difference between the simplified calculation and the field tests. Figure 5.59 shows a bar chart of the different velocities determined in these tests. It can be seen that the CTH and momentum calculations are a conservative estimate of velocity. When used as a simplified approximation for the velocity, it is a very conservative value.

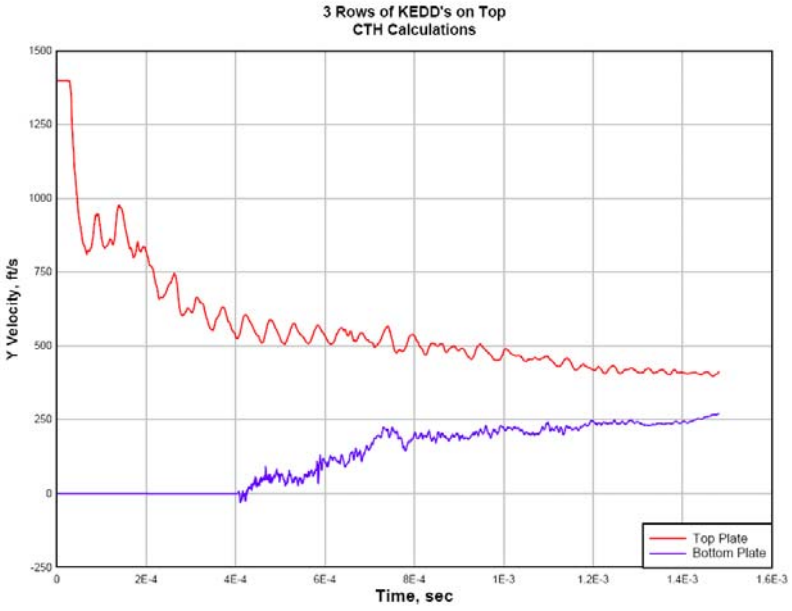

Figure 5.58: 2 Plate Test, Three rows of KEDD's on top – velocity profile of top and bottom plate

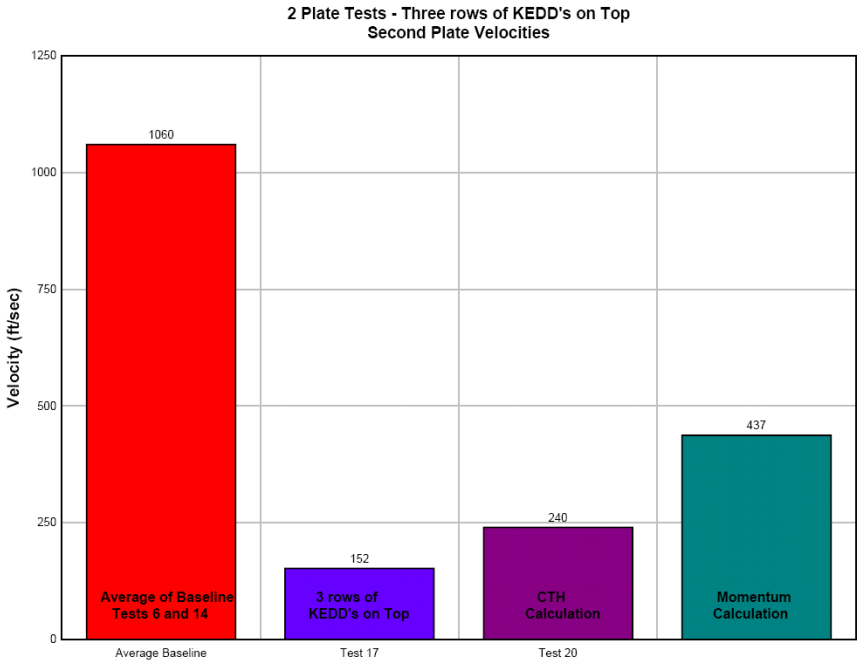

Figure 5.59: Three rows of KEDD's on top, velocities (field, CTH, and Calculation)

5.3.11 WALL OF WATER SIMPLIFIED CALCULATION

The final configuration was a solid wall of water. It utilized the same model set-up as the previous test and is shown in Figure 5.60. The first steel plate is placed 12" above the top surface of the second plate. A 3" x 9" mass of water was placed directly behind the first plate. Like the KEDD set-ups, only the water was modeled, not the device that would contain it.

A series of six plots from this calculation are shown in Figure 5.61 and they are set-up in the same as the previous calculations. The first row of plots shows the formation of the high speed ejecta. The tips of the jets moving outward from the KEDD's, in the X direction, have a velocity around 600 m/sec, or 2,000 ft/sec. These jets are traveling near the same velocity as the incoming plate. While the jets form with this set-up, it is important to note that they are not traveling at as high of a velocity as the same jets formed with the KEDD's. The

color maps, to the right of these plots, have been consistent throughout the calculations. In the tests with the KEDD's, the tips of those jets were red and thin as opposed to the thick green jets shown in Figure 5.61and Figure 5.62 (a). In the second row of plots, of Figure 5.61, some vertical water jets are forming at a slow velocity. The wall of water is applying an upward pressure on the steel plate, causing it to deform. The final row of plots in this figure show the top plate folded in half and a substantial water mass interacting with the second plate. The mass of the wall of water is only slightly larger than the mass of three rows of KEDD's; however, the behavior is very different. Because the water is not able to form high speed, transverse ejecta, due to its geometry, the water is trapped between the two plates and interacts with the second plate. This calculation also shows that there is more to this retrofit solution than just adding mass.

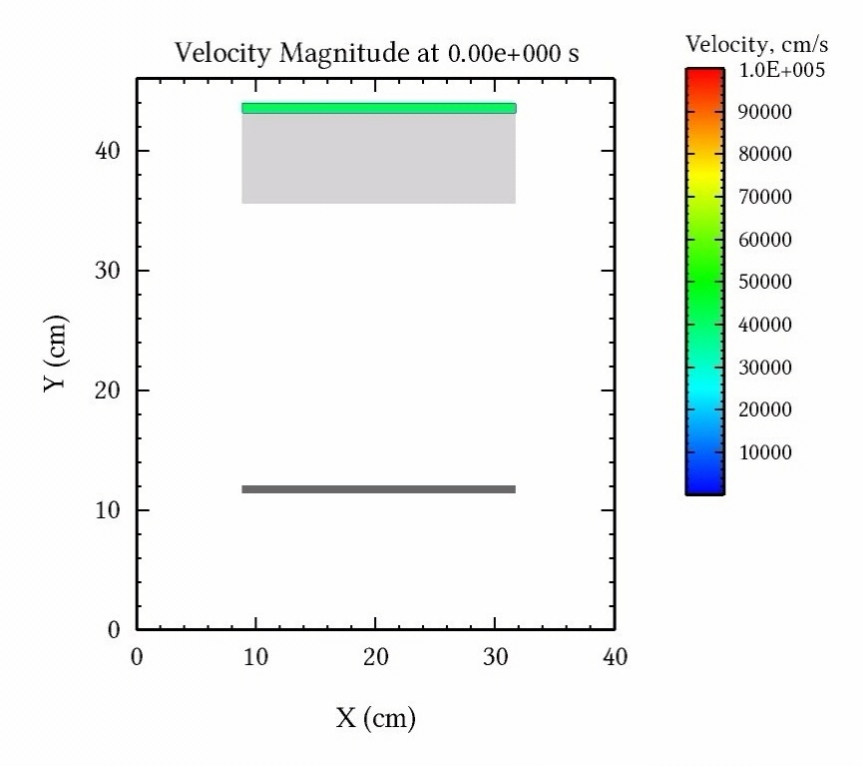

Figure 5.60: One solid wall of water, test set-up

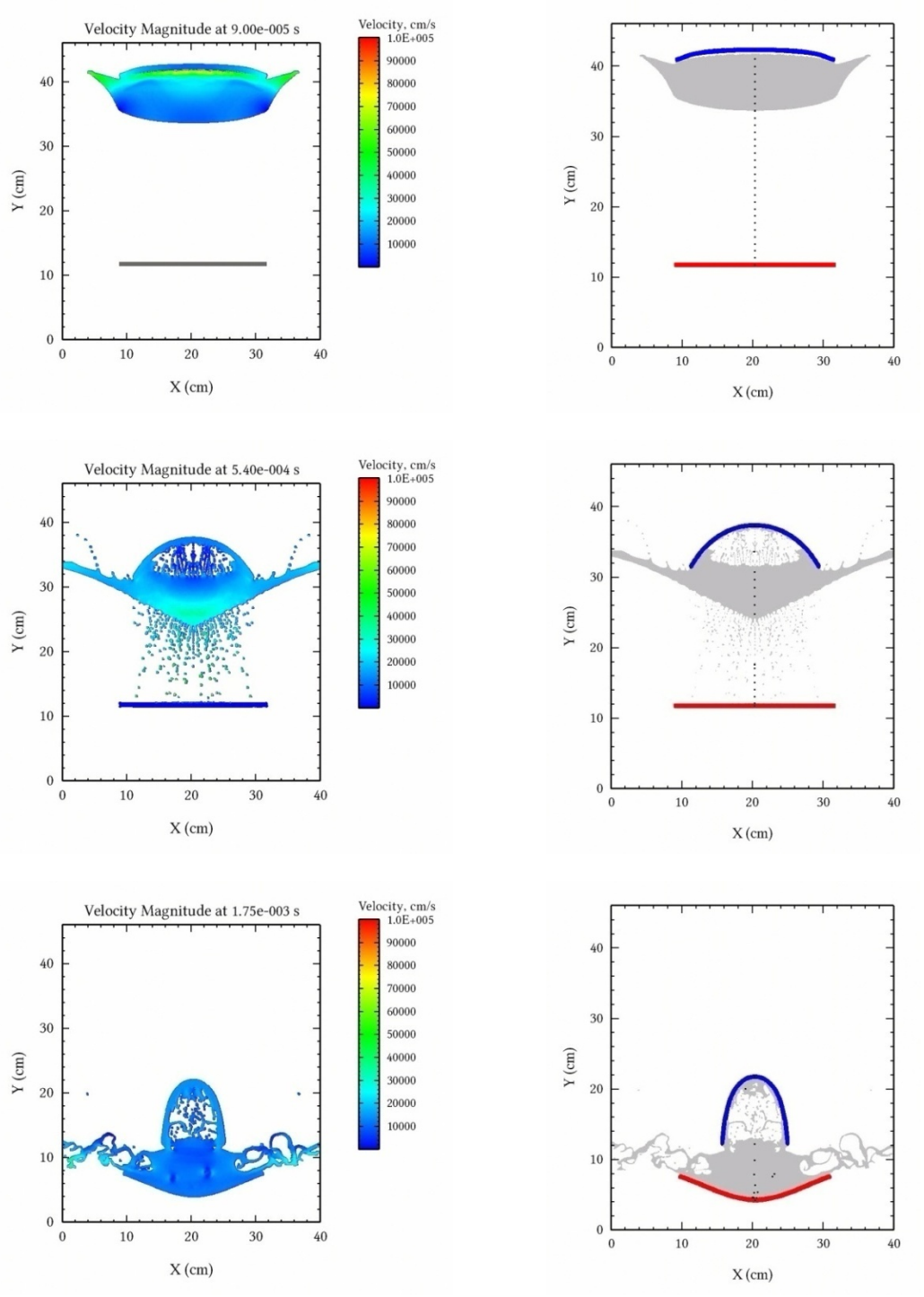

a) Velocity magnitude **b) Materials**

Figure 5.61: One solid wall of water

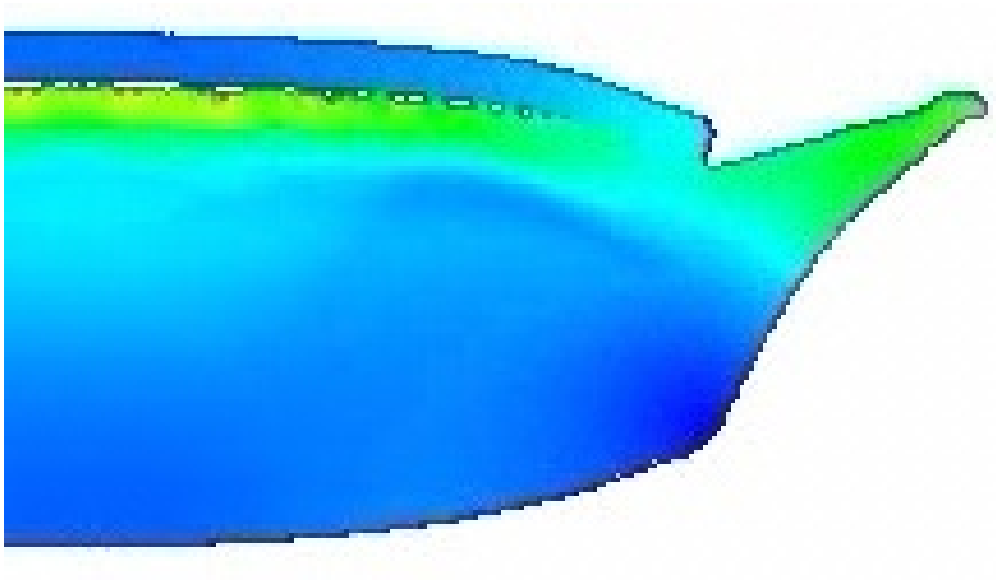

Figure 5.62: Close-up of velocity magnitude for a solid wall of water

The velocity profile of the first and second plate is shown in Figure 5.63. There is a sharp initial deceleration upon impact with the wall of water; however, there is an immediate jump in velocity after the impact which increases over time. The velocity of the plate is determined at the center point of the plate and tracks only the plate movement. The second plate behaves in a similar manner to the previous tests. The only difference is in the magnitude of the oscillations near the end of the calculation. The calculations show that the second plate has a velocity of 355 ft/s. This can be compared to the test with three rows of KEDD's on top as their mass is approximately equal. In that test, the CTH calculations showed that the velocity of the second plate was 240 ft/s. That is a 32% difference between the three rows of KEDD's calculation and the wall of water calculation. If using a solid mass of water was as effective as using a periodic array of open and filled cells (i.e. – the KEDD system), then the results of these computations would be similar. The simplified momentum calculations predict a velocity of 355 ft/s of the second plate; this is 15% difference between the hand calculation and the CTH computation.

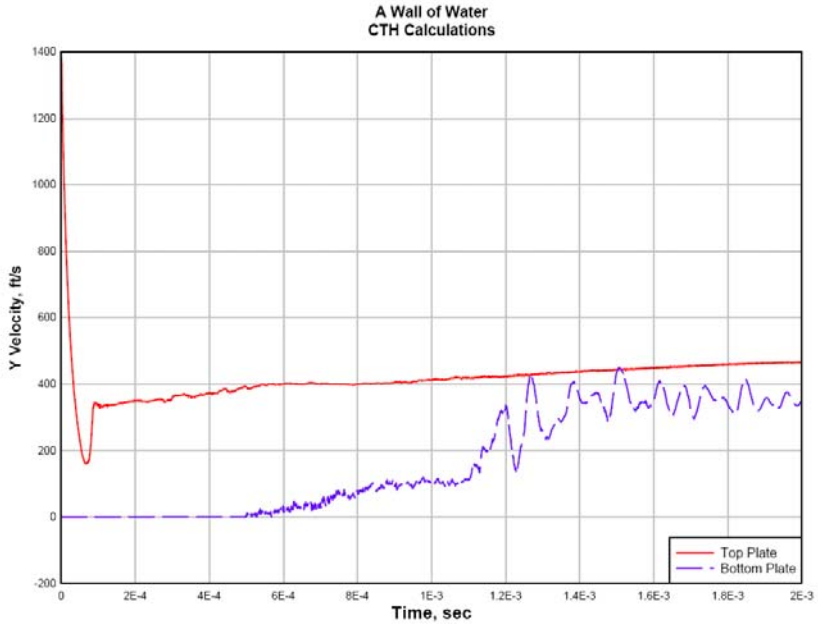

Figure 5.63: One solid wall of water – velocity profile of top and bottom plate

5.4 2 PLATE TEST COMPARISONS

5.4.1 FIELD TEST COMPARISONS

A total of fourteen 2 Plate Tests were performed to determine the most effective location for the KEDD systems. The devices were placed directly behind the first plate in rows of one, two, and three. They were also placed directly in front of the second plate, and one set of tests placed the KEDD's in both locations, in back of the first plate and in front of the second plate. The previous sections have discussed each pair of tests and made comparisons between them, overall comparisons of the field tests will now be discussed. The best way to evaluate the initial effectiveness of the KEDD system and the ideal location is to observe the type of damage the specimens experienced. Figure 5.64 and Figure 5.65 show a representative photo from each of the tests. Both figures are arranged in the same manner: first left was a baseline test (a), top right had a KEDD on top (b), middle left had a KEDD on bottom (c), middle right had two rows of KEDD's on top (d), bottom left had a row of KEDD's on the top and the bottom (e), and bottom right had three rows of KEDD's on top (f).

The failure modes and the effectiveness of the KEDD can be observed the best in these photos. Figure 5.64 shows that the tests with the KEDD's on top typically fail in the same manner. There is significant bowing in the first plate and there is one large hole where a flyer plate is created. It should be noted that the size of the hole is larger than the 9"x9" cake pan that the charge was placed in. In contrast, the baseline test shows the fragmentation of the first plate from the charge. This picture shows at least five pieces and three flyer plates. Figure 5.64(c) shows some bending of the plate, but also significant shearing of along the edges of the plate. There might have been small fragments that also sheared off from the plate but were not found in the test bed since the flyer plate appears to be smaller than the opening.

Figure 5.64(e) shows significant damage, similar to the KEDD's on the bottom test [Figure 5.64(c)]. In this test a large flyer plate was formed out of the center of the plate, in addition to shearing and petalling. It is unclear why the first plate of the test with the KEDD at the top and bottom, did not behave in a similar manner as the test with one row of KEDD's at the top. Additional damage to the first plate may have occurred from the dissipation of the water within the KEDD. Computer models have shown that not only does the water move in a perpendicular direction to the incoming projectile; small jets also move parallel to the projectile. These comparison photos exhibit one of the, unintended, advantages of the KEDD system; the ability to alter the manner in which the top plate fails. If this did not occur, the failure modes of the top plates would exhibit some of the behaviors observed in the as-built condition. Instead, none of the first plates formed multiple fragments. By mitigating the number of smaller flyer plates that are created, the KEDD system is decreasing the velocity of the flyer plate by creating larger fragments, before the first KEDD is activated. If the effectiveness of the KEDD system was based solely on damage to the first plate, the option where the KEDD is placed on top would be the preferred location.

Figure 5.65 shows the failures of the second plate. Both the baseline test [Figure 5.65(a)] and the test with the KEDD on the bottom [Figure 5.65(c)] failed in a similar manner. When the flyer plate impacted the second plate there was a significant amount of petalling and deformation. In the baseline test, a large flyer plate was formed. In the test with the KEDD on the bottom, a very small flyer plate was created. The second plates in the other tests all behaved in a similar manner. When the flyer plate impacted the second plate it caused the plate to deform and release from its supports. It then "fell" onto the plywood base at varying velocities, depending on the speed of the incoming flyer plate. The deformation of the second plate was minimized when the three KEDD's on top were used; however, some cracks were

found in the plate for these tests. Photos show the flyer plate still trapped within the second plate. Through the use of the KEDD's on top the failure, or deformation, of the second plate was significantly reduced. If the boundary conditions represented the generic cellular steel structure, then the deformation of these plates may have been reduced. Once again, if the effectiveness of the KEDD system was based solely on the deformation of the second plate, the tests with the KEDD's on top would appear to be the preferred location. However, the test with a row of KEDD's at the top and the bottom might be considered equally as ideal a location.

Comparison photos were taken of the second plates from the following test series: two rows of KEDD's at the top (a and d), one row of KEDD's on top and bottom (b and e), and three rows of KEDD's on top (c and f). Figure 5.66 shows the amount of damage that occurred to the second plate. Figure 5.66(a) was damaged the most. The other two plates, Figure 5.66(b and c), show similar amounts of damage. Figure 5.67 shows both of the second plates for this test series. It demonstrates that, with the exception of the test shown in Figure 5.67(f), the plates all behaved in a similar manner from test to test.

a)

b)

c)

d)

e)

f)

Figure 5.64: First plates from all tests (from left to right)

a) Baseline Test b) KEDD's on top c) KEDD's on bottom

d) Two rows of KEDD's on top e) KEDD's on top and bottom f) Three rows of KEDD's on top

Figure 5.65: Second plates from all tests (from left to right)

a) Baseline Test b) KEDD's on top c) KEDD's on bottom

d) Two rows of KEDD's on top e) KEDD's on top and bottom f) Three rows of KEDD's on top

Figure 5.66: Comparison of second plates a) Two rows of KEDD's on top b) One row of KEDD's, on top and bottom c) Three rows of KEDD's on top

Figure 5.67: Comparison of second plates a) Two rows of KEDD's on top b) One row of KEDD's, on top and bottom c) Three rows of KEDD's on top d) Two rows of KEDD's top e) Two rows of KEDD's, one top and bottom f) Three rows of KEDD's on top

The comparison of damage is an important measure of the effectiveness of the KEDD for these experimental tests, but it is not the only measure. The comparison of the velocities of the second plate is equally important. The primary goal of the KEDD system is to reduce the velocity of the flyer plates, thereby, reducing the amount of damage that can occur to the structure. The optimum location of the KEDD system should not only limit the type of damage that occurs to the steel plates, but also reduce the velocity of those plates. Figure 5.68 and Table 5.8 shows the different average velocities of the 2 Plate Tests. The first bar, in the chart, is from the baseline tests which had a velocity of 1,060 ft/sec. The second bar is from the KEDD on bottom tests and the third bar is from the tests with one row of KEDD's on top and bottom. The average velocities for these tests are 609 ft/sec and 586 ft/sec. It is interesting to note that even though there were twice as many KEDD's added to the test shown in the third bar, the reduction in velocity was not significant. The fourth, fifth and sixth bars represent the series of tests with the KEDD's on top. The fourth bar had one row of KEDD's, the fifth bar had two rows of KEDD's and the sixth bar had three rows of KEDD's. The average velocities for these tests are 453 ft/sec, 215 ft/sec, and 152 ft/sec. The decrease in velocity, by adding additional rows of KEDD's, follows the trends that would be expected.

Table 5.8: Velocity reductions due to KEDD's

Test Description	Velocity of First Plate	Velocity of Second Plate (Average)	Velocity Reduction from First Plate	Velocity Reduction from Baseline	Velocity Reduction from Previous Test
Baseline	1764 ft/sec	1060 ft/sec	40%		
KEDD on Bottom	1764 ft/sec	609 ft/sec	65%	43%	
KEDD's on Top and Bottom	1764 ft/sec	586 ft/sec	67%	45%	4%
KEDD on Top	1764 ft/sec	453 ft/sec	74%	57%	
Two KEDD's on Top	1764 ft/sec	215 ft/sec	88%	80%	53%
Three KEDD's on Top	1764 ft/sec	152 ft/sec	91%	86%	29%

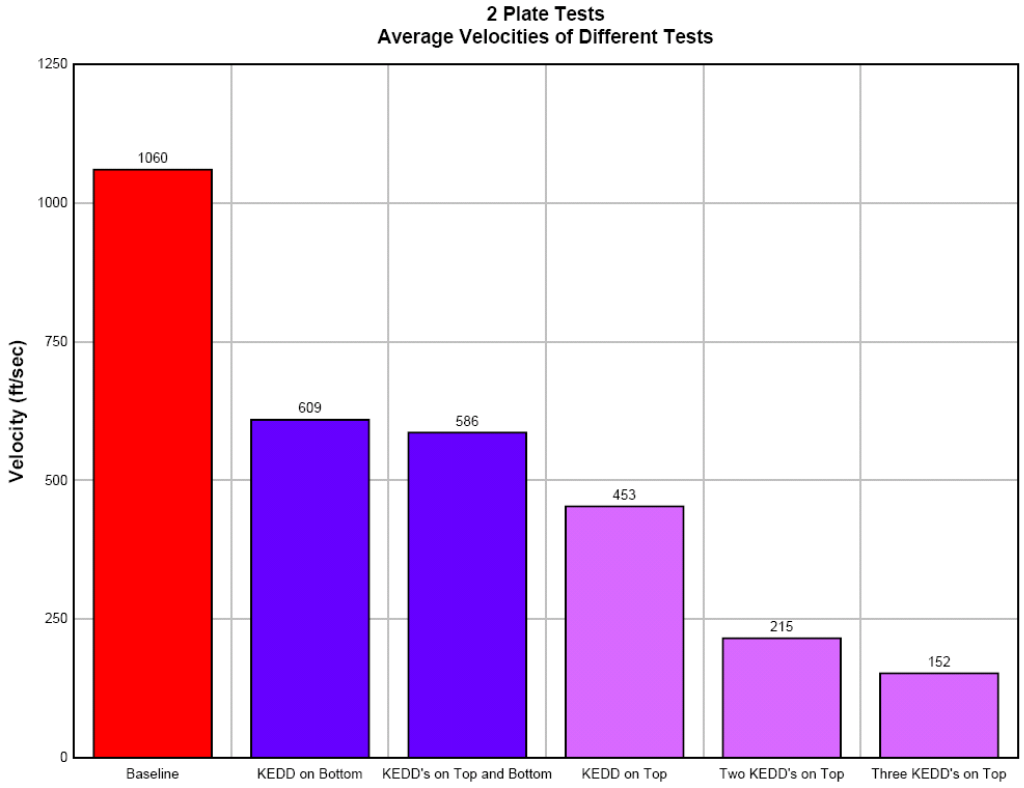

Figure 5.68:Average velocities of all 2 Plate Tests

From the velocities of the second plate the reduction in velocity compared to the base line tests can be determined and is shown in Table 5.8. The use of the KEDD on the bottom whether alone, or in conjunction with a KEDD on top, only reduces the velocity by 43-45%. If one KEDD is used at the top, of the cell, the reduction in velocity increases to 57%. When two rows of KEDD's are used on top the velocity reduction is increased to 80%, and when three rows of KEDD's are used on top the reduction in velocity, when compared to the baseline test, is 86%. The velocity reduction between when the tests with the KEDD's on the bottom of the cell, is not as significant as when the KEDD's are placed at the top of the cell. This could be attributed to the phenomenology of the KEDD. When the KEDD's are activated, the water is expelled from those containers. The majority of the water moves in a

direction perpendicular to the incoming flyer plate, while the rest moves in a direction parallel to the plate. It is imperative that the water has space so that it can expand. If the water is placed directly in front of the steel plate it applies additional force to the plate before it is dissipated and can be trapped between the flyer plate and the second plate. The entrapment of a portion of the water between the plates could act as a small "wall of water" on the second plate. This could transmit the velocity of the flyer plate to the second plate, which accounts for the similarities between the tests with the KEDD's on the bottom, since a similar amount of water should be trapped between the plates.

A similar phenomenon could be seen when comparing the reduction in velocity when additional rows of KEDD's are placed directly behind the top plate. In this case, by adding an additional row of KEDD's (2 rows total) the velocity is reduced by 50% when compared to the test with only one KEDD. This reduction of 50% meets the predictions as the mass of the KEDD's were doubled. However, when an additional row of KEDD's are used (3 rows total) the reduction of velocity is only 30%, not the 50% that was shown in the previous test. The inability of the water to dissipate affects the velocity of the second plate. The entrapment experienced in the tests with the KEDD's on the bottom is experienced here as well. As stated before, the arrangement of three rows of KEDD's is impractical to construct in an existing structure.

The final comparison, in the reduction of velocity from the plates, can be compared to the estimated velocity of the initial flyer plate. In the Calibration Tests, the velocity of the first plate was determined to be 1,764 ft/sec. This value was compared to the velocity of the second plate, whether it is a fragment of the plate or the plate itself, to determine a reduction in velocity. In the baseline test, the reduction is 40%. The use of a KEDD on the bottom increased the reduction in velocity to 65%. When there was a row of KEDD's at the top and

bottom the reduction in velocity was 67%. When one, two and three KEDD's were placed at the top the reduction in velocity was 74%, 88%, and 91%, respectively. This decrease in velocity is a significant reduction and will help contain the failure to a localized area of the structure.

These test shave shown that the KEDD arrangement using two rows at the top of the cell is the most effective arrangement that has been studied. While one row of KEDD's at the top of the cell is an effective mitigation technique, the added benefit of the additional row of cells is significant. The final field test used this arrangement for the retrofitted cells.

5.4.2 SIMPLIFIED CALCULATIONS SUMMARY

Calculations were performed on the six 2 Plate Test set-ups and one wall of water. They captured the behavior of the transverse high speed jets and demonstrated how the water interacts with structure. A justification for placing the KEDD's at the top was discussed and plots showed that when the KEDD is placed at the bottom the water does not have time to disperse before interacting with the second plate. An additional calculation was performed that showed the disadvantages of placing a solid mass, or wall, of water behind the first plate. The high speed jets form, but travel at a much slower velocity than when the KEDD's were used. These calculations predicted outgoing velocities of the second plate. Table 5.9 shows the results of the CTH calculations in tabular form, while Figure 5.69 shows the velocities in a bar chart. Simplified momentum calculations were also performed that predicted the outgoing velocity of the second plates. Both of these calculations (CTH and Momentum) provide a lower bound estimation of velocity.

A comparison of the velocities of the three different methods is shown in Table 5.10 and Figure 5.70. The three types of tests are: the CTH Calculations, field test data, and

simplified momentum calculations. This data shows that with the exception of the test with the KEDD's on the top and bottom, both the CTH and momentum calculations over-predict the velocity of the outgoing flyer plate. If a rough estimate of the velocity of the second plate was desired, these are acceptable, lower bound, methods. These calculations continue to show that the test set-up with two rows of KEDD's on top is still the ideal location. (The data presented in the following tables and graphs, have been discussed above. They are presented now as a measure for comparison that the reader can evaluate at their leisure.)

Table 5.9: Velocity reduction of the second plate (CTH calculations)

Description	Velocity of Second Plate	Velocity Reduction from Top Plate	Velocity Reduction from Baseline	Velocity Reduction from Previous Test	Difference between CTH and Tests
Baseline	1,034 ft/s	26%			2%
KEDD on Bottom	658 ft/s	53%	36%		8%
KEDD on Top and Bottom	445 ft/s	68%	57%	32%	24%
One row of KEDD on Top	670 ft/s	52%	35%		48%
Two rows of KEDD's on Top	380 ft/s	73%	63%	43%	43%
Three rows of KEDD's on Top	240 ft/s	83%	77%	37%	37%
Wall of Water	355 ft/s	75%	66%		

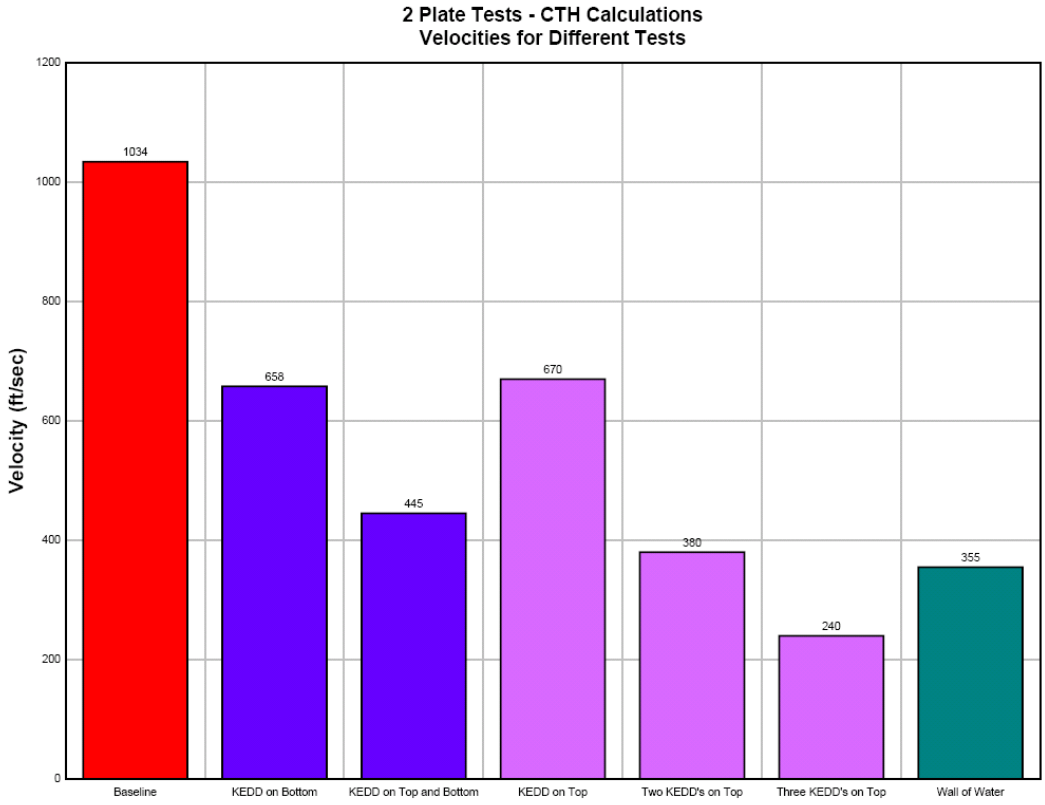

Figure 5.69: 2 Plate Test calculations – second plate velocities

Table 5.10: Comparing velocity reduction of the second plate with CTH, field tests, and momentum calculations

Description	Velocity of Second Plate		
	CTH	Field Tests	Momentum Calculations
Baseline	1,034 ft/s	1,060 ft/s	1,058 ft/s
KEDD on Bottom	658 ft/s	609 ft/s	690 ft/s
KEDD on Top and Bottom	445 ft/s	586 ft/s	512 ft/s
KEDD on Top	670 ft/s	453 ft/s	690 ft/s
Two KEDD's on Top	380 ft/s	215 ft/s	560 ft/s
Three KEDD's on Top	240 ft/s	152 ft/s	437 ft/s
Wall of Water	355 ft/s		418 ft/s

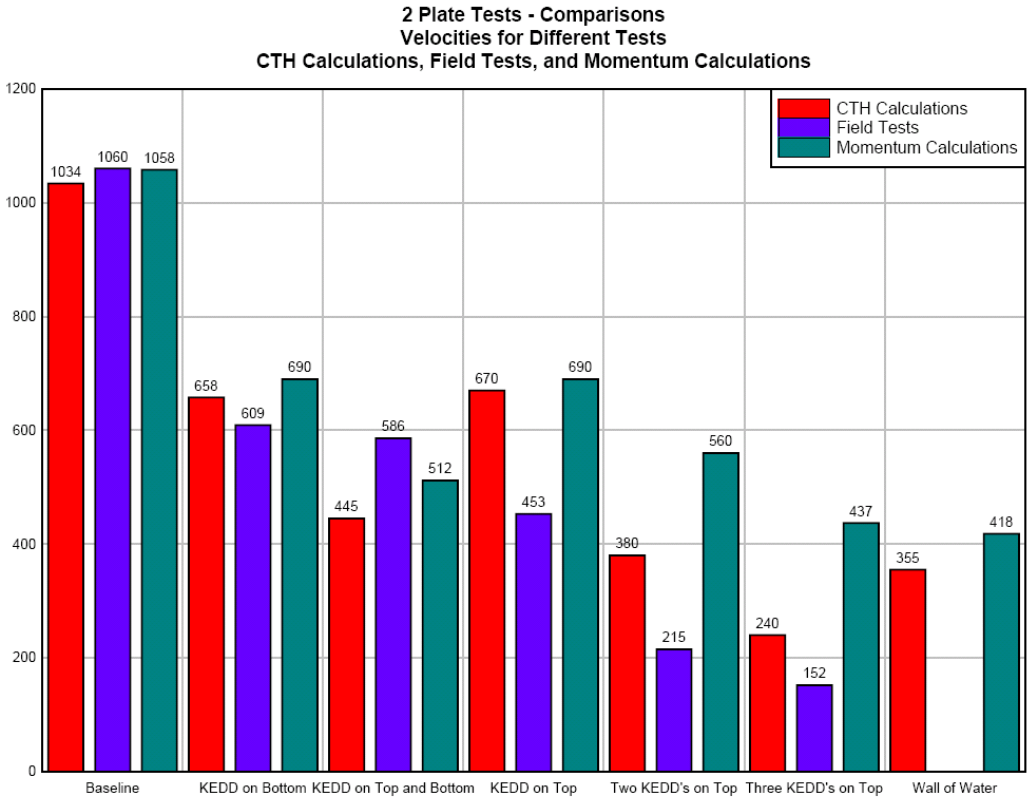

Figure 5.70: Comparing velocity reduction of the second plate with CTH, field tests, and momentum calculations

5.5 CONCEPTUAL DESIGN GUIDELINES

Current computational tools are not sufficiently developed to properly model the fluid and structural interaction of this system. Therefore, it is necessary to develop a conceptual design methodology, which is presented below. It is an empirical based equation that was developed in conjunction with the laboratory and field tests. It can be used as a conceptual guideline; however, it should not be considered a final design for implementation in a specific structure. The final design should be developed in conjunction with the structure owner and based on the unique blast retrofit concept presented herein.

The calculations were determined based on the initial design of the KEDD system for the full scale field test. It was developed to achieve the largest mass, while still allowing for sufficient space between KEDD's. The initial spacing was developed based on the laboratory tests, and used a linear scaling method to achieve the full scale field test design. These design process has been simplified to relate to directly relate to the thickness of the steel plate that interacts with the KEDD. It should be noted, that while the initial calculation was based on assuming only one row of KEDD's, it is recommended that two rows of KEDD's are used, if there is sufficient space in the specific structure.

The design equations, presented below, is based on the KEDD's having a circular shape and assumed that the weight of the KEDD system is 70% of the steel plate. With this assumption, the diameter of the KEDD can be calculated based on the thickness of the steel plate that the KEDD is behind. Once the diameter of the KEDD system has been determined, the spacing between KEDD's can be calculated. The equations for the diameter and spacing of the KEDD are:

$$\text{Diameter of KEDD} = 9 \times \text{thickness of steel plate} \quad (4.3)$$

$$\text{KEDD Spacing} = 1.33 \times \text{diameter} \quad (4.4)$$

Table 5.11 shows the spacing and diameter of the KEDD's for a variety of plate thicknesses. This equation can be used no matter how many rows of KEDD's have been chosen since the equation is based on the plate thickness.

Table 5.11: Diameter and spacing of KEDD system for different plate thicknesses

Plate Thickness, t_p	Diameter	Spacing
0.250 in.	2.250 in.	3.0 in.
0.375 in.	3.375 in.	4.5 in.
0.500 in.	4.500 in.	6.0 in.
0.625 in.	5.625 in.	7.5 in.
0.750 in.	6.750 in.	9.0 in.
0.875 in.	7.875 in.	10.5 in.
1.000 in.	9.000 in.	12.0 in.
1.250 in.	11.250 in.	15.0 in.
1.375 in.	12.375 in.	16.5 in.

5.6 BIBLIOGRAPHY

1. **Morril, Ken.** *Water Slug Write-up.* Karagozian and Case. Burbank, CA : s.n.

2. **Livermore Science Technology Cooperation.** *LS-DYNA Theory Manual.* Livermore, CA : s.n., 2006.

3. **Livermore Science Technology Cooperation**. *LS-DYNA Keyword Users Manual.* Livermore, CA : s.n., 2007.

4. **J. Wolfson, G. Hegemier, F. Seible.** *Kinetic Energy Defeat Device (KEDD) Proof of Concept Tests.* Department of Structural Engineering, University of California, San Diego. San Diego, CA : s.n., 2007.

5. **Sears.** Wearever 9" Comercial Square Cake Pan. *Sears website.* [Online] [Cited: May 26, 2008.] http://www.sears.com/shc/s/p_10153_12605_00807863000P?vName=Appliances&cName=Cookware,Bakeware&Gadgets&sName=Bakeware&psid=MSNSHOPPING01&sid=IPx20070925x00002b.

6. **Sandia National Laboratories.** *CTH Course Notes.* Sandia, NM : Sandia National Laboratories, 2007.

6. FULL-SCALE RETROFITTED FIELD TESTS (EMRTC) FIELD TEST 3

6.1 TEST SET-UP

This test specimen represents a full scale portion of a cellular steel structure and consisted of nine cells in a square pattern (3 x 3) and was tested at EMRTC in May 2008. The specimen was constructed from 7/8" thick A36 steel plates. Each plate was 3' – 6" wide and 8' long. They were supported, at the interior corners, by 8" x 8" x 1/2" A36 steel angles. The plates were connected to the angles by 1" diameter A307 bolts placed at 4" on center. The entire specimen was connected to the concrete foundation through the use of T sections and was anchored to the foundation by 1" diameter anchor rods, with 8" embedment, located at 8" on center.

For this test, a more realistic construction scheme was used, compared to previous tests where a non-continuous top plate was used. In many existing structures, the first plate is continuous across the top three cells. To achieve this, the first plate was divided into two pieces. Each piece was 4' x 10' – 7 3/4" x 7/8" thick, they were placed flush together and were continuous over the vertical supports. The plates were bolted to the interior angles in order to secure the plate to the specimen. In existing structures there would be a continuous splice plate across the seam and bolted into place. This technique was not used for this test. It was determined that bolts connecting the splice plate to the top plate would fail instantaneously, and not offer any additional containment. By not using the splice or "continuity plate" the test set-up is conservative. The test set-up is shown in Figure 6.1 this view is taken from the "front" of the specimen facing the phantom camera. A detailed construction drawing of the test elevation is shown in Figure 6.2.

Key Plan of Structure.
Viewed from the front of
the structure.

1	4	7
2	5	8
3	6	9

Figure 6.1: EMRTC field Test 3 structure elevation (photo)

This test utilized the Kinetic Energy Defeat Device (KEDD) in the center bays of the specimen. Two rows of KEDD's were used in each bay as discussed in Section 4.2.3. Each KEDD system weighed approximately 1,500 lbs per level. This set-up was chosen based on the initial 2 Plate Tests performed in the Proof-of-concept test series. Those tests showed the KEDD's were most effective when placed at the top of the cell. A study was also performed that evaluated the effects of adding multiple rows of KEDD's. It was determined that while one row of KEDD's is acceptable, the addition of the second row of KEDD's yields optimum results. There was a decrease in velocity of 50% between one and two rows of KEDD's., of the second plates. Based on those tests it was chosen to use two rows of KEDD's on top for these tests. KEDD hangers were placed in each cell as a control measure to ascertain if they influence the behavior of the test specimen.

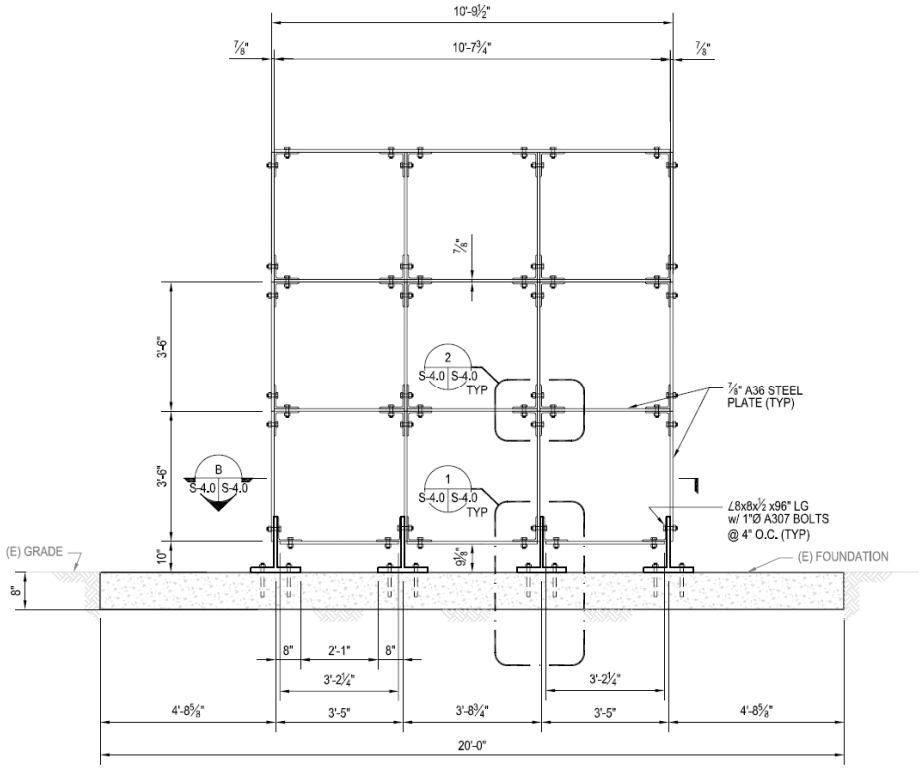

Figure 6.2: EMRTC field Test 3 structure elevation (drawing)

6.2 CHARGE SET-UP

The charge size for this test was a TNT equivalent of 2.1X at a close standoff[2]. The charge size was chosen based on a series of large scale FEA computations preformed by SAIC, in an effort to predict the type of deformation that should occur. A variety of charge sizes and standoffs were evaluated. The parameters chosen for this test predicted destruction of the first three (as-built) plates, but that the fourth plate in the bottom cell would remain intact. It was desirable to have a portion of the specimen in place as it aids in determining its post-test behavior. The charge was placed in a box with interior dimensions of 4' wide by 10' 7 3/4" long. The base was constructed out of 3/8" plywood, while the sides were constructed out of 2" x 8" (nominal) pieces. The wood pieces were connected to the plywood by 3" screws. The box was centered off of the seam in the first plate of the structure. The charge extended 2' past the seam to the front and back. The charge was placed inside of the box using a staggered formation as shown in Figure 6.3. A small booster was placed in the center of the charge to ensure proper detonation of the explosive material.

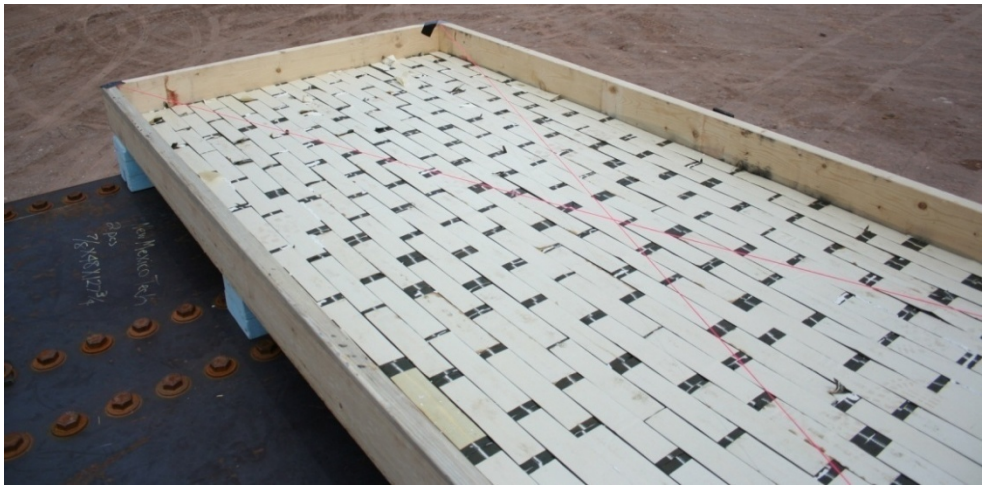

Figure 6.3: EMRTC Test 3 charge in place

[2] For specific information see EMRTC Field Test 3 report (through TSWG)

6.3 PHANTOM CAMERAS

High speed video was captured with one Phantom camera (Vision Research). It was located south of the test bed and was placed to record a close-up of the specimen in an attempt to gather useful information. The camera was placed a short distance from the test specimen and was placed behind a steel barricade. It was set-up perpendicular to the test specimen and used an angled mirror to capture the data as shown in Figure 6.4. Because a mirror was used, the frames in the video are reversed from the actual configuration. When looking at Figure 6.5, instead of the numbering scheme that starts in the upper left hand corner and continuing down and to the left, it starts on the upper right hand side with Cell 1 and continues down and to the right. Figure 6.5 shows the test specimen at initial detonation and Figure 6.6 shows the specimen during the explosion. The bottom two rows of cells are shown in this photo

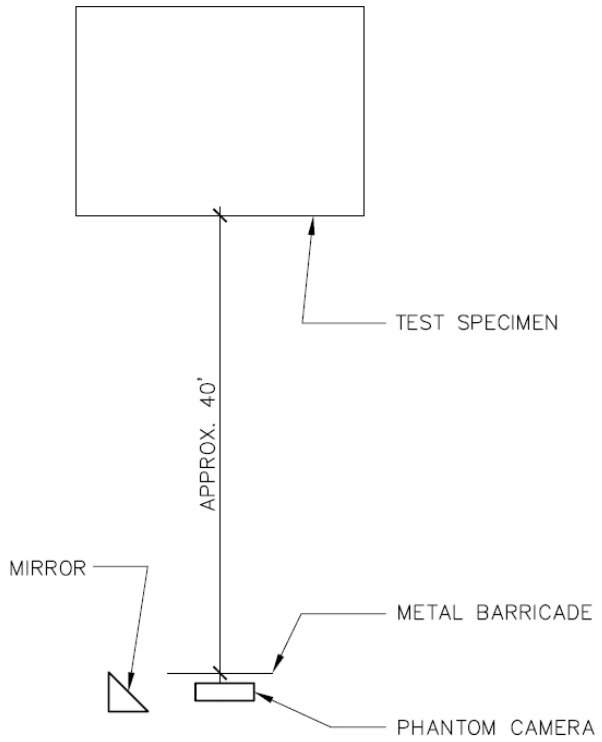

Figure 6.4: EMRTC Field Test 3 camera location (Not to Scale)

Figure 6.5: Image from the Phantom camera at initial detonation

Figure 6.6: Image from the Phantom camera showing the bottom two rows of cells

6.4 TEST RESULTS

This test utilized a 9 celled structure (3 columns by 3 rows). Each cell has been assigned a specific number for future reference. The numbering scheme is the same as that was described in the instrumentation section and is repeated here for convenience Starting at the upper left corner, when looking at the front of the specimen, the first cell is numbered Cell 1. The numbering scheme then continues down the column for Cells 2 and 3. The fourth cell is at the center of the top row. The cells below it, in the second column, are labeled Cell 5 and Cell 6. The cell in the upper right corner is labeled Cell 7. The cells directly below that are labeled Cell 8 and Cell 9. Cells 1-3 and Cells 7-9 represent as-built sections. Cells 4-6 utilized a blast mitigation technique. This numbering scheme is shown in Figure 6.1 and again in Figure 6.8. These will be referenced in future discussions about the specimen behavior, both in the text and in the photos.

Severe damage occurred to the outer cells of the test article during the explosive event. The center cell suffered less damage due to the blast mitigation techniques that were employed. Figure 6.7 shows the entire test specimen “post-test”. This photo is used again in Figure 6.8 with a color coded Key Plan that points out the specific cells. There are no easily identifiable portions of Cells 1, 4, or 7, so they are not referred in the photo. The portions of the specimen, to the right and left of the center cell, in the photo are what remained of the outer as-built cells. In Figure 6.8 they are identified as cells 2 and 8, using the orange colored arrow and numbers. These segments of the structure fell to the sides when the A307 bolts, connecting them to the center section, failed. The center column of cells (Cells 4-6) is shown in the center of the photo in Figure 6.8. It shows that Cell 6 remained intact and that Cell 5 suffered minor damage. The pink arrow and number correspond to the center cell, or Cell 5, and the purple arrow and number correspond to the intact Cell 6. A discussion of the specific

type of damage that occurred to each cell is discussed below. These pictures show the test articles where they landed after the test. A detailed post-mortem of the specimen will be included in a subsequent report.

Figure 6.7: Test specimen post-test

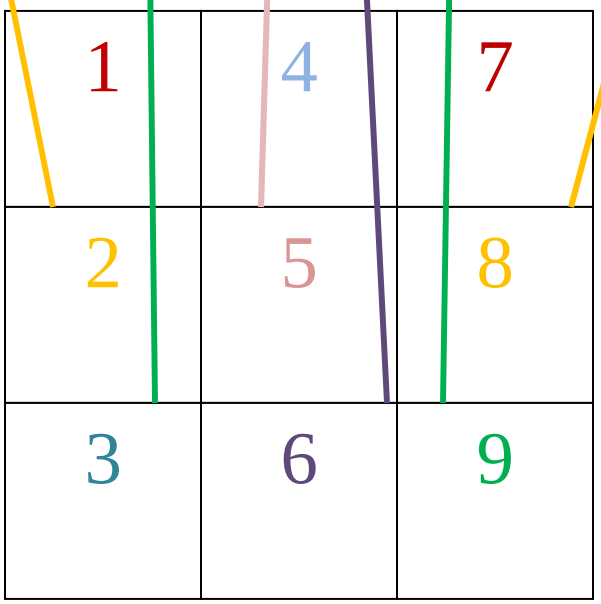

Simplified Key Plan

Figure 6.8: Test specimen post-test with Key Plan

Figure 6.9 shows the remnants of Cells 1 and 2 from the test article, this photo was taken from the side of the test article. The fragments from the first plate from Cell 1, directly under the charge, have not been located in their entirety. Many large flyer plates were found near the test specimen, most of these are from the top plates of Cells 1 and 7. The high speed video captured some data from the bottom two cells during the explosion. It shows that there are two, well formed, flyer plates that move through the structure. Figure 6.10 shows an image from the high speed video that captures flyer plates moving through the third cell at 9.638 ms after initial detonation. Figure 6.11 shows the same flyer plates at 13.838 ms near the bottom of the cell. If the distance that the flyer plates travel is assumed to be 22" (which is conservative), then the estimated velocity of those plates is over 440 ft/sec. As a reminder, the video frames are reversed in comparison to the photos (as described in the instrumentation section).

Figure 6.12 shows the bottom plate from Cell 3 (which will be discussed in more detail below). It shows that there is damage to the edge of the third steel plate, but that the center of that plate is intact. The fracture on the edge was caused by the impact of the flyer plates shown in Figure 6.11. These flyer plates are not located in the center of the cell, but instead occur at the edge of the cell. It is an example of the degree of angular momentum that was observed in this test; this is in contrast to the previous field tests wherein the charge created specific flyer plates with little or no rotation. This could be due to the seam at the center of the top plate, which can represent an actual construction practice. The photo in Figure 6.11 shows that, while the flyer plates have traversed the entire length of the specimen (all 3 cells), the third steel plate in the retrofitted cell (bottom of Cell 5) has not moved.

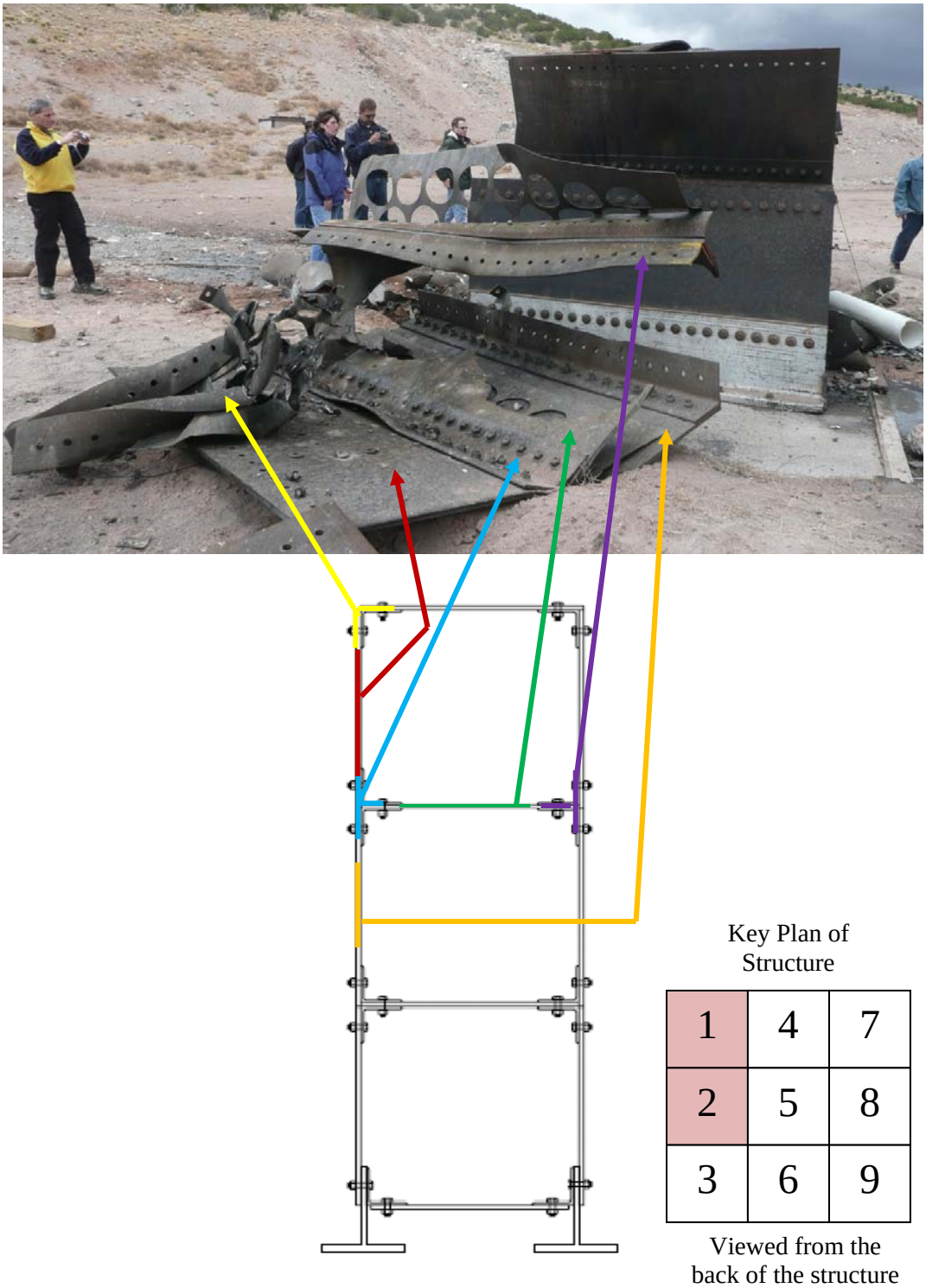

Figure 6.9: Test specimen post-test cells 1 and 2

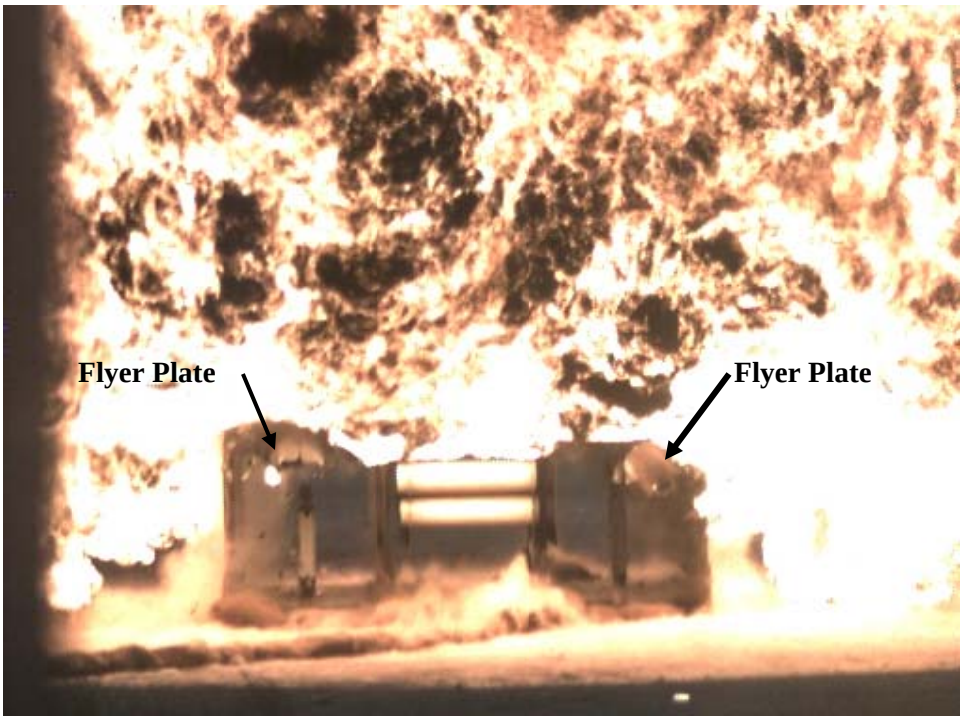

Figure 6.10: Test specimen during the test with initial flyer plates (time = 9.638 ms)

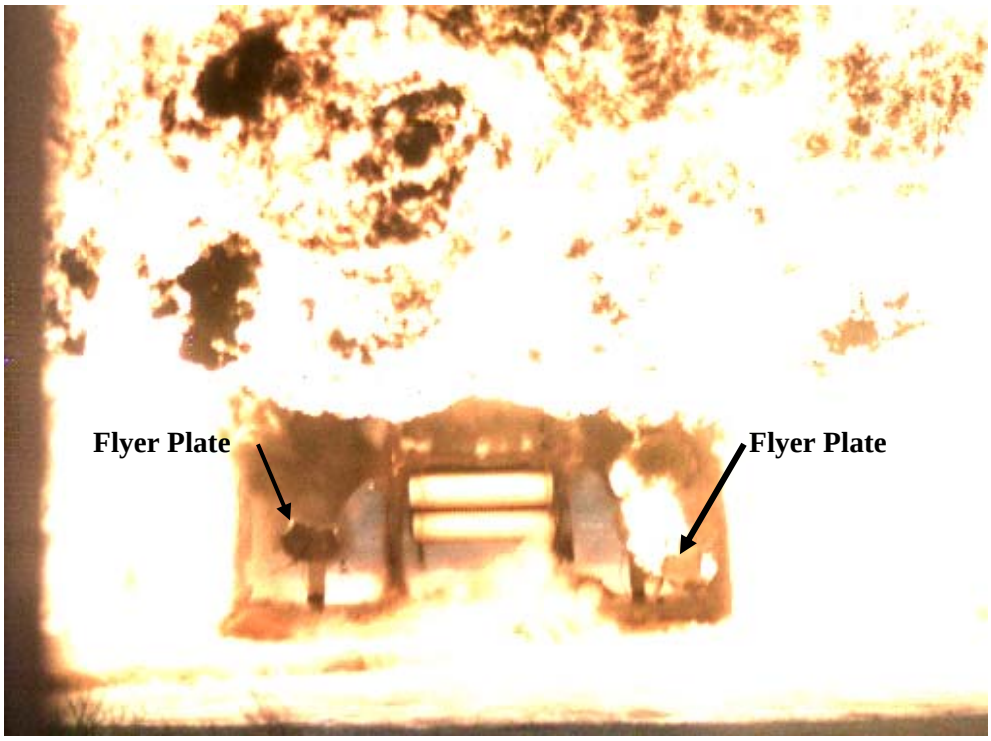

Figure 6.11: Test specimen during the test with initial flyer plates (time = 13.838 ms)

The portions of the test specimen shown in Figure 6.9 are still connected to the second plate in the test article. That plate, designated by the green arrow in Figure 6.9, is what remains of the second plate in the test specimen (the bottom plate in Cell 1 or the top plate of Cell 2). The majority of this plate has been breached and all that remains is the outer portion of the plate. This was created by the incoming flyer plates. Examples of brittle failure can be seen in the sharp edges along with the loss of the portion of plate. Near the back of the plate (back of the photo) there are some signs of ductile behavior, or petalling.

The remaining outer supports, shown by the red and orange arrows, appear to be relatively undamaged. The supporting angles, identified by the blue arrow, continue to connect all three segments from the outside portion of the cell. The supporting angles on the other side, the interior side that connected Cell 2 to Cell 5 (identified by the purple arrow), however, were separated from the supporting plate. They are still connected through the bolts along the second plate. In addition, the connecting supports between Cell 1 and 4 were also damaged along with the angle identified in the photo by the yellow arrow. Notice the torsional and longitudinal deformation of the angle. The failure of the supporting angles (that connected the angled supports of the outer cells to the inner cells) affects the behavior of the retrofitted cells, as discussed below.

Figure 6.12 shows the remnants of Cell 3 from the test article, this photo is taken from the opposite side as the photo in Figure 6.9, which is why the Key Plan is reversed. The top plate of Cell 3, or bottom plate of Cell 2, is shown in this photo. It has been designated by the blue arrow. This photo shows that the plate suffered minor damage, but was not fully breached. As discussed above, this damage is most likely from the impact of the flyer plate shown in Figure 6.10. The perpendicular supports of Cell 3, designated by the red and yellow arrows, shows very little damage to the vertical plates. The angles that connected Cell 2 with Cell 3 (orange arrow) show significant deformation, along with the loss of all the bolts that held the top plate (blue arrow) in place. The fourth plate of the structure, bottom plate of Cell 3, shown by the green arrow, is still intact. The majority of the connecting bolts are still in place, with a few exceptions.

Figure 6.13 shows the remnants of Cells 7 and 8 from the test article. Similar to Cell 1, the top plate of Cell 7 has not been located in its entirety. The photos in Figure 6.10 and Figure 6.11 show a flyer plate that was created from the top plate. Figure 6.13 shows portions of the test specimen that are still connected to the second plate. That second plate is also identified as the bottom plate in Cell 7 or the top plate of Cell 8, which is shown by the green arrow in the photo. There is a large hole in the center of the plate. It was created from the incoming flyer plates from the plate above. This plate behaved in the same manner as Cell 2, except that the edges of the plate are still intact. There are examples of both brittle and ductile failures.

The remaining outer supports behaved in the same manner as Cells 1 and 2. The orange and purple arrows, pointing to the exterior vertical supports, are, again relatively undamaged. The exterior supporting angles, identified by the yellow arrow, are still connecting all three segments. The bolts that connected the second plate (Cell 7 or Cell 8) to

the center cells (Cell 4 or Cell 5) through the interior angles, identified by the blue arrow, have all failed. The angle segment shown in the left side of the photo, identified by the red arrow, is from the top plate. The loss of these bolts resulted in the failure of the adjacent angles, as seen in Cells 1 and 2, which will be discussed below.

This test has shown that the plates parallel to the explosive charge sustain more damage than the perpendicular plates. The time scale in which the plate is damaged and the flyer plates are formed is sufficiently short that it does not allow the perpendicular supports to react before the plates have failed. As a retrofit the strengthening of the vertical plates, is not considered to be effective.

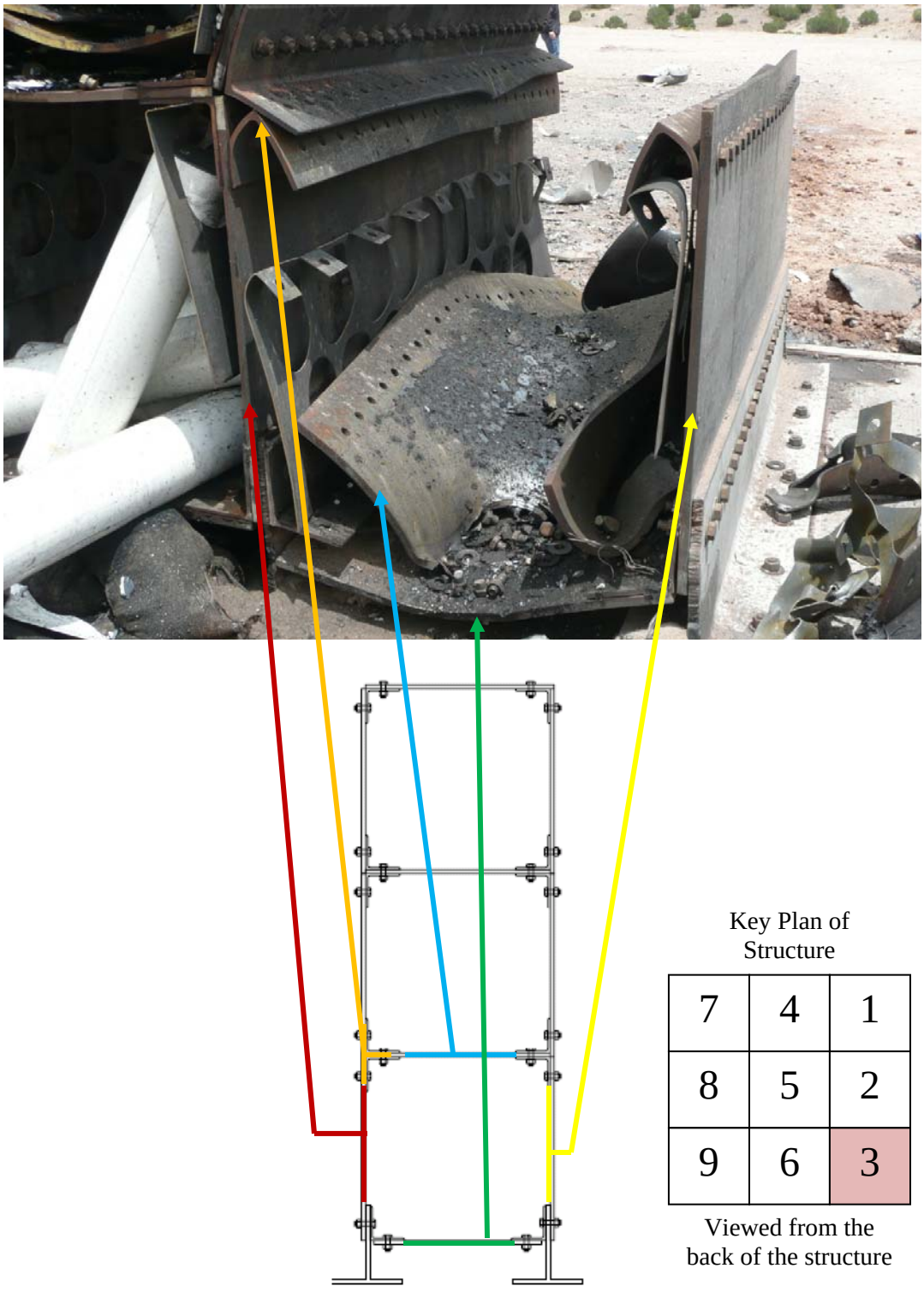

Figure 6.12: Test specimen post-test cell 3

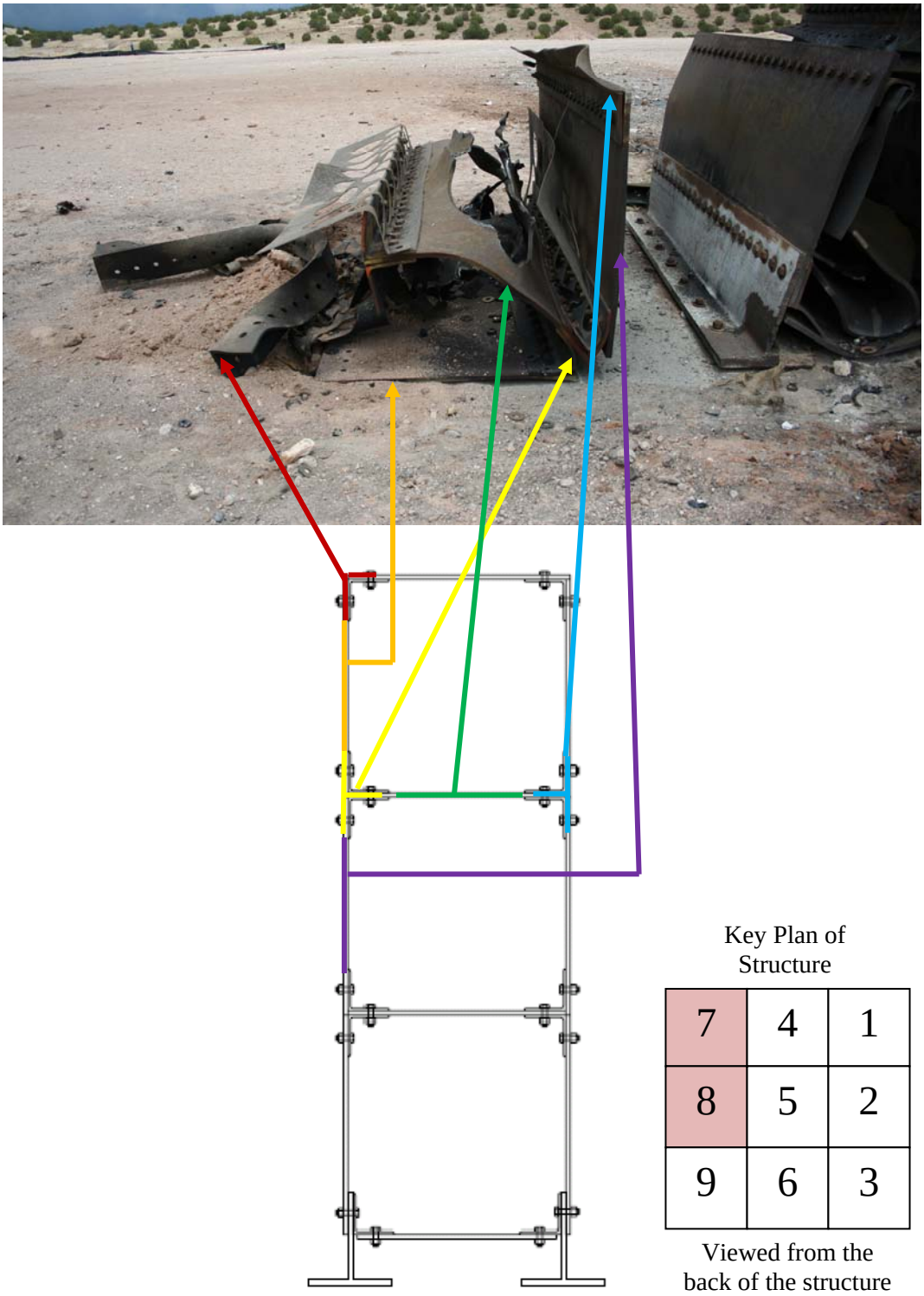

Figure 6.13: Test specimen post-test cells 7 and 8

Figure 6.14 shows the remnants of Cell 9 from the test article. This photo was taken from the front of the structure. It shows that Cell 9 behaved in a similar manner to Cell 3. The top plate of Cell 9, or bottom plate of Cell 8, is shown in this photo, as designated by the yellow arrow. It shows that the plate suffered moderate damage along some edges, but was not fully breached. This is similar to the discussion of Cell 3. The large flyer plate impacted the third plate and caused the damage in the plate. While the behavior of the outer cells was symmetrical, this plate suffered more deformation along its length than its counterpart in Cell 3. This is due to the creation of a larger flyer plate in this row of cells, as opposed to the other set of cells. Figure 6.15 shows the relative size of the flyer plates. The flyer plate created on this side of the specimen is also shown in Figure 6.15 and is designated by the yellow circle. The perpendicular supports of Cell 9 (in Figure 6.14) designated by the red and purple arrows, shows very little damage to those plates. The angles that connected Cell 8 with Cell 9 (orange and blue arrows) show significant deformation, along with the loss of all the bolts that held the third plate (identified by the yellow arrow) in place. The fourth plate in the structure, bottom plate of Cell 9 shown by the green arrow, is still intact. The majority of the connecting bolts are still in place, with a few exceptions. It is interesting to note that the test showed symmetrical results. .

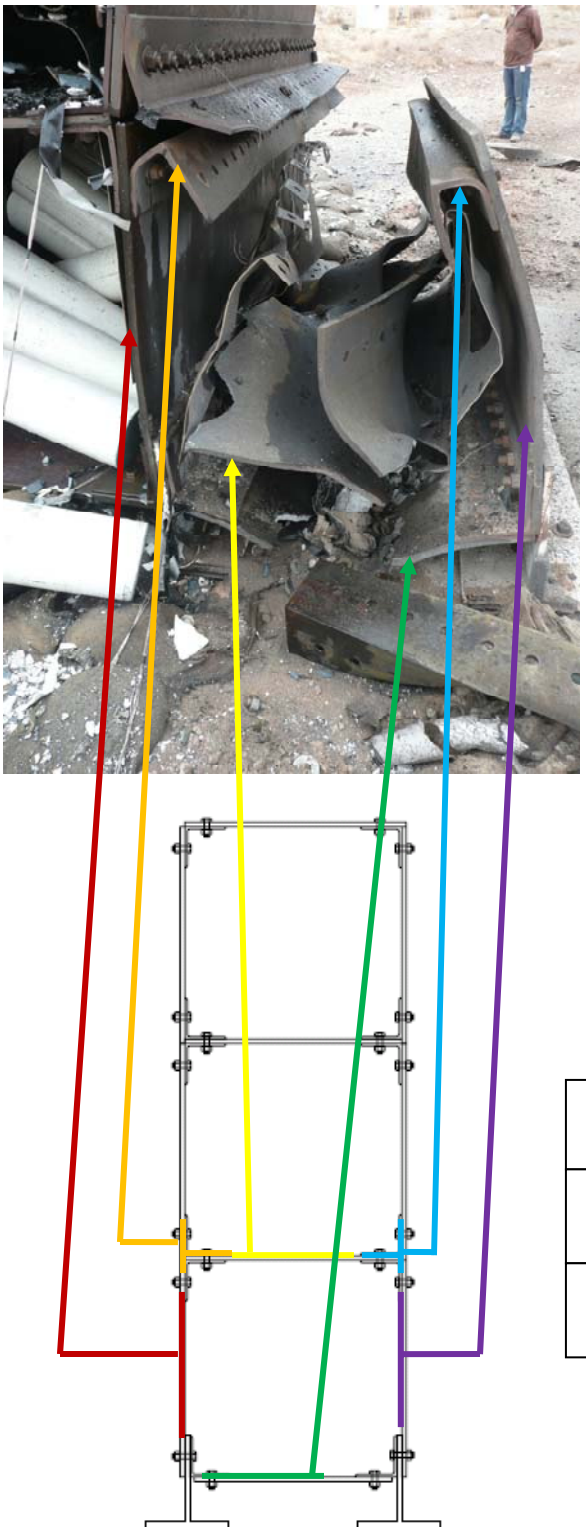

Key Plan of Structure

1	4	7
2	5	8
3	6	9

Viewed from the front of the structure

Figure 6.14: Test specimen post-test cell 9

Portions of the top plates of Cells 1 and 7 were found throughout the test bed. Some of the larger pieces were found close to the test article, while others were found much farther away. Figure 6.15 shows the test specimen post-test and some of the flyer plates that were found nearby. In order to help distinguish the flyer plates, or top plate fragments, from the rest of the test article, they have been circled in the photo. Figure 6.16 show the flyer plates found in front of the test specimen (taken while standing in front of the specimen and looking away.) The fragments from the top plates that were found near the test specimen were significantly larger than the segments that were found at much farther distances. All of the fragments that were found showed signs of both brittle and ductile failure. They have sharp edges where they were formed from the top plate, but also show signs of plastic deformation as demonstrated in the twisting and curling of the plates.

Smaller flyer plates were found at significant distances from the test article. These fragments are much smaller than the ones found closer to the test article, but they indicate that the energy created by the explosion was sufficiently large to launch steel fragments these significant distances. These pieces were formed from the first plate which impacted subsequent plates and eventually rebounded off of the test structure to land at these varied locations. Two fragments were found approximately 400’ – 500’ from the test article. A different portion of the top plate was located almost 1,000’ feet from the test article.

Figure 6.15: Test specimen and miscellaneous flyer plates

Figure 6.16: Miscellaneous flyer plates

This test exhibited two very different types of failures. The outer cells showed the brittle and ductile fractures that can be expected in an as-built specimen. The center cells showed the blast damage mitigation potential of the Kinetic Energy Defeat Device (KEDD). While there are inherent differences in the manner in which each column of cells will behave, the center cells vs. the outer cells. Conclusions can still be made that show the effectiveness of the KEDD system.

In the as-built cells (outer cells), portions of the top plates, in the form of flyer plates, were found throughout the test bed. The remaining support structure was found to the left and right of the test set-up. They are no longer in place because the connecting bolts that held the specimen to the center cell, failed.

The behavior of the center cell was very different from the outer cells; the majority of the support structure of the center cell collapsed straight down onto Cell 5, as opposed to being strewn throughout the test bed. Figure 6.19 shows the center cell (Cells 4 and 5) post-test. The first thing that should be noticed in this photo is that the majority of the miscellaneous pieces shown in the photo are relatively intact. This is due to the effectiveness of the KEDD device. Instead of the first plate fragmenting into many small pieces it appears, from the initial investigation, that only the bolts sheared along the edge of the plate, causing the edges of the plate to bow through ductile deformation. Two large sections of the top plate were found. The separation of the two pieces is not due to fragmentation, but from the joint between the two plates in the test specimen. One of those pieces is shown in Figure 6.19 and is denoted by the blue arrow. It is unclear the extent of the damage to the top plate beyond what is shown in the figure, but it appears to have deformed plastically around the sides. The second top plate is located in the back of the cell, but is not shown in this photo.

One of the unintended effects of the KEDD system is that it changes the failure mechanisms of the first plate. This was initially exhibited in the 2 Plate Tests (see Figure 5.64) and is shown here as well. Instead of the brittle fractures seen in the baseline tests, more ductile deformation occurs when the KEDD's are used. The ductile behavior, exhibited by petalling and other large plastic deformations, consumes significant amounts of energy, which helps decelerate the fragments that are formed. Those large first plates interacted with the KEDD system as they tried to move through the cell. The KEDD system appears to have worked in a similar manner as in the 2 Plate Tests.

The high speed video captured some of the water expulsion of the KEDD system in the second cell (Cell 5) as shown in Figure 6.17 which occurred at 14.338 ms. Approximately 0.5 ms after the flyer plates in the outer cells had impacted the bottom plate. The outer flyer plates have traveled over 6' more than the flyer plate in the center cell over the same time scale. If it is assumed that the flyer plate in the center cell has traveled 4' when the first row of KEDD's was activated in the center cell, then the velocity of that plate at 14.338 ms is approximately 280 ft/s. (4'/0.014338sec) This results in a difference in velocity, from the flyer plates to the activation of the first row of KEDD's in the second cell, of approximately 36%. The water is highlighted by the blue circle and appears to be the entire width of the specimen and is moving down its length. Evidence shows that that water jetted out the length of the specimen and traveled significant distances as demonstrated by Figure 6.16. It shows water jets extending approximately 50' past the end of the specimen. The width of the water jets extended beyond the 3'- 2" length of the KEDD and came closer to expanding the width of the specimen as shown in Figure 6.18. The jets were moving at such a high velocity, near the structure, that they were able to carve small valleys into the soil in front of, and behind, the structure.

Portions of the PVC pipe were also found throughout the test bed. Some of the fragments were quite small, while others pieces were significant in size. Due to the number of the fragments that were observed, as opposed to the 2 Plate Tests where few fragments were found, it would not be recommended to use a KEDD that is stronger than the Schedule 40 PVC pipe.

Figure 6.17: High speed video capturing water expulsion by the KEDD system

After the first plate activated the KEDD system, it decelerated and continued to move through the structure until impact with the second plate (bottom plate of Cell 4 or top plate of Cell 5). The second plate, exhibited in Figure 6.19 by the yellow arrow, was only slightly damaged. The plate was deformed, but not breached. One of the difficulties with this test set-up was that each cell interacts with the other. In this case, the baseline cells caused more damage to their supporting angles which in turn affects the center cell. As stated above, all of the support bolts that connected Cell 2 to Cell 5 and Cell 5 to Cell 8 were sheared off. When these bolts failed, it caused the angles that supported the KEDD's to collapse. The support

angles between Cell 4 and 5 are shown in Figure 6.19 designated by the purple arrows. It can be seen that these angles appear to be undamaged, and that they probably collapsed through the cell subsequent to the bolt failures. Based on Figure 6.17, it appears that the second plate activated the KEDD system before the collapse. In the future, this test should be performed with KEDD's in all cells. This would ensure that there are no unintended consequences from the behavior of the adjacent cells.

Figure 6.18: Jets formed by KEDD system

The bottom plate shown in Figure 6.19 and designated by the green arrow, shows that it is completely intact. The only damage that it appears to have suffered is from the impact of the mass above it. All of the angles and bolts that support this intersection remain intact. This occurrence is also exhibited in the vertical support plates of Cell 5 that are still in place, as shown by the red arrows. These supports are no longer vertical, but that is due to the effects of the angles and plates inside the cell.

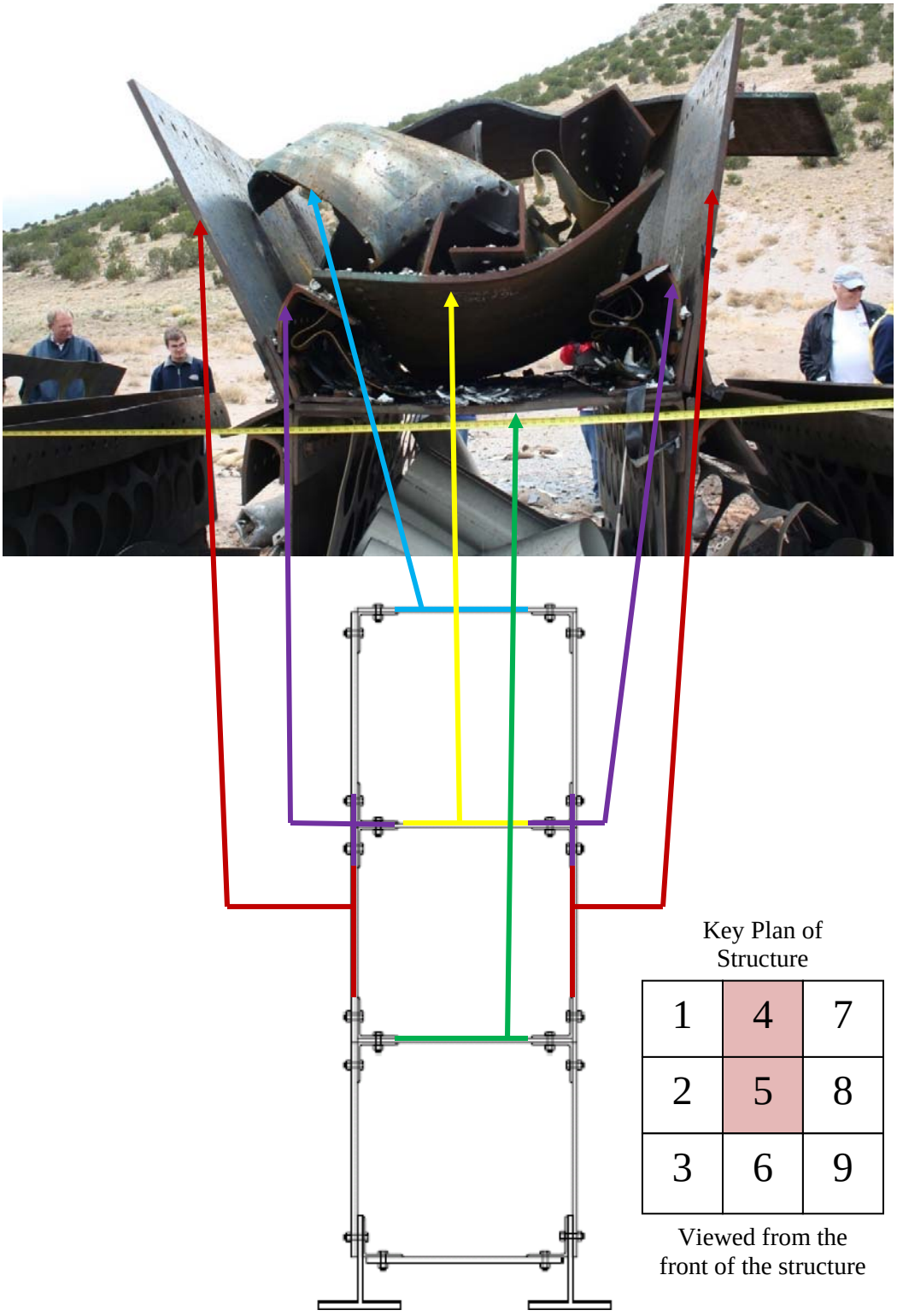

Figure 6.19: Test specimen post-test cells 4and 5

Figure 6.20 shows Cells 4, 5, and 6 post-test. This photo exhibits the entire behavior of the retrofitted specimen. At the very top of the photo, located by the yellow arrow, is one of the vertical supports from Cell 4. It is most likely the support between Cell 4 and 7, but this is not certain. It shows that the plate has not been breached, yet exhibits only minor deformation. The latter could be from the force of jets expelled out of the KEDD, but it is probably from the interaction with other pieces of the specimen. As stated earlier, the vertical supports are still attached to their connecting angles at the intersection of Cells 5 and 8 as well as Cells 5 and 2. This figure also shows portions of the first plate which came to rest inside of Cell 5, as shown by the green arrow. The second plate is shown by the orange arrow and the third plate is pointed to by the purple arrow.

Figure 6.20 is important because it shows the complete and undamaged Cell 6. It should be noted that all of the KEDD's fell out of their supports. In future designs of similar experiments, a better support system should be used that ensures that the KEDD's stay in place. In addition, the KEDD design was not ideal; some of the end caps of the KEDD's detached from the pipe and allowed the water to flow out. Instead of using an adhesive solvent to attach the end caps to the PVC pipe, a better option is to fuse the plastics together, providing a tighter seal. The caps that were screwed into the KEDD's after the water was filled could be fused in the same manner to prevent long term leaking.

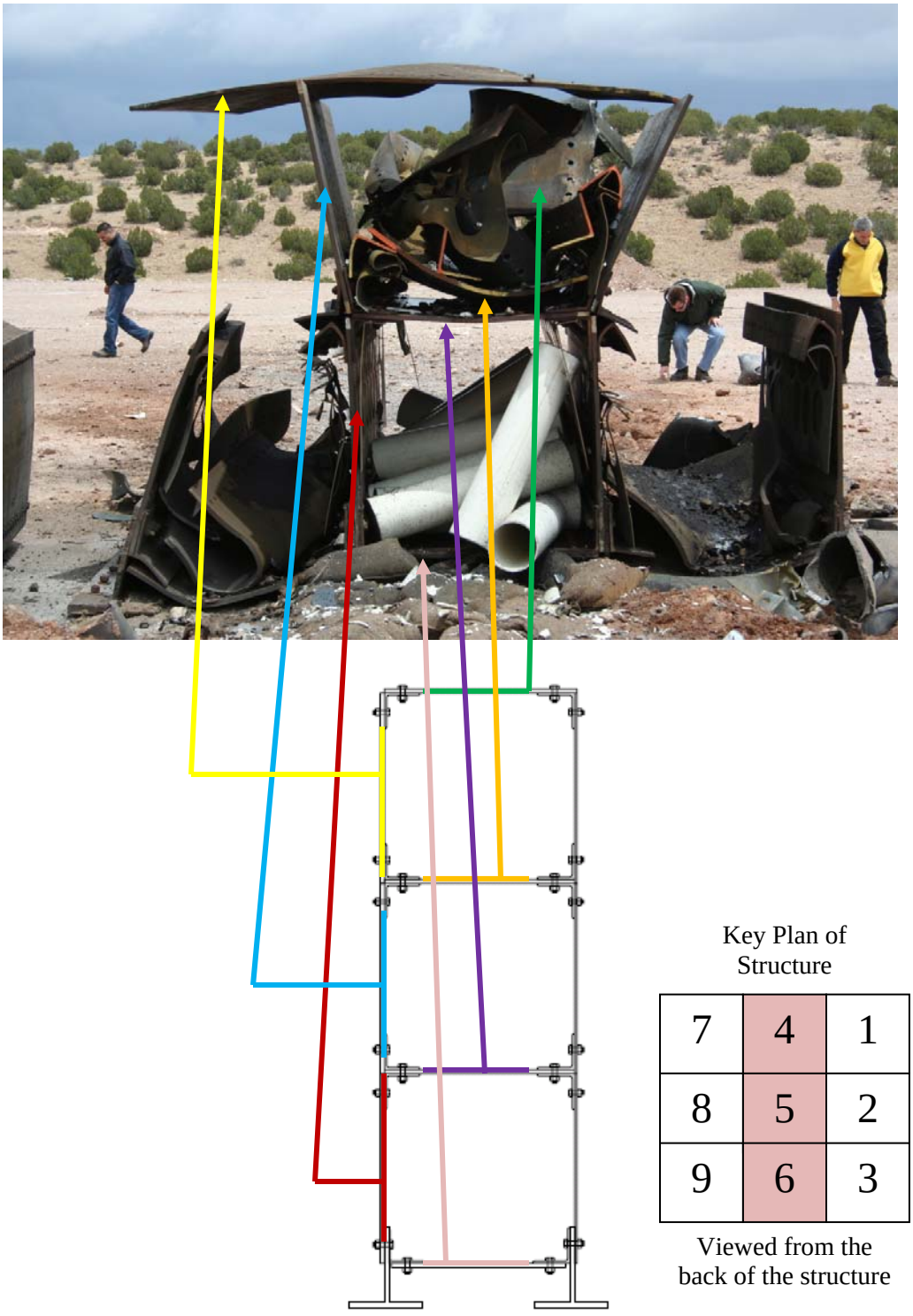

Figure 6.20: Test specimen post-test cells 4, 5, and 6

6.5 ADDITIONAL MITIGATION TECHNIQUES

In addition to the development and continued design improvement of the KEDD system, other steps could be taken to increase the strength and ductility of existing built-up cellular steel structures. Most of the structures consist of riveted, or low strength, connections. In order to improve the ability of the structure to respond to extreme loads, the bolt strength should be increased. Chapter 3 discussed the added benefit of changing from low strength to high strength bolts which allows more deformation to occur in the plate before it is released from the supports. In the laboratory tests, it was shown that the high strength bolts can survive almost twice as long compared to the low strength bolts in a simulated explosive event. (Low strength bolts fail in 5 ms while high strength bolts fail in 10 ms under similar loading conditions, see Chapter 3 for more information) There are additional methods to increase the strength and ductility of these bolts. At the third EMRTC field test, suggestions were made of ways to improve the behavior of the bolts. One idea that was suggested is to use longer bolts with a stack of washers, making it more difficult to shear the bolt by not having the threads in the shear plane. Mike Stanley, from EMRTC, suggested that adding some neoprene between the washers will also increase the ability of the bolts to restrain the steel plates. Both of these ideas, along with others, could easily be tested in the UCSD Blast Simulator utilizing their higher energy, second generation, Blast Generator's (BG50). Once the strength of the bolts is increased, the support angles may need to be strengthened as well. A specific design has not been developed or tested, but it could involve using stiffeners along the length of the angle to restrain it from rotating due to the force of the connecting plate (parallel to the charge).

There are other improvements that can be made to this system; however, the purpose of this research endeavor was to develop a viable retrofit concept, not to develop a completed design protocol for a specific structure.

6.6 SUMMARY

This test showed the effectiveness of the new KEDD system inside a realistic, full scale structure. The structure consisted of nine cells in a 3x3 arrangement. The inner column of the specimen employed the retrofit device, while the outer sections remained in their as-built condition. After the explosive event portions of the first plate, from the as-built specimen, were found throughout the test bed. The high speed video shows that these flyer plates moved through the structure impacting other steel members. The damage to each plate of the as-built structure is summarized here: the first plate fractured into many fragments and impacted the plates below, a large hole formed in the second plate allowing the fragments to move through the cell and impact the plate below, minimal damage occurred to the third plate in the structure; however, enough energy was imparted into the specimen to shear all of the supporting bolts and allow the entire plate to impact the fourth (and last) plate. The last plate was damaged, but still retained most of the bolts that connected it to the structure.

The cells that utilized the new blast mitigation technique behaved quite differently than the outer (or as-built) cells. The first plate (which was already in two distinct pieces by construction) sheared the bolts along the angled supports and impacted the KEDD system below. The first plate showed signs of significant ductile deformation as opposed to the brittle fracture exhibited in the first plate of the as-built specimen. The second plate separated from the angled supports and moved through the cell interacting with the KEDD's. There was limited damage to the angles that supported the second plate. If the strength of the bolts were increased, then additional damage mitigation would occur. The force of the second plate, and other pieces of the specimen on the third plate caused minor deflections of the plate. The entire bottom cell (third and fourth plates) was intact and undamaged.

It is evident, as shown in the previous EMRTC field tests and the baseline Proof-of-concept tests, that the structures in their as-built conditions are very susceptible to significant levels of damage from near-contact charges. When the KEDD system is employed, it improves the behavior of the entire system and limits the damage. If additional blast mitigation techniques were employed along with the KEDD system, it would continue to mitigate damage to the structure as a whole.

6.7 BIBLIOGRAPHY

1. **Morril, Ken.** *Water Slug Write-up.* Karagozian and Case. Burbank, CA : s.n.

2. **Livermore Science Technology Cooperation.** *LS-DYNA Theory Manual.* Livermore, CA : s.n., 2006.

3 **Livermore Science Technology Cooperation**. *LS-DYNA Keyword Users Manual.* Livermore, CA : s.n., 2007.

4. **J. Wolfson, G. Hegemier, F. Seible.** *Kinetic Energy Defeat Device (KEDD) Proof of Concept Tests.* Department of Structural Engineering, University of California, San Diego. San Diego, CA : s.n., 2007.

5. **Sears.** Wearever 9" Comercial Square Cake Pan. *Sears website.* [Online] [Cited: May 26, 2008.] http://www.sears.com/shc/s/p_10153_12605_00807863000P?vName=Appliances&cName=Cookware,Bakeware&Gadgets&sName=Bakeware&psid=MSNSHOPPING01&sid=IPx20070925x00002b.

6. **Sandia National Laboratories.** *CTH Course Notes.* Sandia, NM : Sandia National Laboratories, 2007.

7. CONCLUSIONS AND RECOMMENDATIONS

7.1 CONCLUSION

The main purpose of this research project was to develop a retrofit strategy for built-up cellular steel structures. The retrofit needed to somehow mitigate the damage caused by a flyer plate impacting the structure at high velocities. It also needed to conform to the restrictions associated with these structures: the retrofit must be compact and able to be installed in small spaces, it must be temporary as it will need to be removed for inspections, and it cannot affect the overall behavior of the structure. Within these limitations a retrofit system has been developed that can help mitigate the damage to these structures. Without such a retrofit a reasonable sized near-contact explosive could destroy the entire structure; with it that damage could be contained to a local failure, preventing collapse.

A classically elegant retrofit device has been developed for this very complicated problem. The novel concept of the Kinetic Energy Defeat Device (KEDD) has been demonstrated to be effective both in the laboratory and the field. Tests have also shown that the behavior of the KEDD system works with a variety of plate thicknesses making this retrofit applicable to many different built-up cellular steel structures. Design equations for the KEDD system have been developed that are based on plate thicknesses. Different layouts of KEDD's have been evaluated and it has been determined that the most efficient layout of a KEDD system is two rows directly behind a steel plate.

The main purpose of the twenty-four varying field tests was to determine the effectiveness of the KEDD system. Tests were performed comparing the types of damage that occurred in the baseline tests to tests using the KEDD system. While those tests successfully determined the effectiveness of the KEDD system, they also provided additional information

on the behavior of steel plates under these extreme loads. The baseline data from those tests has provided information of the steel phenomenology that was previously unknown. Currently, the data from the different baseline tests are being used to improve existing high fidelity computer models and is improving material models. Analyses are being performed to replicate the type of damage seen in these tests. It is the Author's hope that eventually the computational tools will be verified and validated to the point that field testing is not necessary; however, we are not yet at that point.

In addition to the successful development of the KEDD system, other useful data has been gathered that can be used to improve existing computer models. New material models can be developed based on strain rate and bolt data from laboratory tests. There are over 600 bolts in varying degrees of failure available for future research.

7.2 RECOMMENDATIONS

A wealth of information was developed in this research; however, there are still aspects that should be evaluated. The strain rate data gathered in the laboratory tests is highly useful information as it shows the strain rates for an entire system instead of a sample of the material. This data can help predict the overall structural behavior of a steel system taking into account the connection type. If this data was used to improve existing material models, it would be useful to many people both academic and professional. Those models could be based on the failure mechanisms of low and high strength bolts. Additionally, the behavior of the steel plate within a structural system can be determined and a better steel model constructed.

Additional research should also be performed on the KEDD system through the use of computational analyses along with laboratory and field tests. Items that should be evaluated are: KEDD shape, KEDD spacing and size relationship, KEDD location, and effectiveness of the system based on incoming velocity. Investigations should be conducted on the structural systems that support the steel plates to determine their weakness. Connections are an integral part of these structures and are one of the basic failure modes, as discussed in the third chapter. Studies should be performed to determine if strengthening the connections and the support angles could limit further damage. Some of those studies should evaluate the effectiveness of longer bolts with a large number of washers to determine the increase in ductility. In addition, studies should be performed to determine the effectiveness of applying neoprene between the washers to continue to increase the effective ductility/strength of the bolts under explosive loads. Strengthening of the support angles may also provide added benefit allowing the steel plate to continue to plastically deform before the supporting angles and bolts fail.

This novel concept was developed for a specific class of structures, however, it does not mean that it cannot be modified and improved for other applications.

A. APPENDIX A- CHAPTER 3

A.1 BRITTLE AND DUCTILE FRACTURE MODES

Figure A.1: Examples of brittle fragments

Figure A.2: Examples of brittle failures

Figure A.3: Example of ductile fractures

A.2 FIELD TESTS

A.2.1.1 TEST SET-UP

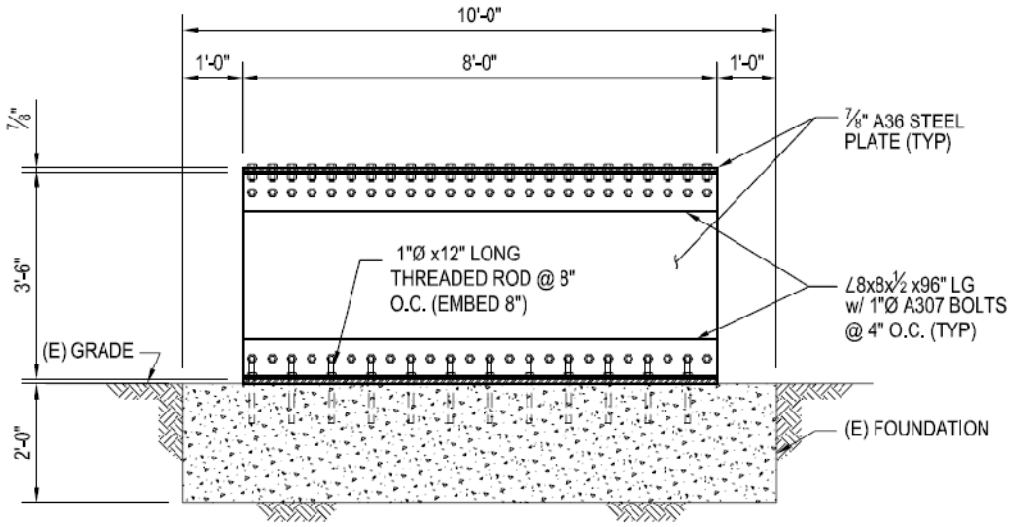

Figure A.4: EMRTC field Test 1 set-up section

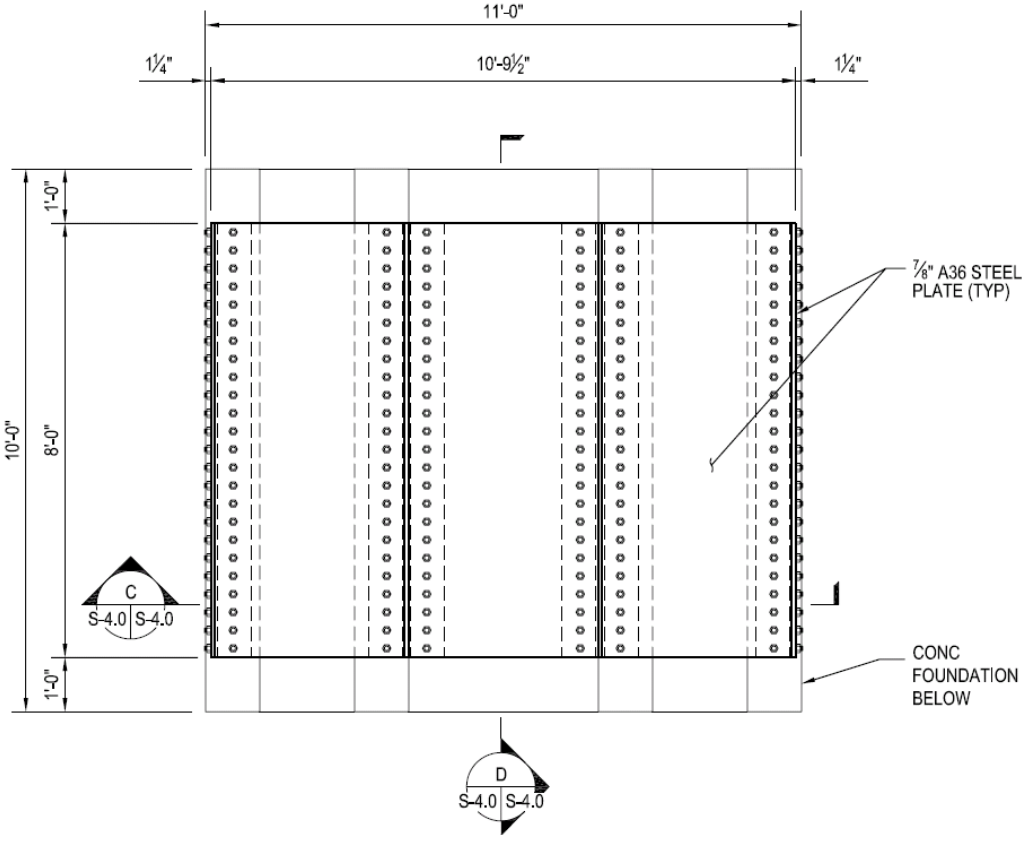

Figure A.5: EMRTC field Test 1 set-up plan view

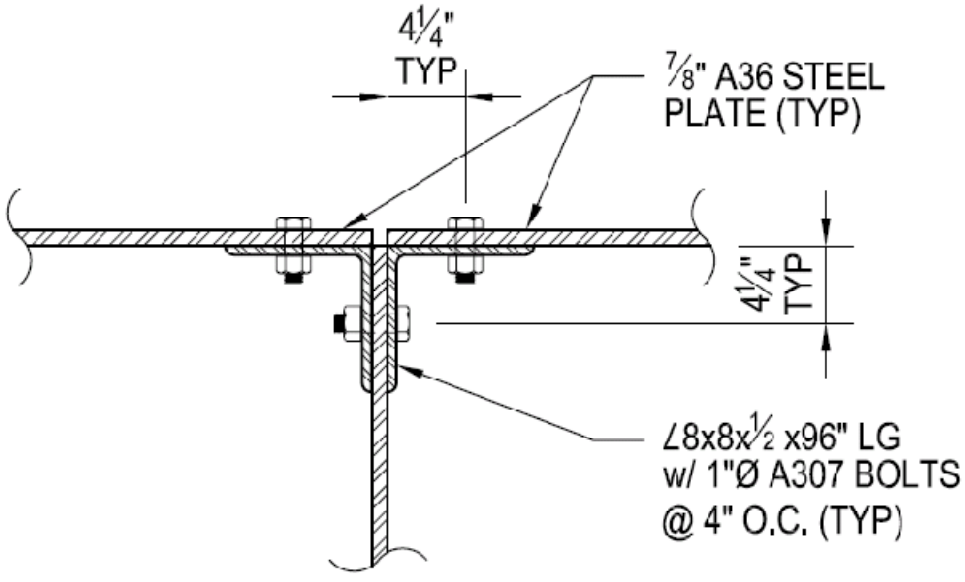

Figure A.6: EMRTC field Test 1 set-up detail

Figure A.7: EMRTC field Test 1 set-up (photo)

A.2.1.2 CHARGE SET-UP

Figure A.8: Test 1set-up with explosive charge in place

A.2.1.3 TEST RESULTS

Figure A.9: Flyer plate created from EMRTC Test 1

Figure A.10: EMRTC Test 1 – post-test

Figure A.11: Portion of structure from EMRTC Test 1

a) Specimen outside of the test bed b) Specimen still in the test bed

Figure A.12: Failures from EMRTC Test 1 – post-test

A.2.2 FIELD TEST 2

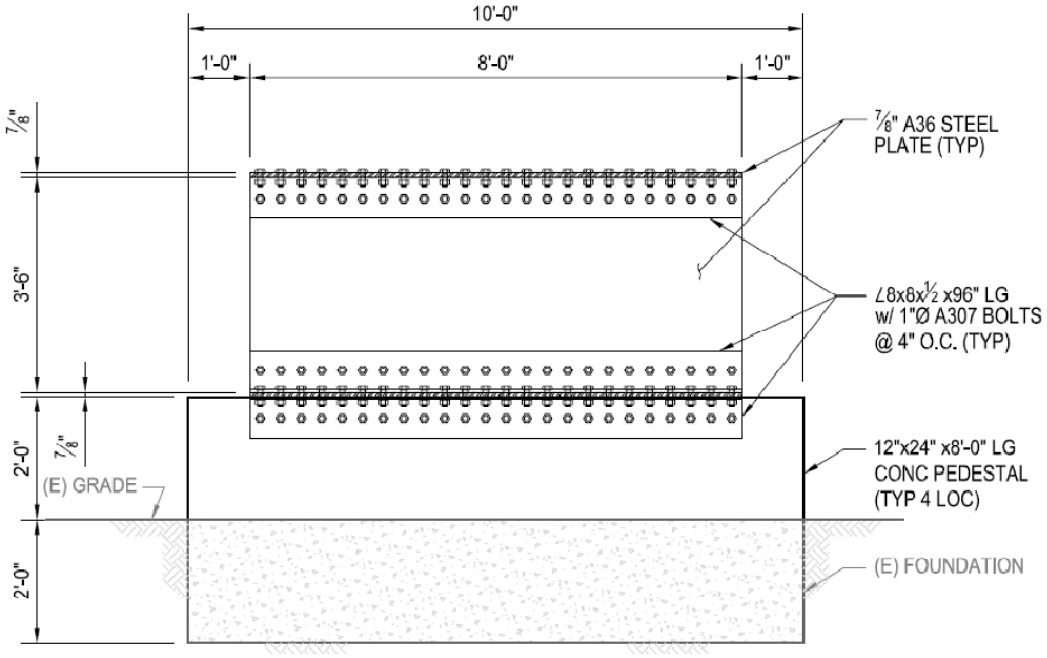

Figure A.13: EMRTC field Test 2 set-up section

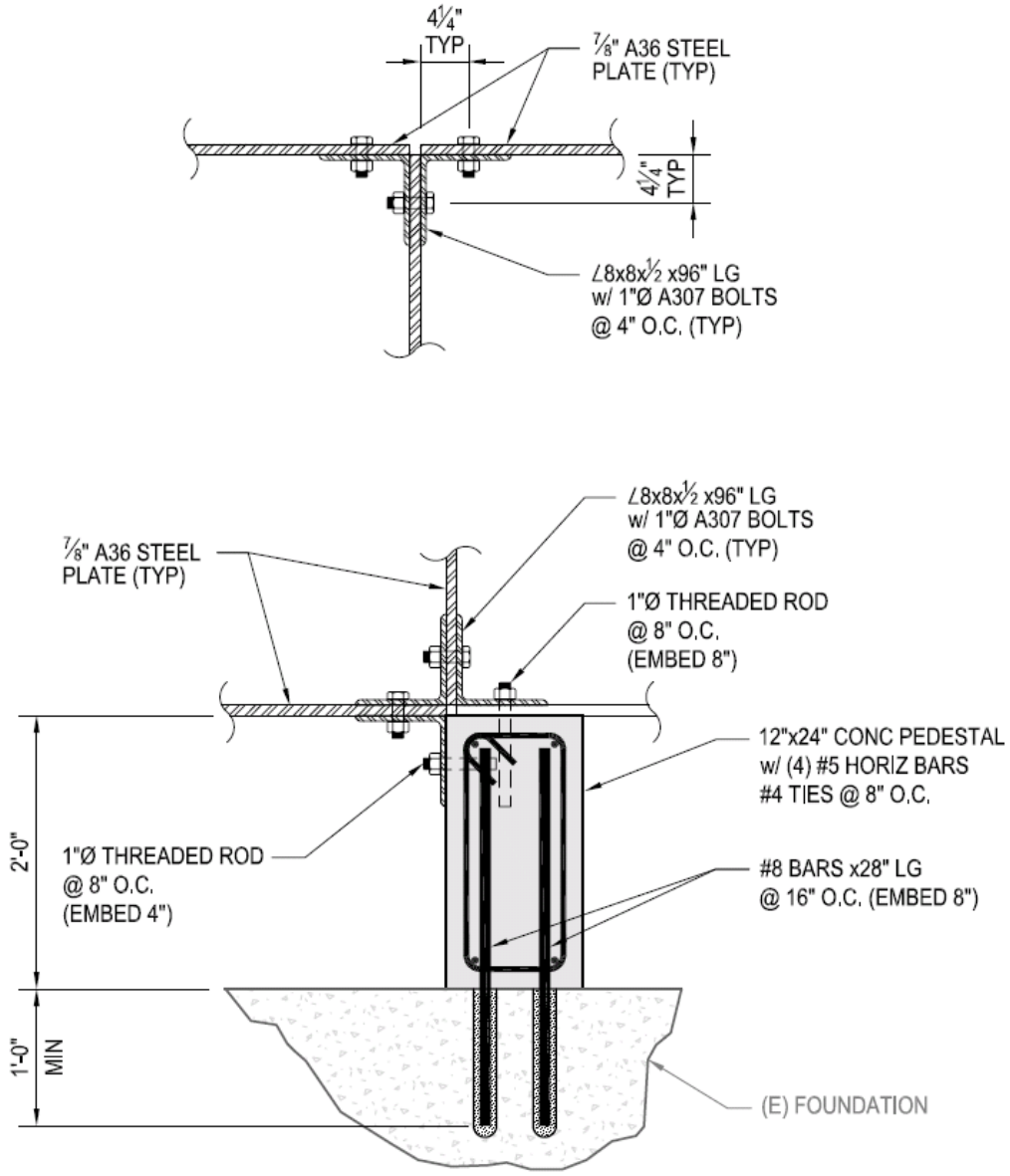

Figure A.14: EMRTC field Test 2 set-up details

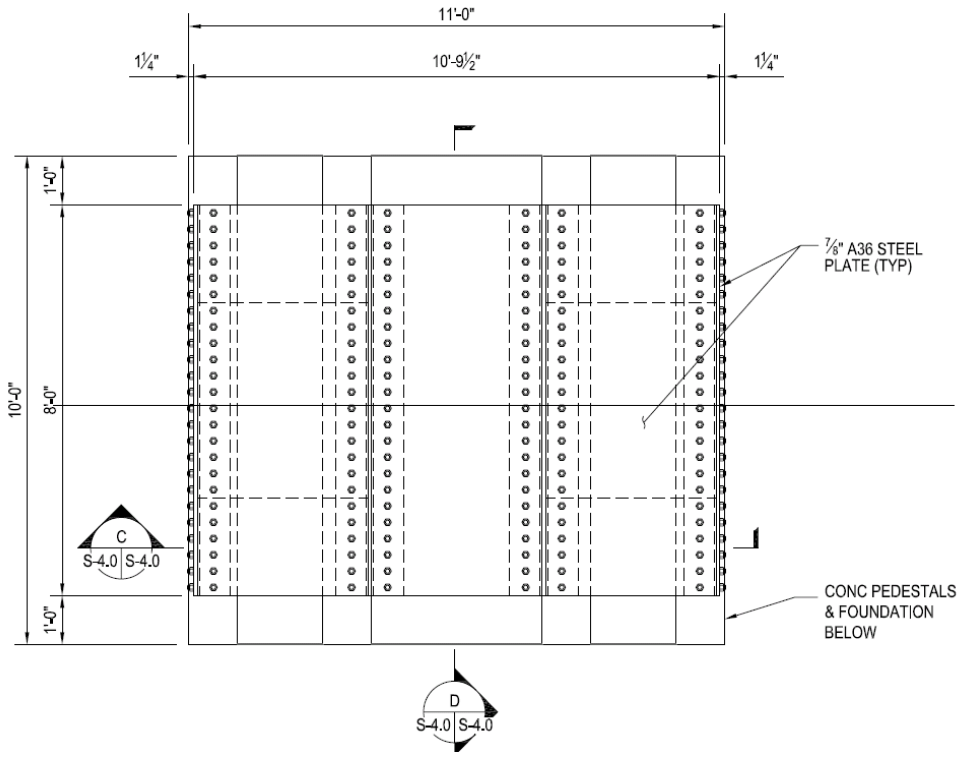

Figure A.15: EMRTC field Test 2 set-up plan view

A.2.2.1 CHARGE SET-UP

Figure A.16: Test charge for EMRTC Test 2

A.2.2.2 TEST RESULTS

Figure A.17: Top plate fragment found approximately 16' from test specimen

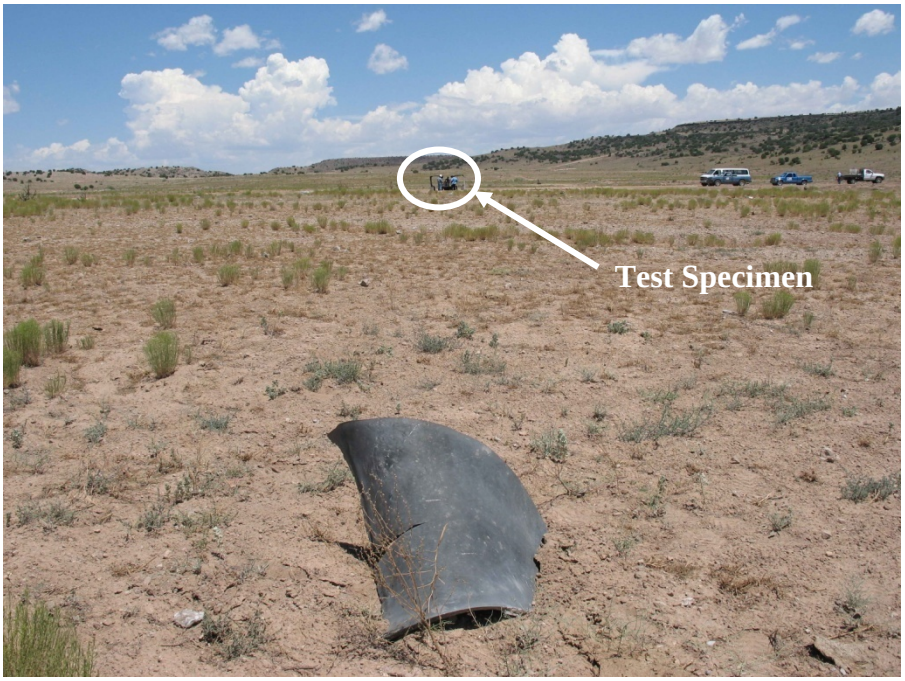

Figure A.18: Top plate fragment found approximately 400' from test specimen

Figure A.19: Failures from EMRTC Test 2 – post-test

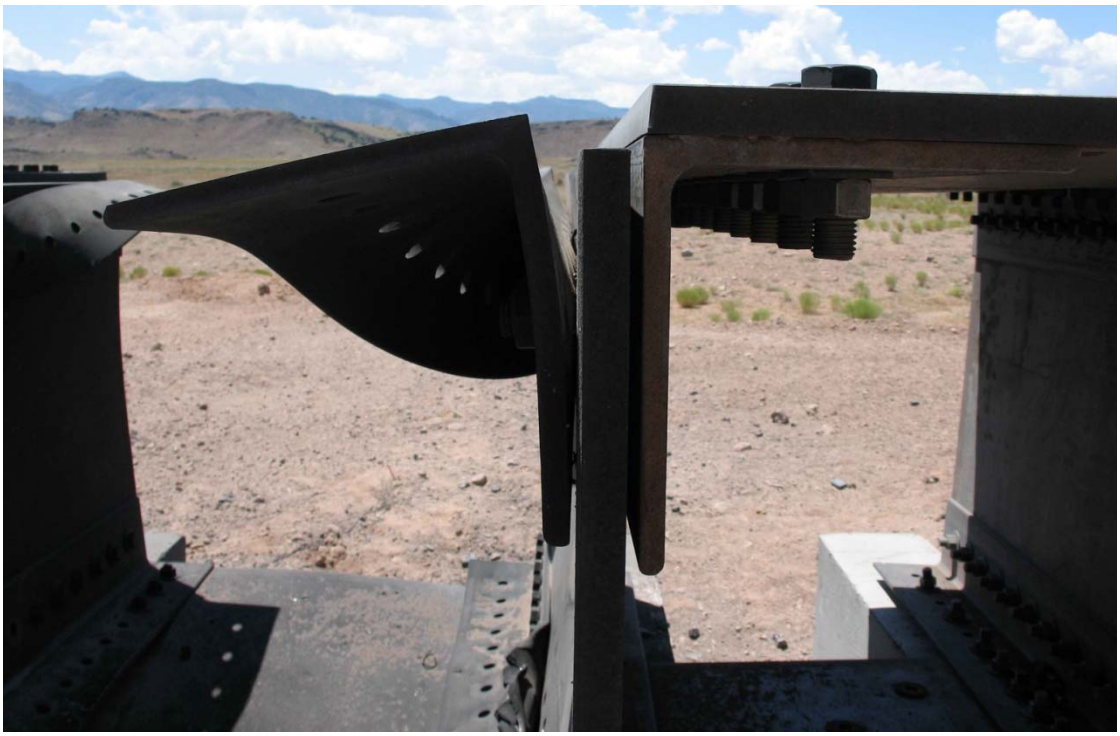

Figure A.20: Demonstration of localized failures from EMRTC Test 2

A.3 LAB TESTS

A.3.1 TEST SET-UP

Table A.1: Ballistic Loading Tests – Type 1 test matrix

Test Number	Plate Thickness	Bolt Type	Goal Velocity	Actual Velocity
1	0.25 in.	Grade 5	10 m/s	
2	0.25 in	Grade 5	10 m/s	9.60 m/s
3	0.25 in	Grade 5	15 m/s	17.14 m/s
4	0.25 in	Grade 5	28 m/s	28.10 m/s
5	0.25 in	Grade 5	19 m/s	18.07 m/s
6	0.5 in	Grade 5	34 m/s	-
7	0.5 in	Grade 5	34 m/s	30.17 m/s
8	0.5 in	Grade 5	28 m/s	27.20 m/s
9	0.5 in	Grade 5	28 m/s	27.50 m/s
10	0.5 in	Grade 5	28 m/s	28.20 m/s
11	0.5 in	Grade 5	28 m/s	27.50 m/s
12	0.25 in	Grade 5	28 m/s	27.80 m/s
13	0.25 in	Grade 5	28 m/s	28.10 m/s
14	0.25 in	A307	28 m/s	28.10 m/s
15	0.5 in	A307	28 m/s	27.70 m/s
16	0.25 in	A307	19.5 m/s	18.60 m/s
17	0.25 in	A307	15 m/s	14.21 m/s
18	0.5 in	A307	25 m/s	25.70 m/s
19	0.5 in	A307	23 m/s	23.00 m/s
20	0.5 in	A307	19.5 m/s	18.40 m/s
21	0.75 in	A307	28 m/s	27.90 m/s
22	0.75 in	A307	25 m/s	24.90 m/s
23	0.75 in	A307	25 m/s	23.00 m/s
24	0.25 in	A307	19.5 m/s	19.50 m/s
25	0.25 in	A307	19.5 m/s	18.50 m/s
26	0.5 in	A307	19.5 m/s	17.93 m/s
27	0.5 in	A307	23 m/s	24.04 m/s
28	0.75 in	A307	28 m/s	27.66 m/s
29	0.75 in	A307	25 m/s	25.83 m/s
30	0.75 in	A307	28 m/s	28.50 m/s
31	0.875 in	A307	28 m/s	27.49 m/s
32	0.875 in	A307	28 m/s	27.46 m/s
33	0.875 in	A307	28 m/s	28.01 m/s
34	0.25 in	A307	20 m/s	23.75 m/s
51	0.25 in	A307	9 m/s	9.00 m/s

Table A.2: Ballistic Loading Tests – Type 2 test matrix

Test Number	Plate Thickness	Bolt Type	Goal Velocity	Actual Velocity
35	0.25 in.	A307	23 m/s	21.50 m/s
36	0.5 in.	A307	25 m/s	22.70 m/s
37	0.5 in.	A307	29 m/s	26.80 m/s
38	0.5 in.	A307	29 m/s	27.10 m/s
39	0.5 in.	A307	29 m/s	27.48 m/s
45	0.5 in.	A307	29 m/s	26.98 m/s

Table A.3: Bolt material properties

Bolt Type	Size	Proof Load Stress	Yield Strength	Min. Tensile Strength
SAE J429 Grade 5	1/2”	85 ksi	92 ksi	120 ksi
ASTM A307	1/2”	60 ksi	--	60 ksi
ASTM A325	1/2”	85 ksi	92 ksi	120 ksi
ASTM A490	1 1/4”	120 ksi	130 ksi	150ksi - 170ksi

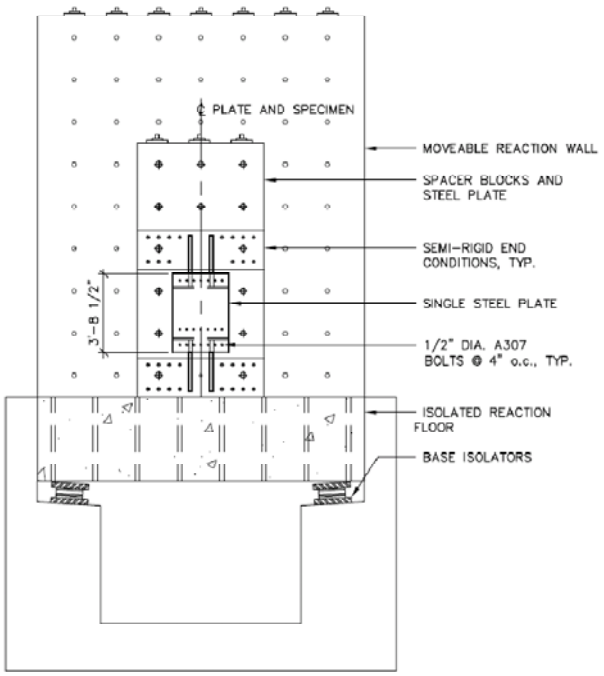

Figure A.21: Ballistic Loading Type 1 and 2 test set-up – east elevation

Figure A.22: Ballistic Loading Type 1 and 2 test set-up

A.3.2 BLAST GENERATOR DESCRIPTION

The blast simulator system consists of four Blast Generator (BG) units that can be arranged in arrays of one to four units depending on the type of test article. A blast generator is essentially a hydraulic actuator with an impact mass on the front which can reach a high velocity in a relatively short stroke. A blast generator without the impact mass attached is shown in Figure A.23(a). The impacting mass and velocity determine the magnitude of the impulse.

The shape of the force-time curve of the mass-to-specimen impact is controlled by means of a non-linear spring (a polyurethane pad) commonly referred to as a “programmer”. The programmer produces an impulse with critical characteristics of the impulse from an explosion. One important characteristic of the programmer is a soft initiation that helps prevent high frequency content during the initial contact with the specimen. This is accomplished in part by the textured front surface that increases stiffness nonlinearities, shown

in Figure A.23(b). The second characteristic of the programmer design is the spring rate of the material, which determines the time period of the pulse and the peak force. The blast generator accelerates the mass and programmer assembly to the velocity required for the desired transfer of momentum and the programmer controls the shape (amplitude and duration) of the impulse imparted onto the specimen.

The control system is used to control the servo-valves that meter oil into the actuators, trigger the data acquisition system, and monitor the sensors used to control and record the performance of the test. The control system software provides real-time control of the servo-valves and provides a user interface for the user to enter the settings necessary to achieve the desired impact velocity.

Figure A.23: a) Blast Generator unit prior to installation. b) Profile and front view of programmer.

A.3.3 INSTRUMENTATION

A.3.3.1 BG ACCELERATIONS

Acceleration for the impacting mass was determined in the Ballistic Loading Tests – Type 1. They were measured with 10Kg piezoelectric shock accelerometers. Up to four accelerometers could be attached to the back of the plate at one time. The different locations were: 4" to the right and left of the centroid and 6" above and below the centroid. The cables that transmit the acceleration signal to the data acquisition system were fastened to the BGs to minimize artificial signals in the data caused by their vibration. At the beginning of the test series, four accelerometers were used to measure data, however, as testing progressed many of the accelerometers became damaged and it was decided to use one accelerometer placed within a steel pipe for protection. Figure A.24 shows two different accelerometer layouts. Figure A.24(b) shows the accelerometer in the location used for the majority of the tests. The photo shows the accelerometer in place with the steel pipe that was installed to protect the accelerometer. The accelerometers are located by circles in Figure A.24 Information regarding the specific instrumentation layout can be found in Appendix A.

A.3.3.2 BG VELOCITIES

The Track Eye Motion Analysis (TEMA) software package, from Image Systems, was used to obtain graphical displacement and velocity measurements from the video capture. For each BG, a point is selected on the impact mass and the software records its displacement-time history. The software then differentiates the displacement-time history using a 7 point numerical differentiation scheme to obtain the velocity time history.

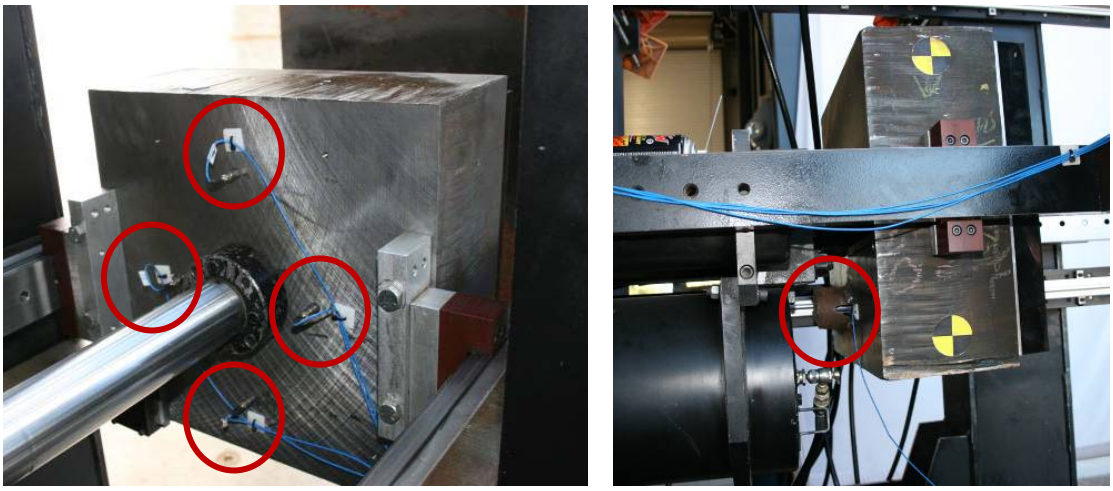

Figure A.24: Location of BG accelerometers

A.3.3.3 PLATE DISPLACEMENTS

The videos from the Phantom cameras were used in conjunction with the TEMA software to measure specimen displacements at several different locations. Targets were attached to 2" x 2" x 1/4" steel plates that were welded to the side of the test specimen, as shown in Figure A.25, to assist in tracking the specimen displacements. The targets were placed at five locations along the plates at approximately four equidistant intervals. The specific location of each target can be found in Appendix A and B. Additional targets were attached to the semi-rigid end conditions in order to track the amount of movement that occurs during a test.

A.3.3.4 STRAIN GAGES

The strain in the steel plate was measured using 5mm strain gage rosettes (YEFRA-5 produced by Texas Measurements.) They are high yield, 0˚, 45˚, 90˚ rosettes with a 5mm gage length and a 2mm width. These strain gages will measure strain until the specimen stretches 10 – 15%. There were up to five gages on each test specimen. They were placed in

a total of twenty-two different locations. The variation in locations was performed in order to gather additional behavior of the strain in the plates. The initial locations (Gages 1 -7) were chosen because they were centered behind the location of the impacting mass. Gages 4 and 5 were outside the "footprint" of the programmer. The initial tests using these gages did not show the strain rates that were expected. It was then determined to try locations even closer to the center of the plate (Gages 8-11) and were quickly discarded in an attempt to capture higher strain rates. Gages 12-15 tried to determine what the stresses were on the front of the specimen between the bolt holes. The goal for the next location that was tried was to gather strain rate behavior near the bolt holes, to determine if this is where the maximum stain rates would occur. To achieve this Gages 17 and 18 were placed centered 2" across from two bolt holes and 2" down (or up depending on location) from that row of bolts. The majority of the test had the strain gages at these locations. During the test series it was decided to determine the axial and bending stresses occurring through the plate. To achieve that gages needed to be placed in the same location on the front and back of the steel plate. This is exhibited in Gage pairs 19 and 21, or 20 and 22. It was still important to gather data near the bolt holes, however, because of the support conditions the gages could not be in the same place as Gages 17 and 18. They were still located between two bolt holes, but were located 7" below (or above) the bolt line. Specific strain gage information, including the additional information gathered from gages 19-22 is located in Appendix E and F. A schematic drawing of the different locations is show in Figure A.26

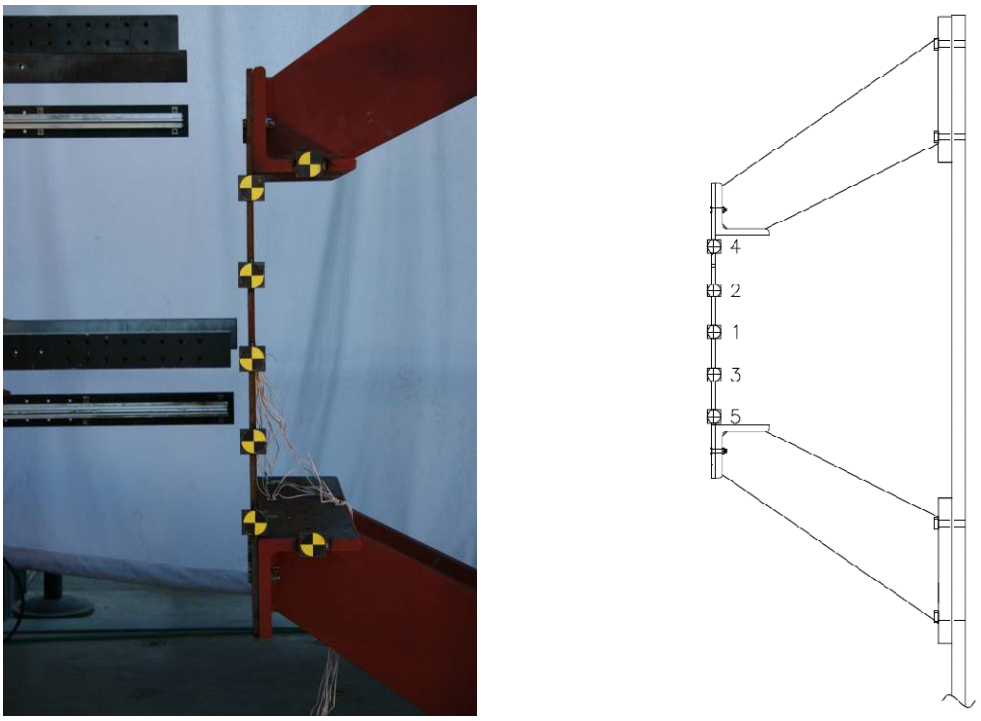

Figure A.25: TEMA target locations a) Photo b) Drawing

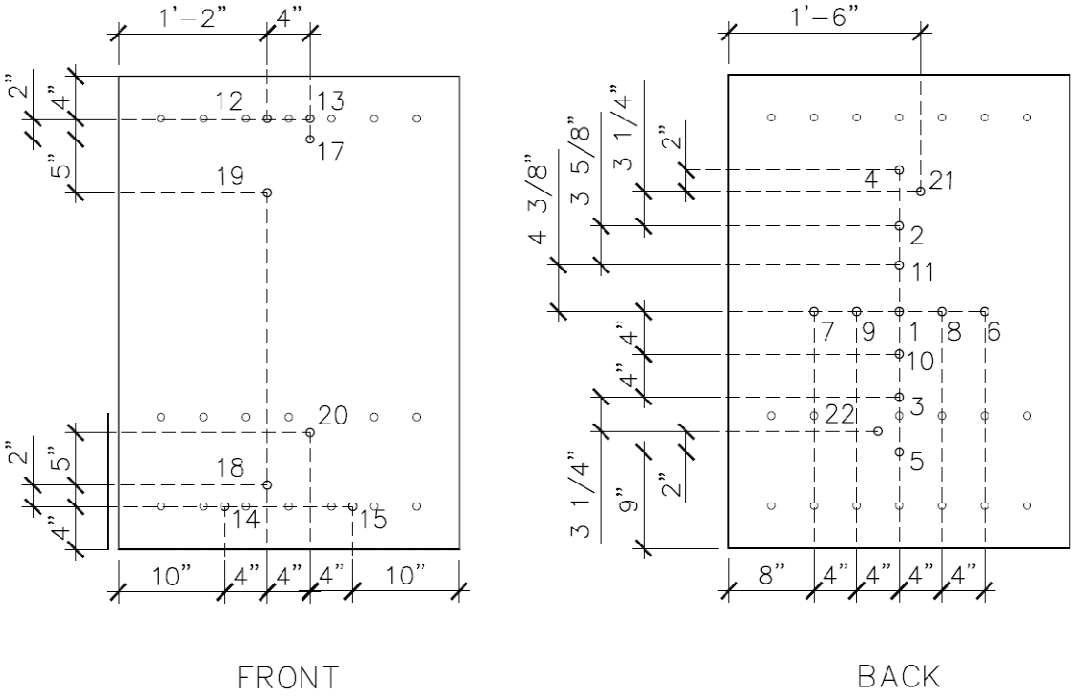

Figure A.26: Strain gage locations

A.3.4 BANDPASS FILTERS

A.3.4.1 ACCELERATION

In an attempt to minimize noise in the acceleration data, a bandpass filter was applied in the data processing program DPlot. The upper bound of the frequency was determined by calculating the speed of sound through the material and dividing it by the wavelength as shown below.

$$f = \frac{c}{\lambda} \tag{2.1}$$

and

$$c = \sqrt{\frac{E}{\rho}} \tag{2.2}$$

Table A.4 shows the different frequencies used for the different impacting masses. Wavelength is determined by assuming the wave bounces through the thickness of the plate 8 times.

Figure A.27 shows the unfiltered acceleration data from a typical test. Figure A.28 shows the data filtered using the bandpass filter as explained above. As can be seen in the graphs, all of the major peaks and valleys are captured in the filtered data. The data shown, in Appendix A, has been filtered using this method.

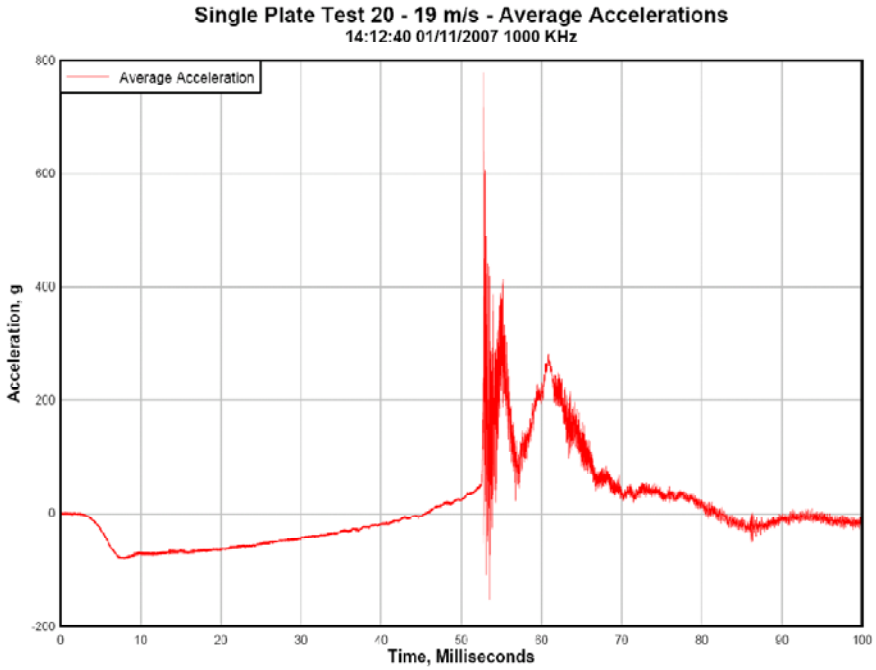

Figure A.27: Unfiltered acceleration data from a typical test

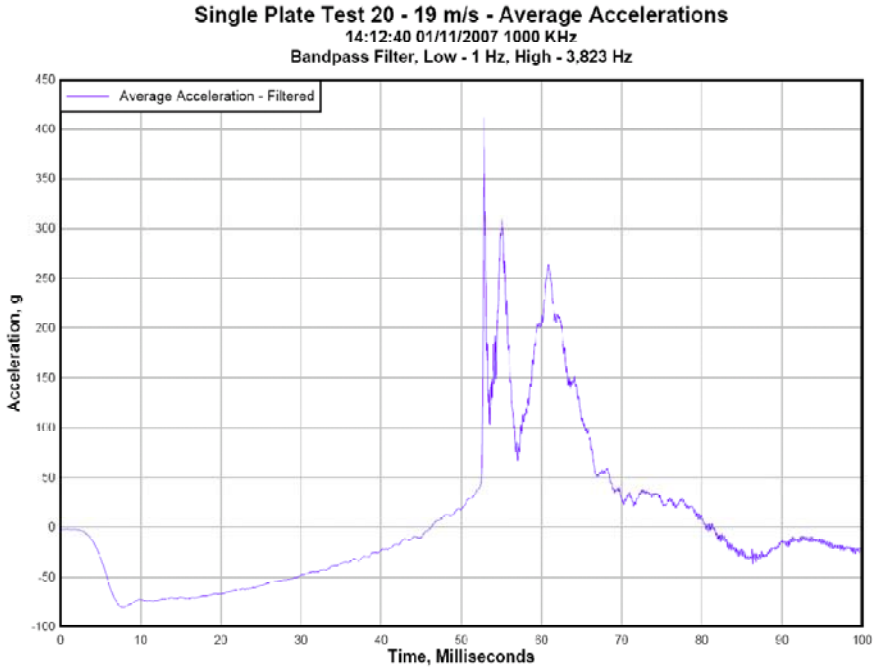

Figure A.28: Filtered acceleration data from a typical test.

Table A.4: Frequencies used for acceleration bandpass filter

Description	Material	Young's Modulus (ksi)	Density (lb/ft^3)	Speed of Sound (ft/s)	Material Thick. (in.)	Number of Passes	Frequency (Hz.)
Impacting Mass 1	Steel	29,000	490	16,566	6.5	8	3,823
Impacting Mass 2	Steel	29,000	490	16,566	6.5	8	3,823
Impacting Mass 3	Alum.	10,000	162	16,903	2.5	8	10,142

A.3.4.2 STRAIN GAGE

In an attempt to minimize noise in the strain gage data, a bandpass filter was applied in the data processing program DPlot. The noise in the signal can be from a variety of different sources i.e., the signal conditioner, acoustical noise, vibration of the wires, the gage factors, or even the settings on the data processor. In order to determine what frequency the data should be filtered at, a series of FFT's were performed on a sample of strain gage data. These samples included different plate thicknesses and bolt types from different tests.

Through the use of the FFT, the cut-off frequency was determined to be 10,000 Hz. The following graphs show strain data from five different tests. These tests had plate thicknesses of 1/4", 1/2", 3/4" and 7/8". Two of the tests employed high strength bolts (Grade 5) supporting the plate, while the other four tests used low strength bolts (A307). Figure A.29 shows the unfiltered data of the Maximum Principal Strain. Figure A.30 shows that same data using the bandpass filter. Figure A.31 and Figure A.32 show the Minimum Principal Strain both unfiltered and filtered. As shown in the graphs, all of the major peaks and valleys are captured in the filtered data. All data that will be discussed has been filtered using this method.

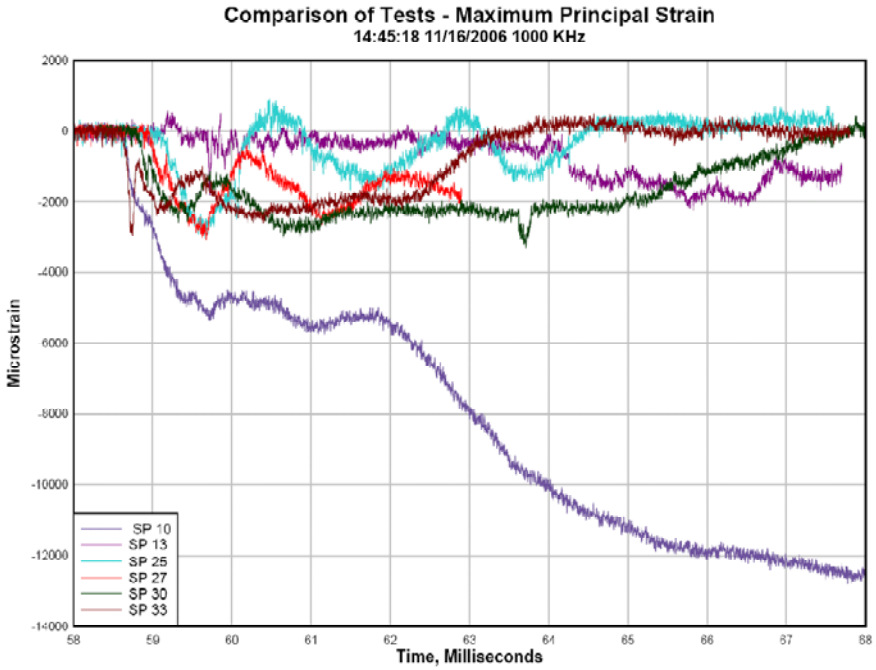

Figure A.29: Collection of maximum principal strain data

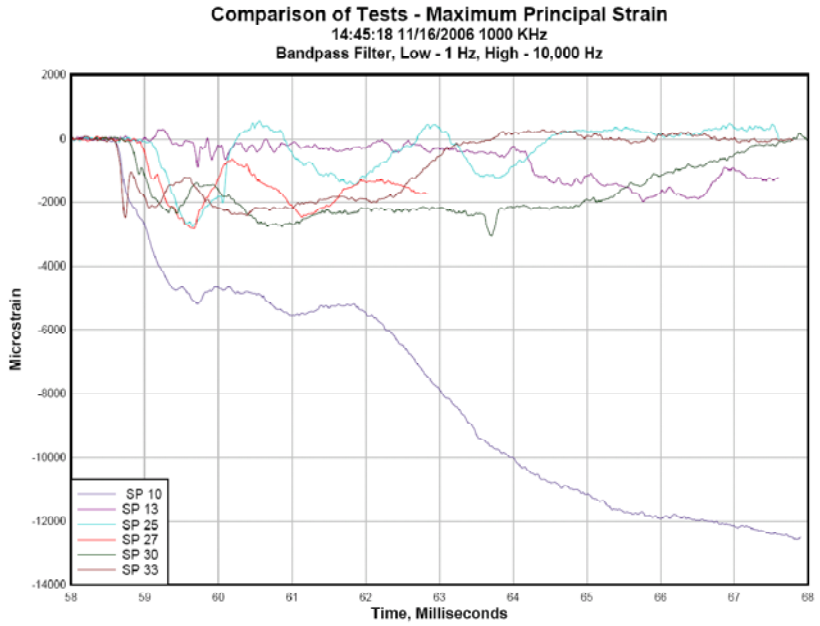

Figure A.30: Collection of maximum principal strain data using a bandpass filter

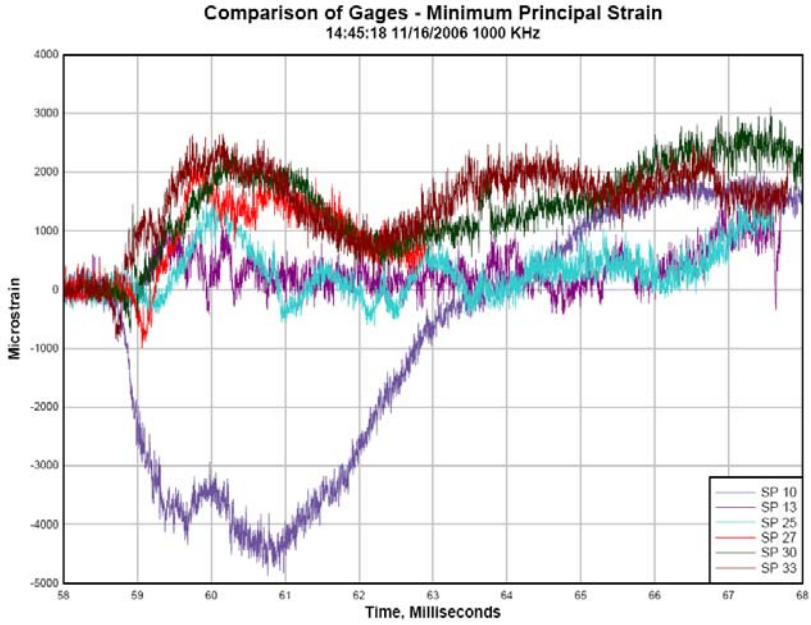

Figure A.31: Collection of minimum principal strain data

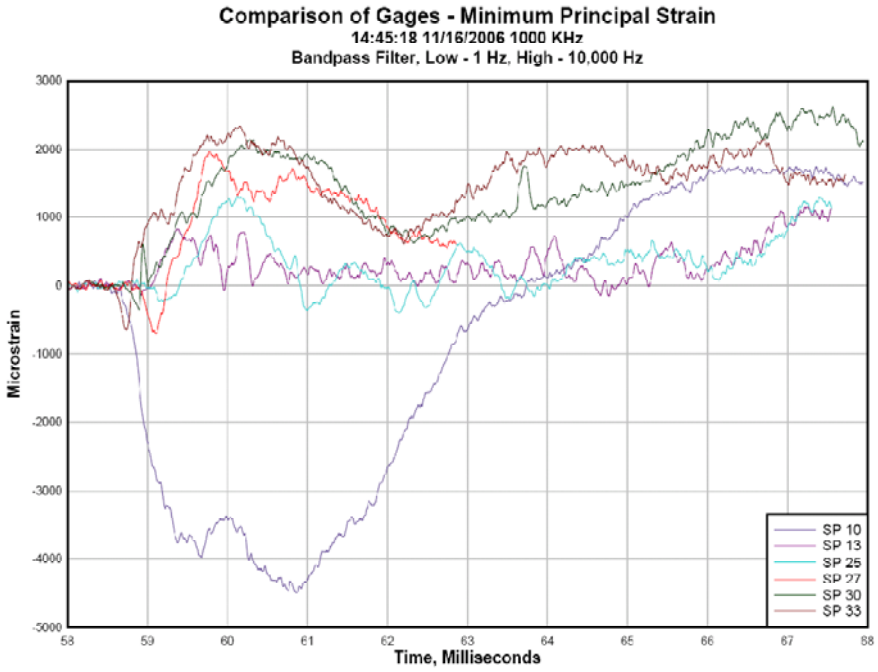

Figure A.32: Collection of minimum principal strain data using a bandpass filter

A.3.5 STRAIN GAGE DATA

The following sections will describe the strain rate behavior from forty different tests. A total of 107 gages yielded useful data. The strain gage data for each test was plotted and the largest strain rate was determined for the maximum and minimum principal strain. A plot of the filtered strain gage data for each applicable test can be found in Appendix A and B. The strain rate was determined by locating the steepest slope in the filtered data near before the plate began plastic deformation (near the beginning of the data). All of the strain rates were eventually computed and placed in a table. They were then sorted by and compared using the different test variables. Those variables included gage location, plate thickness, and bolt type. Each of these variables were plotted against the actual velocity upon impact of the impacting mass. The data provided interesting trends when the plate thickness and the bolt type was compared to velocity and is presented below. There were no discernable trends when evaluating the strain gage location to velocity, and those comparisons are not presented.

A.3.5.1 1/4" PLATE

A total of seventeen 1/4" plates were tested in the series. Six of these plates used Grade 5 bolts and the other eleven used A307 bolts. Twelve of the tests used Ballistic Loading Type 1 while the remaining five tests used Ballistic Loading Type 2. Table A.5 shows information about each test including the test number, bolt type, loading type, the goal and actual velocity, and the failure type. The actual velocity of the impacting mass, upon contact with the 1/4" plate, for these tests ranged from 9 m/s to 28.1 m/s and encompassed all types of failure modes.

Table A.5: 1/4" Plate – test matrix

Test Number	Plate Thickness	Bolt Type	Loading Type	Goal Velocity	Actual Velocity	Failure Type
1	0.25 in.	Grade 5	1	10 m/s	n/a	Remained Attached
2	0.25 in.	Grade 5	1	10 m/s	9.60 m/s	Remained Attached
3	0.25 in.	Grade 5	1	15 m/s	17.14 m/s	Remained Attached
4	0.25 in.	Grade 5	1	28 m/s	28.10 m/s	Complete Failure
5	0.25 in.	Grade 5	1	19 m/s	18.07 m/s	Remained Attached
12	0.25 in.	Grade 5	1	28 m/s	27.80 m/s	Partial Failure
13	0.25 in.	Grade 5	1	28 m/s	28.10 m/s	Complete Failure
14	0.25 in.	A307	1	28 m/s	28.10 m/s	Complete Failure
16	0.25 in.	A307	1	20 m/s	18.60 m/s	Complete Failure
17	0.25 in.	A307	1	15 m/s	14.21 m/s	Partial Failure
24	0.25 in.	A307	1	20 m/s	19.50 m/s	Complete Failure
25	0.25 in.	A307	1	20 m/s	18.50 m/s	Partial Failure
35	0.25 in.	A307	2	23 m/s	21.50 m/s	Complete Failure
40	0.25 in.	A307	2	20 m/s	19.68 m/s	Partial Failure
43	0.25 in.	A307	2	20 m/s	19.87 m/s	Partial Failure
50	0.25 in.	A307	2	15 m/s	15.00 m/s	Remained Attached
51	0.25 in.	A307	2	9 m/s	9.00 m/s	Remained Attached

The maximum strain rate that was determined from the data for the 1/4" plate is shown in Table A.6. A graph of the maximum strain rate of each gage versus the actual velocity for each test was created and is shown in Figure A.33. The data shown in red, using low strength bolts, experienced much higher strain rates than the data in blue, which used high strength bolts. In order to ascertain if there were any trends in the data, a variety of regression analyses were applied to the data using the tools included in the computer program DPlot. After evaluating a variety of different regressions it was determined that a quadratic regression had the highest correlation factor for this data. That trend line is shown by the dotted line through the red data in Figure A.33. The data using the high strength bolts had a linear regression applied to it using DPolt and is exhibited in Figure A.33 by the dashed line through the blue data. This data also includes some tests using results from tests that used Ballistic Impact Tests – Type 2 loading method. Those tests used low strength bolts, but did not follow

the trend of the low strength bolts that used the other loading method, and will be discussed further below. The different trend lines demonstrates that the specimens behaved differently when Grade 5 (high strength) bolts were used compared to A307 bolts (low strength). The bolts that were weaker had a higher strain rate than the stronger bolts when impacted with the Impacting Mass 1. The flexibility of the 1/4" plate in comparison to the stiffness of the end supports plays an important part in the strain rate behavior. When the lighter impacting mass is used, the force applied to the plate is less, which will limit the amount of deflection that the plate will experience. This in turn limits the rate at which the strain is applied to the plate.

In order to ascertain why the 1/4" steel plate behaves differently when high and low strength bolts are used, the movement of the semi-rigid end supports of two tests were studied, Test 13 and 14. They were both impacted at 28 m/s. Test 13 used Grade 5 bolts and Test 14 used A307. Figure A.34 and Figure A.35 show a comparison of those movements up until the bolts fail. The figures show that when high strength bolts were used the end supports displaced twice as much as when low strength bolts were used. This led to the 1/4" plate initially elongating more when A307 bolts were used as compared to the Grade 5 bolts. This rapid, initial, elongation is perceived to account for the higher strain rates. The non-linear trend of the strain rates, when the A307 bolts were used, shows that there may be a point where increased velocity will not lead to increase strain rates, which can be related to the time it takes the bolts to fail. In Test 13 the impact velocity was 28.1 m/s and the bolts failed at 2.8 msec after initial impact. In Test 14, when high strength bolts were used, the time from initial impact to failure almost doubled to 5.4 msec. Since the bolts shear and the plate fails so rapidly, when using A307 bolts, it can be inferred that an increase in the initial velocity of the impact mass will not lead to an increase in strain rates since the plate does not have enough time to respond. In other words, when the incoming velocity is increased, the length of time

to cause the bolts to fail decreases. This shows that the effect of bolt strength on thin plates is significant with respect to strain rate behavior. This same behavior is not seen in further tests where the plate is not as flexible; here the strain rate behavior tends to trend linearly with impact velocity.

Table A.6: 1/4" Plate – strain rate data

Test Number	Strain Gage	Velocity	Plate Thickness	Bolt Type	Loading Type	Max Strain Rate
3	1	17.13 m/s	.25 in.	Grade 5	1	5.80 1/sec
3	2	17.13 m/s	.25 in.	Grade 5	1	4.14 1/sec
3	3	17.13 m/s	.25 in.	Grade 5	1	7.00 1/sec
4	1	28.1 m/s	.25 in.	Grade 5	1	21.46 1/sec
4	2	28.1 m/s	.25 in.	Grade 5	1	9.46 1/sec
4	3	28.1 m/s	.25 in.	Grade 5	1	9.36 1/sec
4	4	28.1 m/s	.25 in.	Grade 5	1	6.46 1/sec
5	1	18.07 m/s	.25 in.	Grade 5	1	9.51 1/sec
5	6	18.07 m/s	.25 in.	Grade 5	1	7.90 1/sec
5	7	18.07 m/s	.25 in.	Grade 5	1	9.44 1/sec
12	10	27.8 m/s	.25 in.	Grade 5	1	9.34 1/sec
12	11	27.8 m/s	.25 in.	Grade 5	1	9.98 1/sec
13	12	28.1 m/s	.25 in.	Grade 5	1	5.78 1/sec
13	13	28.1 m/s	.25 in.	Grade 5	1	5.40 1/sec
13	14	28.1 m/s	.25 in.	Grade 5	1	5.68 1/sec
13	15	28.1 m/s	.25 in.	Grade 5	1	5.69 1/sec
14	17	28.1 m/s	.25 in.	A307	1	32.18 1/sec
14	18	28.1 m/s	.25 in.	A307	1	31.57 1/sec
16	17	18.6 m/s	.25 in.	A307	1	27.16 1/sec
16	18	18.6 m/s	.25 in.	A307	1	29.95 1/sec
17	17	14.21 m/s	.25 in.	A307	1	20.45 1/sec
17	18	14.21 m/s	.25 in.	A307	1	19.05 1/sec
25	19	18.5 m/s	.25 in.	A307	1	26.44 1/sec
25	20	18.5 m/s	.25 in.	A307	1	22.99 1/sec
51	17	9. m/s	.25 in.	A307	1	6.14 1/sec
51	18	9. m/s	.25 in.	A307	1	12.13 1/sec
40	17	19.68 m/s	.25 in.	A307	2	5.59 1/sec
40	18	19.68 m/s	.25 in.	A307	2	6.22 1/sec
43	17	19.87 m/s	.25 in.	A307	2	8.06 1/sec
43	18	19.87 m/s	.25 in.	A307	2	10.14 1/sec

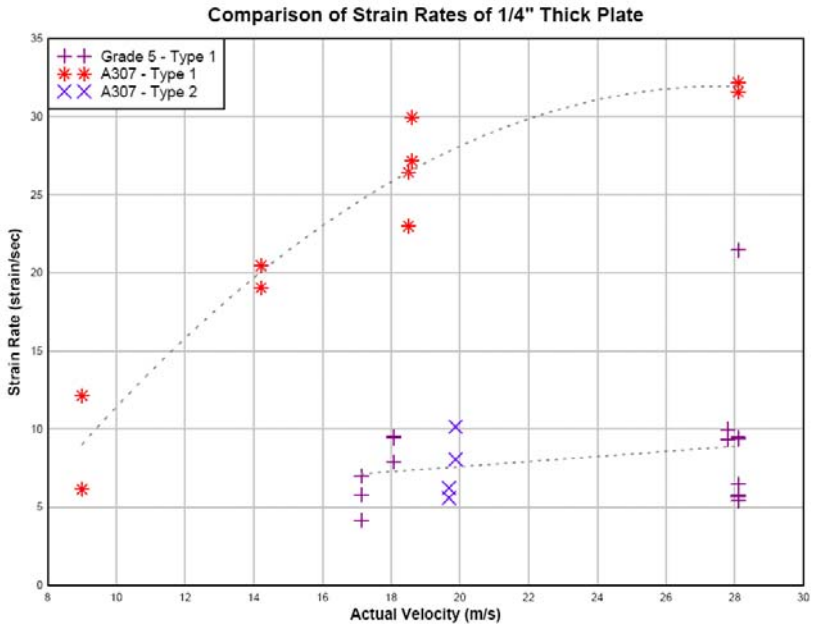

Figure A.33: Strain rate vs. impact velocity for 1/4” thick plate

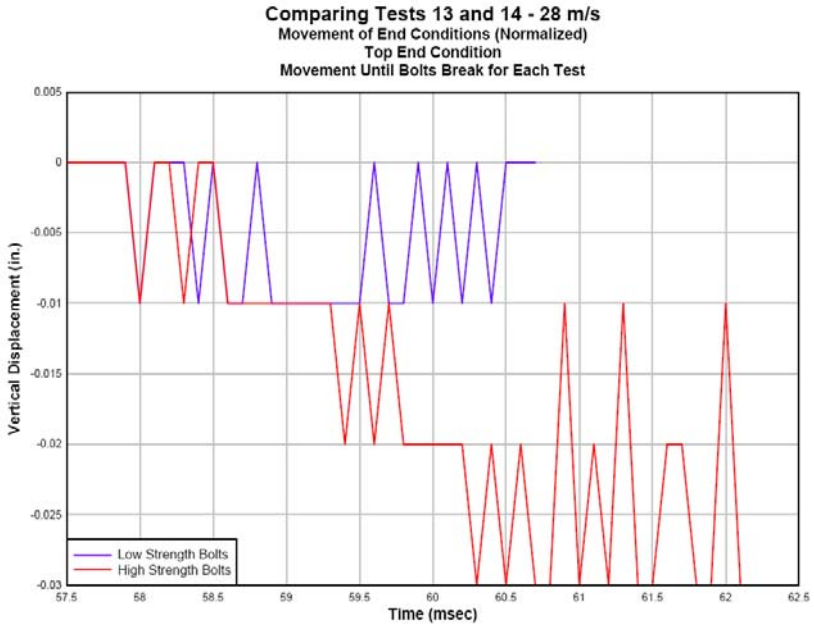

Figure A.34: Comparing displacements of end supports

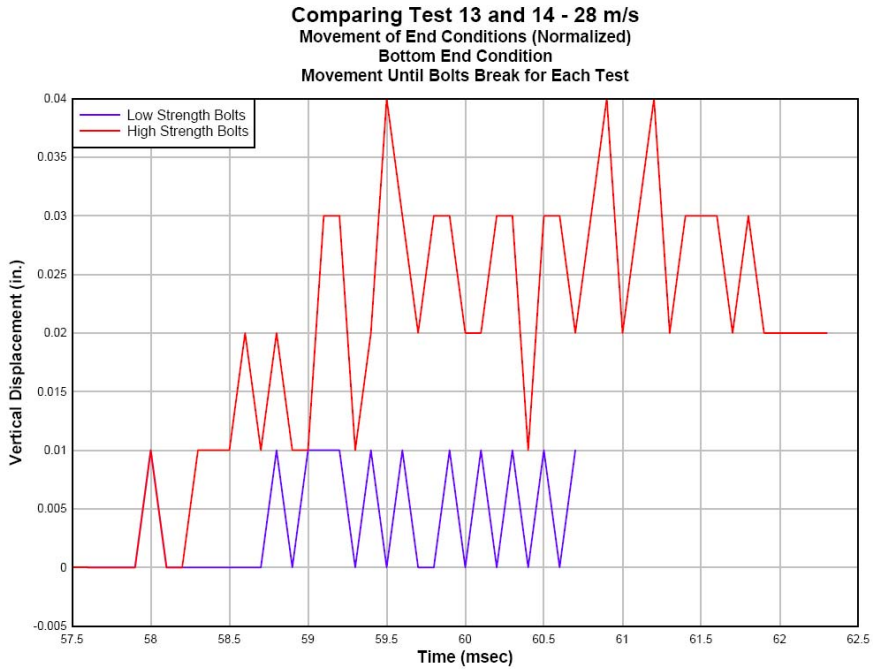

Figure A.35: Comparing displacements of end supports

A.3.5.2 1/2" PLATE

A total of seventeen 1/2" plates were tested in the series. Six of these plates used Grade 5 bolts and the other eleven used A307 bolts. Twelve of the tests used Ballistic Loading – Type 1 while the remaining five tests used Ballistic Loading – Type 2. Table A.7 shows information about each test including the test number, bolt type, loading type, the goal and actual velocity, and failure type. The actual velocities of the impacting mass, upon contact with the 1/2" plate, ranged from 17.93 m/s to 30.17 m/s and encompassed all types of failure modes.

The maximum strain rate that was determined from the data for the 1/2" plate is shown in Table A.8 and Table A.9. A graph of the maximum strain rate of each gage versus the actual velocity for each test was created and is shown in Figure A.36. The linear relation,

between strain rate and impact velocity, for both bolt types and loading methods is demonstrated in the graph. A linear regression was performed on the data using the tool in the computer program DPlot. That trend line is shown in Figure A.36 by the dotted line. The trend can be described as follows: when the velocity increases the rate at which the plate elongates, or strains, increases. Unlike the 1/4" plate tests, there is no obvious difference between bolt types for tests that use the 1/2" plate, or thicker.

Table A.7: 1/2" Plate – test matrix

Test Number	Plate Thickness	Bolt Type	Loading Type	Goal Velocity	Actual Velocity	Failure Type
6	0.50 in.	Grade 5	1	34 m/s	n/a	Remained Attached
7	0.50 in.	Grade 5	1	34 m/s	30.17 m/s	Remained Attached
8	0.50 in.	Grade 5	1	28 m/s	27.20 m/s	Complete Failure
9	0.50 in.	Grade 5	1	28 m/s	27.50 m/s	Partial Failure
10	0.50 in.	Grade 5	1	28 m/s	28.20 m/s	Partial Failure
11	0.50 in.	Grade 5	1	28 m/s	27.50 m/s	Complete Failure
15	0.50 in.	A307	1	28 m/s	27.70 m/s	Complete Failure
18	0.50 in.	A307	1	25 m/s	25.70 m/s	Complete Failure
19	0.50 in.	A307	1	23 m/s	23.00 m/s	Complete Failure
20	0.50 in.	A307	1	20 m/s	18.40 m/s	Partial Failure
26	0.50 in.	A307	1	20 m/s	17.93 m/s	Remained Attached
27	0.50 in.	A307	1	23 m/s	24.04 m/s	Complete Failure
36	0.50 in.	A307	2	25 m/s	22.70 m/s	Remained Attached
37	0.50 in.	A307	2	29 m/s	26.80 m/s	Remained Attached
38	0.50 in.	A307	2	29 m/s	27.10 m/s	Partial Failure
39	0.50 in.	A307	2	29 m/s	27.48 m/s	Partial Failure
45	0.50 in.	A307	2	29 m/s	26.98 m/s	Partial Failure

The effect of the deformation of end supports during three different tests was evaluated (Tests 11, 15, and 39). Test 11 used high strength bolts and had an impact velocity of 27.5 m/s. Test 15 used low strength bolts and had an impact velocity of 27.7 m/s. Both of these tests used Ballistic Loading – Type 1. Test 39 used Ballistic Loading – Type 2 and low strength bolts, with an impact velocity of 27.48 m/s. Figure A.37 shows the movement of the

top end support. In this figure it can be seen, that the increased strength of the Grade 5 bolts caused the end support to move 1 1/2 times more than the similar test using A307 bolts.

This same phenomenon also occurs in the bottom end support as seen in Figure A.38. It is important to note in this figure, that peak displacements are almost twice as large as the top end support for all three tests; this could be attributed to the geometric arrangement of the end support and its stiffness. Due to the increased movement of the bottom end support the strain rates, in the gages that are located closer to the bottom, tend to be higher than their counterparts in this test series. This is most apparent in the points on the graph shown in Figure A.36 for the Grade 5 bolts at the 26.8 m/s and 28.2 m/s values.

Table A.8: 1/2” Plate – strain rate data (Part 1)

Test Number	Strain Gage	Velocity	Plate Thickness	Bolt Type	Loading Type	Max Strain Rate
6	1	30. m/s	.5 in.	Grade 5	1	29.02 1/sec
6	6	30. m/s	.5 in.	Grade 5	1	14.06 1/sec
6	7	30. m/s	.5 in.	Grade 5	1	9.99 1/sec
7	1	30.17 m/s	.5 in.	Grade 5	1	30.71 1/sec
7	2	30.17 m/s	.5 in.	Grade 5	1	10.87 1/sec
7	3	30.17 m/s	.5 in.	Grade 5	1	8.77 1/sec
7	4	30.17 m/s	.5 in.	Grade 5	1	11.23 1/sec
7	5	30.17 m/s	.5 in.	Grade 5	1	11.54 1/sec
8	2	27.2 m/s	.5 in.	Grade 5	1	12.47 1/sec
8	3	27.2 m/s	.5 in.	Grade 5	1	12.46 1/sec
8	4	27.2 m/s	.5 in.	Grade 5	1	12.54 1/sec
8	5	27.2 m/s	.5 in.	Grade 5	1	8.99 1/sec
9	6	27.5 m/s	.5 in.	Grade 5	1	13.54 1/sec
9	7	27.5 m/s	.5 in.	Grade 5	1	11.88 1/sec
10	8	28.2 m/s	.5 in.	Grade 5	1	18.76 1/sec
10	9	28.2 m/s	.5 in.	Grade 5	1	10.85 1/sec
11	8	27.5 m/s	.5 in.	Grade 5	1	14.89 1/sec
11	9	27.5 m/s	.5 in.	Grade 5	1	12.45 1/sec
15	17	27.7 m/s	.5 in.	A307	1	11.73 1/sec
15	18	27.7 m/s	.5 in.	A307	1	10.89 1/sec
18	17	25.7 m/s	.5 in.	A307	1	9.75 1/sec
18	18	25.7 m/s	.5 in.	A307	1	10.99 1/sec
19	17	23. m/s	.5 in.	A307	1	12.74 1/sec
19	18	23. m/s	.5 in.	A307	1	9.14 1/sec
20	17	18.4 m/s	.5 in.	A307	1	6.46 1/sec
20	18	18.4 m/s	.5 in.	A307	1	9.46 1/sec
26	19	17.93 m/s	.5 in.	A307	1	8.31 1/sec
26	20	17.93 m/s	.5 in.	A307	1	6.86 1/sec
26	21	17.93 m/s	.5 in.	A307	1	10.01 1/sec
26	22	17.93 m/s	.5 in.	A307	1	6.70 1/sec
27	19	24.04 m/s	.5 in.	A307	1	14.24 1/sec
27	20	24.04 m/s	.5 in.	A307	1	8.92 1/sec
27	21	24.04 m/s	.5 in.	A307	1	9.58 1/sec
27	22	24.04 m/s	.5 in.	A307	1	14.21 1/sec

Table A.9: 1/2” Plate – strain rate data (Part 2)

Test Number	Strain Gage	Velocity	Plate Thickness	Bolt Type	Loading Type	Max Strain Rate
36	19	22.7 m/s	.5 in.	A307	2	9.87 1/sec
36	20	22.7 m/s	.5 in.	A307	2	8.17 1/sec
37	1	26.8 m/s	.5 in.	A307	2	11.16 1/sec
37	2	26.8 m/s	.5 in.	A307	2	16.94 1/sec
37	3A	26.8 m/s	.5 in.	A307	2	13.38 1/sec
37	4	26.8 m/s	.5 in.	A307	2	12.24 1/sec
37	5A	26.8 m/s	.5 in.	A307	2	10.56 1/sec
38	1	27.1 m/s	.5 in.	A307	2	13.38 1/sec
38	6	27.1 m/s	.5 in.	A307	2	10.64 1/sec
38	7	27.1 m/s	.5 in.	A307	2	11.40 1/sec
39	1	27.48 m/s	.5 in.	A307	2	13.89 1/sec
39	6	27.48 m/s	.5 in.	A307	2	12.39 1/sec
39	7	27.48 m/s	.5 in.	A307	2	11.58 1/sec
45	3A	26.98 m/s	.5 in.	A307	2	16.54 1/sec
45	1	26.98 m/s	.5 in.	A307	2	9.70 1/sec
45	2	26.98 m/s	.5 in.	A307	2	10.99 1/sec
45	4	26.98 m/s	.5 in.	A307	2	8.06 1/sec

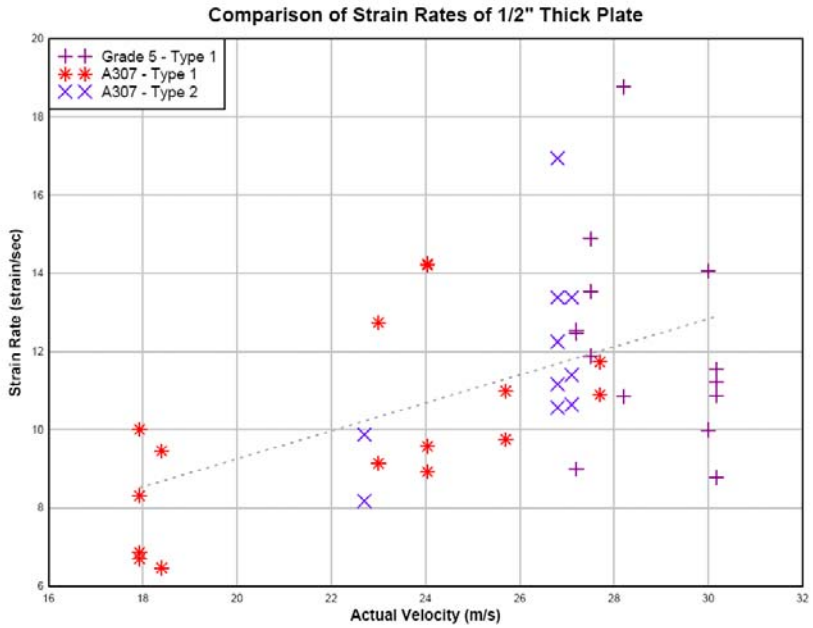

Figure A.36: Strain rate vs. impact velocity for 1/2” thick plate

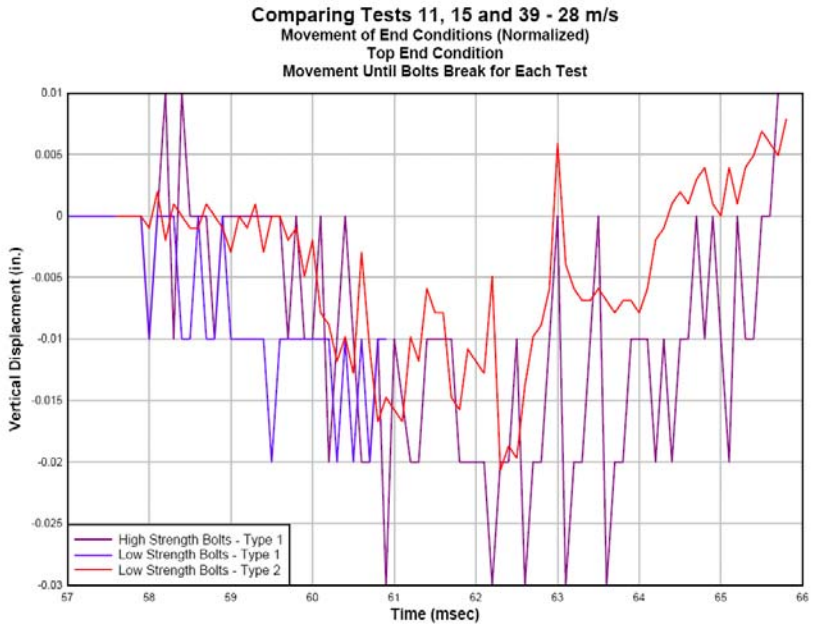

Figure A.37: Comparing displacements of end supports

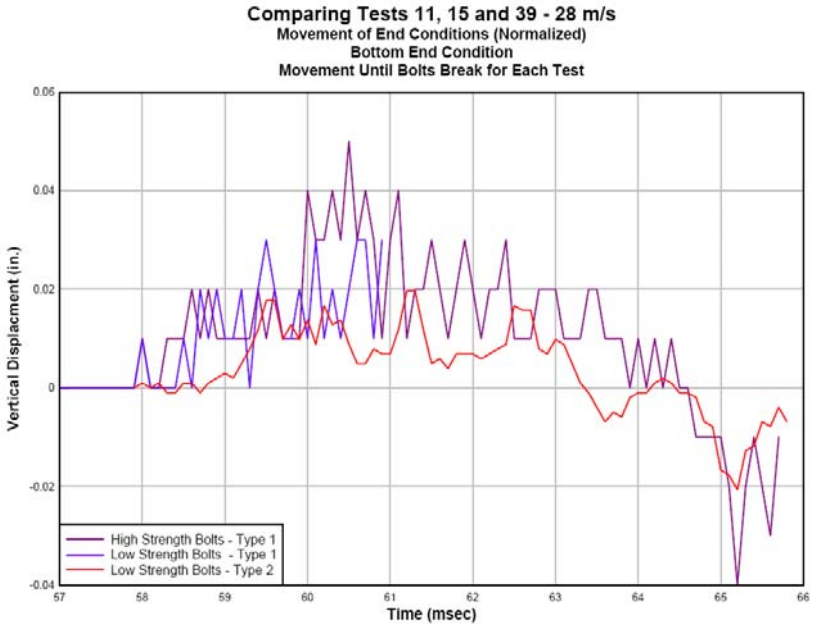

Figure A.38: Comparing displacements of end supports

A.3.5.3 3/4" PLATE

A total of six 3/4" plates were tested in the series. All of these plates used A307 bolts and Ballistic Loading – Type 1. Table A.10 provides information about each test, including the test number, bolt type, loading type, the goal and actual velocity, and failure type. The actual velocities of the impacting mass, upon contact with the 3/4" plate, ranged from 23.00 m/s to 28.50 m/s which resulted in the complete failure of all the test specimens.

Table A.10: 3/4" Plate – test matrix

Test Number	Plate Thickness	Bolt Type	Loading Type	Goal Velocity	Actual Velocity	Failure Type
21	0.75 in.	A307	1	28 m/s	27.90 m/s	Complete Failure
22	0.75 in.	A307	1	25 m/s	24.90 m/s	Complete Failure
23	0.75 in.	A307	1	25 m/s	23.00 m/s	Complete Failure
28	0.75 in.	A307	1	28 m/s	27.66 m/s	Complete Failure
29	0.75 in.	A307	1	25 m/s	25.83 m/s	Complete Failure
30	0.75 in.	A307	1	28 m/s	28.50 m/s	Complete Failure

The maximum strain rate that was determined from the data for the 3/4" plate is shown in Table A.11. A graph of the maximum strain rate of each gage versus the actual velocity for each test was created and is shown in Figure A.39. A linear regression was performed on this data using the same method in the previous section. The trend line of the ¾" plate is exhibited in Figure A.39 by the dotted line. Only two velocities were tested using this plate thickness. Due to the varying conditions that are involved in running the blast generator a total of six different velocities were achieved. The linear relation between strain rate and impact velocity is shown in that graph. This can be described as follows: when the velocity increases then the rate at which the plate elongates, or strains, increases. This is the same trend found in the 1/2" plate and the 1/4" plate when high strength bolts were used.

Table A.11: 3/4” Plate – strain rate data

Test Number	Strain Gage	Velocity	Plate Thickness	Bolt Type	Loading Type	Max Strain Rate
21	17	27.9 m/s	.75 in.	A307	1	10.43 1/sec
21	18	27.9 m/s	.75 in.	A307	1	13.52 1/sec
22	17	24.9 m/s	.75 in.	A307	1	9.28 1/sec
22	18	24.9 m/s	.75 in.	A307	1	10.18 1/sec
28	19	27.66 m/s	.75 in.	A307	1	16.31 1/sec
28	20	27.66 m/s	.75 in.	A307	1	14.70 1/sec
28	21	27.66 m/s	.75 in.	A307	1	11.53 1/sec
28	22	27.66 m/s	.75 in.	A307	1	7.94 1/sec
29	19	25.83 m/s	.75 in.	A307	1	13.80 1/sec
29	20	25.83 m/s	.75 in.	A307	1	9.01 1/sec
29	21	25.83 m/s	.75 in.	A307	1	12.38 1/sec
29	22	25.83 m/s	.75 in.	A307	1	12.53 1/sec
30	19	28.5 m/s	.75 in.	A307	1	14.75 1/sec
30	20	28.5 m/s	.75 in.	A307	1	10.84 1/sec
30	21	28.5 m/s	.75 in.	A307	1	13.70 1/sec
30	22	28.5 m/s	.75 in.	A307	1	14.36 1/sec

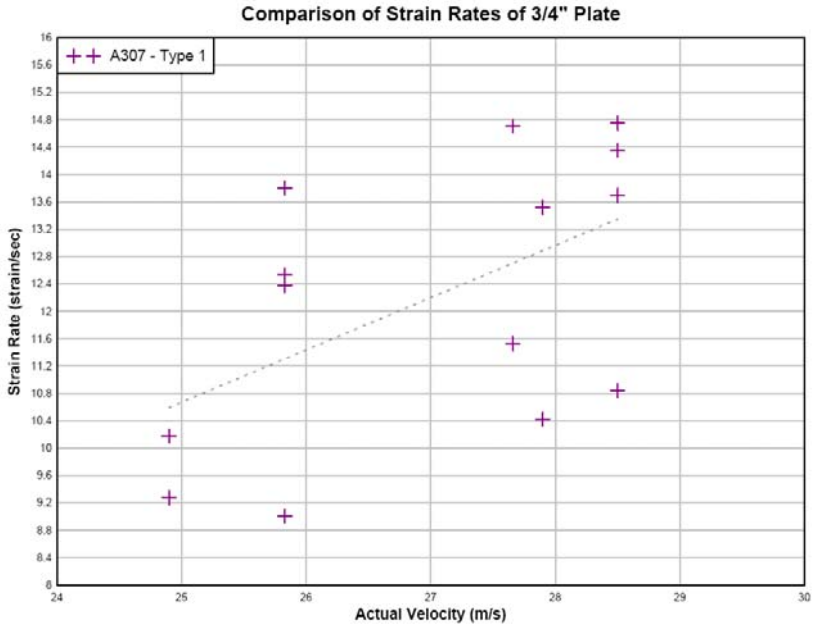

Figure A.39: Strain rate vs. impact velocity for 3/4” thick plate

A.3.5.4 7/8" PLATE

A total of three 7/8" plates were tested in the series. All of these plates used A307 bolts and Ballistic Loading – Type 1. Table A.12 shows information about each test including the test number, bolt type, loading type, the goal and actual velocity, and failure type. The actual velocities of the impacting mass were approximately 28 m/s which resulted in the complete failure of all the test specimens.

Table A.12: 7/8" Plate – test matrix

Test Number	Plate Thickness	Bolt Type	Loading Type	Goal Velocity	Actual Velocity	Failure Type
31	0.875 in.	A307	1	28 m/s	27.49 m/s	Complete Failure
32	0.875 in.	A307	1	28 m/s	27.46 m/s	Complete Failure
33	0.875 in.	A307	1	28 m/s	28.01 m/s	Complete Failure

The maximum strain rate that was determined from the data for the 7/8" plate is shown in Table A.13. A graph of the maximum strain rate of each gage versus the actual velocity for each test was created and is shown in Figure A.40. A linear trend is observed in the data; however, the actual velocities vary only by 0.5 m/s. Therefore, this should not be evaluated as an overall trend since there is no significant variation of velocity.

Table A.13: 7/8” Plate – strain rate data

Test Number	Strain Gage	Velocity	Plate Thickness	Bolt Type	Loading Type	Max Strain Rate
31	19	27.49 m/s	.875 in.	A307	1	14.01 1/sec
31	21	27.49 m/s	.875 in.	A307	1	13.42 1/sec
31	22	27.49 m/s	.875 in.	A307	1	12.10 1/sec
32	19	27.46 m/s	.875 in.	A307	1	14.94 1/sec
32	20	27.46 m/s	.875 in.	A307	1	18.53 1/sec
32	21	27.46 m/s	.875 in.	A307	1	11.86 1/sec
32	22	27.46 m/s	.875 in.	A307	1	15.07 1/sec
33	19	28.01 m/s	.875 in.	A307	1	17.13 1/sec
33	20	28.01 m/s	.875 in.	A307	1	29.60 1/sec
33	21	28.01 m/s	.875 in.	A307	1	15.88 1/sec
33	22	28.01 m/s	.875 in.	A307	1	10.57 1/sec

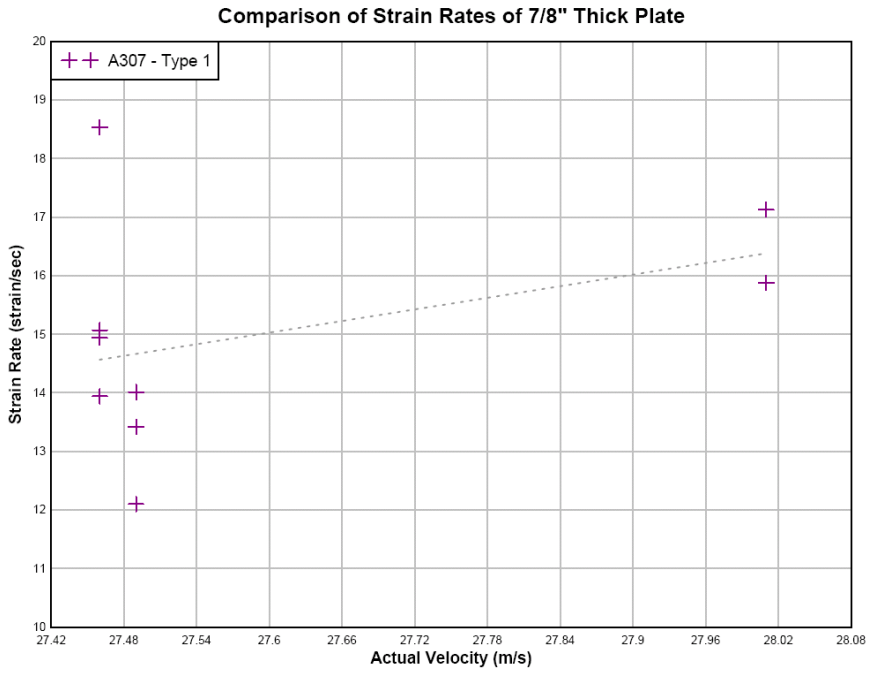

Figure A.40: Strain rate vs. impact velocity for 7/8” thick plate

B. APPENDIX B – CHAPTER 4

B.1 KEDD FIELD SCALE FIELD TEST SET-UP

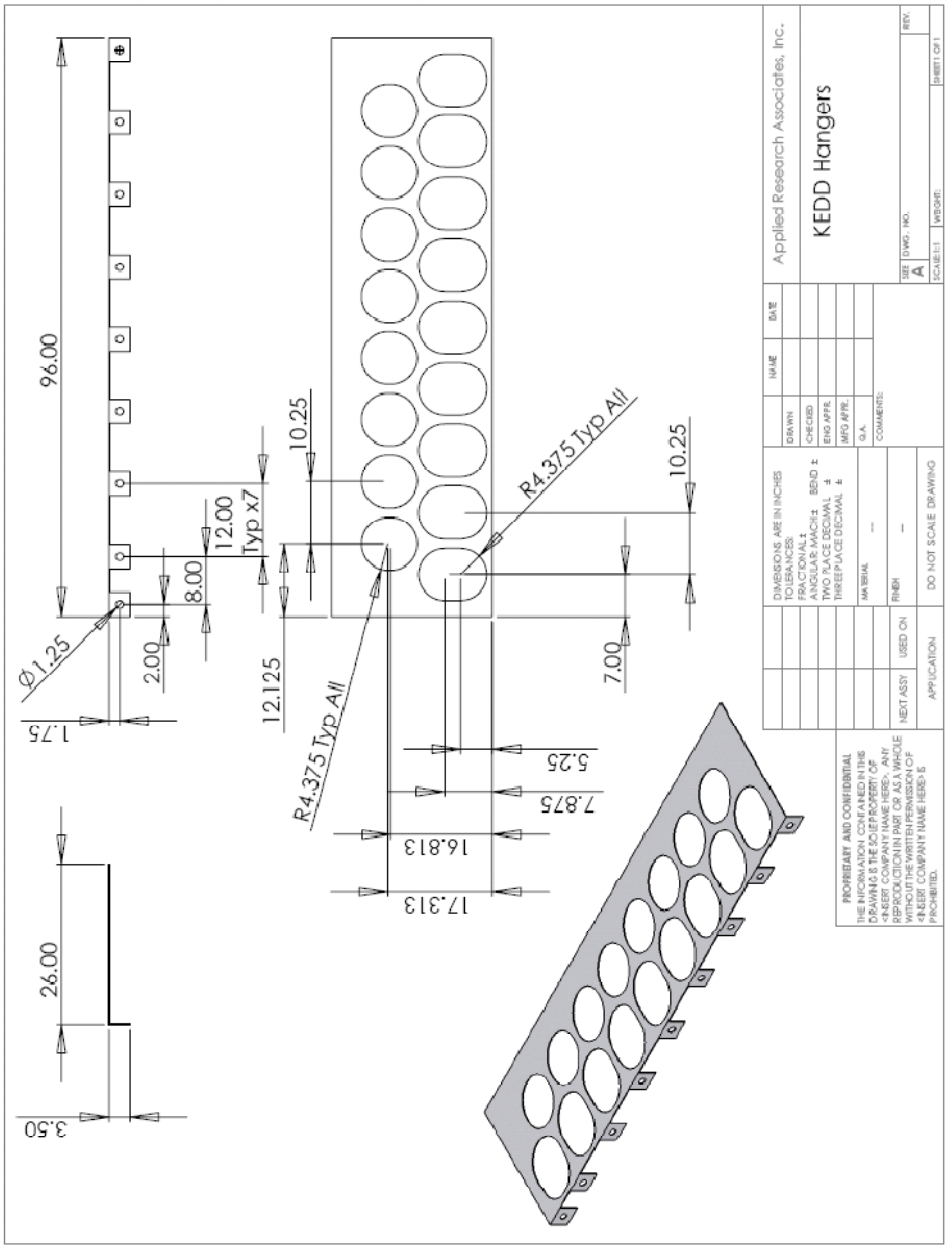

Figure B.1: KEDD hanger assembly drawing (EMRTC)

Figure B.2: KEDD hanger assembly (EMRTC)

Figure B.3: 2 Rows of KEDD's on top (EMRTC)

B.1.1 KEDD SCALED FIELD TESTS SET-UP (PROOF OF CONCEPT TESTS)

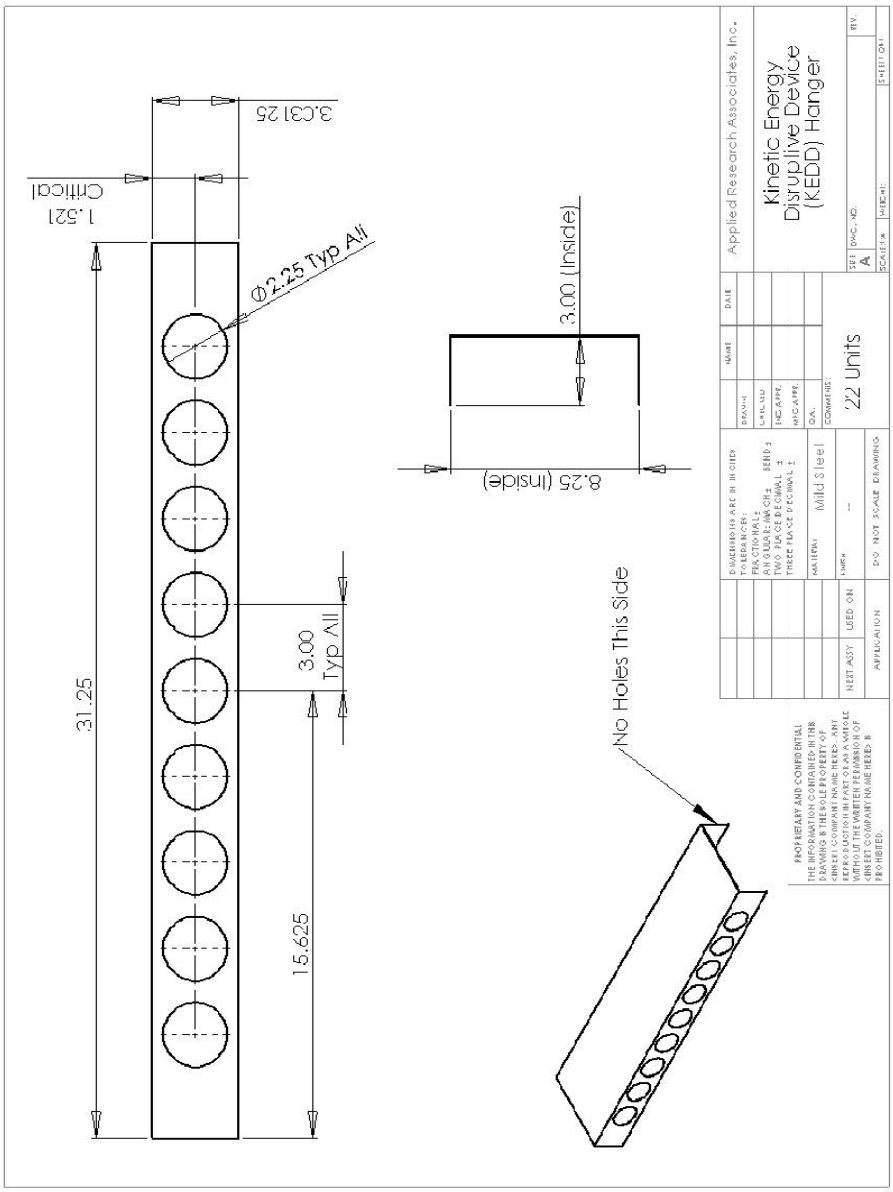

Figure B.4: KEDD hanger assembly drawing

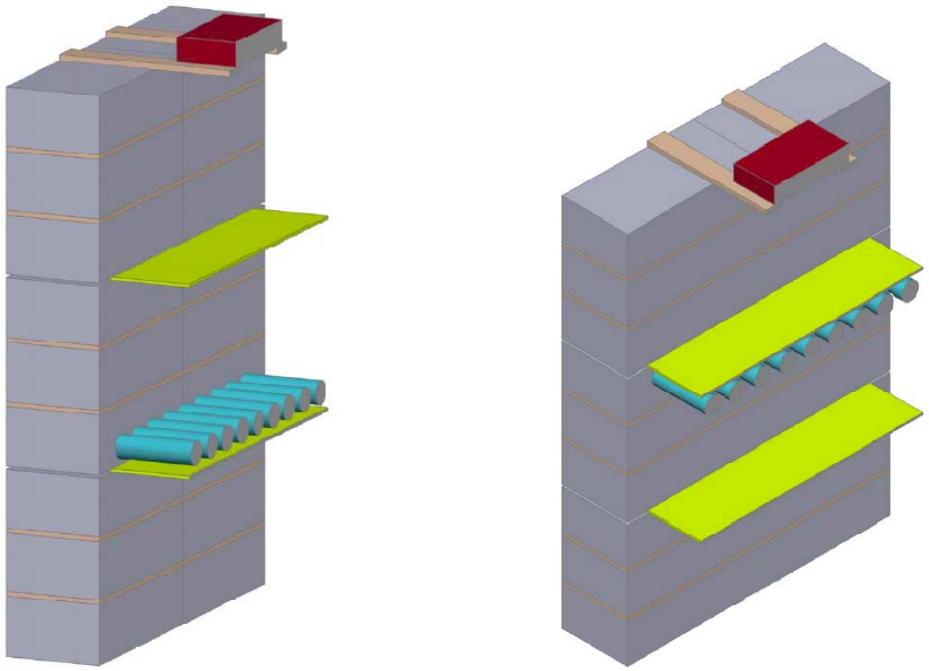

Figure B.5: KEDD layout a) 1 row bottom b) 1 row top

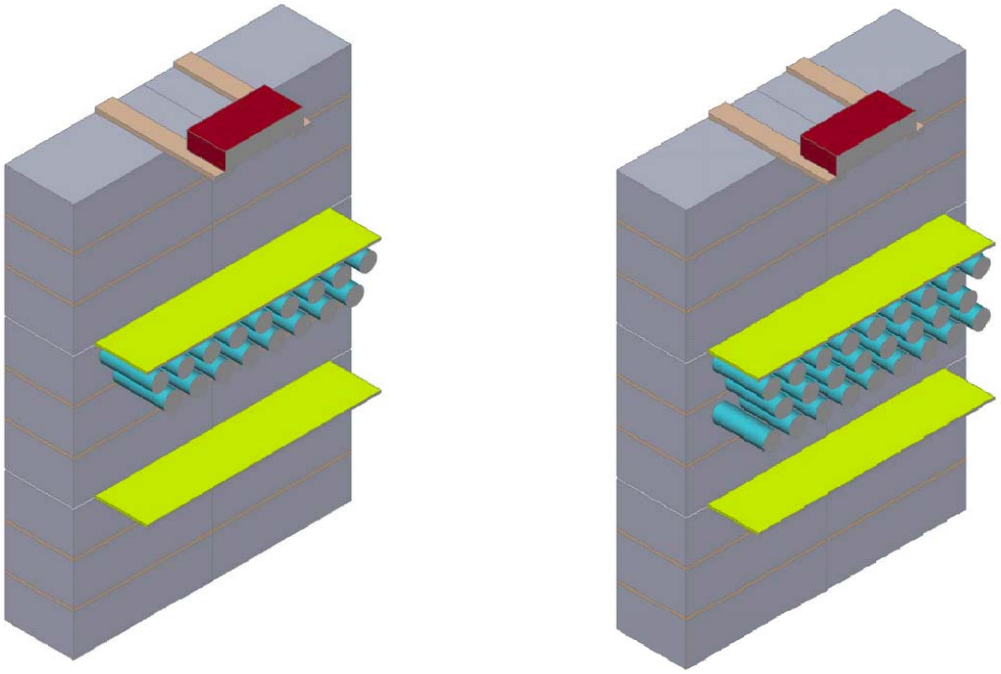

Figure B.6: KEDD layout a) 2-row top b) 3-row top

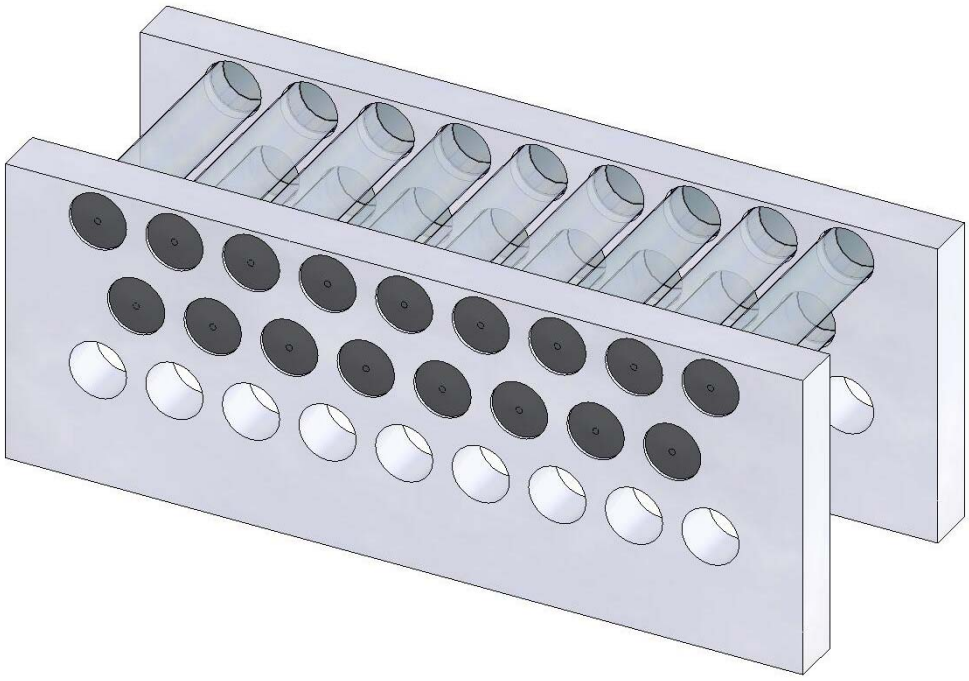

Figure B.7: KEDD 2-row top layout (3-d drawing)

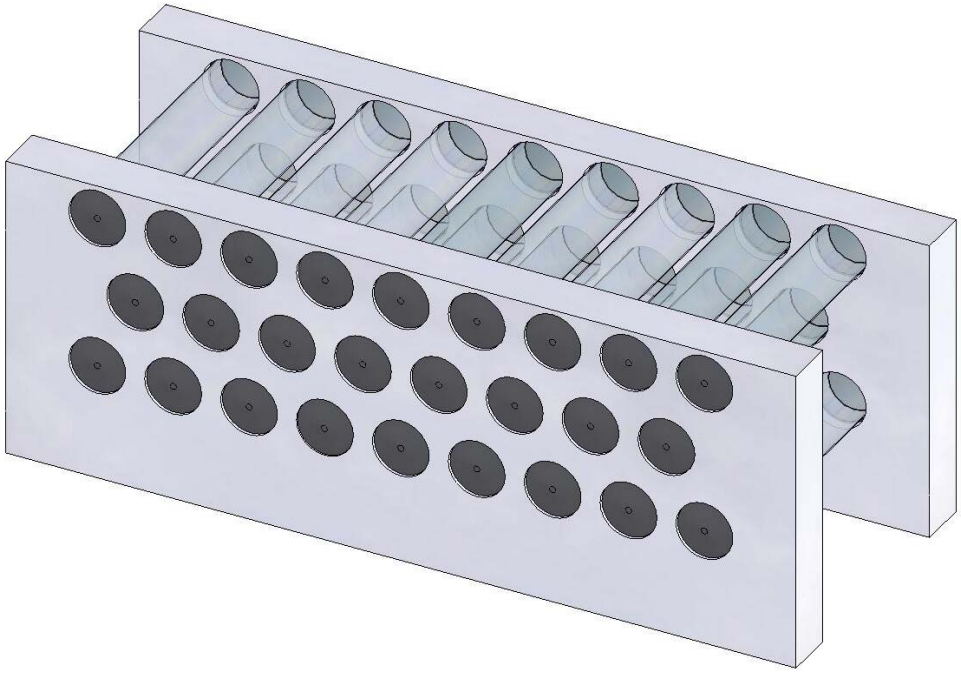

Figure B.8: KEDD 3-row top layout (3-d drawing)

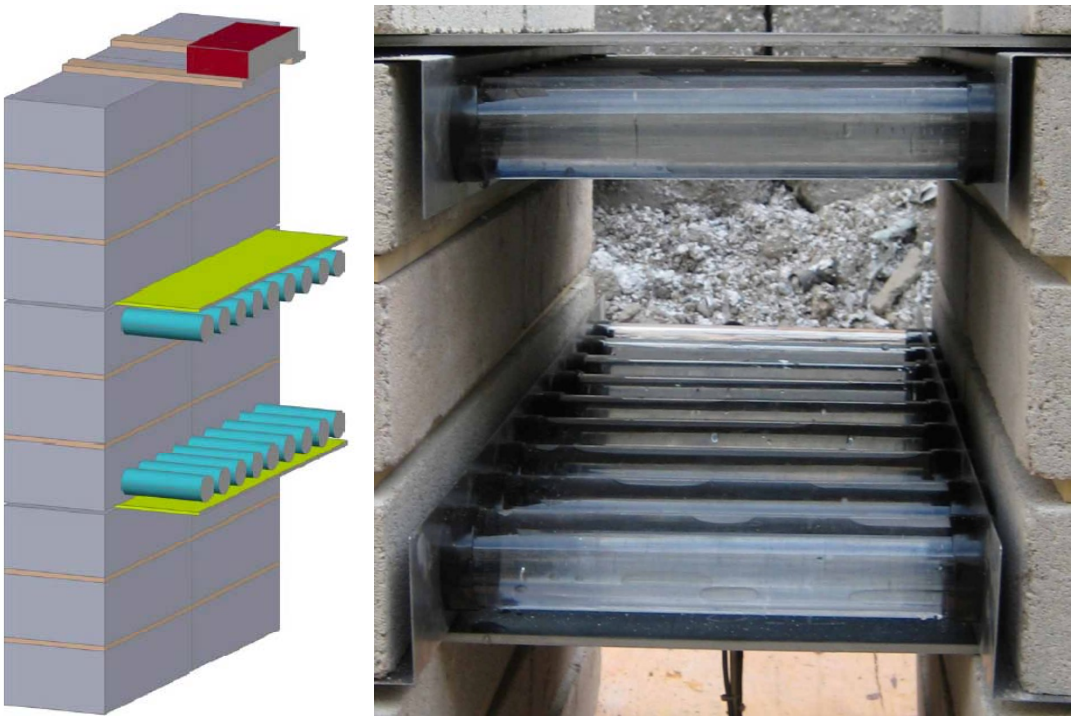

Figure B.9: KEDD top and bottom layout a) drawing b) photo

C. APPENDIX C – CHAPTER 5

C.1 CALIBRATION TEST

C.1.1.1 TEST SET-UP

Four tests (Tests 1 - 4) were performed using this test set-up to determine what initial charge should be used for subsequent tests. It consisted of one 1/4" thick A36 steel plate supported 12" above the base of the set-up. A photo, a schematic drawing, and a drawing of the test set-up can be found in Figure C.1, Figure C.2, and Figure C.3.

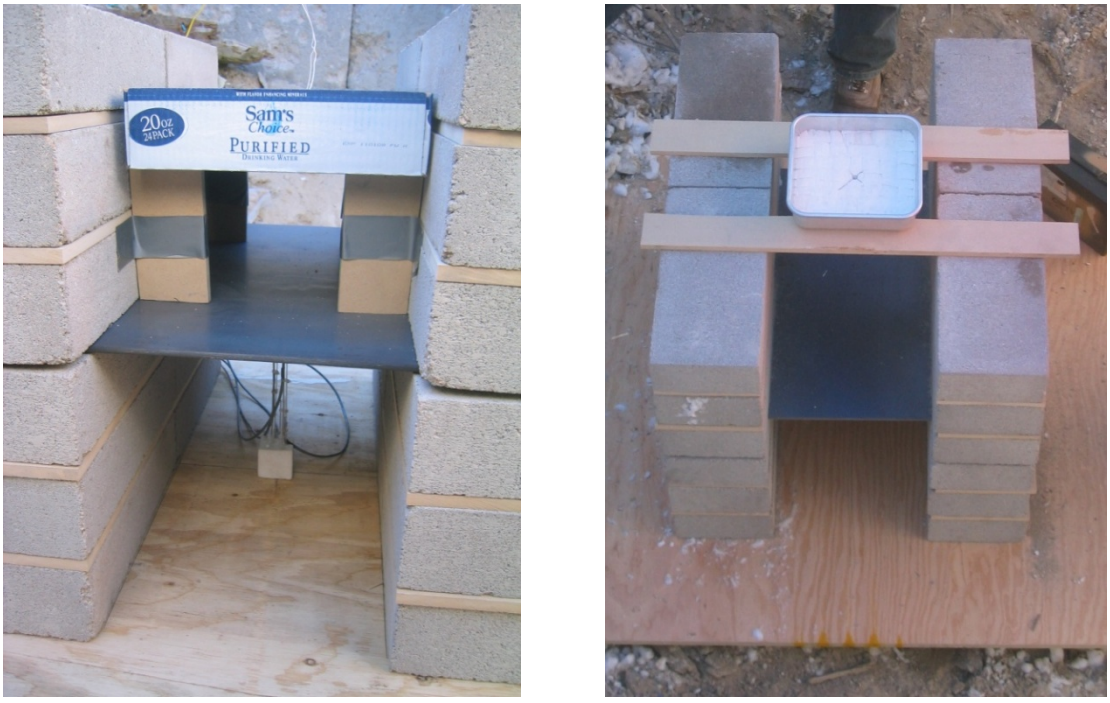

Figure C.1: Calibration Test set-up – photo

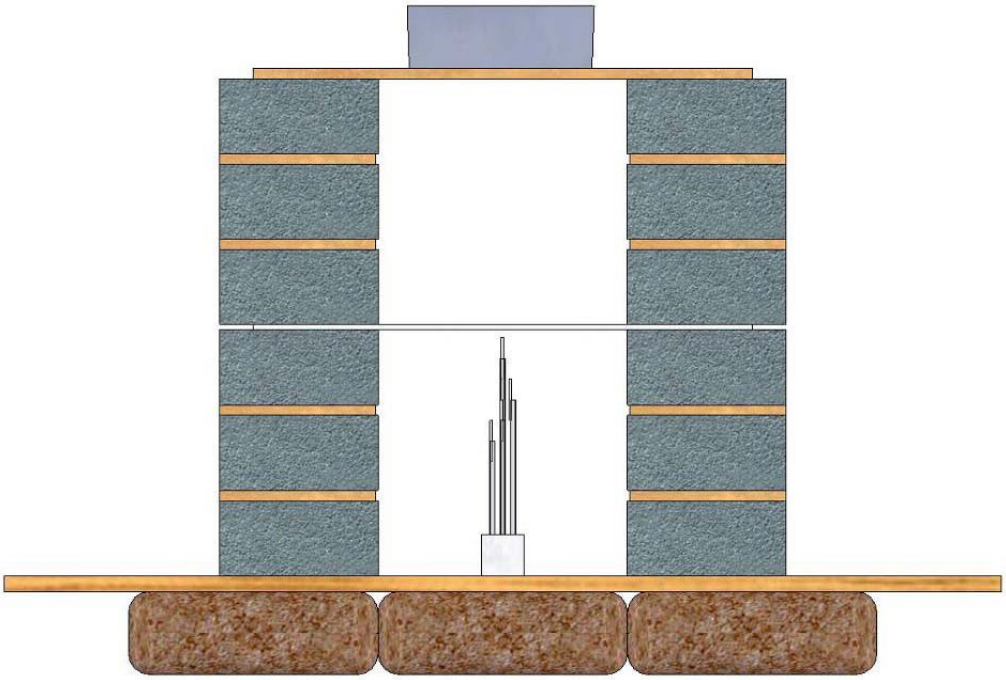

Figure C.2: Calibration Test set-up – schematic drawing

C.1.1.2 TEST RESULTS

Three different charge sizes and two standoff distances were used in the Calibration Tests (Tests 1 – 4). A set of Time of Arrival (TOA) pins were placed behind each plate, in the "lower spacing" arrangement to determine the velocity of the fragments. Figure C.4 shows a chart of the different velocities determined from the tests. As expected, when the standoff was increased and the charge size decreased, the velocity of the fragments formed decreased. The type of failure that occurred in the plate changed along with the changes in charge size and standoff.

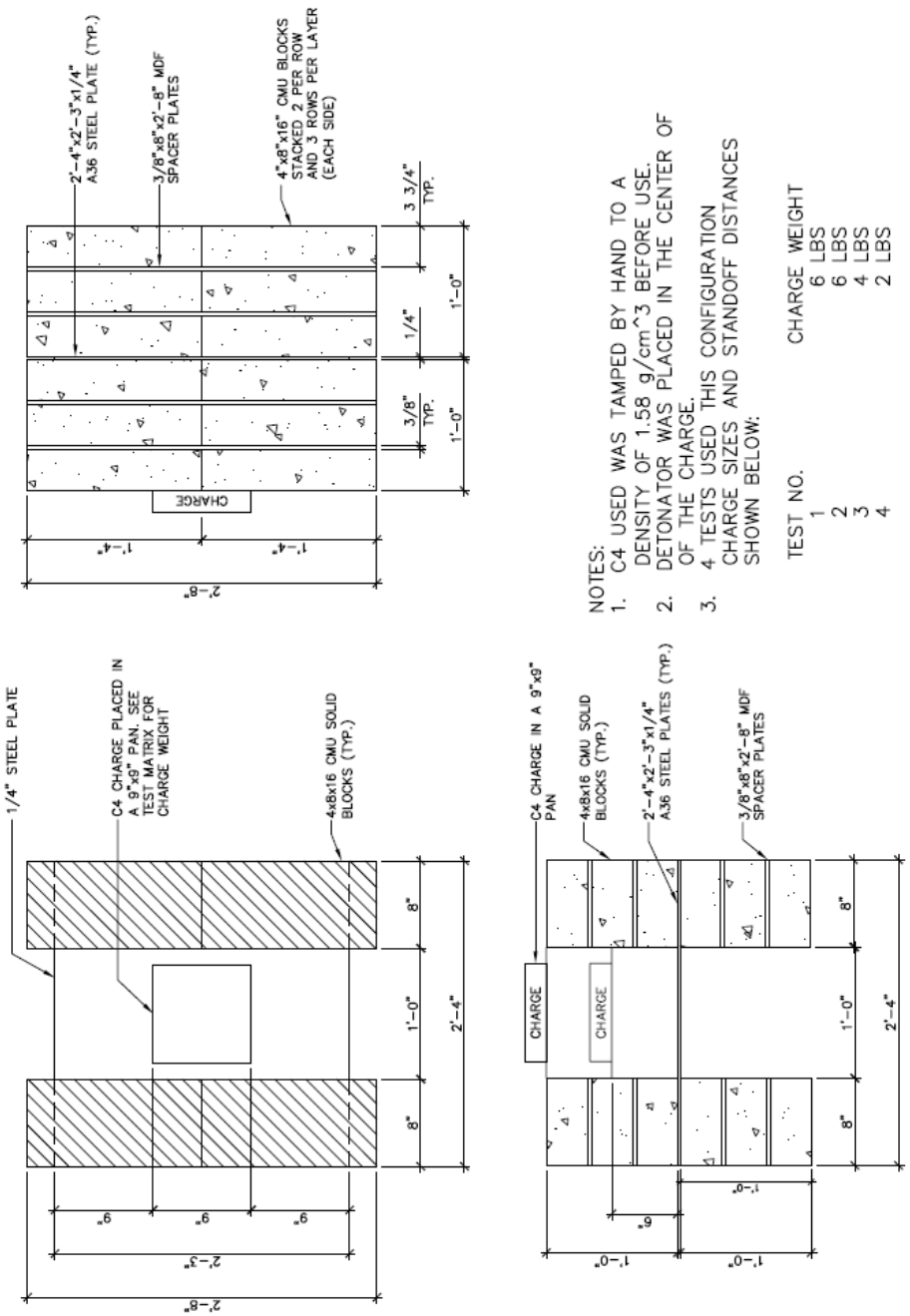

Figure C.3: Calibration Test set-up –drawing

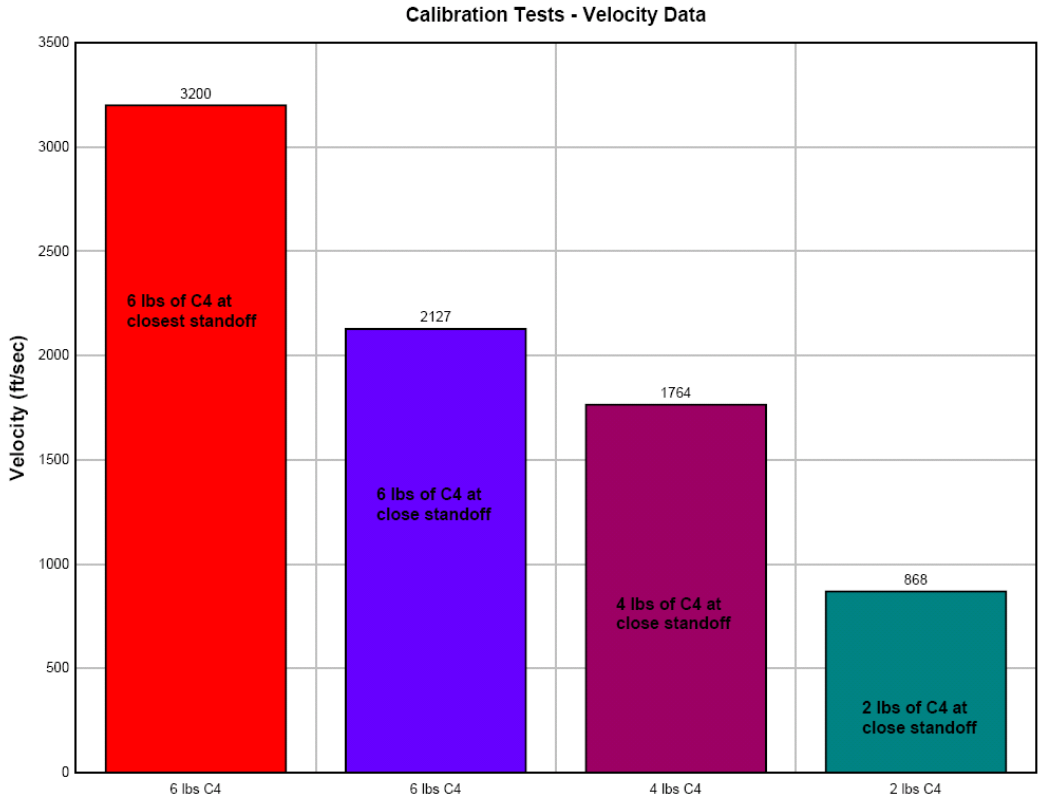

Figure C.4: Fragment velocities from Calibration Tests

The goal of these tests was to determine what charge size and standoff would create one large flyer plate; similar to what was formed in the full scale EMRTC tests. The first test used 0.034X pounds of equivalent TNT at the closest standoff. However, instead of forming one large flyer plate, many small flyer plates were formed. A small sample of those fragments, or flyer plates, can be seen in Figure C.5. The second test used 0.034X pounds of equivalent TNT at a close standoff. The charge formed larger flyer plates in the first plate, yet still too many to achieve our goal. Those flyer plates can be seen in Figure C.6. The third test used 0.023X pounds of equivalent TNT at the same standoff as the previous test. This charge arrangement created even larger flyer plates, but still too many. The entire first plate,

reassembled, can be seen in Figure C.7. The final calibration shot used 0.011X pounds of equivalent TNT at the same standoff as the previous two tests. This test formed one large, classical, flyer plate which was the expected, and desired, failure mode when multiple plates were used. To ensure that the explosive charge would be sufficient to fracture through a series of four plates the charge was increased to 0.014X pounds of equivalent TNT and was implemented in the first specimen test.

Figure C.5: Fragments formed from Calibration Test 1

Figure C.6: Fragments formed from Calibration Test 2

Figure C.7: Fragments formed from Calibration Test 3

Figure C.8: Fragments formed from Calibration Test 4

C.1.2 4 PLATE TEST

C.1.2.1 TEST SET-UP

Test 5 was performed using four 1/4” steel plates. Each plate was spaced 12” above the previous plate, or the plywood base for the first plate. A photo, a drawing, and a schematic drawing of the test set-up can be found in Figure C.9, Figure C.10 and Figure C.11. The picture shows the test set-up reflected in a mirror. Due to the size constraint of the test bunker, this was the only way to get a picture of the entire test specimen. A phantom camera was used to record this test, but even at the lowest exposure setting the data was not useful.

Figure C.9: 4 Plate Test set-up – photo

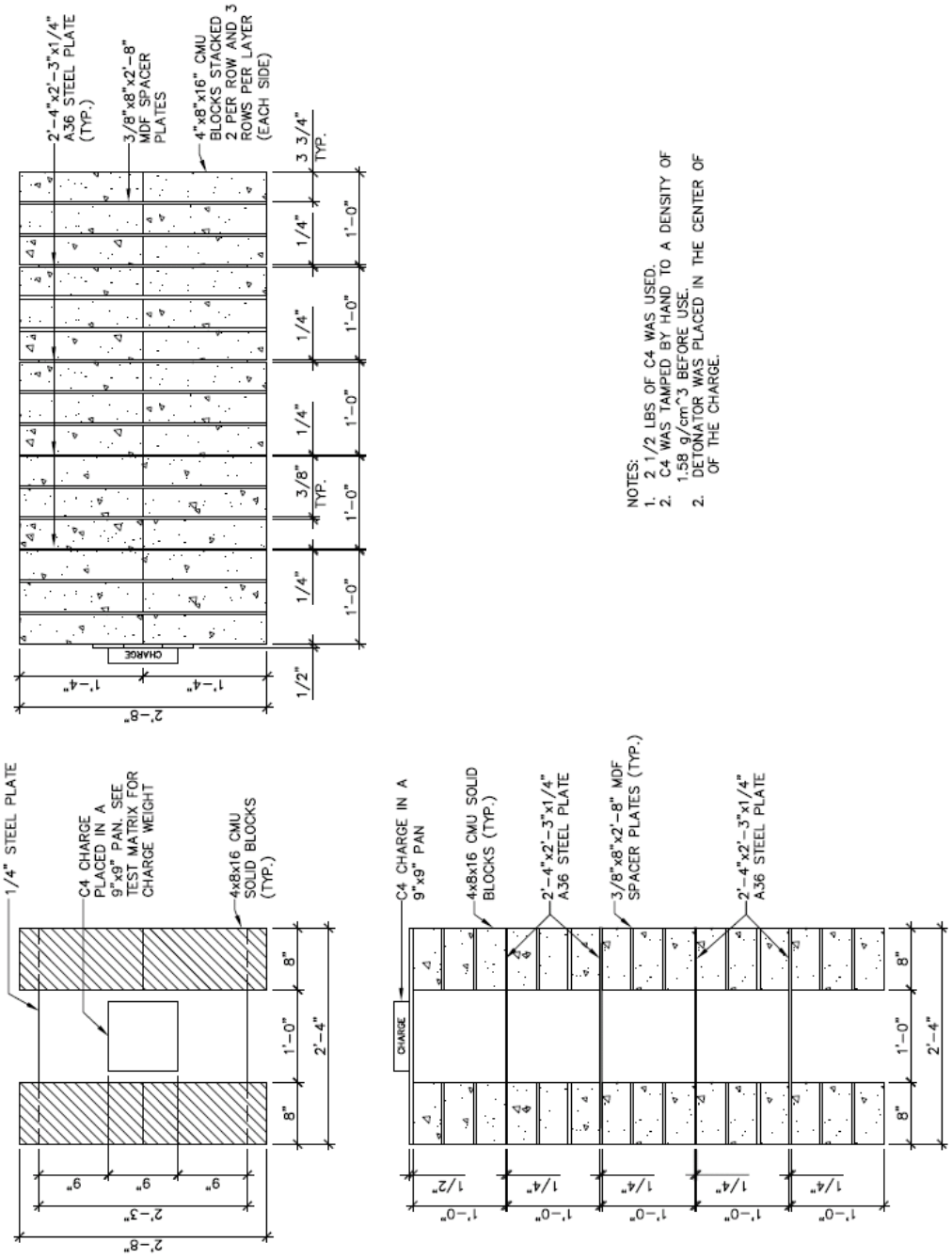

Figure C.10: 4 Plate Test set-up –Drawing

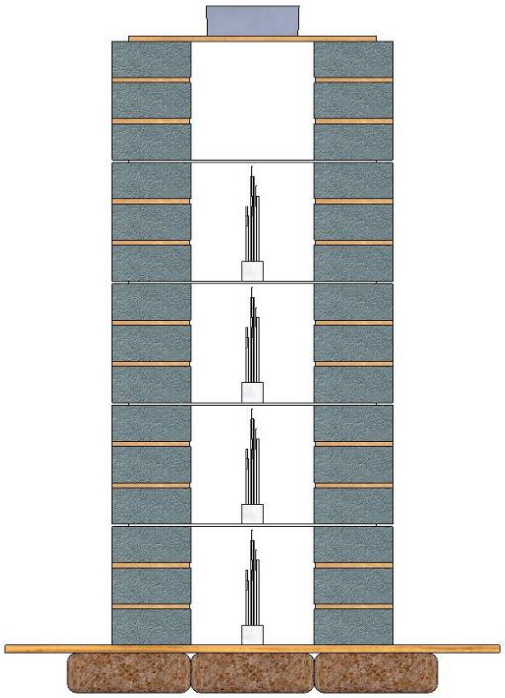

Figure C.11: 4 Plate Test set-up – schematic drawing

C.1.2.2 TEST RESULTS

After the calibration shots, it was thought that 0.014X pounds of equivalent TNT at a close standoff would provide enough energy to fracture a series of four steel plates. Unfortunately, this test did not cause as much damage as was initially anticipated. Only the first three plates were damaged as shown in Figure C.12(a) and Figure C.13. The charge caused a large, or classical, flyer plate to form in the first plate. It subsequently impacted the second plate and caused it to bend in half, with a small fracture in the middle; see Figure C.12(b) and Figure C.13. The weight of the second plate landing on the third plate caused it to deflect, but did not release itself from the support. No damage occurred to the fourth plate.

Due to the minimal damage that occurred in this test, only the first set of Time of Arrival (TOA) pins captured any useful data. According to the data, the initial flyer plate was

traveling at 1,116 ft/sec. The purpose of these tests was to determine the viability of the KEDD concept and determine the ideal layout of the system. Initially, the test had been designed to simulate the full scale test; therefore, the goal was to represent three complete cells. After this baseline test did not fracture through all four steel plates, as hoped, it became necessary to develop a new test plan. There were many limitations including a limited number of steel plates and TOA pins a 2 Plate test plan was developed. This plan met the minimum needs of the test by evaluating one "complete" cell. The test set-up had a first and second plate spaced at 1' where the location of the KEDD system could be evaluated.

Figure C.12: 4 Plate Test a) Post test b) Second, third and fourth plate

Figure C.13: First three plates of 4 Plate Test

C.1.3 2 PLATE TEST

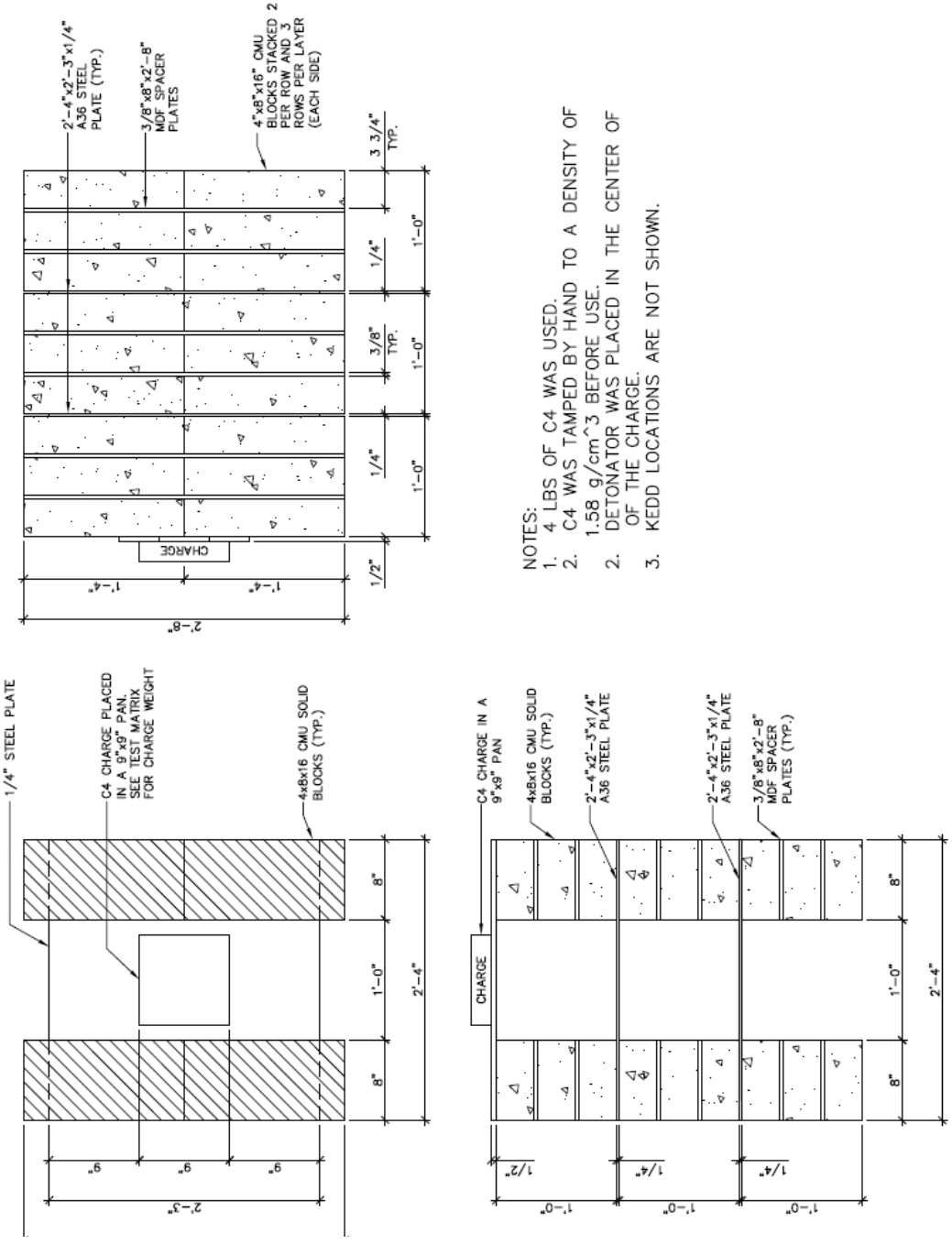

Figure C.14: 2 Plate Test set-up –drawing

Figure C.15: Baseline test set-ups a) Test 6 b) Test 13 c) Test 14 d) Test 18

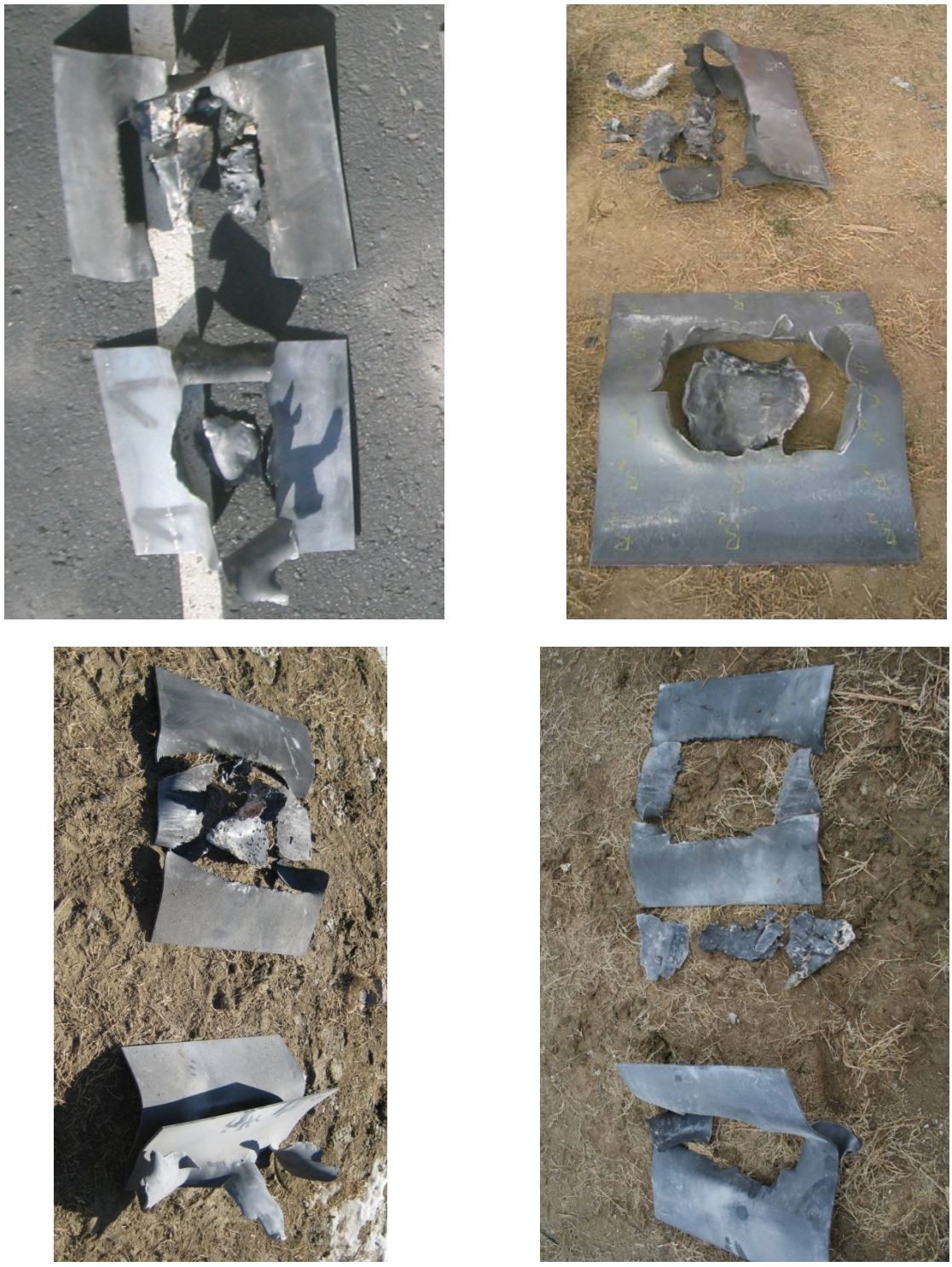

Figure C.16: Baseline tests, first and second plate a) Test 6 b) Test 13 c) Test 14 d) Test 18

C.1.3.1 KEDD ON TOP TEST RESULTS

Figure C.17: KEDD on top test set-ups a) Test 8 b) Test 11

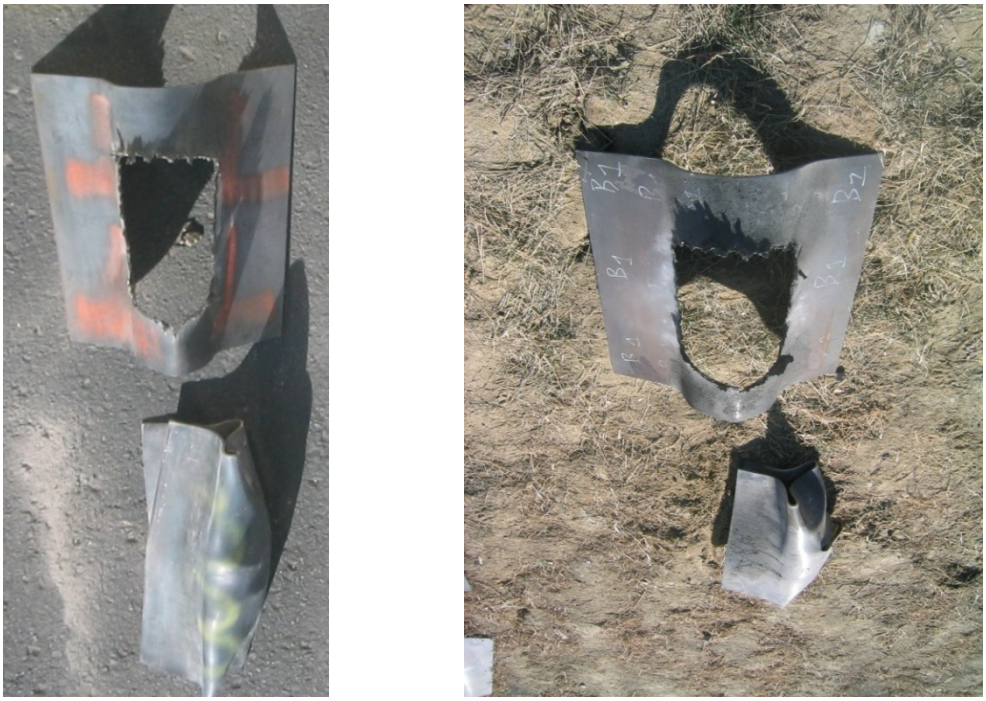

Figure C.18: KEDD on top tests, first and second plate a) Test 8 b) Test 11

C.1.3.2 KEDD ON BOTTOM TEST RESULTS

Figure C.19: KEDD on bottom tests, first and second plate a) Test 7 b) Test 12

C.1.4 KEDD ON TOP – 2- ROW TEST RESULTS

Figure C.20: Two rows of KEDD's on top test set-ups

Figure C.21: Two rows of KEDD's on top tests, first and second plate a) Test 15 b) Test 19

C.1.4.1 KEDD ON TOP AND BOTTOM TEST RESULTS

Figure C.22: One row of KEDD's on top and bottom, first and second plate

a) Test 16 b) Test 21

C.1.5 2 PLATE TEST COMPARISONS

Figure C.23:Two rows of KEDD's on top, second plate a) Top view b) Bottom view

Figure C.24: One row of KEDD's on top and bottom, second plate a) Top view b) Bottom view

Figure C.25:Three rows of KEDD's on top, second plate a) Top view b) Bottom view

C.1.6 3 PLATE TEST

C.1.6.1 TEST SET-UP

Two tests (Test 9 and 10) were performed using three 1/4" steel plates. Each 1/4" plate was spaced 12" above the previous plate, or the plywood base for the first plate. A photo, a drawing, and a schematic drawing of the test set-up can be found in Figure C.27, Figure C.26, and Figure C.28. These test specimens used 0.034X pounds of equivalent TNT at the closest standoff. One of the tests was a baseline test, while the other test had a row of KEDD's placed directly behind the first plate and second plate. These tests were performed before any of the tests using multiple rows of KEDD's. Upon successful completion of Tests 1-8, it was decided to determine the effects of the KEDD system when placed inside of multiple cells. (This test was originally designed to be the last of the series. Fortunately, additional funding became available that allowed for repeated tests.) Based on the two choices of the KEDD system (KEDD on top or bottom) it was decided to place the KEDD's on top for the retrofitted test. .

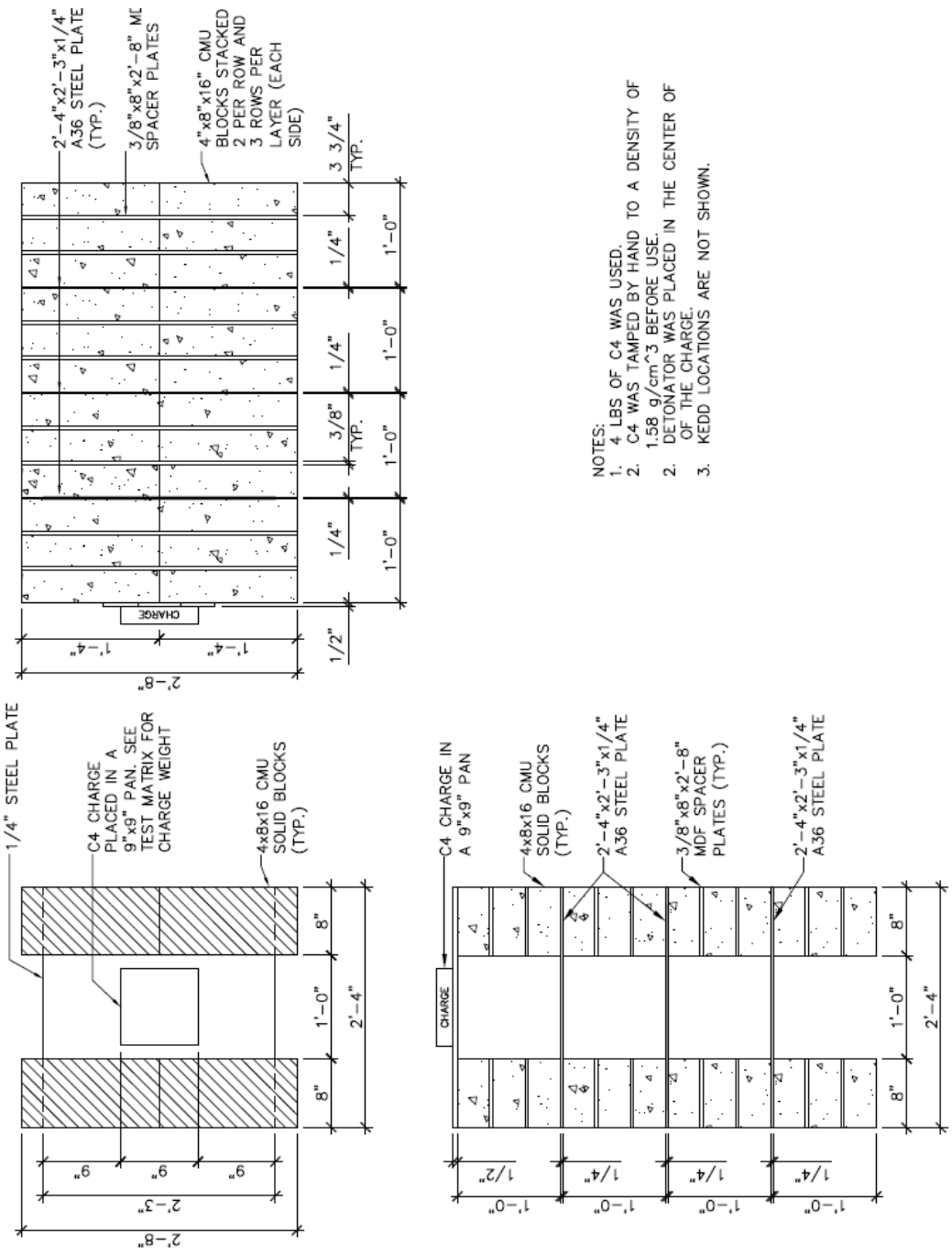

Figure C.26: 3 Plate Test set-up –drawing

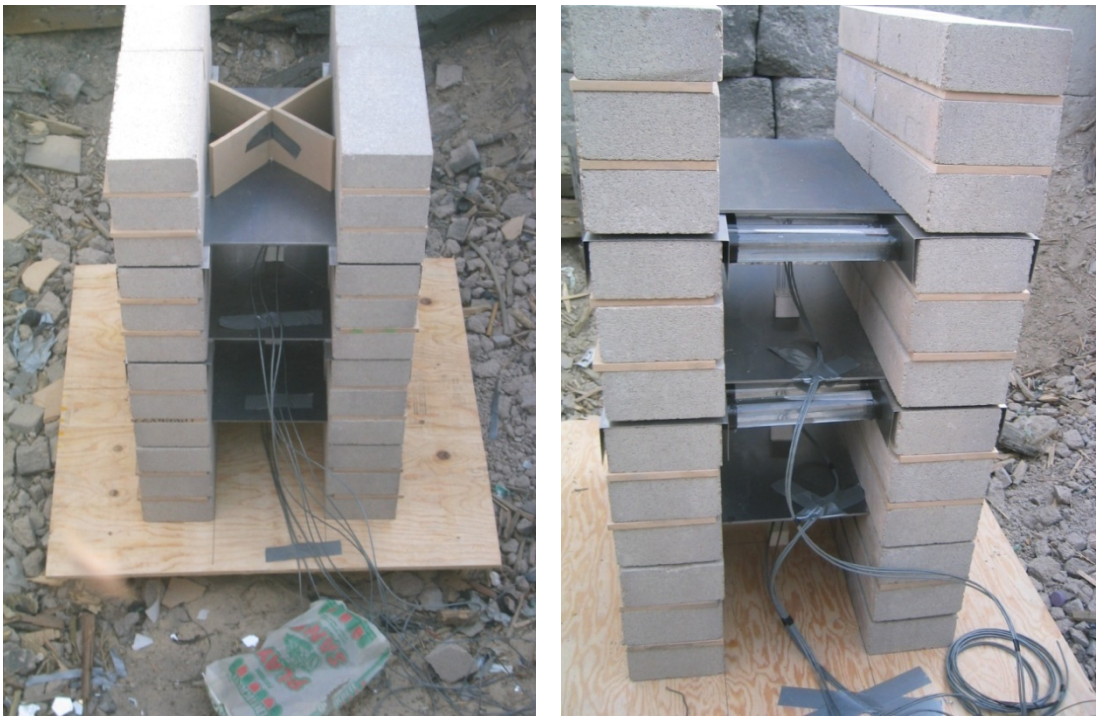

Figure C.27: 3 Plate Test set-up – photo

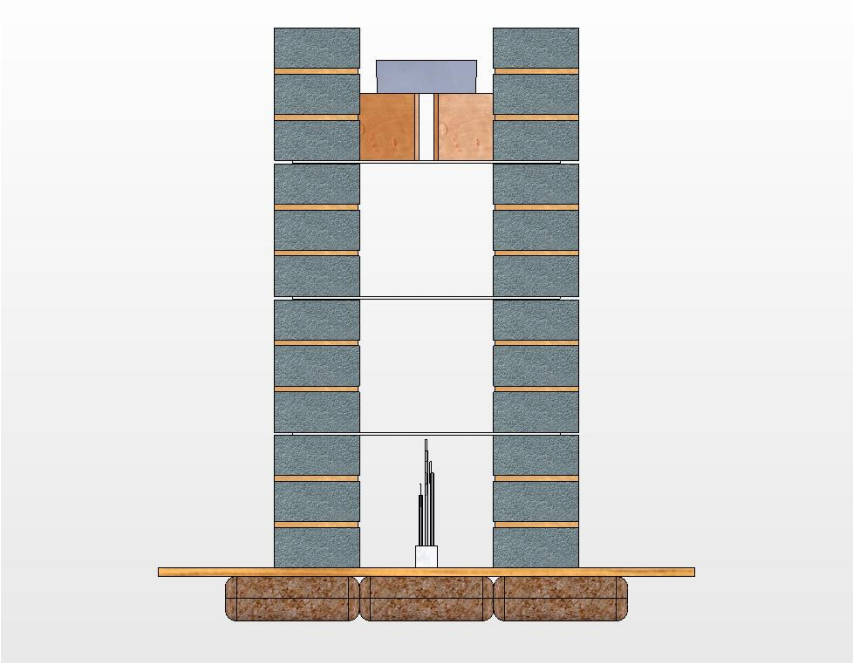

Figure C.28: 3 Plate Test set-up – schematic drawing

C.1.6.2 TEST RESULTS

One way to determine how the retrofit affects the overall behavior of the system is to compare the failure modes of the two specimens. Figure C.29 shows the plates from both tests. The photos are divided into baseline test (left column) and retrofit test (right column). The plates are arranged from first to third down the page.

In the baseline tests the first plate exhibits signs of a brittle failure. Multiple small fragments formed. The second plate also showed signs of a brittle failure, but ductile behavior was also demonstrated by the global deformation of the plate. The third plate failed in a purely ductile manner with petalling along the edges. When compared to the specimens with the KEDD's the difference in failure modes is dramatic.

The first plate of the retrofitted specimen showed exhibited ductile and brittle behavior. A large hole was created in the center of the plate from which several flyer plates were created. Those flyer plates then impacted the second plate and caused in to fold in half while creating a hole in the back of the plate. There was significant deformation of the plate, and some signs of petalling along the edges. The third plate was impacted by the initial and secondary flyer plates. It caused the plate to deform and release from its supports. A crack was formed in the back of the third plate; however, if the plate was secured to its supports there might not have been any additional damage to adjacent plates.

By comparing the types of damage that occurred in the two different tests it is apparent that the KEDD's mitigate damage to the structure. From previous tests we also know that the KEDD system aids in the reduction of velocity of the flyer plates. TOA pins were used in this test; however, the data does not appear to be valid. Velocities were captured that doubled the expected velocity from the Calibration Test. In addition, data gathered after interaction with the second plate does not agree with the data gathered in the 2 Plate Tests, for

either the baseline or KEDD tests.. If a second test had been performed, then the validity of this data could be determined. Without such additional tests, the data needs to be discarded.

Figure C.29: 3 Plate Test comparisons

Left column – baseline tests, first, middle, and third plate

Right column – KEDD tests, first, middle, and third plate

D. APPENDIX D– CHAPTER 6

D.1.1 TEST SET-UP

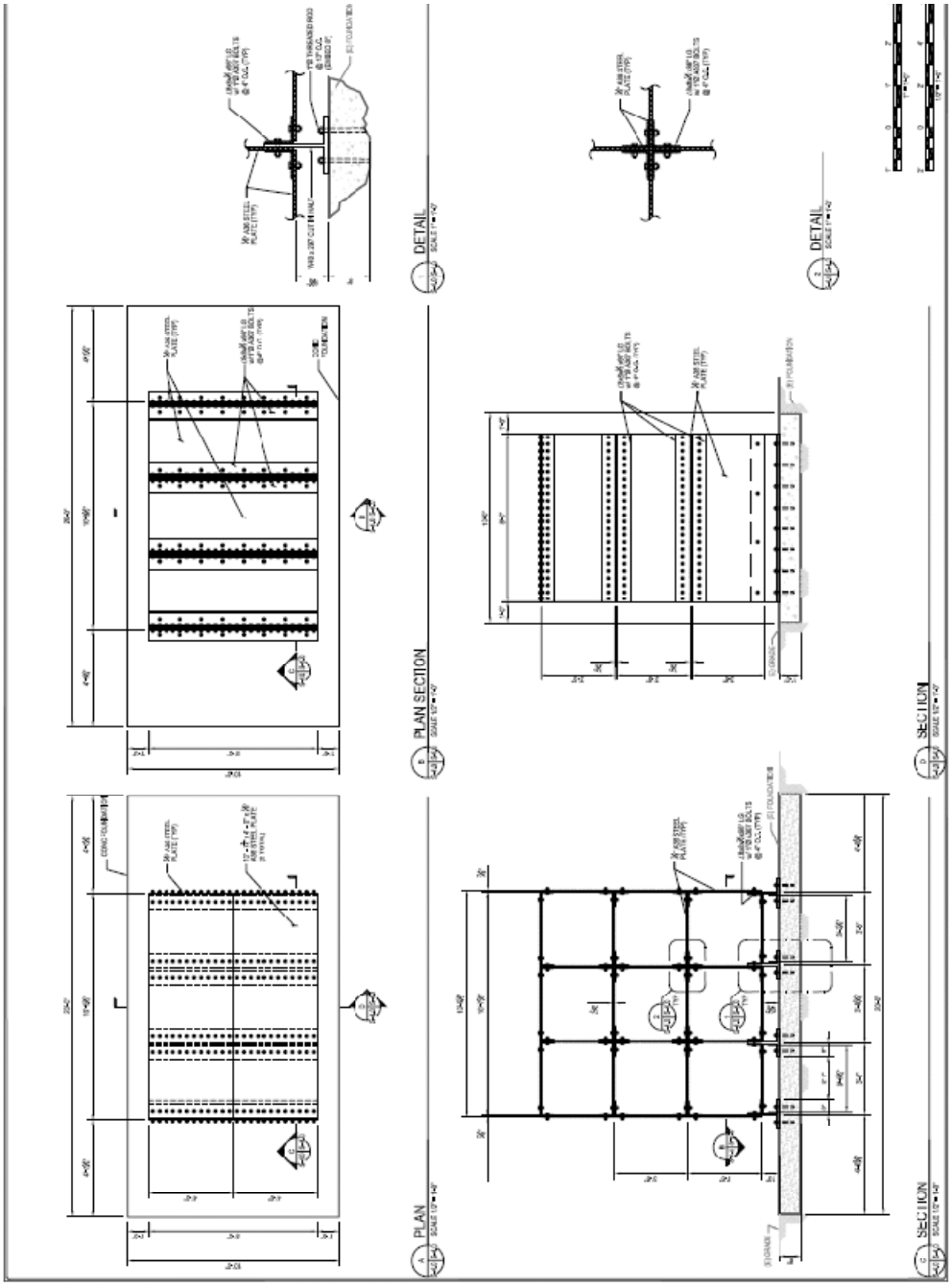

Figure D.1: EMRTC field Test 3 set-up (drawing)

D.1.2 CHARGE SET-UP

Figure D.2: EMRTC Test 3 charge box

D.1.3 INSTRUMENTATION

D.1.3.1 TIME OF ARRIVAL PINS

Ten sets of Time of Arrival (TOA) pins were used for this test series. They recorded the velocity of the steel plates that impacted each array. These pins were the same as the ones used in the Proof of Concept tests. The ARA made TOA pins were chosen over the piezoelectric pins for several reasons; 1) they had already been determined to be effective from the Proof of Concept tests; 2) the instrumentation team was unsure that the piezoelectric pins would accurately capture data in this explosive event; and 3) the manner in which the data is recorded; i.e. - a definite step function is created when the pin creates a short circuit, making the time of impact clear, versus having to discern the difference between noise and

impact when using the piezoelectric pins. In order to calculate the velocity, using the TOA pins, one needs only determine the time of the first and second impact and then divide that value by the distance between the pins.

The TOA pins were held in place by attaching them to a glass rod. These rods are cut at varying lengths in order to achieve a 1/2” spacing between each pin. The typical TOA pin series was placed at 1/2”, 1", and 1 1/2” below the steel plate. There were two arrays that used 4 pins, those pins were located at 1/2”, 1”, 1 1/2”, and 2” below the steel plate. Those arrays are shown in Figure D.3. The arrays were placed in each of the nine cells. The cells were numbered starting with the upper left hand cell continuing down the columns. The first three cells were in the first column of the specimen and are labeled 1, 2, and 3 continuing down the column. The next column of three cells had pin array numbers 4, 5, and 6, where cell 4 was the center cell in the top row. The final column of cells had pin array numbers 7, 8, and 9, where 7 was the last cell in the top row. These pin array numbers also correspond to the cell numbers and will be used as identifying numbers in future sections. Specific information concerning the TOA pins, including cell number, location (front of back) and number of pins, is shown in Figure D.4. The terminology “Front” indicates that the pins are located in the center of the cell, 3’ from the front edge. “Back” indicates that the pins are located in the center of the cell, 7’ from the front edge.

The pin arrays were held in place using two different methods. For the baseline tests (Cells 1-3 and Cells 7-9) the pins were supported by a 3” diameter paper shipping tube that was attached to the bottom steel plate. The pin array shown in Figure D.3 was then attached to the tube by heavy-duty tape. In order to ensure that the tubes would not be blown out of the test article by the blast pressure, they were secured to the test structure by 4 guide wires that were attached to bolts at the bottom of the cell. Figure D.5(a) shows a typical set-up of the TOA

pins on top of the paper tube. In the center cells, the ones with the KEDD's, the TOA pin arrangements were attached to a KEDD. They extended approximately 1" above the top of a KEDD, such that they should be activated before the KEDD is breached. Figure D.5(b) shows the tops of a pin array extending out from between two KEDD's.

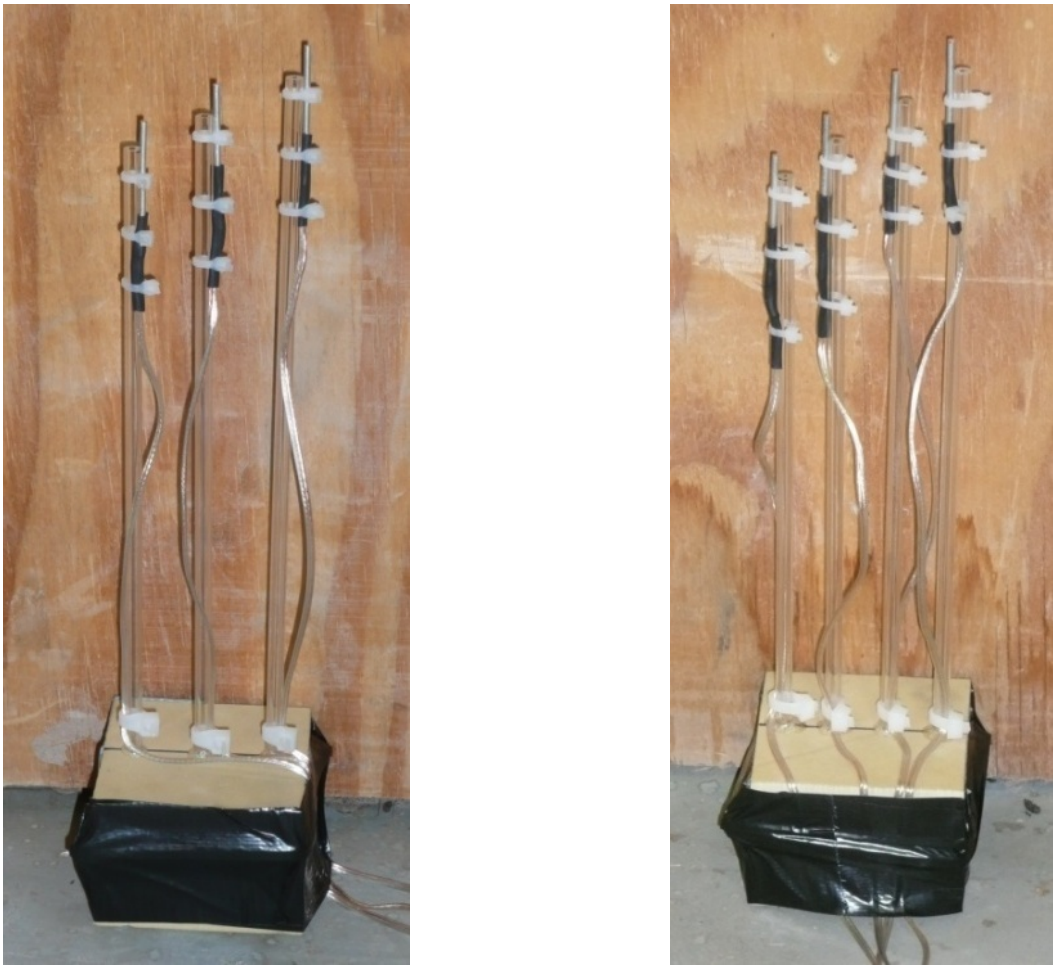

Figure D.3: Time of Arrival pin arrays a) 3 pin array b) 4 pin array

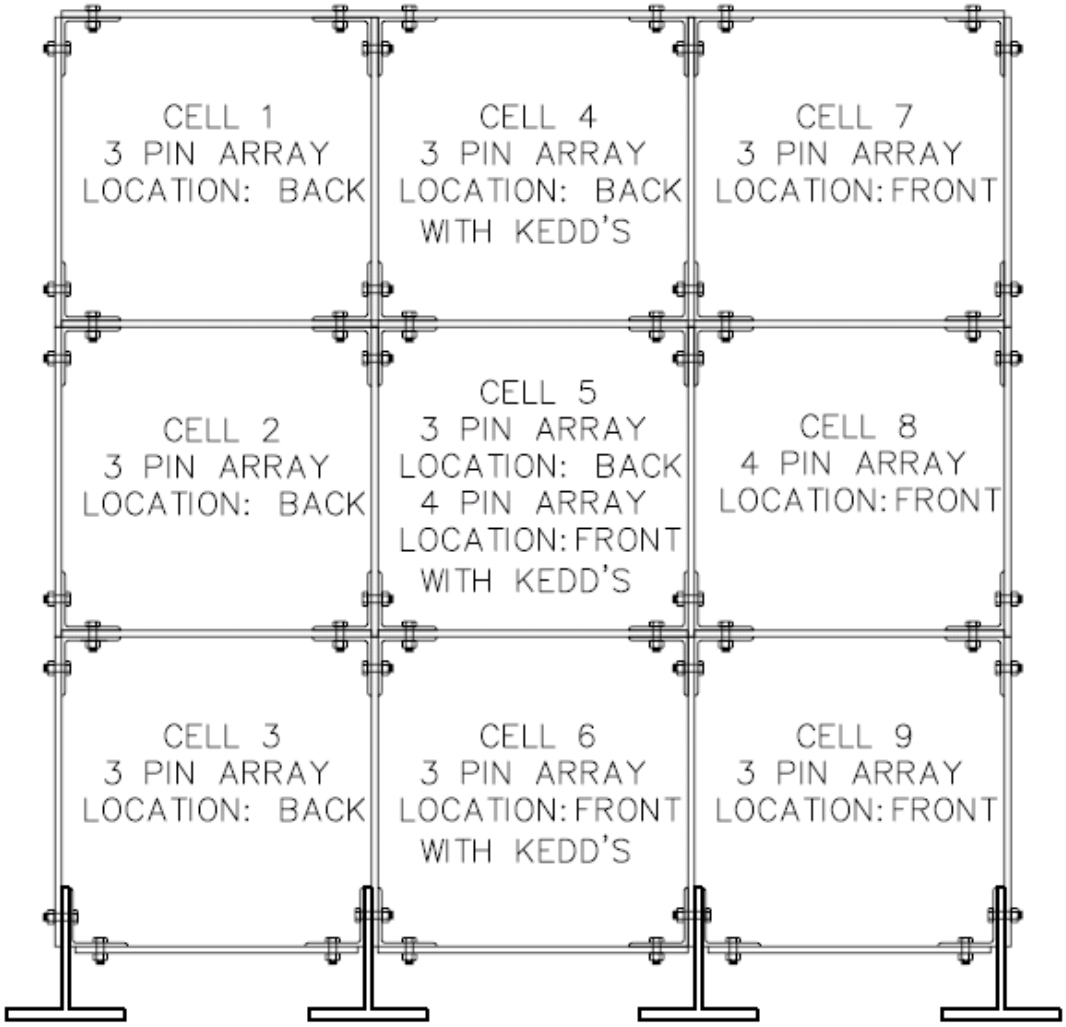

Figure D.4: Time of Arrival pin locations for EMRTC Test 3

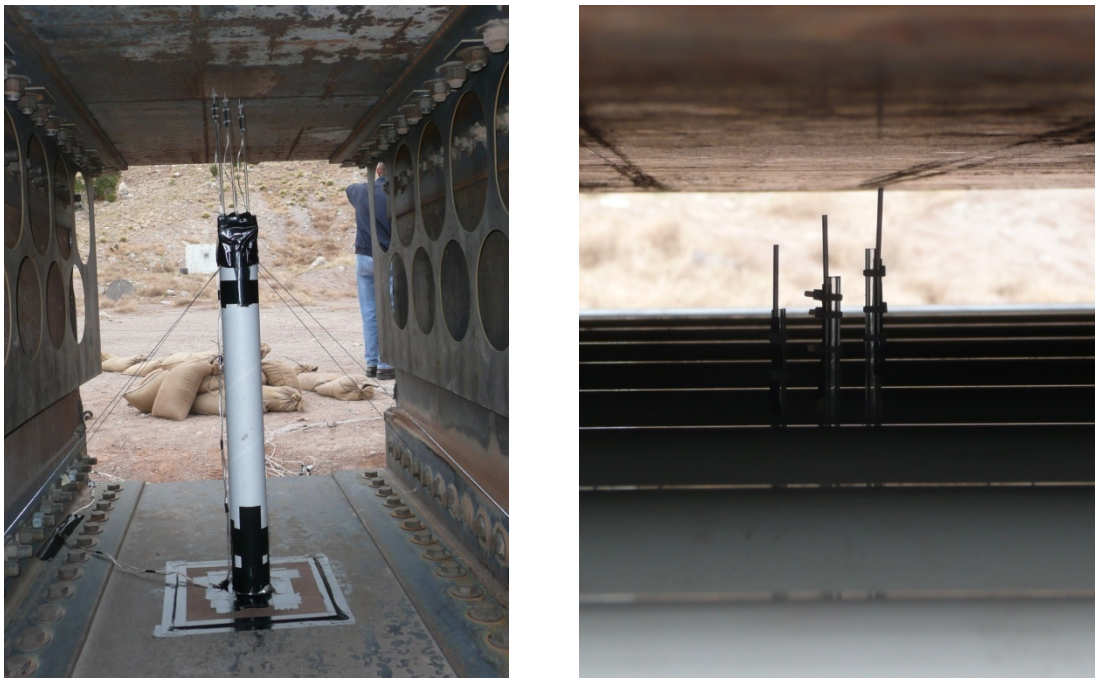

Figure D.5: Time of Arrival pins a) Pin support in outer cells b) Pins located in center cells

The instrumentation design for this test was well thought out and expertly constructed. The decisions on the location and array spacing of the Time of Arrival data were based on the previous tests that were executed successfully. The number of pins available was limited by the number of channels on the data acquisition system, yet they still covered a wide variety of locations. The data that was captured showed definite steps and the data follows well correlated trends; however, it does not match with the deformation that was observed on the high speed video. There are several factors that could explain this situation. One key premise is that, in some instances, a stray bolt, or fragment, activated the TOA pins before the main flyer plate arrived. In other cases, the location of the pin array may have led to completely "missing" the fast moving flyer plate whose velocity we were most interested in. The location of the pins may also have been too close to the steel plate; as a result the TOA pins may have captured the rate of deflection, and not the speed of a flyer plate. Due to such considerations,

and the inability to confirm what portions of the specimen actually interacted with the TOA pins, the data will be disregarded. It is unclear, with the limitations on the available channels for the data collection system, how to improve the instrumentation layouts for future tests. This is one of the drawbacks of live field testing and highlights the importance of the UCSD Blast Simulator, which can simulate these types of events, and document failure process using high speed data recorders.

D.2 TEST RESULTS

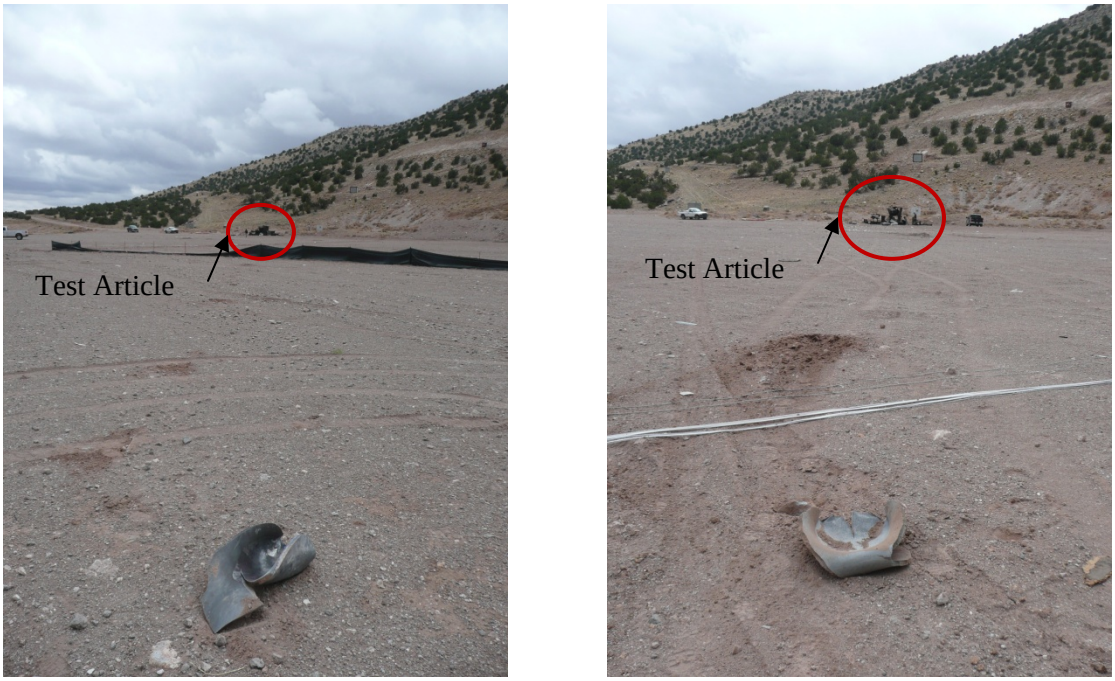

Figure D.6: Flyer plates at extreme distances

Figure D.7: Flyer plates at extreme distances

E TEST RESULTS – BALLISTIC TESTS – TYPE 1

E.1 STEEL TOWER SINGLE PLATE: TEST 1 (SP1)

E.1.1 INTRODUCTION

The first test of the Steel Tower Single Plate test series was performed on October 24th, 2006. The test specimen was a ¼" thick steel plate labeled SP1. The Impacting Mass 1 was attached to the BG with a specimen target velocity of 32.8 ft/sec (10 m/sec). Figure E.1 shows the steel plate prior to impact.

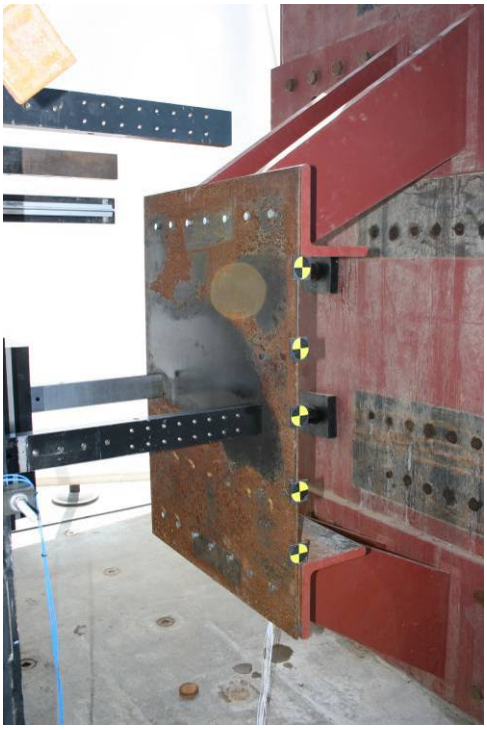

Figure E.1: 1/4" thick steel plate pre test for Test 1

E.1.2 INSTRUMENTATION

E.1.2.1 PHANTOM CAMERAS

The first camera recorded in black and white at a rate of 10,000 frames per second at a resolution of 512x384. This camera was used in order to determine the maximum velocity of the impacting mass and the movement in the plate including the maximum displacement. The second camera recorded in color at a rate of 5,000 frames per second at a resolution of 512x384. This camera recorded the deflection from the back of the plate and was not used to gather any specific. A picture from each of the camera locations are show in Figure E.2**.**

Figure E.2: Phantom cameras for tests a) Camera One b) Camera Two

E.1.2.2 TARGET LOCATIONS

Five targets were welded onto the side of the steel plate as show in Figure E.1**.** They were spaced at the intervals shown in Figure E.3. That figure also shows the location of the targets for the impacting mass.

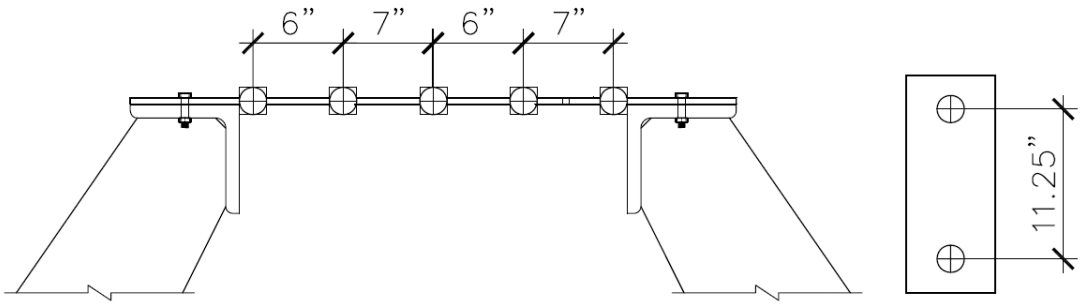

Figure E.3: Target layout on plate and impacting mass for Test 1

E.1.2.3 ACCELERATIONS

For this test there were a total of four accelerometers used. Two of the accelerometers were placed 6” to the north and south of the centroid while the other two accelerometers are placed 4” east and west of the centroid as shown in Figure E.4. The accelerometer data from this test was unusable.

This test does not impart an impulsive load as would be expected from a typical blast test. Instead, this test simulates the behavior of a flyer plate moving through the structure after the initial impact at the front plate of the outer cell of the structure. Therefore we are not determining the initial impulsive load from the accelerometers on the BG.

E.1.2.4 STRAIN GAGE LOCATIONS

There was no strain gage data for this test.

E.1.2.5 BOLT TYPE

A total of fourteen Grade 5 bolts (High Strength Bolts) were used for this test.

Figure E.4: Accelerometer location for Test 1

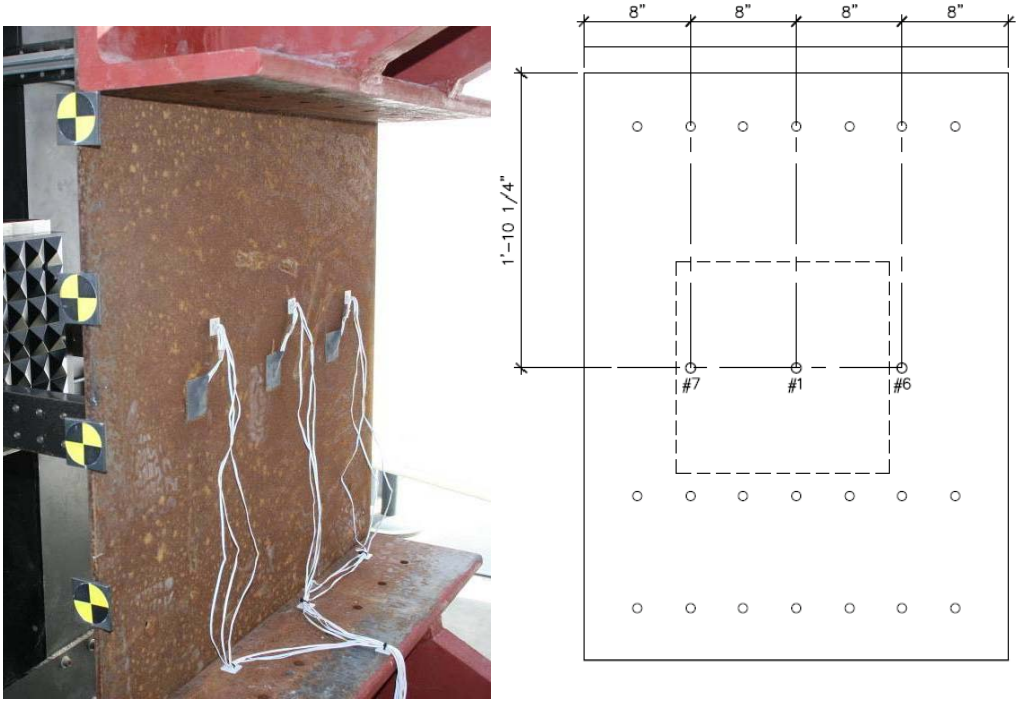

Figure E.5: Strain gage layout for Test 1

E.1.3 BLAST GENERATOR DATA

The initial impact of the single BG was 33.51 ft/sec (10.21 m/sec) with a goal velocity of 10 m/s. It had four accelerometers mounted to the back side of the impact plate as discussed in Section E.1.2.3. The average impact velocity for the impacting mass and the steel plate was calculated using the TEMA Track Eye tracking software.

E.1.4 SPECIMEN BEHAVIOR

The loading of the BG plate imparted an initial velocity of 33.51 ft/sec (10.21 m/s) to the specimen. This caused plate to deform in both directions. The longitudinal deflection (in the north-south direction) behaved in a typical one-way flexural shape. The plate bends horizontally where there is plate that is not being impacted by the programmer. The specimen had an approximate maximum midspan deflection of 1.4" during the test and a permanent deflection of 11/16", Figure E.6 displays the specimen after the test. The progression of damage recorded by Phantom Camera One is shown in Figure E.7. There were not enough breakaway bolts placed between the BG and the impacting mass. Four bolts were used instead of the eight needed due to the forces required to pull the mass back. When the rod began to pull the mass back it broke all of the bolts. It also caused very little damage to the plate; therefore this plate was used again in Steel Plate Test 2

Figure E.6: Steel plate post test for Test 1

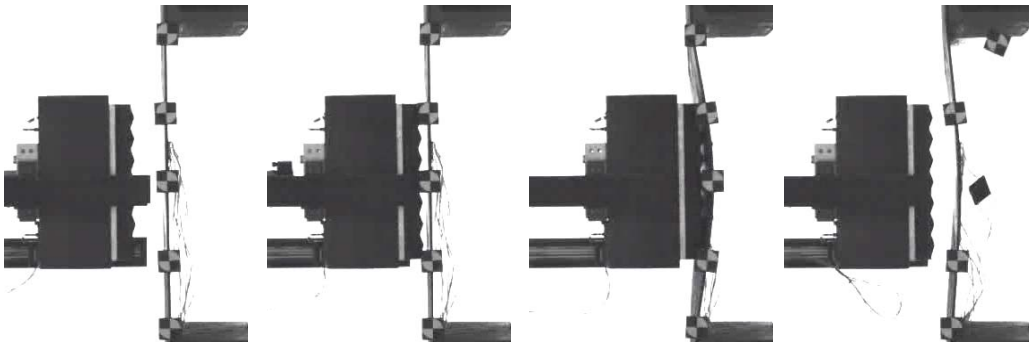

Figure E.7: Progression of damage for Test 1

E.2 STEEL TOWER SINGLE PLATE: TEST 2 (SP2)

E.2.1 INTRODUCTION

The second test of the Steel Tower Single Plate test series was performed on October 25th, 2006. The test specimen was the same that was tested in the first test performed on October 24th, 2006; it had a residual deflection of 11/16" at the midspan. The test specimen was ¼" thick steel plate re-labeled SP2. The Impacting Mass 1 was attached to the BG with a specimen target velocity of 32.8 ft/sec (10 m/sec). Figure E.8 shows the steel plate prior to impact.

Figure E.8: 1/4" thick steel plate pre test for Test 2

E.2.2 INSTRUMENTATION

E.2.2.1 PHANTOM CAMERAS

The first camera recorded in black and white at a rate of 5,000 frames per second at a resolution of 512x384. This camera was used in order to determine the maximum velocity of the impacting mass and the movement in the plate including the maximum displacement. The second camera recorded in color at a rate of 4,000 frames per second at a resolution of 512x384. This camera captured data on the front side of the plate but was not used to gather any specific data.. The third camera recorded in color at a rate of 4,000 frames per second at a resolution of 512x400.This camera recorded the deflection from the back of the plate and was not used to gather any specific data. A picture from each of the camera locations are shown in Figure E.9.

E.2.2.2 TARGET LOCATIONS

Five targets were welded onto the side of the steel plate as show in Figure E.8. They were spaced at the intervals shown in Figure E.10. That figure also shows the location of the targets for the impacting mass.

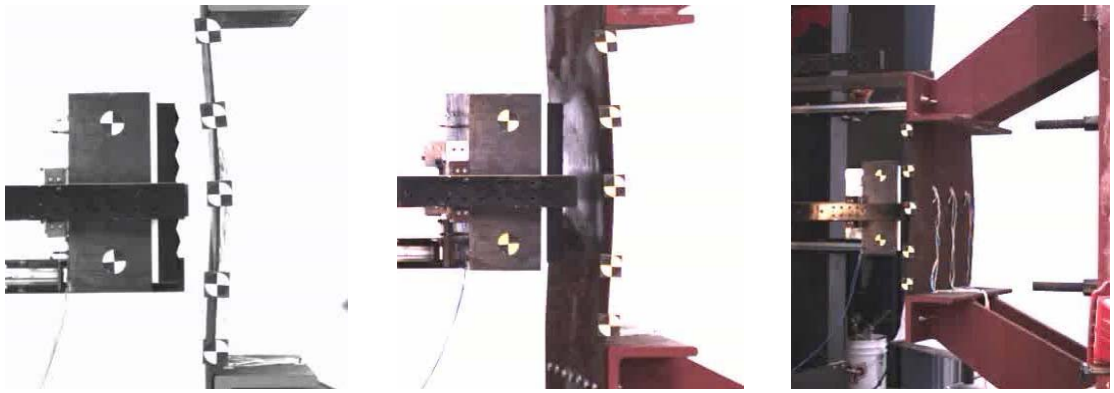

Figure E.9: Phantom cameras for Test 2 a) Camera One b) Camera Two c) Camera Three

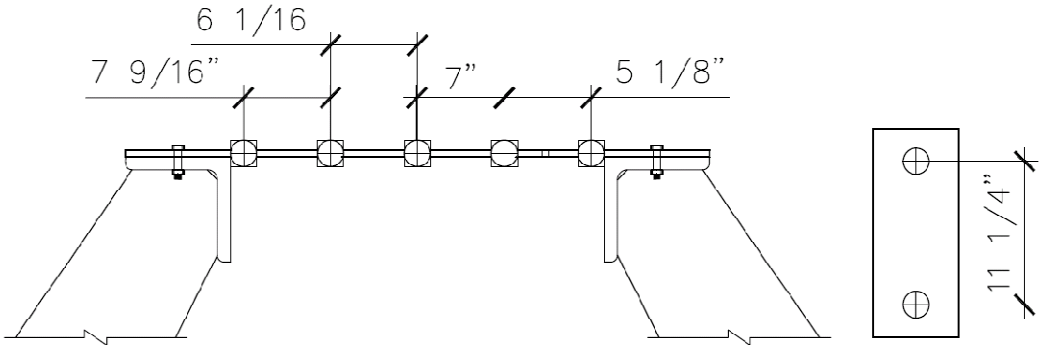

Figure E.10: Target layout on plate and impacting mass for Test 2

E.2.2.3 ACCELERATIONS

For this test there were a total of four accelerometers used. Two of the accelerometers were placed 6" to the north and south of the centroid while the other two accelerometers are placed 4" east and west of the centroid as shown in Figure E.11. The acceleration data from this test was not usable.

This test does not impart an impulsive load as would be expected from a typical blast test. Instead, this test simulates the behavior of a flyer plate moving through the structure after the initial impact at the front plate of the outer cell of the structure. Therefore we are not determining the initial impulsive load from the accelerometers on the BG.

E.2.2.4 BOLT TYPE

A total of fourteen Grade 5 bolts (High Strength Bolts) were used for this test.

E.2.3 BLAST GENERATOR DATA

The initial impact of the single BG was 31.50 ft/sec (9.60 m/sec) with a goal velocity of 10 m/s. It had four accelerometers mounted to the back side of the impact plate as discussed in Section E.2.2.3. The average impact velocity for the impacting mass and the steel plate was calculated using the TEMA Track Eye tracking software.

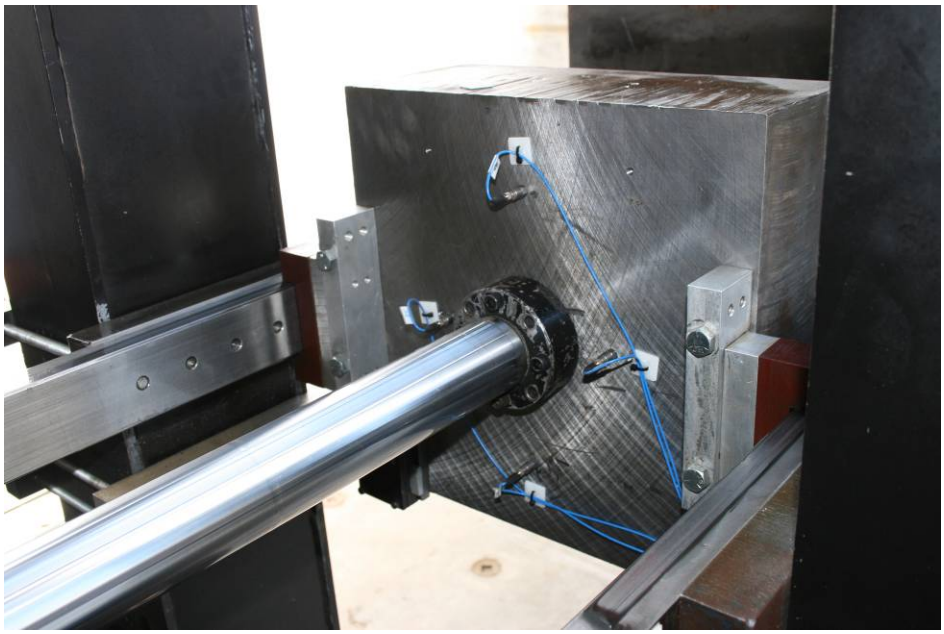

Figure E.11: Accelerometer location for Test 2

E.2.4 SPECIMEN BEHAVIOR

The loading of the BG plate imparted an initial velocity of 31.50 ft/sec (9.60 m/s) to the specimen. This caused plate to deform in both directions. The longitudinal deflection (in the north-south direction) behaved in a typical one-way flexural shape. The plate bends horizontally where there is plate that is not being impacted by the programmer. The specimen had an approximate maximum midspan deflection of 2” during the test, Figure E.12 shows the specimen after the test. The progression of damage recorded by Phantom Camera One can be seen in Figure E.13.

Figure E.12: Steel plate post test for Test 2

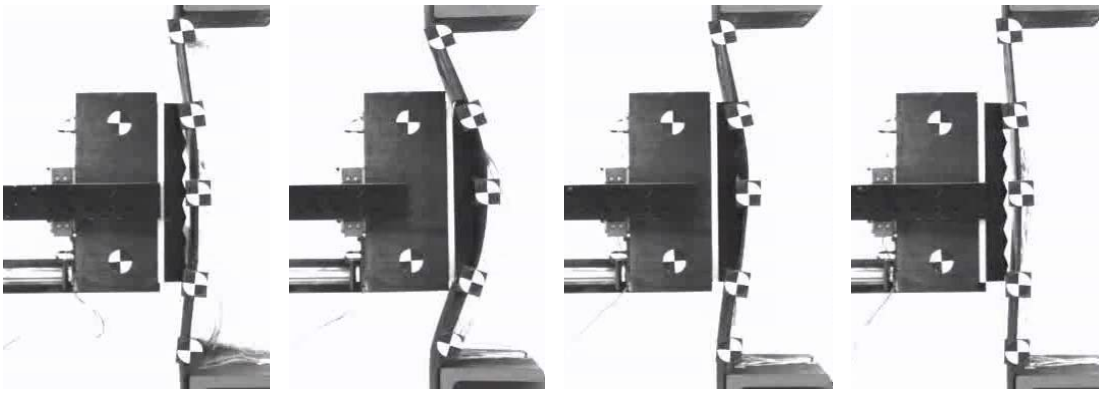

Figure E.13: Progression of damage for Test 2

E.3 STEEL TOWER SINGLE PLATE: TEST 3 (SP3)

E.3.1 INTRODUCTION

The third test of the Steel Tower Single Plate test series was performed on October 25th, 2006. The test specimen was ¼" thick steel plate labeled SP3. The Impacting Mass 1 was attached to the BG with a specimen target velocity of 49.2 ft/sec (15 m/sec). Figure E.14 shows the steel plate prior to impact.

Figure E.14: 1/4" thick steel plate pre test for Test 3

E.3.2 INSTRUMENTATION

E.3.2.1 PHANTOM CAMERAS

The first camera recorded in black and white at a rate of 10,000 frames per second at a resolution of 512x384. This camera was used in order to determine the maximum velocity of the impacting mass and the movement in the plate including the maximum displacement. The second camera recorded in color at a rate of 5,000 frames per second at a resolution of 512x384. This camera captured data on the front side of the test set-up but was not used to gather any specific data. The third camera recorded in color at a rate of 10,000 frames per second at a resolution of 512x400.This camera recorded the deflection from the back of the plate and was not used to gather any specific data. A picture from each of the camera locations are shown in Figure E.15**.**

E.3.2.2 TARGET LOCATIONS

Five targets were welded onto the side of the steel plate as show in Figure E.14. They were spaced at the intervals shown in Figure E.16. That figure also shows the location of the targets for the impacting mass.

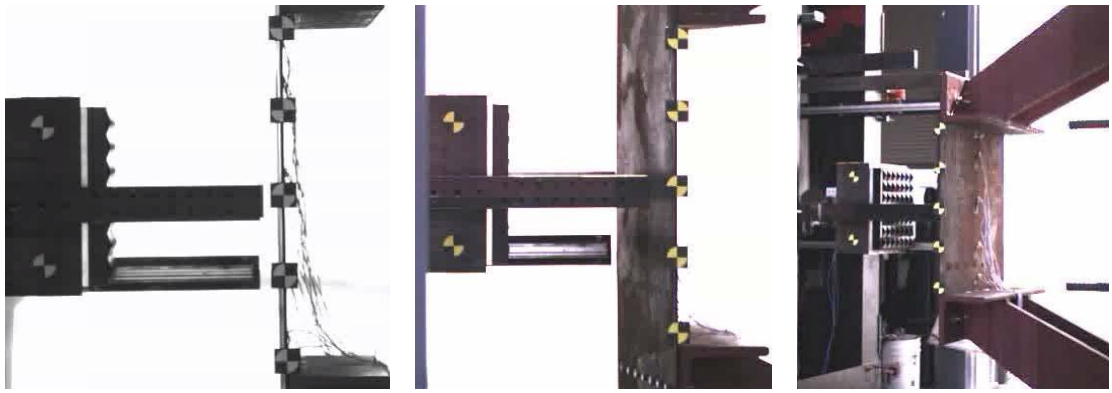

Figure E.15: Phantom Cameras for Test 3 a) Camera One b) Camera Two c) Camera Three

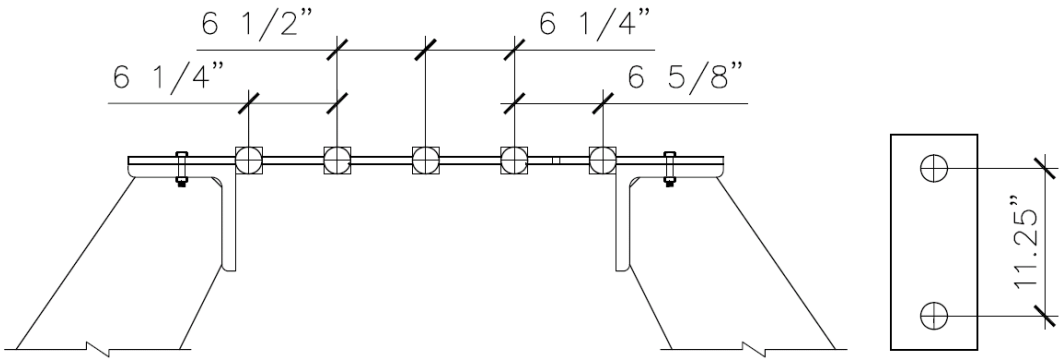

Figure E.16: Target layout on plate and impacting mass for Test 3

E.3.2.3 ACCELERATIONS

For this test there were a total of four accelerometers used. Two of the accelerometers were placed 6” to the north and south of the centroid while the other two accelerometers are placed 4” east and west of the centroid as shown in Figure E.17. The four accelerometers were then averaged together and a filtered was applied as shown in Figure E.18.

This test does not impart an impulsive load as would be expected from a typical blast test. Instead, this test simulates the behavior of a flyer plate moving through the structure after the initial impact at the front plate of the outer cell of the structure. Therefore we are not determining the initial impulsive load from the accelerometers on the BG.

Figure E.17: Accelerometer location for Test

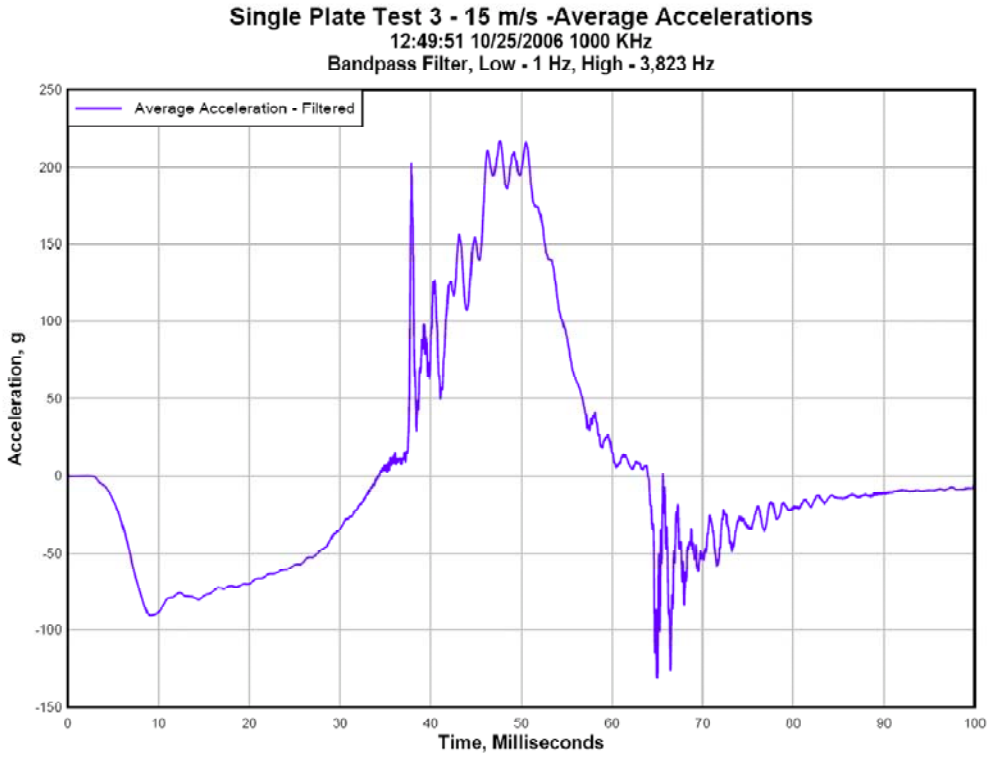

Figure E.18: Filtered accelerometer data for Test 3

E.3.2.4 STRAIN GAGE LOCATIONS

For this test there were five strain gauges used labeled 1, 2, 3, 4 and 5. The strain gauges, and their locations, are shown in Figure E.19. Strain Gage 4 was damaged during this test. Strain Gage 5 showed unreasonable data, those gauges have been discarded. Table E.1 shows the specific information about this test, including the time and velocity at impact, if, and when, the bolts failed along with the maximum and minimum principal strain rates. The largest maximum principal strain rate for this test was 5.80 1/sec and was located at strain gage 1 while the largest minimum strain rate for this test was 7.00 located at strain gage 3. The maximum principal strains for gauges 1, 2 and 3 can be found in
Figure E.20 and the minimum principal strains for the same gauges can be found in
Figure E.21.

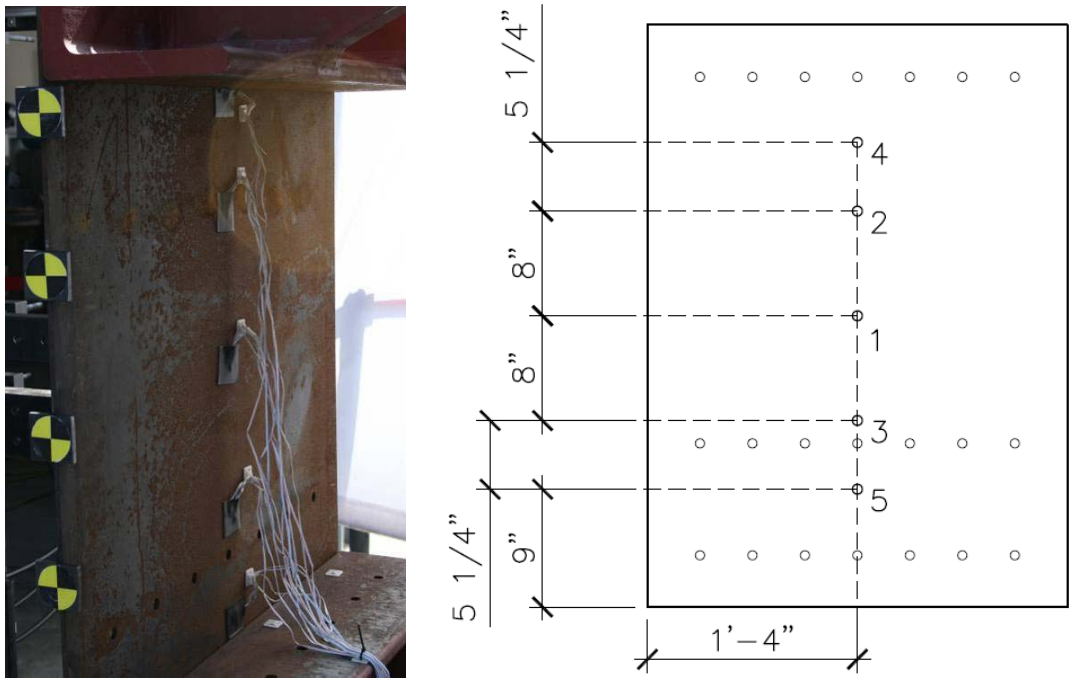

Figure E.19: Strain gage layout for Test 3

Table E.1: Stain rate information for Test 3

Strain Gage Number	Actual Velocity	Initial Impact	Shear Wave at Gage	Bolts Break	Maximum Principal Strain Rate	Minimum Principal Strain Rate
1	17.1 m/s	37.8 msec	-	-	-5.80 1/sec	-5.16 1/sec
2	17.1 m/s	37.8 msec	-	-	-4.14 1/sec	3.82 1/sec
3	17.1 m/s	37.8 msec	-	-	-3.73 1/sec	-7.00 1/sec

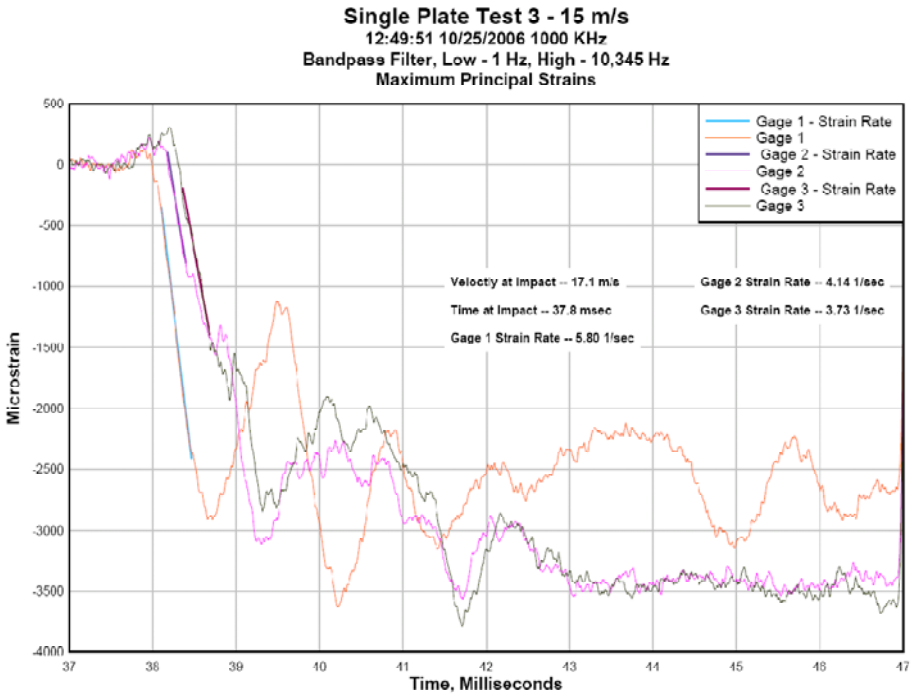

Figure E.20: Maximum principal strains and strain rates for Test 3

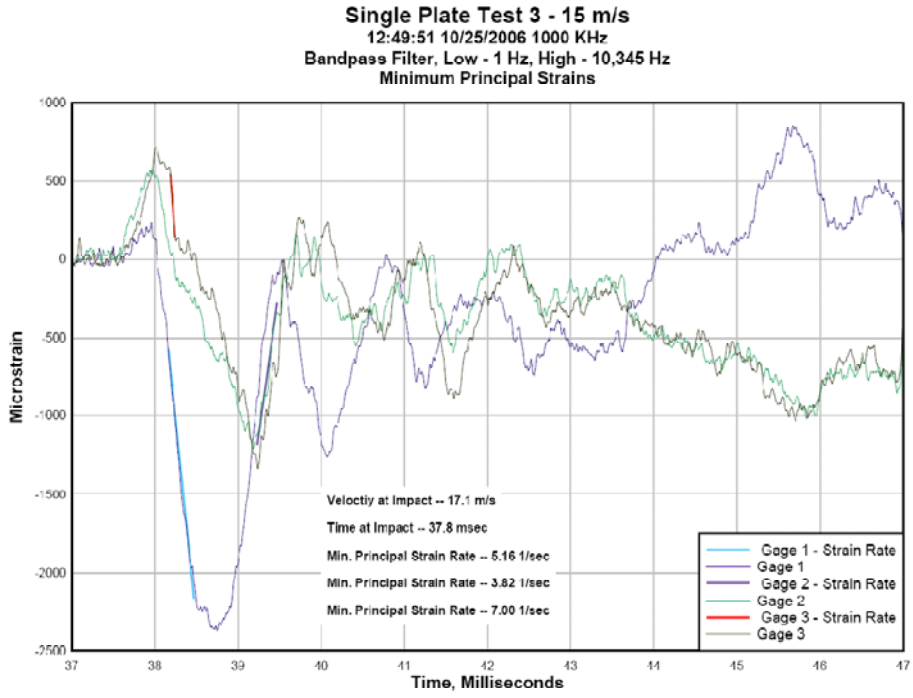

Figure E.21: Minimum principal strains and strain rates for Test 3

E.3.2.5 BOLT TYPE

A total of fourteen Grade 5 bolts (High Strength Bolts) were used for this test.

E.3.3 BLAST GENERATOR DATA

The initial impact of the single BG was 56.23 ft/sec (17.14 m/sec) with a goal velocity of 15 m/s. It had four accelerometers mounted to the back side of the impact plate as discussed in Section E.3.2.3. The average impact velocity for the impacting mass and the steel plate was calculated using the TEMA Track Eye tracking software.

E.3.4 SPECIMEN BEHAVIOR

The loading of the BG plate imparted an initial velocity of 56.23 ft/sec (17.14 m/sec) to the specimen. This caused plate to deform in both directions. The longitudinal deflection (in the north-south direction) behaved in a typical one-way flexural shape. The plate bends horizontally where there is plate that is not being impacted by the programmer. The specimen had an approximate maximum midspan deflection of 4" during the test and a permanent deflection of 1 11/16". It is difficult to determine a more accurate determination of the deflection during the test since the target located at the midspan of the plate became detached from the specimen during the test. Figure E.22 shows the specimen after the test. The progression of damage recorded by Phantom Camera One can be seen in Error! Reference source not found..

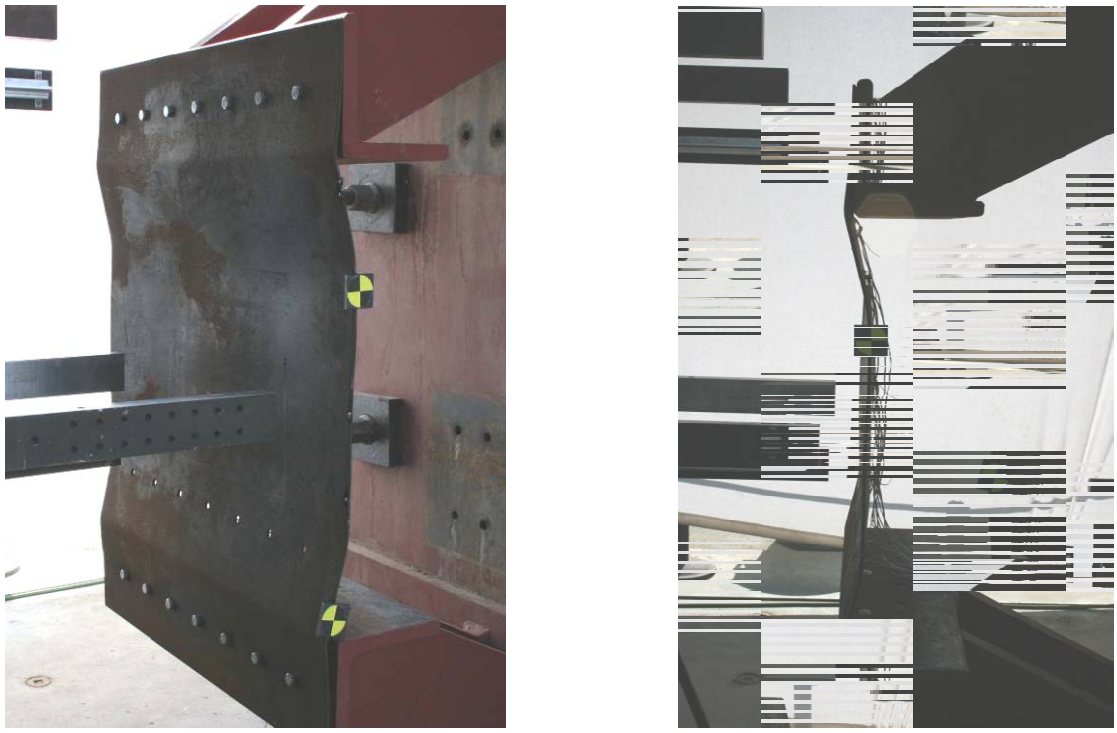

Figure E.22: Steel plate post test for Test 3

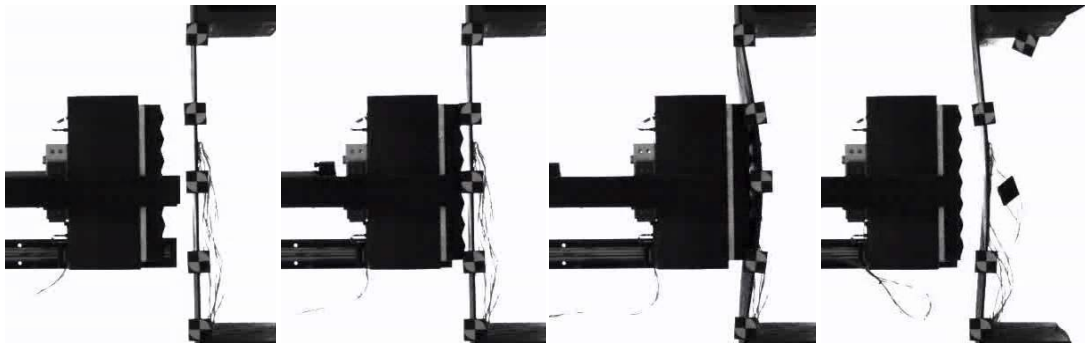

Figure A- E.1: Progression of damage for Test 3

E.4 STEEL TOWER SINGLE PLATE: TEST 4 (SP4)

E.4.1 INTRODUCTION

The fourth test of the Steel Tower Single Plate test series was performed on October 25th, 2006. The test specimen was a ¼" thick steel plate labeled SP4. The Impacting Mass 1 was attached to the BG with a specimen target velocity of 91.86 ft/sec (28 m/sec). Figure E.23 shows the steel plate prior to impact.

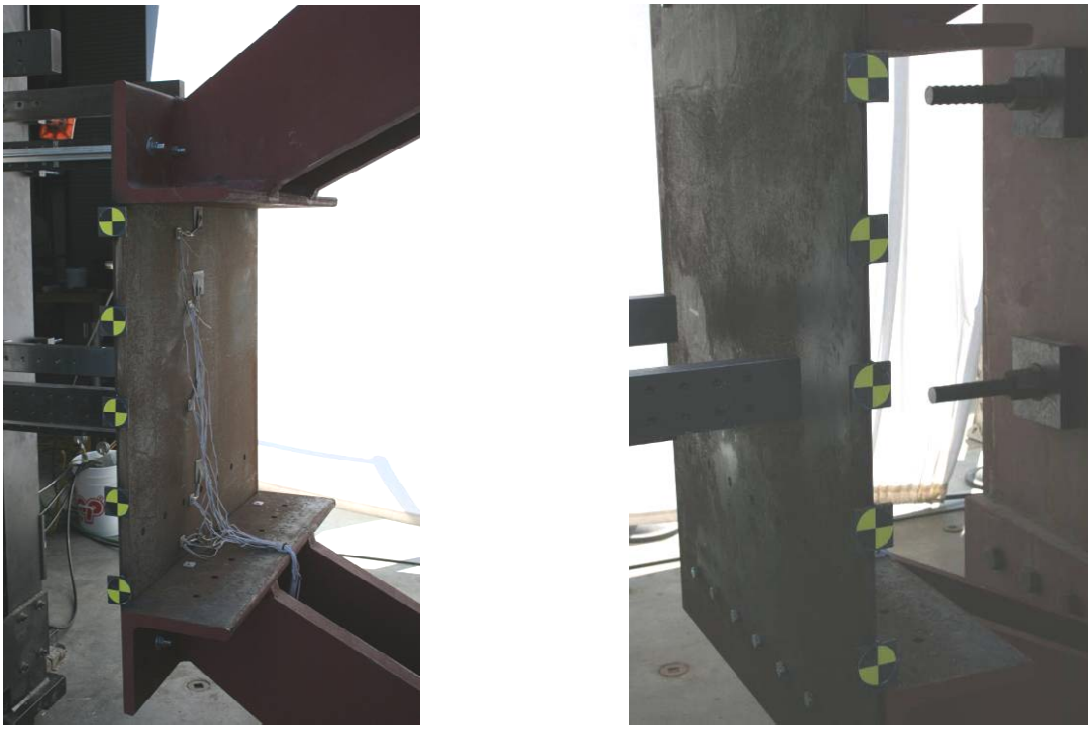

Figure E.23: 1/4" thick steel plate pre test for Test 4

E.4.2 INSTRUMENTATION

E.4.2.1 PHANTOM CAMERAS

The first camera recorded in black and white at a rate of 10,000 frames per second at a resolution of 512x384. This camera was used in order to determine the maximum velocity of the impacting mass and the movement in the plate including the maximum displacement. The second camera recorded in color at a rate of 6,006 frames per second at a resolution of 512x384. This camera recorded the deflection from the back of the plate and was not used to gather any specific data. The third camera recorded in color at a rate of 10,000 frames per second at a resolution of 512x400. This camera captured data on the front side of the but was not used to gather any specific data.. A picture from each of the camera locations are shown in Figure E.24.

E.4.2.2 TARGET LOCATIONS

Five targets were welded onto the side of the steel plate as show in Figure E.23. They were spaced at the intervals shown in Figure E.25. That figure also shows the location of the targets for the impacting mass.

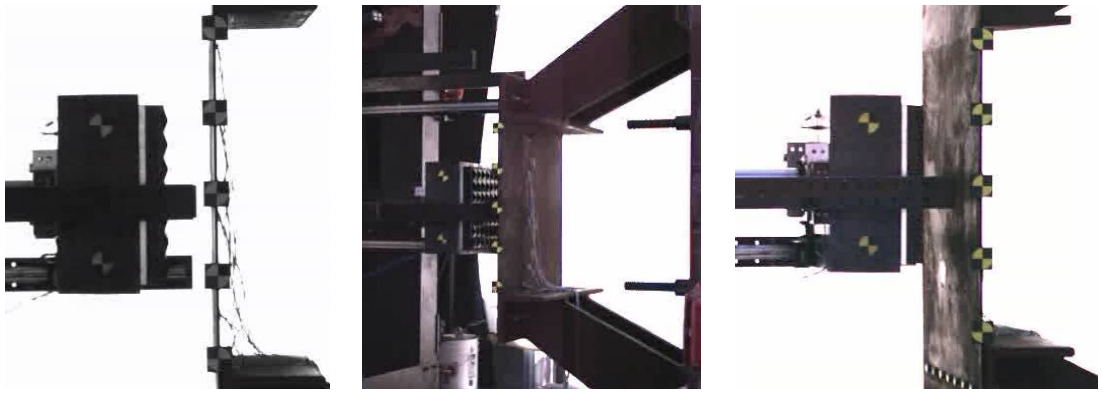

Figure E.24: Phantom Cameras for Test 4 a) Camera One b) Camera Two c) Camera Three

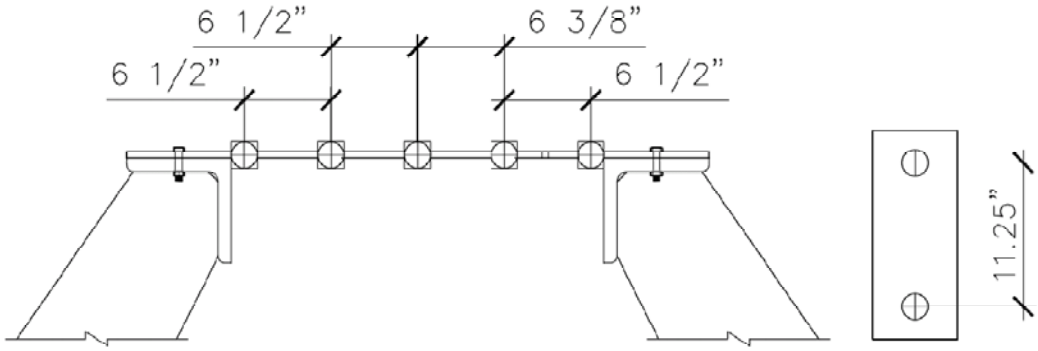

Figure E.25: Target layout on plate and impacting mass for Test 4

E.4.2.3 ACCELERATIONS

For this test there were a total of four accelerometers used. Two of the accelerometers were placed 6" to the north and south of the centroid while the other two accelerometers are placed 4" east and west of the centroid as shown in Figure E.26. The four accelerometers were then averaged together and a filtered was applied as shown in Figure E.27.

This test does not impart an impulsive load as would be expected from a typical blast test. Instead, this test simulates the behavior of a flyer plate moving through the structure after the initial impact at the front plate of the outer cell of the structure. Therefore we are not determining the initial impulsive load from the accelerometers on the BG.

Figure E.26: Accelerometer location for Test 4

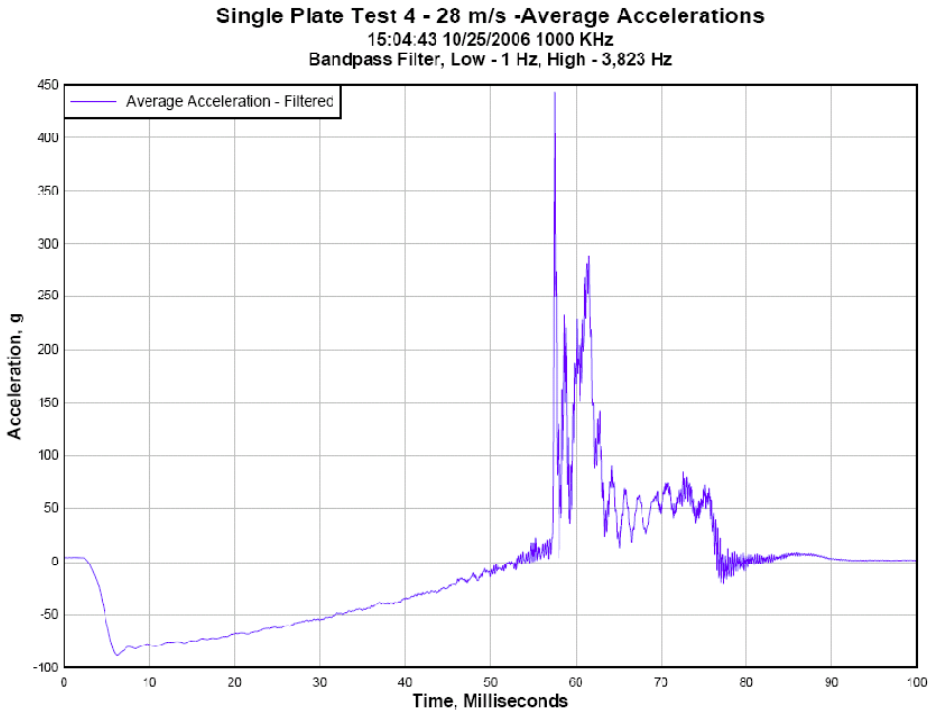

Figure E.27: Filtered accelerometer data for Test 4

E.4.2.4 STRAIN GAGE LOCATIONS

For this test there were five strain gauges labeled 1,2,3,4 and 5. The strain gauges, and their locations, are shown in Figure E.28. Strain gage 5 was damaged during this test and has been discarded. Table E.2 shows the specific information about this test, including the time and velocity at impact, if, and when, the bolts failed along with the maximum and minimum principal strain rates. The largest maximum principal strain rate for this test was 21.46 1/sec and was located at strain gage 1 while the largest minimum strain rate for this test was 15.29 1/sec located at strain gage 1. The maximum principal strains for gauges 1,2,3 and 4 can be found in Figure E.29 and the minimum principal strains for the same gauges can be found in Figure E.30.

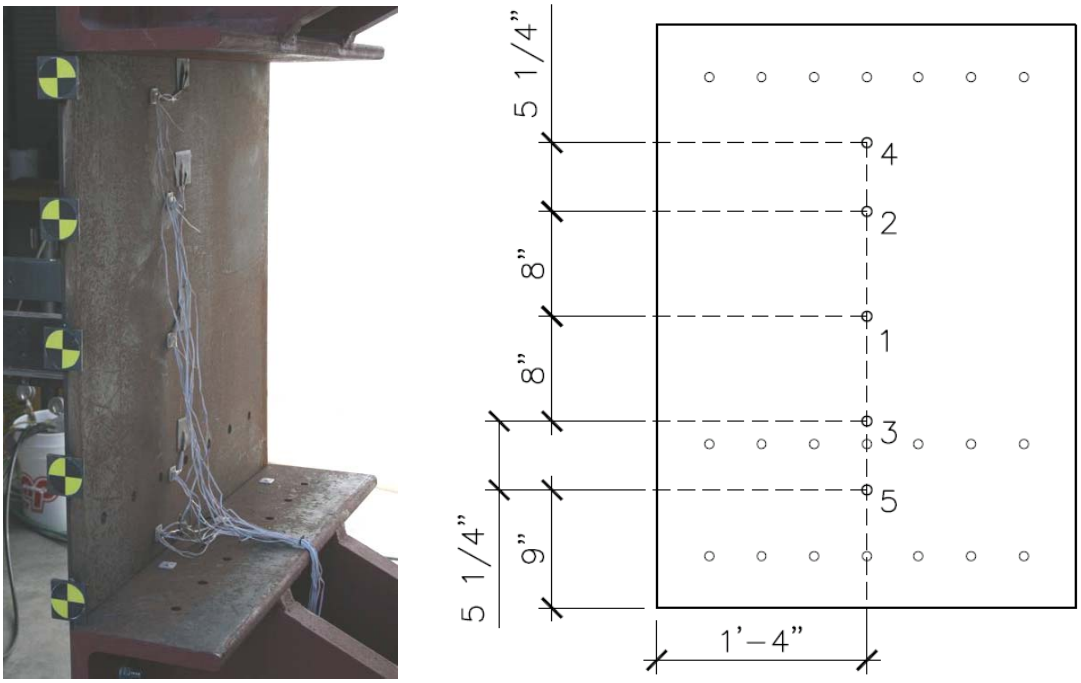

Figure E.28: Strain gage layout for Test 4

Table E.2: Stain rate information for Test 4

Strain Gage Number	Actual Velocity	Initial Impact	Shear Wave at Gage	Bolts Break	Maximum Principal Strain Rate	Minimum Principal Strain Rate
1	28.1 m/s	57.30 msec	-	62.70 msec	-21.46 1/sec	-15.29 1/sec
2	28.1 m/s	57.30 msec	-	62.70 msec	-9.46 1/sec	5.75 1/sec
3	28.1 m/s	57.30 msec	-	62.70 msec	-9.36 1/sec	6.22 1/sec
4	28.1 m/s	57.30 msec	-	62.70 msec	6.46 1/sec	5.49 1/sec

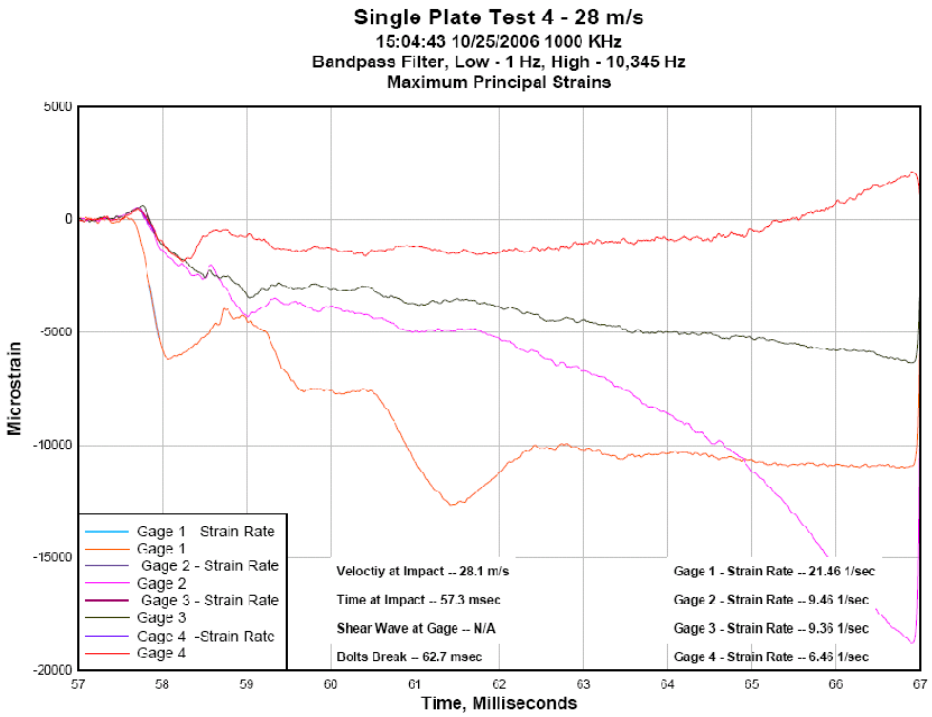

Figure E.29: Maximum principal strains and strain rates for Test 4

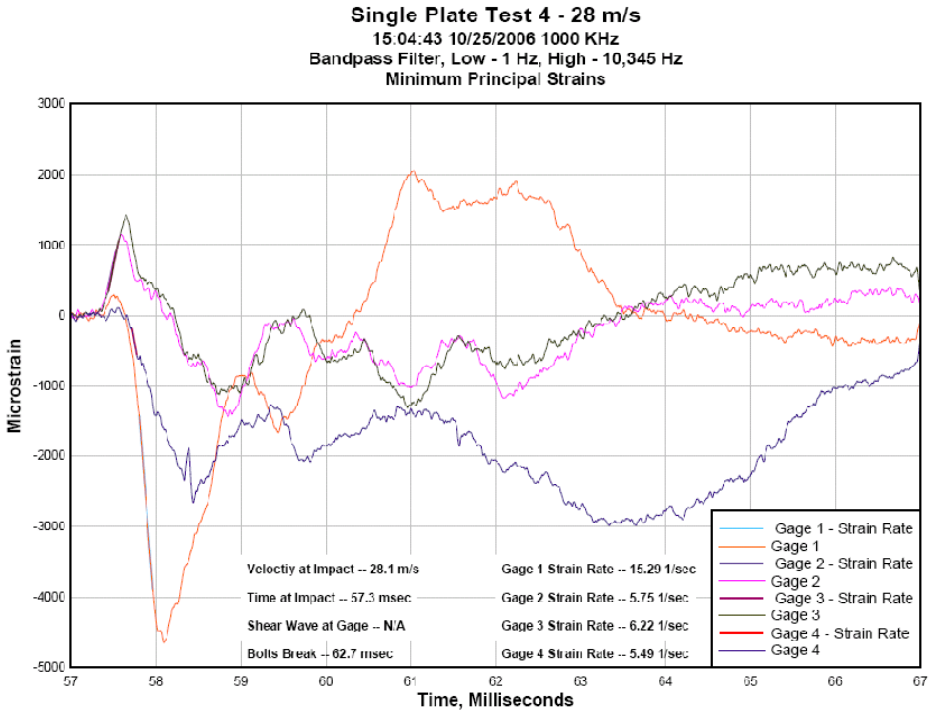

Figure E.30: Minimum principal strains and strain rates for Test 4

E.4.2.5 BOLT TYPE

A total of fourteen Grade 5 bolts (High Strength Bolts) were used for this test.

E.4.3 BLAST GENERATOR DATA

The initial impact of the single BG was 92.19 ft/sec (28.10 m/sec) with a goal velocity of 28 m/s. It had four accelerometers mounted to the back side of the impact plate as discussed in Section E.4.2.3. The average impact velocity for the impacting mass and the steel plate was calculated using the TEMA Track Eye tracking software.

E.4.4 SPECIMEN BEHAVIOR

The loading of the BG plate imparted an initial velocity of 92.19 ft/sec (28.10 m/sec) to the specimen. This caused plate to deform in both directions. The longitudinal deflection (in the north-south direction) behaved in a typical one-way flexural shape. In order to get the velocity as high as needed the test was designed to have the impacting mass break free from the BG and launch itself into the plate. This imparted enough energy into the system that all fourteen Grade 5 bolts failed. The plate and impacting mass continued to travel as one until they hit the back plate. After the test was completed the plate was found on the ground bent into a U-shape. The two ends of the plate folded around the impacting mass during the test. Figure E.31 and Figure E.32 show the test specimen and impacting mass after the test. Figure E.33 shows the progression of damage for this test.

During the test, pieces of bolts flew approximately 6’ directly north of the test set-up and 6 ½’ south of the test set-up. Bolts were also found 7’ away from the test set-up in the lab work area on the south side of the test while another piece was found in the lab on the north side of the test set-up 9 ½’ away. The bolts were discarded after this test since there was no way of discerning how the different bolts fit together. In future tests each bolt will be easily identifiable so that the exact type of failure per bolt at a specific location can be determined.

Figure E.31: Steel plate post test for Test 4

Figure E.32: Steel plate post test for Test 4

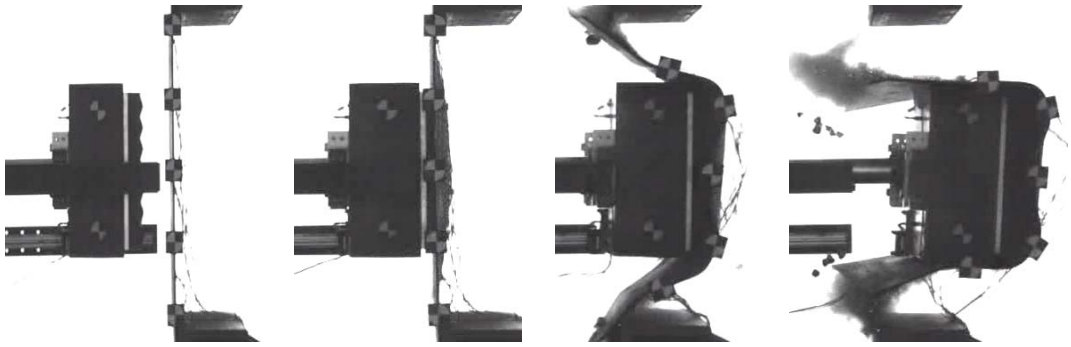

Figure E.33: Progression of damage for Test 4

E.5 STEEL TOWER SINGLE PLATE: TEST 5 (SP5)

E.5.1 INTRODUCTION

The fifth test of the Steel Tower Single Plate test series was performed on October 26th, 2006. The test specimen was a ¼" thick steel plate labeled SP5. The Impacting Mass 1 was attached to the BG with a specimen target velocity of 91.86 ft/sec (28 m/sec). Figure E.34 shows the steel plate prior to impact.

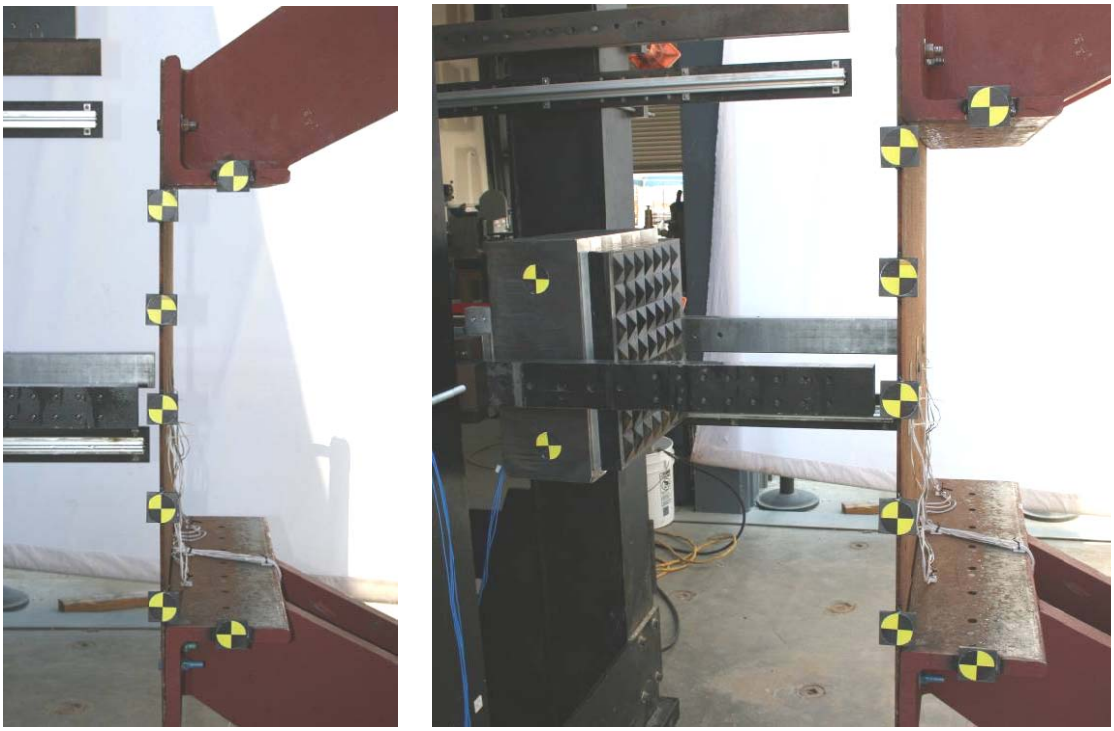

Figure E.34: 1/4" thick steel plate pre test for Test 5

E.5.2 INSTRUMENTATION

E.5.2.1 PHANTOM CAMERAS

The first camera recorded in black and white at a rate of 10,000 frames per second at a resolution of 512x384. This camera was used in order to determine the maximum velocity of the impacting mass and the movement in the plate including the maximum displacement. The second camera recorded in color at a rate of 1,000 frames per second at a resolution of 512x384. This camera captured data on the front side of the plate but was not used to gather any specific data. The third camera recorded in color at a rate of 5,000 frames per second at a resolution of 512x400. This camera recorded the deflection from the back of the plate and was not used to gather any specific data. A picture from each of the camera locations are shown in Figure E.35.

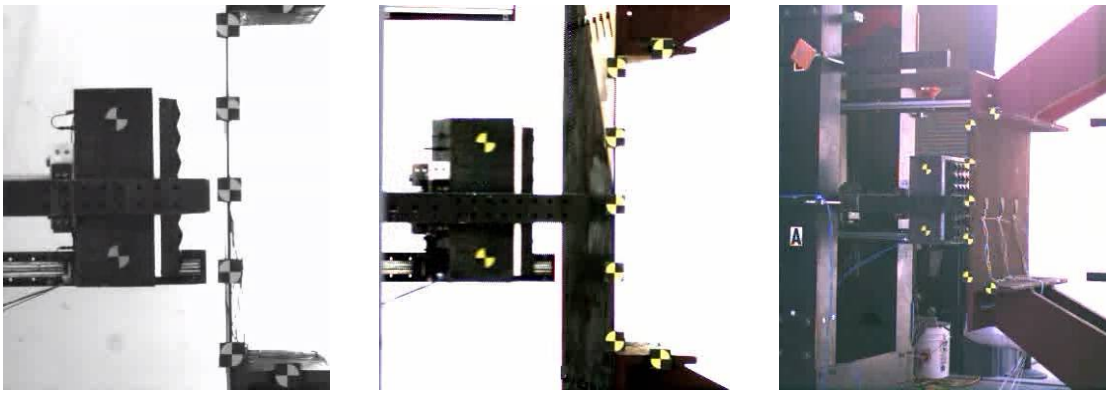

Figure E.35: Phantom Cameras for Test 5 a) Camera One b) Camera Two c) Camera Three

E.5.2.2 TARGET LOCATIONS

Five targets were welded onto the side of the steel plate as show in Figure E.34. They were spaced at the intervals shown in Figure E.36. That figure also shows the location of the targets for the impacting mass. An additional two targets were placed on the angle of the top and the bottom end conditions. The distance between these two points is 74.93 cm (29 ½").

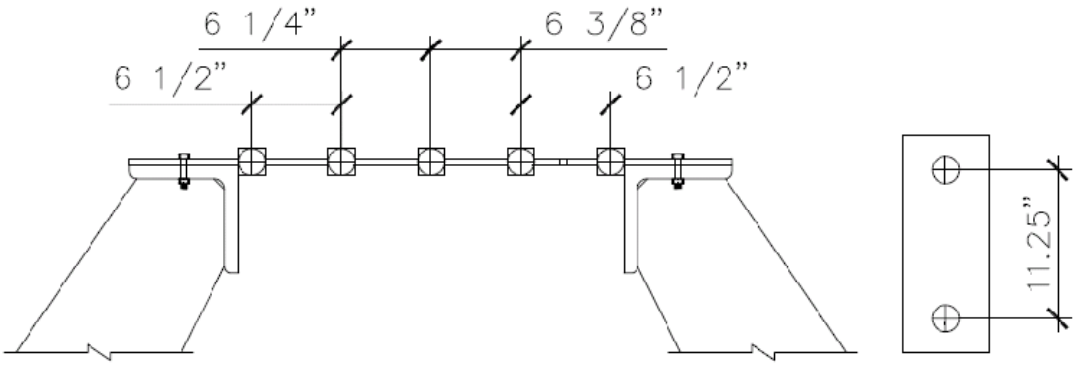

Figure E.36: Target layout on plate and impacting mass for Test 5

E.5.2.3 ACCELERATIONS

For this test there were a total of four accelerometers used. Two of the accelerometers were placed 6" to the north and south of the centroid while the other two accelerometers are placed 4" east and west of the centroid as shown in Figure E.37. The four accelerometers were then averaged together and a filtered was applied as shown in Figure E.38.

This test does not impart an impulsive load as would be expected from a typical blast test. Instead, this test simulates the behavior of a flyer plate moving through the structure after the initial impact at the front plate of the outer cell of the structure. Therefore we are not determining the initial impulsive load from the accelerometers on the BG.

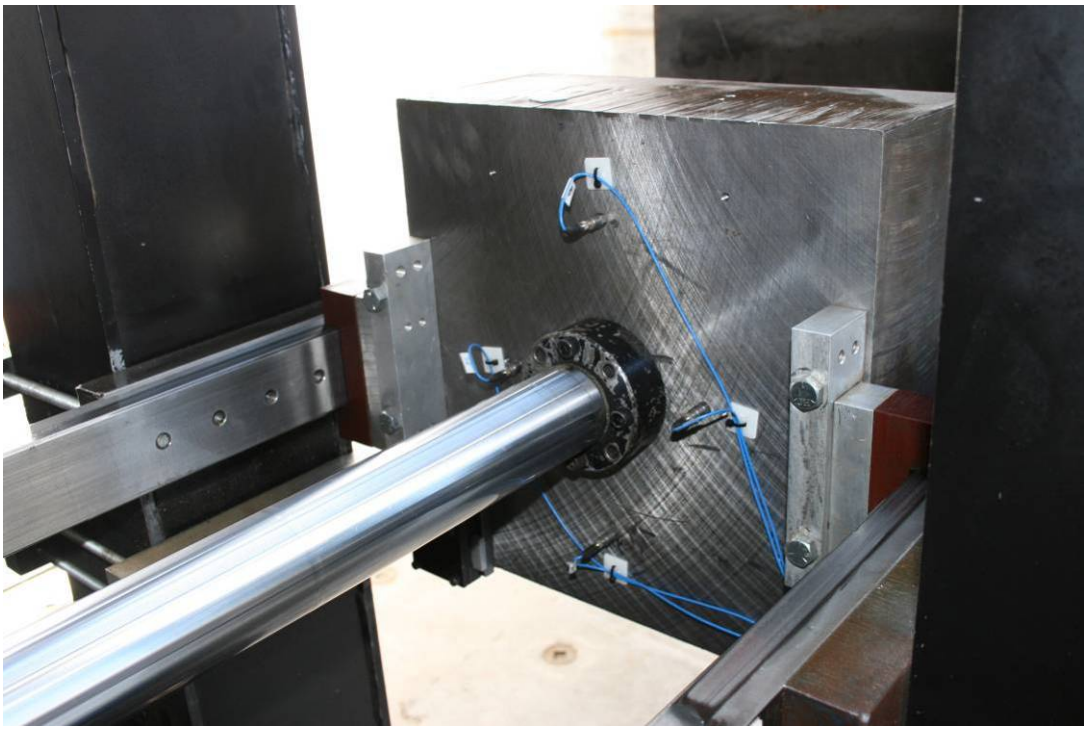

Figure E.37: Accelerometer location for Test 5

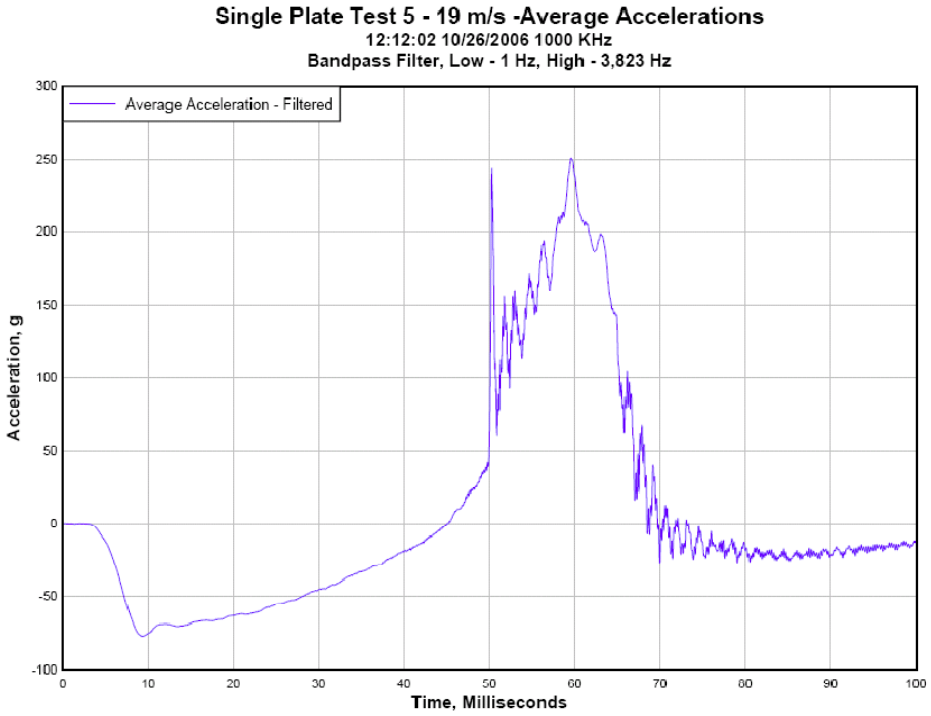

Figure E.38: Filtered accelerometer data for Test 5

E.5.2.4 STRAIN GAGE LOCATIONS

For this test there were three strain gauges labeled 1, 6 and 7. The strain gauges, and their locations, are shown in Figure E.39. Table E.3 shows the specific information about this test, including the time and velocity at impact, if, and when, the bolts failed along with the maximum and minimum principal strain rates. The largest maximum principal strain rate for this test was 8.84 1/sec and was located at strain gage 1 while the largest minimum strain rate for this test was 9.51 1/sec located at strain gage 1. The maximum principal strains for gauges 1,6 and 7 can be found in Figure E.40 and the minimum principal strains for the same gauges can be found in Figure E.41.

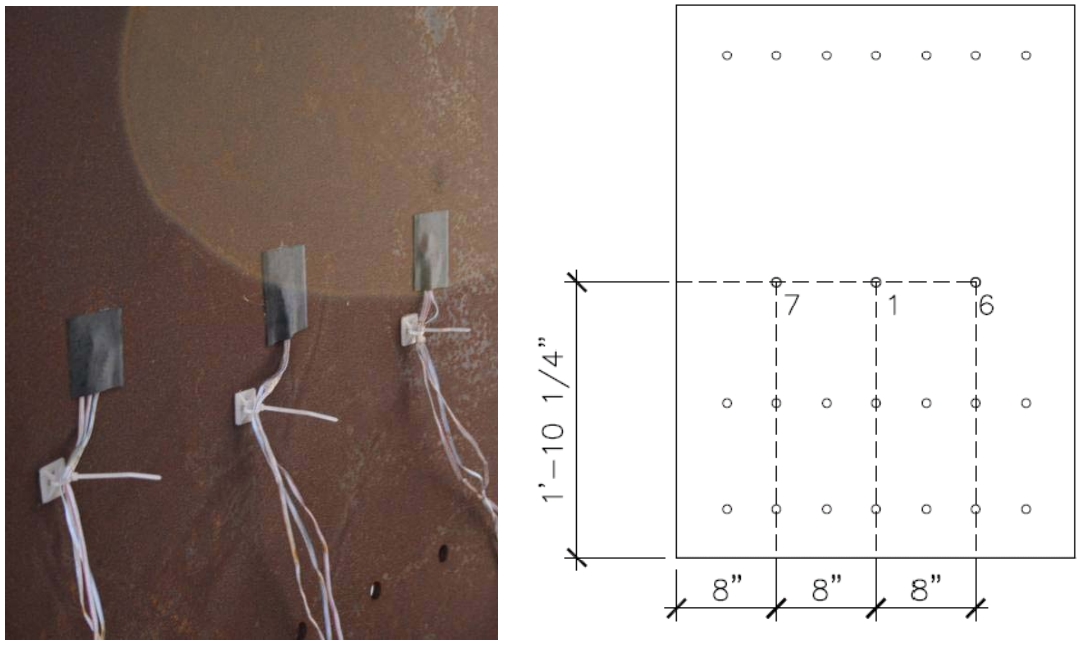

Figure E.39: Strain gage layout for Test 5

Table E.3: Stain rate information for Test 5

Strain Gage Number	Actual Velocity	Initial Impact	Shear Wave at Gage	Bolts Break	Maximum Principal Strain Rate	Minimum Principal Strain Rate
1	18.07 m/s	50.30 msec	-	-	-8.84 1/sec	-9.51 1/sec
6	18.07 m/s	50.30 msec	-	-	-7.90 1/sec	-4.62 1/sec
7	18.07 m/s	50.30 msec	-	-	-5.66 1/sec	-9.44 1/sec

E.5.2.5 BOLT TYPE

A total of fourteen Grade 5 bolts (High Strength Bolts) were used for this test.

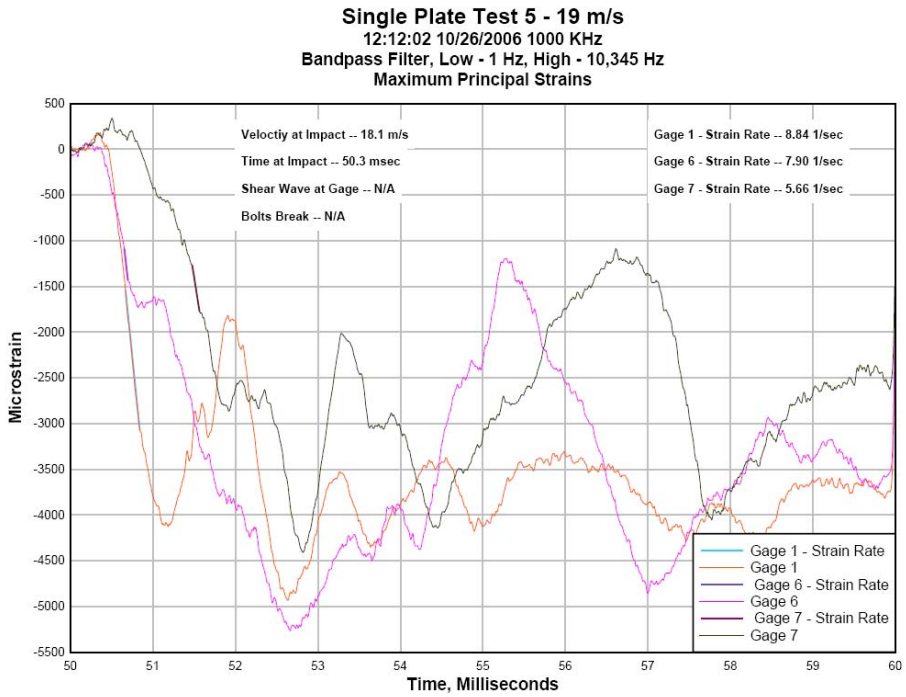

Figure E.40: Maximum principal strains and strain rates for Test 5

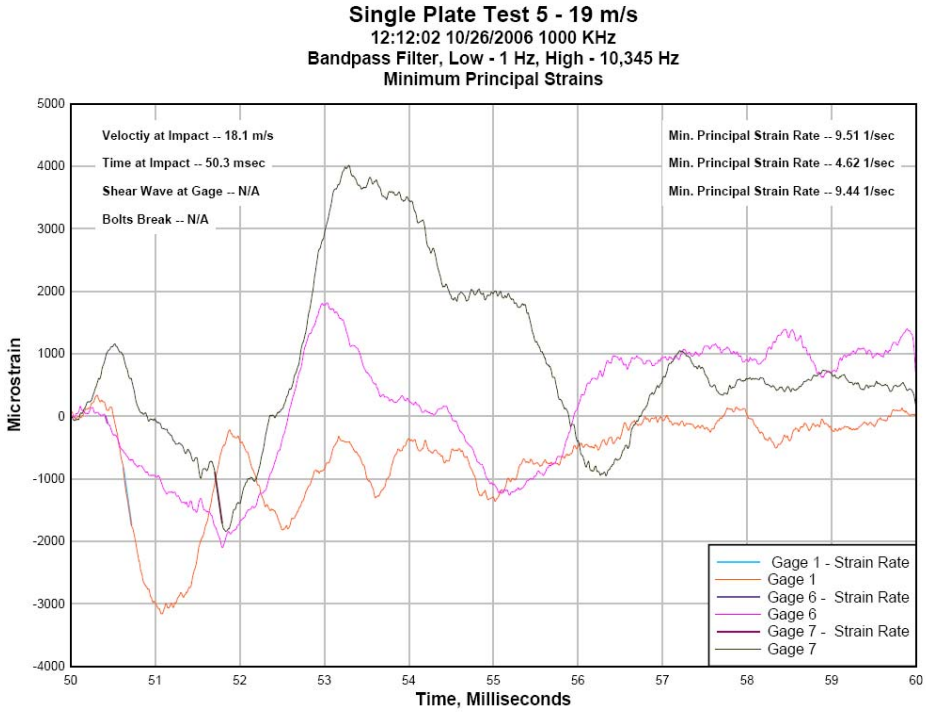

Figure E.41: Minimum principal strains and strain rates for Test 5

E.5.3 BLAST GENERATOR DATA

The initial impact of the single BG was 59.28 ft/sec (18.07 m/sec) with a goal velocity of 19 m/s. It had four accelerometers mounted to the back side of the impact plate as discussed in Section E.5.2.3. The average impact velocity for the impacting mass and the steel plate was calculated using the TEMA Track Eye tracking software.

E.5.4 SPECIMEN BEHAVIOR

The loading of the BG plate imparted an initial velocity of 59.28 ft/sec (18.07 m/sec) to the specimen. This caused the plate to deform in both directions. The longitudinal deflection (in the north-south direction) behaved in a typical one-way flexural shape. The specimen had an approximate maximum midspan deflection of 4 ½" during the test and a permanent deflection of 1 3/8". After the test was completed the plate was still connected to the end conditional with a slight bow in the center as shown in Figure E.42. Figure E.43 shows the progression of damage for this test from Camera 1. Figure E.44 shows the progression of damage for this test from Camera 2.

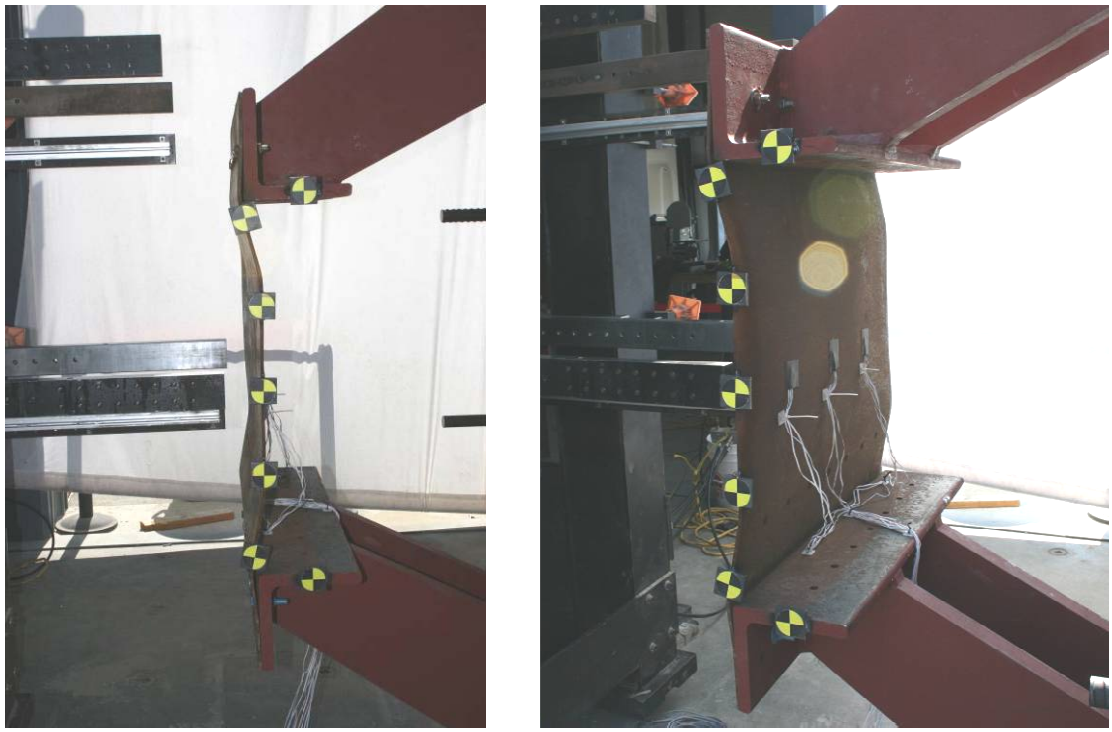

Figure E.42: Steel plate post test for Test 5

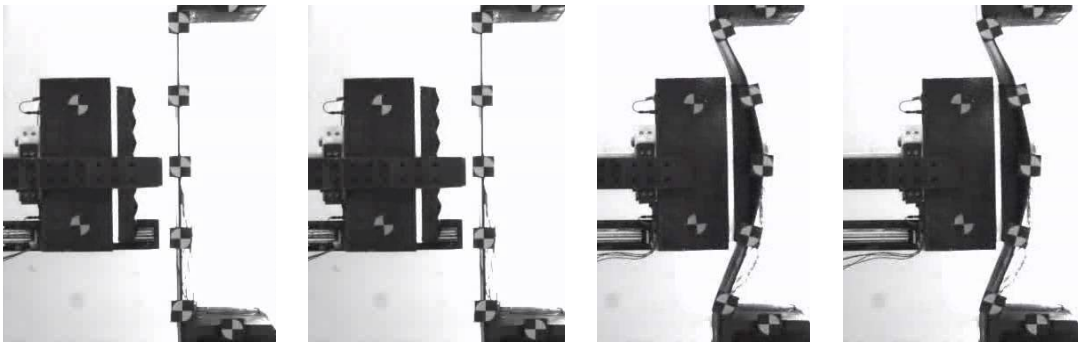

Figure E.43: Progression of damage for Test 5 from Camera 1

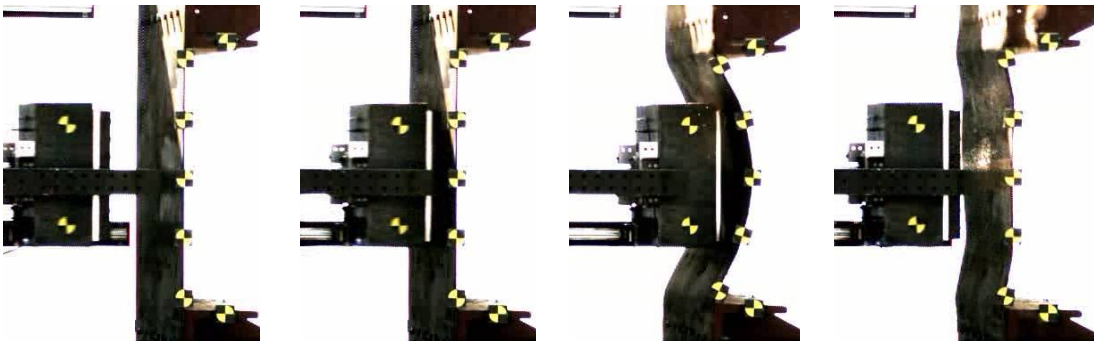

Figure E.44: Progression of damage for Test 5 from Camera 2

E.6 STEEL TOWER SINGLE PLATE: TEST 6 (SP6)

E.6.1 INTRODUCTION

The sixth test of the Steel Tower Single Plate test series was performed on October 27th, 2006. The test specimen was a ½" thick steel plate labeled SP6. The Impacting Mass 3 was attached to the BG with a specimen target velocity of 104.99 ft/sec (32 m/sec). Figure E.45 shows the steel plate prior to impact.

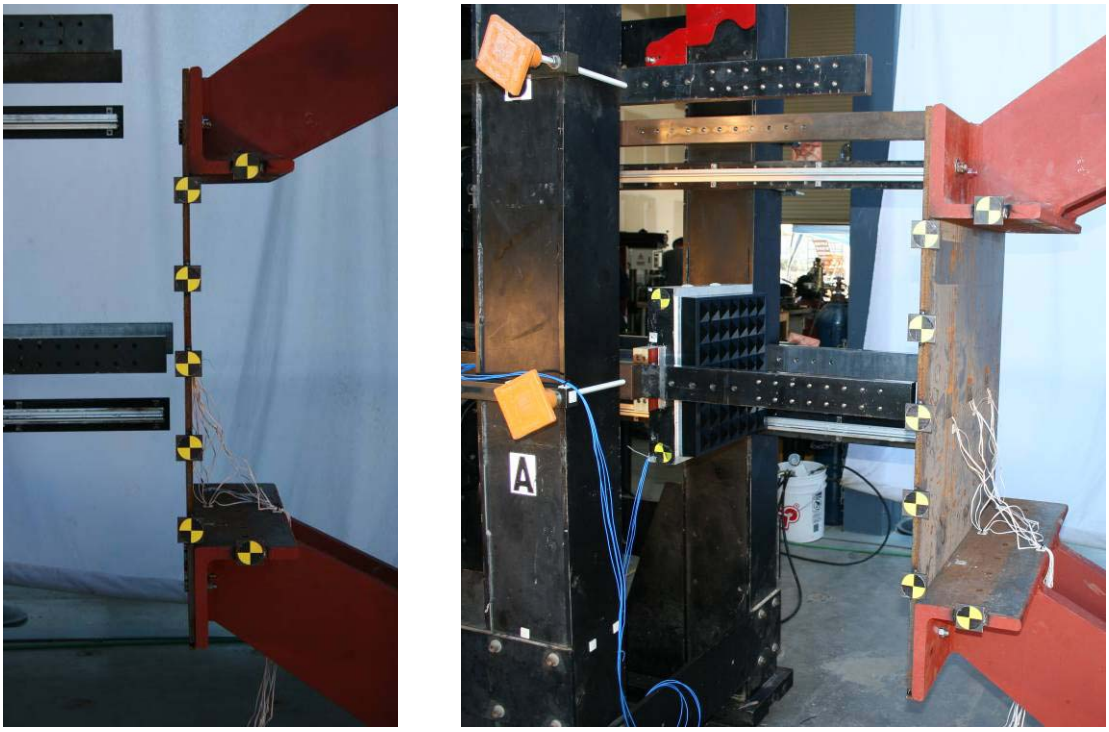

Figure E.45: 1/2" thick steel plate pre test for Test 6

E.6.2 INSTRUMENTATION

E.6.2.1 PHANTOM CAMERAS

There was a problem with this test and the Phantom Camera's did not capture any data.

E.6.2.2 TARGET LOCATIONS

Five targets were welded onto the side of the steel plate as show in Figure E.45. They were spaced at the intervals shown in Figure E.46. That figure also shows the location of the targets for the impacting mass. An additional two targets were placed on the angle of the top and the bottom end conditions. The distance between these two points is 74.93 cm (29 ½").

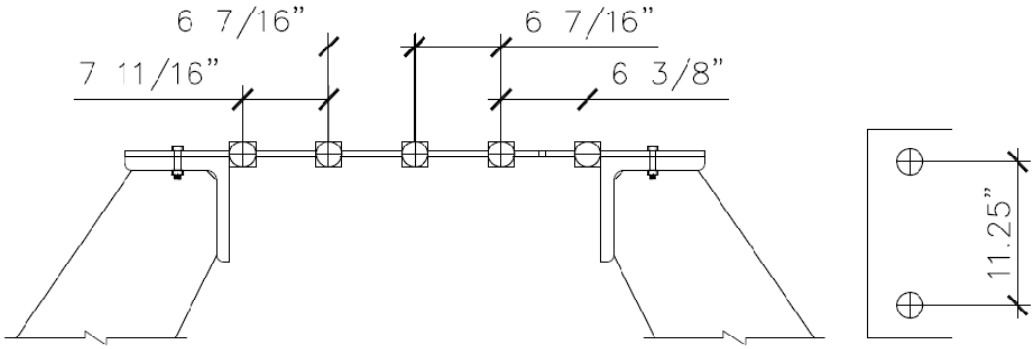

Figure E.46: Target layout on plate and impacting mass for Test 6

E.6.2.3 ACCELERATIONS

For this test there were a total of four accelerometers used. Two of the accelerometers were placed 6" to the north and south of the centroid while the other two accelerometers are placed 4" east and west of the centroid as shown in Figure E.47. The four accelerometers were then averaged together and a filtered was applied as shown in Figure E.48.

This test does not impart an impulsive load as would be expected from a typical blast test. Instead, this test simulates the behavior of a flyer plate moving through the structure after the initial impact at the front plate of the outer cell of the structure. Therefore we are not determining the initial impulsive load from the accelerometers on the BG.

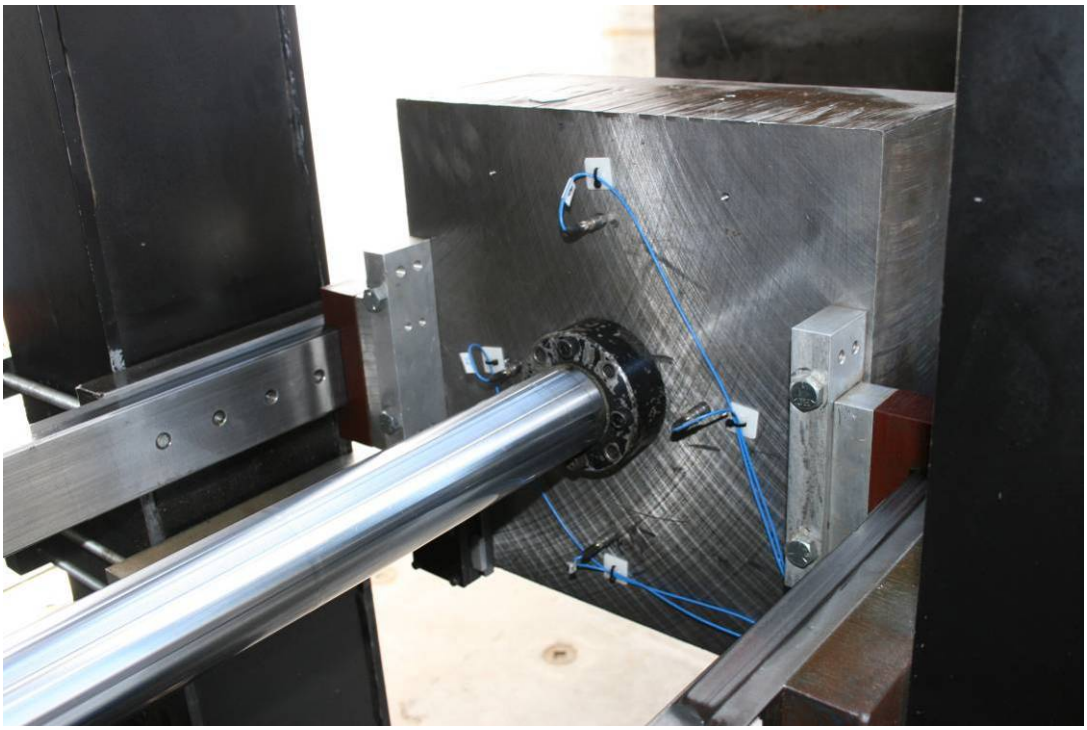

Figure E.47: Accelerometer location for Test 6

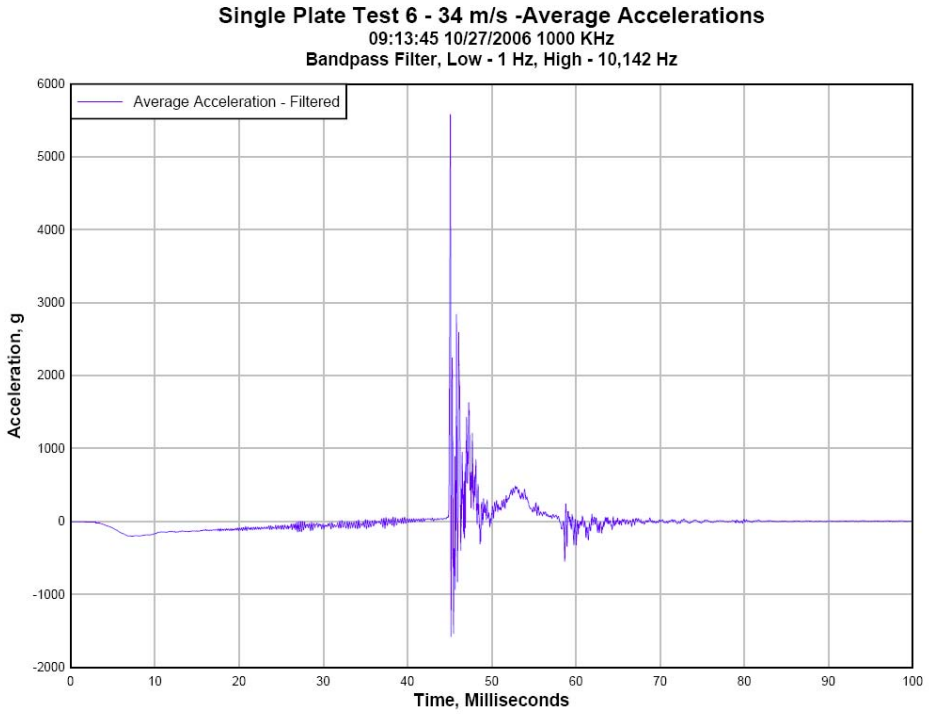

Figure E.48: Filtered accelerometer data for Test 6

E.6.2.4 STRAIN GAGE LOCATIONS

For this test there were three strain gauges labeled 1,6 and 7. The strain gauges, and their locations, are shown in Figure E.49. Table E.4 shows the specific information about this test, including the time and velocity at impact, if, and when, the bolts failed along with the maximum and minimum principal strain rates. The largest maximum principal strain rate for this test was 28.96 1/sec and was located at strain gage 1 while the largest minimum strain rate for this test was 29.02 1/sec located at strain gage 1. The maximum principal strains for gauges 1,6 and 7 can be in Figure E.50and the minimum principal strains for the same gauges can be found in Figure E.51.

Table E.4: Stain rate information for Test 6

Strain Gage Number	Actual Velocity	Initial Impact	Shear Wave at Gage	Bolts Break	Maximum Principal Strain Rate	Minimum Principal Strain Rate
1	-	-	-	-	-28.96 1/sec	-29.02 1/sec
6	-	-	-	-	-14.06 1/sec	-10.50 1/sec
7	-	-	-	-	-5.93 1/sec	-9.99 1/sec

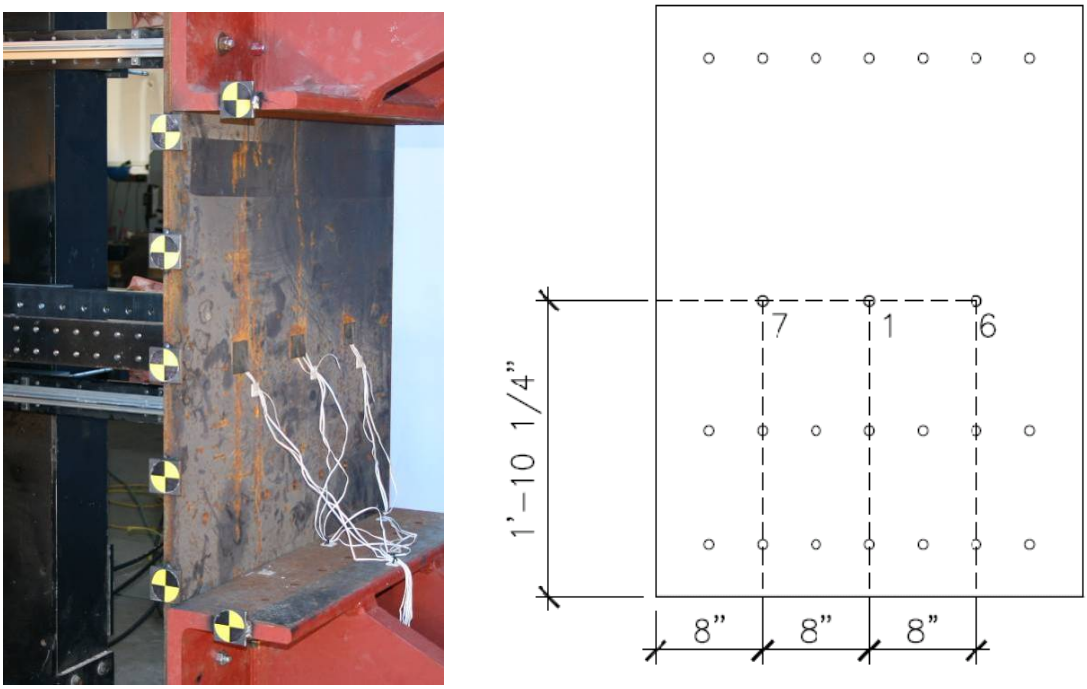

Figure E.49: Strain gage layout for Test 6

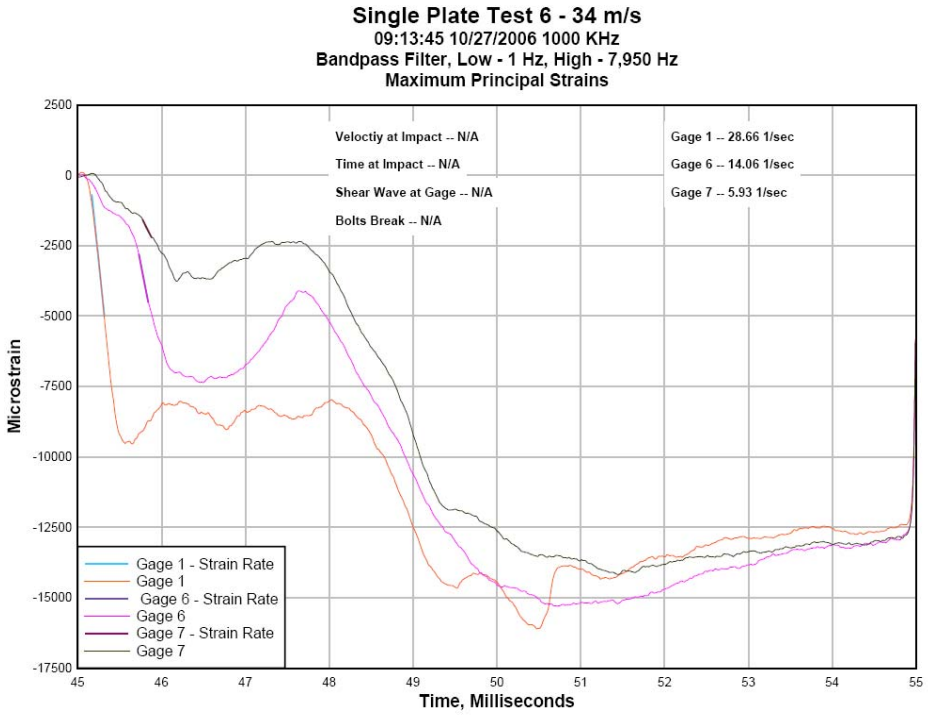

Figure E.50: Maximum principal strains and strain rates for Test 6

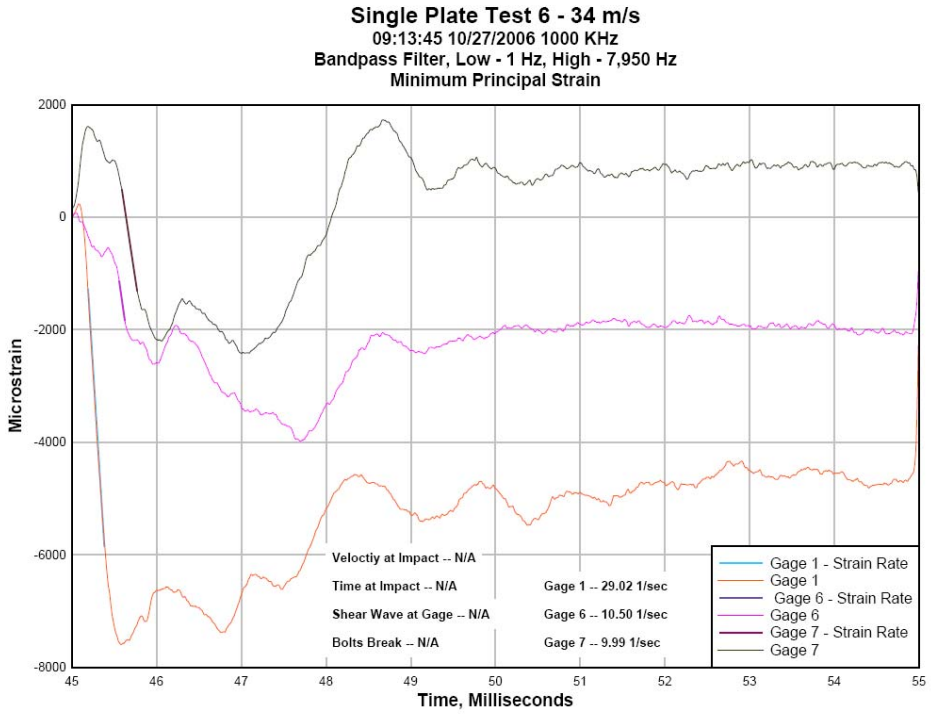

Figure E.51: Minimum principal strains and strain rates for Test 6

E.6.2.5 BOLT TYPE

A total of fourteen Grade 5 bolts (High Strength Bolts) were used for this test.

E.6.3 BLAST GENERATOR DATA

The initial impact of the single BG is unknown due to the failure of the video cameras.

E.6.4 SPECIMEN BEHAVIOR

The loading of the BG plate caused the plate to deform in both directions. The longitudinal deflection (in the north-south direction) behaved in a typical one-way flexural shape. The specimen had a permanent deflection of 2 3/8**”**.

E.7 STEEL TOWER SINGLE PLATE: TEST 7 (SP7)

E.7.1 INTRODUCTION

The seventh test of the Steel Tower Single Plate test series was performed on October 27th, 2006. The test specimen was a ½" thick steel plate labeled SP7. The Impacting Mass 3 was attached to the BG with a specimen target velocity of 104.98 ft/sec (32 m/sec). Figure E.52 shows the steel plate prior to impact.

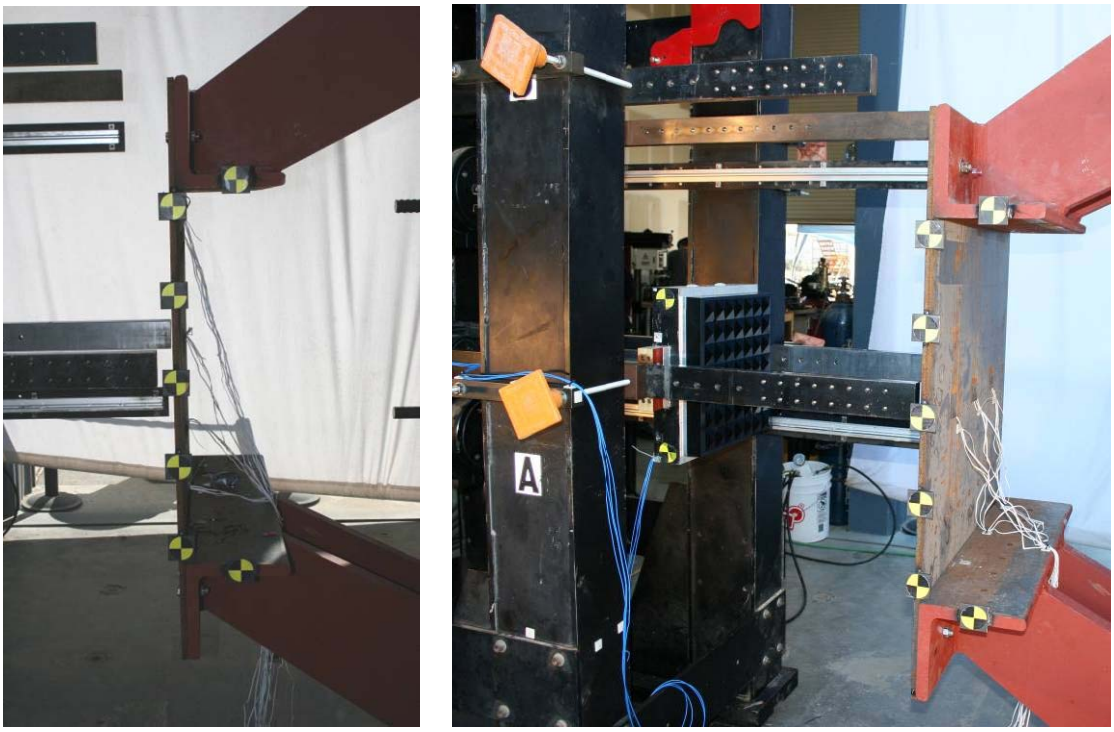

Figure E.52: 1/2" thick steel plate pre test for Test 7

E.7.2 INSTRUMENTATION

E.7.2.1 PHANTOM CAMERAS

The first camera recorded in black and white at a rate of 10,000 frames per second at a resolution of 512x384. This camera was used to determine the maximum velocity of the impacting mass and the movement of the plate including the maximum displacement. The second camera recorded in color at a rate of 5,000 frames per second at a resolution of 512x384. This camera captured data on the back side of the plate but was not used to gather any specific data. The third camera recorded in color at a rate of 10,000 frames per second at a resolution of 512x400. This camera recorded the data from the front side of the plate at an angle. A picture from each of the camera locations are shown in Figure E.53.

E.7.2.2 TARGET LOCATIONS

Five targets were welded onto the side of the steel plate as show in Figure E.52. They were spaced at the intervals shown in Figure E.54. That figure also shows the location of the targets for the impacting mass. An additional two targets were placed on the angle of the top and the bottom end conditions. The distance between these two points is 74.93 cm (29 ½").

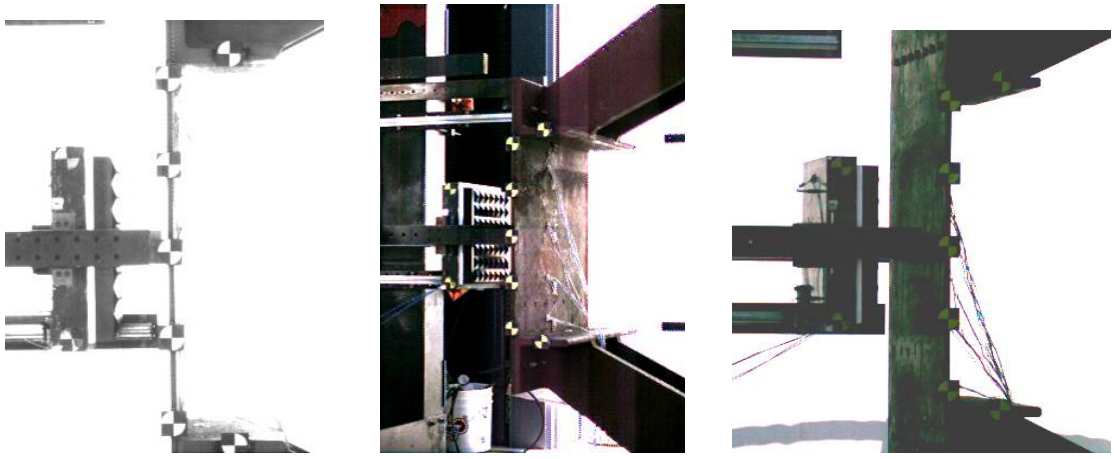

Figure E.53: Phantom Cameras for Test 7 a) Camera One b) Camera Two c) Camera Three

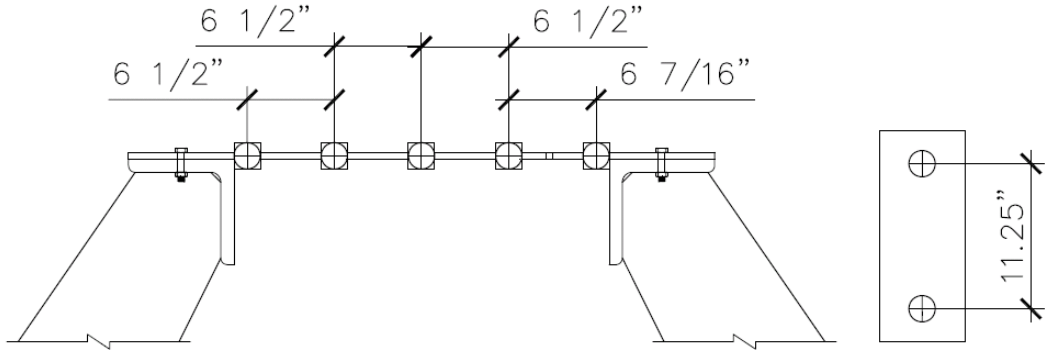

Figure E.54: Target layout on plate and impacting mass for Test 7

E.7.2.3 ACCELERATIONS

For this test there were a total of four accelerometers used. Two of the accelerometers were placed 6" to the north and south of the centroid while the other two accelerometers are placed 4" east and west of the centroid as shown in Figure E.55. The four accelerometers were then averaged together and a filtered was applied as shown in Figure E.56.

This test does not impart an impulsive load as would be expected from a typical blast test. Instead, this test simulates the behavior of a flyer plate moving through the structure after the initial impact at the front plate of the outer cell of the structure. Therefore we are not determining the initial impulsive load from the accelerometers on the BG.

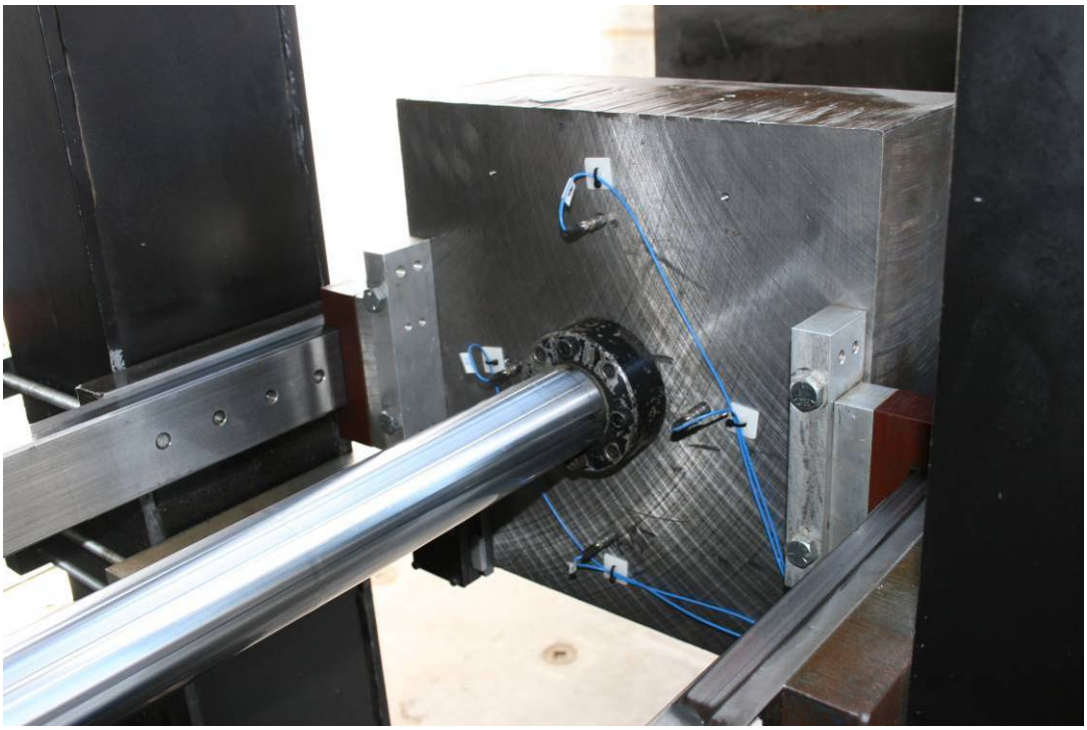

Figure E.55: Accelerometer location for Test 7

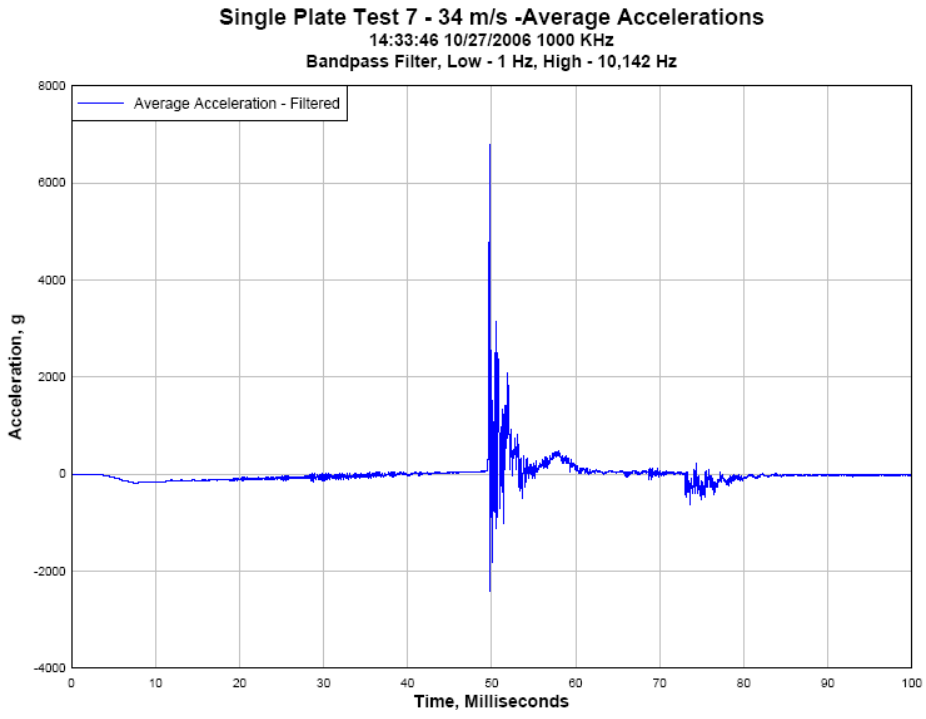

Figure E.56: Filtered accelerometer data for Test 7

E.7.2.4 STRAIN GAGE LOCATIONS

For this test there were five strain gauges labeled 1,2,3,4 and 5. The strain gauges, and their locations, are shown in Figure E.57. Table E.5 shows the specific information about this test, including the time and velocity at impact, if, and when, the bolts failed along with the maximum and minimum principal strain rates. The largest maximum principal strain rate for this test was 30.71 1/sec and was located at strain gage 1 while the largest minimum strain rate for this test was 20.91 1/sec located at strain gage 1. The maximum principal strains for gauges 1,2,3,4 and 5 can be in Figure E.58 and the minimum principal strains for the same gauges can be found in
Figure E.59.

Table E.5: Stain rate information for Test 7

Strain Gage Number	Actual Velocity	Initial Impact	Shear Wave at Gage	Bolts Break	Maximum Principal Strain Rate	Minimum Principal Strain Rate
1	30.17 m/s	49.50 msec	-	-	-30.71 1/sec	-20.91 1/sec
2	30.17 m/s	49.50 msec	-	-	-7.67 1/sec	-10.87 1/sec
3	30.17 m/s	49.50 msec	-	-	-8.77 1/sec	6.86 1/sec
4	30.17 m/s	49.50 msec	-	-	-11.23 1/sec	-9.73 1/sec
5	30.17 m/s	49.50 msec	-	-	-11.54 1/sec	-4.38 1/sec

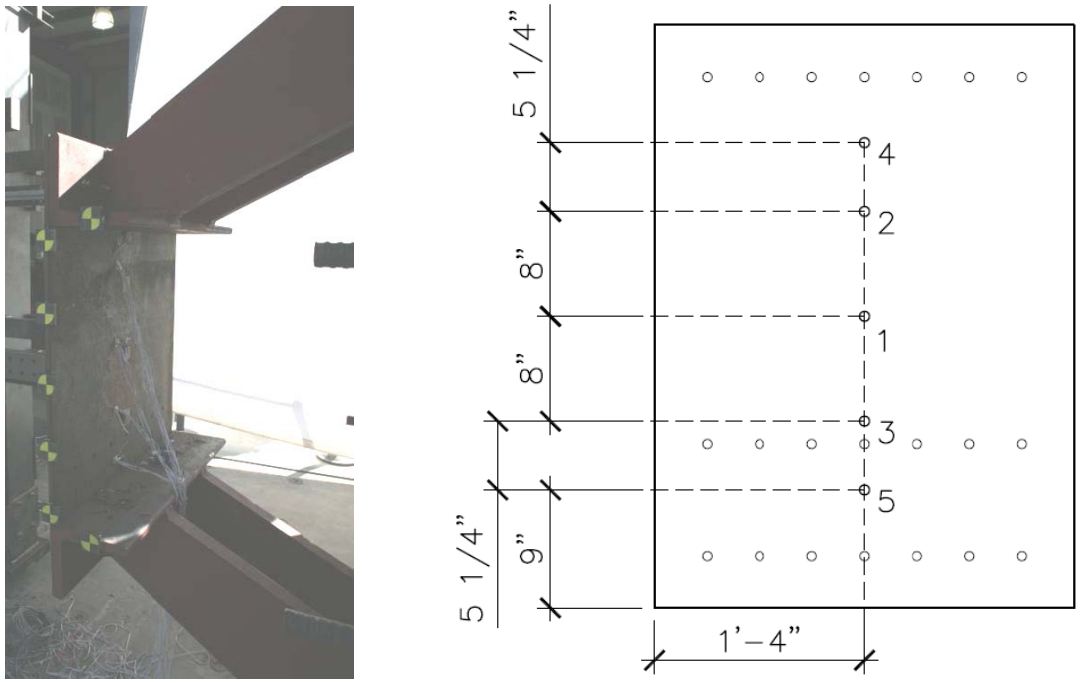

Figure E.57: Strain gage layout for Test 7

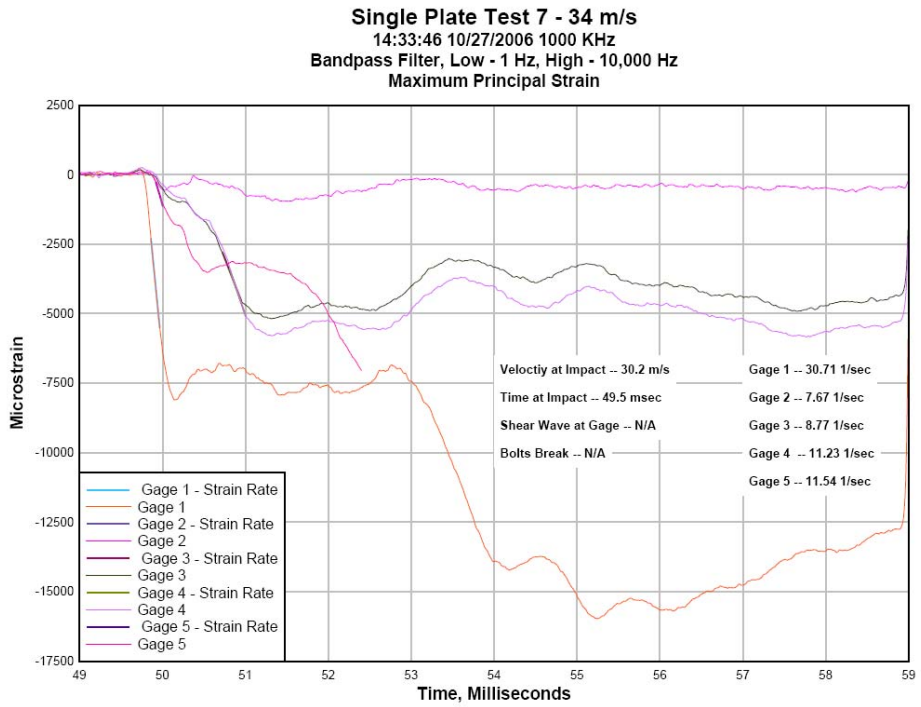

Figure E.58: Maximum principal strains and strain rates for Test 7

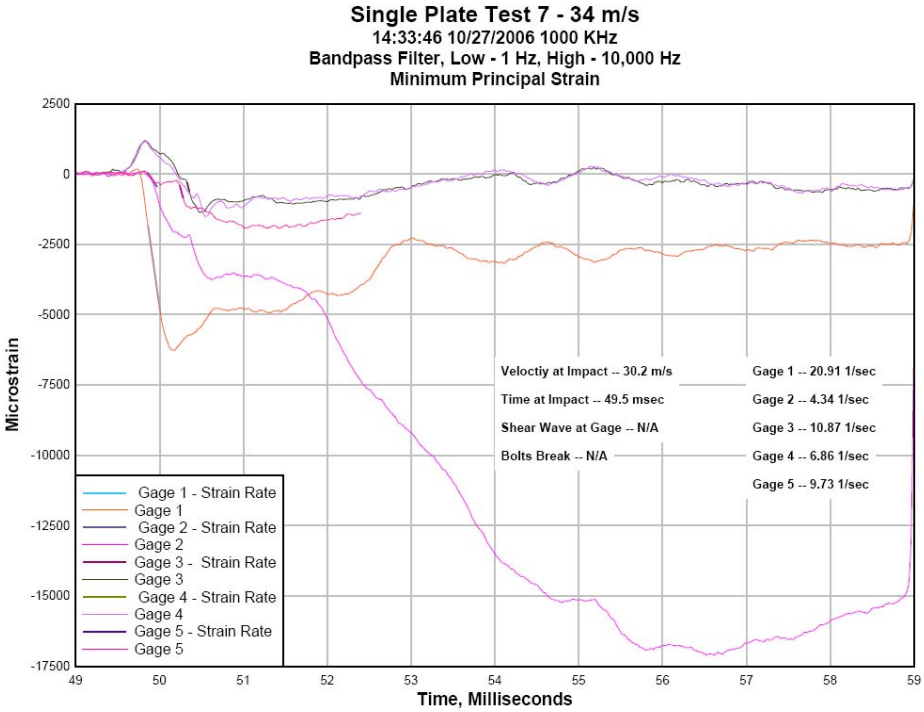

Figure E.59: Minimum principal strains and strain rates for Test 7

E.7.2.5 BOLT TYPE

A total of fourteen Grade 5 bolts (High Strength Bolts) were used for this test.

E.7.3 BLAST GENERATOR DATA

The initial impact of the single BG was 98.98 ft/sec (30.17 m/sec) with a goal velocity of 104.97 ft/sec (32 m/s). It had four accelerometers mounted to the back side of the impact plate as discussed in Section E.6.2.3. The average impact for the impacting mass and the steel plate was calculated using the TEMA Track Eye tracking software.

E.7.4 SPECIMEN BEHAVIOR

The loading of the BG plate caused the plate to deform in both directions. The longitudinal deflection (in the north-south direction) behaved in a typical one-way flexural shape. The specimen had an approximate maximum deflection of 4" during the test and a permanent deflection of 2 ½". After the test was completed the plate was still connected to the end conditions with a slight bow as shown in Figure E.60. Figure E.61 shows the progression of damage for this test from Phantom Camera One. Figure E.62 shows the progression of damage for this test from Phantom Camera Two. Figure E.63 shows the progression of damage for this test from Phantom Camera Three.

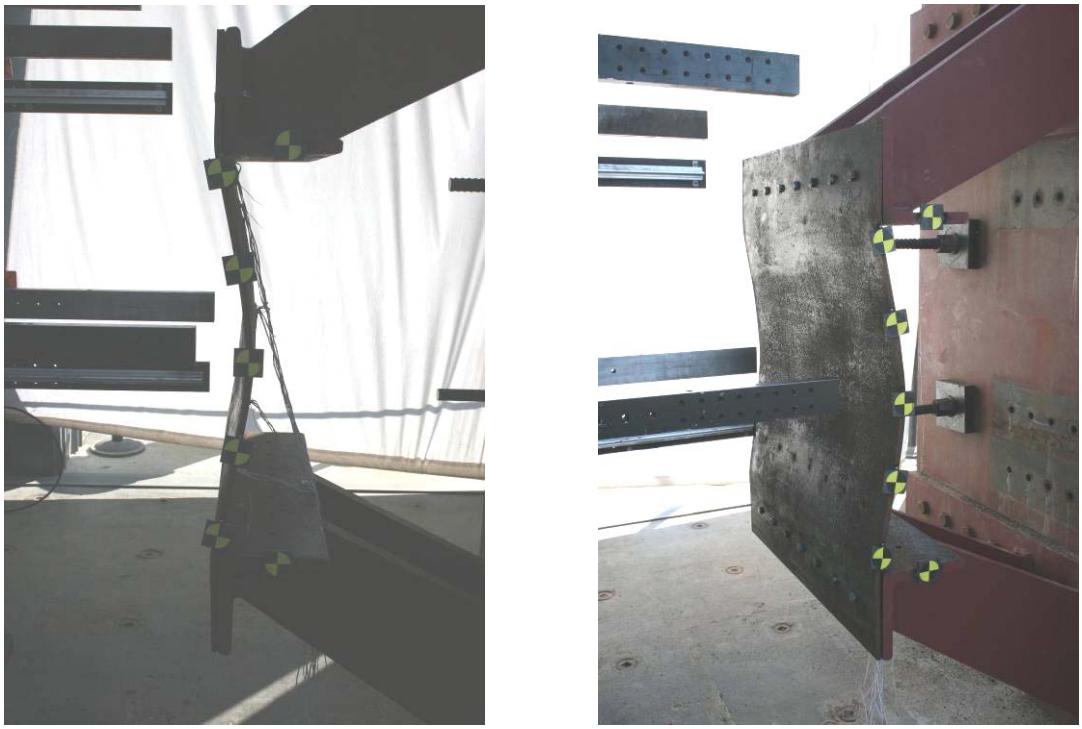

Figure E.60: Steel Plate post test for Test 7

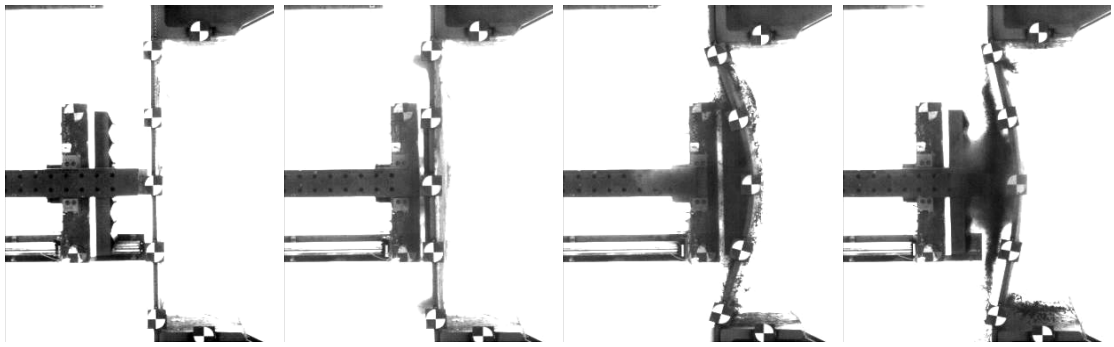

Figure E.61: Progression of damage for Test 7 from Camera 1

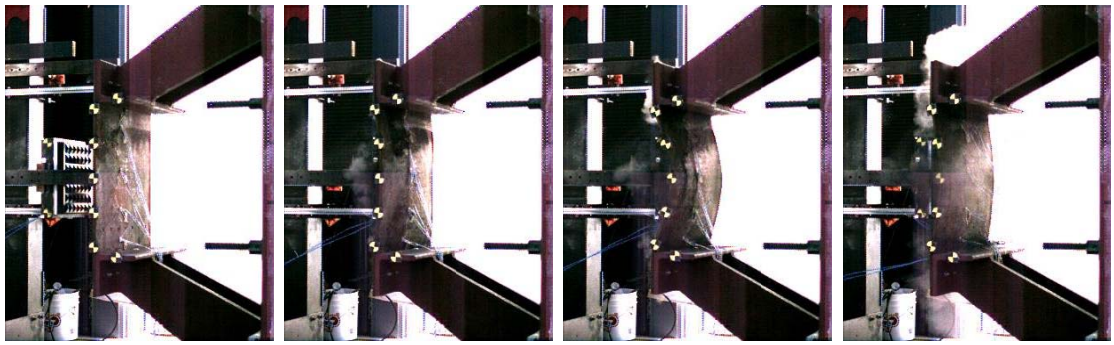

Figure E.62: Progression of damage for Test 7 from Camera 2

Figure E.63: Progression of damage for Test 7 from Camera 3

E.8 STEEL TOWER SINGLE PLATE: TEST 8 (SP8)

E.8.1 INTRODUCTION

The eighth test of the Steel Tower Single Plate test series was performed on November 7th, 2006. The test specimen was a ½" thick steel plate labeled SP8. The Impacting Mass 1 was attached to the BG with a specimen target velocity of 91.86 ft/sec (28 m/sec). Figure E.64 shows the steel plate prior to impact.

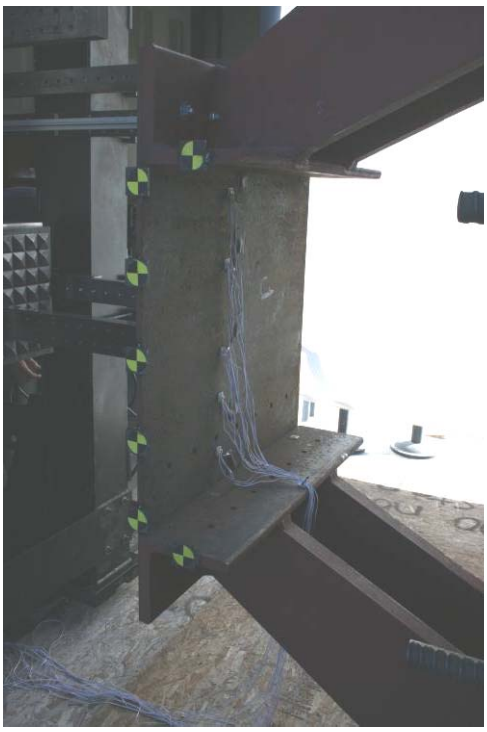

Figure E.64: 1/2" thick steel plate pre test for Test 8

E.8.2 INSTRUMENTATION

E.8.2.1 PHANTOM CAMERAS

The first camera recorded in black and white at a rate of 10,000 frames per second at a resolution of 512x384. This camera was used in order to determine the maximum velocity of the impacting mass and the movement in the plate including the maximum displacement. The second camera recorded in color at a rate of 5,000 frames per second at a resolution of 512x384. This camera recorded the overall deformation of the plate and was not used to gather any specific data. The third camera recorded in color at a rate of 5,000 frames per second at a resolution of 512x400. This camera captured data on the front side of the plate to capture the bolt failures. A picture from each of the camera locations are shown in Figure E.65.

Figure E.65: Phantom Cameras for Test 8 a) Camera One b) Camera Two c) Camera Three

E.8.2.2 TARGET LOCATIONS

Five targets were welded onto the side of the steel plate as show in Figure E.64. They were spaced at the intervals shown in Figure E.66. That figure also shows the location of the targets for the impacting mass. An additional two targets were placed on the angle at the top and the bottom end conditions. The distance between these two points is 74.93 cm (29 ½")

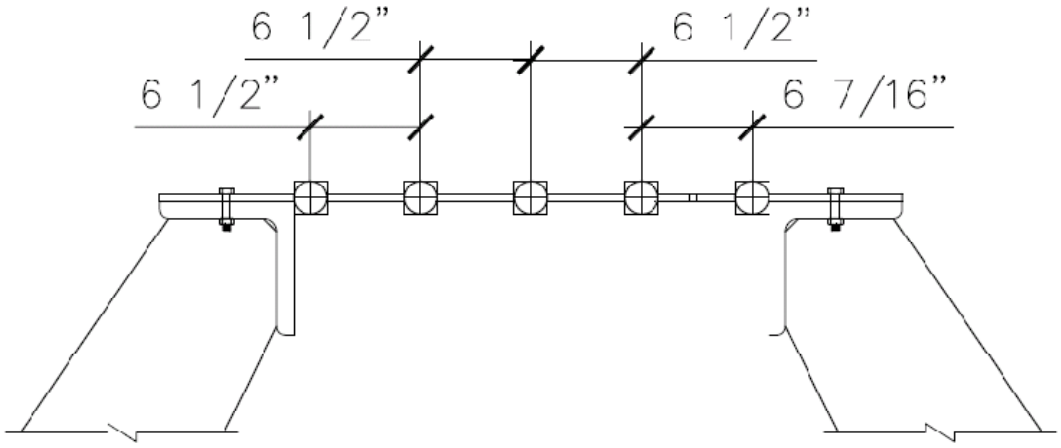

Figure E.66: Target layout on plate and impacting mass for Test 8

E.8.2.3 ACCELERATIONS

For this test one accelerometer was used. This accelerometer was placed 6" south of the centroid of the impacting mass as shown in Figure E.67. The data from this gage was then filtered as shown in Figure E.68.

This test does not impart an impulsive load as would be expected from a typical blast test. Instead, this test simulates the behavior of a flyer plate moving through the structure after the initial impact at the front plate of the outer cell of the structure. Therefore we are not determining the initial impulsive load from the accelerometers on the BG.

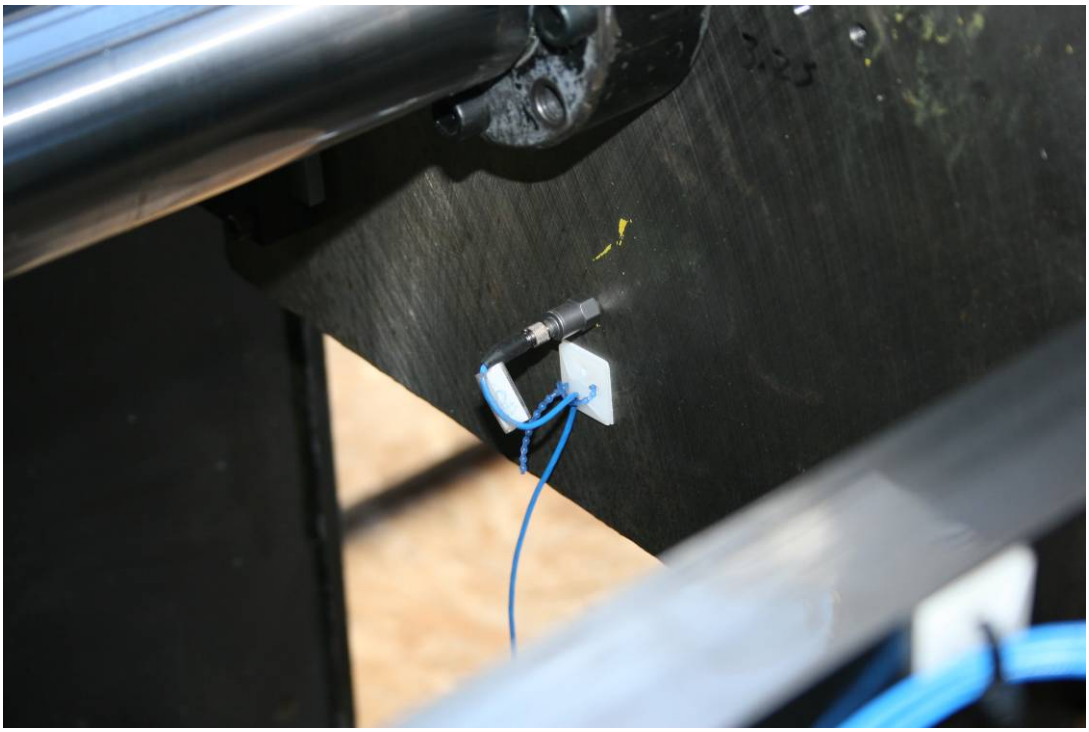

Figure E.67: Accelerometer location for Test 8

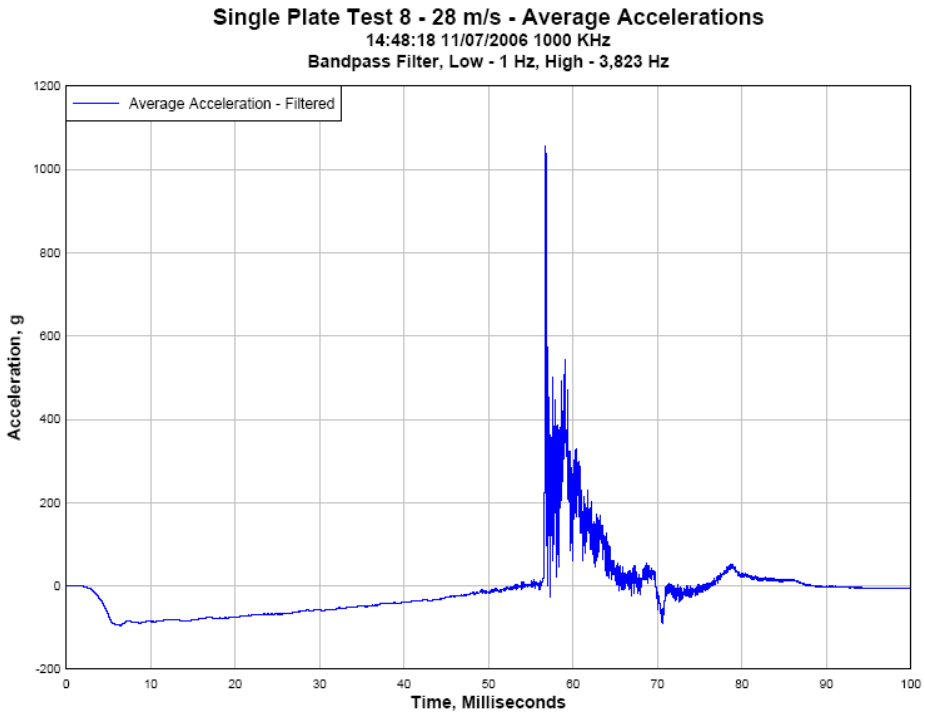

Figure E.68: Filtered accelerometer data for Test 8

E.8.2.4 STRAIN GAGE LOCATIONS

For this test there were five strain gauges labeled 1,2,3,4 and 5. The strain gauges, and their locations, are shown in Figure E.69. Strain gage 1 was damaged during this test and has been discarded. Table E.6 shows the specific information about this test, including the time and velocity at impact, if, and when, the bolts failed along with the maximum and minimum principal strain rates. The largest maximum principal strain rate for this test was 12.47 1/sec and was located at strain gage 2 while the largest minimum strain rate for this test was 12.54 1/sec located at strain gage 4. The maximum principal strains for gauges 2,3,4 and 5 can be found in Figure E.70 and the minimum principal strains for the same gauges can be found in
Figure E.71.

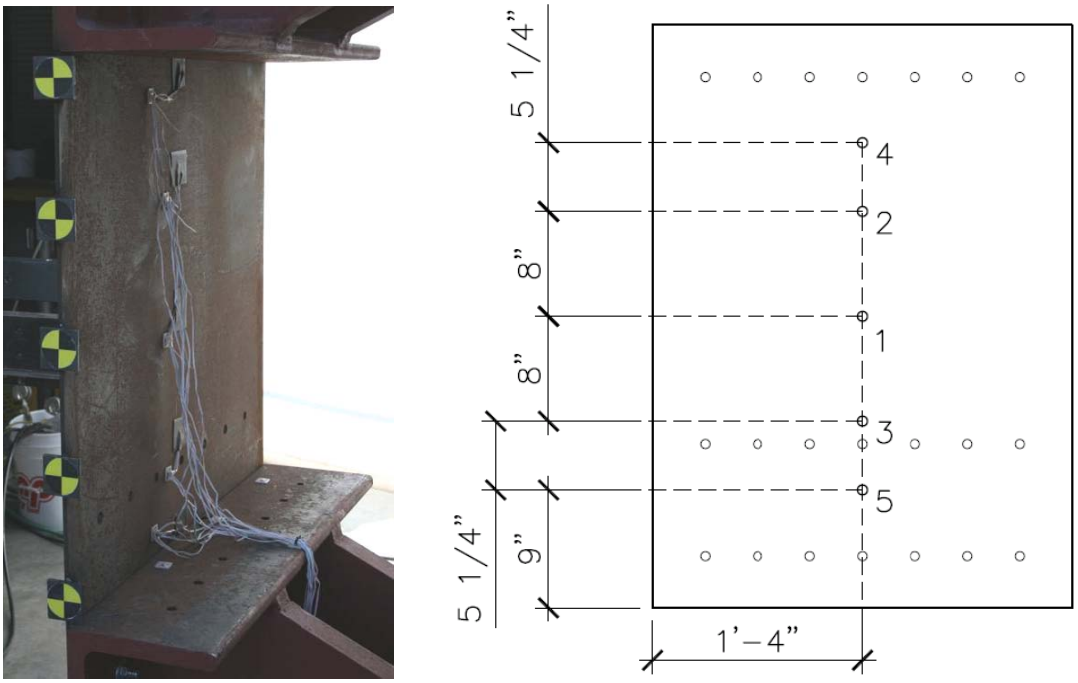

Figure E.69: Strain gage layout for Test 8

Table E.6: Stain rate information for Test 8

Strain Gage Number	Actual Velocity	Initial Impact	Shear Wave at Gage	Bolts Break	Maximum Principal Strain Rate	Minimum Principal Strain Rate 1/sec
2	27.2 m/s	56.50 msec	-	62.70 msec	-12.47 1/sec	7.48 1/sec
3	27.2 m/s	56.50 msec	-	62.70 msec	-9.27 1/sec	-12.46 1/sec
4	27.2 m/s	56.50 msec	-	62.70 msec	-9.87 1/sec	12.54 1/sec
5	27.2 m/s	56.50 msec	-	62.70 msec	-8.99 1/sec	-6.96 1/sec

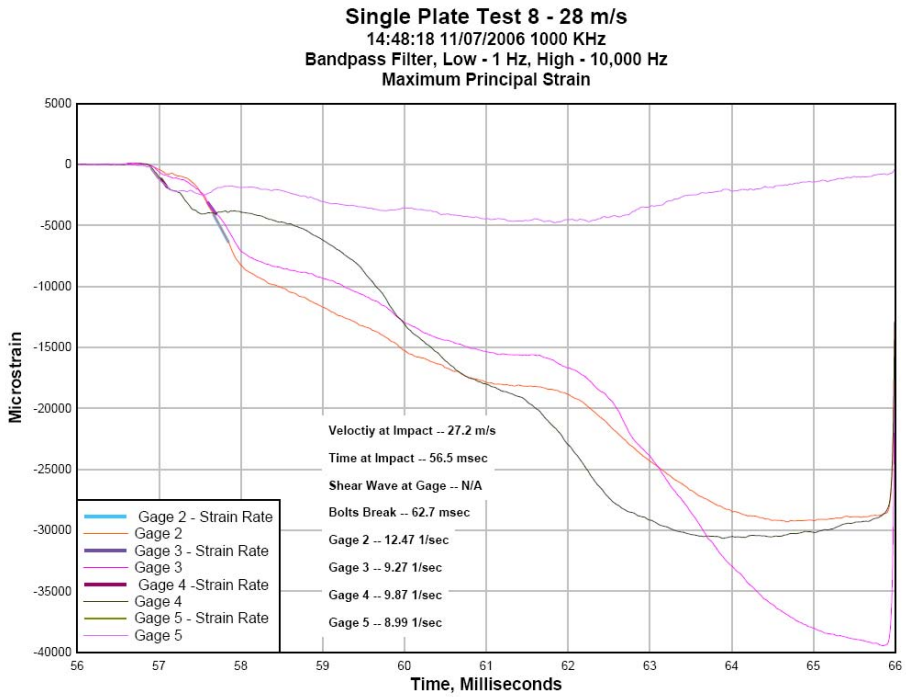

Figure E.70: Maximum principal strains and strain rates for Test 8

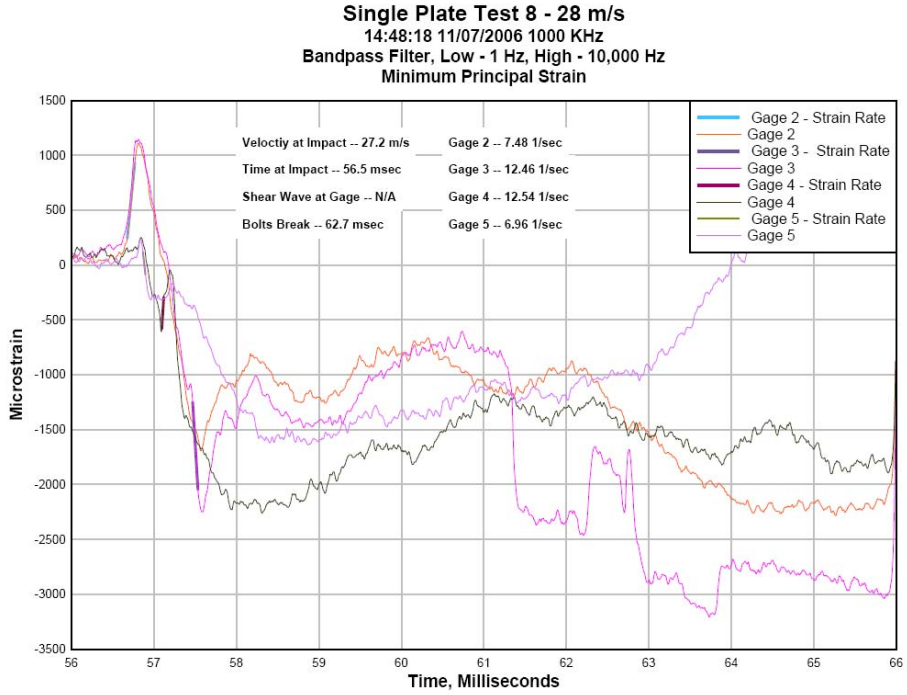

Figure E.71: Minimum principal strains and strain rates for Test 8

E.8.2.5 BOLT TYPE

A total of fourteen Grade 5 bolts (High Strength Bolts) were used for this test.

E.8.3 BLAST GENERATOR DATA

The initial impact of the single BG was 89.24 ft/sec (27.20 m/sec) with a goal velocity of 28 m/s. It had one accelerometer mounted to the back side of the impact plate as discussed in Section E.8.2.3. The average impact velocity for the impacting mass and the steel plate was calculated using the TEMA Track Eye tracking software.

E.8.4 SPECIMEN BEHAVIOR

The loading of the BG plate imparted an initial velocity of 89.24 ft/sec (27.20 m/sec) to the specimen. This caused plate to deform in both directions. The longitudinal deflection (in the north-south direction) behaved in a typical one-way flexural shape. In order to get the velocity as high as needed the test was designed to have the impacting mass break free from the BG and launch itself into the plate. This imparted enough energy into the system that all fourteen Grade 5 bolts failed. It appears that the bottom bolts failed first and then the top set of bolts failed. This caused the impacting mass and plate to rotate upwards. This rotation caused the bottom plate to move up enough that it was no longer supported by the bottom rigid end condition. The plate and impacting mass continued to rotate until the plate and mass fell to the ground. The approximate maximum deflection of the plate before the bolts broke was 6 1/8”. Figure E.72 shows the plate and impacting mass where they landed after the test.

During the test pieces of bolts flew approximately 40’ directly north of the test set-up and 8 ½’ south of the test set-up. Bolts were also found around 25’ away from the test set-up back into the lab work area on the south side of the test. After the test the bolts were pieced together and categorized for future analysis. During the test three different phantom cameras were used to capture the failure modes from three different angles. Figure E.73 shows the progression of damage for this test from Phantom Camera One. Figure E.74 shows the progression of damage for this test from Phantom Camera Two. Figure E.75 shows the progression of damage for this test from Phantom Camera Three.

Figure E.72: Steel plate post test for Test 8

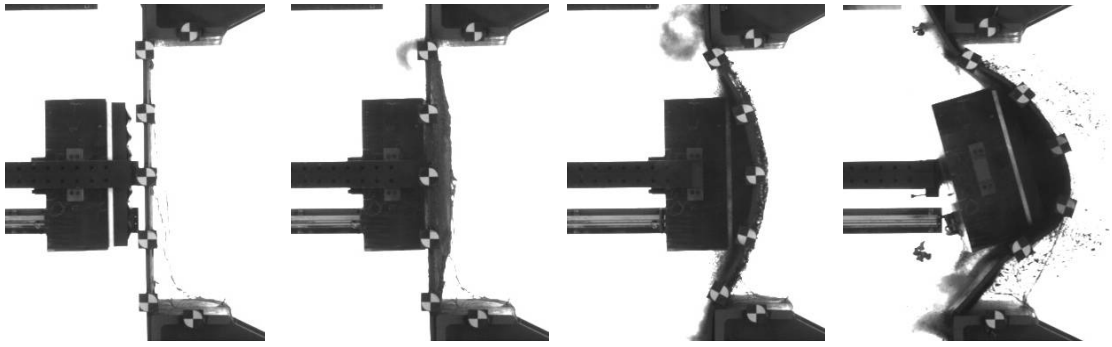

Figure E.73: Progression of damage for Test 8 from Camera 1

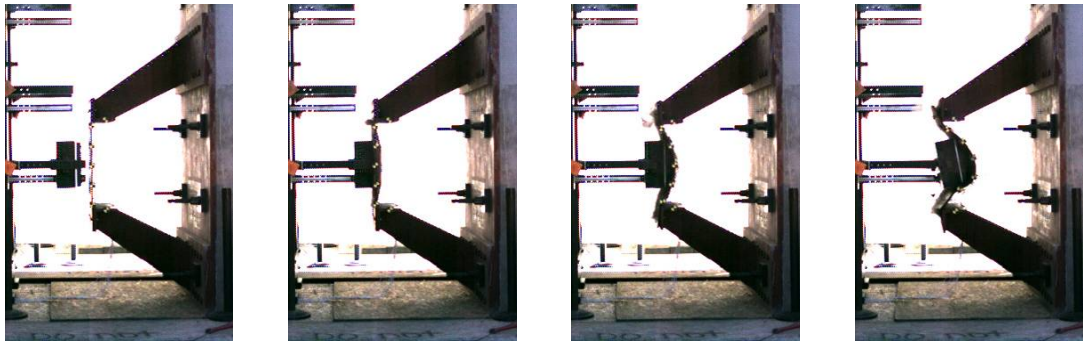

Figure E.74: Progression of damage for Test 8 from Camera 2

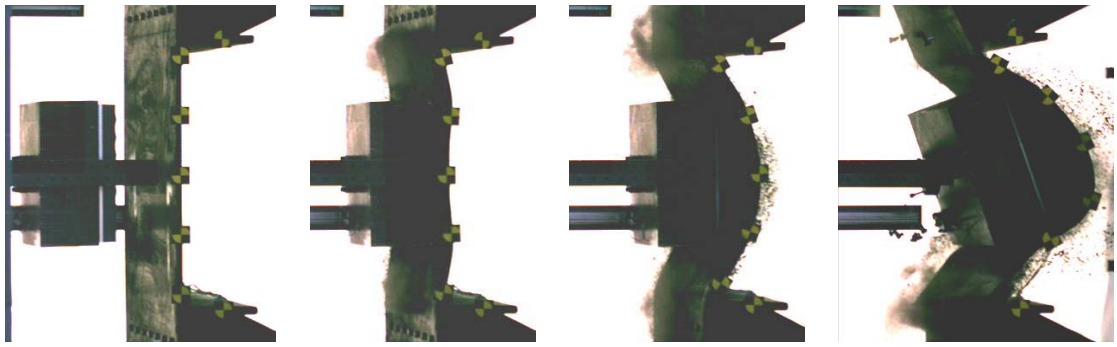

Figure E.75: Progression of damage for Test 8 from Camera 3

E.9 STEEL TOWER SINGLE PLATE: TEST 9 (SP9)

E.9.1 INTRODUCTION

The ninth test of the Steel Tower Single Plate test series was performed on November 13th, 2006. The test specimen was a ½" thick steel plate labeled SP9. The Impacting Mass 2 was attached to the BG with a specimen target velocity of 91.86 ft/sec (28 m/sec). Figure E.76 shows the steel plate prior to impact.

Figure E.76: 1/2" thick steel plate pre test for Test 9

E.9.2 INSTRUMENTATION

E.9.2.1 PHANTOM CAMERAS

The first camera recorded in black and white at a rate of 6,006 frames per second at a resolution of 512x384. This camera was used in order to determine the maximum velocity of the impacting mass and the movement in the plate including the maximum displacement. The second camera recorded in color at a rate of 6,006 frames per second at a resolution of 512x384. This camera recorded the overall deformation of the plate from the back and was not used to gather any specific data. The third camera recorded in color at a rate of 5,000 frames per second at a resolution of 512x400. This camera captured data on the front side of the plate to capture the bolt failures. A picture from each of the camera locations are shown in Figure E.77.

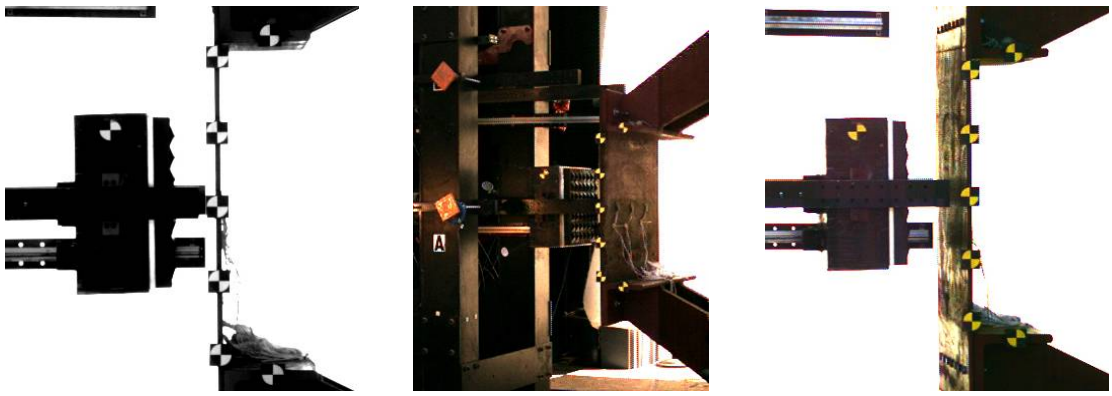

Figure E.77: Phantom Cameras for Test 9 a) Camera One b) Camera Two c) Camera Three

E.9.2.2 TARGET LOCATIONS

Five targets were welded onto the side of the steel plate as show in Figure E.76. They were spaced at the intervals shown in Figure E.78. That figure also shows the location of the targets for the impacting mass. An additional two targets were placed on the angle at the top and the bottom end conditions. The distance between these two points is 74.93 cm (29 ½")

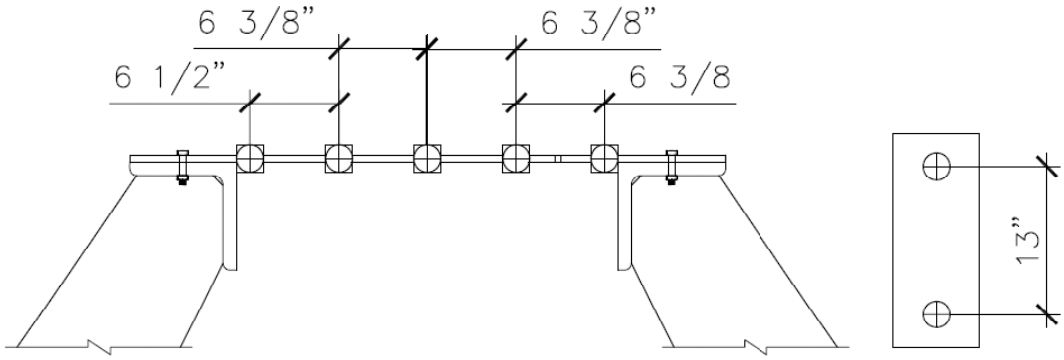

Figure E.78: Target layout on plate and impacting mass for Test 9

E.9.2.3 ACCELERATIONS

For this test one accelerometer was used. This accelerometer was placed 6" south of the centroid of the impacting mass as shown in Figure E.79. The pipe is to protect the accelerometer during the test. The data from this gage was then filtered as shown in Figure E.80.

This test does not impart an impulsive load as would be expected from a typical blast test. Instead, this test simulates the behavior of a flyer plate moving through the structure after the initial impact at the front plate of the outer cell of the structure. Therefore we are not determining the initial impulsive load from the accelerometers on the BG.

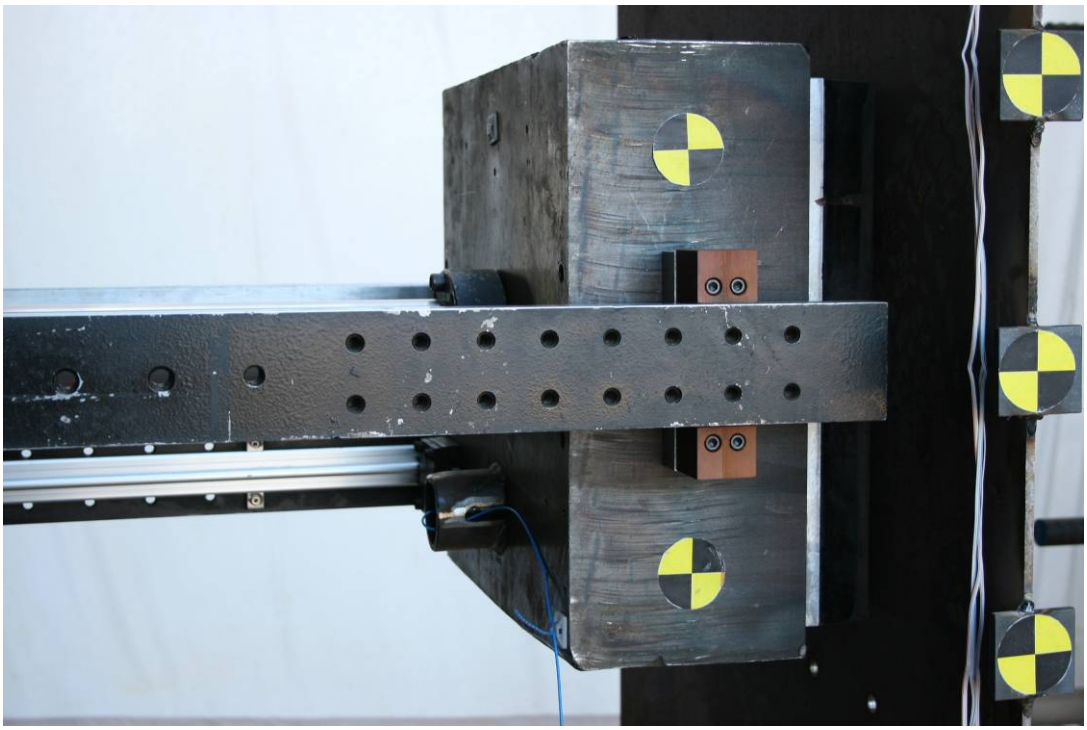

Figure E.79: Accelerometer location for Test 9

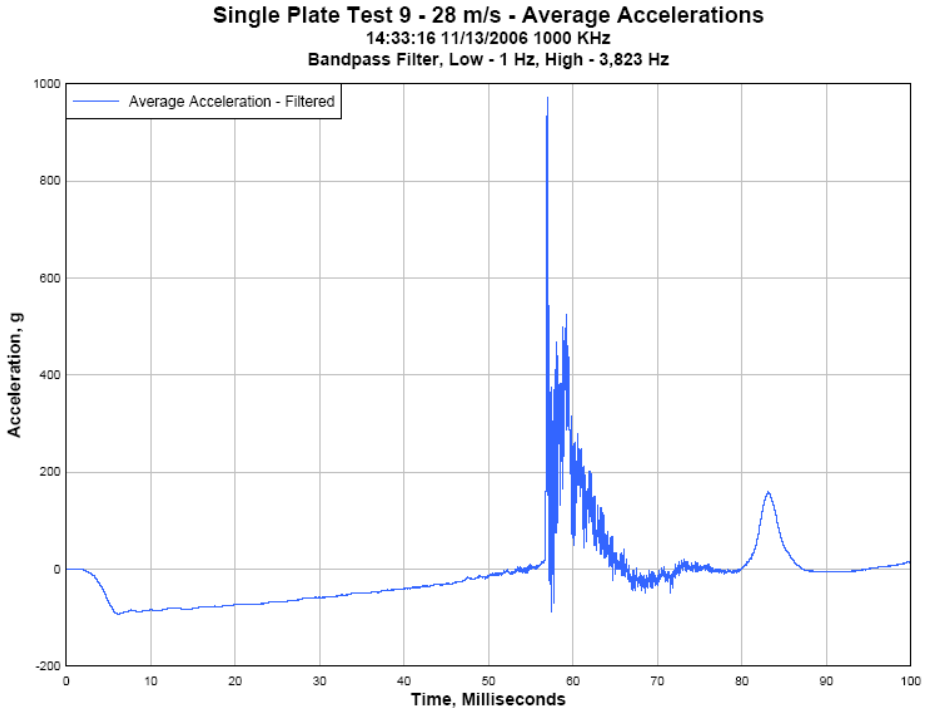

Figure E.80: Filtered accelerometer data for Test 9

E.9.2.4 STRAIN GAGE LOCATIONS

For this test there were three strain gauges labeled 1,6 and 7. The strain gauges, and their locations, are shown in Figure E.81. Strain gage 1 was damaged during this test and has been discarded. Table E.7 shows the specific information about this test, including the time and velocity at impact, if, and when, the bolts failed along with the maximum and minimum principal strain rates. The largest maximum principal strain rate for this test was -13.54 1/sec and was located at strain gage 6 while the largest minimum strain rate for this test was 11.88 1/sec located at strain gage 7. The maximum principal strains for gauges 6 and 7 can be found in Figure E.82 and the minimum principal strains for the same gauges can be found in Figure E.83.

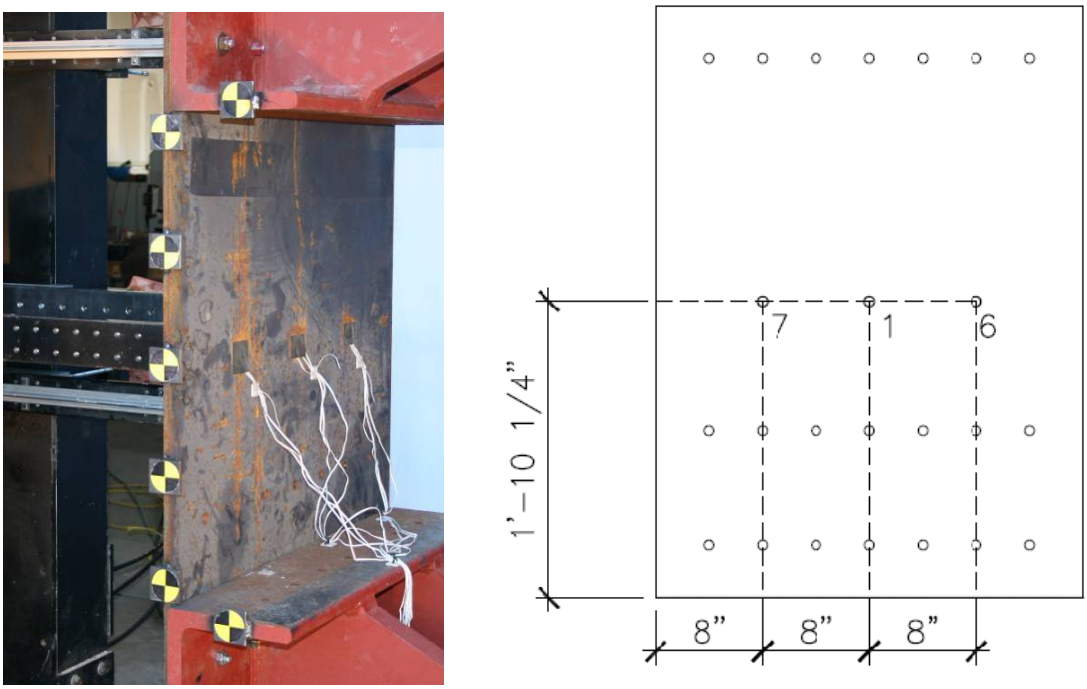

Figure E.81: Strain gage layout for Test 9

Table E.7: Stain rate information for Test 9

Strain Gage Number	Actual Velocity	Initial Impact	Shear Wave at Gage	Bolts Break	Maximum Principal Strain Rate	Minimum Principal Strain Rate
6	27.5 m/s	56.80 msec	-	63.00 msec	-13.54 1/sec	-11.64 1/sec
7	27.5 m/s	56.80 msec	-	63.00 msec	-7.76 1/sec	11.88 1/sec

E.9.2.5 BOLT TYPE

A total of fourteen Grade 5 bolts (High Strength Bolts) were used for this test.

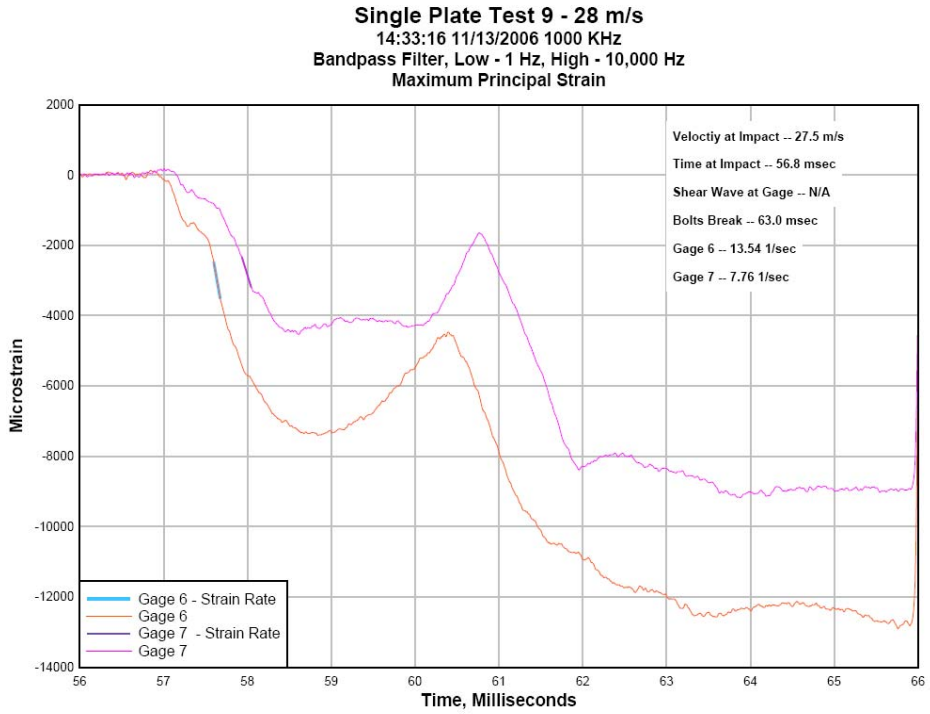

Figure E.82: Maximum principal strains and strain rates for Test 9

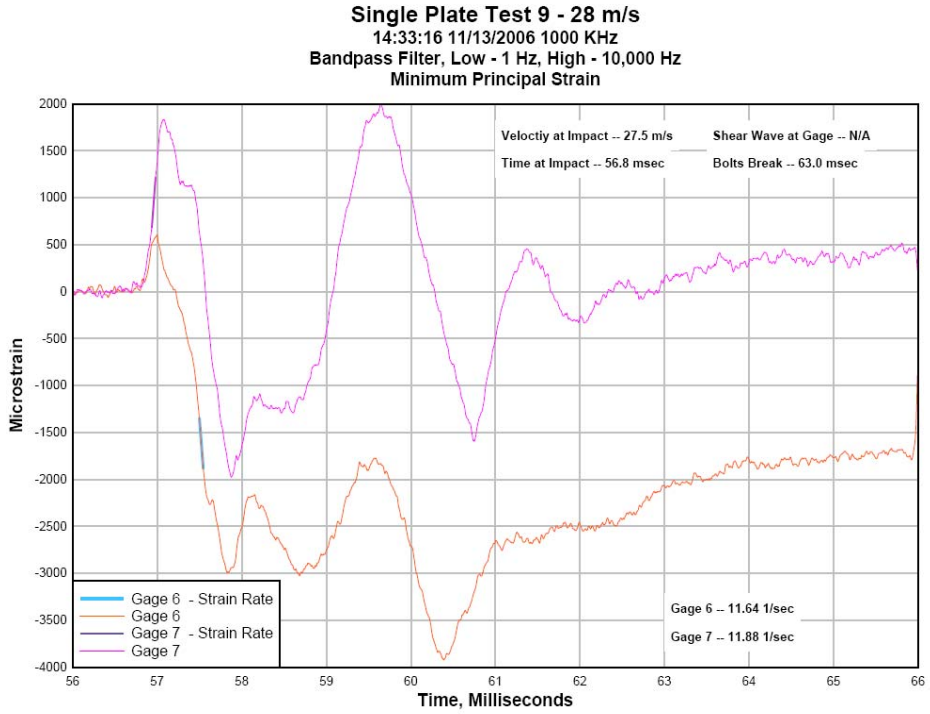

Figure E.83: Minimum principal strains and strain rates for Test 9

E.9.3 BLAST GENERATOR DATA

The initial impact of the single BG was 90.22 ft/sec (27.50 m/sec) with a goal velocity of 28 m/s. It had one accelerometer mounted to the back side of the impact plate as discussed in Section E.9.2.3. The average impact velocity for the impacting mass and the steel plate was calculated using the TEMA Track Eye tracking software.

E.9.4 SPECIMEN BEHAVIOR

The loading of the BG plate imparted an initial velocity of 90.22 ft/sec (27.50 m/sec) to the specimen. This caused plate to deform in both directions. The longitudinal deflection (in the north-south direction) behaved in a typical one-way flexural shape. In order to get the velocity as high as needed the test was designed to have the impacting mass break free from the BG and launch itself into the plate. This imparted enough energy into the system that seven of the Grade 5 bolts failed along the bottom of the plate. During this test the top bolts did not completely fracture. However, some very interesting dislocations did occur. When the Grade 5 bolts and the ½" Steel Plates are used it appears that the energy imparted into the system is at the threshold of failure for this system. Therefore, it is not surprising that the top bolts did not fail completely as occurred in Test 8. Once the bottom bolts broke the impacting mass and plate rotated upwards. The bottom half of the plate and the impacting mass continued to rotate until the plate and mass fell to the ground. The approximate maximum deflection of the plate before the bolts broke was 4".

During the test, pieces of bolts flew approximately 43 ½' directly north of the test set-up and 10' south of the test set-up. Figure E.84 shows the plate and impacting mass where they landed after the test. During the test three different phantom cameras were used to capture the failure modes from three different angles. Figure E.85 shows the progression of damage for this test from Phantom Camera One. Figure E.86 shows the progression of damage for this test from Phantom Camera Two. Figure E.87 shows the progression of damage for this test from Phantom Camera Three.

Figure E.84: Steel plate post test for Test 9

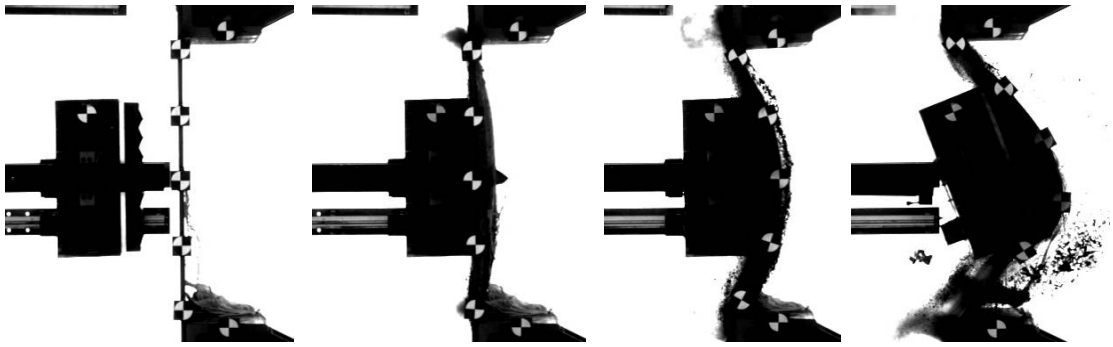

Figure E.85: Progression of damage for Test 9 from Camera 1

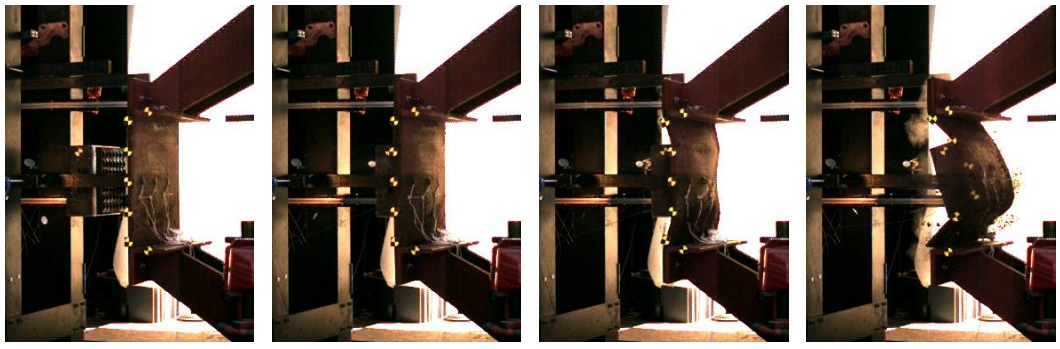

Figure E.86: Progression of damage for Test 9 from Camera 2

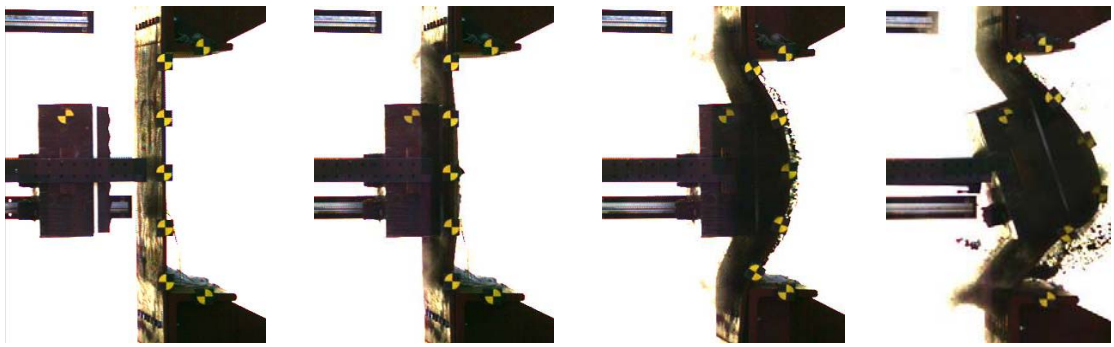

Figure E.87: Progression of damage for Test 9 from Camera 3

E.10 STEEL TOWER SINGLE PLATE: TEST 10 (SP10)

E.10.1 INTRODUCTION

The tenth test of the Steel Tower Single Plate test series was performed on November 16th, 2006. The test specimen was a ½" thick steel plate labeled SP10. The Impacting Mass 2 was attached to the BG with a specimen target velocity of 91.86 ft/sec (28 m/sec). Figure E.88 shows the steel plate prior to impact.

Figure E.88: 1/2" thick steel plate pre test for Test 10

E.10.2 INSTRUMENTATION

E.10.2.1 PHANTOM CAMERAS

The first camera recorded in black and white at a rate of 10,000 frames per second at a resolution of 512x384. This camera was used in order to determine the maximum velocity of the impacting mass and the movement in the plate including the maximum displacement. The second camera recorded in color at a rate of 3,000 frames per second at a resolution of 512x384. This camera recorded the movement at the edge of the bottom support condition. It was not used to gather any specific data. The third camera recorded in color at a rate of 3,000 frames per second at a resolution of 512x400. This camera recorded the movement at the edge of the top support condition. It was not used to gather any specific data. A picture from each of the camera locations are shown in Figure E.89.

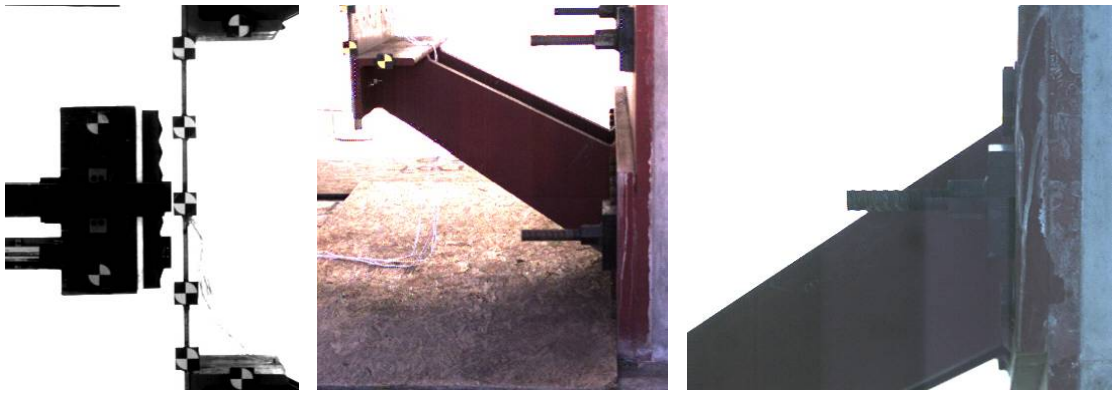

Figure E.89: Phantom Cameras for Test 10 a) Camera One b) Camera Two c) Camera Three

E.10.2.2 TARGET LOCATIONS

Five targets were welded onto the side of the steel plate as show in Figure E.88. They were spaced at the intervals shown in Figure E.90. That figure also shows the location of the targets for the impacting mass. An additional two targets were placed on the angle at the top and the bottom end conditions. The distance between these two points is 74.93 cm (29 ½")

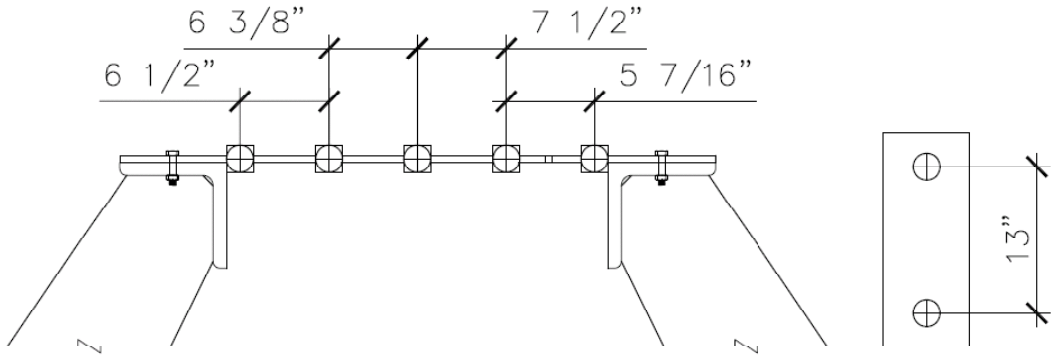

Figure E.90: Target layout on plate and impacting mass for Test 10

E.10.2.3 ACCELERATIONS

For this test one accelerometer was used. This accelerometer was placed 6" south of the centroid of the impacting mass as shown in Figure E.91. The pipe is to protect the accelerometer during the test. The data from this gage was then filtered as shown in Figure E.92.

This test does not impart an impulsive load as would be expected from a typical blast test. Instead, this test simulates the behavior of a flyer plate moving through the structure after the initial impact at the front plate of the outer cell of the structure. Therefore we are not determining the initial impulsive load from the accelerometers on the BG.

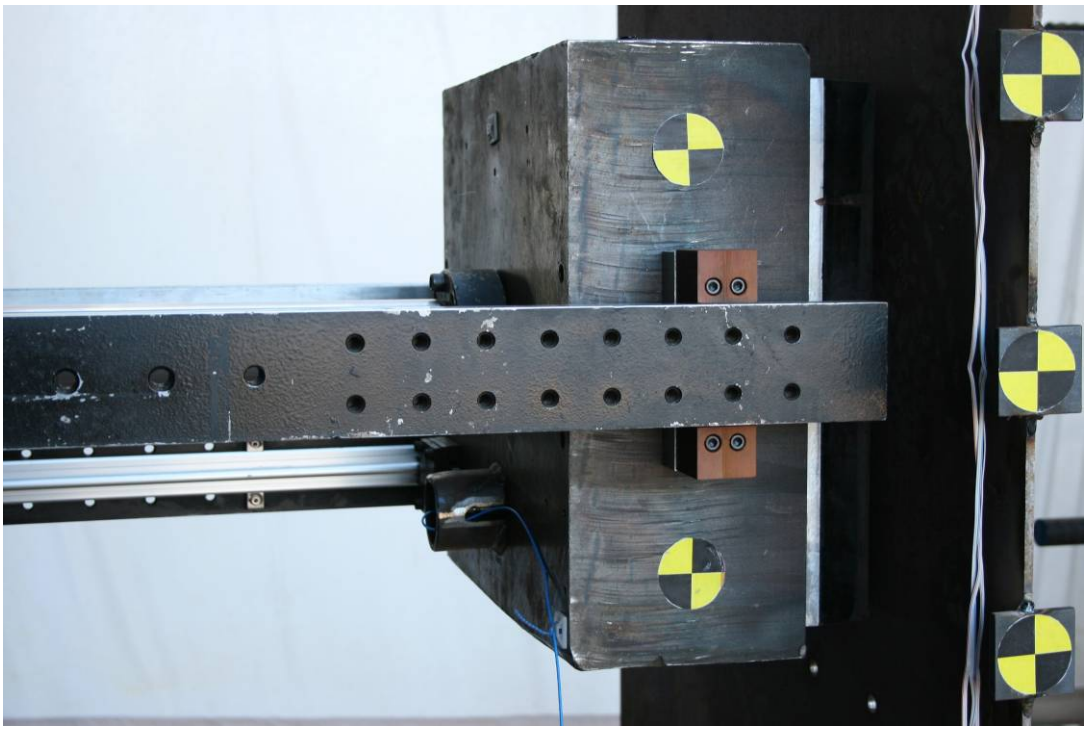

Figure E.91: Accelerometer location for Test 10

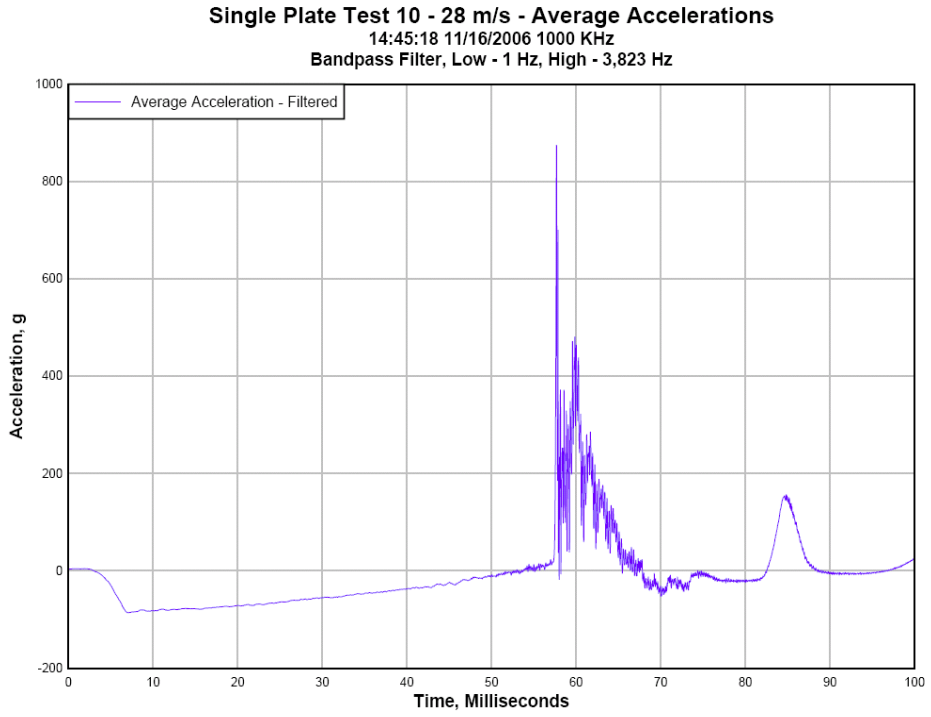

Figure E.92: Filtered accelerometer data for Test 10

E.10.2.4 STRAIN GAGE LOCATIONS

For this test there were two strain gauges labeled 8 and 9. The strain gauges, and their locations, are shown in Figure E.93. Table E.8 shows the specific information about this test, including the time and velocity at impact, if, and when, the bolts failed along with the maximum and minimum principal strain rates. The largest maximum principal strain rate for this test was -18.76 1/sec and was located at strain gage 8 while the largest minimum strain rate for this test was 13.20 1/sec located at strain gage 8. The maximum principal strains for gauges 8 and 9 can be found in Figure E.94 and the minimum principal strains for the same gauges can be found in Figure E.95.

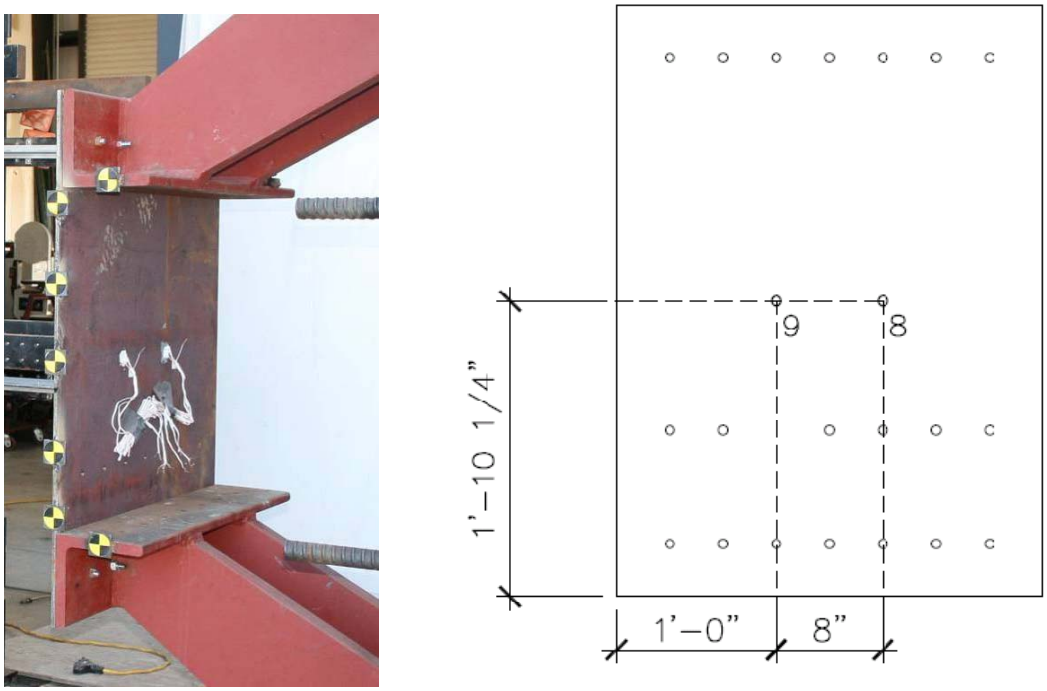

Figure E.93: Strain gage layout for Test 10

Table E.8: Stain rate information for Test 10

Strain Gage Number	Actual Velocity	Initial Impact	Shear Wave at Gage	Bolts Break	Maximum Principal Strain Rate	Minimum Principal Strain Rate
8	28.2 m/s	57.50 msec	-	63.20 msec	-18.76 1/sec	-13.20 1/sec
9	28.2 m/s	57.50 msec	-	63.20 msec	-10.85 1/sec	-9.08 1/sec

E.10.2.5 BOLT TYPE

A total of fourteen Grade 5 bolts (High Strength Bolts) were used for this test.

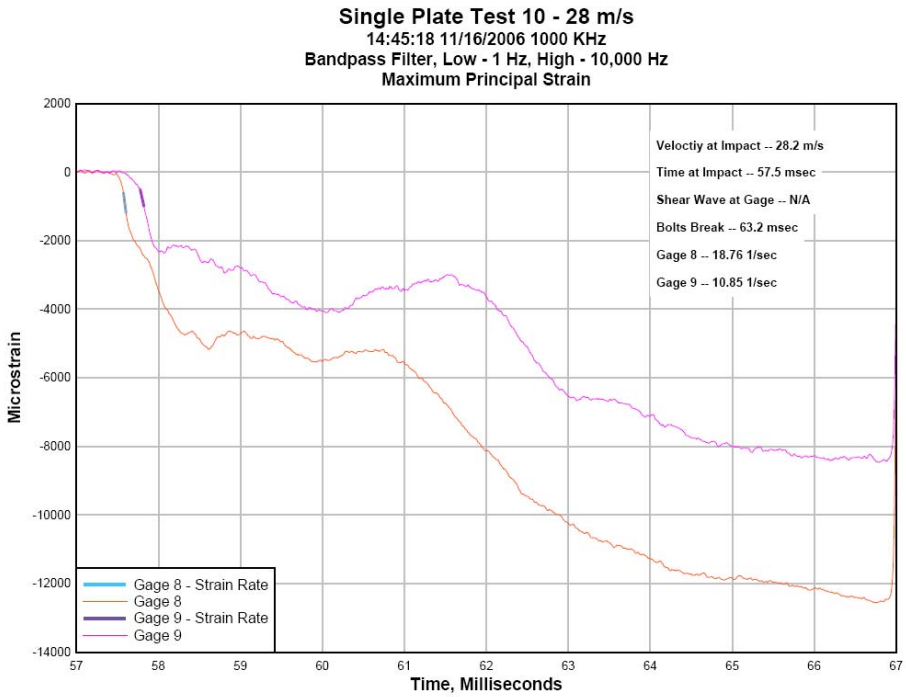

Figure E.94: Maximum principal strains and strain rates for Test 10

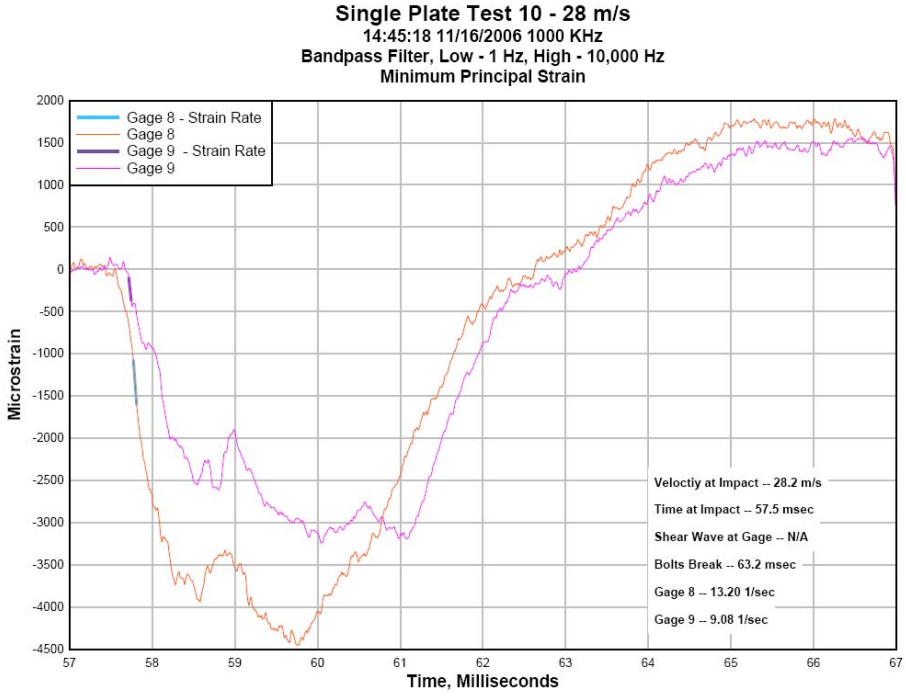

Figure E.95: Minimum principal strains and strain rates for Test 10

E.10.3 BLAST GENERATOR DATA

The initial impact of the single BG was 92.52 ft/sec (28.20 m/sec) with a goal velocity of 28 m/s. It had one accelerometer mounted to the back side of the impact plate as discussed in Section E.10.2.3. The average impact velocity for the impacting mass and the steel plate was calculated using the TEMA Track Eye tracking software.

E.10.4 SPECIMEN BEHAVIOR

The loading of the BG plate imparted an initial velocity of 92.52 ft/sec (28.20 m/sec) to the specimen. This caused plate to deform in both directions. The longitudinal deflection (in the north-south direction) behaved in a typical one-way flexural shape. In order to get the velocity as high as needed the test was designed to have the impacting mass break free from the BG and launch itself into the plate. This imparted enough energy into the system that seven of the Grade 5 bolts failed along the bottom of the plate. During this test the top bolts did not completely fracture. However, some very interesting dislocations did occur. When the Grade 5 bolts and the ½" Steel Plates are used it appears that the energy imparted into the system is at the threshold of failure for this system. Therefore, it is not surprising that the top bolts did not fail completely as occurred in Test 8. Once the bottom bolts broke the impacting mass and plate rotated upwards. The bottom half of the plate and the impacting mass continued to rotate until the plate and mass fell to the ground. The approximate maximum deflection of the plate before the bolts broke was 5 ½". Figure E.96 shows the plate and impacting mass where they landed after the test. During the test a phantom camera was used to capture the failure modes as shown in Figure E.97.

After the test it was discovered that the support rods for the impacting mass might not have been in the exact center of the plate. It appeared that they were located approximately 1 3/8" south of the center of the plate. This might give further explanation as to why the bottom bolts broke and the top bolts did not. In future tests the impacting mass will be checked to make sure that the horizontal center of the plate and programmer impact the steel plate at its horizontal center.

Figure E.96: Steel plate post test for Test 10

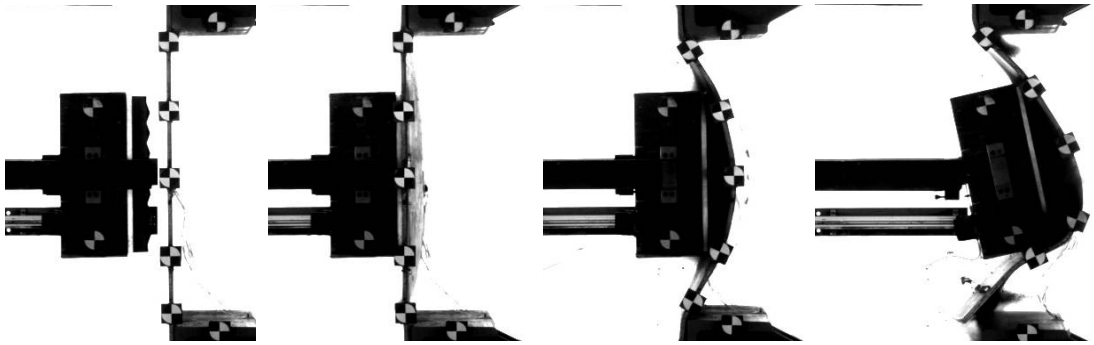

Figure E.97: Progression of damage for Test 10 from Camera 1

E.11 STEEL TOWER SINGLE PLATE: TEST 11 (SP11)

E.11.1 INTRODUCTION

The eleventh test of the Steel Tower Single Plate test series was performed on November 21st, 2006. The test specimen was a ½" thick steel plate labeled SP11. The Impacting Mass 1 was attached to the BG with a specimen target velocity of 91.86 ft/sec (28 m/sec). Figure E.98 shows the steel plate prior to impact.

Figure E.98: 1/2" thick steel plate pre test for Test 11

E.11.2 INSTRUMENTATION

E.11.2.1 PHANTOM CAMERAS

The first camera recorded in black and white at a rate of 10,000 frames per second at a resolution of 512x384. This camera was used in order to determine the maximum velocity of the impacting mass and the movement in the plate including the maximum displacement. The second camera recorded in color at a rate of 5,000 frames per second at a resolution of 512x384. This camera recorded the movement at the edge of the bottom support condition. It was not used to gather any specific data. The third camera recorded in color at a rate of 3,000 frames per second at a resolution of 512x400. This camera recorded the movement at the edge of the top support condition. It was not used to gather any specific data. A picture from each of the camera locations are shown in Figure E.99.

Figure E.99: Phantom Cameras for Test 11 a) Camera One b) Camera Two c) Camera Three

E.11.2.2 TARGET LOCATIONS

Five targets were welded onto the side of the steel plate as show in Figure E.98. They were spaced at the intervals shown in Figure E.100. That figure also shows the location of the targets for the impacting mass. An additional two targets were placed on the angle at the top and the bottom end conditions. The distance between these two points is 74.93 cm (29 ½")

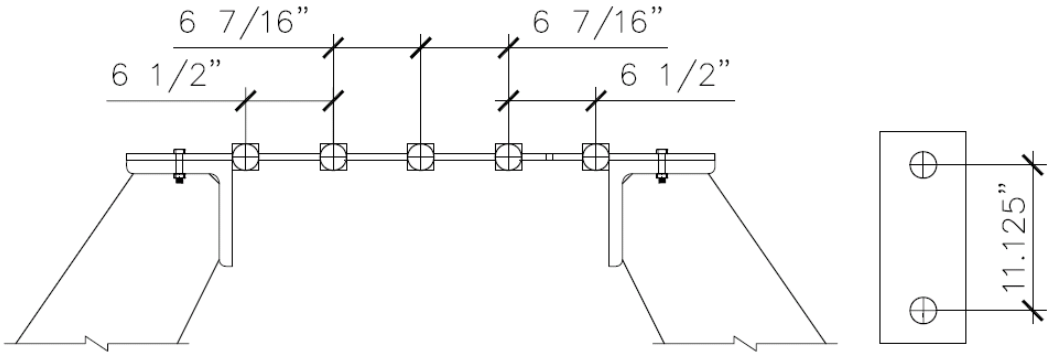

Figure E.100: Target layout on plate and impacting mass for Test 11

E.11.2.3 ACCELERATIONS

For this test one accelerometer was used. This accelerometer was placed 6" south of the centroid of the impacting mass as shown in Figure E.101. The pipe is to protect the accelerometer during the test. The data from this gage was then filtered as shown in Figure E.102.

This test does not impart an impulsive load as would be expected from a typical blast test. Instead, this test simulates the behavior of a flyer plate moving through the structure after the initial impact at the front plate of the outer cell of the structure. Therefore we are not determining the initial impulsive load from the accelerometers on the BG.

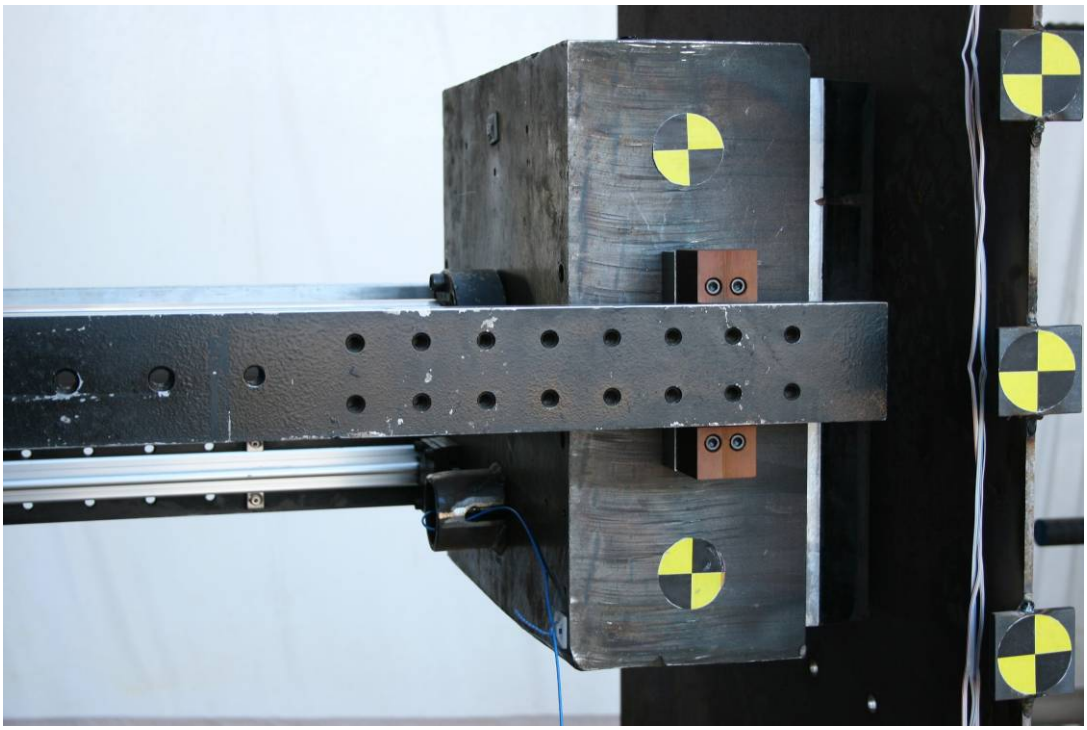

Figure E.101: Accelerometer location for Test 11

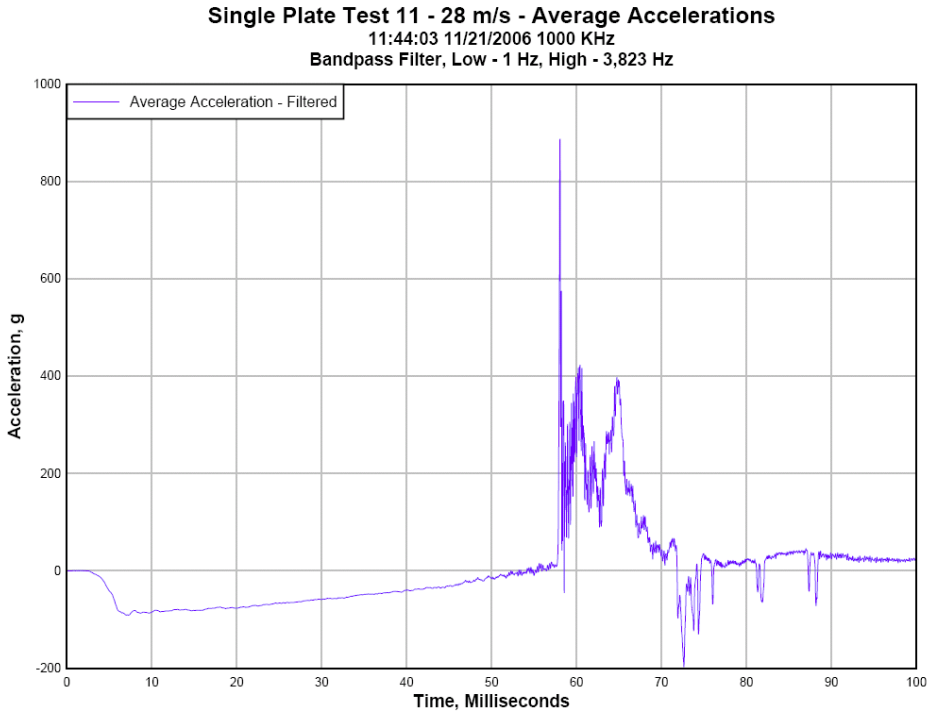

Figure E.102: Filtered accelerometer data for Test 11

E.11.2.4 STRAIN GAGE LOCATIONS

For this test there were two strain gauges labeled 8 and 9. The strain gauges, and their locations, are shown in Figure E.103. Table E.9 shows the specific information about this test, including the time and velocity at impact, if, and when, the bolts failed along with the maximum and minimum principal strain rates. The largest maximum principal strain rate for this test was 14.89 1/sec and was located at strain gage 8 while the largest minimum strain rate for this test was 13.24 1/sec located at strain gage 8. The maximum principal strains for gauges 8 and 9 can be found in Figure E.104 and the minimum principal strains for the same gauges can be found in Figure E.105.

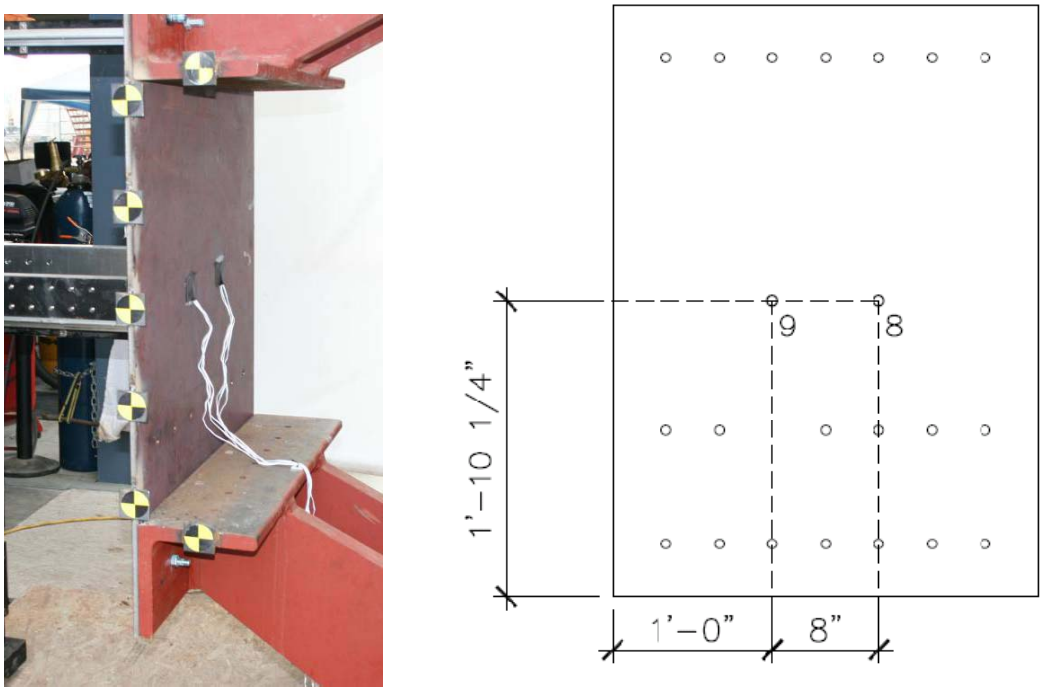

Figure E.103: Strain gage layout for Test 11

Table E.9: Stain rate information for Test 11

Strain Gage Number	Actual Velocity	Initial Impact	Shear Wave at Gage	Bolts Break	Maximum Principal Strain Rate	Minimum Principal Strain Rate
8	27.5 m/s	57.90 msec	-	65.70 msec	-14.89 1/sec	-13.24 1/sec
9	27.5 m/s	57.90 msec	-	65.70 msec	-12.45 1/sec	-9.73 1/sec

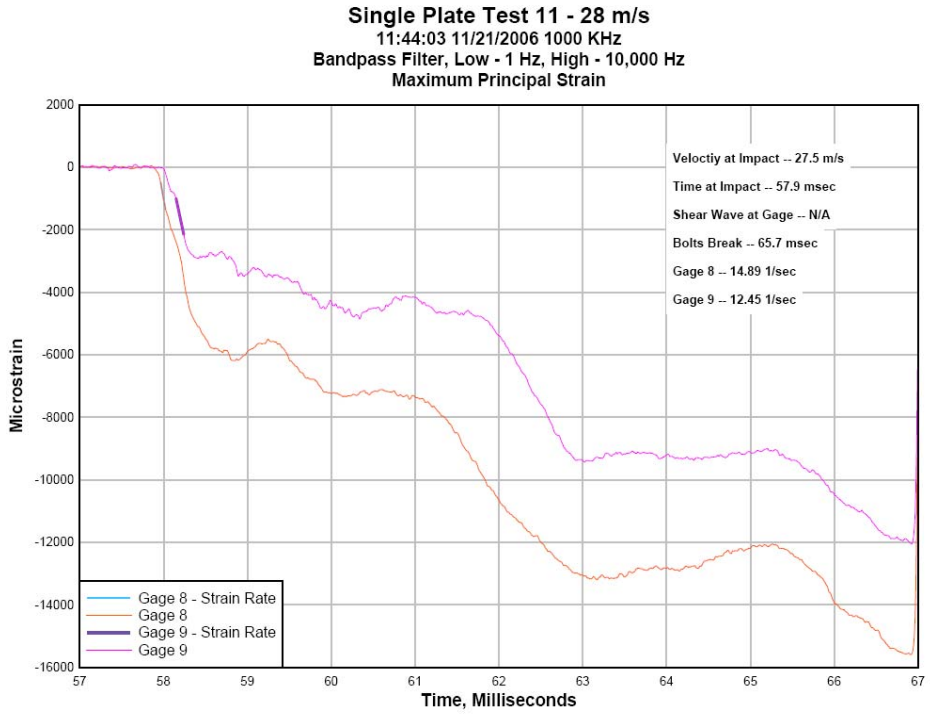

Figure E.104: Maximum principal strains and strain rates for Test 11

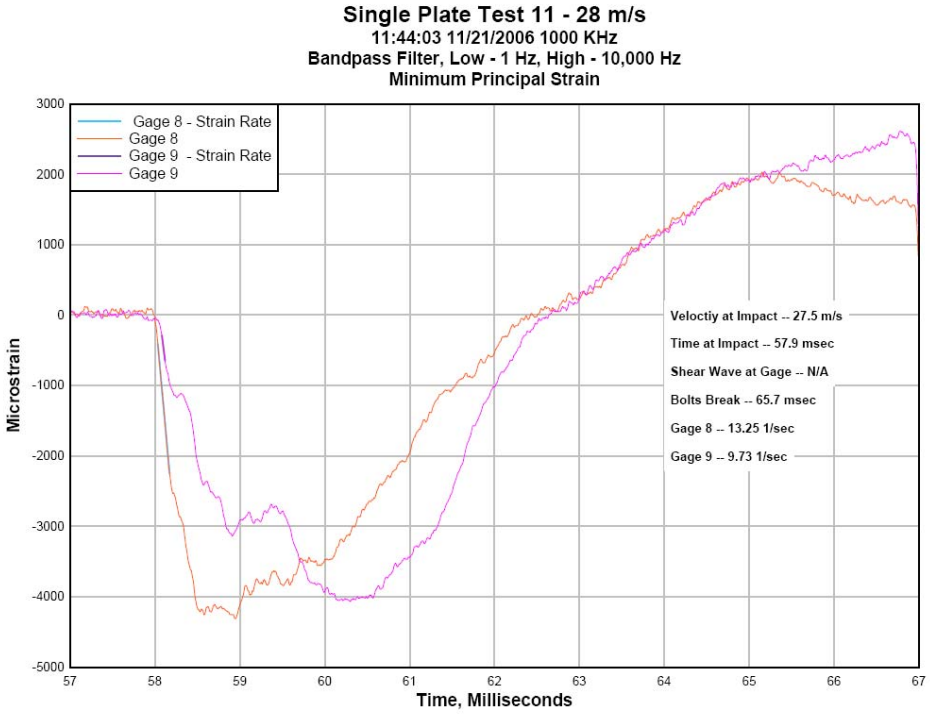

Figure E.105: Minimum principal strains and strain rates for Test 11

E.11.2.5 BOLT TYPE

A total of fourteen Grade 5 bolts (High Strength Bolts) were used for this test. They were all tightened to a torque of 50 ft-lbs.

E.11.3 BLAST GENERATOR DATA

The initial impact of the single BG was 90.22 ft/sec (27.50 m/sec) with a goal velocity of 28 m/s. It had one accelerometer mounted to the back side of the impact plate as discussed in Section E.11.2.3. The average impact velocity for the impacting mass and the steel plate was calculated using the TEMA Track Eye tracking software.

E.11.4 SPECIMEN BEHAVIOR

The loading of the BG plate imparted an initial velocity of 90.22 ft/sec (27.50 m/sec) to the specimen. This caused plate to deform in both directions. The longitudinal deflection (in the north-south direction) behaved in a typical one-way flexural shape. In order to get the velocity as high as needed the test was designed to have the impacting mass break free from the BG and launch itself into the plate. For this test the impacting mass was checked to make sure that the horizontal center of the plate and programmer would impact the steel plate at its horizontal center. The BG and support rails were moved approximately 1 3/8” in order to center the mass. This test imparted enough energy into the system that fourteen of the Grade 5 bolts failed simultaneously. The approximate maximum deflection of the plate before the bolts broke was 5 9/16”.
Figure E.106 shows the plate and impacting mass where they landed after the test. During the test a phantom camera was used to capture the failure modes as shown in Figure E.107.

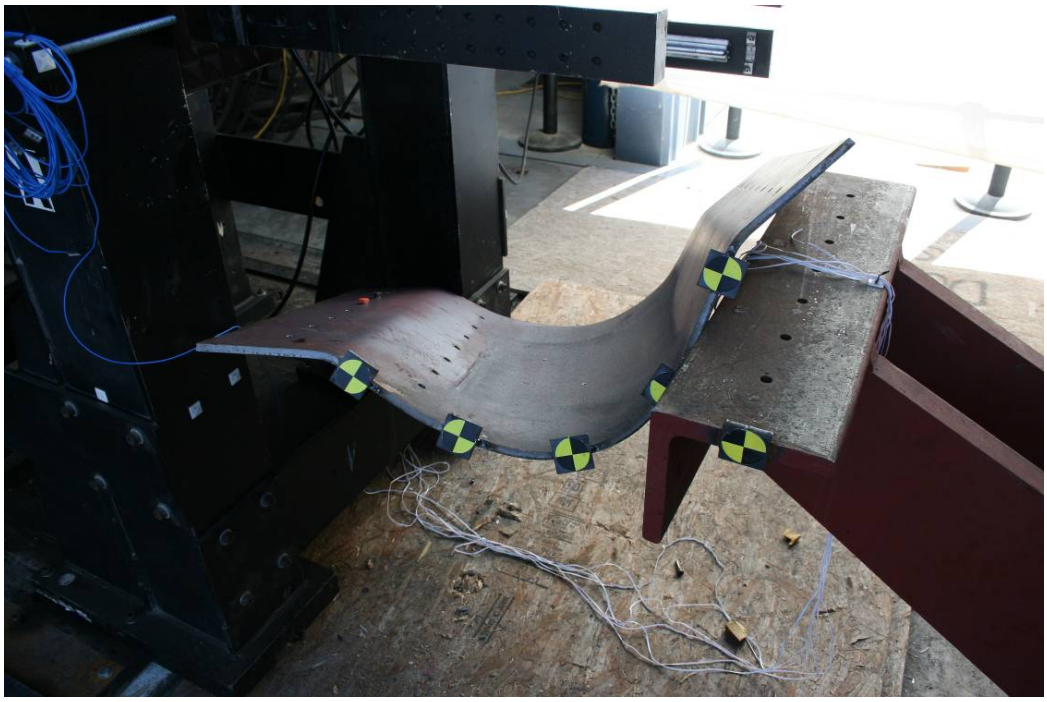

Figure E.106: Steel plate post test for Test 11

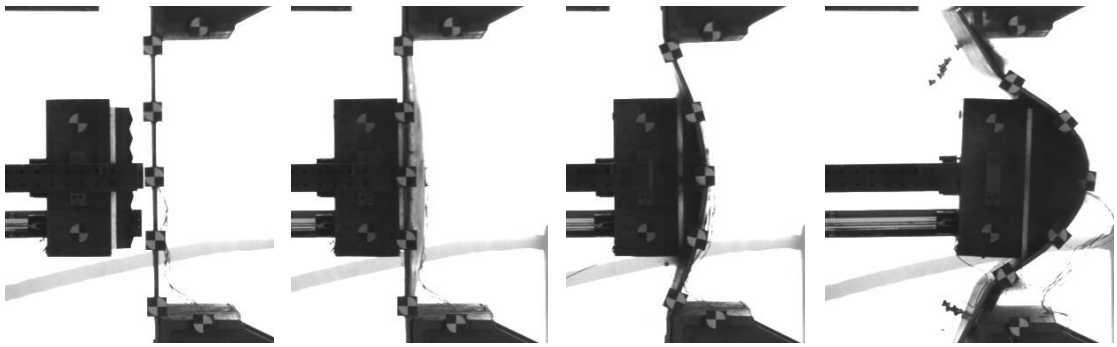

Figure E.107: Progression of damage for Test 11 from Camera 1

E.12 STEEL TOWER SINGLE PLATE: TEST 12 (SP12)

E.12.1 INTRODUCTION

The twelfth test of the Steel Tower Single Plate test series was performed on November 28th, 2006. The test specimen was a ¼" thick steel plate labeled SP12. The Impacting Mass 1 was attached to the BG with a specimen target velocity of 91.86 ft/sec (28 m/sec). Figure E.108 shows the steel plate prior to impact.

Figure E.108: 1/4" thick steel plate pre test for Test 12

E.12.2 INSTRUMENTATION

E.12.2.1 PHANTOM CAMERAS

The first camera recorded in black and white at a rate of 10,000 frames per second at a resolution of 512x384. This camera was used in order to determine the maximum velocity of the impacting mass and the movement in the plate including the maximum displacement. The second camera recorded in color at a rate of 5,000 frames per second at a resolution of 512x384. This camera recorded the movement at the edge of the bottom support condition. It was not used to gather any specific data. The third camera recorded in color at a rate of 2,500 frames per second at a resolution of 512x400. This camera recorded the same information as Camera One. A picture from each of the camera locations are shown in Figure E.109.

Figure E.109: Phantom Cameras for Test 12

a) Camera One b) Camera Two c) Camera Three

E.12.2.2 TARGET LOCATIONS

Five targets were welded onto the side of the steel plate as show in Figure E.108. They were spaced at the intervals shown in Figure E.110. That figure also shows the location of the targets for the impacting mass. An additional two targets were placed on the angle at the top and the bottom end conditions. The distance between these two points is 74.93 cm (29 ½")

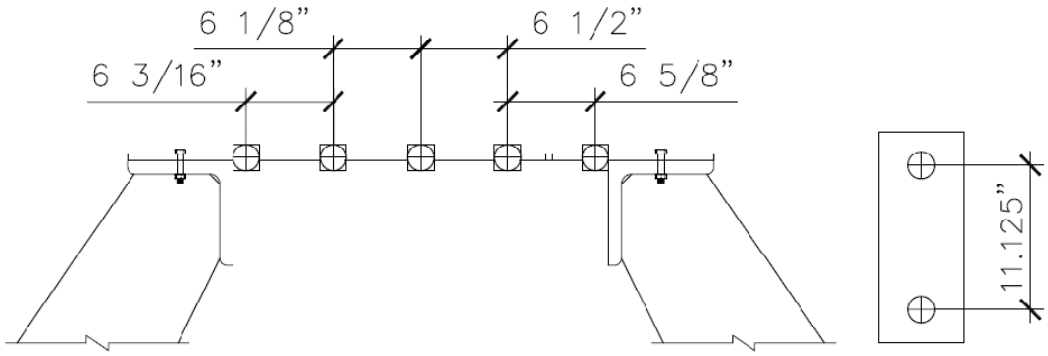

Figure E.110: Target layout on plate and impacting mass for Test 12

E.12.2.3 ACCELERATIONS

For this test one accelerometer was used. This accelerometer was placed 6" south of the centroid of the impacting mass as shown in Figure E.111. The pipe is to protect the accelerometer during the test. The data from this gage was then filtered as shown in Figure E.112.

This test does not impart an impulsive load as would be expected from a typical blast test. Instead, this test simulates the behavior of a flyer plate moving through the structure after the initial impact at the front plate of the outer cell of the structure. Therefore we are not determining the initial impulsive load from the accelerometers on the BG.

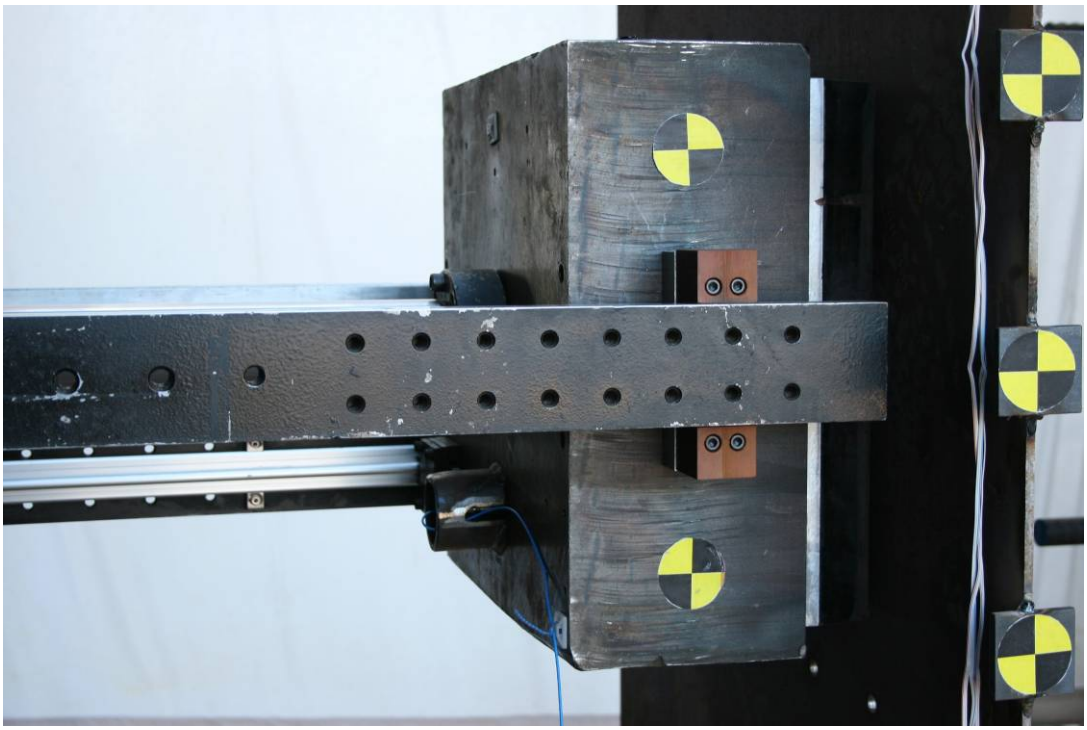

Figure E.111: Accelerometer location for Test 12

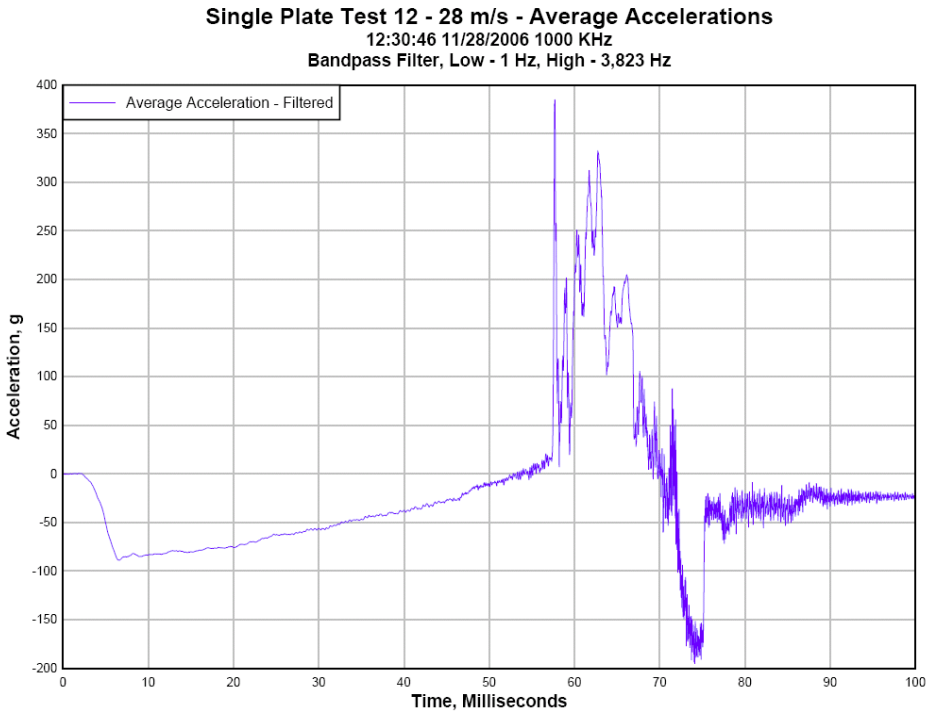

Figure E.112: Filtered accelerometer data for Test 12

E.12.2.4 STRAIN GAGE LOCATIONS

For this test there were two strain gauges labeled 10 and 11. The strain gauges, and their locations, are shown in Figure E.113. Table E.10 shows the specific information about this test, including the time and velocity at impact, if, and when, the bolts failed along with the maximum and minimum principal strain rates. The largest maximum principal strain rate for this test was -9.32 1/sec and was located at strain gage 10 while the largest minimum strain rate for this test was 9.98 1/sec located at strain gage 11. The maximum principal strains for gauges 10 and 11 can be found in Figure E.114 and the minimum principal strains for the same gauges can be found in Figure E.115.

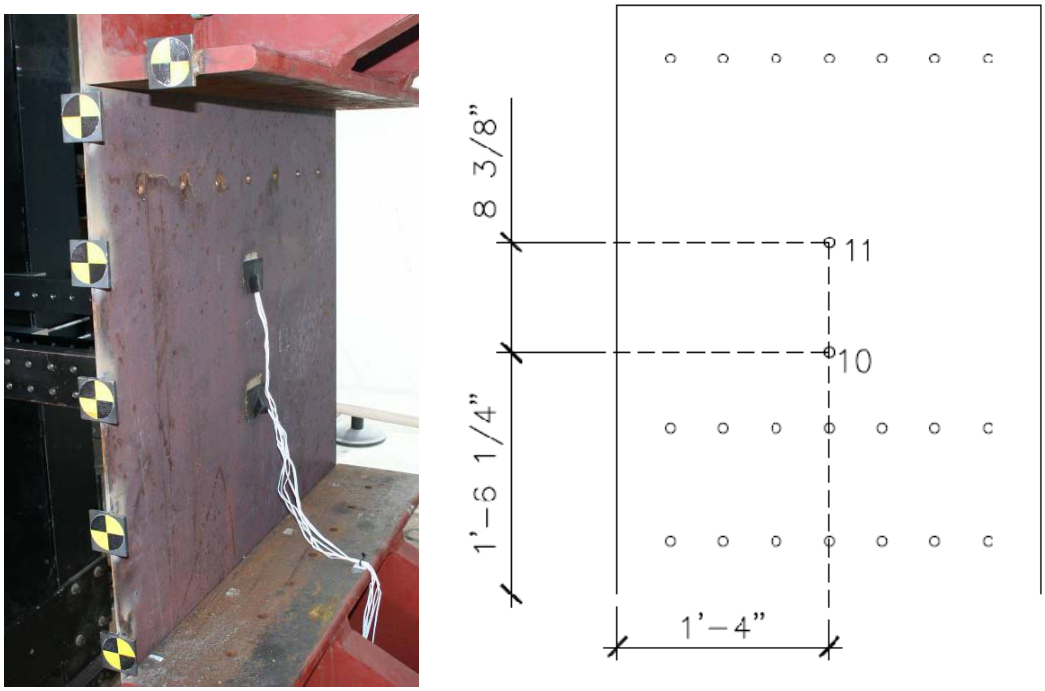

Figure E.113: Strain gage layout for Test 12

Table E.10: Stain rate information for Test 12

Strain Gage Number	Actual Velocity	Initial Impact	Shear Wave at Gage	Bolts Break	Maximum Principal Strain Rate	Minimum Principal Strain Rate
10	27.8 m/s	57.70 msec	-	62.00 msec	-9.32 1/sec	-9.34 1/sec
11	27.8 m/s	57.70 msec	-	62.00 msec	-9.10 1/sec	-9.98 1/sec

E.12.2.5 BOLT TYPE

A total of fourteen Grade 5 bolts (High Strength Bolts) were used for this test. They were all tightened to a torque of 50 ft-lbs.

E.12.3 BLAST GENERATOR DATA

The initial impact of the single BG was 91.20 ft/sec (27.80 m/sec) with a goal velocity of 28 m/s. It had one accelerometer mounted to the back side of the impact plate as discussed in Section E.12.2.3. The average impact velocity for the impacting mass and the steel plate was calculated using the TEMA Track Eye tracking software.

E.12.4 SPECIMEN BEHAVIOR

The loading of the BG plate imparted an initial velocity of 91.20 ft/sec (27.80 m/sec) to the specimen. This caused plate to deform in both directions. The longitudinal deflection (in the north-south direction) behaved in a typical one-way flexural shape. In order to get the velocity as high as needed the test was designed to have the impacting mass break free from the BG and launch itself into the plate. This test imparted enough energy into the system that the top seven bolts broke. For this test the top bolts broke and caused the specimen to rotate and but did not apply enough force to the bottom bolts to cause them to fully shear. The reason that the specimen only broke ½ of the bolts could be due to the fact that the impacting mass was not lined up in the center of the specimen, for some reason that check was missed for this test.

During the test pieces of bolts flew approximately 8’ directly north and 7’ south of the test set-up. Figure E.116 shows the plate and impacting mass where they landed after the test. During the test two different phantom cameras were used to capture the failure modes from two different angles. Figure E.117 shows the progression of damage for this test from Phantom Camera One. Figure E.118 shows the progression of damage for this test from Phantom Camera Three.

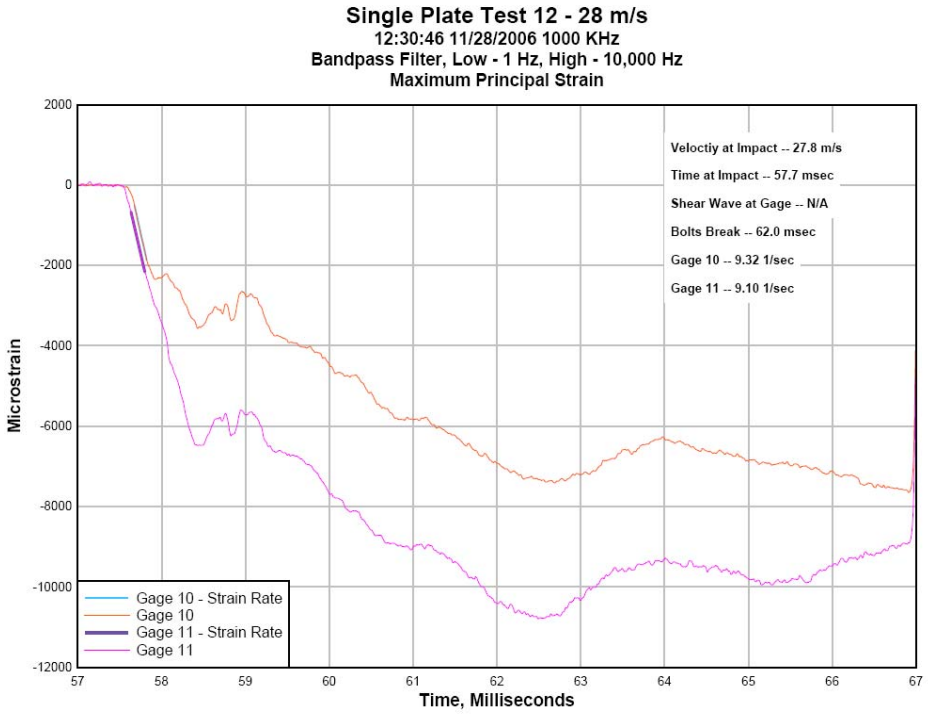

Figure E.114: Maximum principal strains and strain rates for Test 12

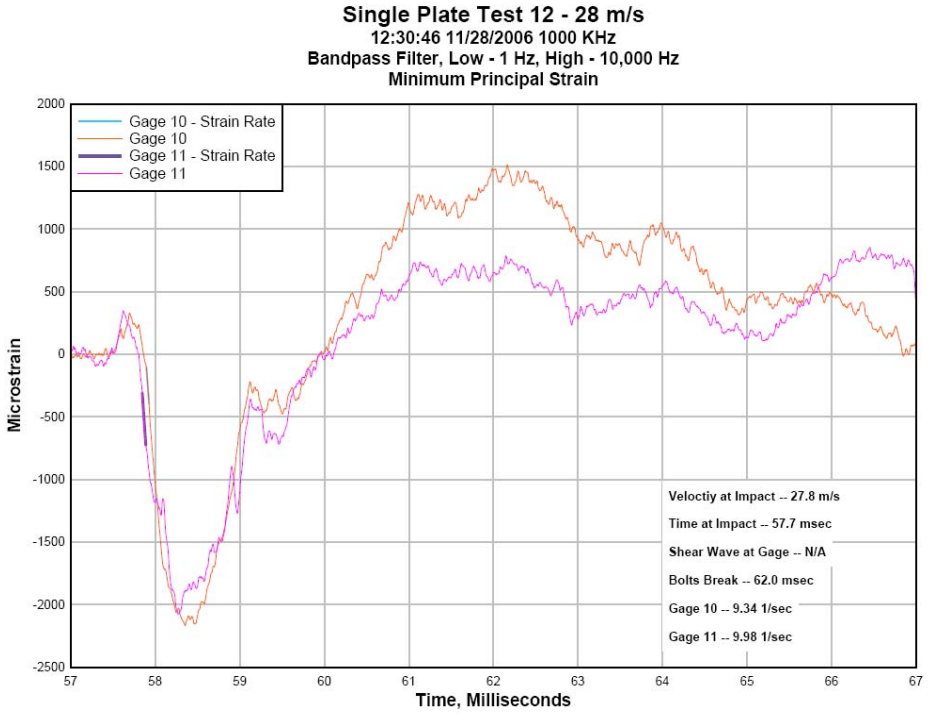

Figure E.115: Minimum principal strains and strain rates for Test 11

Figure E.116: Steel plate post test for Test 12

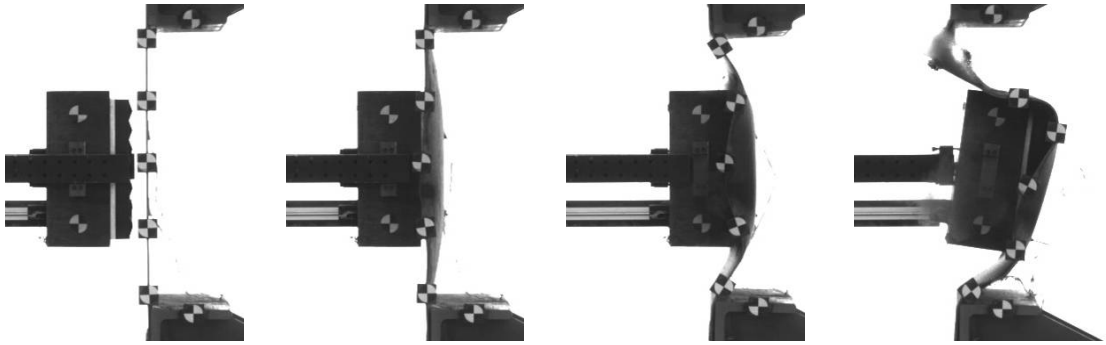

Figure E.117: Progression of damage for Test 12 from Camera 1

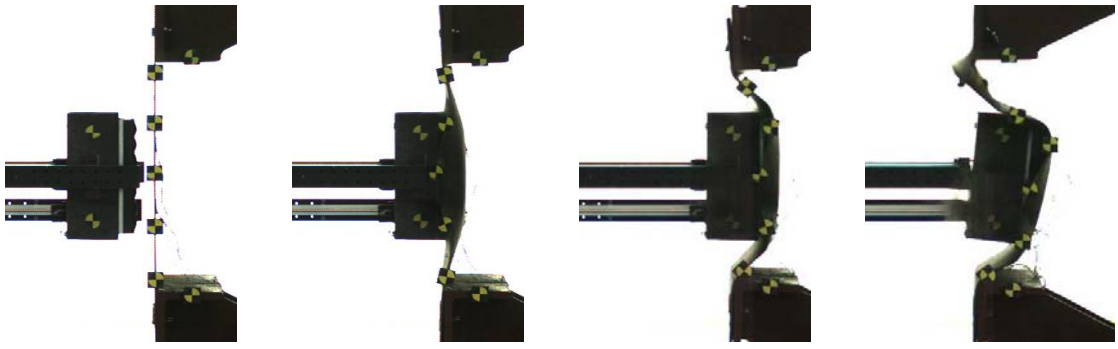

Figure E.118: Progression of damage for Test 12 from Camera 3

E.13 STEEL TOWER SINGLE PLATE: TEST 13 (SP13)

E.13.1 INTRODUCTION

The thirteenth test of the Steel Tower Single Plate test series was performed on November 30th, 2006. The test specimen was a ¼" thick steel plate labeled SP13. The Impacting Mass 1 was attached to the BG with a specimen target velocity of 91.86 ft/sec (28 m/sec). Figure E.119 shows the steel plate prior to impact.

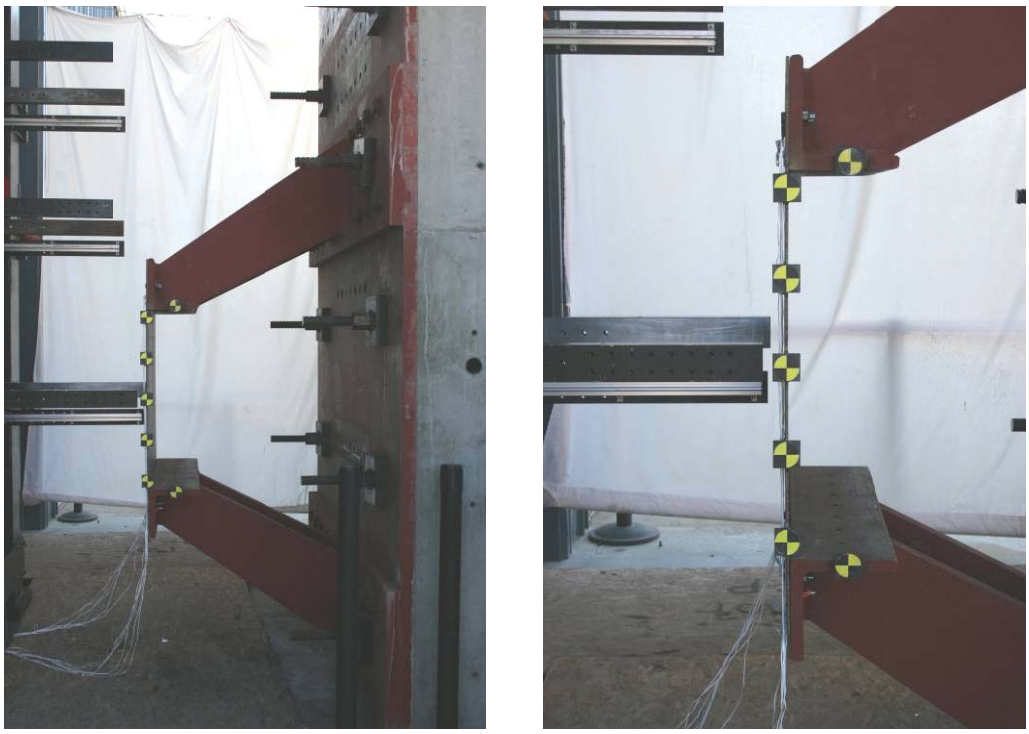

Figure E.119: 1/4" thick steel plate pre test for Test 13

E.13.2 INSTRUMENTATION

E.13.2.1 PHANTOM CAMERAS

The first camera recorded in black and white at a rate of 10,000 frames per second at a resolution of 512x384. This camera was used in order to determine the maximum velocity of the impacting mass and the movement in the plate including the maximum displacement. The second camera recorded in color at a rate of 5,000 frames per second at a resolution of 512x384. This camera recorded the movement at the edge of the bottom support condition. It was not used to gather any specific data. The third camera recorded in color at a rate of 3,000 frames per second at a resolution of 512x384. This camera recorded the same information as Camera One. A picture from each of the camera locations are shown in Figure E.120.

Figure E.120: Phantom Cameras for Test 13

a) Camera One b) Camera Two c) Camera Three

E.13.2.2 TARGET LOCATIONS

Five targets were welded onto the side of the steel plate as show in Figure E.119. They were spaced at the intervals shown in Figure E.121. That figure also shows the location of the targets for the impacting mass. An additional two targets were placed on the angle at the top and the bottom end conditions. The distance between these two points is 74.93 cm (29 ½")

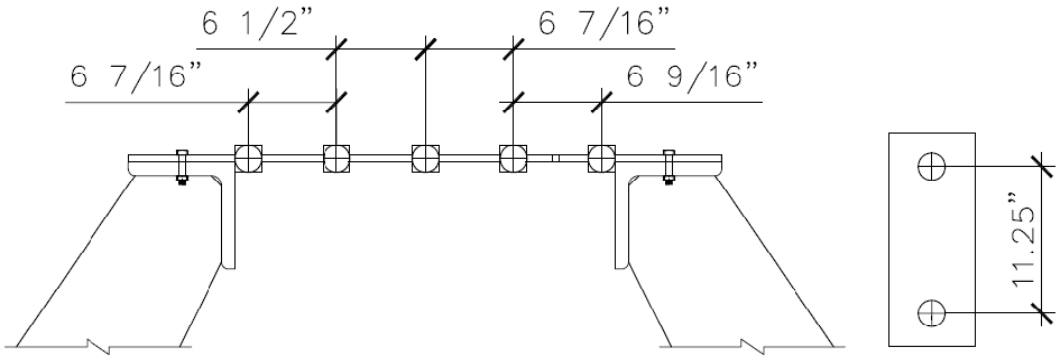

Figure E.121: Target layout on plate and impacting mass for Test 13

E.13.2.3 ACCELERATIONS

For this test one accelerometer was used. This accelerometer was placed 6" south of the centroid of the impacting mass as shown in Figure E.122. The pipe is to protect the accelerometer during the test. The data from this gage was then filtered as shown in Figure E.123.

This test does not impart an impulsive load as would be expected from a typical blast test. Instead, this test simulates the behavior of a flyer plate moving through the structure after

the initial impact at the front plate of the outer cell of the structure. Therefore we are not determining the initial impulsive load from the accelerometers on the BG.

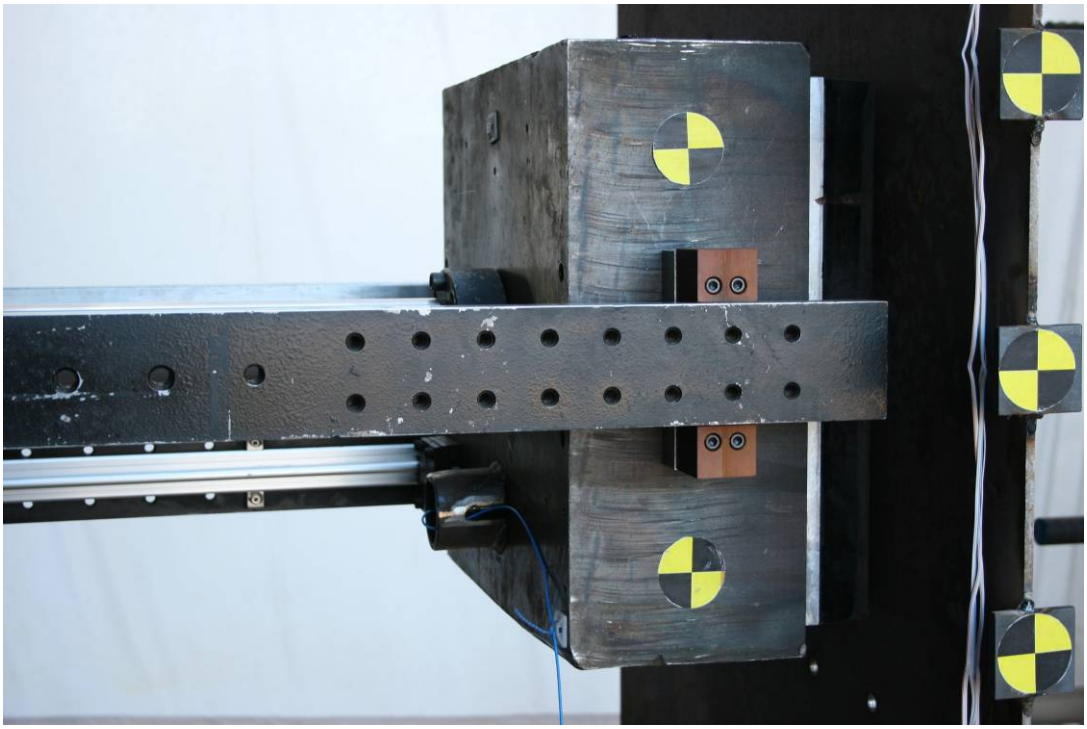

Figure E.122: Accelerometer location for Test 13

E.13.2.4 STRAIN GAGE LOCATIONS

For this test there were four strain gauges labeled 12, 13, 14 and 15. The strain gauges, and their locations, are shown in Figure E.124. Table E.11 shows the specific information about this test, including the time and velocity at impact, if, and when, the bolts failed along with the maximum and minimum principal strain rates. The largest maximum principal strain rate for this test was 5.78 1/sec and was located at strain gage 12 while the largest minimum strain rate for this test was 5.69 1/sec located at strain gage 15. The maximum principal strains for gauges 12, 13, 14 and 15 can be found in Figure E.125 and the minimum principal strains for the same gauges can be found in Figure E.126.

Table E.11: Stain rate information for Test 13

Strain Gage Number	Actual Velocity	Initial Impact	Shear Wave at Gage	Bolts Break	Maximum Principal Strain Rate	Minimum Principal Strain Rate
12	28.1 m/s	57.90 msec	-	62.30 msec	5.78 1/sec	5.45 1/sec
13	28.1 m/s	57.90 msec	-	62.30 msec	4.74 1/sec	5.40 1/sec
14	28.1 m/s	57.90 msec	-	62.30 msec	5.16 1/sec	5.68 1/sec
15	28.1 m/s	57.90 msec	-	62.30 msec	5.62 1/sec	5.69 1/sec

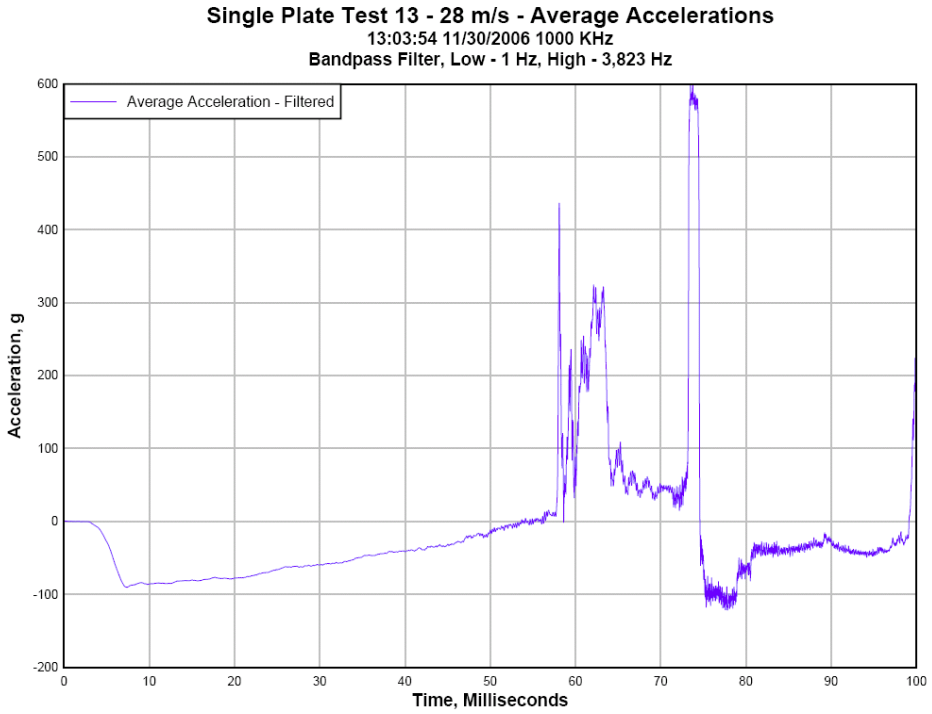

Figure E.123: Filtered accelerometer data for Test 13

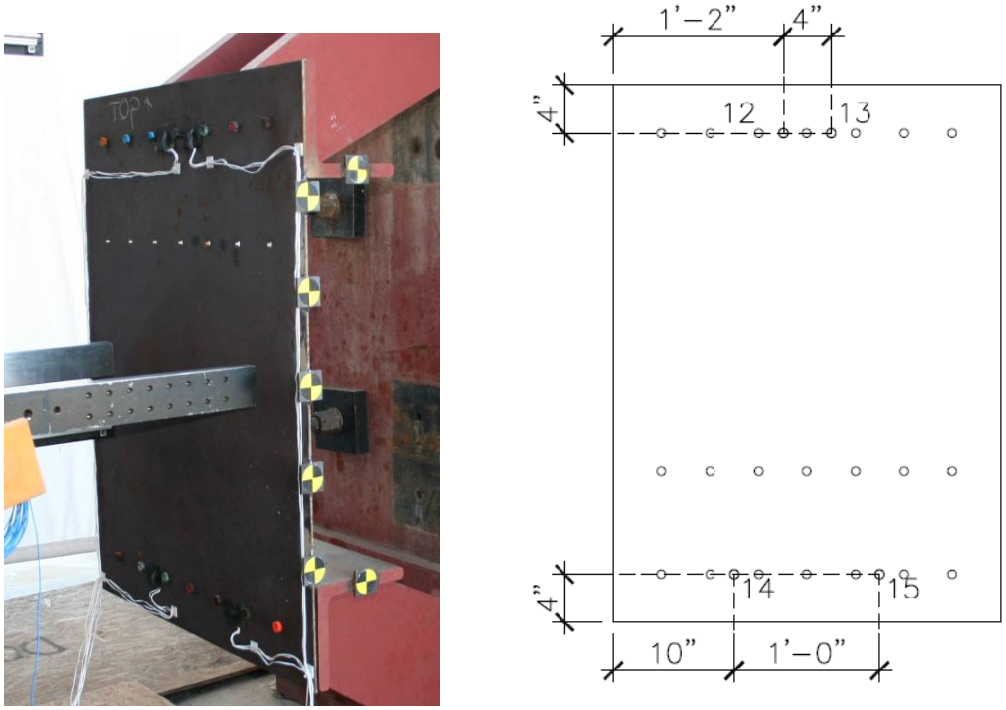

Figure E.124: Strain gage layout for Test 1

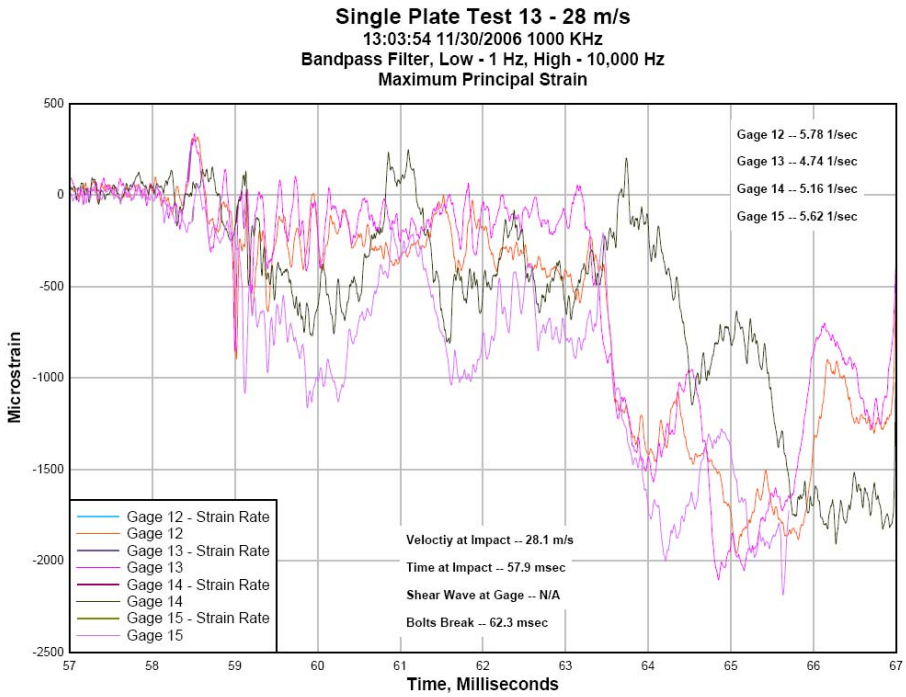

Figure E.125: Maximum principal strains and strain rates for Test 1

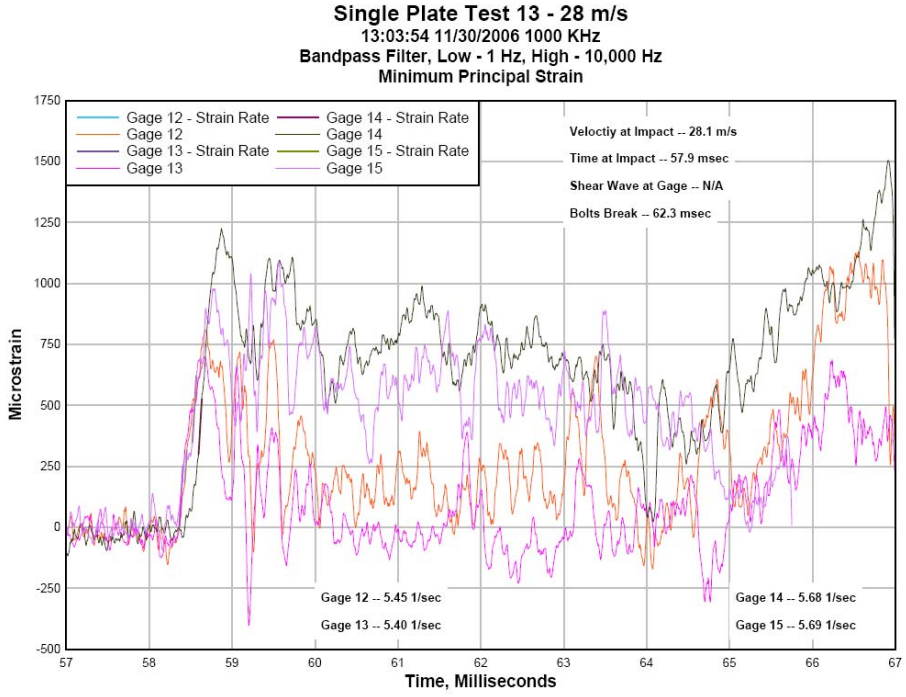

Figure E.126: Minimum principal strains and strain rates for Test 13

E.13.2.5 BOLT TYPE

A total of fourteen Grade 5 bolts (High Strength Bolts) were used for this test. They were all tightened to a torque of 50 ft-lbs.

E.13.3 BLAST GENERATOR DATA

The initial impact of the single BG was 91.67 ft/sec (27.94 m/sec) with a goal velocity of 28 m/s. It had one accelerometer mounted to the back side of the impact plate as discussed in Section E.13.2.3. The average impact velocity for the impacting mass and the steel plate was calculated using the TEMA Track Eye tracking software.

E.13.4 SPECIMEN BEHAVIOR

The loading of the BG plate imparted an initial velocity of 91.67 ft/sec (27.94 m/sec) to the specimen. This caused plate to deform in both directions. The longitudinal deflection (in the north-south direction) behaved in a typical one-way flexural shape. In order to get the velocity as high as needed the test was designed to have the impacting mass break free from the BG and launch itself into the plate. This test imparted enough energy into the system that the all fourteen bolts broke simultaneously. The approximate maximum deflection of the plate before the bolts broke was 5 9/16".

During the test pieces of bolts flew approximately 14' directly north of the test set-up. Figure E.127 shows the plate and impacting mass where they landed after the test. During the test two different phantom cameras were used to capture the failure modes from two different angles. Figure E.128 shows the progression of damage for this test from Phantom Camera One. Figure E.129 shows the progression of damage for this test from Phantom Camera Three

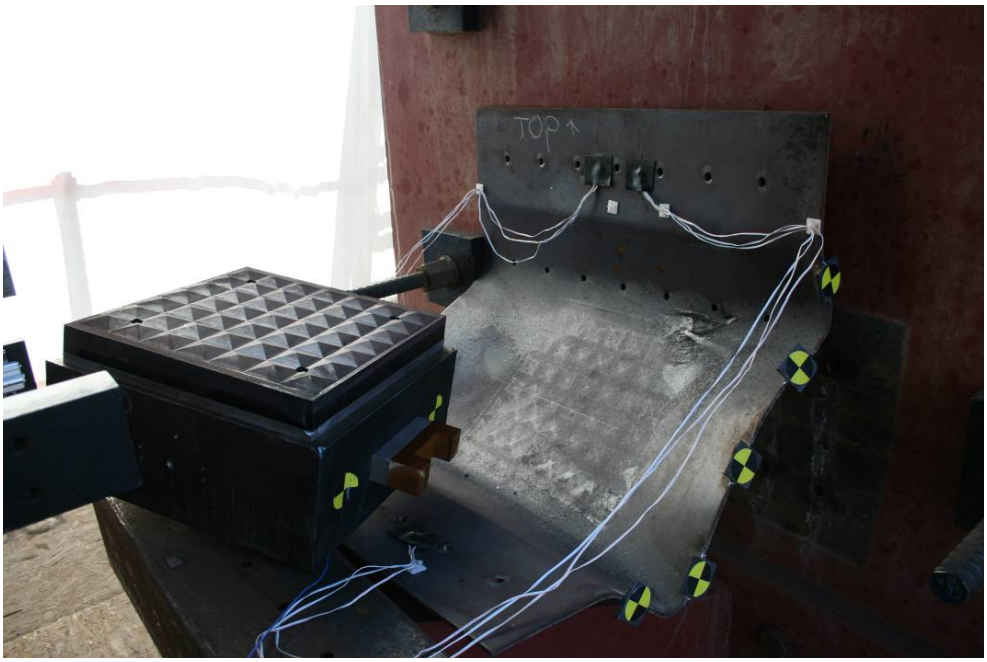

Figure E.127: Steel plate post test for Test 13

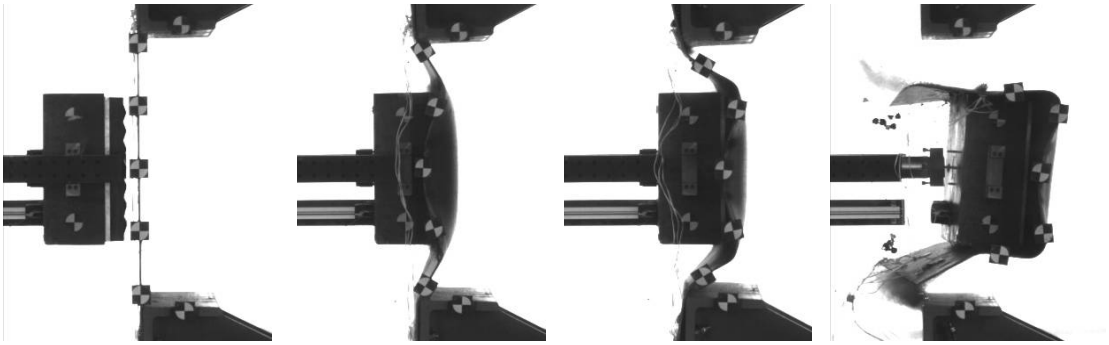

Figure E.128: Progression of damage for Test 13 from Camera 1

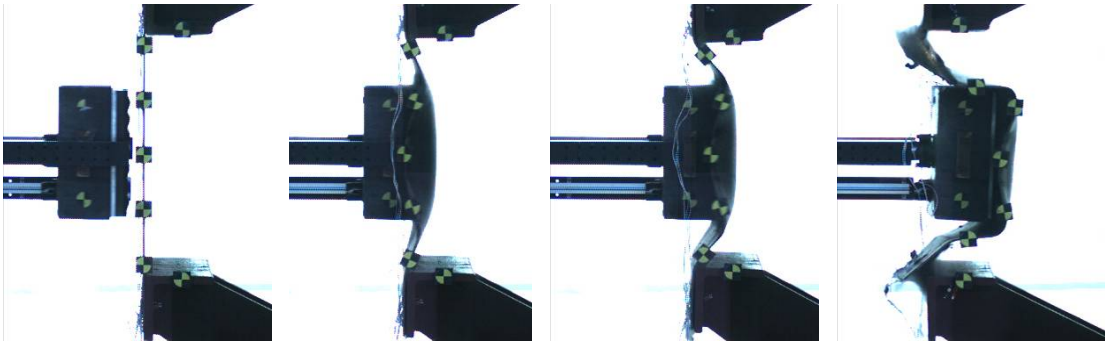

Figure E.129: Progression of damage for Test 13 from Camera 3

E.14 STEEL TOWER SINGLE PLATE: TEST 14 (SP14)

E.14.1 INTRODUCTION

The fourteenth test of the Steel Tower Single Plate test series was performed on December 4th, 2006. The test specimen was a ¼" thick steel plate labeled SP14. The Impacting Mass 1 was attached to the BG with a specimen target velocity of 91.86 ft/sec (28 m/sec). Figure E.130 shows the steel plate prior to impact.

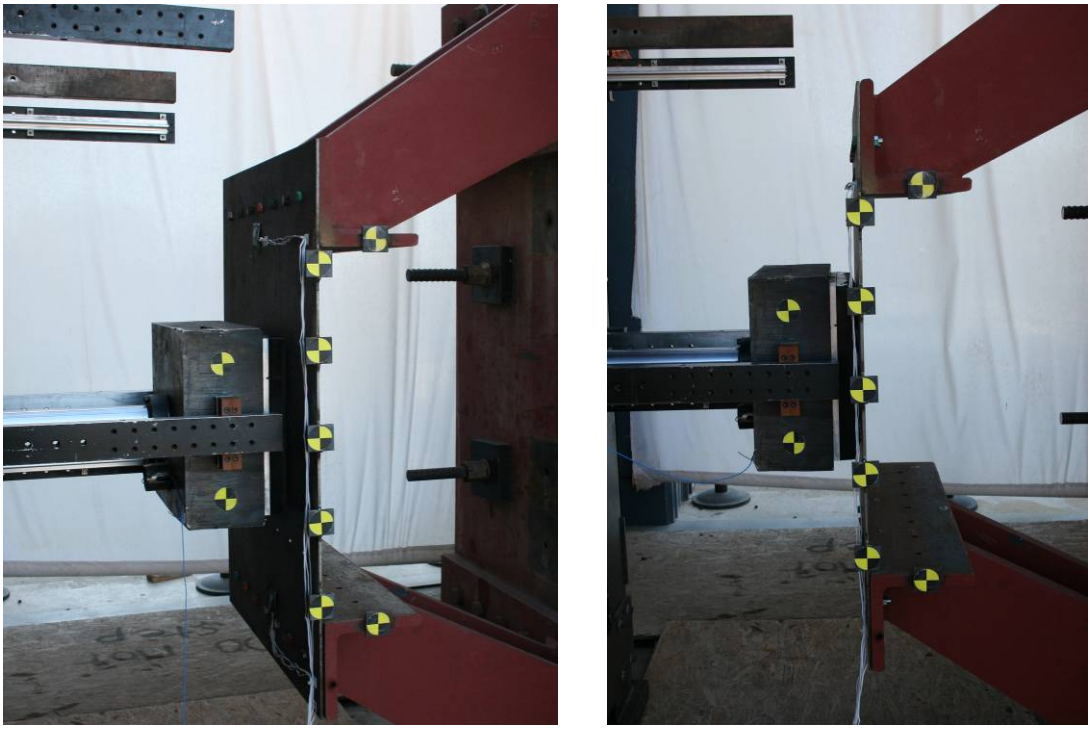

Figure E.130: 1/4" thick steel plate pre test for Test 14

E.14.2 INSTRUMENTATION

E.14.2.1 PHANTOM CAMERAS

The first camera recorded in black and white at a rate of 10,000 frames per second at a resolution of 512x384. This camera was used in order to determine the maximum velocity of the impacting mass and the movement in the plate including the maximum displacement. The second camera recorded in color at a rate of 5,000 frames per second at a resolution of 512x384. This camera recorded the movement at the edge of the bottom support condition. It was not used to gather any specific data. The third camera recorded in color at a rate of 6,006 frames per second at a resolution of 512x384. This camera recorded the same information as Camera One. A picture from each of the camera locations are shown in Figure E.131.

Figure E.131: Phantom Cameras for Test 14

a) Camera One b) Camera Two c) Camera Three

E.14.2.2 TARGET LOCATIONS

Five targets were welded onto the side of the steel plate as show in Figure E.130. They were spaced at the intervals shown in Figure E.132. That figure also shows the location of the targets for the impacting mass. An additional two targets were placed on the angle at the top and the bottom end conditions. The distance between these two points is 74.93 cm (29 ½")

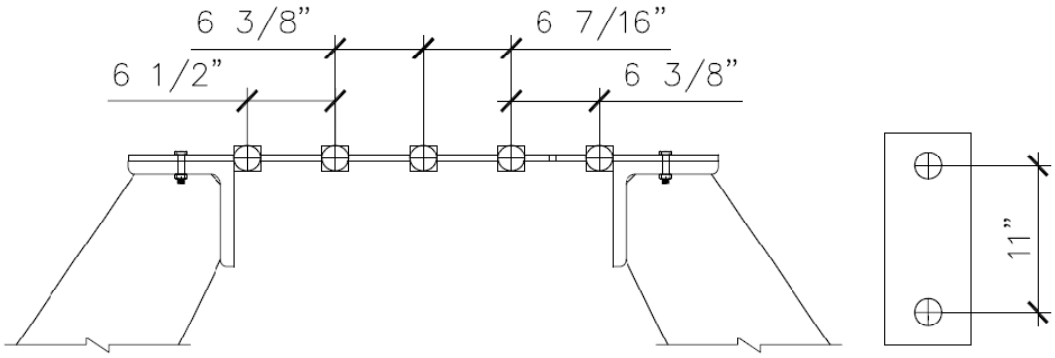

Figure E.132: Target layout on plate and impacting mass for Test 14

E.14.2.3 ACCELERATIONS

For this test one accelerometer was used. This accelerometer was placed 6" south of the centroid of the impacting mass as shown in Figure E.133. The pipe is to protect the accelerometer during the test. The data from this gage was then filtered as shown in Figure E.134.

This test does not impart an impulsive load as would be expected from a typical blast test. Instead, this test simulates the behavior of a flyer plate moving through the structure after the initial impact at the front plate of the outer cell of the structure. Therefore we are not determining the initial impulsive load from the accelerometers on the BG.

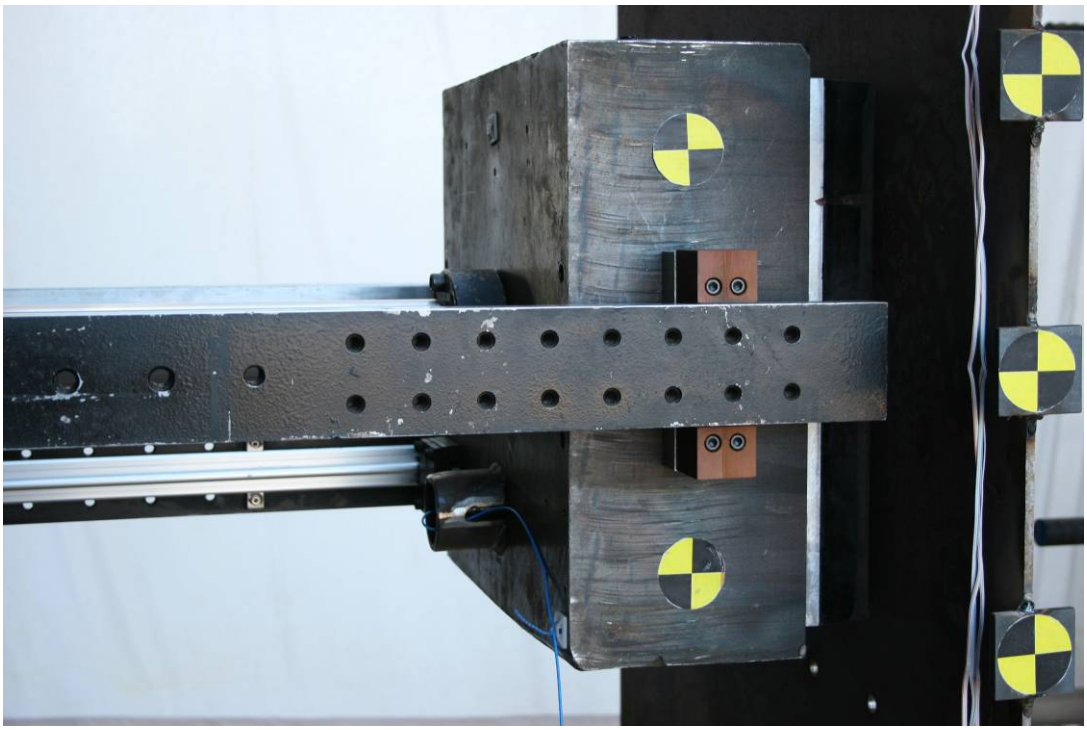

Figure E.133: Accelerometer location for Test 14

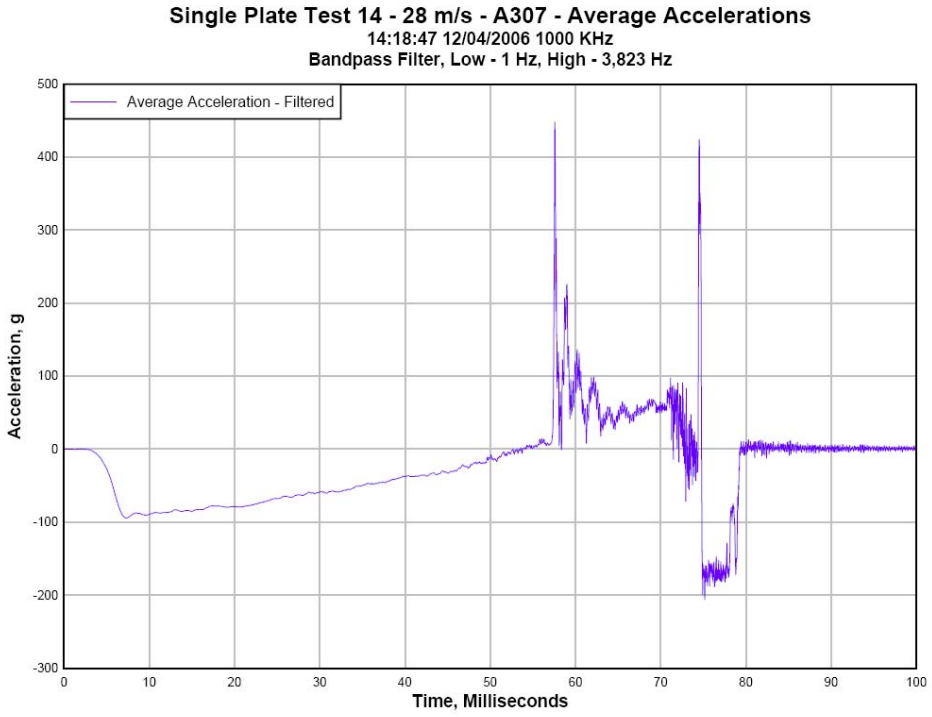

Figure E.134: Filtered accelerometer data for Test 14

E.14.2.4 STRAIN GAGE LOCATIONS

For this test there were two strain gauges labeled 17 and 18. The strain gauges, and their locations, are shown in Figure E.135. Table E.12 shows the specific information about this test, including the time and velocity at impact, if, and when, the bolts failed along with the maximum and minimum principal strain rates. The largest maximum principal strain rate for this test was 32.18 1/sec and was located at strain gage 17 while the largest minimum strain rate for this test was 7.46 1/sec located at strain gage 17. The maximum principal strains for gauges 17 and 18 can be found in Figure E.136 and the minimum principal strains for the same gauges can be found in Figure E.137.

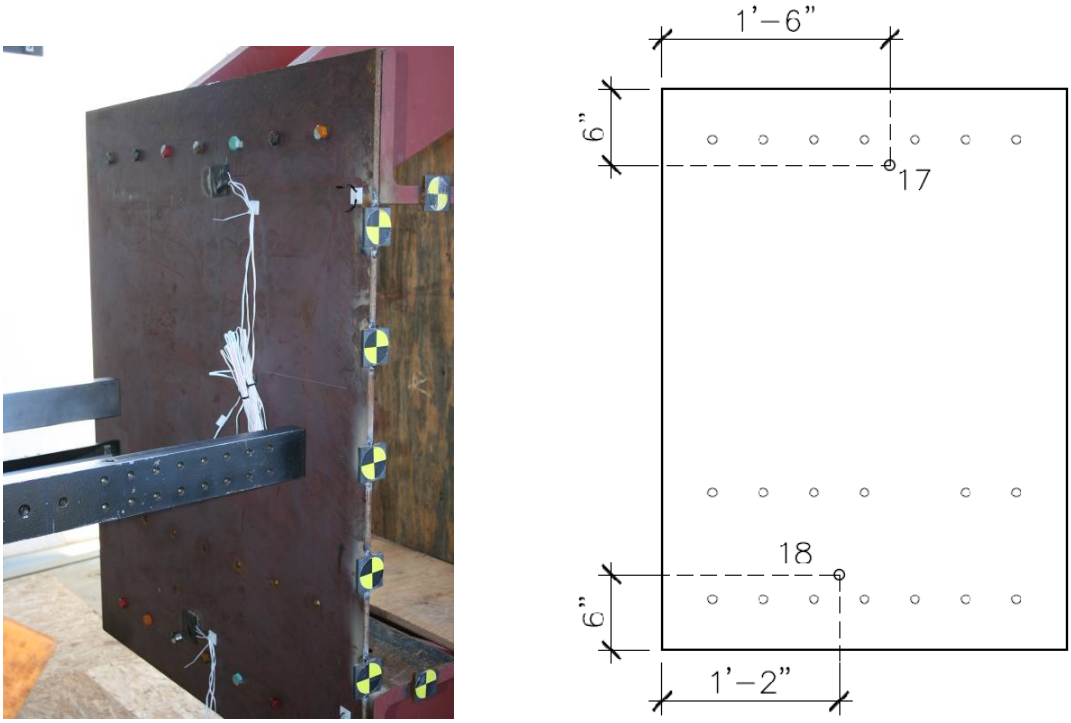

Figure E.135: Strain gage layout for Test 14

Table E.12: Stain rate information for Test 14

Strain Gage Number	Actual Velocity	Initial Impact	Shear Wave at Gage	Bolts Break	Maximum Principal Strain Rate	Minimum Principal Strain Rate
17	28.1 m/s	57.40 msec	-	60.20 msec	32.18 1/sec	7.46 1/sec
18	28.1 m/s	57.40 msec	-	60.20 msec	31.57 1/sec	6.68 1/sec

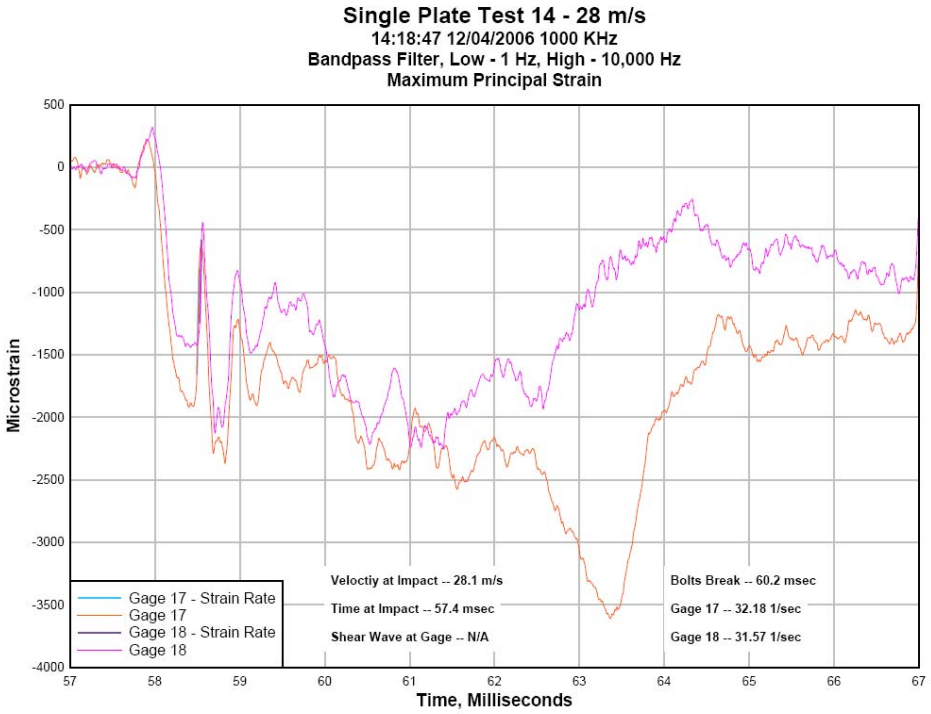

Figure E.136: Maximum principal strains and strain rates for Test 14

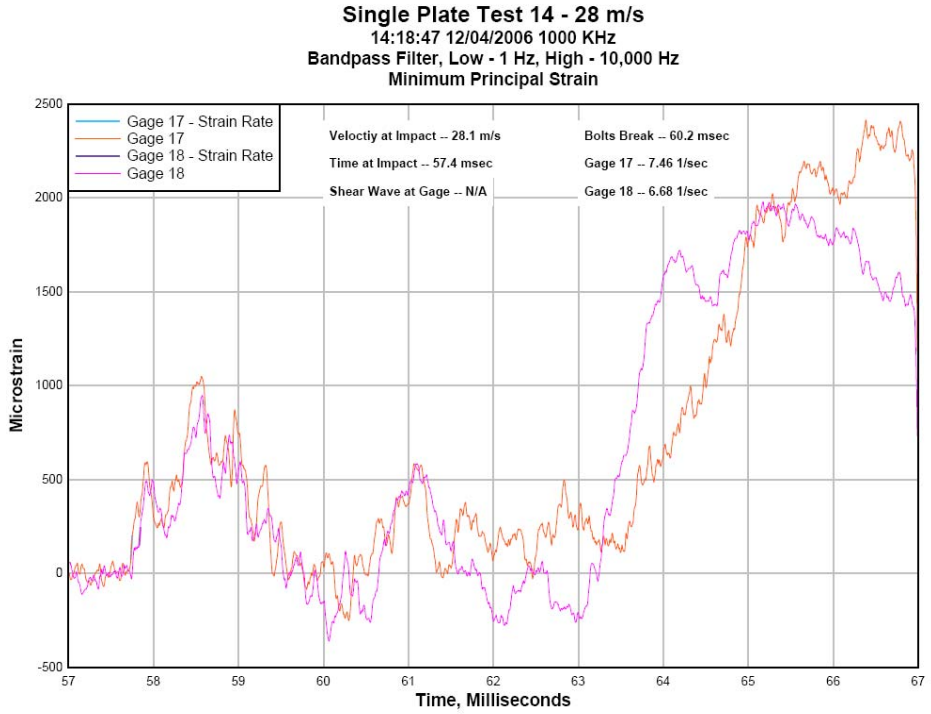

Figure E.137: Minimum principal strains and strain rates for Test 14

E.14.2.5 BOLT TYPE

A total of fourteen A307 bolts (Low Strength Bolts similar to Rivets) were used for this test. They were all tightened to a torque of 40 ft-lbs.

E.14.3 BLAST GENERATOR DATA

The initial impact of the single BG was 92.19 ft/sec (28.10 m/sec) with a goal velocity of 28 m/s. It had one accelerometer mounted to the back side of the impact plate as discussed in Section E.14.2.3. The average impact velocity for the impacting mass and the steel plate was calculated using the TEMA Track Eye tracking software.

E.14.4 SPECIMEN BEHAVIOR

The loading of the BG plate imparted an initial velocity of 92.19 ft/sec (28.10 m/sec) to the specimen. This caused plate to deform in both directions. The longitudinal deflection (in the north-south direction) behaved in a typical one-way flexural shape. In order to get the velocity as high as needed the test was designed to have the impacting mass break free from the BG and launch itself into the plate. This test imparted enough energy into the system that the all fourteen bolts broke simultaneously. It is nearly impossible to get an accurate maximum deflection of the plate when the bolts broke for this test. When the mass impacted the plate the free edges of the plate moved inward. In past tests these edges would then move back before the bolts would break from the plate. That did not occur in this test, therefore the targets that are used in order to determine the maximum deflection were not valid.

During the test pieces of bolts flew approximately 16’-9” northwest of the test set-up, 23’ directly south of the test set-up towards the control room and almost 11’ into the shop area. Figure E.138 shows the plate and impacting mass where they landed after the test. During the test two different phantom cameras were used to capture the failure modes from two different angles. Figure E.139 shows the progression of damage for this test from Phantom Camera One. Figure E.140 shows the progression of damage for this test from Phantom Camera Three.

Figure E.138: Steel plate post test for Test 14

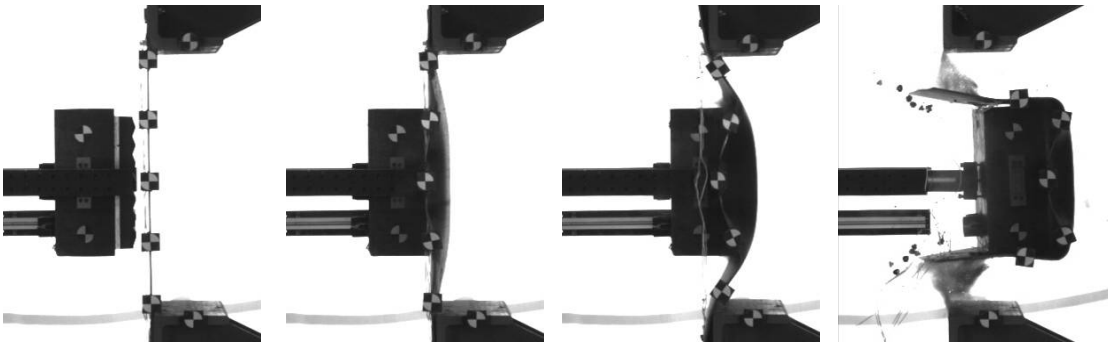

Figure E.139: Progression of damage for Test 14 from Camera 1

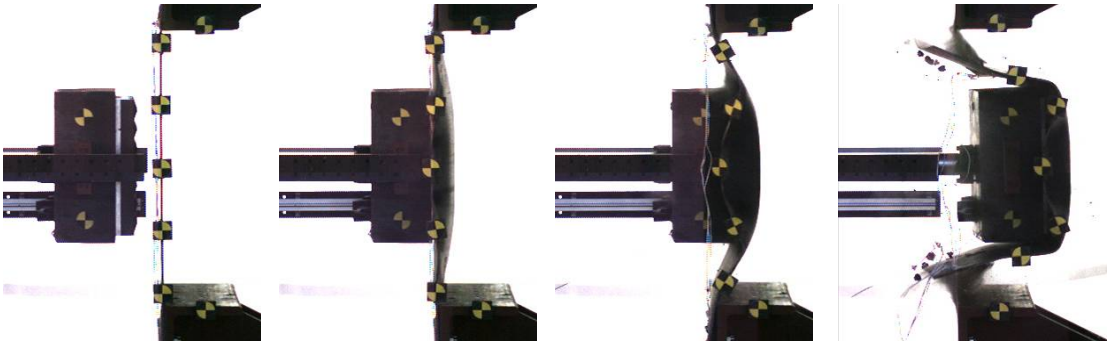

Figure E.140: Progression of damage for Test 14 from Camera 3

E.15 STEEL TOWER SINGLE PLATE: TEST 15 (SP15)

E.15.1 INTRODUCTION

The fifteenth test of the Steel Tower Single Plate test series was performed on December 7th, 2006. The test specimen was a ½" thick steel plate labeled SP15. The Impacting Mass 1 was attached to the BG with a specimen target velocity of 91.86 ft/sec (28 m/sec). Figure E.141 shows the steel plate prior to impact.

Figure E.141: 1/2" thick steel plate pre test for Test 15

E.15.2 INSTRUMENTATION

E.15.2.1 PHANTOM CAMERAS

The first camera recorded in black and white at a rate of 10,000 frames per second at a resolution of 512x384. This camera was used in order to determine the maximum velocity of the impacting mass and the movement in the plate including the maximum displacement. The second camera recorded in color at a rate of 5,000 frames per second at a resolution of 512x384. This camera recorded the movement at the edge of the bottom support condition. It was not used to gather any specific data. The third camera recorded in color at a rate of 10,000 frames per second at a resolution of 512x384. This camera recorded the same information as Camera One. A picture from each of the camera locations are shown in Figure E.142.

Figure E.142: Phantom Cameras for Test 15

a) Camera One b) Camera Two c) Camera Three

E.15.2.2 TARGET LOCATIONS

Five targets were welded onto the side of the steel plate as show in Figure E.141. They were spaced at the intervals shown in Figure E.143. That figure also shows the location of the targets for the impacting mass. An additional two targets were placed on the angle at the top and the bottom end conditions. The distance between these two points is 74.93 cm (29 ½")

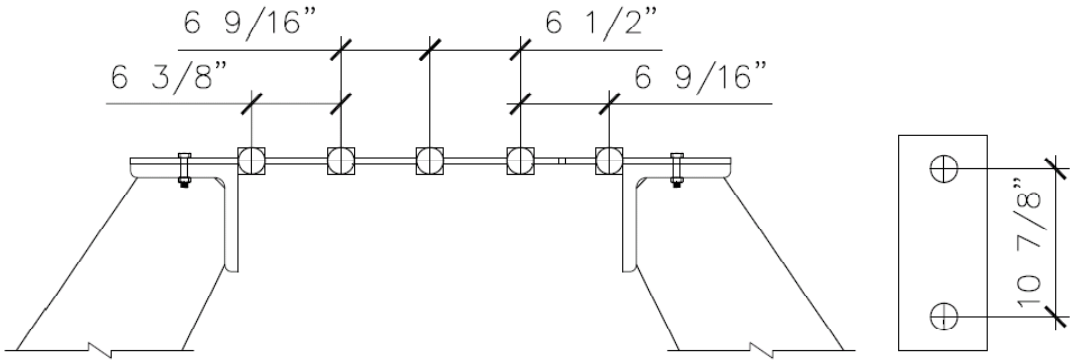

Figure E.143: Target layout on plate and impacting mass for Test 15

E.15.2.3 ACCELERATIONS

For this test accelerometers were not used.

E.15.2.4 STRAIN GAGE LOCATIONS

For this test there were two strain gauges labeled 17 and 18. The strain gauges, and their locations, are shown in Figure E.144. Table E.13 shows the specific information about this test, including the time and velocity at impact, if, and when, the bolts failed along with the maximum and minimum principal strain rates. The largest maximum principal strain rate for this test was 11.73 1/sec and was located at strain gage 17 while the largest minimum strain

rate for this test was 6.49 1/sec located at strain gage 17. The maximum principal strains for gauges 17 and 18 can be found in Figure E.145 and the minimum principal strains for the same gauges can be found in Figure E.146.

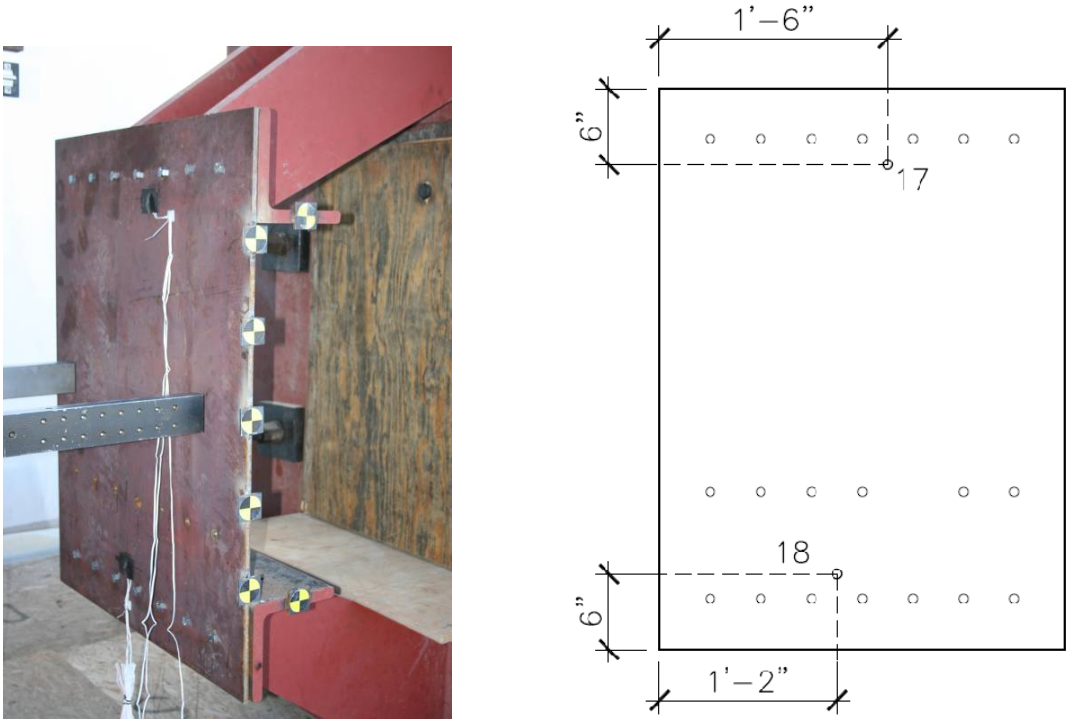

Figure E.144: Strain gage layout for Test 15

Table E.13: Stain rate information for Test 15

Strain Gage Number	Actual Velocity	Initial Impact	Shear Wave at Gage	Bolts Break	Maximum Principal Strain Rate	Minimum Principal Strain Rate
17	27.7 m/s	58.10 msec	-	61.10 msec	-11.73 1/sec	-6.49 1/sec
18	27.7 m/s	58.10 msec	-	61.10 msec	-10.89 1/sec	4.26 1/sec

E.15.2.5 BOLT TYPE

A total of fourteen A307 bolts (Low Strength Bolts similar to Rivets) were used for this test. They were all tightened to a torque of 40 ft-lbs.

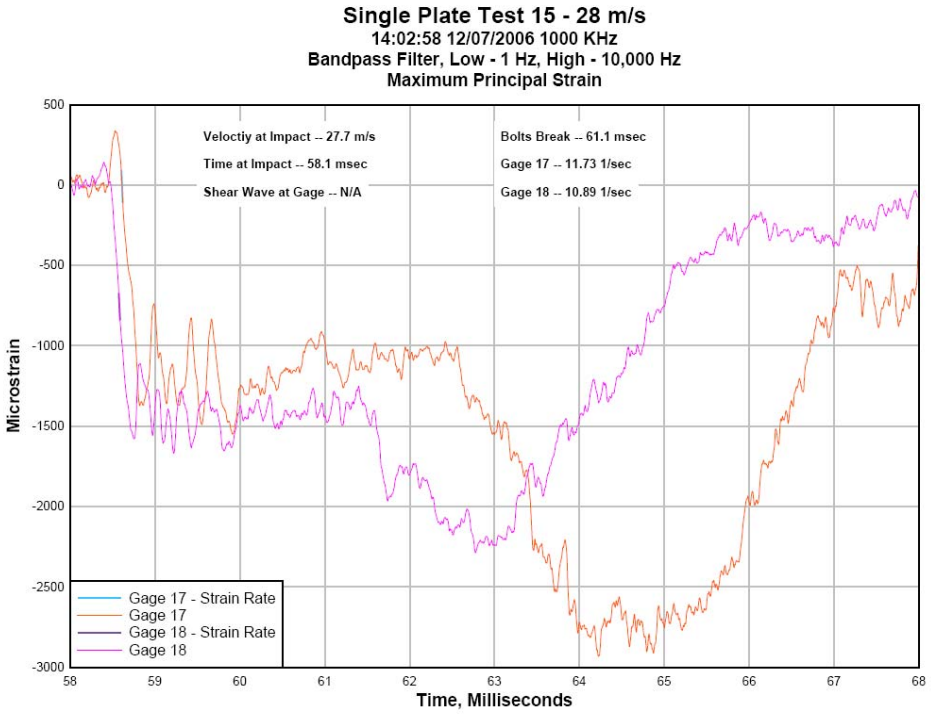

Figure E.145: Maximum principal strains and strain rates for Test 15

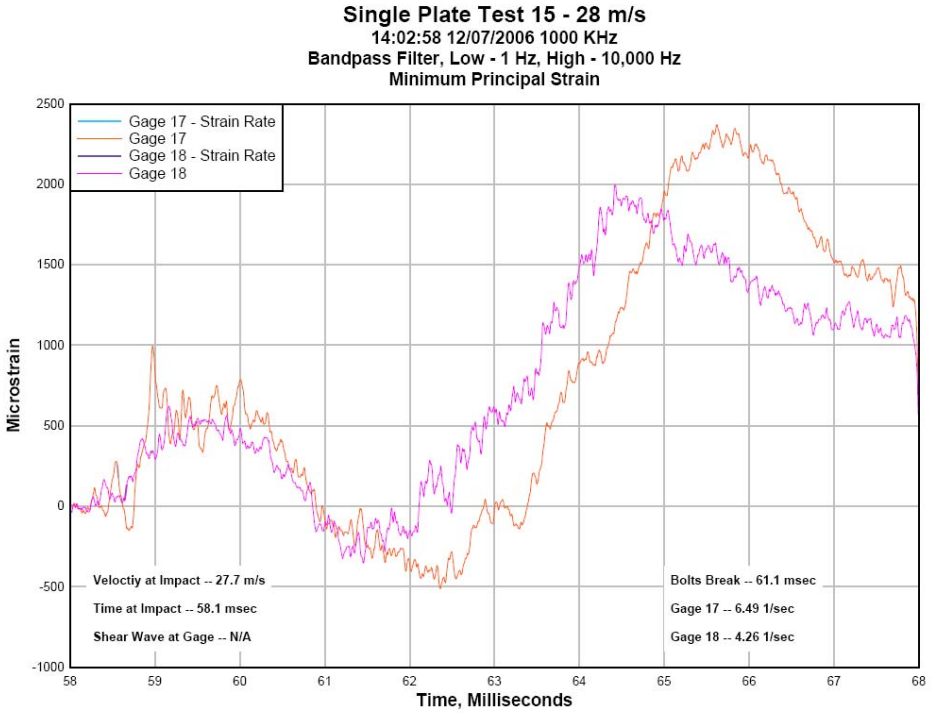

Figure E.146: Minimum principal strains and strain rates for Test 15

E.15.2.6 BLAST GENERATOR DATA

The initial impact of the single BG was 90.88 ft/sec (27.70 m/sec) with a goal velocity of 28 m/s. The average impact velocity for the impacting mass and the steel plate was calculated using the TEMA Track Eye tracking software.

E.15.3 SPECIMEN BEHAVIOR

The loading of the BG plate imparted an initial velocity of 90.88 ft/sec (27.70 m/sec) to the specimen. This caused plate to deform in both directions. The longitudinal deflection (in the north-south direction) behaved in a typical one-way flexural shape. In order to get the velocity as high as needed the test was designed to have the impacting mass break free from the BG and launch itself into the plate. This test imparted enough energy into the system that the all fourteen bolts broke simultaneously. It is nearly impossible to get an accurate maximum deflection of the plate when the bolts broke for this test. When the mass impacted the plate the free edges of the plate moved inward, in past tests these edges would then move back before the bolts would break from the plate. That did not occur in this test; therefore the targets that are used in order to determine the maximum deflection were not valid.

During the test pieces of bolts flew approximately 44’ northwest of the test set-up, 20’ directly south of the test set-up towards the control room. Figure E.147 shows the plate and impacting mass where they landed after the test. During the test two different phantom cameras were used to capture the failure modes from two different angles. Figure E.148 shows the progression of damage for this test from Phantom Camera One. Figure E.149 shows the progression of damage for this test from Phantom Camera Three.

Figure E.147: Steel plate post test for Test 15

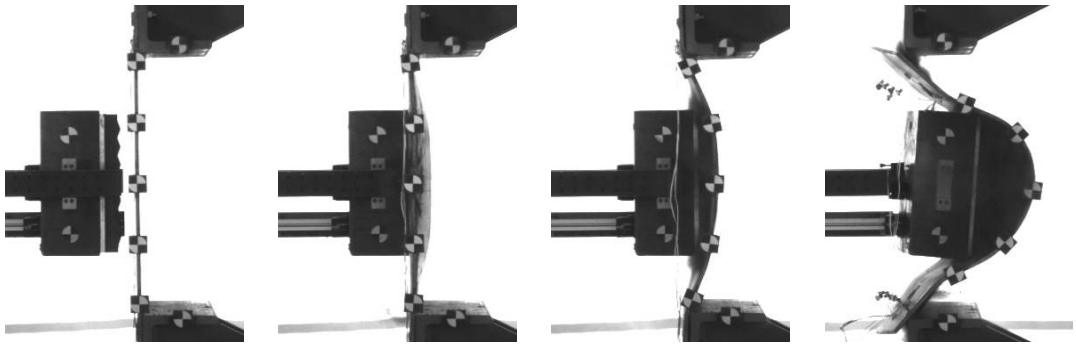

Figure E.148: Progression of damage for Test 15 from Camera 1

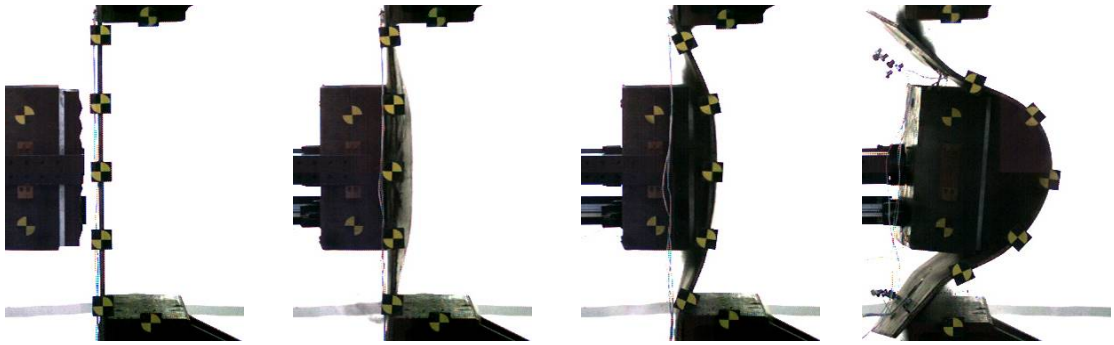

Figure E.149: Progression of damage for Test 15 from Camera 3

E.16 STEEL TOWER SINGLE PLATE: TEST 16 (SP16)

E.16.1 INTRODUCTION

The sixteenth test of the Steel Tower Single Plate test series was performed on December 13th, 2006. The test specimen was a ¼" thick steel plate labeled SP16. The Impacting Mass 1 was attached to the BG with a specimen target velocity of 62.34 ft/sec (19 m/sec). Figure E.150 shows the steel plate prior to impact.

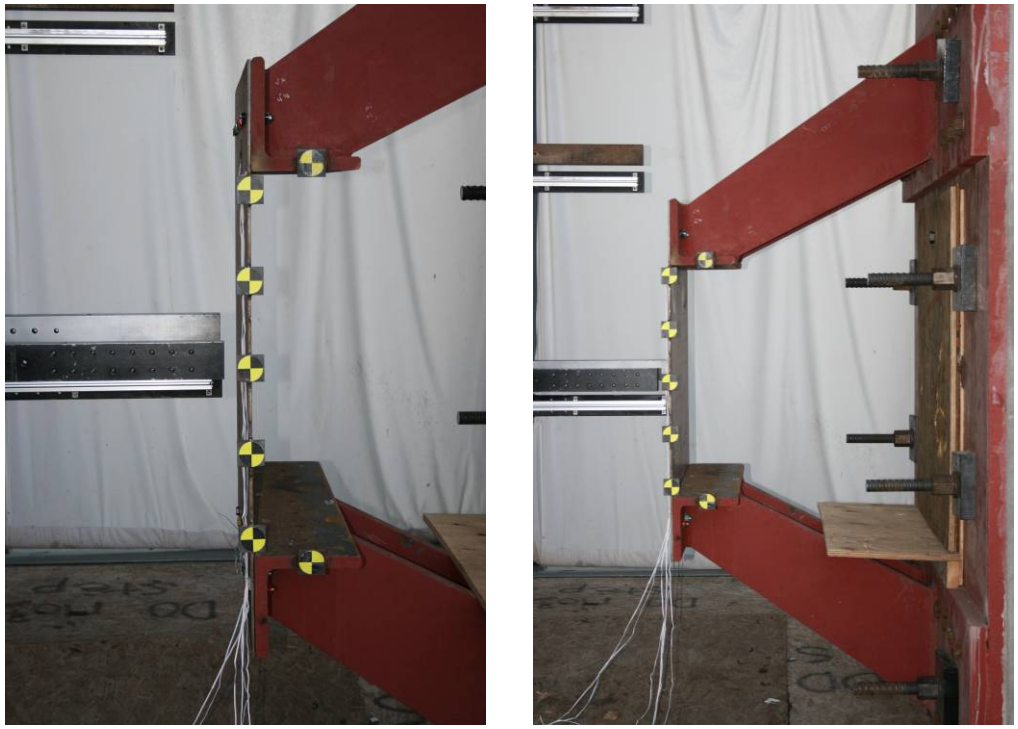

Figure E.150: 1/4" thick steel plate pre test for Test 16

E.16.2 INSTRUMENTATION

E.16.2.1 PHANTOM CAMERAS

The first camera recorded in black and white at a rate of 10,000 frames per second at a resolution of 512x384. This camera was used in order to determine the maximum velocity of the impacting mass and the movement in the plate including the maximum displacement. The second camera recorded in color at a rate of 5,000 frames per second at a resolution of 512x384. This camera recorded the overall behavior of the test specimen. It was not used to gather any specific data. The third camera recorded in color at a rate of 2,006 frames per second at a resolution of 480x480. This camera captured the failure of the bolts. A picture from each of the camera locations are shown in Figure E.151.

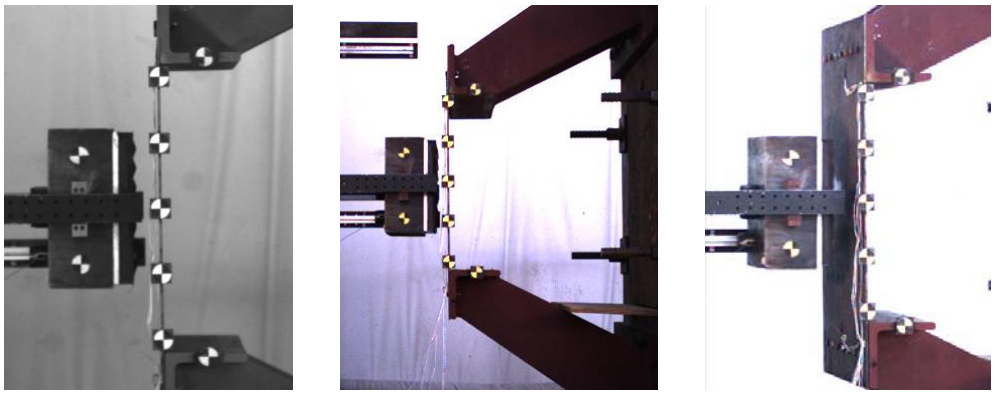

Figure E.151: Phantom Cameras for Test 16

a) Camera One b) Camera Two c) Camera Three

E.16.2.2 TARGET LOCATIONS

Five targets were welded onto the side of the steel plate as show in Figure E.150. They were spaced at the intervals shown in Figure E.152. That figure also shows the location of the targets for the impacting mass. An additional two targets were placed on the angle at the top and the bottom end conditions. The distance between these two points is 74.93 cm (29 ½")

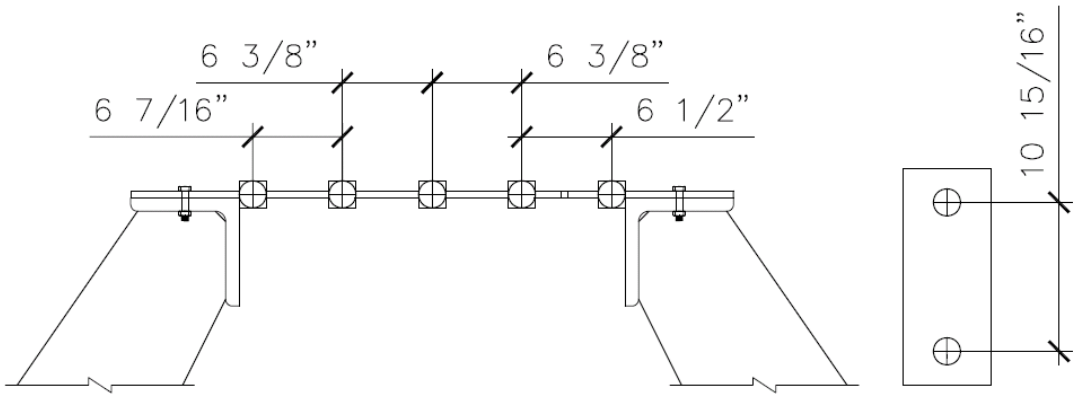

Figure E.152: Target layout on plate and impacting mass for Test 16

E.16.2.3 ACCELERATIONS

For this test one accelerometer was used. This accelerometer was placed 6" south of the centroid of the impacting mass as shown in Figure E.153. The pipe is to protect the accelerometer during the test. The data from this gage was then filtered as shown in Figure E.154.

This test does not impart an impulsive load as would be expected from a typical blast test. Instead, this test simulates the behavior of a flyer plate moving through the structure after the initial impact at the front plate of the outer cell of the structure. Therefore we are not determining the initial impulsive load from the accelerometers on the BG.

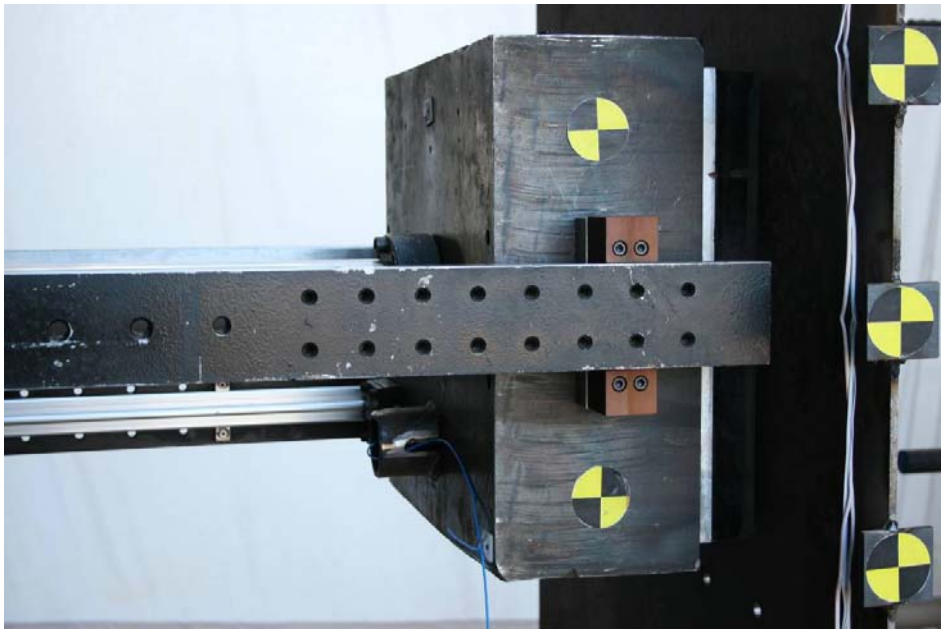

Figure E.153: Accelerometer location for Test 16

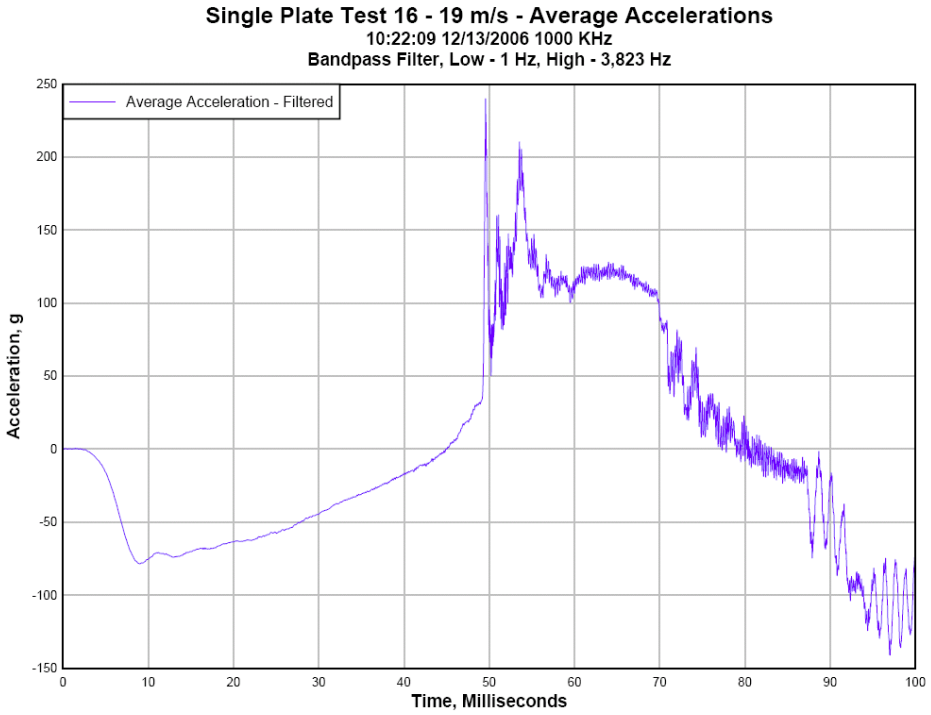

Figure E.154: Filtered accelerometer data for Test 16

E.16.2.4 STRAIN GAGE LOCATIONS

For this test there were two strain gauges labeled 17 and 18. The strain gauges, and their locations, are shown in Figure E.155. Table E.14 shows the specific information about this test, including the time and velocity at impact, if, and when, the bolts failed along with the maximum and minimum principal strain rates. The largest maximum principal strain rate for this test was 29.95 1/sec and was located at strain gage 18 while the largest minimum strain rate for this test was 10.98 1/sec located at strain gage 18. The maximum principal strains for gauges 17 and 18 can be found in Figure E.156 and the minimum principal strains for the same gauges can be found in
Figure E.157.

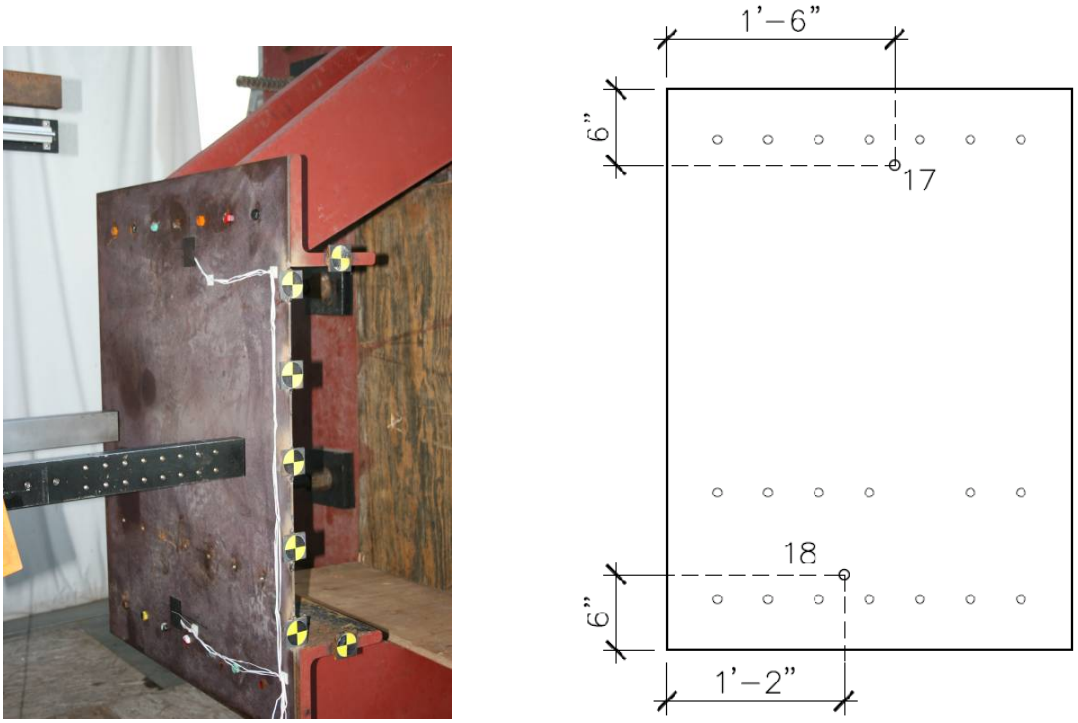

Figure E.155: Strain gage layout for Test 16

Table E.14: Stain rate information for Test 16

Strain Gage Number	Actual Velocity	Initial Impact	Shear Wave at Gage	Bolts Break	Maximum Principal Strain Rate	Minimum Principal Strain Rate
17	18.6 m/s	49.30 msec	53.50 msec	55.10 msec	27.16 1/sec	10.12 1/sec
18	18.6 m/s	49.30 msec	53.50 msec	55.10 msec	29.95 1/sec	10.98 1/sec

E.16.2.5 BOLT TYPE

A total of fourteen A307 bolts (Low Strength Bolts similar to Rivets) were used for this test. They were all tightened to a torque of 40 ft-lbs.

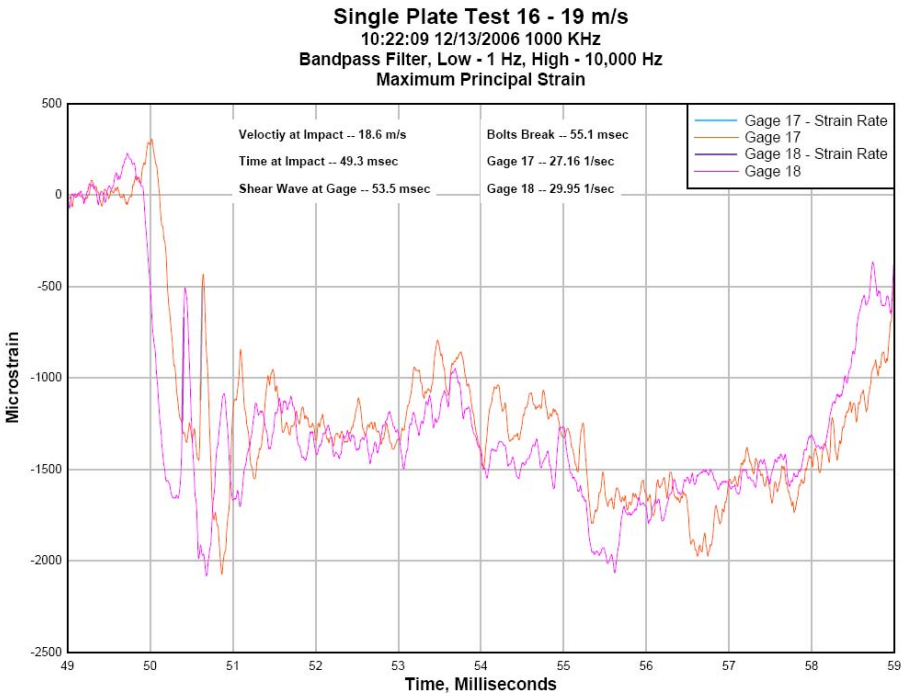

Figure E.156: Maximum principal strains and strain rates for Test 16

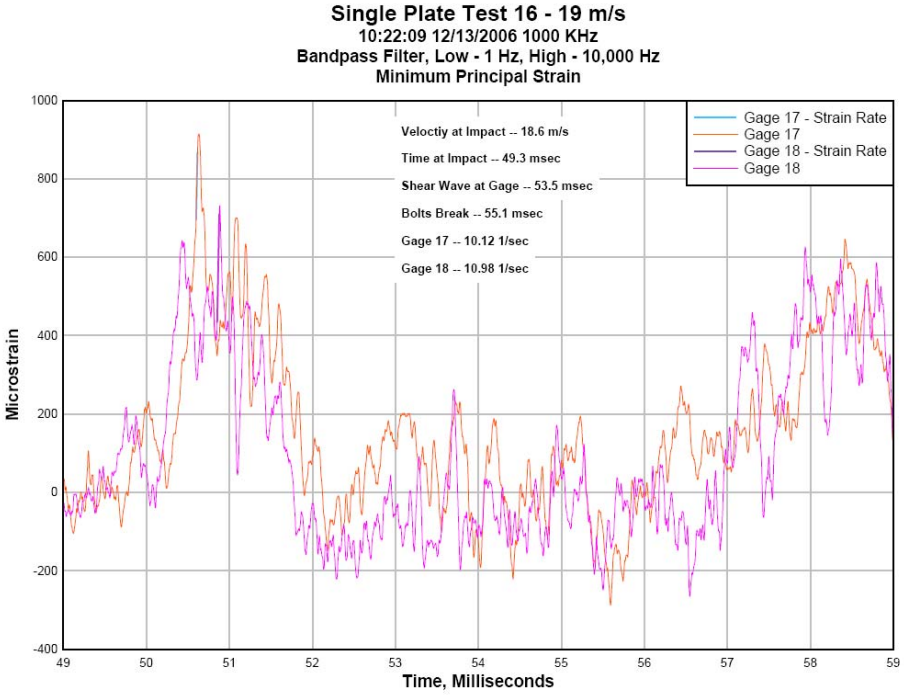

Figure E.157: Minimum principal strains and strain rates for Test 16

E.16.3 BLAST GENERATOR DATA

The initial impact of the single BG was 61.06 ft/sec (18.61 m/sec) with a goal velocity of 19 m/s. It had one accelerometer mounted to the back side of the impact plate as discussed in Section E.16.2.3. The average impact velocity for the impacting mass and the steel plate was calculated using the TEMA Track Eye tracking software.

E.16.4 SPECIMEN BEHAVIOR

The loading of the BG plate imparted an initial velocity of 61.06 ft/sec (18.61 m/sec) to the specimen. This caused plate to deform in both directions. The longitudinal deflection (in the north-south direction) behaved in a typical one-way flexural shape. In order to get the velocity as high as needed the test was designed to have the impacting mass break free from the BG and launch itself into the plate. This test imparted enough energy into the system that the all fourteen bolts broke simultaneously. The maximum dynamic deflection just before the bolts broke was approximately 2 ½". Figure E.158 shows the plate after impact.

During the test three different phantom cameras were used to capture the failure modes from two different angles. Figure E.159 shows the progression of damage for this test from Phantom Camera One. Figure E.160 shows the progression of damage for this test from Phantom Camera Two. Figure E.161 shows the progression of damage for this test from Phantom Camera Three.

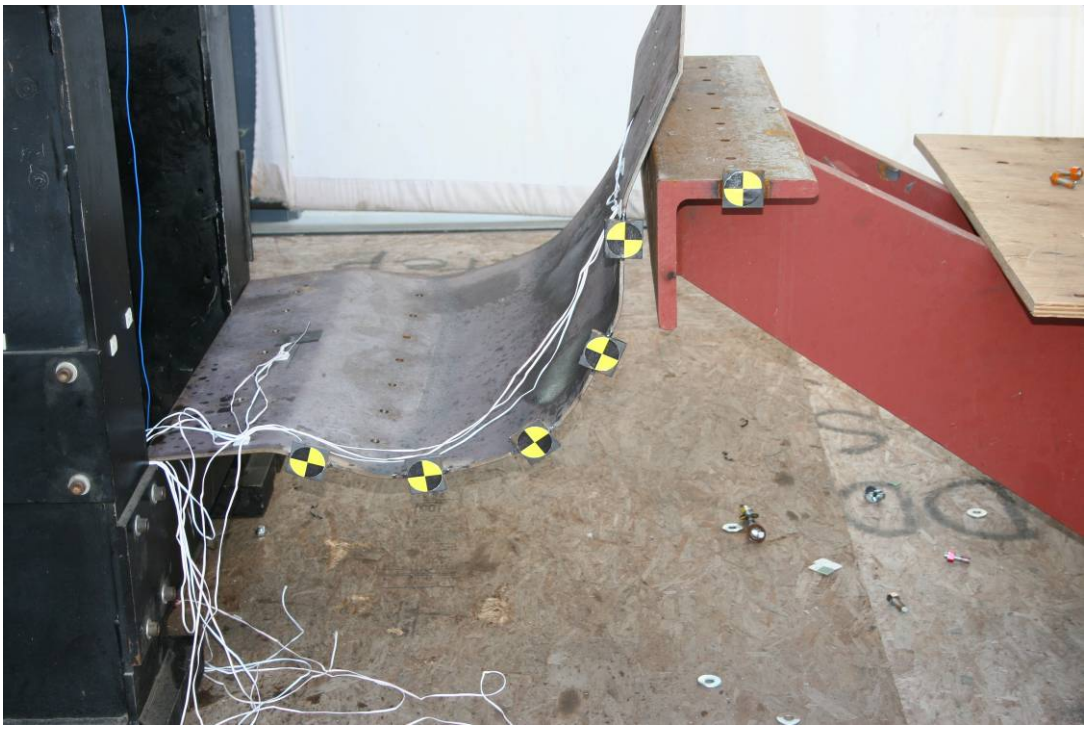

Figure E.158: Steel plate post test for Test 16

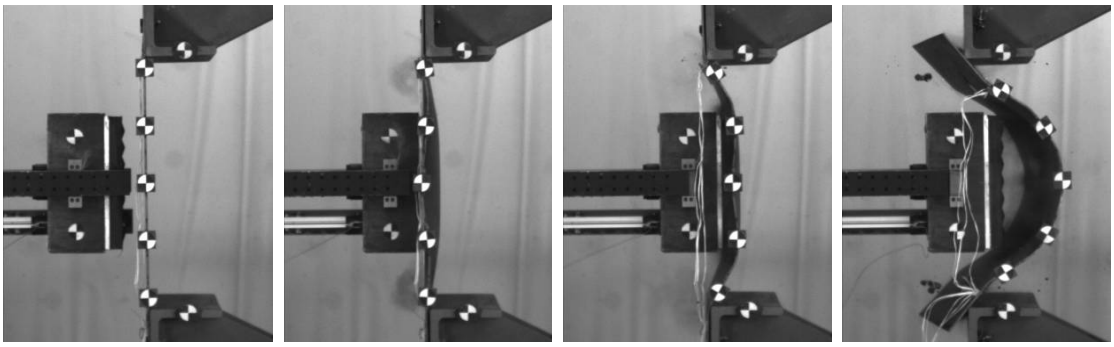

Figure E.159: Progression of damage for Test 16 from Camera 1

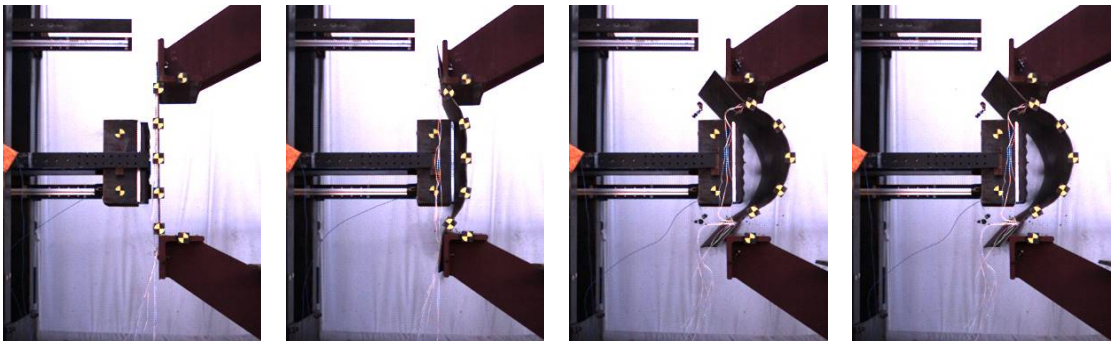

Figure E.160: Progression of damage for Test 16 from Camera 2

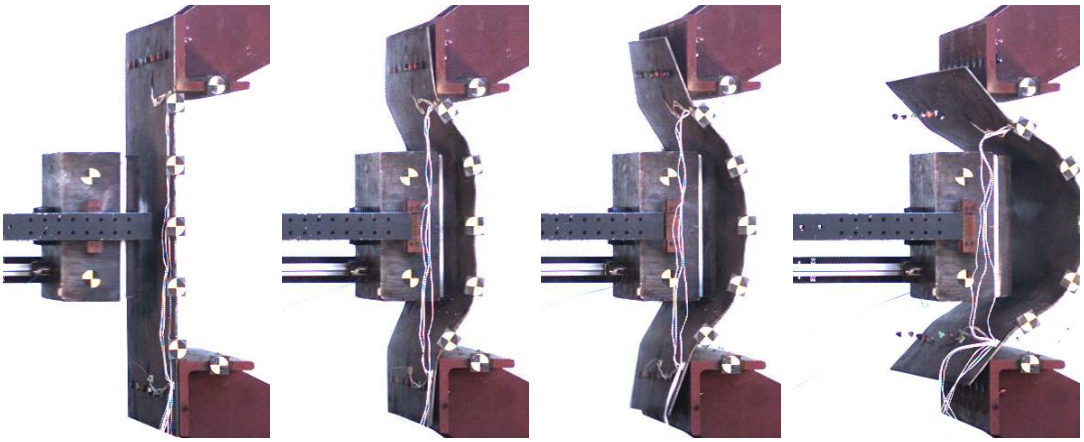

Figure E.161: Progression of damage for Test 16 from Camera 3

E.17 STEEL TOWER SINGLE PLATE: TEST 17 (SP17)

E.17.1 INTRODUCTION

The seventeenth test of the Steel Tower Single Plate test series was performed on December 14th, 2006. The test specimen was a ¼" thick steel plate labeled SP17. The Impacting Mass 1 was attached to the BG with a specimen target velocity of 49.21 ft/sec (15 m/sec). Figure E.162 shows the steel plate prior to impact.

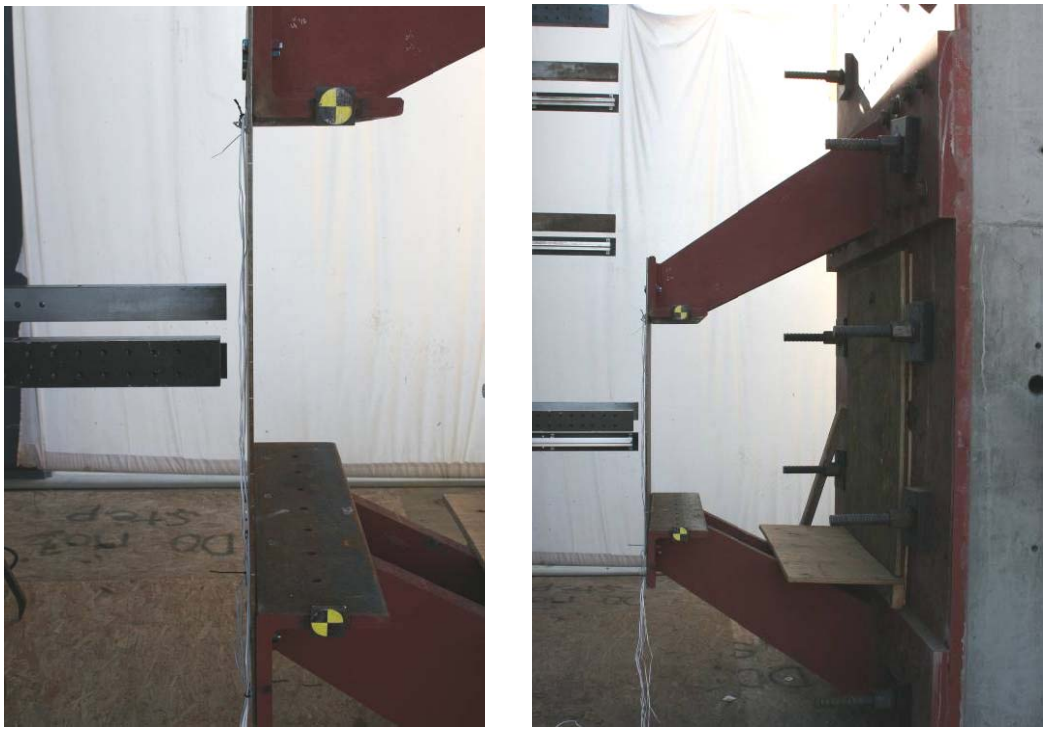

Figure E.162: 1/4" thick steel plate pre test for Test 17

E.17.2 INSTRUMENTATION

E.17.2.1 PHANTOM CAMERAS

The first camera recorded in black and white at a rate of 10,000 frames per second at a resolution of 512x384. This camera was used in order to determine the maximum velocity of the impacting mass and the movement in the plate including the maximum displacement. The second camera recorded in color at a rate of 10,000 frames per second at a resolution of 512x384. This camera recorded the overall behavior of the test specimen. It was not used to gather any specific data. The third camera recorded in color at a rate of 8,000 frames per second at a resolution of 480x480. This camera captured the failure of the bolts. A picture from each of the camera locations are shown in Figure E.163.

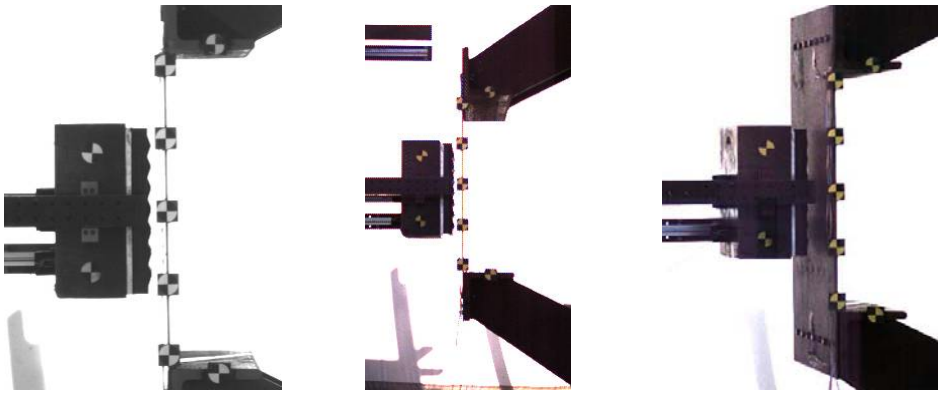

Figure E.163: Phantom Cameras for Test 17

a) Camera One b) Camera Two c) Camera Three

E.17.2.2 TARGET LOCATIONS

Five targets were welded onto the side of the steel plate. They were spaced at the intervals shown in Figure E.164. That figure also shows the location of the targets for the impacting mass. An additional two targets were placed on the angle at the top and the bottom end conditions. The distance between these two points is 74.93 cm (29 ½")

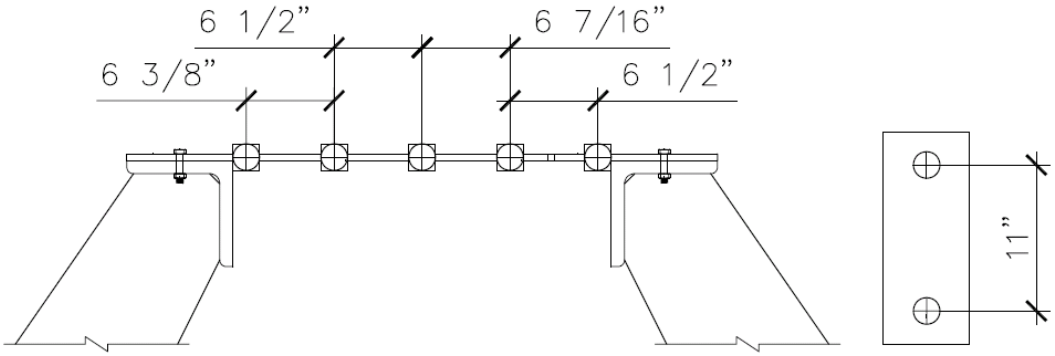

Figure E.164: Target layout on plate and impacting mass for Test 17

E.17.2.3 ACCELERATIONS

For this test one accelerometer was used. This accelerometer was placed 6" south of the centroid of the impacting mass as shown in Figure E.165. The pipe is to protect the accelerometer during the test. The data from this gage was then filtered as shown in Figure E.166.

This test does not impart an impulsive load as would be expected from a typical blast test. Instead, this test simulates the behavior of a flyer plate moving through the structure after the initial impact at the front plate of the outer cell of the structure. Therefore we are not determining the initial impulsive load from the accelerometers on the BG.

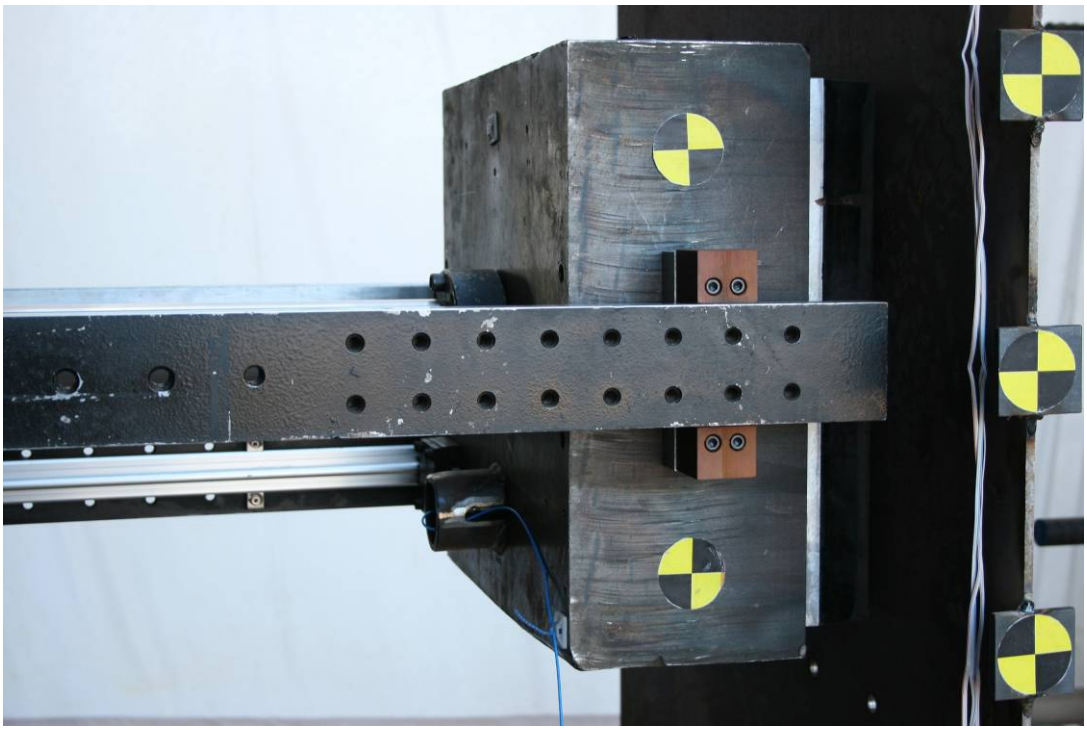

Figure E.165: Accelerometer location for Test 17

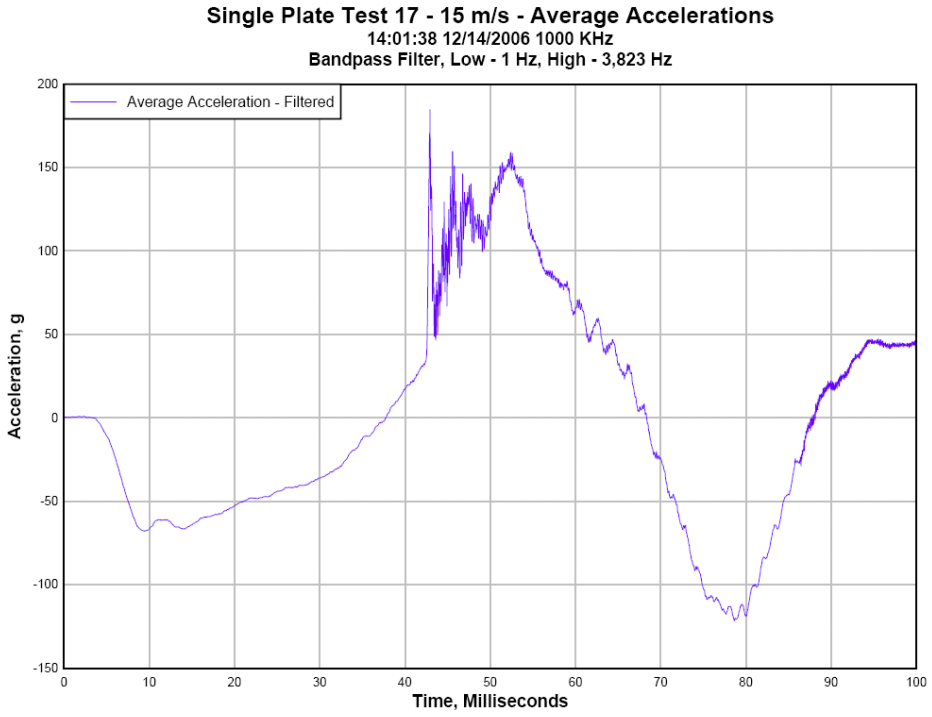

Figure E.166: Filtered accelerometer data for Test 17

E.17.2.4 STRAIN GAGE LOCATIONS

For this test there were two strain gauges labeled 17 and 18. The strain gauges, and their locations, are shown in Figure E.167. Table E.15 shows the specific information about this test, including the time and velocity at impact, if, and when, the bolts failed along with the maximum and minimum principal strain rates. The largest maximum principal strain rate for this test was 20.45 1/sec and was located at strain gage 17 while the largest minimum strain rate for this test was 5.46 1/sec located at strain gage 18. The maximum principal strains for gauges 17 and 18 can be found in Figure E.168 and the minimum principal strains for the same gauges can be found in Figure E.169

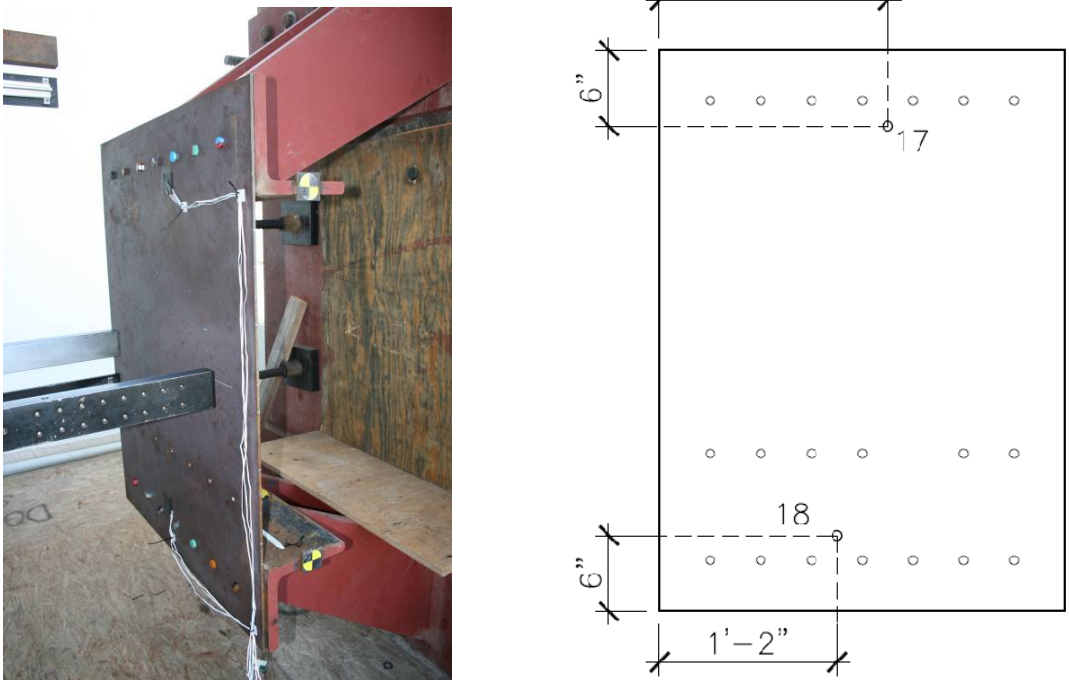

Figure E.167: Strain gage layout for Test 17

Table E.15: Stain rate information for Test 17

Strain Gage Number	Actual Velocity	Initial Impact	Shear Wave at Gage	Bolts Break	Maximum Principal Strain Rate	Minimum Principal Strain Rate
17	14.21 m/s	42.80 msec	-	51.70 msec	20.45 1/sec	5.21 1/sec
18	14.21 m/s	42.80 msec	-	51.70 msec	19.05 1/sec	-5.46 1/sec

E.17.2.5 BLAST BOLT TYPE

A total of fourteen A307 bolts (Low Strength Bolts similar to Rivets) were used for this test. They were all tightened to a torque of 40 ft-lbs.

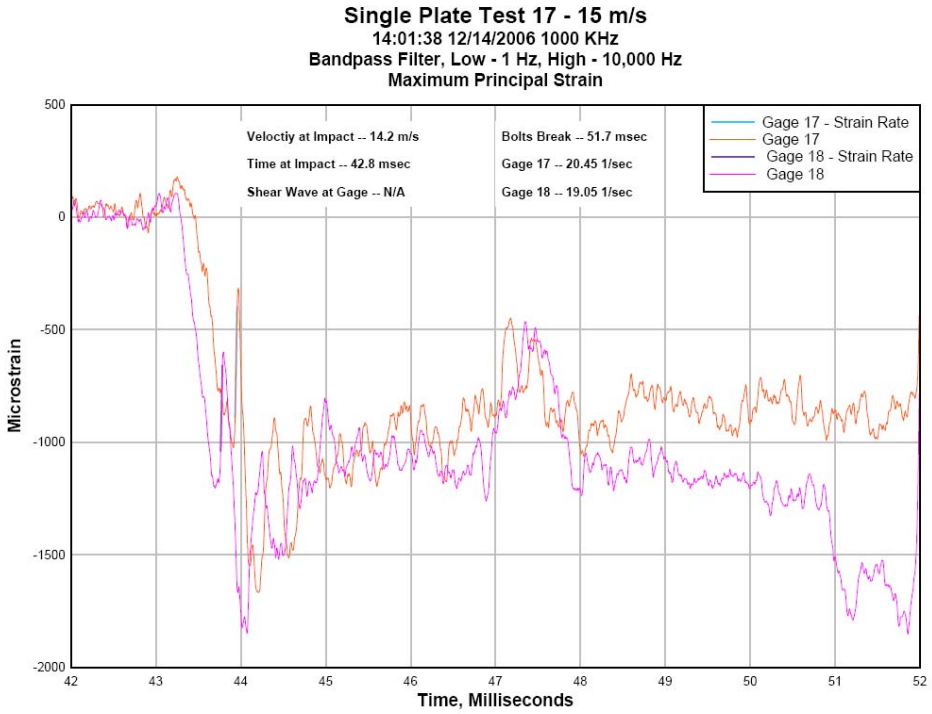

Figure E.168: Maximum principal strains and strain rates for Test 17

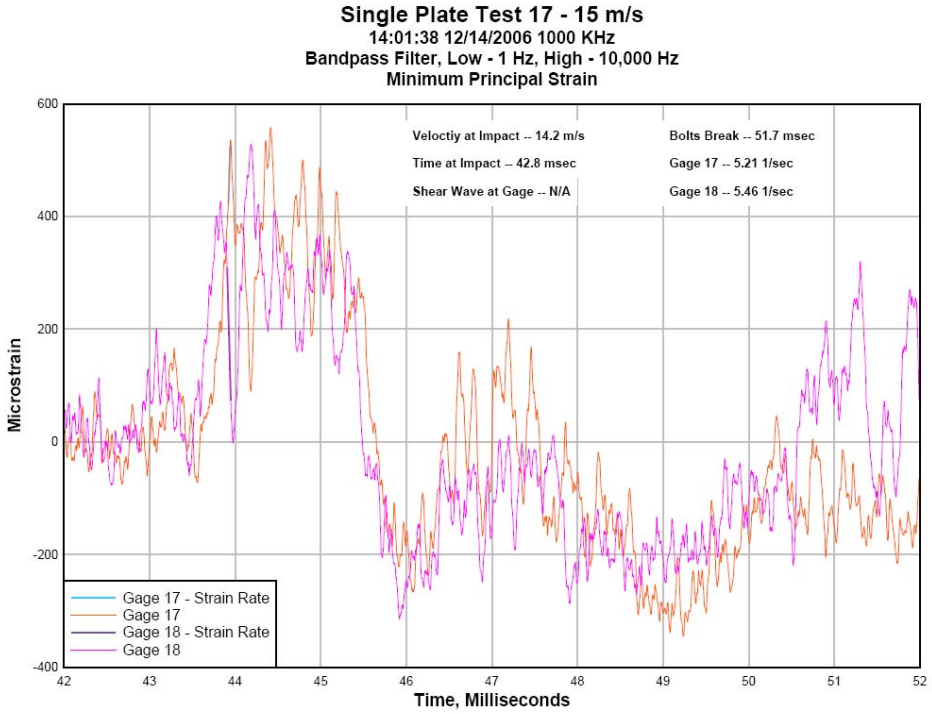

Figure E.169: Minimum principal strains and strain rates for Test 17

E.17.3 GENERATOR DATA

The initial impact of the single BG was 46.62 ft/sec (14.21 m/sec) with a goal velocity of 15 m/s. It had one accelerometer mounted to the back side of the impact plate as discussed in Section E.17.2.3. The average impact velocity for the impacting mass and the steel plate was calculated using the TEMA Track Eye tracking software.

E.17.4 SPECIMEN BEHAVIOR

The loading of the BG plate imparted an initial velocity of 14.21 ft/sec (46.62 m/sec) to the specimen. This caused plate to deform in both directions. The longitudinal deflection (in the north-south direction) behaved in a typical one-way flexural shape. In order to get the velocity as high as needed the test was designed to have the impacting mass break free from the BG and launch itself into the plate. This test imparted enough energy into the system that the top seven bolts broke. The goal of this test was to determine the threshold value for which only half of the bolts would break. That goal was achieved in this test. The maximum dynamic deflection just before the bolts broke was approximately 3 ¾". Figure E.170 shows the plate after impact.

During the test three different phantom cameras were used to capture the failure modes from two different angles. Figure E.171 shows the progression of damage for this test from Phantom Camera One. Figure E.172 shows the progression of damage for this test from Phantom Camera Two. Figure E.173 shows the progression of damage for this test from Phantom Camera Three.

Figure E.170: Steel plate post test for Test 17

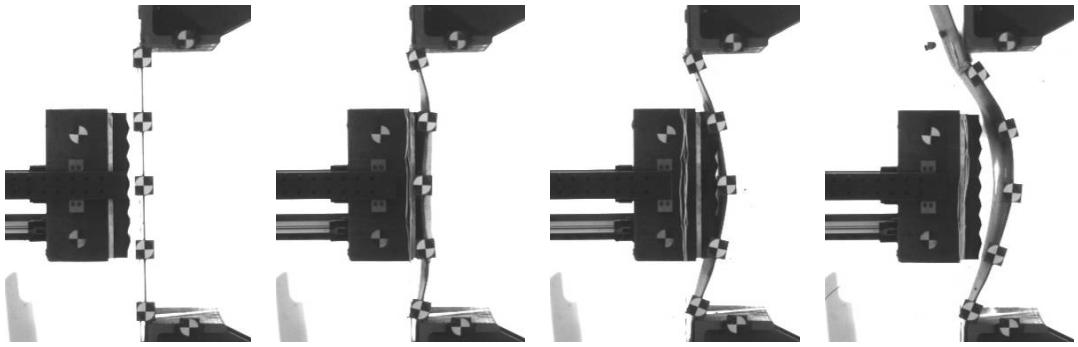

Figure E.171: Progression of damage for Test 17 from Camera 1

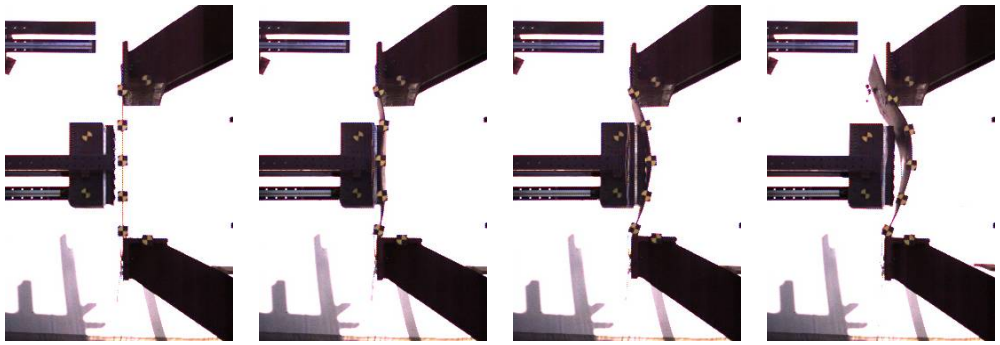

Figure E.172: Progression of damage for Test 17 from Camera 2

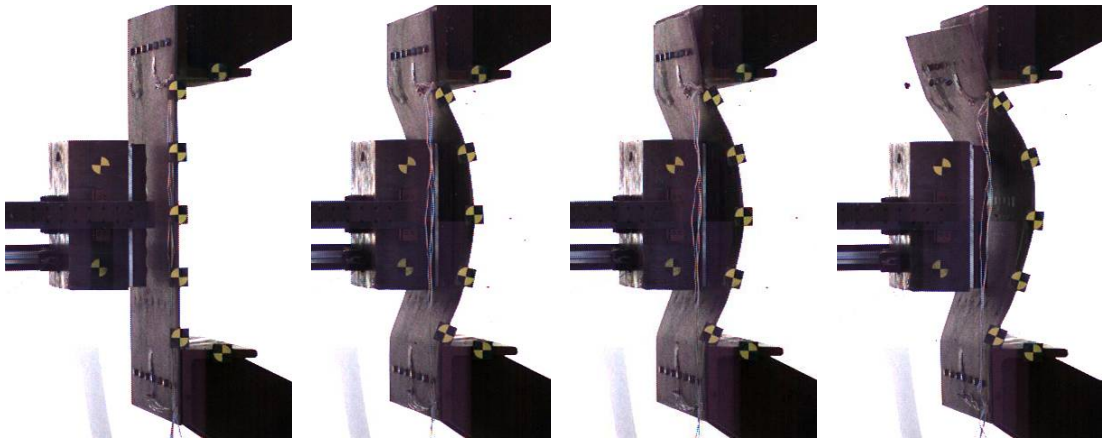

Figure E.173: Progression of damage for Test 17 from Camera 3

E.18 STEEL TOWER SINGLE PLATE: TEST 18 (SP18)

E.18.1 INTRODUCTION

The eighteenth test of the Steel Tower Single Plate test series was performed on December 19th, 2006. The test specimen was a ½" thick steel plate labeled SP18. The Impacting Mass 1 was attached to the BG with a specimen target velocity of 82.02 ft/sec (25 m/sec). The Figure E.174 shows the steel plate prior to impact.

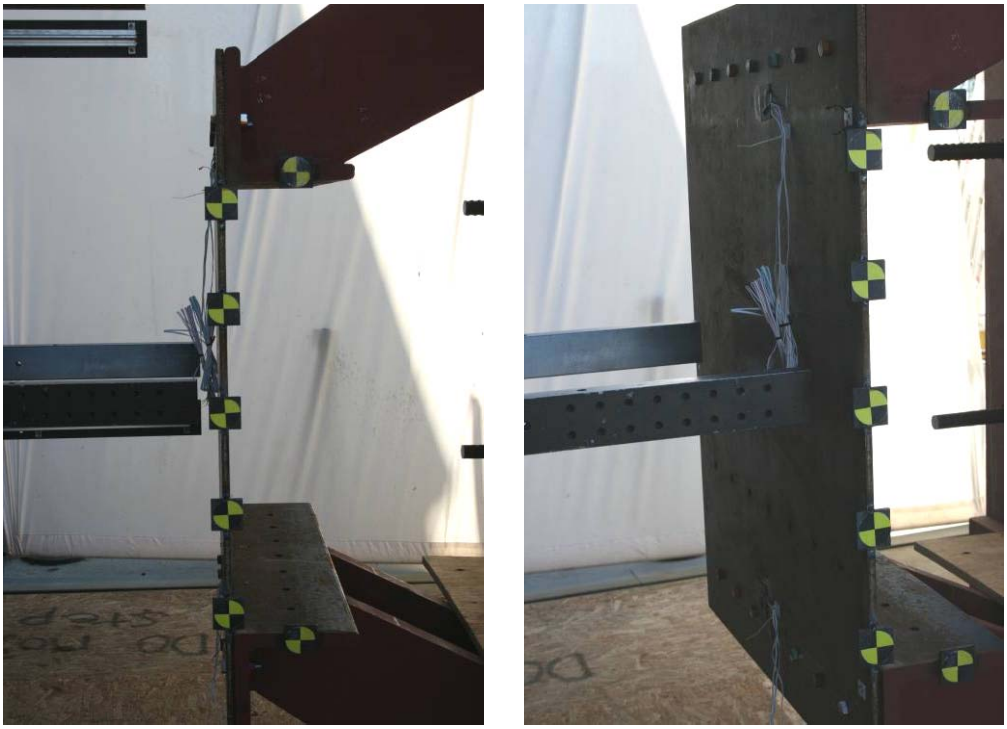

Figure E.174: 1/2" thick steel plate pre test for Test 18

E.18.2 INSTRUMENTATION

E.18.2.1 PHANTOM CAMERAS

The first camera recorded in black and white at a rate of 10,000 frames per second at a resolution of 512x384. This camera was used in order to determine the maximum velocity of the impacting mass and the movement in the plate including the maximum displacement. The second camera recorded in color at a rate of 10,000 frames per second at a resolution of 512x384. This camera recorded the overall behavior of the test specimen. It was not used to gather any specific data. The third camera recorded in color at a rate of 8,000 frames per second at a resolution of 480x480. This camera captured the failure of the bolts. A picture from each of the camera locations are shown in Figure E.175.

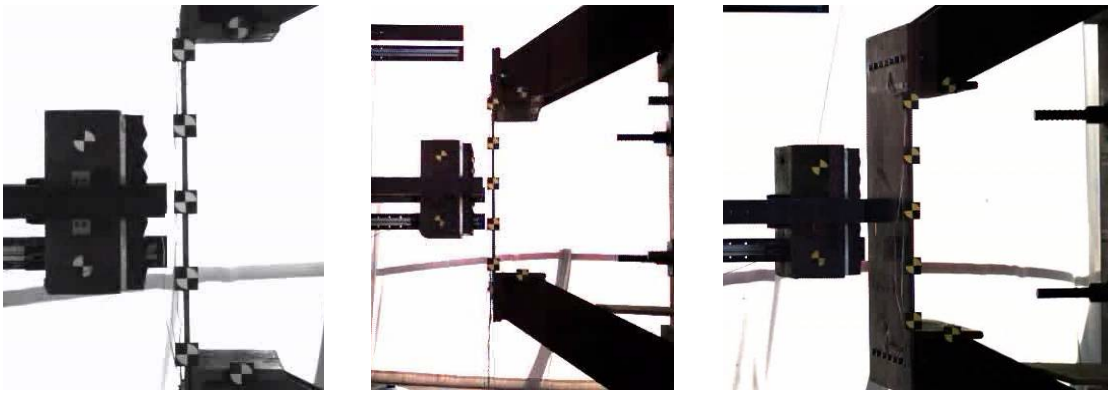

Figure E.175: Phantom Cameras for Test 18

a) Camera One b) Camera Two c) Camera Three

E.18.2.2 TARGET LOCATIONS

Five targets were welded onto the side of the steel plate as show in Figure E.174. They were spaced at the intervals shown in Figure E.176. That figure also shows the location of the targets for the impacting mass. An additional two targets were placed on the angle at the top and the bottom end conditions. The distance between these two points is 74.93 cm (29 ½")

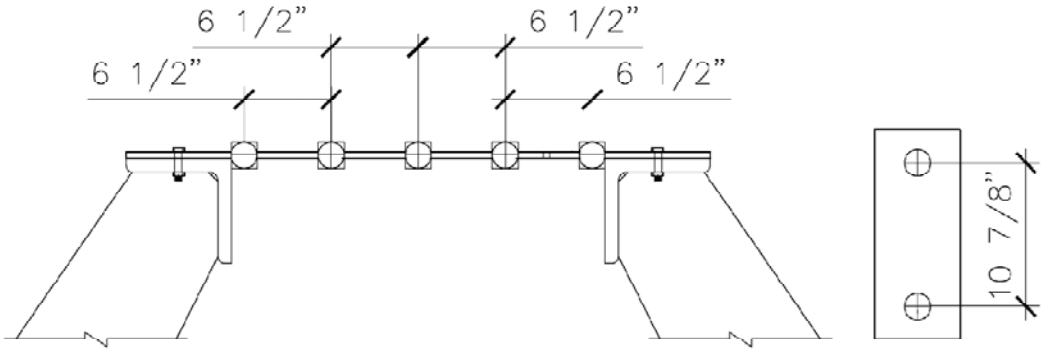

Figure E.176: Target layout on plate and impacting mass for Test 18

E.18.2.3 ACCELERATIONS

For this test one accelerometer was used. It was located 6" south of the centroid as shown in Figure E.177. The pipe is to protect the accelerometer during the test. A filter was applied to the accelerometer data as shown in Figure E.178.

This test does not impart an impulsive load as would be expected from a typical blast test. Instead, this test simulates the behavior of a flyer plate moving through the structure after the initial impact at the front plate of the outer cell of the structure. Therefore we are not determining the initial impulsive load from the accelerometers on the BG.

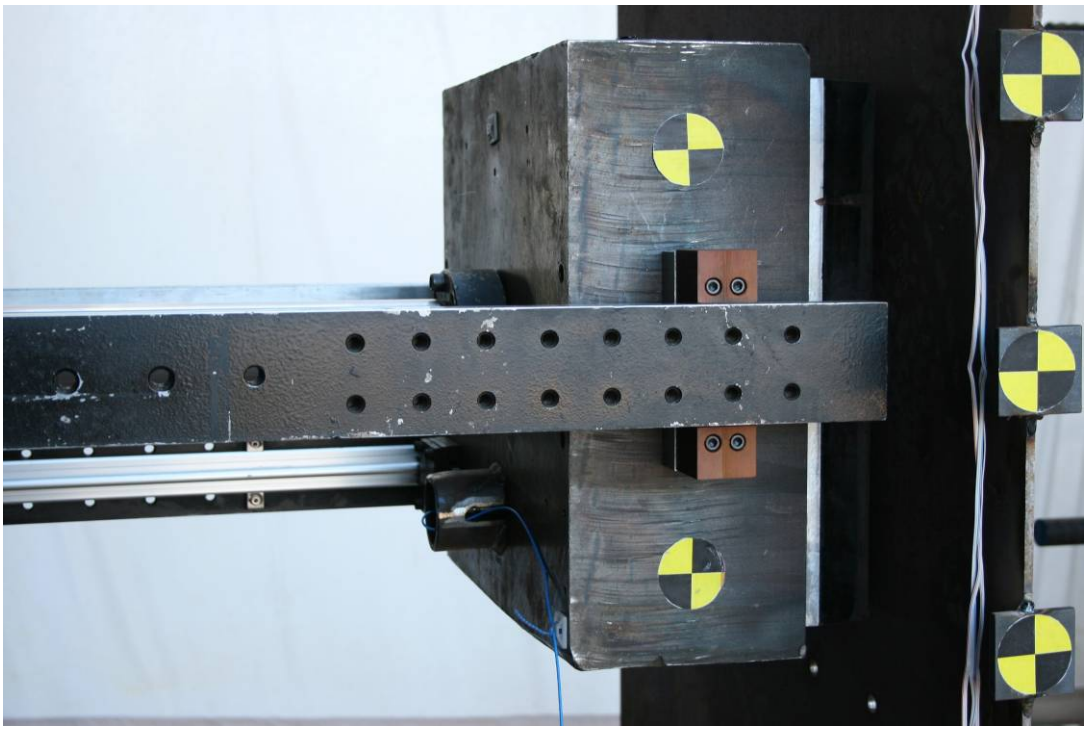

Figure E.177: Accelerometer location for Test 18

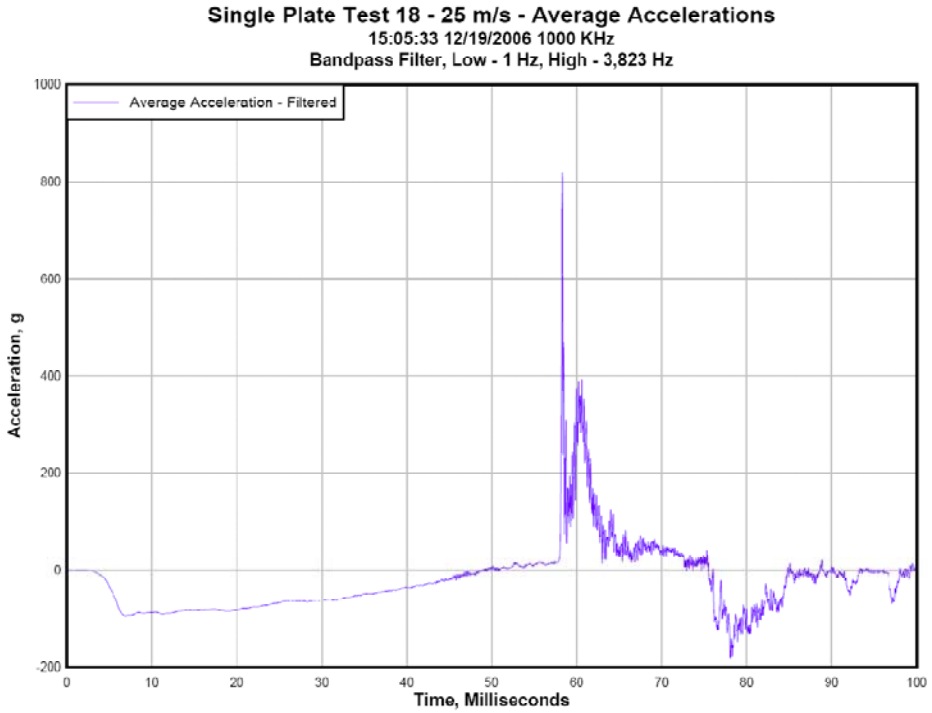

Figure E.178: Filtered accelerometer data for Test 18

E.18.2.4 STRAIN GAGE LOCATIONS

For this test there were two strain gauges labeled 17 and 18. The strain gauges, and their locations, are shown in Figure E.179. Table E.16 shows the specific information about this test, including the time and velocity at impact, if, and when, the bolts failed along with the maximum and minimum principal strain rates. The largest maximum principal strain rate for this test was 10.99 1/sec and was located at strain gage 18 while the largest minimum strain rate for this test was 7.68 1/sec located at strain gage 18. The maximum principal strains for gauges 17 and 18 can be found in Figure E.180and the minimum principal strains for the same gauges can be found in Figure E.181.

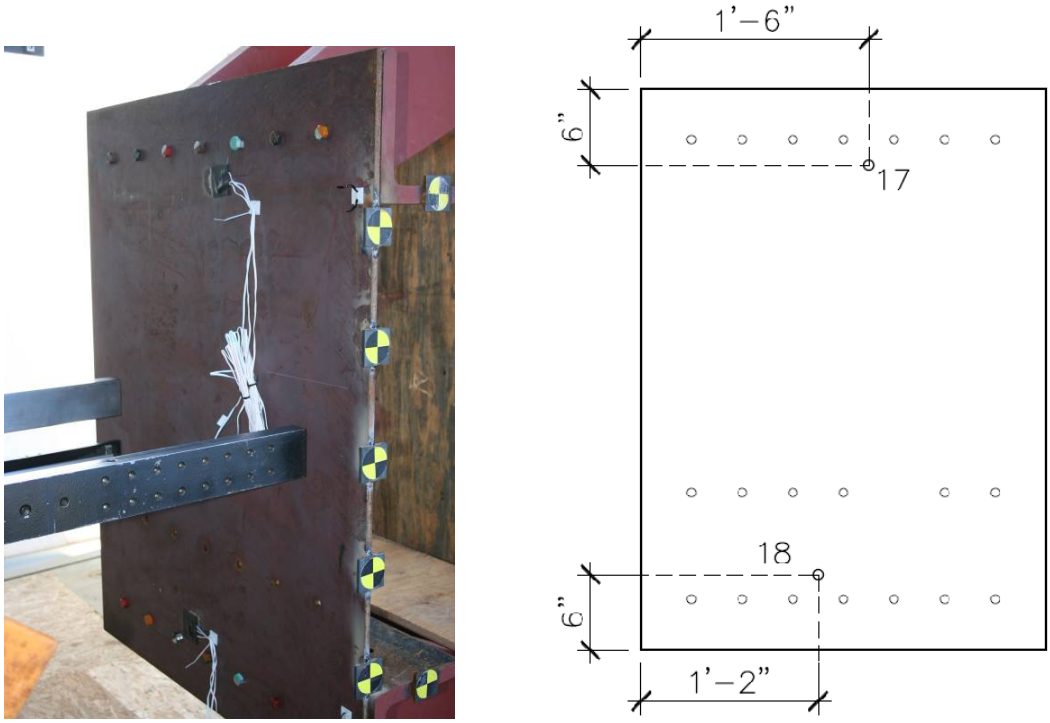

Figure E.179: Strain gage layout for Test 18

Table E.16: Stain rate information for Test 18

Strain Gage Number	Actual Velocity	Initial Impact	Shear Wave at Gage	Bolts Break	Maximum Principal Strain Rate	Minimum Principal Strain Rate
17	25.7 m/s	58.50 msec	61.00 msec	63.60 msec	-9.75 1/sec	3.93 1/sec
18	25.7 m/s	58.50 msec	61.00 msec	63.60 msec	-10.99 1/sec	-7.68 1/sec

E.18.2.5 BOLT TYPE

A total of fourteen A307 bolts (Low Strength Bolts, similar to rivets) were used for this test. They all had a torque of 40 ft-lbs applied to them before the test.

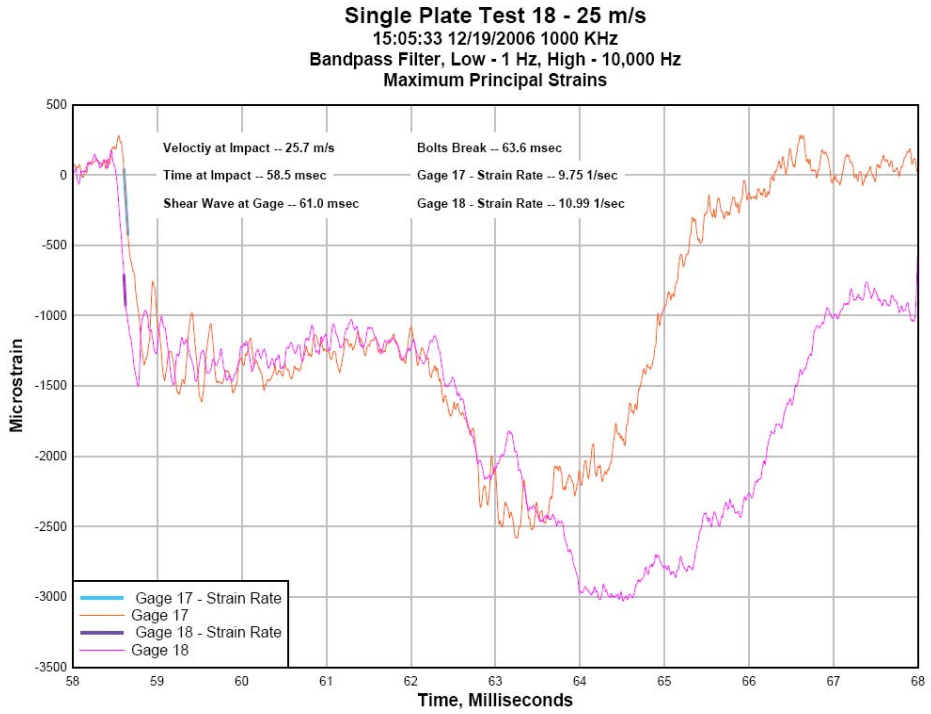

Figure E.180: Maximum principal strains and strain rates for Test 18

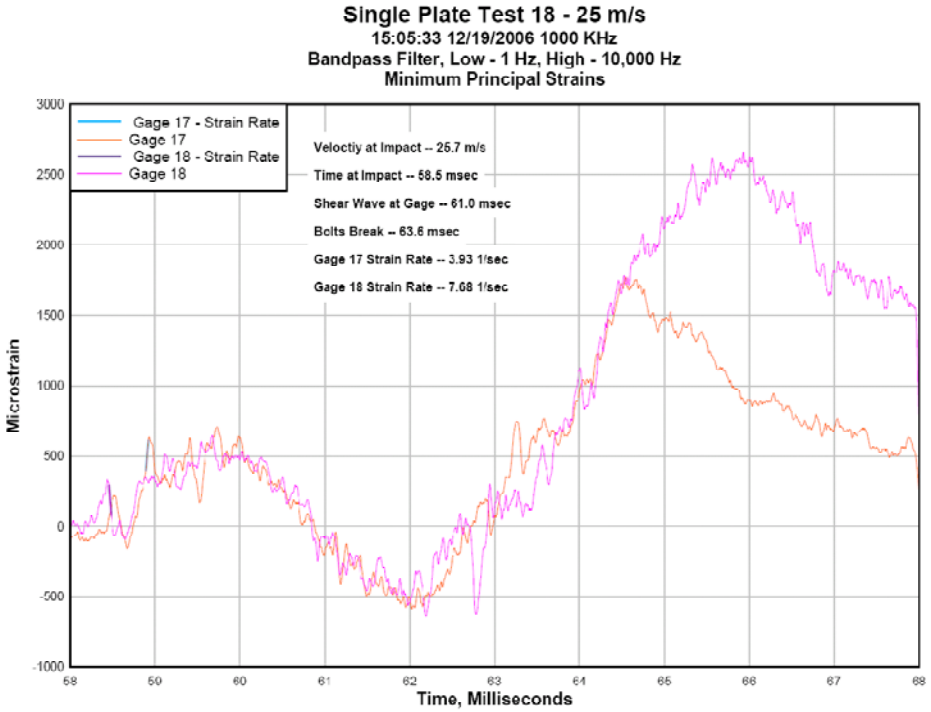

Figure E.181: Minimum principal strains and strain rates for Test 18

E.18.3 BLAST GENERATOR DATA

The initial impact of the single BG was 84.32 ft/sec (25.7 m/sec) with a goal velocity of 25 m/s. It had an accelerometers mounted to the back side of the impact plate as discussed in Section E.18.2.3. The average impact velocity for the impacting mass and the steel plate was calculated using the TEMA Track Eye tracking software.

E.18.4 SPECIMEN BEHAVIOR

The loading of the BG plate imparted an initial velocity of 84.32 ft/sec (25.70 m/sec) to the specimen. This caused plate to deform in both directions. The longitudinal deflection (in the north-south direction) behaved in a typical one-way flexural shape. In order to get the velocity as high as needed the test was designed to have the impacting mass break free from the BG and launch itself into the plate. This imparted enough energy into the system that all fourteen A307 bolts failed. The plate and impacting mass continued to travel as one until they hit the back plate. After the test was completed the plate was found on the ground bent into a V-shape. Figure E.182 shows the test specimen after the test. Some of the bolts that connect the programmer to the mass fractured during the test which allowed the programmer to move into the position shown. Figure E.183 shows the progression of damage from Phantom Camera One while Figure E.184 shows the view from Camera Two.

During the test pieces of bolts flew approximately 14’ directly north of the test set-up and 7’ south of the test set-up. A portion of a bolt was also found northeast of the set-up at approximately 13’.

Figure E.182: Steel plate and Impacting Mass post test for Test 18

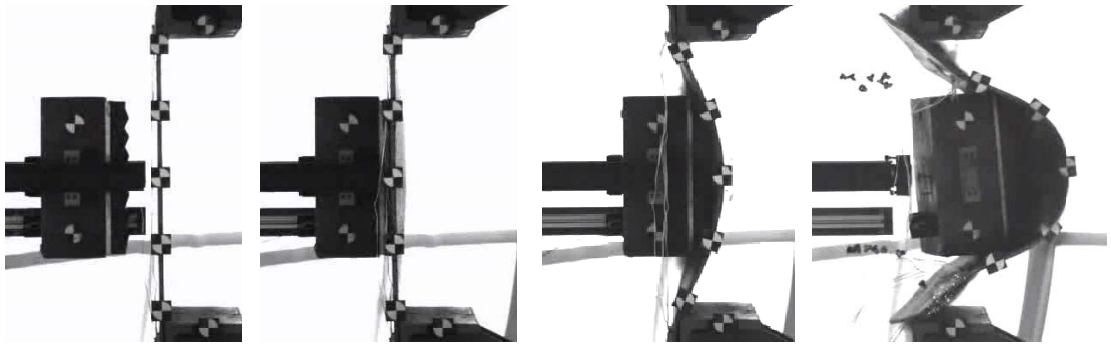

Figure E.183: Progression of damage for Test 18

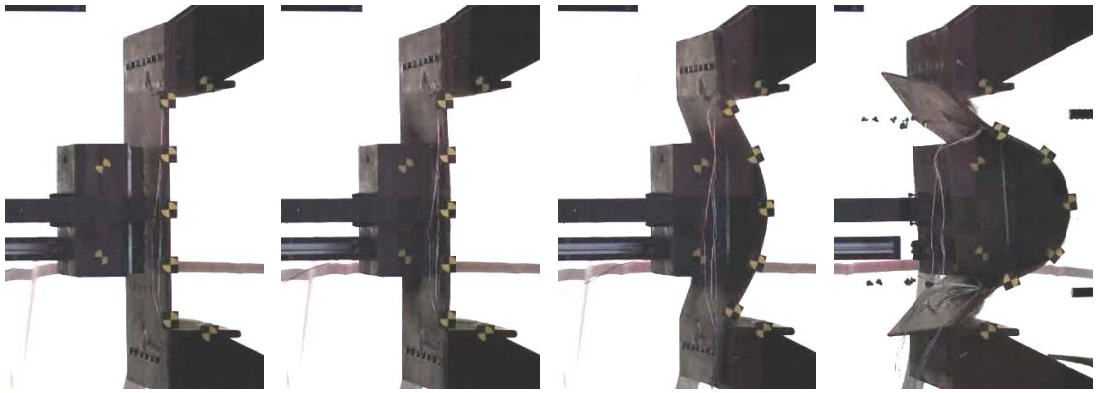

Figure E.184: Progression of damage for Test 18

E.19 STEEL TOWER SINGLE PLATE: TEST 19 (SP19)

E.19.1 INTRODUCTION

The nineteenth test of the Steel Tower Single Plate test series was performed on January 9th, 2007. The test specimen was a ½" thick steel plate labeled SP19. The Impacting Mass 1 was attached to the BG with a specimen target velocity of 75.46 ft/sec (23 m/sec). Figure E.185 shows the steel plate prior to impact.

Figure E.185: 1/2" thick steel plate pre test for Test 19

E.19.2 INSTRUMENTATION

E.19.2.1 PHANTOM CAMERAS

The first camera recorded in black and white at a rate of 5,000 frames per second at a resolution of 512x384. This camera was used in order to determine the maximum velocity of the impacting mass and the movement in the plate including the maximum displacement. The second camera recorded in color at a rate of 5,000 frames per second at a resolution of 512x384. This camera recorded the overall behavior of the test specimen. It was not used to gather any specific data. The third camera recorded in color at a rate of 1,000 frames per second at a resolution of 480x480. This camera captured the failure of the bolts. A picture from each of the camera locations are shown in Figure E.186.

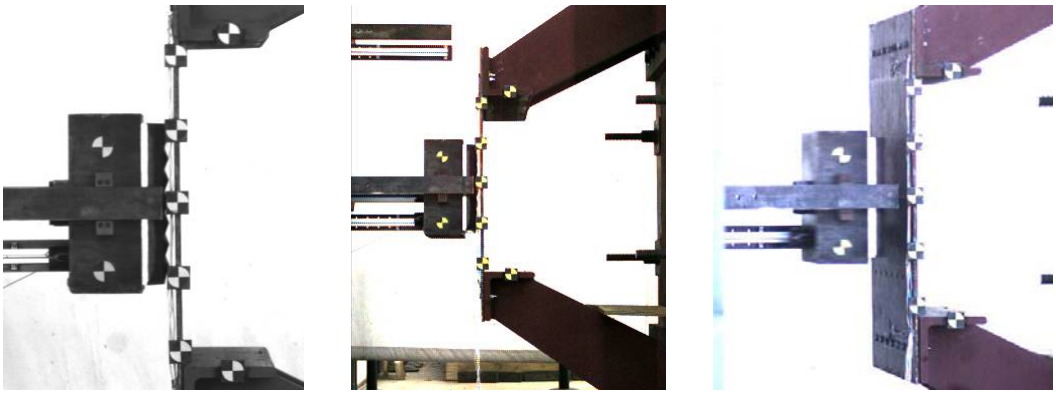

Figure E.186: Phantom Cameras for Test 19

a) Camera One b) Camera Two c) Camera Three

E.19.2.2 TARGET LOCATIONS

Five targets were welded onto the side of the steel plate as shown in Figure E.185. They were spaced at the intervals shown in Figure E.187. That figure also shows the location of the targets for the impacting mass. An additional two targets were placed on the angle at the top and the bottom end conditions. The distance between these two points is 74.93 cm (29 ½")

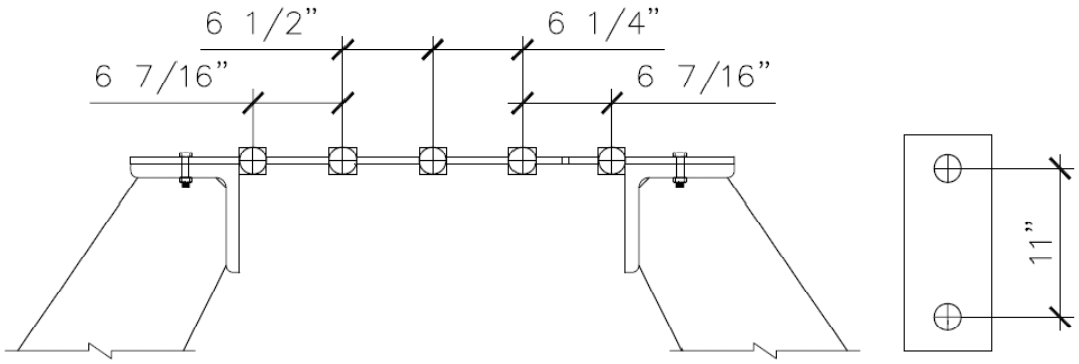

Figure E.187: Target layout on plate and impacting mass for Test 19

E.19.2.3 ACCELERATIONS

For this test one accelerometer was used. This accelerometer was placed 6" south of the centroid of the impacting mass as shown in Figure E.188. The pipe is to protect the accelerometer during the test. The data from this gage was then filtered as shown in Figure E.189.

This test does not impart an impulsive load as would be expected from a typical blast test. Instead, this test simulates the behavior of a flyer plate moving through the structure after the initial impact at the front plate of the outer cell of the structure. Therefore we are not determining the initial impulsive load from the accelerometers on the BG.

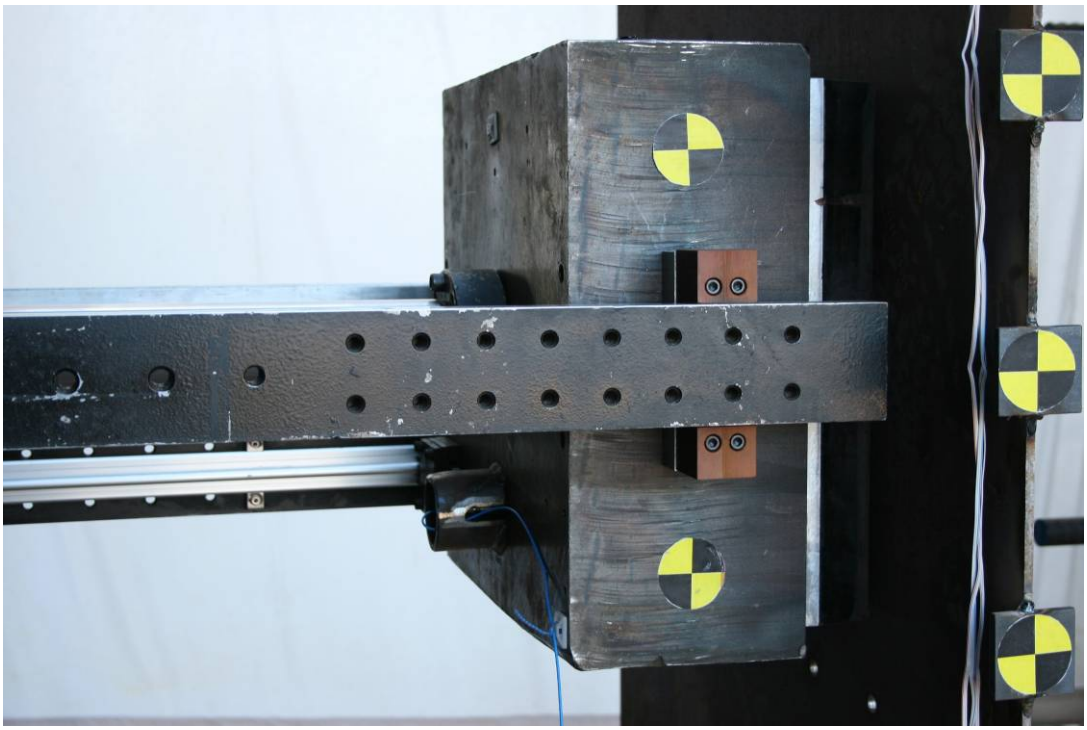

Figure E.188: Accelerometer location for Test 19

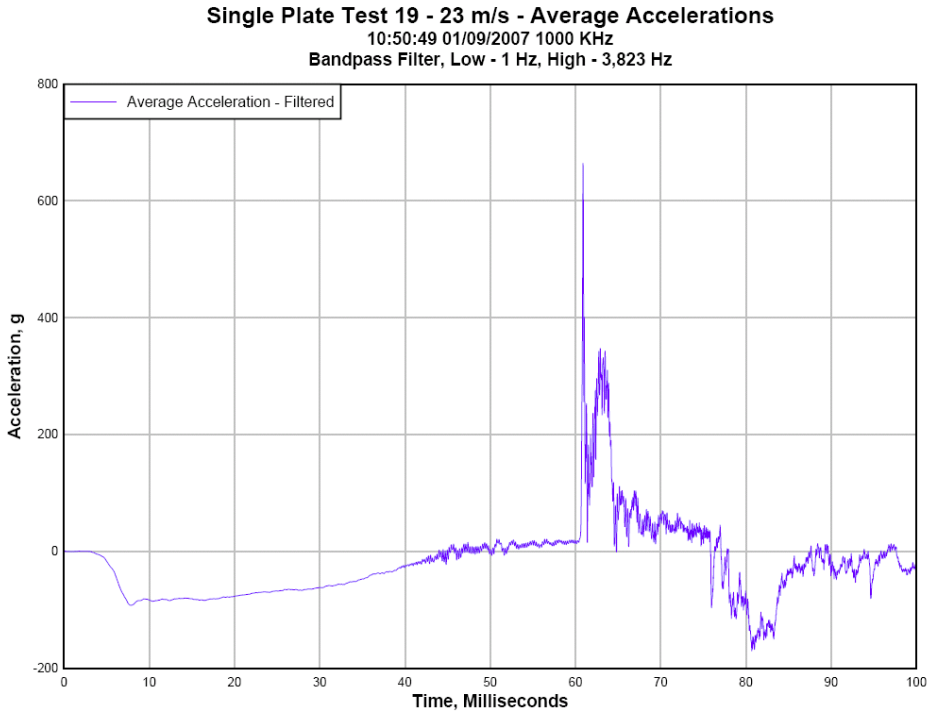

Figure E.189: Filtered accelerometer data for Test 19

E.19.2.4 STRAIN GAGE LOCATIONS

For this test there were two strain gauges labeled 17 and 18. The strain gauges, and their locations, are shown in Figure E.190. Table E.17 shows the specific information about this test, including the time and velocity at impact, if, and when, the bolts failed along with the maximum and minimum principal strain rates. The largest maximum principal strain rate for this test was 12.74 1/sec and was located at strain gage 17 while the largest minimum strain rate for this test was 9.88 1/sec located at strain gage 17. The maximum principal strains for gauges 17 and 18 can be found in Figure E.191 and the minimum principal strains for the same gauges can be found in Figure E.192

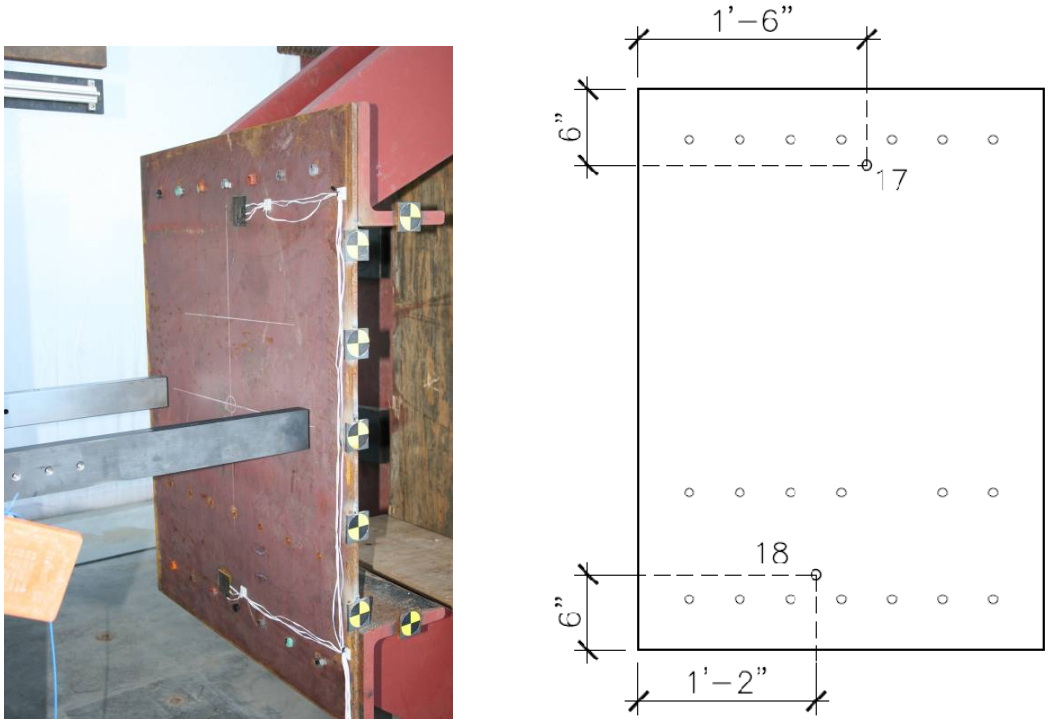

Figure E.190: Strain gage layout for Test 19

Table E.17: Stain rate information for Test 19

Strain Gage Number	Actual Velocity	Initial Impact	Shear Wave at Gage	Bolts Break	Maximum Principal Strain Rate	Minimum Principal Strain Rate
17	23. m/s	60.60 msec	65.00 msec	67.00 msec	12.74 1/sec	-9.88 1/sec
18	23. m/s	60.60 msec	65.00 msec	67.00 msec	-9.14 1/sec	3.49 1/sec

E.19.2.5 BOLT TYPE

A total of fourteen A307 bolts (Low Strength Bolts similar to Rivets) were used for this test. They were all tightened to a torque of 40 ft-lbs.

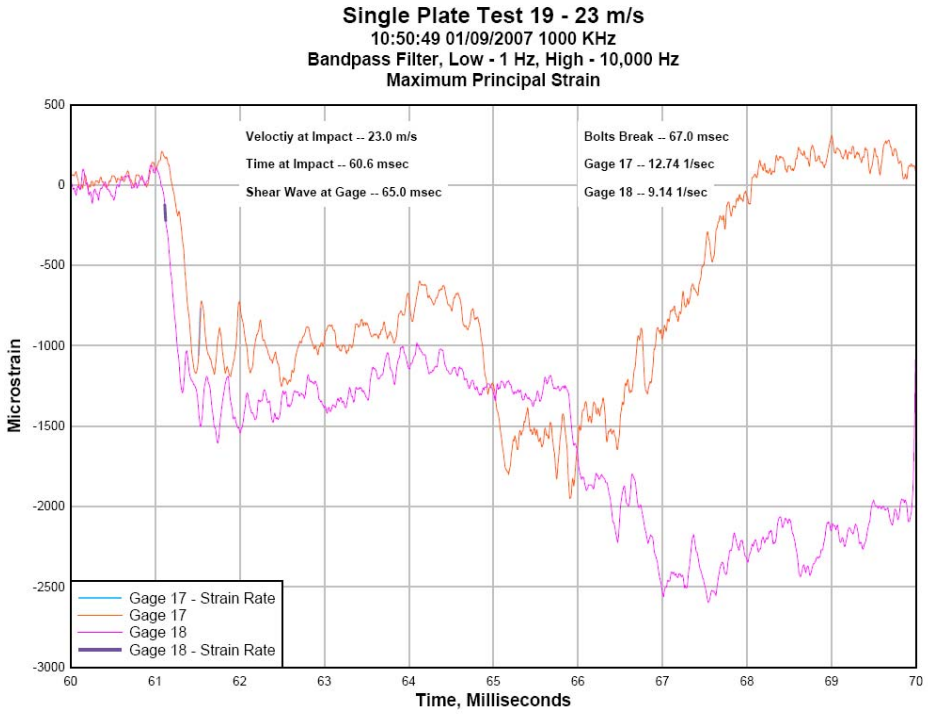

Figure E.191: Maximum principal strains and strain rates for Test 19

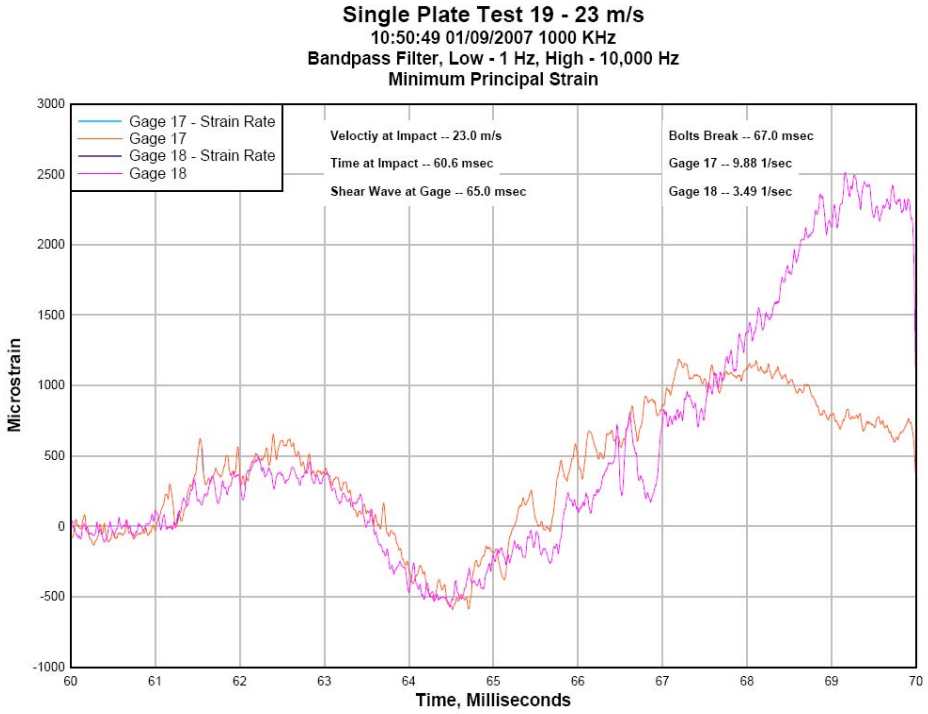

Figure E.192: Minimum principal strains and strain rates for Test 19

E.19.3 BLAST GENERATOR DATA

The initial impact of the single BG was 75.46 ft/sec (23 m/sec) with a goal velocity of 23 m/s. It had one accelerometer mounted to the back side of the impact plate as discussed in Section E.19.2.3. The average impact velocity for the impacting mass and the steel plate was calculated using the TEMA Track Eye tracking software.

E.19.4 SPECIMEN BEHAVIOR

The loading of the BG plate imparted an initial velocity of 75.46 ft/sec (23 m/sec) to the specimen. This caused plate to deform in both directions. The longitudinal deflection (in the north-south direction) behaved in a typical one-way flexural shape. In order to get the velocity as high as needed the test was designed to have the impacting mass break free from the BG and launch itself into the plate. This test imparted enough energy into the system that all fourteen bolts broke as shown in Figure E.193.

During the test pieces of bolts flew approximately 33’ northwest of the test set-up and 11’ directly south of the test set-up beyond the screen. The maximum dynamic deflection just before the bolts broke was approximately 3”. During the test three different phantom cameras were used to capture the failure modes from two different angles. Figure E.194 shows the progression of damage for this test from Phantom Camera One. Figure E.195 shows the progression of damage for this test from Phantom Camera Two. Figure E.196 shows the progression of damage for this test from Phantom Camera Three.

Figure E.193: Steel plate post test for Test 19

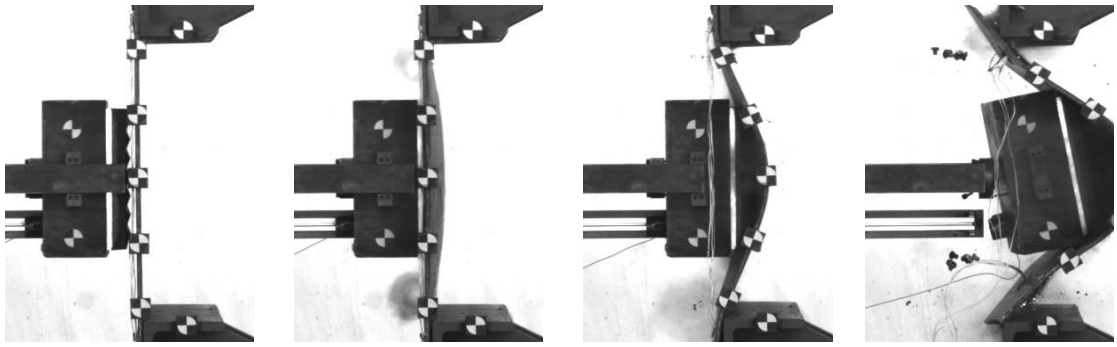

Figure E.194: Progression of damage for Test 19 from Camera 1

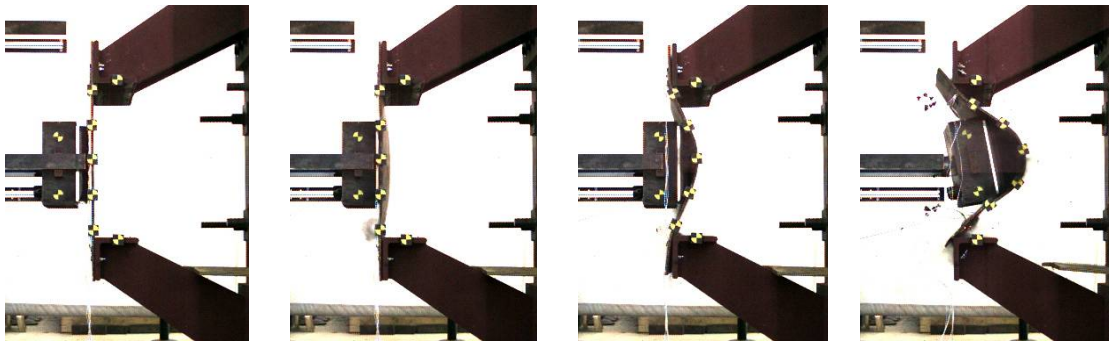

Figure E.195: Progression of damage for Test 19 from Camera 2

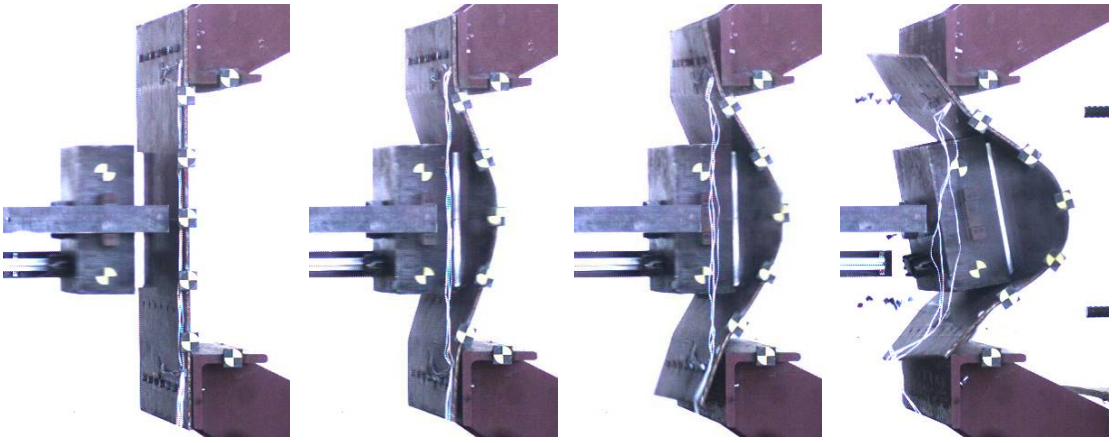

Figure E.196: Progression of damage for Test 19 from Camera 3

E.20 STEEL TOWER SINGLE PLATE: TEST 20 (SP20)

E.20.1 INTRODUCTION

The twentieth test of the Steel Tower Single Plate test series was performed on January 11th, 2007. The test specimen was a ½" thick steel plate labeled SP20. The Impacting Mass 1 was attached to the BG with a specimen target velocity of 63.98 ft/sec (19.5 m/sec). Figure E.197 shows the steel plate prior to impact.

Figure E.197: 1/2" thick steel plate pre test for Test 20

E.20.2 INSTRUMENTATION

E.20.2.1 PHANTOM CAMERAS

The first camera recorded in black and white at a rate of 5,000 frames per second at a resolution of 512x384. This camera was used in order to determine the maximum velocity of the impacting mass and the movement in the plate including the maximum displacement. The second camera recorded in color at a rate of 3,000 frames per second at a resolution of 512x384. This camera recorded the overall behavior of the test specimen. It was not used to gather any specific data. The third camera recorded in color at a rate of 5,000 frames per second at a resolution of 480x480. This camera captured the failure of the bolts. A picture from each of the camera locations are shown in Figure E.198.

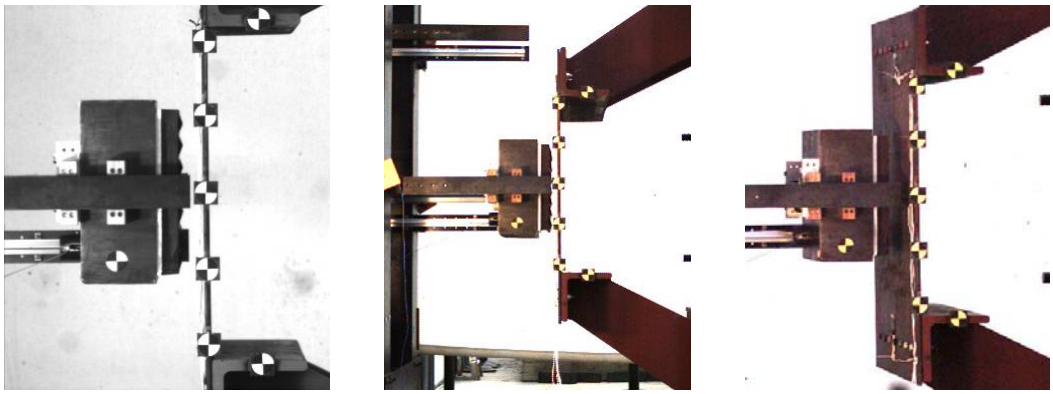

Figure E.198: Phantom Cameras for Test 20

a) Camera One b) Camera Two c) Camera Three

E.20.2.2 TARGET LOCATIONS

Five targets were welded onto the side of the steel plate as shown in Figure E.197. They were spaced at the intervals shown in Figure E.199. That figure also shows the location of the targets for the impacting mass. An additional two targets were placed on the angle at the top and the bottom end conditions. The distance between these two points is 74.93 cm (29 ½")

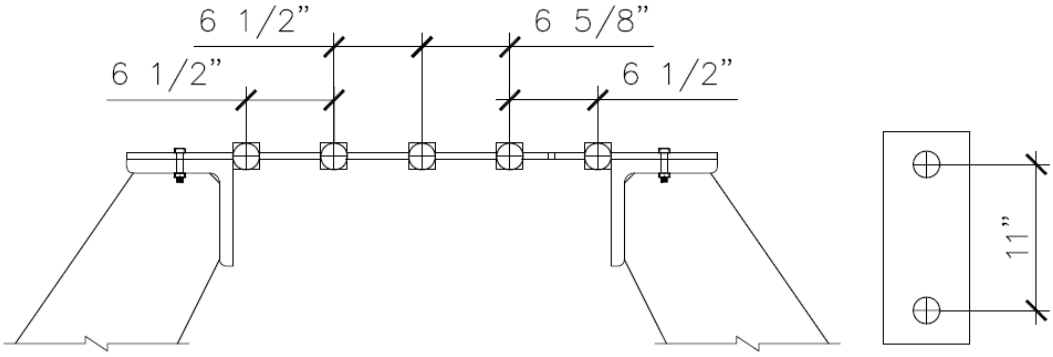

Figure E.199: Target layout on plate and impacting mass for Test 20

E.20.2.3 ACCELERATIONS

For this test one accelerometer was used. This accelerometer was placed 6" south of the centroid of the impacting mass as shown in Figure E.200. The pipe is to protect the accelerometer during the test. The data from this gage was then filtered as shown in Figure E.201.

This test does not impart an impulsive load as would be expected from a typical blast test. Instead, this test simulates the behavior of a flyer plate moving through the structure after the initial impact at the front plate of the outer cell of the structure. Therefore we are not determining the initial impulsive load from the accelerometers on the BG

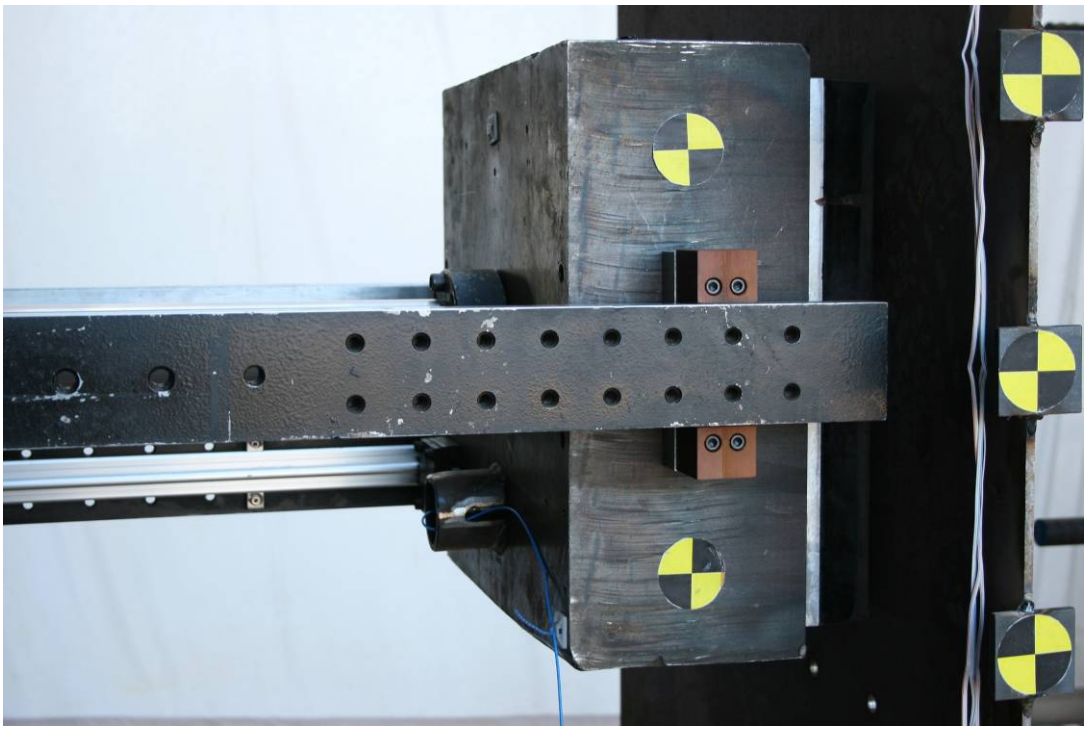

Figure E.200: Accelerometer location for Test 20

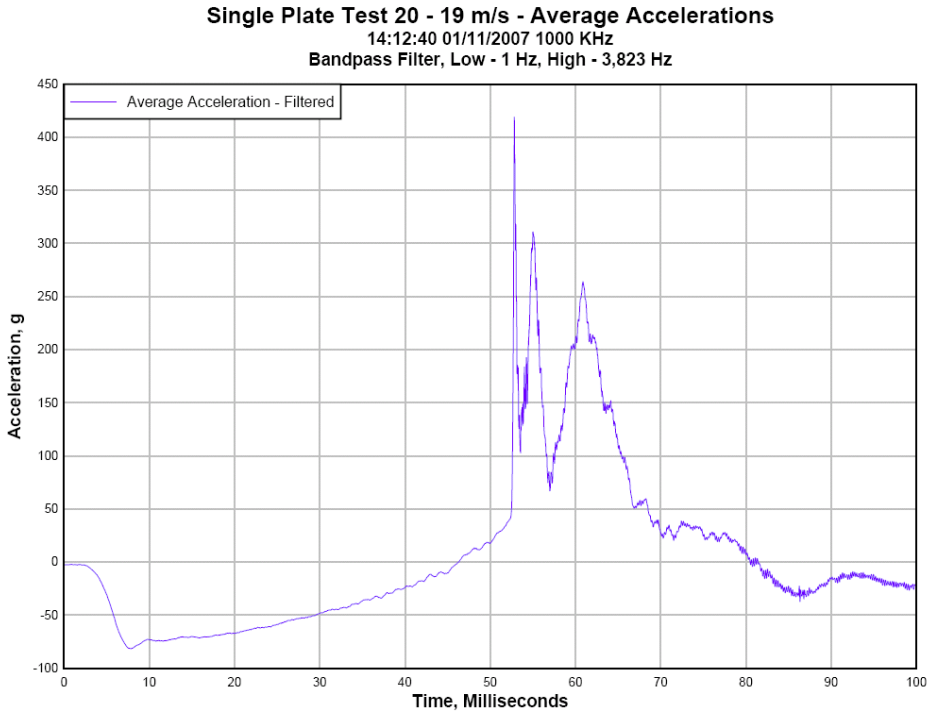

Figure E.201: Filtered accelerometer data for Test 20

E.20.2.4 STRAIN GAGE LOCATIONS

For this test there were two strain gauges labeled 17 and 18. The strain gauges, and their locations, are shown in Figure E.202. Table E.18 shows the specific information about this test, including the time and velocity at impact, if, and when, the bolts failed along with the maximum and minimum principal strain rates. The largest maximum principal strain rate for this test was 9.46 1/sec and was located at strain gage 18 while the largest minimum strain rate for this test was 5.63 1/sec located at strain gage 18. The maximum principal strains for gauges 17 and 18 can be found in Figure E.203 and the minimum principal strains for the same gauges can be found in Figure E.204.

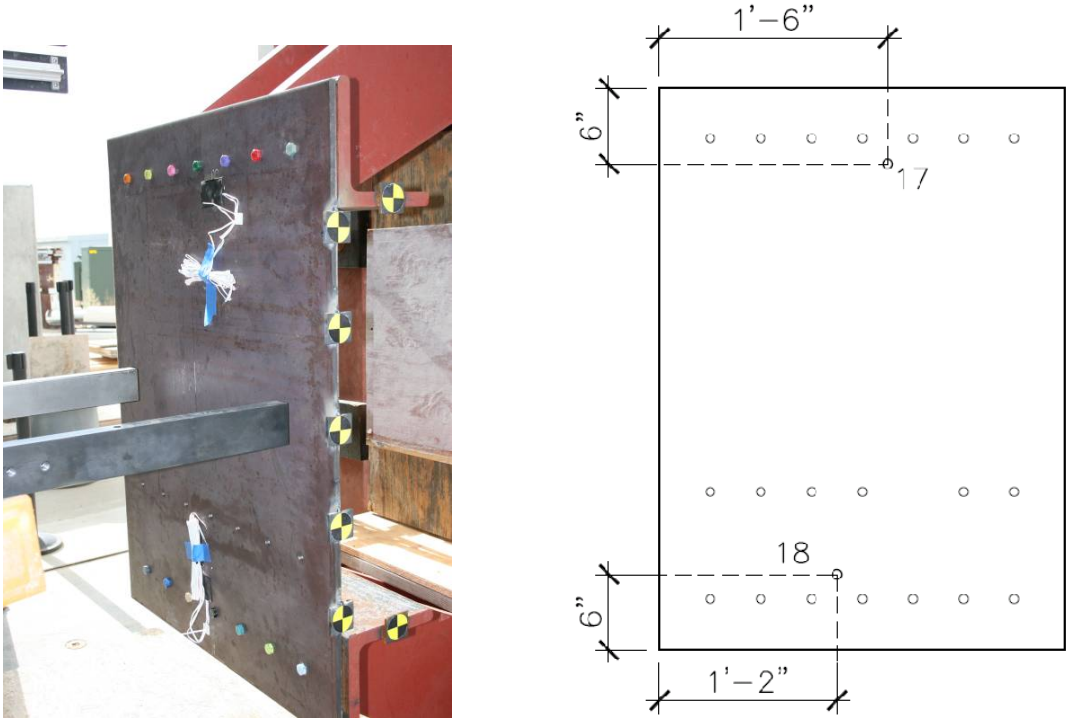

Figure E.202: Strain gage layout for Test 20

Table E.18: Stain rate information for Test 20

Strain Gage Number	Actual Velocity	Initial Impact	Shear Wave at Gage	Bolts Break	Maximum Principal Strain Rate	Minimum Principal Strain Rate
17	18.4 m/s	52.80 msec	58.20 msec	62.40 msec	-6.46 1/sec	4.92 1/sec
18	18.4 m/s	52.80 msec	58.20 msec	62.40 msec	-9.46 1/sec	5.63 1/sec

E.20.2.5 BOLT TYPE

A total of fourteen A307 bolts (Low Strength Bolts similar to Rivets) were used for this test. They were all tightened to a torque of 40 ft-lbs.

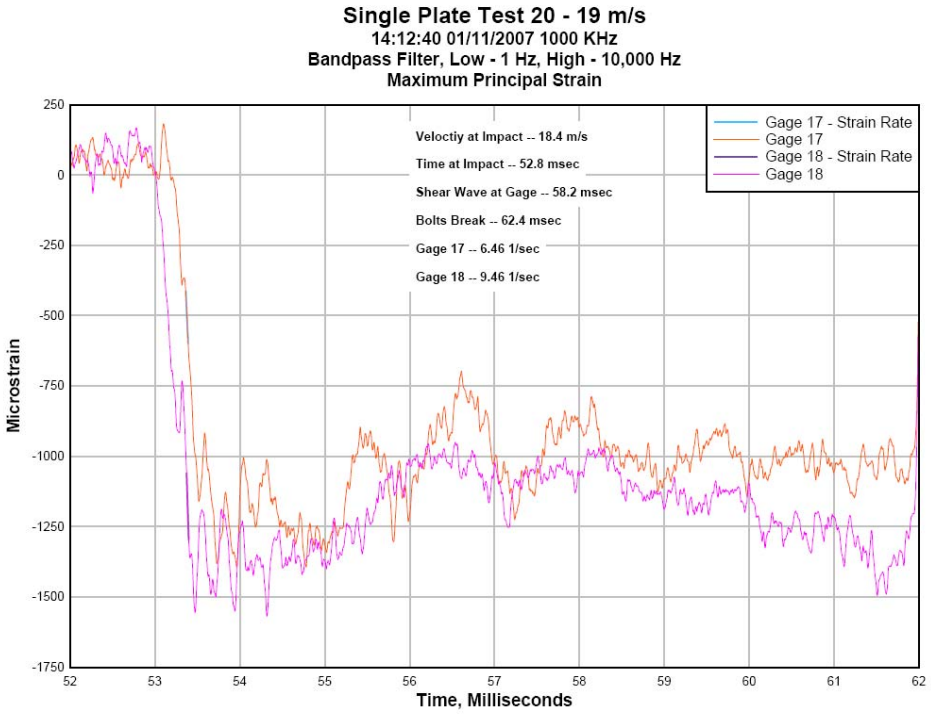

Figure E.203: Maximum principal strains and strain rates for Test 20

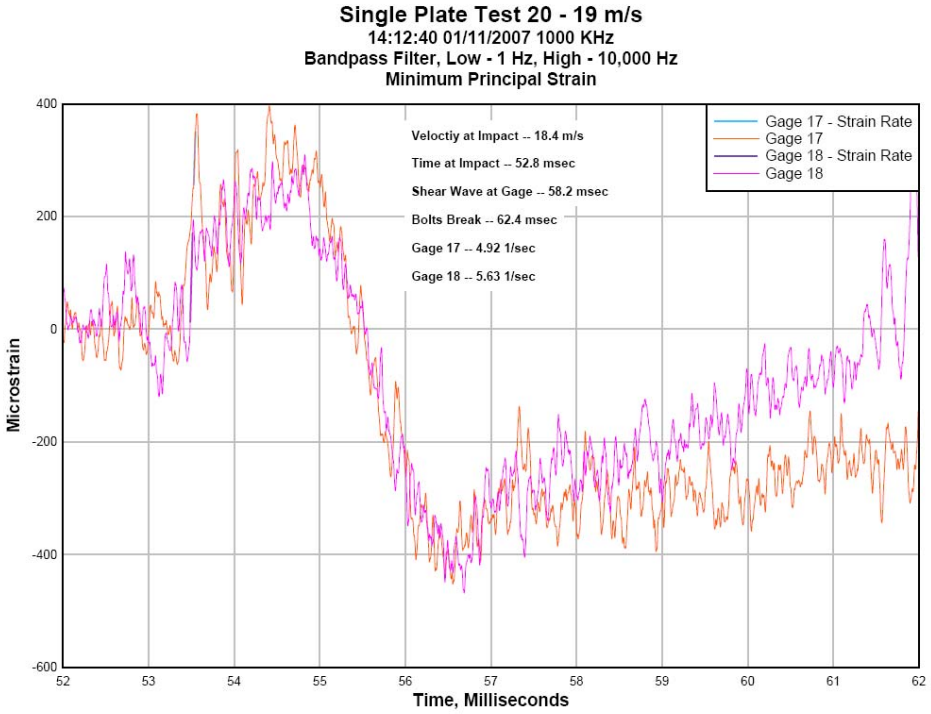

Figure E.204: Minimum principal strains and strain rates for Test 20

E.20.3 BLAST GENERATOR DATA

The initial impact of the single BG was 60.37 ft/sec (18.4 m/sec) with a goal velocity of 19.5 m/s. It had one accelerometer mounted to the back side of the impact plate as discussed in Section E.20.2.3. The average impact velocity for the impacting mass and the steel plate was calculated using the TEMA Track Eye tracking software.

E.20.4 SPECIMEN BEHAVIOR

The loading of the BG plate imparted an initial velocity of 60.37 ft/sec (18.4 m/sec) to the specimen. This caused plate to deform in both directions. The longitudinal deflection (in the north-south direction) behaved in a typical one-way flexural shape. In order to get the velocity as high as needed the test was designed to have the impacting mass break free from the BG and launch itself into the plate. This test imparted enough energy into the system that the top seven bolts broke as shown in Figure E.205. The goal of this test was to determine the threshold value for which only half of the bolts would break. That goal was achieved in this test. The maximum dynamic deflection just before the bolts broke was approximately 4 1/2".

During the test three different phantom cameras were used to capture the failure modes from two different angles. Figure E.206 shows the progression of damage for this test from Phantom Camera One. Figure E.207 shows the progression of damage for this test from Phantom Camera Two. Figure E.208 shows the progression of damage for this test from Phantom Camera Three.

Figure E.205: Steel plate post test for Test 20

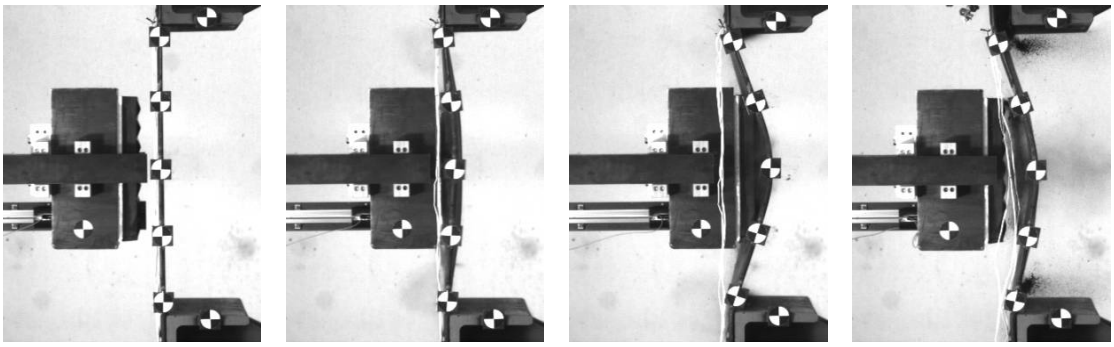

Figure E.206: Progression of damage for Test 20 from Camera 1

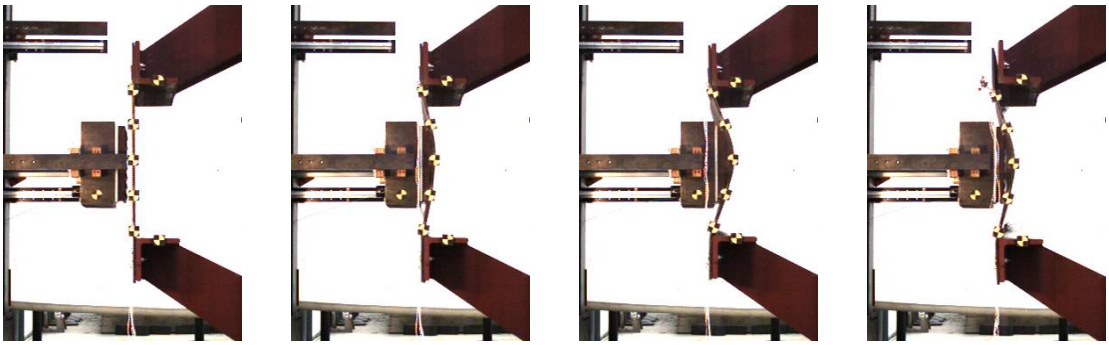

Figure E.207: Progression of damage for Test 20 from Camera 2

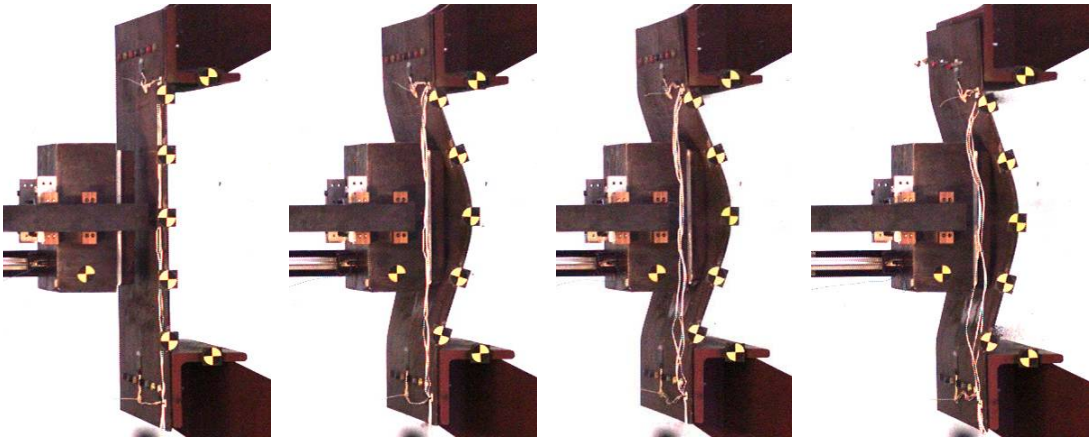

Figure E.208: Progression of damage for Test 20 from Camera 3

E.21 STEEL TOWER SINGLE PLATE: TEST 21 (SP21)

E.21.1 INTRODUCTION

The twenty-first test of the Steel Tower Single Plate test series was performed on January 17th, 2007. The test specimen was a ¾" thick steel plate labeled SP21. The Impacting Mass 1 was attached to the BG with a specimen target velocity of 91.86 ft/sec (28 m/sec). Figure E.209 shows the steel plate prior to impact.

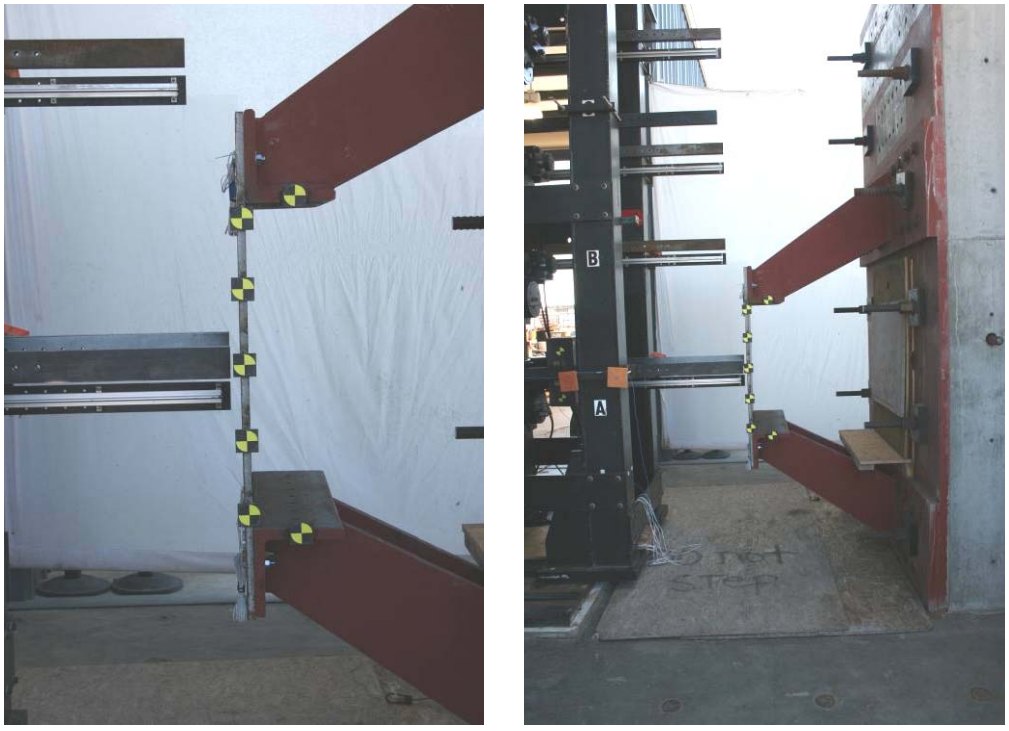

Figure E.209: 3/4" thick steel plate pre test for Test 21

E.21.2 INSTRUMENTATION

E.21.2.1 PHANTOM CAMERAS

The first camera recorded in black and white at a rate of 10,000 frames per second at a resolution of 512x384. This camera was used in order to determine the maximum velocity of the impacting mass and the movement in the plate including the maximum displacement. The second camera recorded in color at a rate of 10,000 frames per second at a resolution of 512x384. This camera recorded the overall behavior of the test specimen. It was not used to gather any specific data. The third camera recorded in color at a rate of 8,000 frames per second at a resolution of 480x480. This camera captured the failure of the bolts. A picture from each of the camera locations are shown in Figure E.210.

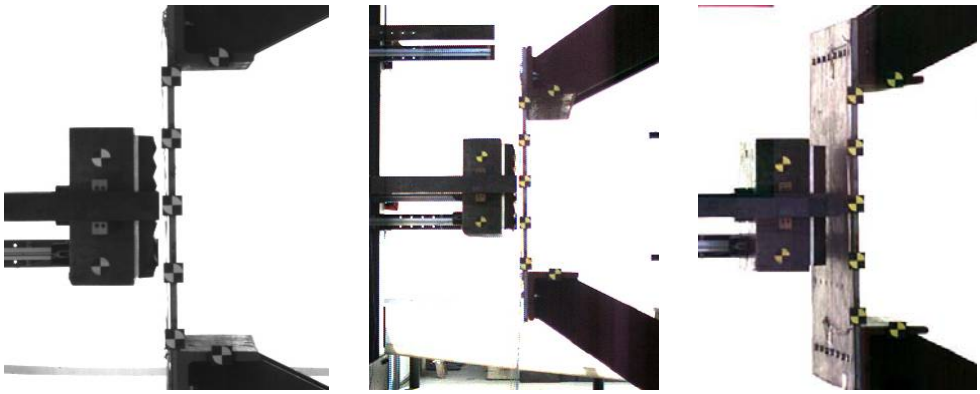

Figure E.210: Phantom Cameras for Test 21

a) Camera One b) Camera Two c) Camera Three

E.21.2.2 TARGET LOCATIONS

Five targets were welded onto the side of the steel plate as shown in Figure E.209. They were spaced at the intervals shown in Figure E.211. That figure also shows the location of the targets for the impacting mass. An additional two targets were placed on the angle at the top and the bottom end conditions. The distance between these two points is 74.93 cm (29 ½")

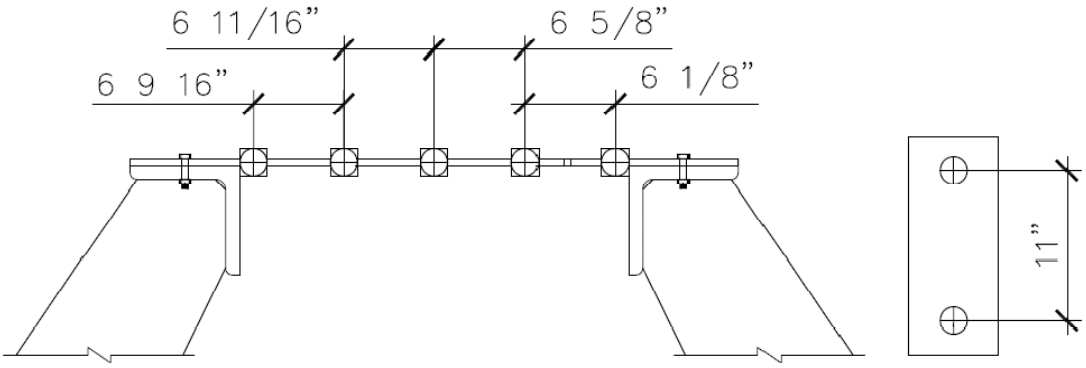

Figure E.211: Target layout on plate and impacting mass for Test 21

E.21.2.3 ACCELERATIONS

For this test one accelerometer was used. This accelerometer was placed 6" south of the centroid of the impacting mass as shown in Figure E.212. The pipe is to protect the accelerometer during the test. The data from this gage was then filtered as shown in Figure E.213.

This test does not impart an impulsive load as would be expected from a typical blast test. Instead, this test simulates the behavior of a flyer plate moving through the structure after the initial impact at the front plate of the outer cell of the structure. Therefore we are not determining the initial impulsive load from the accelerometers on the BG.

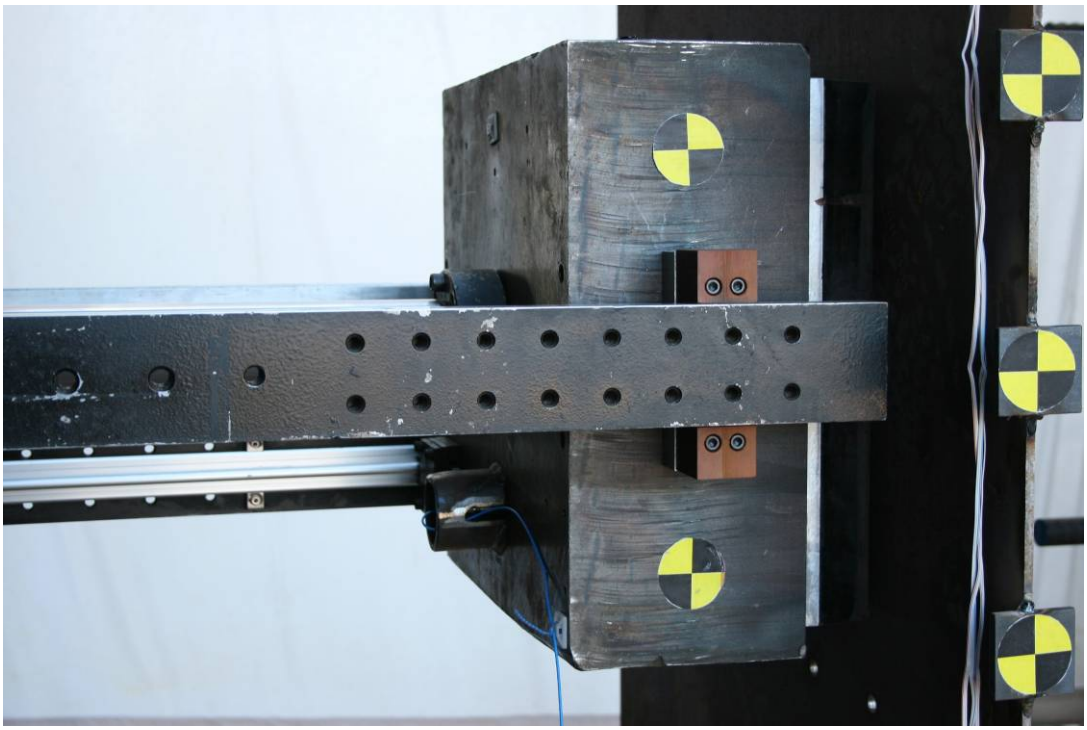

Figure E.212: Accelerometer location for Test 21

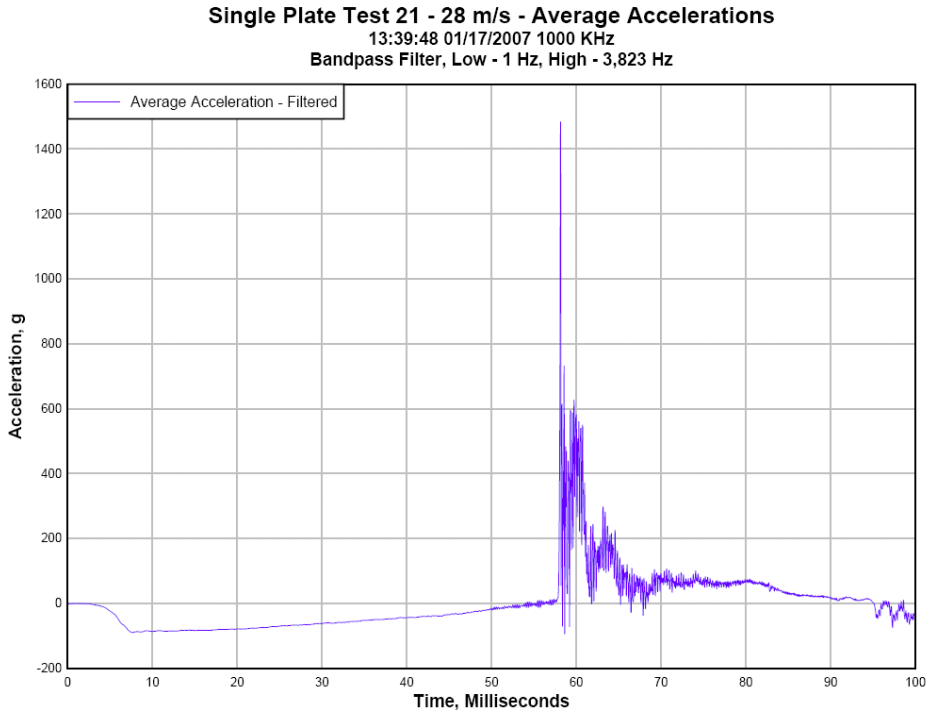

Figure E.213: Filtered accelerometer data for Test 21

E.21.2.4 STRAIN GAGE LOCATIONS

For this test there were two strain gauges labeled 17 and 18. The strain gauges, and their locations, are shown in Figure E.214. Table E.19 shows the specific information about this test, including the time and velocity at impact, if, and when, the bolts failed along with the maximum and minimum principal strain rates. The largest maximum principal strain rate for this test was 13.52 1/sec and was located at strain gage 18 while the largest minimum strain rate for this test was 5.97 1/sec located at strain gage 17. The maximum principal strains for gauges 17 and 18 can be found in Figure E.215 and the minimum principal strains for the same gauges can be found in Figure E.216.

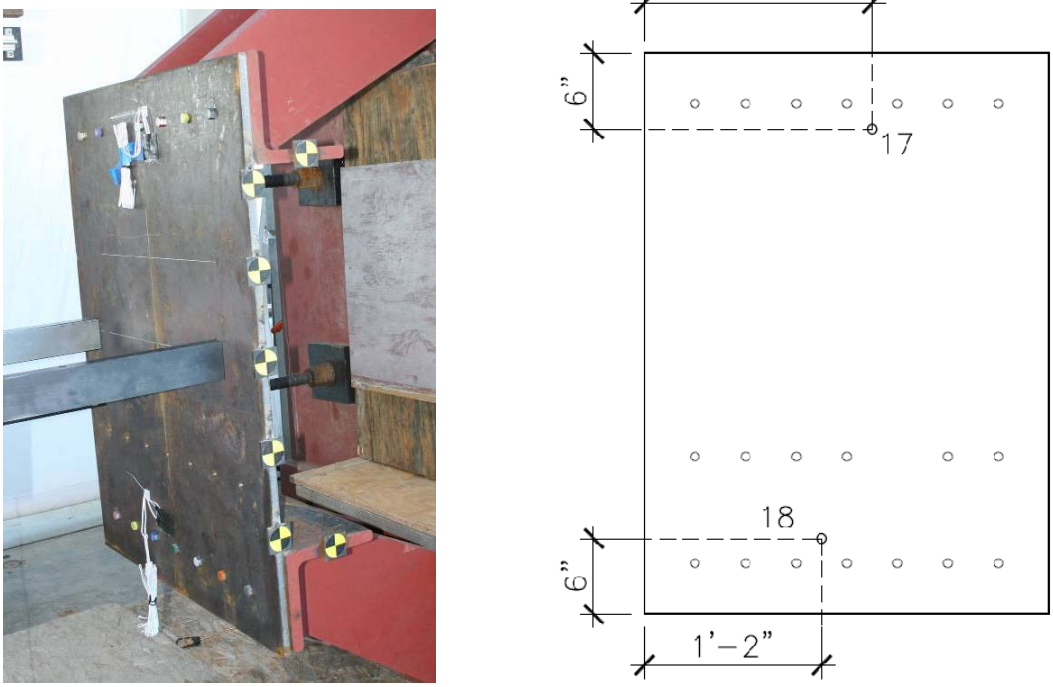

Figure E.214: Strain gage layout for Test 21

Table E.19: Stain rate information for Test 21

Strain Gage Number	Actual Velocity	Initial Impact	Shear Wave at Gage	Bolts Break	Maximum Principal Strain Rate	Minimum Principal Strain Rate
17	27.9 m/s	57.90 msec	60.80 msec	61.30 msec	-10.43 1/sec	5.97 1/sec
18	27.9 m/s	57.90 msec	60.80 msec	61.30 msec	-13.52 1/sec	2.99 1/sec

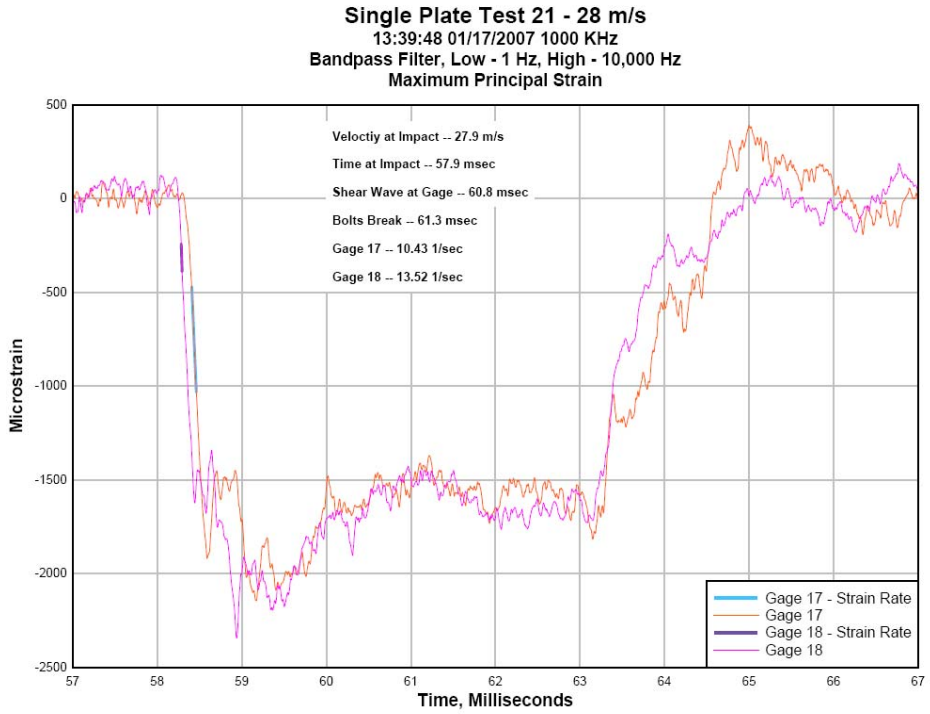

Figure E.215: Maximum principal strains and strain rates for Test 21

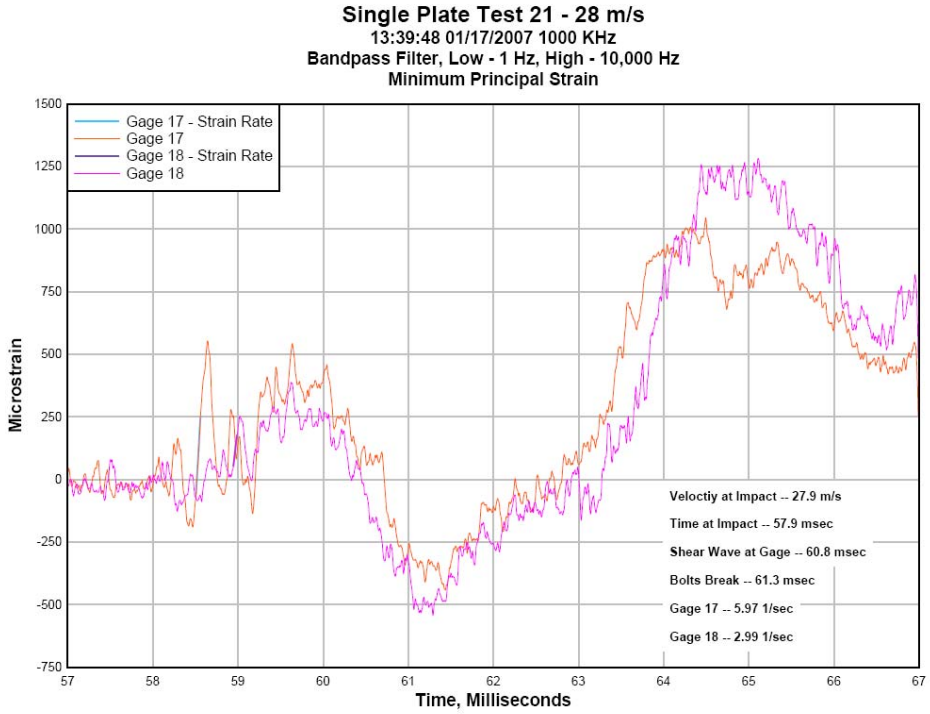

Figure E.216: Minimum principal strains and strain rates for Test 21

E.21.2.5 BOLT TYPE

A total of fourteen A307 bolts (Low Strength Bolts similar to Rivets) were used for this test. They were all tightened to a torque of 40 ft-lbs.

E.21.3 BLAST GENERATOR DATA

The initial impact of the single BG was 91.54 ft/sec (27.9 m/sec) with a goal velocity of 28 m/s. It had one accelerometer mounted to the back side of the impact plate as discussed in Section E.21.2.3. The average impact velocity for the impacting mass and the steel plate was calculated using the TEMA Track Eye tracking software.

E.21.4 SPECIMEN BEHAVIOR

The loading of the BG plate imparted an initial velocity of 91.54 ft/sec (27.9 m/sec) to the specimen. This caused plate to deform in both directions. The longitudinal deflection (in the north-south direction) behaved in a typical one-way flexural shape. In order to get the velocity as high as needed the test was designed to have the impacting mass break free from the BG and launch itself into the plate. . This test imparted enough energy into the system that all fourteen bolts broke as shown in
Figure E.217. The maximum dynamic deflection just before the bolts broke was approximately 2 7/8".

During the test pieces of bolts flew approximately 20" northwest of the test set-up and 16' into the lab area southeast of the test set-up. During the test three different phantom cameras were used to capture the failure modes from three different angles. Figure E.218 shows the progression of damage for this test from Phantom Camera One. Figure E.219 shows the progression of damage for this test from Phantom Camera Two. Figure E.220 shows the progression of damage for this test from Phantom Camera Three.

Figure E.217: Steel plate post test for Test 21

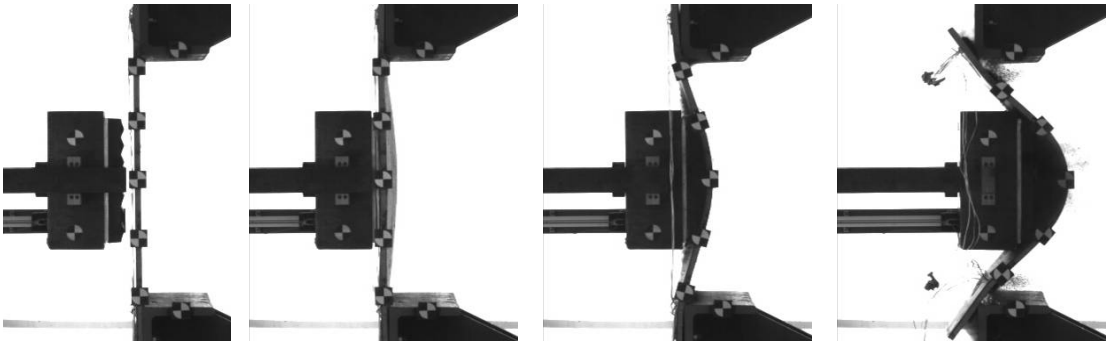

Figure E.218: Progression of damage for Test 21 from Camera 1

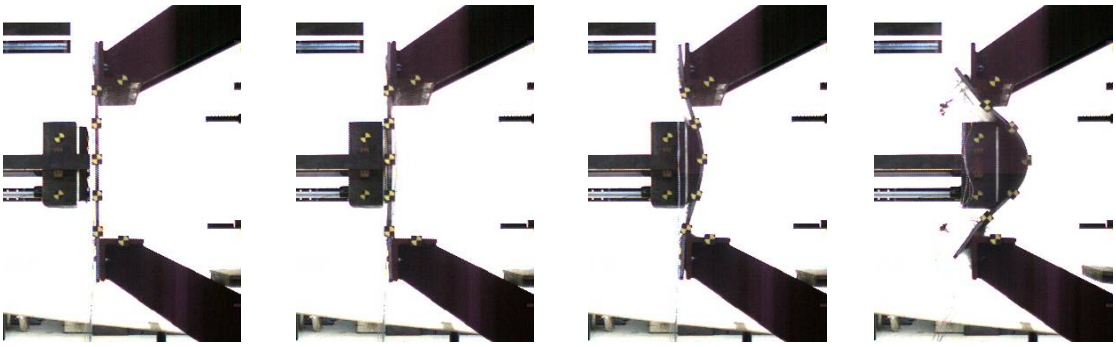

Figure E.219: Progression of damage for Test 21 from Camera 2

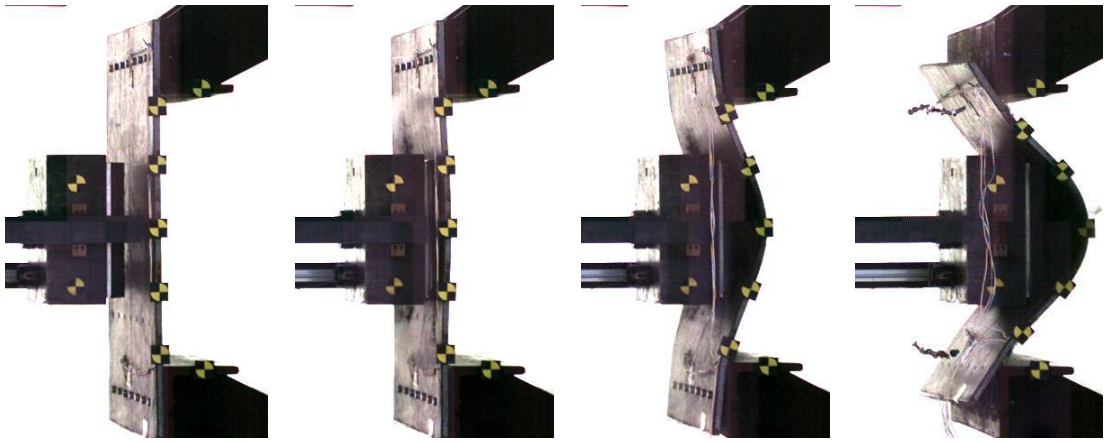

Figure E.220: Progression of damage for Test 21 from Camera 3

E.22 STEEL TOWER SINGLE PLATE: TEST 22 (SP22)

E.22.1 INTRODUCTION

The twenty-second test of the Steel Tower Single Plate test series was performed on January 18th, 2007. The test specimen was a ¾" thick steel plate labeled SP22. The Impacting Mass 1 was attached to the BG with a specimen target velocity of 91.86 ft/sec (28 m/sec). Figure E.221 shows the steel plate prior to impact.

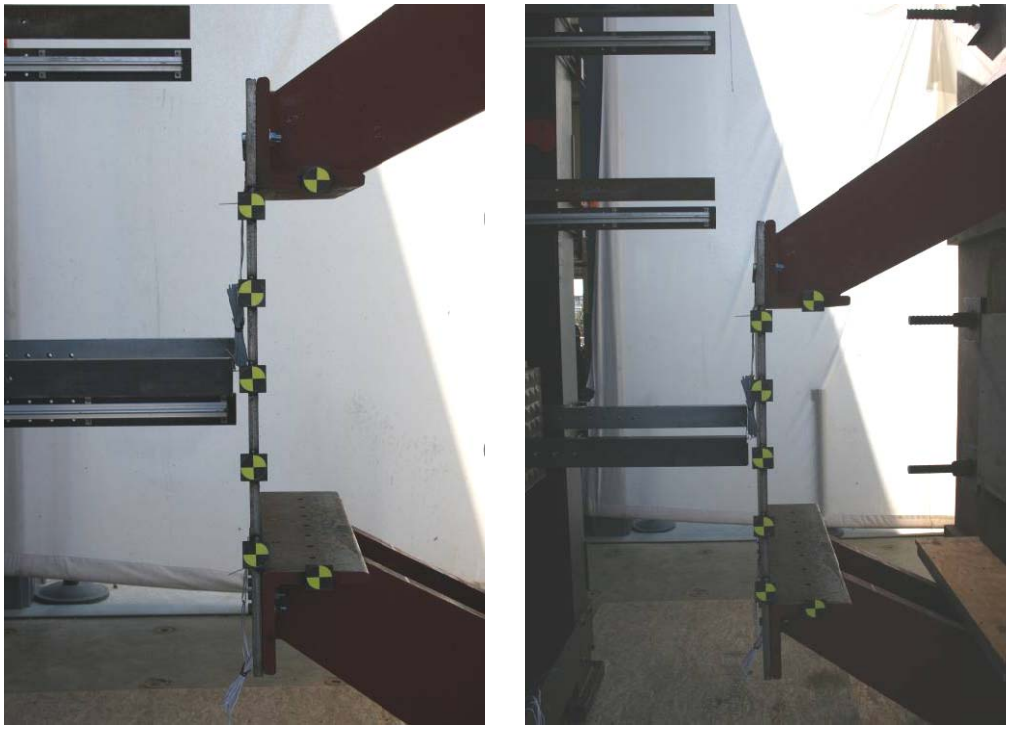

Figure E.221: 3/4" thick steel plate pre test for Test 22

E.22.2 INSTRUMENTATION

E.22.2.1 PHANTOM CAMERAS

The first camera recorded in black and white at a rate of 10,000 frames per second at a resolution of 512x384. This camera was used in order to determine the maximum velocity of the impacting mass and the movement in the plate including the maximum displacement. The second camera recorded in color at a rate of 10,000 frames per second at a resolution of 512x384. This camera recorded the overall behavior of the test specimen. It was not used to gather any specific data. The third camera recorded in color at a rate of 5,000 frames per second at a resolution of 480x480. This camera captured the failure of the bolts. A picture from each of the camera locations are shown in Figure E.222.

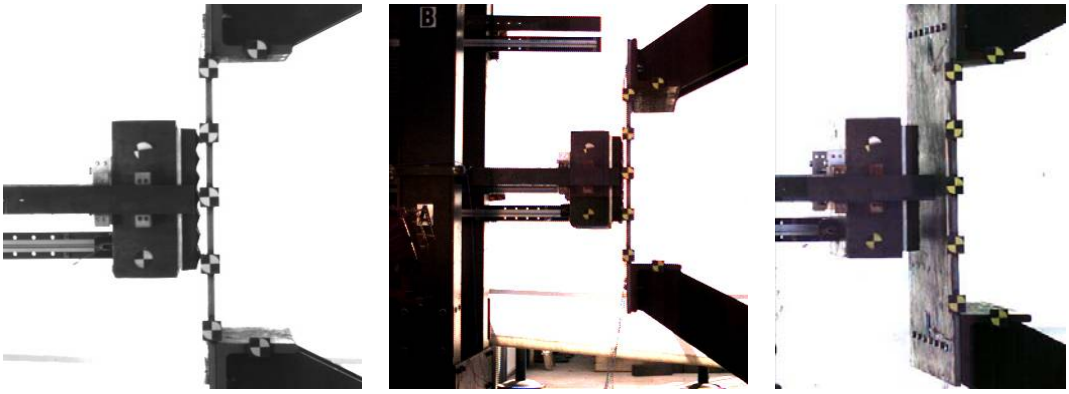

Figure E.222: Phantom Cameras for Test 22

a) Camera One b) Camera Two c) Camera Three

E.22.2.2 TARGET LOCATIONS

Five targets were welded onto the side of the steel plate as shown in Figure E.221. They were spaced at the intervals shown in Figure E.223. That figure also shows the location of the targets for the impacting mass. An additional two targets were placed on the angle at the top and the bottom end conditions. The distance between these two points is 74.93 cm (29 ½")

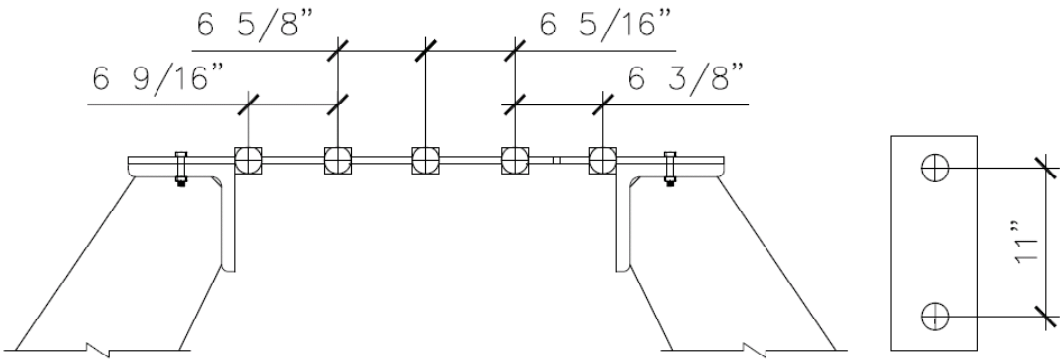

Figure E.223: Target layout on plate and impacting mass for Test 22

E.22.2.3 ACCELERATIONS

For this test accelerometers were not used.

E.22.2.4 STRAIN GAGE LOCATIONS

For this test there were two strain gauges labeled 17 and 18. The strain gauges, and their locations, are shown in Figure E.224. Table E.20 shows the specific information about this test, including the time and velocity at impact, if, and when, the bolts failed along with the maximum and minimum principal strain rates. The largest maximum principal strain rate for this test was 10.18 1/sec and was located at strain gage 18 while the largest minimum strain

rate for this test was 6.76 1/sec located at strain gage 18. The maximum principal strains for gauges 17 and 18 can be found in Figure E.225 and the minimum principal strains for the same gauges can be found in Figure E.226.

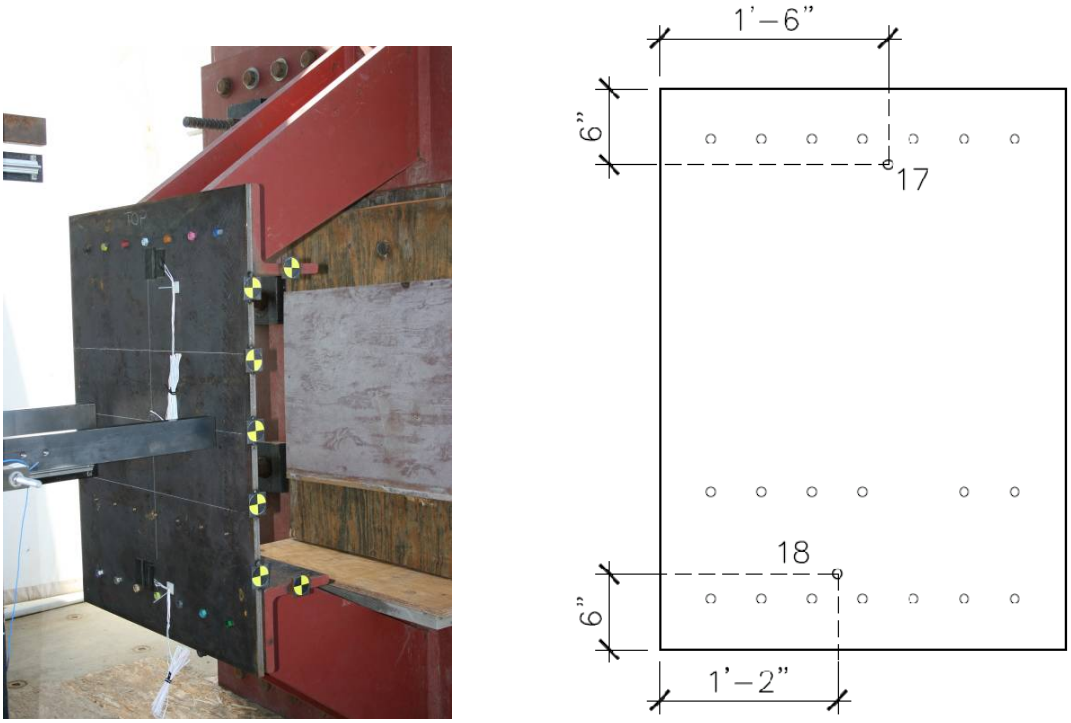

Figure E.224: Strain gage layout for Test 22

Table E.20: Stain rate information for Test 22

Strain Gage Number	Actual Velocity	Initial Impact	Shear Wave at Gage	Bolts Break	Maximum Principal Strain Rate	Minimum Principal Strain Rate
17	24.9 m/s	58.40 msec	61.60 msec	62.10 msec	-9.28 1/sec	4.34 1/sec
18	24.9 m/s	58.40 msec	61.60 msec	62.10 msec	-10.18 1/sec	6.76 1/sec

E.22.2.5 BOLT TYPE

A total of fourteen A307 bolts (Low Strength Bolts similar to Rivets) were used for this test. They were all tightened to a torque of 40 ft-lbs.

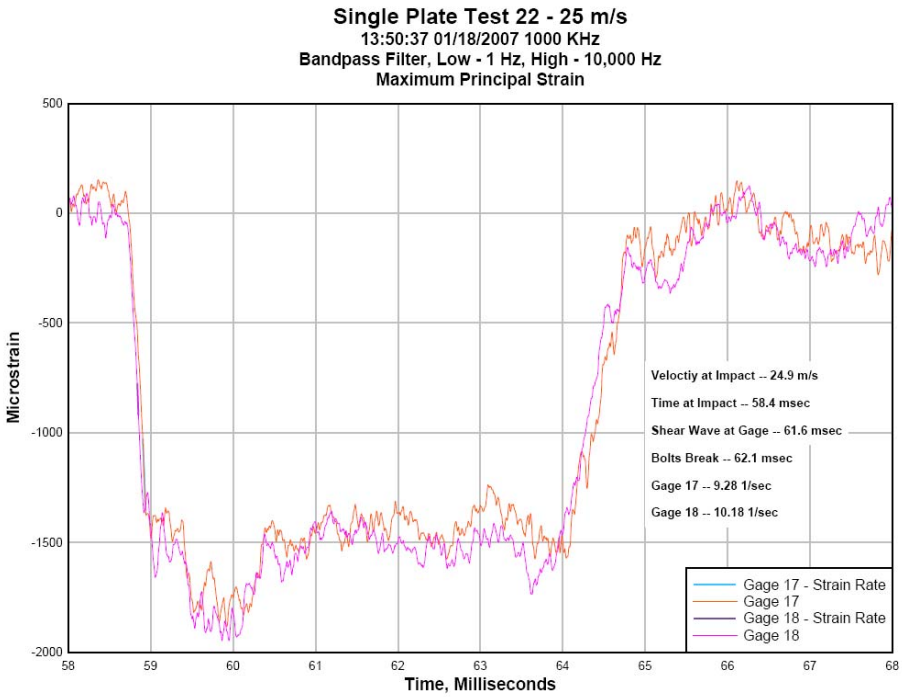

Figure E.225: Maximum principal strains and strain rates for Test 22

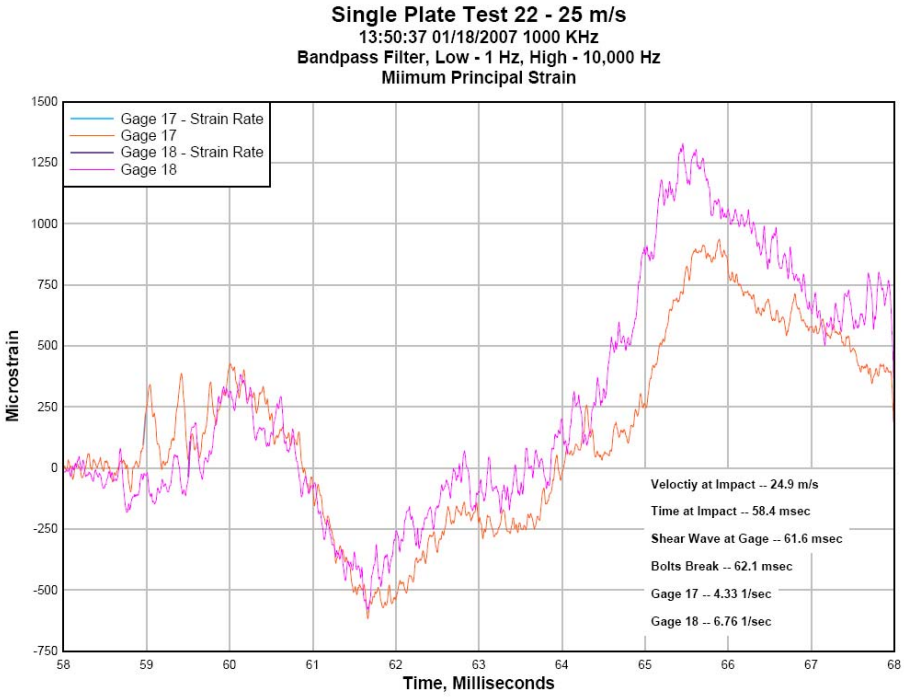

Figure E.226: Minimum principal strains and strain rates for Test 22

E.22.3 BLAST GENERATOR DATA

The initial impact of the single BG was 81.69 ft/sec (24.9 m/sec) with a goal velocity of 28 m/s. The average impact velocity for the impacting mass and the steel plate was calculated using the TEMA Track Eye tracking software.

E.22.4 SPECIMEN BEHAVIOR

The loading of the BG plate imparted an initial velocity of 81.69 ft/sec (24.9 m/sec) to the specimen. This caused plate to deform in both directions. The longitudinal deflection (in the north-south direction) behaved in a typical one-way flexural shape. In order to get the velocity as high as needed the test was designed to have the impacting mass break free from the BG and launch itself into the plate. This test imparted enough energy into the system that all fourteen bolts broke as shown in Figure E.227. The maximum dynamic deflection just before the bolts broke was approximately 3 1/8".

During the test pieces of bolts flew approximately 13' north of the test set-up. During the test three different phantom cameras were used to capture the failure modes from three different angles. Figure E.228 shows the progression of damage for this test from Phantom Camera One. Figure E.229 shows the progression of damage for this test from Phantom Camera Two. Figure E.230 shows the progression of damage for this test from Phantom Camera Three.

Figure E.227: Steel plate post test for Test 22

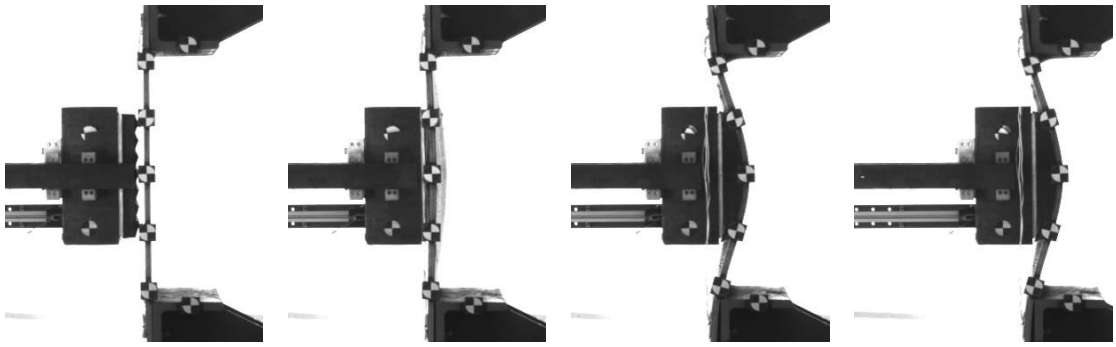

Figure E.228: Progression of damage for Test 22 from Camera 1

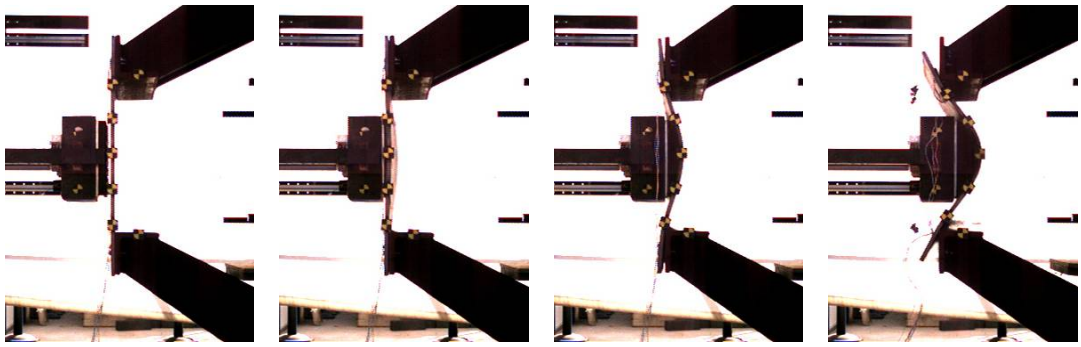

Figure E.229: Progression of damage for Test 22 from Camera 2

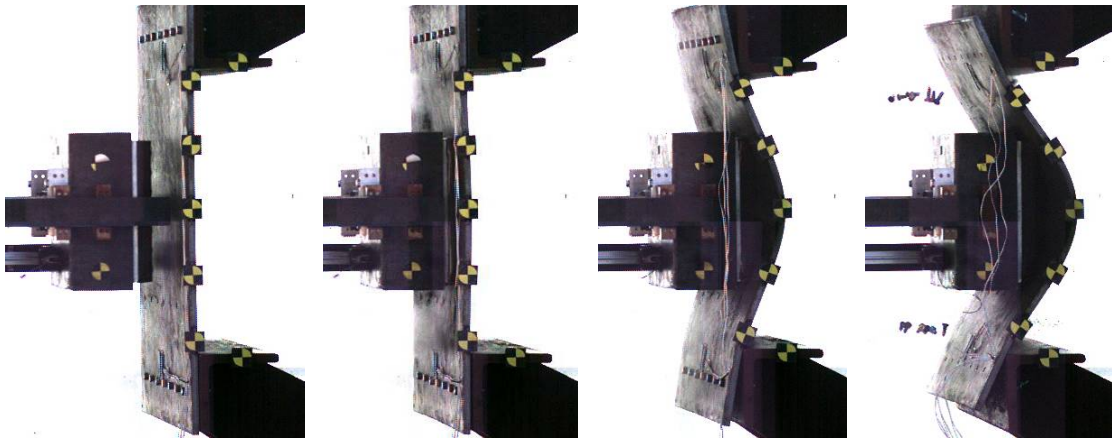

Figure E.230: Progression of damage for Test 22 from Camera 3

E.23 STEEL TOWER SINGLE PLATE: TEST 23 (SP23)

E.23.1 INTRODUCTION

The twenty-third test of the Steel Tower Single Plate test series was performed on January 23rd, 2007. The test specimen was a ¾" thick steel plate labeled SP23. The Impacting Mass 1 was attached to the BG with a specimen target velocity of 82.02 ft/sec (25 m/sec). Figure E.231 shows the steel plate prior to impact.

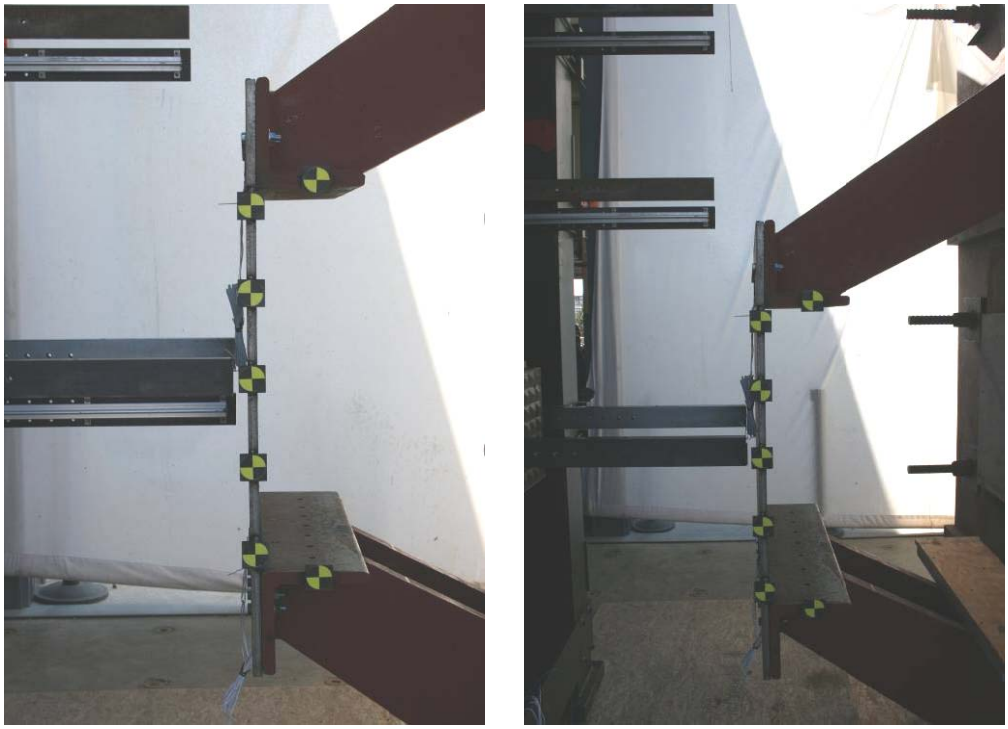

Figure E.231: 3/4" thick steel plate pre test for Test 23

E.23.2 INSTRUMENTATION

E.23.2.1 PHANTOM CAMERAS

The first camera recorded in black and white at a rate of 10,000 frames per second at a resolution of 512x384. This camera was used in order to determine the maximum velocity of the impacting mass and the movement in the plate including the maximum displacement. The second camera recorded in color at a rate of 10,000 frames per second at a resolution of 512x384. This camera recorded the overall behavior of the test specimen. It was not used to gather any specific data. The third camera recorded in color at a rate of 5,000 frames per second at a resolution of 480x480. This camera captured the failure of the bolts. A picture from each of the camera locations are shown in Figure E.232

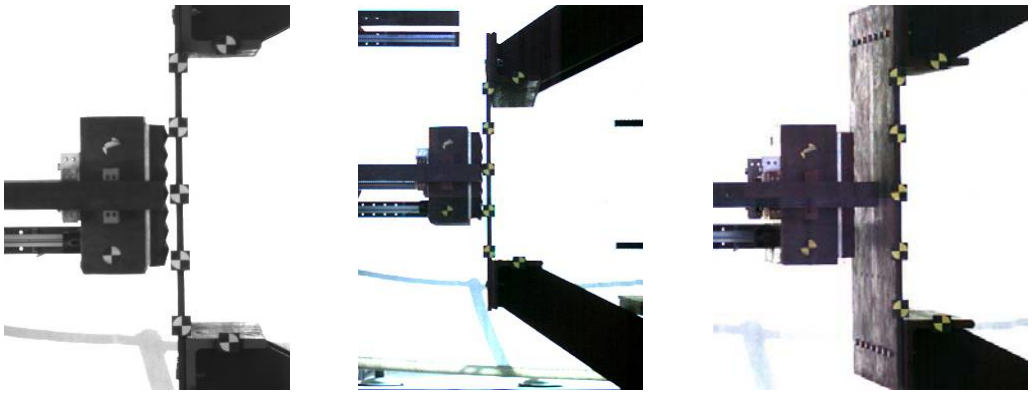

Figure E.232: Phantom Cameras for Test 23

a) Camera One b) Camera Two c) Camera Three

E.23.2.2 TARGET LOCATIONS

Five targets were welded onto the side of the steel plate as shown in Figure E.231. They were spaced at the intervals shown in Figure E.233. That figure also shows the location of the targets for the impacting mass. An additional two targets were placed on the angle at the top and the bottom end conditions. The distance between these two points is 74.93 cm (29 ½")

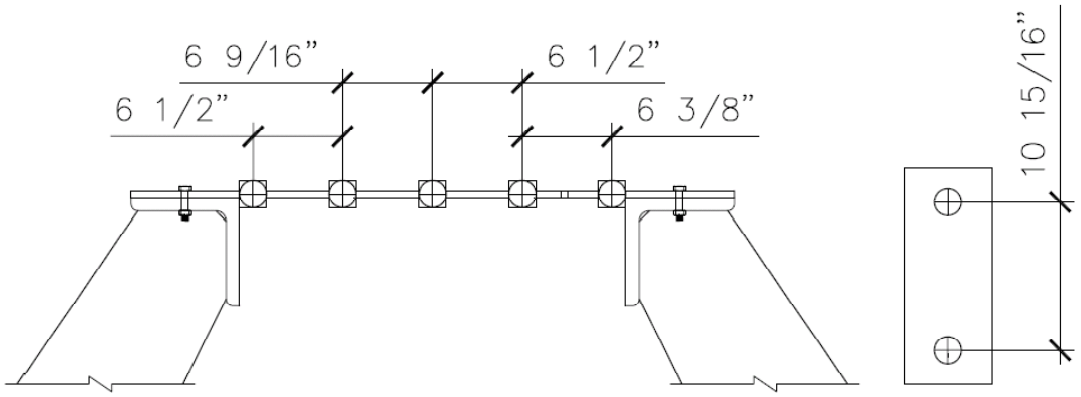

Figure E.233: Target layout on plate and impacting mass for Test 23

E.23.2.3 ACCELERATIONS

For this test accelerometers were not used.

E.23.2.4 STRAIN GAGE LOCATIONS

For this test strain gauges were not used.

E.23.2.5 BOLT TYPE

A total of fourteen A307 bolts (Low Strength Bolts similar to Rivets) were used for this test. They were all tightened to a torque of 40 ft-lbs.

E.23.3 BLAST GENERATOR DATA

The initial impact of the single BG was 75.46 ft/sec (23 m/sec) with a goal velocity of 25 m/s. The average impact velocity for the impacting mass and the steel plate was calculated using the TEMA Track Eye tracking software.

E.23.4 SPECIMEN BEHAVIOR

The loading of the BG plate imparted an initial velocity of 75.46 ft/sec (23 m/sec) to the specimen. This caused plate to deform in both directions. The longitudinal deflection (in the north-south direction) behaved in a typical one-way flexural shape. In order to get the velocity as high as needed the test was designed to have the impacting mass break free from the BG and launch itself into the plate. This test imparted enough energy into the system that all fourteen bolts broke as shown in Figure E.234. During the test three different phantom cameras were used to capture the failure modes from three different angles. Figure E.235 shows the progression of damage for this test from Phantom Camera One. Figure E.236 shows the progression of damage for this test from Phantom Camera Two. Figure E.237 shows the progression of damage for this test from Phantom Camera Three.

Figure E.234: Steel plate post test for Test 23

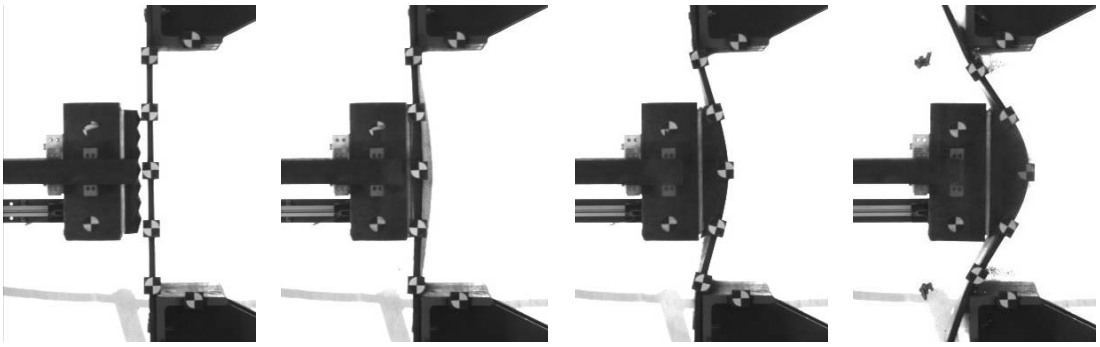

Figure E.235: Progression of damage for Test 23 from Camera 1

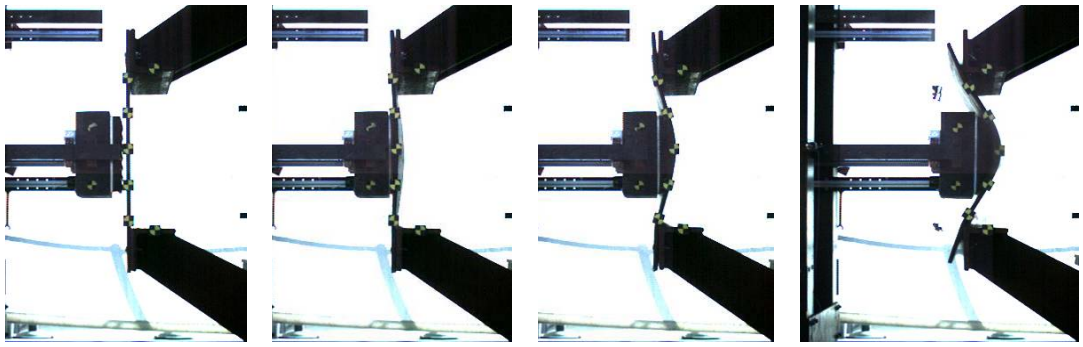

Figure E.236: Progression of damage for Test 23 from Camera 2

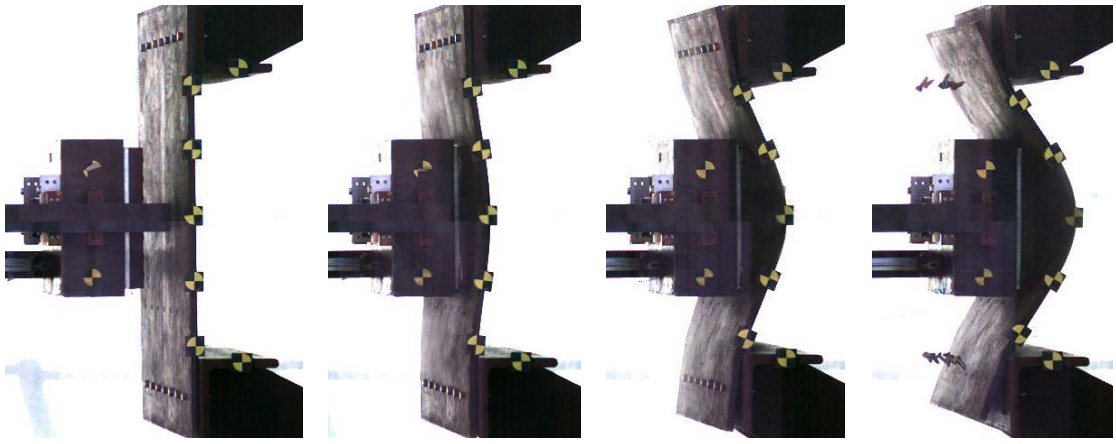

Figure E.237: Progression of damage for Test 23 from Camera 3

E.24 STEEL TOWER SINGLE PLATE: TEST 24 (SP24)

E.24.1 INTRODUCTION

The twenty-fourth test of the Steel Tower Single Plate test series was performed on January 25th, 2007. The test specimen was a ¼" thick steel plate labeled SP24. The Impacting Mass 1 was attached to the BG with a specimen target velocity of 63.98 ft/sec (19.5 m/sec). Figure E.238 shows the steel plate prior to impact.

Figure E.238: 1/4" thick steel plate pre test for Test 24

E.24.2 INSTRUMENTATION

E.24.2.1 PHANTOM CAMERAS

The first camera recorded in black and white at a rate of 10,000 frames per second at a resolution of 512x384. This camera was used in order to determine the maximum velocity of the impacting mass and the movement in the plate including the maximum displacement. The second camera recorded in color at a rate of 5,000 frames per second at a resolution of 512x384. This camera recorded the overall behavior of the test specimen. It was not used to gather any specific data. The third camera recorded in color at a rate of 5,000 frames per second at a resolution of 480x480. This camera captured the failure of the bolts. A picture from each of the camera locations are shown in Figure E.239

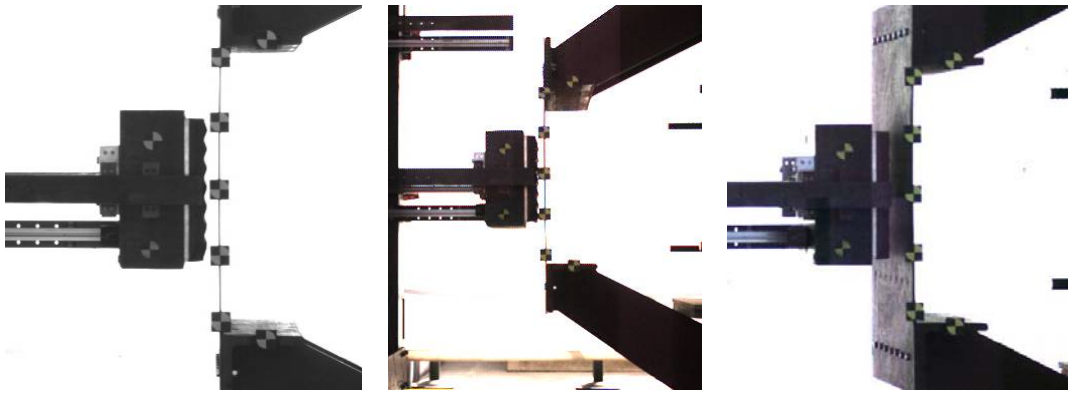

Figure E.239: Phantom Cameras for Test 24

a) Camera One b) Camera Two c) Camera Three

E.24.2.2 TARGET LOCATIONS

Five targets were welded onto the side of the steel plate as shown in Figure E.238. They were spaced at the intervals shown in Figure E.240. That figure also shows the location of the targets for the impacting mass. An additional two targets were placed on the angle at the top and the bottom end conditions. The distance between these two points is 74.93 cm (29 ½")

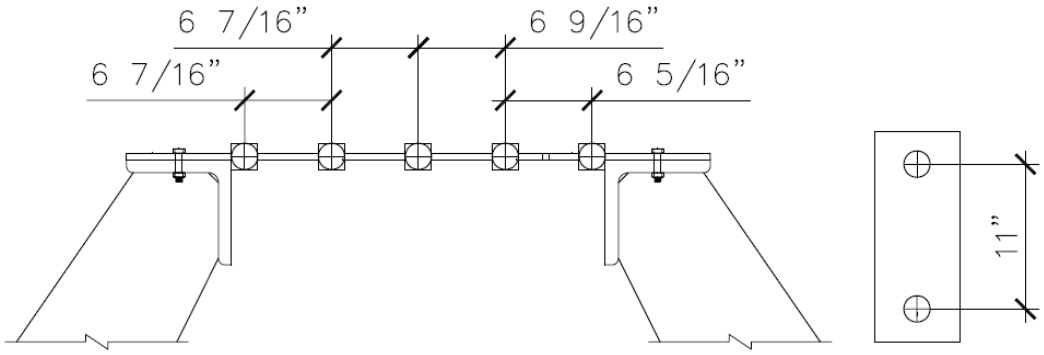

Figure E.240: Target layout on plate and impacting mass for Test 24

E.24.2.3 ACCELERATIONS

For this test one accelerometer was used. This accelerometer was placed 6" south of the centroid of the impacting mass as shown in Figure E.241. The pipe is to protect the accelerometer during the test. The data from this gage was then filtered as shown in Figure E.242.

This test does not impart an impulsive load as would be expected from a typical blast test. Instead, this test simulates the behavior of a flyer plate moving through the structure after the initial impact at the front plate of the outer cell of the structure. Therefore we are not determining the initial impulsive load from the accelerometers on the BG.

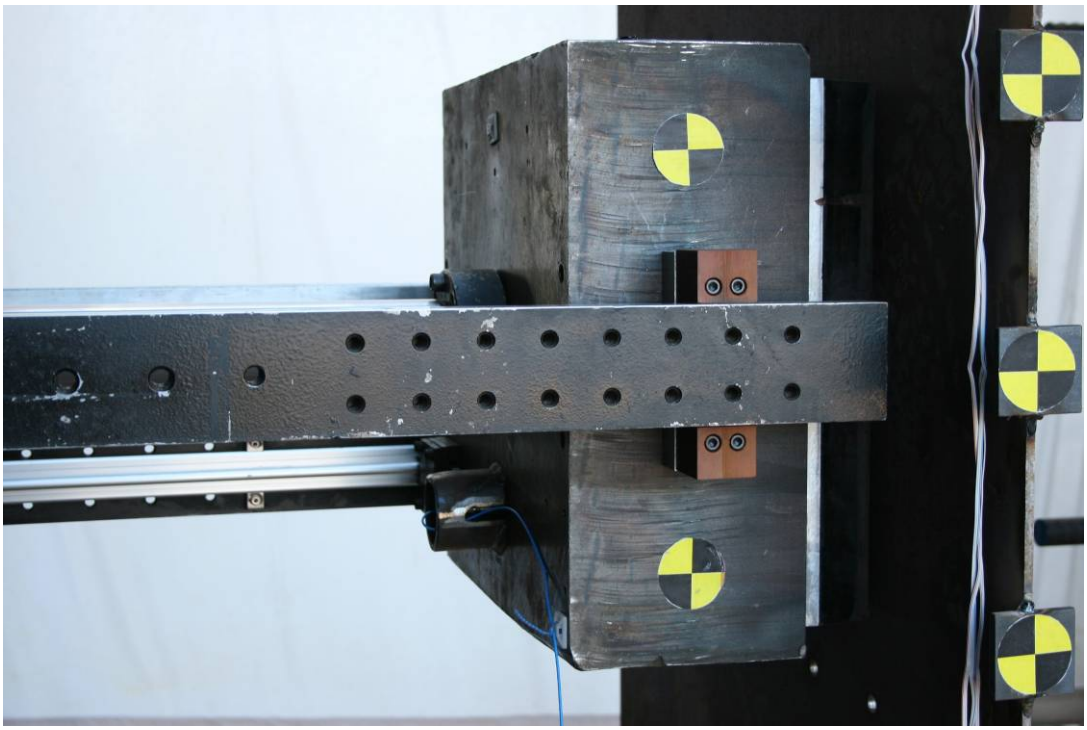

Figure E.241: Accelerometer location for Test 2

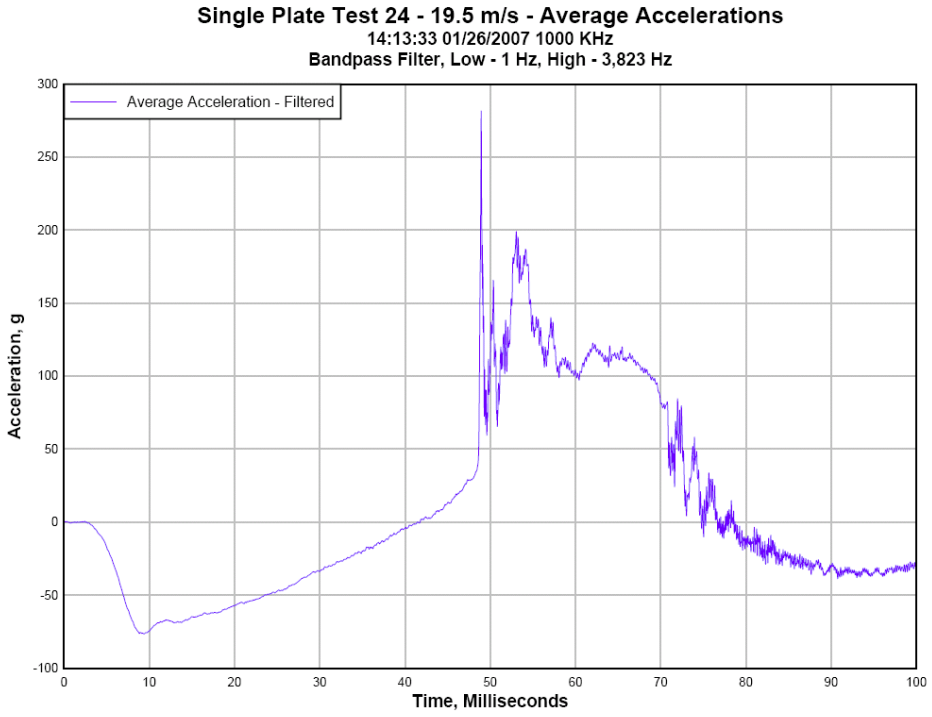

Figure E.242: Filtered accelerometer data for Test 24

E.24.2.4 STRAIN GAGE LOCATIONS

For this test strain gauges were not used.

E.24.2.5 BOLT TYPE

A total of fourteen A307 bolts (Low Strength Bolts similar to Rivets) were used for this test. They were all tightened to a torque of 40 ft-lbs.

E.24.3 BLAST GENERATOR DATA

The initial impact of the single BG was 63.98 ft/sec (19.5 m/sec) with a goal velocity of 19.5 m/s. It had one accelerometer mounted to the back side of the impact plate as discussed in Section E.24.2.3. The average impact velocity for the impacting mass and the steel plate was calculated using the TEMA Track Eye tracking software.

E.24.4 SPECIMEN BEHAVIOR

The loading of the BG plate imparted an initial velocity of 63.98 ft/sec (19.5 m/sec) to the specimen. This caused plate to deform in both directions. The longitudinal deflection (in the north-south direction) behaved in a typical one-way flexural shape. In order to get the velocity as high as needed the test was designed to have the impacting mass break free from the BG and launch itself into the plate. This test imparted enough energy into the system that all fourteen bolts broke as shown in Figure E.243. After the test a bolt head was found 12' north of the set-up and 14' southeast of the test in the lab area.

During the test three different phantom cameras were used to capture the failure modes from three different angles. Figure E.244 shows the progression of damage for this test from Phantom Camera One. Figure E.245 shows the progression of damage for this test from Phantom Camera Two. Figure E.246 shows the progression of damage for this test from Phantom Camera Three.

Figure E.243: Steel plate post test for Test 24

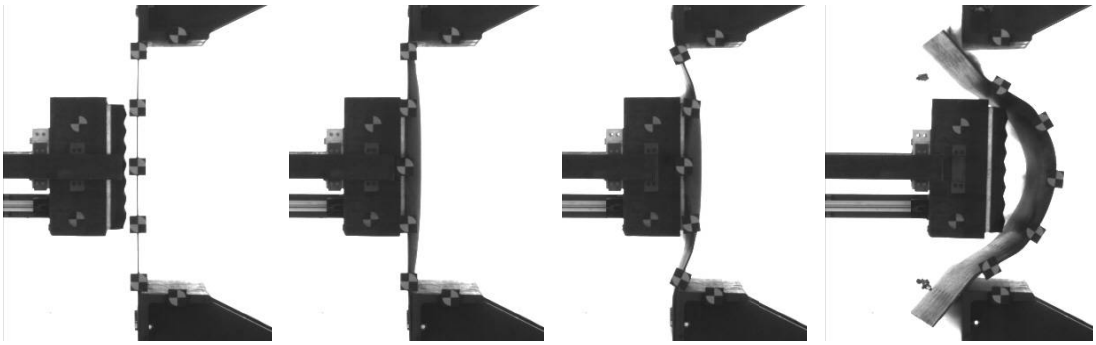

Figure E.244: Progression of damage for Test 24 from Camera 1

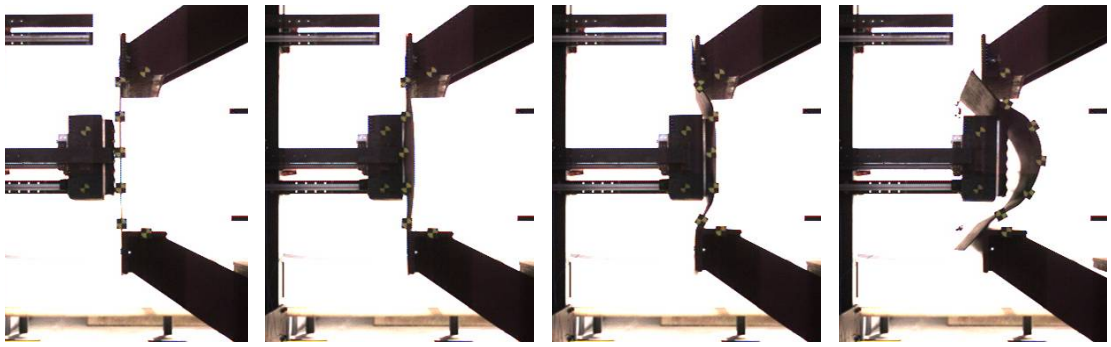

Figure E.245: Progression of damage for Test 24 from Camera 2

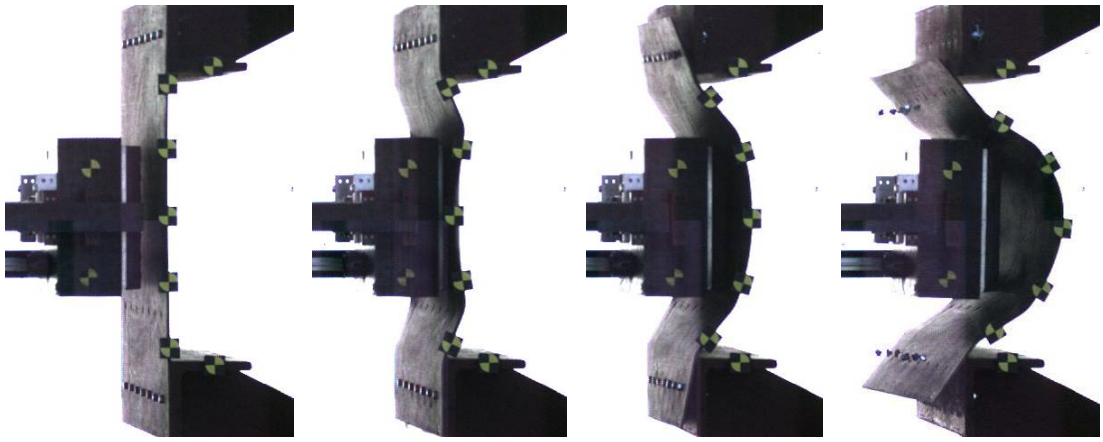

Figure E.246: Progression of damage for Test 24 from Camera 3

E.25 STEEL TOWER SINGLE PLATE: TEST 25 (SP25)

E.25.1 INTRODUCTION

The twenty-fifth test of the Steel Tower Single Plate test series was performed on January 31st, 2007. The test specimen was a ¼" thick steel plate labeled SP25. The Impacting Mass 1 was attached to the BG with a specimen target velocity of 63.98 ft/sec (19.5 m/sec). Figure E.247 shows the steel plate prior to impact.

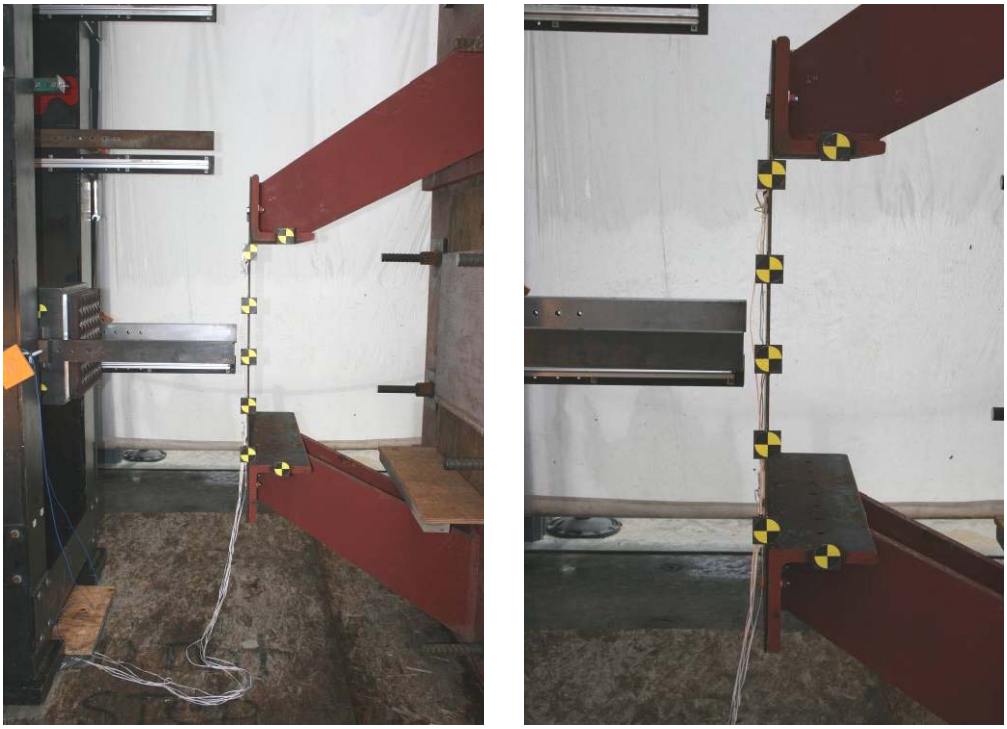

Figure E.247: 1/4" thick steel plate pre test for Test 25

E.25.2 INSTRUMENTATION

E.25.2.1 PHANTOM CAMERAS

The first camera recorded in black and white at a rate of 10,000 frames per second at a resolution of 512x384. This camera was used in order to determine the maximum velocity of the impacting mass and the movement in the plate including the maximum displacement. The second camera recorded in color at a rate of 5,000 frames per second at a resolution of 512x384. This camera recorded the overall behavior of the test specimen. It was not used to gather any specific data. The third camera recorded in color at a rate of 5,000 frames per second at a resolution of 480x480. This camera captured the failure of the bolts. A picture from each of the camera locations are shown in Figure E.248.

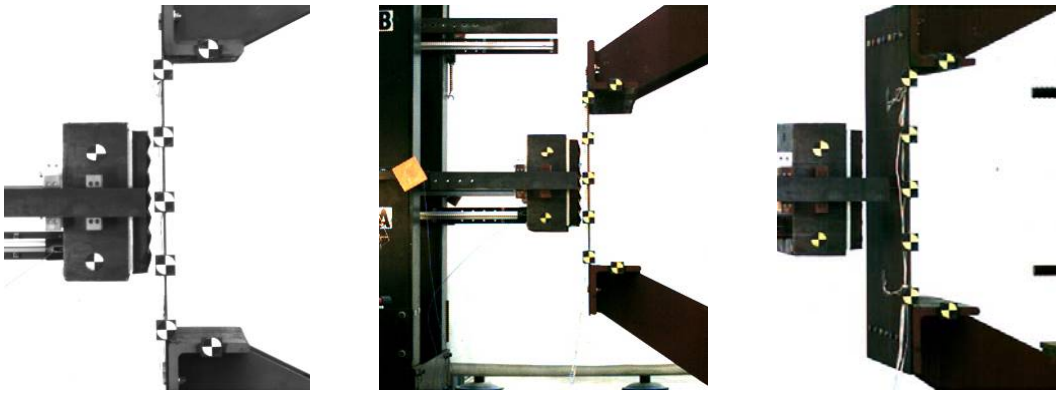

Figure E.248: Phantom Cameras for Test 25

a) Camera One b) Camera Two c) Camera Three

E.25.2.2 TARGET LOCATIONS

Five targets were welded onto the side of the steel plate as shown in Figure E.247. They were spaced at the intervals shown in Figure E.249. That figure also shows the location of the targets for the impacting mass. An additional two targets were placed on the angle at the top and the bottom end conditions. The distance between these two points is 74.93 cm (29 ½")

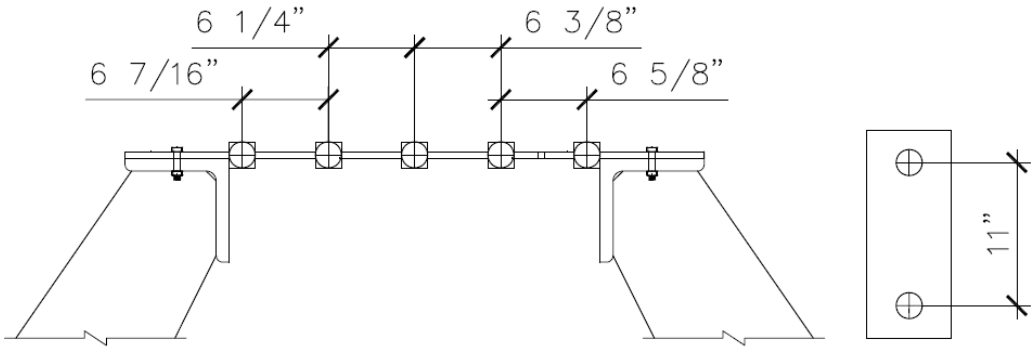

Figure E.249: Target layout on plate and impacting mass for Test 25

E.25.2.3 ACCELERATIONS

For this test one accelerometer was used. This accelerometer was placed 6" south of the centroid of the impacting mass as shown in Figure E.250. The pipe is to protect the accelerometer during the test. The data from this gage was then filtered as shown in Figure E.251.

This test does not impart an impulsive load as would be expected from a typical blast test. Instead, this test simulates the behavior of a flyer plate moving through the structure after the initial impact at the front plate of the outer cell of the structure. Therefore we are not determining the initial impulsive load from the accelerometers on the BG.

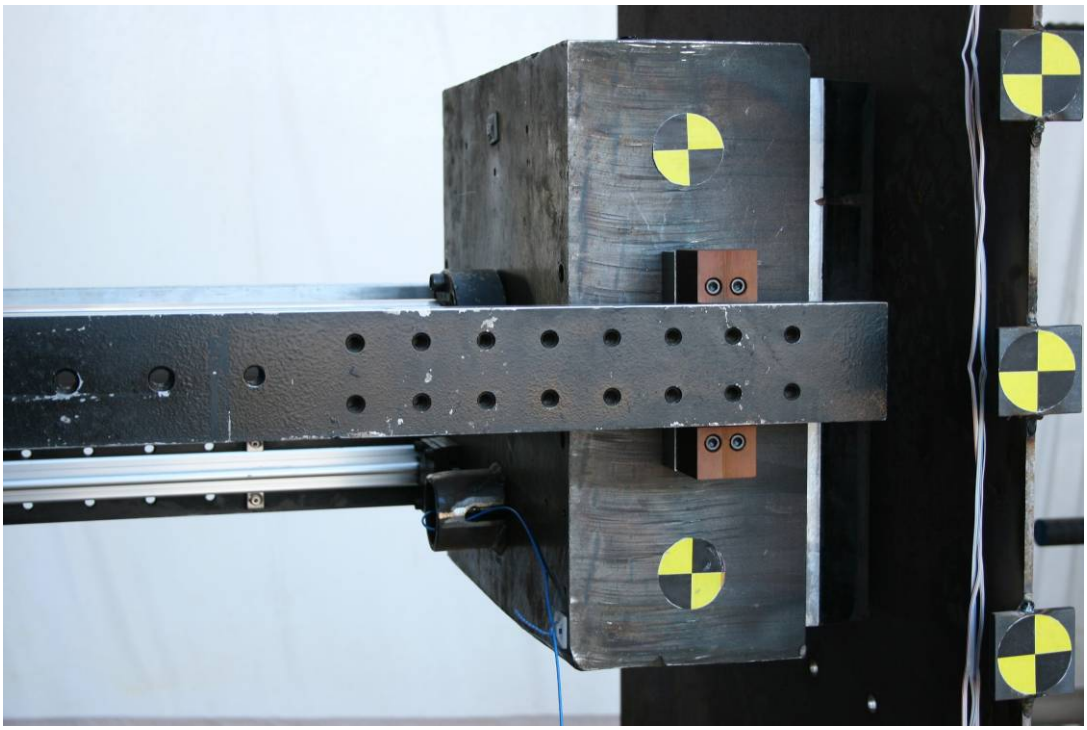

Figure E.250: Accelerometer location for Test 25

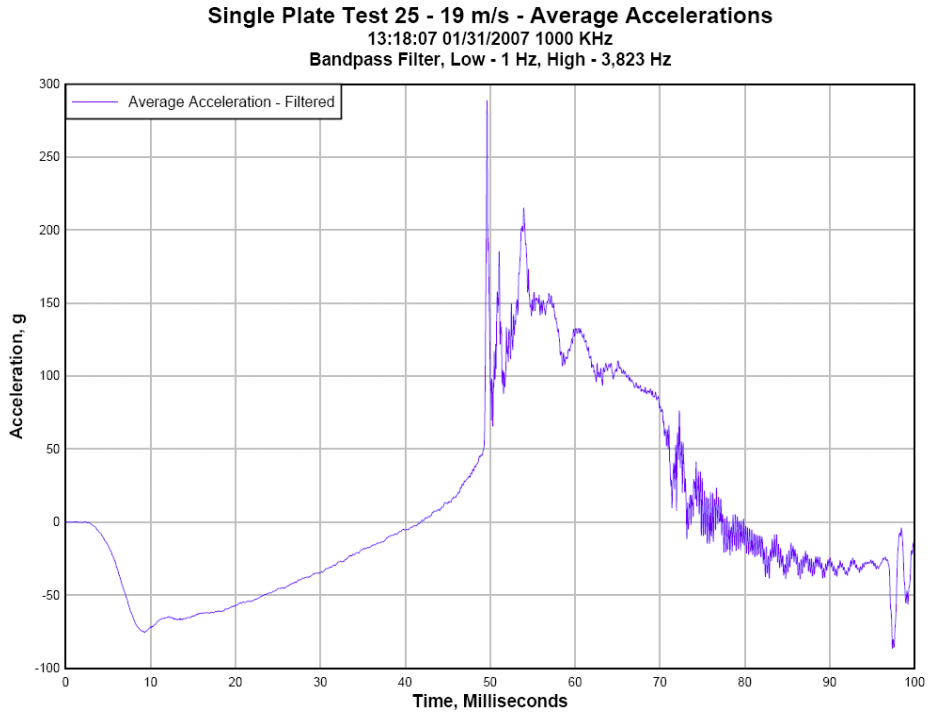

Figure E.251: Filtered accelerometer data for Test 25

E.25.2.4 STRAIN GAGE LOCATIONS

For this test there were two strain gauges labeled 19 and 20. The strain gauges, and their locations, are shown in Figure E.252. Table E.21 shows the specific information about this test, including the time and velocity at impact, if, and when, the bolts failed along with the maximum and minimum principal strain rates. The largest maximum principal strain rate for this test was 26.44 1/sec and was located at strain gage 19 while the largest minimum strain rate for this test was 8.00 1/sec located at strain gage 19. The maximum principal strains for gauges 19 and 20 can be found in Figure E.253 and the minimum principal strains for the same gauges can be found in Figure E.254.

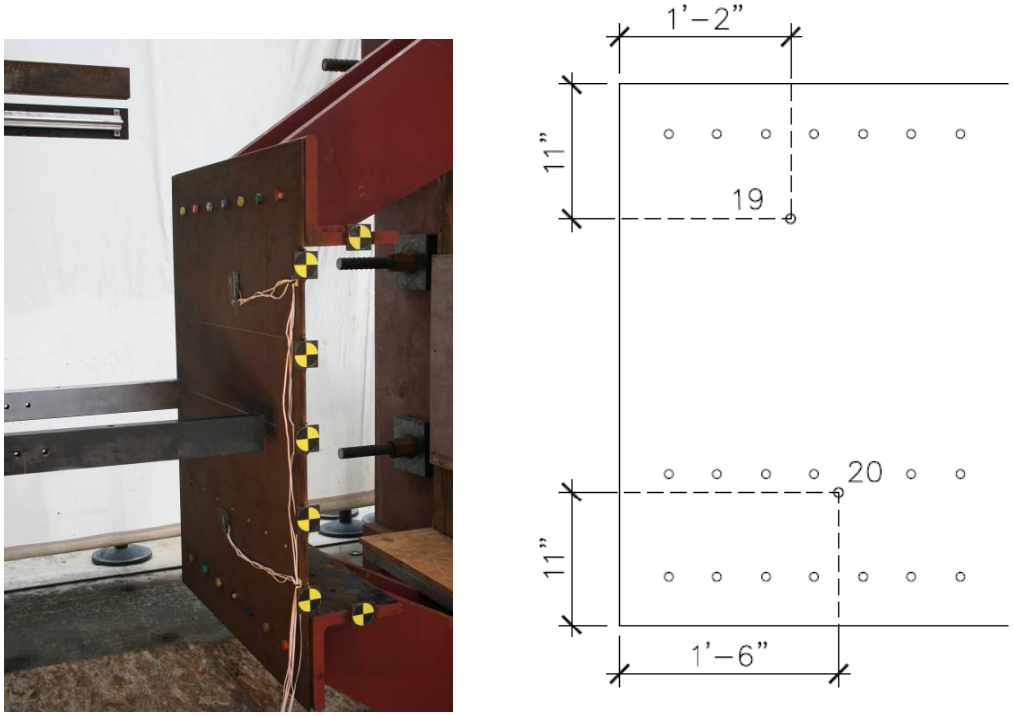

Figure E.252: Strain gage layout for Test 25

Table E.21: Stain rate information for Test 25

Strain Gage Number	Actual Velocity	Initial Impact	Shear Wave at Gage	Bolts Break	Maximum Principal Strain Rate	Minimum Principal Strain Rate
19	18.5 m/s	49.00 msec	49.80 msec	55.00 msec	26.44 1/sec	-8.00 1/sec
20	18.5 m/s	49.00 msec	49.80 msec	55.00 msec	22.99 1/sec	3.75 1/sec

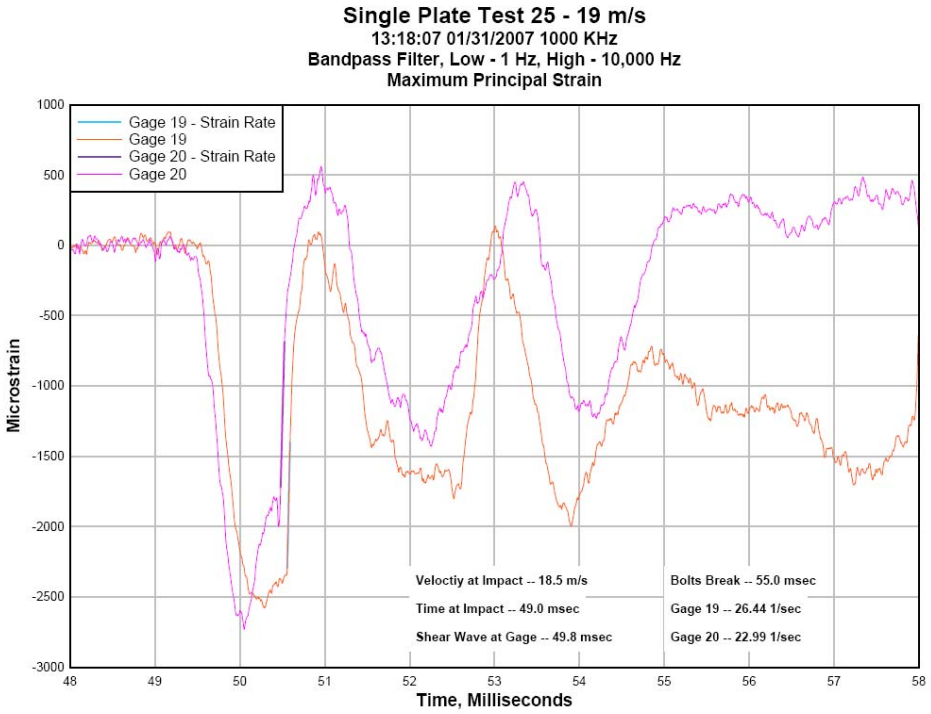

Figure E.253: Maximum principal strains and strain rates for Test 25

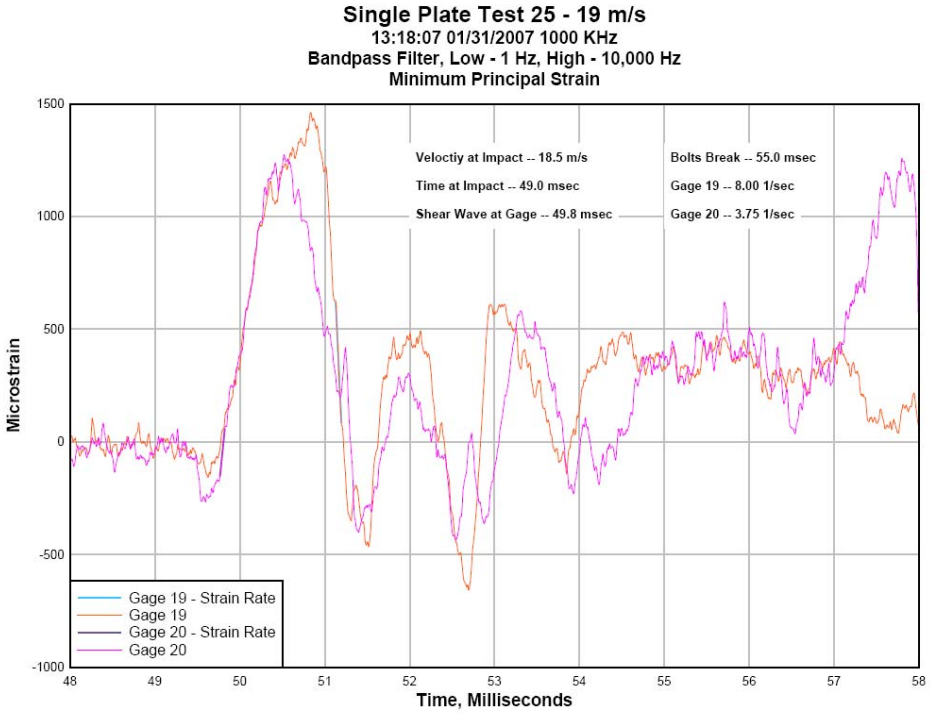

Figure E.254: Minimum principal strains and strain rates for Test 25

E.25.2.5 BOLT TYPE

A total of fourteen A307 bolts (Low Strength Bolts similar to Rivets) were used for this test. They were all tightened to a torque of 40 ft-lbs.

E.25.2.6 BLAST GENERATOR DATA

The initial impact of the single BG was 60.70 ft/sec (18.5 m/sec) with a goal velocity of 19.5 m/s. It had one accelerometer mounted to the back side of the impact plate as discussed in Section E.25.2.3. The average impact velocity for the impacting mass and the steel plate was calculated using the TEMA Track Eye tracking software.

E.25.3 SPECIMEN BEHAVIOR

The loading of the BG plate imparted an initial velocity of 60.70 ft/sec (18.5 m/sec) to the specimen. This caused plate to deform in both directions. The longitudinal deflection (in the north-south direction) behaved in a typical one-way flexural shape. In order to get the velocity as high as needed the test was designed to have the impacting mass break free from the BG and launch itself into the plate. This test imparted enough energy into the system that the top seven bolts broke as shown in Figure E.255.

During the test pieces of bolts flew approximately 24’ north of the test set-up and 8’ south of the test set-up. During the test three different phantom cameras were used to capture the failure modes from three different angles. Figure E.256 shows the progression of damage for this test from Phantom Camera One. Figure E.257 shows the progression of damage for this test from Phantom Camera Two. Figure E.258 shows the progression of damage for this test from Phantom Camera Three.

Figure E.255: Steel plate post test for Test 25

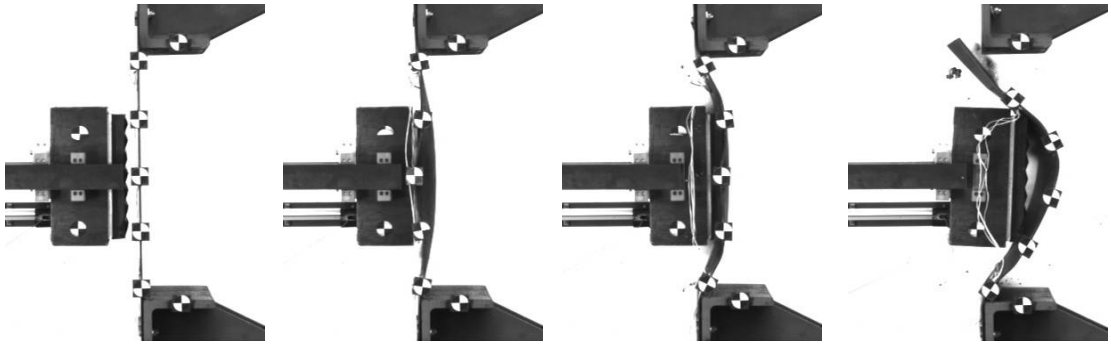

Figure E.256: Progression of damage for Test 25 from Camera 1

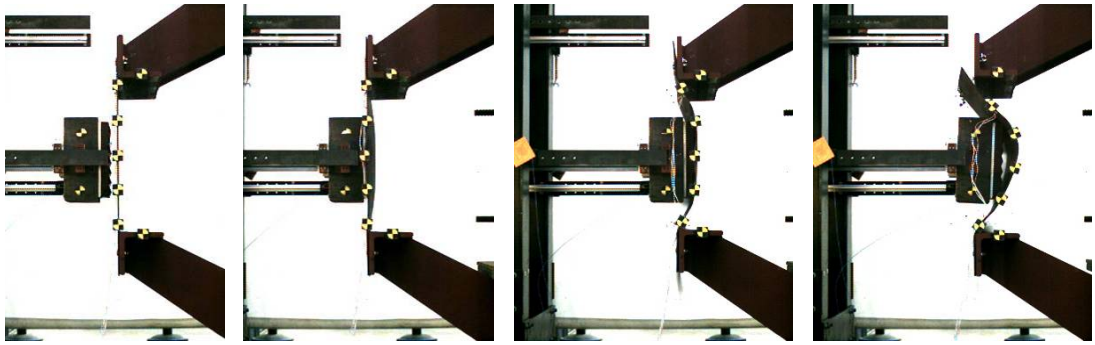

Figure E.257: Progression of damage for Test 25 from Camera 2

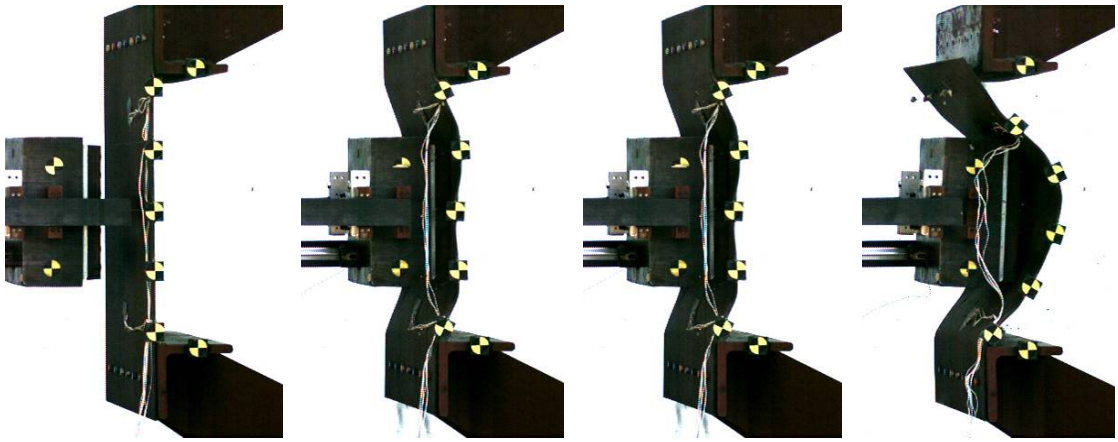

Figure E.258: Progression of damage for Test 25 from Camera 3

E.26 STEEL TOWER SINGLE PLATE: TEST 26 (SP26)

E.26.1 INTRODUCTION

The twenty-sixth test of the Steel Tower Single Plate test series was performed on February 5th, 2007. The test specimen was a ½" thick steel plate labeled SP26. The Impacting Mass 1 was attached to the BG with a specimen target velocity of 63.98 ft/sec (19.5 m/sec). Figure E.259 shows the steel plate prior to impact.

Figure E.259: 1/2" thick steel plate pre test for Test 26

E.26.2 INSTRUMENTATION

E.26.2.1 PHANTOM CAMERAS

The first camera recorded in black and white at a rate of 10,000 frames per second at a resolution of 512x384. This camera was used in order to determine the maximum velocity of the impacting mass and the movement in the plate including the maximum displacement. The second camera recorded in color at a rate of 5,000 frames per second at a resolution of 512x384. This camera recorded the overall behavior of the test specimen. It was not used to gather any specific data. The third camera recorded in color at a rate of 2,500 frames per second at a resolution of 480x480. This camera captured the failure of the bolts. A picture from each of the camera locations are shown in Figure E.260.

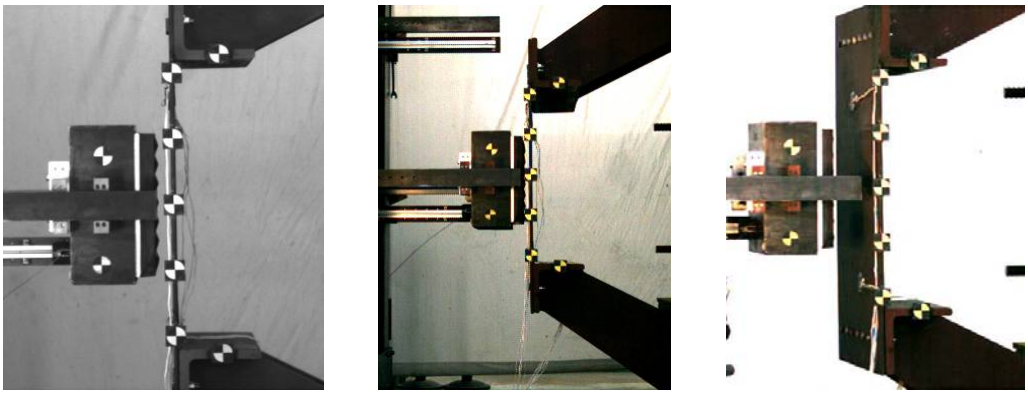

Figure E.260: Phantom Cameras for Test 26

a) Camera One b) Camera Two c) Camera Three

E.26.2.2 TARGET LOCATIONS

Five targets were welded onto the side of the steel plate as shown in Figure E.259. They were spaced at the intervals shown in Figure E.261. That figure also shows the location of the targets for the impacting mass. An additional two targets were placed on the angle at the top and the bottom end conditions. The distance between these two points is 74.93 cm (29 ½")

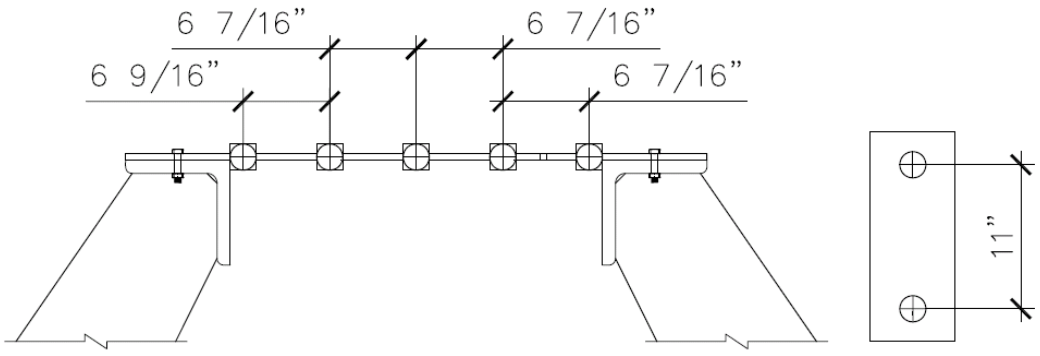

Figure E.261: Target layout on plate and impacting mass for Test 26

E.26.2.3 ACCELERATIONS

For this test one accelerometer was used. This accelerometer was placed 6" south of the centroid of the impacting mass as shown in Figure E.262. The pipe is to protect the accelerometer during the test. The data from this gage was then filtered as shown in Figure E.263.

This test does not impart an impulsive load as would be expected from a typical blast test. Instead, this test simulates the behavior of a flyer plate moving through the structure after the initial impact at the front plate of the outer cell of the structure. Therefore we are not determining the initial impulsive load from the accelerometers on the BG.

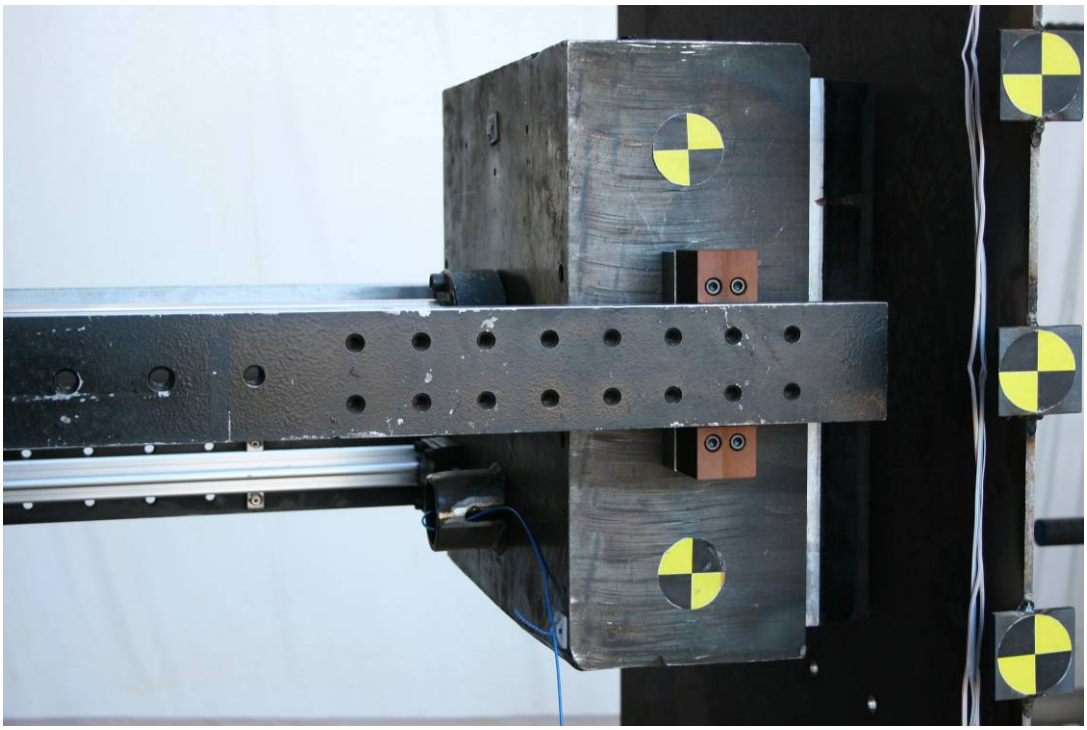

Figure E.262: Accelerometer location for Test 26

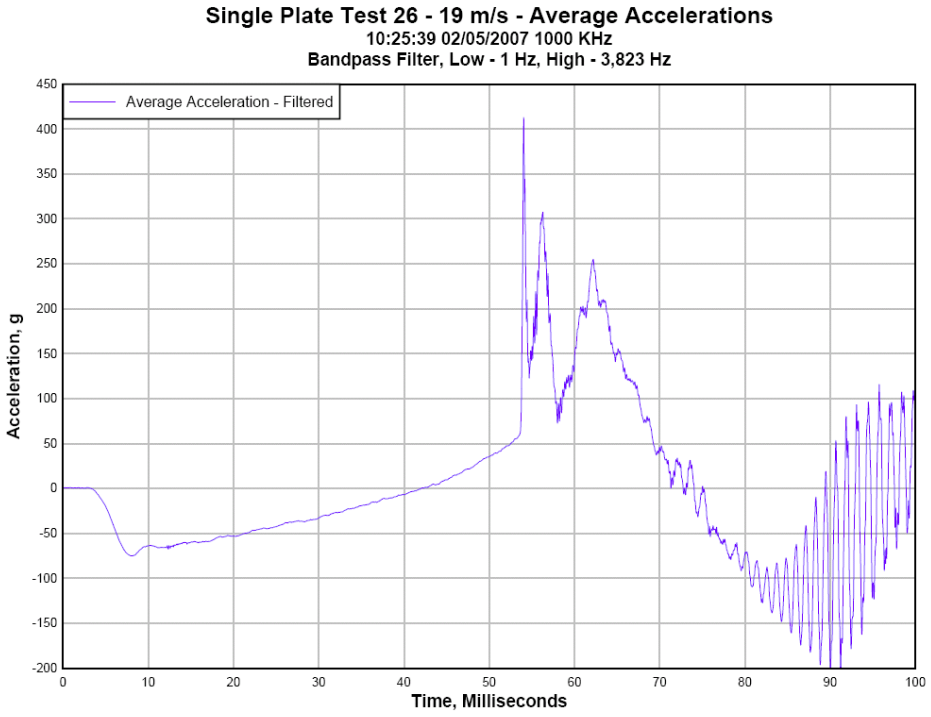

Figure E.263: Filtered accelerometer data for Test 26

E.26.2.4 STRAIN GAGE LOCATIONS

For this test there were four strain gauges labeled 19, 20, 21 and 22. The strain gauges, and their locations, are shown as a drawing in Figure E.264 and as a photo in Figure E.265. Table E.22 shows the specific information about this test, including the time and velocity at impact, if, and when, the bolts failed along with the maximum and minimum principal strain rates. The largest maximum principal strain rate for this test was 10.01 1/sec and was located at strain gage 21 while the largest minimum strain rate for this test was 6.86 1/sec located at strain gage 20. The maximum principal strains for gauges 19, 20 ,21 and 22 can be found in Figure E.266 and the minimum principal strains for the same gauges can be found in Figure E.267.

This test involved the group of test that has gauges on both sides of the plate as discussed in the report. The pure axial strains have been determined and are shown in Figure E.268 for Gauges 19 and 21; and Figure E.269 for Gauges 20 and 22. The actual bending and axial strains were also determined for these tests up until the plate yields. The graphs of the stresses for Gauges 19 and 21, and Gauges 20 and 22 can be found in Figure E.270 and Figure E.271, respectively.

Table E.22: Stain rate information for Test 26

Strain Gage Number	Actual Velocity	Initial Impact	Shear Wave at Gage	Bolts Break	Maximum Principal Strain Rate	Minimum Principal Strain Rate
19	17.93 m/s	53.80 msec	-	-	-8.31 1/sec	6.05 1/sec
20	17.93 m/s	53.80 msec	-	-	-6.25 1/sec	6.86 1/sec
21	17.93 m/s	53.80 msec	-	-	10.01 1/sec	4.40 1/sec
22	17.93 m/s	53.80 msec	-	-	6.70 1/sec	5.55 1/sec

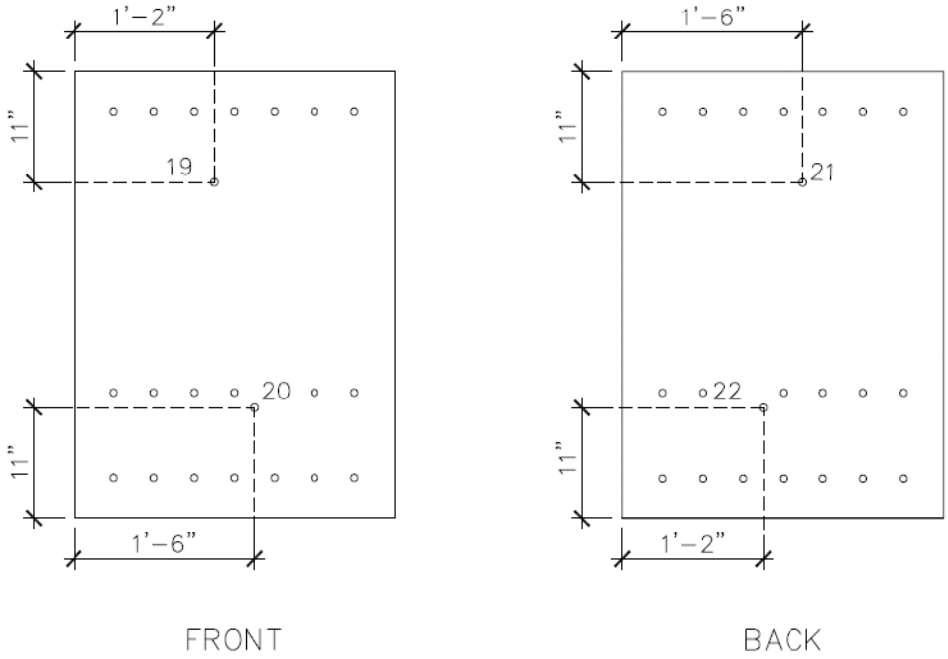

Figure E.264: Strain gage layout for Test 26 (drawing)

Figure E.265: Strain gage layout for Test 26 (pictures)

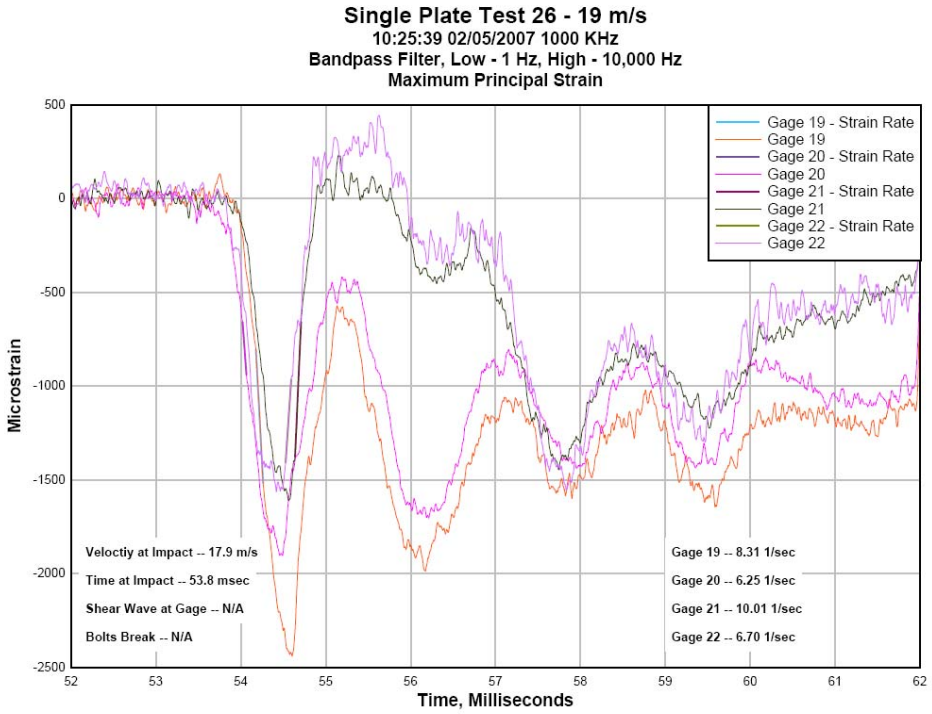

Figure E.266: Maximum principal strains and strain rates for Test 26

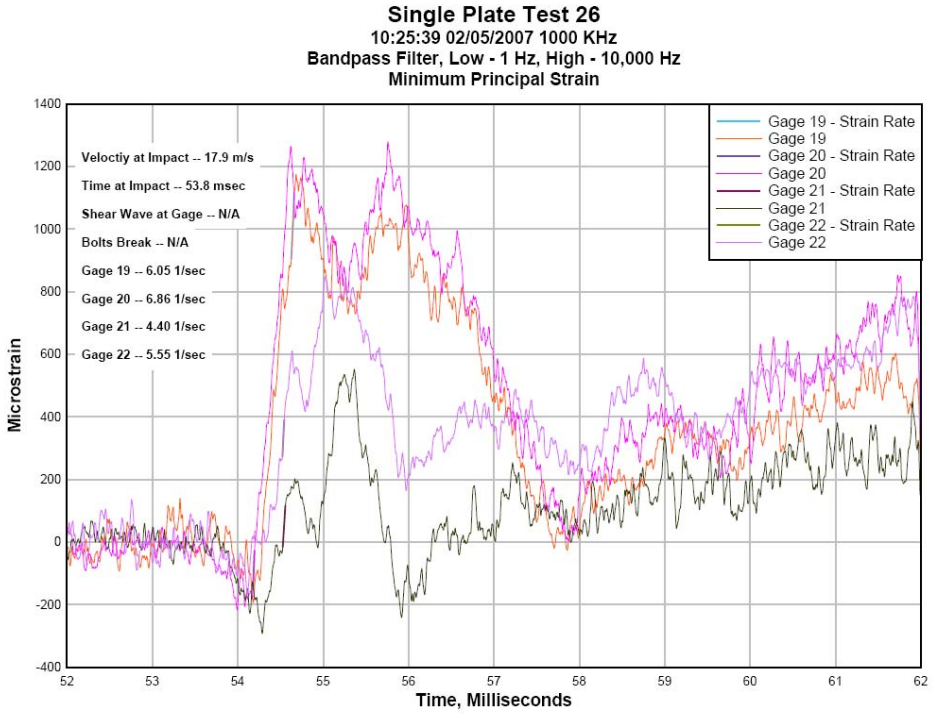

Figure E.267: Minimum principal strains and strain rates for Test 26

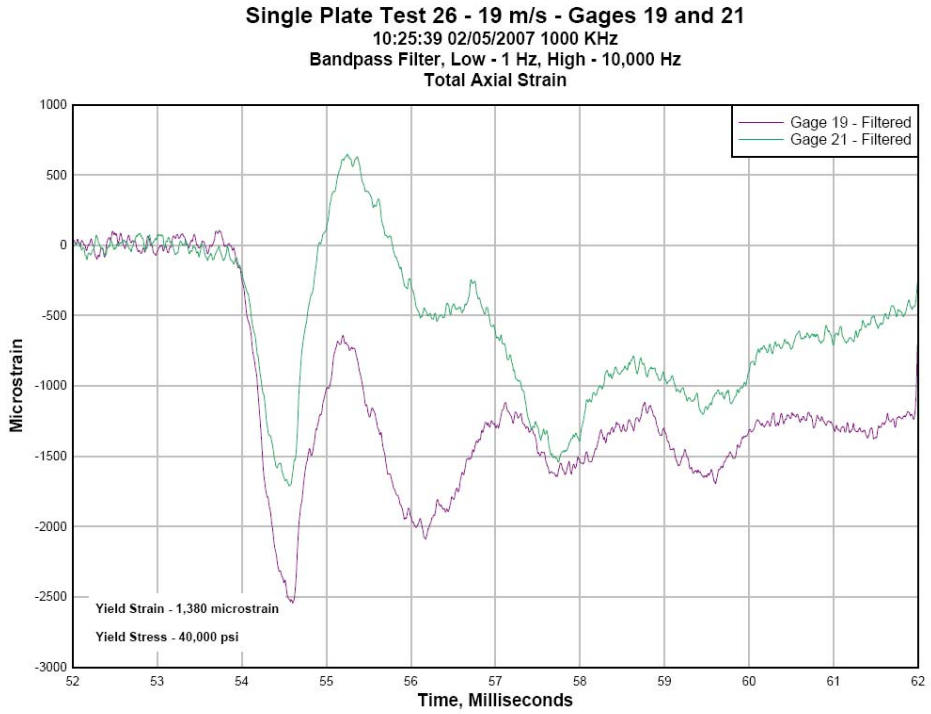

Figure E.268: Combined Axial Strain for Test 26 – Gauges 19 and 21

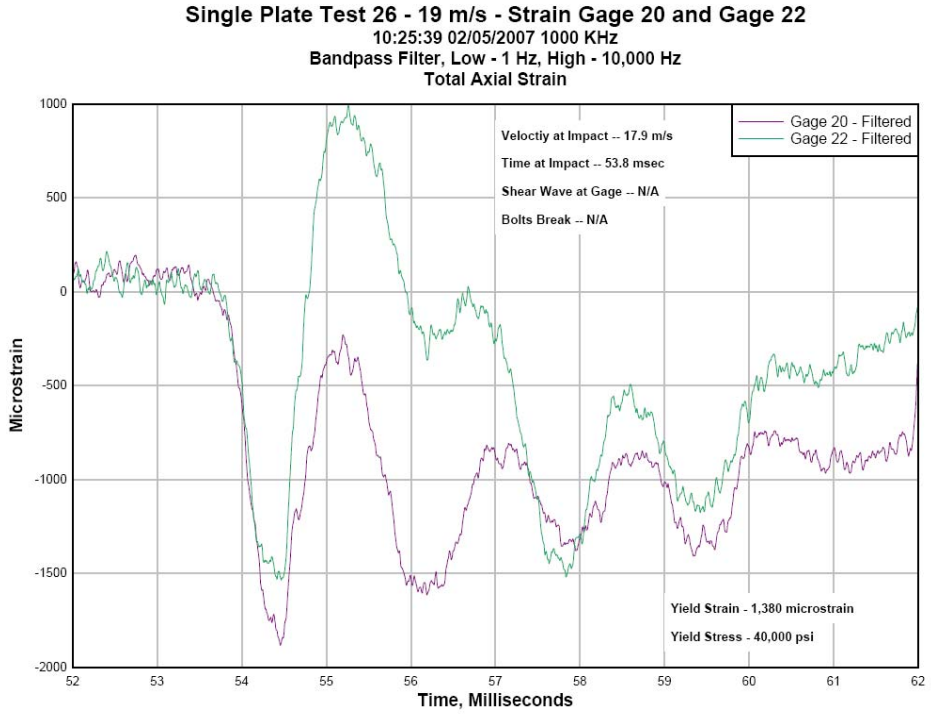

Figure E.269: Combined Axial Strain for Test 26 – Gauges 20 and 22

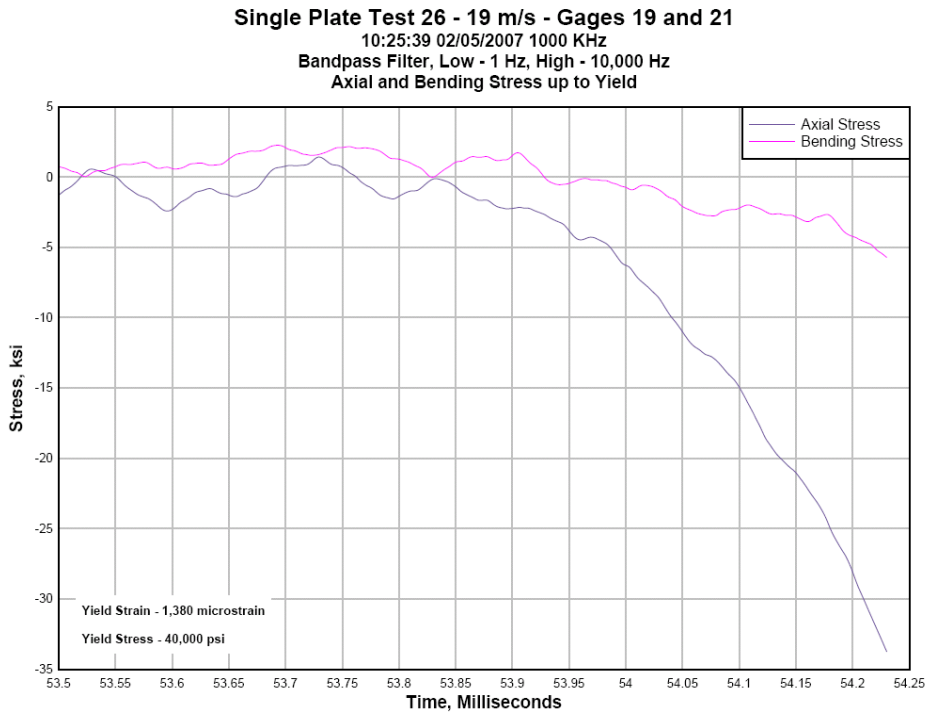

Figure E.270: Truncated Axial and Bending Stresses for Test 26 – Gauges 19 and 21

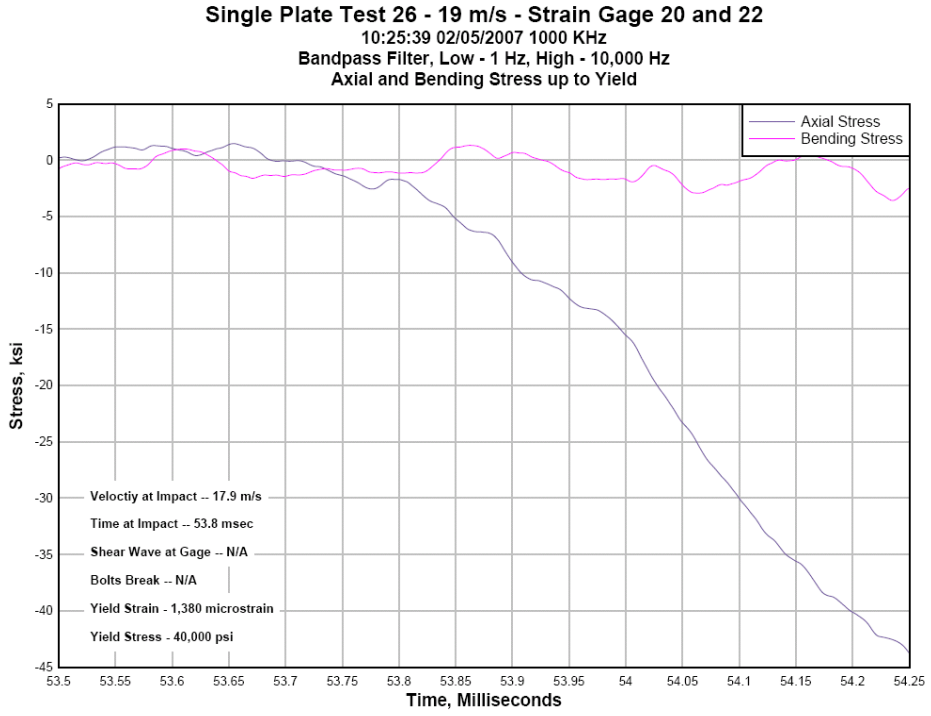

Figure E.271: Truncated Axial and Bending Stresses for Test 26 – Gauges 20 and 22

E.26.2.5 BOLT TYPE

A total of fourteen A307 bolts (Low Strength Bolts similar to Rivets) were used for this test. They were all tightened to a torque of 40 ft-lbs.

E.26.3 BLAST GENERATOR DATA

The initial impact of the single BG was 58.73 ft/sec (17.9 m/sec) with a goal velocity of 19.5 m/s. It had one accelerometer mounted to the back side of the impact plate as discussed in Section E.26.2.3. The average impact velocity for the impacting mass and the steel plate was calculated using the TEMA Track Eye tracking software.

E.26.4 SPECIMEN BEHAVIOR

The loading of the BG plate imparted an initial velocity of 58.73 ft/sec (17.9 m/sec) to the specimen. This caused plate to deform in both directions. The longitudinal deflection (in the north-south direction) behaved in a typical one-way flexural shape. This test did not impart enough energy to break any of the bolts as shown in Figure E.272. The maximum dynamic deflection during the test was approximately 4". During the test three different phantom cameras were used to capture the failure modes from three different angles. Figure E.273 shows the progression of damage for this test from Phantom Camera One. Figure E.274 shows the progression of damage for this test from Phantom Camera Two. Figure E.275 shows the progression of damage for this test from Phantom Camera Three.

Figure E.272: Steel plate post test for Test 26

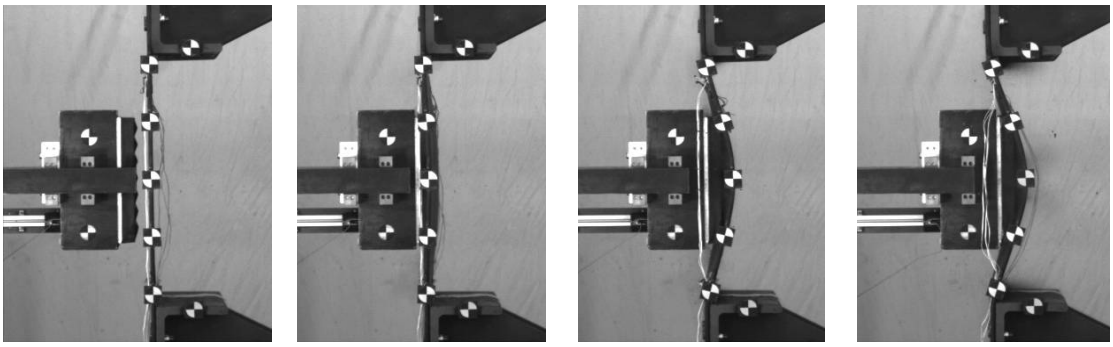

Figure E.273: Progression of damage for Test 26 from Camera 1

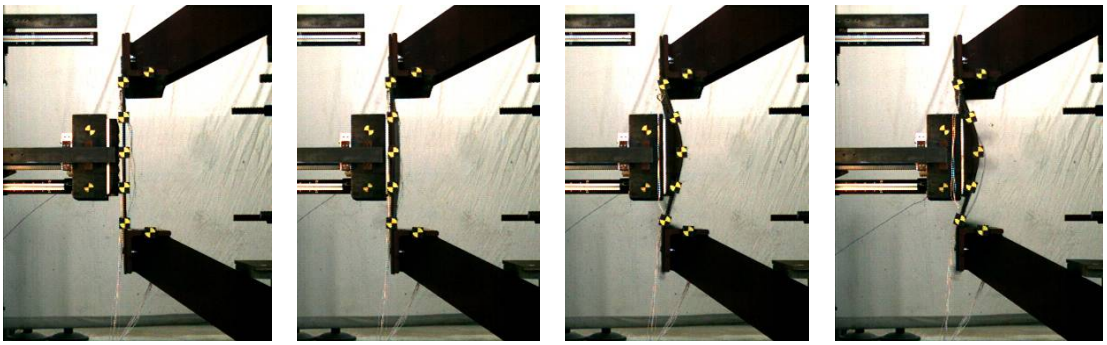

Figure E.274: Progression of damage for Test 26 from Camera 2

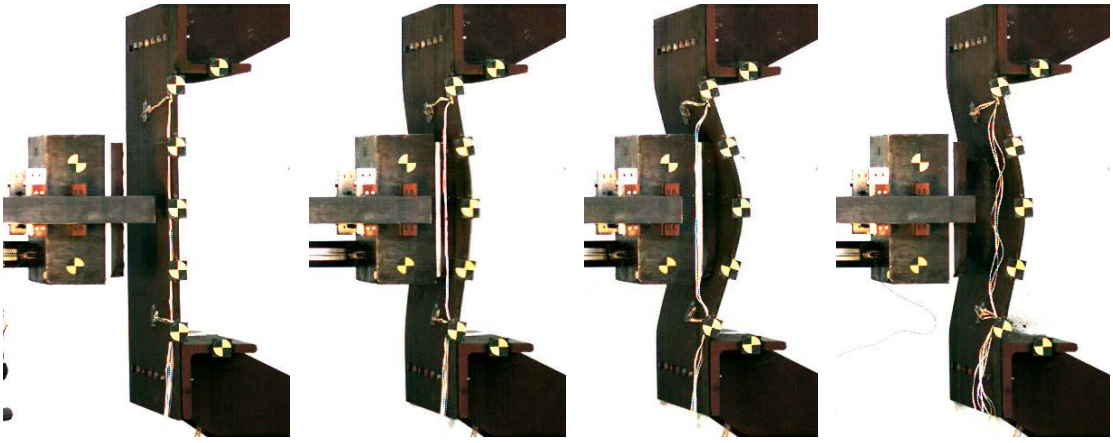

Figure E.275: Progression of damage for Test 26 from Camera 3

E.27 STEEL TOWER SINGLE PLATE: TEST 27 (SP27)

E.27.1 INTRODUCTION

The twenty-seventh test of the Steel Tower Single Plate test series was performed on February 7th, 2007. The test specimen was a ½" thick steel plate labeled SP27. The Impacting Mass 1 was attached to the BG with a specimen target velocity of 75.46 ft/sec (23 m/sec). Figure E.276 shows the steel plate prior to impact.

Figure E.276: 1/2" thick steel plate pre test for Test 27

E.27.2 INSTRUMENTATION

E.27.2.1 PHANTOM CAMERAS

The first camera recorded in black and white at a rate of 10,000 frames per second at a resolution of 512x384. This camera was used in order to determine the maximum velocity of the impacting mass and the movement in the plate including the maximum displacement. The second camera recorded in color at a rate of 10,000 frames per second at a resolution of 512x384. This camera recorded the overall behavior of the test specimen. It was not used to gather any specific data. The third camera recorded in color at a rate of 8,000 frames per second at a resolution of 480x480. This camera captured the failure of the bolts. A picture from each of the camera locations are shown in Figure E.277.

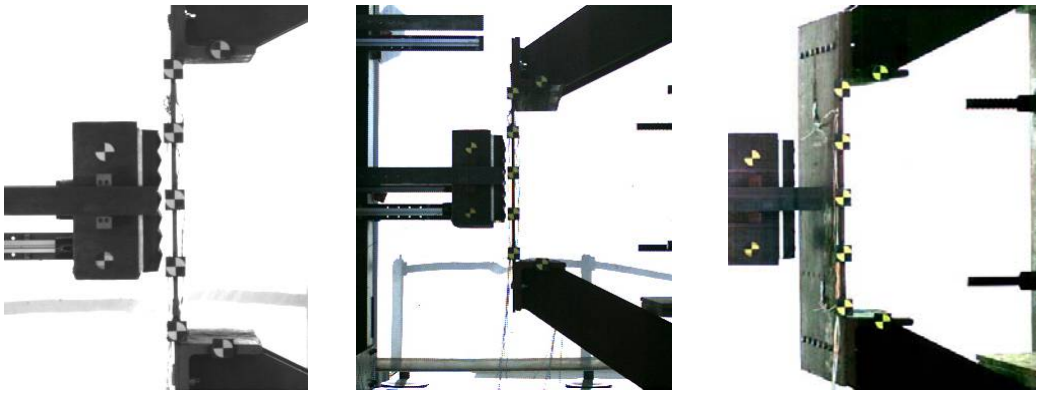

Figure E.277: Phantom Cameras for Test 27

a) Camera One b) Camera Two c) Camera Three

E.27.2.2 TARGET LOCATIONS

Five targets were welded onto the side of the steel plate as shown in Figure E.276. They were spaced at the intervals shown in Figure E.278. That figure also shows the location of the targets for the impacting mass. An additional two targets were placed on the angle at the top and the bottom end conditions. The distance between these two points is 74.93 cm (29 ½")

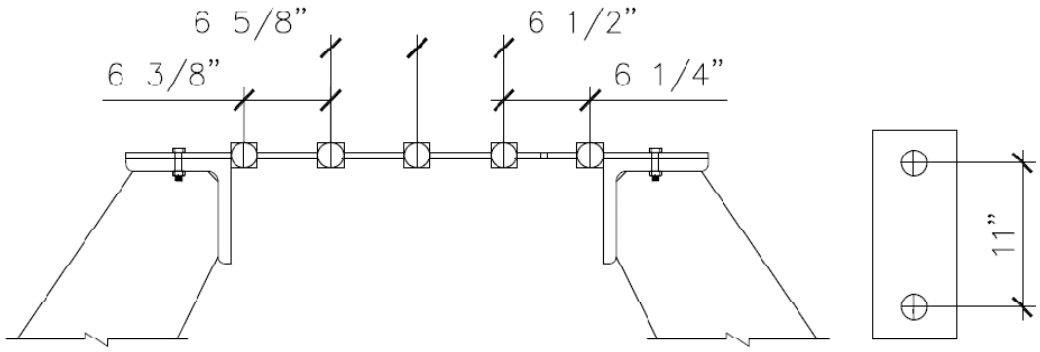

Figure E.278: Target layout on plate and impacting mass for Test 27

E.27.2.3 ACCELERATIONS

For this test one accelerometer was used. This accelerometer was placed 6" south of the centroid of the impacting mass as shown in Figure E.279. The pipe is to protect the accelerometer during the test. The data from this gage was then filtered as shown in Figure E.280.

This test does not impart an impulsive load as would be expected from a typical blast test. Instead, this test simulates the behavior of a flyer plate moving through the structure after the initial impact at the front plate of the outer cell of the structure. Therefore we are not determining the initial impulsive load from the accelerometers on the BG.

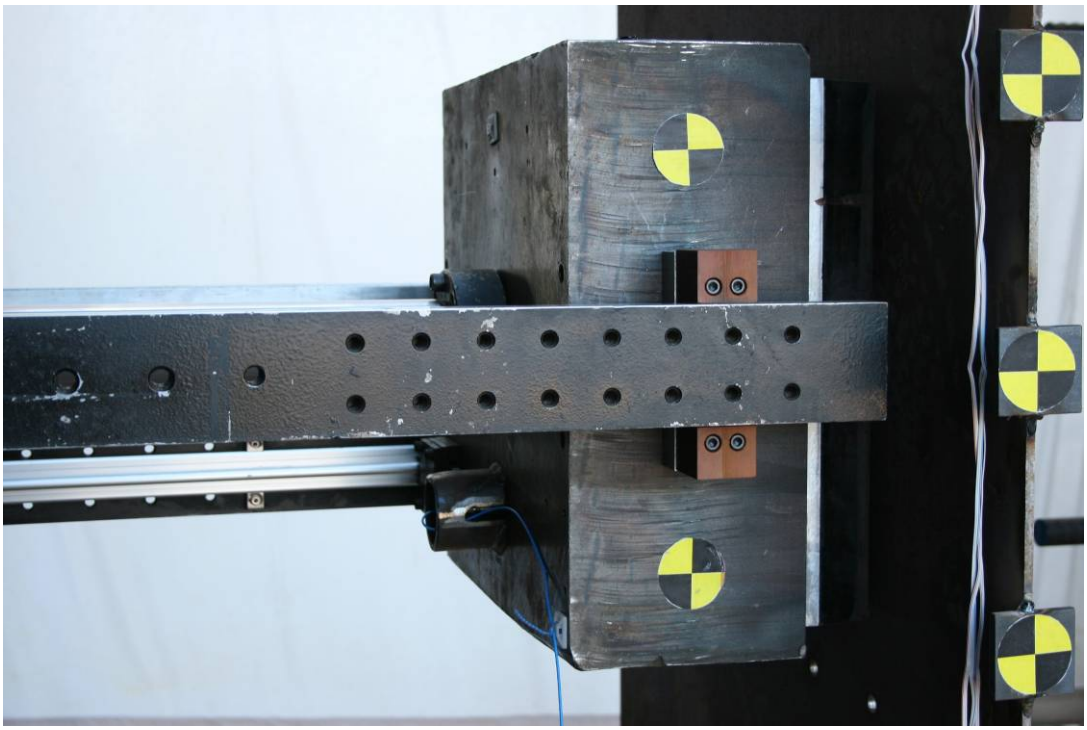

Figure E.279: Accelerometer location for Test 27

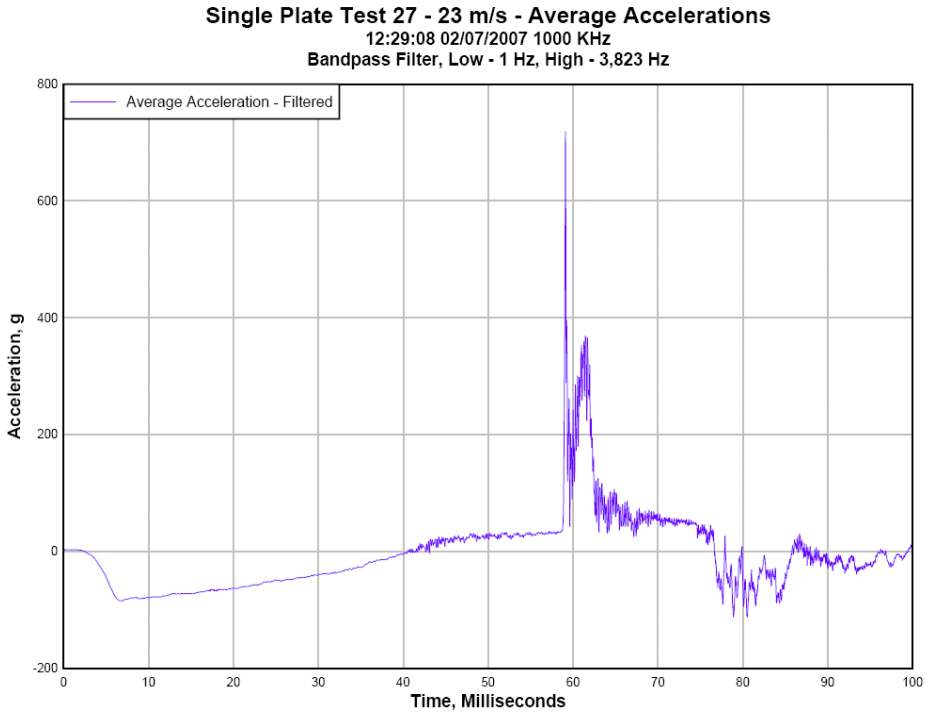

Figure E.280: Filtered accelerometer data for Test 27

E.27.2.4 STRAIN GAGE LOCATIONS

For this test there were four strain gauges labeled 19, 20, 21 and 22. The strain gauges, and their locations, are shown as a drawing in Figure E.281 and as a photo in Figure E.282. Table E.23 shows the specific information about this test, including the time and velocity at impact, if, and when, the bolts failed along with the maximum and minimum principal strain rates. The largest maximum principal strain rate for this test was 14.24 1/sec and was located at strain gage 19 while the largest minimum strain rate for this test was 14.21 1/sec located at strain gage 22. The maximum principal strains for gauges 19, 20, 21 and 22 can be found in Figure E.283 and the minimum principal strains for the same gauges can be found in Figure E.284.

This test involved the group of test that has gauges on both sides of the plate as discussed in the report. The pure axial strains have been determined and are shown in Figure E.285 for Gauges 19 and 21; and Figure E.286 for Gauges 20 and 22. The actual bending and axial strains were also determined for these tests up until the plate yields. The graphs of the stresses for Gauges 19 and 21 and Gauges 20 and 22 can be found in Figure E.287 and Figure E.288, respectively.

Table E.23: Stain rate information for Test 27

Strain Gage Number	Actual Velocity	Initial Impact	Shear Wave at Gage	Bolts Break	Maximum Principal Strain Rate	Minimum Principal Strain Rate
19	24.04 m/s	58.60 msec	59.25 msec	63.20 msec	-14.24 1/sec	6.04 1/sec
20	24.04 m/s	58.60 msec	59.25 msec	63.20 msec	-8.92 1/sec	8.37 1/sec
21	24.04 m/s	58.60 msec	59.25 msec	63.20 msec	7.12 1/sec	9.58 1/sec
22	24.04 m/s	58.60 msec	59.25 msec	63.20 msec	-7.10 1/sec	14.21 1/sec

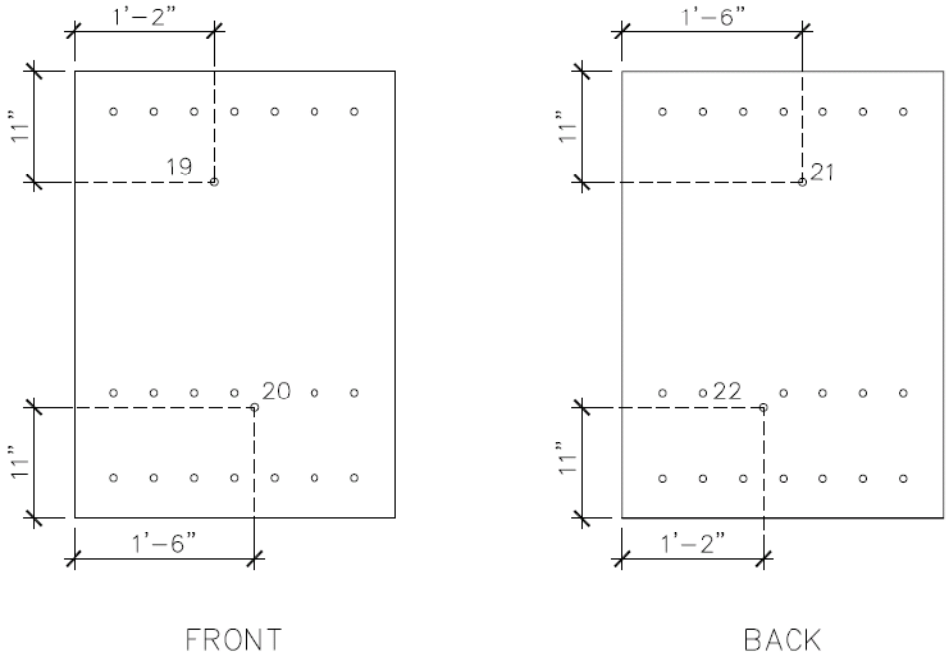

Figure E.281: Strain gage layout for Test 27 (drawing)

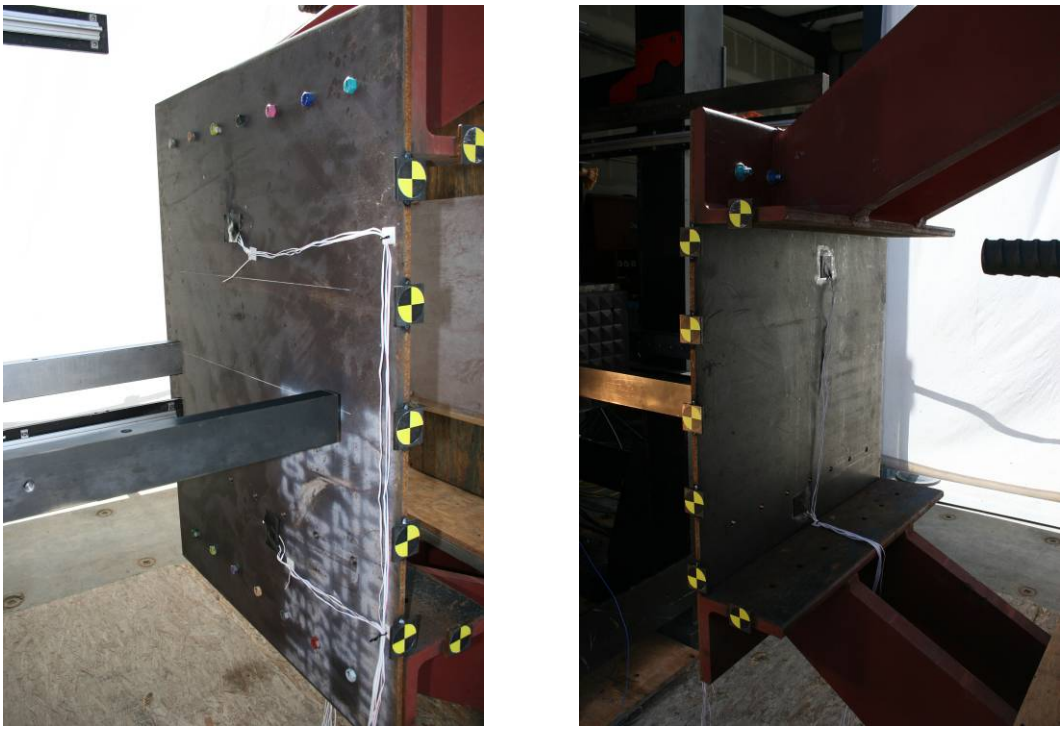

Figure E.282: Strain gage layout for Test 27 (pictures)

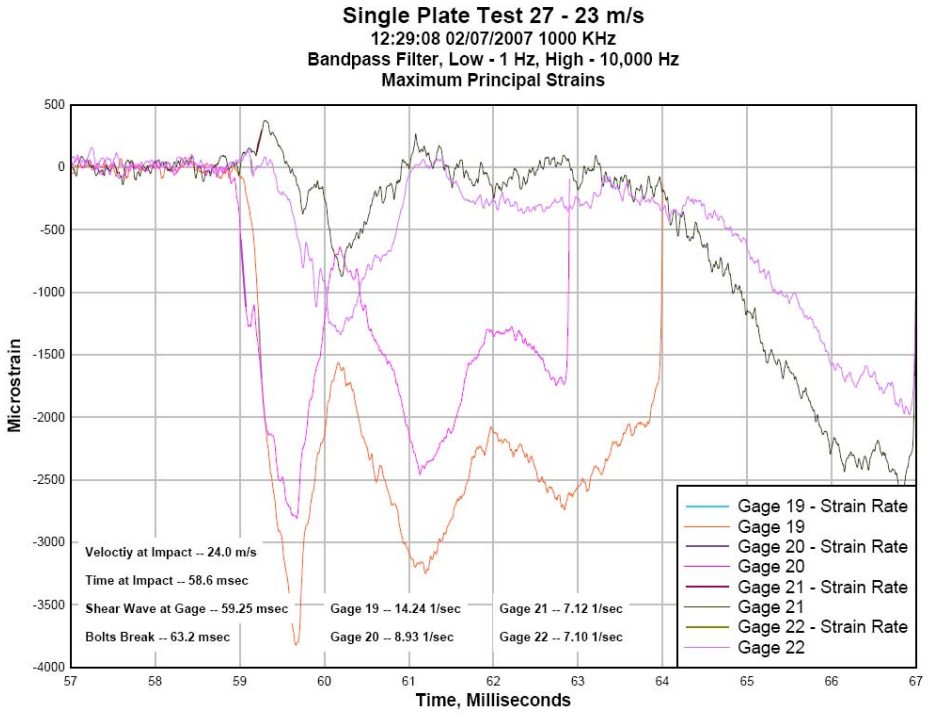

Figure E.283: Maximum principal strains and strain rates for Test 27

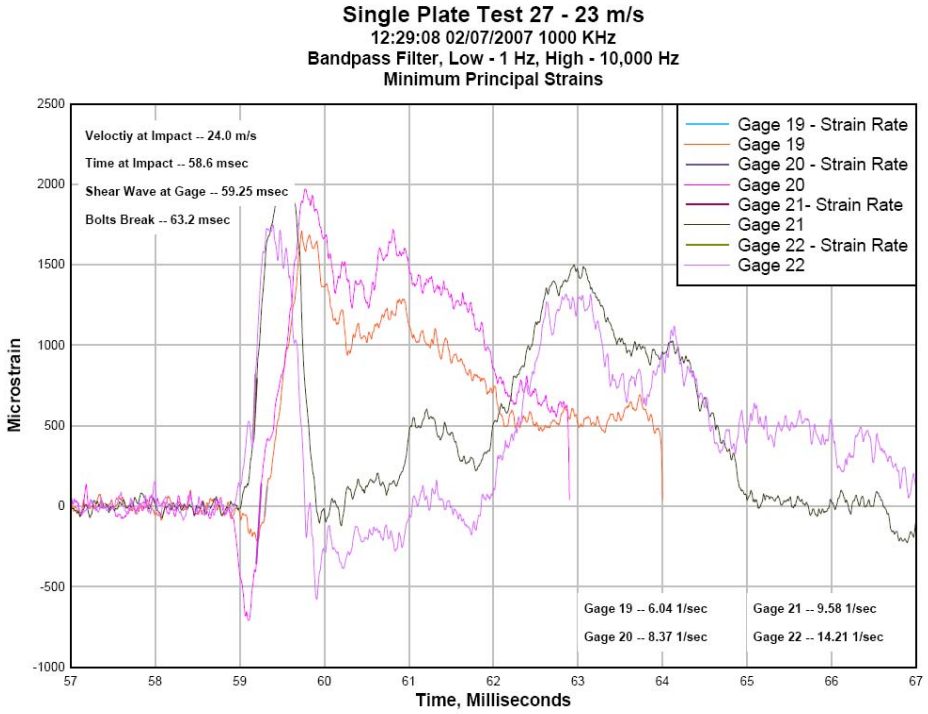

Figure E.284: Minimum principal strains and strain rates for Test 27

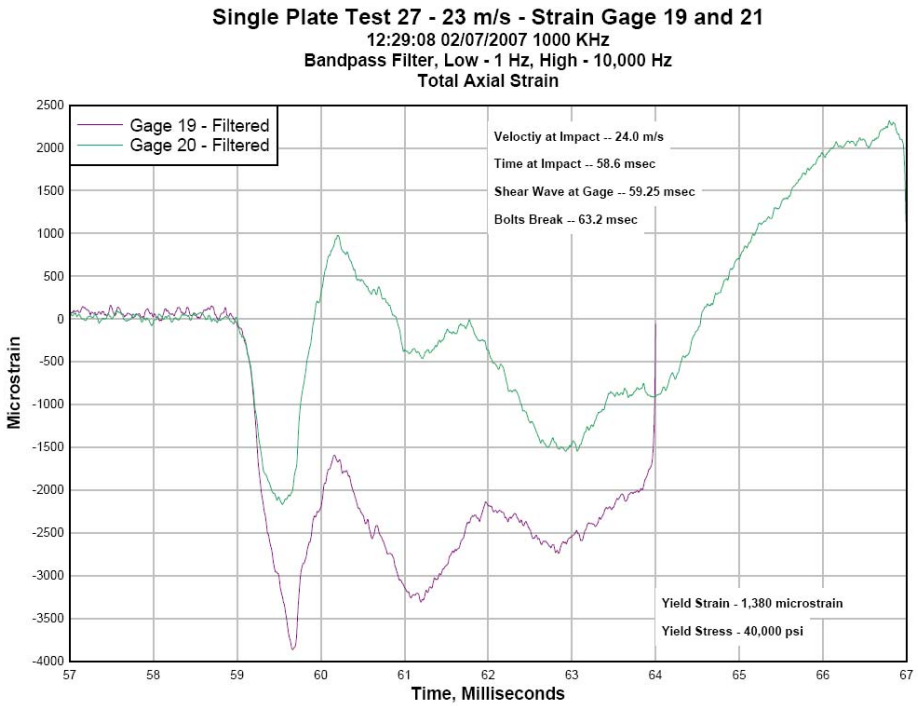

Figure E.285: Combined Axial Strain for Test 27 – Gauges 19 and 21

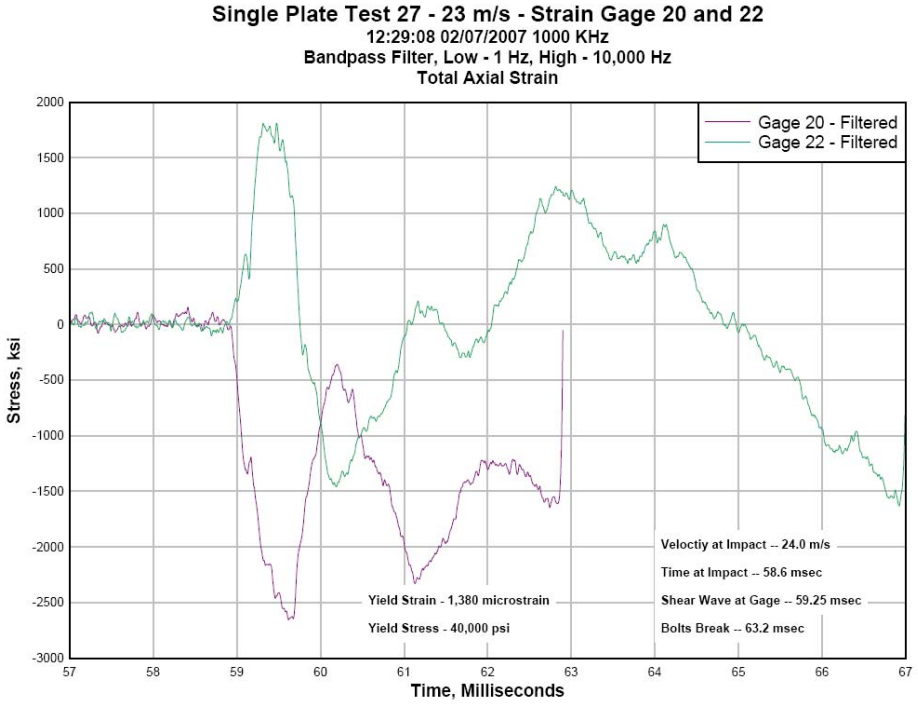

Figure E.286: Combined Axial Strain for Test 27 – Gauges 20 and 22

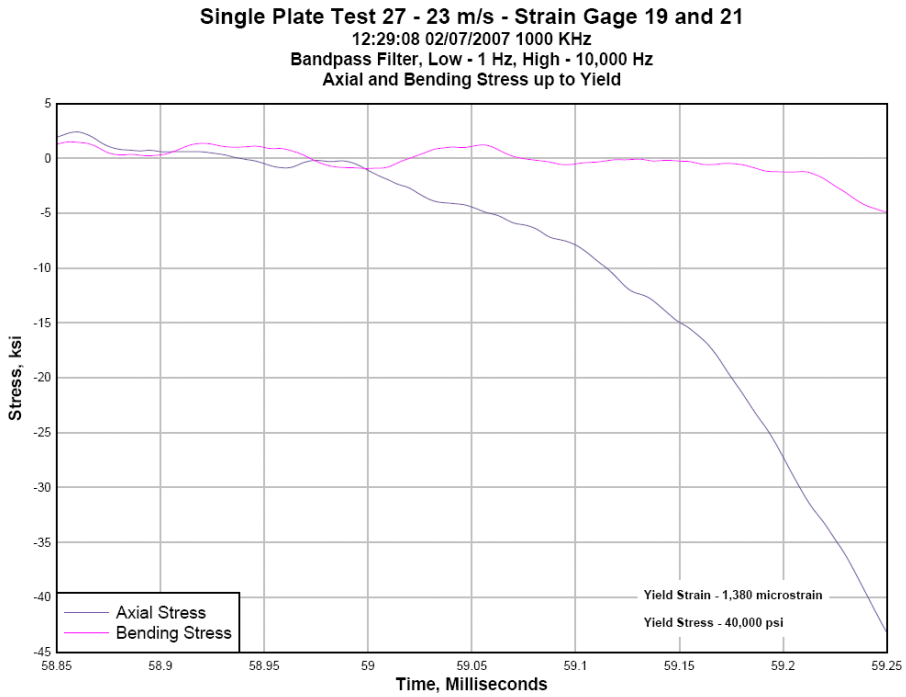

Figure E.287: Truncated Axial and Bending Stresses for Test 27 – Gauges 19 and 21

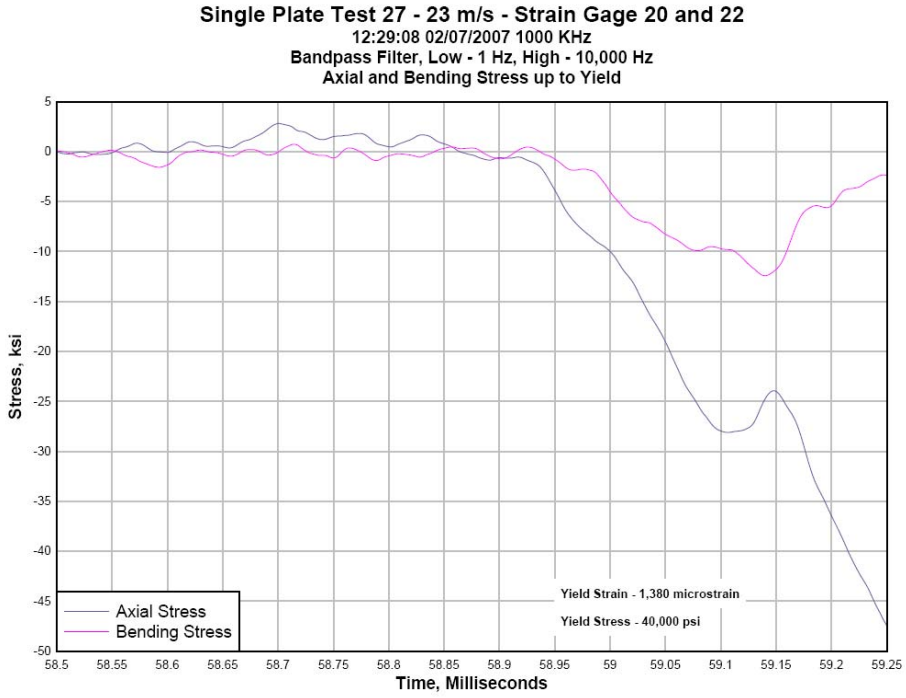

Figure E.288: Truncated Axial and Bending Stresses for Test 27 – Gauges 20 and 22

E.27.2.5 BOLT TYPE

A total of fourteen A307 bolts (Low Strength Bolts similar to Rivets) were used for this test. They were all tightened to a torque of 40 ft-lbs.

E.27.3 BLAST GENERATOR DATA

The initial impact of the single BG was 78.74 ft/sec (24 m/sec) with a goal velocity of 23 m/s. It had one accelerometer mounted to the back side of the impact plate as discussed in Section E.27.2.3. The average impact velocity for the impacting mass and the steel plate was calculated using the TEMA Track Eye tracking software.

E.27.4 SPECIMEN BEHAVIOR

The loading of the BG plate imparted an initial velocity of 78.74 ft/sec (24 m/sec) to the specimen. This caused plate to deform in both directions. The longitudinal deflection (in the north-south direction) behaved in a typical one-way flexural shape. In order to get the velocity as high as needed the test was designed to have the impacting mass break free from the BG and launch itself into the plate. This test imparted enough energy to break all fourteen of the bolts as shown in Figure E.289. The maximum dynamic deflection during the test was approximately 3 5/8".

After the test a bolt head was found approximately 47' northwest of the test set-up near the fence. Another bolt head was found 22' south of the test set-up behind the reaction wall. During the test three different phantom cameras were used to capture the failure modes from three different angles. Figure E.290 shows the progression of damage for this test from Phantom Camera One. Figure E.291 shows the progression of damage for this test from Phantom Camera Two. Figure E.292 shows the progression of damage for this test from Phantom Camera Three.

Figure E.289: Steel plate post test for Test 27

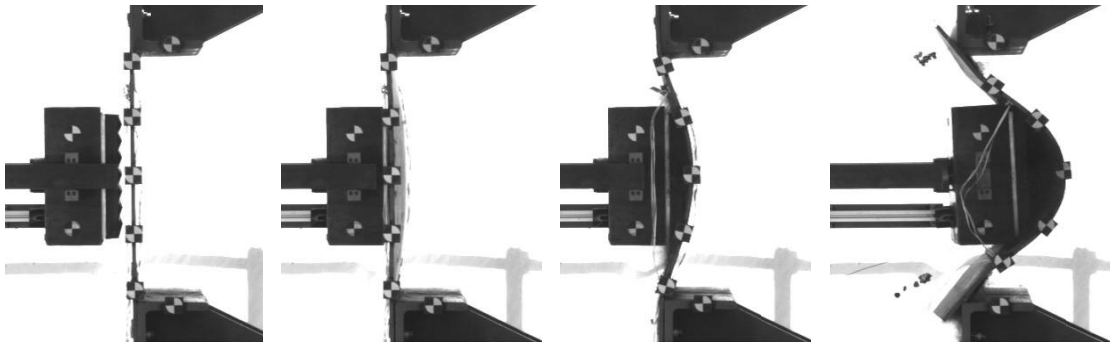

Figure E.290: Progression of damage for Test 27 from Camera 1

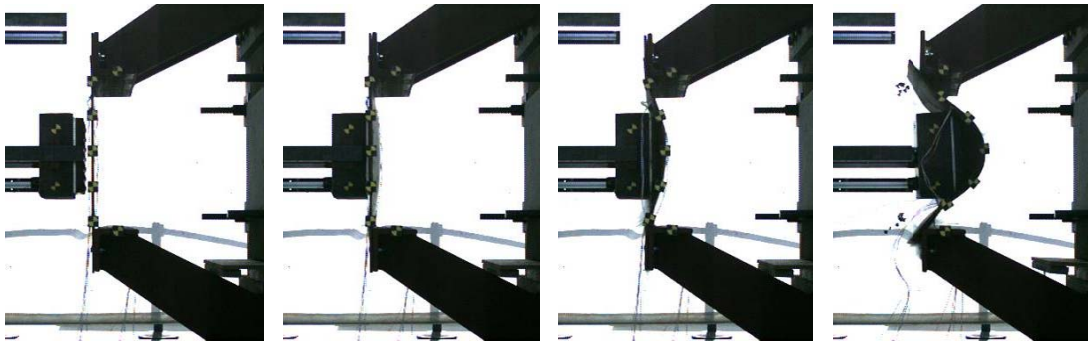

Figure E.291: Progression of damage for Test 27 from Camera 2

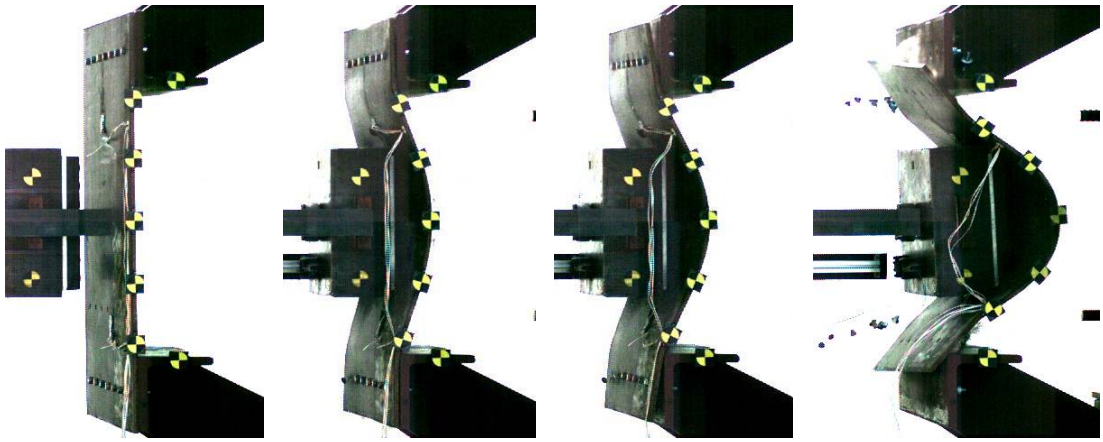

Figure E.292: Progression of damage for Test 27 from Camera 3

E.28 STEEL TOWER SINGLE PLATE: TEST 28 (SP28)

E.28.1 INTRODUCTION

The twenty-eighth test of the Steel Tower Single Plate test series was performed on February 12th, 2007. The test specimen was a ¾" thick steel plate labeled SP28. The Impacting Mass 1 was attached to the BG with a specimen target velocity of 91.86 ft/sec (28 m/sec). Figure E.293 shows the steel plate prior to impact.

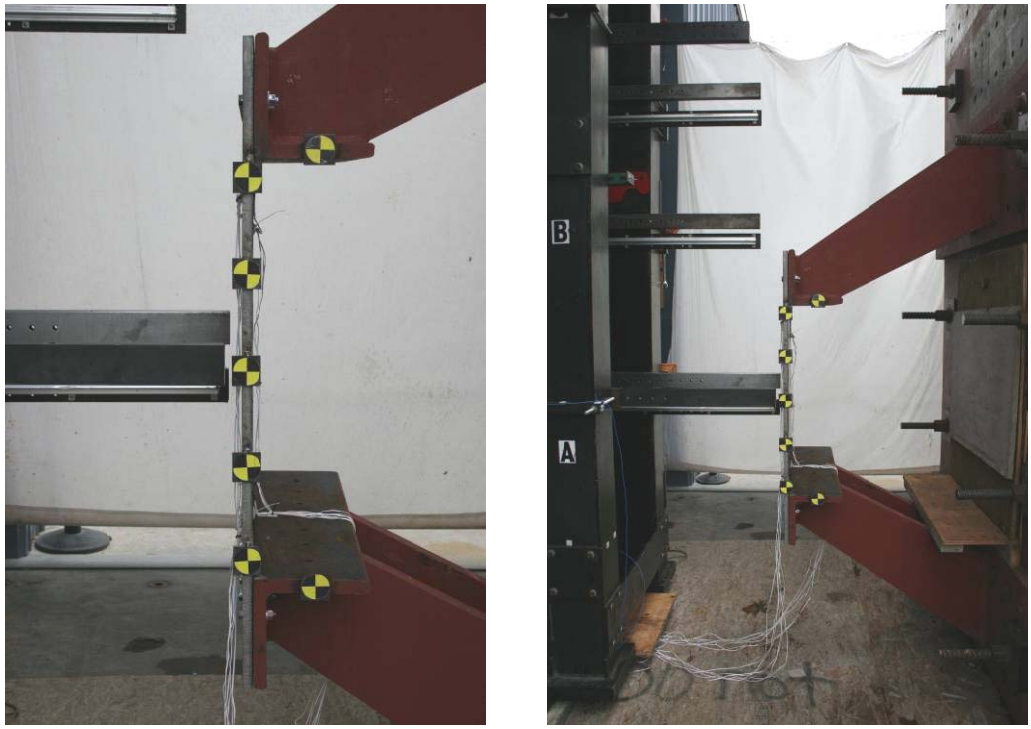

Figure E.293: 3/4" thick steel plate pre test for Test 28

E.28.2 INSTRUMENTATION

E.28.2.1 PHANTOM CAMERAS

The first camera recorded in black and white at a rate of 10,000 frames per second at a resolution of 512x384. This camera was used in order to determine the maximum velocity of the impacting mass and the movement in the plate including the maximum displacement. The second camera recorded in color at a rate of 10,000 frames per second at a resolution of 512x384. A picture from both of the camera locations are shown in Figure E.294.

E.28.2.2 TARGET LOCATIONS

Five targets were welded onto the side of the steel plate as shown in Figure E.293. They were spaced at the intervals shown in
Figure E.295. That figure also shows the location of the targets for the impacting mass. An additional two targets were placed on the angle at the top and the bottom end conditions. The distance between these two points is 74.93 cm (29 ½")

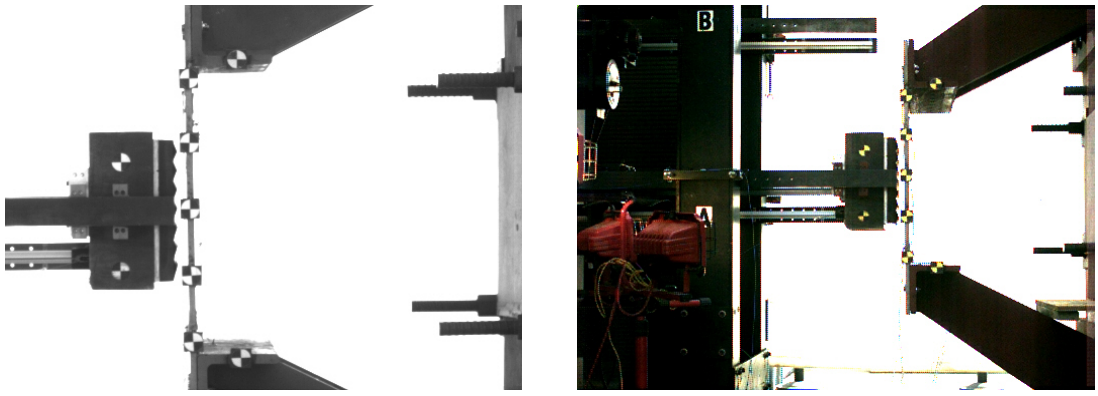

Figure E.294: Phantom Cameras for Test 28 a) Camera One b) Camera Two

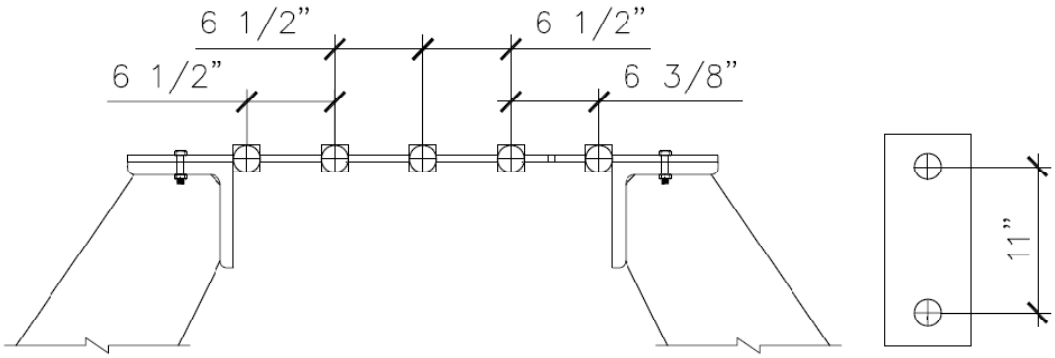

Figure E.295: Target layout on plate and impacting mass for Test 28

E.28.2.3 ACCELERATIONS

Accelerometers were not used for this test.

E.28.2.4 STRAIN GAGE LOCATIONS

For this test there were four strain gauges labeled 19, 20, 21 and 22. The strain gauges, and their locations, are shown as a drawing in Figure E.296 and as a photo in Figure E.297. Table E.24 shows the specific information about this test, including the time and velocity at impact, if, and when, the bolts failed along with the maximum and minimum principal strain rates. The largest maximum principal strain rate for this test was 16.31 1/sec and was located at strain gage 19 while the largest minimum strain rate for this test was 11.33 1/sec located at strain gage 20. The maximum principal strains for gauges 19, 20,21 and 22 can be found in Figure E.298 and the minimum principal strains for the same gauges can be found in Figure E.299.

This test involved the group of test that has gauges on both sides of the plate as discussed in the report. The pure axial strains have been determined and are shown in Figure E.300 for Gauges 19 and 21; and Figure E.301 for Gauges 20 and 22. The actual bending and axial strains were also determined for these tests up until the plate yields. The graphs of the

stresses for Gauges 19 and 21 and Gauges 20 and 22 can be found in Figure E.302 and Figure E.303, respectively.

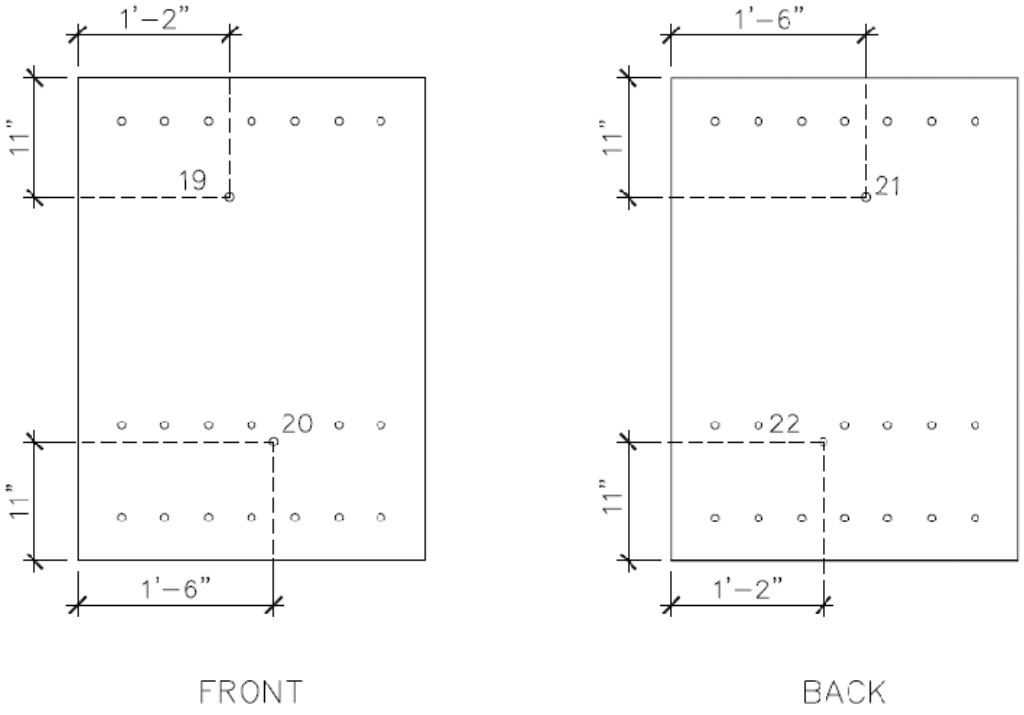

Figure E.296: Strain gage layout for Test 28 (drawing)

Figure E.297: Strain gage layout for Test 28 (pictures)

Table E.24: Stain rate information for Test 28

Strain Gage Number	Actual Velocity	Initial Impact	Shear Wave at Gage	Bolts Break	Maximum Principal Strain Rate	Minimum Principal Strain Rate
19	27.66 m/s	57.50 msec	-	61.40 msec	-16.31 1/sec	8.02 1/sec
20	27.66 m/s	57.50 msec	-	61.40 msec	-14.70 1/sec	11.33 1/sec
21	27.66 m/s	57.50 msec	-	61.40 msec	-11.53 1/sec	7.20 1/sec
22	27.66 m/s	57.50 msec	-	61.40 msec	-7.94 1/sec	7.44 1/sec

E.28.2.5 BOLT TYPE

A total of fourteen A307 bolts (Low Strength Bolts similar to Rivets) were used for this test. They were all tightened to a torque of 40 ft-lbs.

E.28.3 BLAST GENERATOR DATA

The initial impact of the single BG was 90.22 ft/sec (27.5 m/sec) with a goal velocity of 28 m/s. It had one accelerometer mounted to the back side of the impact plate as discussed in Section E.28.2.3. The average impact velocity for the impacting mass and the steel plate was calculated using the TEMA Track Eye tracking software.

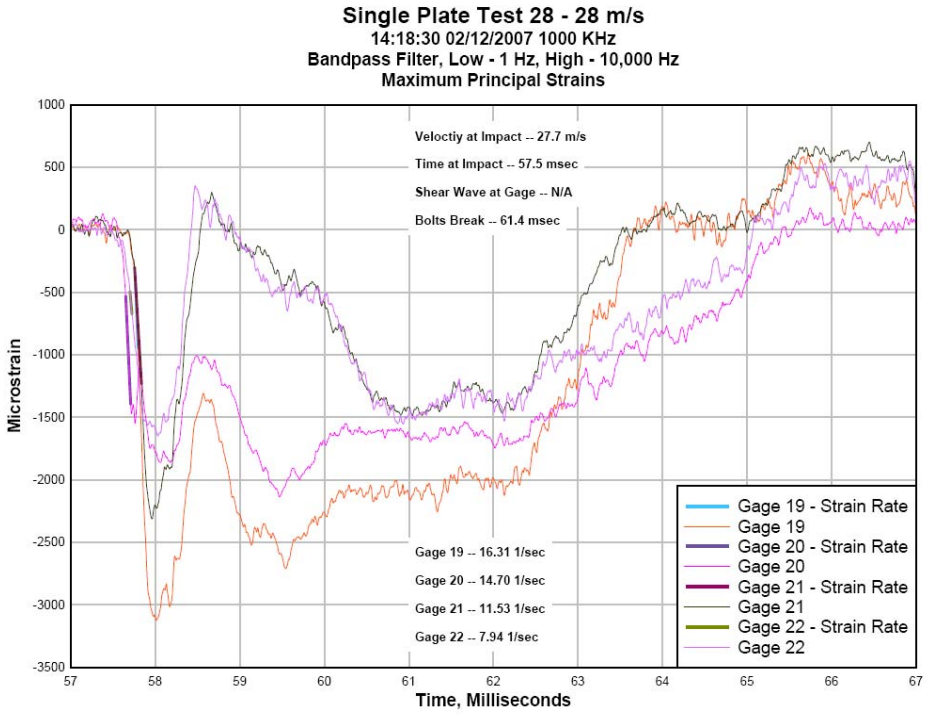

Figure E.298: Maximum principal strains and strain rates for Test 28

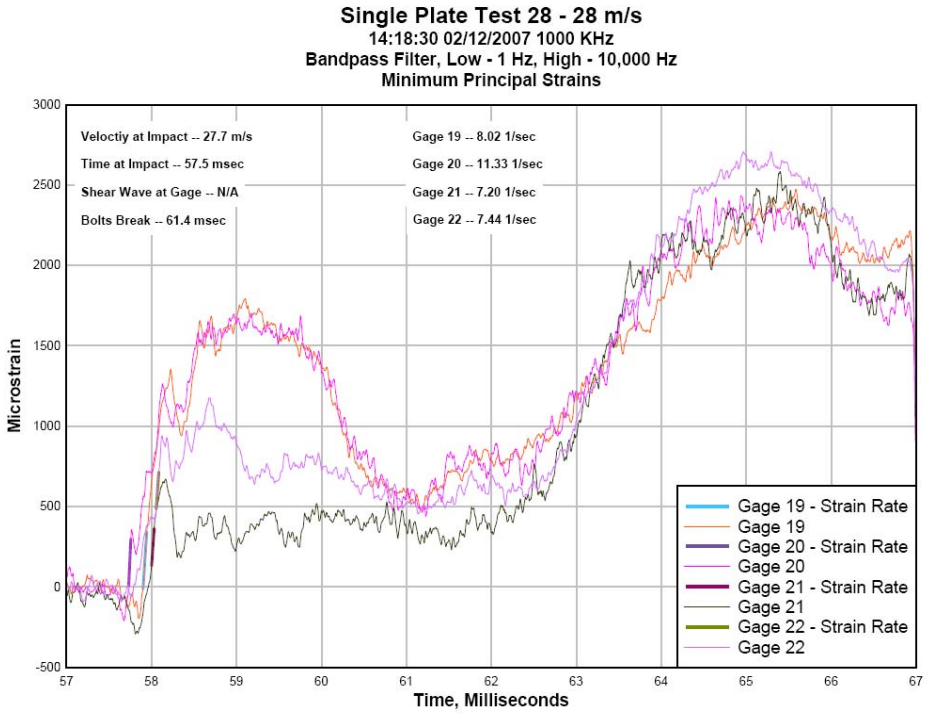

Figure E.299: Minimum principal strains and strain rates for Test 28

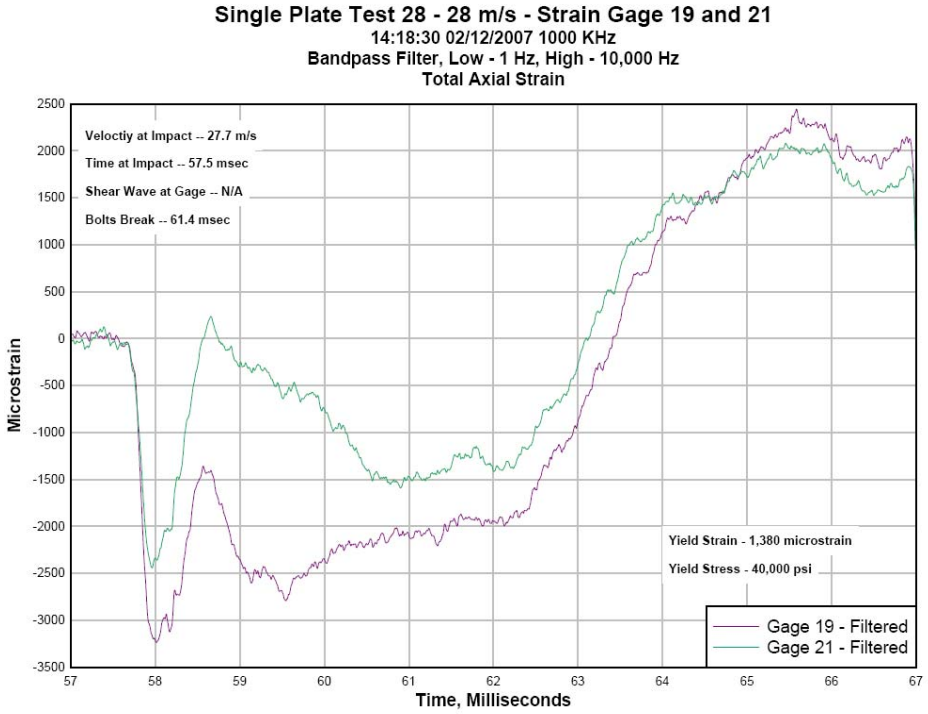

Figure E.300: Combined Axial Strain for Test 28 – Gauges 19 and 21

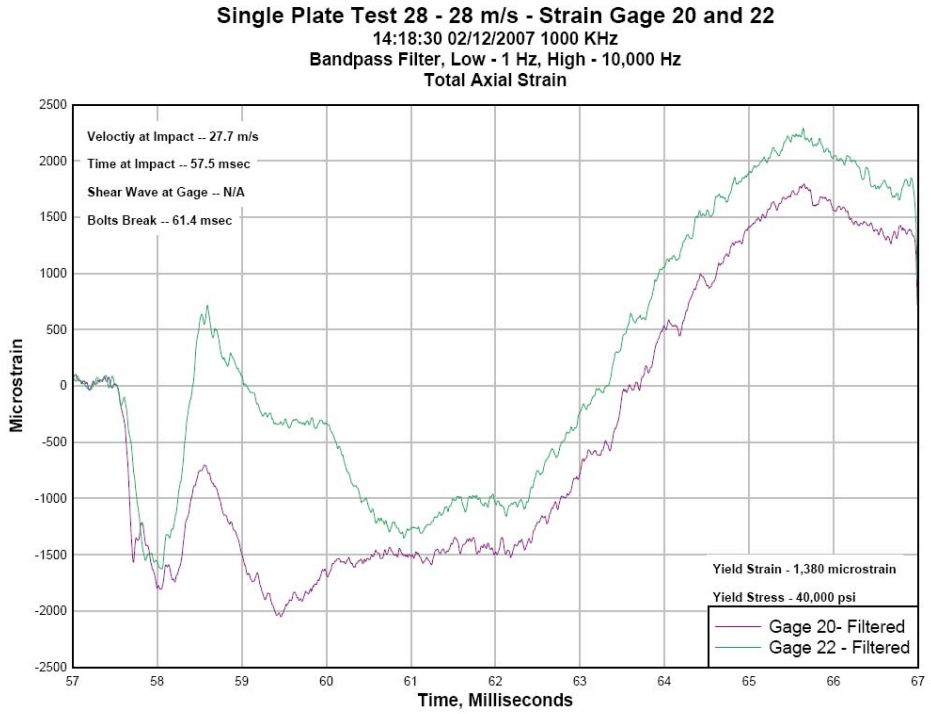

Figure E.301: Combined Axial Strain for Test 28 – Gauges 20 and 22

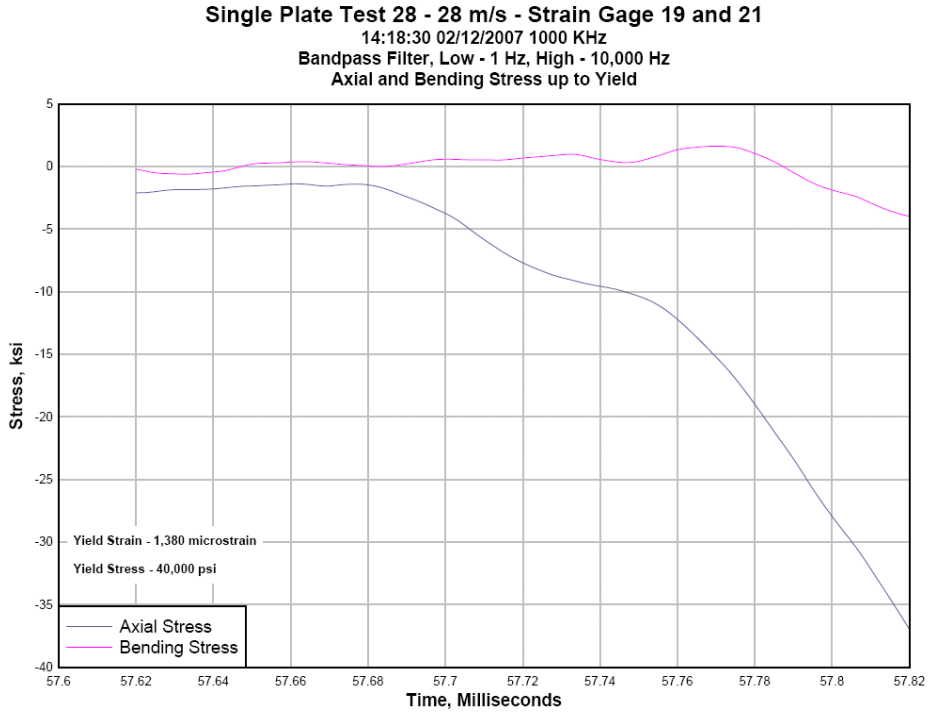

Figure E.302: Truncated Axial and Bending Stresses for Test 28 – Gauges 19 and 21

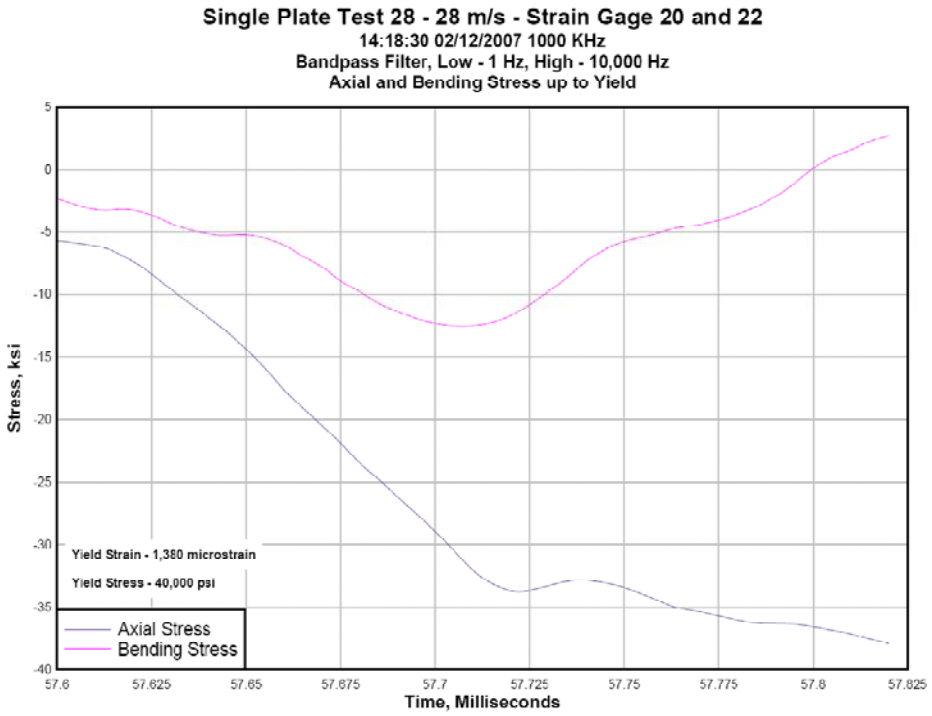

Figure E.303: Truncated Axial and Bending Stresses for Test 28 – Gauges 20 and 22

E.28.4 SPECIMEN BEHAVIOR

The loading of the BG plate imparted an initial velocity of 90.22 ft/sec (27.5 m/sec) to the specimen. This caused plate to deform in both directions. The longitudinal deflection (in the north-south direction) behaved in a typical one-way flexural shape. In order to get the velocity as high as needed the test was designed to have the impacting mass break free from the BG and launch itself into the plate. This test imparted enough energy to break all fourteen of the bolts as shown in Figure E.304. The maximum dynamic deflection during the test was approximately 3 ¾". During the test two different phantom cameras were used to capture the failure modes from three different angles. Figure E.305 shows the progression of damage for this test from Phantom Camera One. Figure E.306 shows the progression of damage for this test from Phantom Camera Two

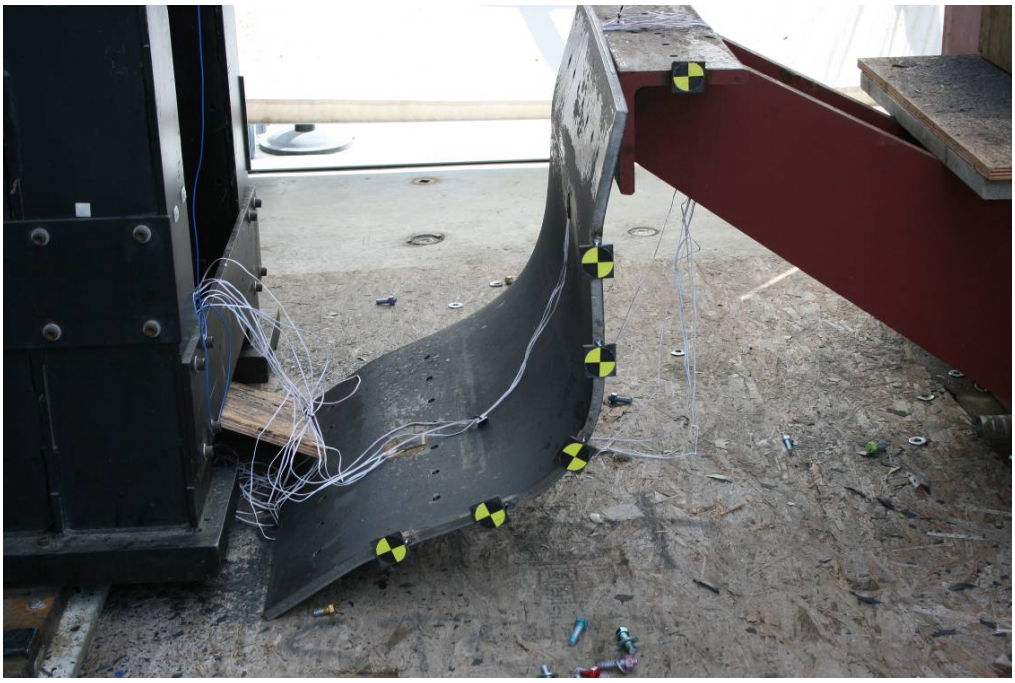

Figure E.304: Steel plate post test for Test 28

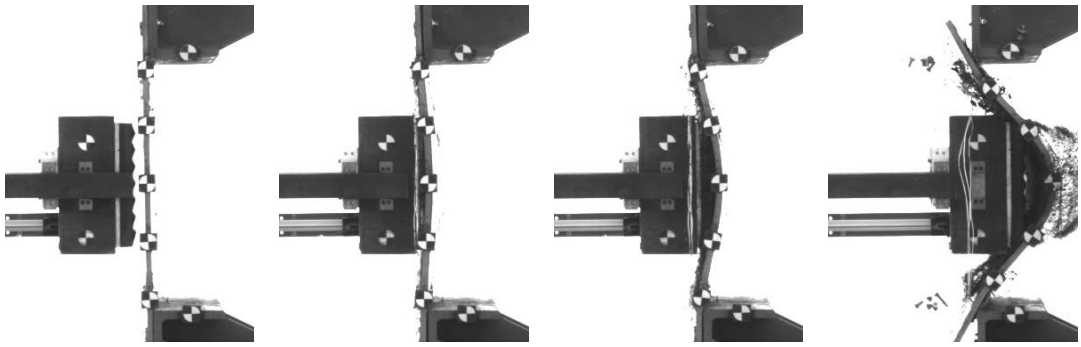

Figure E.305: Progression of damage for Test 28 from Camera 1

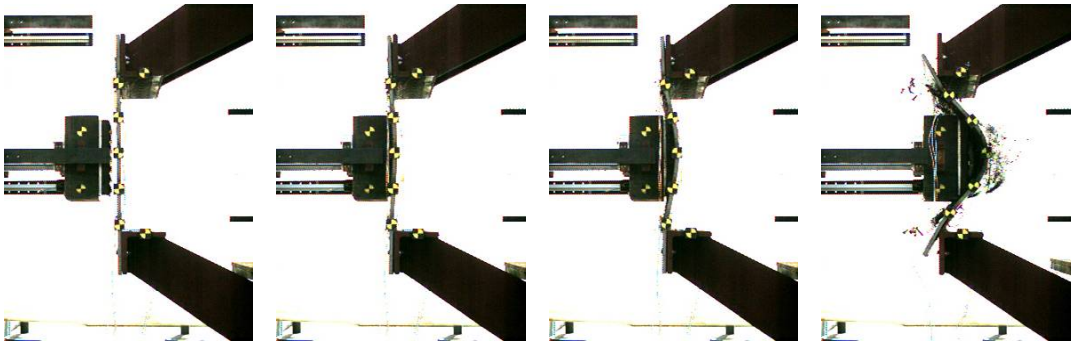

Figure E.306: Progression of damage for Test 28 from Camera 2

E.29 STEEL TOWER SINGLE PLATE: TEST 29 (SP29)

E.29.1 INTRODUCTION

The twenty-ninth test of the Steel Tower Single Plate test series was performed on February 14th, 2007. The test specimen was a ¾" thick steel plate labeled SP29. The Impacting Mass 1 was attached to the BG with a specimen target velocity of 82.02 ft/sec (25 m/sec). Figure E.307 shows the steel plate prior to impact.

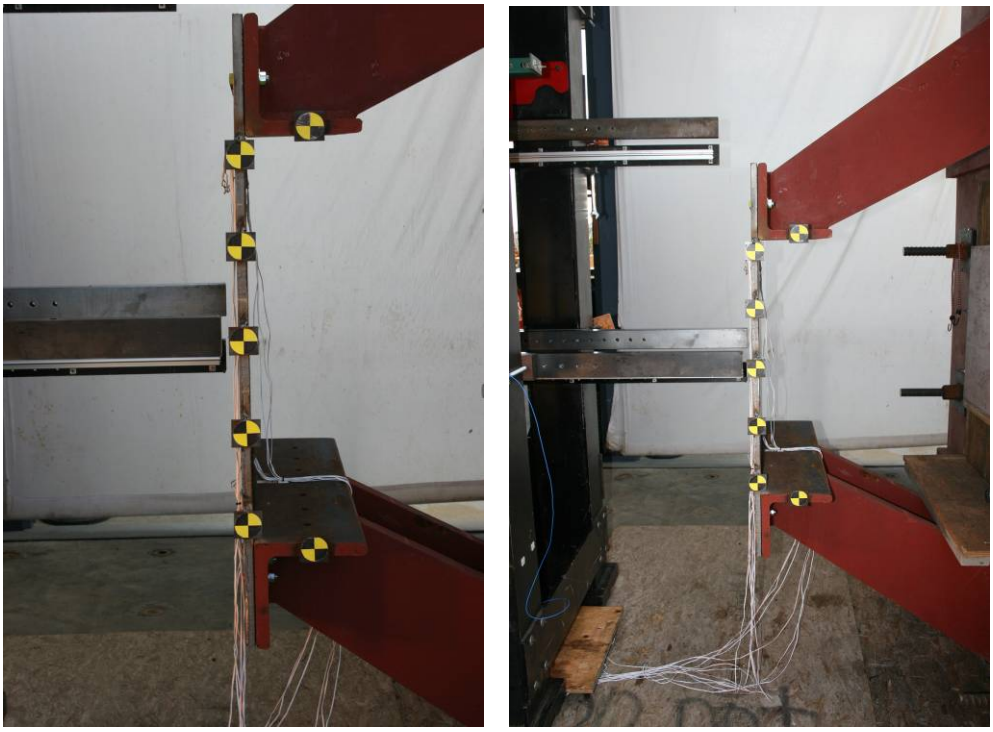

Figure E.307: 3/4" thick steel plate pre test for Test 29

E.29.2 INSTRUMENTATION

E.29.2.1 PHANTOM CAMERAS

The first camera recorded in black and white at a rate of 10,000 frames per second at a resolution of 512x384. This camera was used in order to determine the maximum velocity of the impacting mass and the movement in the plate including the maximum displacement. The second camera recorded in color at a rate of 5,000 frames per second at a resolution of 512x384. This camera recorded the overall behavior of the test specimen. It was not used to gather any specific data. The third camera recorded in color at a rate of 5,000 frames per second at a resolution of 480x480. This camera captured the failure of the bolts. A picture from each of the camera locations are shown in Figure E.308.

E.29.2.2 TARGET LOCATIONS

Five targets were welded onto the side of the steel plate as shown in Figure E.307. They were spaced at the intervals shown in Figure E.309. That figure also shows the location

of the targets for the impacting mass. An additional two targets were placed on the angle at the top and the bottom end conditions. The distance between these two points is 74.93 cm (29 ½")

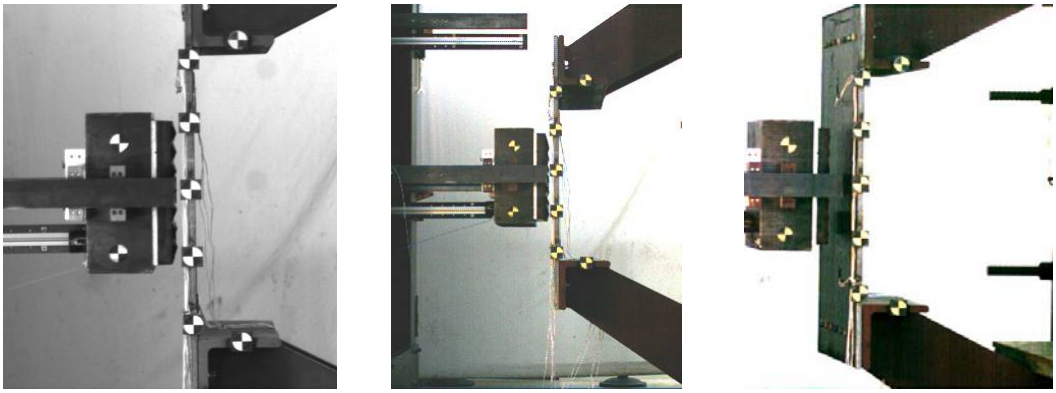

Figure E.308: Phantom Cameras for Test 29

a) Camera One b) Camera Two c) Camera Three

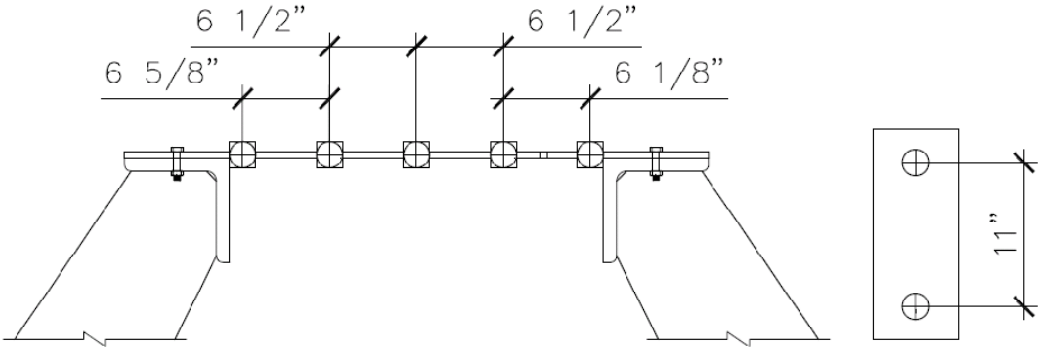

Figure E.309: Target layout on plate and impacting mass for Test 29

E.29.2.3 ACCELERATIONS

For this test one accelerometer was used. This accelerometer was placed 6" south of the centroid of the impacting mass as shown in Figure E.310. The pipe is to protect the accelerometer during the test. The data from this gage was then filtered as shown in Figure E.311.

This test does not impart an impulsive load as would be expected from a typical blast test. Instead, this test simulates the behavior of a flyer plate moving through the structure after the initial impact at the front plate of the outer cell of the structure. Therefore we are not determining the initial impulsive load from the accelerometers on the BG.

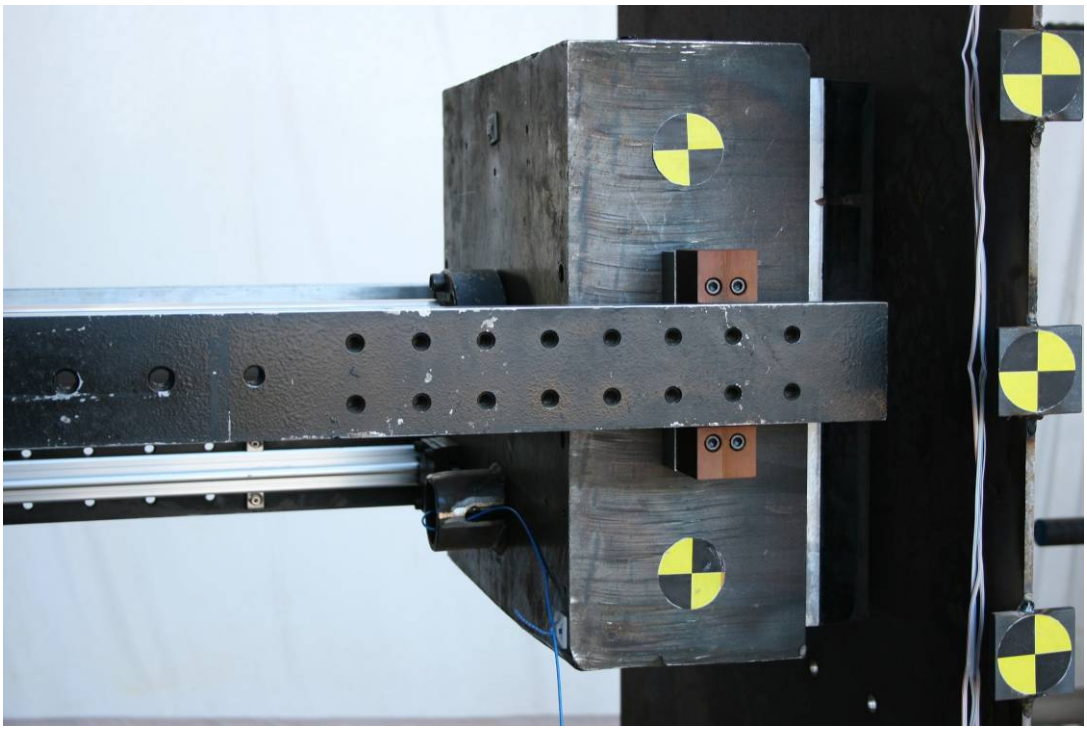

Figure E.310: Accelerometer location for Test 29

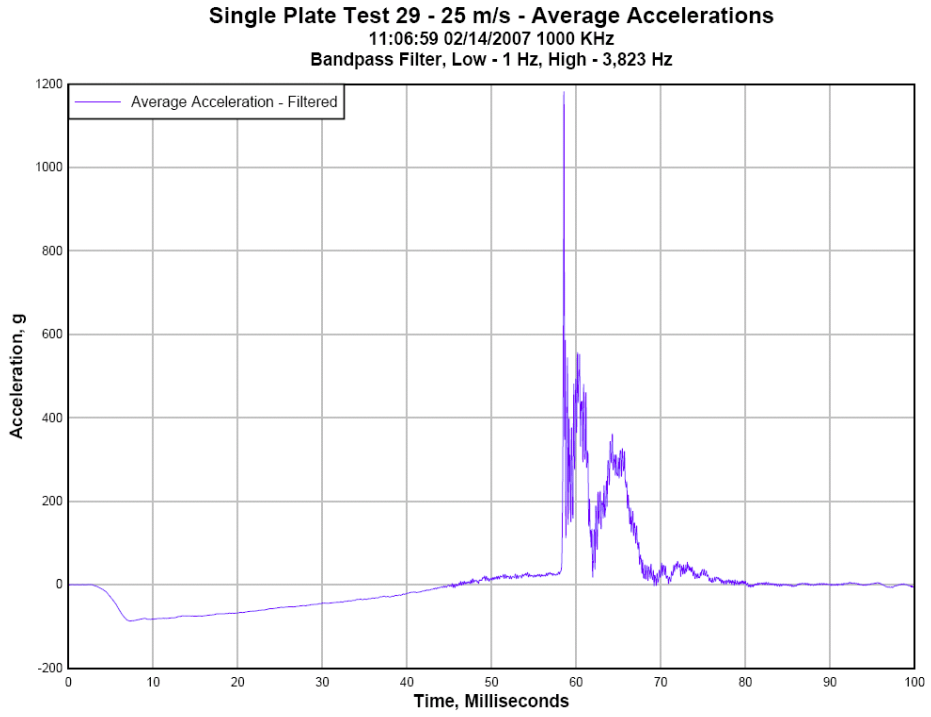

Figure E.311: Filtered accelerometer data for Test 29

E.29.2.4 STRAIN GAGE LOCATIONS

For this test there were four strain gauges labeled 19, 20, 21 and 22. The strain gauges, and their locations, are shown as a drawing in Figure E.312 and as a photo in Figure E.313. Table E.25 shows the specific information about this test, including the time and velocity at impact, if, and when, the bolts failed along with the maximum and minimum principal strain rates. The largest maximum principal strain rate for this test was 13.80 1/sec and was located at strain gage 19 while the largest minimum strain rate for this test was 7.90 1/sec located at strain gage 22. The maximum principal strains for gauges 19, 20,, 21 and 22 can be found in Figure E.314 and the minimum principal strains for the same gauges can be found in Figure E.315.

This test involved the group of test that has gauges on both sides of the plate as discussed in the report. The pure axial strains have been determined and are shown in Figure E.316 for Gauges 19 and 21; and Figure E.317 for Gauges 20 and 22. The actual bending and axial strains were also determined for these tests up until the plate yields. The graphs of the stresses for Gauges 19 and 21 and Gauges 20 and 22 can be found in Figure E.318 and Figure E.319, respectively.

Table E.25: Stain rate information for Test 29

Strain Gage Number	Actual Velocity	Initial Impact	Shear Wave at Gage	Bolts Break	Maximum Principal Strain Rate	Minimum Principal Strain Rate
19	25.83 m/s	57.80 msec	60.20 msec	61.60 msec	-13.80 1/sec	4.30 1/sec
20	25.83 m/s	57.80 msec	60.20 msec	61.60 msec	-9.01 1/sec	7.51 1/sec
21	25.83 m/s	57.80 msec	60.20 msec	61.60 msec	-12.38 1/sec	6.21 1/sec
22	25.83 m/s	57.80 msec	60.20 msec	61.60 msec	-12.53 1/sec	7.90 1/sec

E.29.2.5 BOLT TYPE

A total of fourteen A307 bolts (Low Strength Bolts similar to Rivets) were used for this test. They were all tightened to a torque of 40 ft-lbs.

E.29.3 BLAST GENERATOR DATA

The initial impact of the single BG was 84.74 ft/sec (25.83 m/sec) with a goal velocity of 25 m/s. It had one accelerometer mounted to the back side of the impact plate as discussed in Section E.29.2.3. The average impact velocity for the impacting mass and the steel plate was calculated using the TEMA Track Eye tracking software.

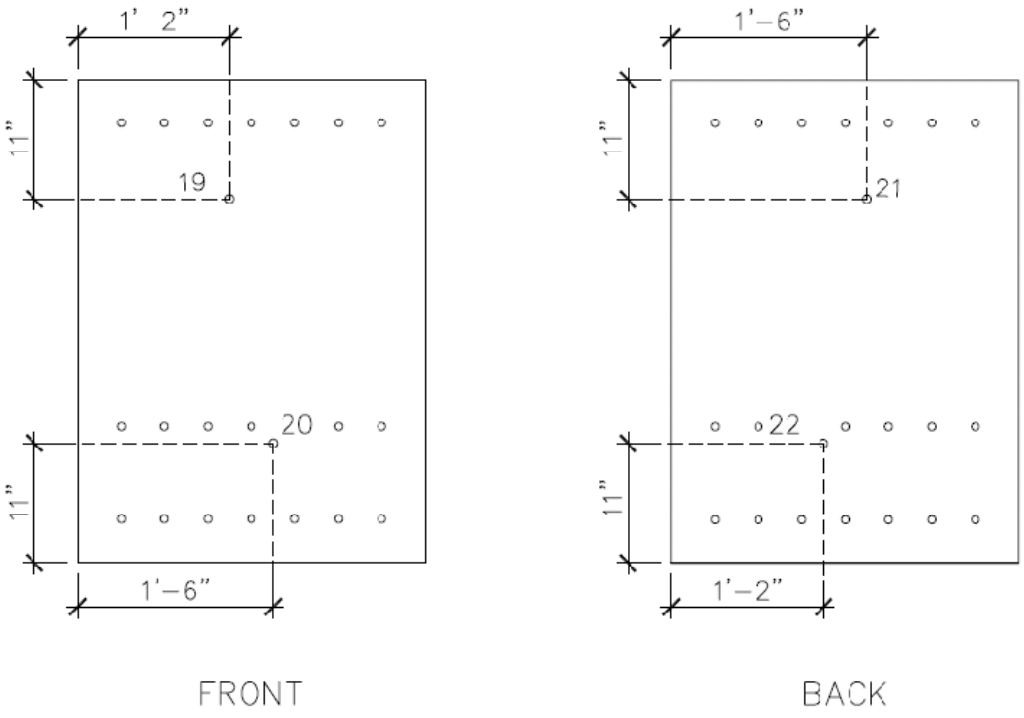

Figure E.312: Strain gage layout for Test 29 (drawing)

Figure E.313: Strain gage layout for Test 29 (pictures)

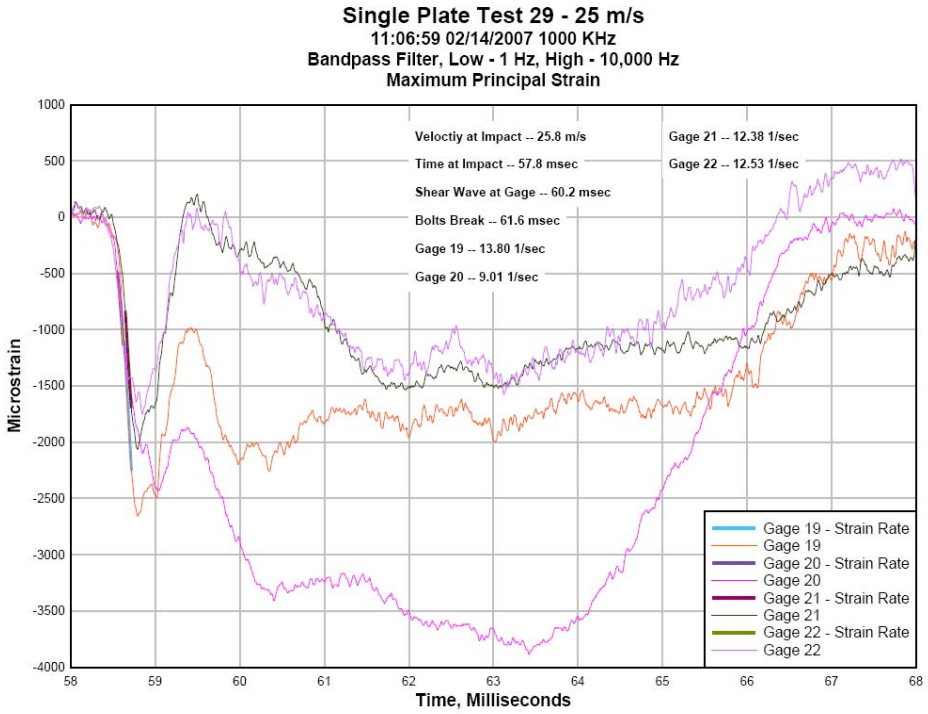

Figure E.314: Maximum principal strains and strain rates for Test 29

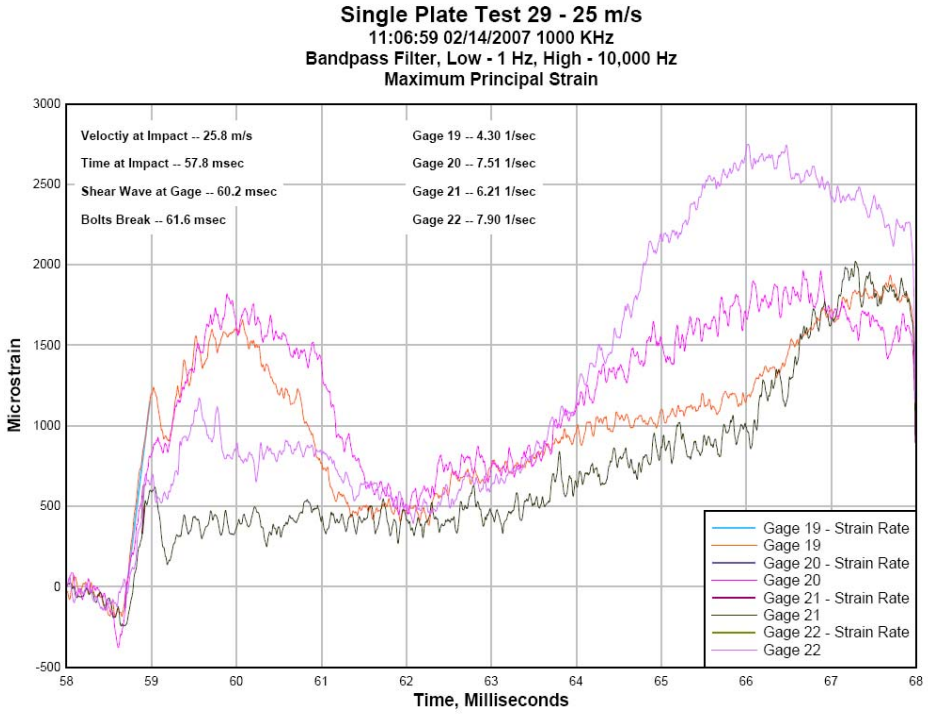

Figure E.315: Minimum principal strains and strain rates for Test 29

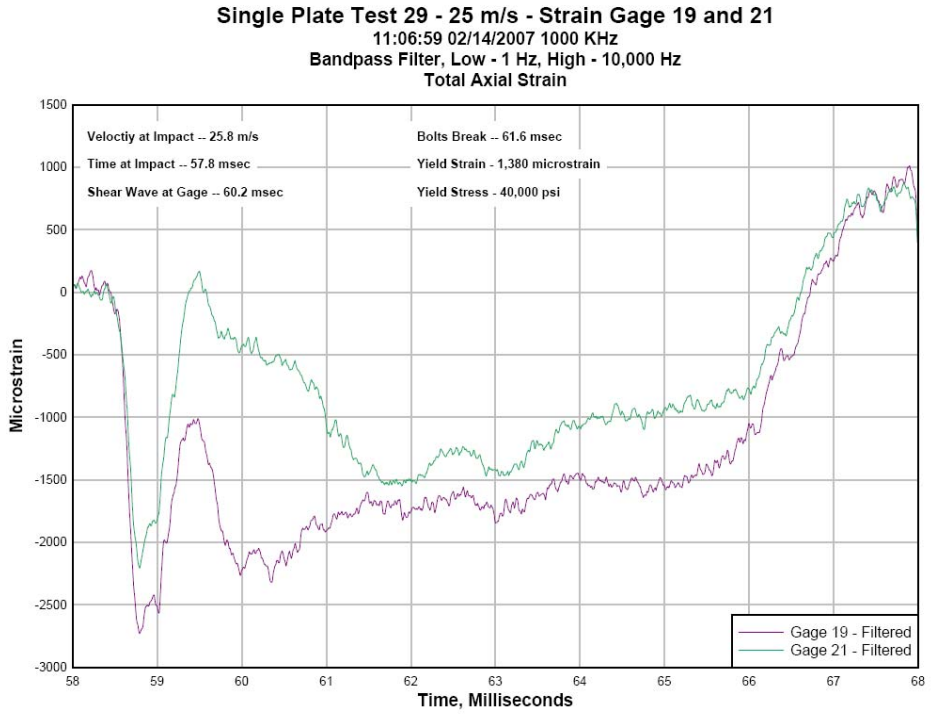

Figure E.316: Combined Axial Strain for Test 29 – Gauges 19 and 21

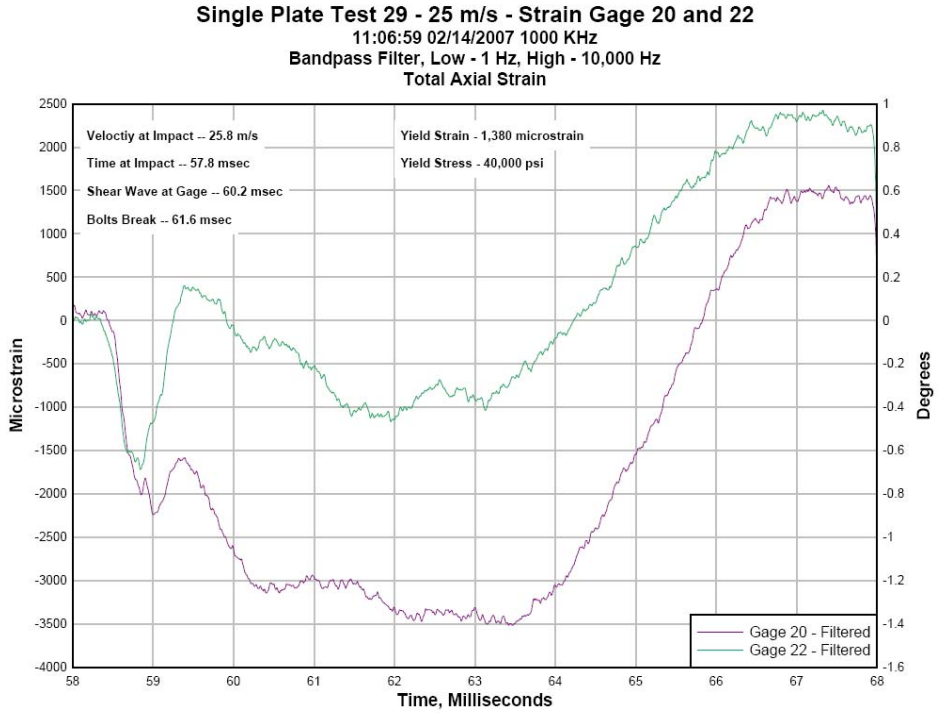

Figure E.317: Combined Axial Strain for Test 29 – Gauges 20 and 22

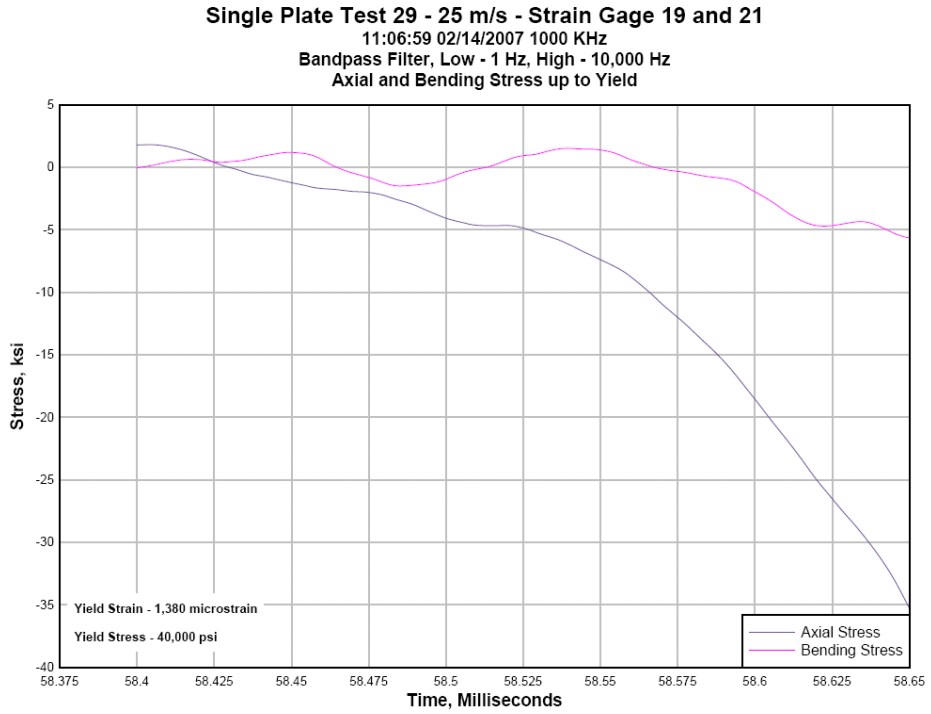

Figure E.318: Truncated Axial and Bending Stresses for Test 29 – Gauges 19 and 21

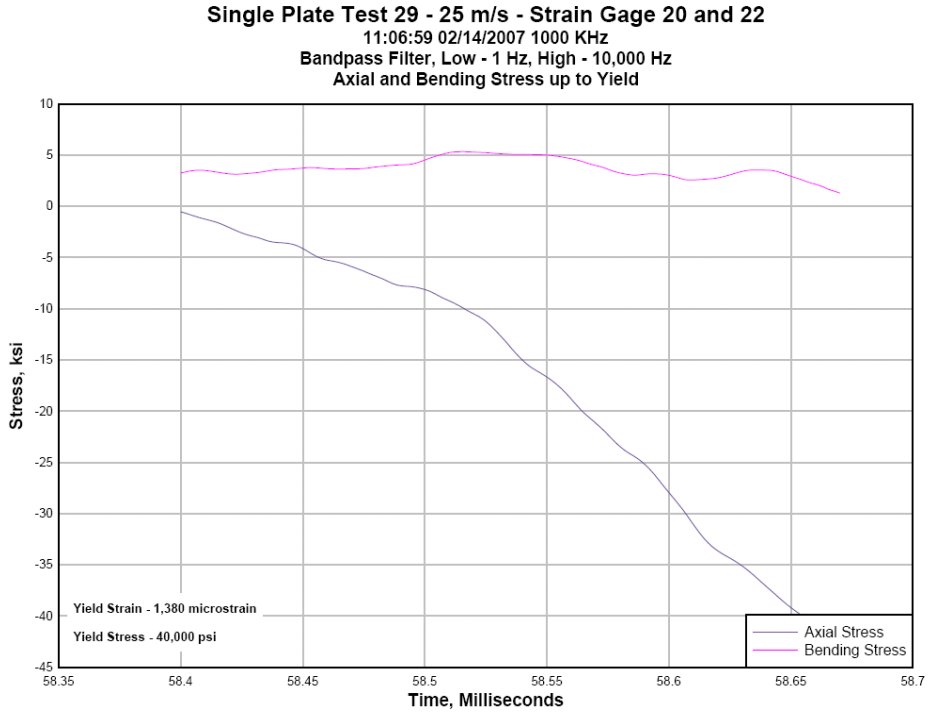

Figure E.319: Truncated Axial and Bending Stresses for Test 29 – Gauges 20 and 22

E.29.4 SPECIMEN BEHAVIOR

The loading of the BG plate imparted an initial velocity of 84.74 ft/sec (28.53 m/sec) to the specimen. This caused plate to deform in both directions. The longitudinal deflection (in the north-south direction) behaved in a typical one-way flexural shape. In order to get the velocity as high as needed the test was designed to have the impacting mass break free from the BG and launch itself into the plate. This test imparted enough energy to break all fourteen of the bolts as shown in Figure E.320. The maximum dynamic deflection during the test was approximately 3 1/8””. During the test three different phantom cameras were used to capture the failure modes from three different angles. Figure E.321 shows the progression of damage for this test from Phantom Camera One. Figure E.322 shows the progression of damage for this test from Phantom Camera Two. Figure E.323 shows the progression of damage for this test from Phantom Camera Three.

Figure E.320: Steel plate post test for Test 29

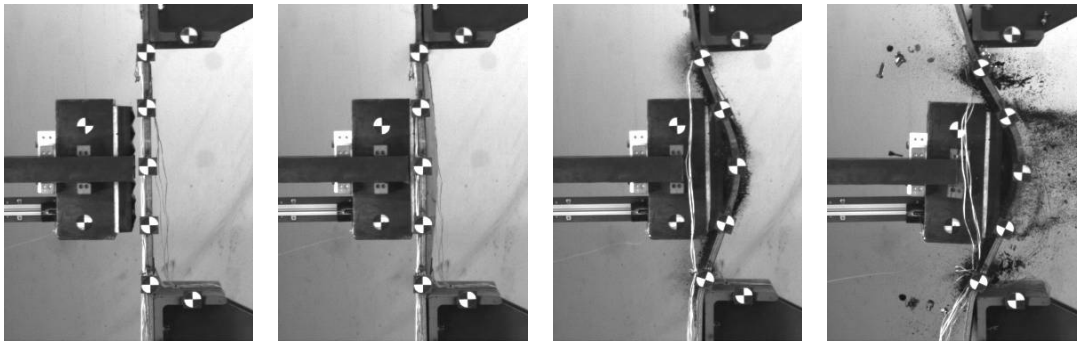

Figure E.321: Progression of damage for Test 29 from Camera 1

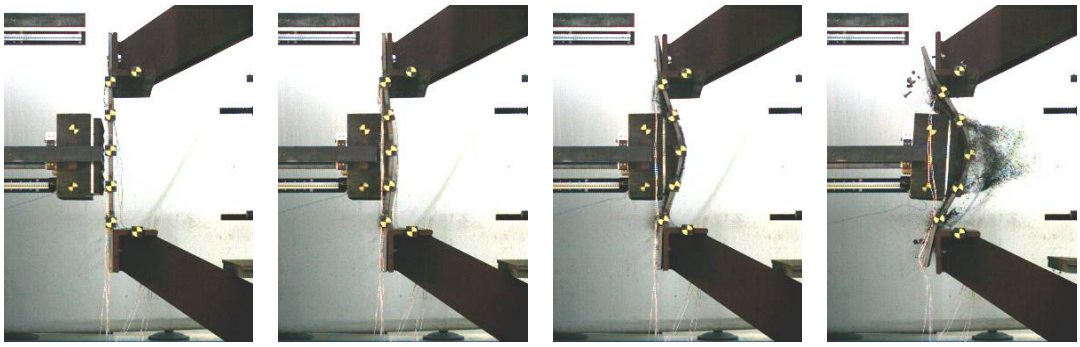

Figure E.322: Progression of damage for Test 29 from Camera 2

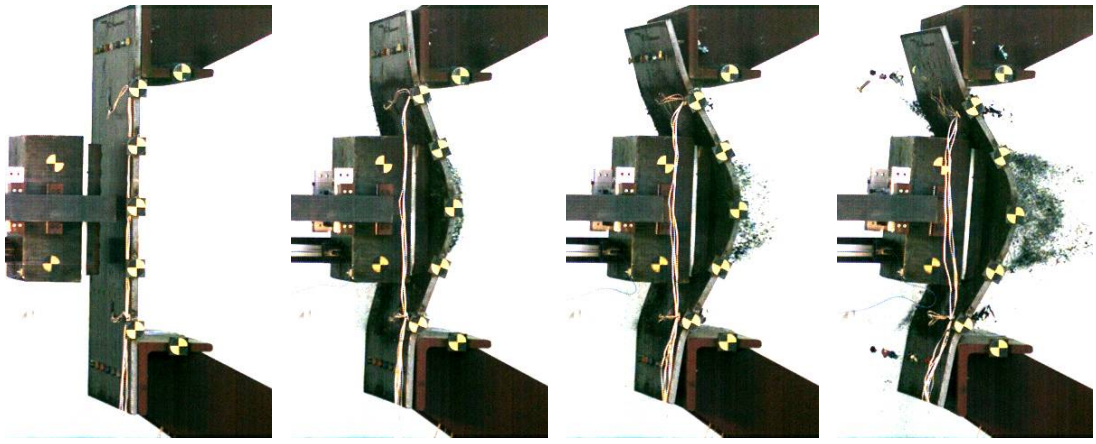

Figure E.323: Progression of damage for Test 29 from Camera 3

E.30 STEEL TOWER SINGLE PLATE: TEST 30 (SP30)

E.30.1 INTRODUCTION

The thirtieth test of the Steel Tower Single Plate test series was performed on February 16th, 2007. The test specimen was a ¾" thick steel plate labeled SP30. The Impacting Mass 1 was attached to the BG with a specimen target velocity of 91.86 ft/sec (28 m/sec). Figure E.324 shows the steel plate prior to impact.

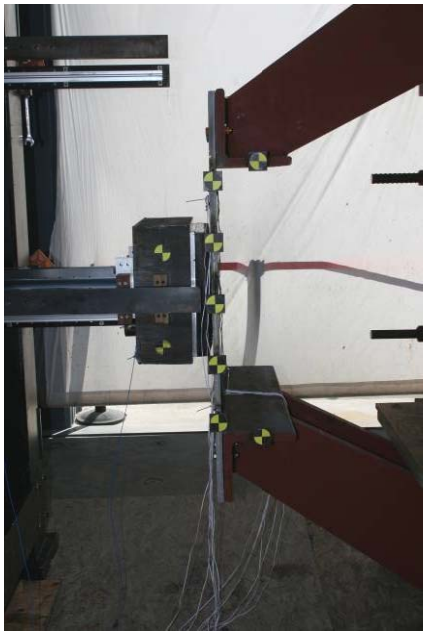

Figure E.324: 3/4" thick steel plate pre test for Test 30

E.30.2 INSTRUMENTATION

E.30.2.1 PHANTOM CAMERAS

The first camera recorded in black and white at a rate of 10,000 frames per second at a resolution of 512x384. This camera was used in order to determine the maximum velocity of the impacting mass and the movement in the plate including the maximum displacement. The second camera recorded in color at a rate of 10,000 frames per second at a resolution of 512x384. This camera recorded similar information as Camera One but with a wider view of the specimen and the test set-up. The third camera recorded in color at a rate of 8,000 frames per second at a resolution of 480x480. This camera captured data on the front side of the plate. Specifically how the bolts failed, but was not used to gather any specific data. A picture from each of the camera locations are shown in Figure E.325.

E.30.2.2 TARGET LOCATIONS

Five targets were welded onto the side of the steel plate as show in Figure E.324. They were spaced at the intervals shown in Figure E.326. That figure also shows the location of the targets for the impacting mass. An additional two targets were placed on the angle at the

top and the bottom end conditions. The distance between these two points is 74.93 cm (29 ½")

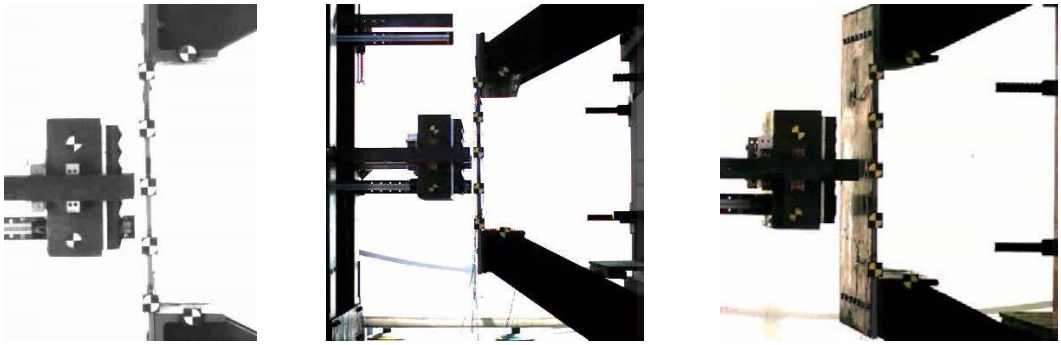

Figure E.325: Phantom Cameras for Test 30

a) Camera One b) Camera Two c) Camera Three

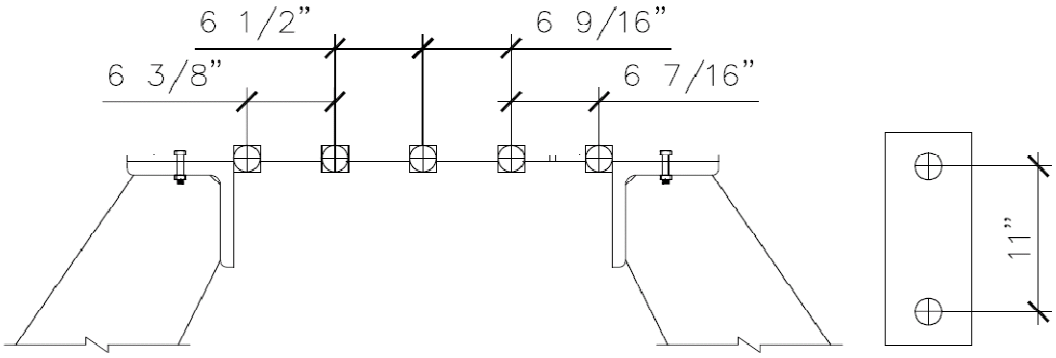

Figure E.326: Target layout on plate and impacting mass for Test 30

E.30.2.3 ACCELERATIONS

For this test one accelerometer was used. It was located 6" south of the centroid as shown in Figure E.327. The pipe is to protect the accelerometer during the test. A filter was applied to the accelerometer data as shown in Figure E.328.

This test does not impart an impulsive load as would be expected from a typical blast test. Instead, this test simulates the behavior of a flyer plate moving through the structure after the initial impact at the front plate of the outer cell of the structure. Therefore we are not determining the initial impulsive load from the accelerometers on the BG.

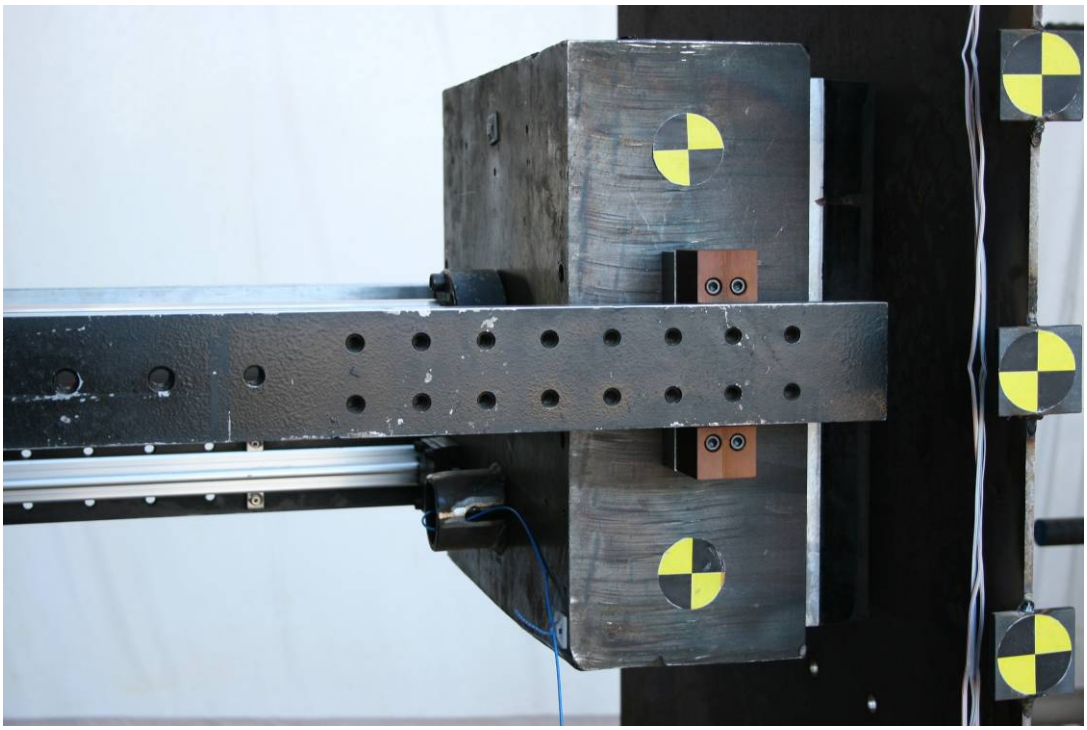

Figure E.327: Accelerometer location for Test 30

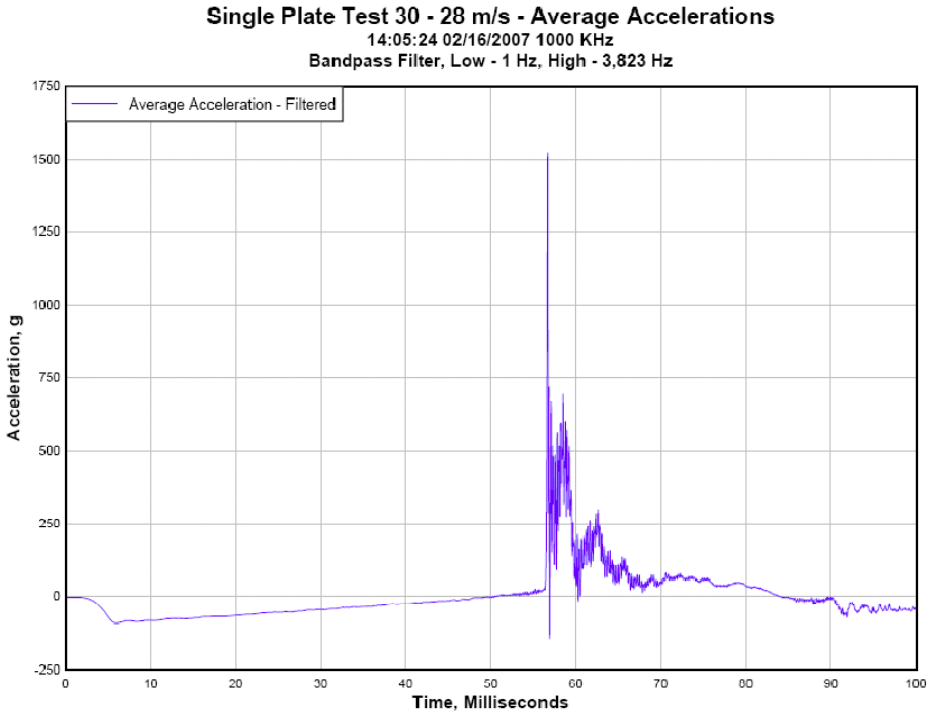

Figure E.328: Filtered accelerometer data for Test 30

E.30.2.4 STRAIN GAGE LOCATIONS

For this test there were four strain gauges labeled 19, 20, 21 and 22. The strain gauges, and their locations, are shown as a drawing in Figure E.329 and as a photo in Figure E.330.
Table E.26 shows the specific information about this test, including the time and velocity at impact, if, and when, the bolts failed along with the maximum and minimum principal strain rates. The largest maximum principal strain rate for this test was 18.01 1/sec and was located at strain gage 19 while the largest minimum strain rate for this test was 11.01 1/sec located at strain gage 22. The maximum principal strains for gauges 19, 20 21 and 22 can be found in Figure E.331 and the minimum principal strains for the same gauges can be found in Figure E.332.

This test involved the group of test that has gauges on both sides of the plate as discussed in the report. The pure axial strains have been determined and are shown in Figure E.333 for Gauges 19 and 21; and Figure E.334 for Gauges 20 and 22. The actual bending and axial strains were also determined for these tests up until the plate yields. The graphs of the stresses for Gauges 19 and 21 and Gauges 20 and 22 can be found in Figure E.335 and Figure E.336, respectively.

Table E.26: Stain rate information for Test 30

Strain Gage Number	Actual Velocity	Initial Impact	Shear Wave at Gage	Bolts Break	Maximum Principal Strain Rate	Minimum Principal Strain Rate
19	28.5 m/s	56.30 msec	57.25 msec	61.25 msec	-14.75 1/sec	7.92 1/sec
20	28.5 m/s	56.30 msec	57.25 msec	61.25 msec	-10.84 1/sec	3.04 1/sec
21	28.5 m/s	56.30 msec	57.25 msec	61.25 msec	-13.70 1/sec	4.54 1/sec
22	28.5 m/s	56.30 msec	57.25 msec	61.25 msec	14.36 1/sec	11.01 1/sec

E.30.2.5 BOLT TYPE

A total of fourteen A307 bolts (Low Strength Bolts, similar to rivets) were used for this test. They all had a torque of 40 ft-lbs applied to them before the test.

E.30.3 BLAST GENERATOR DATA

The initial impact of the single BG was 93.50 ft/sec (28.5 m/sec) with a goal velocity of 28 m/s. It had an accelerometers mounted to the back side of the impact plate as discussed in E.30.2.3. The average impact velocity for the impacting mass and the steel plate was calculated using the TEMA Track Eye tracking software.

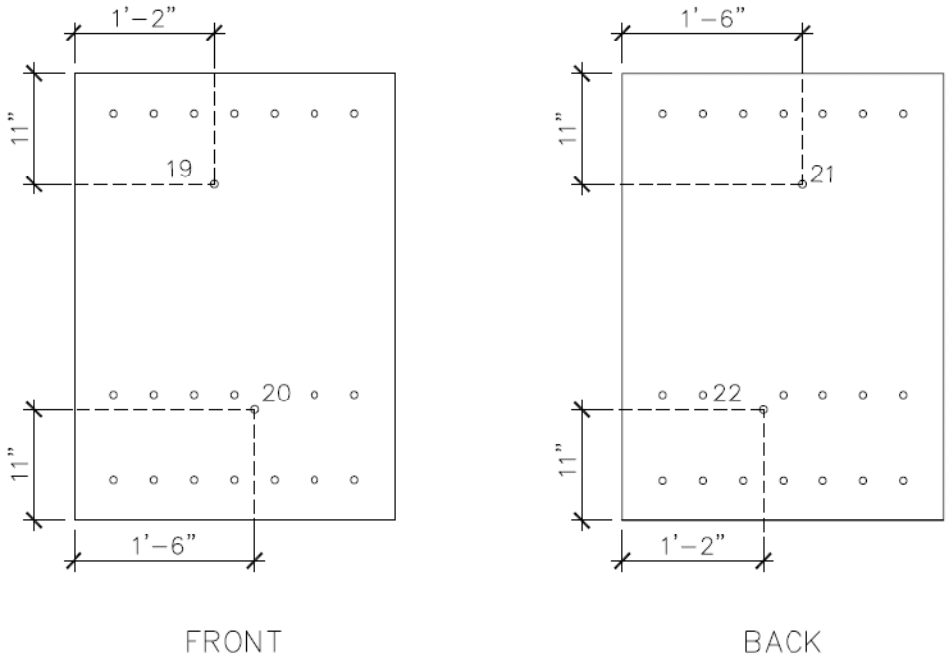

Figure E.329: Strain gage layout for Test 30 (drawing)

Figure E.330: Strain gage layout for Test 30 (pictures)

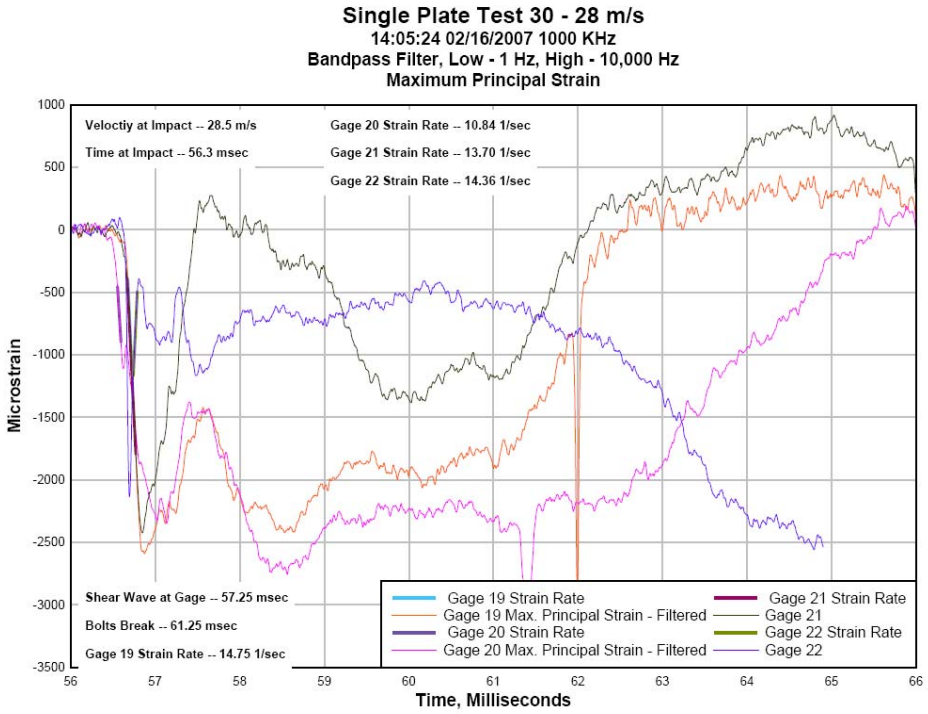

Figure E.331: Maximum principal strains and strain rates for Test 30

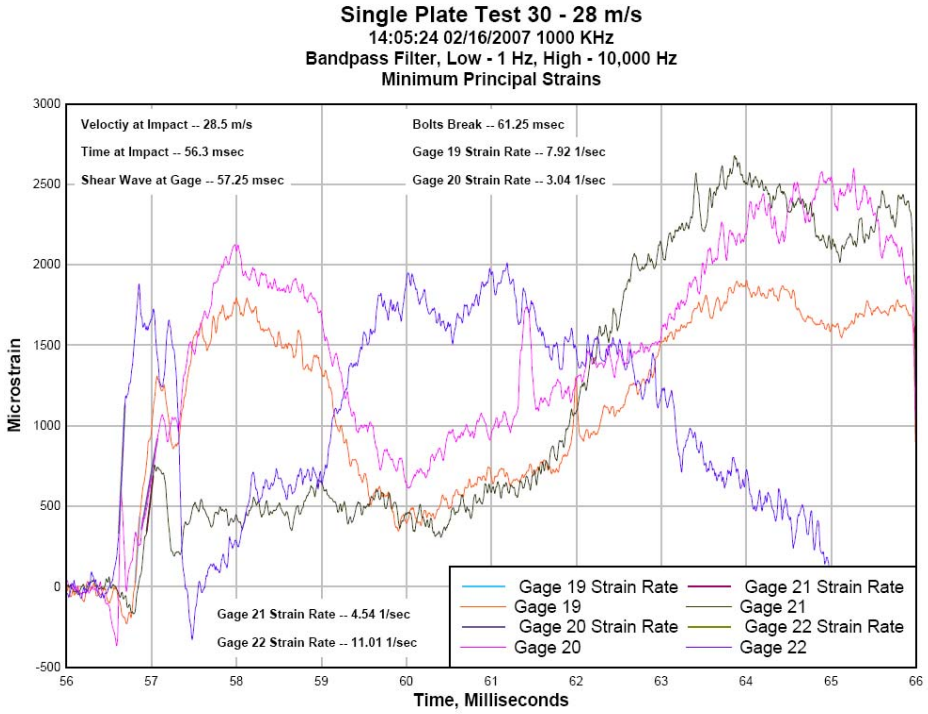

Figure E.332: Minimum principal strains and strain rates for Test 30

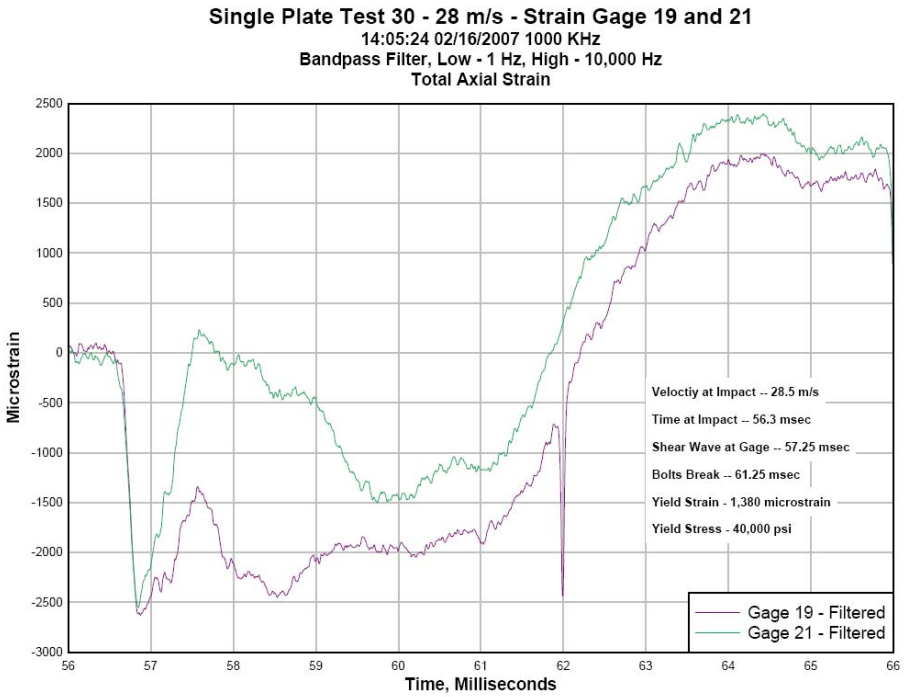

Figure E.333: Combined Axial Strain for Test 30 – Gauges 19 and 21

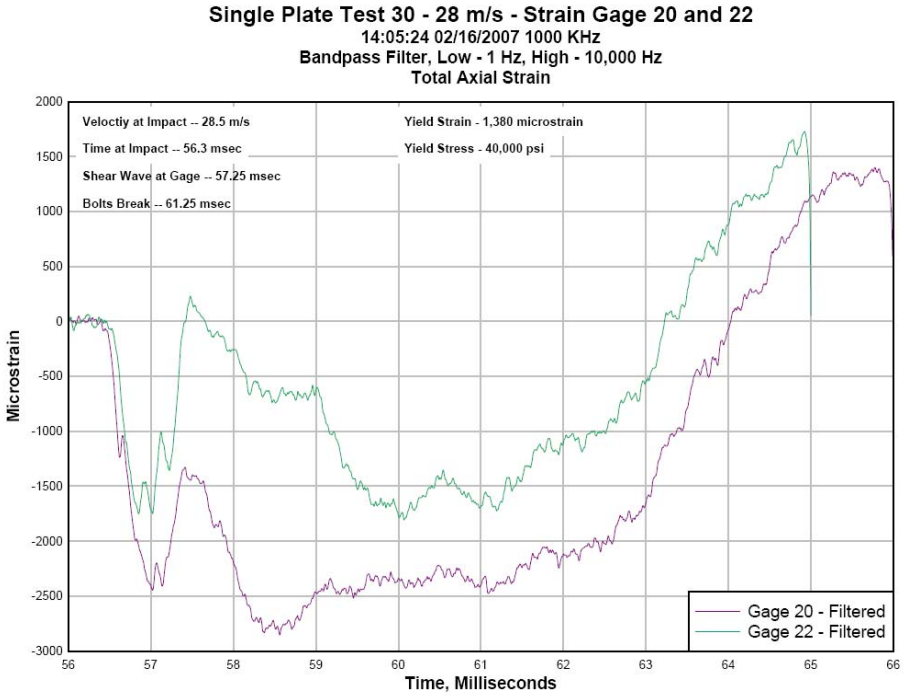

Figure E.334: Combined Axial Strain for Test 30 – Gauges 20 and 22

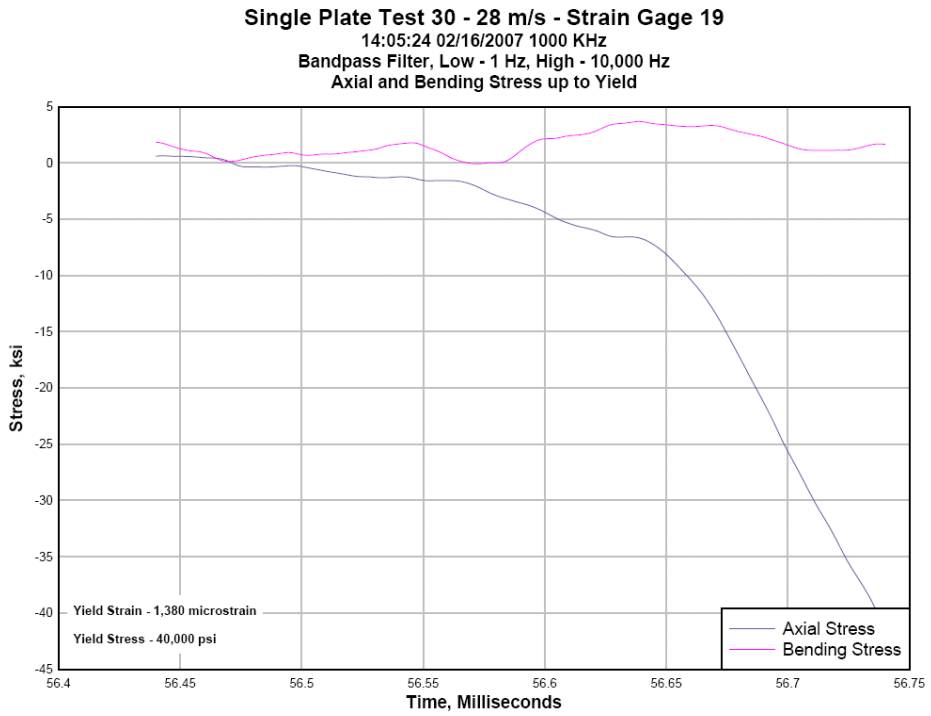

Figure E.335: Truncated Axial and Bending Stresses for Test 30 – Gauges 19 and 21

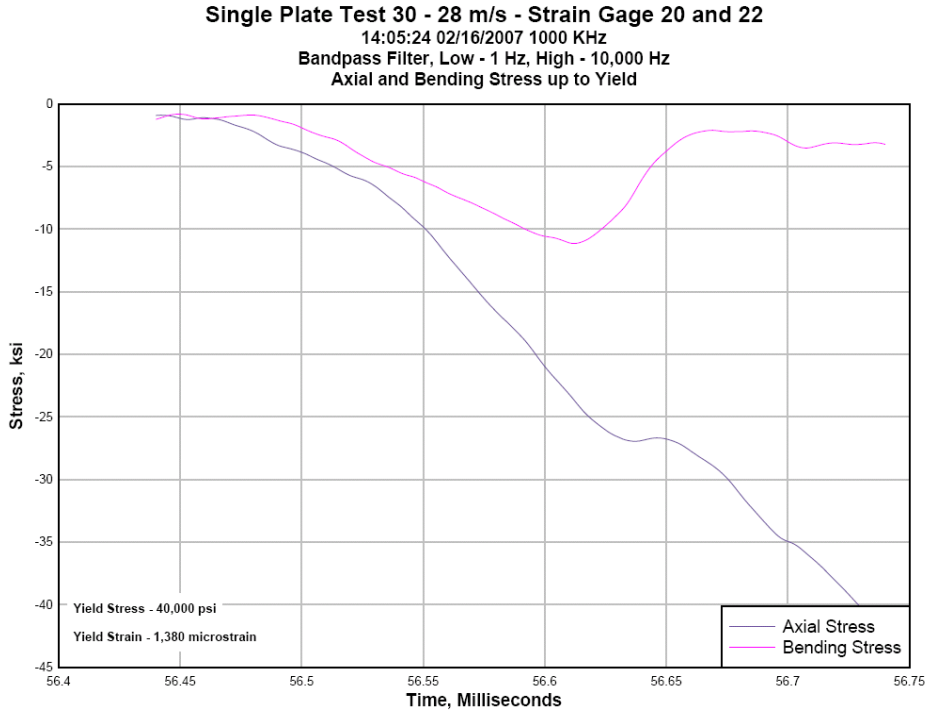

Figure E.336: Truncated Axial and Bending Stresses for Test 30 – Gauges 20 and 22

E.30.4 SPECIMEN BEHAVIOR

The loading of the BG plate imparted an initial velocity of 93.50 ft/sec (28.5 m/sec) to the specimen. This caused plate to deform in both directions. The longitudinal deflection (in the north-south direction) behaved in a typical one-way flexural shape. In order to get the velocity as high as needed the test was designed to have the impacting mass break free from the BG and launch itself into the plate. This imparted enough energy into the system that all fourteen A307 bolts failed. After the test was completed the plate was found on the ground bent into a shallow U-shape. Figure E.337 shows the test specimen after the test. Figure E.338 shows the progression of damage from Phantom Camera One. Figure E.339 shows the progression of damage from Phantom Camera Two. . Figure E.340 shows the progression of damage from Phantom Camera Two.

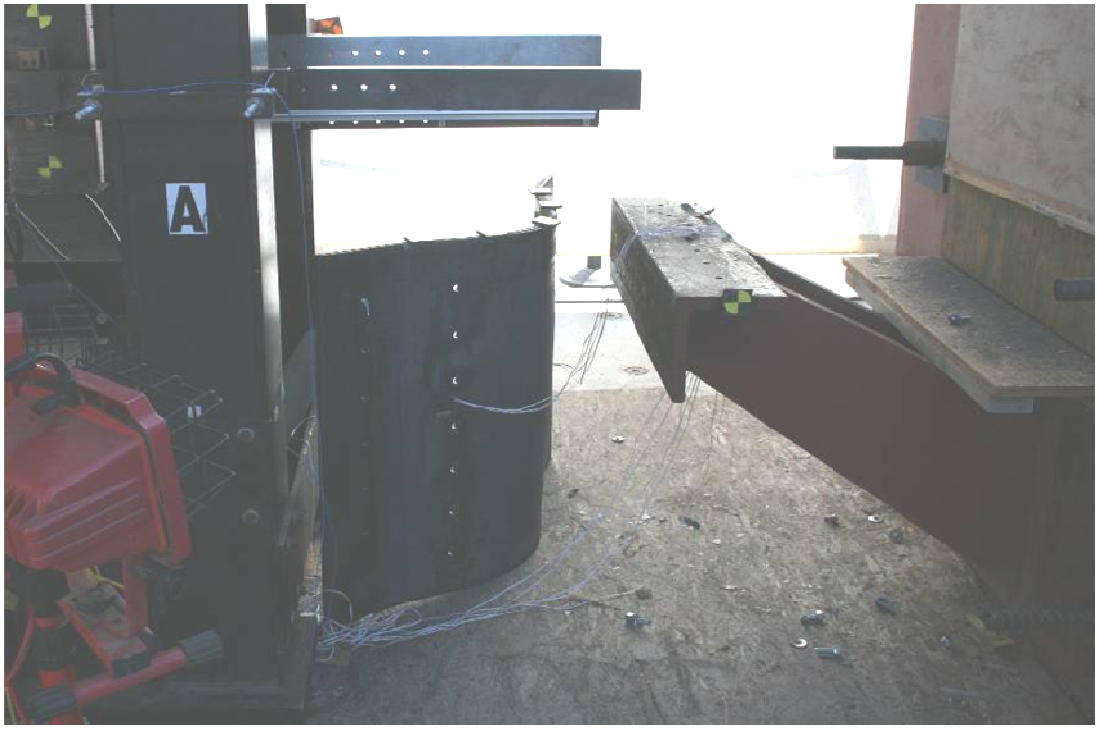

Figure E.337: Steel plate post test for Test 30

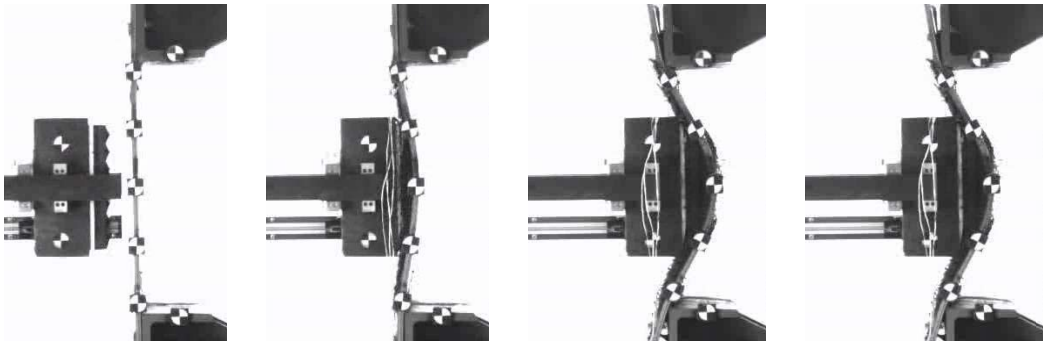

Figure E.338: Progression of damage for Test 30 from Camera 1

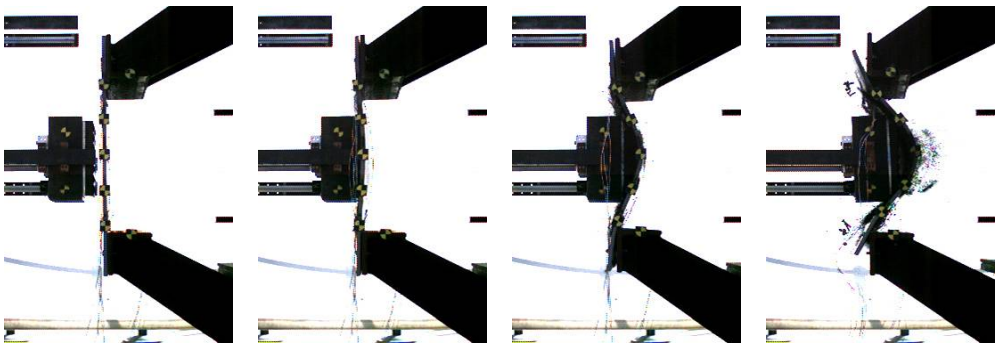

Figure E.339: Progression of damage for Test 29 from Camera 2

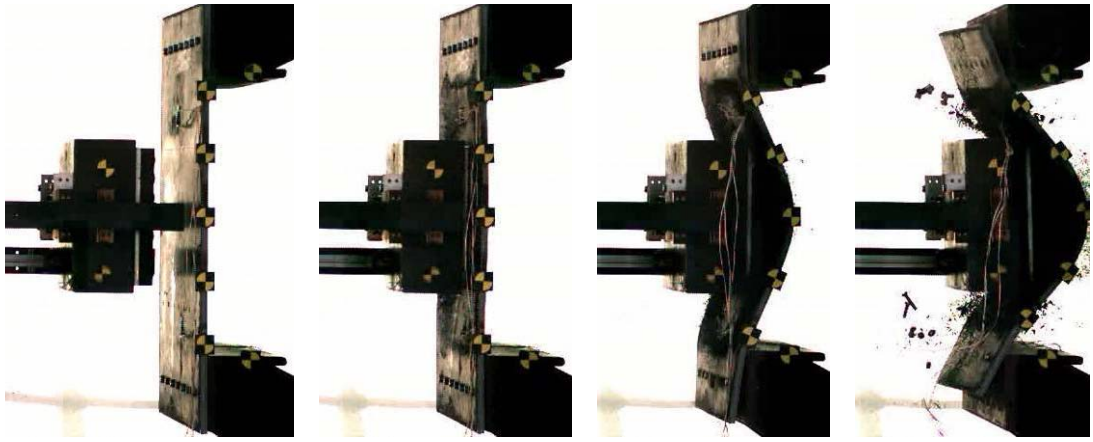

Figure E.340: Progression of damage for Test 30 from Camera 3

E.31 STEEL TOWER SINGLE PLATE: TEST 31 (SP31)

E.31.1 INTRODUCTION

The thirty-first test of the Steel Tower Single Plate test series was performed on February 21st, 2007. The test specimen was a 7/8" thick steel plate labeled SP31. The Impacting Mass 1 was attached to the BG with a specimen target velocity of 91.86 ft/sec (28 m/sec). Figure E.341 shows the steel plate prior to impact.

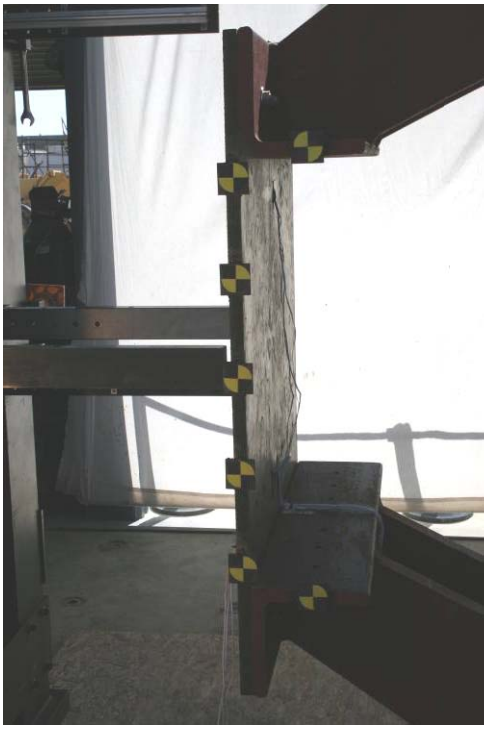

Figure E.341: 7/8" thick steel plate pre test for Test 31

E.31.2 INSTRUMENTATION

E.31.2.1 PHANTOM CAMERAS

The first camera recorded in black and white at a rate of 10,000 frames per second at a resolution of 512x384. This camera was used in order to determine the maximum velocity of the impacting mass and the movement in the plate including the maximum displacement. The second camera recorded in color at a rate of 5,000 frames per second at a resolution of 512x384. This camera recorded the overall behavior of the test specimen. It was not used to gather any specific data. The third camera recorded in color at a rate of 8,000 frames per second at a resolution of 480x480. This camera captured the failure of the bolts. A picture from each of the camera locations are shown in Figure E.342.

E.31.2.2 TARGET LOCATIONS

Five targets were welded onto the side of the steel plate as shown in Figure E.341. They were spaced at the intervals shown in Figure E.343. That figure also shows the location

of the targets for the impacting mass. An additional two targets were placed on the angle at the top and the bottom end conditions. The distance between these two points is 74.93 cm (29 ½")

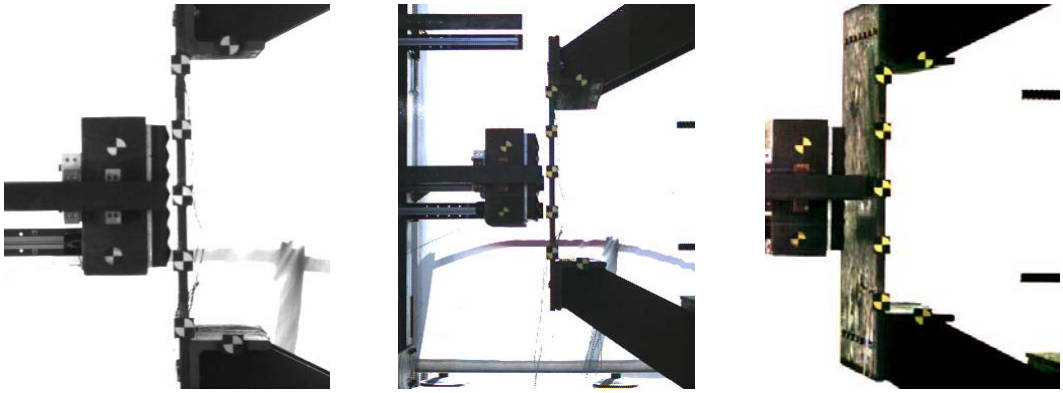

Figure E.342: Phantom Cameras for Test 31

a) Camera One b) Camera Two c) Camera Three

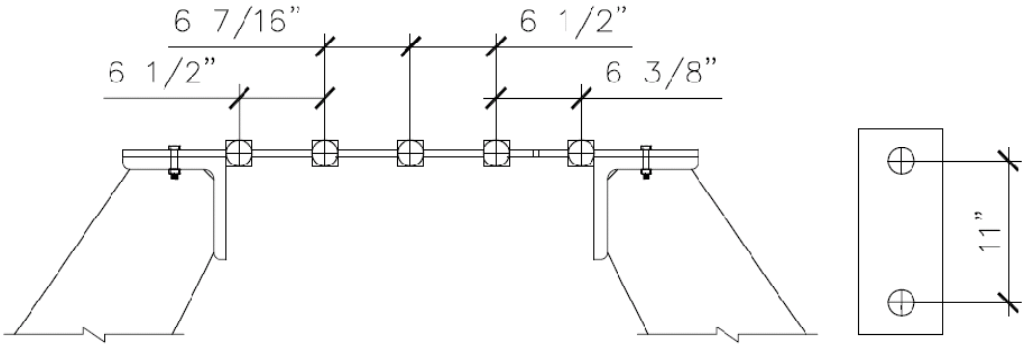

Figure E.343: Target layout on plate and impacting mass for Test 31

E.31.2.3 ACCELERATIONS

For this test one accelerometer was used. This accelerometer was placed 6" south of the centroid of the impacting mass as shown in Figure E.344. The pipe is to protect the accelerometer during the test. The data from this gage was then filtered as shown in Figure E.345.

This test does not impart an impulsive load as would be expected from a typical blast test. Instead, this test simulates the behavior of a flyer plate moving through the structure after the initial impact at the front plate of the outer cell of the structure. Therefore we are not determining the initial impulsive load from the accelerometers on the BG.

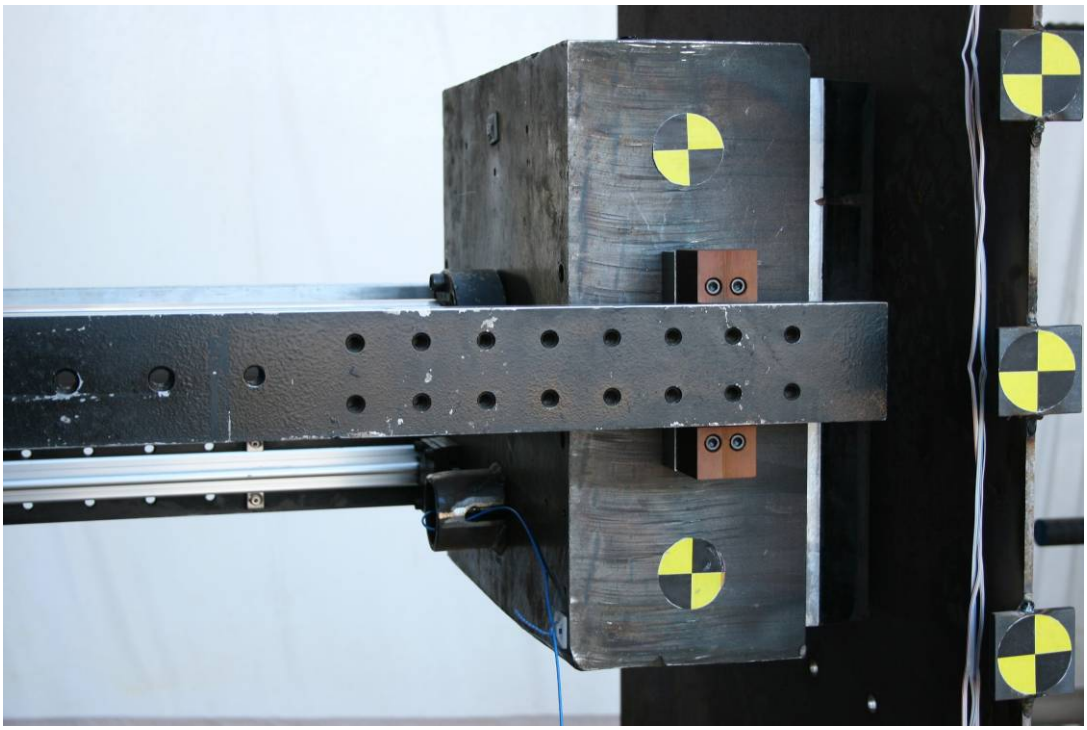

Figure E.344: Accelerometer location for Test 3

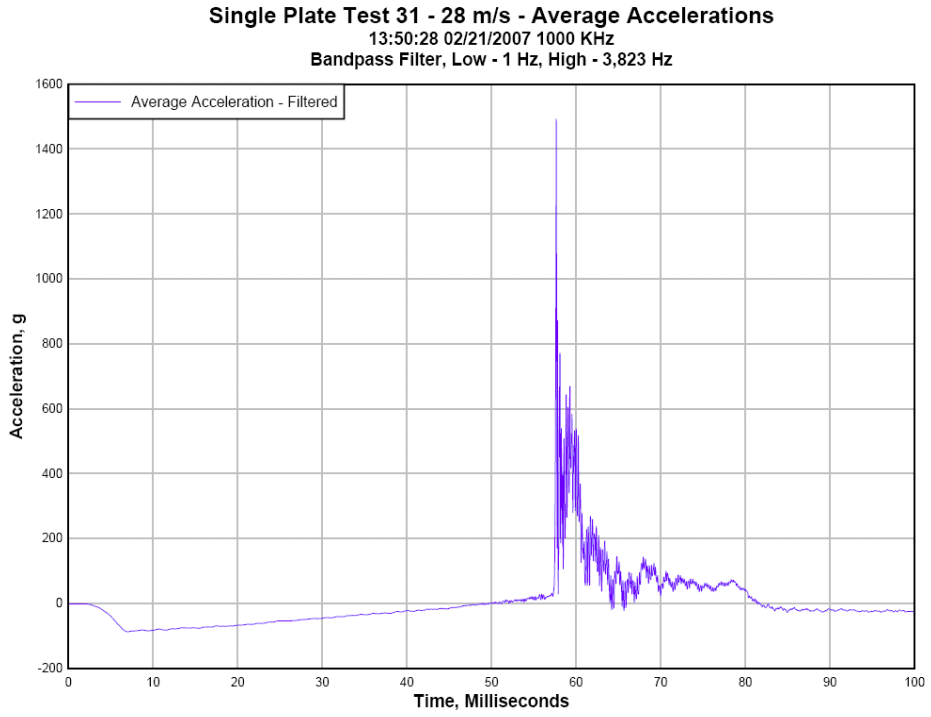

Figure E.345: Filtered accelerometer data for Test 31

E.31.2.4 STRAIN GAGE LOCATIONS

For this test there were four strain gauges labeled 19, 20, 21 and 22. The strain gauges, and their locations, are shown as a drawing in Figure E.346 and as a photo in Figure E.347 Table E.27 shows the specific information about this test, including the time and velocity at impact, if, and when, the bolts failed along with the maximum and minimum principal strain rates. There was no useable information at Gage 20 and therefore it has been discarded. The largest maximum principal strain rate for this test was 14.01 1/sec and was located at strain gage 19 while the largest minimum strain rate for this test was 8.08 1/sec located at strain gage 22. The maximum principal strains for gauges 19, 21 and 22 can be found in Figure E.348 and the minimum principal strains for the same gauges can be found in Figure E.349.

This test involved the group of test that has gauges on both sides of the plate as discussed in the report. The pure axial strains have been determined and are shown in Figure E.350 for Gauges 19 and 21. The actual bending and axial strains were also determined for these tests up until the plate yields. The graphs of the stresses for Gauges 19 and 21 can be found in Figure E.351.

Table E.27: Stain rate information for Test 31

Strain Gage Number	Actual Velocity	Initial Impact	Shear Wave at Gage	Bolts Break	Maximum Principal Strain Rate	Minimum Principal Strain Rate
19	27.49 m/s	57.40 msec	58.25 msec	61.25 msec	-14.01 1/sec	7.82 1/sec
21	27.49 m/s	57.40 msec	58.25 msec	61.25 msec	-13.42 1/sec	-7.93 1/sec
22	27.49 m/s	57.40 msec	58.25 msec	61.25 msec	-12.01 1/sec	8.08 1/sec

E.31.2.5 BOLT TYPE

A total of fourteen A307 bolts (Low Strength Bolts similar to Rivets) were used for this test. They were all tightened to a torque of 40 ft-lbs.

E.31.3 BLAST GENERATOR DATA

The initial impact of the single BG was 90.19 ft/sec (27.49 m/sec) with a goal velocity of 28 m/s. It had one accelerometer mounted to the back side of the impact plate as discussed in Section E.31.2.3. The average impact velocity for the impacting mass and the steel plate was calculated using the TEMA Track Eye tracking software.

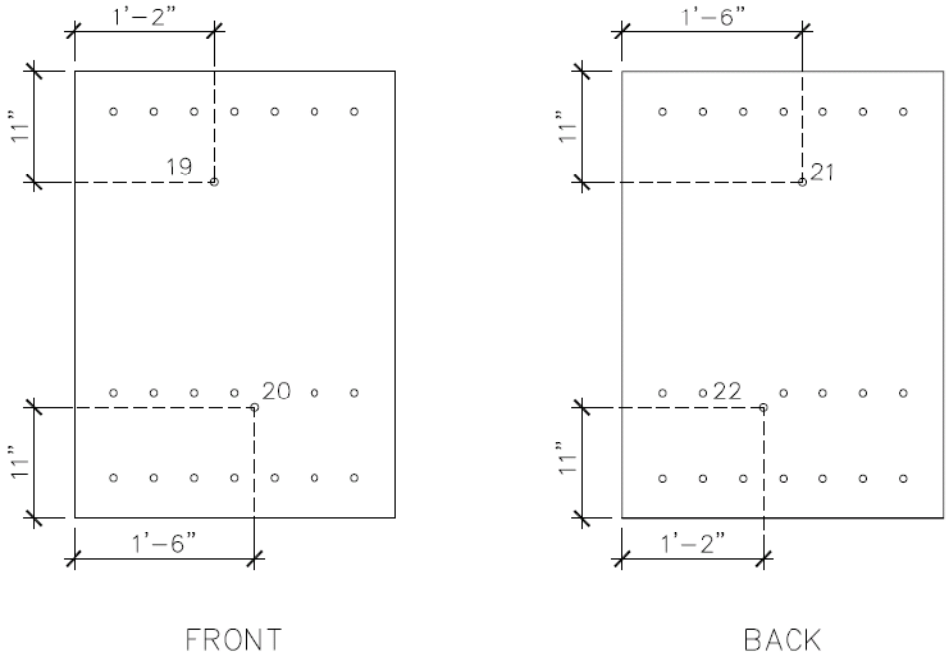

Figure E.346: Strain gage layout for Test 31 (drawing)

Figure E.347: Strain gage layout for Test 31 (pictures)

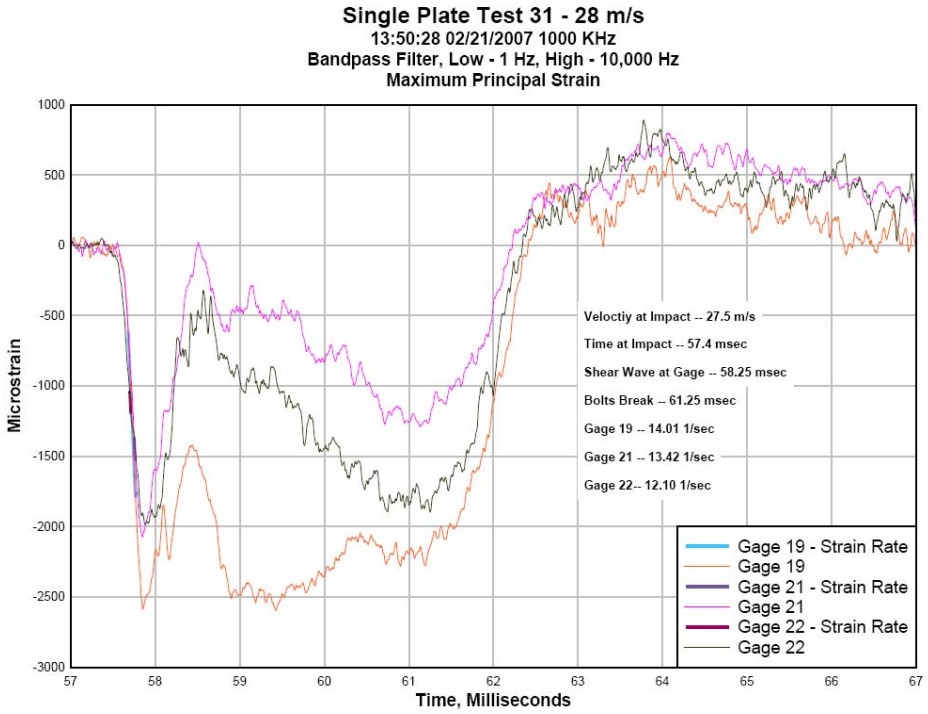

Figure E.348: Maximum principal strains and strain rates for Test 31

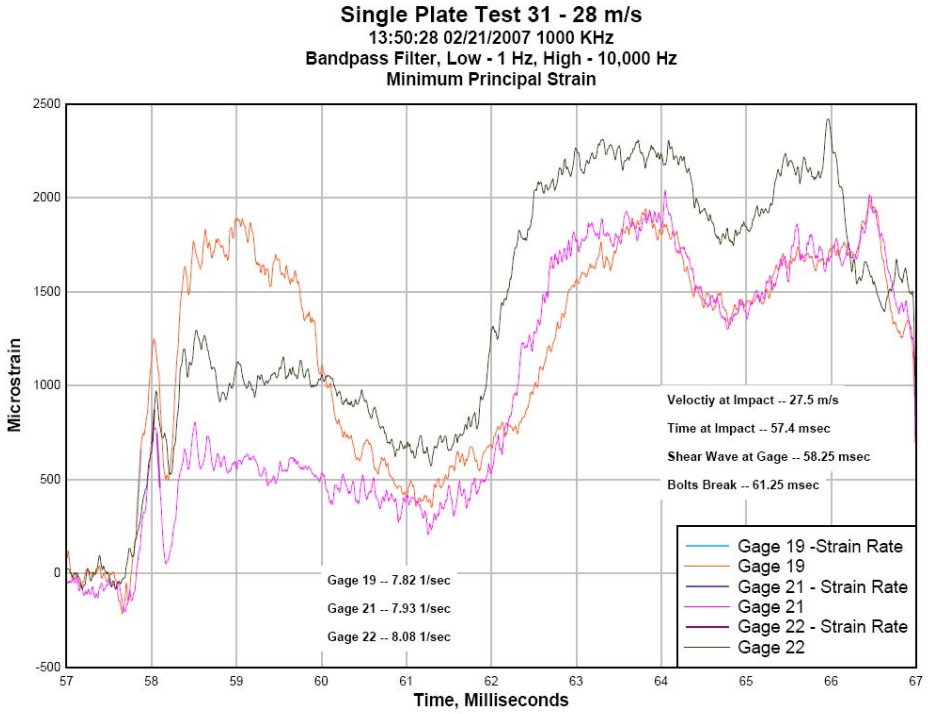

Figure E.349: Minimum principal strains and strain rates for Test 31

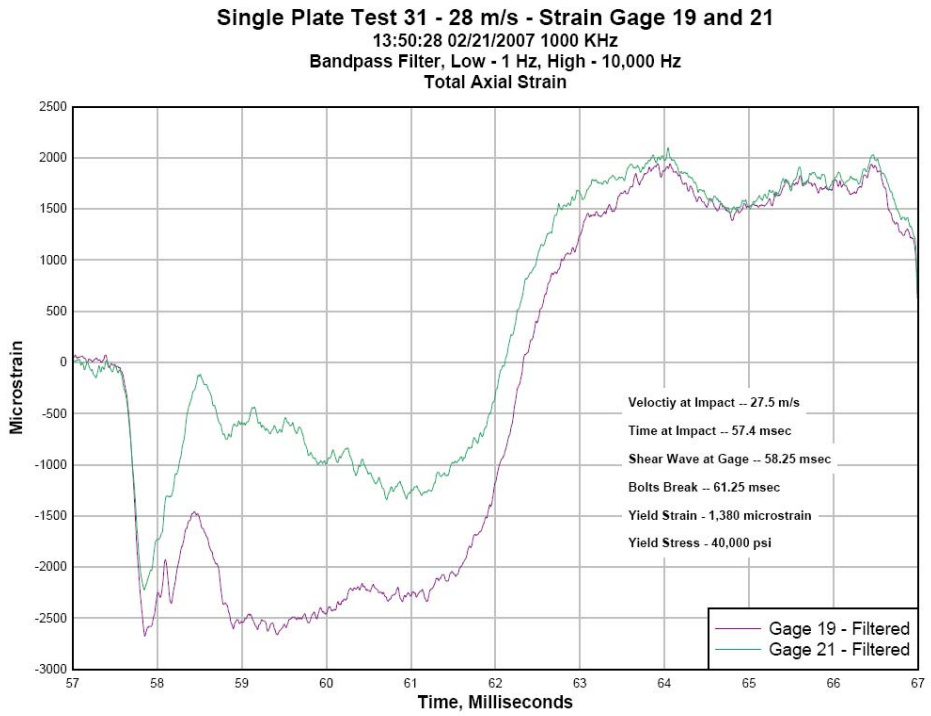

Figure E.350: Combined Axial Strain for Test 31 – Gauges 19 and 21

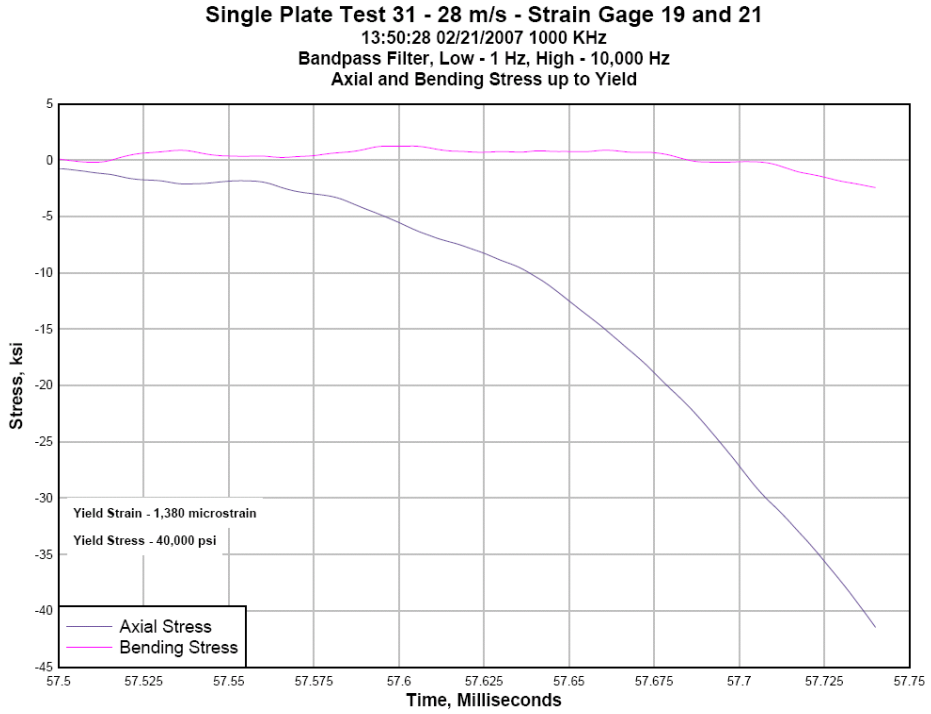

Figure E.351: Truncated Axial and Bending Stresses for Test 31 – Gauges 19 and 21

E.31.4 SPECIMEN BEHAVIOR

The loading of the BG plate imparted an initial velocity of 90.19 ft/sec (27.49 m/sec) to the specimen. This caused plate to deform in both directions. The longitudinal deflection (in the north-south direction) behaved in a typical one-way flexural shape. In order to get the velocity as high as needed the test was designed to have the impacting mass break free from the BG and launch itself into the plate. This test imparted enough energy to break all fourteen of the bolts as shown in Figure E.352. The maximum dynamic deflection during the test was approximately 3".

During the test three different phantom cameras were used to capture the failure modes from three different angles. Figure E.353 shows the progression of damage for this test from Phantom Camera One. Figure E.354 shows the progression of damage for this test from Phantom Camera Two. Figure E.355 shows the progression of damage for this test from Phantom Camera Three.

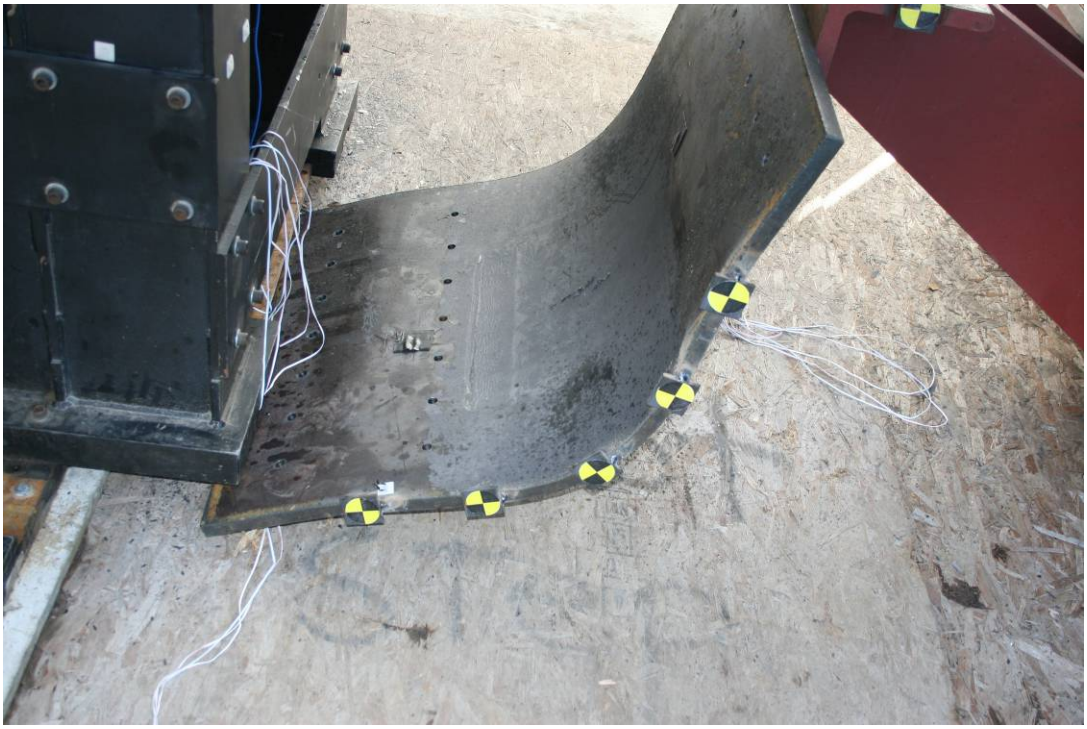

Figure E.352: Steel plate post test for Test 31

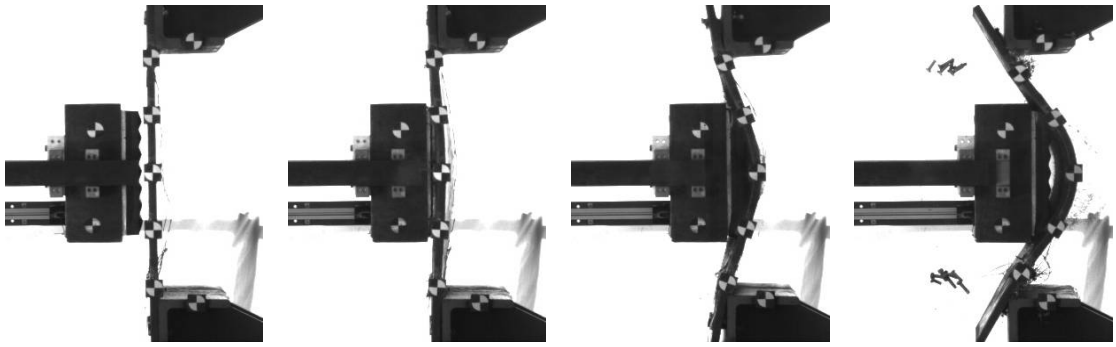

Figure E.353: Progression of damage for Test 31 from Camera 1

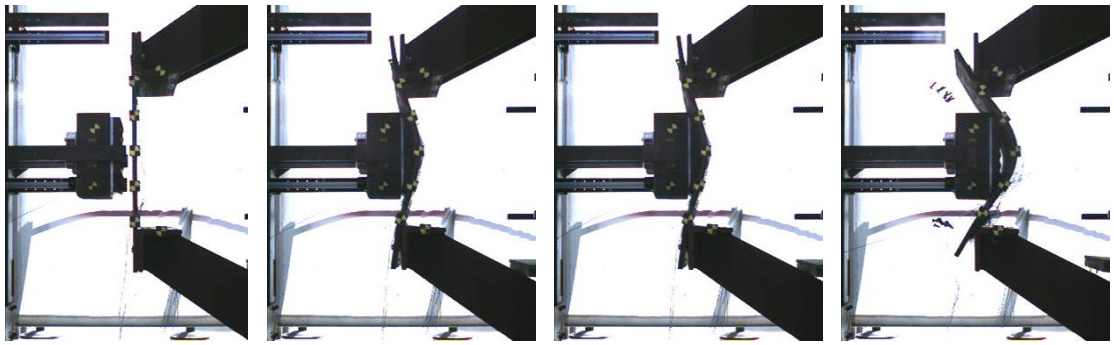

Figure E.354: Progression of damage for Test 31 from Camera 2

Figure E.355: Progression of damage for Test 31 from Camera 3

E.32 STEEL TOWER SINGLE PLATE: TEST 32 (SP32)

E.32.1 INTRODUCTION

The thirty-second test of the Steel Tower Single Plate test series was performed on February 22nd, 2007. The test specimen was a 7/8" thick steel plate labeled SP32. The Impacting Mass 1 was attached to the BG with a specimen target velocity of 91.86 ft/sec (28 m/sec). Figure E.356 shows the steel plate prior to impact.

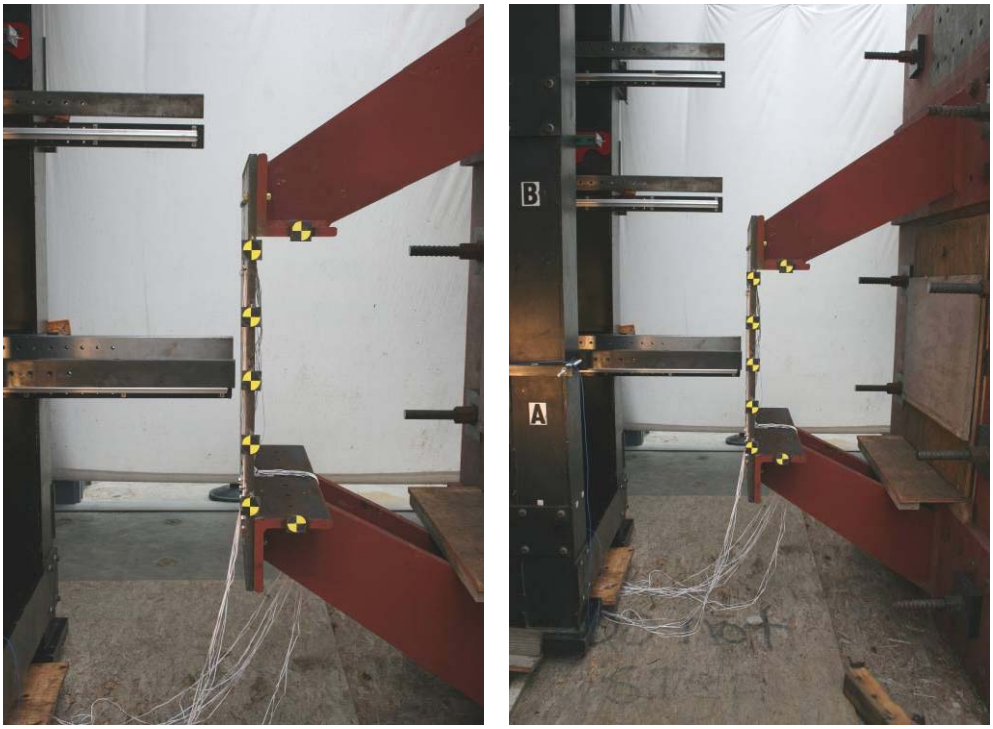

Figure E.356: 7/8" thick steel plate pre test for Test 32

E.32.2 INSTRUMENTATION

E.32.2.1 PHANTOM CAMERAS

The first camera recorded in black and white at a rate of 10,000 frames per second at a resolution of 512x384. This camera was used in order to determine the maximum velocity of the impacting mass and the movement in the plate including the maximum displacement. The second camera recorded in color at a rate of 5,000 frames per second at a resolution of 512x384. This camera recorded the overall behavior of the test specimen. It was not used to gather any specific data. The third camera recorded in color at a rate of 8,000 frames per second at a resolution of 480x480. This camera captured the failure of the bolts. A picture from each of the camera locations are shown in Figure E.357.

E.32.2.2 TARGET LOCATIONS

Five targets were welded onto the side of the steel plate as shown in Figure E.356. They were spaced at the intervals shown in Figure E.358. That figure also shows the location

of the targets for the impacting mass. An additional two targets were placed on the angle at the top and the bottom end conditions. The distance between these two points is 74.93 cm (29 ½")

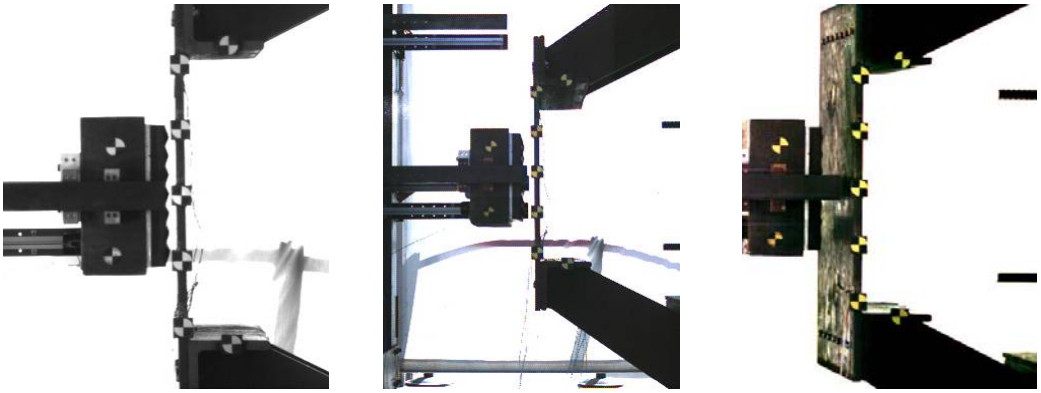

Figure E.357: Phantom Cameras for Test 32

a) Camera One b) Camera Two c) Camera Three

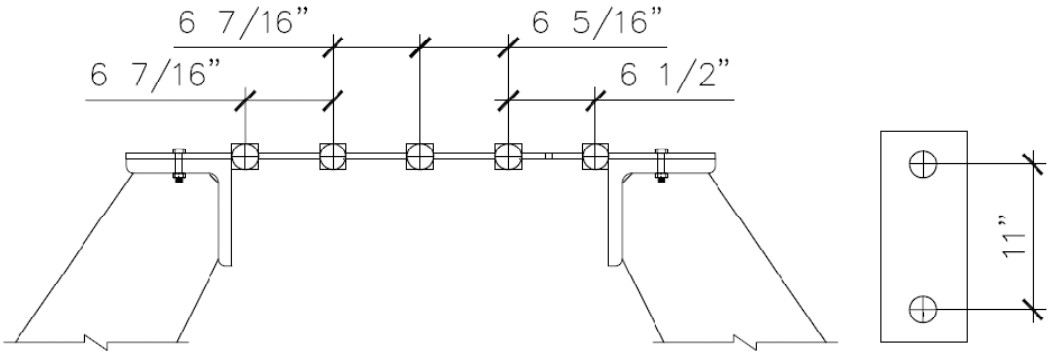

Figure E.358: Target layout on plate and impacting mass for Test 32

E.32.2.3 ACCELERATIONS

For this test one accelerometer was used. This accelerometer was placed 6" south of the centroid of the impacting mass as shown in Figure E.359. The pipe is to protect the accelerometer during the test. The data from this gage was then filtered as shown in Figure E.360.

This test does not impart an impulsive load as would be expected from a typical blast test. Instead, this test simulates the behavior of a flyer plate moving through the structure after the initial impact at the front plate of the outer cell of the structure. Therefore we are not determining the initial impulsive load from the accelerometers on the BG.

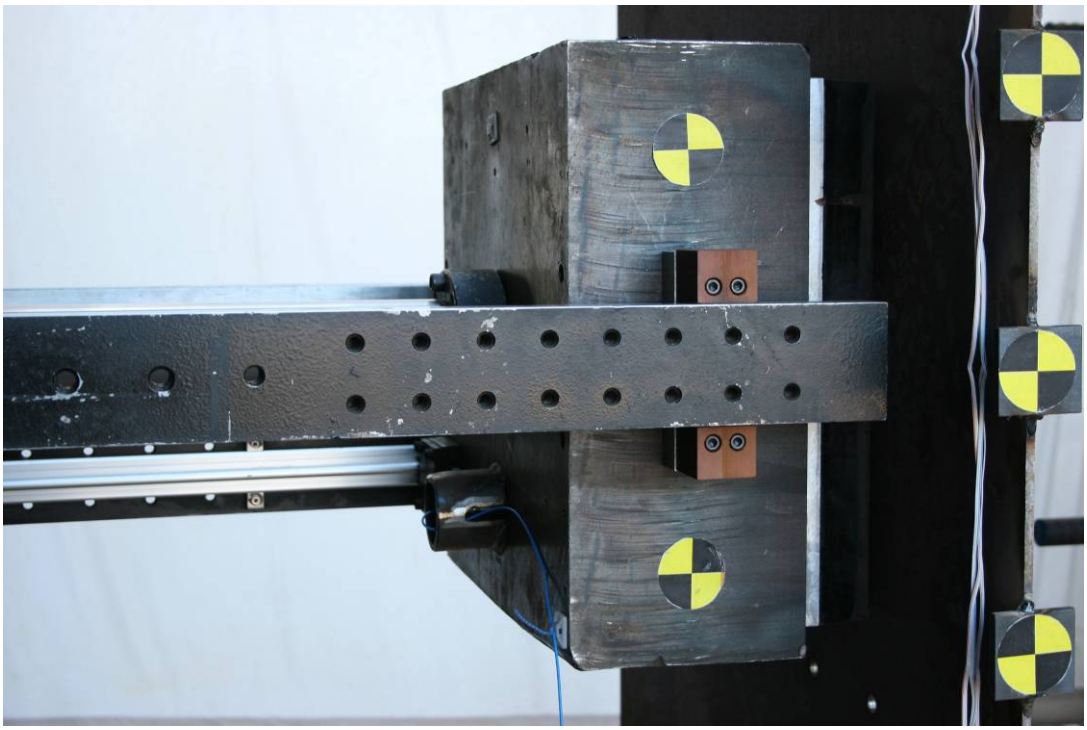

Figure E.359: Accelerometer location for Test 32

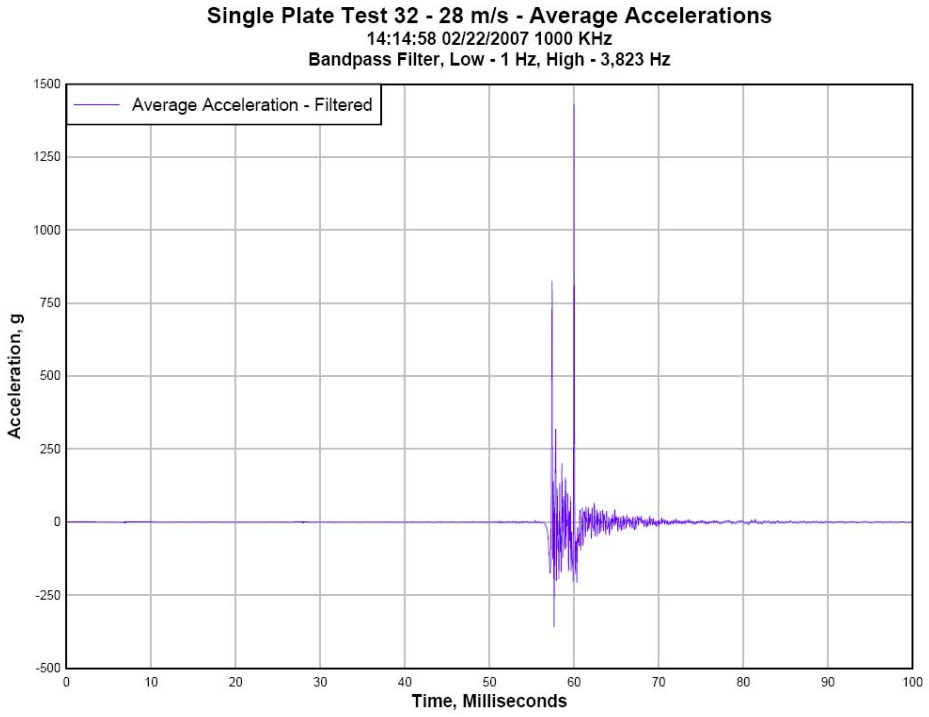

Figure E.360: Filtered accelerometer data for Test 32

E.32.2.4 STRAIN GAGE LOCATIONS

For this test there were four strain gauges labeled 19, 20, 21 and 22. The strain gauges, and their locations, are shown as a drawing in Figure E.361and as a photo in Figure E.362 Table E.28 shows the specific information about this test, including the time and velocity at impact, if, and when, the bolts failed along with the maximum and minimum principal strain rates. The largest maximum principal strain rate for this test was 18.53 1/sec and was located at strain gage 20 while the largest minimum strain rate for this test was 10.59 1/sec located at strain gage 20. The maximum principal strains for gauges 19, 20, 21 and 22 can be found in Figure E.363 and the minimum principal strains for the same gauges can be found in Figure E.364.

This test involved the group of test that has gauges on both sides of the plate as discussed in the report. The pure axial strains have been determined and are shown in Figure E.365 for Gauges 19 and 21; and Figure E.366 for Gauges 20 and 22. The actual bending and axial strains were also determined for these tests up until the plate yields. The graphs of the stresses for Gauges 19 and 21 and Gauges 20 and 22 can be found in Figure E.367 and Figure E.368, respectively.

Table E.28: Stain rate information for Test 32

Strain Gage Number	Actual Velocity	Initial Impact	Shear Wave at Gage	Bolts Break	Maximum Principal Strain Rate	Minimum Principal Strain Rate
19	27.46 m/s	57.30 msec	58.38 msec	61.20 msec	-14.94 1/sec	6.97 1/sec
20	27.46 m/s	57.30 msec	58.38 msec	61.20 msec	-18.53 1/sec	10.59 1/sec
21	27.46 m/s	57.30 msec	58.38 msec	61.20 msec	-13.94 1/sec	-7.34 1/sec
22	27.46 m/s	57.30 msec	58.38 msec	61.20 msec	-15.07 1/sec	6.08 1/sec

E.32.2.5 BOLT TYPE

A total of fourteen A307 bolts (Low Strength Bolts similar to Rivets) were used for this test. They were all tightened to a torque of 40 ft-lbs.

E.32.3 BLAST GENERATOR DATA

The initial impact of the single BG was 90.09 ft/sec (27.46 m/sec) with a goal velocity of 28 m/s. It had one accelerometer mounted to the back side of the impact plate as discussed in Section E.32.2.3. The average impact velocity for the impacting mass and the steel plate was calculated using the TEMA Track Eye tracking software.

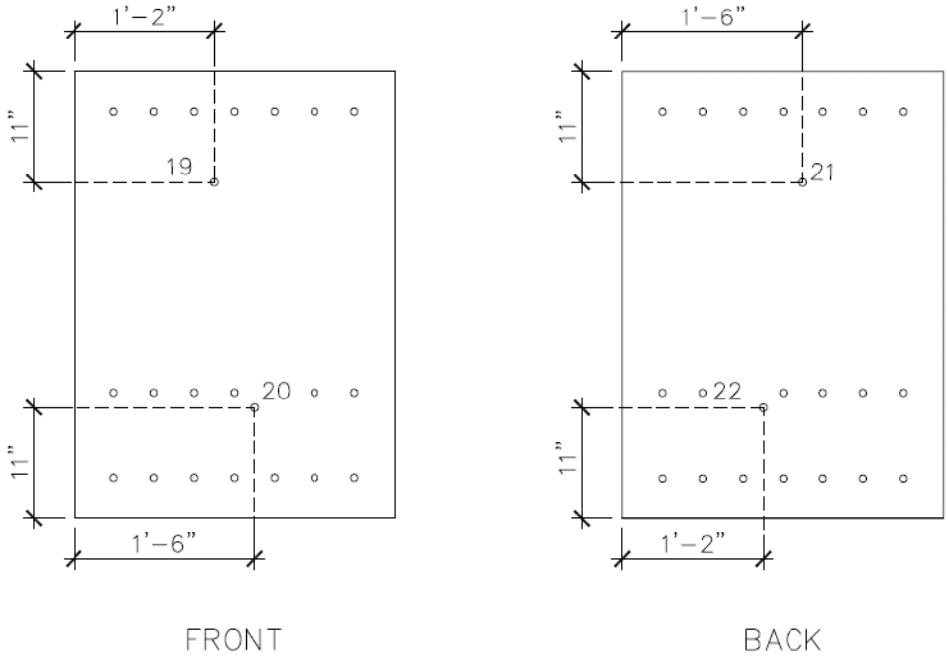

Figure E.361: Strain gage layout for Test 32 (drawing)

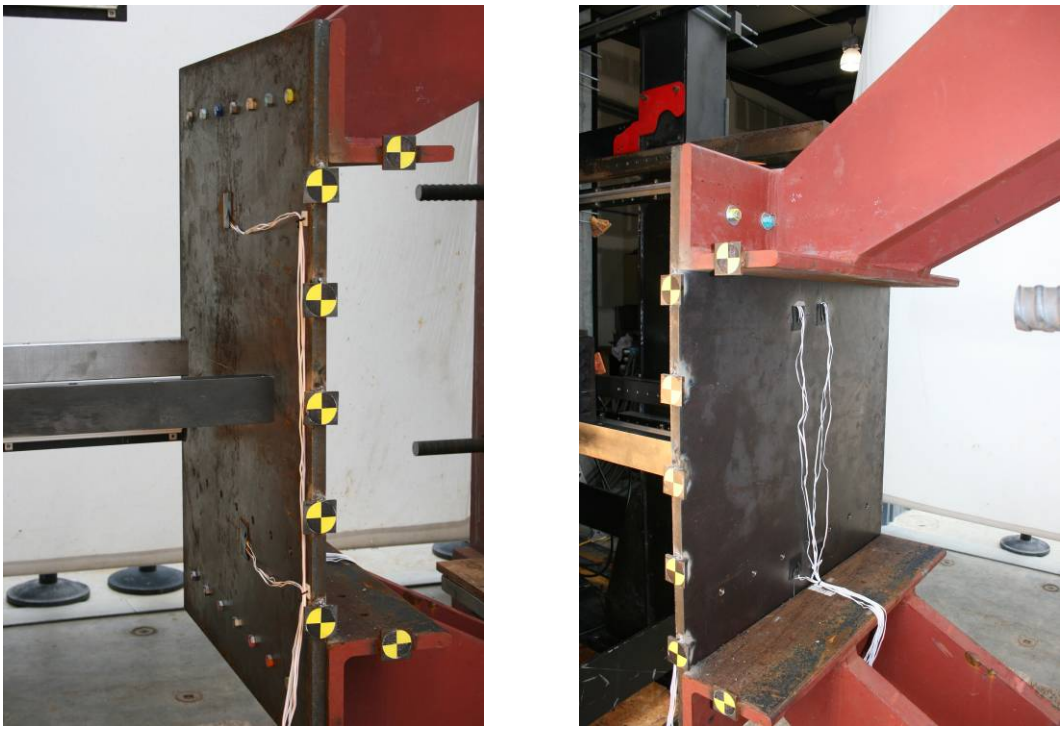

Figure E.362: Strain gage layout for Test 32 (pictures)

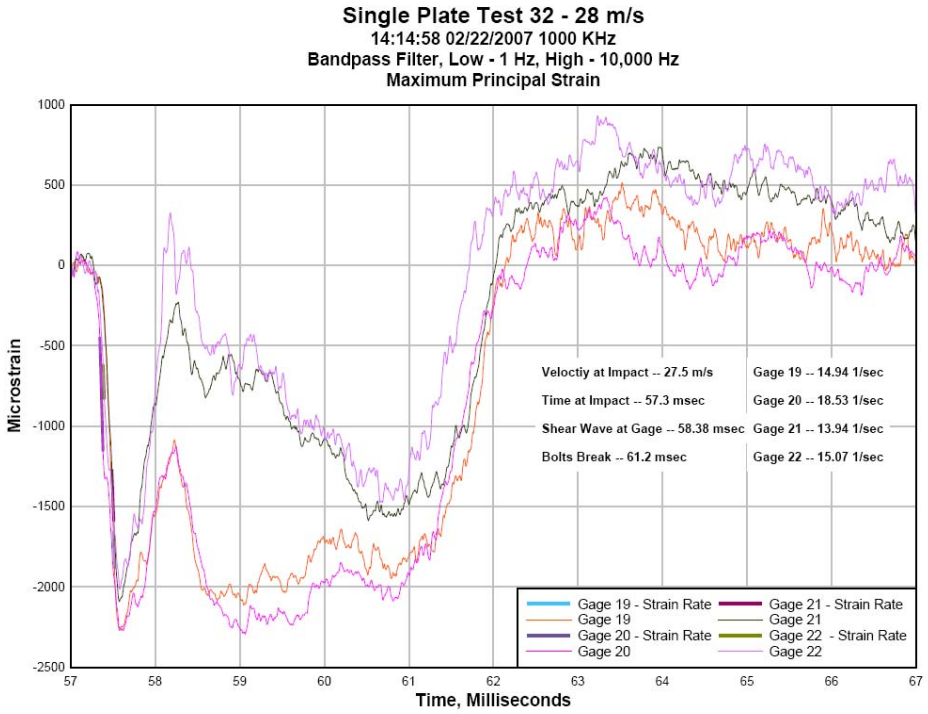

Figure E.363: Maximum principal strains and strain rates for Test 32

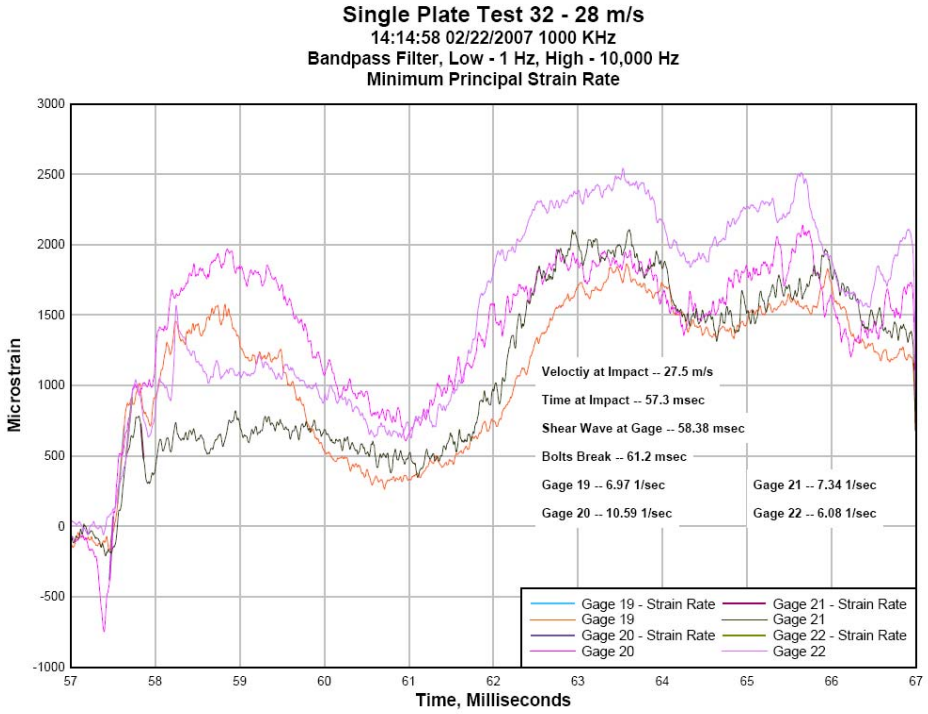

Figure E.364: Minimum principal strains and strain rates for Test 32

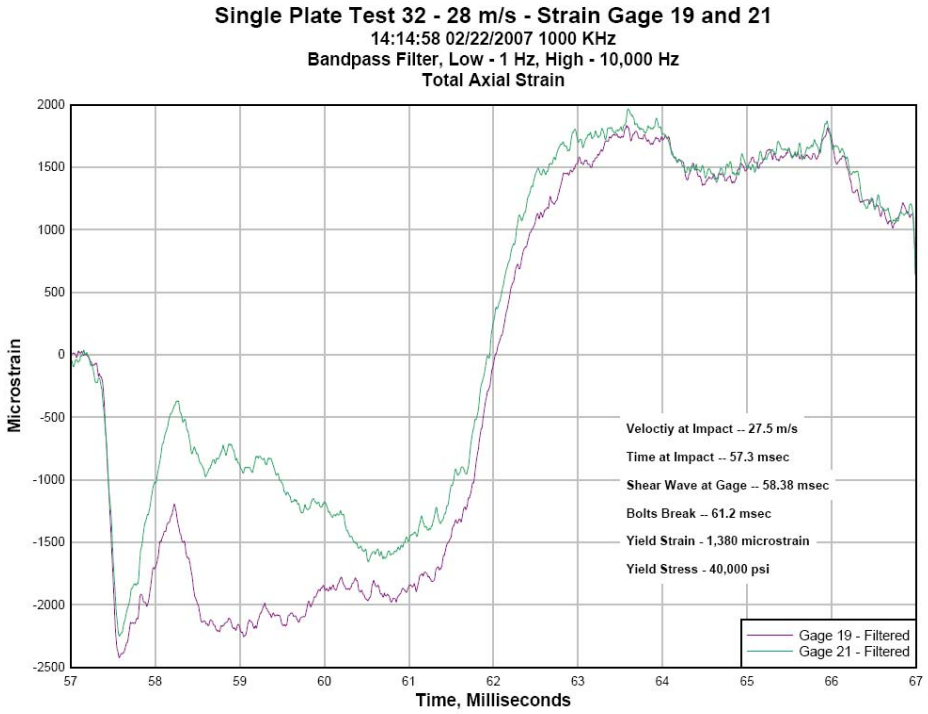

Figure E.365: Combined Axial Strain for Test 32 – Gauges 19 and 21

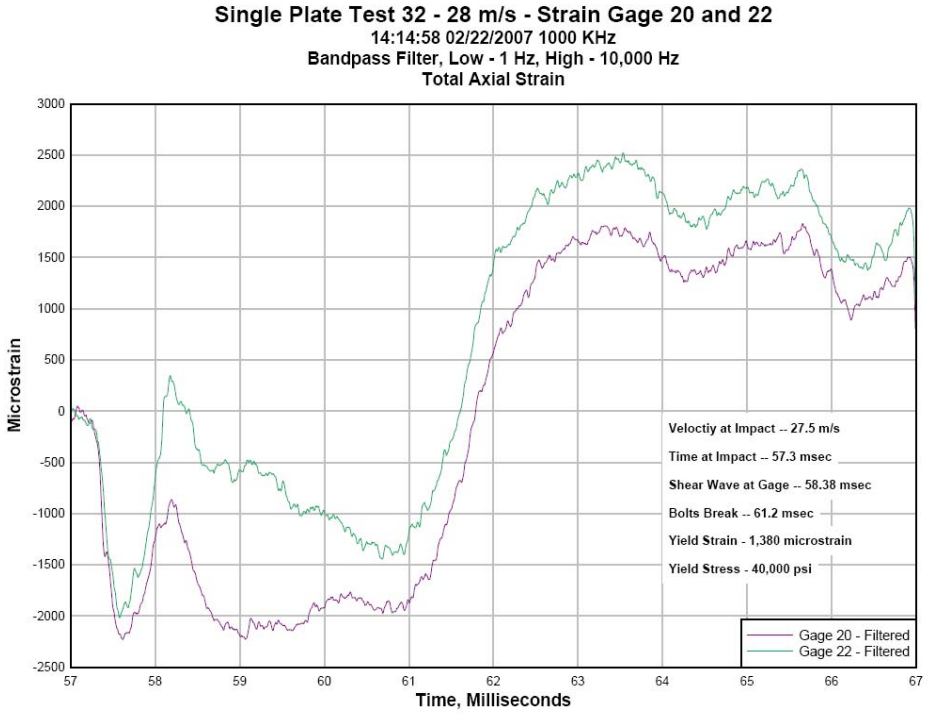

Figure E.366: Combined Axial Strain for Test 32 – Gauges 20 and 22

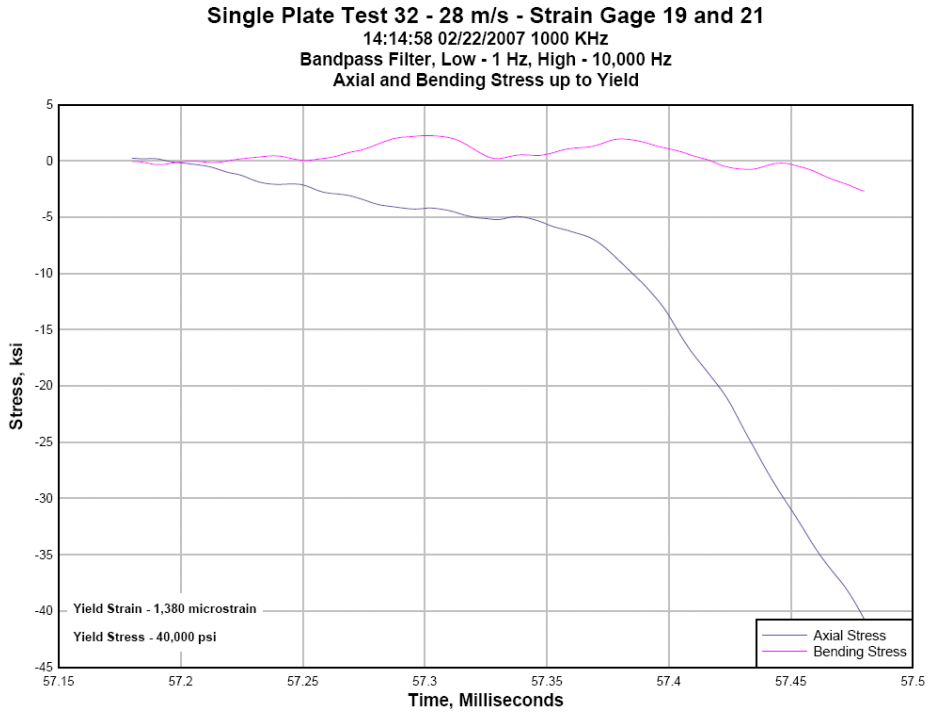

Figure E.367: Truncated Axial and Bending Stresses for Test 32 – Gauges 19 and 21

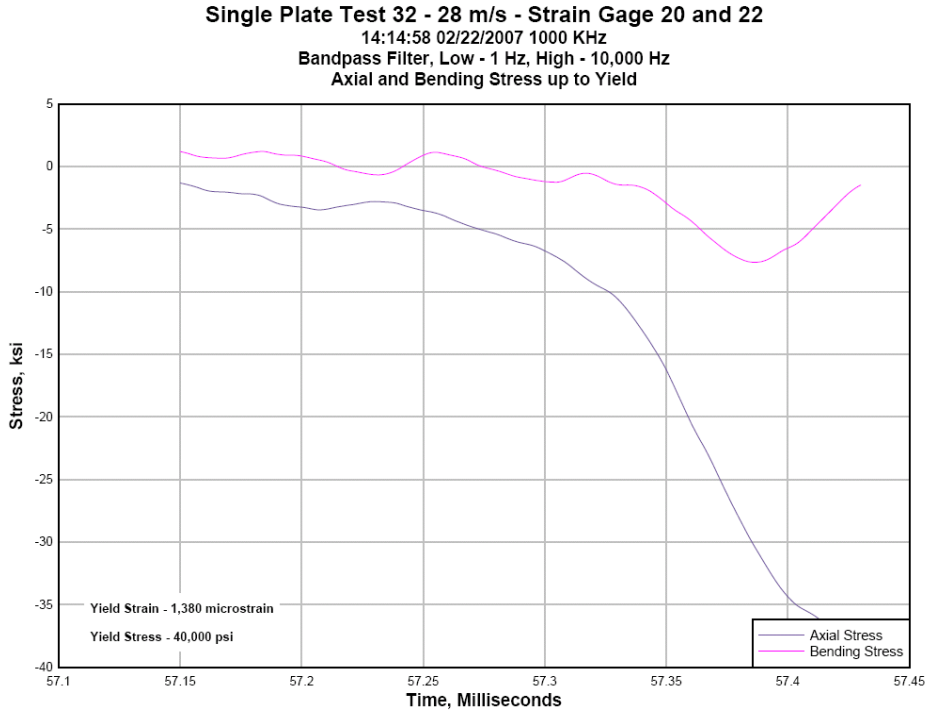

Figure E.368: Truncated Axial and Bending Stresses for Test 32 – Gauges 20 and 22

E.32.4 SPECIMEN BEHAVIOR

The loading of the BG plate imparted an initial velocity of 90.09 ft/sec (27.46 m/sec) to the specimen. This caused plate to deform in both directions. The longitudinal deflection (in the north-south direction) behaved in a typical one-way flexural shape. In order to get the velocity as high as needed the test was designed to have the impacting mass break free from the BG and launch itself into the plate. This test imparted enough energy to break all fourteen of the bolts as shown in Figure E.369. The maximum dynamic deflection during the test was approximately 3 1/4".

During the test three different phantom cameras were used to capture the failure modes from three different angles. Figure E.370 shows the progression of damage for this test from Phantom Camera One. Figure E.371 shows the progression of damage for this test from Phantom Camera Two. Figure E.372 shows the progression of damage for this test from Phantom Camera Three.

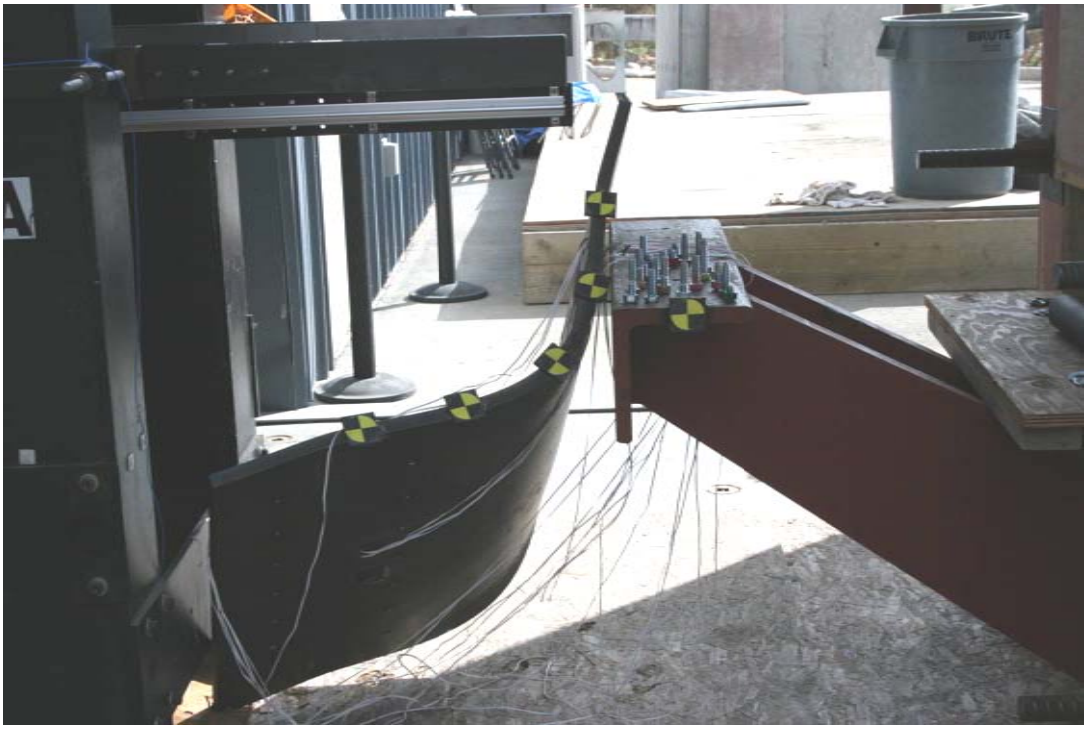

Figure E.369: Steel plate post test for Test 32

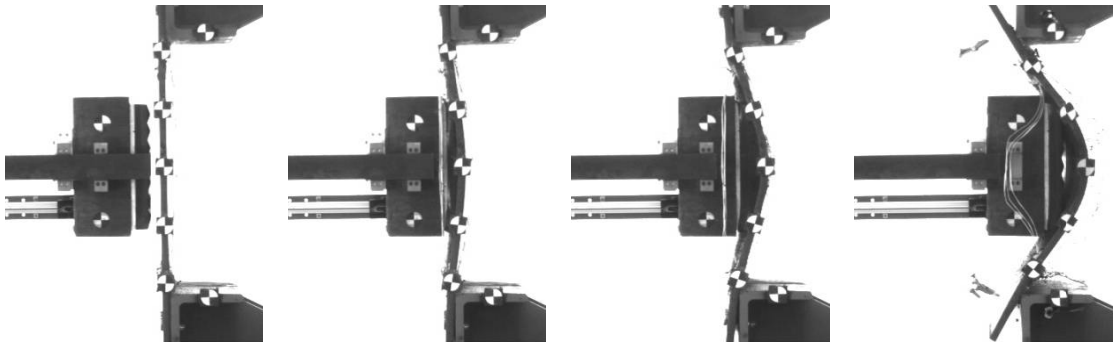

Figure E.370: Progression of damage for Test 32 from Camera 1

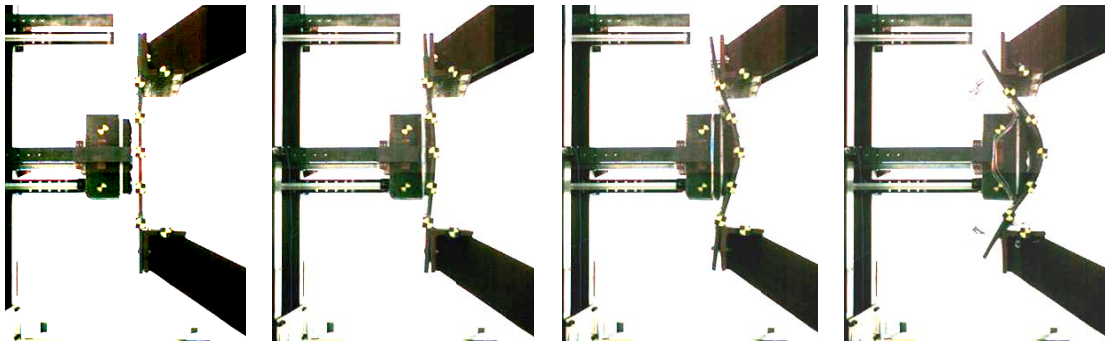

Figure E.371: Progression of damage for Test 32 from Camera 2

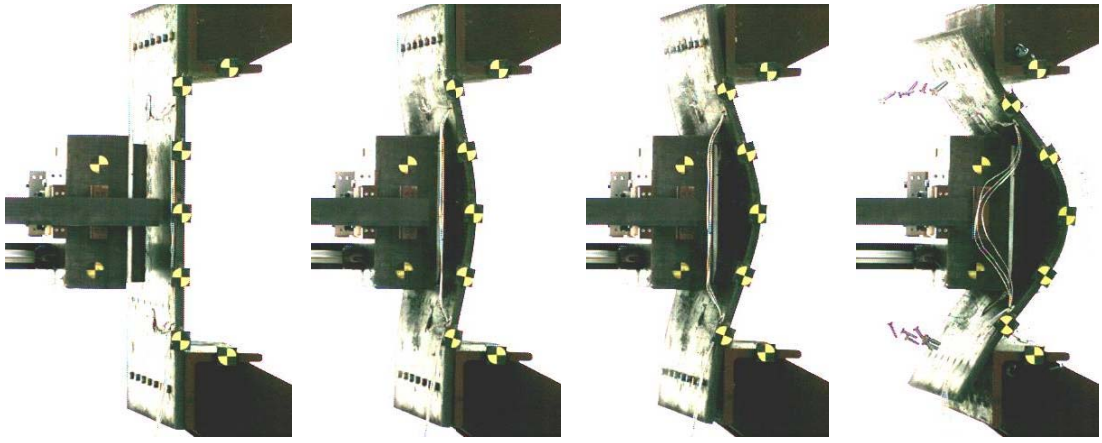

Figure E.372: Progression of damage for Test 32 from Camera 3

E.33 STEEL TOWER SINGLE PLATE: TEST 33 (SP33)

E.33.1 INTRODUCTION

The thirty-third test of the Steel Tower Single Plate test series was performed on February 23rd, 2007. The test specimen was a 7/8" thick steel plate labeled SP33. The Impacting Mass 1 was attached to the BG with a specimen target velocity of 91.86 ft/sec (28 m/sec). Figure E.373 shows the steel plate prior to impact.

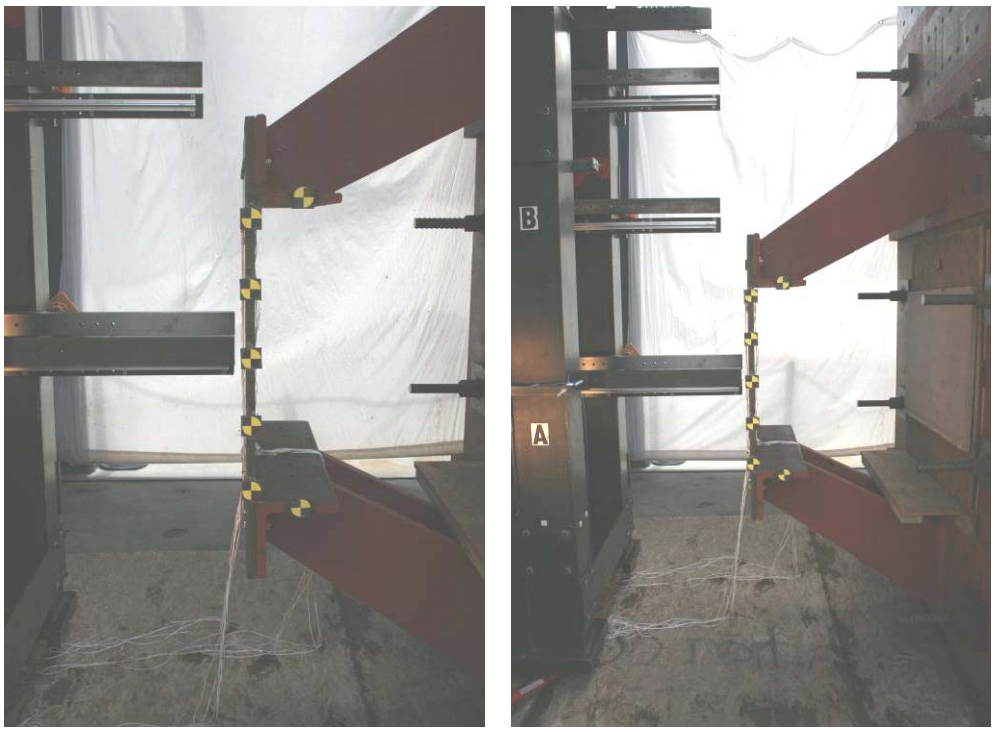

Figure E.373: 7/8" thick steel plate pre test for Test 33

E.33.2 INSTRUMENTATION

E.33.2.1 PHANTOM CAMERAS

The first camera recorded in black and white at a rate of 10,000 frames per second at a resolution of 512x384. This camera was used in order to determine the maximum velocity of the impacting mass and the movement in the plate including the maximum displacement. The second camera recorded in color at a rate of 5,000 frames per second at a resolution of 512x384. This camera recorded the overall behavior of the test specimen. It was not used to gather any specific data. The third camera recorded in color at a rate of 8,000 frames per second at a resolution of 480x480. This camera captured the failure of the bolts. A picture from each of the camera locations are shown in **Figure E**.374.

E.33.2.2 TARGET LOCATIONS

Five targets were welded onto the side of the steel plate as shown in Figure E.373. They were spaced at the intervals shown in Figure E.375. That figure also shows the location

of the targets for the impacting mass. An additional two targets were placed on the angle at the top and the bottom end conditions. The distance between these two points is 74.93 cm (29 ½")

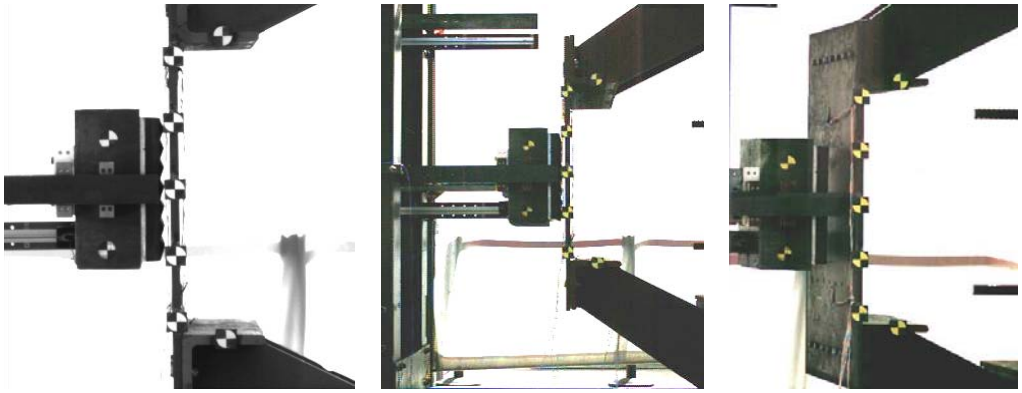

Figure E.374: Phantom Cameras for Test 33 a) Camera One b) Camera Two c) Camera Three

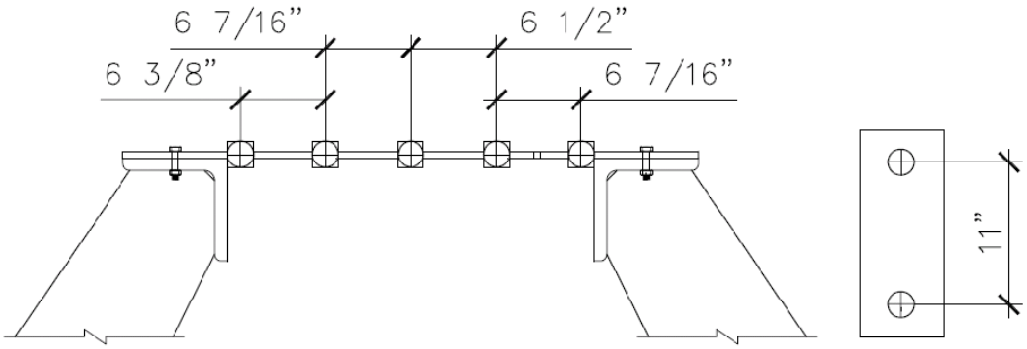

Figure E.375: Target layout on plate and impacting mass for Test 33

E.33.2.3 ACCELERATIONS

For this test one accelerometer was used. This accelerometer was placed 6" south of the centroid of the impacting mass as shown in Figure E.376. The pipe is to protect the accelerometer during the test. The data from this gage was then filtered as shown in Figure E.377.

This test does not impart an impulsive load as would be expected from a typical blast test. Instead, this test simulates the behavior of a flyer plate moving through the structure after the initial impact at the front plate of the outer cell of the structure. Therefore we are not determining the initial impulsive load from the accelerometers on the BG.

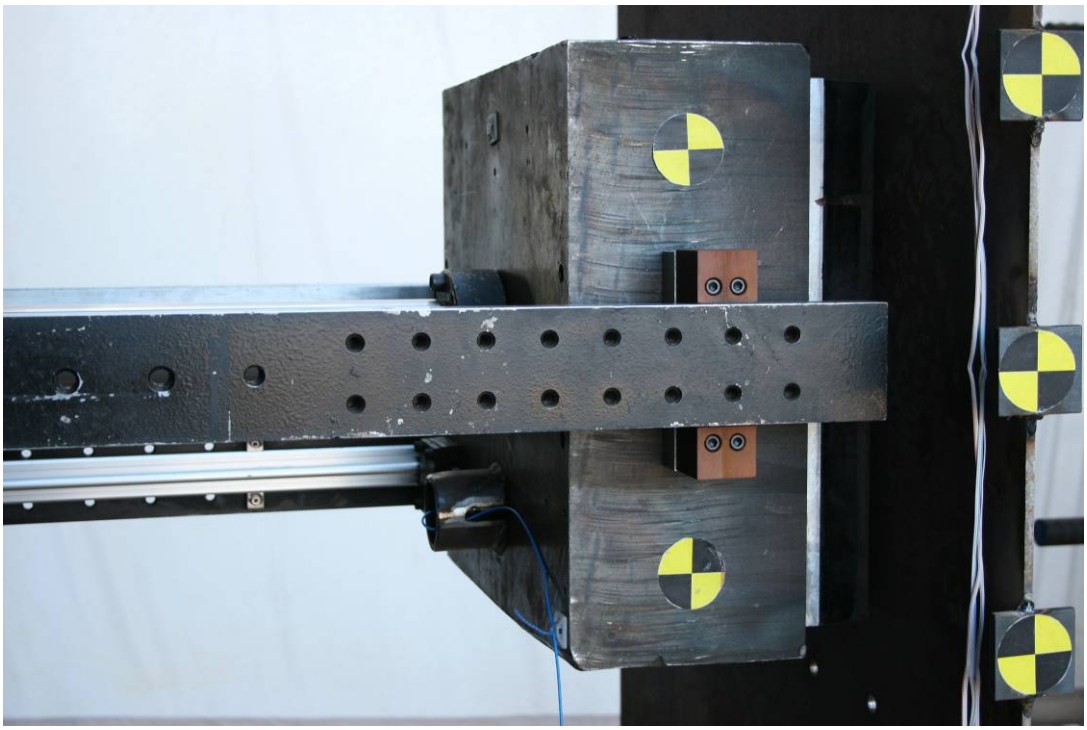

Figure E.376: Accelerometer location for Test 33

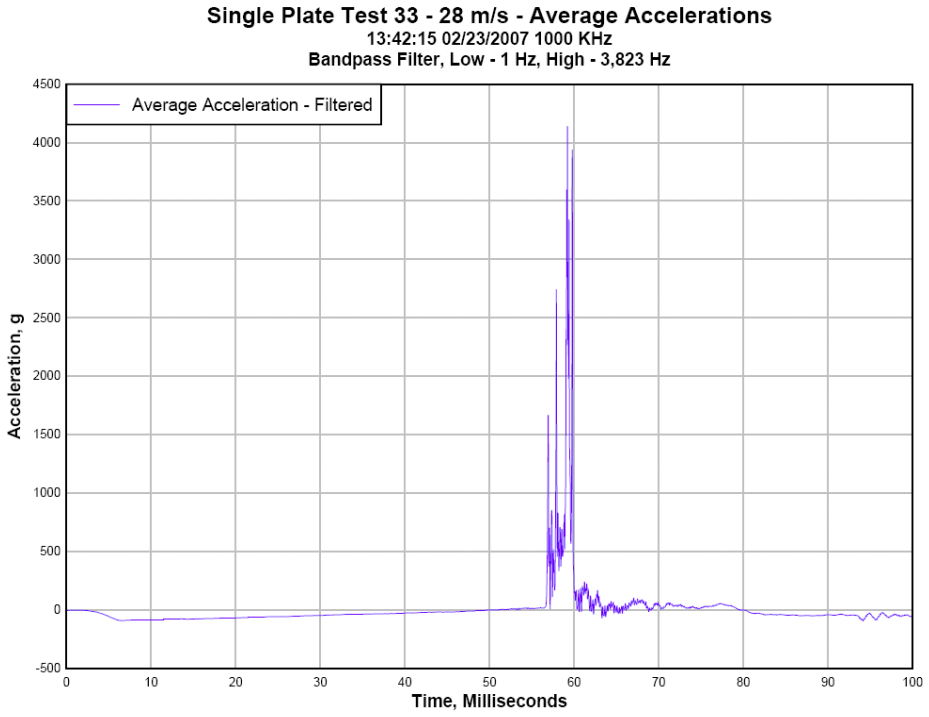

Figure E.377: Filtered accelerometer data for Test 33

E.33.2.4 STRAIN GAGE LOCATIONS

For this test there were four strain gauges labeled 19, 20, 21 and 22. The strain gauges, and their locations, are shown as a drawing in Figure E.378 and as a photo in Figure E.379 Table E.29 shows the specific information about this test, including the time and velocity at impact, if, and when, the bolts failed along with the maximum and minimum principal strain rates. The largest maximum principal strain rate for this test was 29.60 1/sec and was located at strain gage 20 while the largest minimum strain rate for this test was 23.04 1/sec located at strain gage 22. The maximum principal strains for gauges 19, 20, 21 and 22 can be found in Figure E.380 and the minimum principal strains for the same gauges can be found in Figure E.381.

This test involved the group of test that has gauges on both sides of the plate as discussed in the report. The pure axial strains have been determined and are shown in Figure E.382 for Gauges 19 and 21; and Figure E.383 for Gauges 20 and 22. The actual bending and axial strains were also determined for these tests up until the plate yields. The graphs of the stresses for Gauges 19 and 21 and Gauges 20 and 22 can be found in Figure E.384 and Figure E.385, respectively.

Table E.29: Stain rate information for Test 33

Strain Gage Number	Actual Velocity	Initial Impact	Shear Wave at Gage	Bolts Break	Maximum Principal Strain Rate	Minimum Principal Strain Rate
19	28.01 m/s	56.80 msec	57.50 msec	60.75 msec	-17.13 1/sec	6.50 1/sec
20	28.01 m/s	56.80 msec	57.50 msec	60.75 msec	-29.60 1/sec	15.19 1/sec
21	28.01 m/s	56.80 msec	57.50 msec	60.75 msec	-15.88 1/sec	3.40 1/sec
22	28.01 m/s	56.80 msec	57.50 msec	60.75 msec	-10.57 1/sec	23.04 1/sec

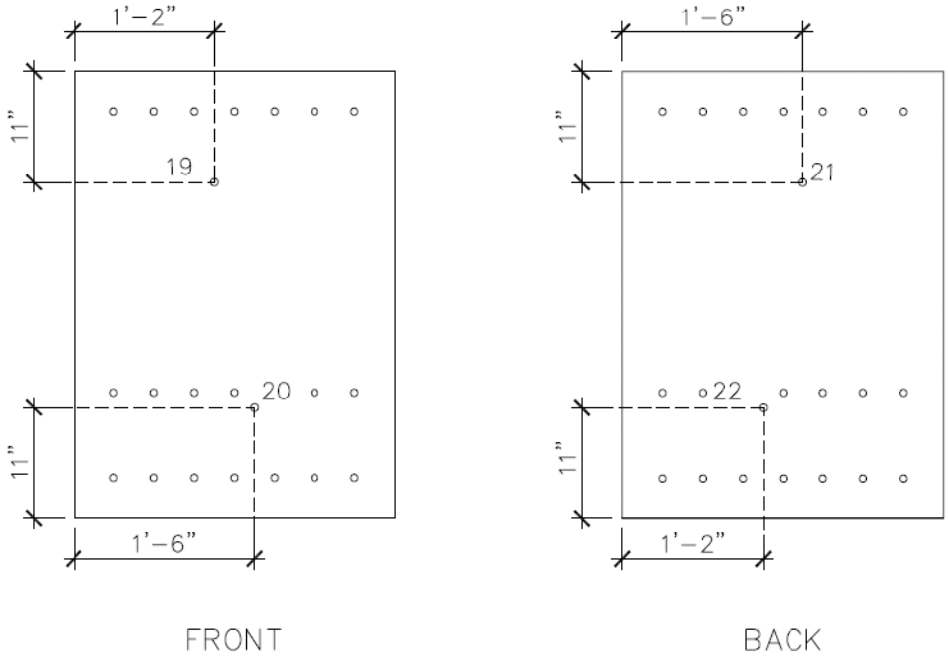

Figure E.378: Strain gage layout for Test 33 (drawing)

Figure E.379: Strain gage layout for Test 33 (pictures)

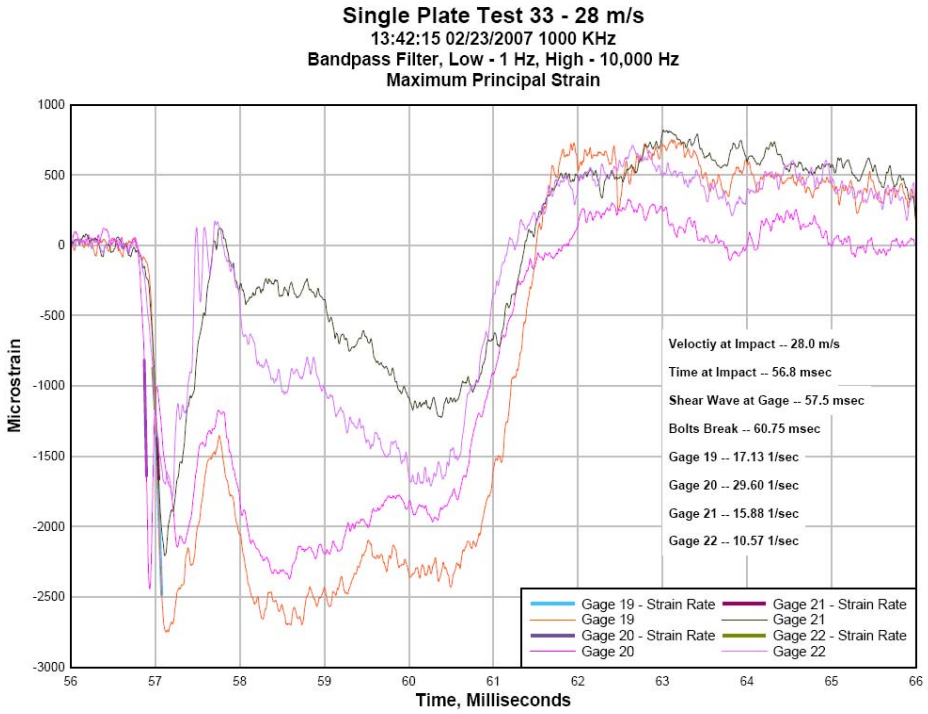

Figure E.380: Maximum principal strains and strain rates for Test 3

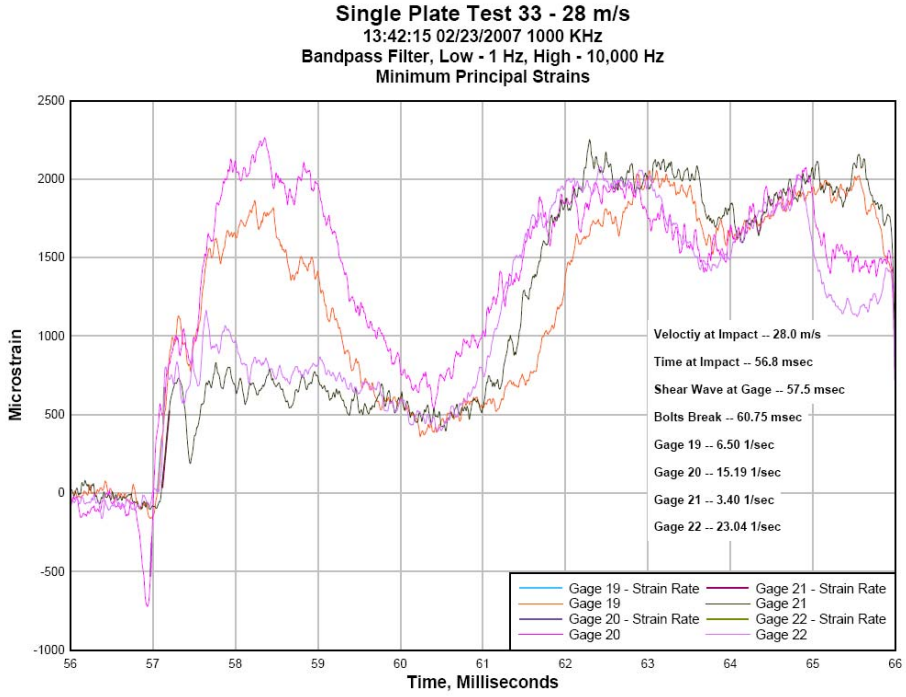

Figure E.381: Minimum principal strains and strain rates for Test 33

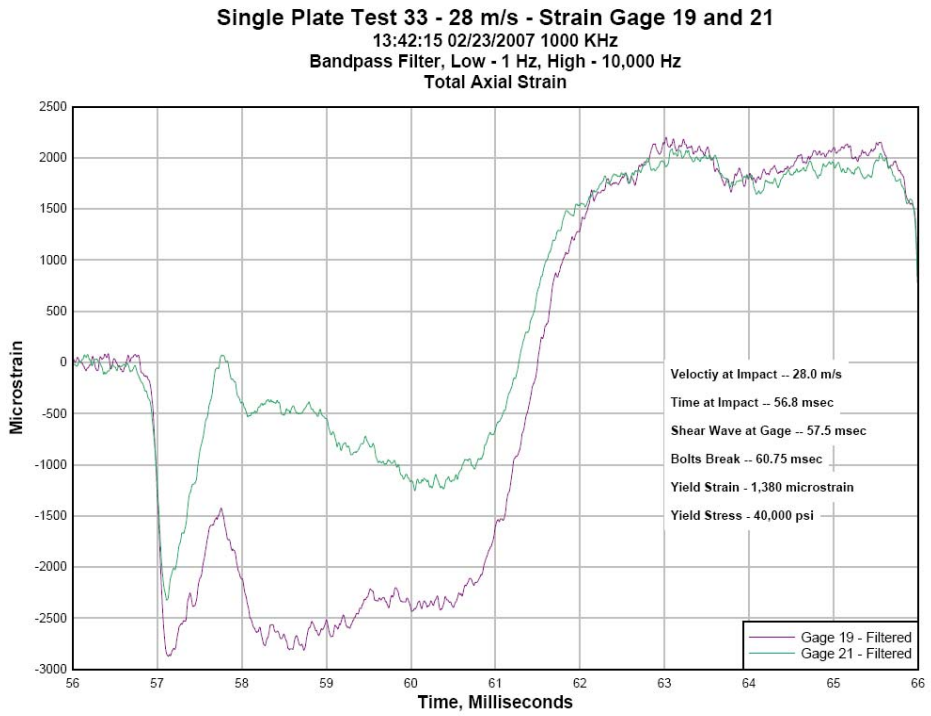

Figure E.382: Combined Axial Strain for Test 33 – Gauges 19 and 21

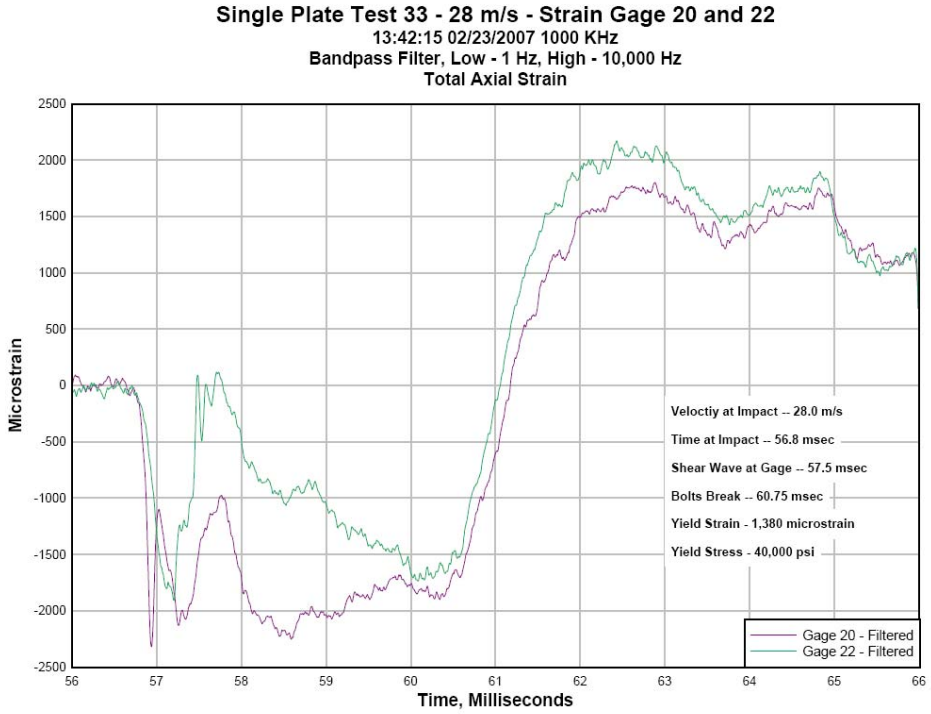

Figure E.383: Combined Axial Strain for Test 33 – Gauges 20 and 22

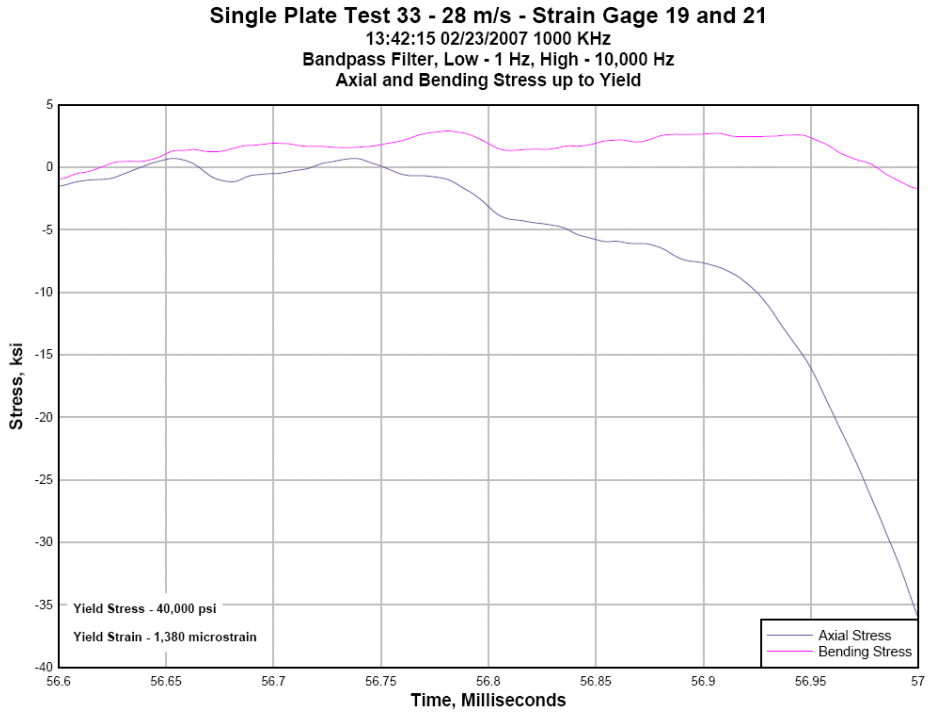

Figure E.384: Truncated Axial and Bending Stresses for Test 33 – Gauges 19 and 21

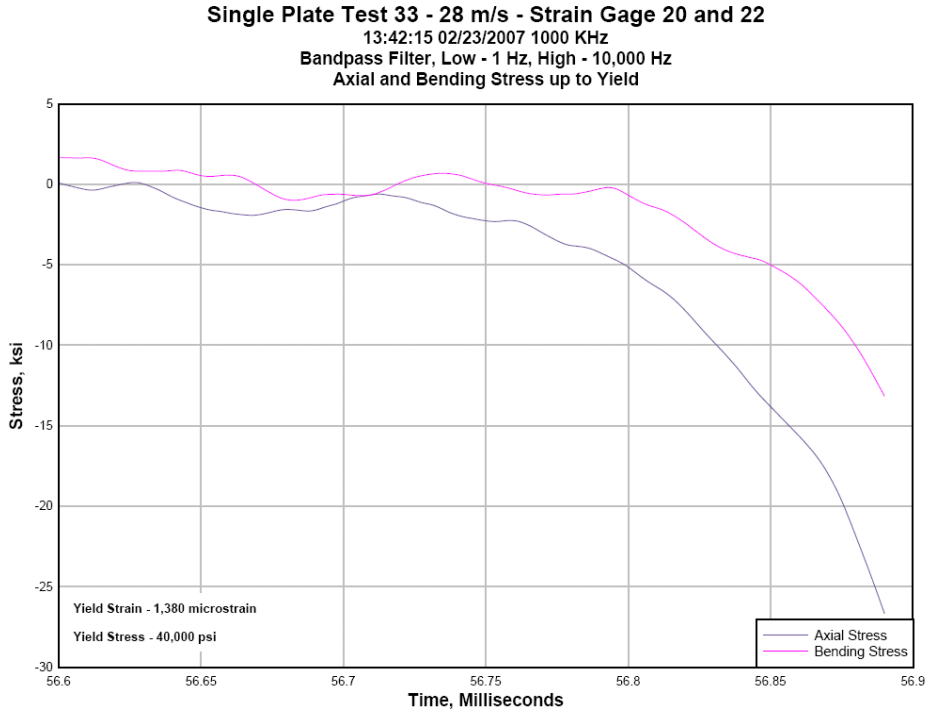

Figure E.385: Truncated Axial and Bending Stresses for Test 33 – Gauges 20 and 22

E.33.2.5 BOLT TYPE

A total of fourteen A307 bolts (Low Strength Bolts similar to Rivets) were used for this test. They were all tightened to a torque of 40 ft-lbs.

E.33.3 BLAST GENERATOR DATA

The initial impact of the single BG was 91.90 ft/sec (28.01 m/sec) with a goal velocity of 28 m/s. It had one accelerometer mounted to the back side of the impact plate as discussed in Section E.33.2.3. The average impact velocity for the impacting mass and the steel plate was calculated using the TEMA Track Eye tracking software.

E.33.4 SPECIMEN BEHAVIOR

The loading of the BG plate imparted an initial velocity of 91.90 ft/sec (28.01 m/sec) to the specimen. This caused plate to deform in both directions. The longitudinal deflection (in the north-south direction) behaved in a typical one-way flexural shape. In order to get the velocity as high as needed the test was designed to have the impacting mass break free from the BG and launch itself into the plate. This test imparted enough energy to break all fourteen of the bolts as shown in Figure E.386. The maximum dynamic deflection during the test was approximately 3 1/2". During the test three different phantom cameras were used to capture the failure modes from three different angles. Figure E.387 shows the progression of damage for this test from Phantom Camera One. Figure E.388 shows the progression of damage for this test from Phantom Camera Two. Figure E.389 shows the progression of damage for this test from Phantom Camera Three.

Figure E.386: Steel plate post test for Test 33

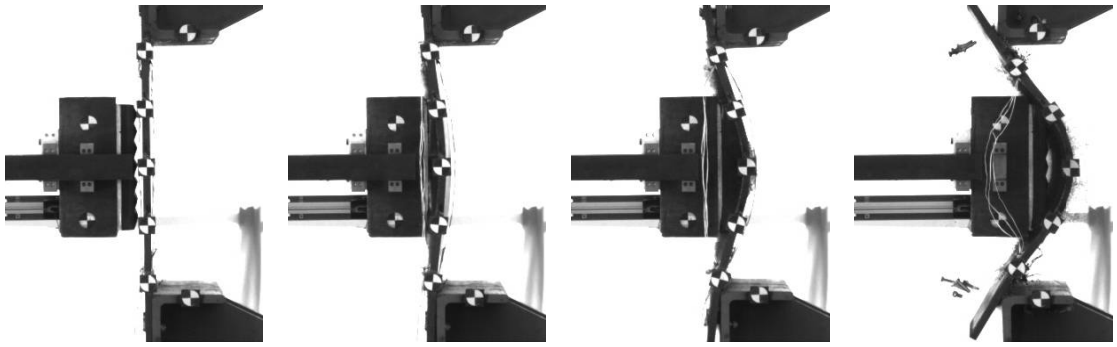

Figure E.387: Progression of damage for Test 33 from Camera 1

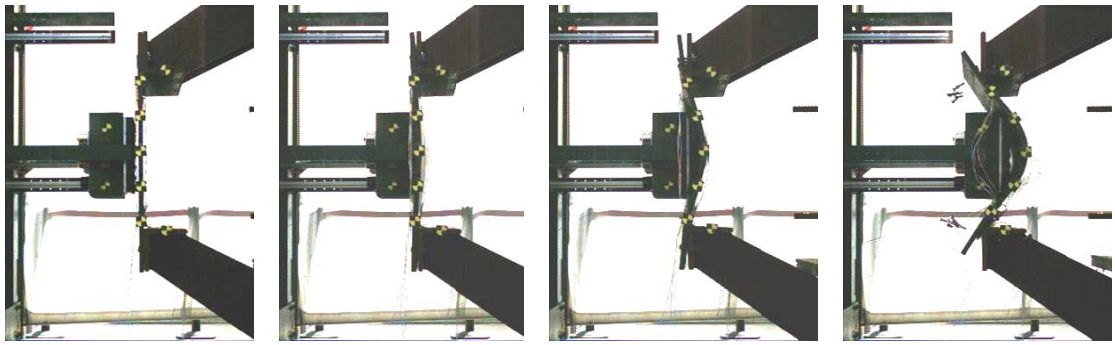

Figure E.388: Progression of damage for Test 33 from Camera 2

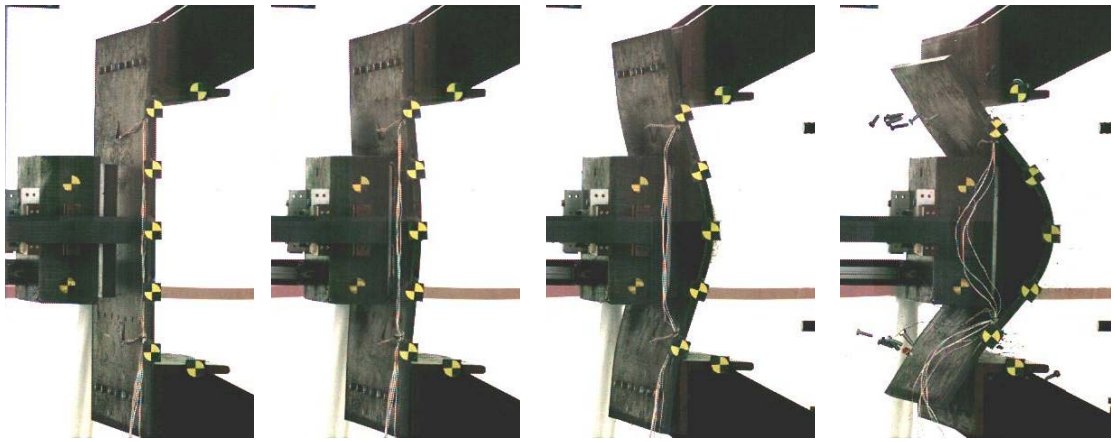

Figure E.389: Progression of damage for Test 33 from Camera 3

E.34 STEEL TOWER SINGLE PLATE: TEST 51 (SP51)

E.34.1 INTRODUCTION

The fifty-first test of the Steel Tower Single Plate test series was performed on April 9th, 2007. The test specimen was a ¼" thick steel plate labeled SP51. The Impacting Mass 1 was attached to the BG with a specimen target velocity of 32.81 ft/sec (10 m/sec). Figure E.390 shows the steel plate prior to impact.

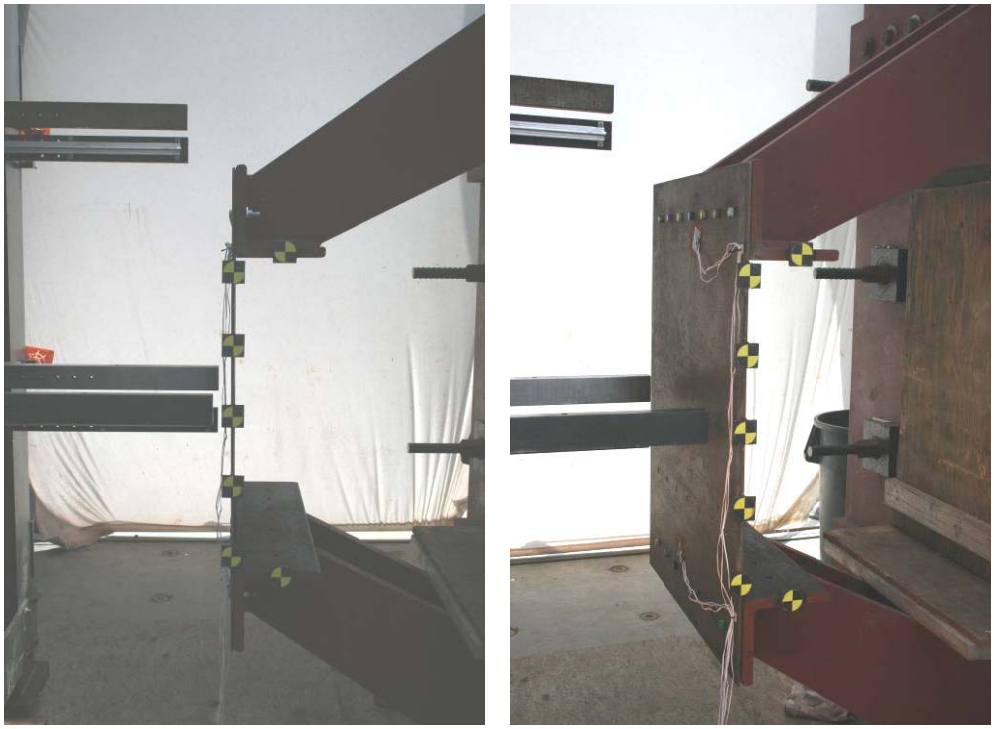

Figure E.390: 1/4" thick steel plate pre test for Test 51

E.34.2 INSTRUMENTATION

E.34.2.1 PHANTOM CAMERAS

The first camera recorded in black and white at a rate of 10,000 frames per second at a resolution of 512x384. This camera was used in order to determine the maximum velocity of the impacting mass and the movement in the plate including the maximum displacement. The second camera recorded in color at a rate of 10,000 frames per second at a resolution of 512x384. This camera recorded the overall behavior of the test specimen. It was not used to gather any specific data. The third camera recorded in color at a rate of 8,000 frames per second at a resolution of 480x480. This camera captured the failure of the bolts. A picture from each of the camera locations are shown in Figure E.391.

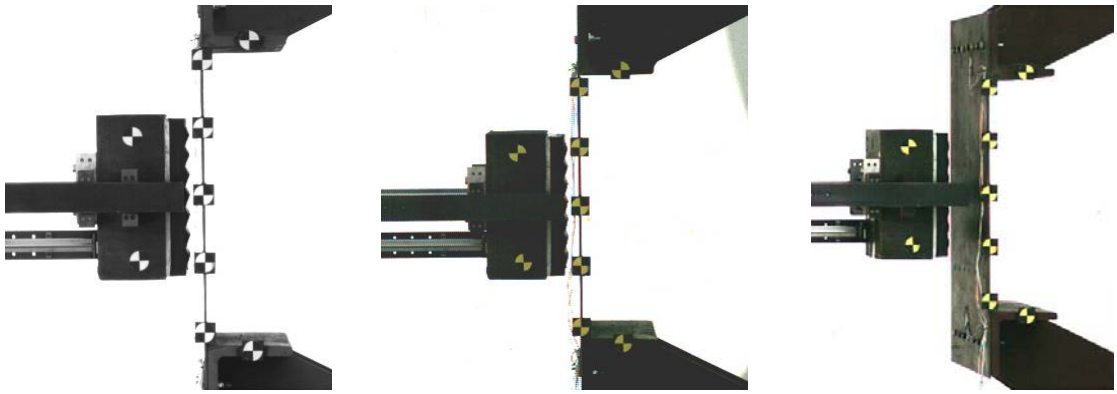

Figure E.391: Phantom Cameras for Test 51

a) Camera One b) Camera Two c) Camera Three

E.34.2.2 TARGET LOCATIONS

Five targets were welded onto the side of the steel plate as shown in Figure E.390. They were spaced at the intervals shown in Figure E.392. That figure also shows the location of the targets for the impacting mass. An additional two targets were placed on the angle at the top and the bottom end conditions. The distance between these two points is 74.93 cm (29 ½")

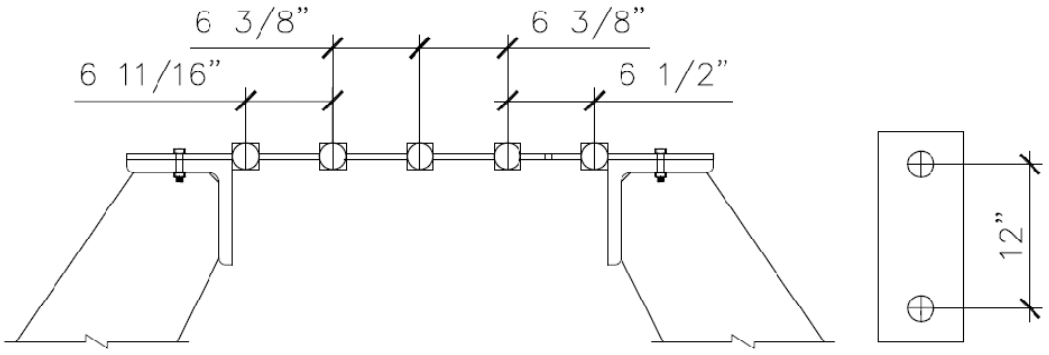

Figure E.392: Target layout on plate and impacting mass for Test 51

E.34.2.3 ACCELERATIONS

For this test there accelerometers were not used.

E.34.2.4 STRAIN GAGE LOCATIONS

For this test there were 2 strain gauges labeled 17 and 18. The strain gauges, and their locations, are shown as a drawing in Figure E.393. Table E.30 shows the specific information about this test, including the time and velocity at impact, if, and when, the bolts failed along with the maximum and minimum principal strain rates. The largest maximum principal strain rate for this test was 12.13 1/sec and was located at strain gage 18 while the largest minimum

strain rate for this test was 5.99 1/sec located at strain gage 18. The maximum principal strains for gauges 17 and 18 can be found in Figure E.394 and the minimum principal strains for the same gauges can be found in Figure E.395.

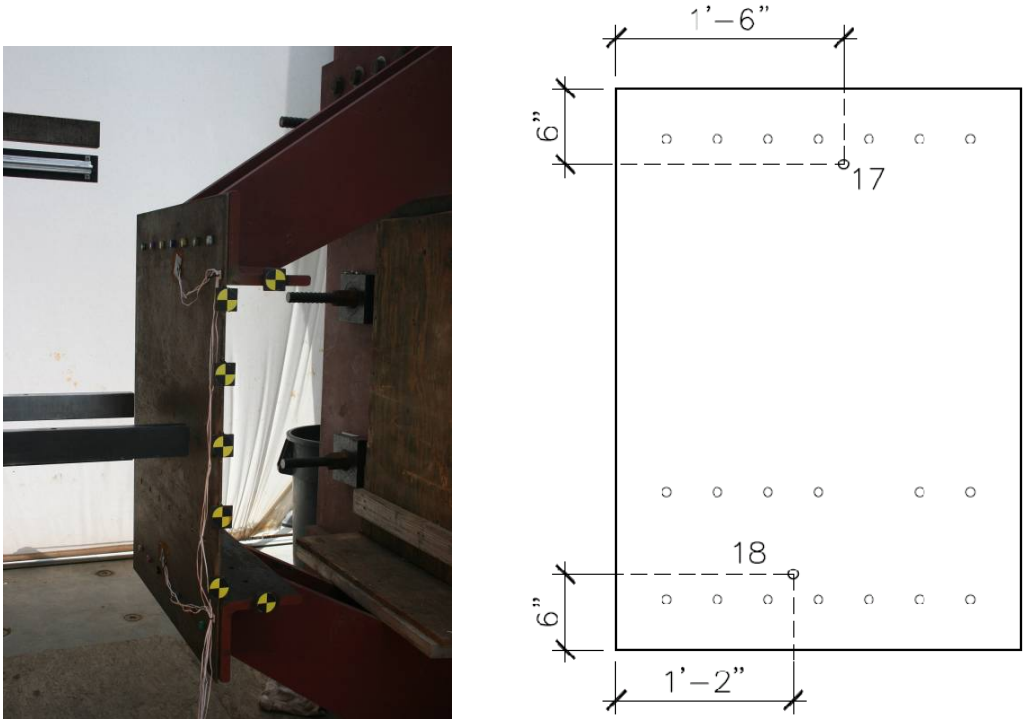

Figure E.393: Strain gage layout for Test 51 (drawing)

Table E.30: Stain rate information for Test 51

Strain Gage Number	Actual Velocity	Initial Impact	Shear Wave at Gage	Bolts Break	Maximum Principal Strain Rate	Minimum Principal Strain Rate
17	9. m/s	68.50 msec	70.50 msec	-	-6.14 1/sec	5.19 1/sec
18	9. m/s	68.50 msec	70.50 msec	-	-12.13 1/sec	5.99 1/sec

E.34.2.5 BOLT TYPE

A total of fourteen A307 bolts (Low Strength Bolts similar to Rivets) were used for this test. They were all tightened to a torque of 40 ft-lbs.

E.34.3 BLAST GENERATOR DATA

The initial impact of the single BG was 29.53 ft/sec (9 m/sec) with a goal velocity of 10 m/s. It had one accelerometer mounted to the back side of the impact plate as discussed in Section E.34.2.3. The average impact velocity for the impacting mass and the steel plate was calculated using the TEMA Track Eye tracking software.

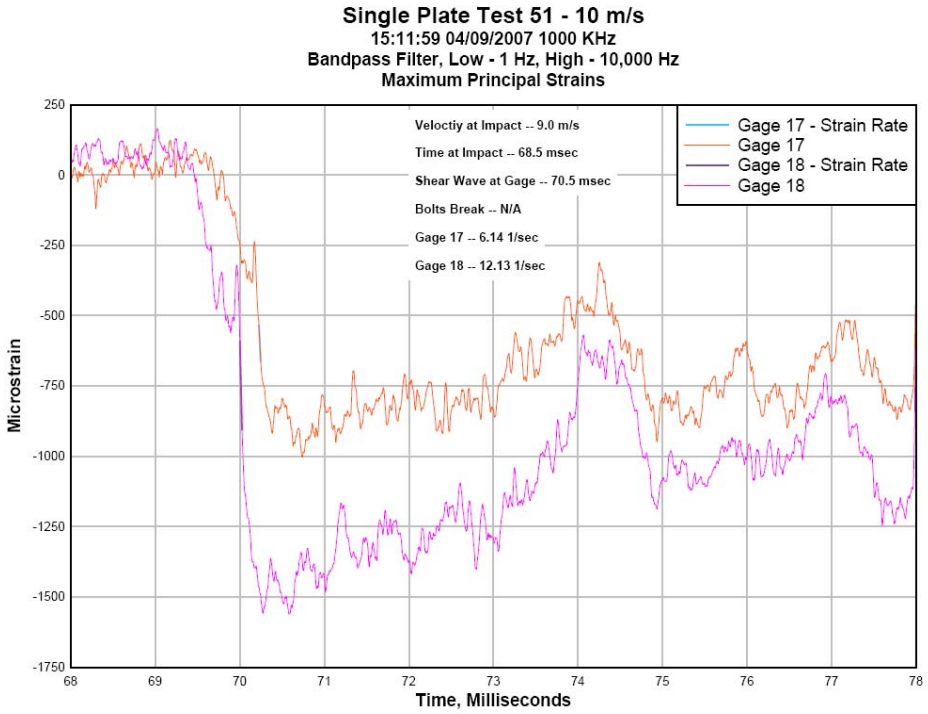

Figure E.394: Maximum principal strains and strain rates for Test 51

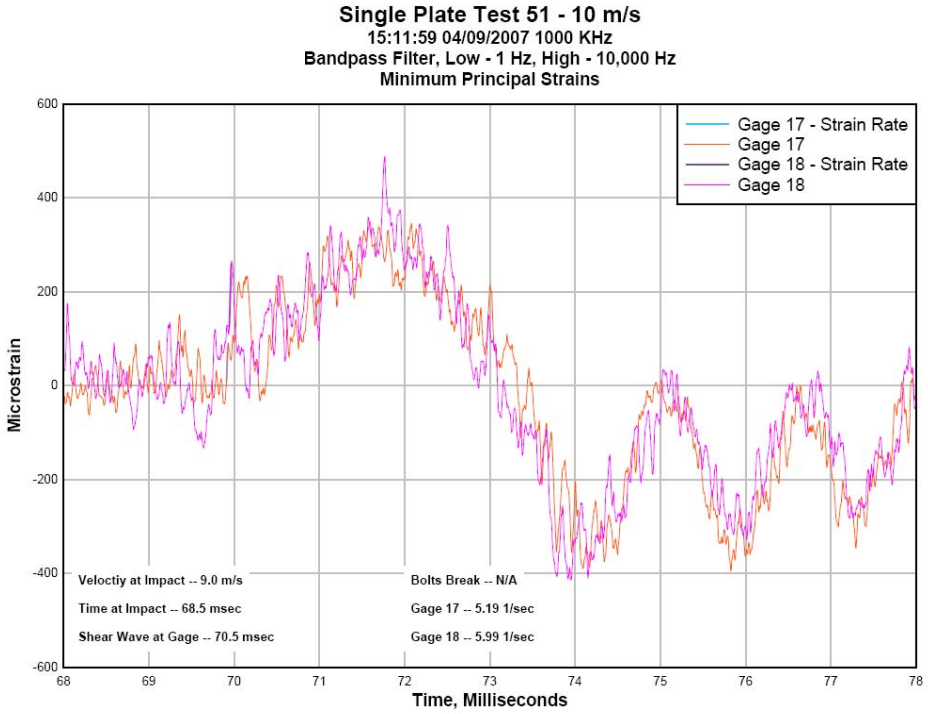

Figure E.395: Minimum principal strains and strain rates for Test 51

E.34.4 SPECIMEN BEHAVIOR

The loading of the BG plate imparted an initial velocity of 29.53 ft/sec (9 m/sec) to the specimen. This caused plate to deform in both directions. The longitudinal deflection (in the north-south direction) behaved in a typical one-way flexural shape. The goal for this test was to be below any previous threshold values so that none of the bolts broke. This test will be useful for developing a single degree of freedom system for the basic experiment. The test had a permanent deflection of 1 ¼". During the test three different phantom cameras were used to capture the failure modes from three different angles. Figure E.397 shows the progression of damage for this test from Phantom Camera One. Figure E.398 shows the progression of damage for this test from Phantom Camera Two. Figure E.399 shows the progression of damage for this test from Phantom Camera Three.

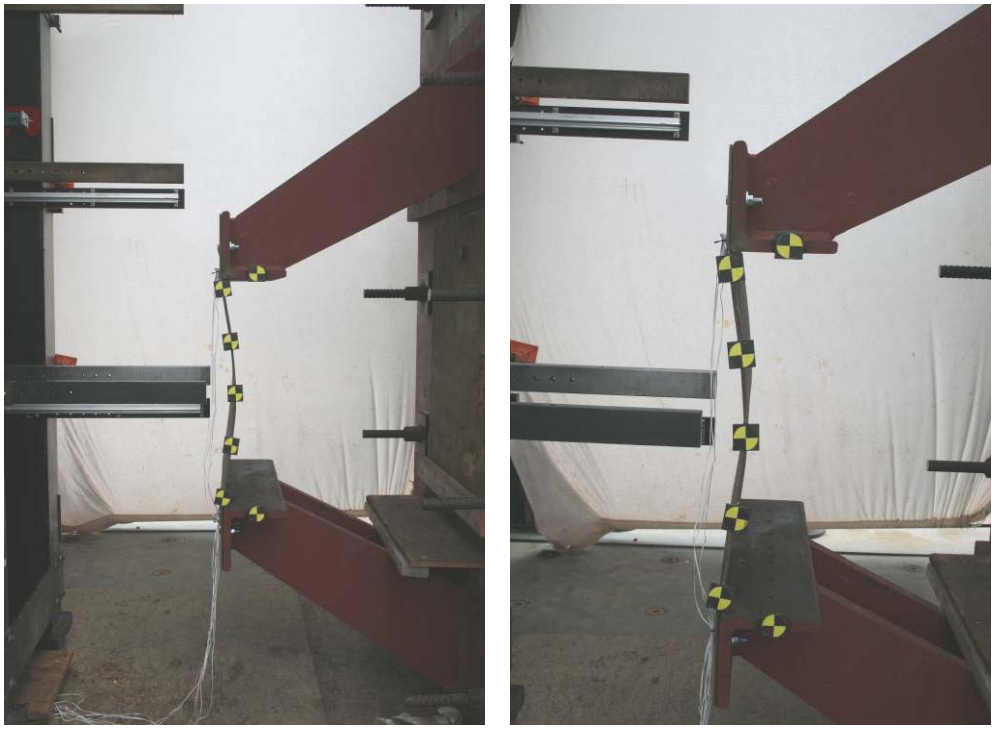

Figure E.396: Steel plate post test for Test 51

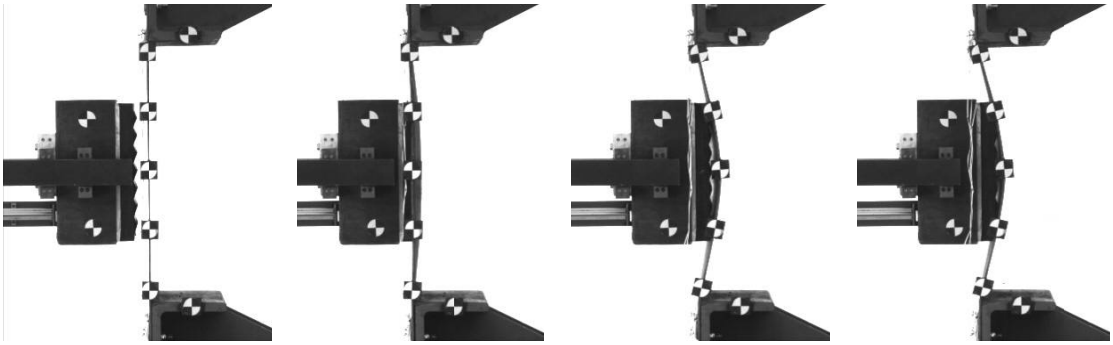

Figure E.397: Progression of damage for Test 51 from Camera 1

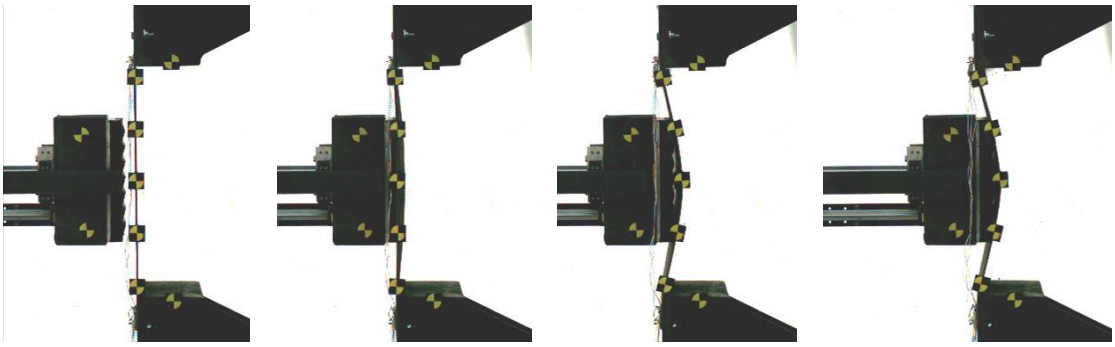

Figure E.398: Progression of damage for Test 51 from Camera 2

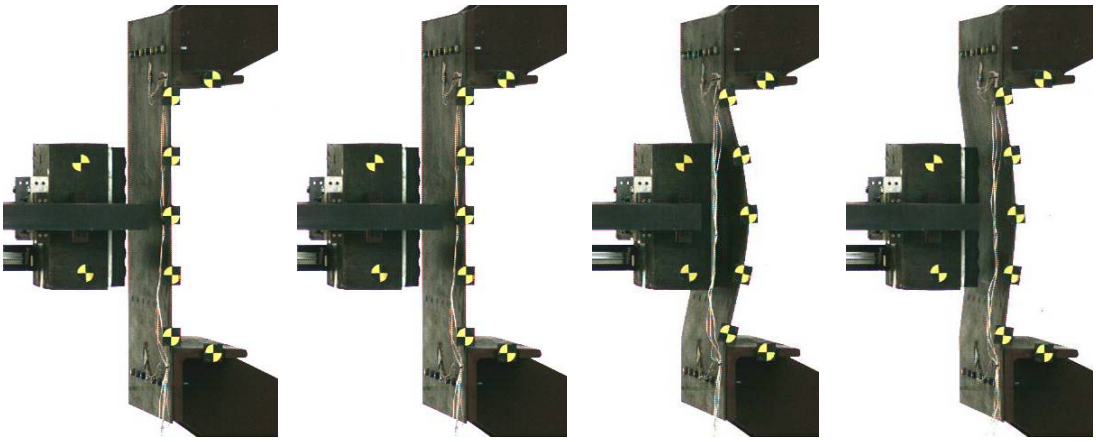

Figure E.399: Progression of damage for Test 51 from Camera 3

F TEST RESULTS – BALLISTIC TESTS – TYPE 2

F.1 STEEL TOWER SINGLE PLATE: TEST 35 (SP35)

F.1.1 INTRODUCTION

The thirty-fifth test of the Steel Tower Single Plate test series was performed on March 1st, 2007. The test specimen was a 1/4" thick steel plate labeled SP35. The Impacting Mass 3 was placed flush with the push plate and accelerated by the BG with a target velocity upon impact with the specimen of 75.46 ft/sec (23 m/s). Figure F.1 shows the steel plate prior to impact.

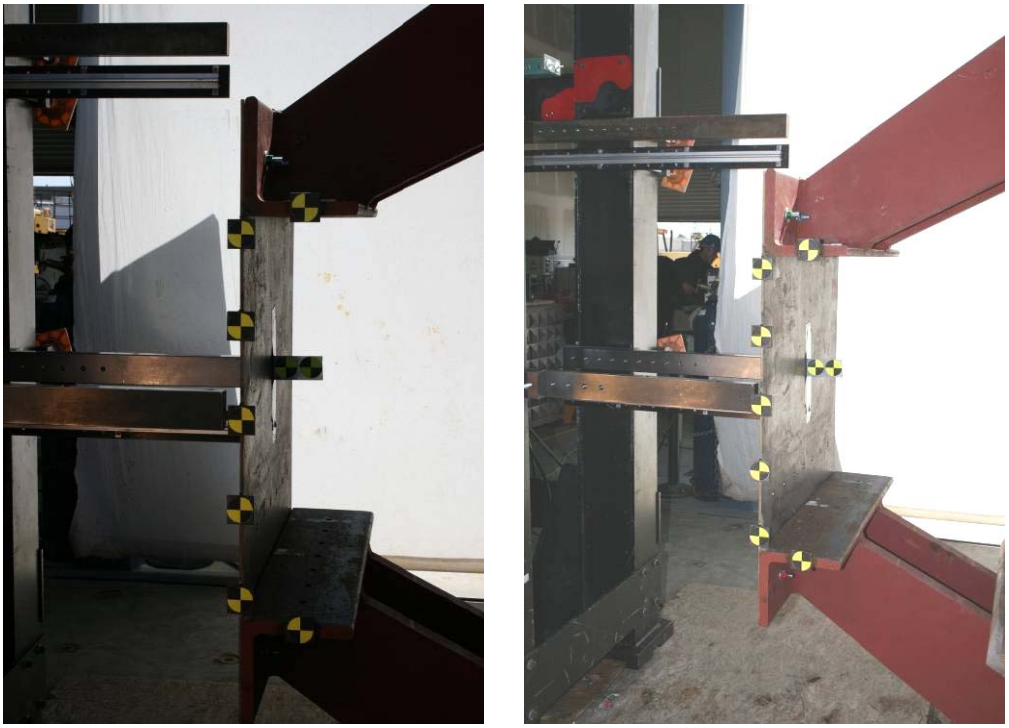

Figure F.1: 1/4" thick steel plate pre test for Test 35

F.1.2 INSTRUMENTATION

F.1.2.1 PHANTOM CAMERAS

The first camera recorded in black and white at a rate of 10,000 frames per second at a resolution of 512x384. This camera was used in order to determine the maximum velocity of the impacting mass and the movement in the plate including the maximum displacement. The second camera recorded in color at a rate of 10,000 frames per second at a resolution of 512x384. This camera recorded the overall behavior of the test specimen. It was not used to gather any specific data. The third camera recorded in color at a rate of 8,000 frames per second at a resolution of 480x480. This camera captured the failure of the bolts. A picture from each of the camera locations are shown in Figure F.2.

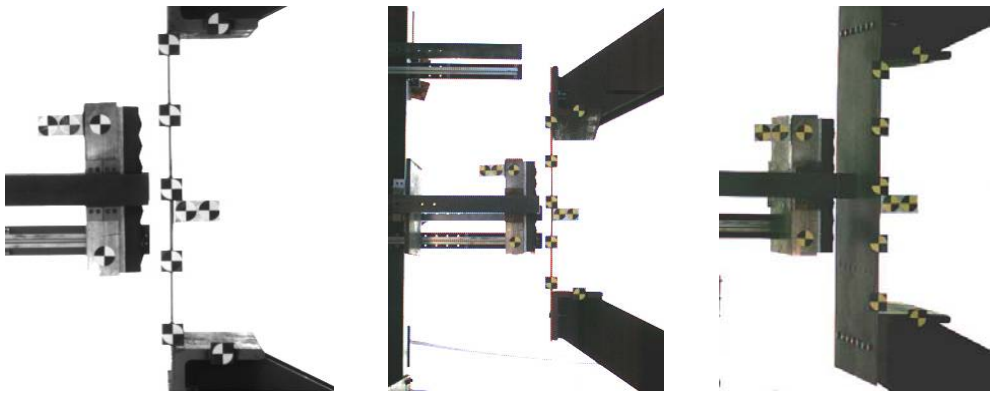

Figure F.2: Phantom Cameras for Test 35 a) Camera One b) Camera Two c) Camera Three

F.1.2.2 TARGET LOCATIONS

Five targets were welded onto the side of the steel plate as shown in Figure F.1. They were spaced at the intervals shown in Figure F.3. That figure also shows the location of the targets for the impacting mass. An additional two targets were placed on the angle at the top and the bottom end conditions. The distance between these two points is 74.93 cm (29 ½"). There are additional targets for this test but their locations are irrelevant.

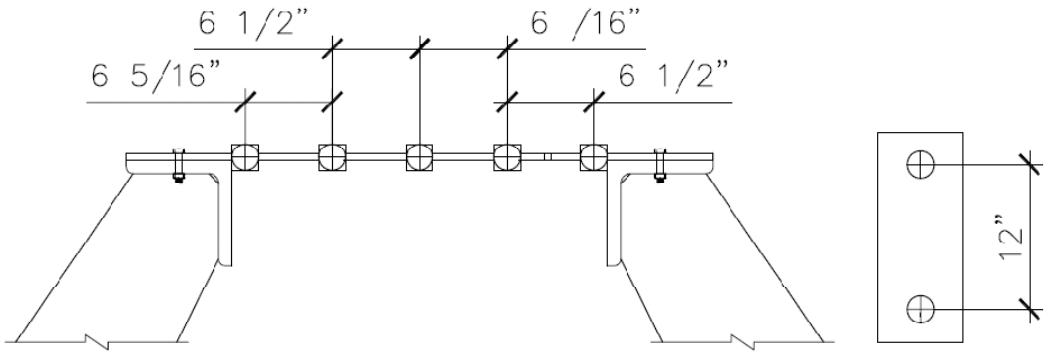

Figure F.3: Target layout on plate and impacting mass for Test 35

F.1.2.3 STRAIN GAGE LOCATIONS

For this test there strain gauges were not used

F.1.2.3.1 BOLT TYPE

A total of fourteen A307 bolts (Low Strength Bolts similar to Rivets) were used for this test. They were all tightened to a torque of 40 ft-lbs.

F.1.3 BLAST GENERATOR DATA

The initial impact of the single BG was 70.54 ft/sec (21.5 m/sec) with a goal velocity of 23 m/s. The average impact velocity for the impacting mass and the steel plate was calculated using the TEMA Track Eye tracking software.

F.1.4 SPECIMEN BEHAVIOR

The loading of the BG plate imparted an initial velocity of 70.54 ft/sec (21.5 m/sec) to the specimen. This caused plate to deform in both directions. The longitudinal deflection (in the north-south direction) behaved in a typical one-way flexural shape. This test imparted enough energy to break all fourteen of the bolts as shown in Figure F.4. The maximum dynamic deflection during the test was approximately 4 ¾". During the test three different phantom cameras were used to capture the failure modes from three different angles. Figure F.5 shows the progression of damage for this test from Phantom Camera One. Figure F.6 shows the progression of damage for this test from Phantom Camera Two. Figure F.7 shows the progression of damage for this test from Phantom Camera Three.

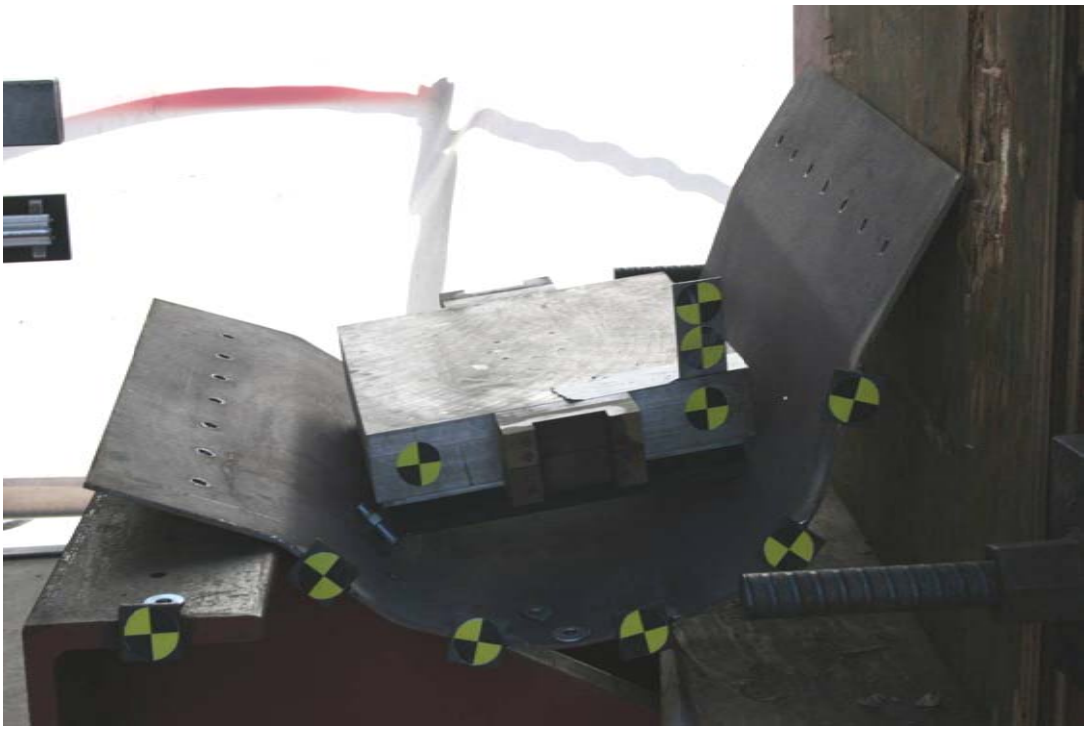

Figure F.4: Steel plate post test for Test 35

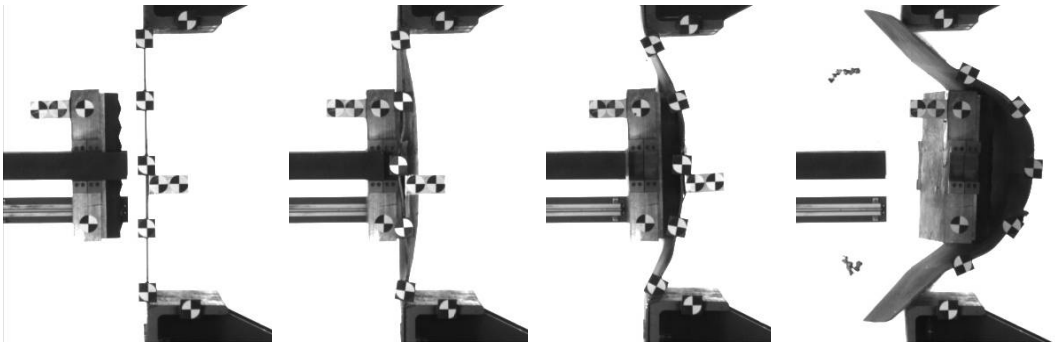

Figure F.5: Progression of damage for Test 35 from Camera 1

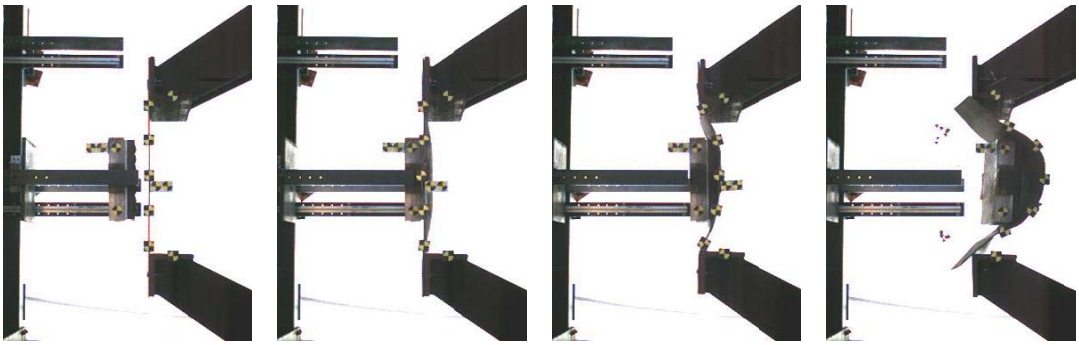

Figure F.6: Progression of damage for Test 35 from Camera 2

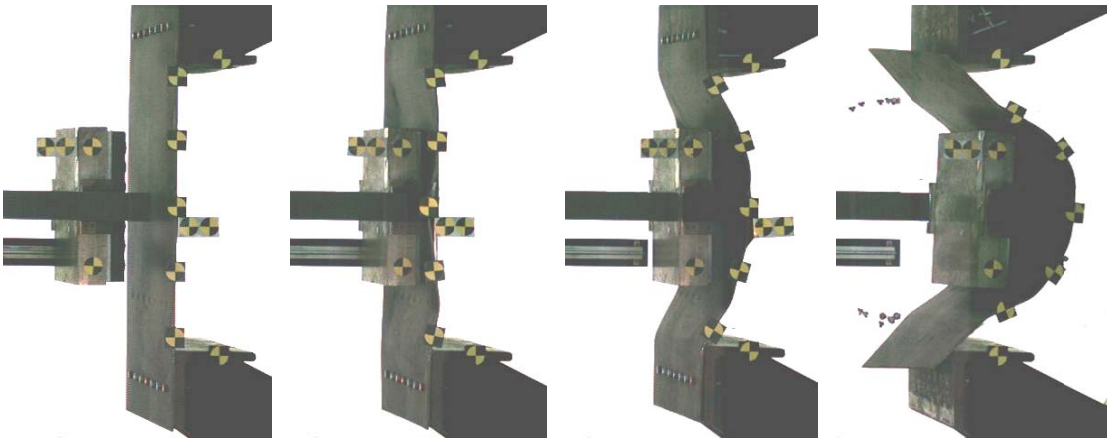

Figure F.7: Progression of damage for Test 35 from Camera 3

F.2 STEEL TOWER SINGLE PLATE: TEST 36 (SP36)

F.2.1 INTRODUCTION

The thirty-sixth test of the Steel Tower Single Plate test series was performed on March 2nd, 2007. The test specimen was a 1/2" thick steel plate labeled SP36. The Impacting Mass 3 was placed flush with the push plate and accelerated by the BG with a target velocity upon impact with the specimen of 82.02 ft/sec (25 m/s). Figure F.8 shows the steel plate prior to impact.

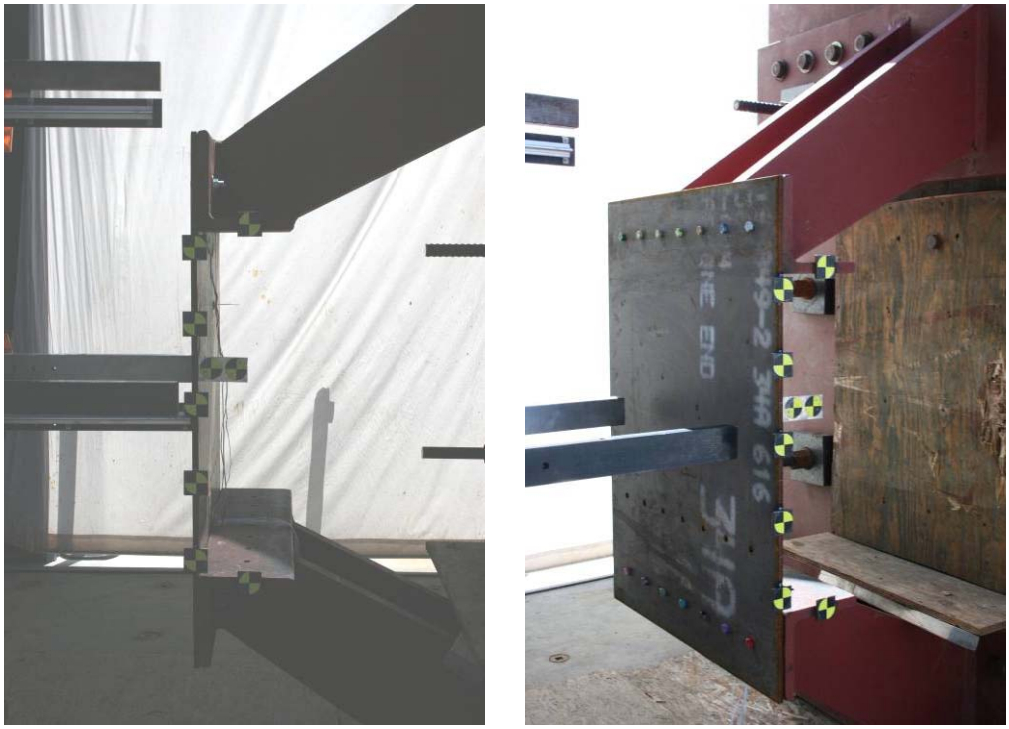

Figure F.8: 1/2" thick steel plate pre test for Test 36

F.2.2 INSTRUMENTATION

F.2.2.1 PHANTOM CAMERAS

The first camera recorded in black and white at a rate of 10,000 frames per second at a resolution of 512x384. This camera was used in order to determine the maximum velocity of the impacting mass and the movement in the plate including the maximum displacement. The second camera recorded in color at a rate of 10,000 frames per second at a resolution of 512x384. This camera recorded the overall behavior of the test specimen. It was not used to gather any specific data. The third camera recorded in color at a rate of 8,000 frames per second at a resolution of 480x480. This camera captured the failure of the bolts. A picture from each of the camera locations are shown in Figure F.9.

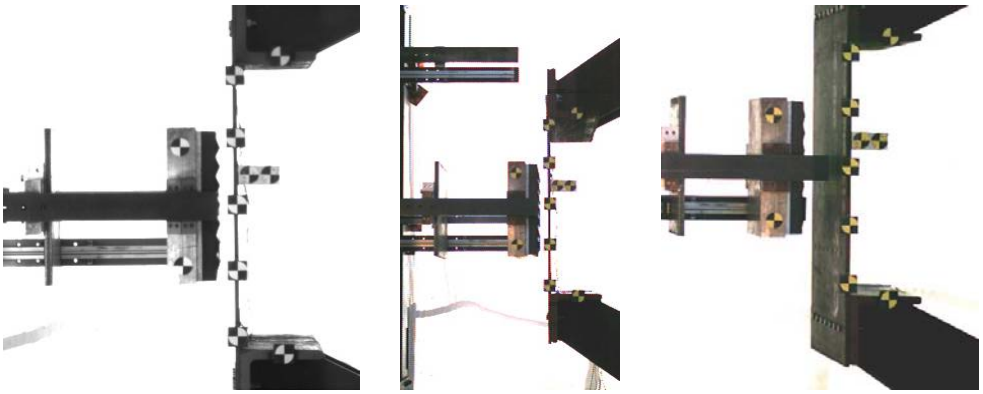

Figure F.9: Phantom Cameras for Test 36 a) Camera One b) Camera Two c) Camera Three

F.2.2.2 TARGET LOCATIONS

Five targets were welded onto the side of the steel plate as shown in Figure F.8. They were spaced at the intervals shown in Figure F.10. That figure also shows the location of the targets for the impacting mass. An additional two targets were placed on the angle at the top and the bottom end conditions. The distance between these two points is 74.93 cm (29 ½"). There are additional targets for this test but their locations are irrelevant.

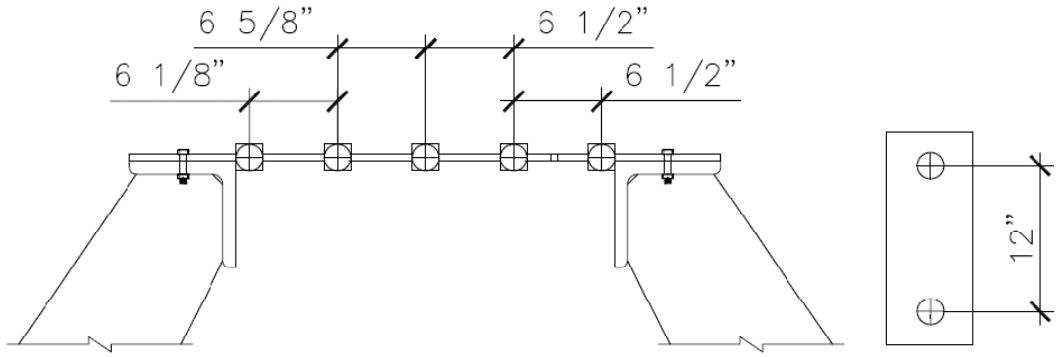

Figure F.10: Target layout on plate and impacting mass for Test 36

F.2.2.3 STRAIN GAGE LOCATIONS

For this test there were two strain gauges labeled 19 and 20. The strain gauges, and their locations, are shown in Figure F.11. Table F.1 shows the specific information about this test, including the time and velocity at impact, if, and when, the bolts failed along with the maximum and minimum principal strain rates. The largest maximum principal strain rate for this test was 9.87 1/sec and was located at strain gage 19 while the largest minimum strain rate for this test was 6.37 1/sec located at strain gage 20. The maximum principal strains for gauges 19 and 20 can be found in Figure F.12 and the minimum principal strains for the same gauges can be found in Figure F.13.

Table F.1: Stain rate information for Test 36

Test Number	Strain Gage Number	Actual Velocity	Initial Impact	Shear Wave at Gage	Bolts Break	Maximum Principal Strain Rate	Minimum Principal Strain Rate
36	19	22.7 m/s	61.80 msec	-	-	-9.87 1/sec	6.19 1/sec
36	20	22.7 m/s	61.80 msec	-	-	-8.17 1/sec	6.37 1/sec

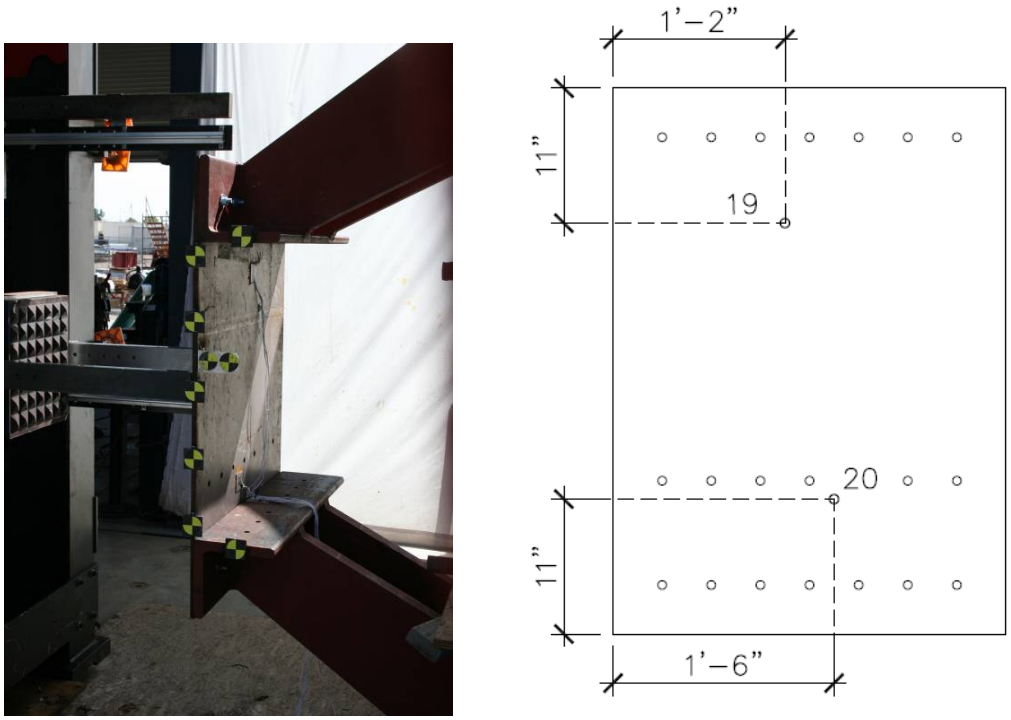

Figure F.11: Strain gage layout for Test 36

F.2.3 BOLT TYPE

A total of fourteen A307 bolts (Low Strength Bolts similar to Rivets) were used for this test. They were all tightened to a torque of 40 ft-lbs.

F.2.4 BLAST GENERATOR DATA

The initial impact of the single BG was 74.78 ft/sec (22.7 m/sec) with a goal velocity of 25 m/s. The average impact velocity for the impacting mass and the steel plate was calculated using the TEMA Track Eye tracking software.

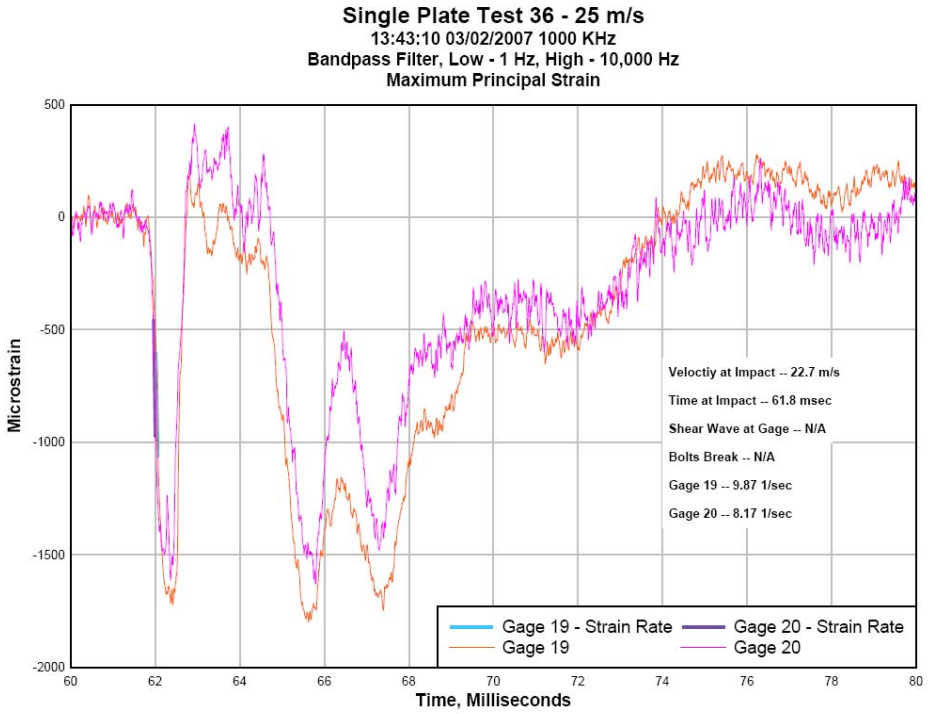

Figure F.12: Maximum principal strains and strain rates for Test 36

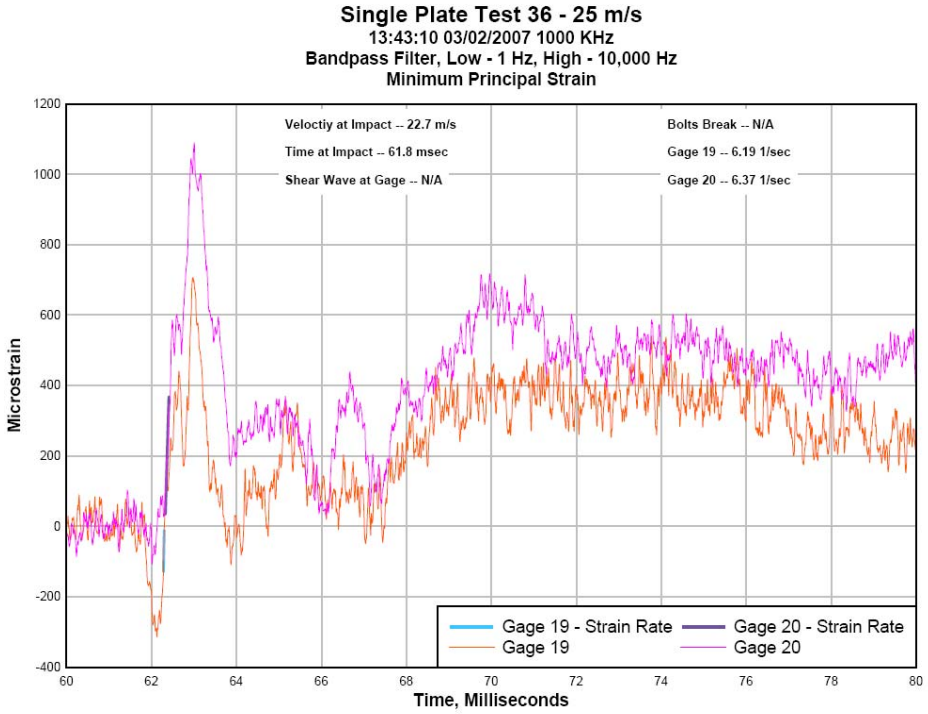

Figure F.13: Minimum principal strains and strain rates for Test 36

F.2.5 SPECIMEN BEHAVIOR

The loading of the BG plate imparted an initial velocity of 74.78 ft/sec (22.7 m/sec) to the specimen. This caused plate to deform in both directions. The longitudinal deflection (in the north-south direction) behaved in a typical one-way flexural shape. This test did not impart enough energy to break any of the bolts as shown in Figure F.14. The maximum dynamic deflection during the test was approximately 3 5/8" with a residual deflection of 2 1/4". During the test three different phantom cameras were used to capture the failure modes from three different angles. Figure F.15 shows the progression of damage for this test from Phantom Camera One. Figure F.16 shows the progression of damage for this test from Phantom Camera Two. Figure F.17 shows the progression of damage for this test from Phantom Camera Three.

Figure F.14: Steel plate post test for Test 36

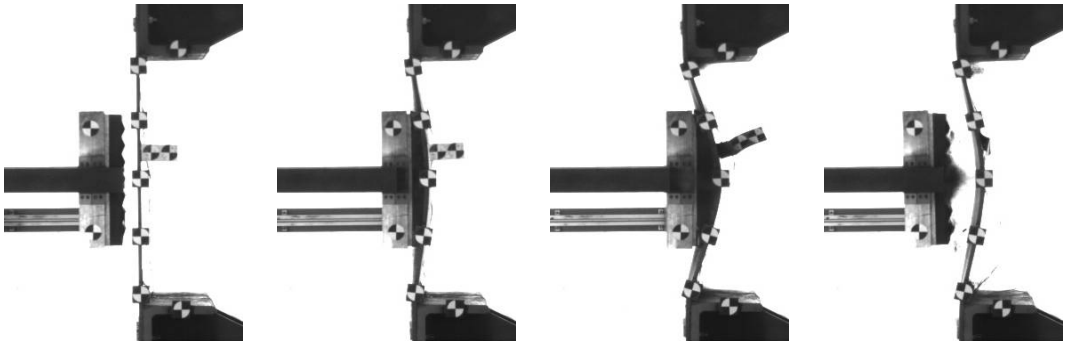

Figure F.15: Progression of damage for Test 36 from Camera 1

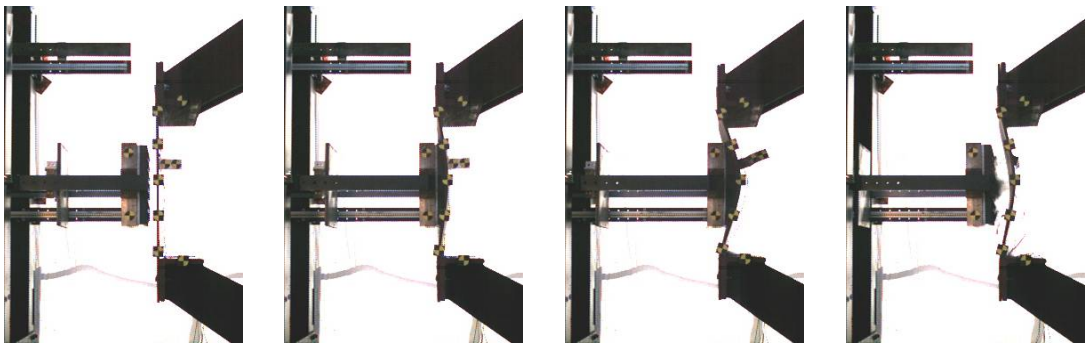

Figure F.16: Progression of damage for Test 36 from Camera 2

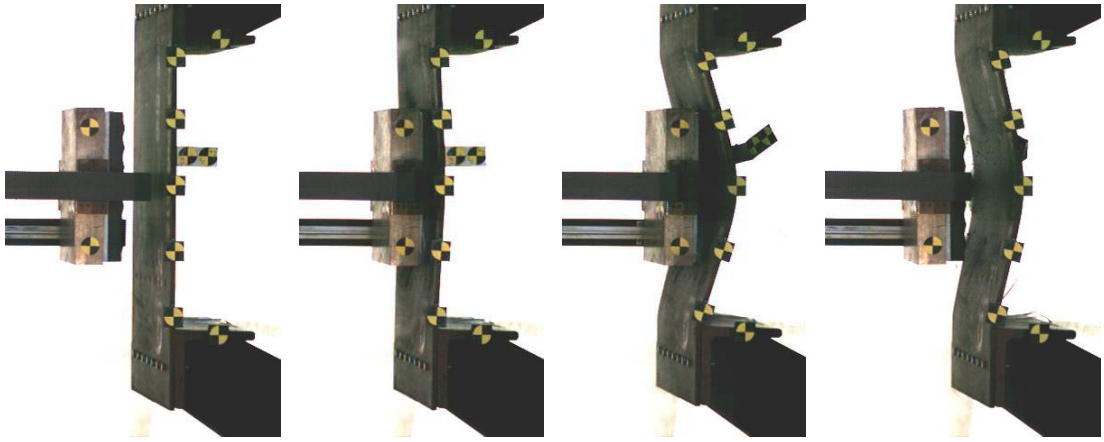

Figure F.17: Progression of damage for Test 36 from Camera 3

F.3 STEEL TOWER SINGLE PLATE: TEST 37 (SP37)

F.3.1 INTRODUCTION

The thirty-seventh test of the Steel Tower Single Plate test series was performed on March 5th, 2007. The test specimen was a 1/2" thick steel plate labeled SP37. The Impacting Mass 3 was placed flush with the push plate and accelerated by the BG with a target velocity upon impact with the specimen of 91.86 ft/sec (28 m/s). Figure F.18 shows the steel plate prior to impact.

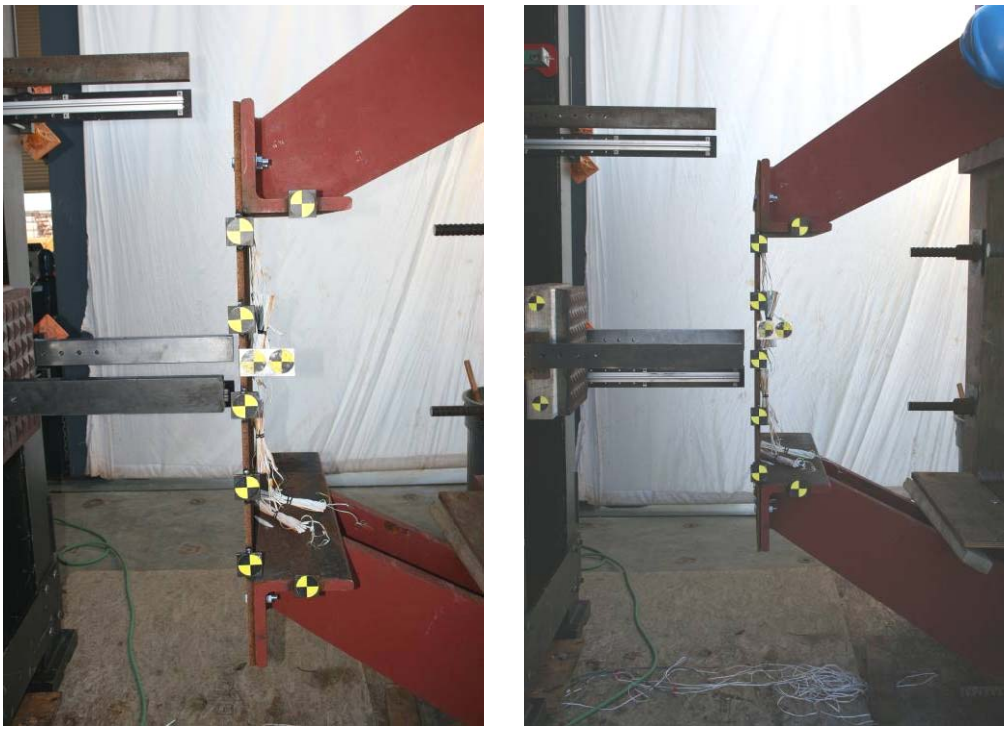

Figure F.18: 1/2" thick steel plate pre test for Test 37

F.3.2 INSTRUMENTATION

F.3.2.1 PHANTOM CAMERAS

The first camera recorded in black and white at a rate of 10,000 frames per second at a resolution of 512x384. This camera was used in order to determine the maximum velocity of the impacting mass and the movement in the plate including the maximum displacement. The second camera recorded in color at a rate of 10,000 frames per second at a resolution of 512x384. This camera recorded the overall behavior of the test specimen. It was not used to gather any specific data. The third camera recorded in color at a rate of 8,000 frames per second at a resolution of 480x480. This camera captured the failure of the bolts. A picture from each of the camera locations are shown in Figure F.19.

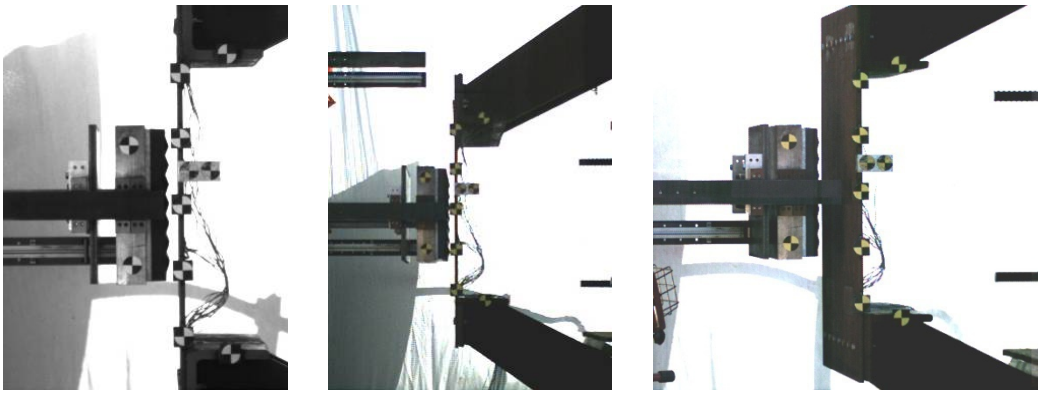

Figure F.19: Phantom Cameras for Test 37 a) Camera One b) Camera Two c) Camera Three

F.3.2.2 TARGET LOCATIONS

Five targets were welded onto the side of the steel plate as shown in Figure F.18. They were spaced at the intervals shown in Figure F.20. That figure also shows the location of the targets for the impacting mass. An additional two targets were placed on the angle at the top and the bottom end conditions. The distance between these two points is 74.93 cm (29 ½”). There are additional targets for this test but their locations are irrelevant.

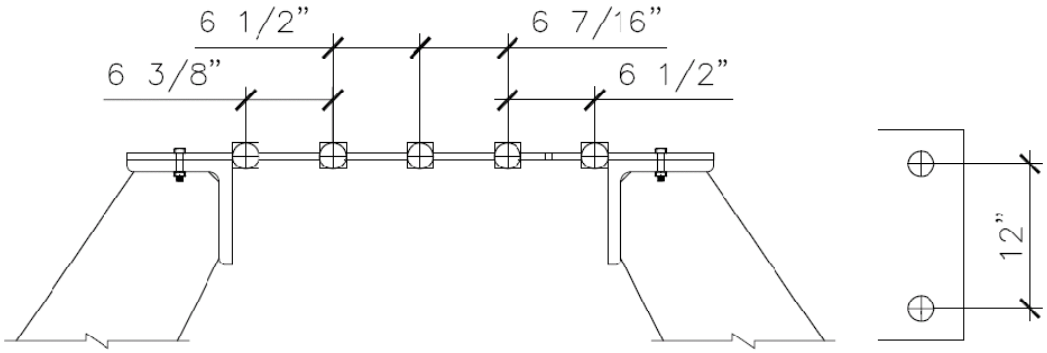

Figure F.20: Target layout on plate and impacting mass for Test 37

F.3.2.3 STRAIN GAGE LOCATIONS

For this test there were five strain gauges labeled 1A, 2A, 3A, 4A and 5A. The strain gauges, and their locations, are shown in Figure F.21. Table F.2 shows the specific information about this test, including the time and velocity at impact, if, and when, the bolts failed along with the maximum and minimum principal strain rates. The largest maximum principal strain rate for this test was 16.94 1/sec and was located at strain gage 2A while the largest minimum strain rate for this test was 13.38 1/sec located at strain gage 3A. The maximum principal strains for gauges 1A, 2A, 3A, 4A and 5A can be found in Figure F.22 and the minimum principal strains for the same gauges can be found in Figure F.23.

Table F.2: Stain rate information for Test 37

Test Number	Strain Gage Number	Actual Velocity	Initial Impact	Shear Wave at Gage	Bolts Break	Maximum Principal Strain Rate	Minimum Principal Strain Rate
37	1A	26.8 m/s	56.10 msec	-	-	-8.37 1/sec	-11.61 1/sec
37	2A	26.8 m/s	56.10 msec	-	-	-16.94 1/sec	-9.91 1/sec
37	3A	26.8 m/s	56.10 msec	-	-	-12.24 1/sec	-13.38 1/sec
37	4A	26.8 m/s	56.10 msec	-	-	-12.24 1/sec	-3.15 1/sec
37	5A	26.8 m/s	56.10 msec	-	-	-10.56 1/sec	6.99 1/sec

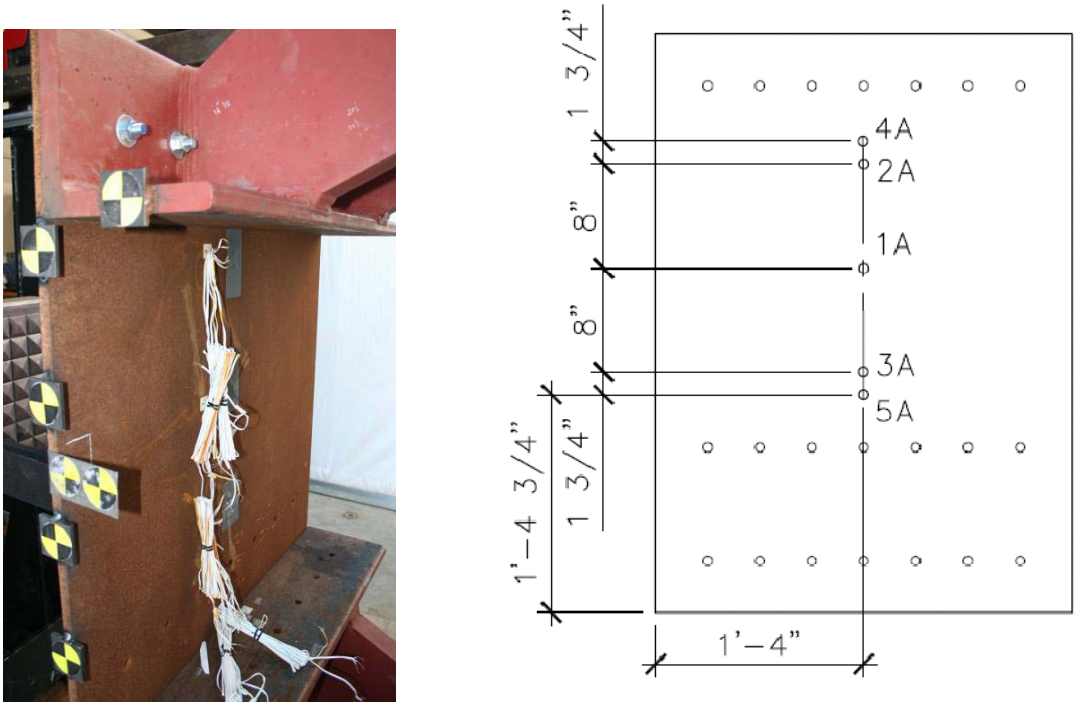

Figure F.21: Strain gage layout for Test 37

F.3.2.4 BOLT TYPE

A total of fourteen A307 bolts (Low Strength Bolts similar to Rivets) were used for this test. They were all tightened to a torque of 40 ft-lbs.

F.3.3 BLAST GENERATOR DATA

The initial impact of the single BG was 87.93 ft/sec (26.8 m/sec) with a goal velocity of 25 m/s. The average impact velocity for the impacting mass and the steel plate was calculated using the TEMA Track Eye tracking software.

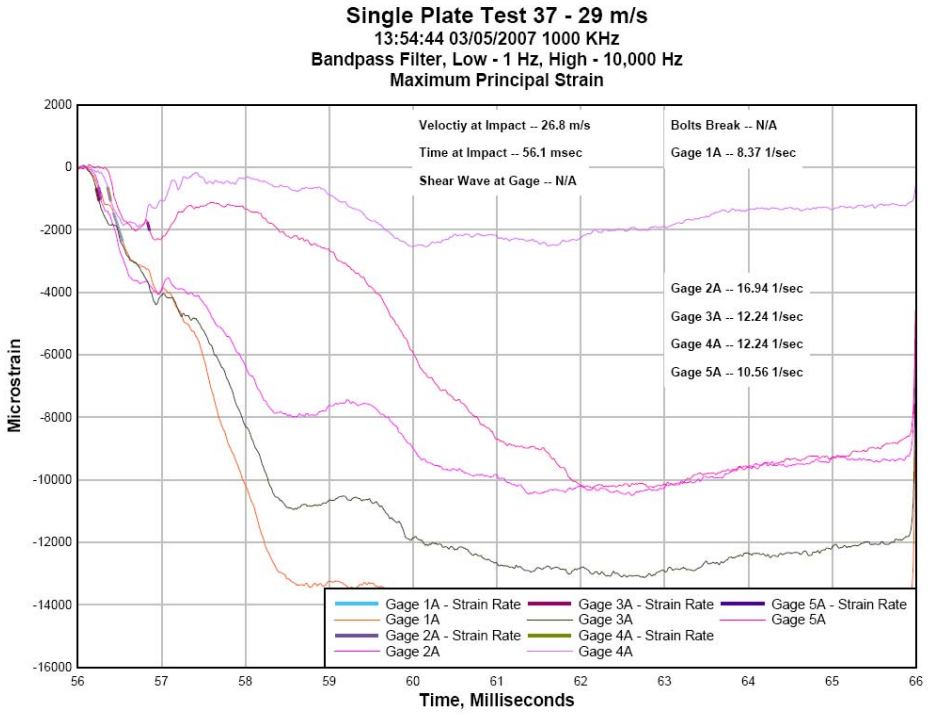

Figure F.22: Maximum principal strains and strain rates for Test 37

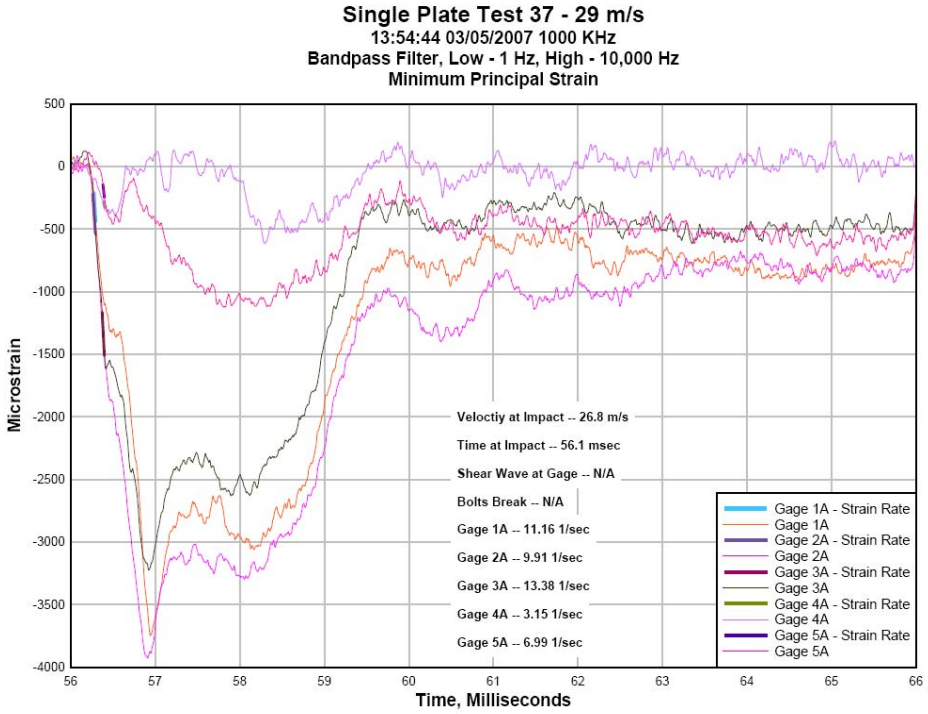

Figure F.23: Minimum principal strains and strain rates for Test 37

F.3.4 SPECIMEN BEHAVIOR

The loading of the BG plate imparted an initial velocity of 87.93 ft/sec (26.8 m/sec) to the specimen. This caused plate to deform in both directions. The longitudinal deflection (in the north-south direction) behaved in a typical one-way flexural shape. This test did not impart enough energy to break any of the bolts as shown in Figure F.24. The maximum dynamic deflection during the test was approximately 3 3/4" with a residual deflection of 2 5/8". During the test three different phantom cameras were used to capture the failure modes from three different angles. Figure F.25 shows the progression of damage for this test from Phantom Camera One. Figure F.26 shows the progression of damage for this test from Phantom Camera Two. Figure F.27 shows the progression of damage for this test from Phantom Camera Three.

Figure F.24: Steel plate post test for Test 37

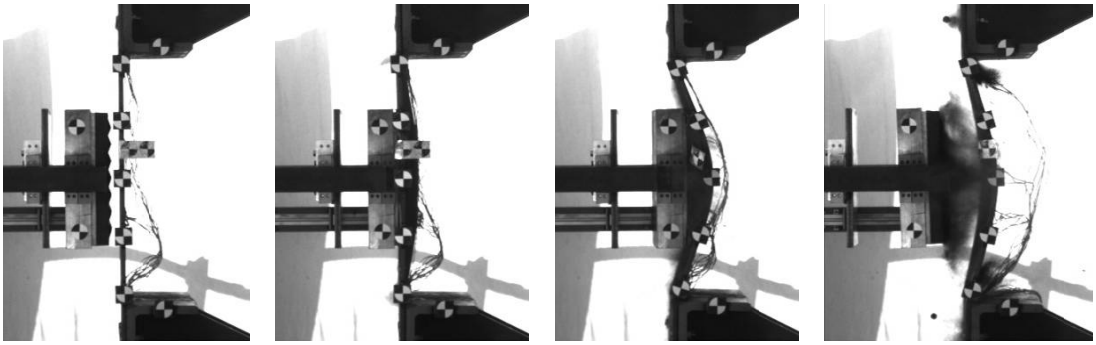

Figure F.25: Progression of damage for Test 37 from Camera 1

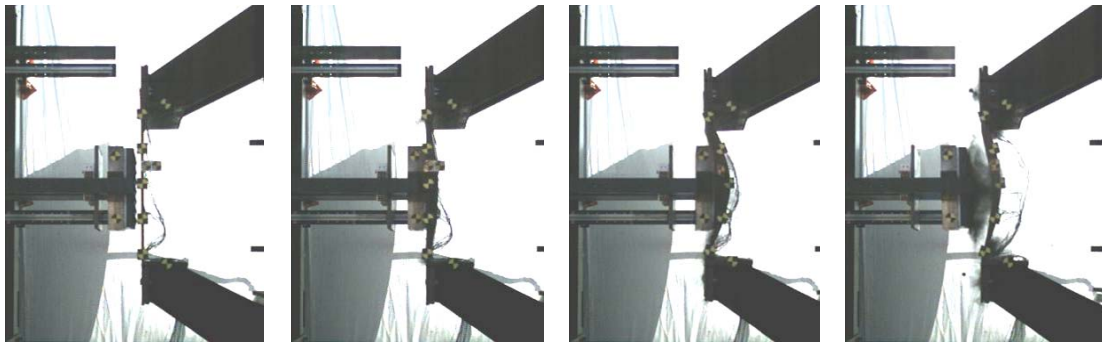

Figure F.26: Progression of damage for Test 37 from Camera 2

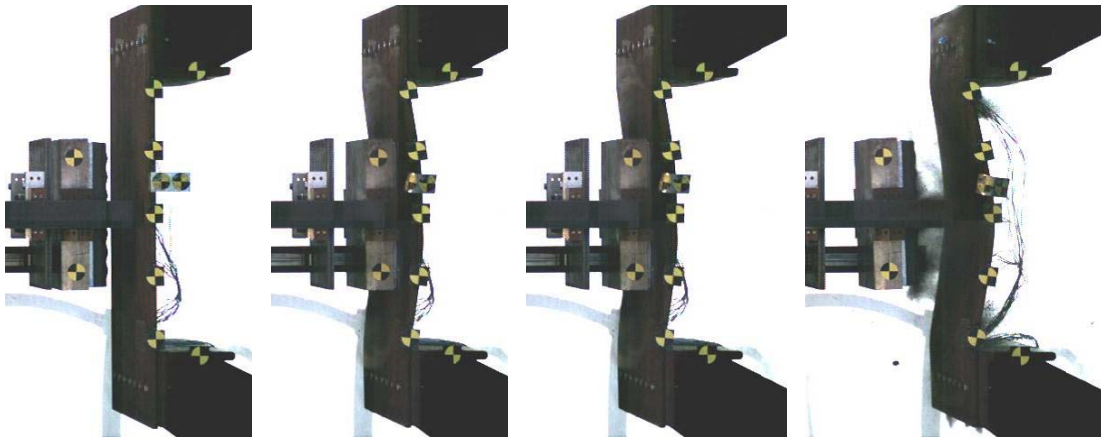

Figure F.27: Progression of damage for Test 37 from Camera 3

F.4 STEEL TOWER SINGLE PLATE: TEST 38 (SP38)

F.4.1 INTRODUCTION

The thirty-eighth test of the Steel Tower Single Plate test series was performed on March 6th, 2007. The test specimen was a 1/2" thick steel plate labeled SP38. The Impacting Mass 3 was placed flush with the push plate and accelerated by the BG with a target velocity upon impact with the specimen of 95.14 ft/sec (29 m/s). Figure F.28 shows the steel plate prior to impact.

Figure F.28: 1/2" thick steel plate pre test for Test 38

F.4.2 INSTRUMENTATION

F.4.2.1 PHANTOM CAMERAS

The first camera recorded in black and white at a rate of 10,000 frames per second at a resolution of 512x384. This camera was used in order to determine the maximum velocity of the impacting mass and the movement in the plate including the maximum displacement. The second camera recorded in color at a rate of 10,000 frames per second at a resolution of 512x384. This camera recorded the overall behavior of the test specimen. It was not used to gather any specific data. The third camera recorded in color at a rate of 8,000 frames per second at a resolution of 480x480. This camera captured the failure of the bolts. A picture from each of the camera locations are shown in Figure F.29.

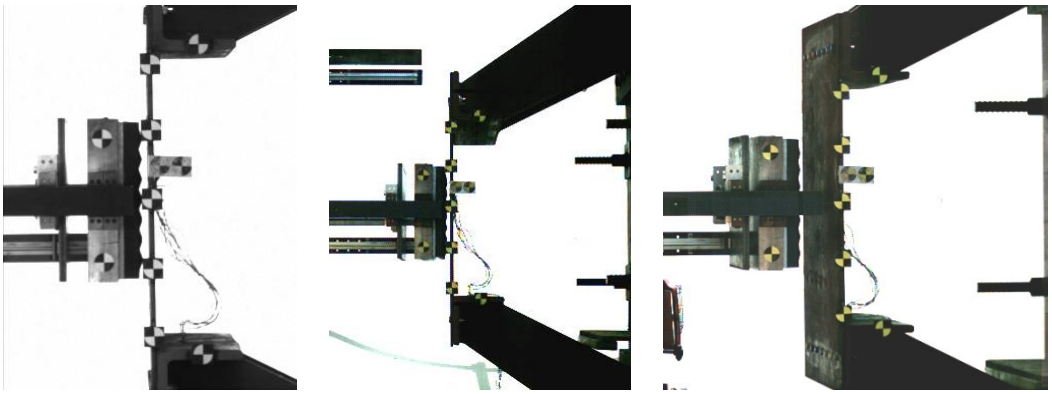

Figure F.29: Phantom Cameras for Test 38 a) Camera One b) Camera Two c) Camera Three

F.4.2.2 TARGET LOCATIONS

Five targets were welded onto the side of the steel plate as shown in Figure F.28. They were spaced at the intervals shown in Figure F.30. That figure also shows the location of the targets for the impacting mass. An additional two targets were placed on the angle at the top and the bottom end conditions. The distance between these two points is 74.93 cm (29 ½”). There are additional targets for this test but their locations are irrelevant.

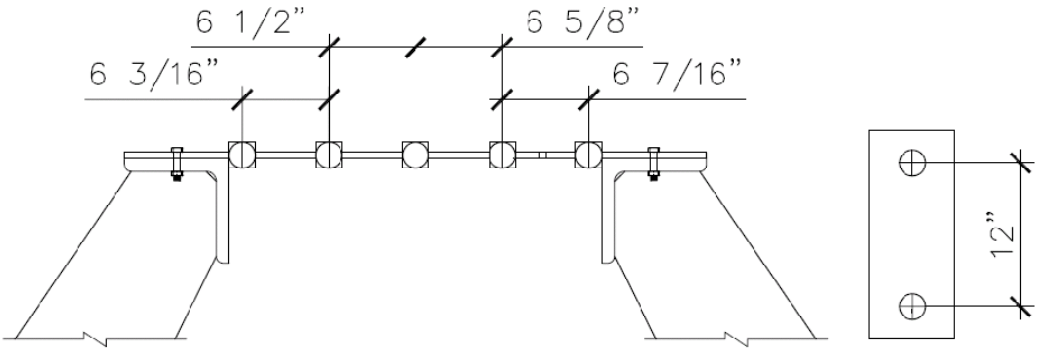

Figure F.30: Target layout on plate and impacting mass for Test 38

F.4.2.3 STRAIN GAGE LOCATIONS

For this test there were three strain gauges labeled 1, 6 and 7. The strain gauges, and their locations, are shown in Figure F.31. Table F.3 shows the specific information about this test, including the time and velocity at impact, if, and when, the bolts failed along with the maximum and minimum principal strain rates. The largest maximum principal strain rate for this test was 13.38 1/sec and was located at strain gage 1 while the largest minimum strain rate for this test was 13.24 1/sec located at strain gage 1. The maximum principal strains for gauges 1, 6 and 7 can be found in Figure F.32 and the minimum principal strains for the same gauges can be found in Figure F.33.

Table F.3: Stain rate information for Test 38

Strain Gage Number	Actual Velocity	Initial Impact	Shear Wave at Gage	Bolts Break	Maximum Principal Strain Rate	Minimum Principal Strain Rate
1	27.1 m/s	55.70 msec	-	62.50 msec	-13.38 1/sec	-13.24 1/sec
6	27.1 m/s	55.70 msec	-	62.50 msec	-10.05 1/sec	-10.64 1/sec
7	27.1 m/s	55.70 msec	-	62.50 msec	-11.40 1/sec	-9.84 1/sec

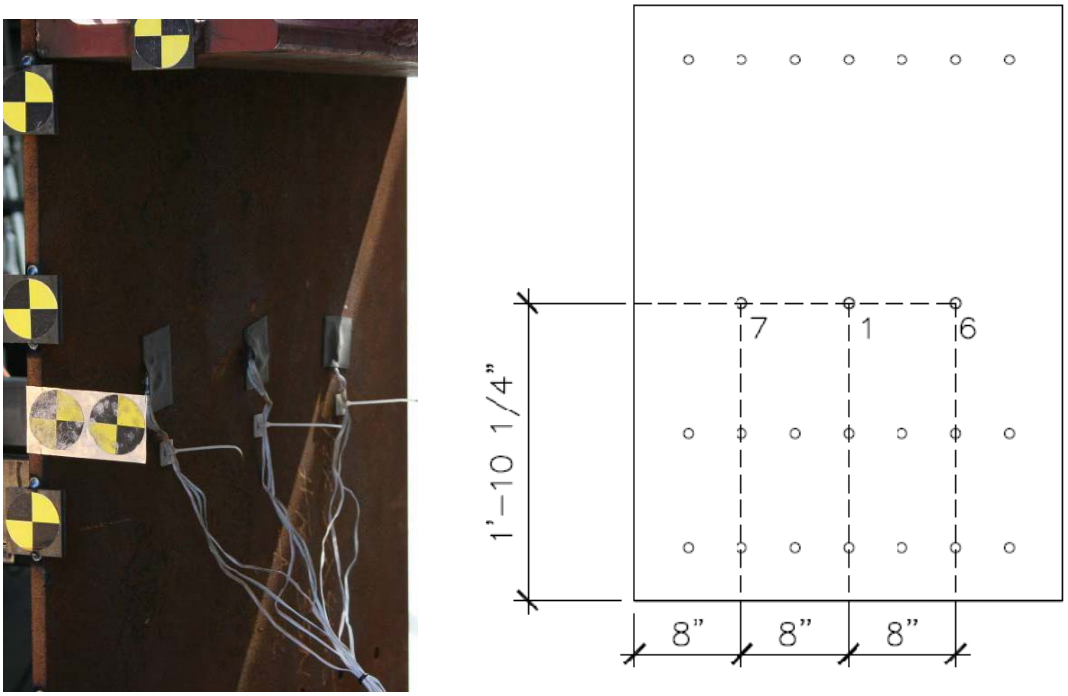

Figure F.31: Strain gage layout for Test 38

F.4.3 BOLT TYPE

A total of fourteen A307 bolts (Low Strength Bolts similar to Rivets) were used for this test. They were all tightened to a torque of 40 ft-lbs.

F.4.4 BLAST GENERATOR DATA

The initial impact of the single BG was 88.91 ft/sec (27.1 m/sec) with a goal velocity of 29 m/s. The average impact velocity for the impacting mass and the steel plate was calculated using the TEMA Track Eye tracking software.

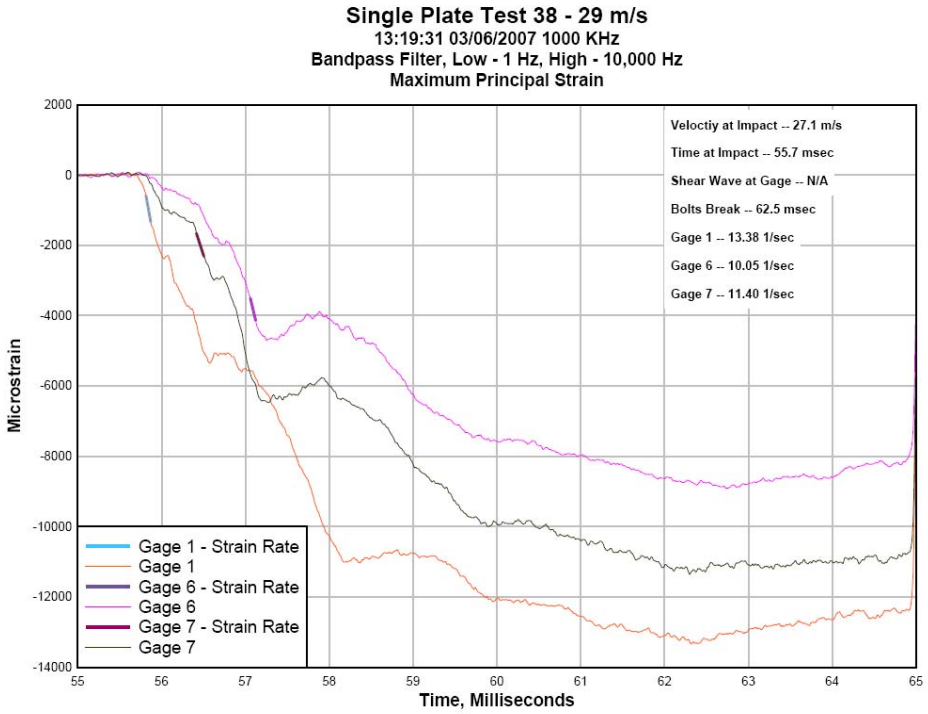

Figure F.32: Maximum principal strains and strain rates for Test 38

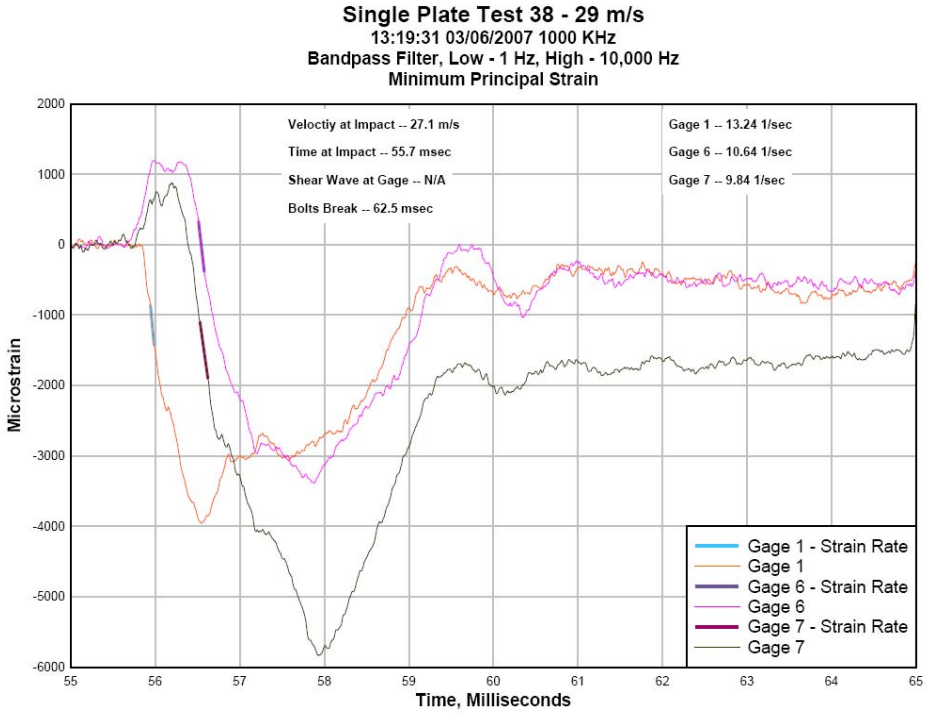

Figure F.33: Minimum principal strains and strain rates for Test 38

F.4.5 SPECIMEN BEHAVIOR

The loading of the BG plate imparted an initial velocity of 88.91 ft/sec (27.1 m/sec) to the specimen. This caused plate to deform in both directions. The longitudinal deflection (in the north-south direction) behaved in a typical one-way flexural shape. This test imparted enough energy to break the bottom seven bolts as shown in Figure F.34. The maximum dynamic deflection during the test was approximately 4 1/4". During the test three different phantom cameras were used to capture the failure modes from three different angles. Figure F.35 shows the progression of damage for this test from Phantom Camera One. Figure F.36 shows the progression of damage for this test from Phantom Camera Two. Figure F.37 shows the progression of damage for this test from Phantom Camera Three.

Figure F.34: Steel plate post test for Test 38

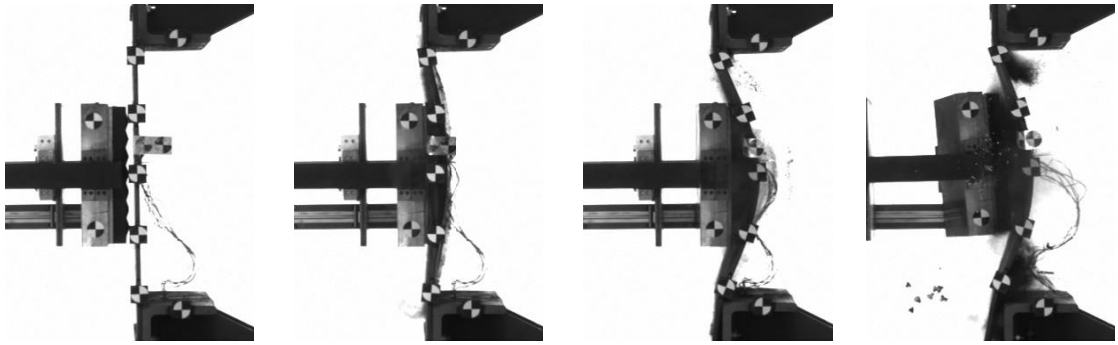

Figure F.35: Progression of damage for Test 38 from Camera 1

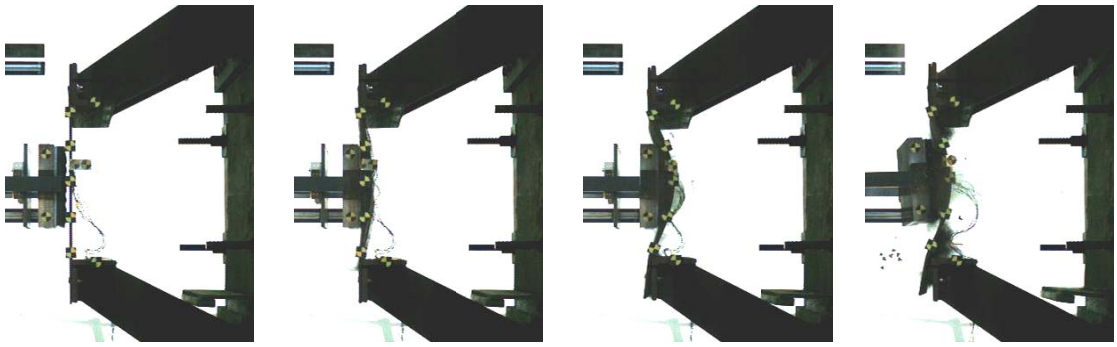

Figure F.36: Progression of damage for Test 38 from Camera 2

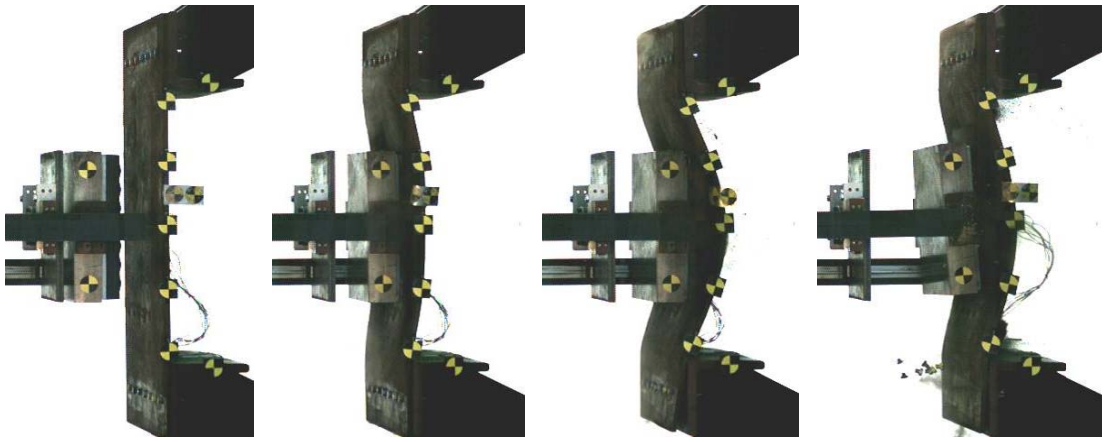

Figure F.37: Progression of damage for Test 38 from Camera 3

F.5 STEEL TOWER SINGLE PLATE: TEST 39 (SP39)

F.5.1 INTRODUCTION

The thirty-ninth test of the Steel Tower Single Plate test series was performed on March 7th, 2007. The test specimen was a 1/2" thick steel plate labeled SP39. The Impacting Mass 3 was placed flush with the push plate and accelerated by the BG with a target velocity upon impact with the specimen of 95.14 ft/sec (29 m/s). Figure F.38 shows the steel plate prior to impact.

Figure F.38: 1/2" thick steel plate pre test for Test 39

F.5.2 INSTRUMENTATION

F.5.2.1 PHANTOM CAMERAS

The first camera recorded in black and white at a rate of 10,000 frames per second at a resolution of 512x394. This camera was used in order to determine the maximum velocity of the impacting mass and the movement in the plate including the maximum displacement. The second camera recorded in color at a rate of 10,000 frames per second at a resolution of 512x394. This camera recorded the overall behavior of the test specimen. It was not used to gather any specific data. A picture from each of the camera locations are shown in Figure F.39.

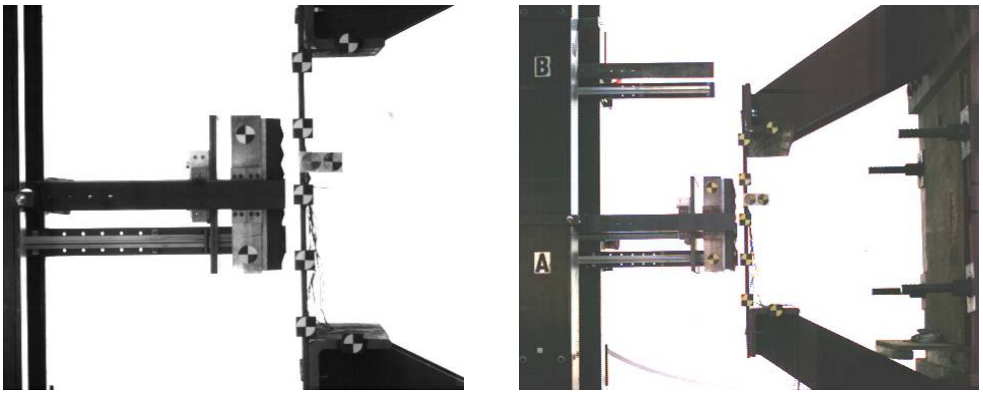

Figure F.39: Phantom Cameras for Test 39 a) Camera One b) Camera Two

F.5.2.2 TARGET LOCATIONS

Five targets were welded onto the side of the steel plate as shown in Figure F.38. They were spaced at the intervals shown in Figure F.40. That figure also shows the location of the targets for the impacting mass. An additional two targets were placed on the angle at the top and the bottom end conditions. The distance between these two points is 74.93 cm (29 ½”). There are additional targets for this test but their locations are irrelevant.

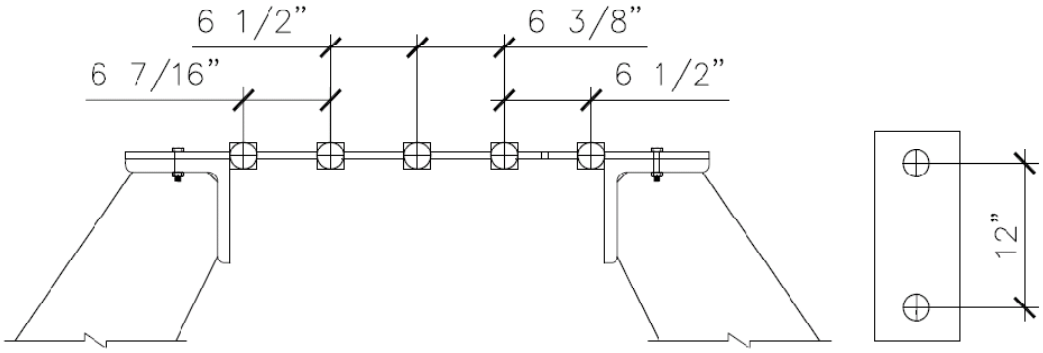

Figure F.40: Target layout on plate and impacting mass for Test 39

F.5.2.3 STRAIN GAGE LOCATIONS

For this test there were three strain gauges labeled 1, 6 and 7. The strain gauges, and their locations, are shown in Figure F.41. Table F.4 shows the specific information about this test, including the time and velocity at impact, if, and when, the bolts failed along with the maximum and minimum principal strain rates. The largest maximum principal strain rate for this test was 13.89 1/sec and was located at strain gage 1 while the largest minimum strain rate for this test was 12.39 1/sec located at strain gage 6. The maximum principal strains for gauges 1, 6 and 7 can be found in Figure F.42 and the minimum principal strains for the same gauges can be found in Figure F.43.

Table F.4: Stain rate information for Test 39

Strain Gage Number	Actual Velocity	Initial Impact	Shear Wave at Gage	Bolts Break	Maximum Principal Strain Rate	Minimum Principal Strain Rate
1	27.48 m/s	55.40 msec	-	63.30 msec	-13.89 1/sec	-8.86 1/sec
6	27.48 m/s	55.40 msec	-	63.30 msec	-7.89 1/sec	-12.39 1/sec
7	27.48 m/s	55.40 msec	-	63.30 msec	-11.58 1/sec	-9.61 1/sec

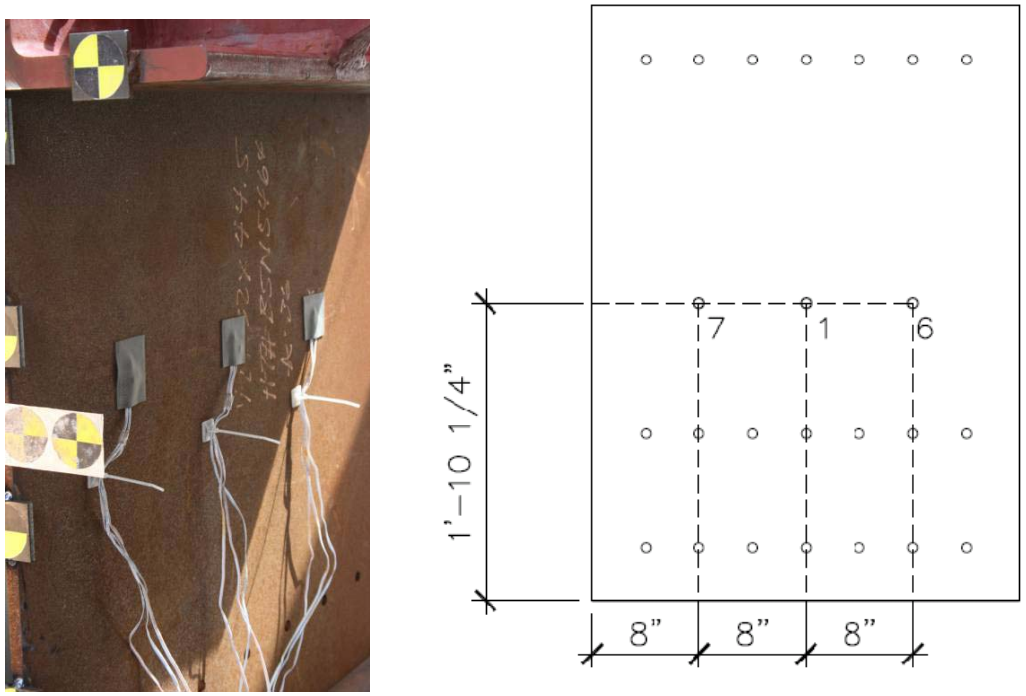

Figure F.41: Strain gage layout for Test 39

F.5.2.4 BOLT TYPE

A total of fourteen A307 bolts (Low Strength Bolts similar to Rivets) were used for this test. They were all tightened to a torque of 40 ft-lbs.

F.5.3 BLAST GENERATOR DATA

The initial impact of the single BG was 90.16 ft/sec (27.48 m/sec) with a goal velocity of 29 m/s. The average impact velocity for the impacting mass and the steel plate was calculated using the TEMA Track Eye tracking software.

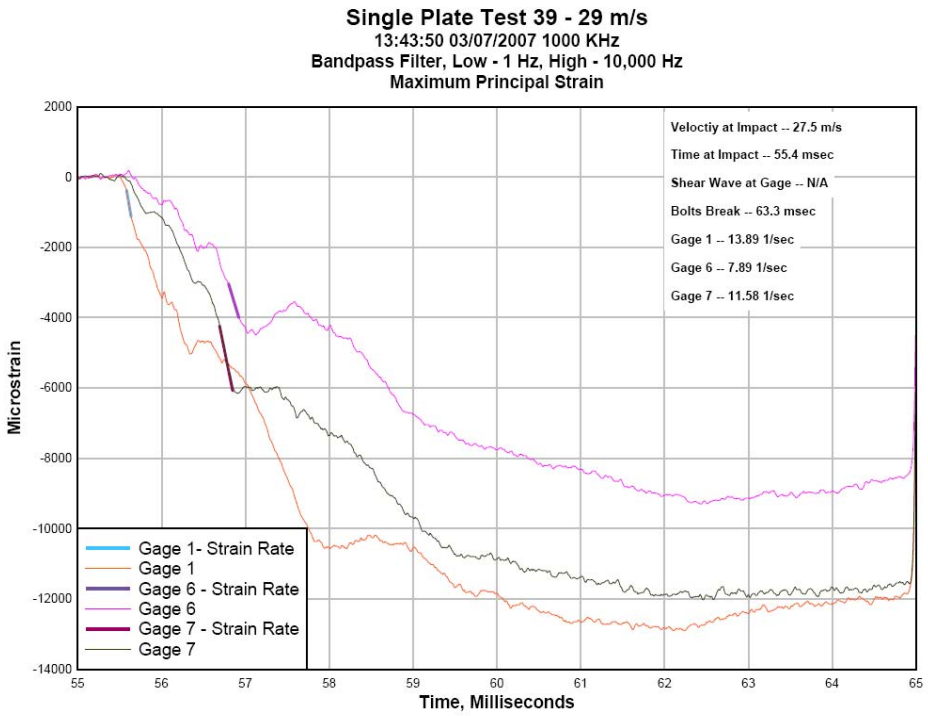

Figure F.42: Maximum principal strains and strain rates for Test 39

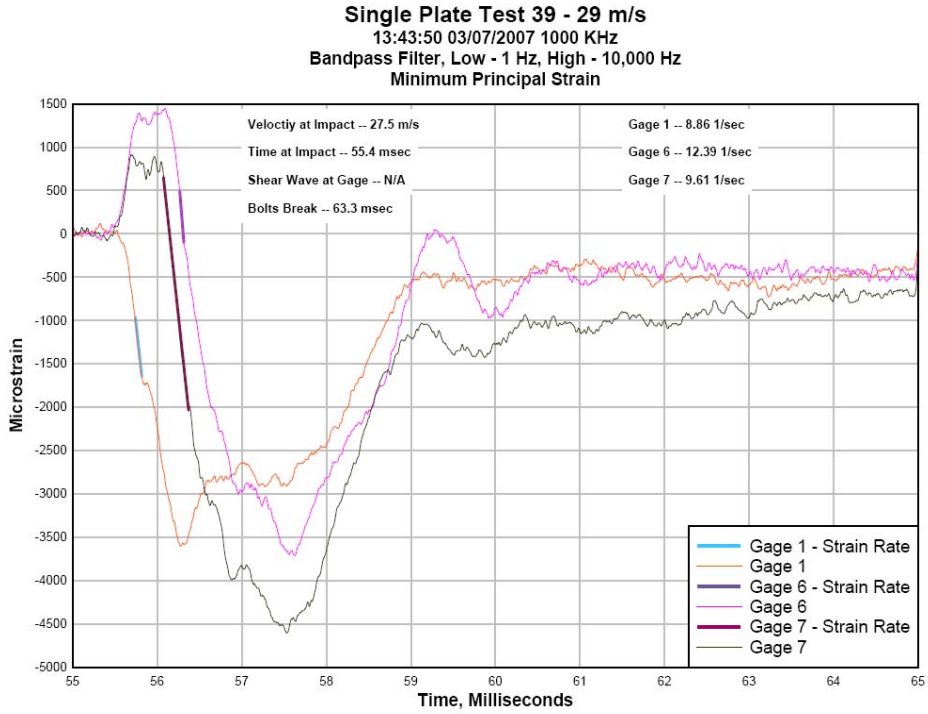

Figure F.43: Minimum principal strains and strain rates for Test 39

F.5.4 SPECIMEN BEHAVIOR

The loading of the BG plate imparted an initial velocity of 90.16 ft/sec (27.48 m/sec) to the specimen. This caused plate to deform in both directions. The longitudinal deflection (in the north-south direction) behaved in a typical one-way flexural shape. This test imparted enough energy to break the bottom seven bolts as shown in Figure F.44. The maximum dynamic deflection during the test was approximately 4 3/4". During the test two different phantom cameras were used to capture the failure modes from two different angles. Figure F.45 shows the progression of damage for this test from Phantom Camera One. Figure F.46 shows the progression of damage for this test from Phantom Camera Two.

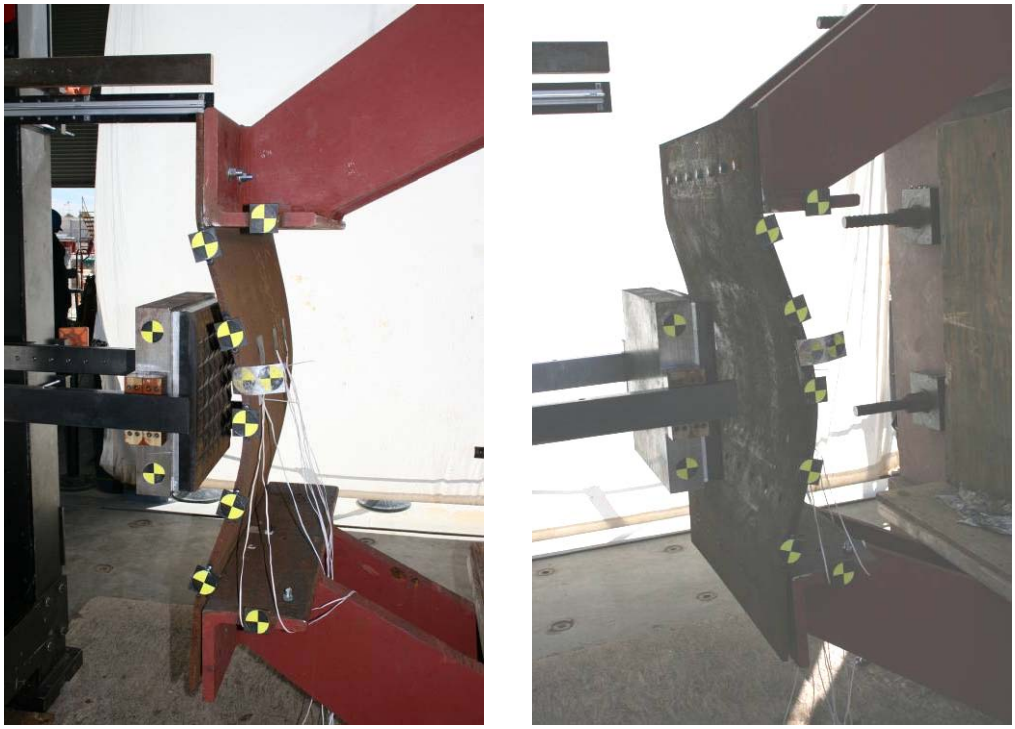

Figure F.44: Steel plate post test for Test 39

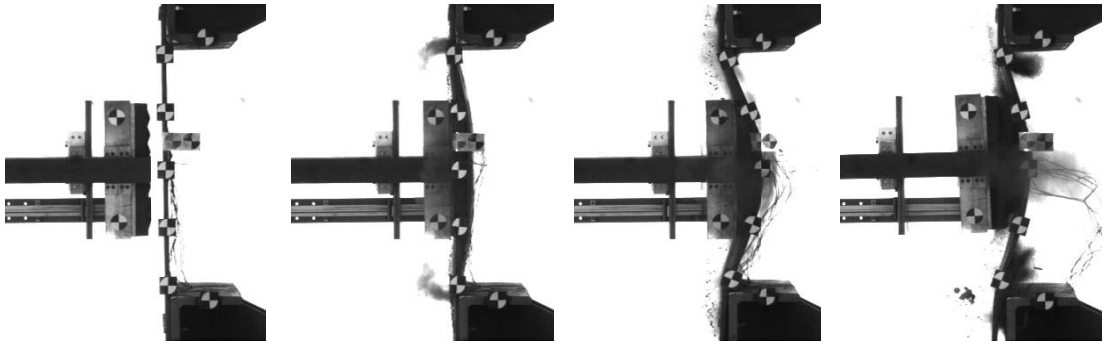

Figure F.45: Progression of damage for Test 39 from Camera 1

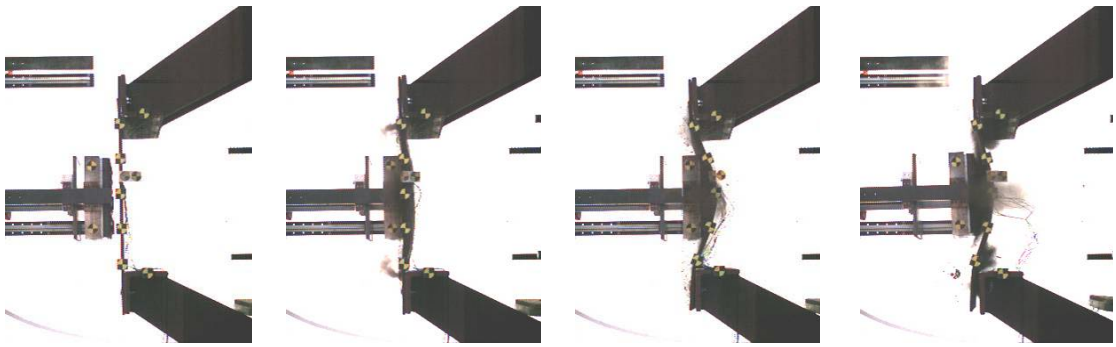

Figure F.46: Progression of damage for Test 39 from Camera 2

F.6 STEEL TOWER SINGLE PLATE: TEST 40 (SP40)

F.6.1 INTRODUCTION

The fortieth test of the Steel Tower Single Plate test series was performed on March 8th, 2007. The test specimen was a 1/4" thick steel plate labeled SP40. The Impacting Mass 3 was placed flush with the push plate and accelerated by the BG with a target velocity upon impact with the specimen of 68.90 ft/sec (21 m/s). Figure F.47 shows the steel plate prior to impact.

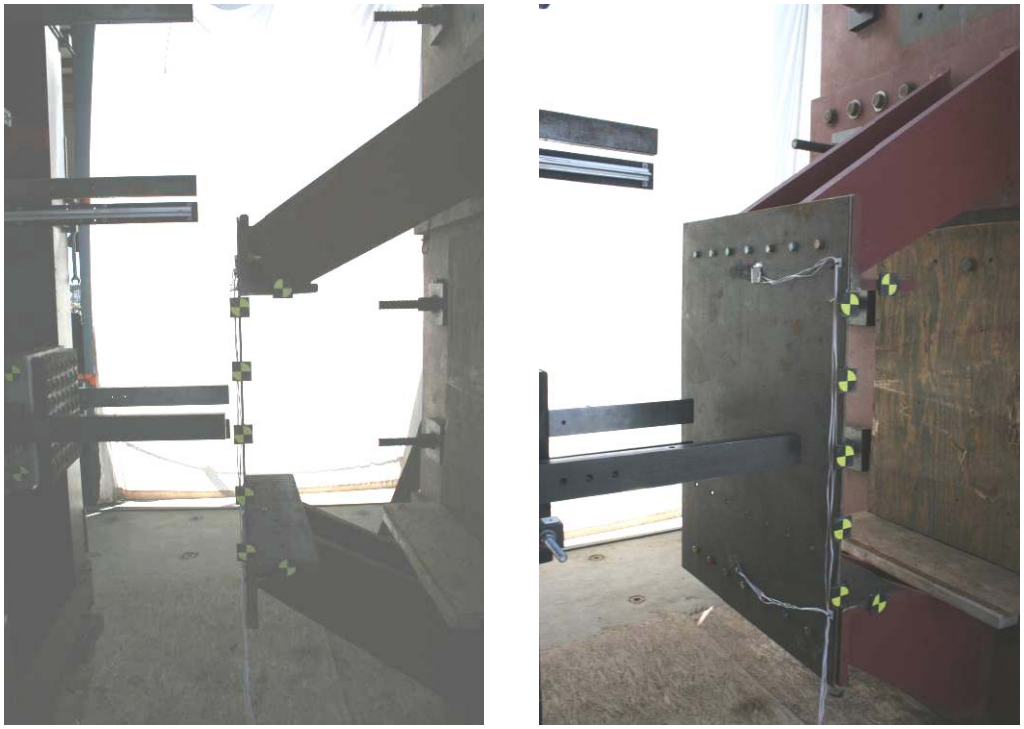

Figure F.47: 1/4" thick steel plate pre test for Test 40

F.6.2 INSTRUMENTATION

F.6.2.1 PHANTOM CAMERAS

The first camera recorded in black and white at a rate of 10,000 frames per second at a resolution of 512x384. This camera was used in order to determine the maximum velocity of the impacting mass and the movement in the plate including the maximum displacement. The second camera recorded in color at a rate of 10,000 frames per second at a resolution of 512x384. This camera recorded the overall behavior of the test specimen. It was not used to gather any specific data. The third camera recorded in color at a rate of 8,000 frames per second at a resolution of 480x480. This camera captured the failure of the bolts. A picture from each of the camera locations are shown in Figure F.48.

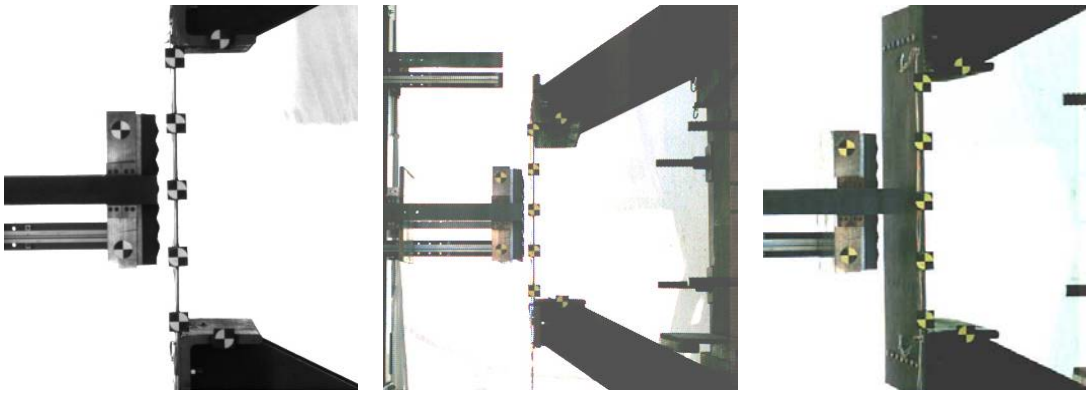

Figure F.48: Phantom Cameras for Test 40 a) Camera One b) Camera Two c) Camera Three

F.6.2.2 TARGET LOCATIONS

Five targets were welded onto the side of the steel plate as shown in Figure F.47. They were spaced at the intervals shown in Figure F.49. That figure also shows the location of the targets for the impacting mass. An additional two targets were placed on the angle at the top and the bottom end conditions. The distance between these two points is 74.93 cm (29 ½").

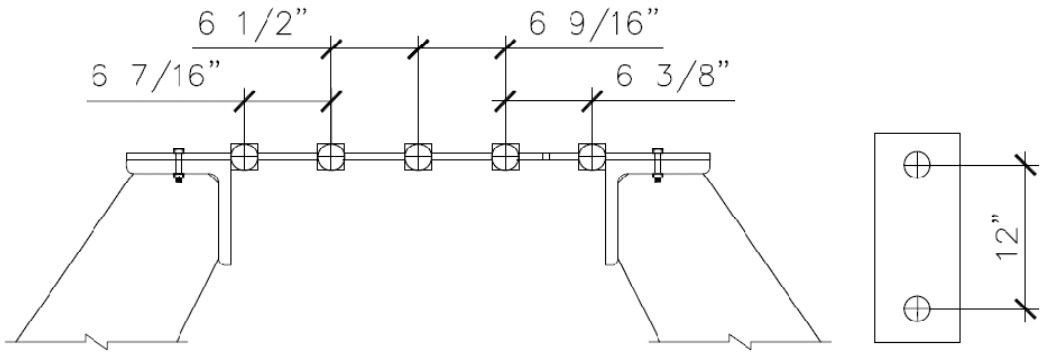

Figure F.49: Target layout on plate and impacting mass for Test 40

F.6.2.3 STRAIN GAGE LOCATIONS

For this test there were two strain gauges labeled 17 and 18. The strain gauges, and their locations, are shown in Figure F.50. Table F.5 shows the specific information about this test, including the time and velocity at impact, if, and when, the bolts failed along with the maximum and minimum principal strain rates. The largest maximum principal strain rate for this test was 6.22 1/sec and was located at strain gage 17 while the largest minimum strain rate for this test was 5.35 1/sec located at strain gage 17. The maximum principal strains for gauges 17 and 18 can be found in Figure F.51 and the minimum principal strains for the same gauges can be found in Figure F.52.

Table F.5: Stain rate information for Test 40

Strain Gage Number	Actual Velocity	Initial Impact	Shear Wave at Gage	Bolts Break	Maximum Principal Strain Rate	Minimum Principal Strain Rate
17	19.68 m/s	65.10 msec	69.00 msec	72.30 msec	5.59 1/sec	-5.35 1/sec
18	19.68 m/s	65.10 msec	69.00 msec	72.30 msec	6.22 1/sec	-2.84 1/sec

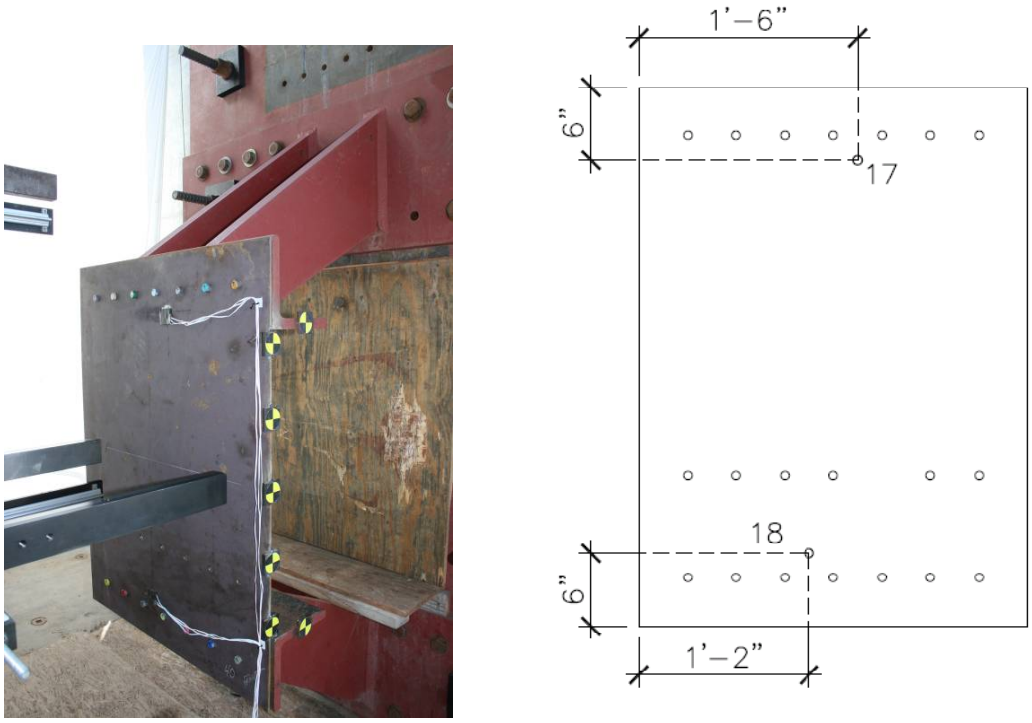

Figure F.50: Strain gage layout for Test 40

F.6.2.4 BOLT TYPE

A total of fourteen A307 bolts (Low Strength Bolts similar to Rivets) were used for this test. They were all tightened to a torque of 40 ft-lbs.

F.6.3 BLAST GENERATOR DATA

The initial impact of the single BG was 64.57 ft/sec (19.68 m/sec) with a goal velocity of 21 m/s. The average impact velocity for the impacting mass and the steel plate was calculated using the TEMA Track Eye tracking software.

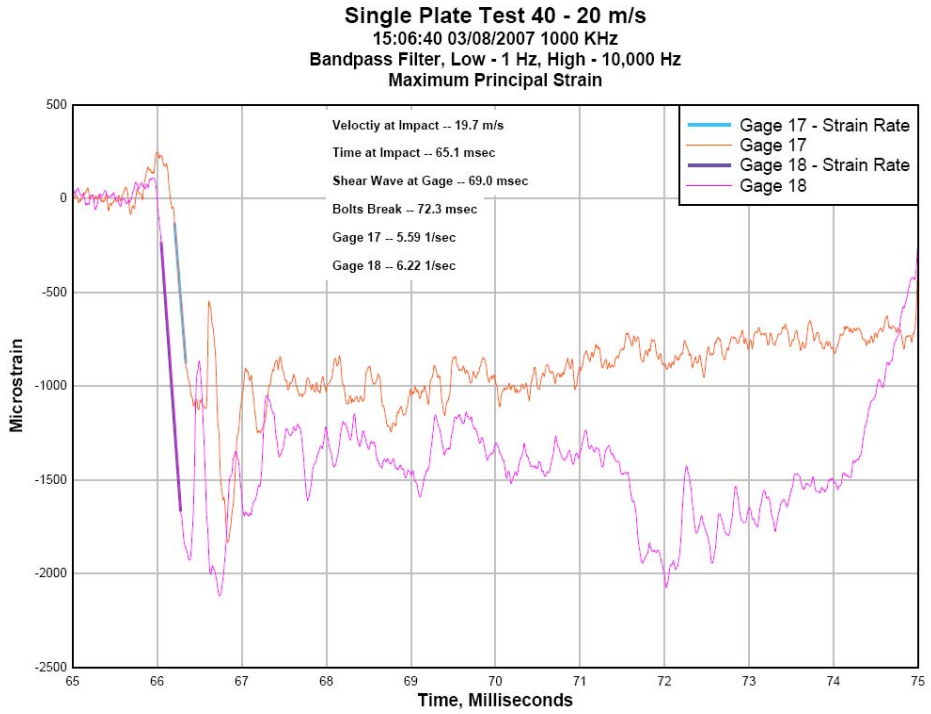

Figure F.51: Maximum principal strains and strain rates for Test 40

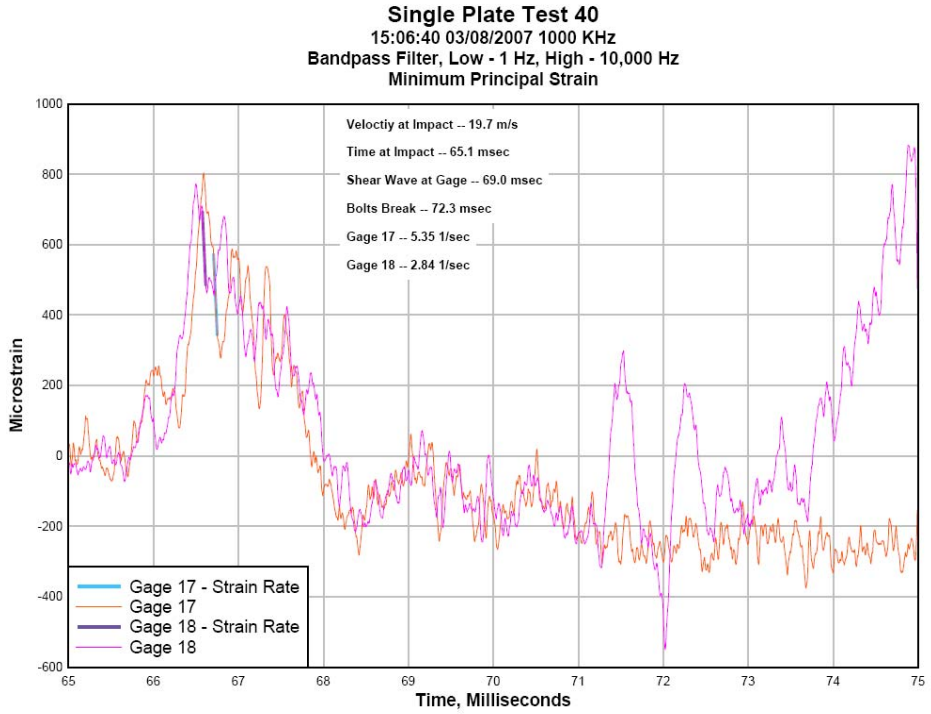

Figure F.52: Minimum principal strains and strain rates for Test 40

F.6.4 SPECIMEN BEHAVIOR

The loading of the BG plate imparted an initial velocity of 64.57 ft/sec (19.68 m/sec) to the specimen. This caused plate to deform in both directions. The longitudinal deflection (in the north-south direction) behaved in a typical one-way flexural shape. This test imparted enough energy to break the top seven bolts as shown in Figure F.53. Due to the flexibility of the ¼" plate the targets on the edge of the plate are not an accurate representation of the maximum dynamic deflection of the plate therefore the maximum dynamic deflection cannot be determined.

During the test three different phantom cameras were used to capture the failure modes from different angles. Figure F.54 shows the progression of damage for this test from Phantom Camera One. Figure F.55 shows the progression of damage for this test from Phantom Camera Two. Figure F.**56** shows the progression of damage for this test from Phantom Camera Three.

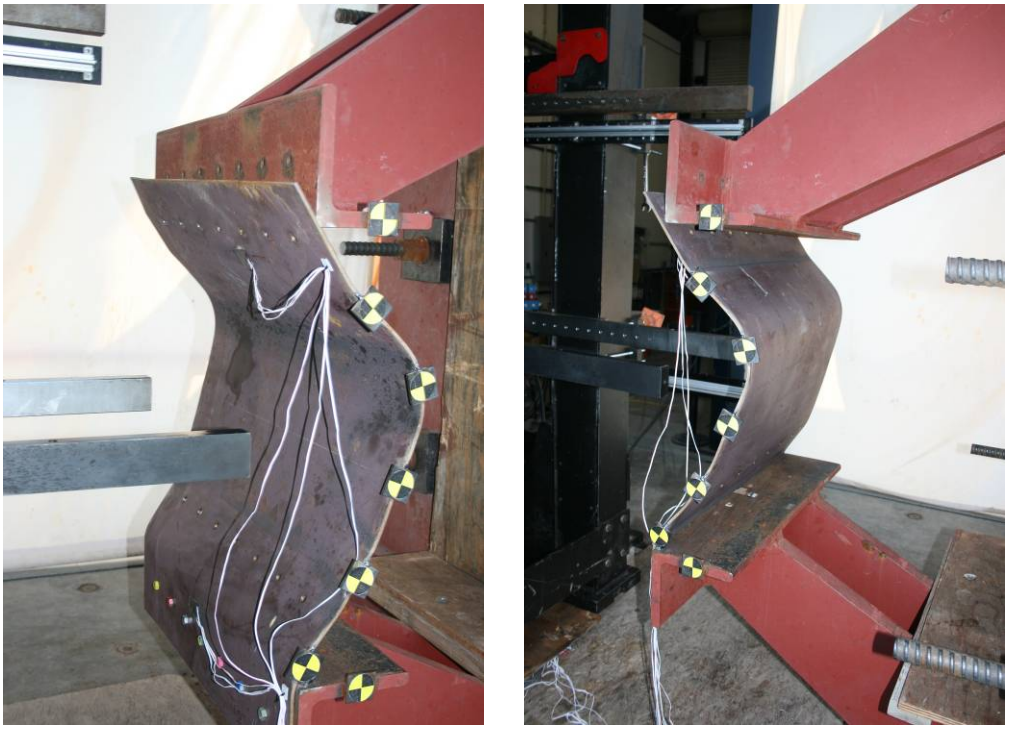

Figure F.53: Steel plate post test for Test 40

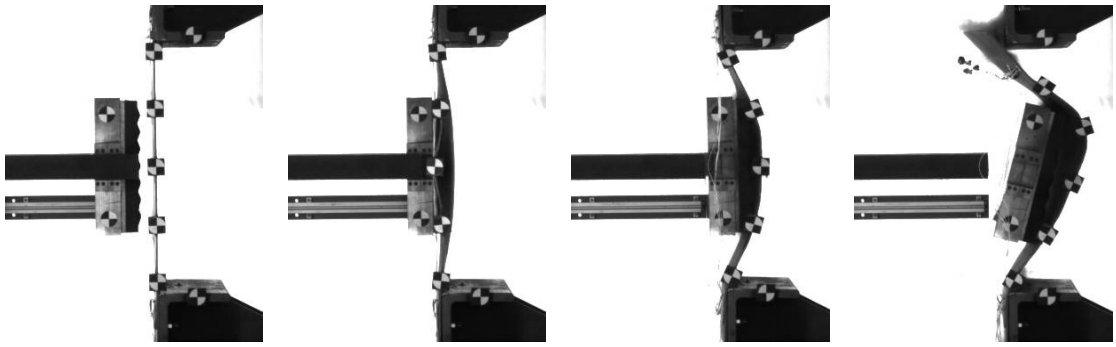

Figure F.54: Progression of damage for Test 40 from Camera 1

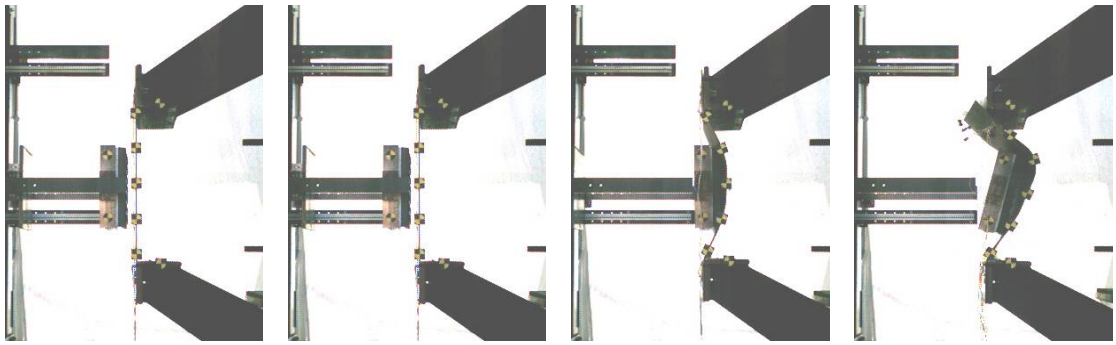

Figure F.55: Progression of damage for Test 40 from Camera 2

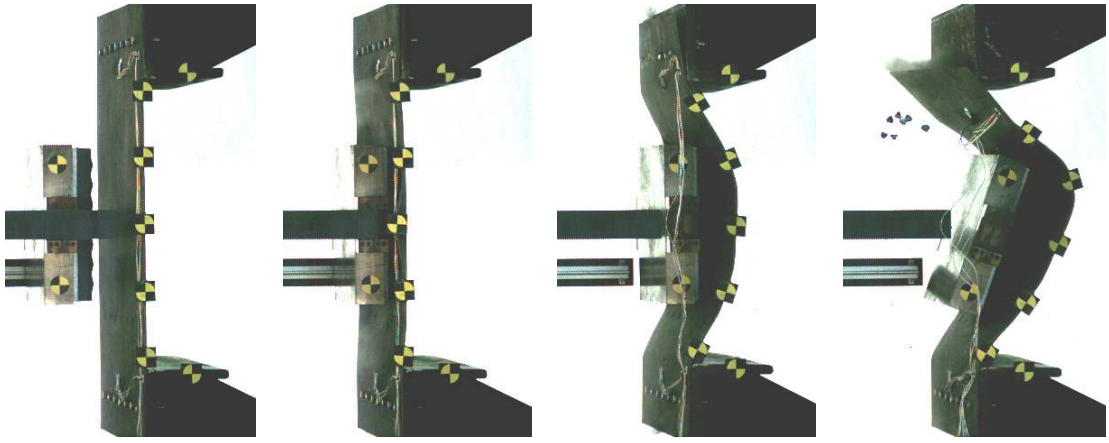

Figure F.56: Progression of damage for Test 40 from Camera 3

F.7 STEEL TOWER SINGLE PLATE: TEST 41 (SP41)

F.7.1 INTRODUCTION

The forty-first test of the Steel Tower Single Plate test series was performed on March 12th, 2007. The test specimen was a 1/4" thick steel plate labeled SP41. The Impacting Mass 3 was placed flush with the push plate and accelerated by the BG with a target velocity upon impact with the specimen of 68.90 ft/sec (21 m/s). Figure F.57 shows the steel plate prior to impact.

F.7.2 KINETIC ENERGY DEFEAT DEVICE (KEDD)

For this test a KEDD filled with cones of sand was used as discussed in Section 2.2. The device is shown in Figure F.57. The impacting mass does not extend the whole height of the KEDD and so it will not interfere with the support structure that the KEDD is sitting on.

Figure F.57: 1/4" thick steel plate and KEDD pre test for Test 41

F.7.3 INSTRUMENTATION

F.7.3.1 PHANTOM CAMERAS

The first camera recorded in black and white at a rate of 10,000 frames per second at a resolution of 512x384. This camera was used in order to determine the maximum velocity of the impacting mass and the movement in the plate including the maximum displacement. The second camera recorded in color at a rate of 10,000 frames per second at a resolution of 512x384. This camera recorded the overall behavior of the test specimen. It was not used to gather any specific data. The third camera recorded in color at a rate of 8,000 frames per

second at a resolution of 480x480. This camera captured the failure of the bolts. A picture from each of the camera locations are shown in Figure F.58.

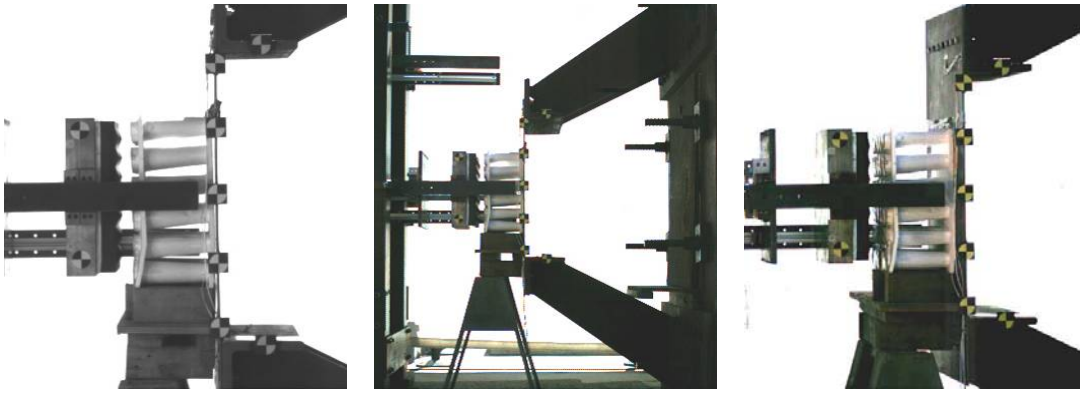

Figure F.58: Phantom Cameras for Test 41 a) Camera One b) Camera Two c) Camera Three

F.7.3.2 TARGET LOCATIONS

Five targets were welded onto the side of the steel plate as shown in Figure F.57. They were spaced at the intervals shown in Figure F.59. That figure also shows the location of the targets for the impacting mass. An additional two targets were placed on the angle at the top and the bottom end conditions. The distance between these two points is 74.93 cm (29 ½").

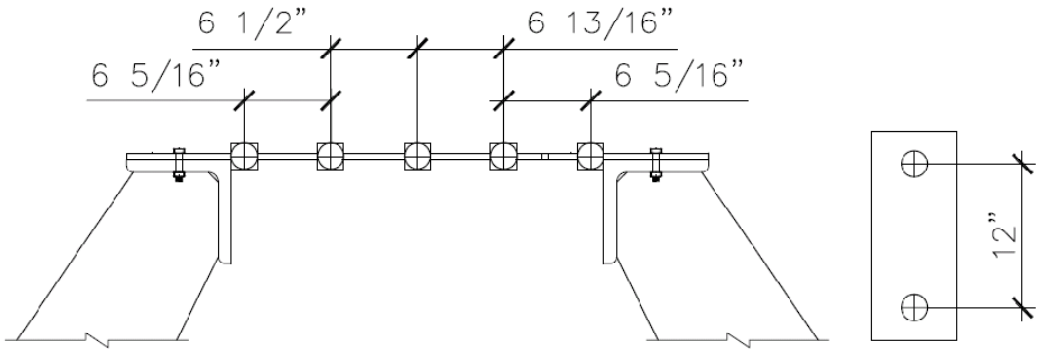

Figure F.59: Target layout on plate and impacting mass for Test 41

F.7.3.3 STRAIN GAGE LOCATIONS

For this test there were two strain gauges labeled 17 and 18. The strain gauges, and their locations, are shown in Figure F.60. Table F.6 shows the specific information about this test, including the time and velocity at impact, if, and when, the bolts failed along with the maximum and minimum principal strain rates. The largest maximum principal strain rate for this test was 2.52 1/sec and was located at strain gage 18 while the largest minimum strain rate for this test was 0.89 1/sec located at strain gage 17. The maximum principal strains for

gauges 17 and 18 can be found in Figure F.61 and the minimum principal strains for the same gauges can be found in Figure F.62.

Table F.6: Stain rate information for Test 41

Strain Gage Number	Actual Velocity	Initial Impact	Shear Wave at Gage	Bolts Break	Maximum Principal Strain Rate	Minimum Principal Strain Rate
17	20.16 m/s	53.30 msec	65.90 msec	70.75 msec	-1.12 1/sec	-0.89 1/sec
18	20.16 m/s	53.30 msec	65.90 msec	70.75 msec	2.52 1/sec	0.77 1/sec

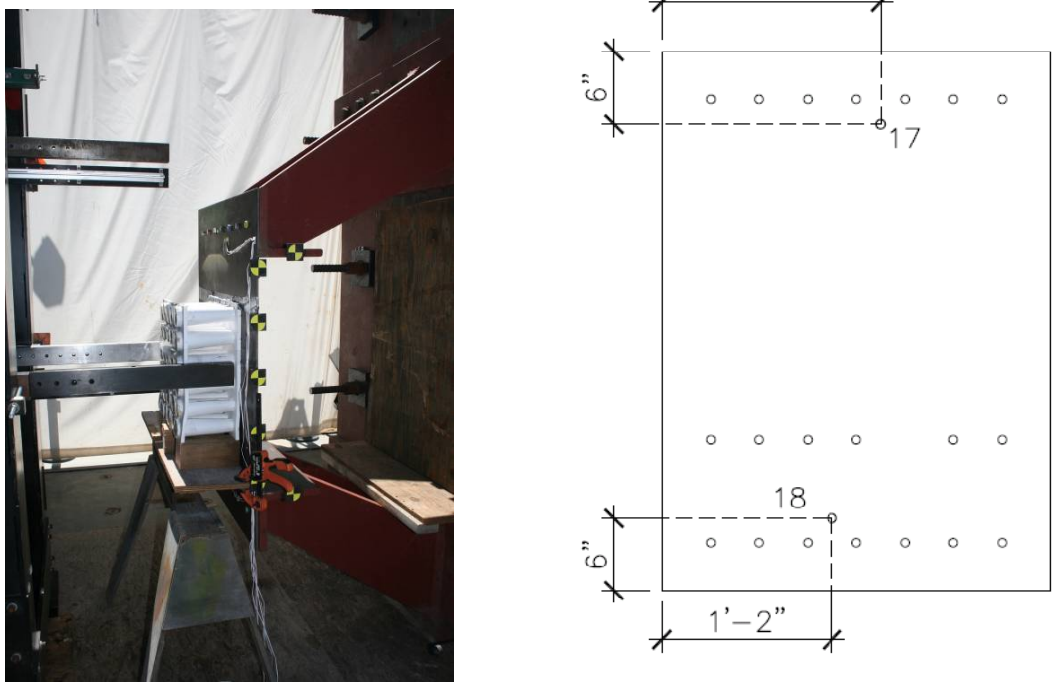

Figure F.60: Strain gage layout for Test 41

F.7.3.4 BOLT TYPE

A total of fourteen A307 bolts (Low Strength Bolts similar to Rivets) were used for this test. They were all tightened to a torque of 40 ft-lbs.

F.7.4 BLAST GENERATOR DATA

The initial impact of the single BG was 66.14 ft/sec (20.16 m/sec) with a goal velocity of 21 m/s. The average impact velocity for the impacting mass and the steel plate was calculated using the TEMA Track Eye tracking software.

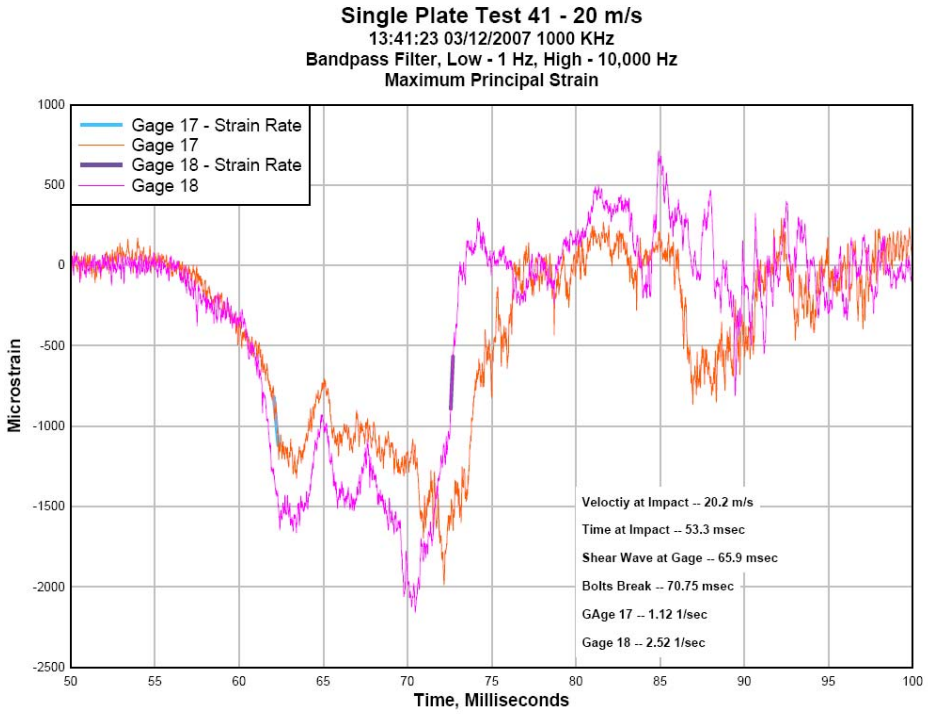

Figure F.61: Maximum principal strains and strain rates for Test 41

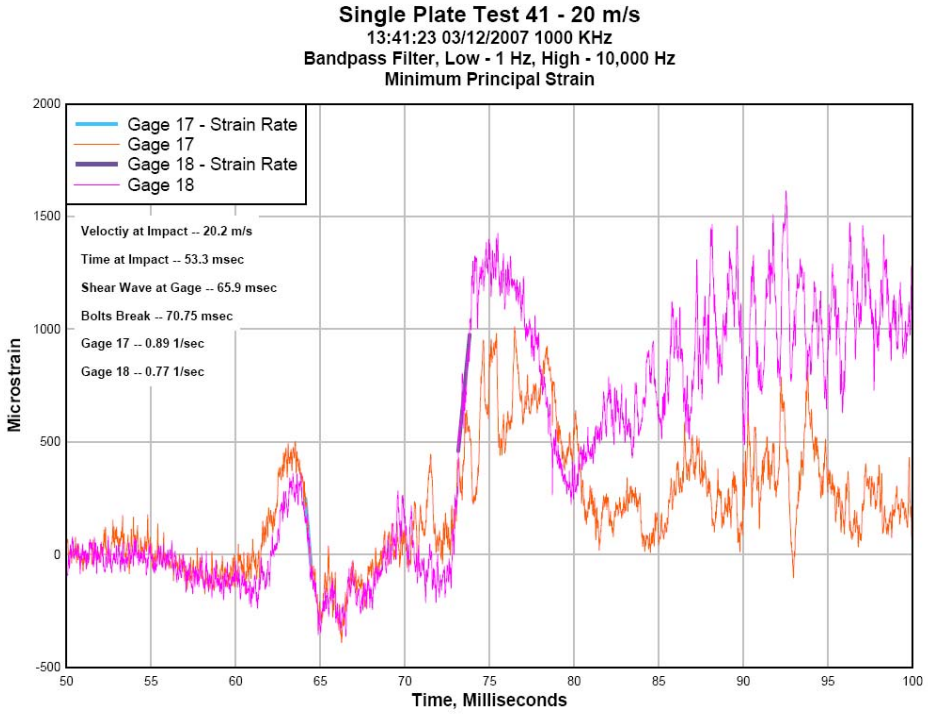

Figure F.62: Minimum principal strains and strain rates for Test 41

F.7.5 BLAST GENERATOR DATA

The loading of the BG plate imparted an initial velocity of 66.14 ft/sec (20.16 m/sec) to the Kinetic Energy Defeat Device (KEDD). This caused plate to deform in both directions. The longitudinal deflection (in the north-south direction) behaved in a typical one-way flexural shape. This test imparted enough energy to break all fourteen bolts as shown in Figure F.63. Due to the flexibility of the ¼" plate and the mass of sand obscuring the cameras, the targets on the edge of the plate were not able to capture the maximum dynamic deflection of the plate.

During the test three different phantom cameras were used to capture the failure modes from three different angles. Figure F.64 shows the progression of damage for this test from Phantom Camera One. Figure F.65 shows the progression of damage for this test from Phantom Camera Two. Figure F.66 shows the progression of damage for this test from Phantom Camera Three.

Figure F.63: Steel plate post test for Test 41

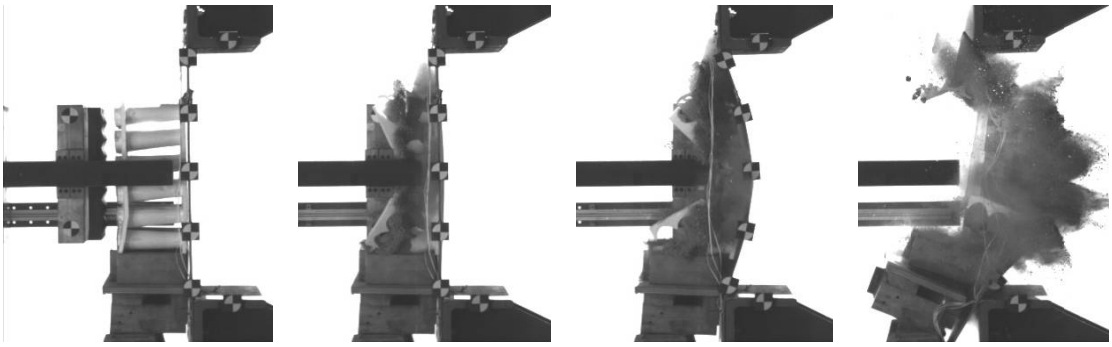

Figure F.64: Progression of damage for Test 41 from Camera 1

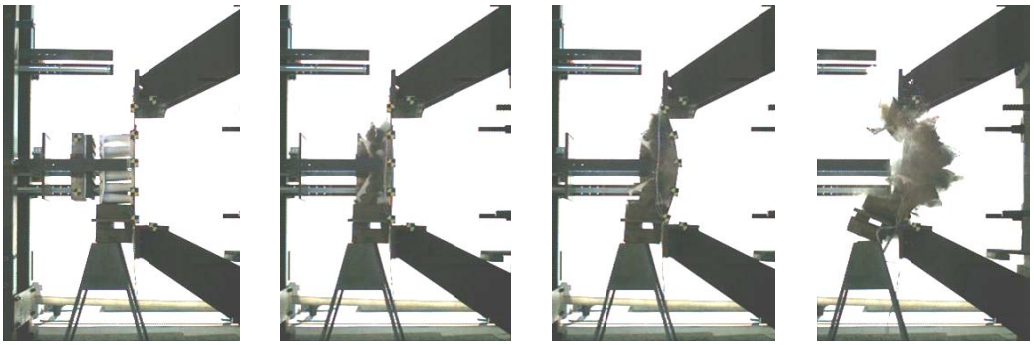

Figure F.65: Progression of damage for Test 41 from Camera 2

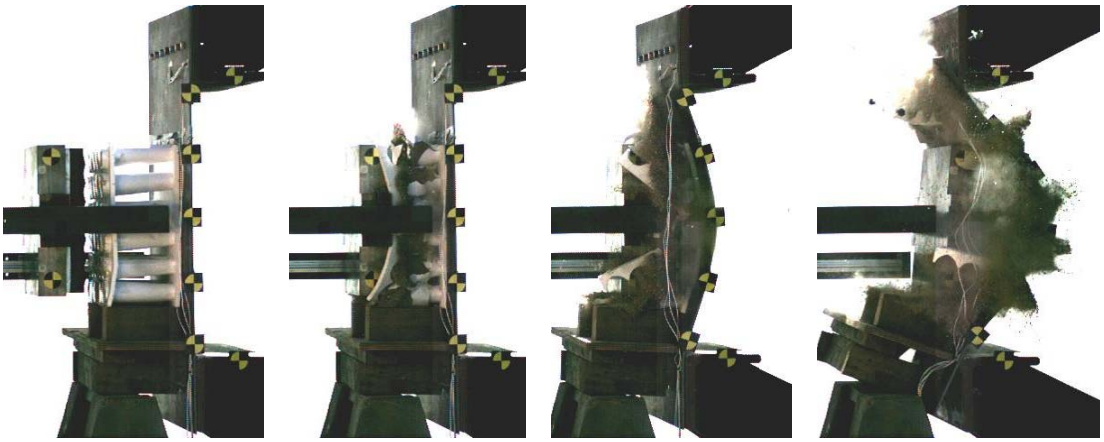

Figure F.66: Progression of damage for Test 41 from Camera 3

F.8 STEEL TOWER SINGLE PLATE: TEST 42 (SP42)

F.8.1 INTRODUCTION

The forty-second test of the Steel Tower Single Plate test series was performed on March 13th, 2007. The test specimen was a 1/4" thick steel plate labeled SP42. The Impacting Mass 3 was placed flush with the push plate and accelerated by the BG with a target velocity upon impact with the specimen of 68.90 ft/sec (21 m/s). Figure F.57 shows the steel plate prior to impact.

F.8.2 KINETIC ENERGY DEFEAT DEVICE (KEDD)

For this test a KEDD filled with bottles of water was used as discussed in Section 2.2. The device is shown in Figure F.67. The impacting mass does not extend the whole height of the KEDD and so it will not interfere with the support structure that the KEDD is sitting on.

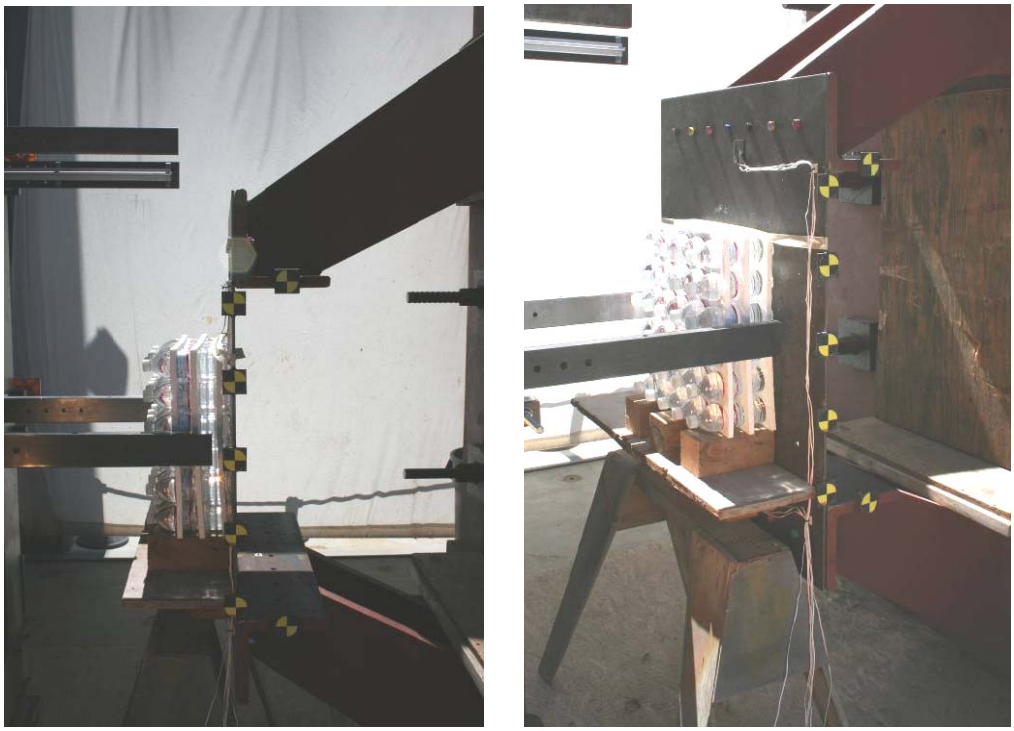

Figure F.67: 1/4" thick steel plate and KEDD pre test for Test 42

F.8.3 INSTRUMENTATION

F.8.3.1 PHANTOM CAMERAS

The first camera recorded in black and white at a rate of 10,000 frames per second at a resolution of 512x384. This camera was used in order to determine the maximum velocity of the impacting mass and the movement in the plate including the maximum displacement. The second camera recorded in color at a rate of 10,000 frames per second at a resolution of 512x384. This camera recorded the overall behavior of the test specimen. It was not used to gather any specific data. The third camera recorded in color at a rate of 8,000 frames per

second at a resolution of 480x480. This camera captured the failure of the bolts. A picture from each of the camera locations are shown in Figure F.68.

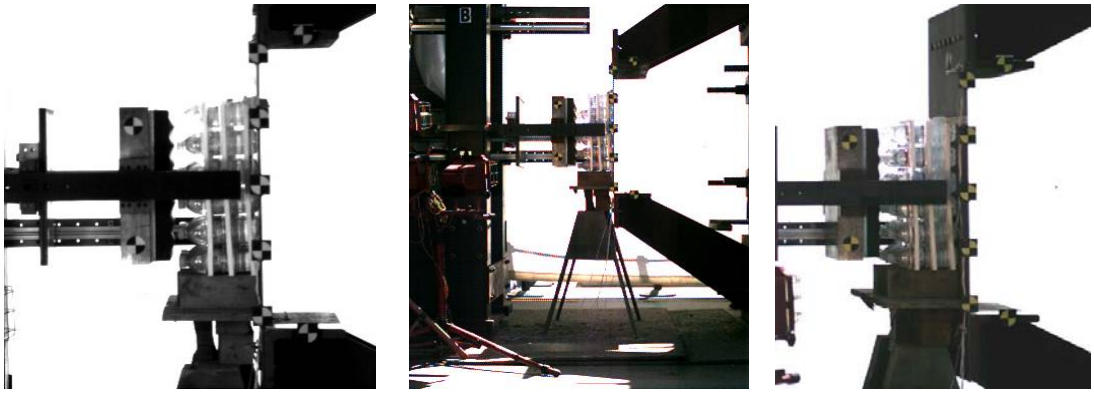

Figure F.68: Phantom Cameras for Test 42 a) Camera One b) Camera Two c) Camera Three

F.8.3.2 TARGET LOCATIONS

Five targets were welded onto the side of the steel plate as shown in Figure F.67. They were spaced at the intervals shown in Figure F**.69**. That figure also shows the location of the targets for the impacting mass. An additional two targets were placed on the angle at the top and the bottom end conditions. The distance between these two points is 74.93 cm (29 ½").

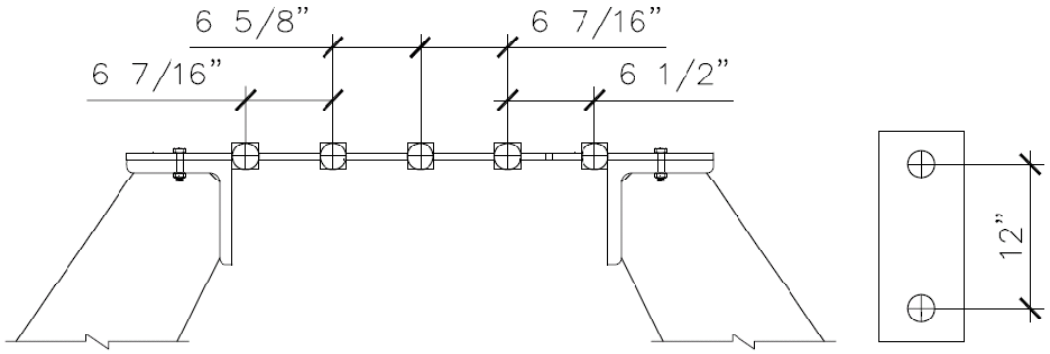

Figure F.69: Target layout on plate and impacting mass for Test 42

F.8.4 STRAIN GAGE LOCATIONS

For this test there were two strain gauges labeled 17, and 18. The strain gauges, and their locations, are shown in Figure F**.70**. Table F.7 shows the specific information about this test, including the time and velocity at impact, if, and when, the bolts failed along with the maximum and minimum principal strain rates. The largest maximum principal strain rate for this test was 2.05 1/sec and was located at strain gage 18 while the largest minimum strain rate for this test was 2.73 1/sec located at strain gage 18. The maximum principal strains for

gauges 17 and 18 can be found in Figure F.71 and the minimum principal strains for the same gauges can be found in Figure F.72.

Table F.7: Stain rate information for Test 42

Strain Gage Number	Actual Velocity	Initial Impact	Shear Wave at Gage	Bolts Break	Maximum Principal Strain Rate	Minimum Principal Strain Rate
17	19.81 m/s	55.10 msec	-	-	-0.80 1/sec	-0.36 1/sec
18	19.81 m/s	55.10 msec	-	-	-2.05 1/sec	2.73 1/sec

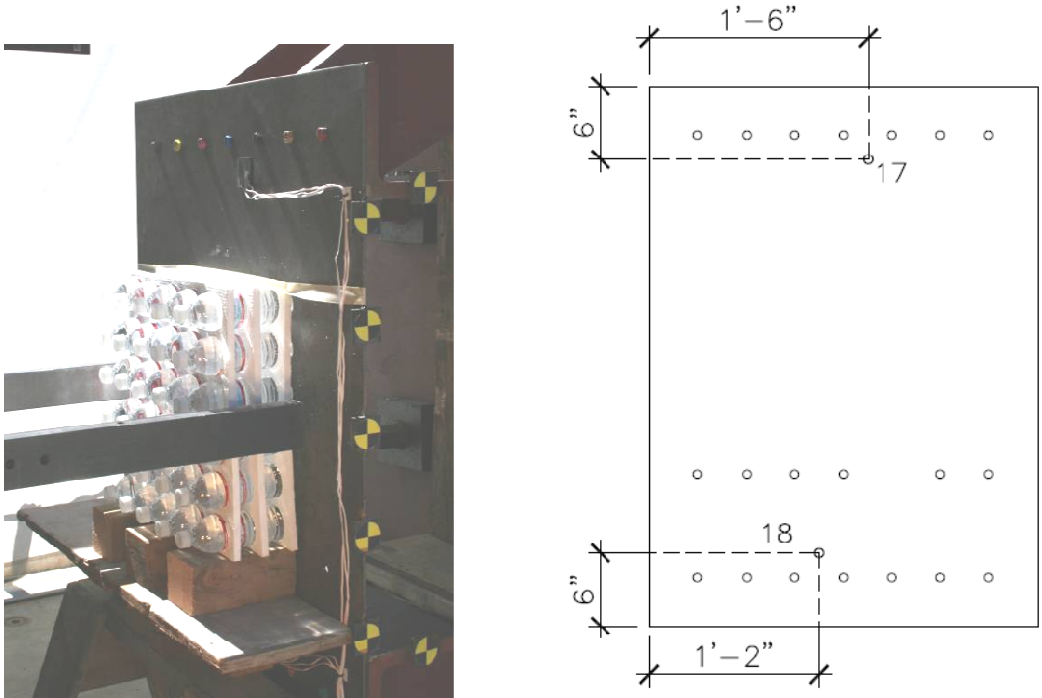

Figure F.70: Strain gage layout for Test 42

F.8.4.1 BOLT TYPE

A total of fourteen A307 bolts (Low Strength Bolts similar to Rivets) were used for this test. They were all tightened to a torque of 40 ft-lbs.

F.8.5 BLAST GENERATOR DATA

The initial impact of the single BG was 64.99 ft/sec (19.81 m/sec) with a goal velocity of 21 m/s. The average impact velocity for the impacting mass and the steel plate was calculated using the TEMA Track Eye tracking software.

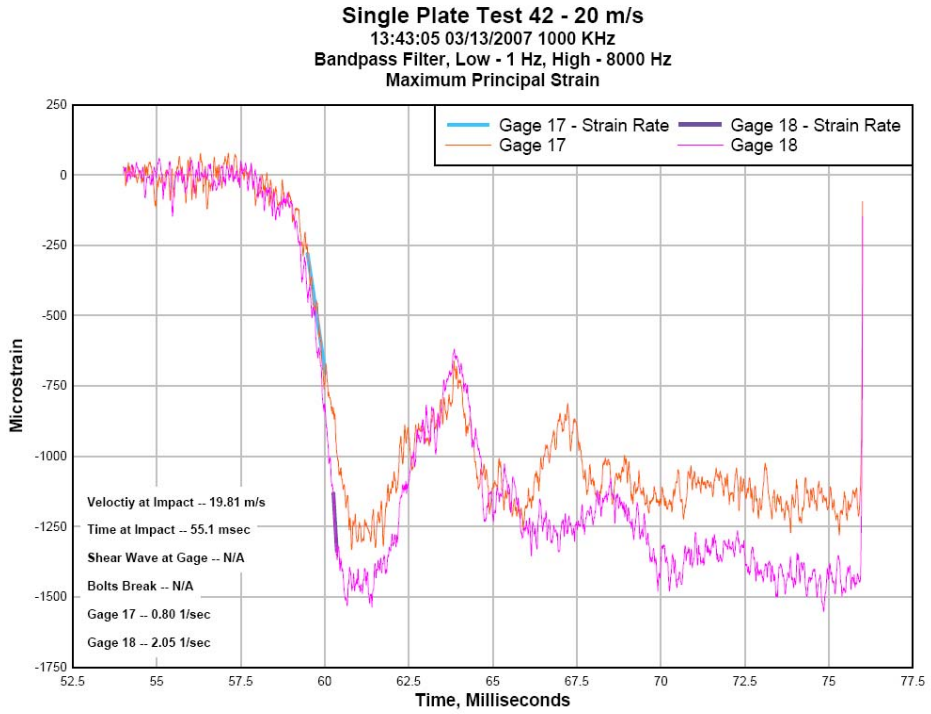

Figure F.71: Maximum principal strains and strain rates for Test 42

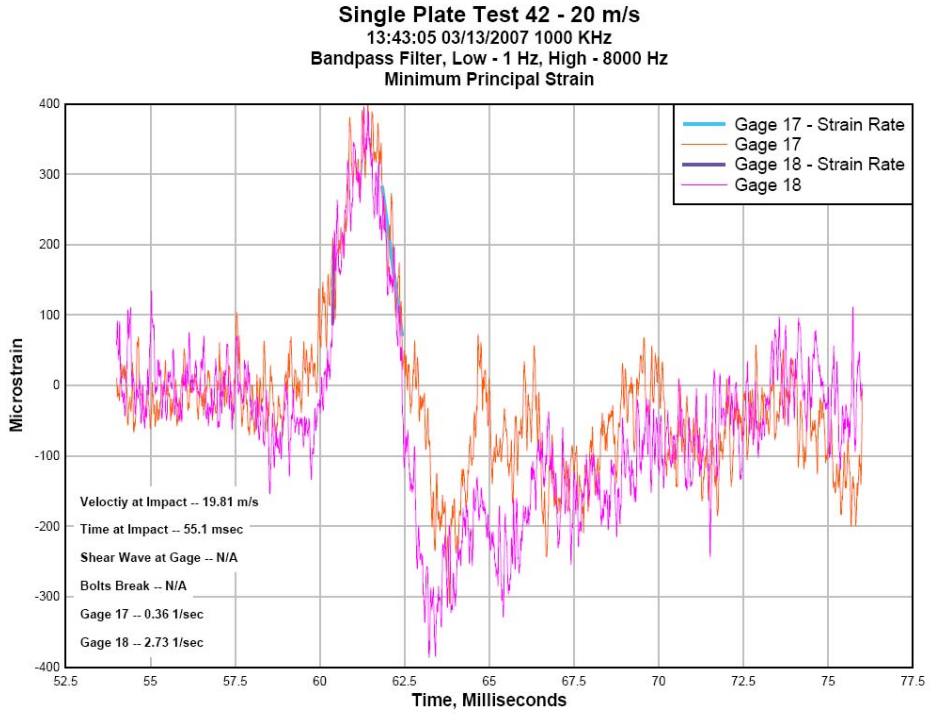

Figure F.72: Minimum principal strains and strain rates for Test 42

F.8.6 BLAST GENERATOR DATA

The loading of the BG plate imparted an initial velocity of 64.99 ft/sec (19.81 m/sec) to the Kinetic Energy Defeat Device (KEDD). This caused the plate to deform in both directions. The longitudinal deflection (in the north-south direction) behaved in a typical one-way flexural shape. This test did not impart enough energy to break any of the bolts as shown in Figure F.73. Due to the flexibility of the ¼" plate and the mass of water obscuring the cameras, the targets on the edge of the plate were not able to capture the maximum dynamic deflection of the plate. The residual deflection of the plate after the test at the midpoint was 2 5/16". The force of the jetting from the KEDD was strong enough to rip down the white background that was placed behind the test specimen.

During the test three different phantom cameras were used to capture the failure modes from three different angles. Figure F.74 shows the progression of damage for this test from Phantom Camera One. Figure F.75 shows the progression of damage for this test from Phantom Camera Two. Figure F.76 shows the progression of damage for this test from Phantom Camera Three.

Figure F.73: Steel plate post test for Test 42

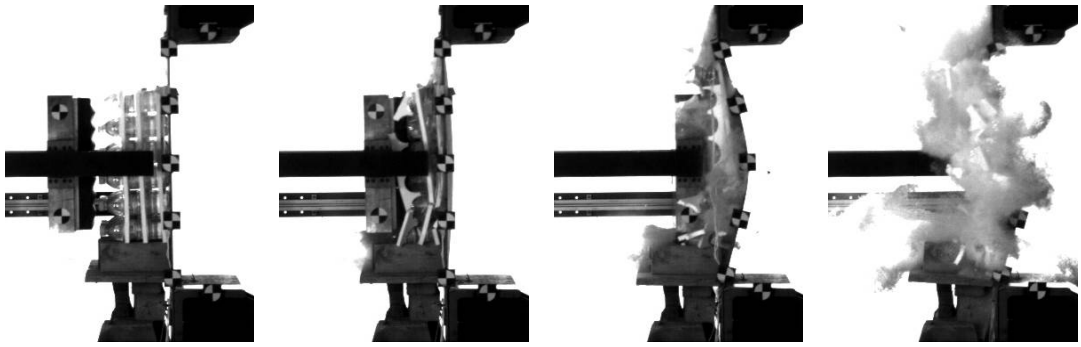

Figure F.74: Progression of damage for Test 42 from Camera 1

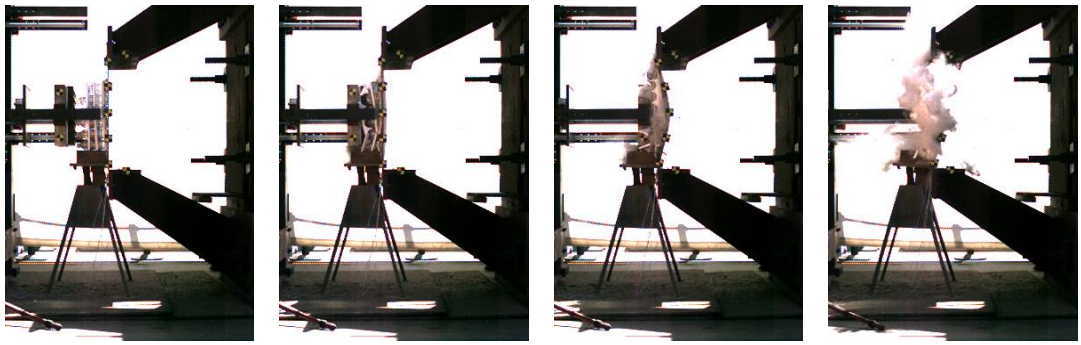

Figure F.75: Progression of damage for Test 42 from Camera 2

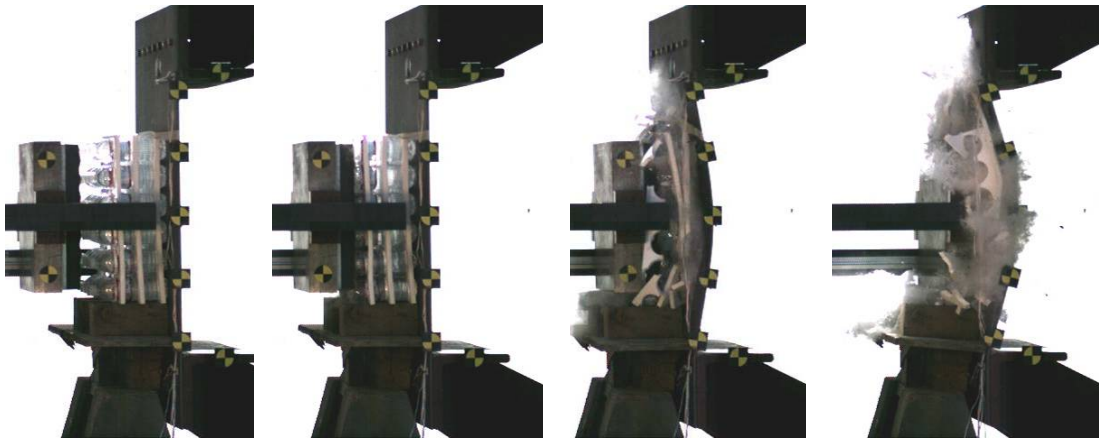

Figure F.76: Progression of damage for Test 42 from Camera 3

F.9 STEEL TOWER SINGLE PLATE: TEST 43 (SP43)

F.9.1 INTRODUCTION

The forty-third test of the Steel Tower Single Plate test series was performed on March 14th, 2007. The test specimen was a 1/4" thick steel plate labeled SP43. The Impacting Mass 3 was placed flush with the push plate and accelerated by the BG with a target velocity upon impact with the specimen of 63.98 ft/sec (19.5 m/s). Figure F.77 shows the steel plate prior to impact.

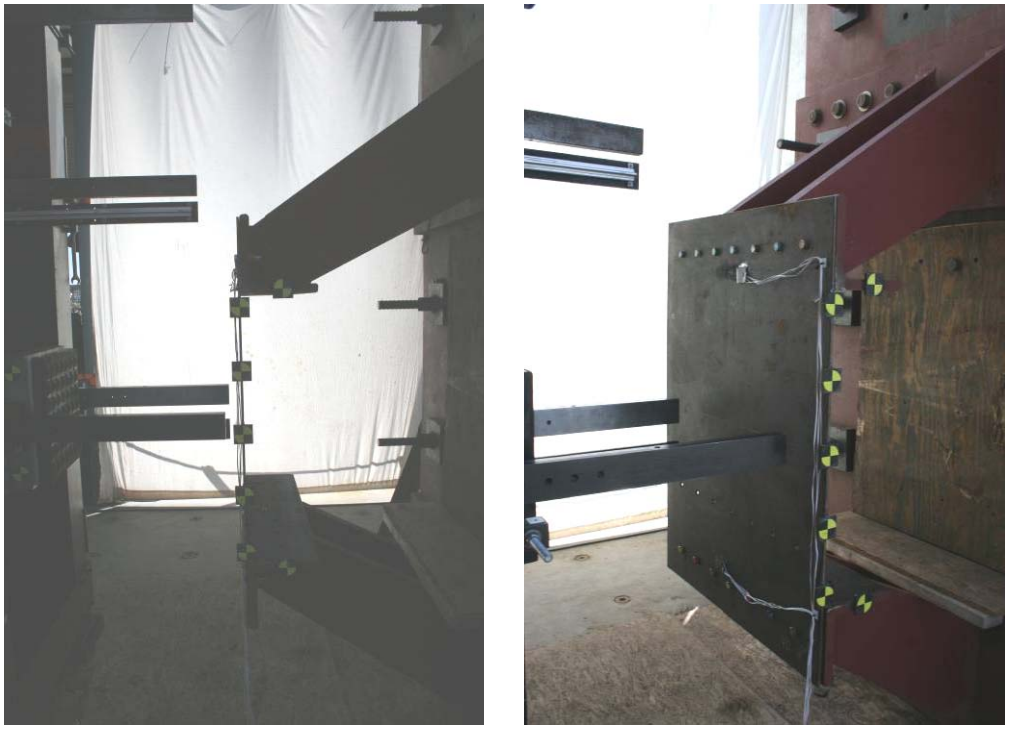

Figure F.77: 1/4" thick steel plate pre test for Test 43

F.9.2 INSTRUMENTATION

F.9.2.1 PHANTOM CAMERAS

The first camera recorded in color at a rate of 10,000 frames per second at a resolution of 512x384. This camera was used in order to determine the maximum velocity of the impacting mass and the movement in the plate including the maximum displacement. The second camera recorded in color at a rate of 8,000 frames per second at a resolution of 480x480. This camera captured the failure of the bolts. A picture from each of the camera locations are shown in Figure F.78.

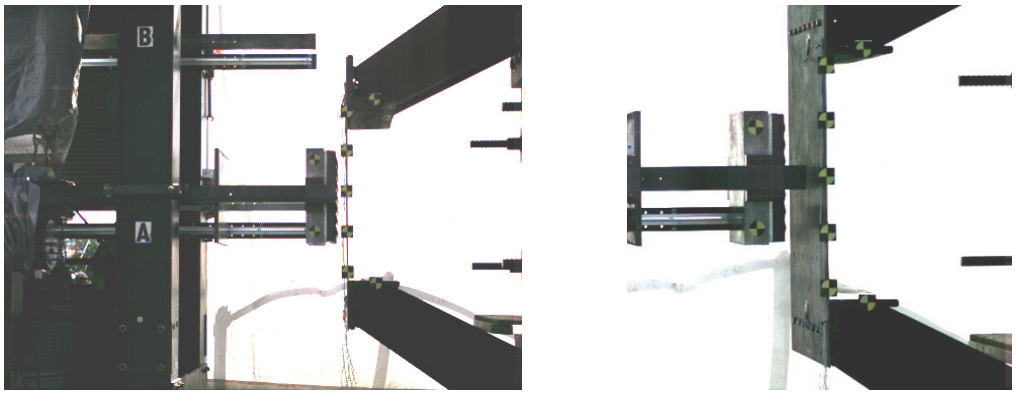

Figure F.78: Phantom Cameras for Test 43 a) Camera One b) Camera Two

F.9.2.2 TARGET LOCATIONS

Five targets were welded onto the side of the steel plate as shown in Figure F.77. They were spaced at the intervals shown in Figure F.79. That figure also shows the location of the targets for the impacting mass. An additional two targets were placed on the angle at the top and the bottom end conditions. The distance between these two points is 74.93 cm (29 ½").

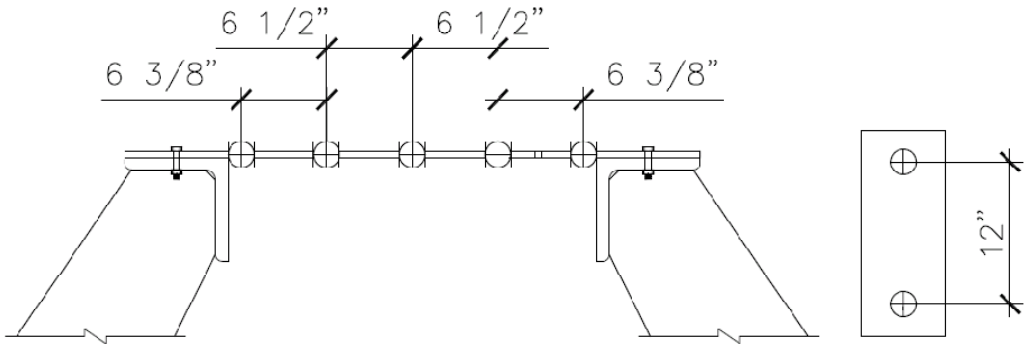

Figure F.79: Target layout on plate and impacting mass for Test 43

F.9.2.3 STRAIN GAGE LOCATIONS

For this test there were two strain gauges labeled 17 and 18. The strain gauges, and their locations, are shown in Figure F.80. Table F.8 shows the specific information about this test, including the time and velocity at impact, if, and when, the bolts failed along with the maximum and minimum principal strain rates. The largest maximum principal strain rate for this test was 10.14 1/sec and was located at strain gage 18 while the largest minimum strain rate for this test was 6.81 1/sec located at strain gage 17. The maximum principal strains for gauges 17 and 18 can be found in Figure F.81 and the minimum principal strains for the same gauges can be found in Figure F.82.

Table F.8: Stain rate information for Test 43

Strain Gage Number	Actual Velocity	Initial Impact	Shear Wave at Gage	Bolts Break	Maximum Principal Strain Rate	Minimum Principal Strain Rate
17	19.87 m/s	64.50 msec	66.38 msec	71.50 msec	8.06 1/sec	6.81 1/sec
18	19.87 m/s	64.50 msec	66.38 msec	71.50 msec	10.14 1/sec	4.66 1/sec

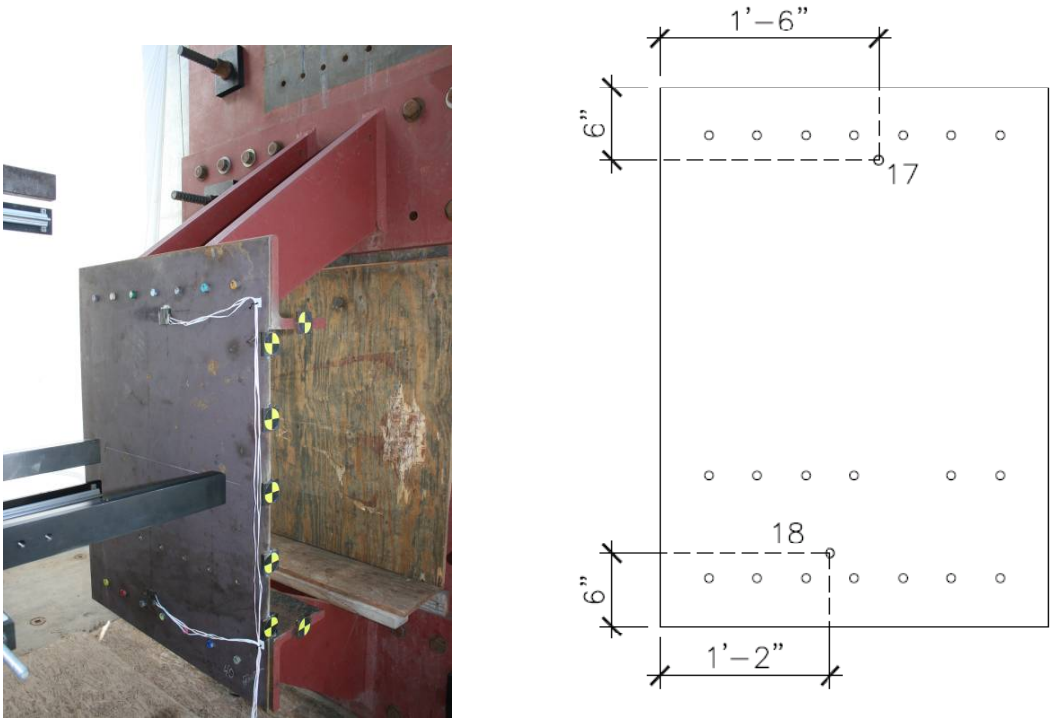

Figure F.80: Strain gage layout for Test 43

F.9.2.4 BOLT TYPE

A total of fourteen A307 bolts (Low Strength Bolts similar to Rivets) were used for this test. They were all tightened to a torque of 40 ft-lbs.

F.9.2.5 BLAST GENERATOR DATA

The initial impact of the single BG was 65.19 ft/sec (19.87 m/sec) with a goal velocity of 19.5 m/s. The average impact velocity for the impacting mass and the steel plate was calculated using the TEMA Track Eye tracking software.

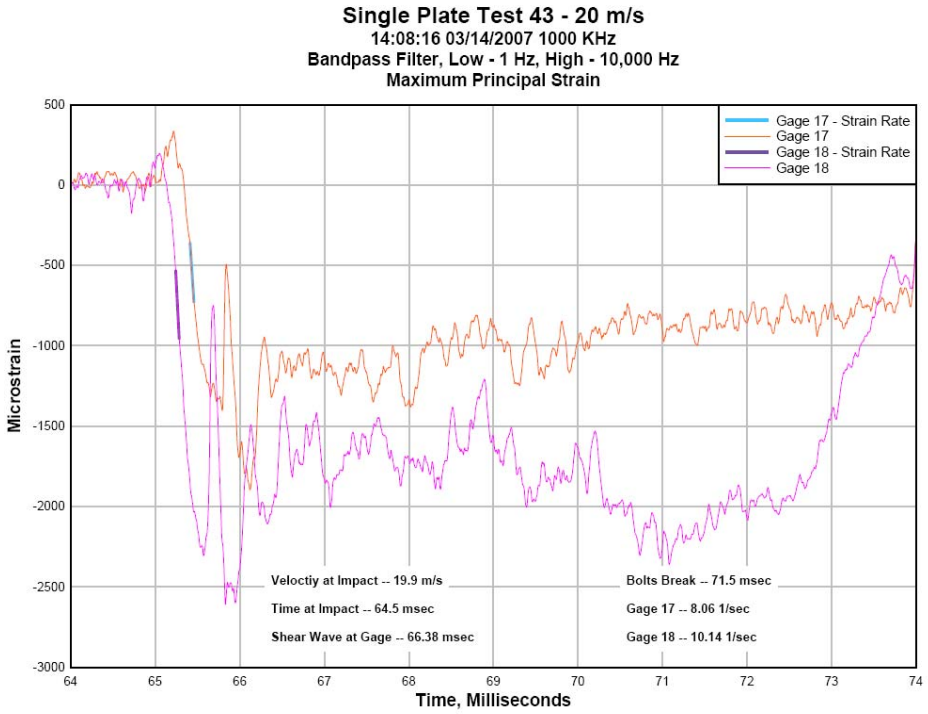

Figure F.81: Maximum principal strains and strain rates for Test 43

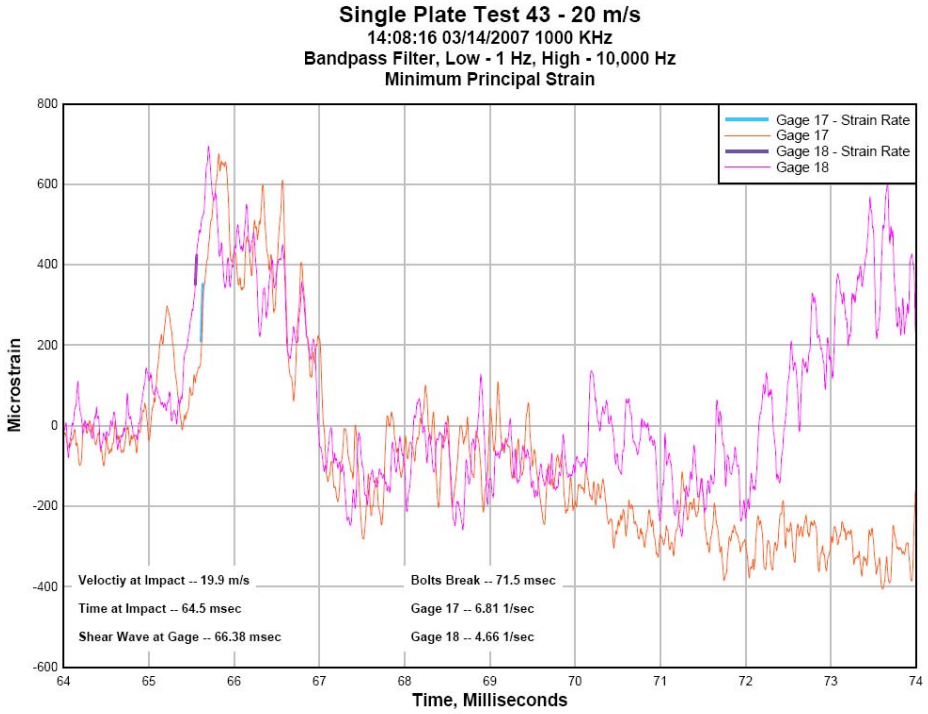

Figure F.82: Minimum principal strains and strain rates for Test 43

F.9.3 SPECIMEN BEHAVIOR

The loading of the BG plate imparted an initial velocity of 64.57 ft/sec (19.68 m/sec) to the specimen. This caused plate to deform in both directions. The longitudinal deflection (in the north-south direction) behaved in a typical one-way flexural shape. This test imparted enough energy to break the top seven bolts as shown in Figure F.83. Due to the flexibility of the ¼" plate the targets on the edge of the plate are not an accurate representation of the maximum dynamic deflection of the plate.

During the test two different phantom cameras were used to capture the failure modes from different angles. Figure F.84 shows the progression of damage for this test from Phantom Camera One. Figure F.85 shows the progression of damage for this test from Phantom Camera Two.

Figure F.83: Steel plate post test for Test 43

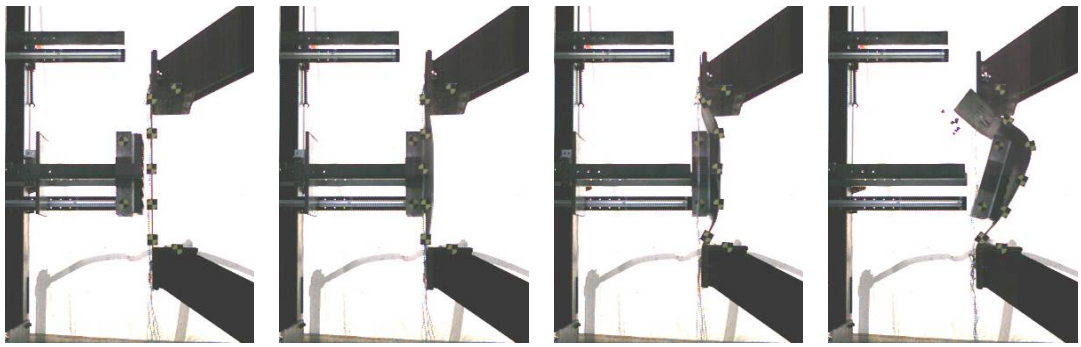

Figure F.84: Progression of damage for Test 43 from Camera 1

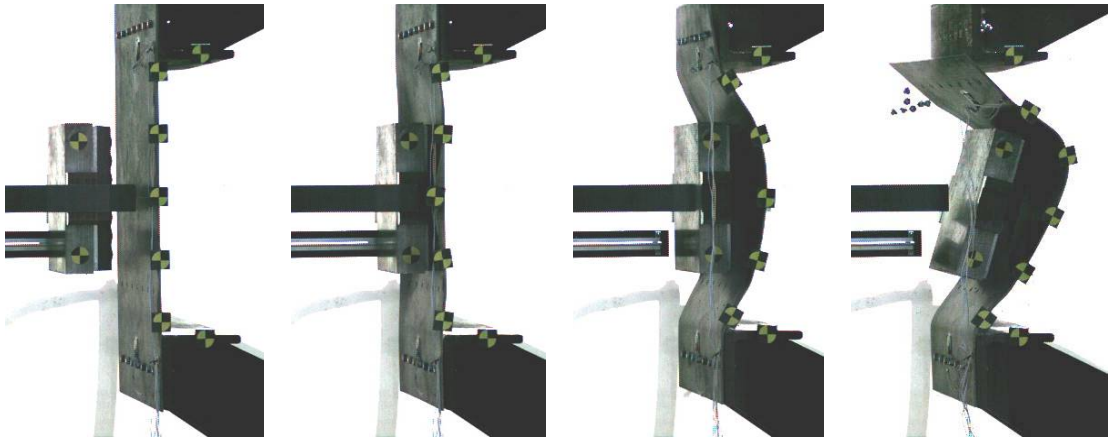

Figure F.85: Progression of damage for Test 43 from Camera 2

F.10 STEEL TOWER SINGLE PLATE: TEST 44 (SP44)

F.10.1 INTRODUCTION

The forty-fourth test of the Steel Tower Single Plate test series was performed on March 15th, 2007. The test specimen was a 1/4" thick steel plate labeled SP44. The Impacting Mass 3 was placed flush with the push plate and accelerated by the BG with a target velocity upon impact with the specimen of 72.18 ft/sec (22 m/s). Figure F.86 shows the steel plate prior to impact.

F.10.2 KINETIC ENERGY DEFEAT DEVICE (KEDD)

For this test a KEDD filled with bottles of water was used as discussed in Section 2.2. The device is shown in Figure F.86. The impacting mass does not extend the whole height of the KEDD and so it will not interfere with the support structure that the KEDD is sitting on. A drop of food coloring was added to each bottle of water to add contrast for the black and white video.

Figure F.86: 1/4" thick steel plate and KEDD pre test for Test 44

F.10.3 INSTRUMENTATION

F.10.3.1 PHANTOM CAMERAS

The first camera recorded in black and white at a rate of 10,000 frames per second at a resolution of 512x384. This camera was used in order to determine the maximum velocity of

the impacting mass and the movement in the plate including the maximum displacement. The second camera recorded in color at a rate of 10,000 frames per second at a resolution of 512x384. This camera recorded the overall behavior of the test specimen. It was not used to gather any specific data. The third camera recorded in color at a rate of 8,000 frames per second at a resolution of 480x480. This camera captured the failure of the bolts. A picture from each of the camera locations are shown in Figure F.87.

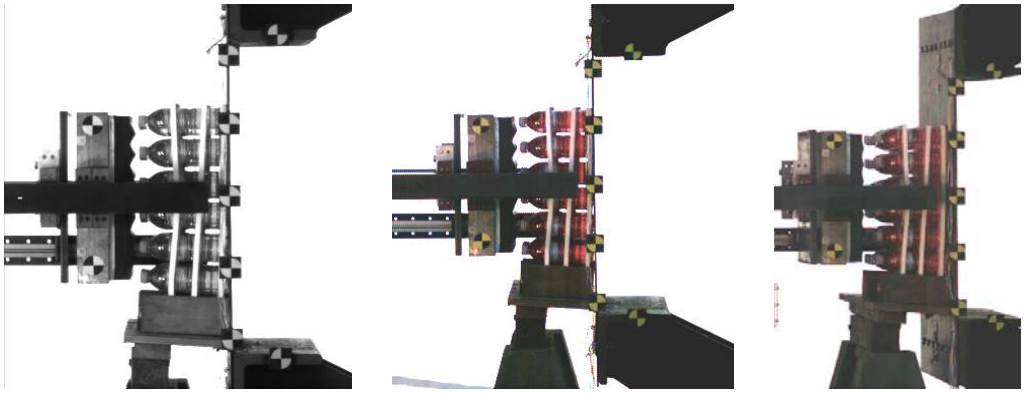

Figure F.87: Phantom Cameras for Test 44 a) Camera One b) Camera Two c) Camera Three

F.10.3.2 TARGET LOCATIONS

Five targets were welded onto the side of the steel plate as shown in Figure F.86. They were spaced at the intervals shown in Figure F.88. That figure also shows the location of the targets for the impacting mass. An additional two targets were placed on the angle at the top and the bottom end conditions. The distance between these two points is 74.93 cm (29 ½").

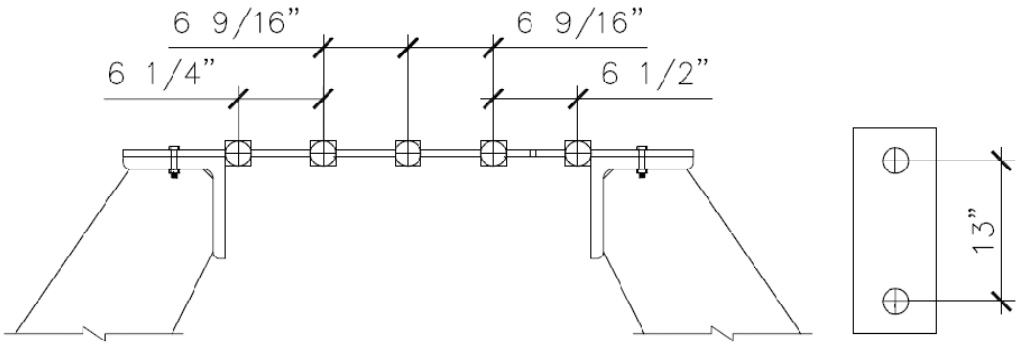

Figure F.88: Target layout on plate and impacting mass for Test 44

F.10.3.3 STRAIN GAGE LOCATIONS

For this test there were two strain gauges labeled 17 and 18. The strain gauges, and their locations, are shown in Figure F.89. Table F.9 shows the specific information about this test, including the time and velocity at impact, if, and when, the bolts failed along with the maximum and minimum principal strain rates. The largest maximum principal strain rate for

this test was 1.45 1/sec and was located at strain gage 18 while the largest minimum strain rate for this test was 1.03 1/sec located at strain gage 18. The maximum principal strains for gauges 17 and 18 can be found in Figure F.90 and the minimum principal strains for the same gauges can be found in Figure F.91.

Table F.9: Stain rate information for Test 44

Strain Gage Number	Actual Velocity	Initial Impact	Shear Wave at Gage	Bolts Break	Maximum Principal Strain Rate	Minimum Principal Strain Rate
17	25.82 m/s	48.70 msec	58.13 msec	62.13 msec	-0.97 1/sec	0.53 1/sec
18	25.82 m/s	48.70 msec	58.13 msec	62.13 msec	-1.45 1/sec	-1.03 1/sec

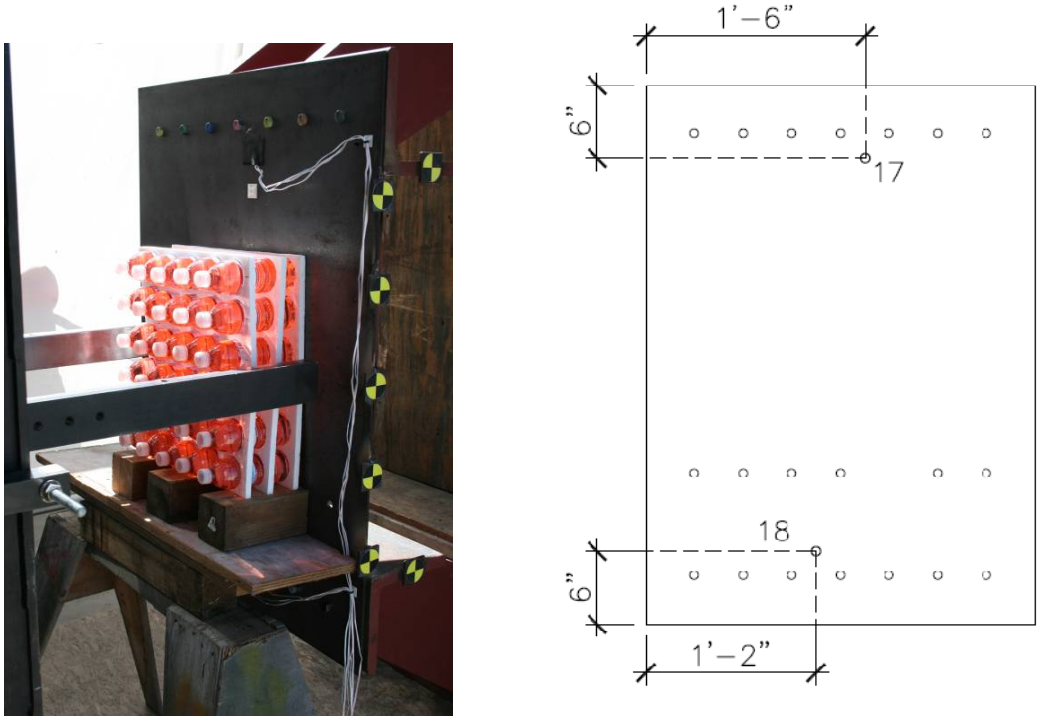

Figure F.89: Strain gage layout for Test 44

F.10.3.4 BOLT TYPE

A total of fourteen A307 bolts (Low Strength Bolts similar to Rivets) were used for this test. They were all tightened to a torque of 40 ft-lbs.

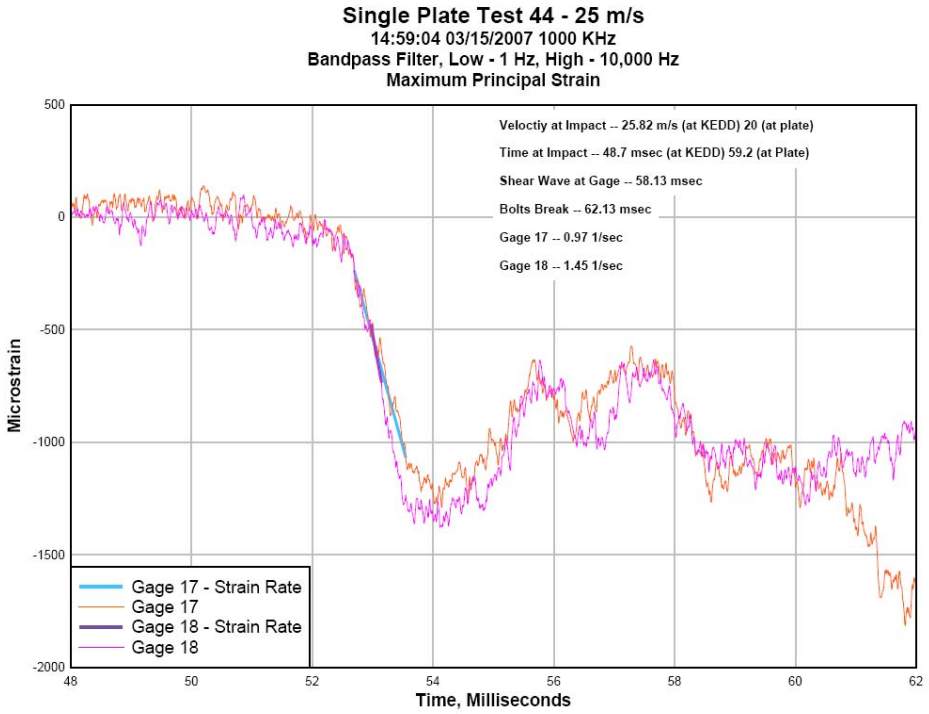

Figure F.90: Maximum principal strains and strain rates for Test 44

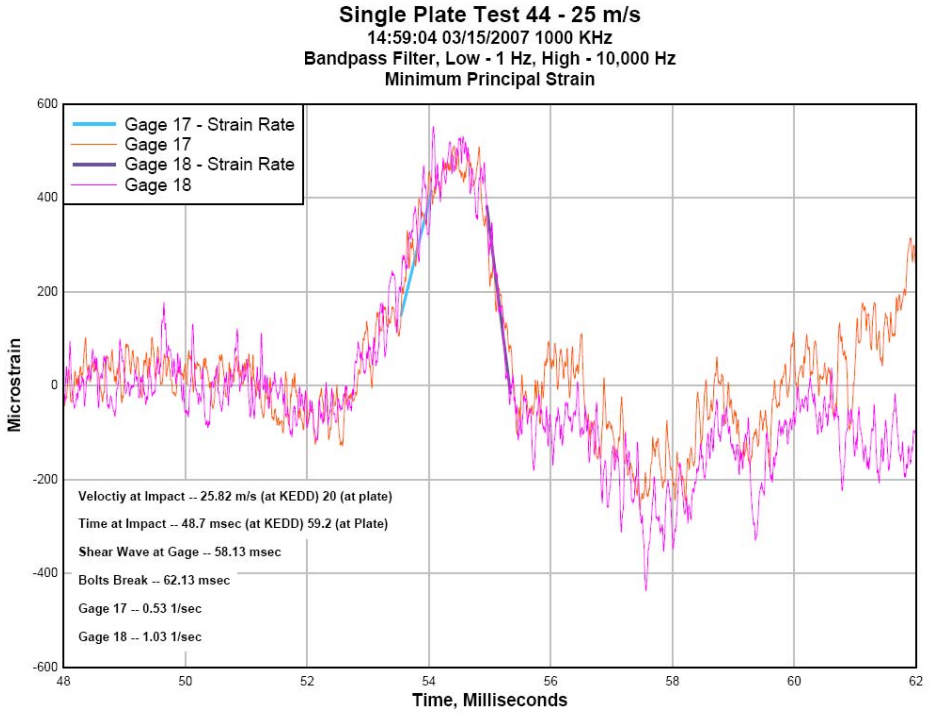

Figure F.91: Minimum principal strains and strain rates for Test 44

F.10.4 BLAST GENERATOR DATA

The initial impact of the single BG was 84.72 ft/sec (25.82 m/sec) with a goal velocity of 22 m/s. The average impact velocity for the impacting mass and the steel plate was calculated using the TEMA Track Eye tracking software.

F.10.5 BLAST GENERATOR DATA

The loading of the BG plate imparted an initial velocity of 84.71 ft/sec (25.82 m/sec) to the Kinetic Energy Defeat Device (KEDD). This caused plate to deform in both directions. The longitudinal deflection (in the north-south direction) behaved in a typical one-way flexural shape. This test imparted enough energy to break the bottom seven bolts as shown in Figure F.92. Due to the flexibility of the ¼" plate and the mass of water obscuring the cameras, the targets on the edge of the plate were not able to capture the maximum dynamic deflection of the plate.

During the test three different phantom cameras were used to capture the failure modes from different angles. Figure F.93 shows the progression of damage for this test from Phantom Camera One. Figure F.94 shows the progression of damage for this test from Phantom Camera Two. Figure F.95 shows the progression of damage for this test from Phantom Camera Three.

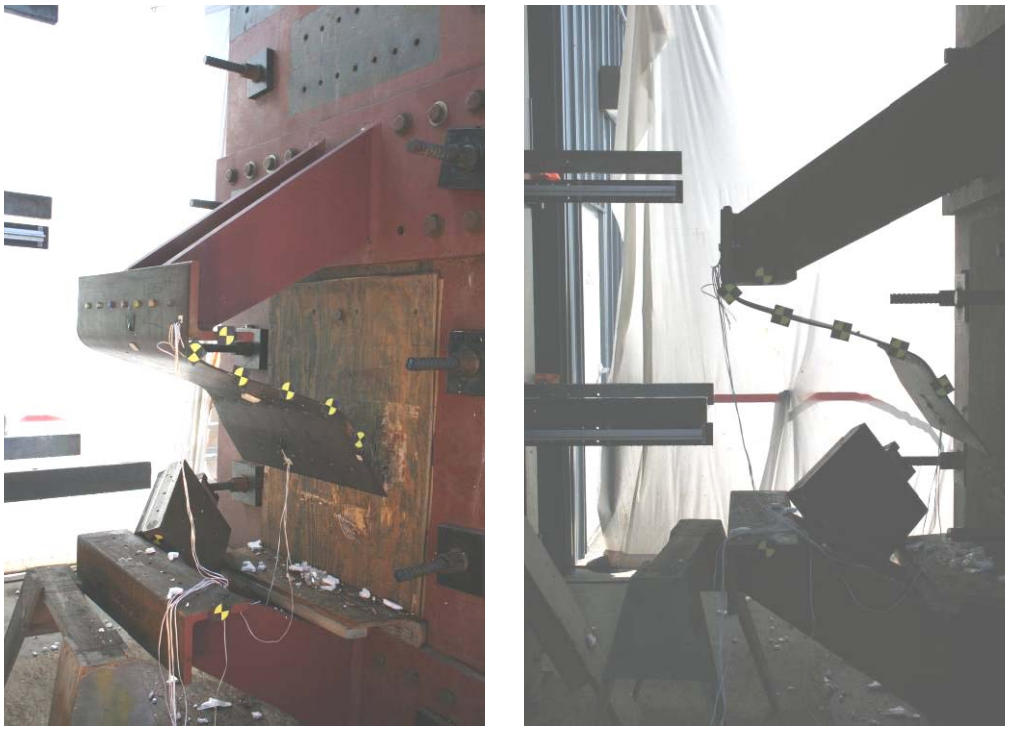

Figure F.92: Steel plate post test for Test 44

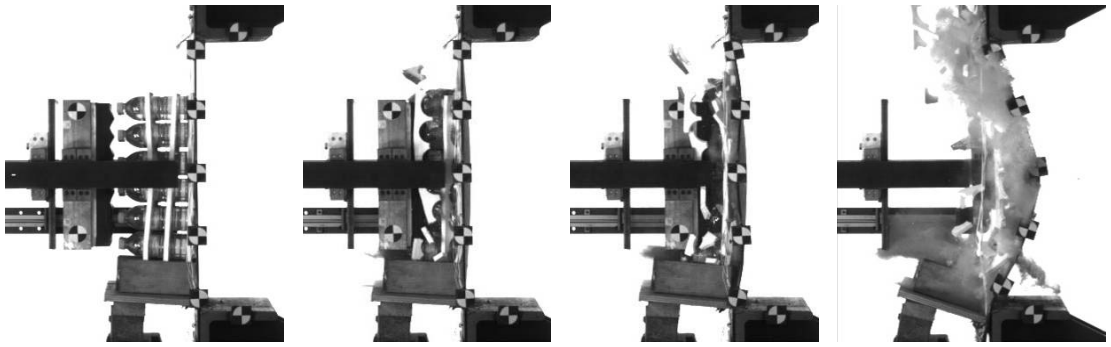

Figure F.93: Progression of damage for Test 44 from Camera 1

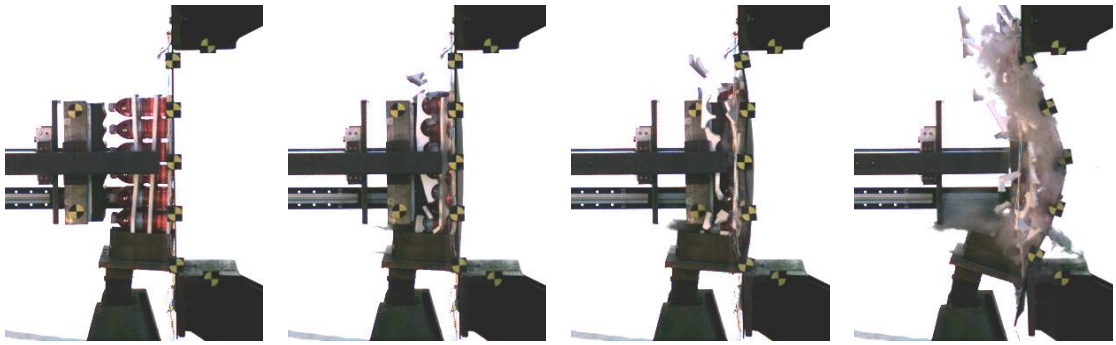

Figure F.94: Progression of damage for Test 44 from Camera 2

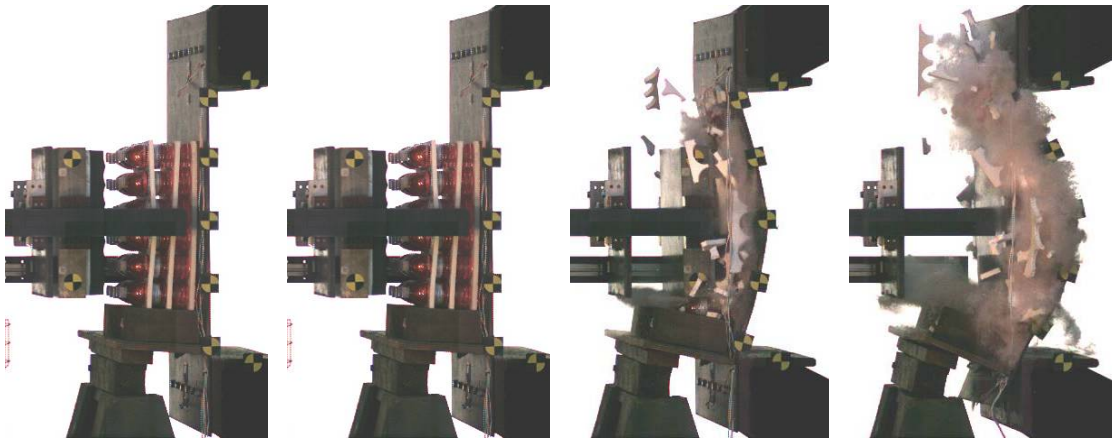

Figure F.95: Progression of damage for Test 44 from Camera 3

F.11 STEEL TOWER SINGLE PLATE: TEST 45 (SP45)

F.11.1 INTRODUCTION

The forty-fifth test of the Steel Tower Single Plate test series was performed on March 16th, 2007. The test specimen was a 1/2" thick steel plate labeled SP45. The Impacting Mass 3 was placed flush with the push plate and accelerated by the BG with a target velocity upon impact with the specimen of 90.22 ft/sec (27.5 m/s). Figure F.96 shows the steel plate prior to impact.

Figure F.96: 1/2" thick steel plate pre test for Test 45

F.11.2 INSTRUMENTATION

F.11.2.1 PHANTOM CAMERAS

The first camera recorded in black and white at a rate of 10,000 frames per second at a resolution of 512x384. This camera was used in order to determine the maximum velocity of the impacting mass and the movement in the plate including the maximum displacement. The second camera recorded in color at a rate of 5,000 frames per second at a resolution of 512x384. This camera recorded the overall behavior of the test specimen. It was not used to gather any specific data. The third camera recorded in color at a rate of 8,000 frames per second at a resolution of 480x480. This camera captured the failure of the bolts. A picture from each of the camera locations are shown in Figure F.97.

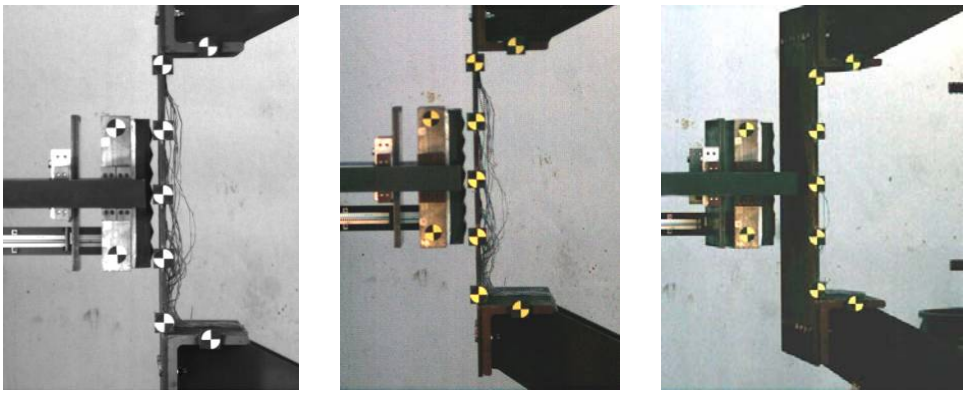

Figure F.97: Phantom Cameras for Test 45 a) Camera One b) Camera Two c) Camera Three

F.11.2.2 TARGET LOCATIONS

Five targets were welded onto the side of the steel plate as shown in Figure F.96. They were spaced at the intervals shown in Figure F.98. That figure also shows the location of the targets for the impacting mass. An additional two targets were placed on the angle at the top and the bottom end conditions. The distance between these two points is 74.93 cm (29 ½").

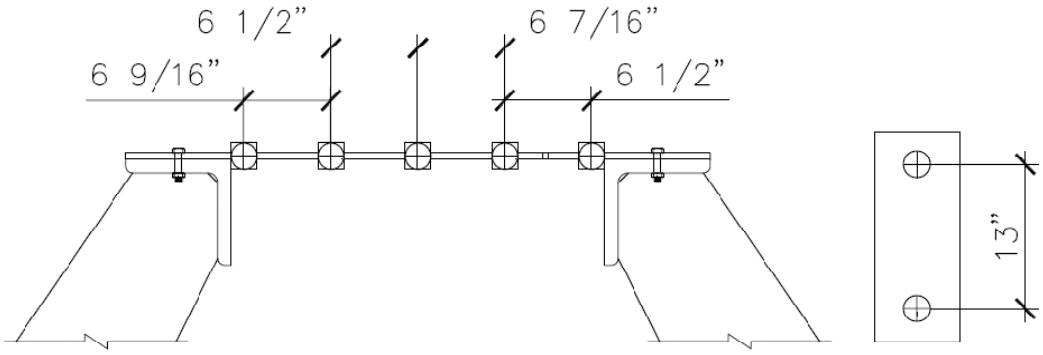

Figure F.98: Target layout on plate and impacting mass for Test 45

F.11.2.3 STRAIN GAGE LOCATIONS

For this test there were five strain gauges labeled 1A, 2A, 3A, 4A and 5A. The strain gauges, and their locations, are shown in Figure F.99. Table F.10 shows the specific information about this test, including the time and velocity at impact, if, and when, the bolts failed along with the maximum and minimum principal strain rates. The data for Gage 5A was discarded due to a damaged gage. The largest maximum principal strain rate for this test was 11.77 1/sec and was located at strain gage 3A while the largest minimum strain rate for this test was 16.54 1/sec located at strain gage 3A. The maximum principal strains for gauges 1A, 2A, 3A and 4A can be found in Figure F.100 and the minimum principal strains for the same gauges can be found in Figure F.101.

Table F.10: Stain rate information for Test 45

Strain Gage Number	Actual Velocity	Initial Impact	Shear Wave at Gage	Bolts Break	Maximum Principal Strain Rate	Minimum Principal Strain Rate
1A	26.98 m/s	57.00 msec	-	64.70 msec	-7.90 1/sec	-9.70 1/sec
2A	26.98 m/s	57.00 msec	-	64.70 msec	-10.99 1/sec	-2.22 1/sec
3A	26.98 m/s	57.00 msec	-	64.70 msec	-11.77 1/sec	-16.54 1/sec
4A	26.98 m/s	57.00 msec	-	64.70 msec	-8.06 1/sec	5.50 1/sec

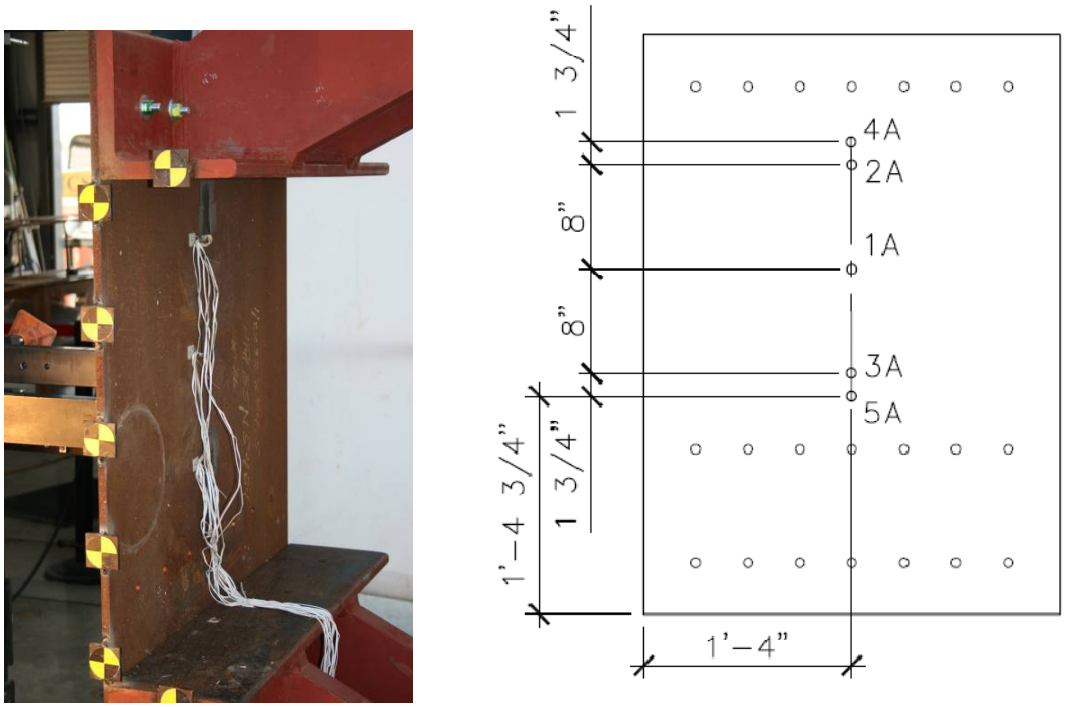

Figure F.99: Strain gage layout for Test 45

F.11.2.4 BOLT TYPE

A total of fourteen A307 bolts (Low Strength Bolts similar to Rivets) were used for this test. They were all tightened to a torque of 40 ft-lbs.

F.11.3 BLAST GENERATOR DATA

The initial impact of the single BG was 88.52 ft/sec (26.98 m/sec) with a goal velocity of 27.5 m/s. The average impact velocity for the impacting mass and the steel plate was calculated using the TEMA Track Eye tracking software.

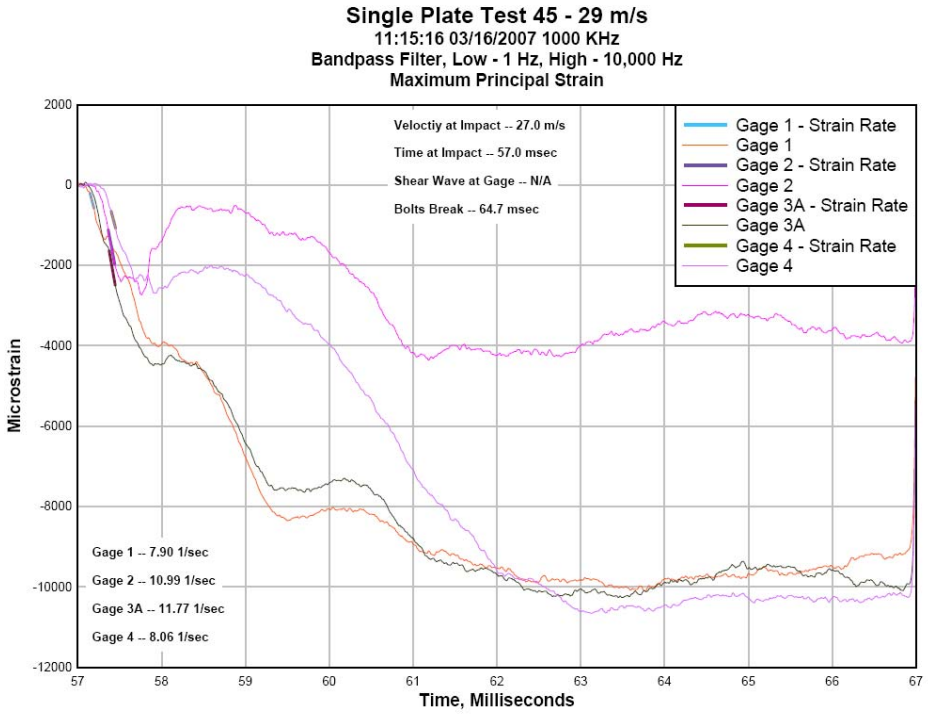

Figure F.100: Maximum principal strains and strain rates for Test 45

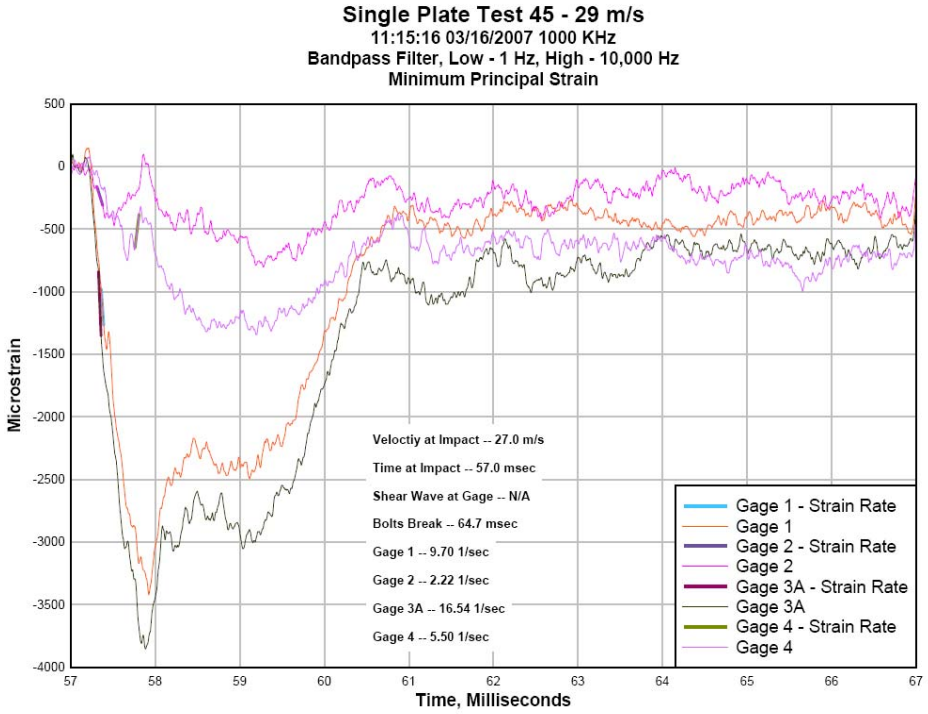

Figure F.101: Minimum principal strains and strain rates for Test 45

F.11.4 SPECIMEN BEHAVIOR

The loading of the BG plate imparted an initial velocity of 88.52 ft/sec (26.98 m/sec) to the specimen. This caused plate to deform in both directions. The longitudinal deflection (in the north-south direction) behaved in a typical one-way flexural shape. This test imparted enough energy to break the bottom seven bolts as shown in Figure F.102. The maximum dynamic deflection of the plate before the bolts broke was 4 ½".

During the test three different phantom cameras were used to capture the failure modes from three different angles. Figure F.103 shows the progression of damage for this test from Phantom Camera One. Figure F.104 shows the progression of damage for this test from Phantom Camera Two. Figure F.105 shows the progression of damage for this test from Phantom Camera Two.

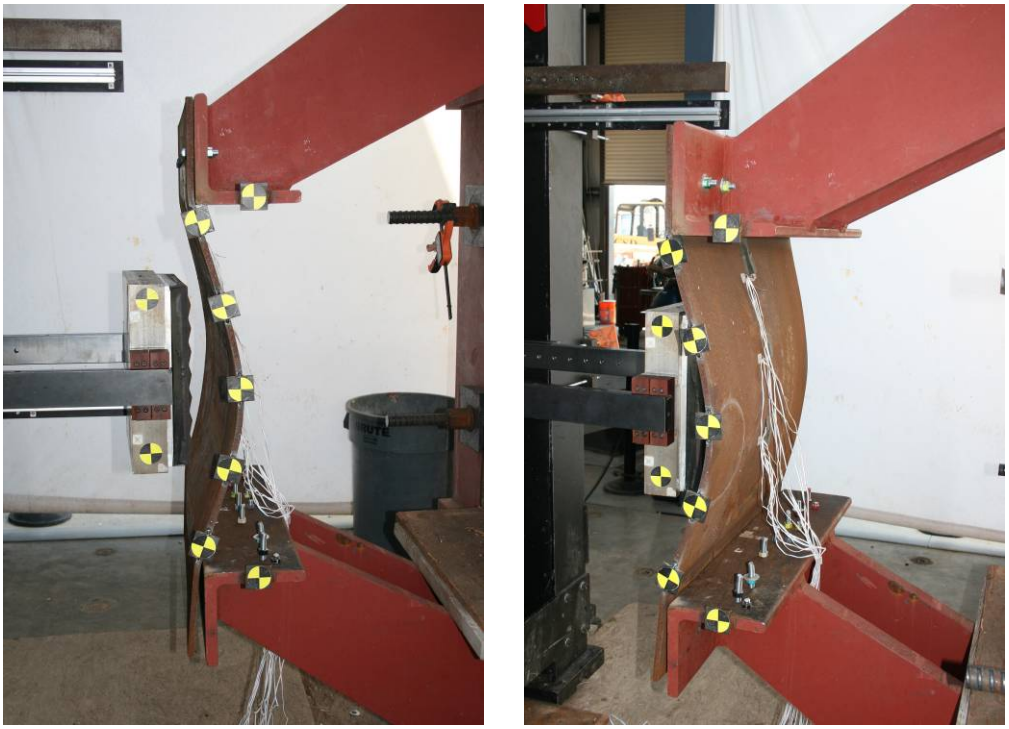

Figure F.102: Steel plate post test for Test 45

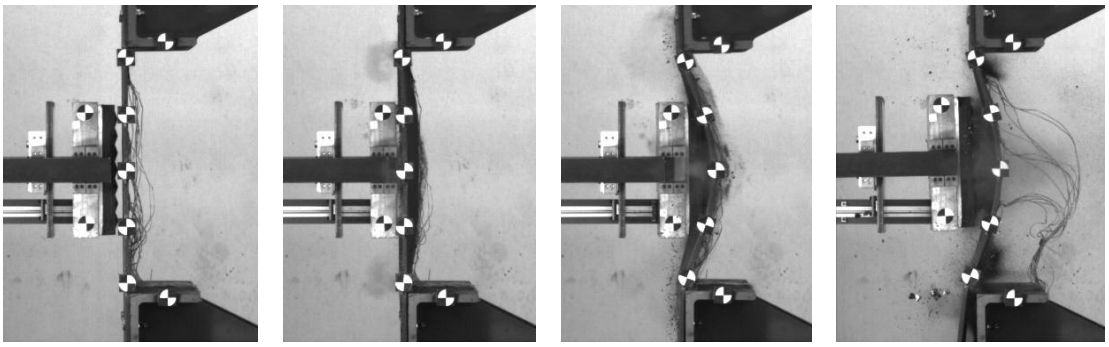

Figure F.103: Progression of damage for Test 45 from Camera 1

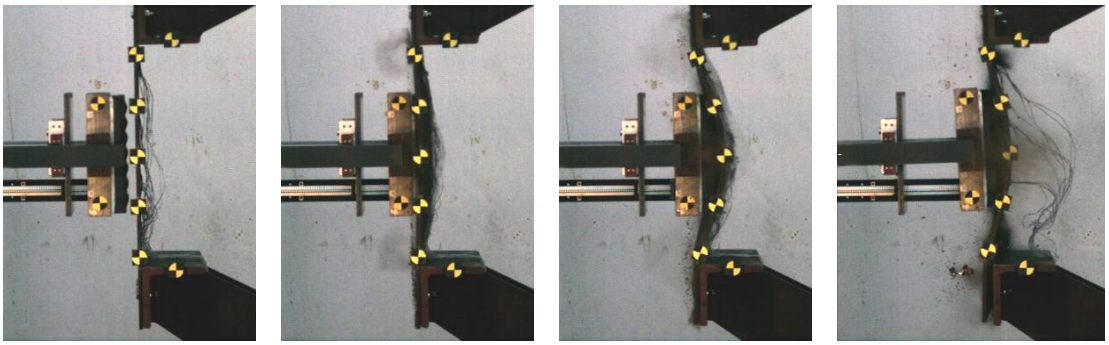

Figure F.104: Progression of damage for Test 45 from Camera 2

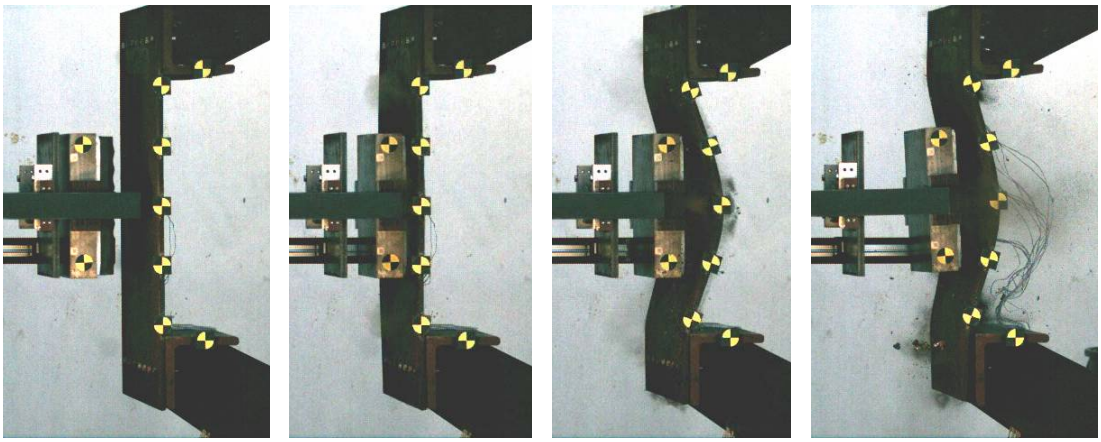

Figure F.105: Progression of damage for Test 45 from Camera 3

F.12 STEEL TOWER SINGLE PLATE: TEST 46 (SP46)

F.12.1 INTRODUCTION

The forty-sixth test of the Steel Tower Single Plate test series was performed on March 27th, 2007. The test specimen was a 1/4" thick steel plate labeled SP46. The Impacting Mass 3 was placed flush with the push plate and accelerated by the BG with a target velocity upon impact with the specimen of 85.30 ft/sec (26 m/s). Figure F.106 shows the steel plate prior to impact.

F.12.2 KINETIC ENERGY DEFEAT DEVICE (KEDD)

For this test a KEDD filled with bottles of water was used as discussed in Section 2.2. The device is shown in Figure F.106. The impacting mass does not extend the whole height of the KEDD and so it will not interfere with the support structure that the KEDD is sitting on. A drop of food coloring was added to each bottle of water to add contrast for the black and white video.

Figure F.106: 1/4" thick steel plate and KEDD pre test for Test 46

F.12.3 INSTRUMENTATION

F.12.3.1 PHANTOM CAMERAS

The first camera recorded in black and white at a rate of 10,000 frames per second at a resolution of 512x384. This camera was used in order to determine the maximum velocity of the impacting mass and the movement in the plate including the maximum displacement. The

second camera recorded in color at a rate of 5,000 frames per second at a resolution of 512x384. This camera recorded the overall behavior of the test specimen. It was not used to gather any specific data. The third camera recorded in color at a rate of 8,000 frames per second at a resolution of 480x480. This camera captured the failure of the bolts. A picture from each of the camera locations are shown in Figure F.107.

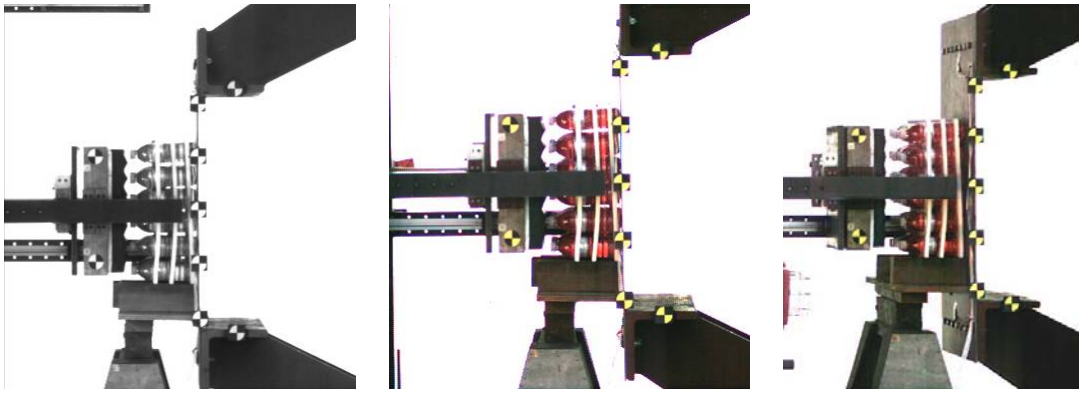

Figure F.107: Phantom Cameras for Test 46

a) Camera One b) Camera Two c) Camera Three

F.12.3.2 TARGET LOCATIONS

Five targets were welded onto the side of the steel plate as shown in Figure F.106. They were spaced at the intervals shown in Figure F.108. That figure also shows the location of the targets for the impacting mass. An additional two targets were placed on the angle at the top and the bottom end conditions. The distance between these two points is 74.93 cm (29 ½").

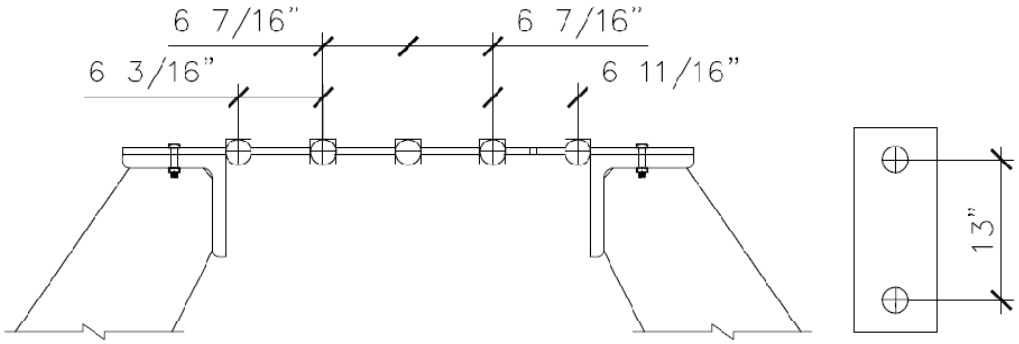

Figure F.108: Target layout on plate and impacting mass for Test 46

F.12.3.3 STRAIN GAGE LOCATIONS

For this test there were two strain gauges labeled 17 and 18. The strain gauges, and their locations, are shown in Figure F.109. Table F.11 shows the specific information about this test, including the time and velocity at impact, if, and when, the bolts failed along with the

maximum and minimum principal strain rates. The largest maximum principal strain rate for this test was 1.76 1/sec and was located at strain gage 18 while the largest minimum strain rate for this test was 0.33 1/sec located at strain gage 18. The maximum principal strains for gauges 17 and 18 can be found in Figure F.110 and the minimum principal strains for the same gauges can be found in Figure F.111.

Table F.11: Stain rate information for Test 46

Strain Gage Number	Actual Velocity	Initial Impact	Shear Wave at Gage	Bolts Break	Maximum Principal Strain Rate	Minimum Principal Strain Rate
17	26.25 m/s	49.40 msec	59.63 msec	63.40 msec	-1.30 1/sec	0.30 1/sec
18	26.25 m/s	49.40 msec	59.63 msec	63.40 msec	-1.76 1/sec	0.33 1/sec

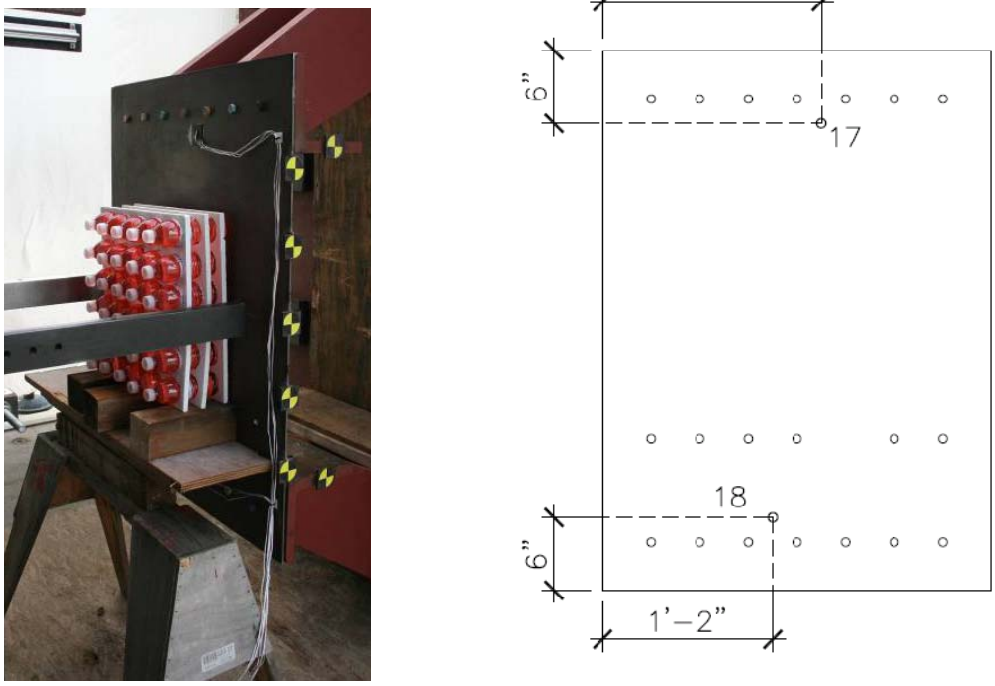

Figure F.109: Strain gage layout for Test 46

F.12.3.4 BOLT TYPE

A total of fourteen A307 bolts (Low Strength Bolts similar to Rivets) were used for this test. They were all tightened to a torque of 40 ft-lbs.

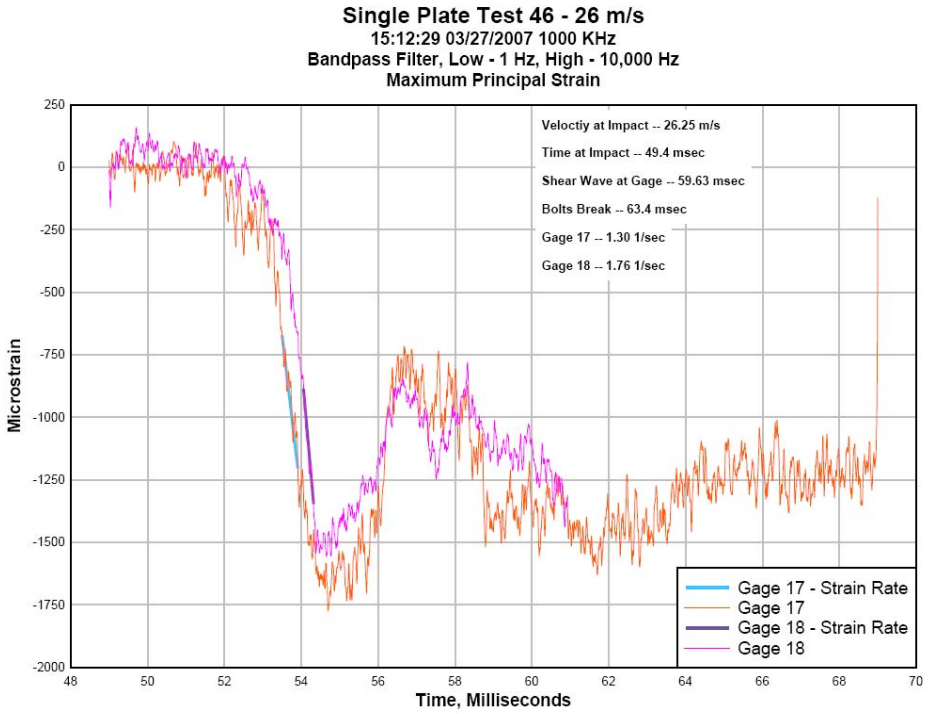

Figure F.110: Maximum principal strains and strain rates for Test 46

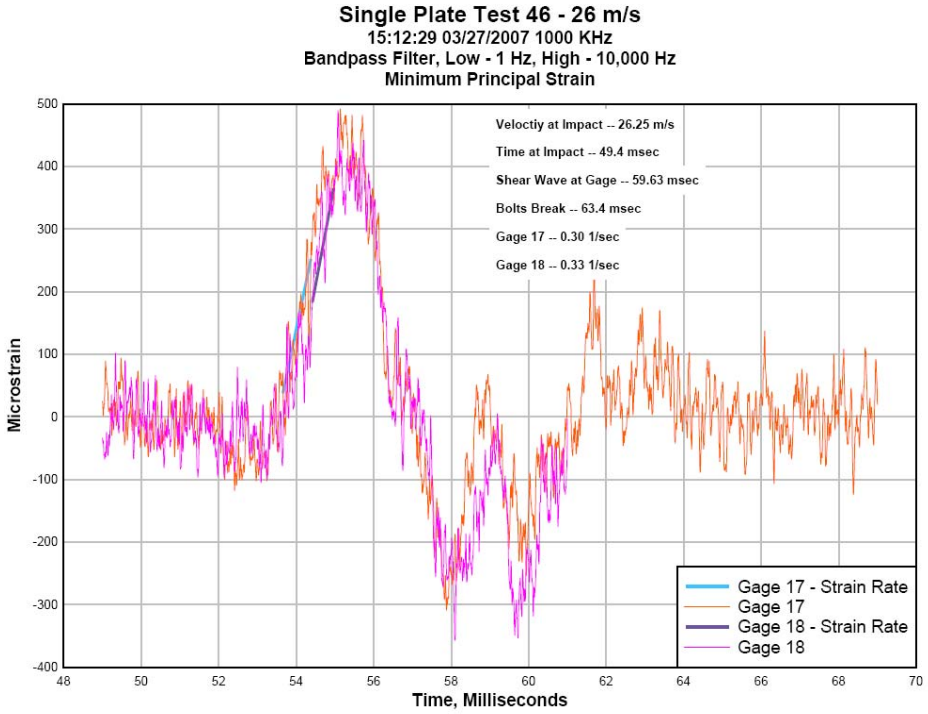

Figure F.111: Minimum principal strains and strain rates for Test 46

F.12.4 BLAST GENERATOR DATA

The initial impact of the single BG was 86.12 ft/sec (26.25 m/sec) with a goal velocity of 26 m/s. The average impact velocity for the impacting mass and the steel plate was calculated using the TEMA Track Eye tracking software.

F.12.5 SPECIMEN BEHAVIOR

The loading of the BG plate imparted an initial velocity of 63.94 ft/sec (19.49 m/sec) to the Kinetic Energy Defeat Device (KEDD). This caused plate to deform in both directions. The longitudinal deflection (in the north-south direction) behaved in a typical one-way flexural shape. This test imparted enough energy to break the top seven bolts as shown in Figure F.112. Due to the flexibility of the ¼" plate and the mass of water obscuring the cameras, the targets on the edge of the plate were not able to capture the maximum dynamic deflection of the plate.

During the test three different phantom cameras were used to capture the failure modes from different angles. Figure F.113 shows the progression of damage for this test from Phantom Camera One. Figure F.114 shows the progression of damage for this test from Phantom Camera Two. Figure F.115 shows the progression of damage for this test from Phantom Camera Three.

Figure F.112: Steel plate post test for Test 46

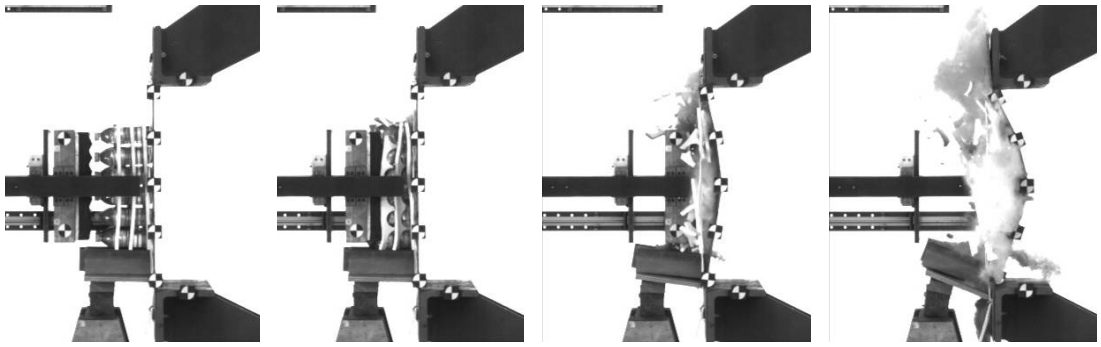

Figure F.113: Progression of damage for Test 46 from Camera 1

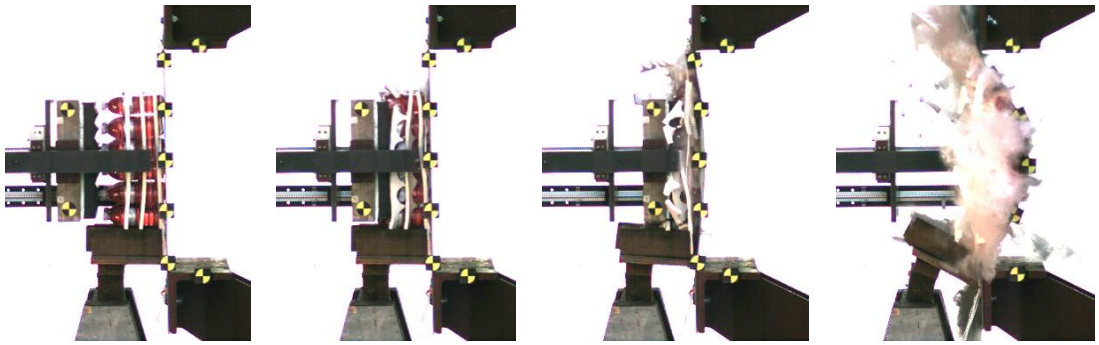

Figure F.114: Progression of damage for Test 46 from Camera 2

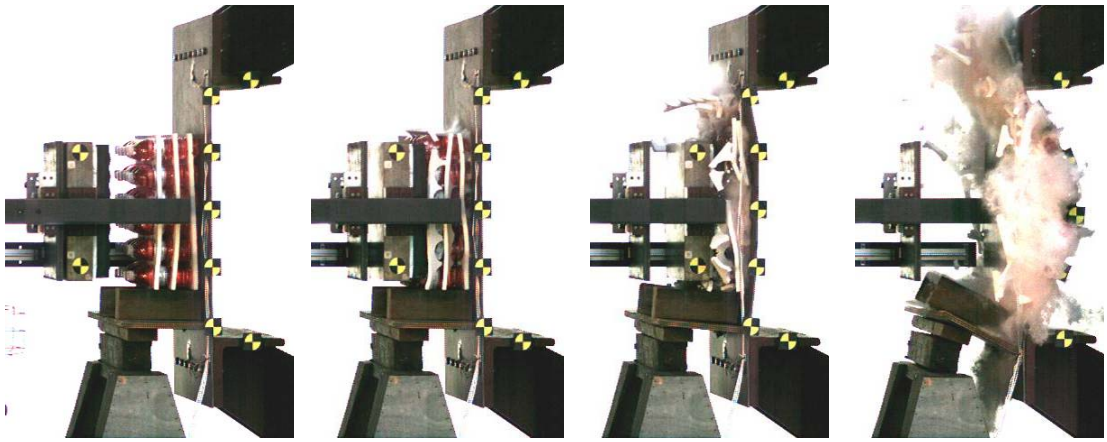

Figure F.115: Progression of damage for Test 46 from Camera 3

F.13 STEEL TOWER SINGLE PLATE: TEST 47 (SP47)

F.13.1 INTRODUCTION

The forty-seventh test of the Steel Tower Single Plate test series was performed on March 28th, 2007. The test specimen was a 1/4" thick steel plate labeled SP47. The Impacting Mass 3 was placed flush with the push plate and accelerated by the BG with a target velocity upon impact with the specimen of 62.34 ft/sec (19 m/s). Figure F.116 shows the steel plate prior to impact.

F.13.2 KINETIC ENERGY DEFEAT DEVICE (KEDD)

For this test a KEDD filled with bottles of water was used as discussed in Section 2.2. The device is shown in Figure F.116. The impacting mass does not extend the whole height of the KEDD and so it will not interfere with the support structure that the KEDD is sitting on. A drop of food coloring was added to each bottle of water to add contrast for the black and white video.

Figure F.116: 1/4" thick steel plate and KEDD pre test for Test 47

F.13.3 INSTRUMENTATION

F.13.3.1 PHANTOM CAMERAS

The first camera recorded in black and white at a rate of 10,000 frames per second at a resolution of 512x384. This camera was used in order to determine the maximum velocity of the impacting mass and the movement in the plate including the maximum displacement. The second camera recorded in color at a rate of 10,000 frames per second at a resolution of

512x384. This camera recorded the overall behavior of the test specimen. It was not used to gather any specific data. The third camera recorded in color at a rate of 8,000 frames per second at a resolution of 480x480. This camera captured the failure of the bolts. A picture from each of the camera locations are shown in Figure F.117.

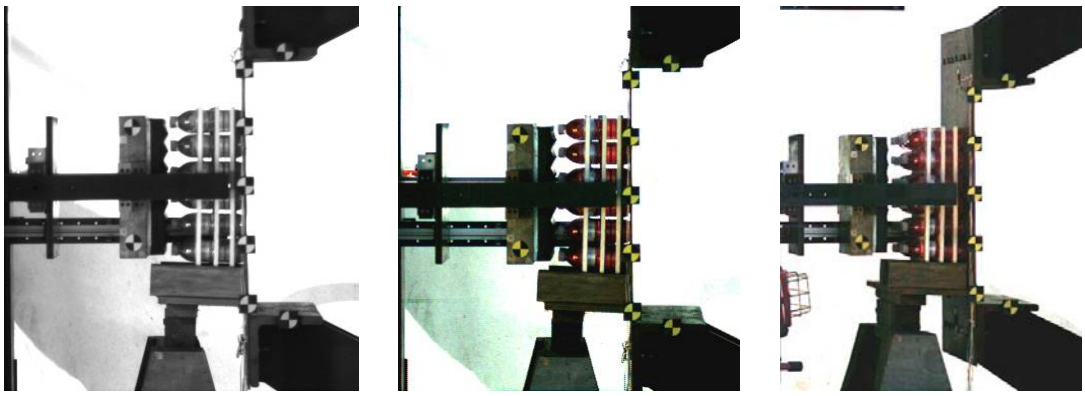

Figure F.117: Phantom Cameras for Test 47

a) Camera One b) Camera Two c) Camera Three

F.13.3.2 TARGET LOCATIONS

Five targets were welded onto the side of the steel plate as shown in Figure F.116. They were spaced at the intervals shown in Figure F.118. That figure also shows the location of the targets for the impacting mass. An additional two targets were placed on the angle at the top and the bottom end conditions. The distance between these two points is 74.93 cm (29 ½").

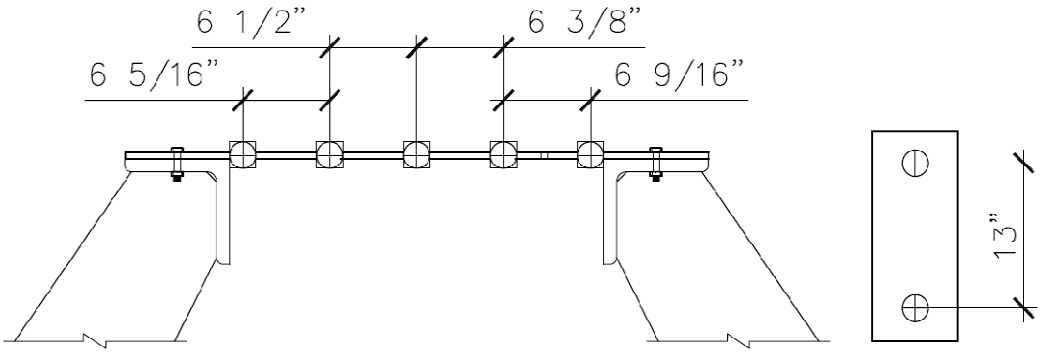

Figure F.118: Target layout on plate and impacting mass for Test 47

F.13.3.3 STRAIN GAGE LOCATIONS

For this test there were two strain gauges labeled 17 and 18. The strain gauges, and their locations, are shown in Figure F.119. Table F.12 shows the specific information about this test, including the time and velocity at impact, if, and when, the bolts failed along with the maximum and minimum principal strain rates. The largest maximum principal strain rate for

this test was 1.30 1/sec and was located at strain gage 18 while the largest minimum strain rate for this test was 0.35 1/sec located at strain gage 18. The maximum principal strains for gauges 17 and 18 can be found in Figure F.120 and the minimum principal strains for the same gauges can be found in Figure F.121.

Table F.12: Stain rate information for Test 47

Strain Gage Number	Actual Velocity	Initial Impact	Shear Wave at Gage	Bolts Break	Maximum Principal Strain Rate	Minimum Principal Strain Rate
17	19.49 m/s	54.80 msec	-	-	-0.72 1/sec	0.22 1/sec
18	19.49 m/s	54.80 msec	-	-	-1.30 1/sec	0.35 1/sec

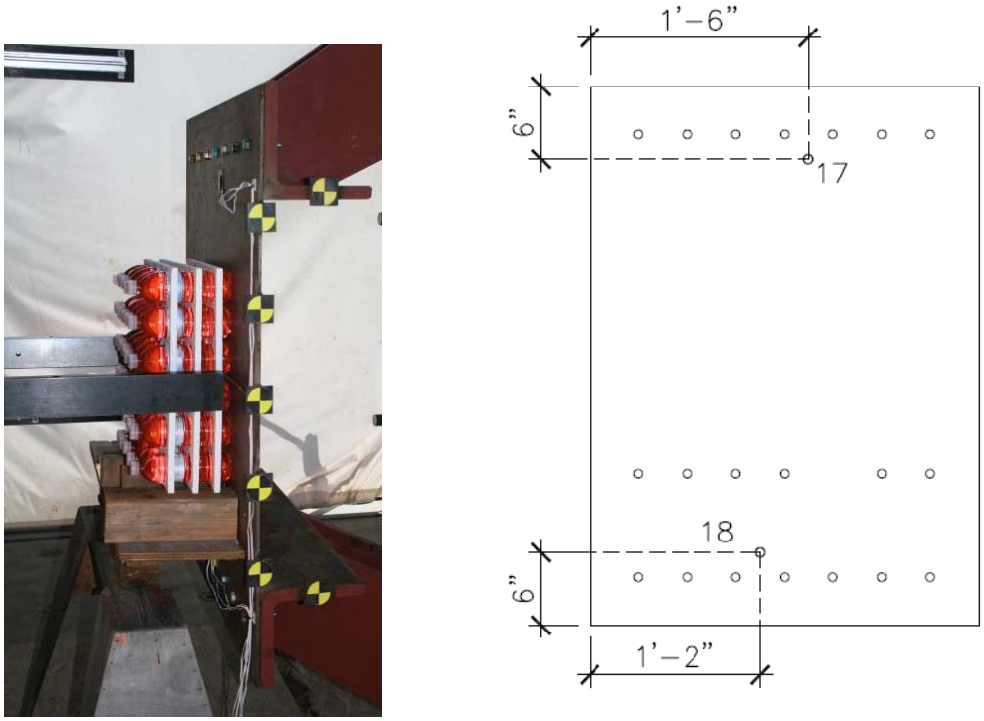

Figure F.119: Strain gage layout for Test 47

F.13.3.4 BOLT TYPE

A total of fourteen A307 bolts (Low Strength Bolts similar to Rivets) were used for this test. They were all tightened to a torque of 40 ft-lbs.

F.13.4 BLAST GENERATOR DATA

The initial impact of the single BG was 63.94 ft/sec (19.49 m/sec) with a goal velocity of 19 m/s. The average impact velocity for the impacting mass and the steel plate was calculated using the TEMA Track Eye tracking software.

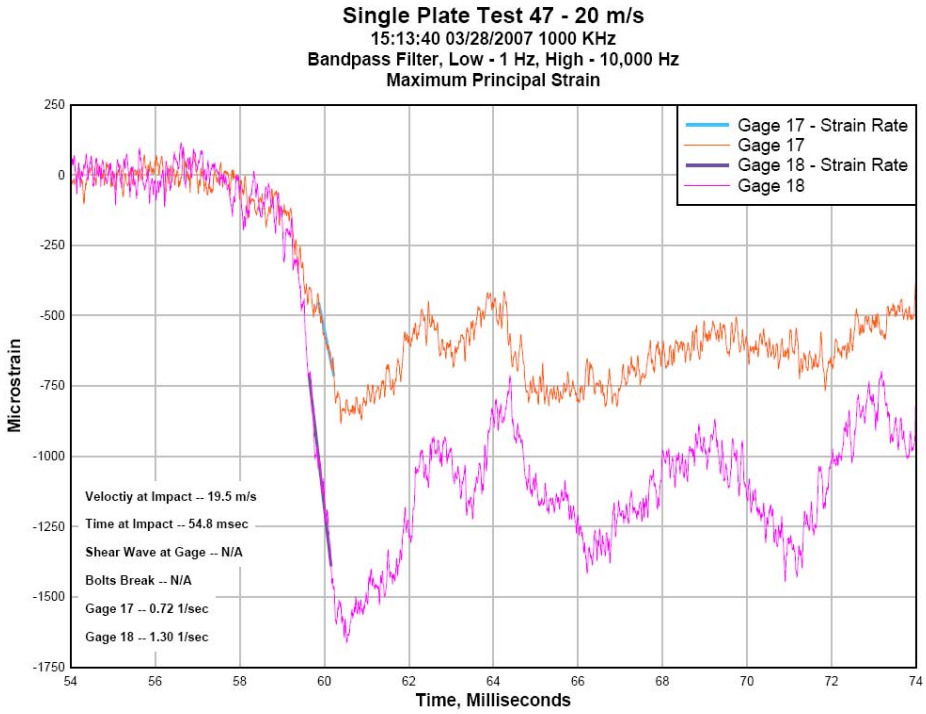

Figure F.120: Maximum principal strains and strain rates for Test 47

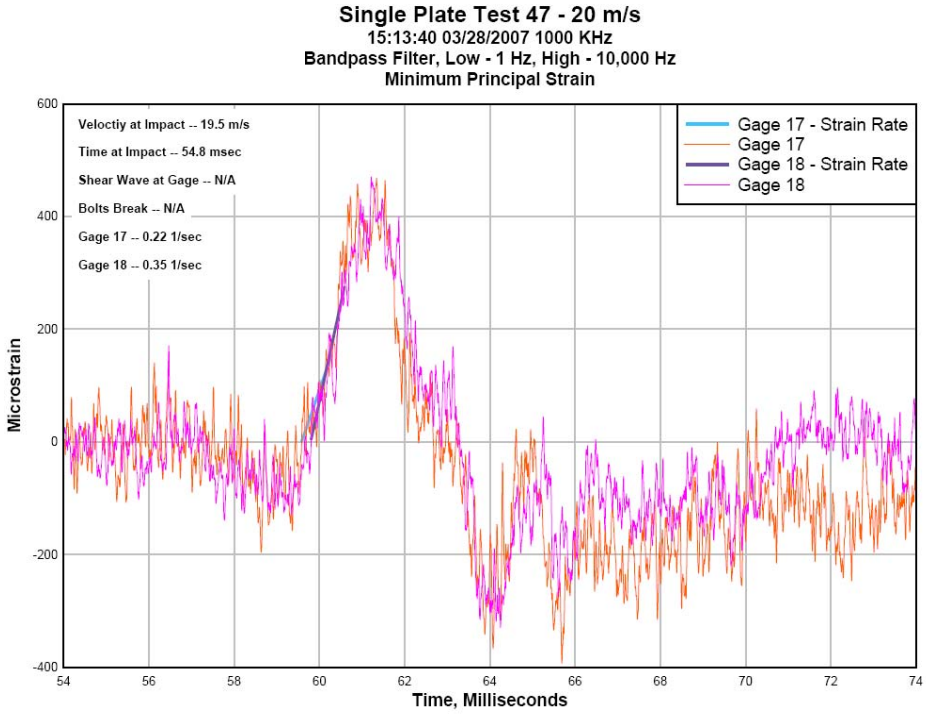

Figure F.121: Minimum principal strains and strain rates for Test 47

F.13.5 BLAST GENERATOR DATA

The loading of the BG plate imparted an initial velocity of 62.34 ft/sec (19.49 m/sec) to the Kinetic Energy Defeat Device (KEDD). This caused plate to deform in both directions. The longitudinal deflection (in the north-south direction) behaved in a typical one-way flexural shape. This test did not impart enough energy to break the any of the bolts as shown in Figure F.122. Due to the flexibility of the ¼" plate and the mass of water obscuring the cameras, the targets on the edge of the plate were not able to capture the maximum dynamic deflection of the plate. The permanent deflection of the plate at midspan was 2 1/8".

During the test three different phantom cameras were used to capture the failure modes from different angles. Figure F.123 shows the progression of damage for this test from Phantom Camera One. Figure F.124 shows the progression of damage for this test from Phantom Camera Two. Figure F.125 shows the progression of damage for this test from Phantom Camera Three.

Figure F.122: Steel plate post test for Test 47

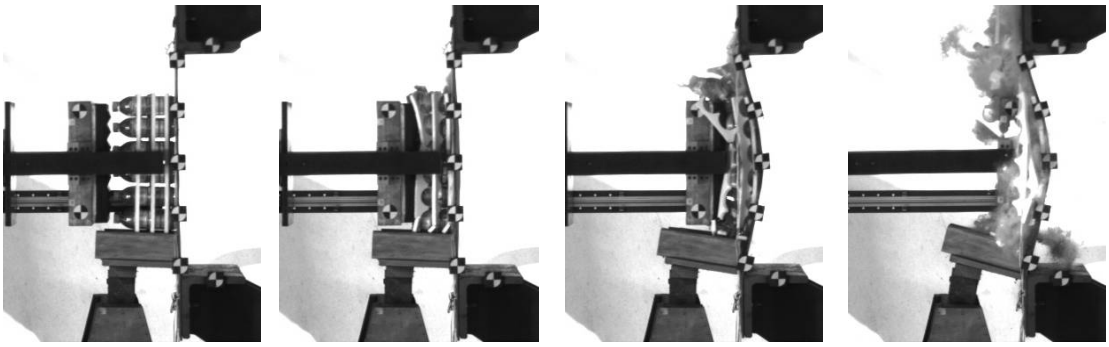

Figure F.123: Progression of damage for Test 47 from Camera 1

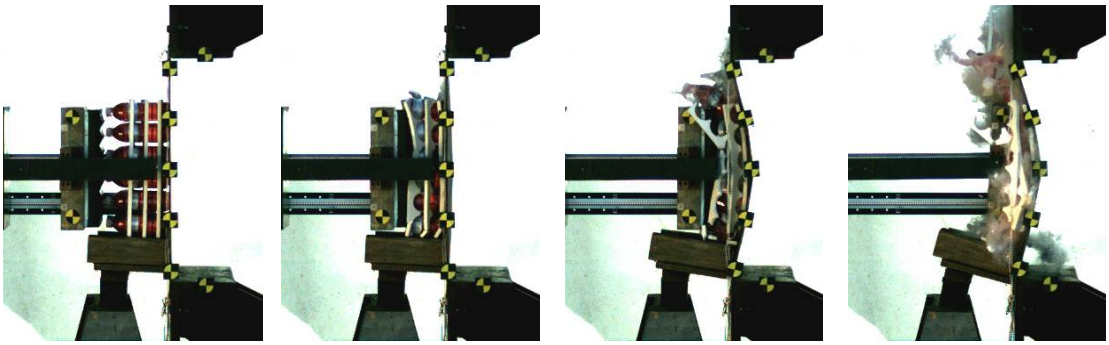

Figure F.124: Progression of damage for Test 47 from Camera 2

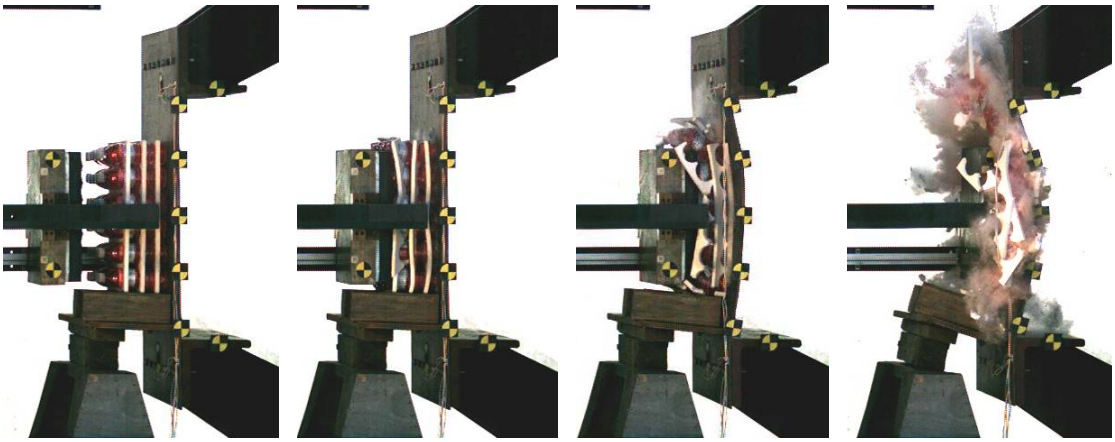

Figure F.125: Progression of damage for Test 47 from Camera 3

F.14 STEEL TOWER SINGLE PLATE: TEST 48 (SP48)

F.14.1 INTRODUCTION

The forty-seventh test of the Steel Tower Single Plate test series was performed on March 29th, 2007. The test specimen was a 1/4" thick steel plate labeled SP48. The Impacting Mass 3 was placed flush with the push plate and accelerated by the BG with a target velocity upon impact with the specimen of 75.46 ft/sec (23 m/s). Figure F.126 shows the steel plate prior to impact.

F.14.2 KINETIC ENERGY DEFEAT DEVICE (KEDD)

For this test a KEDD filled with bottles of water was used as discussed in Section 2.2. The device is shown in Figure F.126. The impacting mass does not extend the whole height of the KEDD and so it will not interfere with the support structure that the KEDD is sitting on. A drop of food coloring was added to each bottle of water to add contrast for the black and white video.

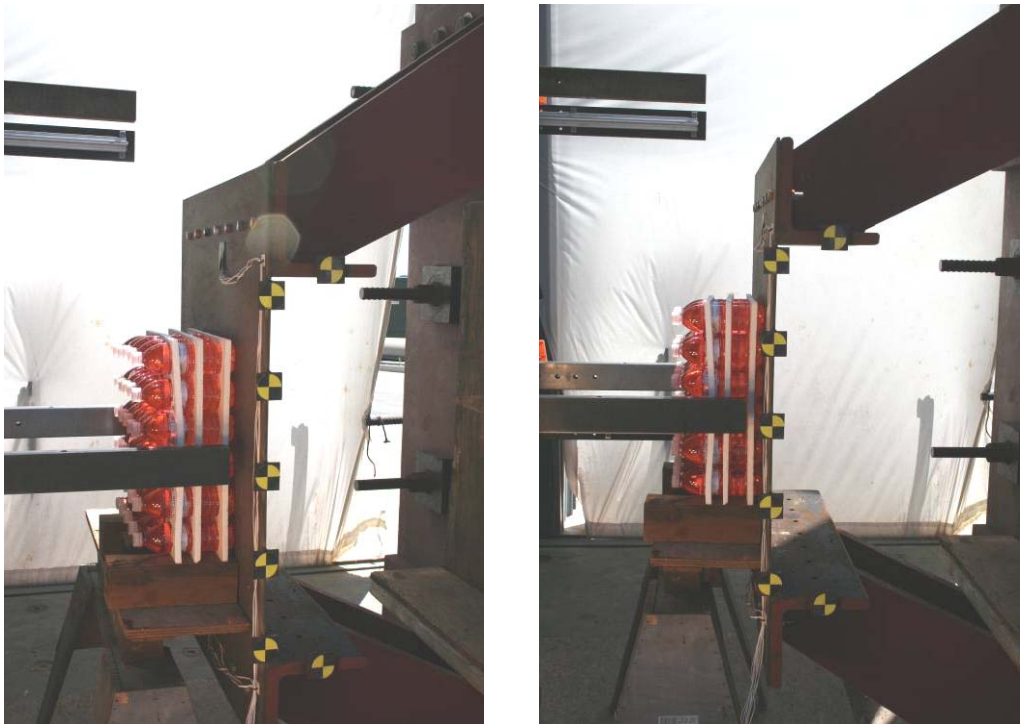

Figure F.126: 1/4" thick steel plate and KEDD pre test for Test 48

F.14.3 INSTRUMENTATION

F.14.3.1 PHANTOM CAMERAS

The first camera recorded in black and white at a rate of 10,000 frames per second at a resolution of 512x384. This camera was used in order to determine the maximum velocity of the impacting mass and the movement in the plate including the maximum displacement. The second camera recorded in color at a rate of 10,000 frames per second at a resolution of

512x384. This camera recorded the overall behavior of the test specimen. It was not used to gather any specific data. The third camera recorded in color at a rate of 8,000 frames per second at a resolution of 480x480. This camera captured the failure of the bolts. A picture from each of the camera locations are shown in Figure F.127.

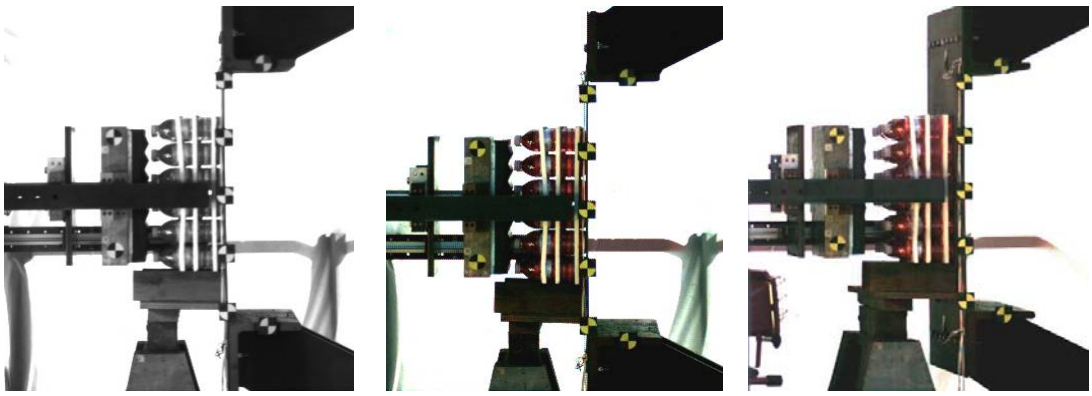

Figure F.127: Phantom Cameras for Test 48

a) Camera One b) Camera Two c) Camera Three

F.14.3.2 TARGET LOCATIONS

Five targets were welded onto the side of the steel plate as shown in Figure F.126. They were spaced at the intervals shown in Figure F.128. That figure also shows the location of the targets for the impacting mass. An additional two targets were placed on the angle at the top and the bottom end conditions. The distance between these two points is 74.93 cm (29 ½").

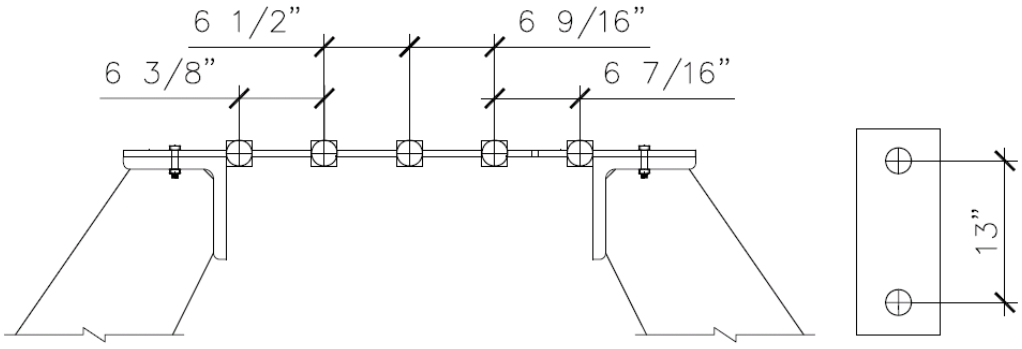

Figure F.128: Target layout on plate and impacting mass for Test 48

F.14.3.3 STRAIN GAGE LOCATIONS

For this test there were two strain gauges labeled 17 and 18. The strain gauges, and their locations, are shown in Figure F.129. Table F.13 shows the specific information about

this test, including the time and velocity at impact, if, and when, the bolts failed along with the maximum and minimum principal strain rates. The largest maximum principal strain rate for this test was 2.21 1/sec and was located at strain gage 17 while the largest minimum strain rate for this test was 1.70 1/sec located at strain gage 18. The maximum principal strains for gauges 17 and 18 can be found in Figure F.130 and the minimum principal strains for the same gauges can be found in Figure F.131.

Table F.13: Stain rate information for Test 48

Strain Gage Number	Actual Velocity	Initial Impact	Shear Wave at Gage	Bolts Break	Maximum Principal Strain Rate	Minimum Principal Strain Rate
17	23.34 m/s	50.60 msec	57.88 msec	70.00 msec	-2.21 1/sec	0.22 1/sec
18	23.34 m/s	50.60 msec	57.88 msec	70.00 msec	-1.89 1/sec	1.70 1/sec

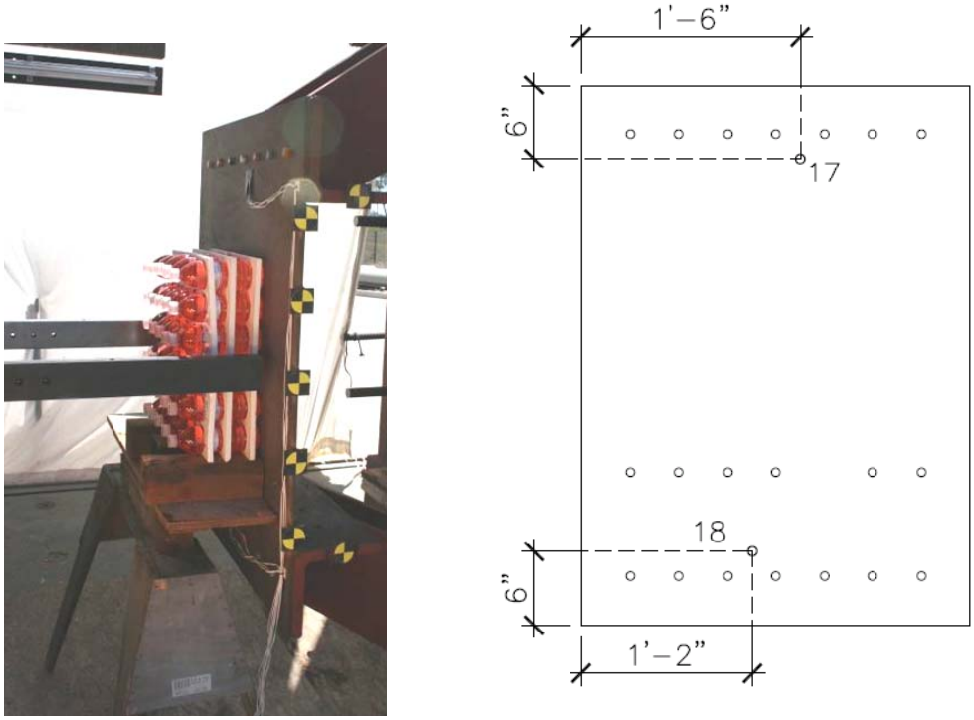

Figure F.129: Strain gage layout for Test 48

F.14.4 BOLT TYPE

A total of fourteen A307 bolts (Low Strength Bolts similar to Rivets) were used for this test. They were all tightened to a torque of 40 ft-lbs.

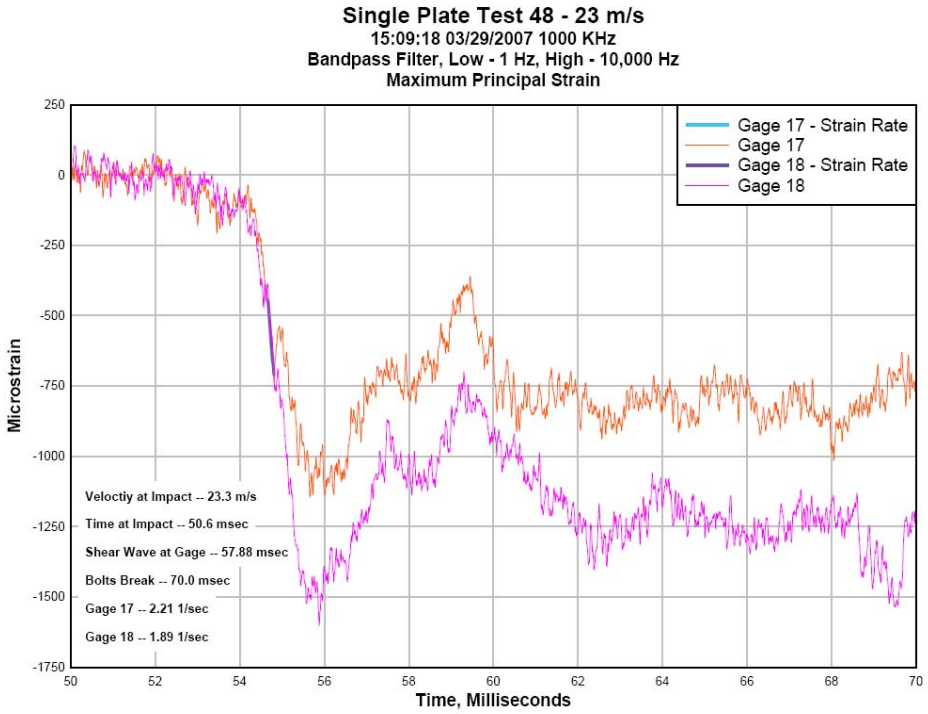

Figure F.130: Maximum principal strains and strain rates for Test 48

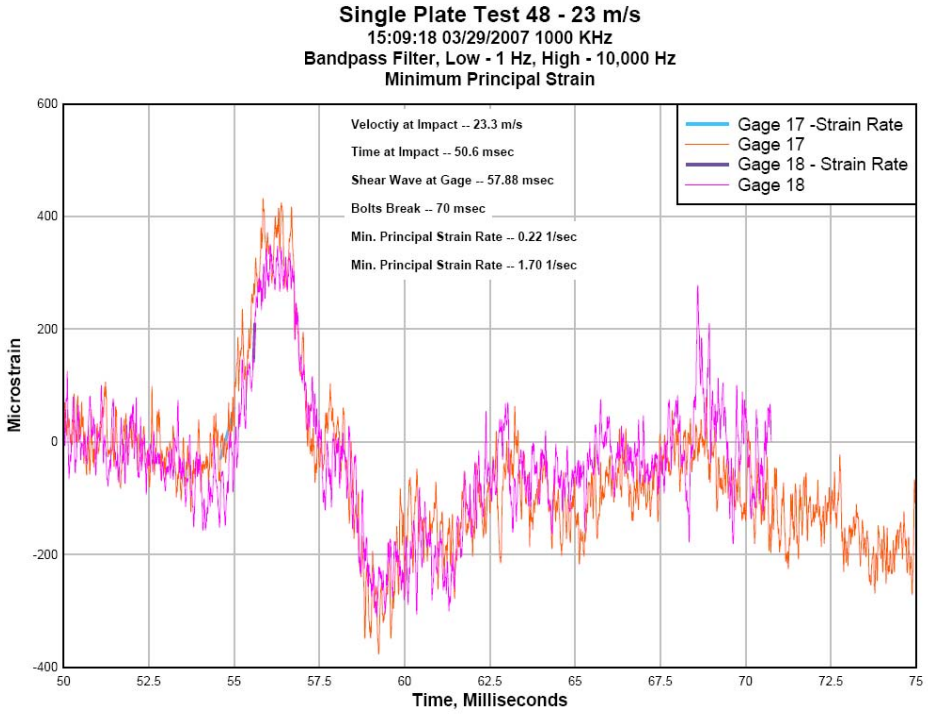

Figure F.131: Minimum principal strains and strain rates for Test 48

F.14.5 BLAST GENERATOR DATA

The initial impact of the single BG was 76.58 ft/sec (23.34 m/sec) with a goal velocity of 23 m/s. The average impact velocity for the impacting mass and the steel plate was calculated using the TEMA Track Eye tracking software.

F.14.6 SPECIMEN BEHAVIOR

The loading of the BG plate imparted an initial velocity of 76.57 ft/sec (23.34 m/sec) to the Kinetic Energy Defeat Device (KEDD). This caused plate to deform in both directions. The longitudinal deflection (in the north-south direction) behaved in a typical one-way flexural shape. This test imparted enough energy to break the top seven bolts as shown in Figure F.132. Due to the flexibility of the ¼" plate and the mass of water obscuring the cameras, the targets on the edge of the plate were not able to capture the maximum dynamic deflection of the plate.

During the test three different phantom cameras were used to capture the failure modes from different angles. Figure F.133 shows the progression of damage for this test from Phantom Camera One. Figure F.134 shows the progression of damage for this test from Phantom Camera Two. Figure F.135 shows the progression of damage for this test from Phantom Camera Three.

Figure F.132: Steel plate post test for Test 48

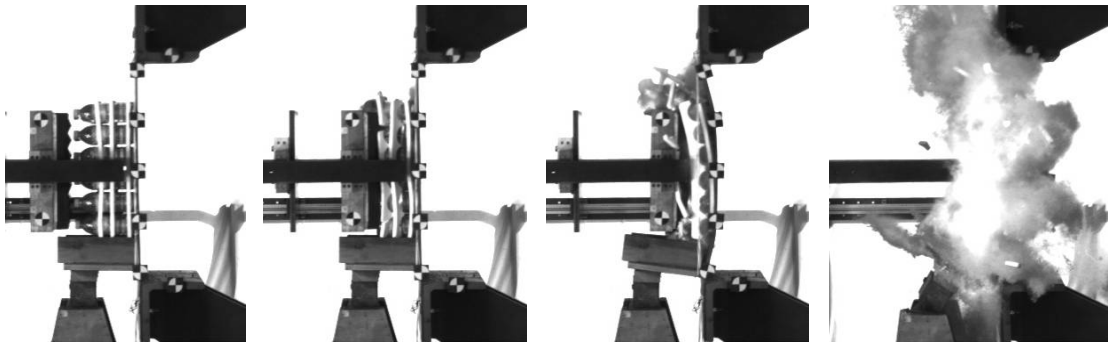

Figure F.133: Progression of damage for Test 48 from Camera 1

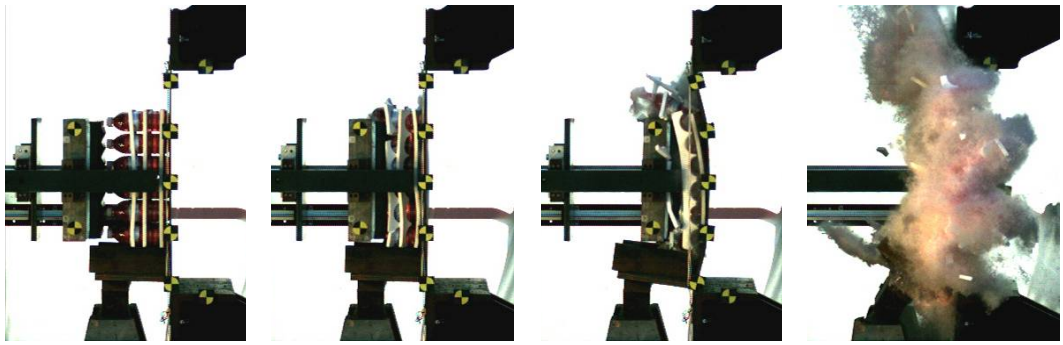

Figure F.134: Progression of damage for Test 48 from Camera 2

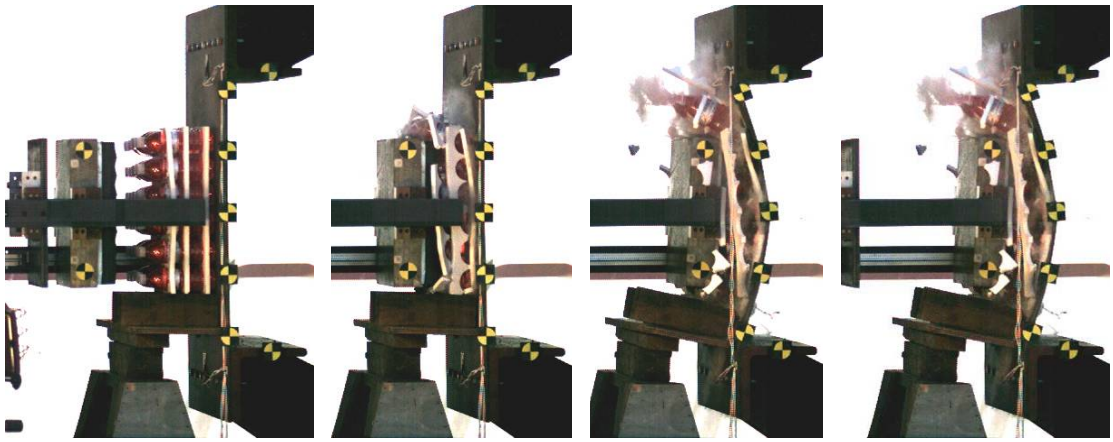

Figure F.135: Progression of damage for Test 48 from Camera 3

F.15 STEEL TOWER SINGLE PLATE: TEST 49 (SP49)

F.15.1 INTRODUCTION

The forty-ninth test of the Steel Tower Single Plate test series was performed on April 4th, 2007. The test specimen was a 1/4" thick steel plate labeled SP49. The Impacting Mass 3 was placed flush with the push plate and accelerated by the BG with a target velocity upon impact with the specimen of 70.54 ft/sec (21.5 m/s). Figure F.136 shows the steel plate prior to impact.

F.15.2 KINETIC ENERGY DEFEAT DEVICE (KEDD)

For this test a KEDD filled with bottles of water was used as discussed in Section 2.2. The device is shown in Figure F.136. The impacting mass does not extend the whole height of the KEDD and so it will not interfere with the support structure that the KEDD is sitting on. A drop of food coloring was added to each bottle of water to add contrast for the black and white video.

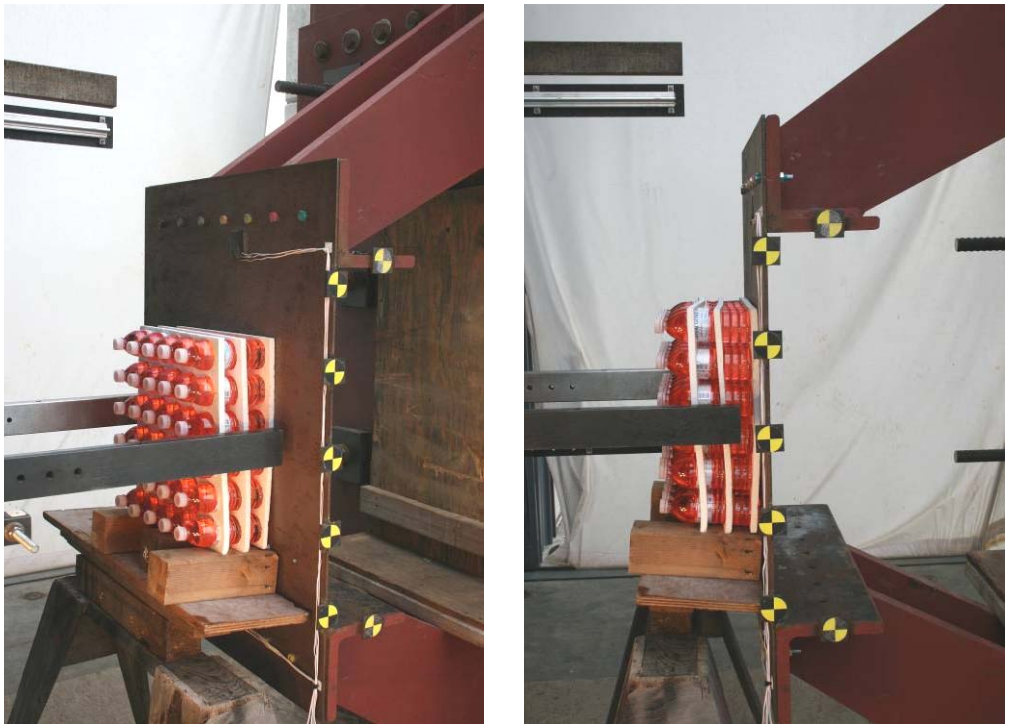

Figure F.136: 1/4" thick steel plate and KEDD pre test for Test 49

F.15.3 INSTRUMENTATION

F.15.3.1 PHANTOM CAMERAS

The first camera recorded in black and white at a rate of 10,000 frames per second at a resolution of 512x384. This camera was used in order to determine the maximum velocity of the impacting mass and the movement in the plate including the maximum displacement. The second camera recorded in color at a rate of 10,000 frames per second at a resolution of

512x384. This camera recorded the overall behavior of the test specimen. It was not used to gather any specific data. The third camera recorded in color at a rate of 5,000 frames per second at a resolution of 480x480. This camera captured the failure of the bolts. A picture from each of the camera locations are shown in Figure F.137.

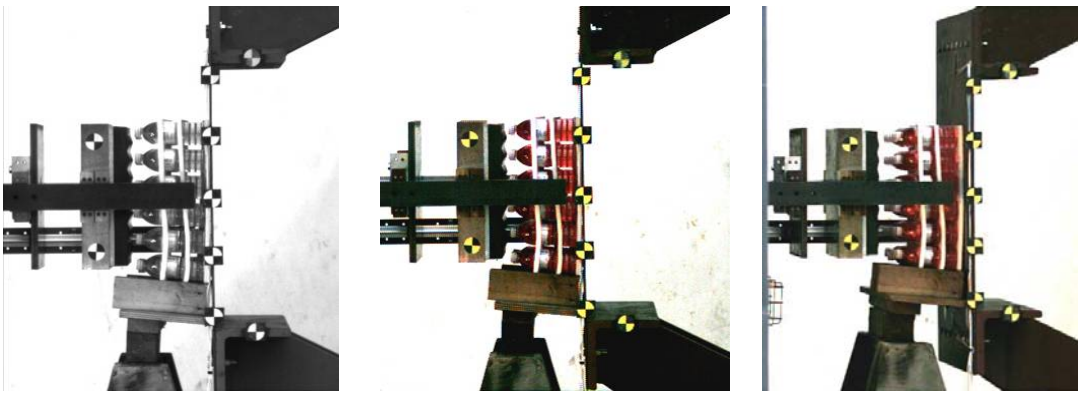

Figure F.137: Phantom Cameras for Test 49

a) Camera One b) Camera Two c) Camera Three

F.15.3.2 TARGET LOCATIONS

Five targets were welded onto the side of the steel plate as shown in Figure F.136. They were spaced at the intervals shown in Figure F.138. That figure also shows the location of the targets for the impacting mass. An additional two targets were placed on the angle at the top and the bottom end conditions. The distance between these two points is 74.93 cm (29 ½").

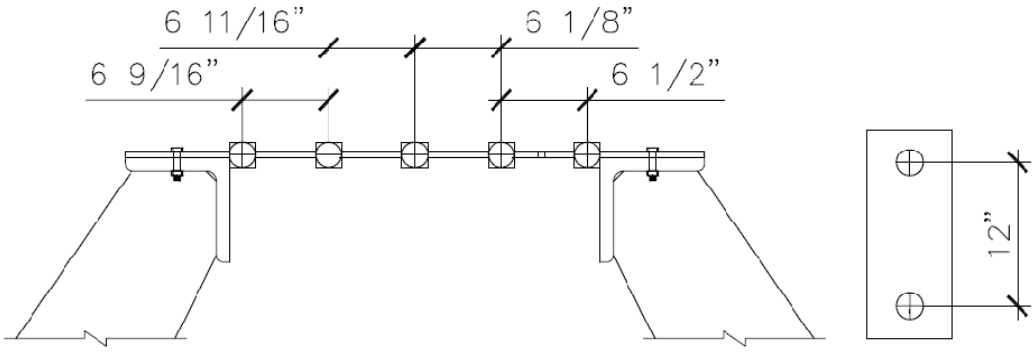

Figure F.138: Target layout on plate and impacting mass for Test 49

F.15.3.3 STRAIN GAGE LOCATIONS

For this test there were two strain gauges labeled 17, and 18. The strain gauges, and their locations, are shown in Figure F.139. Table F.14 shows the specific information about this test, including the time and velocity at impact, if, and when, the bolts failed along with the

maximum and minimum principal strain rates. The largest maximum principal strain rate for this test was 1.14 1/sec and was located at strain gage 18 while the largest minimum strain rate for this test was 0.22 1/sec located at strain gage 17. The maximum principal strains for gauges 17 and 18 can be found in Figure F.140 and the minimum principal strains for the same gauges can be found in Figure F.141.

Table F.14: Stain rate information for Test 49

Strain Gage Number	Actual Velocity	Initial Impact	Shear Wave at Gage	Bolts Break	Maximum Principal Strain Rate	Minimum Principal Strain Rate
17	21.3 m/s	52.30 msec	62.80 msec	-	-0.74 1/sec	0.22 1/sec
18	21.3 m/s	52.30 msec	62.80 msec	-	-1.14 1/sec	0.17 1/sec

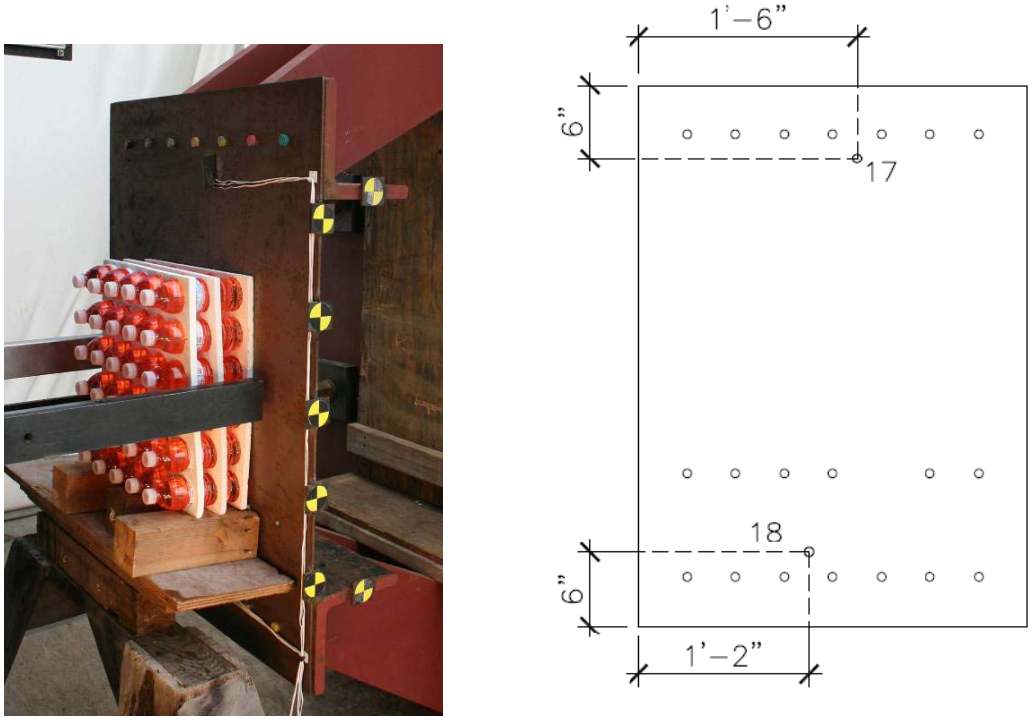

Figure F.139: Strain gage layout for Test 49

F.15.3.4 BOLT TYPE

A total of fourteen A307 bolts (Low Strength Bolts similar to Rivets) were used for this test. They were all tightened to a torque of 40 ft-lbs.

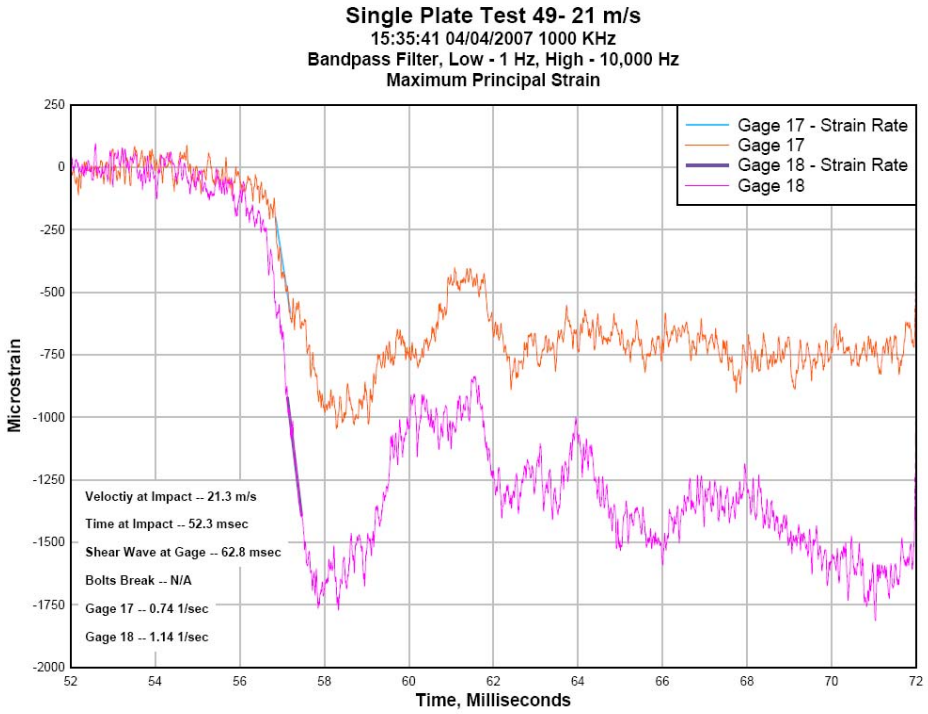

Figure F.140: Maximum principal strains and strain rates for Test 49

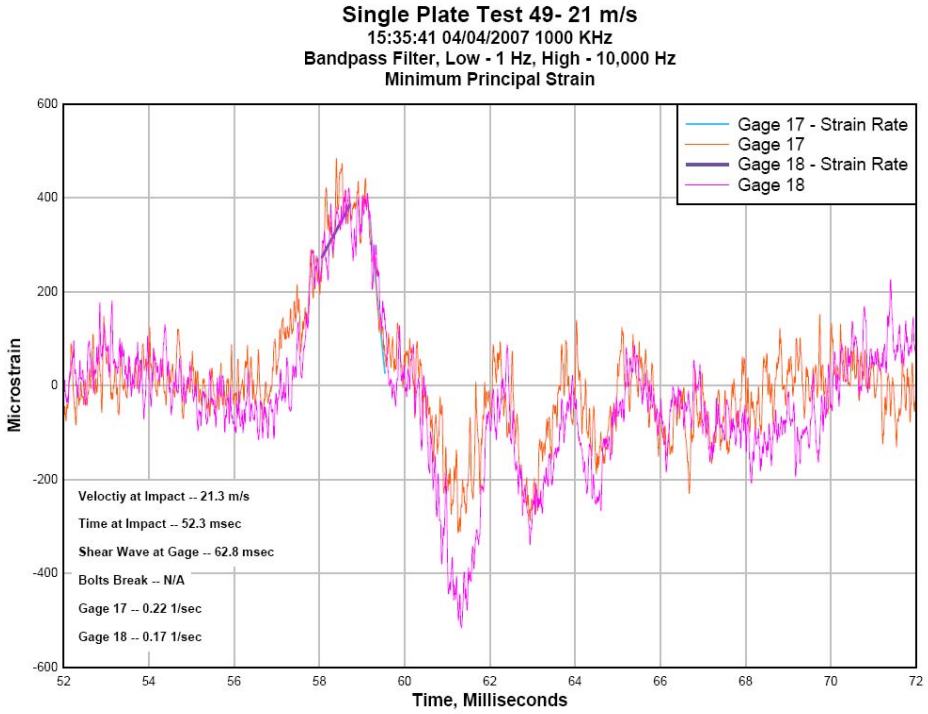

Figure F.141: Minimum principal strains and strain rates for Test 49

F.15.4 BLAST GENERATOR DATA

The initial impact of the single BG was 69.88 ft/sec (21.3 m/sec) with a goal velocity of 21.5 m/s. The average impact velocity for the impacting mass and the steel plate was calculated using the TEMA Track Eye tracking software.

F.15.5 SPECIMEN BEHAVIOR

The loading of the BG plate imparted an initial velocity of 69.88 ft/sec (21.3 m/sec) to the Kinetic Energy Defeat Device (KEDD). This caused plate to deform in both directions. The longitudinal deflection (in the north-south direction) behaved in a typical one-way flexural shape. This test did not impart enough energy to break the any of the bolts as shown in Figure F.142. Due to the flexibility of the ¼" plate and the mass of water obscuring the cameras, the targets on the edge of the plate were not able to capture the maximum dynamic deflection of the plate. The permanent deflection of the plate at midspan was 2 1/8".

During the test three different phantom cameras were used to capture the failure modes from different angles. Figure F.143 shows the progression of damage for this test from Phantom Camera One. Figure F.144 shows the progression of damage for this test from Phantom Camera Two. Figure F.145 shows the progression of damage for this test from Phantom Camera Three.

Figure F.142: Steel plate post test for Test 49

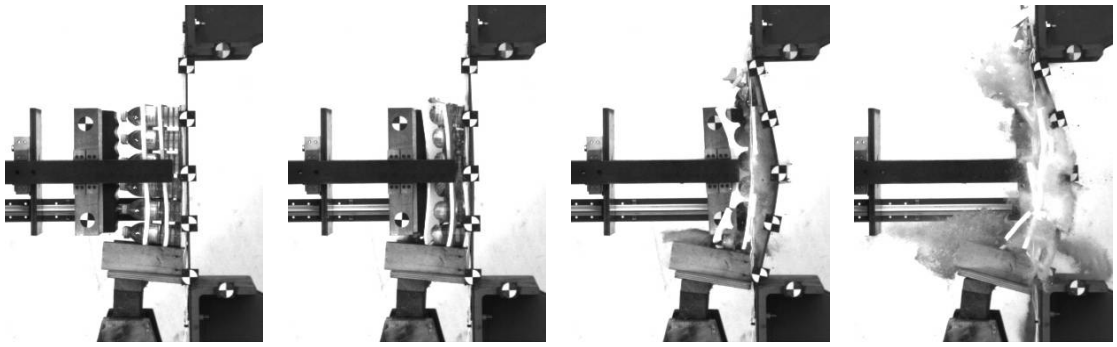

Figure F.143: Progression of damage for Test 49 from Camera 1

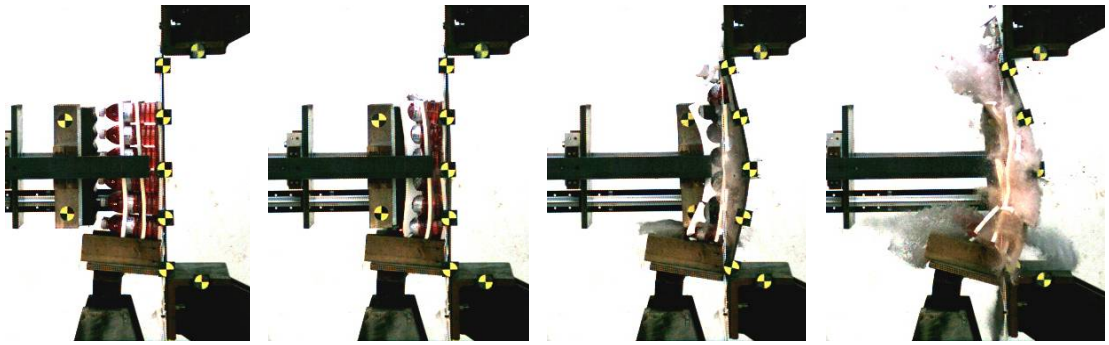

Figure F.144: Progression of damage for Test 49 from Camera 2

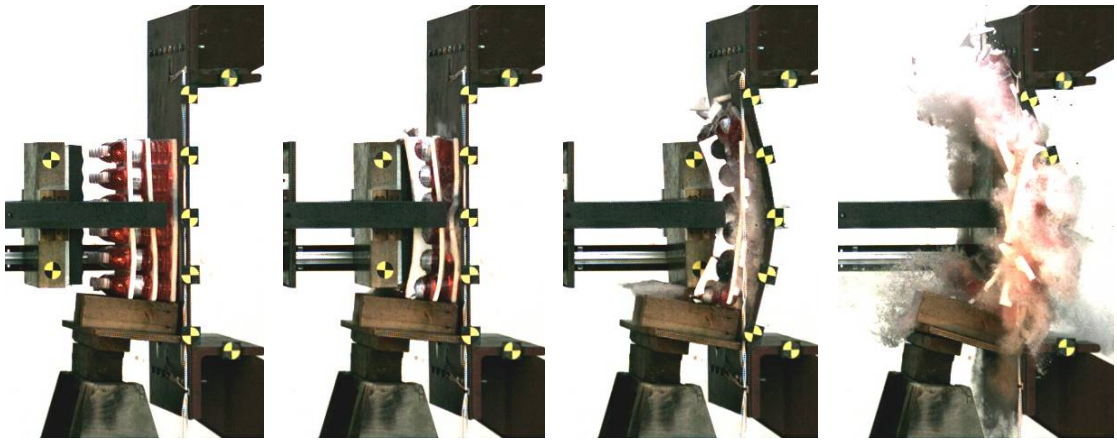

Figure F.145: Progression of damage for Test 49 from Camera 3

F.16 STEEL TOWER SINGLE PLATE: TEST 50 (SP50)

F.16.1 INTRODUCTION

The fiftieth test of the Steel Tower Single Plate test series was performed on April 5th, 2007. The test specimen was a 1/4" thick steel plate labeled SP50. The Impacting Mass 3 was placed flush with the push plate and accelerated by the BG with a target velocity upon impact with the specimen of 49.21 ft/sec (15 m/s). Figure F.146 shows the steel plate prior to impact.

Figure F.146: 1/4" thick steel plate pre test for Test 50

F.16.2 INSTRUMENTATION

F.16.2.1 PHANTOM CAMERAS

The camera's did not trigger properly the video data was not captured for this test.

F.16.2.2 TARGET LOCATIONS

Five targets were welded onto the side of the steel plate as shown in Figure F.146. They were spaced at the intervals shown in Figure F.147. That figure also shows the location of the targets for the impacting mass. An additional two targets were placed on the angle at the top and the bottom end conditions. The distance between these two points is 74.93 cm (29 ½").

F.16.2.3 STRAIN GAGE LOCATIONS

The data acquisition system did not trigger properly the strain gage data was not captured for this test.

F.16.2.4 BOLT TYPE

A total of fourteen A307 bolts (Low Strength Bolts similar to Rivets) were used for this test. They were all tightened to a torque of 40 ft-lbs.

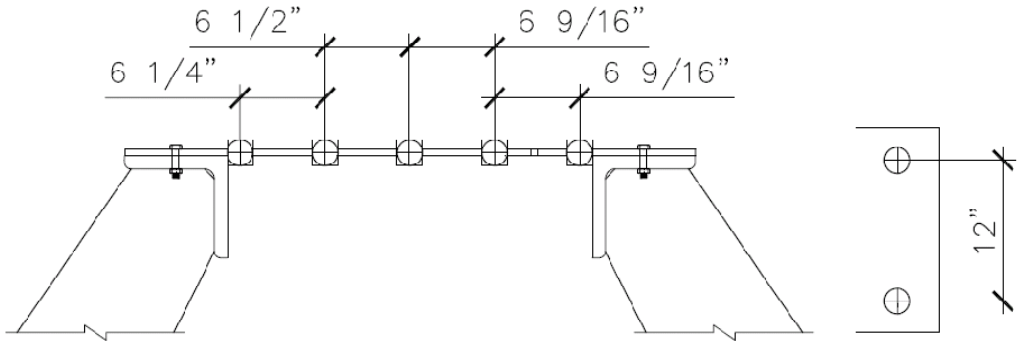

Figure F.147: Target layout on plate and impacting mass for Test 50

F.16.3 BLAST GENERATOR DATA

For this test the cameras failed so there is no data on velocity.

F.16.4 SPECIMEN BEHAVIOR

The loading of the BG plate imparted an approximate initial velocity of 49.21 ft/sec (15 m/sec) to the specimen. This caused plate to deform in both directions. The longitudinal deflection (in the north-south direction) behaved in a typical one-way flexural shape. This test did not impart enough energy to break the any of the bolts as shown in Figure F.148. The permanent deflection of the plate at midspan was 1 1/2".

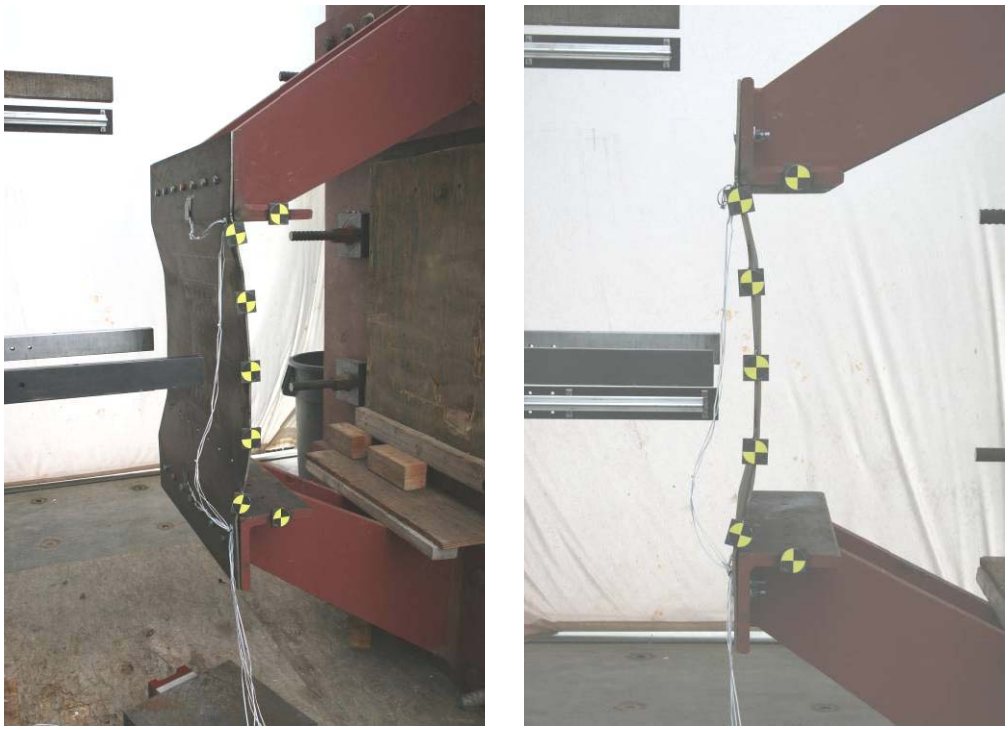

Figure F.148: Steel plate post test for Test 50

G FIELD TEST REPORTS

G.1 TEST 1 (CALIBRATION SHOT 1)

G.1.1 INTRODUCTION

The first Proof of Concept Test was performed at ARA's Rocky Mountain Division test site. It was a calibration shot using an equivalent of 0.034X pounds of TNT, placed in a 9" x 9" aluminum brownie tin, at a close standoff. The explosive material was tamped by hand to a density around 1.58 grams per cubic centimeter. The test specimen was a ¼" thick A36 steel plate supported by solid CMU blocks. A medium density fiberboard (MDF) spacer block was placed in between each course of CMU to achieve a total height of 1' between the steel plate and the supporting plywood. Figure G.1 shows the specimen prior to detonation.

Figure G.1: Test 1 set-up

G.1.2 INSTRUMENTATION

One set of Time of Arrival (TOA) pins were placed behind the plate. They were placed at 10", 7 1/2", 5" and 2 1/2" above the plywood surface below. The data that was retrieved from these pins can be found in Table G.1. The average velocity of the plate fragments, from the TOA pins was 3,200 ft/sec. The arrangement of TOA pins can be seen in Figure G.2

Table G.1: Time of Arrival Data for Test 1

Test	Pin Num	TOA	Plate Number	Pin Interval	Interval Velocity	Average Velocity
1	1	251 microsec	1	2.5 in	3360 ft/sec	3200 ft/sec
	2	313 microsec		2.5 in	3788 ft/sec	
	3	368 microsec		2.5 in	2451 ft/sec	
	4	453 microsec				

Figure G.2: Test 1 Time of Arrival Pins

G.1.3 SPECIMEN BEHAVIOR

The equivalent of 0.034X pounds of TNT used in this test formed a large hole in the center of the plate. As shown in Figure G.3. Figure G.4 and Figure G.5 show multiple fragments of varying sizes were formed from that hole. Figure G.6 demonstrates some of the petalling that was seen in the plate.

Figure G.3: Test 1 plate post test

Figure G.4: Test 1 plate fragmentation

Figure G.5: Test 1 plate fragmentation

Figure G.6: Test 1 plate petalling details

G.2 TEST 2 (CALIBRATION SHOT 2)

G.2.1 INTRODUCTION

The second Proof of Concept Test was performed at ARA's Rocky Mountain Division test site. It was a calibration shot using an equivalent of 0.034X pounds of TNT, placed in a 9" x 9" aluminum brownie tin, at a close standoff. The explosive material was tamped by hand to a density around 1.58 grams per cubic centimeter. The test specimen was a ¼" thick A36 steel plate supported by solid CMU blocks. A medium density fiberboard (MDF) spacer block was placed in between each course of CMU to achieve a total height of 1' between the steel plate and the supporting plywood. Figure G.7 shows the specimen prior to detonation.

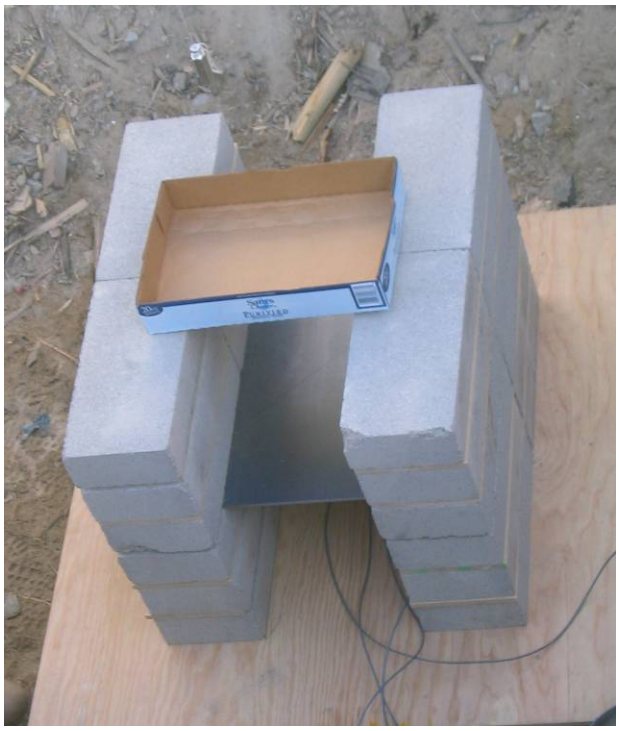

Figure G.7: Test 2 set-up

G.2.2 INSTRUMENTATION

One set of Time of Arrival (TOA) pins were placed behind the plate. They were placed at 10", 7 1/2", 5" and 2 1/2" above the plywood surface below. The data that was retrieved from these pins can be found in Table G.2. The average velocity of the plate fragments, from the TOA pins, was 2,127 ft/sec. The arrangement of TOA pins can be seen in Figure G.8

Table G.2: Time of Arrival Data for Test 2

Test	Pin Num	TOA	Plate Number	Pin Interval	Interval Velocity	Average Velocity
2	1	376 microsec	1	2.5 in	2083 ft/sec	2127 ft/sec
	2	476 microsec		2.5 in	2604 ft/sec	
	3	556 microsec		2.5 in	1694 ft/sec	
	4	679 microsec				

Figure G.8: Test 2 Time of Arrival Pins

G.2.3 SPECIMEN BEHAVIOR

The equivalent of 0.034X pounds of TNT used in this test caused the plate to shear in half, see
Figure G.9. Multiple fragments of varying sizes were formed during this test; they can be seen in Figure G.10 and Figure G.11

Figure G.9: Test 2 plate post test

Figure G.10: Test 2 plate fragments

Figure G.11: Test 2 plate fragments

G.3 TEST 3 (CALIBRATION SHOT 3)

G.3.1 INTRODUCTION

The third Proof of Concept Test was performed at ARA's Rocky Mountain Division test site. It was a calibration shot using an equivalent of 0.023X pounds of TNT, placed in a 9" x 9" aluminum brownie tin, at a close standoff. The explosive material was tamped by hand to a density around 1.58 grams per cubic centimeter. The test specimen was a ¼" thick A36 steel plate supported by solid CMU blocks. A medium density fiberboard (MDF) spacer block was placed in between each course of CMU to achieve a total height of 1' between the steel plate and the supporting plywood. Figure G.12 shows the specimen prior to detonation.

Figure G.12: Test 3 set-up

G.3.2 INSTRUMENTATION

One set of Time of Arrival (TOA) pins were placed behind the plate. They were placed at 10", 7 1/2", 5" and 2 1/2" above the plywood surface below. The data that was retrieved from these pins can be found in Table G.3. The average velocity of the plate fragments, from the TOA pins, was 1,764 ft/sec. The arrangement of TOA pins can be seen in Figure G.13.

Table G.3: Time of Arrival Data for Test 3

Test	Pin Num	TOA	Plate Number	Pin Interval	Interval Velocity	Average Velocity
3	1	440 microsec	1	2.5 in	1894 ft/sec	1764 ft/sec
	2	550 microsec		2.5 in	1911 ft/sec	
	3	659 microsec		2.5 in	1488 ft/sec	
	4	799 microsec				

Figure G.13: Test 3 Time of Arrival Pins

G.3.3 SPECIMEN BEHAVIOR

The equivalent of 0.023X pounds of TNT used in this test caused the plate to shear in half as shown in Figure G.14. A collection of flyer plates were formed from the center section of the plate demonstrated in Figure G.15. One flyer plate of significant size can be found in Figure G.16. The marks on the flyer plate are pits formed from the aluminum cake pan the charge was placed in.

Figure G.14: Test 3 plate post test

Figure G.15: Test 3 plate and fragments

Figure G.16: Test 3 a plate fragment

G.4 TEST 4 (CALIBRATION SHOT 4)

G.4.1 INTRODUCTION

The fourth Proof of Concept Test was performed at ARA's Rocky Mountain Division test site. It was a calibration shot using an equivalent of 0.0114X pounds of TNT, placed in a 9" x 9" aluminum brownie tin, at a close standoff. The explosive material was tamped by hand to a density around 1.58 grams per cubic centimeter. The test specimen was a ¼" thick A36 steel plate supported by solid CMU blocks. A medium density fiberboard (MDF) spacer block was placed in between each course of CMU to achieve a total height of 1' between the steel plate and the supporting plywood. Figure G.17 shows the specimen prior to detonation.

Figure G.17: Test 4 set-up

G.4.2 INSTRUMENTATION

One set of Time of Arrival (TOA) pins were placed behind the plate. They were placed at 10", 7 1/2", 5" and 2 1/2" above the plywood surface below. The data that was retrieved from these pins can be found in Table G.4 Damage occurred to the 3rd and 4th pins as shown in the table below. No data was recorded for these pins; therefore the average velocity was determined from only one interval. The average velocity of the plate fragments, from the TOA pins, was 1,764 ft/sec. The arrangement of TOA pins can be seen in Figure G.18

Table G.4: Time of Arrival Data for Test 4

Test	Pin Num	TOA	Plate Number	Pin Interval	Interval Velocity	Average Velocity
4	1	522 microsec	1	2.5 in	868 ft/sec	868 ft/sec
	2	762 microsec				
	3	n/a				
	4	n/a				

Figure G.18: Test 4 Time of Arrival Pins

G.4.3 SPECIMEN BEHAVIOR

The equivalent of 0.011X pounds of TNT used in this test caused one large flyer plate and a few smaller fragments in the center of the plate as shown in Figure G.19 and Figure G.20. Figure G.21 shows the specimen in the test bed.

Figure G.19: Test 4 plate and fragments

Figure G.20: Test 4 plate fragments

Figure G.21: Test 4 top plate post test

G.5 TEST 5 (FOUR-PLATE TEST)

G.5.1 INTRODUCTION

The fifth Proof of Concept Test was performed at ARA's Rocky Mountain Division test site. It used an equivalent of 0.014X pounds of TNT, placed in a 9" x 9" aluminum brownie tin, at a close standoff. The explosive material was tamed by hand to an approximate density of 1.58 grams/cubic centimeter. The test specimen was a series of four ¼" thick A36 steel plates supported by solid CMU blocks. A medium density fiberboard (MDF) spacer block was placed in between each course of CMU to achieve a total height of 1' between steel plates. Figure G.22 shows the specimen prior to detonation; the picture shown is a reflection of the test set-up from a mirror.

Figure G.22: Test 5 set-up

G.5.2 INSTRUMENTATION

A set of Time of Arrival pins (TOA's) were placed behind each plate, they were spaced at 10", 7 1/2", 5" and 2 1/2" above the surface of each plate below. Figure G.23 shows the array of pins placed on top of the bottom plate. The data gathered from these pins can be found in Table G.5. The only data shown is for the first set of TOA pins. Based on the damage shown in Figure G.24, the data gathered from any additional pins would have been erroneous. The data gathered shows that the fragment from the top plate was traveling at 1,116 ft/sec.

Figure G.23: Test 5 Time of Arrival pins

Table G.5: Time of Arrival Data for Test 5

Test	Pin Num	TOA	Plate Number	Pin Interval	**Interval Velocity**	**Average Velocity**
5	1	400 microsec	1	2.5 in	1190 ft/sec	1116 ft/sec
	2	575 microsec		2.5 in	1042 ft/sec	
	3	775 microsec				
	4	n/a				

G.5.3 SPECIMEN BEHAVIOR

used an equivalent of 0.014X pounds of TNT did not cause as much damage as anticipated. Damage occurred only to the top two plates as shown in Figure G.24. The top plate formed a classical flyer plate, Figure G.25, which impacted, but did not penetrate, the second plate. That plate then separated from its supports and landed on the third plate. There was no damage to the bottom, or fourth, plate.

Figure G.24: Test 5 a) Entire test specimen post test b) Second, third and fourth plates post test

Figure G.25: Test 5 top plate

G.6 TEST 6 (TWO-PLATE TEST – NO KEDD)

G.6.1 INTRODUCTION

The sixth Proof of Concept Test was performed at ARA's Rocky Mountain Division test site. It used an equivalent of 0.023X pounds of TNT, placed in a 9" x 9" aluminum brownie tin, at a close standoff. The test specimen was a series of two ¼" thick A36 steel plates supported by solid CMU blocks. A medium density fiberboard (MDF) spacer block was placed in between each course of CMU to achieve a total height of 1' between steel plates. Figure G.26(a) shows the specimen prior to detonation. Figure G.26(b) shows the charge for the test. The explosive material was tamped by hand to an approximate density of 1.58 grams/ cubic centimeter.

Figure G.26: a) Test 6 set-up b) Charge for Test 6

G.6.2 INSTRUMENTATION

One set of Time of Arrival (TOA) pins were placed behind the bottom plate. They were spaced at 11 1/2", 11", 10 1/2" and 10" above the plywood surface below. The data that was retrieved from these pins can be found in Table G.6. The velocity of the fragments created from the second, or bottom, plate was determined to be traveling at a velocity of 1,036 ft/sec. The arrangement of TOA pins can be seen in Figure G.27

Table G.6: Time of Arrival Data for Test 6

Test	Pin Num	TOA	Plate Number	Pin Interval	Interval Velocity	Average Velocity
6	1	933 microsec	2	0.5 in	1096 ft/sec	1036 ft/sec
	2	971 microsec		0.5 in	1126 ft/sec	
	3	1008 microsec		0.5 in	887 ft/sec	
	4	1055 microsec				

Figure G.27: Test 6 Time of Arrival pins

G.6.3 SPECIMEN BEHAVIOR

The equivalent of 0.023X pounds of TNT used in this test caused large holes to be created in both the top and bottom plates as demonstrated in Figure G.28. The top plate was split into two large pieces with multiple flyer plates, as shown in Figure G.29. The large flyer plate, shown in Figure G.30, impacted the bottom plate and formed an additional, or secondary, flyer plate, see Figure G.31. Figure G.32 and Figure G.33 shows some of the petalling that occurred along the free edges of the bottom plate. Figure G.34 compares the type of damage that occurred to top and bottom plates. The top plate is shown at the top of the photograph and the bottom plate is shown at the bottom. The difference in damage mechanisms due to the velocity of the fragments is demonstrated in this photo. The initial blast forms many fragments, but as the larger one impacts the second plate it forms a slightly smaller flyer plate and the plate behaves in a more ductile manner, which can be seen in the petalling effects of the plate. Figure G.35 shows the two flyer plates. The larger one, folded in half, is from the top plate and the smaller, flatter flyer plate, was formed from the bottom plate and was traveling at a velocity of 1,036 ft/sec.

Figure G.28: Test 6 post test

Figure G.29: Test 6 top plate

Figure G.30: Test 6 top flyer plate

Figure G.31: Test 6 bottom flyer plate

Figure G.32: Test 6 bottom plate

Figure G.33: Test 6 bottom plate petalling details

Figure G.34: Test 6 top and bottom plates

Figure G.35: Test 6 top and bottom flyer plates

G.7 TEST 7 (TWO-PLATE TEST –KEDD ON BOTTOM)

G.7.1 INTRODUCTION

The seventh Proof of Concept Test was performed at ARA's Rocky Mountain Division test site. It used an equivalent of 0.023X pounds of TNT, placed in a 9" x 9" aluminum brownie tin, at a close standoff. The test specimen was a series of two ¼" thick A36 steel plates supported by solid CMU blocks. A medium density fiberboard (MDF) spacer block was placed in between each course of CMU to achieve a total height of 1' between steel plates. Figure G.36 (a) shows the specimen prior to detonation. Figure G.36(b) shows the charge for the test. The explosive material was tamped by hand to an approximate density of 1.58 grams/ cubic centimeter.

Figure G.36: a) Test 7 set-up b) Charge for Test 7

G.7.2 KINETIC ENERGY DEFEAT DEVICE

A Kinetic Energy Defeat Device (KEDD) was used in this test. Each device consists of a 2" diameter thin walled plastic tube, manufactured by VisiPak, filled with water and sealed off on both ends by black plastic caps. The total length of each device was 12". They were then spaced at 3" on center with the middle KEDD placed in the center of the plate. Figure C.37 (a) shows one KEDD, while Figure C.37 (b) shows an array of 9 KEDD's. The array of KEDD's was placed directly above the bottom plate as shown in Figure G.36(a). The metal support system, constructed out of light gage steel, was used to keep each individual KEDD in place.

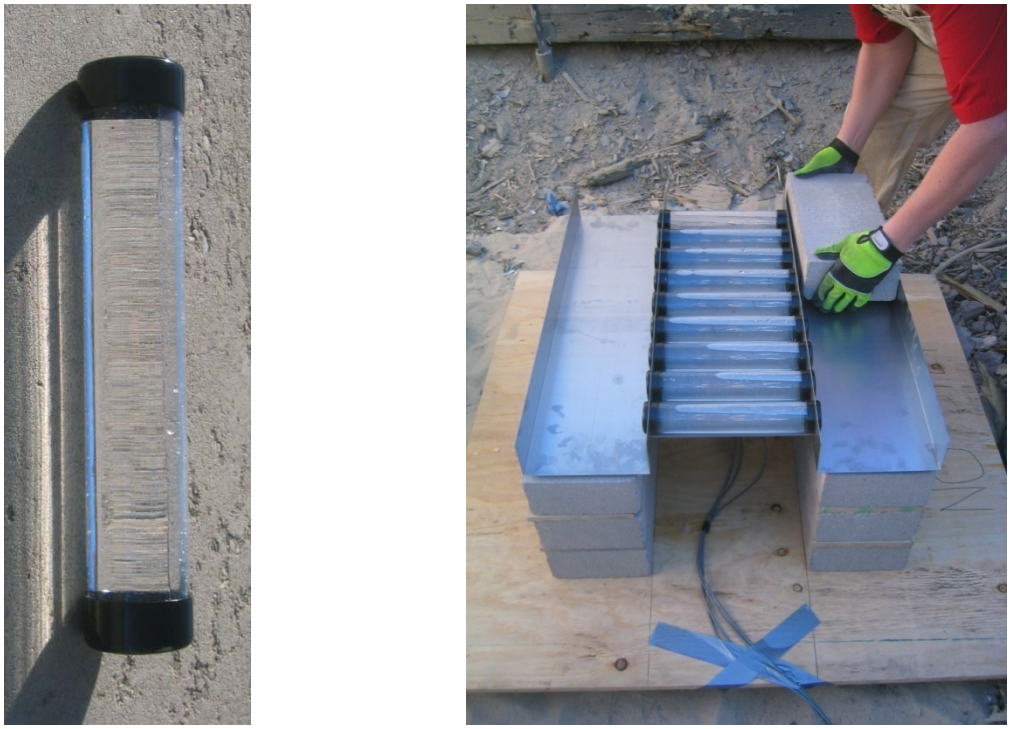

Figure G.37: a) Individual KEDD b) Test 7 Array of 9 KEDD's

G.7.3 INSTRUMENTATION

One set of Time of Arrival (TOA) pins were placed behind the bottom plate. They were spaced at 10", 7 1/2", 5" and 2 1/2" above the plywood surface below. The data that was retrieved from these pins can be found in Table G.7. The velocity of the fragments created from the second, or bottom, plate was determined to be traveling at a velocity of 592 ft/sec. The arrangement of TOA pins can be seen in Figure G.38.

Table G.7: Time of Arrival Data for Test 7

Test	Pin Num	TOA	Plate Number	Pin Interval	Interval Velocity	Average Velocity
7	1	923 microsec	2	0.5 in	772 ft/sec	592 ft/sec
	2	977 microsec		0.5 in	694 ft/sec	
	3	1037 microsec		0.5 in	309 ft/sec	
	4	1172 microsec				

Figure G.38: Test 7 Time of Arrival pins

G.7.4 SPECIMEN BEHAVIOR

The equivalent of 0.023X pounds of TNT caused one large, classical, flyer plate to be formed in the top plate which then impacted the second plate. The plates, still in their final resting position, can be seen in Figure G.39. The flyer plate formed from the top plate, and the remnants of that plate are shown in Figure G.40. That flyer plate then impacted the second plate and caused a large section of the plate to begin to separate from the bottom plate as shown in Figure G.41. The bottom plate behaved in a more ductile manner than previous tests, which could be attributed to the KEDD system. Figure G.42 shows a comparison of the two plates. The plate at the top of the photo was the top plate, while the plate at the bottom was the bottom plate.

Figure G.39: Test 7 post test

Figure G.40: Test 7 top plate

Figure G.41: Test 7 bottom plate

Figure G.42: Test 7 top and bottom plate

G.8 TEST 8 (TWO-PLATE TEST – KEDD ON TOP)

G.8.1 INTRODUCTION

The eighth Proof of Concept Test was performed at ARA's Rocky Mountain Division test site. It used an equivalent of 0.023X pounds of TNT, placed in a 9" x 9" aluminum brownie tin, at a close standoff. The test specimen was a series of two ¼" thick A36 steel plates supported by solid CMU blocks. A medium density fiberboard (MDF) spacer block was placed in between each course of CMU to achieve a total height of 1' between steel plates. Figure G.43(a) shows the specimen prior to detonation. Figure G.43(b) shows the charge for the test. The explosive material was tamped by hand to an approximate density of 1.58 grams/ cubic centimeter.

Figure G.43: a) Test 8 set-up b) Charge for Test 8

G.8.2 KINETIC ENERGY DEFEAT DEVICE

A Kinetic Energy Defeat Device (KEDD) was used in this test. Each device consists of a 2" diameter thin walled plastic tube, manufactured by VisiPak, filled with water and sealed off on both ends by black plastic caps. The total length of each device was 12". They were then spaced at 3" on center with the middle KEDD placed in the center of the plate. Figure G.44(a) shows one KEDD, while Figure G.44(b) shows an array of 9 KEDD's. The top plate will be placed directly above the array of KEDD's as shown in Figure G.43(a). The metal support system, constructed out of light gage steel, was used to keep each individual KEDD in place.

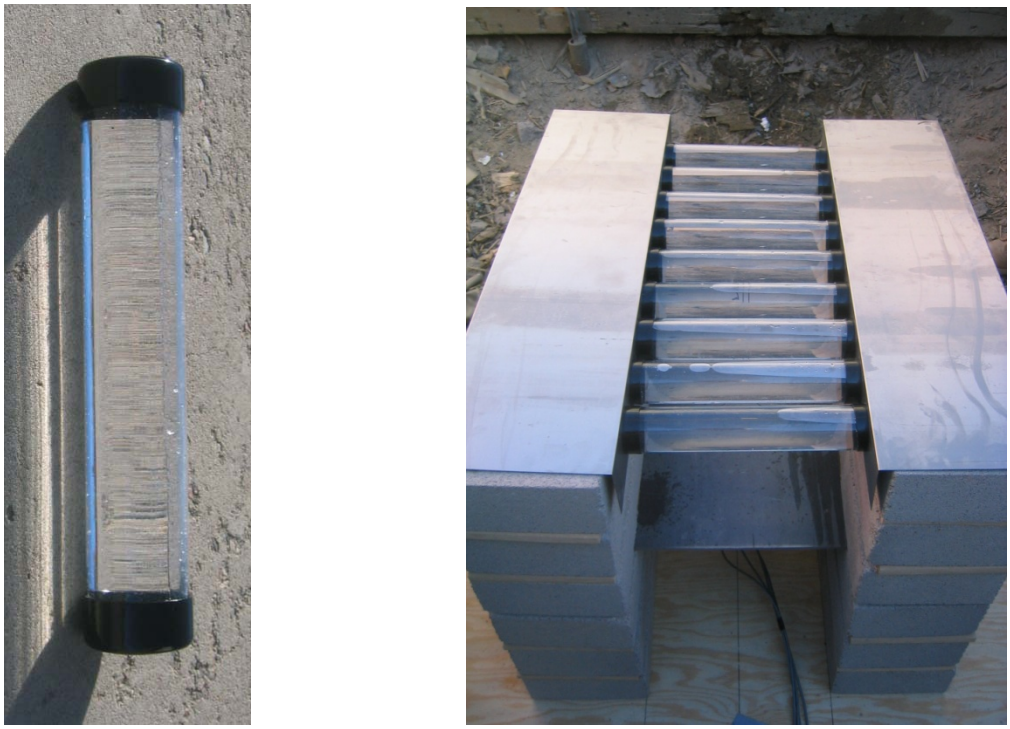

Figure G.44: a) Individual KEDD b) Test 8 Array of 9 KEDD's

G.8.3 INSTRUMENTATION

One set of Time of Arrival (TOA) pins were placed behind the bottom plate. They were spaced at 10", 7 1/2", 5" and 2 1/2" above the plywood surface below. The data that was retrieved from these pins can be found in Table G.8. The velocity of the fragments created from the second, or bottom, plate was determined to be traveling at a velocity of 453 ft/sec. The arrangement of TOA pins can be seen in Figure G.45

Table G.8: Time of Arrival Data for Test 8

Test	Pin Num	TOA	Plate Number	Pin Interval	Interval Velocity	Average Velocity
8	1	1212 microsec	2	0.5 in	239 ft/sec	453 ft/sec
	2	1386 microsec		0.5 in	541 ft/sec	
	3	1463 microsec		0.5 in	579 ft/sec	
	4	1535 microsec				

Figure G.45: Test 8 Time of Arrival pins

G.8.4 SPECIMEN BEHAVIOR

The equivalent of 0.023X pounds of TNT caused one large, classical, flyer plate to be formed in the top plate which then impacted the second plate. The plates, still in their final resting position, can be seen in Figure G.46. The flyer plate formed from the top plate impacted the second plate and caused the second plate to release from its supports and fold in half. The remnants on the top plate can be seen in Figure G.47. The bottom plate is shown in Figure G.48. It is important to note, that while the plate folded in half and separated from the supports, the plate itself did not fracture. If the plate was held in place better, the plate might not have been damaged as severely. The change in amount damage that occurred to the second plate can be attributed to the effectiveness of the KEDD system. As demonstrated in previous tests the damage that occurred to the second plate is less for this test, than previous tests. This can lead to the understanding that the liquid filled KEDD's work better when not placed in front of a steel plate. This enables the liquid to be redirected before it impacts the second plate. Figure G.49 shows a comparison of the two plates. The plate at the top of the photo was the top plate, while the plate at the bottom was the bottom plate.

Figure G.46: Test 8 post test

Figure G.47: Test 8 top plate

Figure G.48: Test 8 bottom plate

Figure G.49: Test 8 top and bottom plate

G.9 TEST 9 (THREE-PLATE TEST – KEDD ON TOP)

G.9.1 INTRODUCTION

The ninth Proof of Concept Test was performed at ARA's Rocky Mountain Division test site. It used an equivalent of 0.034X pounds of TNT, placed in a 9" x 9" aluminum brownie tin, at a close standoff. The test specimen was a series of three ¼" thick A36 steel plates supported by solid CMU blocks. A medium density fiberboard (MDF) spacer block was placed in between each course of CMU to achieve a total height of 1' between steel plates. Figure G.50(a) shows the specimen prior to detonation. Figure G.50(b) shows the test specimen with the charge in place. The explosive material was tamped by hand to an approximate density of 1.58 grams/cubic centimeter.

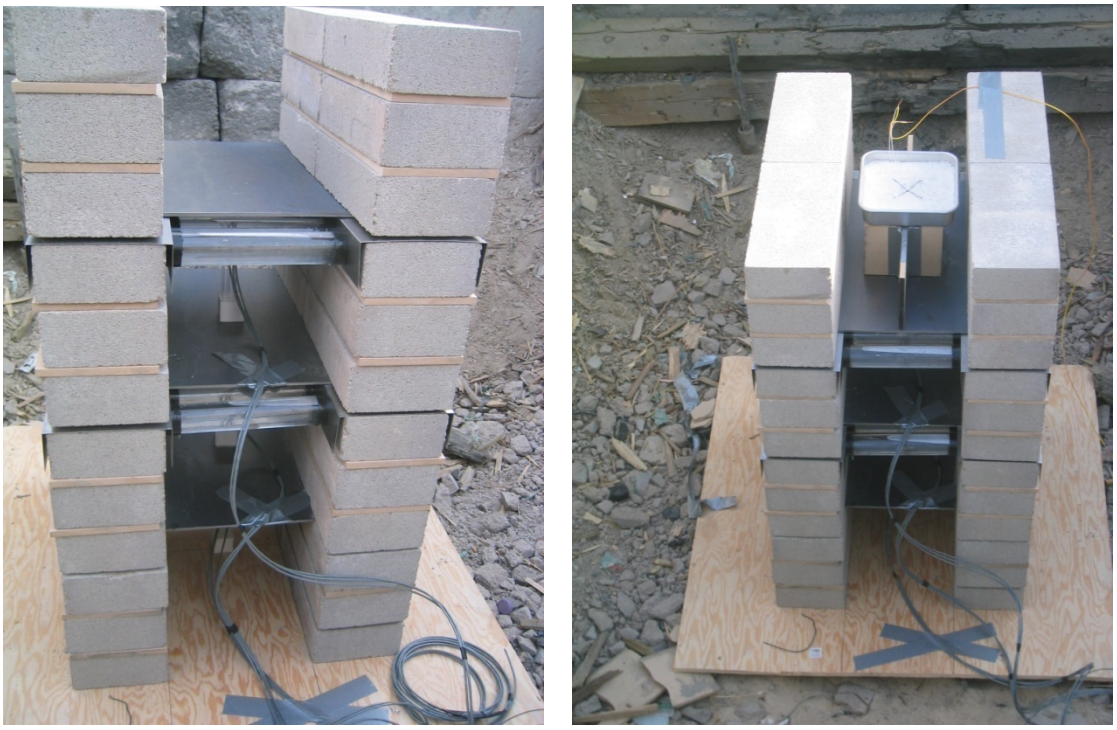

Figure G.50: a) Test 9 set-up b) Test 9 with charge

G.9.1 KINETIC ENERGY DEFEAT DEVICE

A series of two Kinetic Energy Defeat Devices (KEDD's) was used in this test. Each device consists of a 2" diameter thin walled plastic tube, manufactured by VisiPak, filled with water and sealed off on both ends by black plastic caps. The total length of each device was 12". They were then spaced at 3" on center with the middle KEDD placed in the center of the plate. Figure G.51(a) shows one KEDD, while Figure G.51(b) shows an array of 9 KEDD's. The top plate will be placed directly above the array of KEDD's as shown in Figure G.50 and Figure G.52. The metal support system, constructed out of light gage steel, was used to keep each individual KEDD in place.

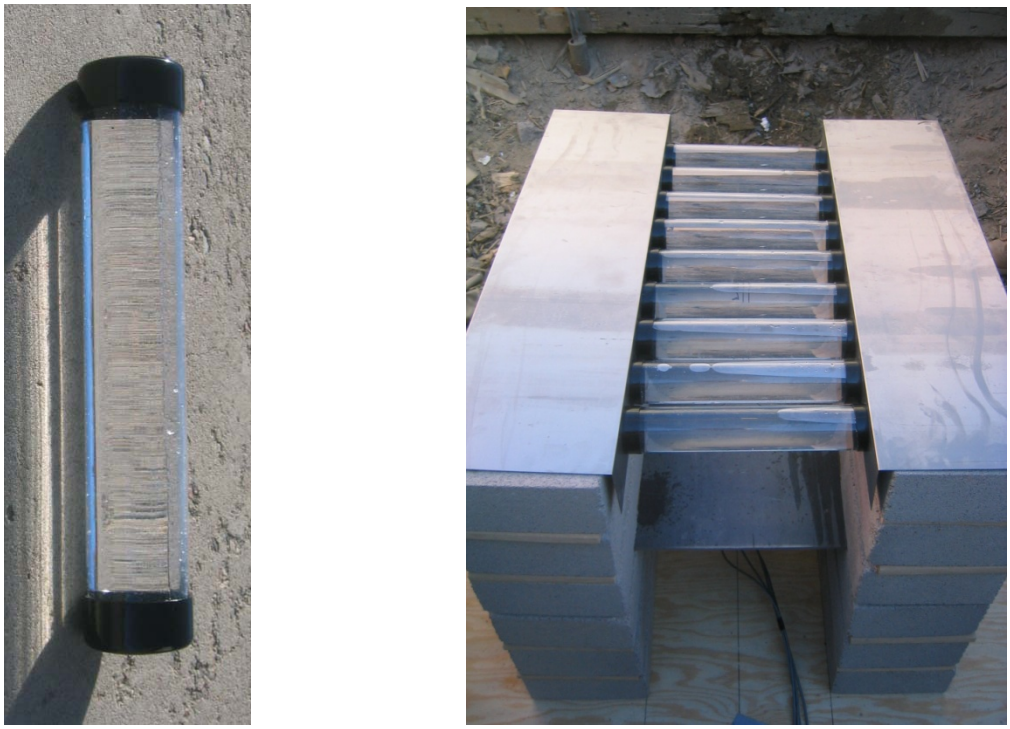

Figure G.51: a) Individual KEDD b) Test 9 Array of 9 KEDD's

G.9.2 INSTRUMENTATION

One set of Time of Arrival (TOA) pins were placed behind each plate. They were spaced at 11 1/2", 11" and 10 1/2" above the surface of the plate below. The arrangements of TOA pins can be seen in Figure G.52. They could not be placed in the center of the plate because a KEDD was located there. Instead they were placed on alternating sides of the center KEDD. They will measure how the velocity is slowed between plate impacts with the KEDD. The data that was retrieved from these pins can be found in Table G.9. The velocity of the fragments created from the top plate was 4,167 ft/sec. They impacted the second plate and created additional flyer plates. The fragments from the second plate traveled at a velocity of 763 ft/sec. The data gathered from the third set of pins was discarded since no fragments were formed.

Table G.9: Time of Arrival Data for Test 9

Test	Pin Num	TOA	Plate Number	Pin Interval	Interval Velocity	Average Velocity
9	1	122 microsec	1	0.5 in	4167 ft/sec	4167 ft/sec
	2	132 microsec		0.5 in	4167 ft/sec	
	3	142 microsec				
	4	516 microsec	2	0.5 in	458 ft/sec	763 ft/sec
	5	607 microsec		0.5 in	1068 ft/sec	
	6	646 microsec				

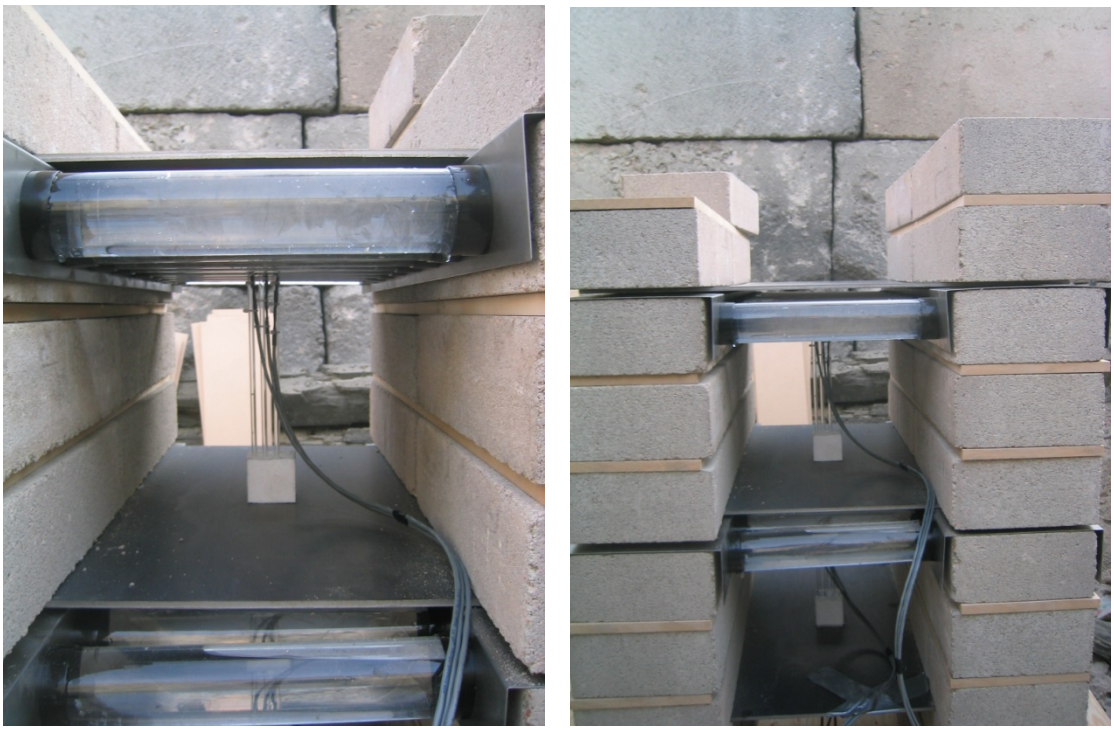

Figure G.52: Test 9 Time of Arrival pins

G.9.3 SPECIMEN BEHAVIOR

The equivalent of 0.034X pounds of TNT caused significant damage to the first two plates. Figure G.53 and Figure G.54 shows the test specimen after the test. Several small flyer plates were formed in the top plate. They were all formed from the center of the plate as demonstrated in Figure G.55. The plate behaved in a ductile manner forming small fragments and exhibiting some petalling around the edges, as shown in Figure G.56. The flyer plates from the top plate impacted the second plate and formed one additional flyer plate. Again, the ductility in the plate, indicative of lower strain rates, was demonstrated in the petalling of the plate. The middle plate was bent in half by the force of the fragment which enabled it to release from the supports. The remnants of the second plate are in Figure G.57. The middle plate then impacted the bottom plate. Figure G.58 shows a small crack in the middle of the bottom plate and the deformation that the second plate caused. Figure G.59 shows a comparison of the tree plates. The plate at the top of the photo was the top plate, the plate in the middle was the middle plate and the plate at the bottom was the bottom plate.

Figure G.53: Test 9 post test

Figure G.54: Test 9 post test

Figure G.55: Test 9 top plate

Figure G.56: Test 9 top plate petalling details

Figure G.57: Test 9 middle plate

Figure G.58: Test 9 bottom plate

Figure G.59: Test 9 top, middle, and bottom plates

G.10 TEST 10 (THREE-PLATE TEST)

G.10.1 INTRODUCTION

The tenth Proof of Concept Test was performed at ARA's Rocky Mountain Division test site. It used an equivalent of 0.034X pounds of TNT, placed in a 9" x 9" aluminum brownie tin, at a close standoff. The test specimen was a series of three ¼" thick A36 steel plates supported by solid CMU blocks. A medium density fiberboard (MDF) spacer block was placed in between each course of CMU to achieve a total height of 1' between steel plates. Figure G.60(a) shows the specimen prior to detonation. Figure G.60(b) shows the test specimen with the charge in place. The explosive material was tamped by hand to an approximate density of 1.58 grams/cubic centimeter.

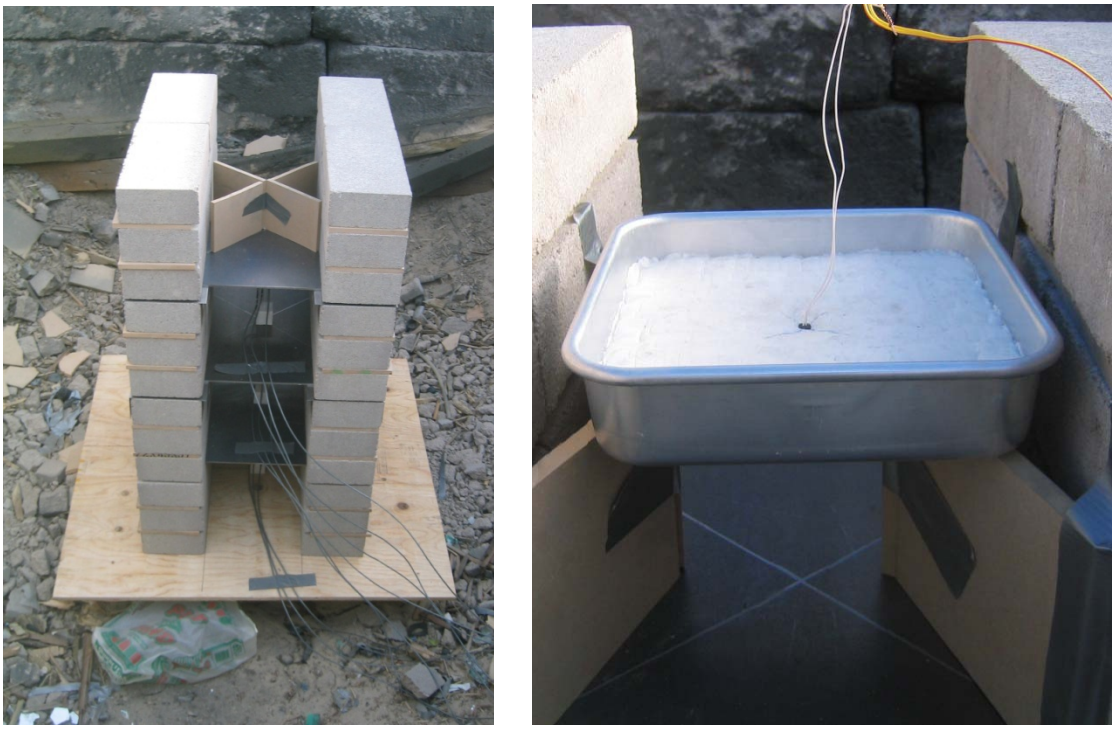

Figure G.60: a) Test 10 set-up b) Charge for Test 10

G.10.2 INSTRUMENTATION

One set of Time of Arrival (TOA) pins were placed behind each plate. They were spaced at 10", 7 1/2" and 5" above the surface of the plate below. The arrangements of TOA pins can be seen in Figure G.61. They were placed in the center of each plate. They will measure how the velocity is slowed between plate impacts. The data can be compared to test 10, but it should be noted that the velocity profiles are taken at different locations. All of the data for Test 9 was gathered before the first pin in Test 10 was impacted. The data that was retrieved from these pins can be found in Table G.10. The velocity of the fragments created from the top plate was 8,695 ft/sec. They impacted the second plate and created additional flyer plates traveling at a velocity of 1,567 ft/sec. The flyer plates from the first and second

plates impacted the third plate and created additional fragments with an average velocity of 1,280 ft/sec.

The KEDD hangers were used in this test to determine if they had any effect on the behavior of the steel supports above them.

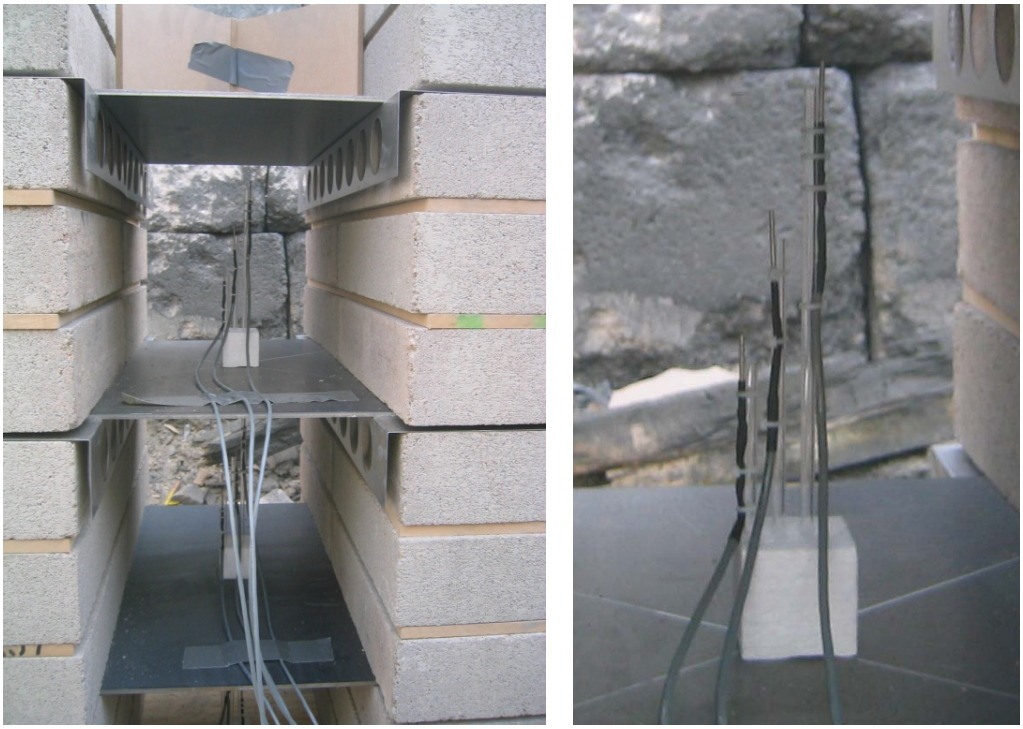

Figure G.61: Test 10 Time of Arrival pins

Table G.10: Time of Arrival Data for Test 10

Test	Pin Num	TOA	Plate Number	Pin Interval	Interval Velocity	Average Velocity
10	1	150 microsec	1	2.5 in	9057 ft/sec	8695 ft/sec
	2	173 microsec		2.5 in	8333 ft/sec	
	3	198 microsec				
	4	552 microsec	2	2.5 in	1520 ft/sec	1567 ft/sec
	5	689 microsec		2.5 in	1614 ft/sec	
	6	818 microsec				
	7	1283 microsec	3	2.5 in	701 ft/sec	1280 ft/sec
	8	1578 microsec		2.5 in	1859 ft/sec	
	9	1689 microsec				

G.10.3 SPECIMEN BEHAVIOR

The equivalent of 0.034X pounds of TNT used in this test caused the complete destruction to all three plates as demonstrated in Figure G.62. The top plate sheared along its supports and fragmented into many pieces as shown in Figure G.63. Details of those fragments can be found in Figure G.64 and Figure G.65. The fragments from the top plate impacted the middle plate and formed slightly larger fragments. As the velocity of the fragments decreases the ductile behavior of the steel increases, this is demonstrated in the ripping and curling of the steel plate around the edges of the opening. Figure G.66 is a good example of this behavior. One can also see that the plate around the edges is bent more than the top plate. The fragments created from the top two plates impacted the bottom plate and caused significant damage to the plate. No identifiable flyer plate was found associated with this plate, but it still incurred significant damage. Figure G.67 and Figure G.68 once again demonstrates the ductile behavior of the plates as shown by the jagged and twisted edges, along with the severe deformation of the plate itself. Figure G.69 shows a comparison of the three plates. The plate at the top of the photo was the top plate, the plate in the middle was the middle plate and the plate at the bottom was the bottom plate.

Figure G.62: Test 10 post test

Figure G.63: Test 10 top plate

Figure G.64: Test 10 top plate fragmentation details

Figure G.65: Test 10 top plate fragmentation details

Figure G.66: Test 10 middle plate

Figure G.67: Test 10 bottom plate

Figure G.68: Test 10 top plate petalling details

Figure G.69: Test 10 top, middle, and bottom plate

G.11 TEST 11 (TWO-PLATE TEST – KEDD ON TOP)

G.11.1 INTRODUCTION

The eleventh Proof of Concept Test was performed at ARA's Rocky Mountain Division test site. It used an equivalent of 0.023X pounds of TNT, placed in a 9" x 9" aluminum brownie tin, at a close standoff. The test specimen was a series of two ¼" thick A36 steel plates supported by solid CMU blocks. A medium density fiberboard (MDF) spacer block was placed in between each course of CMU to achieve a total height of 1' between steel plates. Figure G.70(a) shows the specimen prior to detonation. Figure G.70(b) shows the charge for the test. The explosive material was tamped by hand to an approximate density of 1.58 grams/ cubic centimeter.

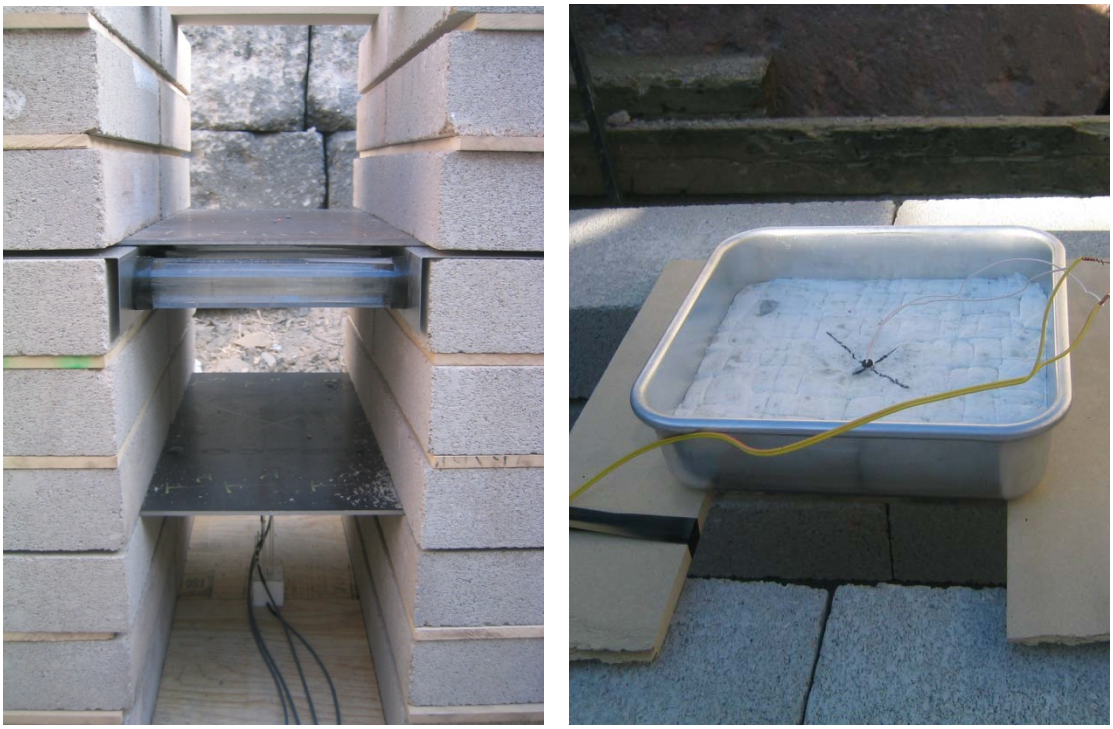

Figure G.70: a) Test 11 set-up b) Charge for Test 11

G.11.2 KINETIC ENERGY DEFEAT DEVICE

A Kinetic Energy Defeat Device (KEDD) was used in this test. Each device consists of a 2" diameter thin walled plastic tube, manufactured by VisiPak, filled with water and sealed off on both ends by black plastic caps. The total length of each device was 12". They were then spaced at 3" on center with the middle KEDD placed in the center of the plate. Figure G.71(a) shows one KEDD, while Figure G.71 (b) shows an array of 9 KEDD's. The top plate will be placed directly above the array of KEDD's as shown in Figure G.70(a). The metal support system, constructed out of light gage steel, was used to keep each individual KEDD in place.

Figure G.71: a) Individual KEDD b) Test 11 Array of 9 KEDD's

G.11.3 INSTRUMENTATION

One set of Time of Arrival (TOA) pins were placed behind the bottom plate. They were spaced at 10", 7 1/2", 5" and 2 1/2" above the plywood surface below. The data that was retrieved from these pins can be found in Table G.11. The velocity of the fragments created from the second, or bottom, plate was determined to be traveling at a velocity of 258 ft/sec. The arrangement of TOA pins can be seen in Figure G.72.

Table G.11: Time of Arrival Data for Test 11

Test	Pin Num	TOA	Plate Number	Pin Interval	Interval Velocity	Average Velocity
11	1	1377 microsec	1	2.5 in	434 ft/sec	258 ft/sec
	2	1857 microsec		2.5 in	191 ft/sec	
	3	2572 microsec		2.5 in	148 ft/sec	
	4	3972 microsec				

Figure G.72: Test 11 Time of Arrival pins

G.11.4 SPECIMEN BEHAVIOR

The equivalent of 0.023X pounds of TNT caused one large, classical, flyer plate to be formed in the top plate which then impacted the second plate. The plates, still in their final resting position, can be seen in Figure G.73. The flyer plate formed from the top plate impacted the second plate and caused the second plate to release from its supports and fold in half. The remnants on the top plate can be seen in Figure G.74. The bottom plate is shown in Figure G.75. It is important to note, that while the plate folded in half and separated from the supports, the plate itself has only one fracture. If the plate was held in place better, the plate might not have been damaged as severely. The change in the amount of damage that occurred to the second plate can be attributed to the effectiveness of the KEDD system. As demonstrated in previous tests the damage that occurred to the second plate is less for this test than previous tests. This can lead to the understanding that the liquid filled KEDD's work better when not placed directly in front of a steel plate. This enables the liquid to be redirected before it impacts the second plate. Figure G.76 shows a comparison of the two plates. The plate at the top of the photo was the top plate, while the plate at the bottom was the bottom plate.

Figure G.73: Test 11 post test

Figure G.74: Test 11 top plate

Figure G.75: Test 11 bottom plate

Figure G.76: Test 11 top and bottom plate

G.12 TEST 12 (TWO-PLATE TEST – KEDD ON BOTTOM)

G.12.1 INTRODUCTION

The twelfth Proof of Concept Test was performed at ARA's Rocky Mountain Division test site. It used an equivalent of 0.023X pounds of TNT, placed in a 9" x 9" aluminum brownie tin, at a close standoff. The test specimen was a series of two ¼" thick A36 steel plates supported by solid CMU blocks. A medium density fiberboard (MDF) spacer block was placed in between each course of CMU to achieve a total height of 1' between steel plates. Figure G.77(a) shows the specimen prior to detonation. Figure G.77(b) shows the charge for the test. The explosive material was tamped by hand to an approximate density of 1.58 grams/ cubic centimeter.

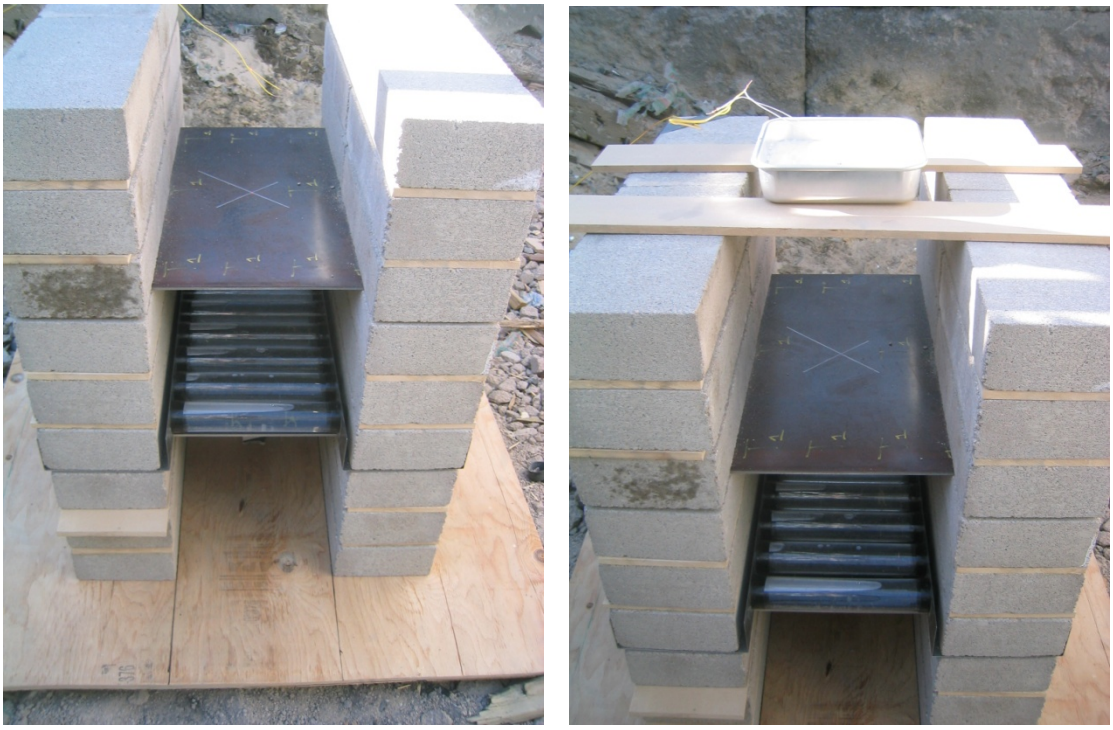

Figure G.77: a) Test 12 set-up b) Test 12 set-up with charge

G.12.2 Kinetic Energy Defeat Device

A Kinetic Energy Defeat Device (KEDD) was used in this test. Each device consists of a 2" diameter thin walled plastic tube, manufactured by VisiPak, filled with water and sealed off on both ends by black plastic caps. The total length of each device was 12". They were then spaced at 3" on center with the middle KEDD placed in the center of the plate. Figure G.80(a) shows one KEDD, while Figure G.80(b) shows an array of 9 KEDD's. The array of KEDD's was placed directly above the bottom plate as shown in Figure G.36(a). The metal support system, constructed out of light gage steel, was used to keep each individual KEDD in place.

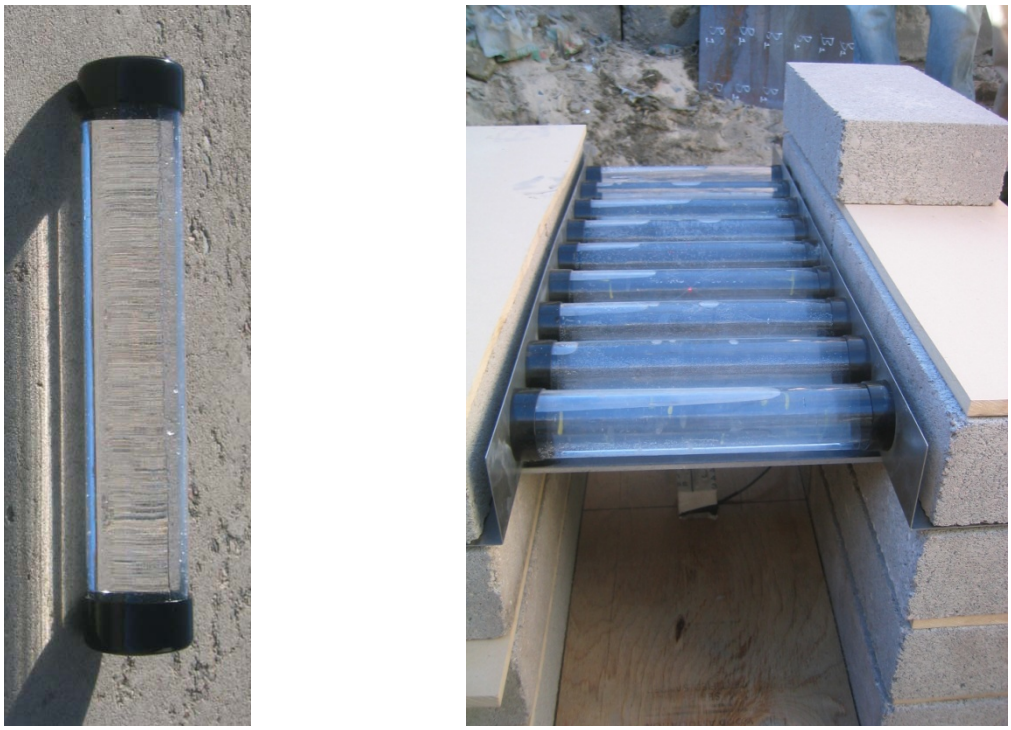

Figure G.78: a) Individual KEDD b) Test 12 Array of 9 KEDD's

G.12.3 INSTRUMENTATION

One set of Time of Arrival (TOA) pins were placed behind the bottom plate. They were spaced at 10", 7 1/2", 5" and 2 1/2" above the plywood surface below. The data that was retrieved from these pins can be found in Table G.12. The velocity of the fragments created from the second, or bottom, plate was determined to be traveling at a velocity of 626 ft/sec. The arrangement of TOA pins can be seen in Figure G.79

Table G.12: Time of Arrival Data for Test 12

Test	Pin Num	TOA	Plate Number	Pin Interval	Interval Velocity	Average Velocity
12	1	1011 microsec	1	2.5 in	598 ft/sec	626 ft/sec
	2	1359 microsec		2.5 in	614 ft/sec	
	3	1698 microsec		2.5 in	667 ft/sec	
	4	2010 microsec				

Figure G.79: Test 12 Time of Arrival pins

G.12.4 SPECIMEN BEHAVIOR

The equivalent of 0.023X pounds of TNT caused one large flyer plate to be formed in the top plate which then impacted the second plate. The bottom plate, still in its final resting place, can be found in Figure G.80. The top plate was found near the entrance of the test bunker. It appears to have impacted a steel plate which might have caused the plate to fold in half. The top plate is shown where it landed in Figure G.81. Figure G.82 and Figure G.83 show the top plate and a close-up of its flyer plate. That flyer plate then impacted the second plate and caused significant petalling to the plate and formed a small flyer plate as demonstrated in Figure G.84. Figure G.85 shows a comparison of the two plates. The plate at the top of the photo was the top plate, while the plate at the bottom was the bottom plate.

Figure G.80: Test 12 bottom plate in test bed

Figure G.81: Test 12 top plate in test bed

\

Figure G.82: Test 12 top plate

Figure G.83: Test 12 flyer plate from top plate

Figure G.84: Test 12 bottom plate

Figure G.85: Test 12 top and bottom plate

G.13 TEST 13 (TWO-PLATE TEST)

G.13.1 INTRODUCTION

The thirteenth Proof of Concept Test was performed at ARA's Rocky Mountain Division test site. It used an equivalent of 0.023X pounds of TNT, placed in a 9" x 9" aluminum brownie tin, at a close standoff. The test specimen was a series of two ¼" thick A36 steel plates supported by solid CMU blocks. A medium density fiberboard (MDF) spacer block was placed in between each course of CMU to achieve a total height of 1' between steel plates. Figure G.86(a) shows the specimen prior to detonation. Figure G.86(b) shows the charge for the test. The explosive material was tamped by hand to an approximate density of 1.58 grams/ cubic centimeter.

Figure G.86: a) Test 13 set-up b) Charge for Test 13

G.13.2 INSTRUMENTATION

One set of Time of Arrival (TOA) pins were placed behind the bottom plate. They were spaced at 10", 7 1/2", 5" and 2 1/2" above the plywood surface below. The data that was retrieved from these pins can be found in Table G.13. The velocity of the fragments created from the second, or bottom, plate was determined to be traveling at a velocity of 635 ft/sec. The arrangement of TOA pins can be seen in Figure G.87

Table G.13: Time of Arrival Data for Test 13

Test	Pin Num	TOA	Plate Number	Pin Interval	Interval Velocity	Average Velocity
13	1	922 microsec	1	2.5 in	593 ft/sec	635 ft/sec
	2	1273 microsec		2.5 in	659 ft/sec	
	3	1589 microsec		2.5 in	653 ft/sec	
	4	1908 microsec				

Figure G.87: Test 13 Time of Arrival pins

G.13.3 SPECIMEN BEHAVIOR

The equivalent of 0.023X pounds of TNT used in this test caused the complete destruction of the test specimen as shown in Figure G.88. The explosion formed large holes in both the top and bottom plates. The top plate was folded in half with multiple flyer plates, as shown in Figure G.89 and Figure G.90. The flyer plates impacted the bottom plate and formed an additional, or secondary, flyer plate, see Figure G.91. Figure G.92 compares the type of damage that occurred to top and bottom plates. The top plate is shown at the top of the photograph and the bottom plate is shown at the bottom. The difference in damage mechanisms due to the velocity of the fragments is demonstrated in this photo. The initial blast forms many fragments, but as the larger one impacts the second plate it forms a slightly smaller flyer plate and the plate behaves in a more ductile manner, which can be seen in the petalling effects of the plate.

Figure G.88: Test 13 test specimen post test

Figure G.89: Test 13 top plate

Figure G.90: Test 13 top plate fragments

Figure G.91: Test 13 bottom plate

Figure G.92: Test 13 top and bottom plate

G.14 TEST 14 (TWO-PLATE TEST)

G.14.1 INTRODUCTION

The fourteenth Proof of Concept Test was performed at ARA's Rocky Mountain Division test site. It used an equivalent of 0.023X pounds of TNT, placed in a 9" x 9" aluminum brownie tin, at a close standoff. The test specimen was a series of two ¼" thick A36 steel plates supported by solid CMU blocks. A medium density fiberboard (MDF) spacer block was placed in between each course of CMU to achieve a total height of 1' between steel plates. Figure G.93(a) shows the specimen prior to detonation. Figure G.93(b) shows the charge for the test. The explosive material was tamped by hand to an approximate density of 1.58 grams/ cubic centimeter.

Figure G.93: a) Test 14 set-up b) Charge for Test 14

G.14.2 INSTRUMENTATION

One set of Time of Arrival (TOA) pins were placed behind the bottom plate. They were spaced at 11 1/2", 11", 10 1/2" and 10" above the plywood surface below. The data that was retrieved from these pins can be found in Table G.14. The velocity of the fragments created from the second, or bottom, plate was determined to be traveling at a velocity of 1,083 ft/sec. The arrangement of TOA pins can be seen in Figure G.94.

Table G.14: Time of Arrival Data for Test 14

Test	Pin Num	TOA	Plate Number	Pin Interval	Interval Velocity	Average Velocity
14	1	891 microsec	2	0.5 in	1302 ft/sec	1083 ft/sec
	2	923 microsec		0.5 in	1096 ft/sec	
	3	961 microsec		0.5 in	850 ft/sec	
	4	1010 microsec		0.5 in		

Figure G.94: Test 14 Time of Arrival pins

G.14.3 SPECIMEN BEHAVIOR

The equivalent of 0.023X pounds of TNT used in this test caused the complete destruction of the test specimen as shown in Figure G.95. Figure G.96 shows where one half of the top plate landed after the test. The explosion caused multiple flyer plates to be created from the top plate, as shown in Figure G.97. They impacted the second plate and caused severe damage to that plate. Figure G.98 shows the second plate. There was significant tearing in the plate; however, no flyer plate was produced. Figure G.99 shows a section of the second plate where a flyer plate might have been created. Cracks on both sides of the plate can be seen in the photo. Figure G.100 compares the type of damage that occurred to the top and bottom plates. The top plate is shown on the left of the photograph and the bottom plate is shown on the right.

Figure G.95: Test 14 test specimen post test

Figure G.96: Test 14 top plate in test bed

Figure G.97: Test 14 top plate

Figure G.98: Test 14 bottom plate

Figure G.99: Test 14 bottom plate petalling and shearing details

Figure G.100: Test 14 top and bottom plate

G.15 TEST 15 (TWO-PLATE TEST –2 ROWS OF KEDD'S ON TOP)

G.15.1 INTRODUCTION

The fifteenth Proof of Concept Test was performed at ARA's Rocky Mountain Division test site. It used an equivalent of 0.023X pounds of TNT, placed in a 9" x 9" aluminum brownie tin, at a close standoff. The test specimen was a series of two ¼" thick A36 steel plates supported by solid CMU blocks. A medium density fiberboard (MDF) spacer block was placed in between each course of CMU to achieve a total height of 1' between steel plates. Figure G.101(a) shows the specimen prior to detonation. Figure G.101(b) shows the charge for the test. The explosive material was tamped by hand to an approximate density of 1.58 grams/ cubic centimeter.

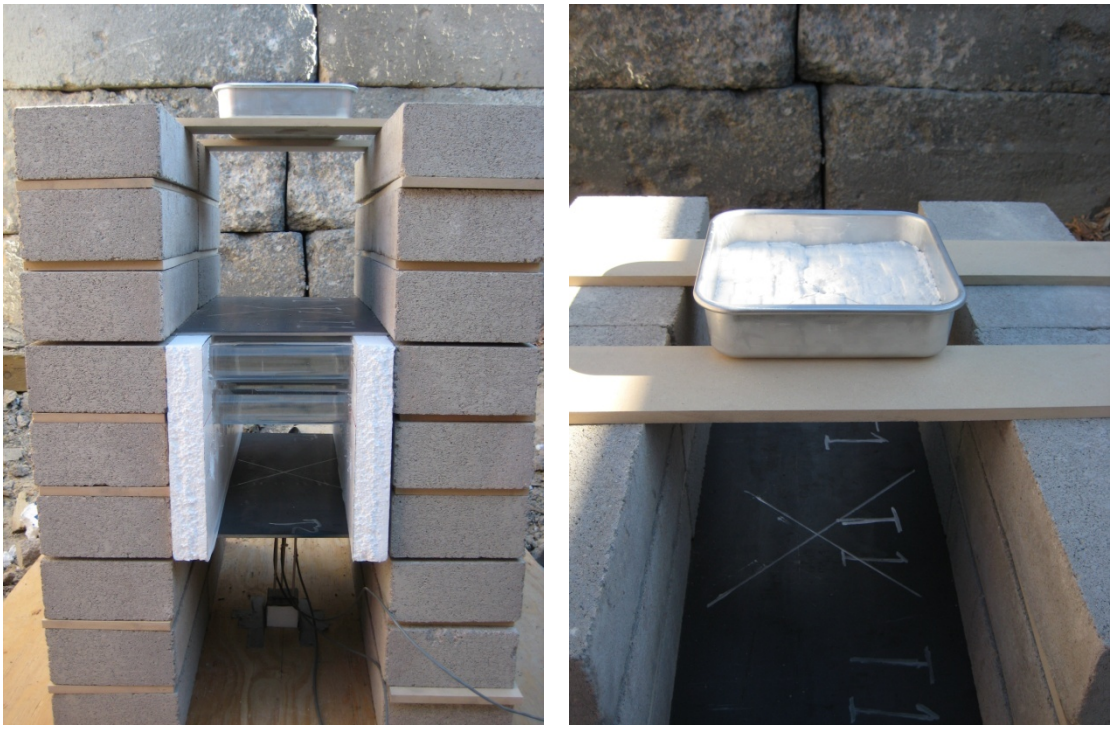

Figure G.101: a) Test 15 set-up b) Charge for Test 15

G.15.2 KINETIC ENERGY DEFEAT DEVICE

A series of Kinetic Energy Defeat Devices (KEDD's) were used in this test. Each device consists of a 2" diameter thin walled plastic tube, manufactured by VisiPak, filled with water and sealed off on both ends by black plastic caps. The total length of each device was 12". Each row was spaced at 3" on center with the middle KEDD placed in the center of the plate for a total of 9 KEDD's in the top row. The second row of KEDD's were placed 3" below the top row and were off-set by 3" for a total of 8 KEDD's. Figure G.102(a) shows one KEDD, while Figure G.102 (b) shows an array of 17 KEDD's. The top plate will be placed directly above the array of KEDD's as shown in Figure G.101(a). The KEDD's were held in place by Styrofoam supports.

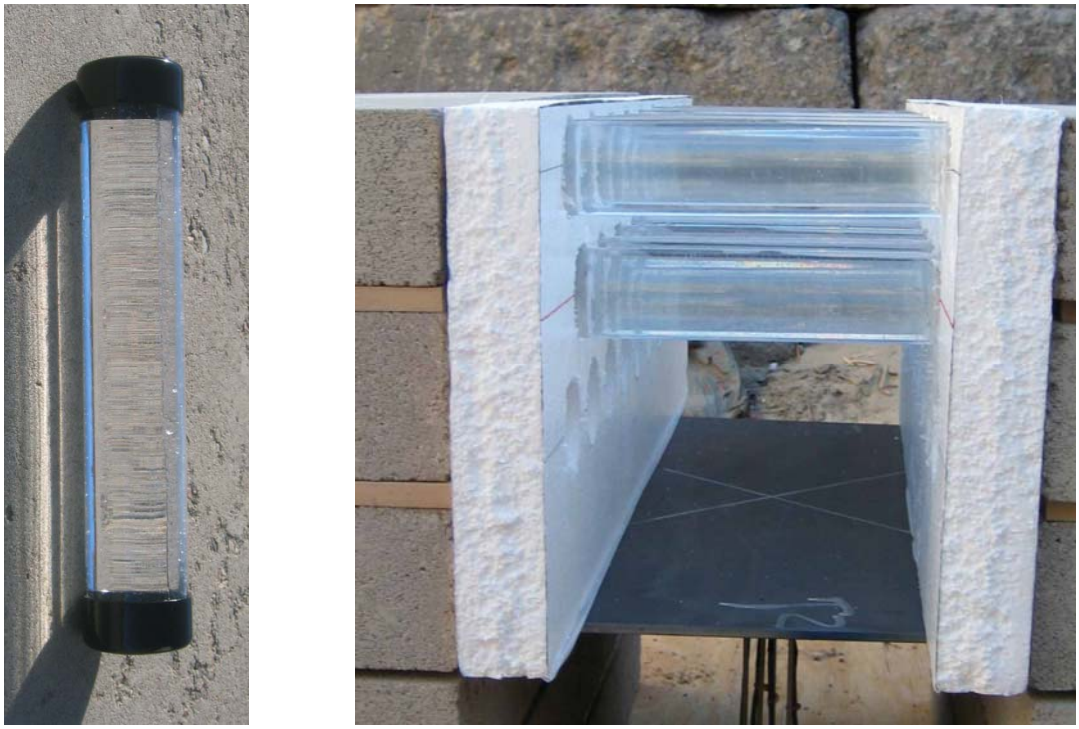

Figure G.102: a) Individual KEDD b) Test 15 - Two rows of KEDD's

G.15.3 INSTRUMENTATION

One set of Time of Arrival (TOA) pins were placed behind the bottom plate. They were spaced at 11 1/2", 11", 10 1/2" and 10" above the plywood surface below. The data that was retrieved from these pins can be found in Table G.15. The velocity of the fragments created from the second, or bottom, plate was determined to be traveling at a velocity of 215 ft/sec. The arrangement of TOA pins can be seen in Figure G.103.

Table G.15: Time of Arrival Data for Test 15

Test	Pin Num	TOA	Plate Number	Pin Interval	Interval Velocity	Average Velocity
15	1	1007 microsec	2	0.5 in	184 ft/sec	215 ft/sec
	2	1234 microsec		0.5 in		
	3	n/a		0.5 in	245 ft/sec	
	4	1574 microsec				

Figure G.103: Test 15 Time of Arrival pins

G.15.4 SPECIMEN BEHAVIOR

The equivalent of 0.023X pounds of TNT caused one large flyer plate to be formed in the top plate which then impacted the second plate. The top and bottom plates, still in their final resting place, can be found in Figure G.104. The top plate sheared into two pieces with a large square hole in the middle where a flyer plate was created as seen in Figure G.105. That flyer plate then impacted the second plate and caused significant deformation as shown in Figure G.106. It is important to note, that while the plate folded in half and separated from the supports, the plate itself did not fracture. If the plate was held in place better, the plate might not have been damaged as severely. The change in amount damage that occurred to the second plate can be attributed to the effectiveness of the KEDD system. Figure G.107 shows a comparison of the two plates. The plate on the left of the photo was the top plate, while the plate on the right was the bottom plate.

Figure G.104: Test 15 post test

Figure G.105: Test 15 top plate

Figure G.106: Test 15 bottom plate

Figure G.107: Test 15 top and bottom plate

G.16 TEST 16 (TWO-PLATE TEST –1 ROWS OF KEDD'S ONE TOP AND BOTTOM)

G.16.1 INTRODUCTION

The sixteenth Proof of Concept Test was performed at ARA's Rocky Mountain Division test site. It used an equivalent of 0.023X pounds of TNT, placed in a 9" x 9" aluminum brownie tin, at a close standoff. The test specimen was a series of two ¼" thick A36 steel plates supported by solid CMU blocks. A medium density fiberboard (MDF) spacer block was placed in between each course of CMU to achieve a total height of 1' between steel plates. Figure G.108(a) shows the specimen prior to detonation. Figure G.108(b) shows the charge for the test. The explosive material was tamped by hand to an approximate density of 1.58 grams/ cubic centimeter.

Figure G.108: a) Test 16 set-up b) Charge for Test 16

G.16.2 KINETIC ENERGY DEFEAT DEVICE

A series of Kinetic Energy Defeat Devices (KEDD's) were used in this test. Each device consists of a 2" diameter thin walled plastic tube, manufactured by VisiPak, filled with water and sealed off on both ends by black plastic caps. The total length of each device was 12". Each row was spaced at 3" on center with the middle KEDD placed in the center of the plate for a total of 9 KEDD's in each row. One row of KEDD's was placed on top of the bottom plate. The other row of KEDD's' was placed directly behind the top plate. There were a total of 18 KEDD's used in this test. Figure G.109(a) shows one KEDD, while Figure G.109(b) shows the two rows of KEDD's. Figure G.108 shows the KEDD's in the test specimen. The metal support system, constructed out of light gage steel, was used to keep each individual KEDD in place.

Figure G.109: a) Individual KEDD b) Test 16 - Two rows of KEDD's (one on top and bottom)

G.16.3 INSTRUMENTATION

One set of Time of Arrival (TOA) pins were placed behind the bottom plate. They were spaced at 11 1/2", 11", and 10 1/2" above the plywood surface below. The data that was retrieved from these pins can be found in Table G.16. The velocity of the fragments created from the second, or bottom, plate was determined to be traveling at a velocity of 630 ft/sec. The arrangement of TOA pins can be seen in Figure G.110.

Table G.16: Time of Arrival Data for Test 16

Test	Pin Num	TOA	Plate Number	Pin Interval	Interval Velocity	Average Velocity
16	1	1120 microsec	2	0.5 in	968 ft/sec	630 ft/sec
	2	1163 microsec		0.5 in	291 ft/sec	
	3	1312 microsec		0.5 in		

Figure G.110: Test 16 Time of Arrival pins

G.16.4 SPECIMEN BEHAVIOR

The equivalent of 0.023X pounds of TNT caused one large flyer plate to be formed in the top plate which then impacted the second plate. The top and bottom plates, still in their final resting place, can be found in Figure G.111. The top plate was bent in half with a large hole in the middle where the flyer plate was formed. Along one of the edges another flyer plate was almost created as shown in Figure G.112 and Figure G.113. The flyer plate created from the top plate then impacted the second plate and caused significant deformation as shown in Figure G.114. The flyer plate can be seen in the photo. Figure G.115 shows a comparison of the two plates. The plate on the left of the photo was the top plate, while the plate on the right was the bottom plate.

Figure G.111: Test 16 post test

Figure G.112: Test 16 top plate in test bed

Figure G.113: Test 16 top plate

Figure G.114: Test 16 bottom plate

Figure G.115: Test 16 top and bottom plate

G.17 TEST 17 (TWO-PLATE TEST –3 ROWS OF KEDD'S ON TOP)

G.17.1 INTRODUCTION

The seventeenth Proof of Concept Test was performed at ARA's Rocky Mountain Division test site. It used an equivalent of 0.023X pounds of TNT, placed in a 9" x 9" aluminum brownie tin, at a close standoff. The test specimen was a series of two ¼" thick A36 steel plates supported by solid CMU blocks. A medium density fiberboard (MDF) spacer block was placed in between each course of CMU to achieve a total height of 1' between steel plates. Figure G.116(a) shows the specimen prior to detonation. Figure G.116(b) shows the charge for the test. The explosive material was tamped by hand to an approximate density of 1.58 grams/ cubic centimeter.

Figure G.116: a) Test 17 set-up b) Charge for Test 17

G.17.2 KINETIC ENERGY DEFEAT DEVICE

A series of Kinetic Energy Defeat Devices (KEDD's) were used in this test. Each device consists of a 2" diameter thin walled plastic tube, manufactured by VisiPak, filled with water and sealed off on both ends by black plastic caps. The total length of each device was 12". Each row was spaced at 3" on center with the middle KEDD placed in the center of the plate for a total of 9 KEDD's in the top row. The second row of KEDD's were placed 3" below the top row and were off-set by 3" for a total of 8 KEDD's. The third row of KEDD's were spaced in the same manner as the top row for a total 9 KEDD's in that row and 26 KEDD's total. Figure G.117(a) shows one KEDD, while Figure G.117(b) shows an array of 26 KEDD's. The top plate is placed directly above the array of KEDD's as shown in Figure G.116(a). The KEDD's were held in place by Styrofoam supports.

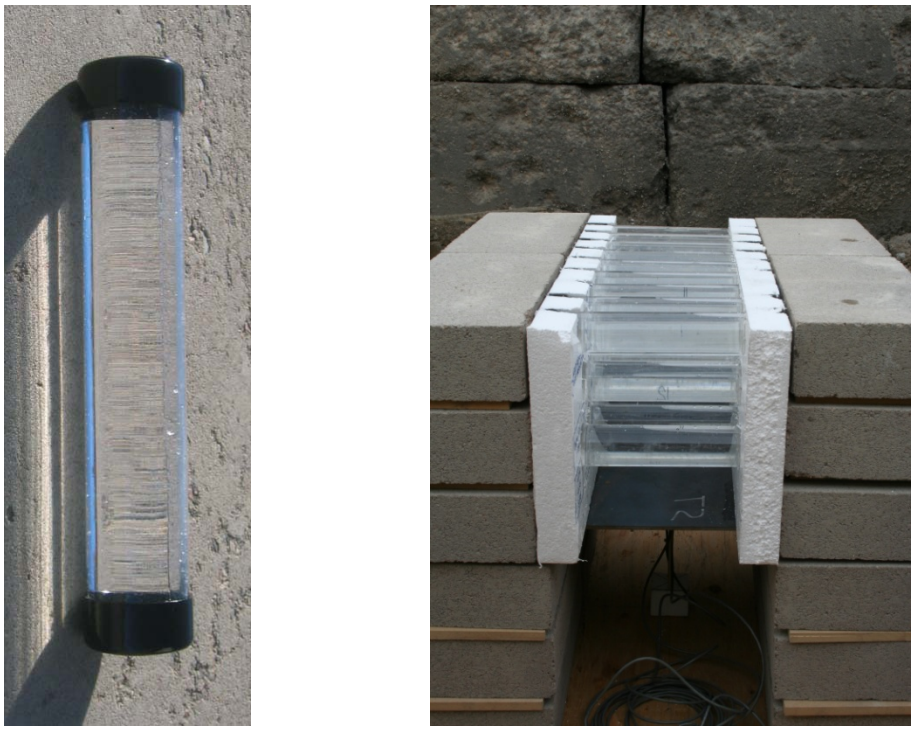

Figure G.117: a) Individual KEDD b) Test 17 - Three rows of KEDD's

G.17.3 INSTRUMENTATION

One set of Time of Arrival (TOA) pins were placed behind the bottom plate. They were spaced at 11 1/2", 11" and 10 1/2" above the plywood surface below. The data that was retrieved from these pins can be found in Table G.17. The velocity of the fragments created from the second, or bottom, plate was determined to be traveling at a velocity of 152 ft/sec. The arrangement of TOA pins can be seen in Figure G.118.

Table G.17: Time of Arrival Data for Test 17

Test	Pin Num	TOA	Plate Number	Pin Interval	Interval Velocity	Average Velocity
17	1	1259 microsec	2	0.5 in	152 ft/sec	152 ft/sec
	2	1533 microsec		0.5 in		
	3	n/a				

Figure G.118: Test 17 Time of Arrival pins

G.17.4 SPECIMEN BEHAVIOR

The equivalent of 0.023X pounds of TNT caused one large flyer plate to be formed in the top plate which then impacted the second plate. The top and bottom plate, still in their final resting place, can be found in Figure G.119. The top plate is in one piece with a large square hole in the middle, where a flyer plate was created, as seen in Figure G.120. That flyer plate then impacted the second plate causing the plate to deform as shown in Figure G.121. It is important to note, that while the plate folded in half and separated from the supports, the plate itself did not fracture. If the plate was held in place better, the plate might not have been damaged as severely. Figure G.122 shows a comparison of the two plates. The plate on the top of the photo was the top plate, while the plate on the bottom was the bottom plate.

Figure G.119: Test 17 post test

Figure G.120: Test 17 top plate

Figure G.121: Test 17 bottom plate

Figure G.122: Test 17 top and bottom plate

G.18 TEST 18 (TWO-PLATE TEST)

G.18.1 INTRODUCTION

The eighteenth Proof of Concept Test was performed at ARA's Rocky Mountain Division test site. It used an equivalent of 0.023X pounds of TNT, placed in a 9" x 9" aluminum brownie tin, at a close standoff. The test specimen was a series of two ¼" thick A36 steel plates supported by solid CMU blocks. A medium density fiberboard (MDF) spacer block was placed in between each course of CMU to achieve a total height of 1' between steel plates. Figure G.123(a) shows the specimen prior to detonation. Figure G.123(b) shows the charge for the test. The explosive material was tamped by hand to an approximate density of 1.58 grams/ cubic centimeter.

Figure G.123: a) Test 18 set-up b) Charge for Test 18

G.18.2 INSTRUMENTATION

One set of Time of Arrival (TOA) pins were placed behind the bottom plate. They were spaced at 11 1/2", 11", and 10 1/2" above the plywood surface below. The data that was retrieved from these pins can be found in Table G.18. The velocity of the fragments created from the second, or bottom, plate was determined to be traveling at a velocity of 1,605 ft/sec. The arrangement of TOA pins can be seen in Figure G.124.

Table G.18: Time of Arrival Data for Test 18

Test	Pin Num	TOA	Plate Number	Pin Interval	Interval Velocity	Average Velocity
18	1	866 microsec	2	0.5 in	1984 ft/sec	1605 ft/sec
	2	887 microsec		0.5 in	1225 ft/sec	
	3	921 microsec				

Figure G.124: Test 18 Time of Arrival pins

G.18.3 SPECIMEN BEHAVIOR

The equivalent of 0.023X pounds of TNT used in this test caused the complete destruction of the test specimen as shown in Figure G.125. However, it caused more damage than the other 2 plate tests that did not use a KEDD (Tests 6,13 and 14). This could be because the velocity of the second plate was much higher in this test (1,605 ft/sec) than the average of the other tests (1,060 ft/sec). Why this test had a higher velocity is unknown but can be seen in the type of damage that occurred to the specimen. Figure G.126 shows a portion of the top plate that bounced of the test support and lodged itself in the concrete wall of the test bunker. Figure G.127 shows the top plate that was sheared along the concrete supports and the five flyer plates that it created. They impacted the second plate and caused severe damage to that plate. Figure G.128 shows the bottom plate in the test bed. It can be seen that there was significant petalling and tearing of the plate. Figure G.129 shows the secondary flyer plate. Figure G.130 compares the type of damage that occurred to top and bottom plates. The top plate is shown on the left of the photograph and the bottom plate is shown on the right.

Figure G.125: Test 18 test specimen post test

Figure G.126: Test 18 section of top plate embedded in wall

Figure G.127: Test 18 top plate

Figure G.128: Test 18 bottom plate

Figure G.129: Test 18 bottom plate fragment

Figure G.130: Test 18 top and bottom plate

G.19 TEST 19 (TWO-PLATE TEST –2 ROWS OF KEDD'S ON TOP)

G.19.1 INTRODUCTION

The nineteenth Proof of Concept Test was performed at ARA's Rocky Mountain Division test site. It used an equivalent of 0.023X pounds of TNT, placed in a 9" x 9" aluminum brownie tin, at a close standoff. The test specimen was a series of two ¼" thick A36 steel plates supported by solid CMU blocks. A medium density fiberboard (MDF) spacer block was placed in between each course of CMU to achieve a total height of 1' between steel plates. Figure G.131(a) shows the specimen prior to detonation. Figure G.131(b) shows the charge for the test. The explosive material was tamped by hand to an approximate density of 1.58 grams/ cubic centimeter.

Figure G.131: a) Test 19 set-up b) Charge for Test 19

G.19.2 KINETIC ENERGY DEFEAT DEVICE

A series of Kinetic Energy Defeat Devices (KEDD's) were used in this test. Each device consists of a 2" diameter thin walled plastic tube, manufactured by VisiPak, filled with water and sealed off on both ends by black plastic caps. The total length of each device was 12". Each row was spaced at 3" on center with the middle KEDD placed in the center of the plate for a total of 9 KEDD's in the top row. The second row of KEDD's were placed 3" below the top row and were off-set by 3" for a total of 8 KEDD's. Figure G.132(a) shows one KEDD, while Figure G.132(b) shows an array of 17 KEDD's. The top plate will be placed directly above the array of KEDD's as shown in Figure G.131 (a). The KEDD's were held in place by Styrofoam supports.

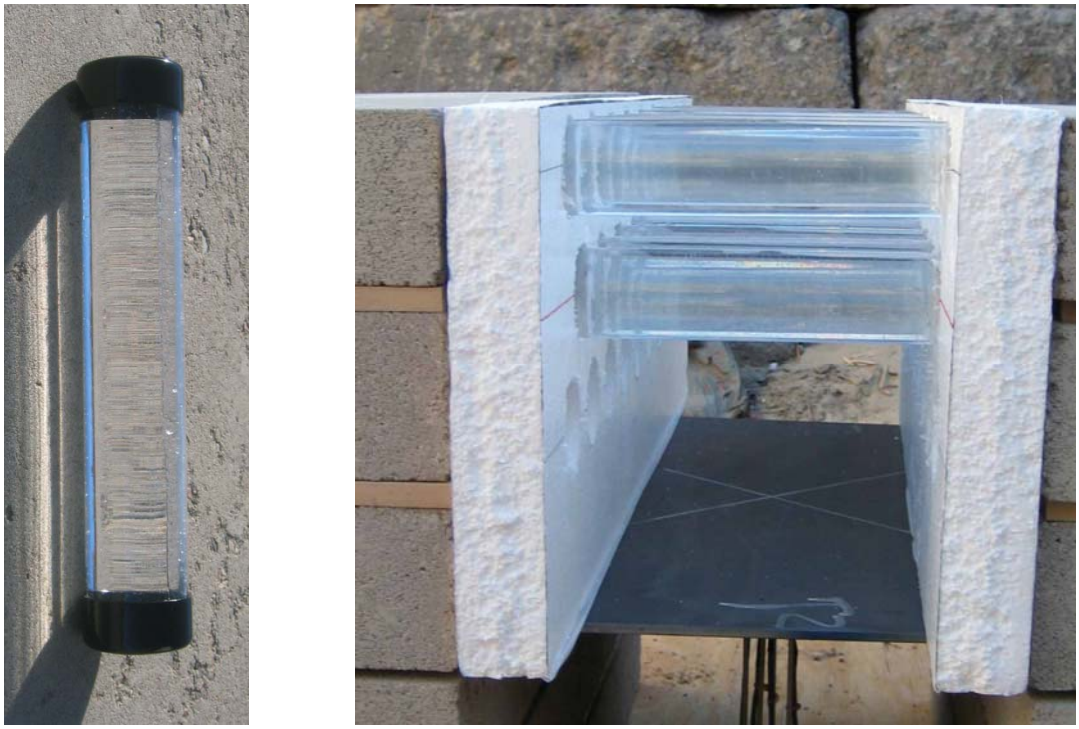

Figure G.132: a) Individual KEDD b) Test 19 - Two rows of KEDD's

G.19.3 INSTRUMENTATION

One set of Time of Arrival (TOA) pins were placed behind the bottom plate. They were spaced at 11 1/2", 11", and 10 1/2" above the plywood surface below. The data that was retrieved from these pins can be found in Table G.19. The velocity of the fragments created from the second, or bottom, plate was determined to be traveling at a velocity of 465 ft/sec. The arrangement of TOA pins can be seen in Figure G.133.

Table G.19: Time of Arrival Data for Test 19

Test	Pin Num	TOA	Plate Number	Pin Interval	Interval Velocity	Average Velocity
19	1	1234 microsec	2	0.5 in	298 ft/sec	465 ft/sec
	2	1374 microsec		0.5 in	631 ft/sec	
	3	1440 microsec				

Figure G.133: Test 19 Time of Arrival pins

G.19.4 SPECIMEN BEHAVIOR

The equivalent of 0.023X pounds of TNT caused one large flyer plate to be formed in the top plate which then impacted the second plate. The top and bottom plate, still in their final resting place, can be found in Figure G.134. The top plate sheared into two pieces with a large square hole in the middle where a flyer plate was created as seen in Figure G.135. That flyer plate then impacted the second plate and caused significant deformation as shown in Figure G.136. It is important to note, that while the plate folded in half and separated from the supports, the plate itself did not fracture. If the plate was held in place better, the plate might not have been damaged as severely. Figure G.137 shows a comparison of the two plates. The plate at the top of the photo was the top plate, while the plate at the bottom was the bottom plate.

Figure G.134: Test 19 post test

Figure G.135: Test 19 top plate

Figure G.136: Test 19 bottom plate in test bed

Figure G.137: Test 19 top and bottom plate

G.20 TEST 20 (TWO-PLATE TEST –3 ROWS OF KEDD'S ON TOP)

G.20.1 INTRODUCTION

The twentieth Proof of Concept Test was performed at ARA's Rocky Mountain Division test site. It used an equivalent of 0.023X pounds of TNT, placed in a 9" x 9" aluminum brownie tin, at a close standoff. The test specimen was a series of two ¼" thick A36 steel plates supported by solid CMU blocks. A medium density fiberboard (MDF) spacer block was placed in between each course of CMU to achieve a total height of 1' between steel plates. Figure G.138(a) shows the specimen prior to detonation. Figure G.138(b) shows the charge for the test. The explosive material was tamped by hand to an approximate density of 1.58 grams/ cubic centimeter.

Figure G.138: a) Test 20 set-up b) Charge for Test 20

G.20.2 KINETIC ENERGY DEFEAT DEVICE

A series of Kinetic Energy Defeat Devices (KEDD's) were used in this test. Each device consists of a 2" diameter thin walled plastic tube, manufactured by VisiPak, filled with water and sealed off on both ends by black plastic caps. The total length of each device was 12". Each row was spaced at 3" on center with the middle KEDD placed in the center of the plate for a total of 9 KEDD's in the top row. The second row of KEDD's were placed 3" below the top row and were off-set by 3" for a total of 8 KEDD's. The third row of KEDD's were spaced in the same manner as the top row for a total 9 KEDD's in that row and 26 KEDD's total. Figure G.139(a) shows one KEDD, while Figure G.139(b) shows an array of 26 KEDD's. The top plate is placed directly above the array of KEDD's as shown in Figure G.138(a). The KEDD's were held in place by Styrofoam supports.

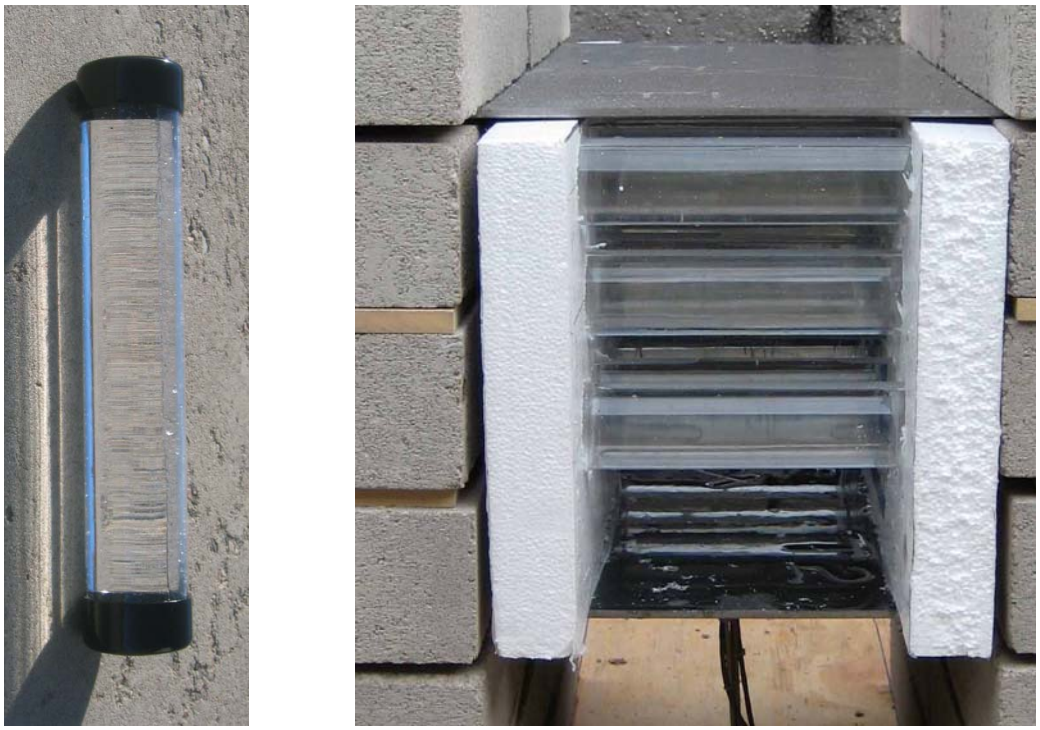

Figure G.139: a) Individual KEDD b) Test 20 - Three rows of KEDD's

G.20.3 INSTRUMENTATION

One set of Time of Arrival (TOA) pins were placed behind the bottom plate. They were spaced at 11 1/2", 11" and 10 1/2" above the plywood surface below. The data that was retrieved from these pins can be found in Table G.20. The velocity of the fragments created from the second, or bottom, plate was determined to be traveling at a velocity of 277 ft/sec. The arrangement of TOA pins can be seen in Figure G.140.

Table G.20: Time of Arrival Data for Test 20

Test	Pin Num	TOA	Plate Number	Pin Interval	Interval Velocity	Average Velocity
20	1	1408 microsec	2	0.5 in	331 ft/sec	277 ft/sec
	2	1534 microsec		0.5 in	223 ft/sec	
	3	1721 microsec				

Figure G.140: Test 20 Time of Arrival pins

G.20.4 SPECIMEN BEHAVIOR

The equivalent of 0.023X pounds of TNT caused one large flyer plate to be formed in the top plate which then impacted the second plate. The top and bottom plate, still in their final resting place, can be found in Figure G.141. The top plate appears to have one large hole in it as seen in its final resting place in Figure G.142. However, when the plate is moved and flipped over it is apparent that some additional damage was done to the plate as show in Figure G.143. A flyer plate was created out of the top plate and is shown on its own in Figure G.144. Figure G.145 shows the bottom plate after the flyer plate was removed.

Figure G.141: Test 20 post test

Figure G.142: Test 20 top plate in test bed

Figure G.143: Test 20 top plate

Figure G.144: Test 20 top plate flyer plate

Figure G.145: Test 20 bottom plate

G.21 TEST 21 (TWO-PLATE TEST –1 ROWS OF KEDD'S ONE TOP AND BOTTOM)

G.21.1 INTRODUCTION

The twenty-first Proof of Concept Test was performed at ARA's Rocky Mountain Division test site. It used an equivalent of 0.023X pounds of TNT, placed in a 9" x 9" aluminum brownie tin, at a close standoff. The test specimen was a series of two ¼" thick A36 steel plates supported by solid CMU blocks. A medium density fiberboard (MDF) spacer block was placed in between each course of CMU to achieve a total height of 1' between steel plates. Figure G.(a) shows the specimen prior to detonation. Figure G. (b) shows the charge for the test. The explosive material was tamped by hand to an approximate density of 1.58 grams/ cubic centimeter.

Figure G.146: a) Test 21 set-up b) Charge for Test 21

G.21.2 KINETIC ENERGY DEFEAT DEVICE

A series of Kinetic Energy Defeat Devices (KEDD's) were used in this test. Each device consists of a 2" diameter thin walled plastic tube, manufactured by VisiPak, filled with water and sealed off on both ends by black plastic caps. The total length of each device was 12". Each row was spaced at 3" on center with the middle KEDD placed in the center of the plate for a total of 9 KEDD's in each row. One row of KEDD's was placed on top of the bottom plate. The other row of KEDD's' was placed directly behind the top plate. There were a total of 18 KEDD's used in this test. Figure G.147(a) shows one KEDD, while Figure G.147(b) shows the two rows of KEDD's. Figure G. shows the KEDD's in the test specimen. The metal support system, constructed out of light gage steel, was used to keep each individual KEDD in place.

Figure G.147: a) Individual KEDD b) Test 21 - Two rows of KEDD's (one on top and bottom)

G.21.3 INSTRUMENTATION

One set of Time of Arrival (TOA) pins were placed behind the bottom plate. They were spaced at 11 1/2", 11", and 10 1/2" above the plywood surface below. The data that was retrieved from these pins can be found in Table G.21. The velocity of the fragments created from the second, or bottom, plate was determined to be traveling at a velocity of 541 ft/sec. The arrangement of TOA pins can be seen in Figure G.148.

Table G.21: Time of Arrival Data for Test 21

Test	Pin Num	TOA	Plate Number	Pin Interval	Interval Velocity	Average Velocity
21	1	n/a	2	0.5 in		541 ft/sec
	2	1240 microsec		0.5 in	541 ft/sec	
	3	1317 microsec				

Figure G.148: Test 21 Time of Arrival pins

G.21.4 SPECIMEN BEHAVIOR

The equivalent of 0.023X pounds of TNT caused one large flyer plate to be formed in the top plate which then impacted the second plate. The top and bottom plates, still in their final resting place, can be found in Figure G.149 The KEDD supports are shown in the photo as part of the wreckage. The top plate was bent in half with a large hole in the middle where the flyer plate was formed, shown in Figure G.150. The flyer plate created from the top plate then impacted the second plate and caused significant deformation, as shown in Figure G.151. Figure G.152 shows the flyer plate caught in the plate. Figure G.153 shows a crack that was formed in the back of the second plate. Figure G.154 shows a comparison of the two plates. The plate on the left of the photo was the top plate, while the plate on the right was the bottom plate.

Figure G.149: Test 21 post test

Figure G.150: Test 21 top plate in test bed

Figure G.151: Test 21 bottom plate in test bed

Figure G.152: Test 21 bottom plate with flyer plate in test bed

Figure G.153: Test 21 crack in bottom plate

Figure G.154: Test 21 top and bottom plate

H EMRTC FIELD TEST REPORTS

H.1 EMRTC TEST 1

H.1.1.1 INTRODUCTION

The first EMRTC field test consisted of a 3 cell structure that was open on the bottom. It was comprised of A36 steel plates that were 3'-6" wide, 8' long, and 7/8" thick. They were supported at the interior corners by 8" x 8" x 1/2" A36 steel angles. The entire assembly was connected by 1" diameter A307 (low strength) bolts spaced at 4" on center. Photos of the test article in place are shown in Figure H.1. Construction drawings are shown in Figure H.3.

Figure H.1: EMRTC Test 1 structure (photo)

The test article was connected to a 2' foot thick un-reinforced concrete foundation with 1" diameter threaded rods. The rods were spaced at 8" on center and were embedded 8" into the concrete structure and secured with epoxy (Red Head Epcon C6). In order to simulate the real structure sand bags were placed at the end of the openings as shown in Figure H.2.

Figure H.2: EMRTC Test 1 structure with sand bags

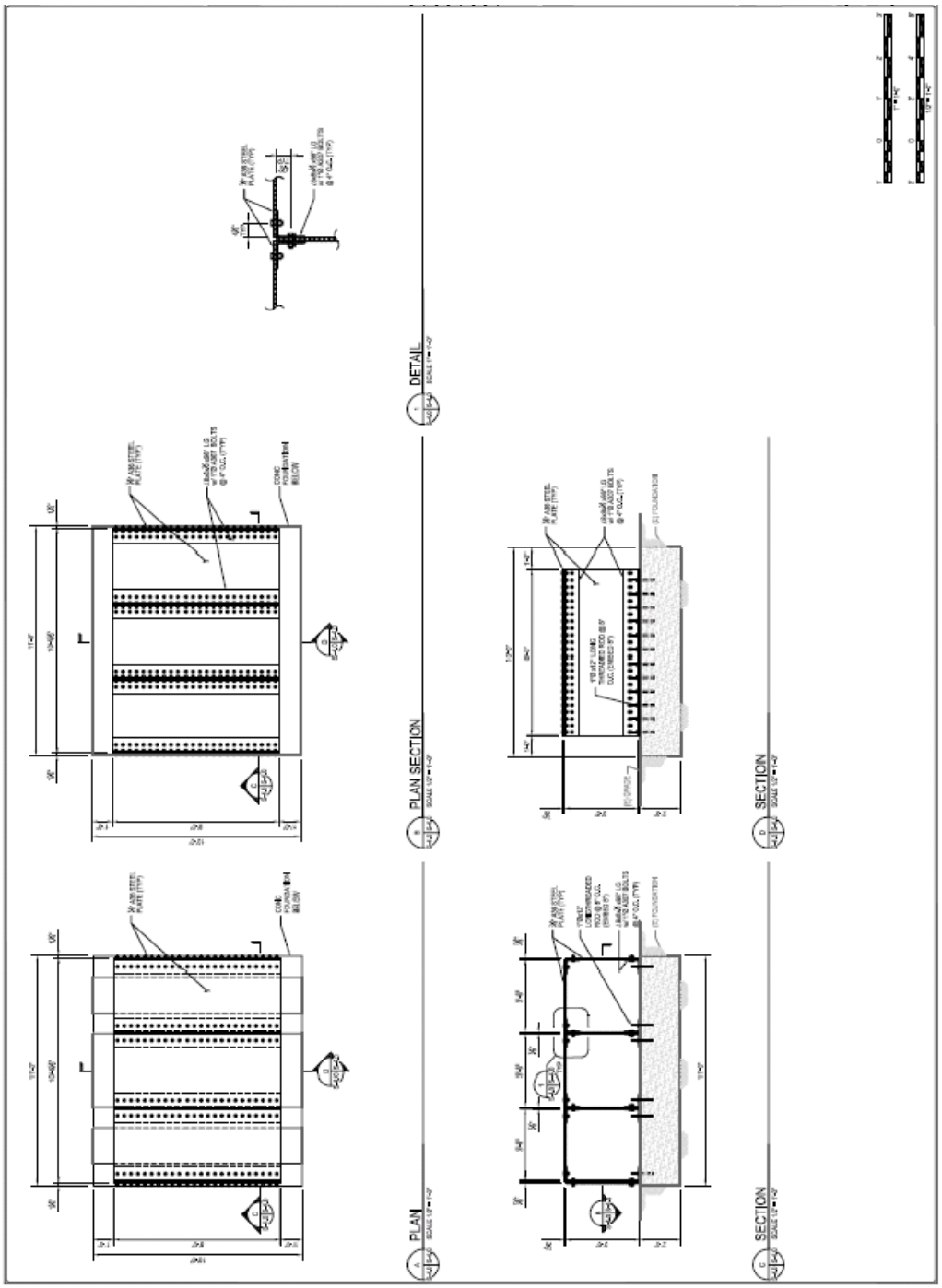

Figure H.3: EMRTC Test 1 structure (drawing)

H.1.2 CHARGE DETAILS

The charge size for this test was a TNT equivalent of X at a short standoff. The charge was placed inside a rectangular box constructed out of 3/4" plywood. The interior dimensions of the box were 26" x 26" x 18". The charge was placed in a conical shape and a

C4 booster charge was placed at the top of that cone to ensure proper ignition of the charge. The charge was placed this way with the desire of producing a planar wave. The TNT and C4 charge is shown in Figure H.4. It was placed at midspan of the center cell as shown in Figure H.5.

Figure H.4: EMRTC Test 1 charge

Figure H.5: Test article and charge

H.1.3 INSTRUMENTATION

H.1.3.1 SENSORS

Field Test 1 used a total of 6 channels of active sensors. Four PCB sensors were installed in rectangular aluminum mounts that were placed at the center and edge of both the central and left bays. Two PVDF-Piezo film gages were laced adjacent to the two centerline PCB gages. The locations are shown in Figure H.6. Table H.1 shows the name, type, and location of each sensor. Unfortunately, the gages failed to report any data.

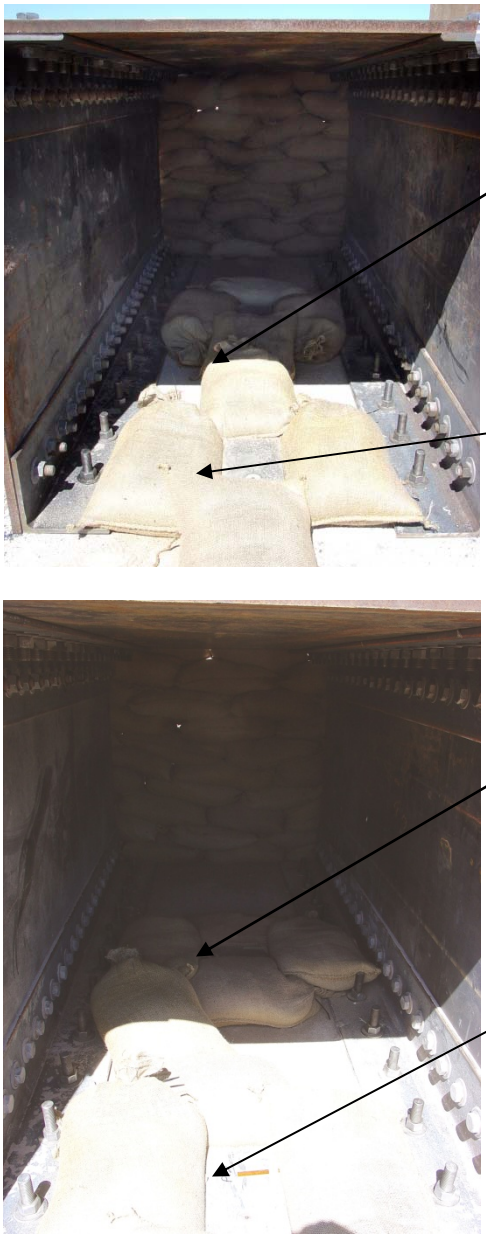

Figure H.6: Test 1 pressure gage locations

Table H.1: Sensors used for EMRTC Test 1

Gage ID	Description	Location
RP 1	Reflected Pressure Gage, 10,000 psi	Central Bay; Centrally Located
RP 2	Reflected Pressure Gage, 10,000 psi	Central Bay; Centered Near Opening
RP 3	Reflected Pressure Gage, 10,000 psi	South Bay; Centrally Located
RP 4	Reflected Pressure Gage, 10,000 psi	South Bay, Centered Near Opening
RPF 5	PVDF-Piezo Film Gage, 10,000 psi	Central Bay; Centrally Located
RPF 6	PVDF-Piezo Film Gage, 10,000 psi	Central Bay; Centered Near Opening

H.1.3.2 PHANTOM CAMERA

One high speed Phantom Camera was used for Test 1. It was located southeast of the test bed. This purpose of this camera was to capture the entire response of the explosive event.

Figure H.7: Test article pictures from Phantom Camera

H.1.4 SPECIMEN BEHAVIOR

The test showed that a flyer plate was formed out of the top plate due to the force of the explosion. The flyer plate was approximately 24" square, which is similar to the 26" square box that the charge was placed in. The flyer plate is shown in Figure H.8(a). The indentation in the flyer plate is from the impact with the pressure gage that was located directly below the charge. The flyer plate impacted the concrete foundation of the test bed and then bounced off of the concrete foundation and was found approximately 50 feet east of the concrete foundation. The individual pieces of the top plate were located around the test article and were reassembled to show there the pieces were originally located. (Figure H.8(b))

Figure H.8: EMRTC Test 1 post test a) Flyer plate b) Reassembled top plate

A majority of the A307 bolts that connected the steel plate and angles of the central bay were found sheared and scattered throughout the test bed. The bolts from the outer cells remained intact and those portions of the specimen remained generally unscathed.

The adhesively anchored threaded rod proved a less than ideal rigid connection to the foundation. The two outer bays of the test specimen were thrown to the north and south of the specimen. The only piece that remained in place from the test was one vertical piece from the center bay as shown in
Figure H.9. Figure H.10 shows how the concrete foundation was pulverized due to the impact of the top plate fragments.

Figure H.9: EMRTC Test 1 post-test

Figure H.10: EMRTC Test 1 post-test, concrete foundation

H.2 EMRTC TEST 2

H.2.1 INTRODUCTION

The second EMRTC field test consisted of a 3 cell structure that was closed on the bottom and placed on elevated supports. It was comprised of A36 steel plates that were 3'-6" wide, 8' long, and 7/8" thick. They were supported at the interior corners by 8" x 8" x 1/2" A36 steel angles. The entire assembly was connected by 1" diameter A307 (low strength) bolts spaced at 4" on center. The entire assembly was elevated 2' above the existing concrete foundation by way of new concrete pedestals. The pedestals allowed for a second plate to be placed in each cell, thereby forming a complete closed cell. This second plate was to determine if an additional flyer plate would be created. Photos of the test article in place are shown in Figure H.11. Construction drawings are shown in Figure H.12.

Figure H.11: EMRTC Test 2 structure (photo)

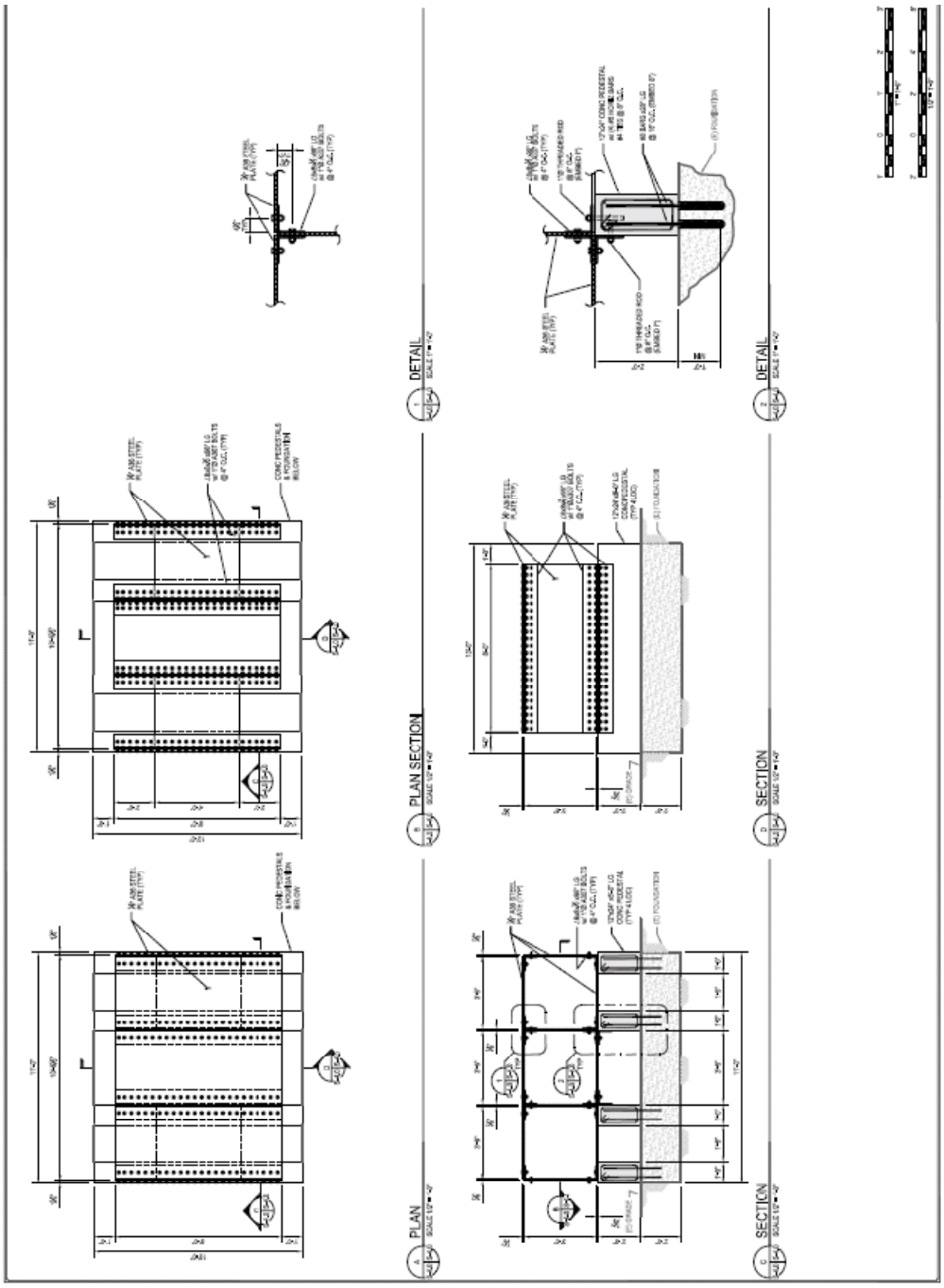

Figure H.12: EMRTC Test 2 structure (drawing)

The test article was connected to a 1’ foot wide and 2’ tall concrete pedestal with 1” diameter threaded rods. The rods were spaced at 8” on center and were embedded 8” into the concrete pedestal.

H.2.2 CHARGE DETAILS

The charge size for this test was a TNT equivalent of X at a short standoff. The charge was placed inside a rectangular box constructed out of 3/4" plywood. The interior dimensions of the box were 26" x 26" x 18". The charge was placed in a conical shape and a C4 booster charge was placed at the top of that cone to ensure proper ignition of the charge. The charge was placed this way with the desire of producing a planar wave. The charge is shown in Figure H.13. It was placed at midspan of the center cell as shown in Figure H.11.

Figure H.13: EMRTC Test 2 charge

H.2.3 INSTRUMENTATION

H.2.3.1 SENSORS

Due to the amount of damage that occurred to the pressure transducers experienced in Field Test 1, they were not used for this test. In attempt to determine the velocity of the initial and secondary flyer plates 3 arrays of Time of Arrival (TOA) pins were used. They were placed directly behind the charge in the central bay. The TOA array is shown in Figure H.14. The pins were mounted to a frame built out of expanded polystyrene. Each array used 12 pins arranged in pairs with a 1/2" spacing between pins. There was a lateral spacing of 5" between sets of pins which is shown in Figure H.15. The arrays were placed behind the top plate, above the second plate, and below the second plate as described in Figure H.16.

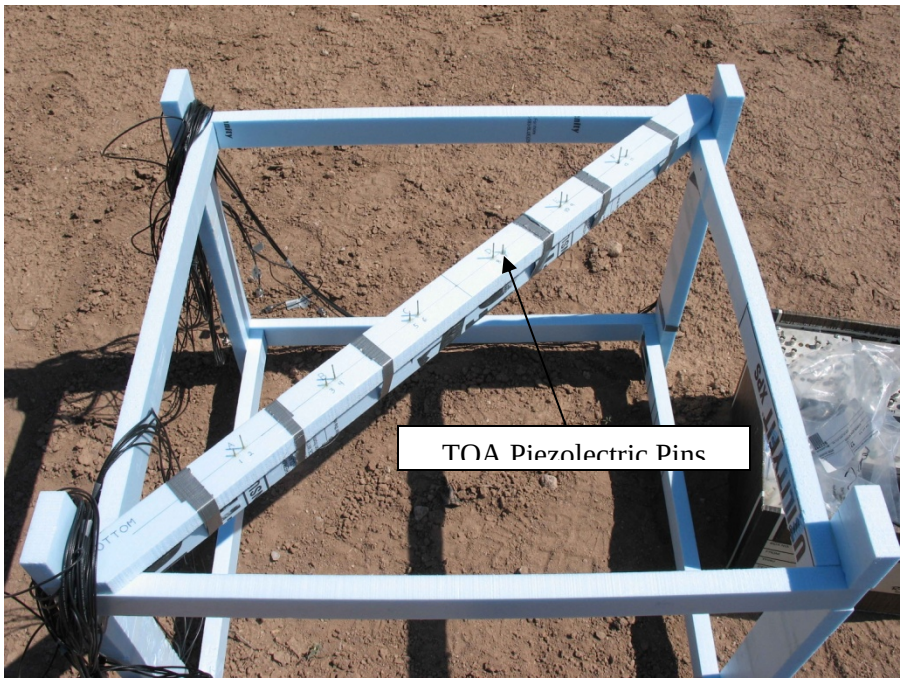

Figure H.14: EMRTC Test 2 Time of Arrival pins

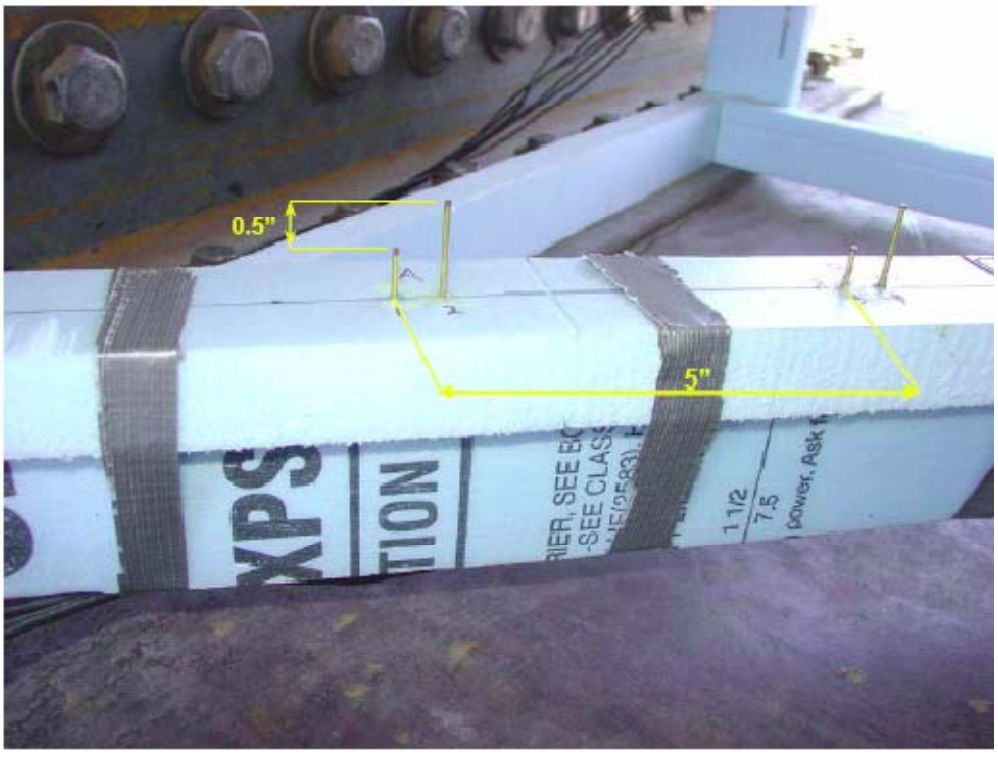

Figure H.15: EMRTC Test 2 Time of Arrival pin dimensions

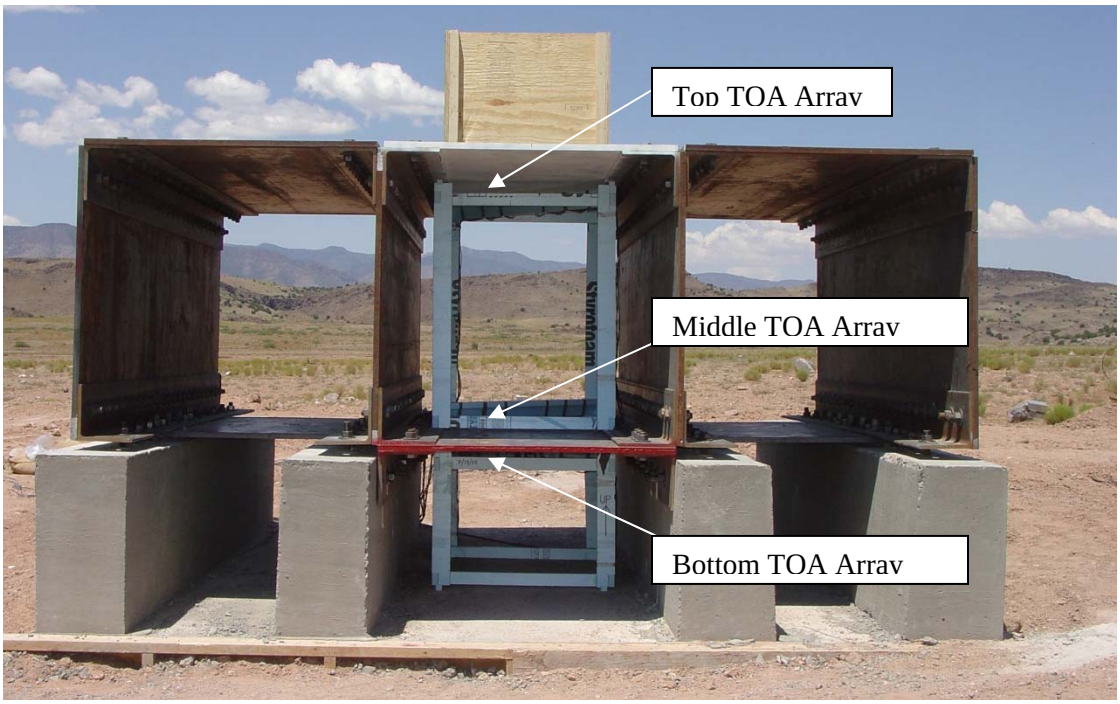

Figure H.16: EMRTC Test 2 Time of Arrival pin array locations

Due to a miscalculation by the instrumentation personnel, the duration of recording time of the data acquisition system was set to an interval that was not long enough to capture all of the data. They overestimated the expected velocity of the flyer plate velocity. Consequently, a significant portion of the data was not captured from the middle and bottom arrays. Eleven of the twelve pin sets on the top TOA array were successfully recorded as well as one gage on the middle array. Table H.2 below shows the results of the 36 gages. It is evident in the first array of gages that a symmetric bulge in the steel plate is formed. From the data gathered in the first array of pins, the flyer plate had an approximate velocity of 1,300 ft/s. If the only other data point is used (M9) which is located on the middle array the velocity of the flyer plate at the second array can be estimated to be 3,400 ft/s.

Table H.2: Time of Arrival pin data

Location	Group	Pin #	Time of Arrival (µs)	Velocity (ft/s)
Top	A	T1	55.961	1344.78
		T2	24.977	
	B	T3	41.537	1296.17
		T4	9.391	
	C	T5	31.143	1337.91
		T6	0.000	
	D	T7	31.401	1346.30
		T8	0.452	
	E	T9	44.334	1276.43
		T10	11.691	
	F	T11	58.831	-
		T12	n/a	
Middle	A	M1	n/a	n/a
		M2	n/a	
	B	M3	n/a	n/a
		M4	n/a	
	C	M5	n/a	n/a
		M6	n/a	
	D	M7	n/a	n/a
		M8	n/a	
	E	M9	916.791	-
		M10	n/a	
	F	M11	n/a	n/a
		M12	n/a	
Bottom	A	B1	n/a	n/a
		B2	n/a	
	B	B3	n/a	n/a
		B4	n/a	
	C	B5	n/a	n/a
		B6	n/a	
	D	B7	n/a	n/a
		B8	n/a	
	E	B9	n/a	n/a
		B10	n/a	
	F	B11	n/a	n/a
		B12	n/a	

H.2.3.2 PHANTOM CAMERAS

High speed video was captured with one Phantom camera (Vision Research). It was located southeast of the test bed and was placed to recode the entire response of the explosive event as shown in Figure H.17.

Figure H.17: Test article pictures from Phantom Camera

H.2.4 SPECIMEN BEHAVIOR

The second EMRTC field test behaved in a similar manner as the first test, except that the specimen remained securely attached to its foundation. Figure H.18 shows the specimen after the test. This photo shows that the damage was contained in the central cell, where the charge was placed. When the charge is contained over one cell there is very little interaction with the other cells. The section of steel seen in the foreground, in Figure H.18, is a fragment from the 7/8" thick top plate. Also evident in this photo is a large square hole in the bottom of the second plate. This occurred from the impact of the initial flyer plate onto the second plate. The secondary flyer plate was found directly below that hole, the initial flyer plate was found resting on the opposite side of the test article as shown in Figure H.19 and Figure H.20. When the flyer plate was removed from the test bed it revealed that the concrete foundation at that point had been pulverized indicating that the residual velocity of the secondary flyer plate was significant.

Figure H.18: EMRTC Test 2 post test

The concrete pedestals used to secure the test article to the foundation proved to be adequate. There was some residual cracking in one of the pedestals, but they were generally in good condition. The epoxy anchorage that was used for this test proved to be sufficient in keeping the test article in place.

The flyer plates that were created were similar to the one created in EMRTC Field Test 1. The initial flyer plate was 24" x 24 1/2" in size and weighed approximately 120 lbs. The secondary flyer plate had slightly larger dimensions; it was 25 1/2" x 25 1/4" and weighed approximately 124.5 lbs. The size of the box that the charge was placed in was 26" x 26". The size of the flyer plates, for EMRTC Field Test 1 and 2, are governed by the size of the box that the charge has been placed in.

Figure H.19: EMRTC Test 2 close up of secondary flyer plate

Figure H.20: EMRTC Test 2 initial flyer plate

Figure H.21: EMRTC Test 2 flyer plates a) Initial flyer plate b) Secondary flyer plate

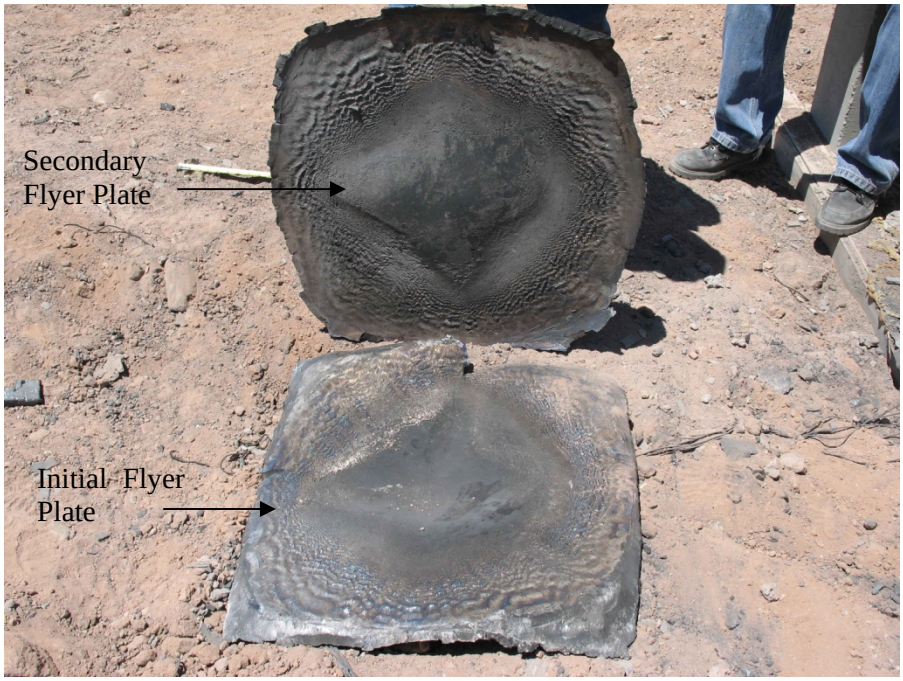

Figure H.22: EMRTC Test 2 flyer plates

A steel fragment that was an original piece of the top plate was found approximately 400’ to the west of the steel bridge assembly. Another fragment from the top plate was found approximately 16’ from the test article. The steel fragments and the test article are shown in Figure H.23. These fragments along with the initial flyer plate, and the large section of top plate shown in Figure H.18 were reassembled to form the top plate as shown in Figure H.24.

Figure H.23: EMRTC Test 2 top plate fragments

Figure H.24: EMRTC Test 2 reassembled top plate

H.3 EMRTC TEST 3

H.3.1 INTRODUCTION

The third EMRTC field test consisted of a 9 cell structure. This structure had a similar construction to the previous tests. Each cell was 3' – 6" wide by 3' – 6" tall and 8' long, constructed out of 7/8" steel plate. They were supported at the interior angles corners by 8" x 8" x 1/2" A36 steel angles. The entire assembly was connected by 1" diameter A307 (low strength) bolts spaced at 4" on center. The only exception to this layout was along the top plate. One of the purposes of this test was to determine the effects on the cells when a charge is placed across all of the cells. In addition, the top plate was to be continuous across those cells. In order to achieve that goal, two steel plates were placed across the top cells, perpendicular to the rest of the plates. These two top plates were 4' x 10'-7 3/4" x 7/8". They were placed flush with each other. The entire specimen was connected to the concrete foundation through the use of T sections. They were connected to the foundation by 1" diameter anchor rods located at 8" on center; they were embedded 8" into the foundation. The test set-up is shown in Figure H.25 and a detailed construction drawing of the test elevation is shown in Figure H.26. The construction drawings for the entire test specimen are shown in Figure H.27.

Figure H.25: EMRTC Test 3 structure elevation (photo)

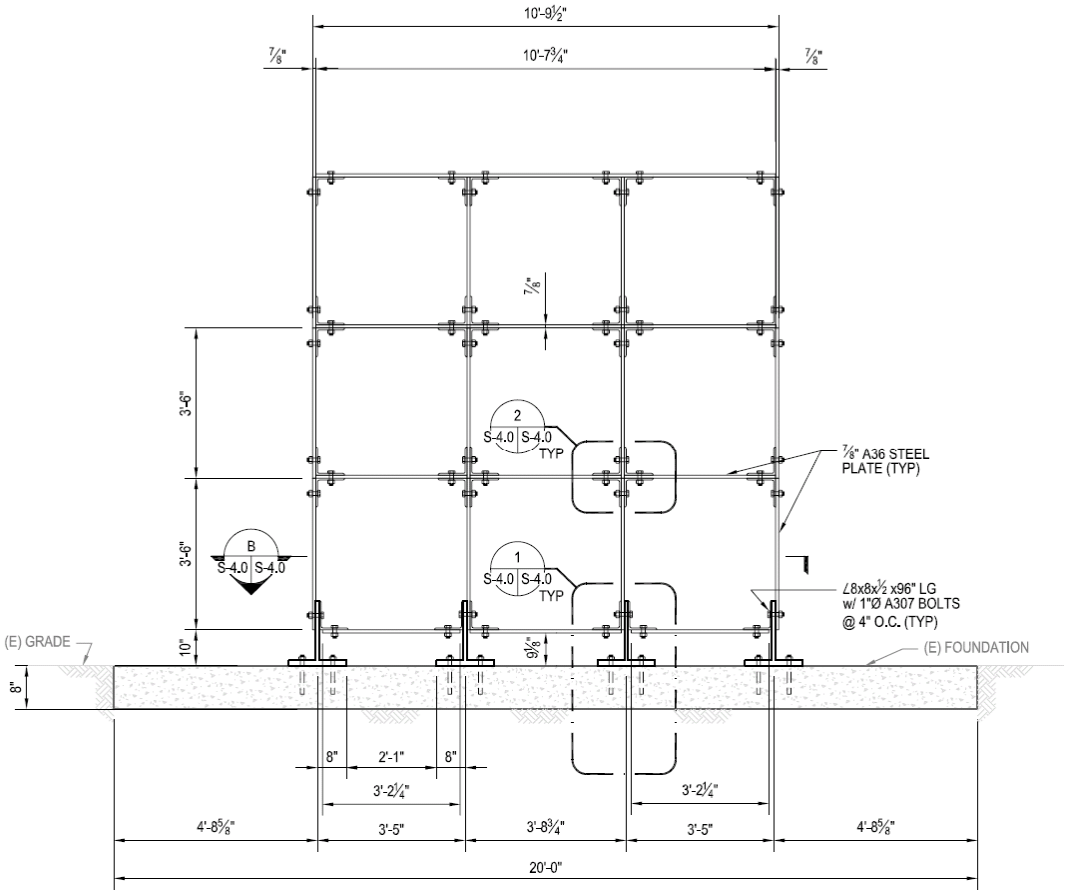

Figure H.26: EMRTC Test 3 structure elevation (drawing)

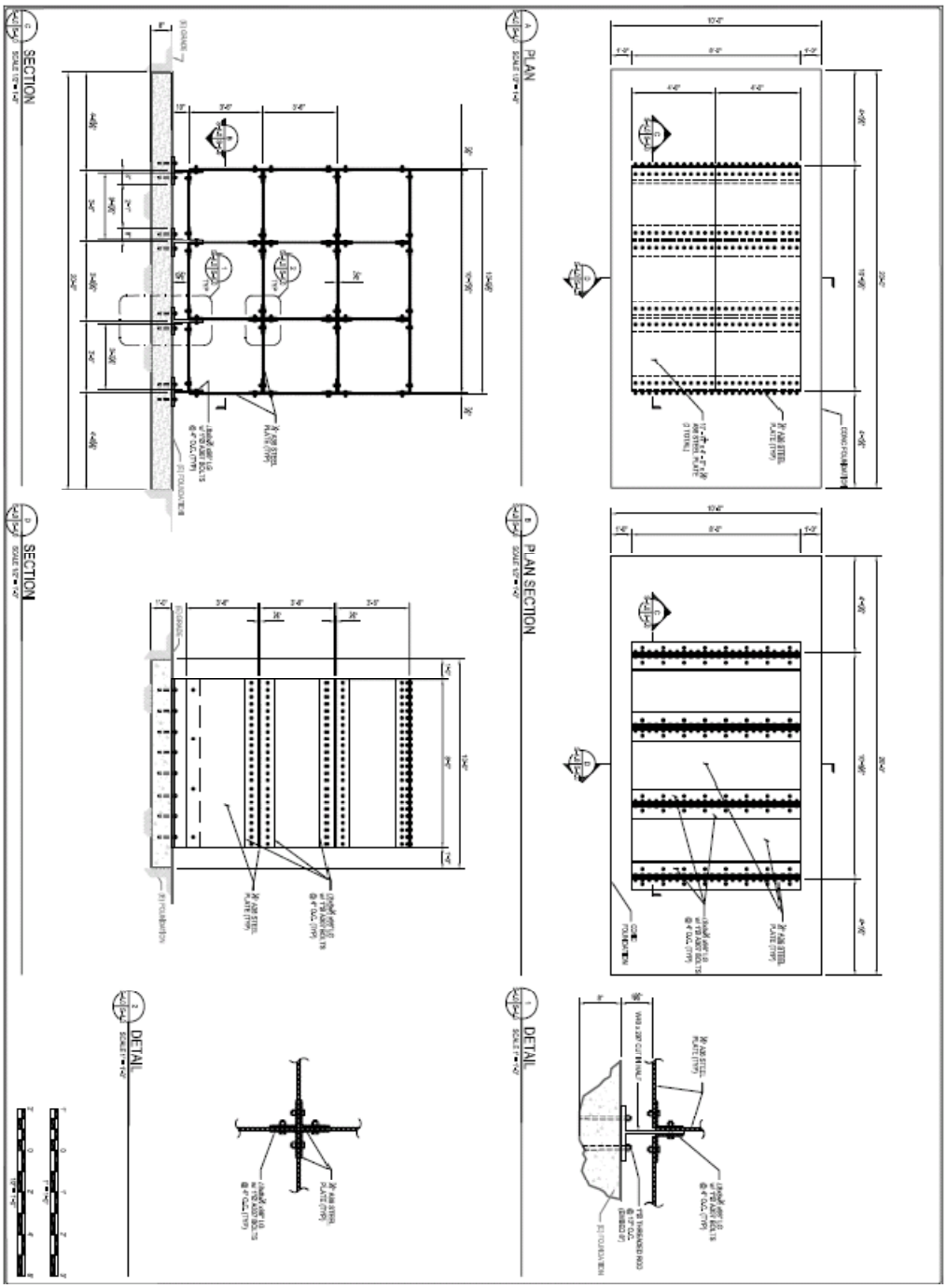

Figure H.27: EMRTC Test 3 structure (drawing)

H.3.2 KEDD FIELD TESTS SET-UP

The Kinetic Energy defeat Device (KEDD) system was constructed out of nominal 8" diameter Schedule 40 PVC pipe. The inside diameter of the tube is 7.943" with an outside diameter of 8.625", and a wall thickness of 0.682". Each pipe was placed in an array where

the center of the pipe is located 10 1/4" away from each other and staggered in two rows. Each pipe had caps constructed out of 3/8" PVC to fit into the ends of the pipes; they extended past the pipe approximately 3/16". One of the end caps had two holes drilled into the ends the KEDD's were filled using those holes (one for air to escape and one for water to enter) and then were sealed with 3/8" NPT blind pipe plugs that had Teflon tape around the edges to protect from leaks. The total KEDD length is 3' 1 3/4" and is shown in Figure H.28. This test used two rows of KEDD's in a staggered pattern. Figure H.29 shows two cells with KEDD's installed. The weight of the KEDD alone is 20 lbs, when filled with water they weigh approximately 88 lbs, the total array of 17 KEDD's is 1,500 lbs.

Figure H.28: KEDD – EMRTC Test 3

Figure H.29: 2 Rows of KEDD's on top EMRTC Test 3

H.3.3 CHARGE DETAILS

The charge size for this test was a TNT equivalent of 2.1X at a short standoff. The charge was placed in a box with interior dimensions of 4' wide by 10' 7 3/4" long. The base was constructed out of 3/8" plywood, while the sides were constructed out of 2" x 8"

(nominal) pieces. The wood was connected to the plywood by 3" screws. The box was centered on the center of the specimen. The charge was placed in the box in a staggered formation. A small booster was placed in the center of the charge to ensure proper detonation of the explosive material. The plywood box before the charge was placed in it is shown in Figure H.30. The completed charge is shown in Figure H.31.

Figure H.30: EMRTC Test 3 charge box

Figure H.31: EMRTC Test 3 charge in place

H.3.4 INSTRUMENTATION

H.3.4.1 TIME OF ARRIVAL PINS

Ten sets of Time of Arrival (TOA) pins were used for this test series. They recorded the velocity of the steel plates. The TOA pins were held in place by attaching them to a glass rod, as shown cut at varying lengths in order to have a 1/2” spacing between each pin. The typical TOA pin series was placed at 1/2", 1", and 1 1/2" below the steel plate. There were two arrays that used 4 pins. Those pins were located at 1/2”, 1”, 1 1/2”, and 2” below the steel plate. Those arrays are shown in Figure H.32. The arrays were placed in each of the nine cells. The cells were numbered starting with the upper left hand cell and moved down the columns. The first three cells were in the first column of the specimen and are labeled 1,2, and 3 moving down the column. The next column of three cells had pin array numbers 4, 5, and 6, where cell 4 was the center cell in the top row. The final column of cells had pin array numbers 7,8, and 9, where 7 was the last cell in the top row. The specific information with regards to the TOA pins including, cell number, location (front of back) and number of pins, is shown in Figure H.33. Front means that the pins are located in the center of the cell, 3’ in from the front edge. Back means that the pins are located in the center of the cell, 7’ in from the front edge.

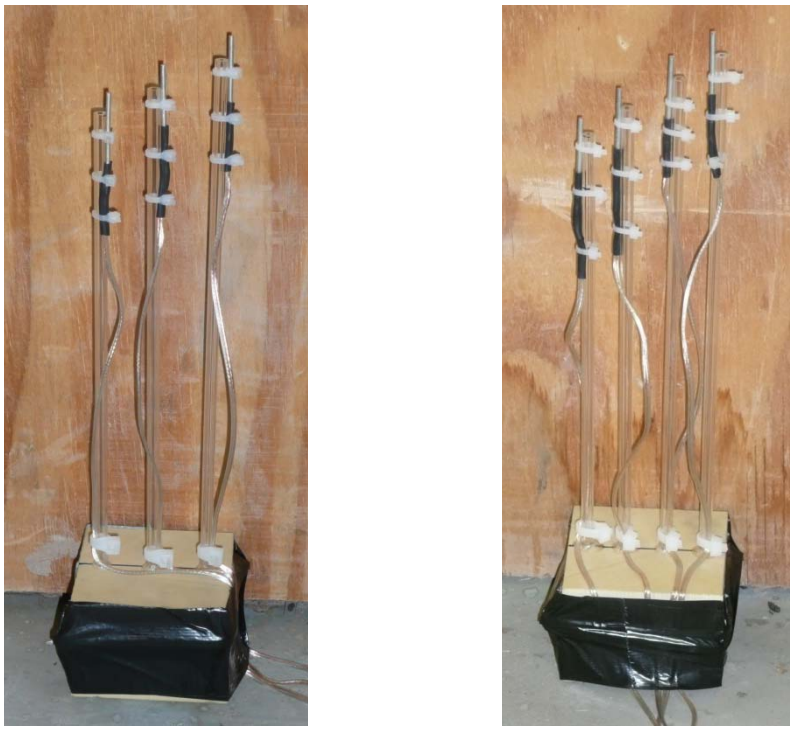

Figure H.32: Time of Arrival pin arrays a) 3 pin array b) 4 pin array

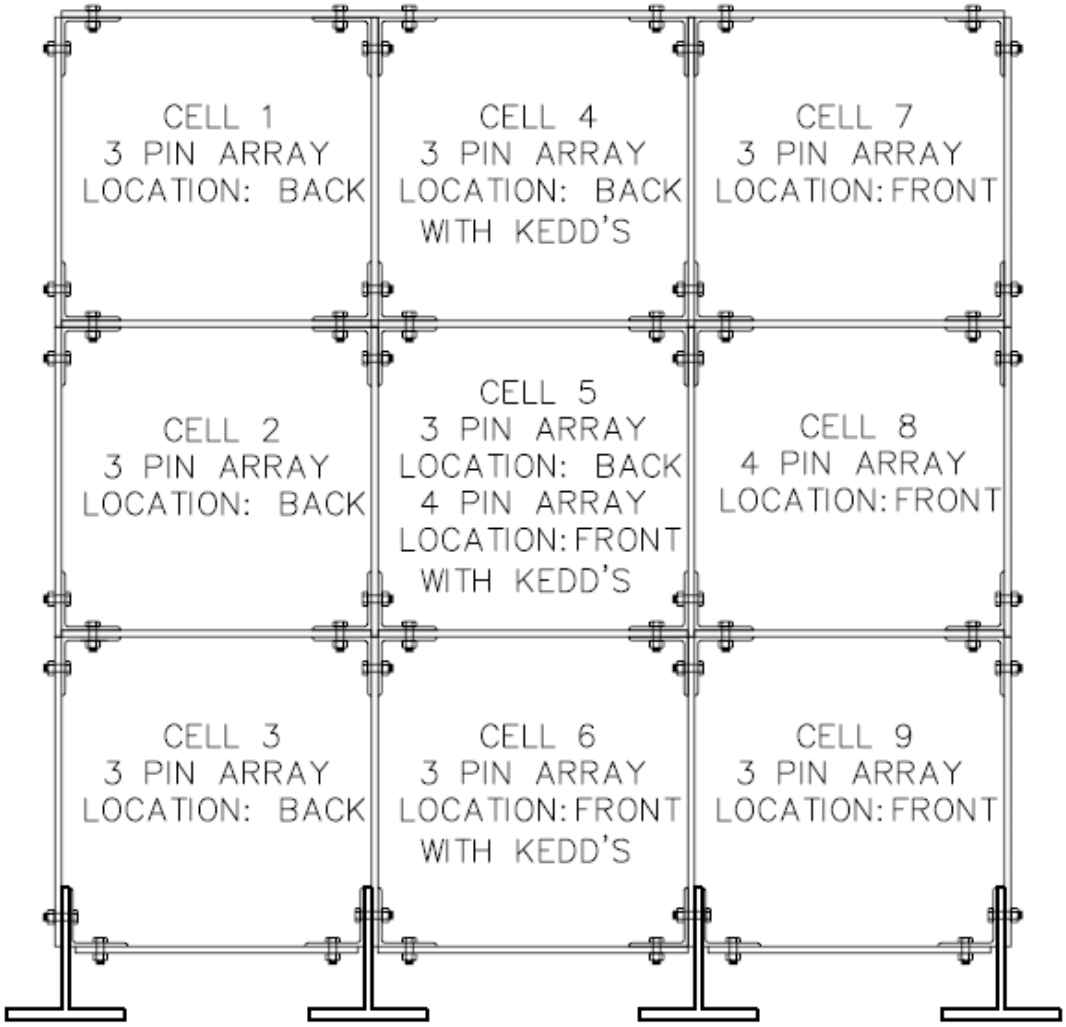

Figure H.33: Time of Arrival pin locations for EMRTC Test 3

The pin arrays were held in place using two different methods. For the baseline tests (Cells 1-3 and Cells 7-9) the pins were supported by a 3" diameter paper shipping tube that was attached to the bottom steel plate. The pin array shown in Figure H.32 was then attached to the tube by tape. In order to ensure that the tube would not be blown out of the test article by the blast pressures they were secured to the test structure by 4 guide wires that were attached to bolts at the bottom of the cell. Figure H.34(a) shows a typical set-up of the TOA pins on top of the paper tube. In the center cells, the ones with the KEDD's, the TOA pin arrangements were attached to a KEDD. They extended approximately 1" above the top of a KEDD, such that they should be activated before the KEDD is breached. Figure H.34(b) shows the tops of a pin array peeking out from between two KEDD's.

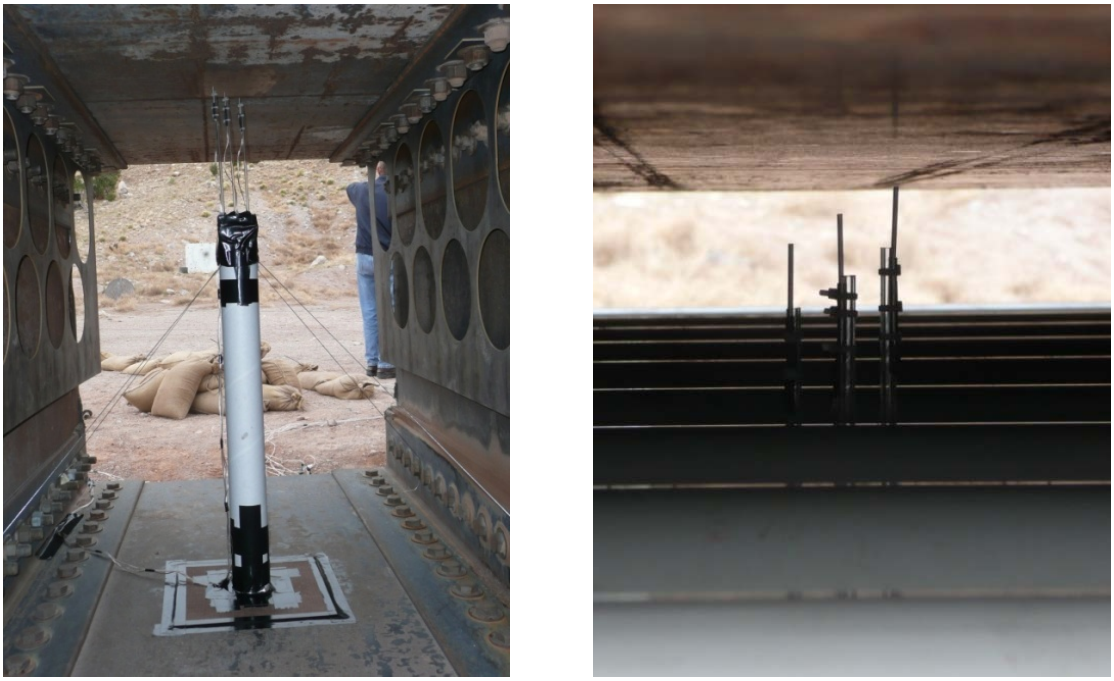

Figure H.34: Time of Arrival pins a) Pin support in outer cells b) Pins located in center cells

Time of Arrival data was gathered in from this test. The data that was retrieved from these pins can be found in Table H.3. No data was recorded from Cell 6 since that plate was not breached.

H.3.4.2 PHANTOM CAMERA

High speed video was captured with one Phantom camera (Vision Research). It was located south of the test bed and was placed to record a close-up of the specimen in an attempt to gather useful information.

Table H.3: EMRTC Field Test 3 Time of Arrival pin data

Cell Number	Pin Number	TOA (microseconds)	Time Interval (microseconds)	Velocity Interval (FPS)	Average Velocity (fps)
1	1	272			1370
	2	304	32	1302	
	3	333	29	1437	
2	4	3141			176
	5	3399	258	161	
	6	3617	218	191	
3	7	11666			178
	8	11912	246	169	
	9	12134	222	187	
4	10	150			1029
	11	191	41	1016	
	12	231	40	1042	
5	13	2820			80
	14	3801	981	42	
	15	4367	566	74	
	16	4707	340	123	
	30	3041			83
	31	3706	665	63	
	32	4108	402	103	
7	20	265			1111
	21	303	38	1096	
	22	340	37	1126	
8	23	3108			189
	24	3371	263	158	
	25	3561	190	219	
9	27	11404			802
	28	11478	74	563	
	29	11518	40	1041	

H.3.5 TEST RESULTS

This test utilized a 9 celled structure (3 columns by 3 rows). Each cell has been assigned a specific number for future reference. Starting at the upper left corner, when looking at the front of the specimen, the first cell is numbered Cell 1. The numbering scheme then moves down the column for Cells 2 and 3. The fourth cell is at the center of the top row. The cells below it, in the second column, are labeled Cell 5 and Cell 6. The cell in the upper right corner is labeled Cell 7. The cells directly below that are labeled Cell 8 and Cell 9. This numbering scheme is shown in Figure H.33 and again in Figure H.36. It will also be referenced in future discussions about the specimen behavior, both in the text and in the photos.

Severe damage occurred to the outer cells of the test article. The center cell suffered less damage due to the blast mitigation techniques that were used. Figure H.35 shows the entire test specimen after the explosive event. That photo is used again in Figure H.36 with a color coded Key Plan that points out the specific cells. The portions of the specimen, to the right and left of the center cell in the photo, are what remain of the outer cells. In Figure H.36 they are identified as cells 2 and 8, using the orange colored arrow and number. These pieces of the structure fell to the sides when the A307 bolts that connected them to the center section, failed. These outer cells (Cells 1-3 and 7-9) were used as a baseline, or reference, for what type of damage would occur without a retrofit device. The center column of cells (Cells 4-6) is shown in the center of the photo in Figure H.36. It shows that Cell 6 remained intact and that Cell 5 suffered minor damage. This is also exhibited in Figure H.36 where the pink arrow and number correspond to the center cell, or Cell 5. The purple arrow and number correspond to the intact Cell 6. A discussion of the specific type of damage that occurred to each cell will be discussed below. These pictures show the test articles where they landed after the test. A detailed post-mortem of the specimen has not occurred the only information on the behavior of the specimen is what is shown in the following photos.

Figure H.35: Test specimen post-test

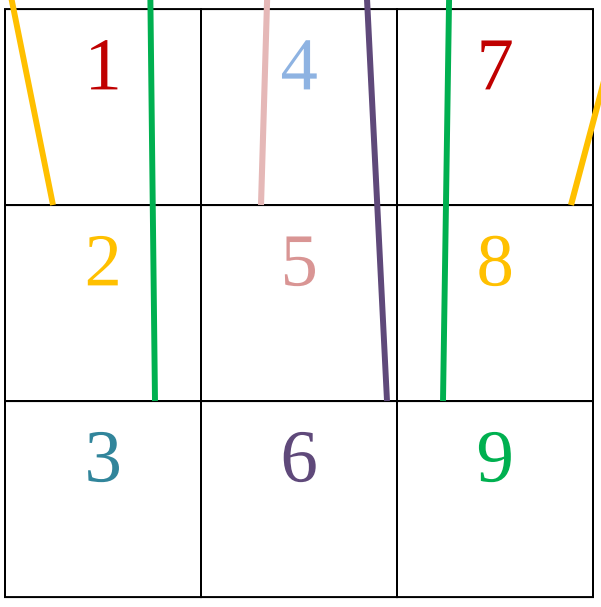

Simplified Key Plan

Figure H.36: Test specimen post-test with Key Plan

Figure H.37 shows the remnants of Cells 1 and 2 from the test article, this photo was taken from the side of the test article. The top plate of Cell 1, from directly under the charge, has not been located in its entirety. Many large flyer plates were found near the test specimen, these are most likely from the top plates of Cells 1 and 7. Eventually, after this document is finalized, a post-mortem of these specimens should occur, where each of the top plates will be reassembled. The portions of the test specimen shown in Figure H.37 are connected to the second plate in the test article. The middle plate in Figure H.37 used to be the second plate in the test specimen, the bottom plate in Cell 1 or the top plate of Cell 2. It is identified by the green arrow in the photo. The majority of this plate has been breached, and all that remains is the outer portion of the plate. This was created from the incoming flyer plates from the plate above. The sharp edges, shown in the closer portion of the photo, are examples of brittle failure. Another example of brittle failure is the loss of the portion of plate shown in the front portion of the picture. Near the back of the plate, back of the photo, there are some signs of ductile behavior in the plate.

The remaining outer supports, the red and orange arrows, are relatively unscathed. The supporting angles, identified by the blue arrow, are still connecting all three pieces on that side. The supporting angles on the other side, the side that connected Cell 8 to Cell 5 identified by the purple arrow, were separated from the supporting plate. They are still connected to each other through the connecting bolts along with staying connected to the second plate. The bolts that connected the second plate (Cell 1 or Cell 2) to the center cells (Cell 4 or Cell 5) were all sheared off. This affects the behavior of the center cells, or retrofitted cells, and will be discussed below. The piece of angle shown in the left side of the photo, identified by the yellow arrow, is from the top plate. Notice the deformation not only along the length of the angle; but also in the structure of the angle. It is an example of the amount of force that was exerted on the unretrofitted cells.

Figure H.38 shows the remnants of Cells from the test article, this photo is taken from the opposite side as the photo in Figure H.37, which is why the Key Plan is reversed. The top plate of Cell 3, or bottom plate of Cell 2, is shown in this photo. It has been designated by the blue arrow. This photo shows that the plate suffered minor damage, but was not fully breached. There is a small portion of that plate, shown at the front of the photo; that was damaged. The perpendicular supports of Cell 3 designated by the red and yellow arrows, shows very little damage to those plates. The angles that connected Cell 2 with Cell 3 (orange arrow) show significant deformation, along with the loss of all the bolts that held the top plate (blue arrow) in place. The bottom plate in the structure, bottom plate of Cell 3 shown by the green arrow, is still intact. The majority of the connecting bolts are still in place, with a few exceptions. There was not enough energy to break through the fourth plate.

The original simulations, performed by SAIC, predicted that with this equivalent TNT charge that the bottom plate of the structure would not be breached. It was the desire of the researcher, and the experts associated with this test, that there was some portion of the unretrofitted test specimen intact after the test. This charge weight and size achieved that goal.

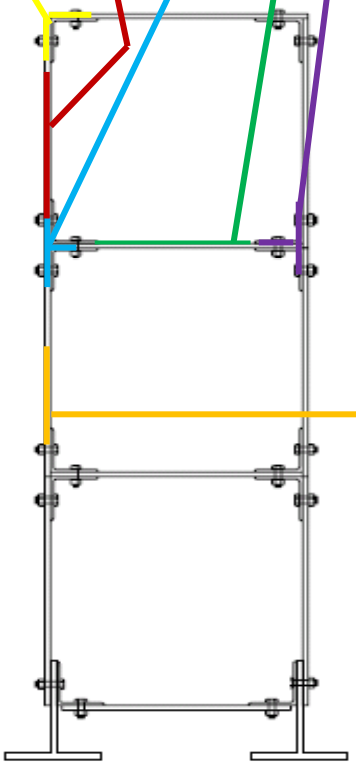

Key Plan of Structure

1	4	7
2	5	8
3	6	9

Looking from the back of the structure

Figure H.37: Test specimen post-test cells 1 and 2

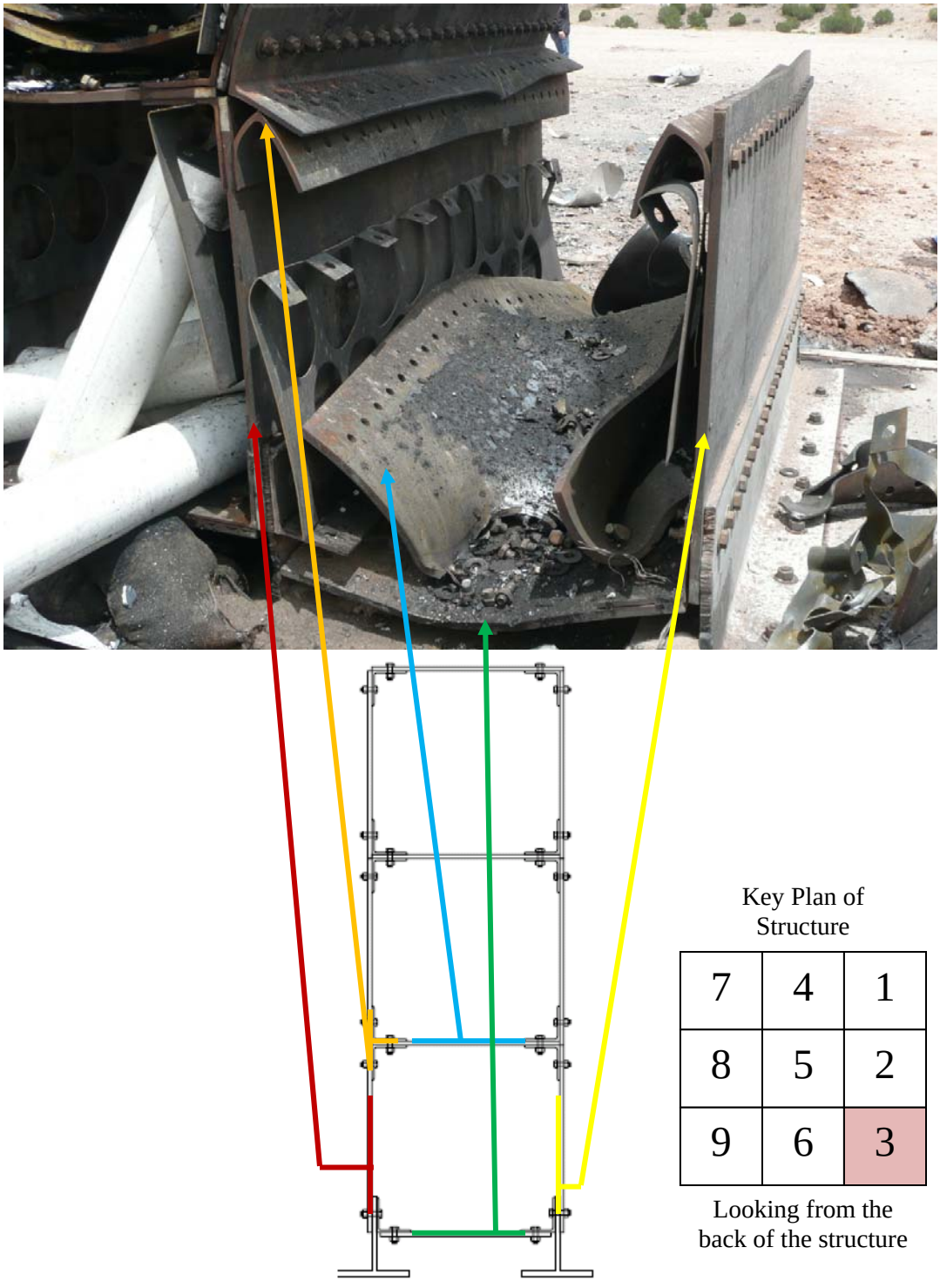

Figure H.38: Test specimen post-test cell 3

Figure H.39 shows the remnants of Cells 7 and 8 from the test article. The top plate of Cell 7, from directly under the charge, has not been located in its entirety. Many large flyer plates were found near the test specimen, these are most likely from the top plates of Cells 1 and 7. The portions of the test specimen shown in Figure H.39 are connected to the second plate in the test article. The middle plate in Figure H.39 used to be the second plate in the test specimen, the bottom plate in Cell 7 or the top plate of Cell 8. It is identified by the green arrow in the photo. There is a large hole in the center of the plate. It was created from the incoming flyer plates from the plate above. The sharp edges, shown in the closer portion of the photo, are examples of brittle failure. Near the back of the plate, back of the photo, there are some signs of ductile behavior in the plate.

The remaining outer supports, the orange and purple arrows, are relatively unscathed. The supporting angles, identified by the yellow arrow, are still connecting all three pieces. The bolts that connected the second plate (Cell 7 or Cell 8) to the center cells (Cell 4 or Cell 5) were all sheared off as identified by the blue arrow. This affects the behavior of the center cells, or retrofitted cells, and will be discussed below. The piece of angle shown in the left side of the photo, identified by the red arrow, is from the top plate. Notice the deformation not only along the length of the angle; but also in the structure of the angle. It is an example of the amount of force that was exerted on the unretrofitted cells. This test has shown that the plates parallel to the explosive charge sustain more damage than the adjacent plates. The flyer plates are created so quickly that they move through the structure before the vertical supports have time to react. The strengthening of those plates, as a retrofit technique, may not be ideal as other portions of the structure are more heavily damaged than those plates.

Figure H.40 shows the remnants of Cells from the test article, this photo is taken from the front of the structure. The top plate of Cell 9, or bottom plate of Cell 8, is shown in this photo. It has been designated by the yellow arrow. This photo shows that the plate suffered moderate damage along some edges, but was not fully breached. There is a small portion of that plate, shown at the front of the photo; that was damaged. There are a few sections where portions of the steel are missing, as seen in the front of the plate. This plate suffered more deformation along its length than its counterpart in Cell 3. In addition, when compared to the damage that occurred in Cell 3, this plate lost more of the connecting bolts between the plate and angles. The perpendicular supports of Cell 9 designated by the red and purple arrows, shows very little damage to those plates. The angles that connected Cell 8 with Cell 9 (orange and blue arrows) show significant deformation, along with the loss of all the bolts that held the top plate (yellow arrow) in place. The bottom plate in the structure, bottom plate of Cell 9 shown by the green arrow, is still intact. The majority of the connecting bolts are still in place, with a few exceptions. There was not enough energy to break through the fourth plate.

It is interesting to note, that while the test was symmetrical the results shown in the two baseline columns are not the same. There was more damage to the top steel plate of Cell 2 than there was for the corresponding plate in Cell 8. At the same time, there was more damage to the top plate of Cell 9 than there was with Cell 3.

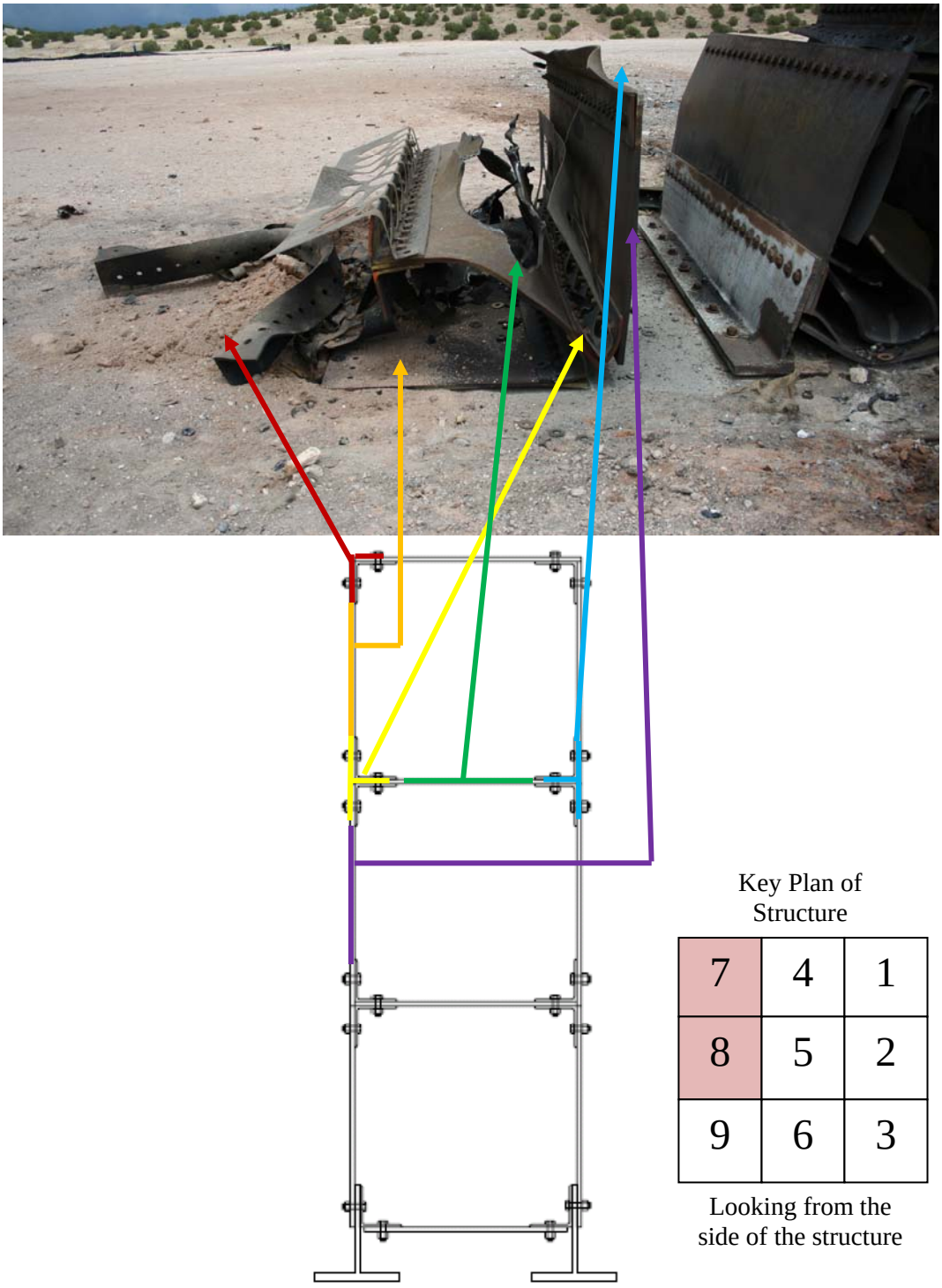

Figure H.39: Test specimen post-test cells 7 and 8

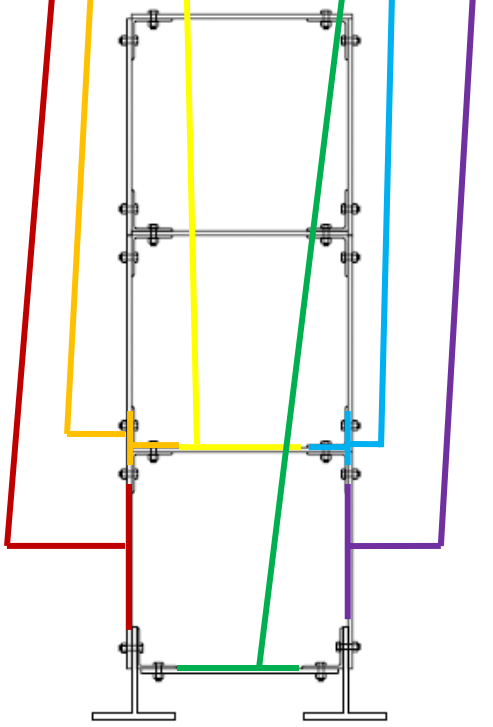

Key Plan of Structure

1	4	7
2	5	8
3	6	9

Looking from the front of the structure

Figure H.40: Test specimen post-test cell 9

Portions of the top plates of Cells 1 and 7 were found throughout the test bed. Some of the larger pieces were found close to the test article, while others were found much farther away. Figure H.41 shows the test specimen post-test and some of the flyer plates that were found nearby. In order to help distinguish the flyer plates, or top plate fragments, from the rest of the test article they have been circled in Figure H.41. Figure H.42 and Figure H.43 show the flyer plates found in front of the test specimen. Both of these photos show the same flyer plates, just from different angles. The fragments from the top plates that were found near the test specimen were significantly larger than the pieces that were found at much farther distances. All of the fragments that were found showed signs of both brittle and ductile failure. They all have sharp edges where they were formed from the top plate, but they also show signs of plastic deformation as demonstrated in the twisting and curling of the plates. This is highlighted in Figure H.42 and Figure H.43.

Smaller flyer plates were found at significant distances from the test article. Those flyer plates are shown in Figure H.44 and Figure H.45, in these photos the areas that are circled is the original location of the test article. These fragments are much smaller than the ones found closer to the test article, but they show the amount of energy these pieces exhibited. These pieces were most likely formed from the top plate which impacted a subsequent plate, at some point they then rebounded off of the test structure to land at these varied locations. The fragments shown in Figure H.44 are approximately 400' – 500' from the test article. The portion of the top plate shown in Figure H.45 was closer to 1,000' feet from the test article. This piece was formed near the edge of the pate as bolt holes are evident in close-up pictures of that piece (Figure H.46).

Figure H.41: Test specimen and miscellaneous flyer plates

Figure H.42: Test specimen and miscellaneous flyer plates

Figure H.43: Miscellaneous flyer plates

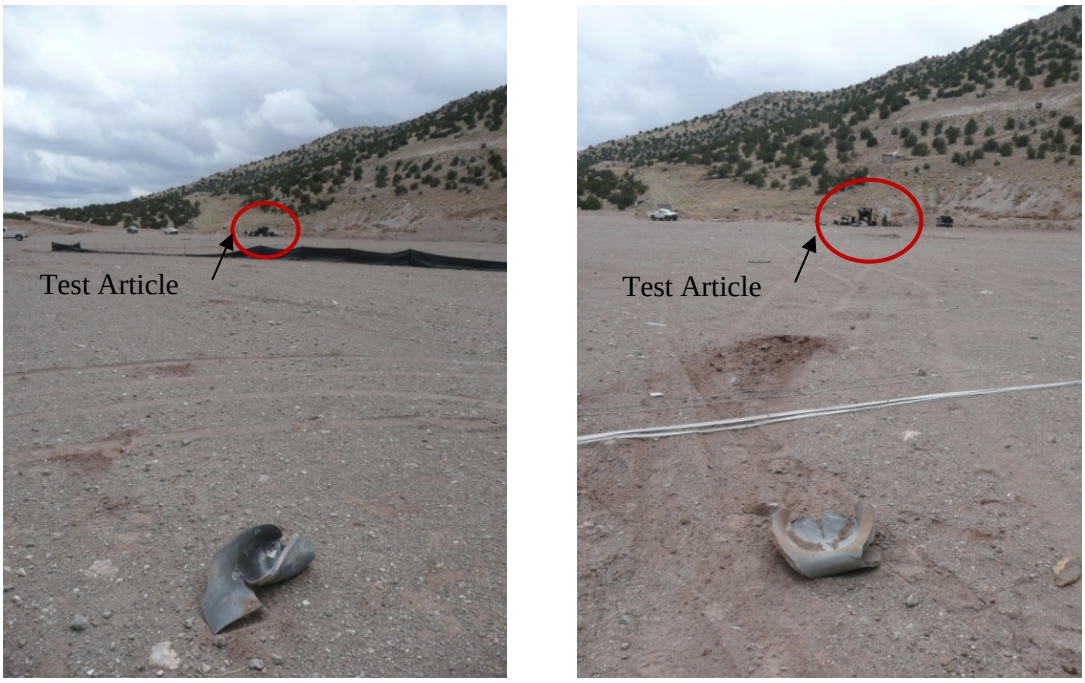

Figure H.44: Flyer plates at extreme distances

Figure H.45: Flyer plates at extreme distances

Figure H.46: Close up of flyer plate

This test exhibited two very different types of failures, the outer cells showed brittle and ductile fractures of an unretrofitted specimen, while the center cells showed the promise of the Kinetic Energy Defeat Device (KEDD). While there are inherent differences in the manner in which each column will behave, based solely on end conditions, conclusions can still be made that show the effectiveness of the KEDD system. In the baseline tests, the top plate could not be fully accounted for immediately after the test. It is assumed, that they flyer plates found throughout the test bed correspond with that top plate. In addition, the support structure of those outer cells was found to the left and right of the test set-up. This is most likely from the loss of the support bolts that held the specimen together.

The behavior of the center cell was very different from the outer cells; the majority of the support structure of the center cell fell straight down into Cell 5, as opposed to being strewn throughout the test bed. Figure H.48 shows the center cell (Cells 4 and 5) post-test. The first thing that should be noticed in this photo is that the majority of the miscellaneous pieces shown in the photo are relatively intact. This is due to the effectiveness of the KEDD device. Instead of the top plate fragmenting into many small pieces, it appears, from the initial investigation that it only sheared the bolts along the edge supports of the plate. Two large pieces were found that appear to be the top plate. The separation of the two pieces is not because of fragmentation, but because of the joint between the two plates that was centered on the test specimen. One of those pieces is shown in Figure H.48 and is denoted by the blue arrow. It is unclear the extent of the damage to the top plate beyond what is shown in the figure, but it appears to have plastic deformation around the sides. It would not be surprising if a small flyer plate was found, but that has not been determined yet. The second half of the top plate is located in the back of the cell, but is not shown in this photo. One of the

unintended effects of the KEDD system, is that it changes the behavior of the shock wave of the top plate. Those larger plates then interacted with the KEDD system as they tried to move through the cell. The KEDD system appears to have worked in a similar manner as the 2 Plate Tests. The jets from the KEDD system traveled approximately 50' out both the front and the back of the test specimen. Figure H.43 shows some of the puddles of water that were formed by the jet. The photo shows a large width of water with some residual mud puddles. The width of the water jets extended beyond the 3'- 2" length of the KEDD and came closer to expanding the width of the specimen as shown in Figure H.47. The jets were moving at such a high velocity near the structure that they were able to carve small valleys into the soil in front of, and behind, the structure. Portions of the PVC pipe were also found throughout the test bed. Some of the fragments were quite small, while others were of a non-trivial size. Due to the amount of the fragments that were seen, as opposed to the 2 Plate Tests where hardly any fragments were found, it would not be recommended to use a KEDD that is stronger than the Schedule 40 PVC pipe that was used.

After the top plate interacted with the KEDD's it continued to move through the structure until impact with the second plate (bottom plate of Cell 4 or top plate of Cell 5). The second plate, exhibited in Figure H.48 by the yellow arrow, was only slightly damaged. The plate was deformed, but was not breached. One of the difficulties with this test set-up was that each cell interacts with the other. In this case the baseline cells caused more damage to their supports which in turn affects the center cell. As stated above, all of the support bolts that connected Cell 2 to Cell 5 and Cell 5 to Cell 8 were sheared off. This was due to the force that the baseline tests experienced. When these bolts failed, it caused the angles that supported the KEDD's to fall. It is not known if this occurred prior to the second plate being impacted or not. The support angles between Cell 4 and 5 are shown in Figure H.48 designated by the purple arrows. It can be seen that these angles appear to be undamaged, and that they probably fell through the cell when their support bolts failed. The KEDD's in Cell 5 were most likely activated by the falling through the cell, as opposed to being activated by the plate above it. In the future, this test should be performed with KEDD's in all cells. This would ensure that there are no unintended consequences from the behavior of the adjacent cells.

The bottom plate shown in Figure H.48 and designated by the green arrow, shows that it is completely intact. The only damage that it appears to have suffered is from the impact of the mass above it. All of the angles and bolts that support this intersection remain intact. This is also exhibited in the vertical support plates of Cell 5 are still in place, as shown by the red and blue arrows. These supports are no longer vertical, but that is due to the effects of the angles and plates inside the cell.

Figure H.49 shows Cells 4, 5, and 6 post-test. This picture exhibits the entire behavior of the retrofitted specimen. At the very top of the photo, exhibited by the yellow arrow, is one of the vertical supports from Cell 4. It is most likely the support between Cell 4 and 7, but it is impossible to be certain. As you can see, it has not been breached and shows only minor deformation. That could be from the force of jets form the KEDD, but it is most likely from the interaction with other pieces of the specimen. As stated earlier, the vertical supports are still attached to their connecting angles at the intersection of Cells 5 and 6 as well as Cells 5 and 2. This figure also shows portions of the top plate which came to rest inside of Cell 5, as shown by the green arrow. The second plate is shown by the orange arrow and the third plate is pointed to by the purple arrow.

The importance of Figure H.49 is that is shows the complete, and undamaged, Cell 6. It shows that all of the supports are still intact and undamaged. It should also be noted that the KEDD's fell out of their supports. In future designs of similar experiments a better support system should be used that ensures that the KEDD's stay in place. In addition, the KEDD design was not ideal; some of the end caps of the KEDD's detached from the KEDD and allowed the water to seep out. Instead of using a solvent to attach the caps to the PVC pipe another option could be to fuse, or melt, the plastics together. That would give it a tighter seal. The caps that were screwed into the KEDD's after the water was filled could be fused in the same manner to prevent long term leaking.

Figure H.47: Jets formed by KEDD system

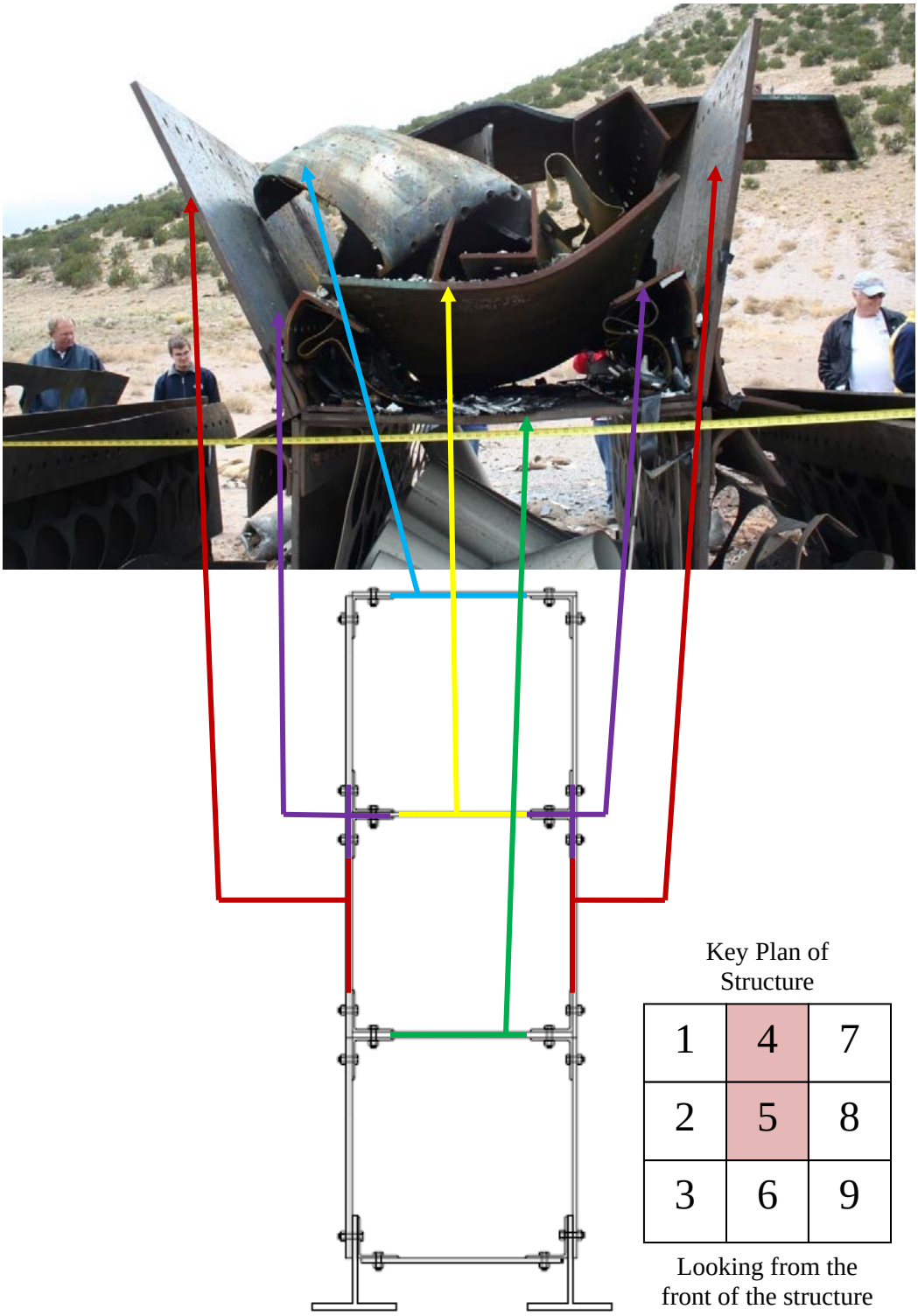

Figure H.48: Test specimen post-test cells 4and 5

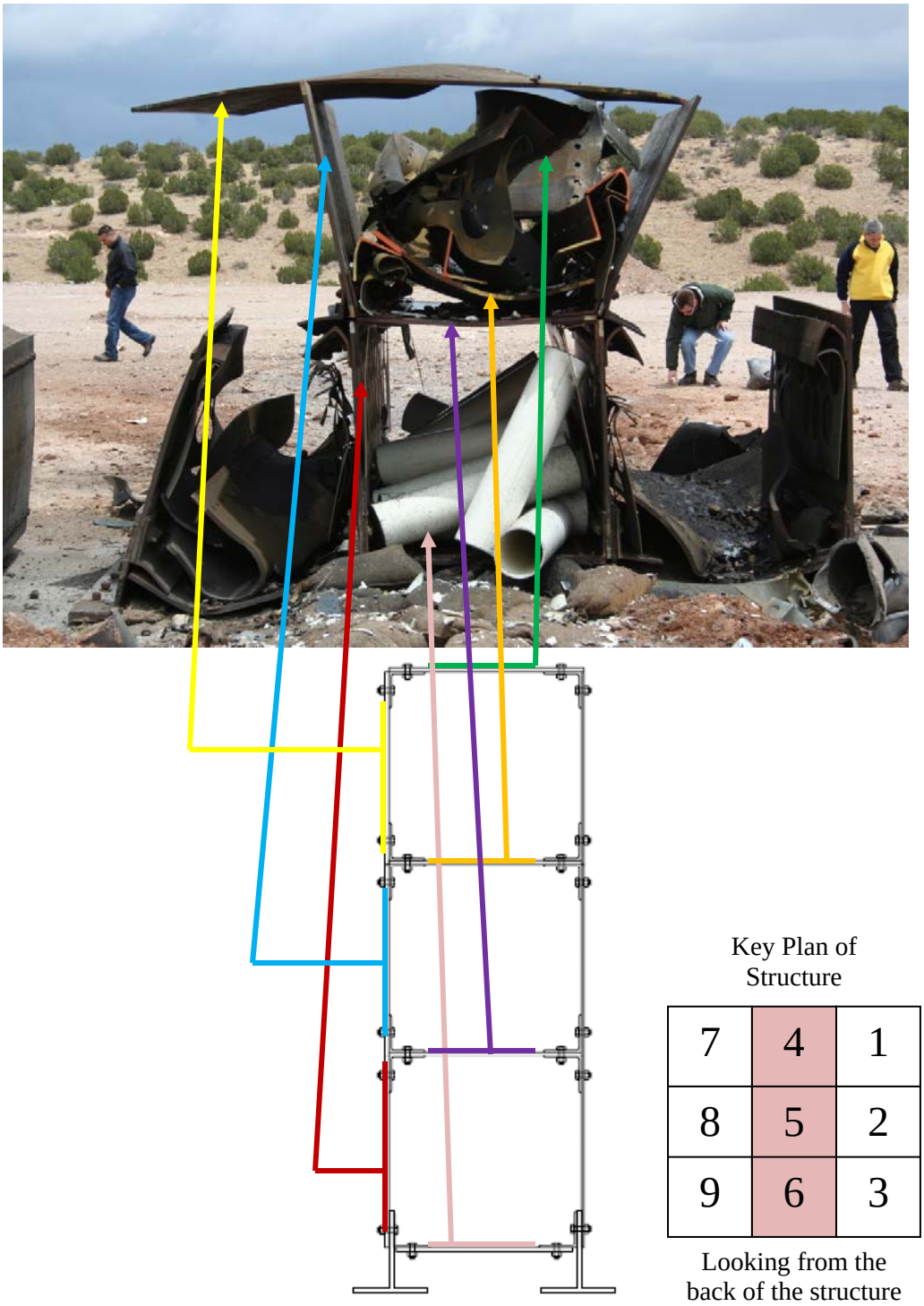

Figure H.49: Test specimen post-test cells 4, 5, and 6